

General Disclaimer

One or more of the Following Statements may affect this Document

- This document has been reproduced from the best copy furnished by the organizational source. It is being released in the interest of making available as much information as possible.
- This document may contain data, which exceeds the sheet parameters. It was furnished in this condition by the organizational source and is the best copy available.
- This document may contain tone-on-tone or color graphs, charts and/or pictures, which have been reproduced in black and white.
- This document is paginated as submitted by the original source.
- Portions of this document are not fully legible due to the historical nature of some of the material. However, it is the best reproduction available from the original submission.

Bibliography of Lewis Research Center Technical Publications Announced in 1979

(NASA-TM-81525) BIBLIOGRAPHY OF LEWIS
RESEARCH CENTER TECHNICAL PUBLICATIONS
ANNOUNCED IN 1979 (NASA) 376 p
HC A17/MF A01

N81-17942

CSSL 05B

G3/82

Unclass
15675

May 1980



NASA

PREFACE

In 1979, Lewis' 1050 research authors published 448 technical publications which were announced to and reached the worldwide scientific community. This number was our typical output even though we had a slight decrease in staff. In recent years, the trend in Lewis publishing has been that each year the number of technical presentations given at seminars, society symposia, and Lewis-hosted conferences has surpassed the record set the previous year. Lewis authors publish almost 60 percent of their research contributions in outside publications and the rest as NASA research reports. Lewis authors primarily use society proceedings, seminar presentations, and journal and transactions articles to describe their work.

In 1979, the production of 294 contractor-authored research reports was higher than the previous year's output of 267. In addition, 51 patent applications were filed, and 32 patents were issued, typical numbers for Lewis patent contributions.

In 1979, the annual award for Best Lewis Publication was presented to Walton L. Howes for his paper "Loudness of Steady Sounds - A New Theory," which delves deeply into the physical and physiological basis of sound perception. This journal article appeared in *Acustica*, volume 41, 1979, and is described in abstract A79-39375 (p. 176) in this bibliography. An expanded version of the journal article, entitled "Overall Loudness of Steady Sounds According to Theory and Experiment," was published as NASA RP-1001; it is described in abstract N79-25753 (p. 163) in this bibliography.

And in 1979, the Joint Propulsion Conference, sponsored by the American Institute of Aeronautics and Astronautics, the Society of Automotive Engineers, and the American Society of Mechanical Engineers, presented its award for Best Paper of the Year to James J. Pelouch, Jr., for his study "Low-Thrust Chemical Orbit Transfer Propulsion." This paper describes a unique Lewis capability to take the lead in generating the knowledge for low-thrust chemical propulsion. This presentation, AIAA Paper 79-1182, is described in abstract A79-39815 (p. 55) in this bibliography.

All the publications in this collection were announced in the 1979 issues of STAR (Scientific and Technical Aerospace Reports) and/or IAA (International Aerospace Abstracts).

The arrangement of the material is by NASA subject category, as noted in the Contents. The Lewis-authored items are listed first, followed by the contractor items. Within each of these groups is listed report literature, in N-number sequence, followed by the journal and conference presentations, in A-number sequence.

The various indexes will help locate specific publications by subject, author, contractor organization, contract number, and report number.

George Mandel
Chief, Management Services Division

CONTENTS

	Page
AERONAUTICS (GENERAL)	1
AERODYNAMICS	2
AIR TRANSPORTATION AND SAFETY	8
AIRCRAFT COMMUNICATIONS AND NAVIGATION	10
AIRCRAFT DESIGN, TESTING AND PERFORMANCE	11
AIRCRAFT INSTRUMENTATION	12
AIRCRAFT PROPULSION AND POWER	13
AIRCRAFT STABILITY AND CONTROL	38
RESEARCH AND SUPPORT FACILITIES (AIR)	39
ASTRONAUTICS (GENERAL)	40
ASTRODYNAMICS	41
LAUNCH VEHICLES AND SPACE VEHICLES	42
SPACE TRANSPORTATION	43
SPACECRAFT COMMUNICATIONS, COMMAND AND TRACKING	44
SPACECRAFT DESIGN, TESTING AND PERFORMANCE	46
SPACECRAFT INSTRUMENTATION	51
SPACECRAFT PROPULSION AND POWER	52
CHEMISTRY AND MATERIALS (GENERAL)	59
COMPOSITE MATERIALS	61
INORGANIC AND PHYSICAL CHEMISTRY	68
METALLIC MATERIALS	73
NONMETALLIC MATERIALS	81
PROPELLANTS AND FUELS	89
ENGINEERING (GENERAL)	93
COMMUNICATIONS	94
ELECTRONICS AND ELECTRICAL ENGINEERING	97
FLUID MECHANICS AND HEAT TRANSFER	102
INSTRUMENTATION AND PHOTOGRAPHY	109
LASERS AND MASERS	112
MECHANICAL ENGINEERING	113
QUALITY ASSURANCE AND RELIABILITY	125
STRUCTURAL MECHANICS	126
EARTH RESOURCES	131
ENERGY PRODUCTION AND CONVERSION	133
ENVIRONMENT POLLUTION	157
GEOPHYSICS	160
METEOROLOGY AND CLIMATOLOGY	161
OCEANOGRAPHY	162
BEHAVIORAL SCIENCES	163
MAN/SYSTEM TECHNOLOGY AND LIFE SUPPORT	164
COMPUTER OPERATIONS AND HARDWARE	165
COMPUTER PROGRAMMING AND SOFTWARE	166
NUMERICAL ANALYSIS	168

	Page
STATISTICS AND PROBABILITY	169
SYSTEMS ANALYSIS	170
PHYSICS (GENERAL)	171
ACOUSTICS	172
ATOMIC AND MOLECULAR PHYSICS	179
NUCLEAR AND HIGH-ENERGY PHYSICS	180
PLASMA PHYSICS	181
SOLID-STATE PHYSICS	184
THERMODYNAMICS AND STATISTICAL PHYSICS	187
URBAN TECHNOLOGY AND TRANSPORTATION	188
GENERAL	190
SUBJECT INDEX (KEYWORDS)	A-1
PERSONAL AUTHOR INDEX (INCLUDES LEWIS AND CONTRACTOR AUTHORS)	B-1
CORPORATE SOURCE INDEX (CONTRACTOR ORGANIZATIONS)	C-1
CONTRACT NUMBER INDEX	D-1
REPORT/ACCESSION NUMBER INDEX (INCLUDES PATENTS)	E-1

01 AERONAUTICS (GENERAL)

N79-16796* National Aeronautics and Space Administration. Lewis Research Center, Cleveland, Ohio.

GENERATION OF LINEAR DYNAMIC MODELS FROM A DIGITAL NONLINEAR SIMULATION

Carl J. Daniele and Susan M. Krosel Feb. 1979 95 p refs (NASA-TP-1388; E-9490) Avail: NTIS HC A05/MF A01 CSCL 02A

The results and methodology used to derive linear models from a nonlinear simulation are presented. It is shown that averaged positive and negative perturbations in the state variables can reduce numerical errors in finite difference, partial derivative approximations and, in the control inputs, can better approximate the system response in both directions about the operating point. Both explicit and implicit formulations are addressed. Linear models are derived for the F 100 engine, and comparisons of transients are made with the nonlinear simulation. The problem of startup transients in the nonlinear simulation in making these comparisons is addressed. Also, reduction of the linear models is investigated using the modal and normal techniques. Reduced-order models of the F 100 are derived and compared with the full-state models. J.M.S.

N79-20008* National Aeronautics and Space Administration. Lewis Research Center, Cleveland, Ohio.

MATERIALS AND STRUCTURAL ASPECTS OF ADVANCED GAS-TURBINE HELICOPTER ENGINES

John C. Freche (US Army Aviation Res. and Develop. Command, Cleveland) and John Acurio 1979 65 p refs To be presented at the Intern. Congr. in Aeron., Paris, 6-8 Jun. 1979 (NASA-TM-79100; AVRADCOM-TR-79-4) Avail: NTIS HC A04/MF A01 CSCL 21E

The key to improved helicopter gas turbine engine performance lies in the development of advanced materials and advanced structural and design concepts. The modification of the low temperature components of helicopter engines (such as the inlet particle separator), the introduction of composites for use in the engine front frame, the development of advanced materials with increased use-temperature capability for the engine hot section, can result in improved performance and/or decreased engine maintenance cost. A major emphasis in helicopter engine design is the ability to design to meet a required lifetime. This, in turn, requires that the interrelated aspects of higher operating temperatures and pressures, cooling concepts, and environmental protection schemes be integrated into component design. The major material advances, costings, and design life-prediction techniques pertinent to helicopter engines are reviewed; the current state-of-the-art is identified; and when appropriate, progress, problems, and future directions are assessed. A.R.H.

02 AERODYNAMICS

Includes aerodynamics of bodies, combinations, wings, rotors, and control surfaces; and internal flow in ducts and turbomachinery.

For related information see also 34 *Fluid Mechanics and Heat Transfer*.

N79-10022* National Aeronautics and Space Administration, Lewis Research Center, Cleveland, Ohio.

AERODYNAMIC PERFORMANCE OF A 1.35-PRESSURE-RATIO AXIAL-FLOW FAN STAGE

Walter M. Osborn, Royce D. Moore, and Ronald J. Steinke Oct. 1978 108 p refs
(NASA-TP-1259; E-9025) Avail: NTIS HC A06/MF A01 CSCL 01A

The overall blade element performances and the aerodynamic design parameters are presented for a 1.35-pressure-ratio fan stage. The fan stage was designed for a weight flow of 32.7 kilograms per second and a tip speed of 302.8 meters per second. At design speed the stage peak efficiency of 0.879 occurred at a pressure ratio of 1.329 and design flow. Stage stall margin was approximately 14 percent. At design flow rotor efficiency was 0.94 and the pressure ratio was 1.360. B.B.

N79-10023* National Aeronautics and Space Administration, Lewis Research Center, Cleveland, Ohio.

A COMPUTER PROGRAM FOR THE CALCULATION OF THE FLOW FIELD IN SUPERSONIC MIXED-COMPRESSION INLETS AT ANGLE OF ATTACK USING THE THREE-DIMENSIONAL METHOD OF CHARACTERISTICS WITH DISCRETE SHOCK WAVE FITTING

Joseph Vadyak (Purdue Univ., West Lafayette, Ind.), Joe D. Hoffman (Purdue Univ., West Lafayette, Ind.), and Allan R. Bishop Jun. 1978 173 p refs
(Grant NGR-15-005-191)
(NASA-TM-78947; E-8694) Avail: NTIS HC A08/MF A01 CSCL 01A

The calculation procedure is based on the method of characteristics for steady three-dimensional flow. The bow shock wave and the internal shock wave system were computed using a discrete shock wave fitting procedure. The general structure of the computer program is discussed, and a brief description of each subroutine is given. All program input parameters are defined, and a brief discussion on interpretation of the output is provided. A number of sample cases, complete with data deck listings, are presented. G.G.

N79-11000* National Aeronautics and Space Administration, Lewis Research Center, Cleveland, Ohio.

SUPERSONIC UNSTALLED FLUTTER

J. J. Adamczyk, M. E. Goldstein, and M. J. Hartmann 1978 24 p refs Presented at the 52d Meeting of the Propulsion and Energetics Panel, Cleveland, 23-27 Oct. 1978; sponsored by AGARD
(NASA-TM-79001; E-9785) Avail: NTIS HC A02/MF A01 CSCL 01A

Flutter analyses were developed to predict the onset of supersonic unstalled flutter of a cascade of two-dimensional airfoils. The first of these analyzes the onset of supersonic flutter at low levels of aerodynamic loading (i.e., backpressure), while the second examines the occurrence of supersonic flutter at moderate levels of aerodynamic loading. Both of these analyses are based on the linearized unsteady inviscid equations of gas dynamics to model the flow field surrounding the cascade. These analyses are utilized in a parametric study to show the effects of cascade geometry, inlet Mach number, and backpressure on the onset of single and multi degree of freedom unstalled supersonic flutter. Several of the results are correlated against experimental qualitative observation to validate the models. J.M.S.

N79-11001* National Aeronautics and Space Administration, Lewis Research Center, Cleveland, Ohio.

AERODYNAMIC AND ACOUSTIC EFFECTS OF ELIMINATING CORE SWIRL FROM A FULL SCALE 1.8 STAGE PRESSURE RATIO FAN (QF-5A)

Richard P. Woodward, Loren W. Acker, and Edward G. Stakolich Sep. 1978 35 p refs
(NASA-TM-78991; E-9774) Avail: NTIS HC A03/MF A01 CSCL 01A

Fan QF-5A was a modification of fan QF-5 which had an additional core stator and adjusted support struts to turn the core exit flow from a 30 deg swirl to the axial direction. This modification was necessary to eliminate the impingement of the swirling core flow on the axial support pylon of the NASA-Lewis Quiet Fan Facility that caused aerodynamic, acoustic and structural problems with the original fan stage at fan speeds greater than 85 percent of design. The redesigned fan QF-5A did obtain the design bypass ratio with an increased core airflow suggesting that the flow problem was resolved. Acoustically, the redesigned stage showed a low frequency broadband noise reduction compared to the results for fan QF-5 at similar operating conditions. Author

N79-12015* National Aeronautics and Space Administration, Lewis Research Center, Cleveland, Ohio.

EFFECT OF ROTOR TIP CLEARANCE AND CONFIGURATION ON OVERALL PERFORMANCE OF A 12.77-CENTIMETER TIP DIAMETER AXIAL-FLOW TURBINE

Jeffrey E. Haas (Army Aviation Research and Development Command) and Milton G. Kofskey 1978 14 p refs To be presented at 24th Ann. Intern. Conf., San Diego, Calif., 11-15 Mar. 1979; sponsored by Am. Soc. of Mech. Engr.
(NASA-TM-79025; E-9181-1; AVRADCOM-TR-78-54) Avail: NTIS HC A02/MF A01 CSCL 01A

The rotor tip clearance was obtained by use of a recess in the casing above the rotor blades and also by use of a reduced blade height. For the recessed casing configuration, the optimum rotor blade height was found to be the one where the rotor tip diameter was equal to the stator tip diameter. The tip clearance loss associated with this optimum recessed casing configuration was less than that for the reduced blade height configuration. G.G.

N79-12016* National Aeronautics and Space Administration, Lewis Research Center, Cleveland, Ohio.

WIND TUNNEL TESTS OF A BLADE SUBJECTED TO MIDCHORD TORSIONAL OSCILLATION AT HIGH SUBSONIC STALL FLUTTER CONDITIONS

D. R. Boldman and A. E. Buggele Oct. 1978 33 p refs
(NASA-TM-78998; E-9782) Avail: NTIS HC A03/MF A01 CSCL 01A

A mechanical drive system for oscillating blades in a wind tunnel at frequencies up to 767 hertz and amplitudes of + or - 1.2 deg is described. High-speed motion pictures of schlieren images of the flow over a double-circular arc blade oscillating in harmonic motion about the midchord revealed extensive shock patterns at a nominal free stream Mach number of 0.7, a mean angle of attack of 4 deg, and reduced frequency of about 0.7. A phase lag resulting from the slow response of the flow to the motion of the blade increased with increasing reduced frequency. This phase lag, based on the difference between the time the blade attained its maximum angle of attack and the time required for the normal shock to reach its extreme downstream position, was nominally 100 deg at the above conditions. Author

N79-12020* National Aeronautics and Space Administration, Lewis Research Center, Cleveland, Ohio.

AN APPROACH TO OPTIMUM SUBSONIC INLET DESIGN

R. W. Luidens, N. O. Stockman, and J. H. Diedrich 1978 14 p refs Proposed for presentation at the 24th Ann. Intern. Gas Turbine Conf. and 1st Solar Energy Conf., 11-15 Mar. 1979; sponsored by Am. Soc. of Mech. Engr.

(NASA-TM-79051; E-9850) Avail: NTIS HC A02/MF A01 CSCL 01A

Inlet operating requirements are compared with estimated inlet separation characteristics to identify the most critical inlet operating condition. This critical condition is taken to be the design point and is defined by the values of inlet mass flow, free-stream velocity and inlet angle of attack. Optimum flow distributions on the inlet surface were determined to be a high, flat top Mach number distribution on the inlet lip to turn the flow quickly into the inlet and a flat bottom skin-friction distribution on the diffuser wall to diffuse the flow rapidly and efficiently to the velocity required at the fan face. These optimum distributions are then modified to achieve other desirable flow characteristics. Example applications are given. G.G.

N79-13003* National Aeronautics and Space Administration, Lewis Research Center, Cleveland, Ohio.

ANALYSIS OF SUPERSONIC STALL BENDING FLUTTER IN AXIAL-FLOW COMPRESSOR BY ACTUATOR DISK THEORY

John J. Adamczyk Nov. 1978 58 p refs
(NASA-TP-1345; E-9186) Avail: NTIS HC A04/MF A01 CSCL 01A

An analytical model was developed for predicting the onset of supersonic stall bending flutter in axial-flow compressors. The analysis is based on two-dimensional, compressible, unsteady actuator disk theory. It is applied to a rotor blade row by considering a cascade of airfoils. The effects of shock waves and flow separation are included in the model. Calculations show that the model predicts the onset, in an unshrouded rotor, of a bending flutter mode that exhibits many of the characteristics of supersonic stall bending flutter. The validity of the analysis for predicting this flutter mode is demonstrated. Author

N79-14996* National Aeronautics and Space Administration, Lewis Research Center, Cleveland, Ohio.

THEORETICAL STUDY OF VTOL TILT-NACELLE AXISYMMETRIC INLET GEOMETRIES

J. Dennis Hawk and Norbert O. Stockman Jan. 1979 29 p refs
(NASA-TP-1380; E-9756) Avail: NTIS HC A03/MF A01 CSCL 01A

A systematic theoretical study of VTOL tilt-nacelle inlet design parameters is reported. The parameters considered are internal-lip contraction ratio, internal-lip major-to-minor axis ratio, diffuser-exit-area to throat-area ratio, maximum diffuser wall angle and shape. Each of the inlets was analyzed at the same given flow condition of free-stream velocity, angle between the free stream and centerline of the inlet, and diffuser-exit Mach number. The effects of these geometric parameters on surface static-pressure distribution, peak surface Mach number, diffusion velocity ratio, and tendency for the inlet flow to separate are presented. Author

N79-14999* National Aeronautics and Space Administration, Lewis Research Center, Cleveland, Ohio.

AERODYNAMIC PERFORMANCE OF SCARF INLETS

John M. Abbott 1979 22 p refs Presented at 17th Aerospace Sci. Meeting, New Orleans, La., 15-17 Jan. 1979; sponsored by AIAA
(NASA-TM-79055; E-9865) Avail: NTIS HC A02/MF A01 CSCL 01A

A scarf inlet is characterized by having a longer lower lip than upper lip leading to both aerodynamic and acoustic advantages. Aerodynamically, a scarf inlet has higher angle of attack capability and is less likely to ingest foreign objects while the aircraft is on the ground. Acoustically, a scarf inlet provides for reduced inlet radiated noise levels below the engine as a result of upward reflection and refraction of inlet radiated noise. Results of a wind tunnel test program are presented which illustrate the aerodynamic performance of two different scarf inlet designs. Based on these results, scarf inlet performance is summarized in a way to illustrate the advantages and limitations of a scarf inlet compared to an axisymmetric inlet. Author

N79-14998* National Aeronautics and Space Administration, Lewis Research Center, Cleveland, Ohio.

EFFECT OF LIP AND CENTERBODY GEOMETRY ON AERODYNAMIC PERFORMANCE OF INLETS FOR TILTING-NACELLE VTOL AIRCRAFT

Richard R. Burley 1979 27 p Presented at the 7th Aerospace Sci. Meeting, New Orleans, 15-17 Jan. 1979; sponsored by AIAA

(NASA-TM-79056; E-9866; AIAA-Paper-79-0381) Avail: NTIS HC A03/MF A01 CSCL 01A

Inlets for tilt-nacelle VTOL aircraft must operate over a wide range of incidence angles and engine weight flows without internal flow separation. Wind tunnel tests of scale model inlets were conducted to evaluate the effectiveness of three geometric variables to provide this capability. Increasing the lip contraction ratio increased the separation angle at all engine weight flows. The optimum axial location of the centerbody occurred when its leading edge was located just downstream of the inlet lip. Compared with a short centerbody, the optimum location of the centerbody resulted in an increase in separation angle at all engine weight flows. Decreasing the lip major-to-minor-axis ratio increased the separation angle at the lower engine weight flows. Author

N79-20089* National Aeronautics and Space Administration, Lewis Research Center, Cleveland, Ohio.

WIND TUNNEL PERFORMANCE OF FOUR ENERGY EFFICIENT PROPELLERS DESIGNED FOR MACH 0.8 CRUISE

Robert J. Jeracki, Daniel C. Mikkelsen, and Bernard J. Blaha 1979 24 p refs Presented at the Business Aircraft Meeting, Wichita, Kansas, 3-6 Apr. 1979; sponsored by the Soc. of Automotive Engrs.

(NASA-TM-79124; E-9960) Avail: NTIS HC A02/MF A01 CSCL 01A

Several advanced aerodynamic and acoustic concepts were investigated in recent wind tunnel tests performed in the NASA-Lewis Research Center 8x6 foot wind tunnel. These concepts included aerodynamically integrated propeller/nacelles, area-ruling, blade sweep, reduced blade thickness, and power (disk) loadings several times higher than conventional designs. Four eight-bladed propeller models were tested to determine aerodynamic performance. Relative noise measurements were made on three of the models at cruise conditions. Three of the models were designed with swept blades and one with straight blades. At the design Mach number of 0.8, power coefficient c_P 1.7, and advance ratio of 3.06, the straight bladed model had the lowest net efficiency of 75.8 percent. Increasing the sweep to 30 deg improved the performance to near 77 percent. Installation of an area-ruled spinner on a 30 deg sweep model further improved the efficiency to about 78 percent. The model with the highest blade sweep (45 deg) and an area-ruled spinner had the highest net efficiency of 78.7 percent, and at lower power loadings the efficiency exceeded 80 percent. At lower Mach numbers the 30 deg swept model had the highest efficiency. Values near 81 percent were obtained for the design loading at speeds to Mach 0.7. Relative noise measurements indicated that the acoustically designed 45 deg sweep model reduced the near field cruise noise by between 5 and 6 dB. A.R.H.

N79-23911* National Aeronautics and Space Administration, Lewis Research Center, Cleveland, Ohio.

THEORETICAL FAN VELOCITY DISTORTIONS DUE TO INLETS AND NOZZLES

J. Dennis Hawk 1979 12 p refs Presented at the Workshop on V/STOL Aerodyn., Monterey, Calif., 16-18 May 1979
(NASA-TM-79150; E-006) Avail: NTIS HC A02/MF A01 CSCL 01A

Nonuniform velocity profiles imposed on the propulsion system fan can cause fan blade stresses and thrust losses. A theoretical parametric study of the effects of inlets with 0 deg and 90 deg nozzle deflection on the velocity profile at a hypothetical fan is presented. The parameters investigated are fan-to-nozzle spacing and inlet centerline offset. The interaction between the inlet and nozzle is also investigated. The study is made using a two-dimensional analysis. A.R.H.

N79-23912* National Aeronautics and Space Administration, Lewis Research Center, Cleveland, Ohio.

AIRCRAFT ICING

Bernard J. Bleha, comp 1979 147 p refs Workshop held at Cleveland, 19-21 Jul. 1978

(NASA-CP-2086; FAA-RD-78-109; E-027) Avail: NTIS HC A07/MF A01 CSCL 01C

The results of a conference on the problems of aircraft icing are reported. For individual titles, see N79-23913 through N79-23919.

N79-23914* National Aeronautics and Space Administration, Lewis Research Center, Cleveland, Ohio.

EXECUTIVE SUMMARY OF AIRCRAFT ICING SPECIALISTS WORKSHOP

Milton A. Beheim In its Aircraft Icing 1979 p 1-16 (For primary document see N79-23912 15-02)

Avail: NTIS HC A07/MF A01 CSCL 01C

In a period of escalating development costs for new aircraft, there is growing interest in a renewed and coordinated icing research effort to achieve an updating or modernization of each aspect of the technological issues that are involved. This includes the data base, analysis methods, test techniques, and test facilities. L.S.

N79-23920* National Aeronautics and Space Administration, Lewis Research Center, Cleveland, Ohio.

AN EXPERIMENTAL INVESTIGATION OF FORCED MIXING OF A TURBULENT BOUNDARY LAYER IN AN ANNULAR DIFFUSER Ph.D. Thesis - Ohio State Univ.

Robert Joseph Shaw Apr. 1979 182 p refs (NASA-TM-79171; E-9947) Avail: NTIS HC A09/MF A01 CSCL 01A

The forced mixing process of a turbulent boundary layer in an axisymmetric annular diffuser using conventional wing-like vortex generators was studied. Flow field measurements were made at four axial locations downstream of the vortex generators. At each axial location, a total of 25 equally spaced profiles were measured behind three consecutive vortex generators which formed two pairs of vortex generators. Hot film anemometry probes measured the boundary layer turbulence structure at the same locations where pressure measurements were made. Both single and cross film probes were used. The diffuser turbulence data was taken only for a nominal inlet Mach number of 0.3. Three vortex generator configurations were tested. The differences between configurations involved changes in size and relative vortex generator positions. All three vortex generator configurations tested provided increases in diffuser performance. Distinct differences in the boundary layer integral properties and skin friction levels were noted between configurations. The axial turbulence intensity and Reynolds stress profiles measured displayed similarities in trends but differences in levels for the three configurations. A.R.H.

N79-26019* National Aeronautics and Space Administration, Lewis Research Center, Cleveland, Ohio.

COMPUTER PROGRAMS FOR CALCULATING TWO-DIMENSIONAL POTENTIAL FLOW THROUGH DEFLECTED NOZZLES

J. Dennis Hawk and Norbert O. Stockman May 1979 316 p refs

(NASA-TM-79144; E-9999) Avail: NTIS HC A14/MF A01 CSCL 01A

Computer programs to calculate the incompressible potential flow, corrected for compressibility, in two-dimensional nozzles at arbitrary operating conditions are presented. A statement of the problem to be solved, a description of each of the computer programs, and sufficient documentation, including a test case, to enable a user to run the program are included. J.M.S.

N79-27093* National Aeronautics and Space Administration, Lewis Research Center, Cleveland, Ohio.

PERFORMANCE OF A V/STOL TILT NACELLE INLET WITH BLOWING BOUNDARY LAYER CONTROL

Albert L. Johns, Robert C. Williams, and H. C. Potonides (Grumman Aerospace Corp., Bethpage, N. Y.) 1979 13 p refs Presented at the 15th Joint Propulsion Conf., Las Vegas, Nev., 18-20 Jun. 1979; cosponsored by AIAA, SAE and ASME

(NASA-TM-79176; E-043) Avail: NTIS HC A02/MF A01 CSCL 01A

A scale model of a V/STOL tilt nacelle fitted to a 0.508 m single stage fan was tested in the NASA Lewis 9x15 ft low speed wind tunnel to determine the effect of diffuser blowing on the inlet aerodynamics and aeromechanical performance. The test was conducted over a range of freestream speeds (up to 120 knots) and angles of attack (up to 120 deg). Diffuser blowing had a beneficial effect on all performance parameters. The angle of attack range for separation free flow substantially increased, and the fan face distortion significantly reduced with a corresponding increase in total pressure recovery. Discrete narrow band blade stress peaks which were common to the nonblowing (baseline) configuration were eradicated with diffuser blowing. S.E.S.

N79-28146* National Aeronautics and Space Administration, Lewis Research Center, Cleveland, Ohio.

WING AERODYNAMIC LOADING CAUSED BY JET-INDUCED LIFT ASSOCIATED WITH STOL-OTW CONFIGURATIONS

U. vonGlahn and D. Groesbeck 1979 40 p refs Presented at Atmospheric Flight Mech. Conf., Boulder, Colo., 6-8 Aug. 1979; sponsored by AIAA

(NASA-TM-79218; E-110) Avail: NTIS HC A03/MF A01 CSCL 01A

Surface pressure distributions were obtained with model-scale STOL-OTW configurations using various nozzles designed to promote flow attachment to the wing/flap surface. The nozzle configurations included slot-types and both circular and slot nozzles with external flow deflectors. The wing aerodynamic loading caused by the jet-induced lift is presented in conventional terms of delta p/q as a function of chordwise surface distance in the nozzle centerline plane as well as outboard of the nozzle centerline. Nozzle roof/deflector angle, chordwise location of the nozzle, wing size, and flap deflection angle are included in the geometric variables affecting the wing loading. A.R.H.

N79-29143* National Aeronautics and Space Administration, Lewis Research Center, Cleveland, Ohio.

RECENT APPLICATIONS OF THEORETICAL ANALYSIS TO V/STOL INLET DESIGN

Norbert O. Stockman 1979 18 p refs Presented at Workshop on V/STOL Aerodyn., Monterey, Calif. 16-18 May 1979; sponsored by Naval Air Develop. Center

(NASA-TM-79211; E-096) Avail: NTIS HC A02/MF A01 CSCL 01A

The theoretical analysis methods, potential flow, and boundary layer, used at Lewis are described. Recent application to Navy V/STOL aircraft, both fixed and tilt nacelle configurations, are presented. A three dimensional inlet analysis computer program is described and preliminary results presented. An approach to optimum design of inlets for high angle of attack operations is discussed. M.M.M.

A79-12599 * Supersonic unstalled flutter. J. J. Adamczyk, M. E. Goldstein, and M. J. Hartmann (NASA, Lewis Research Center, Cleveland, Ohio). NATO, AGARD, Meeting of the Propulsion and Energetics Panel, 52nd, Cleveland, Ohio, Oct. 23-27, 1978, Paper. 23 p. 8 refs.

Recently two flutter analyses have been developed at NASA Lewis Research Center to predict the onset of supersonic unstalled flutter of a cascade of two-dimensional airfoils. The first of these analyzes the onset of supersonic flutter at low levels of aerodynamic loading (i.e., backpressure), while the second examines the occur-

rence of supersonic flutter at moderate levels of aerodynamic loading. Both of these analyses are based on the linearized unsteady inviscid equations of gas dynamics to model the flow field surrounding the cascade. The details of the development of the solution to each of these models have been published. The objective of the present paper is to utilize these analyses in a parametric study to show the effects of cascade geometry, inlet Mach number, and backpressure on the onset of single and multi degree of freedom unstalled supersonic flutter. Several of the results from this study are correlated against experimental qualitative observation to validate the models. (Author)

A79-16047 * # Unsteady flow in a supersonic cascade with subsonic leading-edge locus. J. J. Adamczyk and M. E. Goldstein (NASA, Lewis Research Center, Cleveland, Ohio). *AIAA Journal*, vol. 16, Dec. 1978, p. 1248-1254. 14 refs.

Linearized theory is used to predict the unsteady flow in a supersonic cascade with subsonic axial flow velocity. A closed-form analytical solution is obtained by using a double application of the Wiener-Hopf technique. Although numerical and semianalytical solutions of this problem have already appeared in the literature, this paper contains the first completely analytical solution. It has been stated in the literature that the blade source should vanish at the infinite duct resonance condition. The present analysis shows that this does not occur. This apparent discrepancy is explained in the paper. (Author)

A79-19452 * Unsteady vortical and entropic distortions of potential flows round arbitrary obstacles. M. E. Goldstein (NASA, Lewis Research Center, Cleveland, Ohio). *Journal of Fluid Mechanics*, vol. 89, Dec. 13, 1978, p. 433-468. 16 refs.

The analysis concerns the alterations produced when small amplitude disturbances, including entropy and vorticity disturbances, are imposed on steady potential flows. For the most general non-acoustic incident distortion field that can be imposed on the uniform upstream flow, it is shown that the perturbation velocity at any point of the resulting unsteady compressible and vortical flow consists of a part that is a known function of the imposed upstream distortion field and the mean flow variables and a potential part that can be found by solving a linear inhomogeneous wave equation with a dipole-type source term whose strength is a known function of the imposed upstream distortion field. The theory is applied to the unsteady flow past a corner, and a closed-form analytical solution is found. P.T.H.

A79-19495 * # High speed smoke flow visualization for the determination of cascade shock losses. J. A. Slovisky (Notre Dame, University, Notre Dame, Ind.), W. B. Roberts (Nielsen Engineering and Research, Inc., Mountain View, Calif.), and J. E. Crouse (NASA, Lewis Research Center, Fan and Compressor Branch, Cleveland, Ohio). *American Institute of Aeronautics and Astronautics, Aerospace Sciences Meeting, 17th, New Orleans, La., Jan. 15-17, 1979, Paper 79-0042*. 11 p. 17 refs. Grant No. NSG-3133.

A flow visualization technique has been developed by which quantitative cascade shock loss data can be ascertained without the interference effects of intrusive probes. The technique is first proven feasible by studying the high speed wind tunnel flow around a variety of two-dimensional shapes. Applicability is demonstrated by the testing of a 5% thick sharp-edged flat plate cascade at an upstream Mach number of about 1.3. Results are compared with the relevant theory and total pressure probe data. (Author)

A79-19524 * # An efficient user-oriented method for calculating compressible flow about three-dimensional inlets. J. L. Hess (Douglas Aircraft Co., Long Beach, Calif.) and N. O. Stockman (NASA, Lewis Research Center, Low Speed Aerodynamics Branch, Cleveland, Ohio). *American Institute of Aeronautics and Astronautics, Aerospace Sciences Meeting, 17th, New Orleans, La., Jan. 15-17, 1979, Paper 79-0081*. 7 p. Contract No. NAS3-21135.

tics, Aerospace Sciences Meeting, 17th, New Orleans, La., Jan. 15-17, 1979, Paper 79-0081. 7 p. Contract No. NAS3-21135.

This method uses a so-called panel method to calculate incompressible flow about arbitrary three-dimensional inlets with or without centerbodies for four fundamental flow conditions: unit onset flows parallel to each of the coordinate axes plus static operation. The computing time is scarcely longer than for a single solution. A linear superposition of these solutions quite rigorously gives incompressible flow about the inlet for any angle of attack, angle of yaw, and mass flow rate. Compressibility is accounted for by applying a well-proven correction to the incompressible flow. Since the computing times for the combination and the compressibility correction are small, flows at a large number of inlet operating conditions are obtained very cheaply. A number of graphical output features are provided to aid the user, including streamline tracing and automatic generation of curves of constant pressure, Mach number, and flow inclination at selected inlet cross sections. This paper describes the method in some detail and presents calculated results. (Author)

A79-19533 * # Reynolds number, scale and frequency content effects on F-15 inlet instantaneous distortion. C. H. Stevens, E. D. Spong (McDonnell Douglas Corp., St. Louis, Mo.), J. Nugent (NASA, Flight Research Center, Edwards, Calif.), and H. E. Neumann (NASA, Lewis Research Center, Cleveland, Ohio). *American Institute of Aeronautics and Astronautics, Aerospace Sciences Meeting, 17th, New Orleans, La., Jan. 15-17, 1979, Paper 79-0104*. 11 p. 6 refs.

An inlet instantaneous distortion study program sponsored by NASA was recently completed using an F-15 fighter aircraft. Peak distortion data from subscale inlet model wind tunnel tests are shown to be representative of full-scale flight test peak distortion. The effects on peak distortion are investigated for engine presence, Reynolds number, scale and frequency content. Data are presented which show that: (1) the effect of engine presence on total pressure recovery, peak distortion, and turbulence is small but favorable, (2) increasing the Reynolds number increases total pressure recovery, decreases peak distortion, and decreases turbulence, and (3) increasing the filter cutoff frequency increases the calculated values of both peak distortion and turbulence. (Author)

A79-23510 * # Aerodynamic performance of scarf inlets. J. M. Abbott (NASA, Lewis Research Center, Cleveland, Ohio). *American Institute of Aeronautics and Astronautics, Aerospace Sciences Meeting, 17th, New Orleans, La., Jan. 15-17, 1979, Paper 79-0380*. 21 p.

A scarf inlet is characterized by having a longer lower lip than upper lip leading to both aerodynamic and acoustic advantages. Aerodynamically, a scarf inlet has higher angle of attack capability and is less likely to ingest foreign objects while the aircraft is on the ground. Acoustically, a scarf inlet provides for reduced inlet radiated noise levels below the engine as a result of upward reflection and refraction of inlet radiated noise. Results of a wind tunnel test program are presented which illustrate the aerodynamic performance of two different scarf inlet designs. Based on these results, scarf inlet performance is summarized in a way to illustrate the advantages and limitations of a scarf inlet compared to an axisymmetric inlet. (Author)

A79-29007 * # Evaluation of MOSTAS computer code for predicting dynamic loads in two-bladed wind turbines. K. R. V. Kaza (NASA, Lewis Research Center, Cleveland; Toledo, University, Toledo, Ohio), D. C. Janetzke, and T. L. Sullivan (NASA, Lewis Research Center, Wind Energy Projects Office, Cleveland, Ohio). In: *Structures, Structural Dynamics, and Materials Conference, 20th, St. Louis, Mo., April 4-6, 1979, Technical Papers on Structures and Materials*. (A79-29002 11-39) New York, American Institute of Aeronautics and Astronautics, Inc., 1979, p. 53-63. 13 refs. (AIAA 79-0733)

Calculated dynamic blade loads are compared with measured loads over a range of yaw stiffnesses of the DOE/NASA Mod-0 wind turbine to evaluate the performance of two versions of the MOSTAS computer code. The first version uses a time-averaged coefficient approximation in conjunction with a multiblade coordinate transformation for two-bladed rotors to solve the equations of motion by standard eigenanalysis. The results obtained with this approximate analysis do not agree with dynamic blade load amplifications at or close to resonance conditions. The results of the second version, which accounts for periodic coefficients while solving the equations by a time history integration, compare well with the measured data.

(Author)

A79-30504 * # Axial-flow compressor turning angle and loss by inviscid-viscous interaction blade-to-blade computation. E. C. Hansen, G. K. Serovy (Iowa State University of Science and Technology, Ames, Iowa), and P. M. Sockol (NASA, Lewis Research Center, Cleveland, Ohio). *American Society of Mechanical Engineers, Gas Turbine Conference and Exhibit and Solar Energy Conference, San Diego, Calif., Mar. 12-15, 1979, Paper 79-GT-5*, 7 p. 27 refs. Members, \$1.50; nonmembers, \$3.00. Grants No. F45G-3033; No. AF-FOSR-78-3609; Contract No. F33615-76-C-2090.

A method for computation of the flow field around an arbitrary airfoil cascade on an axially symmetric blade-to-blade surface was developed which takes into account the development and separation of the blade surface boundary layers and mixing in the wake. The method predicts the overall fluid turning and total pressure loss in the context of an inviscid-viscous interaction scheme. The inviscid flow solution is obtained from a compressible flow matrix method. The viscous flow is obtained from a differential boundary layer method which calculates laminar, transitional and turbulent boundary layers. Provisions for the calculation of laminar and turbulent separation regions were added to the viscous scheme. The combined inviscid-viscous interaction scheme described yields results which are quantitatively consistent with experimental data. This suggests that the physical basis for the interactive system is correct and justifies continued exploration and use of the method.

(Author)

A79-30527 * # An approach to optimum subsonic inlet design. R. W. Luidens, N. O. Stockman, and J. H. Diedrich (NASA, Lewis Research Center, Cleveland, Ohio). *American Society of Mechanical Engineers, Gas Turbine Conference and Exhibit and Solar Energy Conference, San Diego, Calif., Mar. 12-15, 1979, Paper 79-GT-51*, 10 p. 21 refs. Members, \$1.50; nonmembers, \$3.00.

The approach consists of comparing inlet operating requirements with estimated inlet separation characteristics to identify the most critical inlet operating condition. This critical condition is taken to be the design point and is defined by the values of inlet mass flow, free stream velocity, and inlet angle of attack. Optimum flow distributions on the inlet surface are determined to be a high, flat top Mach number distribution on the inlet lip to turn the flow quickly into the inlet and a low, flat bottom skin friction distribution on the diffuser wall to diffuse the flow rapidly and efficiently to the velocity required at the fan face. These optimum distributions are then modified to achieve other desirable flow characteristics. Example applications are given. Extension of the method is suggested.

(Author)

A79-39810 * # Theoretical fan velocity distortions due to inlets and nozzles. J. D. Hawk (NASA, Lewis Research Center, Cleveland, Ohio). *Workshop on V/STOL Aerodynamics, Monterey, Calif., May 16-18, 1979, Paper*, 10 p.

Nonuniform velocity profiles imposed on the propulsion system fan can cause fan blade stresses and thrust losses. This paper presents a theoretical parametric study of the effects of inlets with 0 deg and 90 deg nozzle deflection on the velocity profile at a hypothetical fan. The parameters investigated are fan-to-nozzle spacing and inlet centerline offset. The interaction between the inlet and nozzle is also investigated. The study is made using a two-dimensional analysis.

(Author)

A79-47346 * # Wing aerodynamic loading caused by jet-induced lift associated with STOL-OTW configurations. U. von Glehn and D. Groesbeck (NASA, Lewis Research Center, Cleveland, Ohio). *American Institute of Aeronautics and Astronautics, Atmospheric Flight Mechanics Conference, Boulder, Colo., Aug. 6-8, 1979, Paper 79-1664*, 38 p. 5 refs.

Surface pressure distributions were obtained with model-scale STOL-OTW configurations using various nozzles designed to promote flow attachment to the wing-flap surface. The nozzle configurations included slot-types and both circular and slot nozzles with external flow deflectors. The wing aerodynamic loading caused by the jet-induced lift is presented in conventional terms of delta p/q as a function of chordwise surface distance in the nozzle centerline plane as well as outboard of the nozzle centerline. Included in the geometric variables affecting the wing loading are nozzle roof/deflector angle, chordwise location of the nozzle, wing size, and flap deflection angle.

(Author)

A79-47347 * # Performance of a V/STOL tilt nacelle inlet with blowing boundary layer control. A. L. Johns, R. C. Williams (NASA, Lewis Research Center, Cleveland, Ohio), and H. C. Potonides (Grumman Aerospace Corp., Bethpage, N.Y.). *AIAA, SAE, and ASME, Joint Propulsion Conference, 15th, Las Vegas, Nev., June 18-20, 1979, AIAA Paper 79-1163*, 11 p. 5 refs.

A scale model of a V/STOL tilt nacelle fitted to a 0.508 m single stage fan was tested in the NASA Lewis low speed wind tunnel to determine the effect of diffuser blowing on the inlet aerodynamics and aeromechanical performance. The test was conducted over a range of freestream speeds (up to 120 knots) and angles of attack (up to 12 deg). In general, diffuser blowing had a beneficial effect on all performance parameters. The angle-of-attack range for a separation-free flow substantially increased, and the fan face distortion reduced with a corresponding increase in total pressure recovery. Discrete narrow band blade stress peaks which were common to the nonblowing (baseline) configuration were eradicated with diffuser blowing.

V.T.

A79-49530 * # Recent applications of theoretical analysis to V/STOL inlet design. N. O. Stockman (NASA, Lewis Research Center, Cleveland, Ohio). *U.S. Navy, Workshop on V/STOL Aerodynamics, Monterey, Calif., May 16-18, 1979, Paper*, 16 p. 17 refs.

A brief description of the axisymmetric potential flow and boundary layer analysis methods used at the NASA Lewis Research Center, is presented. Application of this method to inlet problems arising from both tilt-nacelle and fixed-nacelle V/STOL aircraft configurations is illustrated. A three-dimensional inlet analysis computer program is described and the preliminary results presented. Finally, a suggested approach to optimum design of inlets for high angle-of-attack operation is discussed.

M.E.P.

N79-12014 * # General Dynamics/Fort Worth, Tex. **EXPERIMENTAL INVESTIGATION OF A 0.15-SCALE MODEL OF AN UNDERFUSELAGE NORMAL-SHOCK INLET** Final Report

P. C. Leamer and I. G. Kennon 1978 332 p refs (Contract NAS3-21139)

(NASA-CR-3049) Avail: NTIS HC A15/MF A01 CSCL 01A

A 0.15 scale model of an underfuselage inlet designed for a single-engine fighter airplane was tested. The inlet was a fixed-geometry, normal-shock configuration designed to operate at flight speeds up to Mach 2.0. Performance data for the basic inlet and several configuration variations are presented as a function of angle of attack, angle of sideslip, and airflow in the 0.6 to 2.0 Mach number range. The configuration variations included boundary-layer diverter height, cowl and splitter-plate modifications, and inlet bleed system variations. Flow-field characteristics at the simulated engine face, at the inlet throat, at the splitter-plate leading edge, and forward of the inlet are presented. The pressure recovery of the inlet is approximately equal to the product of theoretical normal-shock and duct pressure recoverable at cruise angle of attack. Very good performance at

high angle of attack was obtained. Pressure distortion and turbulence at the engine face were low, and the inlet remained stable at all engine airflows over the flight maneuver envelope of the aircraft for which the inlet was designed. G.G.

03 AIR TRANSPORTATION AND SAFETY

Includes passenger and cargo air transport operations; and aircraft accidents.

For related information see also 16 Space Transportation and 85 Urban Technology and Transportation.

N79-15013* National Aeronautics and Space Administration, Lewis Research Center, Cleveland, Ohio.

AIRCRAFT CABIN OZONE MEASUREMENTS ON B747-100 AND B747-SP AIRCRAFT: CORRELATIONS WITH ATMOSPHERIC OZONE AND OZONE ENCOUNTER STATISTICS

Porter J. Perkins, J. D. Holdeman, and Daniel J. Gauntner Jan. 1978 41 p refs Presented at a Tech. Briefing on Ozone, Cleveland, Ohio, 19 Jan. 1978 (NASA-TM-79060; E-9875) Avail: NTIS HC A03/MF A01 CSCL 06F

Simultaneous measurements of atmospheric (outside) ozone concentration and ozone levels in the cabin of the B747-100 and B747-SP airliners were made by NASA to evaluate the aircraft cabin ozone contamination problem. Instrumentation on these aircraft measured ozone from an outside probe and at one point in the cabin. Average ozone in the cabin of the B747-100 was 39 percent of the outside. Ozone in the cabin of the B747-SP measured 82 percent of the outside, before corrective measures. Procedures to reduce the ozone in this aircraft included changes in the cabin air circulation system, use of the high-temperature 15th stage compressor bleed, and charcoal filters in the inlet cabin air ducting, which as separate actions reduced the ozone to 58, 19 and 5 percent, respectively. The potential for the NASA instrumented B747 aircraft to encounter high levels of cabin ozone was derived from atmospheric ozone measurements on these aircraft. Encounter frequencies for two B747-100's were comparable even though the route structures were different. The B747-SP encountered high ozone than did the B747-100's.

Author

N79-21022* National Aeronautics and Space Administration, Lewis Research Center, Cleveland, Ohio.

OZONE CONTAMINATION IN AIRCRAFT CABINS: OBJECTIVES AND APPROACH

Porter J. Perkins In *its Ozone Contamination in Aircraft Cabins* Mar. 1979 p 1-2 (For primary document see N79-21021 12-03) Avail: NTIS HC A05/MF A01 CSCL 06S

Three panels were developed to solve the problem of ozone contamination in aircraft cabins. The problem is defined from direct in-flight measurements of ozone concentrations inside and outside airliners in their normal operations. Solutions to the cabin ozone problem are discussed under two areas: (1) flight planning to avoid high ozone concentrations, and (2) ozone destruction techniques installed in the cabin air systems. S.E.S.

N79-21025* National Aeronautics and Space Administration, Lewis Research Center, Cleveland, Ohio.

OZONE CONTAMINATION IN AIRCRAFT CABINS: SUMMARY OF RECOMMENDATIONS

Porter J. Perkins In *its Ozone Contamination in Aircraft Cabins* Mar. 1979 p 11-12 (For primary document see N79-21021 12-03) Avail: NTIS HC A05/MF A01 CSCL 06S

Recommendations from the three panels on in-flight measurements, flight planning to avoid high ozone, and ozone destruction techniques are summarized. S.E.S.

N79-21027* National Aeronautics and Space Administration, Lewis Research Center, Cleveland, Ohio.

OZONE CONTAMINATION IN AIRCRAFT CABINS: POST WORKSHOP REVIEW OF RECOMMENDATIONS

Porter J. Perkins In *its Ozone Contamination in Aircraft Cabins* Mar. 1979 p 13-16 (For primary document see N79-21021 12-03)

Avail: NTIS HC A05/MF A01 CSCL 06S

The recommendations, level of priority for accomplishment, and recommended approaches and responsibility for implementation as established by the review are presented. S.E.S.

N79-21029* National Aeronautics and Space Administration, Lewis Research Center, Cleveland, Ohio.

OZONE CONTAMINATION IN AIRCRAFT CABINS. APPENDIX B: OVERVIEW PAPERS. IN-FLIGHT MEASUREMENTS

Porter J. Perkins In *its Ozone Contamination in Aircraft Cabins* Mar. 1979 p 21-29 (For primary document see N79-21021 12-03)

Avail: NTIS HC A05/MF A01 CSCL 06S

The NASA Global Atmospheric Sampling Program ozone measurements were obtained to establish to characteristics of the ambient ozone concentration during routine operations and to determine the attenuation of ambient concentrations of cabin air systems from simultaneous ambient and in cabin measurements. The characteristics of ambient ozone include: (1) maximum concentration; (2) duration of ozone encounters; (3) frequency of ozone during a flight; (4) variability of ozone during a flight; (5) in relation to routes, altitude, and meteorological conditions. S.E.S.

N79-33171* National Aeronautics and Space Administration, Lewis Research Center, Cleveland, Ohio.

PROCEDURES FOR ESTIMATING THE FREQUENCY OF COMMERCIAL AIRLINE FLIGHTS ENCOUNTERING HIGH CABIN OZONE LEVELS

James D. Holdeman Oct. 1979 56 p refs (NASA-TP-1560; E-9991) Avail: NTIS HC A04/MF A01 CSCL 01C

Three analytical problems in estimating the frequency at which commercial airline flights will encounter high cabin ozone levels are formulated and solved, namely, estimating flight-segment mean levels, estimating maximum-per-flight levels, and estimating the maximum average level over a specified flight interval. For each problem, solution procedures are given for different levels of input information - from complete cabin ozone data, which provides a direct solution, to limited ozone information, such as ambient ozone means and standard deviations, with which several assumptions are necessary to obtain the required estimates. Each procedure is illustrated by an example case calculation that uses simultaneous cabin and ambient ozone data obtained by the NASA Global Atmospheric Sampling Program. Critical assumptions are discussed and evaluated, and the several solutions for each problem are compared. Example calculations are also performed to illustrate how variations in latitude, altitude, season, retention ratio, flight duration, and cabin ozone limits affect the estimated probabilities. Author

A79-27571 * Simultaneous measurements of ozone outside and inside cabins of two B-747 airliners and a Gates Learjet business jet. P. J. Perkins and D. Briehl (NASA, Lewis Research Center, Cleveland, Ohio). In: Conference on Atmospheric Environment of Aerospace Systems and Applied Meteorology, New York, N.Y., November 14-16, 1978, Preprints. (A79-27571 10-47) Boston, Mass., American Meteorological Society, 1978, p. 39-44, 15 refs.

Recently, passengers and crew members on long-distance commercial flights have filed complaints after suffering symptoms of ozone sickness. Studies were conducted to determine the frequency and concentration of ozone in commercial jet transports. The airliner problem with ozone prompted NASA to determine the ozone concentrations that might be encountered in the cabin of a small business jet. Simultaneous measurements of atmospheric ozone levels

and ozone levels in the cabins of jet aircraft were necessary because of the wide and rapid variability of atmospheric ozone in flight. It was found that the atmospheric ozone concentrations in the case of B-747 airliners vary widely during a flight. A constant difference, or ratio, between ozone concentrations outside and inside the cabin does not exist.

G.R.

**N79-23940*# Boeing Commercial Airplane Co., Seattle, Wash.
INFLIGHT FUEL TANK TEMPERATURE SURVEY DATA Final
Report**

A. J. Fasion May 1979 60 p refs
(Contract NAS3-20815)

(NASA-CR-159569; D6-48611)

Avail: NTIS

HC A04/MF A01 CSCL 01C

Statistical summaries of the fuel and air temperature data for twelve different routes and for different aircraft models (B747, B707, DC-10 and DC-8), are given. The minimum fuel, total air and static air temperature expected for a 0.3% probability were summarized in table form. Minimum fuel temperature extremes agreed with calculated predictions and the minimum fuel temperature did not necessarily equal the minimum total air temperature even for extreme weather, long range flights. R.E.S.

04 AIRCRAFT COMMUNICATIONS AND NAVIGATION

Includes digital and voice communication with aircraft; air navigation systems (satellite and ground based); and air traffic control.

For related information see also 17 *Spacecraft Communications, Command, and Tracking* and 32 *Communications*.

N79-31185* National Aeronautics and Space Administration. Lewis Research Center, Cleveland, Ohio.

UHF COPLANAR-SLOT ANTENNA FOR AIRCRAFT-TO-SATELLITE DATA COMMUNICATIONS

Poyce W. Myhre 1979 21 p refs Presented at the Printed Circuit Antenna Technol. Workshop, Las Cruces, N. Mex., 17-19 Oct. 1979; sponsored by New Mexico State Univ. and the Army Res. Office Physical Sci. Lab. (NASA-TM-79239; E-146) Avail: NTIS HC A02/MF A01 CSCL 176

A lightweight low drag coplanar slot antenna was developed for use on commercial jet aircraft that will provide upper hemisphere coverage in the UHF band at frequencies of 402 and 468 MHz is described. The antenna is designed to transmit meteorological data from wide body jet aircraft to ground users via synchronous meteorological data relay satellites. The low profile antenna (23.5 cm wide by 38.1 cm long slot by 1.9 cm high) is a conformal antenna utilizing the coplanar approach with the advantages of broad frequency bandwidth and improved electrical integrity over wide range of temperature. The antenna is circular polarized, has anon axis gain of near +2.5 dB, and a HPBW greater than 90 deg. Areas discussed include antenna design, radiation characteristics, flight testing, and system performance. K.L.

N79-33185* National Aeronautics and Space Administration. Lewis Research Center, Cleveland, Ohio.

MULTIPLE SPEED EXPANDABLE BIT SYNCHRONIZER

James M. Bundinger Aug. 1979 13 p refs (NASA-TM-79262; E-176) Avail: NTIS HC A02/MF A01 CSCL 17G

A multiple speed bit synchronizer was designed for installation in an inertial navigation system data decoder to extract non-return-to-zero level data and clock signal from biphasic level data. The circuit automatically senses one of four pre-determined biphasic data rates and synchronizes the proper clock rate to the data. Through a simple expansion of the basic design, synchronization of more than four binarily related data rates can be accomplished. The design provides an easily adaptable, low cost, low power alternative to external bit synchronizers with additional savings in size and weight. A.R.H.

A79-14949 * An airborne meteorological data collection system using satellite relay (ASDAR). J. W. Bagwell and B. G. Lindow (NASA, Lewis Research Center, Cleveland, Ohio). *Instrument Society of America, International Telemetry Conference, Los Angeles, Calif., Nov. 14-16, 1978, Paper*. 16 p.

The paper describes the aircraft to satellite data relay (ASDAR) project which processes information collected by the navigation and data systems of widebody jet aircraft which cross data-sparse areas of the tropics and southern hemisphere. The ASDAR system consists of a data acquisition and control unit to acquire, store, and format latitude, longitude, altitude, wind speed, wind direction, and outside air temperature data; a transmitter to relay the formatted data via satellite to the ground; and a clock to time the data sampling and transmission periods. M.L.

A79-17092 * Automated meteorological data from commercial aircraft via satellite - Present experience and future implications. R. Steinberg (NASA, Lewis Research Center, Cleveland, Ohio). In: *International Conference on Maritime and Aeronautical Satellite Communication and Navigation*, London, England, March 7-9, 1978, *Proceeding* (A79-17086 05-04) London, Institution of Electrical Engineers, 1978, p. 33-36.

The National Aeronautics and Space Administration has developed a low-cost communications system to provide meteorological data from commercial aircraft, in near real-time, on a fully automated basis. The complete system including the low profile antenna and all installation hardware weighs 34 kg. The prototype system has been installed on a Pan American B-747 aircraft and has been providing meteorological data (wind angle and velocity, temperature, altitude and position as a function of time) on a fully automated basis for the past several months. The results have been exceptional. This concept is expected to have important implications for operational meteorology and airline route forecasting. (Author)

05 AIRCRAFT DESIGN, TESTING AND PERFORMANCE

Includes aircraft simulation technology.
For related information see also 18 *Spacecraft Design, Testing and Performance* and 39 *Structural Mechanics*.

N79-24978* National Aeronautics and Space Administration, Lewis Research Center, Cleveland, Ohio.

SELF STABILIZING SONIC INLET Patent

Brent A. Miller, inventor (to NASA) Issued 15 May 1979 5 p
Filed 29 Mar. 1978

(NASA-Case-LEW-11890-1; US-Patent-4,154,256;

US-Patent-Appl-SN-891244; US-Patent-Class-137-15.1;

US-Patent-Class-244-53B) Avail: US Patent and Trademark Office CSCL 01C

An inlet suitable for a turbine engine in a STOL VTOL or CTOL aircraft is described. A circumferentially extended slot is provided in the inner surface of the air inlet at the windward side and downstream of the throat region. The slot communicates with a circumferential plenum chamber formed in the front of the air inlet just behind the lip. Circumferentially extending rows of apertures are provided on the lip establishing two sets of apertures spaced circumferentially away from the slot in opposite directions. The slot removes the boundary layer from the critical portion of the diffuser to minimize or eliminate flow pressure loss or separations resulting from diffusion or turning. The apertures are in a region of low static pressure on the lip of the inlet and serve as a source of suction to cause air flow into the slot.

Official Gazette of the U.S. Patent and Trademark Office

A79-28970* # Investigation of wing shielding effects on CTOL engine noise. H. E. Bloomer (NASA, Lewis Research Center, Cleveland, Ohio). *American Institute of Aeronautics and Astronautics, Aeroacoustics Conference, 5th, Seattle, Wash., Mar. 12-14, 1979, Paper 79-0669*. 33 p. 9 refs.

A full scale engine wing shielding investigation was conducted at the Lewis Research Center using a 97,900 N (22,000 lb) thrust turbofan engine and a simulated wing section sized around a conventional-take-off type four-engine narrow body airplane. Sound data were obtained for the wing placed at seven positions in a plane parallel to the engine axis, and were compared to data obtained without the wing at both take off and approach power. In addition the engine was operated with and without extensive acoustic treatment including a sonic inlet in order to evaluate wing shielding effectiveness with a highly suppressed engine. The wing shielding effectiveness was also calibrated using a 3.8 cm diam air nozzle as a sound source. Results indicated that even though about 10 dB broad band shielding was achieved, the equivalent flyover noise reduction was less than 3.0 EPNdB for most configurations. (Author)

06 AIRCRAFT INSTRUMENTATION

Includes cockpit and cabin display devices; and flight instruments.

For related information see also 19 *Spacecraft Instrumentation and 35 Instrumentation and Photography*.

N79-23963* National Aeronautics and Space Administration, Lewis Research Center, Cleveland, Ohio.

COMBINED PRESSURE AND TEMPERATURE DISTORTION EFFECTS ON INTERNAL FLOW OF A TURBOFAN ENGINE
W. M. Braithwaite and Ronald H. Soeder 1979 19 p refs Presented at the 15th Joint Propulsion Conf., Las Vegas, 18-20 Jun. 1979; cosponsored by AIAA, the Soc. of Automotive Engr., and ASME (NASA-TM-79136; E-9984) Avail: NTIS HC A02/MF A01 CSCL 21E

An additional data base for improving and verifying a computer simulation developed by an engine manufacturer was obtained. The multisection parallel compressor simulation was designed to predict the effects of steady-state circumferential inlet total-pressure and total-temperature distortions on the flows into and through a turbofan compression system. It also predicts the degree of distortion that will result in surge of the compressor. The effect of combined 180 deg square-wave distortion patterns of total pressure and total temperature in various relative positions is reported. The observed effects of the combined distortion on a unitary bypass ratio turbofan engine are presented in terms of total and static pressure profiles and total temperature profiles at stations ahead of the inlet guide vanes as well as through the fan-compressor system. These observed profiles are compared with those predicted by the complex multisection model. The effects of relative position of the two components comprising the combined distortion on the degree resulting in surge are discussed. Certain relative positions required less combined distortion than either a temperature or pressure distortion by itself. S.E.S.

N79-23965* National Aeronautics and Space Administration, Lewis Research Center, Cleveland, Ohio.

EFFECT OF DEGREE OF FUEL VAPORIZATION UPON EMISSIONS FOR A PREMIXED PREVAPORIZED COMBUSTION SYSTEM
L. P. Cooper 1979 17 p refs Presented at the 15th Joint Propulsion Conf. Las Vegas, 18-20 Jun. 1979; cosponsored by AIAA, SAE and ASME (NASA-TM-79154; E-010) Avail: NTIS HC A02/MF A01 CSCL 21E

An experimental and analytical study of the combustion of partially vaporized fuel-air mixtures was performed to assess the impact of the degree of fuel vaporization upon emissions for a premixing-prevaporizing flame-tube combustor. Data collected show near linear increases in nitrogen oxide emissions with decreasing vaporization at equivalence ratios of 0.6. For equivalence ratio of 0.72, the degree of vaporization had very little impact on nitrogen oxide emissions. A simple mechanism which accounts for the combustion of liquid droplets in partially vaporized mixtures was found to agree with the measured results with fair accuracy with respect to both trends and magnitudes. Author

A79-50333* Airborne atmospheric sampling system. U. R. C. Gustafsson (United Airlines, Inc., San Francisco, Calif.), P. J. Perkins, T. W. Nyland, M. W. Tiefermann, and T. J. Dudzinski (NASA, Lewis Research Center, Cleveland, Ohio). In: Learning to use our environment; Proceedings of the Twenty-fifth Annual Technical Meeting, Seattle, Wash., April 30-May 2, 1979. (A79-50326 22-42) Mount Prospect, Ill., Institute of Environmental Sciences, p. 48-57.

The atmospheric sampling system developed for use on board commercial airliners as part of the Global Atmospheric Sampling Program (GASP) is described. The automated air-constituent measur-

ing system is installed in a Boeing 747 airliner below the passenger cabin floor near the nose wheel well. It consists of an air sample flow system, composed of air inlet and pressurization systems, computerized data acquisition and system control units which direct system operation in 15 modes, and commercial instruments significantly modified to measure low levels of atmospheric constituents (ozone, water vapor, nitrogen oxides, carbon monoxide, chlorofluoromethanes, particulates, condensation nuclei, sulfates and nitrates). Flight and meteorological data, including air temperature and altitude, are also recorded. The system is designed for servicing at 14-day intervals, and to require a minimum of aircrew involvement. A.L.W.

N79-12084* Pratt and Whitney Aircraft Group, East Hartford, Conn. Commercial Products Div.
ENERGY EFFICIENT ENGINE PRELIMINARY DESIGN AND INTEGRATION STUDY

D. E. Gray et al Nov. 1978 36? p (Contract NAS3-20628) (NASA-CR-135396; PWA-5500-18) Avail: NTIS HC A16/MF A01 CSCL 21E

The technology and configurational requirements of an all new 1990's energy efficient turbofan engine having a twin spool arrangement with a directly coupled fan and low-pressure turbine, a mixed exhaust nacelle, and a high 38.6:1 overall pressure ratio were studied. Major advanced technology design features required to provide the overall benefits were a high pressure ratio compression system, a thermally actuated advanced clearance control system, lightweight shroudless fan blades, a low maintenance cost one-stage high pressure turbine, a short efficient mixer and structurally integrated engine and nacelle. A conceptual design analysis was followed by integration and performance analyses of geared and direct-drive fan engines with separate or mixed exhaust nacelles to refine previously designed engine cycles. Preliminary design and more detailed engine-aircraft integration analysis were then conducted on the more promising configurations. Engine and aircraft sizing, fuel burned, and airframe noise studies on projected 1990's domestic and international aircraft produced sufficient definition of configurational and advanced technology requirements to allow immediate initiation of component technology development. A.R.H.

N79-12087* Battelle Columbus Labs., Ohio.
COMPUTER-AIDED ANALYSIS AND DESIGN OF THE SHAPE ROLLING PROCESS FOR PRODUCING TURBINE ENGINE AIRFOILS Final Report, 1 Oct. 1976 - 30 Jun. 1978

G. D. Lahoti, N. Akgerman, and T. Altan Dec. 1978 251 p refs (Contract NAS3-20380) (NASA-CR-159445) Avail: NTIS HC A12/MF A01 CSCL 21E

Mild steel (AISI 1018) was selected as model cold rolling material and Ti-6Al-4V and Inconel 718 were selected as typical hot rolling and cold rolling alloys, respectively. The flow stress and workability of these alloys were characterized and friction factor at the roll/workpiece interface was determined at their respective working conditions by conducting ring tests. Computer-aided mathematical models for predicting metal flow and stresses, and for simulating the shape rolling process were developed. These models utilized the upper bound and the slab methods of analysis, and were capable of predicting the lateral spread, roll separating force, roll torque, and local stresses, strains and strain rates. This computer-aided design system was also capable of simulating the actual rolling process, and thereby designing the roll pass schedule in rolling of an airfoil or a similar shape. J.A.M.

07 AIRCRAFT PROPULSION AND POWER

Includes prime propulsion systems and systems components, e.g., gas turbine engines and compressors; and on-board auxiliary power plants for aircraft.

For related information see also 20 *Spacecraft Propulsion and Power*, 28 *Propellants and Fuels*, and 44 *Energy Production and Conversion*.

N79-100C7* National Aeronautics and Space Administration, Lewis Research Center, Cleveland, Ohio.

APPARATUS AND METHOD FOR REDUCING THERMAL STRESS IN A TURBINE ROTOR Patent

Jack A. Heller, inventor (to NASA) Issued 3 Oct. 1978 6 p Filed 4 Mar. 1977 Supersedes N77-18160 (15 - 09, p 1135)

(NA SA-Case-LEW-12232-1; US-Patent-4,117,669;

US Patent-Appl-SN-776029; US-Patent-Class-60-39.14;

US-Patent-Class-415-115; US-Patent-Class-415-116) Avail: US Patent Office CSCL 21E

A gas turbine is described wherein the thermal stresses in the turbine rotor are reduced. The rotor includes a central disc with a peripheral rim, and a plurality of blades extending radially outward from the rim. To reduce thermal stresses, a duct arrangement is provided which selectively directs hot gases from the turbine combustor to the rim during the turbine start up. The hot gases from the combustor serve to heat the rim, and decrease the start up period necessary to bring the temperature profile of the rotor into the operating temperature range. After the start up period, the duct arrangement is then used to direct cool gases from the turbine compressor to the rim of the rotor in order to maintain a lower rotor equilibrium temperature.

Official Gazette of the U.S. Patent Office

N79-10060* National Aeronautics and Space Administration, Lewis Research Center, Cleveland, Ohio.

PERFORMANCE OF SINGLE-STAGE AXIAL-FLOW TRANSONIC COMPRESSOR WITH ROTOR AND STATOR ASPECT RATIOS OF 1.19 AND 1.26, RESPECTIVELY, AND WITH DESIGN PRESSURE RATIO OF 1.82

Lonnie Reid and Royce D. Moore Nov. 1978 103 p refs

(NASA-TP-1338; E-9461) Avail: NTIS HC A06/MF A01 CSCL 21E

The overall and blade-element performance of a low-aspect-ratio transonic compressor stage is presented over the stable operating flow range at 70, 90, and 100 percent design speeds. At design speed the rotor and stage achieved peak efficiencies of 0.872 and 0.845 at pressure ratios of 1.875 and 1.842, respectively. The stage stall margin at design speed was 21.8 percent.

Author

N79-11043* National Aeronautics and Space Administration, Lewis Research Center, Cleveland, Ohio.

INFRARED SUPPRESSOR EFFECT ON T63 TURBOSHAFT ENGINE PERFORMANCE

Everett E. Bailey, Kestutis C. Cevinskas, and Curtis L. Walker Sep. 1978 14 p ref

(NASA-TM-78970; E-9730; AVRADCOM-TR-78-38(PL)) Avail: NTIS HC A02/MF A01 CSCL 21E

Tests were conducted to determine if there are performance penalties associated with the installation of infrared (IR) suppressors on the T63-A-700 turboshaft engine. The testing was done in a sea-level, static test cell. The same engine (A-E402808 B) was run with the standard OH-58 aircraft exhaust stacks and with the ejector-type IR suppressors in order to make a valid comparison. Repeatability of the test results for the two configurations was verified by rerunning the conditions over a period of days. Test results showed no measurable difference in performance between the standard exhaust stacks and the IR suppressors.

Author

N79-11057* National Aeronautics and Space Administration, Lewis Research Center, Cleveland, Ohio.

GAS PATH SEALING IN TURBINE ENGINES

Lawrence P. Ludwig In AGARD Seal Technol. in Gas Turbine Eng. Aug. 1978 41 p refs (For primary document see N79-11056 02-07)

Avail: NTIS HC A13/MF A01 CSCL 21E

Gas path seals are discussed with emphasis on sealing clearance effects on engine component efficiency, compressor pressure ratio, and stall margin. Various case-rotor relative displacements, which affect gas path seal clearances, are identified. Forces produced by nonuniform sealing clearances and their effect on rotor stability are examined qualitatively, and recent work on turbine-blade-tip sealing for high temperatures is described. The need for active clearance control and for engine structural analysis is discussed. The functions of the internal-flow system and its seals are reviewed.

A.R.H.

N79-11070* National Aeronautics and Space Administration, Lewis Research Center, Cleveland, Ohio.

SELF-ACTING SHAFT SEALS

Lawrence P. Ludwig In AGARD Seal Technol. in Gas Turbine Eng. Aug. 1973 29 p refs (For primary document see N79-11056 02-07)

Avail: NTIS HC A13/MF A01 CSCL 131

The operating principle and design of the self-acting seal is reviewed. Mathematical models for obtaining a seal force balance and the equilibrium operating film thickness are outlined. Particular attention is given to primary ring response (seal vibration) to rotating seat face runout. This response analysis reveals three different vibration modes with secondary seal friction being an important parameter. Leakage flow inlet pressure drop and effects of axisymmetric and nonaxisymmetric sealing face deformations are discussed. Experimental data on self-acting face seals operating under simulated gas turbine conditions are given; these data show the feasibility of operating the seal at conditions of 345 N/sq cm (500 psi) and 152 m/sec (500 ft/sec) sliding speed. Also, a spiral groove seal design operated to 244 m/sec (800 ft/sec) is described.

A.R.H.

N79-12083* National Aeronautics and Space Administration, Lewis Research Center, Cleveland, Ohio.

PRELIMINARY STUDY OF OPTIMUM DUCTBURNING TURBOFAN ENGINE CYCLE DESIGN PARAMETERS FOR SUPERSONIC CRUISING

Laurence H. Fishbach Nov. 1978 26 p refs

(NASA-TM-79047; E-9856) Avail: NTIS HC A03/MF A01 CSCL 21E

The effect of turbofan engine overall pressure ratio, fan pressure ratio, and ductburner temperature rise on the engine weight and cruise fuel consumption for a Mach 2.0 supersonic transport was investigated. Design point engines, optimized purely for the supersonic cruising portion of the flight where the bulk of the fuel is consumed, are considered. Based on constant thrust requirements at cruise, fuel consumption considerations would favor medium bypass ratio engines (1.5 to 1.8) of overall pressure ratio of about 16. Engine weight considerations favor low bypass ratio (0.6 or less) and low overall pressure ratio (8). Combination of both effects results in bypass ratios of 0.6 to 0.8 and overall pressure ratio of 12 being the overall optimum.

A.R.H.

N79-12085* National Aeronautics and Space Administration, Lewis Research Center, Cleveland, Ohio.

EFFECT OF FLIGHT LOADS ON TURBOFAN ENGINE PERFORMANCE DETERIORATION

E. G. Stakolich, A. Jay (Pratt and Whitney Aircraft, East Hartford, Conn.), E. S. Todd (Pratt and Whitney Aircraft, East Hartford, Conn.), P. G. Kafka (Boeing Com. Airplane Co., Renton, Wash.), and J. L. White (Boeing Com. Airplane Co., Renton, Wash.) 1979 22 p refs Proposed for presentation at the 24th Ann. Intern. Gas Turbine Conf., San Diego, Calif., 11-15 Mar. 1979; sponsored by the Am. Soc. of Mech. Engrs.

(NASA-TM-79041; E-9844) Avail: NTIS HC A02/MF A01 CSCL 21E

A significant percentage of high bypass ratio, turbofan engine performance deterioration was caused by an increase in operating clearance between fan/compressor and turbine blades and their outer air seals. These increased clearances resulted from ruts induced by a combination of engine power transients and aircraft flight loads. An analytical technique for predicting the effect of quasi-steady state aircraft flight loads on engine performance deterioration was developed and is presented. Thrust, aerodynamic and inertia loads were considered. Analytical results are shown and compared to actual engine test experience. J.A.M.

N79-12006* National Aeronautics and Space Administration, Lewis Research Center, Cleveland, Ohio.
NASA RESEARCH ON GENERAL AVIATION POWER PLANTS

Warner L. Stewart, Richard J. Weber, Edward A. Willis, and Gilbert K. Sievers 1978 14 p refs Proposed for presentation at the 15th Ann. Meeting and Tech. Display, Washington, D. C., 5-8 Feb. 1979; sponsored by AIAA (NASA-TM-79031; E-9828) Avail. NTIS HC A02/MF A01 CSCL 21A

Propulsion systems are key factors in the design and performance of general aviation airplanes. NASA research programs that are intended to support improvements in these engines are described. Reciprocating engines are by far the most numerous powerplants in the aviation fleet; near-term efforts are being made to lower their fuel consumption and emissions. Longer-term work includes advanced alternatives, such as rotary and lightweight diesel engines. Work is underway on improved turboprops and turboprops. Author

N79-13046* National Aeronautics and Space Administration, Lewis Research Center, Cleveland, Ohio.
LOW-CYCLE FATIGUE OF THERMAL-BARRIER COATINGS AT 982 DEG C

Albert Kaufman, Curt H. Liebert, and Alfred J. Nachtigall Dec. 1978 20 p refs (NASA-TP-1322; E-9888) Avail. NTIS HC A02/MF A01 CSCL 21E

The low-cycle fatigue lives of $ZrO_2-NiCrAlY$ and $Al_2O_3-ZrO_2-NiCrAlY$ thermal-barrier coatings in air at 982 C were determined from cyclic flexural tests of coated TAZ-8A strips. Strains were computed as a function of specimen displacements from a nonlinear, three-dimensional stress analysis program. Fatigue resistances of thermal-barrier coatings applied to the strips were compared with those of uncoated and $NiCrAlY$ -coated strips. The results indicate that ZrO_2 is about four times greater in fatigue life than TAZ-8A at 982 C, that ZrO_2 would probably

N79-13049* National Aeronautics and Space Administration, Lewis Research Center, Cleveland, Ohio.

COLD-AIR PERFORMANCE OF FREE POWER TURBINE DESIGNED FOR 112-KILOWATT AUTOMOTIVE GAS-TURBINE ENGINE 3: EFFECT OF STATOR VANE END CLEARANCES ON PERFORMANCE

Milton G. Kofskey and Kerry L. McLallin Dec. 1978 41 p refs (Contract EC-77-A-31-1011) (NASA-TM-78956; DOE/NASA/1011-78/29) Avail. NTIS HC A03/MF A01 CSCL 21A

An experimental investigation of a free power turbine designed for a 112-kW, automotive, gas turbine engine was made to determine the penalty in performance due to the stator vane end clearances. Tests were made over a range of mean section stator vane angles from 26 deg to 50 deg (as measured from the plane of rotation) with the vane end clearances filled. These results were compared with test results of the same turbine with vane end clearances open. At design equivalent values of rotational speed and pressure ratio and at a vane angle of 35 deg, the mass flow with the vane end clearances filled was about 8 percent lower than mass flow with vane end clearances open. The decrease in mass flow was mitigated by increasing the

N79-14086* National Aeronautics and Space Administration, Lewis Research Center, Cleveland, Ohio.

CAM-OPERATED PITCH-CHANGE APPARATUS Patent
 Philip E. Barnes, inventor (to NASA) (United Technologies Corp., Windsor Locks, Conn.) Issued 7 Nov. 1978 8 p Filed 9 Oct. 1974 Published under the second Trial Voluntary Patent Program as B 513, 346, 9 Mar. 1976 Sponsored by NASA (NASA-Case-LEW-13050-1; US-Patent-4,124,330; US-Patent-Appl-SN-513346; US-Patent-Class-416-157B; US-Patent-Class-416-162; US-Patent-Class-416-160; US-Patent-Class-416-167) Avail. US Patent and Trademark Office CSCL 01C

A pitch-change apparatus for a ducted thrust fan having a plurality of variable pitch blades employs a camming ring mounted coaxially at the hub at an axially fixed station along the hub axis for rotation about the hub axis both with the blades and relative to the blades. The ring has a generally spherical outer periphery and a plurality of helical camming grooves extending in a generally spherical plane on the periphery. Each of the variable pitch blades is connected to a pitch-change horn having a cam follower mounted on its outer end, and the camming ring and the horns are so arranged about the hub axis that the plurality of followers on the horns engage respectively the plurality of helical camming grooves. Rotary drive means rotates the camming ring relative to the blades to cause blade pitch to be changed through the cooperative operation of the camming grooves on the ring and the cam followers on the pitch-change horns. Official Gazette of the U.S. Patent and Trademark Office

N79-14086* National Aeronautics and Space Administration, Lewis Research Center, Cleveland, Ohio.

INTEGRATED GAS TURBINE ENGINE-NACELLE Patent
 Arthur P. Adamaon (GE, Cincinnati), Donald F. Sergisson (GE, Cincinnati), and Charles L. Stotler, Jr., inventors (to NASA) (GE, Cincinnati) Issued 2 Jan. 1979 9 p Filed 22 Dec. 1976 Continuation of abandoned US Patent Appl. SN-522106, filed 8 Nov. 1974 Sponsored by NASA (NASA-Case-LEW-12389-3; US-Patent-4,132,069; US-Patent-Appl-SN-753452; US-Patent-Class-60-226R; US-Patent-Class-60-226A; US-Patent-Class-60-39.31; US-Patent-Class-244-54; US-Patent-Class-137-15.1; US-Patent-Class-415-201; US-Patent-Class-415-200; US-Patent-Appl-SN-552108) Avail. US Patent and Trademark Office CSCL 21E

A nacelle for use with a gas turbine engine is provided with an integral webbed structure resembling a spoked wheel for rigidly interconnecting the nacelle and engine. The nacelle is entirely supported in its spacial relationship with the engine by means of the webbed structure. The inner surface of the nacelle defines the outer limits of the engine motive fluid flow annulus, while the outer surface of the nacelle defines a streamlined envelope for the engine.

Official Gazette of the U.S. Patent and Trademark Office

N79-14087* National Aeronautics and Space Administration, Lewis Research Center, Cleveland, Ohio.

VARIABLE AREA EXHAUST NOZZLE Patent
 Everett A. Johnston, inventor (to NASA) (GE, Cincinnati) Issued 2 Jan. 1979 8 p Filed 30 Apr. 1975 Sponsored by NASA (NASA-Case-LEW-12378-1; US-Patent-4,132,068; US-Patent-Appl-SN-573029; US-Patent-Class-60-226A; US-Patent-Class-239-265.39) Avail. US Patent and Trademark Office CSCL 21E

An exhaust nozzle for a gas turbine engine comprises a number of arcuate flaps pivotally connected to the trailing edge of a cylindrical casing which houses the engine. Seals disposed within the flaps are spring biased and extensible beyond the side edges of the flaps. The seals of adjacent flaps are maintained in sealing engagement with each other when the flaps are adjusted between positions defining minimum nozzle flow area and the cruise position. Extensible, spring biased seals are also disposed within the flaps adjacent to a supporting pylon to thereby engage the pylon in a sealing arrangement. The flaps are hinged to the casing at the central portion of the flaps' leading edges and are connected to actuators at opposed outer portions of the leading

edges to thereby maximize the mechanical advantage in the actuation of the flaps.

Official Gazette of the U.S. Patent and Trademark Office

N79-14088* National Aeronautics and Space Administration, Lewis Research Center, Cleveland, Ohio.

CERAMIC COATING EFFECT ON LINER METAL TEMPERATURES OF FILM-COOLED ANNULAR COMBUSTOR

Russell W. Claus, Jerrold D. Wear, and Curt H. Liebert Jan. 1979 24 p refs (NASA-TP-1323; E-9732) Avail: NTIS HC A03/MF A01 CSCL 21E

An experimental and analytical investigation was conducted to determine the effect of a ceramic coating on the average metal temperatures of full annular, film cooled combustion chamber liner. The investigation was conducted at pressures from 0.50 to 0.062. At all test conditions, experimental results indicate that application of a ceramic coating will result in significantly lower wall temperatures. In a simplified heat transfer analysis, agreement between experimental and calculated liner temperatures was achieved. Simulated spalling of a small portion of the ceramic coating resulted in only small increases in liner temperature because of the thermal conduction of heat from the hotter, uncoated liner metal.

Author

N79-14089* National Aeronautics and Space Administration, Lewis Research Center, Cleveland, Ohio.

EFFECT OF SWIRLER-MOUNTED MIXING VENTURI ON EMISSIONS OF FLAME-TUBE COMBUSTOR USING JET A FUEL

David B. Ercogovic Jan. 1979 23 p refs (NASA-TP-1393; AVRADCOM-TR-78-41; E-9762) Avail: NTIS HC A02/MF A01 CSCL 21E

Six headplate modules in a flame-tube combustor were evaluated. Unburned hydrocarbons, carbon monoxide, and oxides of nitrogen were measured for three types of fuel injectors both with and without a mixing venturi. Tests were conducted using jet A fuel at an inlet pressure of 0.69 megapascal, an inlet temperature of 478 K, and an isothermal static pressure drop of 3 percent. Oxides of nitrogen were reduced by over 50 percent with a mixing venturi with no performance penalties in either other gaseous emissions or pressure drop.

G.G.

N79-15046* Boeing Military Airplane Development, Seattle, Wash.

A METHOD TO ESTIMATE WEIGHT AND DIMENSIONS OF LARGE AND SMALL GAS TURBINE ENGINES

Final Report
E. Onat and G. W. Klees Jan. 1979 136 p refs (Contract NAS3-21205) (NASA-CR-159481) Avail: NTIS HC A07/MF A01 CSCL 21E

A computerized method was developed to estimate weight and envelope dimensions of large and small gas turbine engines within + or - 5% to 10%. The method is based on correlations of component weight and design features of 29 data base engines. Rotating components were estimated by a preliminary design procedure which is sensitive to blade geometry, operating conditions, material properties, shaft speed, hub tip ratio, etc. The development and justification of the method selected, and the various methods of analysis are discussed.

B.B.

N79-15047* National Aeronautics and Space Administration, Lewis Research Center, Cleveland, Ohio.

THE ADVANCED LOW-EMISSIONS CATALYTIC-COMBUSTOR PROGRAM. PHASE 1: DESCRIPTION AND STATUS

Andrew J. Szanislo 1979 13 p refs To be presented at the 24th Ann. Intern. Gas Turbine Conf. and 1st Solar Energy Conf., San Diego, Calif., 11-15 Mar. 1979; sponsored by the Am. Soc. of Mech. Engr. (NASA-TM-79049; E-9853) Avail: NTIS HC A02/MF A01 CSCL 21E

An overview of the ongoing program is presented. Objectives, plan, schedule, pollution and performance goals, catalyst advantages, present problems, and the present status of identified combustor concepts are discussed. The possible increase in upper atmosphere oxides of nitrogen (NOx) levels due to aircraft number density increases was predicted to adversely decrease ozone concentration levels. A technique for achieving low NOx emission levels was experimentally demonstrated with a lean, premixing prevaporizing flame-tube combustor.

B.B.

N79-15048* National Aeronautics and Space Administration, Lewis Research Center, Cleveland, Ohio.

NASA THERMAL BARRIER COATINGS: SUMMARY AND UPDATE

Francis S. Stepka 1978 23 p refs Presented at Proj. SQUID (ONR) Workshop on Cooling Problems in Aircraft Gas Turbines, Monterey, Calif., 27-28 Sep. 1978; sponsored by AFOSR, Naval Air Systems Command, and ONR (NASA-TM-79053; E-9862) Avail: NTIS HC A02/MF A01 CSCL 21E

A durable, two-layer, plasma-sprayed coating consisting of a ceramic layer over a metallic layer was developed that has the potential of insulating hot engine parts and thereby reducing metal temperatures and coolant flow requirements and/or permitting use of less costly and complex cooling configurations and materials. The results are summarized of analytical and experimental investigations of the coatings on flat metal specimens, turbine vanes and blades, and combustor liners. Discussed are results of investigations to determine coating adherence and durability, coating thermal, strength and fatigue properties, and chemical reactions of the coating with oxides and sulfates. Also presented are the effect of the coating on aerodynamic performance of a turbine vane, measured vane and combustor liner temperatures with and without the coating, and predicted turbine metal temperatures and coolant flow reductions potentially possible with the coating. Included also are summaries of some current research related to the coating and potential applications for the coating.

Author

N79-15049* National Aeronautics and Space Administration, Lewis Research Center, Cleveland, Ohio.

EFFECT OF FORWARD VELOCITY AND CROSSWIND ON THE REVERSE-THRUST PERFORMANCE OF A VARIABLE-PITCH FAN ENGINE

D. C. Reemsnyder and D. A. Sagerser 17 Jan. 1979 21 p refs Presented at the 17th Aerospace Sci. Meeting, New Orleans, 15-17 Jan. 1979; sponsored by Am. Inst. of Aeron. and Astronautics (NASA-TM-79059; E-9873; AIAA-79-0105) Avail: NTIS HC A02/MF A01 CSCL 21E

A full-size variable-pitch fan engine was tested in the Ames 40 by 80 foot wind tunnel to determine the effect of forward velocity and crosswind on reverse-thrust performance. Two flight-type inlet configurations were tested, and a flared fan nozzle was installed as an inlet for reverse-thrust operation. Steady-state reverse-thrust performance was obtained up to 54 m/s (105 knots). An abrupt decrease in reverse thrust occurred at about 30 m/s (60 knots). Reverse thrust was established following forward-to-reverse thrust transients both statically and with forward velocities only up to 30 m/s.

Author

N79-15050* National Aeronautics and Space Administration, Lewis Research Center, Cleveland, Ohio.

THE NASA HIGH PRESSURE FACILITY AND TURBINE TEST RIG

Francis S. Stepka 1978 17 p refs Presented at the Project SQUID (ONR) Workshop on Cooling Probl. in Aircraft Gas Turbines, Monterey, Calif., 27-28 September 1978; sponsored by AFOSR, Naval Air Systems Command, and ONR (NASA-TM-79054; E-9863) Avail: NTIS HC A02/MF A01 CSCL 21E

A description of the facility and turbine test rig is presented. Also discussed is the turbine cooling test program.

L.S.

N79-15051* National Aeronautics and Space Administration, Lewis Research Center, Cleveland, Ohio.

PRELIMINARY QCGAT PROGRAM TEST RESULTS

R. W. Koenig and G. K. Sievers 1979 19 p refs To be presented at the Business Aircraft Meeting, Wichita, Kas., 3-6 Apr. 1979; sponsored by SAE

(NASA-TM-79013; E-9802) Avail: NTIS HC A02/MF A01 CSCL 21E

NASA Lewis Research Center is conducting a program to demonstrate that large commercial engine technology can be applied to general aviation engines to reduce noise, emissions and fuel consumption and to develop new technology where required. The overall engine program, design, and technology incorporated into the QCGAT engines are described. In addition, preliminary engine test results are presented and compared to the technical requirements the engines were designed to meet.

S.E.S.

N79-15052* Teledyne Continental Motors, Mobile, Ala.
COMPUTER SIMULATION OF AN AIRCRAFT ENGINE FUEL INJECTION SYSTEM Final Report

David D. Hester Jun. 1978 93 p refs

(Contracts NAS3-19755; DOT-FA74NA-1091)

(NASA-CR-157641; AD-A060452; FAA-NA-78-156;

FAA-RD-78-67) Avail: NTIS HC A05/MF A01 CSCL 21/7

An analytical model of the Teledyne Continental fuel system was studied to provide a basis for quantitatively exploring deficiencies in the system response which lead to poor exhaust emission characteristics. A computer model of the fuel system was developed based on component testing and found to give accurate predictions for pressures and flow rates within the system. The model was used to investigate modifications to the system for improved fuel management and reduced exhaust emissions. The effect of improved fuel management on engine exhaust emissions is evaluated.

F.O.S.

N79-15957* National Aeronautics and Space Administration, Lewis Research Center, Cleveland, Ohio.

MEASURED AND PREDICTED NOISE OF THE AVCO-LYCOMING YF-102 TURBOFAN NOISE

Bruce J. Clark, Jack G. McArdle, and Leonard Homyak 1979 18 p refs Presented at 5th Aeroacoustics Conf., Seattle, 12-14 Mar. 1979; sponsored by AIAA

(NASA-TM-79069; E-9885; AIAA-Paper-79-0641) Avail: NTIS HC A02/MF A01

Acoustic testing of the AVCO-Lycoming YF-102 turbofan engine was done on a static test stand in support of the quiet short-haul research aircraft acoustic design. Overall noise levels were dominated by the fan noise emanating from the exhaust duct, except at high power settings when combination tones were generated in the fan inlet. Component noise levels, calculated by noise prediction methods were in reasonable agreement with the measured results. Far-field microphones placed at ground level were found superior to those at engine centerline height, even at high frequencies.

J.A.M.

N79-15958* National Aeronautics and Space Administration, Lewis Research Center, Cleveland, Ohio.

THE GATE STUDIES: ASSESSING THE POTENTIAL OF FUTURE SMALL GENERAL AVIATION TURBINE ENGINES

William C. Strack 1979 24 p refs Presented at the Intern. Ann. Gas Turbine Conf., San Diego, Calif., 11-15 Mar. 1979; sponsored by Am. Soc. of Mechanical Engineers

(NASA-TM-79075; E-9892) Avail: NTIS HC A02/MF A01 CSCL 21E

Four studies were completed that explore the opportunities for future General Aviation turbine engines (GATE) in the 150-1000 SHP class. These studies forecasted the potential impact of advanced technology turbine engines in the post-1988 market, identified important aircraft and missions, desirable engine sizes, engine performance, and cost goals. Parametric evaluations of various engine cycles, configurations, design features, and advanced technology elements defined baseline conceptual engines for each of the important missions identified by the

market analysis. Both fixed-wing and helicopter aircraft, and turboshaft, turboprop, and turbofan engines were considered. Sizable performance gains (e.g., 20% SFC decrease), and large engine cost reductions of sufficient magnitude to challenge the reciprocating engine in the 300-500 SHP class were predicted.

J.A.M.

N79-15959* National Aeronautics and Space Administration, Lewis Research Center, Cleveland, Ohio.

APPLICATIONS OF VELOCITY POTENTIAL FUNCTION TO ACOUSTIC DUCT PROPAGATION AND RADIATION FROM INLETS USING FINITE ELEMENT THEORY

K. J. Baumeister and R. K. Majjigi (GE Co., Cincinnati, Ohio) 1979 12 p refs Presented at the 5th Aeroacoustics Conf., Seattle, Wash., 12-14 Mar. 1979; sponsored by AIAA

(NASA-TM-79071; E-9888) Avail: NTIS HC A02/MF A01 CSCL 21E

A finite element velocity potential program was developed to study acoustic wave propagation in complex geometries. For irrotational flows, relatively low sound frequencies, and plane wave input, the finite element solutions showed significant effects of inlet curvature and flow gradients on the attenuation of a given acoustic liner in a realistic variable area turbofan inlet. The velocity potential approach can not be used to estimate the effects of rotational flow on acoustic propagation, since the potential acoustic disturbances propagate at the speed of the media in sheared flow. Approaches are discussed that are being considered for extending the finite element solution to include the far field, as well as the internal portion of the duct. A new matrix partitioning approach is presented that can be incorporated in previously developed programs to allow the finite element calculation to be marched into the far field. The partitioning approach provided a large reduction in computer storage and running times.

J.A.M.

N79-15960* National Aeronautics and Space Administration, Lewis Research Center, Cleveland, Ohio.

ANALYSIS OF RADIATION PATTERNS OF INTERACTION TONES GENERATED BY INLET RODS IN THE JT15D ENGINE

M. F. Heidmann and A. V. Saule 1979 27 p refs Presented at the 5th Aeroacoustics Conf., Seattle, 12-14 Mar. 1978; sponsored by AIAA

(NASA-TM-79074; E-9891) Avail: NTIS HC A03/MF A01 CSCL 21E

Interaction tones were intentionally generated by circumferential arrays of equally spaced rods that protrude radially from the inlet wall near the face of the 28-blade fan. Arrays of 28 and 41 rods, selected to give specific far field radiation properties, were tested. The expected properties were readily apparent in the measured radiation patterns. A more detailed analysis of the test data showed both the precision and limitations of the applied acoustic theory. Rods protruding 23 percent of the radius predominantly generated only lowest radial order modes, as expected. Measured and predicted radiation patterns were generally in good agreement. The agreement, however, depended on a significant degree of implied refraction due to inlet velocity gradients. Refraction, if present, would impact static-flight noise comparisons.

Author

N79-15961* National Aeronautics and Space Administration, Lewis Research Center, Cleveland, Ohio.

THE ROTARY COMBUSTION ENGINE: A CANDIDATE FOR GENERAL AVIATION

1978 190 p refs Symp held at Cleveland, Ohio, 28 Feb 1978

(NASA-CP-2067; E-9800) Avail: NTIS HC A09/MF A01 CSCL 21A

The state of development of the rotary combustion engine is discussed. The nonturbine engine research programs for general aviation and future requirements for general aviation powerplants are emphasized. For individual titles, see N79-15962 through N79-15968

N79-15969*# National Aeronautics and Space Administration. Lewis Research Center, Cleveland, Ohio.
EVALUATION OF TWO INFLOW CONTROL DEVICES FOR FLIGHT SIMULATION OF FAN NOISE USING A JT15D ENGINE

W. L. Jones, J. G. McArdle, and L. Homyak 1979 17 p refs
 Presented at 5th Aeroacoustics Conf., Seattle, Washington, 12-14 Mar. 1978; sponsored by AIAA
 (NASA-TM-79072; E-9889) Avail: NTIS HC A02/MF A01 CSCL 21E

The program was developed to accurately simulate flight fan noise on ground static test stands. The results generally indicated that both the induct and external ICD's were effective in reducing the inflow turbulence and the fan blade passing frequency tone generated by the turbulence. The external ICD was essentially transparent to the propagating fan tone but the induct ICD caused attenuation under most conditions. Author

N79-16849*# National Aeronautics and Space Administration. Lewis Research Center, Cleveland, Ohio.

NEW OPPORTUNITIES FOR FUTURE SMALL CIVIL TURBINE ENGINES: OVERVIEWING THE GATE STUDIES
 William C. Strack 1979 36 p Proposed for presentation at the Business and Aircraft Meeting, Wichita, Kans., 3-6 Apr. 1979; sponsored by Soc. of Automotive Engineers, Inc.
 (NASA-TM-79073; E-9890) Avail: NTIS HC A03/MF A01 CSCL 21E

An overview of four independent studies forecasts the potential impact of advanced technology turbine engines in the post 1988 market, identifies important aircraft and missions, desirable engine sizes, engine performance, and cost goals. Parametric evaluations of various engine cycles, configurations, design features, and advanced technology elements defined baseline conceptual engines for each of the important missions identified by the market analysis. Both fixed-wing and helicopter aircraft, and turboshaft, turboprop, and turbofan engines were considered. Sizable performance gains (e.g., 20% SFC decrease), and large engine cost reductions of sufficient magnitude are predicted to challenge the reciprocating engine in the 300-500 SHP class. G.G.

N79-16852*# National Aeronautics and Space Administration. Lewis Research Center, Cleveland, Ohio.

EFFECT OF CASING TREATMENT ON PERFORMANCE OF A TWO-STAGE HIGH-PRESSURE-RATIO FAN
 Donald C. Urasek Feb. 1979 68 p refs
 (NASA-TP-1409; E-8997) Avail: NTIS HC A04/MF A01 CSCL 21E

A two-stage fan, previously tested with a solid casing, was tested with a casing with circumferential grooves over the tips of both rotors (casing treatment). Tests were conducted at 80 and 100 percent of design speed with uniform flow. The casing treatment improved the flow range and stall margin significantly without changing the characteristics overall performance curves of total-pressure and efficiency as functions of weight flow, other than extending them to lower weight flows. Author

N79-17859*# National Aeronautics and Space Administration. Lewis Research Center, Cleveland, Ohio.

COLD-AIR PERFORMANCE OF FREE POWER TURBINE DESIGNED FOR 112-KILOWATT AUTOMOTIVE GAS-TURBINE ENGINE. 2: EFFECTS OF VARIABLE STATOR-VANE-CHORD SETTING ANGLE ON TURBINE PERFORMANCE Final Report
 Kerry L. McLallin and Milton G. Kofskey Feb. 1979 53 p refs

(Contract EC-77-A-31-1011)
 (NASA-TM-78993, DOE/NASA/1011-78/28, E-9775) Avail: NTIS HC A04/MF A01 CSCL 21A

The cold-air performance of an axial-flow power turbine with a variable stator designed for a 112-kW automotive gas-turbine engine was determined at speeds from 30 to 110 percent of design and at pressure ratios from 1.11 to 2.67. Performance is presented in terms of equivalent mass flow, torque, power,

and efficiency for stator-vane-chord setting angles of 26 degs, 30 degs, 35 degs (design), 40 degs, 45 degs, and 50 degs. Turbine braking performance at a nominal stator setting angle of 107 degs is also presented. Turbine efficiency increased with increasing stator setting angle. A 10-point efficiency increase was obtained by opening the stator from the design setting angle of 35 degs to a setting angle of 45 degs. Author

N79-20114*# National Aeronautics and Space Administration. Lewis Research Center, Cleveland, Ohio.

PARAMETRIC PERFORMANCE OF A TURBOJET ENGINE COMBUSTOR USING JET A AND A DIESEL FUEL
 Helmuth F. Butze and Francis M. Humenik Mar. 1979 44 p refs
 (NASA-TM-79089; E-9913) Avail: NTIS HC A03/MF A01 CSCL 21E

The performance of a single-can JT8D combustor was evaluated with Jet A and a high-aromatic diesel fuel over a parametric range of combustor-inlet conditions. Performance parameters investigated were combustion efficiency, emissions of CO, unburned hydrocarbons, and NOx, as well as liner temperatures and smoke. At all conditions the use of diesel fuel instead of Jet A resulted in increases in smoke numbers and liner temperatures; gaseous emissions, on the other hand, did not differ significantly between the two fuels. Author

N79-20118*# National Aeronautics and Space Administration. Lewis Research Center, Cleveland, Ohio.

TESTS OF NASA CERAMIC THERMAL BARRIER COATING FOR GAS-TURBINE ENGINES
 Curt H. Liebert 1979 10 p refs Presented at the Intern. Conf. on Met. Coatings, San Diego, Calif., 23-27 Apr. 1979
 (NASA-TM-79116; E-9846-1) Avail: NTIS HC A02/MF A01 CSCL 21E

A two-layer thermal barrier coating system with a bond coating of nickel-chromium-aluminum-yttrium and a ceramic coating of yttria-stabilized zirconia was tested for corrosion protection, thermal protection and durability. Full-scale gas-turbine engine tests demonstrated that this coating eliminated burning, melting, and warping of uncoated parts. During cyclic corrosion resistance tests made in marine diesel fuel products of combustion in a burner rig, the ceramic cracked on some specimens. Metallographic examination showed no base metal deterioration. S.E.S.

N79-22099*# National Aeronautics and Space Administration. Lewis Research Center, Cleveland, Ohio.

PERFORMANCE OF A VORTEX-CONTROLLED DIFFUSER IN AN ANNULAR SWIRL-CAN COMBUSTOR AT INLET MACH NUMBERS UP TO 0.53
 John M. Smith Washington Apr. 1979 17 p refs
 (NASA-TP-1452; E-9832) Avail: NTIS HC A02/MF A01 CSCL 21E

A short, annular dump diffuser with suction stabilized vortices in the region of abrupt area change was tested with a full scale, annular swirl can combustor. The prediffuser area ratio was 1.4. Performance data were obtained for both isothermal and burning conditions at inlet temperatures of 589 to 895 K and pressures of 0.5 to 1.0 MPa for a range of diffuser inlet Mach numbers from 0.25 to 0.53. Suction rates were 0 to 20 percent of the total diffuser mass flow rate. Diffuser effectiveness increased from 47 percent without suction to approximately 80 percent for a total suction rate of 14 percent. Combustor total pressure loss for the same total suction rate was reduced from 6.8 percent without suction to 4.0 percent at an inlet Mach number of 0.40. Author

N79-23985* National Aeronautics and Space Administration, Lewis Research Center, Cleveland, Ohio.
EFFECT OF PRIMARY-ZONE EQUIVALENCE RATIO ON POLLUTANT FORMATION
 Russell W. Claus May 1979 20 p refs
 (NASA-TP-1463; E-9896) Avail: NTIS HC A02/MF A01 CSCL 21E

Test were conducted to determine the effect of primary-zone equivalence ratio on the formation of smoke and other gaseous pollutants in an experimental can combustor. Several fuel injection techniques were examined at primary-zone equivalence ratios from 0.8 to 2.0. The main emphasis was on reducing fuel-rich-combustion smoke levels. Two of the four fuel injection configurations studied produced smoke levels below a smoke number of 20 at a primary-zone equivalence ratio of about 1.7. As the fuel mixing and atomization were recorded at primary-zone equivalence ratios as high as 2.0. The gaseous emissions of unburned hydrocarbons, carbon monoxide, and oxides of nitrogen were quite sensitive to the fuel injection configuration as well as to the primary-zone equivalence ratio. Author

N79-23983* National Aeronautics and Space Administration, Lewis Research Center, Cleveland, Ohio.
COMBINED PRESSURE AND TEMPERATURE DISTORTION EFFECTS ON INTERNAL FLOW OF A TURBOFAN ENGINE
 W. M. Braithwaite and Ronald H. Soeder 1979 19 p refs
 Presented at the 15th Joint Propulsion Conf., Las Vegas, 18-20 Jun. 1979; cosponsored by AIAA, the Soc. of Automotive Engr., and ASME
 (NASA-TM-79136; E-9984) Avail: NTIS HC A02/MF A01 CSCL 21E

An additional data base for improving and verifying a computer simulation developed by an engine manufacturer was obtained. The multisegment parallel compressor simulation was designed to predict the effects of steady-state circumferential inlet total-pressure and total-temperature distortions on the flows into and through a turbofan compression system. It also predicts the degree of distortion that will result in surge of the compressor. The effect of combined 180 deg square-wave distortion patterns of total pressure and total temperature in various relative positions is reported. The observed effects of the combined distortion on a unitary bypass ratio turbofan engine are presented in terms of total and static pressure profiles and total temperature profiles at stations ahead of the inlet guide vanes as well as through the fan-compressor system. These observed profiles are compared with those predicted by the complex multisegment model. The effects of relative position of the two components comprising the combined distortion on the degree resulting in surge are discussed. Certain relative positions required less combined distortion than either a temperature or pressure distortion by itself. S.E.S.

N79-23964* National Aeronautics and Space Administration, Lewis Research Center, Cleveland, Ohio.
LEAN, PREMIXED, PREVAPORIZED COMBUSTION FOR AIRCRAFT GAS TURBINE ENGINES
 Edward J. Mularz 1979 18 p refs. Presented at the 15th Propulsion Conf., Las Vegas, 18-20 Jun. 1979; cosponsored by AIAA, the Soc. of Automotive Engr., and ASME. Prepared in cooperation with Army Aviation Res. and Develop. Command, St. Louis, Mo.
 (NASA-TM-79148; E-004; AVRADCOM-TR-79-18) Avail: NTIS HC A02/MF A01 CSCL 21E

The application of lean, premixed, prevaporized combustion to aircraft turbine engine systems can result in benefits in terms of superior combustion performance, improved combustor and turbine durability, and environmentally acceptable pollutant emissions. Lean, premixed prevaporized combustion is particularly attractive for reducing the oxides of nitrogen emissions during high altitude cruise. The NASA stratospheric cruise emission reduction program will evolve and demonstrate lean, premixed, prevaporized combustion technology for aircraft engines. This multiphased program is described. In addition, the various elements of the fundamental studies phase of the program are reviewed, and results to date of many of these studies are summarized. Author

N79-23965* National Aeronautics and Space Administration, Lewis Research Center, Cleveland, Ohio.
EFFECT OF DEGREE OF FUEL VAPORIZATION UPON EMISSIONS FOR A PREMIXED PREVAPORIZED COMBUSTION SYSTEM
 L. P. Cooper 1979 17 p refs. Presented at the 15th Joint Propulsion Conf. Las Vegas, 18-20 Jun. 1979; cosponsored by AIAA, SAE and ASME
 (NASA-TM-79154; E-010) Avail: NTIS HC A02/MF A01 CSCL 21E

An experimental and analytical study of the combustion of partially vaporized fuel-air mixtures was performed to assess the impact of the degree of fuel vaporization upon emissions for a premixing-prevaporizing flametube combustor. Data collected show near linear increases in nitrogen oxide emissions with decreasing vaporization at equivalence ratios of 0.6. For equivalence ratio of 0.72, the degree of vaporization had very little impact on nitrogen oxide emissions. A simple mechanism which accounts for the combustion of liquid droplets in partially vaporized mixtures was found to agree with the measured results with fair accuracy with respect to both trends and magnitudes. Author

N79-23966* National Aeronautics and Space Administration, Lewis Research Center, Cleveland, Ohio.
EFFECT OF SHOCKS ON FILM COOLING OF A FULL SCALE TURBOJET EXHAUST NOZZLE HAVING AN EXTERNAL EXPANSION SURFACE
 David M. Straight 1979 20 p refs. Presented at the 15th Joint Propulsion Conf., Las Vegas, 18-20 Jun. 1979; cosponsored by AIAA, SAE, and ASME
 (NASA-TM-79157; E-013) Avail: NTIS HC A02/MF A01 CSCL 21E

Experimental film cooling data obtained during exploratory testing with an axisymmetric plug nozzle having external expansion and installed on an afterburning turbojet engine in an altitude test facility is presented. The shocks and local hot gas stream conditions had a marked effect on film cooling effectiveness. An existing film cooling correlation was adequate at some operating conditions but inadequate at other conditions such as in separated flow regions resulting from shock boundary layer interactions. R.E.S.

N79-23967* National Aeronautics and Space Administration, Lewis Research Center, Cleveland, Ohio.
PERFORMANCE OF TWO-STAGE FAN WITH LARGER DAMPERS ON FIRST-STAGE ROTOR
 Donald C. Urasick, Walter S. Cunnah, and William Stevens May 1979 81 p refs
 (NASA-TP-1399; E-8958) Avail: NTIS HC A05/MF A01 CSCL 21E

The performance of a two stage, high pressure-ratio fan, having large, part-span vibration dampers on the first stage rotor is presented and compared with an identical aerodynamically designed fan having smaller dampers. Comparisons of the data for the two damper configurations show that with increased damper size (1) very high losses in the damper region reduced overall efficiency of first stage rotor by approximately 3 points, (2) the overall performance of each blade row, downstream of the damper was not significantly altered, although appreciable differences in the radial distributions of various performance parameters were noted, and (3) the lower performance of the first stage rotor decreased the overall fan efficiency more than 1 percentage point. Author

N79-23968* National Aeronautics and Space Administration, Lewis Research Center, Cleveland, Ohio.
EFFECTS OF STEADY-STATE PRESSURE DISTORTION ON THE STALL MARGIN OF A J85-21 TURBOJET ENGINE
 George A. Bobula Mar 1979 28 p refs. Prepared in cooperation with Army Aviation Research and Development Command, Cleveland, St. Louis, Mo.
 (NASA-TM-79123; E-9958; AVRADCOM-TR-79-12) Avail: NTIS HC A03/MF A01 CSCL 21E

The effects of the inlet pressure distortions, induced by five screen patterns, on the performance of a J85-21 turbojet engine was conducted at the NASA Lewis Research Center. Testing was in support of the HiMAT RPRV program at Dryden Flight Research Center. Distortion patterns were chosen based on anticipated application of test results of the HiMAT installation.

Tests were conducted at a simulated Mach number and altitude condition of 0.9 and 10 973 meters. Results are presented in terms of distortion levels and standard compressor performance parameters. Author

N79-23969* National Aeronautics and Space Administration, Lewis Research Center, Cleveland, Ohio.

EFFECT OF STEADY-STATE PRESSURE DISTORTION ON FLOW CHARACTERISTICS ENTERING A TURBOFAN ENGINE

Ronald H. Soeder and George A. Bobula Apr. 1979 34 p refs Prepared in cooperation with Army Aviation Research and Development Command, St. Louis, Mo. (NASA-TM-79134; E-9982; AVRADCOM-TR-79-19) Avail. NTIS HC A03/MF A01 CSCL 21E

Flow angle, static-pressure, and total-pressure distributions were measured in the passage ahead of a turbofan engine operating with inlet pressure distortion. Distortions were generated with five screen configurations and one solid plate configuration. The screens and solid plate were circumferential and mounted on a rotatable assembly. Reynolds Number Index upstream of the distortion device was maintained at 0.5, 0.35, or 0.2, and engine corrected low rotor speeds were held at 6000 rpm and 8600 rpm. Near the engine inlet, flow angle was largest at the hub and increased as flow approached the engine. The magnitude of static-pressure distortion measured along the inlet-duct and extended bullet nose walls increased exponentially as the flow approached the engine. Wall static-pressure distortion was also a function of distortion harmonic. Author

N79-24994* National Aeronautics and Space Administration, Lewis Research Center, Cleveland, Ohio.

PREMIXED PREVAPORIZED COMBUSTOR TECHNOLOGY FORUM

1979 262 p refs Conf. held at Cleveland, Ohio, 9-10 Jan. 1979

(NASA-CP-2078; E-9933) Avail. NTIS HC A12/MF A01 CSCL 21E

The Forum was held to present the results of recent and current work intended to provide basic information required for demonstration of lean, premixed prevaporized combustors for aircraft gas turbine engine application. Papers are presented which deal with the following major topics: (1) engine interfaces, (2) fuel-air preparation, (3) autoignition, (4) lean combustion, and (5) concept design studies. For individual titles, see N79-24995 through N79-25014.

N79-24995* Pratt and Whitney Aircraft Group, East Hartford, Conn.

TURBULENCE CHARACTERISTICS OF COMPRESSOR DISCHARGE FLOWS

Howard P. Grant In NASA Lewis Res. Center Premixed Prevaporized Combustor Technol. Forum 1979 p 5-31 (For primary document see N79-24994 16-07) Avail. NTIS HC A12/MF A01 CSCL 21E

Turbulence measurements were conducted in a large gas turbine engine (JT9D) at the entrance to the diffuser duct, joining the compressor discharge to the combustor inlet. Hot film probe and hot wire probe measurements were obtained at temperatures from 450K (350F) (idle) to 608K (635F) (rich approach). At I.D. (25 percent span) and mid-span locations, the turbulence intensity increased slightly from 6 + or - percent at idle condition to 7 or - 1 percent at rich approach. At O.D. (75 percent span) the turbulent intensity increased more rapidly, from 7.5 + or - 0.5 percent at idle to 15 + or - 0.5 percent at rich approach. The spectra showed turbulent energy distributed uniformly over a 0.1 to 5 KHz bandwidth (down 3db) at all operating conditions, corresponding to random turbulence with velocity wave lengths of 2 cm to 1 meter travelling at the mean velocity of 100 m/sec. Tests results are given in tables and graphs. A.R.H.

N79-24996* General Electric Co., Cincinnati, Ohio.

TURBULENCE MEASUREMENTS IN THE COMPRESSOR EXIT FLOW OF A GENERAL ELECTRIC CF6-50 ENGINE

Jack R. Taylor In NASA Lewis Res. Center Premixed Prevaporized Combustor Technol. Forum 1979 p 33-45 (For primary document see N79-24994 16-07) Avail. NTIS HC A12/MF A01 CSCL 21E

Ruggedized cooled film probes were used to measure CF6-50 compressor exit turbulence properties at three different engine idle condition test points. The turbulence probe was coupled to a constant temperature anemometer and signal conditioning system. An on-line readout system connected to the anemometer was used to check the data as it was acquired. At engine idle conditions, the turbulence intensity ranged from 4.8 percent to 5.6 percent and the length scale ranged from 5.64 cm to 6.95 cm. The length scale values are somewhat larger than the passage height at the measurement plane (5.54 cm), which indicates that the shape of the turbulent eddies are elongated in the axial direction. The microscale values range from about 0.73 cm to about 0.98 cm. Power spectral density distributions show that a large proportion of the turbulent energy at the measurement plane is concentrated at frequencies below one kilohertz. A.R.H.

N79-24997* Solar Turbines International, San Diego, Calif.

FUEL SPRAY DATA WITH LDV

David A. Rohy and John G. Meier In NASA Lewis Res. Center Premixed Prevaporized Combustor Technol. Forum 1979 p 47-55 (For primary document see N79-24994 16-07) Avail. NTIS HC A12/MF A01 CSCL 21E

Droplet size and two component velocities in the severe environment of an operating gas turbine combustor system can be measured simultaneously using the solar laser morphokinometer (SLM) which incorporates the following capabilities: (1) measurement of a true two-dimensional velocity vector with a range of + or - (0.01-200 m/sec); (2) measurement of particle size (range 5 to 300 micron m) simultaneously with the measurement of velocity; (3) specification of probe volume position coordinates with a high degree of accuracy (+ or - 0.5 mm); (4) immediate on-line data checks; and (5) rapid computer storage of acquired data. The optical system of the SLM incorporates an ultrasonic beam splitter to allow the measurement of a two-dimensional velocity vector simultaneously with particle size. A microprocessor with a limited storage capability permits immediate analysis of test data in the test cell. A.R.H.

N79-24998* United Technologies Research Center, East Hartford, Conn.

MODELING OF PREMIXING-PREVAPORIZING FUEL-AIR MIXING PASSAGES

O. L. Anderson, J. B. McVey, D. E. Edwards, and L. M. Chiappetta In NASA Lewis Res. Center Premixed Prevaporized Combustor Technol. Forum 1979 p 57-65 (For primary document see N79-24994 16-07) Avail. NTIS HC A12/MF A01 CSCL 21E

The development of a computer program for the analytical prediction of the distribution of liquid and vapor fuel in the premixing-prevaporizing passage by the direct injection method is described. The technical approach adopted for this program is to separate the problem into three parts each with its own computer code. These three parts are: calculation of the two-dimensional or axisymmetric air flow, calculation of the three-dimensional fuel droplet evaporation, and calculation of the fuel vapor diffusion. This method of approach is justified because premixing passages operate at lean equivalence ratios. Hence, a weak interaction assumption can be made wherein the airflow can affect the fuel droplet behavior but the fuel droplet behavior does not affect the airflow. A.R.H.

N79-24999* Michigan Univ., Ann Arbor.

EFFECT OF FUEL SPRAYS ON EMISSIONS

J. A. Nicholls *In* NASA Lewis Res. Center Premixed Prevaporized Combustor Technol. Forum 1979 p 67-84 refs (For primary document see N79-24994 16-07)
(Grant NSG-3148)

Avail: NTIS HC A12/MF A01 CSCL 21E

A research gas turbine combustor was operated under realistic conditions such that the influence of individual variables (in particular, fuel spray characteristics) on emissions could be determined. The special combustor allows independent control over drop size, fuel-air ratio, air inlet temperature, pressure, reference velocity, and residence time. Also, it lends itself to theoretical modeling and turbulent intensity measurements through use of laser velocimetry. Emission results for a range of operations are presented. A number of graphs show which show the variations of emissions levels with one variable at a time are included. In every case, the fuel is jet A, the pressure is atmospheric, and combustion is limited to a primary zone. A.R.H.

N79-25000* National Aeronautics and Space Administration, Lewis Research Center, Cleveland, Ohio.

PERFORMANCE OF A MULTIPLE VENTURI FUEL-AIR PREPARATION SYSTEM

Robert R. Tacina *In* its Premixed Prevaporized Combustor Technol. Forum 1979 p 85-93 refs (For primary document see N79-24994 16-07)

Avail: NTIS HC A12/MF A01 CSCL 21E

Spatial fuel-air distributions, degree of vaporization, and pressure drop were measured 16.5 cm downstream of the fuel injection plane of a multiple Venturi tube fuel injector. Tests were performed in a 12 cm tubular duct. Test conditions were: a pressure of 0.3 MPa, inlet air temperature from 400 to 800K, air velocities of 10 and 20 m/s, and fuel-air ratios of 0.010 and 0.020. The fuel was Diesel #2. Spatial fuel-air distributions were within + or - 20 percent of the mean at inlet air temperatures above 450K. At an inlet air temperature of 400K, the fuel-air distribution was measured when a 50 percent blockage plate was placed 9.2 cm upstream of the fuel injection plane to distort the inlet air velocity profile. Vaporization of the fuel was 50 percent complete at an inlet air temperature of 400K and the percentage increased linearly with temperature to complete vaporization at 600K. The pressure drop was 3 percent at the design point which was three times greater than the designed value and the single tube experiment value. No autoignition or flashback was observed at the conditions tested. A.R.H.

N79-25001* United Technologies Research Center, East Hartford, Conn.

AUTOIGNITION OF FUELS

Louis J. Spadaccini *In* NASA Lewis Res. Center Premixed Prevaporized Combustor Technol. Forum 1979 p 95-107 ref (For primary document see N79-24994 16-07)

Avail: NTIS HC A12/MF A01 CSCL 21E

An autoignition test section and a premixing fuel injector developed to determine the autoignition characteristics of a variety of aircraft fuels are described. Parametric tests to map the ignition delay characteristics of Jet-A fuel were conducted at pressures of 10, 15, 20, 25, and 30 atm, inlet air temperatures up to 900K and fuel-air equivalence ratios of 0.3, 0.5, 0.7, and 1.0. Residence times in the range of 1 to 50 msec were obtained by interchanging spool pieces to create six different mixer/vaporizer lengths (6, 23, 53, 84, 99, and 130 cm) and by testing at two different airflow rates (0.5 and 1.0 kg/sec). The resulting free-stream velocities were in the range 20 to 100 m/sec. As expected, the results indicate that the ignition delay times decrease with increasing air temperature and pressure. Also, the data show that, for lean mixtures, ignition delay times decrease with increasing equivalence ratios. A.R.H.

N79-25002* General Applied Science Labs., Inc., Westbury, N. Y.

EMISSIONS MEASUREMENTS FOR A LEAN PREMIXED PROPANE/AIR SYSTEM AT PRESSURES UP TO 30 ATMOSPHERES

Gerald Roffe *In* NASA Lewis Res. Center Premixed Prevaporized Combustor Technol. Forum 1979 p 109-125 Forum 1979 p 109-125 (For primary document see N79-24994 16-07)
Avail: NTIS HC A12/MF A01 CSCL 21E

A series of experiments was conducted in which the emissions of a lean premixed system of propane and air were measured at pressures of 5, 10, 20 and 30 atm in a flametube apparatus. Measurements were made for inlet temperatures between 600K and 1000K and combustor residence times from 1.0 to 3.0 msec. A schematic of the test rig is presented along with graphs showing emissions measurements for nitric oxide, carbon monoxide, and UHC as functions of combustor residence time for various equivalence ratios, entrance temperatures and pressures; typical behavior of emissions as a function of equivalence ratio for a fixed residence time. Correlations of nitric oxide emission index with adiabatic flame temperature for a fixed residence time of 2 msec and pressures from 5 to 30 atm; and adiabatic flame temperature corresponding to CO breakpoint conditions for 2 msec residence time as a function of inlet temperature. A.R.H.

N79-25003* National Aeronautics and Space Administration, Lewis Research Center, Cleveland, Ohio.

EFFECT OF DEGREE OF FUEL VAPORIZATION ON EMISSIONS FOR A PREMIXED-PREVAPORIZED COMBUSTOR SYSTEM

Larry P. Cooper *In* its Premixed Prevaporized Combustor Technol. Forum 1979 p 127-130 (For primary document see N79-24994 16-07)

Avail: NTIS HC A12/MF A01 CSCL 21E

The impact of the degree of fuel vaporization upon emission from a flametube combustor was studied using an inlet air pressure of 3×10^5 to the 5th power pascals, inlet air temperatures of 600K and 700K, a reference velocity of 35 meters per second and equivalence ratios of .6 and .72 using Jet A fuel. Incoming air was preheated to temperatures from 600K to 700K by a nonvitiating preheater. Jet A fuel was injected into this airstream through two different fuel injectors manifolded together and mounted in series upstream of a watercooled perforated plate flameholder. The fuel-air mixture burner in a watercooled combustor section. Samples of the fuel-air mixture upstream of the flameholder were obtained for analysis to determine the local degree of fuel vaporization and the fuel-air ratio. Samples of the combustion products were analyzed to determine gaseous emissions. The effects of vaporization on carbon monoxide and nitric oxide, carbon monoxide and nitric oxide emissions are presented. A.R.H.

N79-25004* National Aeronautics and Space Administration, Lewis Research Center, Cleveland, Ohio.

EFFECT OF FUEL/AIR NONUNIFORMITY ON NITRIC OXIDE EMISSIONS

Valerie J. Lyons *In* its Premixed Prevaporized Combustor Technol. Forum 1979 p 131-134 (For primary document see N79-24994 16-07)

Avail: NTIS HC A12/MF A01 CSCL 21E

A flame tube combustor holding jet A fuel was used in experiments performed at a pressure of 3 Mpa and a reference velocity of 25 meters/second for three inlet air temperatures of 600, 700, and 800 K. The gas sample measurements were taken at locations 18 cm and 48 cm downstream of the perforated plate flameholder. Nonuniform fuel/air profiles were produced using a fuel injector by separately fueling the inner five fuel tubes and the outer ring of twelve fuel tubes. Six fuel/air profiles were produced for nominal overall equivalence ratios of .5 and .6. An example of three of these profiles and their resultant nitric oxide NOx emissions are presented. The uniform fuel/air profile cases produced uniform and relatively low profile levels. When the profiles were either center-peaked or edge-peaked, the overall mass-weighted nitric oxide levels increased. A.R.H.

N79-25005* General Applied Science Labs., Inc., Westbury, N. Y.

EFFECTS OF FLAMEHOLDER GEOMETRY ON EMISSIONS AND PERFORMANCE OF LEAN PREMIXED COMBUSTORS

K. S. Venkataramani / In NASA. Lewis Res. Center Premixed Prevaporized Combustor Technol. Forum 1979 p 135-155 (For primary document see N79-24994 16-07)

Avail: NTIS HC A12/MF A01 CSCL 21E

Emission levels and performance of twelve flameholder designs were investigated in a lean, premixed propane-air system at inlet conditions of 800K and 10 atm. The flameholder tested represents six design concepts with two values of blockage for each concept. The design concept consists of the following geometries: perforated plate, wire grid, single cone, multiple cone, vee gutter and swirl cone. Measurements were made at reference velocities of 35 m/s, 25 m/s and 20 m/s at combustor stations 10 cm and 30 cm downstream of the flameholder. G.Y.

N79-25006* National Aeronautics and Space Administration, Lewis Research Center, Cleveland, Ohio.

EFFECTS OF FLAMEHOLDER BLOCKAGE ON EMISSIONS AND PERFORMANCE OF LEAN PREMIXED-PREVAPORIZED COMBUSTORS

Robert A. Duerr / In its Premixed Prevaporized Combustor Technol. Forum 1979 p 157-162 (For primary document see N79-24994 16-07)

Avail: NTIS HC A12/MF A01 CSCL 21E

The results from a parametric study are presented. Tests were conducted at inlet air pressure of 300,000 and 500,000 pascals, inlet air temperatures of 600K, 700K and 800K, reference velocities from 20 to 35 meters per second, and equivalent ratios from the lean stability limit to 0.7 using Jet A fuel. The tests were conducted in a closed duct test facility. Results from the test support the theory that flameholder blockage is one of the major determinants of the size and shape of the recirculation zone. The test data show that higher blockage with its larger recirculation zone provides more residence time which leads to more NO_x formation. G.Y.

N79-25007* United Technologies Research Center, East Hartford, Conn.

LEAN STABILITY AUGMENTATION STUDY

John B. McVey and Jan B. Kennedy / In NASA. Lewis Res. Center Premixed Prevaporized Combustor Technol. Forum 1979 p 163-177 (For primary document see N79-24994 16-07)

Avail: NTIS HC A12/MF A01 CSCL 21E

An analytical and experimental program was conducted to investigate techniques and develop technology for improving the lean combustion limits of premixing, prevaporizing combustors applicable to gas turbine engine main burners. Three concepts for improving lean stability limits were selected for experimental evaluation among twelve approaches considered. Concepts were selected on the basis of the potential for improving stability limits and achieving emission goals, the technological risks associated with development of practical burners employing the concepts, and the penalties to airline direct operating costs resulting from decreased combustor performance, increased engine cost, increased maintenance cost and increased engine weight associated with implementation of the concepts. Tests of flameholders embodying the selected concepts were conducted. G.Y.

N79-25008* Massachusetts Inst. of Tech., Cambridge.
MODELLING TURBULENT FLAME IGNITION AND BLOW-OUT

Krishnan Radhakrishnan and John B. Heywood / In NASA. Lewis Res. Center Premixed Prevaporized Combustor Technol. Forum 1979 p 179-186 refs (For primary document see N79-24994 16-07)

(Grant NGR-22-009-378)

Avail: NTIS HC A12/MF A01 CSCL 21E

A statistical mixing model incorporating an overall rate equation to describe the fuel oxidation process was developed for studies of ignition and blowout in a combustor primary zone.

This zone is treated as a partially stirred reactor whose composition is described by a statistical ensemble of equal mass fluid elements. This ensemble experiences mixing interactions, which represent the turbulent mixing process, at time intervals governed by an empirically determined mixing frequency. Each mixing interaction is computed by randomly selecting two different elements which are then allowed to mix completely so that they reach a mean composition depending on their thermodynamic states prior to mixing. The two elements then separate, and the chemical kinetics proceed depending on their new composition and temperature. G.Y.

N79-25011* General Electric Co., Cincinnati, Ohio.

ADVANCED LOW EMISSIONS CATALYTIC COMBUSTOR PROGRAM AT GENERAL ELECTRIC

W. J. Dodds / In NASA. Lewis Res. Center Premixed Prevaporized Combustor Technol. Forum 1979 p 215-227 refs (For primary document see N79-24994 16-07)

Avail: NTIS HC A12/MF A01 CSCL 21E

The Advanced Low Emissions Catalytic Combustors Program (ALECC) is being undertaken to evaluate the feasibility of employing catalytic combustion technology in aircraft gas turbine engines as a means to control emission of oxides of nitrogen during subsonic stratospheric cruise operation. The ALECC Program is being conducted in three phases. The first phase, which was completed in November, 1978, consisted of a design study to identify catalytic combustor designs having the greatest potential to meet the emissions and performance goals specified. The primary emissions goal of this program was to obtain cruise NO emissions of less than 1g/kg (compared with levels of 15 to 20 g/kg obtained with current designs). However, good overall performance and feasibility for engine development were heavily weighted in the evaluation of combustor designs. G.Y.

N79-25012* Pratt and Whitney Aircraft Group, East Hartford, Conn.

ADVANCED LOW EMISSIONS CATALYTIC COMBUSTOR PROGRAM AT PRATT AND WHITNEY

G. J. Sturgess / In NASA. Lewis Res. Center Premixed Prevaporized Combustor Technol. Forum 1979 p 229-245 (For primary document see N79-24994 16-07)

Avail: NTIS HC A12/MF A01 CSCL 21E

The feasibility of employing catalytic combustion technology to control the emissions of oxides of nitrogen for subsonic, stratospheric cruise aircraft operations is the objective of this NASA contract. The existing Environmental Protection Agency standards for the landing and takeoff cycle were also required to be satisfied. Work for the first phase of a proposed three phase effort is reported and is concerned with analytical design studies. G.Y.

N79-25013* Pratt and Whitney Aircraft Group, East Hartford, Conn.

LEAN, PREMIXED, PREVAPORIZED COMBUSTOR CONCEPTUAL DESIGN STUDY

Anthony J. Fiorentino / In NASA. Lewis Res. Center Premixed Prevaporized Combustor Technol. Forum 1979 p 247-254 (For primary document see N79-24994 16-07)

Avail: NTIS HC A12/MF A01 CSCL 21E

The seven month study program has the objective to identify and evaluate promising lean, premixed, prevaporized combustor concepts utilizing variable geometry and/or other flow control techniques. The general approach taken to accomplish this objective is outlined and consists of combustor design, design analysis and design ranking. The schedule being taken to achieve this program is shown. Although the ultimate goal of this program is the significant reduction of cruise oxides of nitrogen, both the EPA emission standards and combustor performance levels outlined are retained as goals as well. G.Y.

N79-25014* General Electric Co., Cincinnati, Ohio.

LEAN, PREMIXED, PREVAPORIZED COMBUSTOR CONCEPTUAL DESIGN STUDY

E. E. Ekstedt / In NASA, Lewis Res. Center Premixed Prevaporized Combustor Technol. Forum 1979 p 255-263 (For primary document see N79-24994 16-07)

Avail: NTIS HC A12/MF A01 CSCL 21E

Phase 1 of the Lean Premixed-Prevaporized Combustor Design Study is a nine month analytical study effort with no experimental or testing activities included. The program has the objective to design and analyze advanced combustor concepts with features for fuel premixing and prevaporization upstream of the combustion zone for use in future subsonic aircrafts with features for fuel premixing and prevaporization upstream of the combustion zone for use in future subsonic aircraft engines. All of the designs also embody some form of variable geometry for combustor flow modulation. The primary criterion for these designs is low oxides of nitrogen emissions at stratospheric cruise conditions. Four combustor concepts are being designed for the NASA/GE Energy Efficient Engine (EEE) envelope and cycle. Current status of the program is that the four concepts sized for the EEE were designed and are currently undergoing analysis and evaluation.

G.Y.

N79-25015* National Aeronautics and Space Administration, Lewis Research Center, Cleveland, Ohio.

MULTIVARIABLE CONTROL ALTITUDE DEMONSTRATION ON THE F100 TURBOFAN ENGINE

B. Lehtinen, R. L. DeHoff (Systems Control, Inc., Palo Alto, Calif.), and R. D. Hackney (Pratt and Whitney Aircraft Group, West Palm Beach, Fla.) 1979 31 p refs Presented at the 15th Joint Propulsion Conf., Las Vegas, Nev., 18-20 Jun. 1979; sponsored by AIAA, Soc. of Automotive Engr., and ASME (NASA-TM-79183; E-050) Avail: NTIS HC A03/MF A01 CSCL 21E

The F100 Multivariable control synthesis (MVCS) program, was aimed at demonstrating the benefits of LGR synthesis theory in the design of a multivariable engine control system for operation throughout the flight envelope. The advantages of such procedures include: (1) enhanced performance from cross-coupled controls, (2) maximum use of engine variable geometry, and (3) a systematic design procedure that can be applied efficiently to new engine systems. The control system designed, under the MVCS program, for the Pratt & Whitney F100 turbofan engine is described. Basic components of the control include: (1) a reference value generator for deriving a desired equilibrium state and an approximate control vector, (2) a transition model to produce compatible reference point trajectories during gross transients, (3) gain schedules for producing feedback terms appropriate to the flight condition, and (4) integral switching logic to produce acceptable steady-state performance without engine operating limit exceedance.

J.A.M.

N79-25016* National Aeronautics and Space Administration, Lewis Research Center, Cleveland, Ohio.

FUNDAMENTALS OF GAS TURBINE COMBUSTION

Melvin Gerstein (Univ. of Southern Calif., Los Angeles) 1979 52 p Workshop held at Cleveland, 6-7 Feb. 1979

(NASA-CP-2087; E-026) Avail: NTIS HC A04/MF A01 CSCL 21E

Combustion problems and research recommendations are discussed in the areas of atomization and vaporization, combustion chemistry, combustion dynamics, and combustion modelling. The recommendations considered of highest priority in these areas are presented.

S.E.S.

N79-25022* National Aeronautics and Space Administration, Lewis Research Center, Cleveland, Ohio.

OPERATING CONDITIONS AND GEOMETRY EFFECTS ON LOW-FREQUENCY AFTERBURNER COMBUSTION INSTABILITY IN A TURBOFAN AT ALTITUDE

Richard R. Cullom and Roy L. Johnson Jun 1979 31 p refs (NASA-TP-1475; E-9886) Avail: NTIS HC A03/MF A01 CSCL 21E

Three afterburner configurations were tested in a low-bypass-ratio turbofan engine to determine the effect of various fuel distributions, inlet conditions, flameholder geometry, and fuel injection location on combustion instability. Tests were conducted at simulated flight conditions of Mach 0.75 and 1.3 at altitudes from 11,580 to 14,020 m (38,000 to 46,000 ft). In these tests combustion instability with frequency from 28 to 90 Hz and peak-to-peak pressure amplitude up to 46.5 percent of the afterburner inlet total pressure level was encountered. Combustion instability was suppressed in these tests by varying the fuel distribution in the afterburner.

Author

N79-25023* National Aeronautics and Space Administration, Lewis Research Center, Cleveland, Ohio.

INDUSTRY TESTS OF NASA CERAMIC THERMAL BARRIER COATING

Curt H. Liebert and Francis S. Stepka Jun 1979 26 p refs Presented at 6th Intern. Vacuum Metallurgy Conf., San Diego, Calif., 23-27 Apr. 1979; Sponsored by Am. Vacuum Soc. (NASA-TP-1425; E-9846) Avail: NTIS HC A03/MF A01 CSCL 21E

Ceramic thermal barrier coating (TBC) system was tested by industrial and governmental organizations for a variety of aeronautical, marine, and ground-based gas turbine engine applications. This TBC is a two-layer system with a bond coating of nickel-chromium-aluminum-yttrium (Ni-16Cr-6Al-0.6Y, in wt. percent) and a ceramic coating of yttria-stabilized zirconia (ZrO₂-12Y₂O₃, in wt. percent). Seven tests evaluated the system's thermal protection and durability. Five other tests determined thermal conductivity, vibratory fatigue characteristics, and corrosion resistance of the system. The information presented includes test results and photographs of the coated parts. Recommendations are made for improving the coating procedures.

J.M.S.

N79-27140* National Aeronautics and Space Administration, Lewis Research Center, Cleveland, Ohio.

TURBINE ENGINE ALTITUDE CHAMBER AND FLIGHT TESTING WITH LIQUID HYDROGEN

E. William Conrad 1979 22 p refs Presented at the Intern. DGLR/DFVLR Symp. on Hydrogen in Air Transportation, Stuttgart, 11-14 Sep. 1979

(NASA-TM-79196; E-062) Avail: NTIS HC A02/MF A01 CSCL 21E

Flight engine experiments using liquid hydrogen fuel were reviewed. A few implications of the results to modern turbine engines are presented. A subsequent contract dealing with a positive displacement pump operating on liquid hydrogen is discussed, and some aspects of liquid hydrogen propellant systems, reflected by rocket booster experience are treated.

S.E.S.

N79-27141* National Aeronautics and Space Administration, Lewis Research Center, Cleveland, Ohio.

ENERGY EFFICIENT AIRCRAFT ENGINES

Roger Chamberlin and Brent Miller 1979 21 p refs Presented at Aircraft Systems Meeting, New York, 20-22 Aug. 1979; sponsored by AIAA

(NASA-TM-79204; E-089) Avail: NTIS HC A02/MF A01 CSCL 21E

The three engine programs that constitute the propulsion portion of NASA's Aircraft Energy Efficiency Program are described, their status indicated, and anticipated improvements in SFC discussed. The three engine programs are (1) Engine Component Improvement-directed at current engines, (2) Energy Efficiency Engine directed at new turbofan engines, and (3) Advanced Turboprops-directed at technology for advanced turboprop-powered aircraft with cruise speeds to Mach 2.8. Unique propulsion system interactive ties to the airframe, deriving from engine design features to reduce fuel consumption, are discussed. Emphasis is placed on the advanced turboprop since it offers the largest potential fuel savings of the three propulsion programs and also has the strongest interactive ties to the airframe.

Author

N79-27142* National Aeronautics and Space Administration, Lewis Research Center, Cleveland, Ohio.

FLOW VISUALIZATION OF DISCRETE-HOLE FILM COOLING WITH SPANWISE INJECTION OVER A CYLINDER

Louis M. Russell Jul. 1975 15 p refs

(NASA-TP-1491; E-9946) Avail: NTIS HC A02/MF A01 CSCL 21E

Insight into the fluid mechanics encountered when film air from a single row of holes is injected over a cylinder in a mainstream at conditions simulating a film cooled, turbulent-vane leading edge was investigated. Smoke was added to the cooling air to visualize its flow path. Film was injected in the spanwise direction at angles of 30 deg and 45 deg to the surface; at angular locations of 15 deg, 30 deg, 45 deg, and 60 deg from the stagnation line; and at various blowing ratios. The observations were related to the measured heat transfer data of others. The results indicate that, in addition to the expected growth in film thickness and the greater penetration of the boundary layer with increasing blowing ratio, there was an absence of spanwise spreading and only a small spanwise deflection of the injected film. S.E.S.

N79-27143* National Aeronautics and Space Administration, Lewis Research Center, Cleveland, Ohio.

PERFORMANCE OF TWO-STAGE FAN HAVING LOW-ASPECT-RATIO FIRST-STAGE ROTOR BLADING

Donald C. Urasek, William T. Gorrell (Army Aviation Res. and Develop. Command, Cleveland), and Walter S. Cunniff Aug. 1979 132 p Prepared in cooperation with US Army Aviation Research and Development Command, Cleveland

(NASA-TP-1493; AVRADCOM-TR-78-49; E-9237) Avail: NTIS HC A07/MF A01 CSCL 21E

The NASA two stage fan was tested with a low aspect ratio first stage rotor having no midspan dampers. At design speed the fan achieved an adiabatic design efficiency of 0.846, and peak efficiencies for the first stage and rotor of 0.870 and 0.906, respectively. Peak efficiency occurred very close to the stall line. In an attempt to improve stall margin, the fan was retested with circumferentially grooved casing treatment and with a series of stator blade resets. Results showed no improvement in stall margin with casing treatment but increased to 8 percent with stator blade reset. Author

N79-27179* National Aeronautics and Space Administration, Lewis Research Center, Cleveland, Ohio.

REVIEW OF THE AGARD 5 AND M PANEL EVALUATION PROGRAM OF THE NASA-LEWIS SRP APPROACH TO HIGH-TEMPERATURE LCF LIFE PREDICTION

Marvin H. Hirschberg In AGARD Stresses, Vibrations, Struct. Integration and Eng. Integrity (Including Aeroelasticity and Flutter) Apr. 1979 9 p refs (For primary document see N79-27148 18-07)

Avail: NTIS HC A21/MF A01 CSCL 21E

The strain range partitioning SRP method method presented is a significant step forward in high temperature low cycle fatigue life prediction. Several concerns and recommendations regarding SRP were described. These dealt primarily with the problems associated with the application of SRP to cases involving small inelastic strains (and therefore long lives). The difficulties associated with partitioning these narrow hysteresis loops and the present inability of SRP to handle mean stress effects were also noted. M.M.M.

N79-27181* National Aeronautics and Space Administration, Lewis Research Center, Cleveland, Ohio.

SUPERSONIC UNSTALLED FLUTTER

J. J. Adamczyk, M. E. Goldstein, and M. J. Hartmann In AGARD Stresses, Vibrations, Struct. Integration and Eng. Integrity (Including Aeroelasticity and Flutter) Apr. 1979 14 p refs (For primary document see N79-27148 18-07)

Avail: NTIS HC A21/MF A01 CSCL 21E

A parametric study to show the effects of cascade geometry, inlet Mach number, and backpressure on the onset of single

and multi degree of freedom unstalled supersonic flutter is presented. Several of the results are correlated against experimental qualitative observation to validate the models. M.M.M.

N79-28176* National Aeronautics and Space Administration, Lewis Research Center, Cleveland, Ohio.

A THROAT-BYPASS STABILITY-BLEED SYSTEM USING RELIEF VALVES TO INCREASE THE TRANSIENT STABILITY OF A MIXED-COMPRESSION INLET

George H. Neiner, Miles O. Dustin, and Gary L. Cole Jul. 1979 47 p refs

(NASA-TP-1083; E-8950) Avail: NTIS HC A03/MF A01 CSCL 21E

A stability-bleed system was installed in a YF-12 flight inlet that was subjected to internal and external airflow disturbances in the NASA Lewis 10 by 10 foot supersonic wind tunnel. The purpose of the system is to allow higher inlet performance while maintaining a substantial tolerance (without unstart) to internal and external disturbances. At Mach numbers of 2.47 and 2.76, the inlet tolerance to decreases in diffuser-exit corrected airflow was increased by approximately 10 percent of the operating-point airflow. The stability-bleed system complemented the terminal-shock-control system of the inlet and did not show interaction problems. For disturbances which caused a combined decrease in Mach number and increase in angle of attack, the system with valves operative kept the inlet started 4 to 28 times longer than with the valves inoperative. Hence, the stability system provides additional time for the inlet control system to react and prevent unstart. This was observed for initial Mach numbers of 2.55 and 2.68. For slow increase in angle of attack at Mach 2.47 and 2.76, the system kept the inlet started beyond the steady-state unstart angle. However, the maximum transient angles of attack without unstart could not be determined because wind-tunnel mechanical-stop limits for angle of attack were reached. A.R.H.

N79-28177* National Aeronautics and Space Administration, Lewis Research Center, Cleveland, Ohio.

EFFECT OF ROTOR MERIDIONAL VELOCITY RATIO ON RESPONSE TO INLET RADIAL AND CIRCUMFERENTIAL DISTORTION

Nelson, L. Sanger Jul. 1979, 73 p refs

(NASA-TP-1278; E-8987) Avail: NTIS HC A04/MF A01 CSCL 21E

Three single transonic fan stages, each having a different meridional velocity ratio across its rotor, were tested with two magnitudes of tip radial distortion and with a 90 deg circumferential distortion imposed on the inlet flow. The rotor with the lowest meridional velocity ratio (less than 0.9 at the tip) demonstrated the least degradation of performance due to these distortions. Loss and deviation angle data (as needed for performance prediction with radial distortion) calculated along actual streamlines for radially distorted flow and correlated against diffusion factor, showed consistent agreement with data calculated along design streamlines for undistorted flow. Author

N79-30187* National Aeronautics and Space Administration, Lewis Research Center, Cleveland, Ohio.

EFFECT OF STEADY-STATE TEMPERATURE DISTORTION AND COMBINED DISTORTION ON INLET FLOW TO A TURBOFAN ENGINE

Ronald H. Soeder and George A. Bobula Aug. 1979 43 p refs

(NASA-TM-79237; E-143) Avail: NTIS HC A03/MF A01 CSCL 21E

Flow angle, static pressure, total temperature and total pressure were measured in the inlet duct upstream of a turbofan engine operating with temperature distortion or combined pressure-temperature distortion. Such measurements are useful in the evaluation of analytical models of inlet distortion. A rotating gaseous-hydrogen burner and a circumferential 180 degrees-extent screen configuration mounted on a rotatable assembly generated the distortions. Reynolds number index was maintained at 0.5 and engine corrected low-speed speeds were held

at 6000 and 8000 rpm. The measurements showed that at the entrance to the engine, flow angle was largest in the hub region. As flow approached the engine, yaw angle (circumferential variation) increased and pitch angle (radial variation) decreased. The magnitude of static-pressure distortion measured along the inlet-duct and extended bullet nose walls increased exponentially as flow approached the engine. Author

N79-30188* National Aeronautics and Space Administration, Lewis Research Center, Cleveland, Ohio

A SUMMARY OF NASA/AIR FORCE FULL SCALE ENGINE RESEARCH PROGRAMS USING THE F100 ENGINE

W. J. Deskin (Pratt and Whitney Aircraft Group, West Palm Beach, Fla.) and H. G. Hurrell 1979 24 p refs Presented at 15th Joint Propulsion Conf., Las Vegas, Nev., 18-20 Jun. 1979; Sponsored by AIAA, Am. Soc. of Mech. Engr. (NASA-TM-79267; E-183) Avail. NTIS HC A02/MF A01 CSCL 21E

A full scale engine research (FSER) program conducted with the F100 engine is presented. The program mechanism is described and the F100 test vehicles utilized are illustrated. Technology items were addressed in the areas of swirl augmentation, flutter phenomenon, advanced electronic control logic theory, strain gage technology and distortion sensitivity. The associated test programs are described. The FSER approach utilizes existing state of the art engine hardware to evaluate advanced technology concepts and problem areas. Aerodynamic phenomenon previously not considered by design systems were identified and incorporated into industry design tools. A.W.H.

N79-30191* National Aeronautics and Space Administration, Lewis Research Center, Cleveland, Ohio

PERFORMANCE OF TWO-STAGE FAN WITH A FIRST-STAGE ROTOR REDESIGNED TO ACCOUNT FOR THE PRESENCE OF A PART-SPAN DAMPER

William T. Gorrell and Donald C. Yrasek Sep. 1979 72 p refs (NASA-TP-1483; E-9786; AVRADCOM-TR-79-10) Avail. NTIS HC A04/MF A01 CSCL 21E

The NASA two-stage fan was tested with a redesigned first-stage rotor. The redesign included a new design approach to account for the presence of a part-span damper. At design speed the fan achieved a peak efficiency of 0.803, which is 1.9 percentage points higher than the original design. The peak efficiencies of the first stage and first rotor were 0.789 and 0.821 respectively. An improvement in efficiency of up to 5 percentage points in the damper region was achieved over the original large damper version. The stall margin, based on flow conditions at peak efficiency, was 10 percent at design speed. Author

N79-31210* National Aeronautics and Space Administration, Lewis Research Center, Cleveland, Ohio

AN OVERVIEW OF NASA RESEARCH ON POSITIVE DISPLACEMENT TYPE GENERAL AVIATION ENGINES

E. E. Kempke and E. A. Willis 1979 40 p refs Presented at the Aircraft Systems and Technol. Meeting N. Y., 20-22 Aug. 1979; sponsored by AIAA (NASA-TM-79254; E-165; AIAA-79-1824) Avail. NTIS HC A03/MF A01 CSCL 21E

The general aviation positive displacement engine program encompassing conventional, lightweight diesel, and rotary combustion engines is described. Lean operation of current production type spark ignition engines and advanced alternative engine concepts are emphasized. J.M.S.

N79-31213* National Aeronautics and Space Administration, Lewis Research Center, Cleveland, Ohio

AERODYNAMIC PERFORMANCE OF 1.38-PRESSURE-RATIO, VARIABLE-PITCH FAN STAGE

Royce D. Moore and Walter M. Osborn Sep. 1979 71 p (NASA-TP-1502; E-9700) Avail. NTIS HC A04/MF A01 CSCL 21E

The performance of a variable pitch fan stage tested over a range of blade setting angles, speeds, and flows is presented. The fan was designed for a tip speed of 289.6 m/sec and a flow of 29.6 kg/sec. The measured performance agreed reasonably well with the design point. The stall margin was only 5 percent. Static thrust values along an operating line ranged from less than 15 to over 115 percent of that at design angle as the blade setting angle was varied from 25 degrees (closed) to -8 degrees (opened). The use of casing treatment increased the stall margin to 20 percent but decreased efficiency by 4 percentage points. A.W.H.

N79-31214* National Aeronautics and Space Administration, Lewis Research Center, Cleveland, Ohio

AERODYNAMIC PERFORMANCE OF AXIAL-FLOW FAN STAGE OPERATED AT NINE INLET GUIDE VANE ANGLES

Royce D. Moore and Lonnie Reid Sep. 1979 43 p refs (NASA-TP-1510; E-9714) Avail. NTIS HC A03/MF A01 CSCL 21E

The overall performance of a fan stage with nine inlet guide vane angle settings is presented. These data were obtained over the stable flow range at speeds from 60 to 120 percent of design for vane setting angles from -25 to 42.5 degrees. At design speed and design inlet guide vane angle, the stage has a peak efficiency of 0.892 at a pressure ratio of 1.322 and a flow of 25.31 kg/s. The stall margin based on peak efficiency and stall was 20 percent. Based on an operating line passing through the peak efficiency point at the design setting angle, the useful operating range of the stage at design speed is limited by stall at the positive setting angles and by choke at the negative angles. At design the calculated static thrust along the operating line varied from 68 to 114 percent of that obtained at design setting angle. Author

A79-10792 * Wide range operation of advanced low NOx aircraft gas turbine combustors. P. B. Roberts, R. J. Fiorito (Solar Turbines International, San Diego, Calif.), and H. F. Butze (NASA, Lewis Research Center, Air Breathing Engines Div., Cleveland, Ohio). *American Society of Mechanical Engineers, Gas Turbine Conference and Products Show, London, England, Apr. 9-13, 1978, Paper 78-GT-128*. 13 p. 6 refs. Members, \$150; nonmembers, \$3.00. NASA-supported research.

The paper summarizes the results of an experimental test rig program designed to define and demonstrate techniques which would allow the jet-induced circulation and vortex air blast combustors to operate stably with acceptable emissions at simulated engine idle without compromise to the low NOx emissions under the high-altitude supersonic cruise condition. The discussion focuses on the test results of the key combustor modifications for both the simulated engine idle and cruise conditions. Several range-augmentation techniques are demonstrated that allow the lean-reaction premixed aircraft gas turbine combustor to operate with low NOx emissions at engine cruise and acceptable CO and UHC levels at engine idle. These techniques involve several combinations, including variable geometry and fuel switching designs. S.D.

A79-11600 * Impact of future fuel properties on aircraft engines and fuel systems. R. A. Rudey and J. S. Grobman (NASA, Lewis Research Center, Cleveland, Ohio). *NATO, AGARD, Lecture Series on Energy Conservation in Aircraft Propulsion, 96th, Munich, West Germany, Oct. 26, 27, 1978, Paper, 32 p. 20 refs.*

From current projections of the availability of high-quality petroleum crude oils, it is becoming increasingly apparent that the specifications for hydrocarbon jet fuels may have to be modified. The problems that are most likely to be encountered as a result of these modifications relate to engine performance, component durability and maintenance, and aircraft fuel-system performance. The effect on engine performance will be associated with changes in specific fuel consumption, ignition at relight limits, at exhaust emissions. Durability and maintenance will be affected by increases in combustor liner temperatures, carbon deposition, gum formation

in fuel nozzles, and erosion and corrosion of turbine blades and vanes. Aircraft fuel-system performance will be affected by increased deposits in fuel-system heat exchangers and changes in the pumpability and flowability of the fuel. The severity of the potential problems is described in terms of the fuel characteristics most likely to change in the future. Recent data that evaluate the ability of current-technology aircraft to accept fuel specification changes are presented, and selected technological advances that can reduce the severity of the problems are described and discussed. (Author)

A79-14796 * # Correlation of combustor acoustic power levels inferred from internal fluctuating pressure measurements. U. H. von Glahn (NASA, Lewis Research Center, Cleveland, Ohio). *Acoustical Society of America, Meeting, 96th, Honolulu, Hawaii, Nov. 26-Dec. 1, 1978, Paper, 24 p.* 12 refs.

Combustion chamber acoustic power levels inferred from internal fluctuating pressure measurements are correlated with operating conditions and chamber geometries over a wide range. The variables include considerations of chamber design (can, annular, and reverse-flow annular) and size, number of fuel nozzles, burner staging and fuel split, airflow and heat release rates, and chamber inlet pressure and temperature levels. The correlated data include those obtained with combustion component development rigs as well as engines. (Author)

A79-17029 * Predicted inlet gas temperatures for tungsten fiber reinforced superalloy turbine blades. E. A. Winsa, L. J. Westfall, and D. W. Petrasek (NASA, Lewis Research Center, Cleveland, Ohio). In: ICCM/2, Proceedings of the Second International Conference on Composite Materials, Toronto, Canada, April 16-20, 1978. (A79-16981 05-24) Warrendale, Pa., Metallurgical Society of AIME, 1978, p. 840-857. 23 refs.

A procedure is presented for predicting the magnitude of the turbine inlet gas temperatures potentially achievable using first generation tungsten fiber reinforced superalloys (TFRS) turbine blades. Both uncoated blades and blades with thermal barrier coatings are considered. The thermal conductivities of two representative TFRS were measured over a range of temperatures. The results show that cooled TFRS blades may allow significantly higher gas temperatures than are possible with superalloy blades. For one design, the difference is about 150-200 K. M.L.

A79-19698 * # Calculation of the three-dimensional flow field in supersonic inlets at angle of attack using a bicharacteristic method with discrete shock wave fitting. J. Vadyak, J. D. Hoffman (Purdue University, West Lafayette, Ind.), and A. R. Bishop (NASA, Lewis Research Center, Wind Tunnel and Flight Div., Cleveland, Ohio). *American Institute of Aeronautics and Astronautics, Aerospace Sciences Meeting, 17th, New Orleans, La., Jan. 15-17, 1979, Paper 79-0379.* 11 p. 11 refs. Grants No. NGR-15-005-162; No. NGR-15-005-191.

An analysis is presented for calculating the flow field in supersonic mixed-compression aircraft inlets operating at angle of attack. The flow field is computed by a steady three-dimensional bicharacteristic method. The bow shock wave and the reflected internal shock wave system are computed by a three-dimensional discrete shock wave fitting procedure. Viscous and thermal diffusion may be included as source terms in the bicharacteristic method. A production type computer program capable of determining the flow field in a variety of axisymmetric mixed-compression supersonic inlets is available. The results of the present analysis agree well with those produced by the two-dimensional method of characteristics when axisymmetric flow fields are computed. For three-dimensional flow fields, the results of the present analysis agree well with experimental data except in regions of high viscous interaction and boundary layer removal. The present analysis does not compute the boundary layer, nor does it account for boundary layer bleed. (Author)

A79-20078 * # Fuel conservative aircraft engine technology. D. L. Nored (NASA, Lewis Research Center, Cleveland, Ohio). In: International Council of the Aeronautical Sciences, Congress, 11th, Lisbon, Portugal, September 10-16, 1978, Proceedings, Volume 1. (A79-20076 06-01) Cologne, International Council of the Aeronautical Sciences Secretariat (DGLR), 1978, p. 11-26. 22 refs.

NASA's Aircraft Energy Efficiency Program, initiated in an effort to minimize the adverse impact of the worldwide fuel crisis, will develop technology for more fuel-efficient subsonic transport aircraft. The program includes three major propulsion projects: (1) Engine Component Improvement, directed at current engines, (2) Energy Efficient Engine, directed at new turbofan engines, and (3) Advanced Turboprops, directed at technology for advanced turboprop-powered aircraft. The present paper reviews the current status of each of these projects and describes some of the technologies and recent accomplishments. B.J.

A79-20880 * # Impact behavior of filament-wound graphite/epoxy fan blades. K. J. Bowles (NASA, Lewis Research Center, Cleveland, Ohio). *Society for the Advancement of Material and Process Engineering, National Symposium and Exhibition, 23rd, Anaheim, Calif., May 2-4, 1978, Paper.* 18 p.

The fabrication and impact tests of graphite/epoxy filament wound fan blades are discussed. Blades which were spin tested at tip speeds up to 305 m/sec retained their structural integrity. Two blades were each impacted with a 454-g slice of a 908-g simulated bird at a tip speed of 263 deg and impact angles of 22 deg and 32 deg. The impact tests were recorded with high-speed movie film. The blade which was impacted at 22 deg sustained some root delamination but remained intact. The 32 deg impact separated the blade from the root. No local damage other than leading-edge debonding was observed for either blade. The results of a failure mode analysis are also discussed. (Author)

A79-23509 * # Effect of lip and centerbody geometry on aerodynamic performance of inlets for tilting-nacelle VTOL aircraft. R. R. Burley (NASA, Lewis Research Center, Cleveland, Ohio). *American Institute of Aeronautics and Astronautics, Aerospace Sciences Meeting, 17th, New Orleans, La., Jan. 15-17, 1979, Paper 79-0381.* 25 p. 8 refs.

Inlets for tilt-nacelle VTOL aircraft must operate over a wide range of incidence angles and engine weight flows without internal flow separation. Wind tunnel tests of scale model inlets were conducted to evaluate the effectiveness of three geometric variables to provide this capability. Increasing the lip contraction ratio increased the separation angle at all engine weight flows. The optimum axial location of the centerbody occurred when its leading edge was located just downstream of the inlet lip. Compared with a short centerbody, the optimum location of the centerbody resulted in an increase in separation angle at all engine weight flows. Decreasing the lip major-to-minor-axis ratio increased the separation angle at the lower engine weight flows. (Author)

A79-23512 * # Effect of forward velocity and crosswind on the reverse-thrust performance of a variable-pitch fan engine. D. C. Reemsnyder and D. A. Sagerser (NASA, Lewis Research Center, Cleveland, Ohio). *American Institute of Aeronautics and Astronautics, Aerospace Sciences Meeting, 17th, New Orleans, La., Jan. 15-17, 1979, Paper 79-0105.* 20 p. 12 refs.

Variable-pitch-fan engines may be attractive for future short-haul aircraft if sufficient reverse thrust is available for aircraft deceleration after touchdown. Thrust reversal is obtained in these engines by changing fan blade pitch about 90 deg, which causes the fan airflow to enter the fan duct nozzle and exhaust through the fan inlet. This capability would eliminate the heavy and costly thrust reverser system required for current fixed-pitch turbofan engines. NASA has, therefore, supported the development of advanced technology for a quiet, clean, high-bypass-ratio turbofan engine for future short-haul aircraft. In connection with this program, tests

were conducted to determine the effect of forward velocity and angle of attack on steady-state reverse-thrust performance. Other objectives of the tests were related to the determination of the effect of forward velocity on forward-to-reverse thrust transient performance and the determination of the effectiveness of an overshoot blade angle technique to establish reverse thrust during a transient. The results of the tests are discussed. G.R.

A79-25856 * # Lean combustion limits of a confined premixed-prevaporized propane jet. K. L. Huck (NASA, Lewis Research Center, Cleveland, Ohio; Martin Marietta Aerospace, Bethesda, Md.). *American Institute of Aeronautics and Astronautics, Annual Meeting and Technical Display, 15th, Washington, D.C., Feb. 6-8, 1979, Paper 79-0538*. 9 p. 10 refs.

An experimental study was carried out to determine the effects of jet velocity and confinement on lean premixed-prevaporized propane/air blowout limits. The combustor consisted of a single hole flameholder within a quartz liner. Five flameholder plates and two quartz liners were used. Lean stability limits were mapped for confined propane jet in cylindrical combustor. Three zones of flame stability were observed depending on the liner and jet Reynolds number and the combustor geometry. At low Reynolds number the combustor was jet stabilized. As the Reynolds number was increased the combustor became either recirculation zone stabilized, or for small recirculation zone step sizes, the combustor was wall stabilized. The factors affecting stability seem to be the Reynolds numbers of the liner and inlet jet along with the flameholder step size. Stability was achieved at both laminar and turbulent conditions. S.D.

A79-25870 * # NASA research on general aviation power plants. W. L. Stewart, R. J. Weber, E. A. Willis, and G. K. Sievers (NASA, Lewis Research Center, Cleveland, Ohio). *American Institute of Aeronautics and Astronautics, Annual Meeting and Technical Display, 15th, Washington, D.C., Feb. 6-8, 1979, Paper 79-0561*. 10 p. 7 refs.

Research activities within NASA to support general aviation industry in improving propulsion engines are described. Near-term objectives include improvements of gasoline piston engines to achieve fuel savings and reduce emissions well below EPA levels. To meet the longer term goals, advanced combustion research has been considered as essential in obtaining further improvements in BSFC (break specific fuel consumption). Modifications of an aircraft rotary engine were tested and it was found that by increasing the compression ratio and other refinements the BSFC was improved by 15%. The applicability of available large turbofan engine technology to small engines in order to obtain significant reductions in noise and pollutant emissions is being tested. Studies have been conducted at exploring the possibility of achieving high improvements in cost and performance for turboprop engines of less than 1000 horsepower. A.A.

A79-25880 * Prop-fan propulsion - Its status and potential. J. F. Dugan, Jr. (NASA, Lewis Research Center, Cleveland, Ohio), B. S. Gatzert, and W. M. Adamson (United Technologies Corp., Hartford, Conn.). *Society of Automotive Engineers, Aerospace Meeting, San Diego, Calif., Nov. 27-30, 1978, Paper 780995*. 27 p. 43 refs.

Studies have established that advanced turboprop (prop-fan) equipped aircraft will reduce fuel consumption by 15 to 20 percent compared to aircraft equipped with high-bypass turbofan engines of equivalent technology. A reduction in direct operating costs of approximately 10 percent has been identified for commercial aircraft as well as approximately 20 percent lower gross weight airplane for long endurance military missions. The prop-fan propulsion system is being investigated as part of the NASA Aircraft Energy Efficiency program which includes both analytical studies and experimental tests. The experimental work encompasses performance and acoustic wind tunnel tests on several prop-fan models. The prop-fan technology status is reviewed in the major areas of performance, installed

effects, cabin noise, blade structure and maintenance cost. Also, further activities required to complete the technical validation of prop-fans are described. (Author)

A79-25885 * An in-place recalibration technique to extend the temperature capability of capacitance-sensing, rotor-blade-tip-clearance measurement systems. J. Barranger (NASA, Lewis Research Center, Cleveland, Ohio). *Society of Automotive Engineers, Aerospace Meeting, San Diego, Calif., Nov. 27-30, 1978, Paper 781003*. 14 p.

It is known that capacitance-sensing, rotor-blade-tip-clearance measurement systems suffer from a strong dependency on probe tip temperature and humidity. A novel in-place recalibration technique partly overcomes this problem through a simple modification of the electronics that permits a scale factor correction. The technique is used to reduce the errors in a commercial system by more than 50 percent up to a temperature of 370 C (700 F). A probe design is proposed to further raise the maximum temperature capability of the measurement system. (Author)

A79-26877 * # Measured and predicted noise of the AVCO-Lycoming YF-102 turbofan engine. D. J. Clark, J. G. McArdle, and L. Homyak (NASA, Lewis Research Center, Cleveland, Ohio). *American Institute of Aeronautics and Astronautics, Aeroacoustics Conference, 5th, Seattle, Wash., Mar. 12-14, 1979, Paper 79-0641*. 9 p. 8 refs.

Acoustic testing of the AVCO-Lycoming YF-102 turbofan engine was done on a static test stand at Lewis Research Center in support of the Quiet Short-Haul Research Aircraft (QSRA) acoustic design. Overall noise levels are dominated by the fan noise emanating from the exhaust duct, except at high power settings when combination tones are generated in the fan inlet. Component noise levels, calculated by noise prediction methods developed at Lewis Research Center for the ANOP program, are in reasonable agreement with the measured results. Far-field microphones placed at ground level were found superior to those at engine centerline height, even at high frequencies. (Author)

A79-26881 * # Full-scale engine tests of bulk absorber acoustic inlet treatment. L. J. Heidelberg and L. Homyak (NASA, Lewis Research Center, Cleveland, Ohio). *American Institute of Aeronautics and Astronautics, Aeroacoustics Conference, 5th, Seattle, Wash., Mar. 12-14, 1979, Paper 79-0600*. 10 p. 6 refs.

Three different densities of Kevlar bulk absorber fan inlet treatment were tested on a YF 102 turbofan engine. This bulk absorber material may have potential for flight application. Far-field noise measurements were made and the attenuation properties of the three treatment densities were compared. In addition the best bulk treatment was compared to the best single degree of freedom, SDOF (honeycomb and perforated cover sheet) treatment from another investigation. Although the density was varied over a large range, (3 to 1) the effect on attenuation was small. The highest density treatment, 11.8 lb/cu ft, had a somewhat broader attenuation bandwidth. The comparison of the best bulk and SDOF treatments showed the bulk to have a greater attenuation bandwidth. At the design frequency both types of treatment had almost equal performance. (Author)

A79-26926 * # Evaluation of two inflow control devices for flight simulation of fan noise using a JT15D engine. W. L. Jones, J. G. McArdle, and L. Homyak (NASA, Lewis Research Center, Cleveland, Ohio). *American Institute of Aeronautics and Astronautics, Aeroacoustics Conference, 5th, Seattle, Wash., Mar. 12-14, 1979, Paper 79-0654*. 11 p. 9 refs.

Two inflow control devices, (ICD's) one in-duct and the other external to the duct, were tested on a JT15D engine to determine their ability to remove inflow turbulence without altering the sound

transmission to the far field. The objective of the program was to develop means of accurately simulating flight fan noise on ground static test stands. The results generally indicated that both the in-duct and external ICD's were effective in reducing the inflow turbulence and the fan blade passing frequency tone generated by the turbulence. The external ICD was essentially transparent to the propagating fan tone but the in-duct ICD caused attenuation under most conditions. (Author)

A79-26944 * # Analysis of radiation patterns of interaction tones generated by inlet rods in the JT15D engine. M. F. Heidmann, A. V. Saule, and J. G. McArdle (NASA, Lewis Research Center, Cleveland, Ohio). *American Institute of Aeronautics and Astronautics, Aerodynamics Conference, 5th, Seattle, Wash., Mar. 12-14, 1979, Paper 79-0581*. 14 p. 10 refs.

A79-29383 * # Effect of broadened-specification fuels on aircraft engines and fuel systems. R. A. Rudey (NASA, Lewis Research Center, Cleveland, Ohio). In: *International Symposium on Air Breathing Engines, 4th, Orlando, Fla., April 1-6, 1979, Proceedings*. (A79-29376 11-07) New York, American Institute of Aeronautics and Astronautics, Inc., 1979, p. 53-69. 23 refs. (AIAA 79-7008)

A wide variety of studies on the potential effects of broadened-specification fuels on future aircraft engines and fuel systems are summarized. The compositions and characteristics of aircraft fuels that may be derived from current and future crude-oil sources are described, and the most critical properties that may affect aircraft engines and fuel systems are identified and discussed. The problems that are most likely to be encountered because of changes in selected fuel properties are described; and the related effects on engine performance, component durability and maintenance, and aircraft fuel-system performance are discussed. The ability of current technology to accept possible future fuel-specification changes is discussed, and selected technological advances that can reduce the severity of the potential problems are illustrated. (Author)

A79-29386 * # Characteristics of aeroelastic instabilities in turbomachinery - NASA full scale engine test results. J. F. Lubomski (NASA, Lewis Research Center, Cleveland, Ohio). In: *International Symposium on Air Breathing Engines, 4th, Orlando, Fla., April 1-6, 1979, Proceedings*. (A79-29376 11-07) New York, American Institute of Aeronautics and Astronautics, Inc., 1979, p. 91-102. 8 refs. (AIAA 79-7011)

Several aeromechanical programs have been conducted in the NASA/USAF Joint Engine System Research Programs. The scope of these programs, the instrumentation, data acquisition and reduction, and the test results are discussed. Data pertinent to four different instabilities were acquired; two types of stall flutter, choke flutter and a system mode instability. The data indicates that each instability has its own unique characteristics. These characteristics are described. (Author)

A79-30521 * # Effect of rotor tip clearance and configuration on overall performance of a 12.77-centimeter tip diameter axial-flow turbine. J. E. Haas (USAF, Aero Propulsion Laboratory, Wright-Patterson AFB, Ohio) and M. G. Kofskey (NASA, Lewis Research Center, Cleveland, Ohio). *American Society of Mechanical Engineers, Gas Turbine Conference and Exhibit and Solar Energy Conference, San Diego, Calif., Mar. 12-15, 1979, Paper 79-GT-42*. 9 p. 7 refs. Members, \$1.50; nonmembers, \$3.00.

An extensive experimental investigation was made to determine the effect of varying the rotor tip clearance of a 12.77-cm-tip diameter, single-stage, axial-flow reaction turbine. In this investigation, the rotor tip clearance was obtained by use of a recess in the casing above the rotor blades and also by use of a reduced blade height. For the recessed casing configuration, the optimum rotor blade height was found to be the one where the rotor tip diameter

was equal to the stator tip diameter. The tip clearance loss associated with this optimum recessed casing configuration was less than that for the reduced blade height configuration. (Author)

A79-30553 * # Thermal-structural mission analyses of air-cooled gas turbine blades. A. Kaufman and R. E. Gaugler (NASA, Lewis Research Center, Cleveland, Ohio). *American Society of Mechanical Engineers, Gas Turbine Conference and Exhibit and Solar Energy Conference, San Diego, Calif., Mar. 12-15, 1979, Paper 79-GT-19*. 11 p. 8 refs.

Cyclic temperature and stress-strain states in cooled turbine blades were calculated for a simulated mission of an advanced technology aircraft engine. TACTI (three dimensional heat transfer) and MARC (nonlinear structural analysis) computer programs were used to analyze impingement cooled airfoils, with and without leading-edge film cooling. Creep was the predominant damage mode, particularly around film cooling holes. Radially angled holes exhibited less creep than holes normal to surface. Beam-type analyses of all-impingement cooled airfoils gave fair agreement with MARC results for initial creep. (Author)

A79-30557 * # The Advanced Low-Emissions Catalytic-Combustor Program: Phase I - Description and status. A. J. Szanislo (NASA, Lewis Research Center, Cleveland, Ohio). *American Society of Mechanical Engineers, Gas Turbine Conference and Exhibit and Solar Energy Conference, San Diego, Calif., Mar. 12-15, 1979, Paper 79-GT-192*. 11 p. 22 refs.

The Advanced Low-Emissions Catalytic-Combustor Program is an ongoing three-phase contract effort with the primary objective of evolving the technology required for incorporating catalytic combustors into advanced aircraft gas-turbine engines. Phase I is currently in progress. At the present time, analytical evaluation is being conducted on advanced catalytic-combustor concepts, including variable geometry, with their known inherent potential advantages of low-level pollutant emissions, widened combustion stability limits, and reduced pattern factor for longer turbine life. Phases II and III will consist of experimental evaluation of the most promising concepts. (Author)

A79-30559 * # Effect of flight loads on turbofan engine performance deterioration. E. G. Stakolich (NASA, Lewis Research Center, Cleveland, Ohio), A. Jay, E. S. Todd (United Technologies Corp., Pratt and Whitney Aircraft, East Hartford, Conn.), P. G. Kafka and J. L. White (Boeing Commercial Airplane Co., Renton, Wash.). *American Society of Mechanical Engineers, Gas Turbine Conference and Exhibit and Solar Energy Conference, San Diego, Calif., Mar. 12-15, 1979, Paper*. 21 p.

A significant percentage of high-bypass-ratio turbofan engine performance deterioration is caused by an increase in operating clearance between fan/compressor and turbine blades and their outer air seals. These increased clearances result from rubs induced by a combination of engine power transients and aircraft flight loads. An analytical technique for predicting the effect of quasi-steady state aircraft flight loads on engine performance deterioration has been developed and is presented. Thrust, aerodynamic and inertia loads are considered. Analytical results are shown and compared to actual engine test experience. (Author)

A79-30560 * # The GATE studies - Assessing the potential of future small general aviation turbine engines. W. C. Strack (NASA, Lewis Research Center, Cleveland, Ohio). *American Society of Mechanical Engineers, Gas Turbine Conference and Exhibit and Solar Energy Conference, San Diego, Calif., Mar. 12-15, 1979, Paper*. 22 p.

Four studies have been completed that explore the opportunities for future General Aviation Turbine Engines (GATE) in the 150-1000 SHP class. These studies forecasted the potential impact of advanced technology turbine engines in the post-1988 market, identi-

fied important aircraft and missions, desirable engine sizes, engine performance and cost goals. Parametric evaluations of various engine cycles, configurations, design features, and advanced technology elements defined baseline conceptual engines for each of the important missions identified by the market analysis. Both fixed-wing and helicopter aircraft, and turboshaft, turboprop, and turbofan engines were considered. Key technology areas were recommended for NASA support in order to realize proposed improvements. (Author)

A79-32329 * # An off-design correlation of part span damper losses through transonic axial fan rotors. W. B. Roberts (Nielsen Engineering and Research, Inc., Mountain View, Calif.), J. E. Crouse, and D. M. Sandercock (NASA, Lewis Research Center, Cleveland, Ohio). *American Society of Mechanical Engineers, Gas Turbine Conference and Exhibit and Solar Energy Conference, San Diego, Calif., Mar. 12-15, 1979, Paper 79-GT-6*. 15 p. 21 refs. Members, \$1.50; nonmembers, \$3.00. Grant No. NSG-3133.

The experimental performance of 10 transonic fan rotors was used to correlate losses caused by midchord part-span dampers (PSD) during off-design operation between 50 and 100 percent of design speed. The design tip speed for the rotors used varied from 419 to 425 m/s and the design pressure ratios from 1.6 to 2.0. The loss attributable to the damper and the region influenced along the blade height was correlated with relevant aerodynamic and geometric parameters. The losses at the design point were estimated by a previously reported correlation (Roberts, 1978). Using this as a base, the off-design losses were correlated with variation in blade suction surface incidence. A check with independent data showed that the prediction of damper losses and region of influence was fair to good for most of the off-design data examined. (Author)

A79-36729 * Preliminary QCGAT program test results. R. W. Koenig and G. K. Sievers (NASA, Lewis Research Center, Cleveland, Ohio). *Society of Automotive Engineers, Business Aircraft Meeting and Exposition, Wichita, Kan., Apr. 3-6, 1979, Paper 790596*. 11 p.

The paper presents the NASA Lewis program to demonstrate that large engine technology can be applied to general aviation engines to reduce noise, emissions, and fuel consumption. After a Phase I study, two contractors, Garrett AiResearch and AVCO-Lycoming, were selected to design, manufacture, assemble, test, and deliver their Quiet, Clean, General Aviation Turbofan (QCGAT) engines to NASA. Noise, emissions, and performance goals and how well they were met are discussed. Noise goals involve take off noise 3.5 n. mi. from runway threshold, sideline noise at .25 n. mi. and approach noise 1 n. mi. from the runway at an altitude of 370 ft. The AiResearch engines power a stretched Learjet 35 and the Lycoming a specially conceived Beech executive jet, resulting in differing power goals. Thus the thrust goal for the Lycoming was 1622 lb. while the AiResearch goal was 3937 lb. Cruise thrust goals were 485 lb. at Mach 0.6 at 25,000 ft. and 903 lb. at Mach 0.8 at 40,000 ft. respectively. The design of both engines, based on existing cores, is studied, noting such special QCGAT features as new reduction gears, combustor and power turbine. Test results are given, indicating that while the goals for noise and thrust were met those for emissions were only partially met. M.E.P.

A79-36747 * New opportunities for future small civil turbine engines - Overviewing the GATE studies. W. C. Strack (NASA, Lewis Research Center, Cleveland, Ohio). *Society of Automotive Engineers, Business Aircraft Meeting and Exposition, Wichita, Kan., Apr. 3-6, 1979, Paper 790619*. 14 p.

This paper presents an overview of four independent studies that explore the opportunities for future General Aviation Turbine Engines (GATE) in the 150-1000 SHP class. Detroit Diesel Allison, Garrett/AiResearch, Teledyne CAE, and Williams Research participated along with several airframers. These studies forecasted the potential impact of advanced technology turbine engines in the post-1988 market, identified important aircraft and missions, de-

sirable engine sizes, engine performance and cost goals. Parametric evaluations of various engine cycles, configurations, design features, and advanced technology elements defined baseline conceptual engines for each of the important missions identified by the market analysis. Both fixed-wing and helicopter aircraft, and turboshaft, turboprop, and turbofan engines were considered. All four companies predicted sizable performance gains (e.g., 20% SFC decrease), and three predicted large engine cost reductions of sufficient magnitude to challenge the reciprocating engine in the 300-500 SHP class. Key technology areas were recommended for NASA support in order to realize these improvements. (Author)

A79-36759 * Wind tunnel performance of four energy efficient propellers designed for Mach 0.8 cruise. R. J. Jeracki, D. C. Mikkelsen, and B. J. Blaha (NASA, Lewis Research Center, Cleveland, Ohio). *Society of Automotive Engineers, Business Aircraft Meeting and Exposition, Wichita, Kan., Apr. 3-6, 1979, Paper 790573*. 22 p. 44 refs.

For the advanced turboprop to be competitive with proposed advanced turbofan-powered aircraft, it must have high propulsive efficiency at Mach 0.8 cruise above 9,144-km altitude with an acceptable cabin noise environment. Four 8-bladed propeller models are designed employing various concepts to reduce compressibility losses. Wind tunnel tests are conducted at zero model incidence to the free-stream flow. Aerodynamic and acoustic test results are presented and discussed. It is shown that the aeroacoustically designed configuration (SR-3) with 45 deg of tip sweep and an area-ruled spinner yields the highest propulsive efficiency (78.7% at Mach 0.8, 3.06 advance ratio, and 1.7 power coefficient), with an improvement of about 3% over the straight bladed configuration (SR-2, with zero-degree sweep). The phase-interference concept for noise reduction used in SR-3 yields about 5-6 dB reduction as compared to SR-2. S.D.

A79-36760 * Effects of air injection on a turbocharged Teledyne Continental Motors TSIO-360-C engine. D. V. Cosgrove and E. E. Kempke (NASA, Lewis Research Center, Cleveland, Ohio). *Society of Automotive Engineers, Business Aircraft Meeting and Exposition, Wichita, Kan., Apr. 3-6, 1979, Paper 790607*. 35 p. 7 refs.

Results are presented for tests performed to assess the effects of exhaust manifold injection air flow rate on emissions and on exhaust gas temperature and turbine inlet temperature for a range of engine operating conditions (speed, torque, and fuel-air ratios) of a fuel-injected turbocharged six-cylinder air-cooled Teledyne Continental Motors TSIO-360-C engine. Air injection into the exhaust gas at 80 F resulted in a decrease in hydrocarbons and carbon monoxide while exceeding the maximum recommended turbine inlet temperature of 1650 F at the full rich mixture of the engine. The EPA standards could be met within present turbine inlet temperature limits using commercially available air pumps, provided that the fuel-air ratios were leaned in the taxi, climb, and approach modes. S.D.

A79-38969 * # Effect of shocks on film cooling of a full scale turbojet exhaust nozzle having an external expansion surface. D. M. Straight (NASA, Lewis Research Center, Cleveland, Ohio). *AIAA, SAE, and ASME, Joint Propulsion Conference, 15th, Las Vegas, Nev., June 18-20, 1979, AIAA Paper 79-1170*. 13 p. 17 refs.

Cooling is one of the critical technologies for efficient design of exhaust nozzles, especially for the developing technology of non-axisymmetric (2D) nozzles for future aircraft applications. Several promising 2D nozzle designs have external expansion surfaces which need to be cooled. Engine data are scarce, however, on nozzle cooling effectiveness in the supersonic flow environment (with shocks) that exists along external expansion surfaces. This paper will present experimental film cooling data obtained during exploratory testing with an axisymmetric plug nozzle having external expansion and installed on an afterburning turbojet engine in an altitude test

facility. The data obtained shows that the shocks and local hot gas stream conditions have a marked effect on film cooling effectiveness. An existing film cooling correlation is adequate at some operating conditions but inadequate at other conditions such as in separated flow regions resulting from shock-boundary-layer interactions.

(Author)

A79-38981 * # Test verification of a turbofan partial swirl afterburner. K. J. Hanloser (United Technologies Corp., Pratt and Whitney Aircraft Group, West Palm Beach, Fla.) and R. Cullom (NASA, Lewis Research Center, Cleveland, Ohio). *AIAA, SAE, and ASME, Joint Propulsion Conference, 15th, Las Vegas, Nev., June 18-20, 1979, AIAA Paper 79-1199*. 6 p. 6 refs.

Flamespreading velocities exceeding conventional turbulent flamespreading values were demonstrated in a strong centrifugal flow field. This centrifugal flow field flamespreading concept was integrated into an F100 turbofan engine afterburner by introducing swirling airflow into the afterburner. Successful tests were conducted on F100 Engine P072 at sea level and at altitude conditions in a test chamber. This paper summarizes the design approach, engine design verification tests and performance data. Engine tests showed the swirl afterburner increased fuel-air capability improving combustion stability at adverse conditions for combustion in the engine flight envelope. No engine performance or durability degradation was observed.

(Author)

A79-38984 * # Application of digital controls on the quiet clean short haul experimental engines. A. A. Saunders, Jr. (General Electric Co., Aircraft Engine Group, Cincinnati, Ohio) and A. C. Hoffman (NASA, Lewis Research Center, Cleveland, Ohio). *AIAA, SAE, and ASME, Joint Propulsion Conference, 15th, Las Vegas, Nev., June 18-20, 1979, AIAA Paper 79-1203*. 8 p. 6 refs. Contract No. NAS3-18021.

The digital control systems for the Under-the-Wing (UTW) and Over-the-Wing (OTW) engines developed on the NASA/General Electric Quiet Clean Shorthaul Experimental Engine (QCSEE) program are described. The system to control engine variables includes three major functional parts: system sensors, digital control and system actuators. One of the primary control system functions is to prevent the engine from exceeding speed or temperature limits. The UTW control system also provides fault detection and condition monitoring. The control system requirements for the OTW engine are essentially the same as the UTW engine, however the inlet Mach number control requirement is eliminated, and failure indication and corrective action and full authority digital control are added. The digital controls scheduled the engine variables and maintained engine operation within all physical limits throughout the test program of approximately 200 hours of operation and provided stable and accurate control of both engines.

V.T.

A79-39031 * # Combined pressure and temperature distortion effects on internal flow of a turbofan engine. W. M. Braithwaite and R. H. Soeder (NASA, Lewis Research Center, Cleveland, Ohio). *AIAA, SAE, and ASME, Joint Propulsion Conference, 15th, Las Vegas, Nev., June 18-20, 1979, AIAA Paper 79-1309*. 11 p. 13 refs.

The flow characteristics obtained experimentally for the compression of a 2 spool TF30-P-3 turbofan engine operating with 180 grad combined pressure and temperature distortion in the inlet flow are presented. The analytical model (Mazzawy and Banks, 1976), 'tuned' during Lewis testing, was used for pretest predictions of the effects that these distortions would have on the engine flow characteristics and the limiting distortion values. The effect of inlet flow distortion on the performance of the engine is discussed, including: (1) the flow between a screen mounted in the inlet duct and the inlet guide vanes; (2) the flow through the compression system; and (3) the effects of the combined distortion and its orientation on the compressor stability limits. It is concluded that the model used in this program was capable of predicting the effects of total pressure, total temperature and combined total pressure-total

temperature distortions in terms of flow profiles, inlet flow angles and attenuation of the distortions through the compressor system. It was also capable of predicting the trends of the limiting values experienced with various orientations of the combined distortions.

V.T.

A79-39034 * # Lean, premixed, prevaporized combustion for aircraft gas turbine engines. E. J. Mularz (NASA, Lewis Research Center; U.S. Army, Propulsion Laboratory, Cleveland, Ohio). *AIAA, SAE, and ASME, Joint Propulsion Conference, 15th, Las Vegas, Nev., June 18-20, 1979, AIAA Paper 79-1318*. 13 p. 24 refs.

The application of lean, premixed, prevaporized combustion to aircraft gas turbine engine systems can result in benefits in terms of superior combustion performance, improved combustor and turbine durability, and environmentally acceptable pollutant emissions. Lean, premixed, prevaporized combustion is particularly attractive for reducing the oxides of nitrogen emissions during high altitude cruise. The NASA Stratospheric Cruise Emission Reduction Program will evolve and demonstrate lean, premixed, prevaporized combustion technology for aircraft engines. This multiphased program is described. In addition, the various elements of the Fundamental Studies Phase of the program are reviewed, and results to date of many of these studies are summarized.

(Author)

A79-39804 * # Materials and structural aspects of advanced gas-turbine helicopter engines. J. C. Freche (NASA, Lewis Research Center, Cleveland, Ohio) and J. Acurio (U.S. Army, Propulsion Laboratory, Cleveland, Ohio). *Association Aéronautique et Astronautique de France, International Congress in Aeronautics, Paris, France, June 6-8, 1979, Paper*. 63 p. 122 refs.

Advances in materials, coatings, turbine cooling technology, structural and design concepts, and component-life prediction of helicopter gas-turbine-engine components are presented. Stationary parts including the inlet particle separator, the front frame, rotor tip seals, vanes and combustors and rotating components - compressor blades, disks, and turbine blades - are discussed. Advanced composite materials are considered for the front frame and compressor blades, prealloyed powder superalloys will increase strength and reduce costs of disks, the oxide dispersion strengthened alloys will have 100C higher use temperature in combustors and vanes than conventional superalloys, ceramics will provide the highest use temperature of 1400C for stator vanes and 1370C for turbine blades, and directionally solidified eutectics will afford up to 50C temperature advantage at turbine blade operating conditions. Coatings for surface protection at higher surface temperatures and design trends in turbine cooling technology are discussed. New analytical methods of life prediction such as strain gage partitioning for high temperature prediction, fatigue life, computerized prediction of oxidation resistance, and advanced techniques for estimating coating life are described.

A.T.

A79-39814 * # Multivariable control altitude demonstration on the F100 turbofan engine. B. Lehtinen (NASA, Lewis Research Center, Cleveland, Ohio), R. L. DeHoff (Systems Control, Inc., Palo Alto, Calif.), and R. D. Hackney (United Technologies Corp., Pratt and Whitney Aircraft Group, West Palm Beach, Fla.). *AIAA, SAE, and ASME, Joint Propulsion Conference, 15th, Las Vegas, Nev., June 18-20, 1979, AIAA Paper 79-1204*. 2S p. 16 refs.

The control system designed under the Multivariable Control Synthesis (MVCS) program for the F100 turbofan engine is described. The MVCS program, applied the linear quadratic regulator (LQR) synthesis methods in the design of a multivariable engine control system to obtain enhanced performance from cross coupled controls, maximum use of engine variable geometry, and a systematic design procedure that can be applied efficiently to new engine systems. Basic components of the control system, a reference value generator for deriving a desired equilibrium state and an approximate control vector, a transition model to produce compatible reference point trajectories during gross transients, gain schedules for producing feedback terms appropriate to the flight condition, and integral

switching logic to produce acceptable steady-state performance without engine operating limit exceedance are described and the details of the F100 implementation presented. The engine altitude test phase of the MVCS program, and engine responses in a variety of test operating points and power transitions are presented. A.T.

A79-40488 * # A summary of NASA/Air Force Full Scale Engine Research programs using the F100 engine. W. J. Deskin (United Technologies Corp., Government Products Div., West Palm Beach, Fla.) and H. G. Hurrell (NASA, Lewis Research Center, Cleveland, Ohio). *AIAA, SAF, and ASME, Joint Propulsion Conference, 15th, Las Vegas, Nev., June 18-20, 1979, AIAA Paper 79-1306*. 14 p. 20 refs.

This paper summarizes a joint NASA/Air Force Full Scale Engine Research (FSER) program conducted with the F100 engine during the period 1974 through 1979. The program mechanism is described and the F100 test vehicles utilized are illustrated. Technology items which have been addressed in the areas of swirl augmentation, flutter phenomenon, advanced electronic control logic theory, strain gage technology, and distortion sensitivity are identified and the associated test programs conducted at the NASA-Lewis Research Center are described. Results presented show that the FSER approach, which utilizes existing state-of-the-art engine hardware to evaluate advanced technology concepts and problem areas, can contribute a significant data base for future system applications. Aerodynamic phenomenon previously not considered by current design systems have been identified and incorporated into current industry design tools. (Author)

A79-47918 * # Energy efficient aircraft engines. R. Chamberlin and B. Miller (NASA, Lewis Research Center, Energy Conservative Engines Office, Cleveland, Ohio). *American Institute of Aeronautics and Astronautics, Aircraft Systems and Technology Meeting, New York, N.Y., Aug. 20-22, 1979, Paper 79-1861*. 11 p.

The three engine programs that constitute the propulsion portion of NASA's Aircraft Energy Efficiency Program are described, their status indicated, and anticipated improvements in SFC discussed. The three engine programs are: (1) engine component improvement, directed at current engines, (2) energy efficient engine, directed at new turbofan engines, and (3) advanced turboprops, directed at technology for advanced turboprop-powered aircraft with cruise speeds to Mach 0.8. Unique propulsion system interactive ties to the airframe resulting from engine design features to reduce fuel consumption are discussed. Emphasis is placed on the advanced turboprop since it offers the largest potential fuel savings of the three propulsion programs and also has the strongest interactive ties to the airframe. (Author)

A79-50208 * QCSEE - The key to future short-haul air transport. C. C. Ciepluch (NASA, Lewis Research Center, Quiet, Clean, Short-Haul Experimental Engine Project Office, Cleveland, Ohio) and W. S. Willis (General Electric Co., Aircraft Engine Group, West Lynn, Mass.). *ICAO Bulletin*, vol. 34, Apr. 1979, p. 24-29.

The paper describes the design and test procedure for the QCSEE (quiet, clean, short-haul experimental engine). The engines designed for the YC-14 and YC-15 STOL aircraft, both use a very low fan pressure ratio to keep jet-flap noise about 3 dB below total system noise. Other noise reducing features discussed are the low tip speed fans and a carefully selected number of fan blades and vanes with adequate spacing between them. Attention is also given to the development of a low emissions combustor, and reduction of fan frame weight, through the use of graphite/epoxy material. The YC-15 engine also employs variable pitch fans to provide thrust reversal, thus saving weight. Finally, it is noted that the tests have proven that the engines could be configured to meet the needs of a powered lift system without excessively compromising performance or weight. M.E.P.

A79-50333 * Airborne atmospheric sampling system. U. R. C. Gustafsson (United Airlines, Inc., San Francisco, Calif.), P. J. Perkins, T. W. Nyland, M. W. Tiefermann, and T. J. Dudzinski (NASA, Lewis Research Center, Cleveland, Ohio). In: *Learning to use our environment; Proceedings of the Twenty-fifth Annual Technical Meeting, Seattle, Wash., April 30-May 2, 1979, (A79-50326 22-42)* Mount Prospect, Ill., Institute of Environmental Sciences, p. 48-57.

The atmospheric sampling system developed for use on board commercial airliners as part of the Global Atmospheric Sampling Program (GASP) is described. The automated air-constituent measuring system is installed in a Boeing 747 airliner below the passenger cabin floor near the nose wheel well. It consists of an air sample flow system, composed of air inlet and pressurization systems, computerized data acquisition and system control units which direct system operation in 15 modes, and commercial instruments significantly modified to measure low levels of atmospheric constituents (ozone, water vapor, nitrogen oxides, carbon monoxide, chlorofluoromethanes, particulates, condensation nuclei, sulfates and nitrates). Flight and meteorological data, including air temperature and altitude, are also recorded. The system is designed for servicing at 14-day intervals, and to require a minimum of aircrew involvement. A.L.W.

N79-10058 * # Pratt and Whitney Aircraft Group, West Palm Beach, Fla. Government Products Div. **EVALUATION OF THE CYCLIC BEHAVIOR OF AIRCRAFT TURBINE DISK ALLOYS** Final Report B. A. Cowles, D. L. Sims, and J. R. Warren Oct. 1978 152 p. refs. (Contract NAS3-20367) (NASA-CR-159409; PWA-FR-10299) Avail. NTIS HC A08/MF A01 CSCL 21E

Five aircraft turbine disk alloys representing various strength and processing histories were evaluated at 650 C to determine if recent strength advances in powder metallurgy have resulted in corresponding increases in low cycle fatigue (LCF) capability. Controlled strain LCF tests and controlled load crack propagation tests were performed. Results were used for direct material comparisons and in the analysis of an advanced aircraft turbine disk, having a fixed design and operating cycle. Crack initiation lives were found to increase with increasing tensile yield strength, while resistance to fatigue crack propagation generally decreased with increasing strength. Author

N79-10061 * # Mechanical Technology, Inc., Latham, N. Y. **STUDY OF T53 ENGINE VIBRATION** Final Report Thomas J. Walter Nov. 1978 60 p. refs. (Contract NAS3-20609) (NASA-CR-135449; MTI-78TR66) Avail. NTIS HC A04/MF A01 CSCL 21E

Vibration characteristics for overhauled T53 engines, including rejection rate, principal sources of vibration, and normal procedures taken by the overhaul center to reduce engine vibration are summarized. Analytical and experimental data were compared to determine the engine's dynamic response to unbalance forces with results showing that the engine operates through bending critical speeds. Present rigid rotor balancing techniques are incapable of compensating for the flexible rotor unbalance. A comparison of typical test cell and aircraft vibration levels disclosed significant differences in the engine's dynamic response. A probable spline shift phenomenon was uncovered and investigated. Action items to control costs and reduce vibration levels were identified from analytical and experimental studies. B.B.

N79-11042* General Electric Co., Cincinnati, Ohio Aircraft Engine Group

DEFINITION STUDY OF A VARIABLE CYCLE EXPERIMENTAL ENGINE (VCEE) AND ASSOCIATED TEST PROGRAM AND TEST PLAN Final Report, Sep. 1977 - Mar. 1978

R D Allan Oct 1978 198 p

(Contract NAS3-20810)

(NASA-CR-159419, R78AEG568)

Avail

NTIS

HC A09/MF A01 CSCL 21E

The Definition Study of a Variable Cycle Experimental Engine (VCEE) and Associated Test Program and Test Plan, was initiated to identify the most cost effective program for a follow-on to the AST Test Bed Program. The VCEE Study defined various subscale VCEE's based on different available core engine components, and a full scale VCEE utilizing current technology. The cycles were selected, preliminary design accomplished and program plans and engineering costs developed for several program options. In addition to the VCEE program plans and options, a limited effort was applied to identifying programs that could logically be accomplished on the AST Test Bed Program VCEE to extend the usefulness of this test hardware. Component programs were provided that could be accomplished prior to the start of a VCEE program. Author

N79-11068* Detroit Diesel Allison, Indianapolis, Ind Flow Systems Group

DETERMINING AND IMPROVING LABYRINTH SEAL PERFORMANCE IN CURRENT AND ADVANCED HIGH PERFORMANCE GAS TURBINES

Harold L Stocker In AGARD Seal Technol in Gas Turbine Eng Aug 1978 22 p refs (For primary document see N79-11056 02-07)

(Contracts NAS3-20056, N00140-73-C-005,

N00140-74-C-0759)

Avail NTIS HC A13/MF A01 CSCL 21E

Abradable and honeycomb lands were evaluated with a conventional straight-through seal using a static two dimensional (rectangular flowpath) seal rig and a rotating three dimensional seal rig. Test results show that some abrasible lands leak significantly more than a solid-smooth land. However honeycomb lands were found to reduce leakage up to 24 percent. Through aerodynamic testing, an advanced design labyrinth seal was developed which reduced leakage 54.2 percent compared to a conventional straight-through seal and 26.3 percent compared to a conventional stepped seal. A R H

N79-12088* General Electric Co., Cincinnati, Ohio

EXPERIMENTAL CLEAN COMBUSTOR PROGRAM: PHASE 3: TURBULENCE MEASUREMENT ADDENDUM Final Report

J R Taylor Nov 1978 40 p refs

(Contract NAS3-19736)

(NASA-CR-135422, R78AEG529)

Avail

NTIS

HC A03/MF A01 CSCL 21E

Airflow turbulence parameters were measured in the high pressure, high temperature flow stream leaving the compressor of an operating gas turbine engine. A water cooled hot film turbulence probe was used to determine the turbulence intensity and length scale in the compressor exit flow stream of the CF6-50 engine. Data were obtained only at idle operating conditions. At engine power levels above idle conditions, durability problems and erratic data readings were encountered with the turbulence measurement probes. Turbulence measurements were made at three radial immersions at a point 15.5 cm downstream of the compressor outlet guide vanes in the compressor exit diffuser. The passage height at this point is 5.54 cm. Data reduction was accomplished with a time-data fast Fourier transform (FFT) system. This system finds the power spectral density distribution (PSD) of a large number of data samples using a direct Fourier transform algorithm and finds the autocorrelation parameter for these data by doing an FFT analysis of the PSD curves for a series of time delay intervals. Author

N79-13048* General Electric Co., Cincinnati, Ohio Aircraft Engine Group

DEFINITION STUDY FOR VARIABLE CYCLE ENGINE TESTBED ENGINE AND ASSOCIATED TEST PROGRAM Final Report

John W. Vdovick Nov. 1978 112 p

(Contract NAS3-20582A)

(NASA-CR-159459, R78AEG551)

Avail:

NTIS

HC A06/MF A01 CSCL 21E

The product/study double bypass variable cycle engine (VCE) was updated to incorporate recent improvements. The effect of these improvements on mission range and noise levels was determined. This engine design was then compared with current existing high-technology core engines in order to define a subscale testbed configuration that simulated many of the critical technology features of the product/study VCE. Detailed preliminary program plans were then developed for the design, fabrication, and static test of the selected testbed engine configuration. These plans included estimated costs and schedules for the detail design, fabrication and test of the testbed engine and the definition of a test program, test plan, schedule, instrumentation, and test stand requirements. Author

N79-13060* Pratt and Whitney Aircraft Group, East Hartford, Conn. Commercial Products Div.

ANALYTICAL EVALUATION OF THE IMPACT OF BROAD SPECIFICATION FUELS ON HIGH BYPASS TURBOFAN ENGINE COMBUSTORS Final Report

R. P. Lohmann, E. J. Szelata, and A. Vranos Dec. 1978 161 p refs

(Contract NAS3-20802)

(NASA-CR-159454, PWA-5565-15)

Avail:

NTIS

HC A08/MF A01 CSCL 21E

The impact of the use of broad specification fuels on the design, performance, durability, emissions and operational characteristics of combustors for commercial aircraft gas turbine engines was assessed. Single stage, vortex and lean premixed prevaporized combustors, in the JT9D and an advanced energy efficient engine cycle were evaluated when operating on Jet A and ERBS (Experimental Referee Broad Specification) fuels. Design modifications, based on criteria evolved from a literature survey, were introduced and their effectiveness at offsetting projected deficiencies resulting from the use of ERBS was estimated. The results indicate that the use of a broad specification fuel such as ERBS, will necessitate significant technology improvements and redesign if deteriorated performance, durability and emissions are to be avoided. Higher radiant heat loads are projected to seriously compromise liner life while the reduced thermal stability of ERBS will require revisions to the engine-airframe fuel system to reduce the thermal stress on the fuel. Smoke and emissions output are projected to increase with the use of broad specification fuels. While the basic geometry of the single stage and vortex combustors are compatible with the use of ERBS, extensive redesign of the front end of the lean premixed prevaporized burner will be required to achieve satisfactory operation and optimum emissions. G.G.

N79 15053* General Electric Co., Evendale, Ohio Aircraft Engine Business Group

ANALYSIS AND PRELIMINARY DESIGN OF AN OPTICAL DIGITAL TIP CLEARANCE SENSOR FOR PROPULSION CONTROL

G L Poppel Sep 1978 28 p

(Contract NAS3-21006)

(NASA-CR-159434, R78AEG518)

Avail:

NTIS

HC A03/MF A01 CSCL 21E

Following the generation of several concepts for passive, digital compatible, optical sensors for propulsion control systems, a tip clearance sensor was chosen for further analysis and preliminary design. Emphasis was placed on application to the TF34 engine compressor section. Laboratory experiments were performed to investigate several optical aspects of the concept. Preliminary design included an assessment of all sensor elements and recommendations for development programs. Quantitative predictions were made of sensor performance. A test plan was written to demonstrate sensor feasibility and that the perform-

ance goals can be met. A continuing experimental and design effort was suggested. Author

N79-16850* Pratt and Whitney Aircraft, East Hartford, Conn. **ENERGY EFFICIENT ENGINE: PROPULSION SYSTEM-AIRCRAFT INTEGRATION EVALUATION** Topical Report, Mar. 1978 - Sep. 1978

R. E. Owens Mar. 1979 311 p refs
(Contract NAS3-20646)
(NASA-CR-159488; PWA-5594-48) Avail: NTIS
HC A14/MF A01 CSCL 21E

Flight performance and operating economics of future commercial transports utilizing the energy efficient engine were assessed as well as the probability of meeting NASA's goals for TSFC, DOC, noise, and emissions. Results of the initial propulsion systems aircraft integration evaluation presented include estimates of engine performance, predictions of fuel burns, operating costs of the flight propulsion system installed in seven selected advanced study commercial transports, estimates of noise and emissions, considerations of thrust growth, and the achievement-probability analysis. A R H.

N79-16853* United Technologies Research Center, East Hartford, Conn.

STUDY OF MEAN- AND TURBULENT-VELOCITY FIELDS IN A LARGE-SCALE TURBINE-VANE PASSAGE Final Report

Douglas A. Bailey Feb. 1979 123 p refs
(Contract NAS3-19752)
(NASA-CR-3067) Avail: NTIS HC A02/MF A01 CSCL 21E

Laser-Doppler velocimetry, and to a lesser extent hot-wire anemometry, were employed to measure three components of the mean velocity and the six turbulent stresses at four planes within the turbine inlet-guide-vane passage. One variation in the turbulent inlet boundary layer thickness and one variation in the blade aspect ratio (span/axial chord) were studied. A longitudinal vortex (passage vortex) was clearly identified in the exit plane of the passage for the three test cases. The maximum turbulence intensities within the longitudinal vortex were found to be on the order of 2 to 4 percent, with large regions appearing nonturbulent. Because a turbulent wall boundary layer was the source of vorticity that produced the passage vortex, these low turbulence levels were not anticipated. For the three test cases studied, the lateral velocity field extended significantly beyond the region of the longitudinal velocity defect. Changing the inlet boundary layer thickness produced a difference in the location, the strength, and the extent of the passage vortex. Changing the aspect ratio of the blade passage had a measurable but less significant effect. The experiment was performed in a 210 mm pitch, 272 mm axial chord model in low speed wind tunnel at an inlet Mach number of 0.07. A R H.

N79-17857* Pratt and Whitney Aircraft Group, West Palm Beach, Fla. Government Products Div.

DESIGN, FABRICATION AND SPIN TESTING OF CERAMIC BLADE METAL DISK ATTACHMENT Final Report

Glenn Calvert Feb. 1979 152 p
(Contract NAS3-19715)
(NASA-CR-159532; FR-10179) Avail: NTIS
HC A08/MF A01 CSCL 21E

A ceramic turbine blade metal disk attachment was designed for small, non-man-rated turbine engine applications. The selected design consisted of a hot pressed silicon nitride blade having a skewed dovetail attachment with a compliant interlayer between the disk and the blade. Two-dimensional and three-dimensional analyses predicted that life goals could be achieved, considering both NDE limitations and crack growth rates for the ceramic material. Twenty ceramic blades were fabricated to closely held manufacturing tolerances. New fracture mechanics data at elevated temperature are presented. S E S

N79-17858* Hamilton Standard, Windsor Locks, Conn. **INTERACTIVE MULTI MODE BLADE IMPACT ANALYSIS** Final Report, Jan. 1976 - Aug. 1977 and Feb. 1978 - Aug. 1978

A. Alexander and R. W. Cornell Aug. 1978 301 p refs
(Contract NAS3-20091)
(NASA-CR-159462) Avail: NTIS HC A16/MF A01 CSCL 21E

The theoretical methodology used in developing an analysis for the response of turbine engine fan blades subjected to soft-body (bird) impacts is reported, and the computer program developed using this methodology as its basis is described. This computer program is an outgrowth of two programs that were previously developed for the purpose of studying problems of a similar nature (a 3-mode beam impact analysis and a multi-mode beam impact analysis). The present program utilizes an improved missile model that is interactively coupled with blade motion which is more consistent with actual observations; it takes into account local deformation at the impact area, blade camber effects, and the spreading of the impacted missile mass on the blade surface. In addition, it accommodates plate-type mode shapes. The analysis capability in this computer program represents a significant improvement in the development of the methodology for evaluating potential fan blade materials and designs with regard to foreign object impact resistance. S E S

N79-18976* Shaker Research Corp., Ballston Lake, N. Y. **TURBOJET BLADE VIBRATION DATA ACQUISITION DESIGN AND FEASIBILITY TESTING** Final Report

J. L. Frarey, N. J. Petersen (Amherst Systems), and D. A. Hess Nov. 1978 72 p
(Contract NAS3-21715)
(NASA-CR-159505; SRC-78-TR-36) Avail: NTIS
HC A04/MF A01 CSCL 21E

A turbojet blade vibration data acquisition system was designed to allow the measurement of blade vibration. The data acquisition system utilizing 96 microprocessors to gather data from optical probes, store, sort and transmit to the central computer is described. Areas of high technical risk were identified and a two-microprocessor system was breadboarded and tested to investigate these areas. Results show that the system was feasible and that low technical risk would be involved in proceeding with the complete system fabrication. S E S

N79-18977* Naval Air Propulsion Test Center, Trenton, N. J. **ROTOR FRAGMENT PROTECTION PROGRAM: STATISTICS ON AIRCRAFT GAS TURBINE ENGINE ROTOR FAILURES THAT OCCURRED IN U.S. COMMERCIAL AVIATION DURING 1976** Final Report, 1976 - 1976

R. A. DeLucia and J. T. Salvino Jul. 1978 30 p
(NASA Order C-41581-B)
(NASA-CR-159474; NACP-PE-9) Avail: NTIS
HC A03/MF A01 CSCL 21E

Statistical information relating to the number of gas turbine engine rotor failures which occurred during 1976 in commercial aviation service use is presented. The predominant failure involved blade fragments, 88 percent of which were contained. Although fewer rotor rim, disk, and seal failures occurred, all were uncontained. Sixty-seven percent of the 186 rotor failures occurred during the takeoff and climb stages of flight. S E S

N79-18978* General Electric Co., Philadelphia, Pa. **CONTAINMENT OF COMPOSITE FAN BLADES** Quarterly Progress Report, 1 Apr. - 30 Jun. 1977

A. P. Coppe and C. L. Stotler 1977 15 p
(Contract NAS3-20118)
(NASA-CR-158168; QPR-4; R77AEG450) Avail: NTIS
HC A02/MF A01 CSCL 21E

The development of containment concepts for use with large composite fan blades, taking into account the fragile nature of composite blades is considered. Aspects of the development program include: (1) an analysis to predict the interaction between a failed fan blade and the blade containment structure; (2) scaling factors to allow impact testing using subscale containment rings

and simulated blades; (3) the design and fabrication of containment systems for further evaluation in a rotating rig test facility; (4) evaluate the test data against the analytically predicted results; and (5) determine overall systems weights and design characteristics of a composite fan stage installation and compare to the requirements of an equivalent titanium fan blade system. Progress in the blade impact penetration tests and the design and fabrication of blade containment systems is reported. J.M.S.

N79-20116* Pratt and Whitney Aircraft Group, East Hartford, Conn. Commercial Products Div.

JT8D AND JT9D JET ENGINE PERFORMANCE IMPROVEMENT PROGRAM. TASK 1: FEASIBILITY ANALYSIS Final Report, Feb. - Dec. 1977

W. O. Gaffin and D. E. Webb Apr. 1979 227 p refs (Contract NAS3-20630)

(NASA-CR-159449; PWA-5518-38) Avail: NTIS HC A11/MF A01 CSCL 21E

JT8D and JT9D component performance improvement concepts which have a high probability of incorporation into production engines were identified and ranked. An evaluation method based on airline payback period was developed for the purpose of identifying the most promising concepts. The method used available test data and analytical models along with conceptual/preliminary designs to predict the performance improvements, weight, installation characteristics, cost for new production and retrofit, maintenance cost, and qualitative characteristics of candidate concepts. These results were used to arrive at the concept payback period, which is the time required for an airline to recover the investment cost of concept implementation. G.Y.

N79-20117* General Electric Co., Evendale, Ohio. Aircraft Engine Group.

THEORY OF LOW FREQUENCY NOISE TRANSMISSION THROUGH TURBINES Final Report

R. K. Matta and R. Mani Mar. 1979 153 p refs (Contract NAS3-20027)

(NASA-CR-159457; R77AEG570) Avail: NTIS HC A08/MF A01 CSCL 21E

Improvements of the existing theory of low frequency noise transmission through turbines and development of a working prediction tool are described. The existing actuator-disk model and a new finite-chord model were utilized in an analytical study. The interactive effect of adjacent blade rows, higher order spinning modes, blade-passage shocks, and duct area variations were considered separately. The improved theory was validated using the data acquired in an earlier NASA program. Computer programs incorporating the improved theory were produced for transmission loss prediction purposes. The programs were exercised parametrically and charts constructed to define approximately the low frequency noise transfer through turbines. The loss through the exhaust nozzle and flow(s) was also considered. Author

N79-21073* Detroit Diesel Allison, Indianapolis, Ind. **STUDY OF AN ADVANCED GENERAL AVIATION TURBINE ENGINE (GATE) Final Report**

J. C. Gill, F. R. Short, D. V. Staton, B. A. Zolezzi, C. E. Curry, M. J. Orsini, J. M. Vaught, and J. M. Humphrey 10 Apr. 1979 147 p refs (Contract NAS3-20756)

(NASA-CR-159558; DDA-EDR-9528) Avail: NTIS HC A07/MF A01 CSCL 21E

The best technology program for a small, economically viable gas turbine engine applicable to the general aviation helicopter and aircraft market for 1985-1990 was studied. Turbo-shaft and turboprop engines in the 112 to 746 kW (150 to 1000 hp) range and turboprop engines up to 6672 N (1500 lbf) thrust were considered. A good market for new turbine engines was predicted for 1988 providing aircraft are designed to capitalize on the advantages of the turbine engine. Parametric engine families were defined in terms of design and off-design performance, mass, and cost. These were evaluated in aircraft design

missions selected to represent important market segments for fixed and rotary-wing applications. Payoff parameters influenced by engine cycle and configuration changes were aircraft gross mass, acquisition cost, total cost of ownership, and cash flow. Significant advantage over a current technology, small gas turbine engines was found especially in cost of ownership and fuel economy for airframes incorporating an air-cooled high-pressure ratio engine. A power class of 373 kW (500 hp) was recommended as the next frontier for technology advance where large improvements in fuel economy and engine mass appear possible through component research and development. S.E.S.

N79-21074* General Electric Co., Cincinnati, Ohio. Aircraft Engine Group.

CF6 JET ENGINE PERFORMANCE IMPROVEMENT PROGRAM. TASK 1: FEASIBILITY ANALYSIS Final Report

W. A. Fasching Mar. 1979 370 p refs (Contract NAS3-20629)

(NASA-CR-159450; R79AEG295) Avail: NTIS HC A13/MF A01 CSCL 21E

Technical and economic engine improvement concepts selected for subsequent development include: (1) fan improvement; (2) short core exhaust; (3) HP turbine aerodynamic improvement; (4) HP turbine roundness control; (5) HP turbine active clearance control; and (6) cabin air recirculation. The fuel savings for the selected engine modification concepts for the CF6 fleet are estimated. S.E.S.

N79-21075* Ford Motor Co., Dearborn, Mich. Research Staff.

EVALUATION OF CERAMICS FOR STATOR APPLICATION: GAS TURBINE ENGINE REPORT Progress Report, 1 Feb. 1978 - 31 Jul. 1978

W. Trela and P. H. Havstad Nov. 1978 36 p refs Prepared for DOE

(Contract DEN-3-00019)

(NASA-CR-159533; DOE/NASA/0019-78/1) Avail: NTIS HC A03/MF A01 CSCL 21E

Current ceramic materials, component fabrication processes, and reliability prediction capability for ceramic stators in an automotive gas turbine engine environment are assessed. Simulated engine duty cycle testing of stators conducted at temperatures up to 1093 C is discussed. Materials evaluated are SiC and Si3N4 fabricated from two near-net-shape processes: slip casting and injection molding. Stators for durability cycle evaluation and test specimens for material property characterization, and reliability prediction model prepared to predict stator performance in the simulated engine environment are considered. The status and description of the work performed for the reliability prediction modeling, stator fabrication, material property characterization, and ceramic stator evaluation efforts are reported. J.M.S.

N79-21076* Pratt and Whitney Aircraft Group, East Hartford, Conn.

JT8D REVISED HIGH-PRESSURE TURBINE COOLING AND OTHER OUTER AIR SEAL PROGRAM

W. O. Gaffin 20 Mar. 1979 59 p refs

(Contract NAS3-20630)

(NASA-CR-159551; PWA-5515-77) Avail: NTIS HC A04/MF A01 CSCL 21E

The JT8D high pressure turbine was revised to reduce leakage between the blade tip shrouds and the outer air seal, and engine testing was performed to determine the effect on performance. The addition of a second knife-edge on the blade tip shroud, the extension of the honeycomb seal land to cover the added knife-edge and an existing spoiler on the shroud, and a material substitution in the seal support ring to improve thermal growth characteristics are included. A relocation of the blade cooling air discharge to insure adequate cooling flow is required. Significant specific fuel consumption and exhaust gas temperature improvements were demonstrated with the revised turbine in sea level and simulated altitude engine tests. Inspection of the revised seal hardware after these tests showed no unusual wear or degradation. S.E.S.

N79-23084* Pratt and Whitney Aircraft Group, East Hartford, Conn. Commercial Products Div.

VARIABLE CYCLE ENGINE TECHNOLOGY PROGRAM PLANNING AND DEFINITION STUDY Final Report

J. S. Westmoreland and A. M. Stern Sep. 1978 89 p

(Contract NAS3-20811)

(NASA-CR-159539, PWA-5581-12)

Avail: NTIS

HC A05/MF A01 CSCL 21E

The variable stream control engine, VSCE-502B, was selected as the base engine, with the inverted flow engine concept selected as a backup. Critical component technologies were identified, and technology programs were formulated. Several engine configurations were defined on a preliminary basis to serve as demonstration vehicles for the various technologies. The different configurations present compromises in cost, technical risk, and technology return. Plans for possible variable cycle engine technology programs were formulated by synthesizing the technology requirements with the different demonstrator configurations. J.M.S.

N79-23085* Pratt and Whitney Aircraft Group, East Hartford, Conn.

STUDY OF BLADE ASPECT RATIO ON A COMPRESSOR FRONT STAGE AERODYNAMIC AND MECHANICAL DESIGN REPORT

G. D. Burger, G. Leo, and D. W. Snow Mar. 1979 84 p refs (Contract NAS3-20809)

(NASA-CR-159555, PWA-5583-25)

Avail: NTIS

HC A05/MF A01 CSCL 21E

A single stage compressor was designed with the intent of demonstrating that, for a tip speed and hub-tip ratio typical of an advanced core compressor front stage, the use of low aspect ratio can permit high levels of blade loading to be achieved at an acceptable level of efficiency. The design pressure ratio is 1.8 at an adiabatic efficiency of 88.5 percent. Both rotor and stator have multiple-circular-arc airfoil sections. Variable IGV and stator vanes permit low speed matching adjustments. The design incorporates an inlet duct representative of an engine transition duct between fan and high pressure compressor. S.E.S.

N79-23970* General Electric Co., Cincinnati, Ohio. Aircraft Engine Group.

FABRICATION OF J79 BORON/ALUMINUM COMPRESSOR BLADES Final Report, Apr. 1975 - Jun. 1978

J. W. Brantley and R. G. Stabrylla May 1979 74 p refs

(Contract NAS3-18943)

(NASA-CR-159566, R79AEG388)

Avail: NTIS

HC A04/MF A01 CSCL 21E

A total of 81 boron/aluminum first stage compressor blades were developed. The processing of the blades and the series designs established for various types of blade tests are described. S.E.S.

N79-25017* Williams Research Corp., Walled Lake, Mich.
ADVANCED GENERAL AVIATION TURBINE ENGINE (GATE) CONCEPTS Final Report

E. J. Lays and G. L. Murray 26 Jun 1979 182 p refs

(Contract NAS3-20758)

(NASA-CR-159603, WRC-78-113-15)

Avail: NTIS

HC A09/MF A01 CSCL 21E

Concepts are discussed that project turbine engine cost savings through use of geometrically constrained components designed for low rotational speeds and low stress to permit manufacturing economies. Aerodynamic development of geometrically constrained components is recommended to maximize component efficiency. Conceptual engines, airplane applications, airplane performance, engine cost, and engine related life cycle costs are presented. The powerplants proposed offer encouragement with respect to fuel efficiency and life cycle costs, and make possible remarkable airplane performance gains. M.M.M.

N79-25018* Solar Turbines International, San Diego, Calif.
INTERNALLY COATED AIR-COOLED GAS TURBINE BLADING Final Report, Aug. 1977 - Dec. 1978

L. Hsu, W. G. Stevens, and A. R. Stetson Mar 1979 102 p refs

(NASA-CR-159574, SR79-R-4655-15)

Avail: NTIS

HC A06/MF A01 CSCL 21E

Ten candidate modified nickel-aluminide coatings were developed using the slip pack process. These coatings contain additives such as silicon, chromium, and columbium in a nickel-aluminum coating matrix with directionally solidified MAR-M200 - Hf as the substrate alloy. Following a series of screening tests which included strain tolerance, dynamic oxidation and hot corrosion testing, the Ni-19Al-1Cb (nominal composition) coating was selected for application to the internal passages of the first-stage turbine blades. Process development results indicate that a dry pack process is suitable for internal coating application resulting in 18 percent or less reduction in air flow. Coating uniformity, based on coated air-cooled blades, was within + or - 20 percent. Test results show that the presence of additives (silicon, chromium or columbium) appeared to improve significantly the ductility of the NiAl matrix. However, the environmental resistance of these modified nickel-aluminides were generally inferior to the simple aluminides. A.R.H.

N79-25020* General Electric Co., Cincinnati, Ohio. Aircraft Engine Group.

DESIGN STUDY AND PERFORMANCE ANALYSIS OF A HIGH-SPEED MULTISTAGE VARIABLE-GEOMETRY FAN FOR A VARIABLE CYCLE ENGINE Final Report

T. J. Sullivan and D. E. Parker Mar 1979 228 p refs

(Contract NAS3-20041, R79AEG288)

(NASA-CR-159545) Avail: NTIS HC A11/MF A01 CSCL 21E

A design technology study was performed to identify a high speed, multistage, variable geometry fan configuration capable of achieving wide flow modulation with near optimum efficiency at the important operating condition. A parametric screening study of the front and rear block fans was conducted in which the influence of major fan design features on weight and efficiency was determined. Key design parameters were varied systematically to determine the fan configuration most suited for a double bypass, variable cycle engine. Two and three stage fans were considered for the front block. A single stage, core driven fan was studied for the rear block. Variable geometry concepts were evaluated to provide near optimum off design performance. A detailed aerodynamic design and a preliminary mechanical design were carried out for the selected fan configuration. Performance predictions were made for the front and rear block fans. Author

N79-26055* Pratt and Whitney Aircraft Group, East Hartford, Conn.

ROTOR REDESIGN FOR A HIGHLY LOADED 1800 FT/SEC TIP SPEED FAN. 1: AERODYNAMIC AND MECHANICAL DESIGN REPORT

J. M. Norton, U. Tari, and R. M. Weber Apr 1979 104 p refs

(Contract NAS3-20591)

(NASA-CR-159596, PWA-5523-42)

Avail: NTIS

HC A06/MF A01 CSCL 21E

A quasi three dimensional design system and multiple-circular-arc airfoil sections were used to design a fan rotor. An axisymmetric intrablade flow field calculation modeled the shroud of an isolated splitter and radial distribution. The structural analysis indicates that the design is satisfactory for evaluation of aerodynamic performance of the fan stage in a test facility. S.E.S.

N79-30185* Pratt and Whitney Aircraft Group, East Hartford, Conn.

AERODYNAMIC AND ACOUSTIC INVESTIGATION OF INVERTED VELOCITY PROFILE COANNULAR EXHAUST NOZZLE MODELS AND DEVELOPMENT OF AERODYNAMIC AND ACOUSTIC PREDICTION PROCEDURES, COMPREHENSIVE DATA REPORT, VOLUME 1

Richard S. Larson, Douglas P. Nelson, and Bradley S. Stevens
Jun 1979 312 p 2 Vol.
(Contract NAS3-20061)
(NASA-CR-159515; PWA-5550-16-Vol-1) Avail: NTIS
HC A14/MF A01 CSCL 21E

The experimental data necessary to establish aerodynamic and acoustic prediction systems for coannular exhaust nozzles with inverted velocity profiles are presented in graphical form.

F. E.S.

N79-30186* Pratt and Whitney Aircraft Group, East Hartford, Conn.

AERODYNAMIC AND ACOUSTIC INVESTIGATION OF INVERTED VELOCITY PROFILE COANNULAR EXHAUST NOZZLE MODELS AND DEVELOPMENT OF AERODYNAMIC AND ACOUSTIC PREDICTION PROCEDURES, COMPREHENSIVE DATA REPORT, VOLUME 2

Richard S. Larson, Douglas P. Nelson, and Bradley S. Stevens
Jun 1979 225 p refs

(Contract NAS3-20061)
(NASA-CR-159516; PWA-5550-17-Vol-2) Avail: NTIS
HC A10/MF A01 CSCL 21E

The experimental data necessary to establish aerodynamic and acoustic prediction systems for coannular exhaust nozzles with inverted velocity profiles are presented in tabular form. The acoustic data are corrected to a 'theoretical day' and scaled to full engine size.

R.E.S.

N79-30189* Pratt and Whitney Aircraft Group, East Hartford, Conn. Commercial Products Div.

ENERGY EFFICIENT ENGINE FLIGHT PROPULSION SYSTEM PRELIMINARY ANALYSIS AND DESIGN REPORT Progress Report, Mar. 1978 - Feb. 1979

W B Gardner Apr 1979 480 p refs

(Contract NAS3-20646)
(NASA-CR-159487; PWA-5594-49) Avail: NTIS
HC A21/MF A01 CSCL 21E

A flight propulsion system preliminary design was established that meets the program goals of at least a 12 percent reduction in thrust specific fuel consumption, at least a five percent reduction in direct operating cost, and one-half the performance deterioration rate of the most efficient current commercial engines. The engine provides a high probability of meeting the 1978 noise rule goal. Smoke and gaseous emissions defined by the EPA proposed standards for engines newly certified after 1 January 1981 are met with the exception of NOx, despite incorporation of all known NOx reduction technology.

F.O.S.

N79-31207* General Electric Co., Cincinnati, Ohio.
EXPERIMENTAL CLEAN COMBUSTOR PROGRAM (ECCP), PHASE 3 Final Report

C C Gleason and D W Bahr 1 Jun 1979 201 p refs

(Contract NAS3-19736)
(NASA-CR-135384; R79AEG410) Avail: NTIS
HC A10/MF A01 CSCL 21E

A double annular advanced technology combustor with low pollutant emission levels was evaluated in a series of CF6-50 engine tests. Engine lightoff was readily obtained and no difficulties were encountered with combustor staging. Engine acceleration and deceleration were smooth, responsive and essentially the same as those obtainable with the CF6-50 combustor. The emission reductions obtained in carbon monoxide, hydrocarbons, and nitrogen oxide levels were 55, 95, and 30 percent, respectively, at an idle power setting of 33 percent of takeoff power on an EPA parameter basis. Acceptable smoke levels were also obtained. The exit temperature distribution of the combustor was found to be its major performance deficiency. In all other important combustion system performance aspects, the combustor was found to be generally satisfactory.

K.L.

N79-31212* United Technologies Corp., East Hartford, Conn.
AERODYNAMIC AND ACOUSTIC INVESTIGATION OF INVERTED VELOCITY PROFILE COANNULAR EXHAUST NOZZLE MODELS AND DEVELOPMENT OF AERODYNAMIC AND ACOUSTIC PREDICTION PROCEDURES Final Report

Richard S. Larson, Douglas P. Nelson, and Bradley S. Stevens
Washington NASA Aug 1979 223 p refs

(Contract NAS3-20061)
(NASA-CR-3168; PWA-5550-8) Avail: NTIS
HC A10/MF A01 CSCL 21E

Five co-annular nozzle models, covering a systematic variation of nozzle geometry, were tested statically over a range of exhaust conditions including inverted velocity profile (IVP) (fan to primary stream velocity ratio > 1) and non IVP profiles. Fan nozzle pressure ratio (FNPR) was varied from 1.3 to 4.1 at primary nozzle pressure ratios (PNPR) of 1.53 and 2.0. Fan stream temperatures of 700 K (1260 deg R) and 1089 K (1960 deg R) were tested with primary stream temperatures of 700 K (1260 deg R), 811 K (1460 deg R), and 1089 K (1960 deg R). At fan and primary stream velocities of 610 and 427 m/sec (2000 and 1400 ft/sec), respectively, increasing fan radius ratio from 0.69 to 0.83 reduced peak perceived noise level (PNL) 3 dB, and an increase in primary radius ratio from 0 to 0.81 (fan radius ratio constant at 0.83) reduced peak PNL an additional 1.0 dB. There were no noise reductions at a fan stream velocity of 853 m/sec (2800 ft/sec). Increasing fan radius ratio from 0.69 to 0.83 reduced nozzle thrust coefficient 1.2 to 1.5% at a PNPR of 1.53, and 1.7 to 2.0% at a PNPR of 2.0. The developed acoustic prediction procedure collapsed the existing data with standard deviation varying from + or - 8 dB to + or - 7 dB. The aerodynamic performance prediction procedure collapsed thrust coefficient measurements to within + or - .004 at a FNPR of 4.0 and a PNPR of 2.0.

Author

N79-32211* Pratt and Whitney Aircraft Group, East Hartford, Conn. Commercial Products Div.

LEAN, PREMIXED, PREVAPORIZED FUEL COMBUSTOR CONCEPTUAL DESIGN STUDY Final Report

A J Fiorentino, W. Greene, and J Kim Washington NASA
Aug 1979 63 p refs

(Contract NAS3-21256)
(NASA-CR-159647; PWA-5626-12) Avail: NTIS
HC A04/MF A01 CSCL 21E

Four combustor concepts, designed for the energy efficient engine, utilize variable geometry or other flow modulation techniques to control the equivalence ratio of the initial burning zone. Lean conditions are maintained at high power to control oxides of nitrogen while near stoichiometric conditions are maintained at low power for low CO and THC emissions. Each concept was analyzed and ranked for its potential in meeting the goals of the program. Although the primary goal of the program is a low level of nitric oxide emissions at stratospheric cruise conditions, both the ground level EPA emission standards and combustor performance and operational requirements typical of advanced subsonic aircraft engines are retained as goals as well. Based on the analytical projections made, two of the concepts offer the potential of achieving the emission goals; however, the projected operational characteristics and reliability of any concept to perform satisfactorily over an entire aircraft flight envelope would require extensive experimental substantiation before engine adaptation can be considered.

A.R.H.

N79-32212* Cincinnati Univ., Ohio. Dept of Aerospace Engineering and Applied Mechanics
FLOW IN NONROTATING PASSAGES OF RADIAL INFLOW TURBINES

E Baskharone, A Hamed, and W Tabakoff Sep 1979 104 p refs

(Grant NsG-3066)
(NASA-CR-159679) Avail: NTIS HC A06/MF A01 CSCL 21E

This analysis of irrotational incompressible flow field in the stator unit of a radial inflow turbine is presented. The solution in the combined scroll-nozzle assembly is complicated by the domain geometry and by its multiconnectivity. This model is

necessary, however, in order to provide a better understanding of the mutual interaction effects of these two components on the flow field. The finite element method is used in the solution which is limited to the two dimensional case. A substructuring technique is adopted in the computational procedure and results in considerable savings in both computer time and core storage requirements. The results are presented for the flow velocity magnitude and direction in the scroll and through the various nozzles, for two nozzle blade geometries. In addition, the mass flow rates in the different nozzles are computed and their deviations from the mean value determined. Author

A79-26925 * # Reduction of rotor-turbulence interaction noise in static fan noise testing. R. A. Kantola and R. E. Warren (GE Corporate Research and Development Center, Schenectady, N.Y.). *American Institute of Aeronautics and Astronautics, Aeroacoustics Conference, 5th, Seattle, Wash., Mar. 12-14, 1979, Paper 79-0656*. 18 p. 22 refs. Contract No. NAS3-17853.

Three effective inlet cleanup methods are described. A flared reverse cone inlet is used to eliminate wakes from the fan casings and/or probe supports. Boundary layer suction is employed ahead of the fan rotor and on the outer flare of the cone to reduce the boundary layer turbulence and remove any residual wakes. To reduce the midstream turbulent intensity and length scales, a turbulence control structure is used which is constructed with both a layer of honeycomb and a fine mesh screen. The effects of these cleanup methods are quantified by measuring the far-field noise in an anechoic chamber, using a high-speed 20-in.-diam fan of the current high passband type. The changes in the turbulent field impinging on this rotor are quantified by mapping the streamwise and transverse turbulent properties (spectra, intensity and length scale) with crossed hot film probes. It is convincingly shown that it is possible to clean up the inlet flow of a static fan noise test facility to a point where the static acoustic data simulate flight data. S.D.

A79-36737 * Concepts for reducing exhaust emissions and fuel consumption of the aircraft piston engine. B. J. Rezy, K. J. Stuckas, J. R. Tucker, and J. E. Meyers (Teledyne Continental Motors, Mobile, Ala.). *Society of Automotive Engineers, Business Aircraft Meeting and Exposition, Wichita, Kan., Apr. 3-6, 1979, Paper 790605*. 35 p. 23 refs. Research supported by the Teledyne Continental Motors; Contract No. NAS3-19755.

A study was made to reduce exhaust emissions and fuel consumption of a general aviation aircraft piston engine by applying known technology. Fourteen promising concepts such as stratified charge combustion chambers, cooling cylinder head improvements, and ignition system changes were evaluated for emission reduction and cost effectiveness. A combination of three concepts, improved fuel injection system, improved cylinder head with exhaust port liners and exhaust air injection was projected as the most cost effective and safe means of meeting the EPA standards for CO, HC and NO. The fuel economy improvement of 4.6% over a typical single engine aircraft flight profile does not though justify the added cost of the three concepts, and significant reductions in fuel consumption must be applied to the cruise mode where most of the fuel is used. The use of exhaust air injection in combination with exhaust port liners reduces exhaust valve stem temperatures which can result in longer valve guide life. The use of exhaust port liners alone can reduce engine cooling air requirements by 11% which is the equivalent of a 1.5% increase in propulsive power. The EPA standards for CO, HC and NO can be met in the IO-520 engine using air injection alone or the Simmonds improved fuel injection system. A.T.

A79-36749 * A review of Curtiss-Wright rotary engine developments with respect to general aviation potential. C. Jones (Curtiss-Wright Corp., Wood-Ridge, N.J.). *Society of Automotive Engineers, Business Aircraft Meeting and Exposition, Wichita, Kan., Apr. 3-6, 1979, Paper 790621*. 23 p. 21 refs. Contracts No. NAS3-20030, No. NAS3-20808.

Aviation related rotary (Wankel-type) engine tests, possible growth directions and relevant developments at Curtiss-Wright have been reviewed. Automotive rotary engines including stratified charge are described and flight test results of rotary aircraft engines are presented. The current 300 HP engine prototype shows basic durability and competitive performance potential. Recent parallel developments have separately confirmed the geometric advantages of the rotary engine for direct injected unthrottled stratified charge. Specific fuel consumption equal to or better than pr- or swirl-chamber diesels, low emission and multi-fuel capability have been shown by rig tests of similar rotary engine. A.T.

A79-39035 * # Lean stability augmentation for premixing, prevaporizing combustors. J. B. McVey and J. B. Kennedy (United Technologies Research Center, East Hartford, Conn.). *AIAA, SAE, and ASME, Joint Propulsion Conference, 15th, Las Vegas, Nev., June 18-20, 1979, AIAA Paper 79-1319*. 12 p. 5 refs. Contract No. NAS3-20804.

An experimental program was conducted to investigate techniques for improving the lean combustion limits of premixing, prevaporizing combustors applicable to gas turbine engine main burners. Augmented flameholders employing recessed perforated plates, catalyzed tube bundles, and configurations in which pilot fuel was injected into the wakes of V-gutters or perforated plates were designed and tested. Stable operation of the piloted designs was achieved at equivalence ratios as low as 0.25, NOx emissions of less than 1.0 g/kg at simulated turbine engine cruise conditions were obtained. A piloted perforated plate employing four percent pilot fuel flow produced the best performance while meeting severe NOx constraints. (Author)

A79-40483 * # Causes of high pressure compressor deterioration in service. J. H. Richardson, G. P. Sallee, and F. K. Smakula (United Technologies Corp., Pratt and Whitney Aircraft Group, East Hartford, Conn.). *AIAA, SAE, and ASME, Joint Propulsion Conference, 15th, Las Vegas, Nev., June 18-20, 1979, AIAA Paper 79-1234*. 8 p. Contract No. NAS3-20632.

The high mechanical reliability and low deterioration rate of the JT9D high-pressure compressor results in long utilization without exceeding engine operational limits. The increasing cost and decreasing supply of fuel have focused attention on the fuel burned implications of such high time use without refurbishment. The paper presents the results of JT9D high pressure compressor studies. The mechanical deterioration of the JT9D high-pressure compressor gaspath parts versus increasing service usage, documented from inspection of service parts, is presented and discussed including changes in airfoil roughness, blade length, airfoil contour and outer air seal trench characteristics. An estimate of the performance loss versus usage is related to each type of damage. The combined estimated high-pressure compressor performance loss for all mechanisms determined from part inspection is compared to historical engine test data to establish the validity of the predicted loss levels. The effect of cold section refurbishment on engine fuel consumption recovery and the results of an optimization study to determine the appropriate interval for high pressure compressor refurbishment are also reported. (Author)

A79-40759 * # Progress on Variable Cycle Engines. J. S. Westmoreland, R. A. Howlett, and R. P. Lohmann (United Technologies Corp., Pratt and Whitney Aircraft Group, East Hartford, Conn.). *AIAA, SAE, and ASME, Joint Propulsion Conference, 15th, Las Vegas, Nev., June 18-20, 1979, AIAA Paper 79-1312*. 11 p. 9 refs. Contracts No. NAS3-20061, No. NAS3-20602, No. NAS3-20048.

Progress in the development and future requirements of the Variable Stream Control Engine (VSCE) are presented. The two most critical components of this advanced system for future supersonic transports, the high performance duct burner for thrust augmentation, and the low jet conannular nozzle were studied. Nozzle model tests substantiated the jet noise benefit associated with the unique

velocity profile possible with a coannular nozzle system on a VSCE. Additional nozzle model performance tests have established high thrust efficiency levels only at takeoff and supersonic cruise for this nozzle system. An experimental program involving both isolated component and complete engine tests has been conducted for the high performance, low emissions duct burner with good results and large scale testing of these two components is being conducted using a F100 engine as the testbed for simulating the VSCE. Future work includes application of computer programs for supersonic flow fields to coannular nozzle geometries, further experimental testing with the duct burner segment rig, and the use of the Variable Cycle Engine (VCE) Testbed Program for evaluating the VSCE duct burner and coannular nozzle technologies.

A.T.

08 AIRCRAFT STABILITY AND CONTROL

Includes aircraft handling qualities; piloting; flight controls; and autopilots.

N79-28186* # National Aeronautics and Space Administration. Lewis Research Center, Cleveland, Ohio.

PREDICTING DYNAMIC PERFORMANCE LIMITS FOR SERVOSYSTEMS WITH SATURATING NONLINEARITIES

John A. Webb, Jr. and Richard A. Blech. Jul. 1979. 52 p. refs (NASA-TP-1488, E-9903) Avail: NTIS HC A04/MF A01 CSCL 01C

A generalized treatment for a system, with a single saturating nonlinearity is presented and compared with frequency response plots obtained from an analog model of the system. Once the amplitude dynamics are predicted with the limit lines, an iterative technique is employed to determine the system phase response. The saturation limit line technique is used in conjunction with velocity and acceleration limits to predict the performance of an electro-hydraulic servosystem containing a single-stage servovalve. Good agreement was obtained between predicted performance and experimental data. S.E.S.

N79-33210* # National Aeronautics and Space Administration. Lewis Research Center, Cleveland, Ohio.

EFFECTS OF DIFFUSION FACTOR, ASPECT RATIO AND SOLIDITY ON OVERALL PERFORMANCE OF 14 COMPRESSOR MIDDLE STAGES

Werner R. Britsch, Walter M. Osborn, and Mark R. Laessig. Washington. Sep. 1979. 148 p. (NASA-TP-1523, E-9943) Avail: NTIS HC A07/MF A01 CSCL 21E

A series of high hub tip radius ratio compressor stages representative of the middle and latter stages of axial flow compressors is discussed. The effects of aspect ratio, diffusion factor, and solidity on rotor and stage performance are determined. Fourteen middle stages are tested to study the effects on performance of varying both diffusion through the rotor and stator blades and blade aspect ratio. The design parameters in the streamline analysis program, the blade geometry program, and the blade coordinate program are presented. A.W.H.

A79-21296 * # The NASA high pressure facility and turbine test rig. F. S. Stepka (NASA, Lewis Research Center, Turbine Cooling Section, Cleveland, Ohio). *U.S. Navy and U.S. Air Force, Workshop on Cooling Problems in Aircraft Gas Turbines, Monterey, Calif., Sept. 27, 28, 1978, Paper*. 16 p. Project SQUID.

NASA Lewis Research Center is presently constructing a test facility for developing turbine-cooling and combustor technology for future-generation aircraft gas-turbine engines. Prototype engine hardware will be investigated in this facility at gas-stream conditions up to 2480 K average turbine inlet temperature and 4.14 million N/sq m turbine inlet pressure. The facility will have the unique features of fully automated control and data acquisition through the use of an integrated system of minicomputers and programmable controllers, which will result in more effective use of operating time and operators and will provide a built-in self-protection safety system. The facility, turbine rig, and turbine-cooling test program are described. (Author)

A79-53750 * # An overview of NASA research on positive displacement type general aviation engines. E. E. Kempke and E. A. Willis (NASA, Lewis Research Center, Cleveland, Ohio). *American Institute of Aeronautics and Astronautics Aircraft Systems and Technology Meeting, New York, N.Y., Aug. 20-22, 1979, Paper* 79-1824. 38 p. 12 refs.

The paper surveys the current status of the aviation positive displacement engine programs underway at the NASA Lewis Research Center. The program encompasses conventional, lightweight

diesel, and rotary combustion engines. Attention is given to topics such as current production type engine improvement, cooling drag reduction, fuel injection, and experimental and theoretical combustion studies. It is shown that the program's two major technical thrusts are directed toward lean operation of current production type spark ignition engines and advanced alternative engine concepts. Finally, an Otto cycle computer model is also covered. M.E.P.

N79-33206* # General Electric Co., Cincinnati, Ohio. Aircraft Engine Group.

CF6 JET ENGINE PERFORMANCE IMPROVEMENT PROGRAM. SHORT CORE EXHAUST NOZZLE PERFORMANCE IMPROVEMENT CONCEPT

W. A. Fasching. Sep. 1979. 113 p. refs.

(Contract NAS3-20628)

(NASA-CR 159564) Avail: NTIS HC A06/MF A01 CSCL 21E

The short core exhaust nozzle was evaluated in CF6-50 engine ground tests including performance, acoustic, and endurance tests. The test results verified the performance predictions from scale model tests. The short core exhaust nozzle provides an internal cruise speed reduction of 0.9 percent without an increase in engine noise. The nozzle hardware successfully completed 1000 flight cycles of endurance testing without any signs of distress. Author

09 RESEARCH AND SUPPORT FACILITIES (AIR)

Includes airports, hangars and runways; aircraft repair and overhaul facilities; wind tunnels; shock tube facilities; and engine test blocks.

For related information see also 14 Ground Support Systems and Facilities (Space).

N79-21084* National Aeronautics and Space Administration. Lewis Research Center, Cleveland, Ohio.

HYPERVELOCITY GUN Patent

Franklin C. Ford (MB Assoc., San Ramon, Calif.) and Arthur J. Biehl, inventors (to NASA) Issued 21 Dec. 1985 3 p filed 7 Jun. 1962 Sponsored by NASA

(NASA-Case-XLE-03186-1; US-Patent-3,224,337;

US-Patent-Appl-SN-200770; US-Patent-Class-89-8) Avail: US Patent and Trademark Office CSCL 14B

A velocity amplifier system which uses both electric and chemical energy for projectile propulsion is provided in a compact hypervelocity gun suitable for laboratory use. A relatively heavy layer of a tamping material such as concrete encloses a loop of an electrically conductive material. An explosive charge at least partially surrounding the loop is adapted to collapse the loop upon detonation of the charge. A source of electricity charges the loop through two leads, and an electric switch which is activated by the charge explosive charge, disconnects the leads from the source of electricity and short circuits them. An opening in the tamping material extends to the loop and forms a barrel. The loop, necked down in the opening, forms the sabot on which the projectile is located. When the loop is electrically charged and the explosive detonated, the loop is short circuited and collapsed thus building up a magnetic field which acts as a sabot catcher. The sabot is detached from the loop and the sabot and projectile are accelerated to hypervelocity.

Official Gazette of the U.S. Patent and Trademark Office

A79-32398 * # Low-turbulence high-speed wind tunnel for the determination of cascade shock losses. J. A. Slovisky (Notre Dame, University, Notre Dame, Ind.), W. B. Roberts (Nielsen Engineering and Research, Inc., Mountain View, Calif.), and D. M. Sandercock (NASA, Lewis Research Center, Fan and Compressor Branch, Cleveland, Ohio). *American Society of Mechanical Engineers, Gas Turbine Conference and Exhibit and Solar Energy Conference, San Diego, Calif., Mar. 12-15, 1979, Paper 79-GT-129*. 11 p. 23 refs. Members, \$1.50; nonmembers, \$3.00.

A low turbulence high-speed wind tunnel, using anti-turbulence screening and a 100:1 contraction ratio, has been found suitable for high-speed smoke flow visualization. The location and strength of normal, oblique, and curved shock waves generated by transonic or supersonic wind tunnel flow over airfoils or through axial compressor cascades is determined by combined shadowgraph and smoke visualization techniques without the interference effects caused by intrusive probes. The Reynolds number based on chord varied between 50,000 and 1,000,000. Preliminary results are compared with the relevant theory and data gathered using a total pressure probe.

(Author)

N79-29189* # Teledyne CAE, Toledo, Ohio

ADVANCED GENERAL AVIATION TURBINE ENGINE (GATE) STUDY Final Report

R. Smith and E. H. Benstein Jun 1979 150 p refs

(Contract NAS3-20757)

(NASA CR-159624; Teledyne-CAE-1600)

Avail NTIS

HC A07/MF A01 CSCL 21E

The small engine technology requirements suitable for general aviation service in the 1987 to 1988 time frame were defined. The market analysis showed potential United States engines sales of 31,500 per year providing that the turbine engine sales price approaches current reciprocating engine prices. An optimum engine design was prepared for four categories of fixed wing aircraft and for rotary wing applications. A common core approach

was derived from the optimum engines that maximizes engine commonality over the power spectrum with a projected price competitive with reciprocating piston engines. The advanced technology features reduced engine cost, approximately 50 percent compared with current technology.

J M S.

N79-29191* # General Electric Co., Evendale, Ohio. Aircraft Engine Group.

NASA CF6 JET ENGINE DIAGNOSTICS PROGRAM: LONG-TERM CF6-8D LOW-PRESSURE TURBINE DETE-RIORATION

Jeffrey J. Smith Aug. 1979 116 p refs

(Contract NAS3-20631)

(NASA-CR-159618; R79AEG356)

Avail: NTIS

HC A06/MF A01 CSCL 21E

Back-to-back performance tests were run on seven airline low pressure turbine (LPT) modules and four new CF6-8D modules. Back-to-back test cell runs, in which an airline LPT module was directly compared to a new production module, were included. The resulting change, measured in fuel burn, equaled the level of LPT module deterioration. Three of the LPT modules were analytically inspected followed by a back-to-back test cell run to evaluate current refurbishment techniques.

Author

12 ASTRONAUTICS (GENERAL)

For extraterrestrial exploration see 91 *Lunar and Planetary Exploration*.

N79-32232* National Aeronautics and Space Administration. Lewis Research Center, Cleveland, Ohio.

MASS DRIVERS. 3: ENGINEERING

c37

William Arhold (Hampshire Coll.), Stuart Bowen, Steve Cohen, Kevin Fine (MIT), David Kaplan (Michigan Univ.), Margaret Kolm (Haverford Coll.), Henry Kolm (MIT), Jonathan Newman (Amherst Coll.), Gerard K. O'Neill (Princeton Univ.), and William Snow (MIT). In NASA. Ames Res. Center. Space Resources and Space Settlements 1979 p 119-157 refs (For primary document see N79-32225 23-12)

Avail. NTIS MF A01; SOD HC CSCL 13I

The last of a series of three papers by the Mass-Driver Group of the 1977 Ames Summer Study is presented. It develops the engineering principles required to implement the basic mass-driver. Optimum component mass trade-offs are derived from a set of four input parameters, and the program used to design a lunar launcher. The mass optimization procedures is then incorporated into a more comprehensive mission optimization program called OPT-4, which evaluates an optimized mass-driver reaction engine and its performance in a range of specified missions. Finally, this paper discusses, to the extent that time permitted, certain peripheral problems: heating effects in buckets due to magnetic field ripple; an approximate derivation of guide force profiles; the mechanics of inserting and releasing payloads; the reaction mass orbits; and a proposed research and development plan for implementing mass drivers.

G Y.

N79-20161* Princeton Combustion Lab., N. J.

DEFINITION OF SMOLDER EXPERIMENTS FOR SPACELAB Progress Report, 18 Apr. - 20 Dec. 1978

M. Summerfield, N. A. Messina, and L. S. Ingram. Jan. 1979. 81 p. refs

(Contract NAS3-21354)

(NASA-CR-159528. PCRL-FR-79-001)

Avail. NTIS

HC A05/MF A01 CSCL 22A

The feasibility of conducting experiments in space on smoldering combustion was studied to conceptually design specific smoldering experiments to be conducted in the Shuttle/Spacelab System. Design information for identified experiment critical components is provided. The analytical and experimental basis for conducting research on smoldering phenomena in space was established. Physical descriptions of the various competing processes pertaining to smoldering combustion were identified. The need for space research was defined based on limitations of existing knowledge and limitations of ground-based reduced-gravity experimental facilities.

S.E.S.

13 ASTRODYNAMICS

includes powered and free-flight trajectories; and orbit and launching dynamics.

N79-26101*# Georgia Inst of Tech., Atlanta. Engineering Experiment Station.

MILLIMETER WAVE SATELLITE CONCEPTS. VOLUME 1: EXECUTIVE SUMMARY Report, Jun. 1978 - Jun. 1978

N. B. Hilsen, L. D. Holland, R. W. Wallace, D. L. Kelly, R. E. Thomas, J. J. Gallagher, and F. H. Vogler. Jun. 1979. 32 p. refs. 2 Vol.

(Contract NAS3-20110; Georgia Tech. Proj. A-1855)

(NASA-CR-159504) Avail. NTIS HC A03/MF A01 CSCL 22B

The objectives of the program were: (1) development of methodology based on the technical requirements of potential services that might be assigned to millimeter wave bands for identifying the viable and appropriate technologies for future NASA millimeter research and development programs, and (2) testing of this methodology with user applications and services. The scope of the program included the entire communications network, both ground and space subsystems. The reports include: (1) cost, weight, and performance models for the subsystems, (2) conceptual design for point-to-point and broadcast communications satellites, (3) analytic relationships between subsystem parameters and an overall link performance, (4) baseline conceptual systems, (5) sensitivity studies, (6) model adjustment analyses, (7) identification of critical technologies and their risks, (8) brief R&D program scenarios for the technologies judged to be moderate or extensive risks. J.A.M.

N79-26102*# Georgia Inst. of Tech., Atlanta. Engineering Experiment Station.

MILLIMETER WAVE SATELLITE CONCEPTS. VOLUME 2: TECHNICAL REPORT Report, Jun. 1978 - Jun. 1978

N. B. Hilsen, L. D. Holland, R. W. Wallace, D. L. Kelly, R. E. Thomas, and F. H. Vogler. May 1979. 40 p. refs. 2 Vol.

(Contract NAS3-20110; Georgia Tech. Proj. A-1855)

(NASA-CR-159503) Avail. NTIS HC A03/MF A01 CSCL 22B

Identification of technologies for millimeter satellite communication systems, and assessment of the relative risks of these technologies, were accomplished through subsystem modeling and link optimization for both point-to-point and broadcast applications. The results, in terms of annual cost per channel to the user from a commercial view point, are described. J.A.M.

15 LAUNCH VEHICLES AND SPACE VEHICLES

Includes boosters; manned orbital laboratories; reusable vehicles; and space stations.

N79-20171* National Aeronautics and Space Administration. Lewis Research Center, Cleveland, Ohio.

SPACE PROPULSION TECHNOLOGY OVERVIEW

J. J. Pelouch, Jr. 1979 10 p refs To be presented at Conf. on Advanced Technol. for Future Space Systems, Hampton, Va., 8-11 May 1979; sponsored by AIAA (NASA-TM-79104; E-9928) Avail: NTIS HC A02/MF A01 CSCL 21H

Chemical and electric propulsion technologies for operations beyond the shuttle's orbit with focus on future mission needs and economic effectiveness is discussed. The adequacy of the existing propulsion state-of-the-art, barriers to its utilization, benefit of technology advances, and the prognosis for advancement are the themes of the discussion. Low-thrust propulsion for large space systems is cited as a new technology with particularly high benefit. It is concluded that the shuttle's presence for at least two decades is a legitimate basis for new propulsion technology, but that this technology must be predicted on an awareness of mission requirements, economic factors, influences of other technologies, and real constraints on its utilization.

Author

16 SPACE TRANSPORTATION

Includes passenger and cargo space transportation e.g., shuttle operations; and rescue techniques.

For related information see also 03 Air Transportation and Safety and 85 Urban Technology and Transportation.

N79-25129* National Aeronautics and Space Administration. Lewis Research Center, Cleveland, Ohio.

LOW-THRUST CHEMICAL ORBIT TRANSFER PROPULSION

J. J. Pelouch, Jr. 1979 22 p refs Presented at the 15th Joint Propulsion Conf., Las Vegas, Nev., 18-20 Jun. 1979; sponsored by AIAA, Soc. of Automotive Engr., and ASME (NASA-TM-79190, E-059) Avail: NTIS HC A02/MF A01 CSCL 22B

The need for large structures in high orbit is reported in terms of the many mission opportunities which require such structures. Mission and transportation options for large structures are presented, and it is shown that low-thrust propulsion is an enabling requirement for some missions and greatly enhancing to many others. Electric and low-thrust chemical propulsion are compared, and the need for an requirements of low-thrust chemical propulsion are discussed in terms of the interactions that are perceived to exist between the propulsion system and the large structure.

S.E.S.

N79-27235* National Aeronautics and Space Administration. Lewis Research Center, Cleveland, Ohio.

HIGH VOLTAGE SURFACE-CHARGED ENVIRONMENT TEST RESULTS FROM SPACE FLIGHT AND GROUND SIMULATION EXPERIMENTS

Norman T. Grier 1979 13 p refs Presented at the High Voltage Workshop, Anaheim, Calif., 26-27 Feb. 1979, sponsored by the AIAA

(NASA-TM-79184, E-051) Avail: NTIS HC A02/MF A01 CSCL 10A

Surface-charged particle interactions were investigated for a small 100 sq cm conventionally constructed solar cell panel in ground facilities and in a flight experiment. The flight data substantiated preflight ground test results showing that at high positive biases the cover glass over each solar cell enhances the coupling current and that, at high negative biases, arcs create large transients in the coupling current.

R.E.S.

N79-27236* National Aeronautics and Space Administration. Lewis Research Center, Cleveland, Ohio.

A THERMAL CONTROL APPROACH FOR A SOLAR ELECTRIC PROPULSION THRUST SUBSYSTEM

Joseph E. Maloy and Jon C. Oglebay Jun 1979 22 p refs (NASA-TM-79175, E-040) Avail: NTIS HC A02/MF A01 CSCL 21C

A thrust subsystem thermal control design is defined for a Solar Electric Propulsion System (SEPS) proposed for the comet Halley Flyby/comet Tempel 2 rendezvous mission. A 114 node analytic model, developed and coded on the systems improved numerical differencing analyzer program, was employed. A description of the resulting thrust subsystem thermal design is presented as well as a description of the analytic model and comparisons of the predicted temperature profiles for various SEPS thermal configurations that were generated using this model. It was concluded that (1) a BIMOD engine system thermal design can be autonomous; (2) an independent thrust subsystem thermal design is feasible; (3) the interface module electronics temperatures can be controlled by a passive radiator and supplementary heaters; (4) maintaining heat pipes above the freezing point would require an additional 322 watts of supplementary heating power for the situation where no thrusters are operating; (5) insulation is required around the power processors, and between the interface module and the avionics module, as well as in those areas which may be subjected to solar heating; and (6) insulation behind the heat pipe radiators is not necessary.

Author

17 SPACECRAFT COMMUNICATIONS, COMMAND AND TRACKING

includes telemetry; space communications networks; astronavigation; and radio blackout.

For related information see also 04 Aircraft Communications and Navigation and 32 Communications.

N79-20176* National Aeronautics and Space Administration, Lewis Research Center, Cleveland, Ohio.

GLOBAL DISASTER SATELLITE COMMUNICATIONS SYSTEM FOR DISASTER ASSESSMENT AND RELIEF COORDINATION

B. E. Leroy 1979 12 p refs Presented at the Intern. Telecommun. Exposition, Dallas, 26 Feb. - 2 Mar. 1979 (NASA-TM-79105; E-9929) Avail: NTIS HC A02/MF A01 CSDL 17B

The global communication requirements for disaster assistance and examines operationally feasible satellite system concepts and the associated system parameters are analyzed. Some potential problems associated with the current method of providing disaster assistance and a scenario for disaster assistance relying on satellite communications are described. Historical statistics are used with the scenario to assess service requirements. Both present and planned commercially available systems are considered. The associated global disaster communication yearly service costs are estimated. S.E.S.

N79-21120* National Aeronautics and Space Administration, Lewis Research Center, Cleveland, Ohio.

THERMAL ANOMALIES OF THE TRANSMITTER EXPERIMENT PACKAGE ON THE COMMUNICATIONS TECHNOLOGY SATELLITE

Robert E. Alexovich and Arthur N. Curren Apr. 1979 113 p refs (NASA-TP-1410; E-9735) Avail: NTIS HC A06/MF A01 CSDL 17B

The causes of four temporary thermal-control-system malfunctions that gave rise to unexpected temperature excursions in the 12-gigahertz, 200-watt transmitter experiment package (TEP) on the Communications Technology Satellite were investigated. The TEP consists of a nominal 200-watt output stage tube (OST), a supporting power-processing system (PPS), and a variable-conductance heat-pipe system (VCHPS). The VCHPS, which uses three heat pipes to conduct heat from the body of the OST to a radiator fin, was designed to maintain the TEP at safe operating temperatures at all operating conditions. On four occasions during 1977, all near the spring and fall equinoxes, the OST body temperature and related temperatures displayed sudden, rapid, and unexpected rises above normal levels while the TEP was operating at essentially constant, normal conditions. The temperature excursions were terminated without TEP damage by reducing the radio frequency (RF) output power of the OST. Between the anomalies and since the fourth, the thermal control system has apparently functioned as designed. The results indicate the most probable cause of the temperature anomalies is depriving of the arteries in the variable-conductance heat pipes. A mode was identified in which the TEP, as presently configured, may operate with stable temperatures and with minimum change in performance level. S.E.S.

N79-23999* National Aeronautics and Space Administration, Lewis Research Center, Cleveland, Ohio.

COMMUNICATIONS TECHNOLOGY SATELLITE: UNITED STATES EXPERIMENTS AND DISASTER COMMUNICATIONS APPLICATIONS

Patrick Donoghue, Henry R. Hunczak, and Guy S. Gurski 1978 45 p refs Presented at the United Regional Seminar on the Use of Satellite Technol. for Disaster Appl., Sao Paulo, Brazil

2-13 Oct. 1978

(NASA-TM-79109; E-9935) Avail: NTIS HC A03/MF A01 CSDL 17B

Ground antennas from 0.6 to 5.0 meters in diameter were used as remote earth terminals by the United States for both wideband (television) and narrowband (voice, data) communication in conjunction with the Canadian Hermes satellite's high power transmitter. Experiments summarized cover teleconferencing and duplex videoconferencing for medical, educational, and civic purposes, as well as the remote interpretation of multilingual broadcasts from the United Nations. The capabilities of the system during real and simulated disasters at airports are assessed. Particular attention is given to miniexperiments for flood control in the Mississippi River basin and in Johnstown, Pennsylvania during the 1977 flood. A.R.H.

N79-31264* National Aeronautics and Space Administration, Lewis Research Center, Cleveland, Ohio.

LIFE CHARACTERISTICS ASSESSMENT OF THE COMMUNICATIONS TECHNOLOGY SATELLITE TRANSMITTER EXPERIMENT PACKAGE

Jerry Smetana and Arthur N. Curren Jul. 1979 52 p refs (NASA-TM-79181; E-049) Avail: NTIS HC A04/MF A01 CSDL 17B

The performance characteristics of the transmitter experiment package (TEP) aboard the Communications Technology Satellite (CTS) measured during its first 2 years in orbit are presented. The TEP consists of a nominal 200 watt output stage tube (OST), a supporting power processing system (PPS), and a variable conductance heat pipe system (VCHPS). The OST, a traveling wave tube augmented with a 10 stage depressed collector has an overall saturated average efficiency of 51.5 percent and an average saturated radio frequency (rf) output power at center band frequency of 240 watts. The PPS operated with a measured efficiency of 86.5 to 88.5 percent. The VCHPS, using three pipes to conduct heat from the PPS and the OST to a 52 by 124 centimeter radiator fin, maintained the PPS baseplate temperature below 50 C for all operating conditions. The TEP performance characteristics presented include frequency response, rf output power, thermal performance, and efficiency. Communications characteristics were evaluated by using both video and audio modulated signals. On four occasions, the TEP experienced temporary thermal control system malfunctions. The anomalies were terminated safely, and the problem was investigated because of the potential for TEP damage due to the significant temperature increases. Safe TEP operating procedures were established. K.L.

A79-20877 * Laboratory studies of electrical properties of insulating materials. J. E. Nanevich, R. C. Adamo (SRI International, Menlo Park, Calif.), and N. Grier (NASA, Lewis Research Center, Cleveland, Ohio). In: Selective application of materials for products and energy; Proceedings of the Twenty-third National Symposium and Exhibition, Anaheim, Calif., May 2-4, 1978. (A79-20801 07-23) Azusa, Calif., Society for the Advancement of Material and Process Engineering, 1978, p. 1190-1201.

The characteristics of satellites are influenced by the electrical properties of the dielectric exterior. It was found in simulated space environment tests that the electrical conductivities of dielectrics are affected as the result of interactions with various components of the environment. The degree to which the conductivity was affected varied with material. In some instances the changes found to occur could be used to advantage, particularly if they could be enhanced. For example, the increased electrical conductivity of Kapton resulting from solar illumination could be used to advantage to eliminate the charge storage leading to electrical breakdown during magnetic substorms. Similarly the relative immunity of FEP Teflon to change from response to the space environment makes it a logical choice as a solar cell cover in a high-voltage solar array. G.R.

A79-51097 * # VHF downlink communication system for SLAR data. R. J. Schertler, T. L. Chase, R. A. Mueller, I. Kramarchuk, R. J. Jirberg, and R. T. Gedney (NASA, Lewis Research Center, Cleveland, Ohio). *University of Michigan, International Symposium on Remote Sensing of Environment, 13th, Ann Arbor, Mich., Apr. 23-27, 1979, Paper. 8 p.*

This paper describes a real-time VHF downlink communication system for transmitting side-looking airborne-radar (SLAR) data directly from an aircraft to a portable ground/shipboard receiving station. Use of this receiving station aboard the U.S. Coast Guard icebreaker Mackinaw for generating real-time photographic quality radar images will be discussed. The system was developed and demonstrated in conjunction with the U.S. Coast Guard and NOAA National Weather Service as part of the Project Icewarn all-weather ice information system for the Great Lakes Winter Navigation Program. (Author)

A79-45374 * # Bilinear tangent yaw guidance. R. G. Brusch (General Dynamics Corp., Convair Div., San Diego, Calif.). In: Guidance and Control Conference, Boulder, Colo., August 6-8, 1979, Collection of Technical Papers. (A79-45351 19-12) New York, American Institute of Aeronautics and Astronautics, Inc., 1979, p. 250-264. 23 refs. Contract No. NAS3-19154. (AIAA 79-1730)

This paper presents a parametric yaw steering law which has been used to provide closed-loop yaw guidance for the launch of the HEAO (High Energy Astronomy Observatory) satellite mission using the Atlas/Centaur launch vehicle. This bilinear tangent steering law provides near optimal yaw steering for maneuvers requiring insertion into orbits with a specified inclination and node. Bilinear tangent steering is shown to be optimal in both the pitch and yaw planes when a uniform gravitational field is assumed. The conditions under which the general bilinear tangent laws degenerate into linear tangent and constant attitude laws are presented. The flight computer implementation of these laws in a rotating coordinate system using real-time integration of the equations of motion is detailed. Explicit solution of the parametric guidance equations requires the inflight solution of (2x2) two-point boundary value problems in the pitch and yaw planes. Excellent results are obtained even for very large (greater than 50 deg) out-of-plane steering angles. (Author)

18 SPACECRAFT DESIGN, TESTING AND PERFORMANCE

Includes spacecraft thermal and environmental control; and attitude control

For life support systems see 54 Man/System Technology and Life Support. For related information see also 05 Aircraft Design, Testing and Performance and 39 Structural Mechanics.

N79-11109* National Aeronautics and Space Administration Lewis Research Center, Cleveland, Ohio
INSULATOR EDGE VOLTAGE GRADIENT EFFECTS IN SPACECRAFT CHARGING PHENOMENA
N. John Stevens, Carolyn K. Purvis, and John V. Staskus 1978 16 p. refs. Presented at the Ann. Conf. on Nucl. and Space Radiation Effects, Albuquerque, N. Mex., 18-21 Jul. 1978, sponsored by IEEE
(NASA-TM 78988, E-9769) Avail. NTIS HC A02/MF A01 CSCL 22B

Insulating surfaces on geosynchronous satellites were charged by geomagnetic substorms to a point where discharges occur. The electromagnetic pulses from these discharges couple into satellite electronic systems disrupting operations are examined. Laboratory tests conducted on insulator charging have indicated that discharges appear to be initiated at insulator edges where voltage gradients can exist. An experimental investigation was conducted to measure edge voltage gradients on silvered Teflon samples as they are charged by monoenergetic electron beams. It was found that the surface voltage at insulator edges can be approximated by an exponential expression based on an electron current density balance. Author

N79-18149* National Aeronautics and Space Administration Lewis Research Center, Cleveland, Ohio
JUPITER PROBE CHARGING STUDY
Carolyn K. Purvis Jan. 1979 38 p. refs.
(NASA-TP-1263, E-9167) Avail. NTIS HC A03/MF A01 CSCL 22B

A model to predict spacecraft charging effects in the Jovian magnetosphere was developed for the preliminary design of a Jupiter probe. Charging calculations made with this model are presented and discussed. Differential potentials between interior and exterior surfaces and between sunlit and dark exterior surfaces are predicted to be in the kilovolt range. Author

N79-18150* National Aeronautics and Space Administration Lewis Research Center, Cleveland, Ohio
SPACE ENVIRONMENTAL INTERACTIONS WITH SPACECRAFT SURFACES
John N. Stevens 1979 23 p. refs. Presented at 17th Aerospace Sci. Meeting, New Orleans, La., 15-17 Jan. 1979. Sponsored by AIAA
(NASA-TM-79016, E-9805) Avail. NTIS HC A02/MF A01 CSCL 22B

Environmental interactions are defined as the response of spacecraft surfaces to the charged-particle environment. These interactions are divided into two broad categories: spacecraft passive, in which the environment acts on the surfaces and spacecraft active, in which the spacecraft or a system on the spacecraft causes the interaction. The principal spacecraft passive interaction of concern is the spacecraft charging phenomenon. The spacecraft active category introduces the concept of interactions with the thermal plasma environment and Earth's magnetic fields, which are important at all altitudes and must be considered the designs of proposed large space structures and space power systems. The status of the spacecraft charging investigations is reviewed along with the spacecraft active interactions. J. M. S.

N79-22097* National Aeronautics and Space Administration Lewis Research Center, Cleveland, Ohio.

DESIGN PROBLEMS OF SMALL TURBOMACHINERY

H. E. Rohlik In: Von Karman Inst. for Fluid Dyn. Closed Cycle Gas Turbines 1970 11 p. refs. (For primary document see N79-22093 13-07)

Avail. NTIS HC A15/MF A01 CSCL 21E

Advanced design and testing techniques developed at NASA Lewis to achieve high efficiency in small turbomachines are described. Small radial and axial turbines and compressors were built for space power systems and associated studies at the Lewis Research Center. A six stage axial compressor of 3.5 inches diameter and axial turbines of 5 and 8.5 inches diameter were included. Radial turbines and compressors ranged from 3.5 to 6 inches. Topics discussed include maximum efficiency as a function of speed, the effect of compressibility on passage size, the use of quasi-orthogonals to calculate cross-channel velocity gradients, a design point velocity diagram study for axial turbines, and estimating off-design performance. Special turbine instruments and calibration procedures were developed to test compressors and turbines, to determine Reynolds and size number effects clearance, specific speed effects, and compressor performance. Laboratory tests conducted to study system operation and shaft and bearing motions are also reviewed. A. R. H.

N79-22188* National Aeronautics and Space Administration Lewis Research Center, Cleveland, Ohio.

LARGE SPACE SYSTEM: CHARGED PARTICLE ENVIRONMENT INTERACTION TECHNOLOGY

N. John Stevens, James C. Roche, and Norman T. Grier 1979 23 p. refs. Presented at the Conf. on Advanced Technol. for Future Space Systems, Hampton, Va., 8-11 May 1979, sponsored by AIAA

(NASA-TM-79156, E-012) Avail. NTIS HCA02/MF A01 CSCL 22B

Large, high voltage space power systems are proposed for future space missions. These systems must operate in the charged-particle environment of space and interactions between this environment and the high voltage surfaces are possible. Ground simulation testing indicated that dielectric surfaces that usually surround biased conductors can influence these interactions. For positive voltages greater than 100 volts, it has been found that the dielectrics contribute to the current collection area. For negative voltages greater than 500 volts, the data indicates that the dielectrics contribute to discharges. A large, high-voltage power system operating in geosynchronous orbit was analyzed. Results of this analysis indicate that very strong electric fields exist in these power systems. S. E. S.

N79-24000* National Aeronautics and Space Administration Lewis Research Center, Cleveland, Ohio.

NASCAP MODELLING OF HIGH-VOLTAGE POWER SYSTEM INTERACTIONS WITH SPACE CHARGED-PARTICLE ENVIRONMENTS

N. John Stevens, James C. Roche, and Myron J. Mandell (Systems, Science and Software, La Jolla, Calif.) 1979 20 p. refs. Presented at the High Voltage Workshop, Anaheim, Calif., 26-27 Feb. 1979, sponsored by IEEE

(NASA-TM-79146, E-001) Avail. NTIS HC A02/MF A01 CSCL 22B

A simple space power system operating in geosynchronous orbit was analyzed. This system consisted of two solar array wings and a central body. Each solar array wing was considered to be divided into three regions operating at 2000 volts. The center body was considered to be an electrical ground with the array voltages both positive and negative relative to ground. The system was analyzed for both a normal environment and a moderate geomagnetic substorm environment. Initial results indicate a high probability of arcing at the interconnects on the negative operating voltage wing. The dielectric strength of the substrate may be exceeded giving rise to breakdown in the bulk of the material. The geomagnetic substorm did not seem to increase the electrical gradients at the interconnects on the negative operating voltage wing but did increase the gradients on the positive operating voltage wing which could result in increased coupling current losses. R. E. S.

N79-24001* National Aeronautics and Space Administration, Lewis Research Center, Cleveland, Ohio.

SPACECRAFT CHARGING TECHNOLOGY, 1978

1979 908 p refs Conf. held at Colorado Springs, Colo., 31 Oct. - 2 Nov. 1978; sponsored by NASA and AFGL (NASA-CP-2071; AFGL-TR-79-0082) Avail: NTIS HC A99/MF A01 CSCL 22B

The interaction of the aerospace environment with spacecraft surfaces and onboard, high voltage spacecraft systems operating over a wide range of altitudes from low Earth orbit to geosynchronous orbit is considered. Emphasis is placed on control of spacecraft electric potential. Electron and ion beams, plasma neutralizers material selection, and magnetic shielding are among the topics discussed. For individual titles, see N79-24002 through N79-24057.

N79-24006* National Aeronautics and Space Administration, Lewis Research Center, Cleveland, Ohio.

SUMMARY OF THE TWO YEAR NASA PROGRAM FOR ACTIVE CONTROL OF ATS-5/6 ENVIRONMENTAL CHARGING

Robert O. Bartlett and Carolyn K. Purvis *In its Spacecraft Charging Technol.*, 1978 1979 p 44-58 refs Prepared in cooperation with NASA, Goddard Space Flight Center (For primary document see N79-24001 15-18)

Avail: NTIS HC A99/MF A01 CSCL 22B

Experiments conducted on the ATS 5 and ATS 6 which have demonstrated the feasibility of modifying or clamping the environmentally induced potential of these spacecraft are described. The results of these experiments indicate that a thermionic electron source is capable of replacing photo-emitted electrons during eclipse. However, the utility of this type of device is limited if its emission is suppressed by local electric fields. On the other hand, it is shown that a plasma source will not only serve as a substitute for photo-emitted electrons but will also suppress differential charging of isolated elements of the spacecraft which would tend to suppress electron emission. This latter device is therefore capable of clamping the potential of a spacecraft without special considerations of its coupling to the ambient plasma. J.M.S.

N79-24011* National Aeronautics and Space Administration, Lewis Research Center, Cleveland, Ohio.

THE CAPABILITIES OF THE NASA CHARGING ANALYZER PROGRAM

I. Katz, J. J. Cassidy, M. J. Mandell, G. W. Schnuelle, P. G. Steen, and J. C. Roche *In its Spacecraft Charging Technol.*, 1978 1979 p 101-122 refs Prepared in cooperation with Systems, Science and Software, La Jolla, Calif. (For primary document see N79-24001 15-18) (Contract NAS3-21050)

Avail: NTIS HC A99/MF A01 CSCL 22B

Desirable features in a spacecraft modeling code are enumerated. The NASCAP is discussed in terms of its approach to the problem. Samples of problem setup and output are provided which demonstrate the ease with which the program can be used. A simple but interesting case of spacecraft charging is examined, and other applications are discussed. Author

N79-24013* National Aeronautics and Space Administration, Lewis Research Center, Cleveland, Ohio.

COMPARISON OF NASCAP PREDICTIONS WITH EXPERIMENTAL DATA

James C. Roche and Carolyn K. Purvis *In its Spacecraft Charging Technol.*, 1978 1979 p 144-157 refs (For primary document see N79-24001 15-18)

Avail: NTIS HC A99/MF A01 CSCL 22B

The NASA charging analyzer program (NASCAP) is a three dimensional, finite element computer code capable of simulating the electrostatic charging of an arbitrary body either in a ground test tank or in the space environment. The code incorporated surface property parameters needed to simulate insulating and conducting materials. These parameters are being updated as required to bring the NASCAP predictions into correspondence

with data from ground tests. NASCAP predictions are also being compared with data from the ATS 5 spacecraft. The significance of these results is discussed. J.A.M.

N79-24021* National Aeronautics and Space Administration, Lewis Research Center, Cleveland, Ohio.

INTERACTIONS BETWEEN SPACECRAFT AND THE CHARGED-PARTICLE ENVIRONMENT

N. John Stevens *In its Spacecraft Charging Technol.*, 1978 1979 p 268-294 refs (For primary document see N79-24001 15-18)

Avail: NTIS HC A99/MF A01 CSCL 22B

Spacecraft-environment interactions are defined as the responses of a spacecraft surface to a charged-particle environment. This response can influence spacecraft system performance. Interactions can be divided into two broad categories: spacecraft passive, in which the environment acts on the spacecraft; and spacecraft active, in which the spacecraft causes the interaction. Passive interactions include the spacecraft-charging phenomenon. Active interactions include the relatively new interactions arising from the use of very large spacecraft and space power systems in future missions. To illustrate active interactions, a large power system operating at elevated voltages is considered. Possible interactions are described, available experimental data are reviewed, and the effect on power system performance is estimated. G.Y.

N79-24022* National Aeronautics and Space Administration, Lewis Research Center, Cleveland, Ohio.

PLASMA INTERACTION EXPERIMENT (PIX) FLIGHT RESULTS

Norman T. Grier and N. John Stevens *In its Spacecraft Charging Technol.*, 1978 1979 p 295-314 refs (For primary document see N79-24001 15-18)

Avail: NTIS HC A99/MF A01 CSCL 22B

An auxiliary payload package called PIX (plasma interaction experiment) was launched on March 5, 1978, on the LANDSAT 3 launch vehicle to study interactions between the space charged-particle environment and surfaces at high applied positive and negative voltages. Three experimental surfaces were used in this package: a plain disk to act as a control; a disk on a Kapton sheet to determine the effect of surrounding insulation on current collection; and a small solar-array segment to evaluate the effect of distributing biased surfaces among an array of insulators. Only half of the results from the 4 hours of PIX operations were recovered. The results did verify effects found in ground simulation testing. The results of this experiment are discussed in detail. G.Y.

N79-24025* National Aeronautics and Space Administration, Lewis Research Center, Cleveland, Ohio.

EFFECT OF PARASITIC PLASMA CURRENTS ON SOLAR-ARRAY POWER OUTPUT

Stanley Domitz and Joseph C. Kolecki *In its Spacecraft Charging Technol.*, 1978 1979 p 358-375 refs (For primary document see N79-24001 15-18)

Avail: NTIS HC A99/MF A01 CSCL 22B

Solar-array voltage-current curves are calculated by assuming the existence of parasitic loads that consist of local currents of charged particles collected by the array. Three cases of interest are calculated to demonstrate how the distribution and magnitude of parasitic currents affect output. Solar array performance degradation became significant when the total parasitic current plus the load current exceeded the short-circuit current. Approximate graphical methods were useful for many applications. Power loss, which was calculated by summing the product of parasitic current and the local potential, underestimated the loss in maximum power. G.Y.

N79-24030* National Aeronautics and Space Administration, Lewis Research Center, Cleveland, Ohio.

STATUS OF MATERIALS CHARACTERIZATION STUDIES
Carolyn K. Purvis. In: *its Spacecraft Charging Technol.*, 1978 1979 p 437-456 refs (For primary document see N79-24001 15-18)

Avail: NTIS HC A99/MF A01 CSCL 22B

In the context of the spacecraft charging technology investigation, studies were made to characterize the response of typical spacecraft surface materials to the charging environment. The objective is to obtain an understanding of the charging and discharging behavior of such materials for the reliable prediction of spacecraft response to charging environments and as a guide for the design of future spacecraft. Materials were characterized in terms of such basic properties as resistivity and secondary emission and in terms of charging and discharging behavior in simulated charging environments. G Y.

N79-24031* National Aeronautics and Space Administration, Lewis Research Center, Cleveland, Ohio.

TEST RESULTS FOR ELECTRON BEAM CHARGING OF FLEXIBLE INSULATORS AND COMPOSITES

John V. Staskus and Frank D. Berkopec. In: *its Spacecraft Charging Technol.*, 1978 1979 p 457-484 refs (For primary document see N79-24001 15-18)

Avail: NTIS HC A99/MF A01 CSCL 22B

Flexible solar-array substrates, graphite-fiber/epoxy - aluminum honeycomb panels, and thin dielectric films were exposed to monoenergetic electron beams ranging in energy from 2 to 20 keV in the Lewis Research Center's geomagnetic-substorm-environment simulation facility to determine surface potentials, dc currents, and surface discharges. The four solar-array substrate samples consisted of Kapton sheet reinforced with fabrics of woven glass or carbon fibers. They represented different construction techniques that might be used to reduce the charge accumulation on the array back surface. Five honeycomb-panel samples were tested, two of which were representative of Voyager antenna materials and had either conductive or nonconductive painted surfaces. A third sample was of Navstar solar-array substrate material. The other two samples were of materials proposed for use on Intelsat V. All the honeycomb-panel samples had graphite-fiber/epoxy composite face sheets. The thin dielectric films were 2.54-micrometer-thick Mylar and 7.62-micrometer-thick Kapton. A R H.

N79-24032* National Aeronautics and Space Administration, Lewis Research Center, Cleveland, Ohio.

AREA SCALING INVESTIGATIONS OF CHARGING PHENOMENA

Paul R. Aron and John V. Staskus. In: *its Spacecraft Charging Technol.*, 1978 1979 p 485-506 refs (For primary document see N79-24001 15-18)

Avail: NTIS HC A99/MF A01 CSCL 22B

The charging and discharging behavior of square, planar samples of silvered, fluorinated ethylene-propylene (FEP) Teflon thermal control tape was measured. The equilibrium voltage profiles scaled with the width of the sample. A wide range of discharge pulse characteristics was observed, and the area dependences of the peak current, charge, and pulse widths are described. The observed scaling of the peak currents with area was weaker than that previously reported. The discharge parameters were observed to depend strongly on the grounding impedance and the beam voltage. Preliminary results suggest that measuring only the return-current-pulse characteristics is not adequate to describe the spacecraft discharging behavior of this material. The seams between strips of tape appear to play a fundamental role in determining the discharging behavior. An approximate propagation velocity for the charge cleanoff was extracted from the data. The samples - 232, 1265, and 5058 square centimeters in area - were exposed at ambient temperature to a 1- to 2-nA/sq cm electron beam at energies of 10, 15, and 20 kilovolts in a 19-meter-long by 4.6-meter diameter simulation facility at the Lewis Research Center. Author

N79-24033* National Aeronautics and Space Administration, Lewis Research Center, Cleveland, Ohio.

CHARGING RATES OF METAL-DIELECTRIC STRUCTURES
Carolyn K. Purvis, John V. Staskus, James C. Roche, and Frank D. Berkopec. In: *its Spacecraft Charging Technol.*, 1978 1979 p 507-523 refs (For primary document see N79-24001 15-18)

Avail: NTIS HC A99/MF A01 CSCL 22B

Metal plates partially covered by 0.01-centimeter-thick fluorinated ethylene-propylene (FEP) Teflon were charged in the Lewis Research Center's geomagnetic substorm simulation facility using 5-, 8-, 10-, and 12-kilovolt electron beams. Surface voltage as a function of time was measured for various initial conditions (Teflon discharged or precharged) with the metal plate grounded or floating. Results indicate that both the charging rates and the levels to which the samples become charged are influenced by the geometry and initial charge state of the insulating surfaces. The experiments are described and the results are presented and discussed. NASA charging analyzer program (NASCAP) models of the experiments have been generated, and the predictions obtained are described. Implications of the study results for spacecraft are discussed. Author

N79-31265* National Aeronautics and Space Administration, Lewis Research Center, Cleveland, Ohio.

NASCAP MODELLING OF ENVIRONMENTAL-CHARGING-INDUCED DISCHARGES IN SATELLITES

N. John Stevens and James C. Roche. 1979 25 p refs Presented at Ann. Conf. on Nucl. and Space Radiation Effects, Santa Cruz, Calif. 17-20 Jul. 1979; sponsored by IEEE (NASA-TM-79247; E-155) Avail: NTIS HC A02/MF A01 CSCL 22B

The charging and discharging characteristics of a typical geosynchronous satellite experiencing time-varying geomagnetic substorms, in sunlight, were studied utilizing the NASA Charging Analyzer Program (NASCAP). An electric field criteria of 150,000 volts/cm to initiate discharges and transfer of 67 percent of the stored charge was used based on ground test results. The substorm characteristics were arbitrarily chosen to evaluate effects of electron temperature and particle density (which is equivalent to current density). It was found that while there is a minimum electron temperature for discharges to occur, the rate of discharges is dependent on particle density and duration times of the encounter. Hence, it is important to define the temporal variations in the substorm environments. J M S.

A79-30139 * Insulator edge voltage gradient effects in spacecraft charging phenomena. N. J. Stevens, C. K. Purvis, and J. V. Staskus (NASA, Lewis Research Center, Cleveland, Ohio). (IEEE, DNA, NASA, and DOE Annual Conference on Nuclear and Space Radiation Effects, 15th, Albuquerque, N. Mex., July 18-21, 1979.) IEEE Transactions on Nuclear Science, vol. NS-25, Dec. 1978, p. 1304-1312. 22 refs.

Insulating surfaces on geosynchronous satellites have been charged by geomagnetic substorms to a point where discharges occur. The electromagnetic pulses from these discharges couple into satellite electronic systems disrupting operations. Laboratory tests conducted on insulator charging have indicated that discharges appear to be initiated at insulator edges where voltage gradients can exist. An experimental investigation has been conducted to measure edge voltage gradients on silvered Teflon samples as they are charged by monoenergetic electron beams. It has been found that the surface voltage at insulator edges can be approximated by an exponential expression based on an electron current density balance. Using this expression at known breakdown conditions results in a discharge voltage gradient down the insulator edge to ground of about 150,000 V/cm. (Author)

A79-30140 * The decrease in effective photocurrents due to saddle points in electrostatic potentials near differentially charged spacecraft. M. J. Mandell, I. Katz, G. W. Schnuelle, P. G. Steen (Systems, Science and Software, La Jolla, Calif.), and J. C. Roche (NASA, Lewis Research Center, Cleveland, Ohio). (IEEE, DNA, NASA, and DOE, Annual Conference on Nuclear and Space Radiation Effects, 15th, Albuquerque, N. Mex., July 18-21, 1978.) IEEE Transactions on Nuclear Science, vol. NS-25, Dec. 1978, p. 1313-1317. 9 refs. Contract No. NAS3-21050.

The reported investigation had the objective to illustrate the presence of important multidimensional effects in spacecraft charging. Two-dimensional codes have been under development by Parker (1976). A description is presented of a calculation which was performed using the three-dimensional NASA Charging Analyzer Program (NASCAP). NASCAP was run to calculate the electrostatic potentials on the surface of, and in the space surrounding, a sunlit Teflon-coated sphere. Currents to the sunlit surfaces were determined on the basis of an approximate photosheath model for strong differential charging. G.R.

A79-23511 * # Space environmental interactions with spacecraft surfaces. N. J. Stevens (NASA, Lewis Research Center, Cleveland, Ohio). American Institute of Aeronautics and Astronautics, Aerospace Sciences Meeting, 17th, New Orleans, La., Jan. 15-17, 1979, Paper 79-0386. 25 p. 47 refs.

The employment of large structures in space, which would be necessary in connection with a number of space missions and space activities currently being contemplated, might involve special problems as a result of the interactions of the structures with the charged particle environment. Such interactions would be particularly significant in the case of high operational voltages. A review is presented of possible interactions between spacecraft surfaces and charged particle environments. The categories of spacecraft-environmental interactions are examined and a description of spacecraft charging interactions is presented. The status of charging investigation is considered, taking into account the environment, aspects of analytical modeling, materials characterization, materials development, space flight experiments, and design guidelines. High voltage surface plasma interactions are also investigated. G.R.

N79-24007*# California Univ., San Diego
OPERATIONS OF THE ATS-6 ION ENGINE
R. C. Olsen, and E. C. Whipple. In NASA, Lewis Res. Center Spacecraft Charging Technol., 1978-1979 p. 59-68. refs (For primary document see N79-24001 15-18)
(Grant NSG-3150)

Avail. NTIS HC A99/MF A01 CSCL 22B

The ion engine experiments on ATS 6 were operated in daylight and eclipse. The effect on particle fluxes to the spacecraft was monitored with the UCSD Auroral Particles Experiment. These data also provide information on the potential of the spacecraft with respect to the ambient plasma and on the local electric fields caused by the charge distribution on the satellite. Daylight operations of the plasma bridge neutralizer and the cesium thruster in fall, 1974 served to hold the spacecraft between -3 and -8 volts with respect to the ambient plasma. Neutralizer operation reduced differential charging effects, while operation of the thruster usually reduced the effects below the detectors sensitivity. Eclipse operations of the neutralizer reduced kilovolt negative potentials to a few volts. Operation of the thruster prevented possible charging of the satellite during substorms, making it possible to study low energy particle spectra which are at times obscured by charging during substorms. J.M.S.

N79-24008*# California Univ., San Diego
CHARACTERISTICS OF DIFFERENTIAL CHARGING OF ATS-6
Bruce Johnson and Elden C. Whipple. In NASA, Lewis Res. Center Spacecraft Charging Technol., 1978-1979 p. 69-79. refs (For primary document see N79-24001 15-18)
(Grant NSG-3150)

Avail. NTIS HC A99/MF A01 CSCL 22B

Thirteen days of data collected by the Auroral Particle Experiment on board the ATS 6 were analyzed emphasizing peculiarities in the electron data attributed to differential charging. On one of these days the satellite was eclipsed by the earth at local midnight. Spectrograms were used to examine the data. It is concluded that differential charging is responsible for returning photoelectrons to the spacecraft up to a couple hundred eV, depending on the spacecraft charge. It is believed that the Minnesota experiment on ATS 6 is largely responsible for producing a potential barrier that returns particles and produces intense spots in the count rates. J.M.S.

N79-24038*# Pennsylvania State Univ., University Park
POTENTIAL MAPPING WITH CHARGED-PARTICLE BEAMS

James W. Robinson and David G. Tillery. In NASA, Lewis Res. Center Spacecraft Charging Technol., 1978-1979 p. 606-620. refs (For primary document see N79-24001 15-18)
(Grant NSG-3166)

Avail. NTIS HC A99/MF A01 CSCL 22B

Experimental methods of mapping the equipotential surfaces near some structure of interest rely on the detection of charged particles which have traversed the regions of interest and are detected remotely. One method is the measurement of ion energies for ions created at a point of interest and expelled from the region by the fields. The ion energy at the detector in eV corresponds to the potential where the ion was created. An ionizing beam forms the ions from background neutrals. The other method is to inject charged particles into the region of interest and to locate their exit points. A set of several trajectories becomes a data base for a systematic mapping technique. An iterative solution of a boundary value problem establishes concepts and limitations pertaining to the mapping problem. A.R.H.

N79-24046*# Pennsylvania State Univ., University Park
STABLE DIELECTRIC CHARGE DISTRIBUTIONS FROM FIELD ENHANCEMENT OF SECONDARY MISSION

James W. Robinson. In NASA, Lewis Res. Center Spacecraft Charging Technol., 1978-1979 p. 734-746. refs (For primary document see N79-24001 15-18)
(Grant NSG-3097)

Avail. NTIS HC A99/MF A01 CSCL 22B

The emission of secondary electrons from dielectrics subject to numerous effects of electric field which are experimentally difficult to control is discussed. Measurements are reported using pulse techniques such that local fields do not build to significant levels, but measurements with fields present are also of interest. A specific series of measurements under controlled conditions are described and their implications in terms of fields, magnitude and angle, near the dielectric surface were examined. The measurements were made for a charged fluorinated ethylene-propylene surface near a grounded aluminum half-round resting on the surface. The geometry produced a stable surface-charge gradient being controlled by a strongly enhanced secondary emission for which a model is constructed. Observations of surface flashovers under various conditions confirm the predictions of some scaling exercises. S.E.S.

N79-24012*# Systems Science and Software, La Jolla, Calif.
CHARGING ANALYSIS OF THE SCATHA SATELLITE
G. W. Schnuelle, D. E. Parks, I. Kaz, M. J. Mandell, P. C. Steen, J. J. Cassidy, and A. G. Rubin (AFGL). In NASA, Lewis Res. Center Spacecraft Charging Technol., 1978-1979 p. 123-143. refs (For primary document see N79-24001 15-18)
(Contract NAS3-21050)

Avail. NTIS HC A99/MF A01 CSCL 22B

A detailed model of the geometrical, material, and electrical properties of the SCATHA satellite for use with the NASA charging analyzer program is described. Charging calculations in an intense magnetospheric substorm environment demonstrated that (1) long booms can significantly perturb the potentials near the spacecraft and (2) discharging by sunlight or by active control can cause serious time-dependent differential charging problems. J.A.M.

N79-24049* # Hiram Coll., Ohio.

**GEOSYNCHRONOUS SATELLITE OPERATING ANOMALIES
CAUSED BY INTERACTION WITH THE LOCAL SPACE-
CRAFT ENVIRONMENT**

Michael A. Grajek and Donald A. McPherson (Science Applications, Inc.) In NASA, Lewis Res. Center Spacecraft Charging Technol., 1978 1979 p 769-782 refs (For primary document see N79-24001 15-18)

(Contracts NAS3-21048; F04071-77-C-0166)

Avail: NTIS HC A99/MF A01 CSCL 22B

The dependence of a spacecraft anomaly or event upon geophysical parameters established on the basis of statistical analysis is presented. Examples are provided for establishing relationships between events and parameters such as geomagnetic activity, local time, and events on other spacecraft. Examples illustrated the potential dangers of not using quantitative statistical techniques it was recommended that the data collection planning and statistical analysis planning be done together. Results demonstrate a high correlation between the events and the geophysical parameter being investigated. S.E.S.

N79-24051* # Science Applications, Inc., La Jolla, Calif.

**SPACECRAFT CHARGING MODELING DEVELOPMENT
AND VALIDATION STUDY**

E. E. O'Donnell In NASA, Lewis Res. Center Spacecraft Charging Technol., 1978 1979 p 797-816 refs (For primary document see N79-24001 15-18)

(Contracts NAS3-21048; F04071-77-C-0166)

Avail: NTIS HC A99/MF A01 CSCL 22B

The effects of spacecraft charging are presented. Analytical models of the magnetospheric environment are used to show the charging interaction between the spacecraft and the plasma sheath, the discharge phenomena, and electromagnetic coupling from the discharge to spacecraft components. Ground tests to validate the models are described. M.M.M.

N79-27234* # General Dynamics/Convair, San Diego, Calif.

ATLAS 5013 TANK CORROSION TEST Final Report

W. M. Sutherland, L. D. Girton, and D. G. Treadway Dec. 1978 133 p refs

(Contract NAS3-20644)

(NASA-CR-158760; CASD-LVP-78-078)

HC A07/MF A01 CSCL 22B

Avail: NTIS

The type and cause of corrosion in spot welded joints were determined by X-ray and chemical analysis. Fatigue and static tests showed the degree of degradation of mechanical properties. The corrosion inhibiting effectiveness of WD-40 compound and required renewal period by exposing typical joint specimens were examined. M.M.M.

19 SPACECRAFT INSTRUMENTATION

For related information see also 06 Aircraft Instrumentation and 35 Instrumentation and Photography.

A79-39806 * # NASCAP modelling of high-voltage power system interactions with space charged-particle environments. N. J. Stevens, J. C. Roche (NASA, Lewis Research Center, Cleveland, Ohio), and M. J. Mandel (System, Science and Software, La Jolla, Calif.). *Institute of Electrical and Electronics Engineers, High Voltage Workshop, Anaheim, Calif., Feb. 26, 27, 1979, Paper.* 18 p. 22 refs.

The NASA Charging Analyzer Program (NASCAP), an engineering tool capable of analyzing the impact of the charged particle environment on spacecraft surfaces and systems, is described. NASCAP is a quasi-static computational program which analyzes the charging of a 3-dimensional complex body as a function of time and system-generated voltages for given space environmental conditions. The material properties of the surfaces are taken into account, the surface potentials, low energy sheath, potential distribution in space and particle trajectories are calculated. An application of NASCAP to a simple space solar power station consisting of two 6 m by 18 m solar array wings surrounding a central body is presented. Each solar array wing is considered to be divided into three regions operating at 2000 volts. Results of NASCAP analysis of the system for a normal environment and a moderate geomagnetic substorm environment are discussed.

C.K.D.

20 SPACECRAFT PROPULSION AND POWER

Includes main propulsion systems and components e.g., rocket engines, and spacecraft auxiliary power sources. For related information see also 07 Aircraft Propulsion, 28 Propellants and Fuels, and 44 Energy Production and Conversion.

N79-10122* National Aeronautics and Space Administration, Lewis Research Center, Cleveland, Ohio.

FUTURE ORBITAL POWER SYSTEMS TECHNOLOGY REQUIREMENTS

Sep 1978 195 p refs Symp. held at Cleveland, 31 May - 1 Jun 1978

(NASA-CF-2058; E-9713) Avail: NTIS HC A09/MF A01 CSCL 10A

NASA is actively involved in program planning for missions requiring several orders of magnitude, more energy than in the past. Therefore, a two-day symposium was held to review the technology requirements for future orbital power systems. The purpose of the meeting was to give leaders from government and industry a broad view of current government supported technology efforts and future program plans in space power. It provided a forum for discussion, through workshops, to comment on current and planned programs and to identify opportunities for technology investment. Several papers are presented to review the technology status and the planned programs. For individual titles, see N79-10123 through N79-10143.

N79-10130* National Aeronautics and Space Administration, Lewis Research Center, Cleveland, Ohio.

A BRIEF SURVEY OF THE SOLAR CELL STATE-OF-THE-ART

Daniel T. Bernatowicz. In its Future Orbital Power Systems Technol. Requirements. Sep. 1978. p 133-146 refs (For primary document see N79-10122 01-20)

Avail: NTIS HC A09/MF A01 CSCL 10A

Modern high performance cells made for space are discussed. The major recent developments that are expected to influence what solar cells will be available in five years or so are described. G Y

N79-10132* National Aeronautics and Space Administration, Lewis Research Center, Cleveland, Ohio.

TECHNOLOGY STATUS: BATTERIES AND FUEL CELLS

J. Stuart Fordyce. In its Future Orbital Power Systems Technol. Requirements. Sep. 1978. p 157-166 refs (For primary document see N79-10122 01-20)

Avail: NTIS HC A09/MF A01 CSCL 10A

The current status of research and development programs on batteries and fuel cells and the technology goals being pursued are discussed. Emphasis is placed upon those technologies relevant to earth orbital electric energy storage applications. G Y

N79-10139* National Aeronautics and Space Administration, Lewis Research Center, Cleveland, Ohio.

AN ECONOMICAL APPROACH TO SPACE POWER SYSTEMS

Fred Teren. In its Future Orbital Power Systems Technol. Requirements. Sep. 1978. p 265-270 (For primary document see N79-10122 01-20)

Avail: NTIS HC A09/MF A01 CSCL 10A

Projected energy demand for all NASA, DoD and civil missions for the time span 1981 to 1995 are illustrated. Typical energy cost range from about \$300 to \$2000 per kW-hr, with an average of about \$800 per kW-hr for long-duration missions. At these levels, the cost of the required energy would be several billion dollars per year by about 1985 and might constrain the number and types of NASA programs to be carried out. NASA is extensively pursuing approaches for reducing nonrecurring costs

Two programs are presented for the development of an economical approach to space power systems. They are: (1) Economical Orbital Power (ECOP) with the objective to demonstrate the applicability of a commercial approach to the development of a low cost photovoltaic space power system; and (2) Space Power Experiment (SPEX) which has the objective to demonstrate the application of industrial hardware for space power systems. G Y

N79-20179* National Aeronautics and Space Administration, Lewis Research Center, Cleveland, Ohio.

CLOSED LOOP SOLAR ARRAY-ION THRUSTER SYSTEM WITH POWER CONTROL CIRCUITRY Patent

Robert P. Gruber, inventor (to NASA). Issued 6 Mar. 1979. 8 p. Filed 29 Mar. 1978. Supersedes N78-22149 (16 - 13, p 1673)

(NASA-Case-LEW-12780-1; US-Patent-4,143,314;

US-Patent-Appl-SN-891370; US-Patent-Class-323-15;

US-Patent-Class-323-20) Avail: US Patent and Trademark Office CSCL 20C

A power control circuit connected between a solar array and an ion thruster receives voltage and current signals from the solar array. The control circuit multiplies the voltage and current signals together to produce a power signal which is differentiated with respect to time. The differentiator output is detected by a zero crossing detector and, after suitable shaping, the detector output is phase compared with a clock in a phase demodulator. An integrator receives no output from the phase demodulator when the operating point is at the maximum power but is driven toward the maximum power point for non-optimum operation. A ramp generator provides minor variations in the beam current reference signal produced by the integrator in order to obtain the first derivative of power.

Official Gazette of the U.S. Patent and Trademark Office

N79-20180* National Aeronautics and Space Administration, Lewis Research Center, Cleveland, Ohio.

AN OXIDE DISPERSION STRENGTHENED ALLOY FOR GAS TURBINE BLADES

T. K. Glasgow. 1979. 13 p refs. Presented at the 20th Structures, Structural Dyn. and Mater. Conf., St. Louis, 4-6 Apr. 1979; sponsored by AIME and the Am. Soc. of Civil Engrs.

(NASA-TM-79088; E-9912) Avail: NTIS HC A02/MF A01 CSCL 21H

The strength of the newly developed alloy MA-6000E is derived from a nickel alloy base, an elongated grain structure, naturally occurring precipitates of gamma prime, and an artificial distribution of extremely fine, stable oxide particles. Its composition is Ni-15Cr-2Mo-2Ta-4W-4.5Al-2.5Ti-0.15Zr-0.05C-0.01B-1.1Y2O3. It exhibits the strength of a conventional nickel-base alloy at 1400 F but is quite superior at 2000 F. Its shear strength is relatively low, necessitating consideration of special joining procedures. Its high cycle, low cycle, and thermal fatigue properties are excellent. The relationship between alloy microstructure and properties is discussed. Author

N79-22190* National Aeronautics and Space Administration, Lewis Research Center, Cleveland, Ohio.

PRIMARY ELECTRIC PROPULSION FOR FUTURE SPACE MISSIONS

David C. Byers, Fred F. Terdan, and Ira T. Myers. 1979. 45 p refs. Presented at the Conf. on Adv. Technol. for Future Space Systems, Langley, Va., 8-11 May 1979; sponsored in part by AIAA.

(NASA-TM-79141; E-9994) Avail: NTIS HC A03/MF A01 CSCL 20C

A general methodology is presented which allows prediction of the overall characteristics of thrust systems employing electron-bombardment ion thrusters. Elements of the thrust system are defined and their characteristics presented in a parametric fashion. Two system approaches are evaluated where power management and control elements and thruster characteristics were substantially different. For an assumed system approach, the methodology presented predicts overall system properties, such as input power and mass, when major mission and thrust

system parameters, such as trip time and specific impulse, are assumed. Author

N79-22191* National Aeronautics and Space Administration, Lewis Research Center, Cleveland, Ohio.

RESULTS FROM SYMPOSIUM ON FUTURE ORBITAL POWER SYSTEMS, TECHNOLOGY REQUIREMENTS

Sol Gorland 1979 8 p refs To be presented at the 14th Intersoc. Energy Conversion Eng. Conf., Boston, 5-10 Aug. 1979; sponsored by the Am. Chem. Soc. (NASA-TM-79125; E-9961) Avail. NTIS HC A02/MF A01 CSCL 10B

The technology requirements for future orbital power systems were reviewed. Workshops were held in 10 technology disciplines to discuss technology deficiencies, adequacy of current programs to resolve those deficiencies and recommendations for tasks that might reduce the testing and risks involved in future orbital energy systems. These recommendations are summarized. J.M.S.

N79-22192* National Aeronautics and Space Administration, Lewis Research Center, Cleveland, Ohio

INCREASED CAPABILITIES OF THE 30-cm DIAMETER Hg ION THRUSTER

Vincent K. Rawlin and Charles E. Hawkins 1979 22 p refs Presented at the Conf. on Advanced Technol. for Future Space Systems, Langley, Va., 8-11 May 1979; sponsored by AIAA (NASA-TM-79142; E-9995) Avail. NTIS HC A02/MF A01 CSCL 21C

Some space flight missions require advanced ion thrusters which operate at conditions much different than those for which the baseline 30-cm Hg thruster was developed. Results of initial tests of a 30-cm Hg thruster with two and three grid ion accelerating systems, operated at higher values of both thrust and power and over a greater range of specific impulse than the baseline conditions are presented. Thruster lifetime at increased input power was evaluated both by extended tests and real time spectroscopic measurements. Author

N79-22193* National Aeronautics and Space Administration, Lewis Research Center, Cleveland, Ohio.

AN ECONOMIC ANALYSIS OF A COMMERCIAL APPROACH TO THE DESIGN AND FABRICATION OF A SPACE POWER SYSTEM

Zimri Putney (Solarrex Corp., Rockville, Md.) and Julian Been 1979 8 p refs Presented at the Conf. on Adv. Technol. for Future Space Systems, Hampton, 8-11 May 1979; sponsored by AIAA (NASA-TM-79153; E-1009) Avail. NTIS HC A02/MF A01 CSCL 10A

A commercial approach to the design and fabrication of an economical space power system is presented. Cost reductions are projected through the conceptual design of a 2 kW space power system built with the capability for having serviceability. The approach to system costing that is used takes into account both the constraints of operation in space and commercial production engineering approaches. The cost of this power system reflects a variety of cost/benefit tradeoffs that would reduce system cost as a function of system reliability requirements, complexity, and the impact of rigid specifications. A breakdown of the system design, documentation, fabrication, and reliability and quality assurance cost estimates are detailed. J.M.S.

N79-23132* National Aeronautics and Space Administration, Lewis Research Center, Cleveland, Ohio

EFFECT OF LOW-STIFFNESS CLOSEOUT OVERWRAP ON ROCKET THRUST-CHAMBER LIFE

Harold J. Kasper and J. Joseph Nota-donato May 1979 23 p refs (NASA-TP-1456; E-9870) Avail. NTIS HC A03/MF A01 CSCL 21H

Three rocket thrust chambers with copper liners and a thrust level of 209 kN were cyclically test fired to failure. Two

of the liners were made from oxygen free, high conductivity (OFHC) copper and from annealed Armzinc. The milled coolant channels were closed out with a thin copper closeout over which a fiberglass composite was wrapped to provide hoop strength only. Experimental data are presented, along with the results of a preliminary analysis that was performed before fabrication to evaluate the life extending potential of a thin copper closeout with a fiberglass overwrap. Author

N79-23133* National Aeronautics and Space Administration, Lewis Research Center, Cleveland, Ohio.

THE ROLE OF FUEL CELLS IN NASA'S SPACE POWER SYSTEMS

Julian F. Been 1979 11 p refs To be presented at the 14th Energy Conversion Eng. Conf., Boston, 5-10 Aug. 1979 (NASA-TM-79182; E-042) Avail. NTIS HC A02/MF A01 CSCL 22B

A history of the fuel cell technology is presented and compared with NASA's increasing space power requirements. The role of fuel cells is discussed in perspective with other energy storage systems applicable for space using such criteria as type of mission, weight, reliability, costs, etc. Potential applications of space fuel cells with projected technology advances were examined. S.E.S.

N79-25131* National Aeronautics and Space Administration, Lewis Research Center, Cleveland, Ohio.

THE 30-CENTIMETER ION THRUST SUBSYSTEM DESIGN MANUAL

Jun. 1979 579 p refs (NASA-TM-79191; E-060) Avail. NTIS HC A25/MF A01 CSCL 09C

The principal characteristics of the 30-centimeter ion propulsion thrust subsystem technology that was developed to satisfy the propulsion needs of future planetary and early orbital missions are described. Functional requirements and descriptions, interface and performance requirements, and physical characteristics of the hardware are described at the thrust subsystem, BIMOD engine system, and component level. G.Y.

N79-28220* National Aeronautics and Space Administration, Lewis Research Center, Cleveland, Ohio.

NATIONAL AERONAUTICS AND SPACE ADMINISTRATION PLANS FOR SPACE COMMUNICATION TECHNOLOGY

Robert E. Alexovich 1979 13 p refs Proposed for presentation at EASCON Session on Communications Satellite Technol., Washington, D. C., 9-11 Oct. 1979; sponsored by IEEE (NASA-TM-79217; E-107) Avail. NTIS HC A02/MF A01 CSCL 17B

A program plan is presented for a space communications application utilizing the 30/20 GHz frequency bands (30 GHz uplink and 20 GHz downlink). Results of market demand studies and spacecraft systems studies which significantly affect the supporting research and technology program are also presented, along with the scheduled activities of the program plan. Author

N79-30290* National Aeronautics and Space Administration, Lewis Research Center, Cleveland, Ohio.

CHARACTERISTICS OF PRIMARY ELECTRIC PROPULSION SYSTEMS

David C. Byers 1979 17 p refs Proposed for Presentation at 14th Intern. Conf. on Elec. Propulsion, Princeton, N. J., 31 Oct. - 2 Nov. 1979; sponsored by AIAA and GLR (NASA-TM-79255; E-166) Avail. NTIS HC A02/MF A01 CSCL 21C

The use of advanced electric propulsion systems is expected to provide cost and performance benefits for future energetic space missions. A methodology to predict the characteristics of advanced electric propulsion systems was developed and programmed for computer calculations to allow evaluation of a broad set of technology and mission assumptions. The impact on overall thrust system characteristics was assessed for variations

of propellant type, total accelerating voltage, thruster area, specific impulse, and power system approach. The data may be used both to provide direction to technology emphasis and allow for preliminary estimates of electric propulsion system properties for a wide variety of applications. Author

N79-31343* National Aeronautics and Space Administration, Lewis Research Center, Cleveland, Ohio.

SPUTTERING IN MERCURY ION THRUSTERS

Maris A. Mantieniks and Vincent K. Rawlin 1979 20 p refs Presented at 14th Intern. Conf. on Electric Propulsion, Princeton, N. J., 31 Oct. - 2 Nov. 1979; sponsored by AIAA and Deutsche Gesellschaft fuer Luft- und Raumfahrt (NASA-TM-79266; E-181) Avail: NTIS HC A02/MF A01 CSCL 21C

A model, which assumes that chemisorption is the dominant mechanism, is applied to the sputtering rate measurements of the screen grid of a 30 cm thruster in the presence of nitrogen. The model utilizes inputs from a variety of experimental and analytical sources. The model of environmental effects on sputtering was applied to thruster conditions of low discharge voltage and a discussion of the comparison of theory and experiment is presented. M M M

N79-33252* National Aeronautics and Space Administration, Lewis Research Center, Cleveland, Ohio

SERT 2 1979 EXTENDED FLIGHT THRUSTER SYSTEM PERFORMANCE

W R Kerslake and L R Ignaczak 1979 22 p refs Presented at 14th Intern. Conf. on Electric Propulsion, Princeton, N. J., 31 Oct. - 2 Nov. 1979; sponsored by AIAA and Deutsche Gesellschaft fuer Luft- und Raumfahrt (NASA-TM-79256; E-168; AIAA-Paper-79-2063) Avail: NTIS HC A02/MF A01 CSCL 21H

Steady state tests of the thruster 2 system on the SERT 2 spacecraft are presented. A direct thrust measurement was obtained for the ion thruster during operations to increase the spacecraft spin rate to maintain spacecraft attitude stability. The continued restart tests of thruster 1 and a report on the general status of all spacecraft systems including the main solar array are presented. A W H

N79-33253* National Aeronautics and Space Administration, Lewis Research Center, Cleveland, Ohio

REDUCED POWER PROCESSOR REQUIREMENTS FOR THE 30-cm DIAMETER Hg ION THRUSTER

Vincent K. Rawlin 1979 14 p refs Presented at the 14th Intern. Conf. on Electric Propulsion, Princeton, N. J., 30 Oct. - 1 Nov. 1979; sponsored by AIAA and Deutsche Gesellschaft fuer Luft- und Raumfahrt (NASA-TM-79257; E-169; AIAA Paper 79-2081) Avail: NTIS HC A02/MF A01 CSCL 21C

An evaluation of simplifications for the thruster power processor interface for a 30 cm Hg ion thruster is presented. Tests on the engine, thruster control, and the power supplies are performed. Reduced power processors requirements are defined and the impact on thruster design, performance and lifetime are assessed. A W H

N79-33254* National Aeronautics and Space Administration, Lewis Research Center, Cleveland, Ohio

PRELIMINARY RESULTS OF THE MISSION PROFILE LIFE TEST OF A 30 cm Hg BOMBARDMENT THRUSTER

R T Bechtel and E L James (Xerox-EOS, Pasadena, Calif.) 1979 23 p refs Presented at 14th Intern. Conf. on Electric Propulsion, Princeton, N. J., 31 Oct. - 2 Nov. 1979; sponsored by AIAA and Deutsche Gesellschaft fuer Luft- und Raumfahrt (NASA-TM-79261; E-175) Avail: NTIS HC A02/MF A01 CSCL 20C

Long term tests were performed on a 30 cm Hg bombardment thruster and a power processing unit to determine lifetime characteristics. The thruster performance data and other operational characteristics taken at various times during the test segment are presented and evaluated with the life limiting mechanisms: discharge chamber erosion, deposition and spalling,

external erosion, cathode degradation, and propellant isolator leakage. The control algorithms for thruster start up, steady state operation, throttle, detection and correction of off normal conditions, and shutdown are discussed. A W H

N79-33255* National Aeronautics and Space Administration, Lewis Research Center, Cleveland, Ohio

NEUTRALIZATION TESTS ON THE SERT 2 SPACECRAFT

William R Kerslake and Stanley Domitz 1979 24 p refs Presented at 14th Intern. Conf. on Electric Propulsion, Princeton, N. J., 31 Oct. - 2 Nov. 1979; sponsored by AIAA and Deutsche Gesellschaft fuer Luft- und Raumfahrt (NASA-TM-79271; E-191; AIAA-Paper-79-2064; Avail: NTIS HC A02/MF A01 CSCL 22B

Neutralization test data obtained on the SERT 2 spacecraft are presented. Tests included ion beam neutralization of a thruster by a close (normal design) neutralizer as well as by a distant (1 meter) neutralizer. Parameters affecting neutralization, such as neutralizer bias voltage, neutralizer anode voltage, local spacecraft plasma density, and solar array voltage configuration were varied and changes in plasma potentials were measured. A plasma model is presented as an approximation of observed results. A W H

A79-10014 * Status of wraparound contact solar cells and arrays. C. R. Baraona (NASA, Lewis Research Center, Cleveland, Ohio) and L. E. Young (NASA, Marshall Space Flight Center, Huntsville, Ala.). In: Intersociety Energy Conversion Engineering Conference, 13th, San Diego, Calif., August 20-25, 1978, Proceedings, Volume 1. (A79-10001 01-44) Warrendale, Pa., Society of Automotive Engineers, Inc., 1978, p. 84-90, 13 refs.

The paper describes the development of wraparound contact solar cell technology. Future development trends are distinguished. The current method of module fabrication with wraparound contact cells is briefly reviewed. The prospects for automated cell assembly are discussed. P.T.H.

A79-34704 * Space propulsion technology overview. J. J. Pelouch, Jr. (NASA, Lewis Research Center, Propulsion Systems Section, Cleveland, Ohio). In: Conference on Advanced Technology for Future Space Systems, Hampton, Va., May 8-10, 1979, Technical Papers. (A79-34701 14-12) New York, American Institute of Aeronautics and Astronautics, Inc., 1979, p. 24-29. (AIAA 79-0860)

This paper discusses Shuttle-era, chemical and electric propulsion technologies for operations beyond the Shuttle's orbit with focus on future mission needs and economic effectiveness. The adequacy of the existing propulsion state-of-the-art, barriers to its utilization, benefit of technology advances, and the prognosis for advancement are the themes of the discussion. Low thrust propulsion for large space systems is cited as a new technology with particularly high benefit. It is concluded that the Shuttle's presence for at least two decades is a legitimate basis for new propulsion technology, but that this technology must be predicated on an awareness of mission requirements, economic factors, influences of other technologies, and real constraints on its utilization. (Author)

A79-34736 * Some effects of cyclic induced deformation in rocket thrust chambers. N. P. Hannum, R. J. Quentmeyer, and H. J. Kasper (NASA, Lewis Research Center, Cleveland, Ohio). In: Conference on Advanced Technology for Future Space Systems, Hampton, Va., May 8-10, 1979, Technical Papers. (A79-34701 14-12) New York, American Institute of Aeronautics and Astronautics, Inc., 1979, p. 290-299, 8 refs. (AIAA 79-0911)

A test program to investigate the deformation process observed in the hot gas wall of rocket thrust chambers was conducted using three different liner materials. Five thrust chambers were cycled to failure using hydrogen and oxygen as propellants at a chamber pressure of 4.14 MN/sq m. The deformation was observed nondestructively at midlife points and destructively after failure occurred. The cyclic life results are presented with an accompanying discussion.

about the types of failure encountered. Data indicating the deformation of the thrust chamber liner as cycles are accumulated are presented for each of the test thrust chambers. (Author)

A79-34737 * # An economic analysis of a commercial approach to the design and fabrication of a space power system. Z. Putney (Solarex Corp., Rockville, Md.) and J. Beer (NASA, Lewis Research Center, Cleveland, Ohio). In: Conference on Advanced Technology for Future Space Systems, Hampton, Va., May 8-10, 1979, Technical Papers. (A79-34701 14-12) New York, American Institute of Aeronautics and Astronautics, Inc., 1979, p. 300-305. 6 refs. (AIAA 79-0914)

This paper discusses a commercial approach to the design and fabrication of an economical space power system. With the advent of the space shuttle, steps can be taken to back away from the presently used space qualified approach in order to reduce cost of space hardware by incorporating, where possible, commercial design, fabrication, and quality assurance methods. Cost reductions are projected through the conceptual design of a 2 kW space power system built with the capability for having serviceability. The approach to system costing that has been used takes into account both the constraints of operation in space and commercial production engineering approaches. The cost of this power system reflects a variety of cost/benefit tradeoffs that would reduce system cost as a function of system reliability requirements, complexity, and the impact of rigid specifications. A breakdown of the system design, documentation, fabrication and reliability and quality assurance cost estimates are detailed. (Author)

A79-34773 * # Primary electric propulsion for future space missions. D. C. Byers, F. F. Terdan, and I. T. Myers (NASA, Lewis Research Center, Cleveland, Ohio). In: Conference on Advanced Technology for Future Space Systems, Hampton, Va., May 8-10, 1979, Technical Papers. New York, American Institute of Aeronautics and Astronautics, Inc., 1979, 43 p. 27 refs. (AIAA 79-0881)

The paper presents data and a methodology to allow preliminary definition of electric propulsion systems. The elements comprising the thrust system are described parametrically. As an example, thruster performance is presented as a function of specific impulse and propellant type. Two power management and control (PMAC) approaches are considered to illustrate the use of the methodology. Power source characteristics are disregarded in the system description. One PMAC concept assumes a dc power input to the thrust system and all thruster power conditioned in a conventional manner; the other PMAC approach assumes an ac power source. S.D.

A79-34774 * # Increased capabilities of the 30-cm diameter Hg ion thruster. V. K. Rawlin and C. E. Hawkins (NASA, Lewis Research Center, Cleveland, Ohio). In: Conference on Advanced Technology for Future Space Systems, Hampton, Va., May 8-10, 1979, Technical Papers. New York, American Institute of Aeronautics and Astronautics, Inc., 1979, 20 p. 21 refs. (AIAA 79-0910)

A 30-cm-diam mercury ion thruster, using two or three grid ion accelerating systems, is operated at increased values of beam current. Comparisons with the SEP (Solar Electric Propulsion) and EPSEP (Extended Performance SEP) baseline thrusters are made with respect to performance and lifetime. It is found that when a third, or decelerator, grid is added to the conventional two-grid optics of a SEP-like thruster, the ion beam focusing properties are improved, as expected from theoretical considerations. The total thruster efficiency as a function of specific impulse, is increased for values of specific impulse in the range 1200-2800 sec. Lifetime test results predict a thruster lifetime, under space conditions, not less than that of the baseline SEP thruster. S.D.

A79-34775 * # Large space system - Charged particle environment interaction technology. N. J. Stevens, J. C. Roche, and N. T. Grier (NASA, Lewis Research Center, Cleveland, Ohio). In: Conference on Advanced Technology for Future Space Systems, Hampton, Va., May 8-10, 1979, Technical Papers. New York, American Institute of Aeronautics and Astronautics, Inc., 1979, 21 p. 31 refs. (AIAA 79-0913)

Large high-voltage space power systems proposed for future applications in both low earth orbit and geosynchronous altitudes must operate in the space charged-particle environment with possible interactions between this environment and the high-voltage surfaces. The paper reviews the ground experimental work to provide indicators for the interactions that could exist in the space power system. A preliminary analytical model of a large space power system is constructed using the existing NASA Charging Analyzer Program, and its performance in geosynchronous orbit is evaluated. The analytical results are used to illustrate the regions where detrimental interactions could exist and to establish areas where future technology is required. S.D.

A79-38972 * # Plug cluster engine concept for in-space missions. C. J. O'Brien (Aerojet Liquid Rocket Co., Sacramento, Calif.) and C. A. Aukerman (NASA, Lewis Research Center, Cleveland, Ohio). AIAA, SAE, and ASME, Joint Propulsion Conference, 15th, Las Vegas, Nev., June 18-20, 1979, AIAA Paper 79-1179, 10 p. 27 refs.

The development of a suitable orbital transfer vehicle (OTV) engine is discussed. The OTV's dimensions are limited by those of the Space Shuttle payload bay on which it will be carried. An approach to utilize the available diameter to achieve high area ratio and thus high engine performance, is presented. Unconventional nozzles, such as clusters of small thrusters around a large diameter contoured plug, are investigated to arrive at engine designs which feature lower chamber pressures, with attendant lower heat flux, lower wall temperature, longer fatigue life, and less critical turbomachinery. Attention is also given to plug nozzle technology, high area ratio module and scarfed bell. Plug Cluster Engine (PCE) concepts, as well as PCE performance, weight, and assessment. A conceptual design of a PCE formed from a cluster of high area ratio, scarfed, bell nozzles proved to be competitive with bell and spike nozzle engines. PCE advantages cited include increased payload length due to shorter engine length, ability to increase or decrease the number of modules and thereby the thrust, and low cost due to utilization of off-the-shelf technology. M.E.P.

A79-39815 * # Low-thrust chemical orbit transfer propulsion. J. J. Pelouch, Jr. (NASA, Lewis Research Center, Space Propulsion and Power Div., Cleveland, Ohio). AIAA, SAE, and ASME, Joint Propulsion Conference, 15th, Las Vegas, Nev., June 18-20, 1979, AIAA Paper 79-1182, 20 p.

The need for large structures in high orbit is discussed in terms of the many mission opportunities which require such structures. Mission and transportation options for large structures are presented, and it is shown that low-thrust propulsion is an enabling requirement for some missions and greatly enhancing to many others. A general comparison of electric and low-thrust chemical propulsion is made and the need for and requirements of low-thrust chemical propulsion are discussed in terms of the interactions that are perceived to exist between the propulsion system and the large structure. (Author)

A79-40984 * # Preliminary evaluation of glass resin materials for solar cell cover use. S. J. Marsik, C. K. Swartz, and C. R. Baraona (NASA, Lewis Research Center, Cleveland, Ohio). In: Photovoltaic Specialists Conference, 13th, Washington, D.C., June 5-8, 1978, Conference Record. (A79-40881 17-44) New York, Institute of Electrical and Electronics Engineers, Inc., 1978, p. 624-627.

Silicon solar cells and silicon wafers coated with a heat-curable resin consisting of alternating Si-O atoms were subjected to three tests to evaluate the potential utility of this coating in space

environments. These included UV irradiation in vacuum at an intensity of 10 air mass zero UV energy-equivalent solar constants for 728 hours followed by a long thermal cycle; 15 thermal shock cycles between 100 C and minus 196 C; and high temperature and humidity (65 C at 90% relative humidity). The UV tests resulted in a 8 to 24% loss in short-circuit current and darkening of the covers. Modification of the resin to provide a better match between the coefficients of expansion of the resin and silicon improved resistance to thermal shock, but also increased the darkening effect under UV irradiation. Silicon wafers coated with the resin were not adversely affected by the temperature/humidity test. C.K.D.

A79-51810 * The role of fuel cells in NASA's space power systems. J. F. Been (NASA, Lewis Research Center, Cleveland, Ohio). In: Intersociety Energy Conversion Engineering Conference, 14th, Boston, Mass., August 5-10, 1979, Proceedings, Volume 1, (A79-51726 23-44) Washington, D.C., American Chemical Society, 1979, p. 544-549, 11 refs.

The advances in fuel cell technology which have expanded the capabilities of the fuel cell from that of power generation to include energy storage also expanded its potential role in space power systems. This paper presents a brief evolutionary history of the fuel cell technology and compares this with NASA's increasing space power requirements. The role of fuel cells is put in perspective with other energy storage systems applicable for space using such criteria as type of mission, weight, reliability, costs, etc. Potential applications of space fuel cells with projected technology advances are examined. (Author)

N79-10120* Xerox Electro Optical Systems, Pasadena, Calif. Electronic Systems Div. **INERT GAS ION SOURCE PROGRAM Final Report, 2 Mar. 1977 - 2 Jan. 1978**

William D. Ramsey 13 Jul 1978 76 p refs
(Contract NAS3-20393)
(NASA CR 159423) XEOS-2361) Avail NTIS
HC A05/MF A01 CSCL 21C

The original 12 cm hexagonal magneto-electrostatic containment discharge chamber has been optimized for argon and xenon operation. Argon mass utilization efficiencies of 65 to 77 percent were achieved at keeper-plus-main discharge energy consumptions of 200 to 458 eV/ion, respectively. Xenon performance of 84 to 96 percent mass utilization was realized at 203 to 350 eV/ion. The optimization process and test results are discussed. G G

N79 11115* Battelle Pacific Northwest Labs. Richland, Wash. **DEVELOPMENT OF SPUTTERING PROCESS TO DEPOSIT STOICHIOMETRIC ZIRCONIA COATINGS FOR THE INSIDE WALL OF REGENERATIVELY COOLED ROCKET THRUST CHAMBERS**

R. Busch 19 Jul 1978 33 p refs
(Contract NAS3 19721)
(NASA CR 159412) Avail NTIS HC A03 MF A01 CSCL 21H

Thermal barrier coatings of yttria stabilized zirconia and zirconia-ceria mixtures were deposited by RF reactive sputtering. Coatings were 1.2 mils thick and were deposited on copper cylinders intended to simulate the inner wall of a regeneratively cooled thrust chamber. Coating stoichiometry and adherence were investigated as functions of deposition parameters. Modest deposition rates (approximately 0.15 mil/hr) and subambient substrate temperatures (180 C) resulted in nearly stoichiometric coatings which remained adherent through thermal cycles between 196 and 400 C. Coatings deposited at higher rates or substrate temperatures exhibited greater oxygen deficiencies, while coatings deposited at lower temperatures were not adherent. Substrate bias resulted in structural changes in the coating and high krypton contents had no clear effect on stoichiometry was observed. Author

N79-14153* Hughes Research Labs., Malibu, Calif. Ion Physics Dept.

ADVANCED ELECTROSTATIC ION THRUSTER FOR SPACE PROPULSION Final Report, 21 May 1976 - 21 Jan. 1978
Tommy D. Masek, Duncan MacPherson, Walter Gelon, Seiji Kami, Robert L. Poeschel, and James W. Ward Apr. 1978 400 p ref

(Contract NAS3-20101)
(NASA-CR-159406) Avail NTIS HC A17/MF A01 CSCL 21C

The suitability of the baseline 30 cm thruster for future space missions was examined. Preliminary design concepts for several advanced thrusters were developed to access the potential practical difficulties of a new design. Useful methodologies were produced for assessing both planetary and earth orbit missions. Payload performance as a function of propulsion system technology level and cost sensitivity to propulsion system technology level are among the topics assessed. A 50 cm diameter thruster designed to operate with a beam voltage of about 2400 V is suggested to satisfy most of the requirements of future space missions. J.M.S.

N79-15152* Colorado State Univ., Fort Collins. Dept. of Mechanical Engineering. **PREDICTION OF PLASMA PROPERTIES IN MERCURY ION THRUSTERS**

Glen Longhurst Dec 1978 118 p refs
(Grant NGR-06-002-112)
(NASA-CR-159448) Avail NTIS HC A06/MF A01 CSCL 21C

A simplified theoretical model was developed which obtains to first order the plasma properties in the discharge chamber of a mercury ion thruster from basic thruster design and controllable operating parameters. The basic operation and design of ion thrusters is discussed, and the important processes which influence the plasma properties are described in terms of the design and control parameters. The conservation for mass, charge and energy were applied to the ion production region, which was defined as the region of the discharge chamber having as its outer boundary the surface of revolution of the innermost field line to intersect the anode. Mass conservation and the equations describing the various processes involved with mass addition and removal from the ion production region are satisfied by a Maxwellian electron density spatial distribution in that region. B B

N79-16913* Colorado State Univ., Fort Collins. Dept. of Mechanical Engineering. **MERCURY ION THRUSTER RESEARCH, 1978 Annual Report, 1 Dec. 1977 - 1 Dec. 1978**

Paul J. Wilbur Dec 1978 110 p refs
(Grant NGR-06-002-112)
(NASA-CR-159485) Avail NTIS HC A06/MF A01 CSCL 21C

The effects of 8 cm thruster main and neutralizer cathode operating conditions on cathode orifice plate temperatures were studied. The effects of cathode operating conditions on insert temperature profiles and keeper voltages are presented for three different types of inserts. The bulk of the emission current is generally observed to come from the downstream end of the insert rather than from the cathode orifice plate. Results of a test in which the screen grid plasma sheath of a thruster was probed as the beam current was varied are shown. Grid performance obtained with a grid machined from glass ceramic is discussed. The effects of copper and nitrogen impurities on the sputtering rates of thruster materials are measured experimentally and a model describing the rate of nitrogen chemisorption on materials in either the beam or the discharge chamber is presented. The results of optimization of a radial field thruster design are presented. Performance of this device is shown to be comparable to that of a divergent field thruster and efficient operation with the screen grid biased to floating potential, where its susceptibility to sputter erosion damage is reduced, is demonstrated. Author

N79-19073* Lockheed Missiles and Space Co., Huntsville, Ala. Research and Engineering Center.
STRUCTURAL ANALYSIS OF CYLINDRICAL THRUST CHAMBERS. VOLUME 1 Final Report, May 1978 - Mar. 1979

W. H. Armstrong Mar. 1979 52 p refs
(Contract NAS3-21361)

(NASA-CR-159522, LMSC-HREC-TR-D56882/Vol-1) Avail.
NTIS HC A04/MF A01 CSCL 21H

Life predictions of regeneratively cooled rocket thrust chambers are normally derived from classical material fatigue principles. The failures observed in experimental thrust chambers do not appear to be due entirely to material fatigue. The chamber coolant walls in the failed areas exhibit progressive bulging and thinning during cyclic firings until the wall stress finally exceeds the material rupture stress and failure occurs. A preliminary analysis of an oxygen free high conductivity (OFHC) copper cylindrical thrust chamber demonstrated that the inclusion of cumulative cyclic plastic effects enables the observed coolant wall thinout to be predicted. The thinout curve constructed from the referent analysis of 10 firing cycles was extrapolated from the tenth cycle to the 200th cycle. The preliminary OFHC copper chamber 10-cycle analysis was extended so that the extrapolated thinout curve could be established by performing cyclic analysis of deformed configurations at 100 and 200 cycles. Thus the original range of extrapolation was reduced and the thinout curve was adjusted by using calculated thinout rates at 100 and 200 cycles. An analysis of the same undeformed chamber model constructed of half-hard Amzirc to study the effect of material properties on the thinout curve is included. A. R. H.

N79-19074* Aerojet Liquid Rocket Co., Sacramento, Calif.
ADVANCED ENGINE STUDY FOR MIXED-MODE ORBIT-TRANSFER VEHICLES Final Report

J. A. Mellish Dec. 1978 228 p refs
(Contract NAS3-21049)

(NASA-CR-159491) Avail. NTIS HC A11/MF A01 CSCL 21H

Engine design, performance, weight and envelope data were established for three mixed-mode orbit-transfer vehicle engine candidates. Engine concepts evaluated are the tripropellant, dual-expander and plug cluster. Oxygen, RP-1 and hydrogen are the propellants considered for use in these engines. Theoretical performance and propellant properties were established for bipropellant and tripropellant mixes of these propellants. RP-1, hydrogen and oxygen were evaluated as coolants and the maximum attainable chamber pressures were determined for each engine concept within the constraints of the propellant properties and the low cycle thermal fatigue (300 cycles) requirement. The baseline engine design and component operating characteristics are determined at a thrust level of 88,964 N (20,000 lbs) and a thrust split of 0.5. The parametric data is generated over ranges of thrust and thrust split of 6.7 to 400 kN (15 to 90 klb) and 0.4 to 0.8, respectively. A. R. H.

N79-26110* Colorado State Univ., Fort Collins, Dept. of Mechanical Engineering

INERT GAS THRUSTERS Annual Report

Harold R. Kaufman Nov. 1978 88 p refs
(Grant NSG-3011)

(NASA-CR-159527) Avail. NTIS HC A05/MF A01 CSCL 21H

Inert gas thrusters have continued to be of interest for space propulsion applications. Xenon is of interest in that its physical characteristics are well suited to propulsion. High atomic weight and low tankage fraction were major factors in this choice. If a large amount of propellant was required, so that cryogenic storage was practical, argon is a more economical alternative. Argon was also the preferred propellant for ground applications of thruster technology, such as sputter etching and deposition. Additional magnetic field measurements are reported. These measurements should be of use in magnetic field design. The diffusion of electrons through the magnetic field above multipole anodes was studied in detail. The data were consistent with Bohm diffusion across a magnetic field. The theory based on Bohm diffusion was simple and easily used for diffusion calculations. Limited startup data

were obtained for multipole discharge chambers. These data were obtained with refractory cathodes, but should be useful in predicting the upper limits for starting with hollow cathodes.

J. A. M.

N79-28224* Aerojet Liquid Rocket Co., Sacramento, Calif.
UNCONVENTIONAL NOZZLE TRADEOFF STUDY

C. J. O'Brien Jul. 1979 311 p refs

(Contract NAS3-20109)

(NASA-CR-159520) Avail. NTIS HC A14/MF A01 CSCL 21H

Plug cluster engine design, performance, weight, envelope, operational characteristics, development cost, and payload capability, were evaluated and comparisons were made with other space tug engine candidates using oxygen/hydrogen propellants. Parametric performance data were generated for existing developed or high technology thrust chambers clustered around a plug nozzle of very large diameter. The uncertainties in the performance prediction of plug cluster engines with large gaps between the modules (thrust chambers) were evaluated. The major uncertainty involves the aerodynamics of the flow from discrete nozzles, and the lack of this flow to achieve the pressure ratio corresponding to the defined area ratio for a plug cluster. This uncertainty was reduced through a cluster design that consists of a plug contour that is formed from the cluster of high area ratio bell nozzles that have been scarfed. Light-weight, high area ratio, bell nozzles were achieved through the use of AGCarb (carbon-carbon cloth) nozzle extensions. Author

N79-31341* Sundstrand Corp., Rockford, Ill.
LIQUID OXYGEN/LIQUID HYDROGEN BOOST/VANE PUMP FOR THE ADVANCED ORBIT TRANSFER VEHICLES AUXILIARY PROPULSION SYSTEM

F. Gluzek, R. G. Mokadam, I. H. To, J. D. Stanitz, and J. Wollschlaeger Sep. 1979 138 p refs

(Contract NAS3-20401)

(NASA-CR-159648) Avail. NTIS HC A07/MF A01 CSCL 21H

A rotating, positive displacement vane pump with an integral boost stage was designed to pump saturated liquid oxygen and liquid hydrogen for auxiliary propulsion system of orbit transfer vehicle. This unit is designed to ingest 10% vapor by volume, contamination free liquid oxygen and liquid hydrogen. The final pump configuration and the predicted performance are included. A. W. H.

A79-22396 * Convective heat flux in a laser-heated thruster. P. K. S. Wu (Physical Sciences, Inc., Woburn, Mass.). *Journal of Spacecraft and Rockets*, vol. 16, Jan.-Feb. 1979, p. 56-58, 7 refs. Contract No. NAS3-19728.

An analysis is performed to estimate the convective heating to the wall in a laser-heated thruster on the basis of a solution of the laminar boundary-layer equations with variable transport properties. A local similarity approximation is used, and it is assumed that the gas phase is in equilibrium. For the thruster described by Wu (1976), the temperature and pressure distributions along the nozzle are obtained from the core calculation. The similarity solutions and heat flux are obtained from the freestream conditions of the boundary layer, in order to determine if it is necessary to couple the boundary losses directly to the core calculation. In addition, the effects of mass injection on the convective heat transfer across the boundary layer with large density-viscosity product gradient are examined. P. T. H.

A79-51907 * Hydrogen recombination in sealed nickel-cadmium aerospace cells. P. F. Ritterman (TRW Defense and Space Systems Group, Redondo Beach, Calif.). In: *Intersociety Energy Conversion Engineering Conference*, 14th, Boston, Mass., August 5-10, 1979, Proceedings, Volume 2. (A79-51726 23-44) Washington, D.C., American Chemical Society, 1979, p. 1288-1291. Contract No. NAS3-21253.

The paper presents a mechanism which offers an explanation of the observed behavior of nickel-cadmium cells during voltage

reversal. Constant current reversals using aerospace Ni-Cd cells showed that at rates of C/100 and temperatures of 20 C, a steady condition of constant pressure is achieved with continuous over-discharge. Results of a test employing a battery pack of thirteen 24 Ah cells at 10 C showed that: (1) no net evolution of H occurs in Ni-Cd cells during overdischarge, (2) as H pressure increases the rate of pressure rise decreases, and (3) after attaining pressure equilibrium at a given overdischarge rate, a pressure decrease is noted when the discharge is lowered. Other tests using varying overdischarge rates were examined and have resulted in the development of a laboratory cell with a safe overdischarge capability of C/20 which is three times as great as state-of-the-art Ni-Cd cells. C.F.W.

A79-51911 * Some practical observations on the accelerated testing of Nickel-Cadmium Cells. P. P. McDermott (Coppin State College, Baltimore, Md.). In: Intersociety Energy Conversion Engineering Conference, 14th, Boston, Mass., August 5-10, 1979, Proceedings. Volume 2. (A79-51726 23-44) Washington, D.C., American Chemical Society, 1979, p. 1305-1309. 12 refs. Grant No. NsG-5051.

A large scale test of 6.0 Ah Nickel-Cadmium Cells conducted at the Naval Weapons Support Center, Crane, Indiana has demonstrated a methodology for predicting battery life based on failure data from cells cycled in an accelerated mode. After examining eight variables used to accelerate failure, it was determined that temperature and depth of discharge were the most reliable and efficient parameters for use in accelerating failure and for predicting life. (Author)

23 CHEMISTRY AND MATERIALS (GENERAL)

Includes biochemistry and organic chemistry.

N79-11119* National Aeronautics and Space Administration, Lewis Research Center, Cleveland, Ohio
A STUDY OF VARIOUS SYNTHETIC ROUTES TO PRODUCE A HALOGEN-LABELED TRACTION FLUID
 William R. Jones, Jr. and Hans Zimmer. Nov. 1978. 10 p. refs. (NASA-TM-79024, E-9821) Avail. NTIS HC A02/MF A01 CSCL 07C

Several synthetic routes were studied for the synthesis of the compound 1, 1, 3-trimethyl-1, 3-dicyclohexyl-2-chloropropane. This halogen-labeled fluid would be of use in the study of high traction lubricants under elastohydrodynamic lubrication conditions using infrared emission spectroscopy. The synthetic routes included: dimerization of alpha-methylstyrene, methanol addition to alpha-methylstyrene, a Wittig reaction, and an organometallic approach. Because of steric hindrance and competing reactions, none of these routes were successful. Author

N79-21128* National Aeronautics and Space Administration, Lewis Research Center, Cleveland, Ohio
THREE METHODS FOR IN SITU CROSS-LINKING OF POLYVINYL ALCOHOL FILMS FOR APPLICATION AS ION-CONDUCTING MEMBRANES IN POTASSIUM HYDROXIDE ELECTROLYTE
 Warren H. Philipp and Li-Chen Hsu. Apr. 1979. 18 p. refs. (NASA-TP-1407, E-9778) Avail. NTIS HC A02/MF A01 CSCL 07D

Three methods of in situ cross-linking polyvinyl alcohol films are presented. They are: (1) acetalization with a dialdehyde such as glutaraldehyde, (2) acetalization with a dehyde groups formed by selective oxidative cleaving of the few percent of 1,2 diol units present in polyvinyl alcohol, and (3) cross-linking by hydrogen abstraction by reaction with hydrogen atoms and hydroxyl radicals from irradiated water. For the third method, improvement in film conductivity in KOH solution at the expense of mechanical strength is obtained by the presence of polyacrylic acid in the polyvinyl alcohol films. Resistivities in 45 percent KOH are given for in situ cross-linked films prepared by each of the three methods. Author

N79-22194* National Aeronautics and Space Administration, Lewis Research Center, Cleveland, Ohio
IMPROVED ADHERENCE OF SPUTTERED TITANIUM CARBIDE COATINGS ON NICKEL- AND TITANIUM-BASE ALLOYS
 Donald R. Wheeler and William A. Brainard. Apr. 1979. 18 p. refs. (NASA-TP-1450, E-9838) Avail. NTIS HC A02/MF A01 CSCL 11F

Rene 41 and Ti-6Al-4V alloys were radio frequency sputter coated with titanium carbide by several techniques in order to determine the most effective. Coatings were evaluated in pin-on-disk tests. Surface analysis by X-ray photoelectron spectroscopy was used to relate adherence to interfacial chemistry. For Rene 41, good coating adherence was obtained when a small amount of acetylene was added to the sputtering plasma. The acetylene carburized the alloy surface and resulted in better bonding to the TiC coating. For Ti-6Al-4V, the best adherence and wear protection was obtained when a pure titanium interlayer was used between the coating and the alloy. The interlayer is thought to prevent the formation of a brittle, fracture-prone aluminum oxide layer. Author

N79-24081* National Aeronautics and Space Administration, Lewis Research Center, Cleveland, Ohio
POLYIMIDE PREPREG MATERIAL HAVING IMPROVED TACK RETENTION Patent Application
 T. T. Serafini and P. Deluigi, inventors (to NASA). Filed 6 Apr. 1979. 10 p. (NASA-Case-LEW-12933-1; US-Patent-Appl-SN 027857) Avail. NTIS HC A02/MF A01 CSCL 07C

A composition, of the type disclosed in U.S. Patent 3,745,149 and which includes a polyfunctional ester, a polyfunctional amine, and an end-capping agent, is impregnated into fibers or fabric and heated to form prepreg material. The tack retention characteristics of this prepreg material are improved by incorporating into the composition a liquid olefinic material comparable with the other ingredients of the composition. The prepreg material is heated at a higher temperature to effect formation of the polyimide resin and the monomeric additive is incorporated in the polyimide polymer structure. NASA

N79-27242* National Aeronautics and Space Administration, Lewis Research Center, Cleveland, Ohio
ELECTROCHEMICAL FLUORINATION OF TRICHLOROETHYLENE AND N, N-DIMETHYLTRIFLUOROACETAMIDE
 Li-Chen Hsu. 1979. 14 p. refs. Presented at the 155th Meeting of the Electrochem. Soc., Boston, 6-11 May 1979. (NASA-TM-79188, E-057) Avail. NTIS HC A02/MF A01 CSCL 07C

Fluorination of trichloroethylene and N, N-dimethyltrifluoroacetamide was carried out on a laboratory scale in an advanced Simons type electrochemical apparatus which could be operated automatically from ambient to 50 psi pressure. A variety of fluorine-substituted products are formed, depending upon electrolysis conditions and concentrations of reactant relative to the NaF, KF, HF electrolyte. A new reaction mechanism of electrochemical fluorination of trichloroethylene is proposed. The solvency-to-fluorine content relationship of fluorinated N, N-dimethyltrifluoroacetamide is described. Author

N79-31345* National Aeronautics and Space Administration, Lewis Research Center, Cleveland, Ohio
CURING AGENT FOR POLYEPOXIDES AND EPOXY RESINS AND COMPOSITES CURED THEREWITH Patent Application
 T. T. Serafini and P. Deluigi, inventors (to NASA). Filed 30 Aug. 1979. 14 p. (NASA-Case-LEW-12226-1; US-Patent-Appl-SN-070771) Avail. NTIS HC A02/MF A01 CSCL 07C

A curing agent for a polyepoxide is described which contains a divalent aryl radical such as phenylene and a tetravalent aryl radical such as a tetravalent benzene radical. An epoxide is cured by admixture with the curing agent. The cured epoxy product retains the usual properties of cured epoxides and, in addition, has a high char residue after burning, on the order of 45% by weight. The high char residue is of value in preventing release to the atmosphere of carbon fibers from carbon fiber-epoxy resin composites in the event of burning of the composite. NASA

N79-31346* National Aeronautics and Space Administration, Lewis Research Center, Cleveland, Ohio
SURFACE CHEMISTRY OF IRON SLIDING IN AIR AND NITROGEN LUBRICATED WITH HEXADECANOL AND HEXADECANOL CONTAINING DIBENZYL DITHIOLATE
 Donald R. Wheeler. Sep. 1979. 15 p. refs. (NASA-TP-1455, E-9956) Avail. NTIS HC A02/MF A01 CSCL 11G

Wear experiments were conducted on iron sliding in hexadecane and hexadecane plus one weight percent dibenzyl dithiolate (DBDS) in atmospheres of air and nitrogen at room temperature. The wear scars and the wear debris were analyzed by X-ray photoelectron spectroscopy. The presence of air reduced wear but increased friction, while DBDS reduced friction but had little effect on wear except that the wear increased somewhat when DBDS was used in air. Wear scar analysis indicated that oxygen and sulfur competed chemically for the surface, with

the oxide predominating. Low wear was associated with a thick oxide layer and low friction with a thin predominantly sulfide layer. Analysis of the wear debris indicated the presence of a sulfate in the high wear case (hexadecane plus DBDS in air), and showed the presence of an organic sulfide in the low wear case (hexadecane plus DBDS in nitrogen). Author

A79-14798 * # Adhesive bonding of ion beam textured metals and fluoropolymers. M. J. Mirtich and J. S. Sovey (NASA, Lewis Research Center, Cleveland, Ohio). *American Vacuum Society, National Vacuum Symposium, 25th, San Francisco, Calif., Nov. 28-Dec. 1, 1978, Paper, 13 p.* 12 refs.

An electron-bombardment argon ion source was used to ion-etch various metals and fluoropolymers. The metal and fluoropolymers were exposed to (0.5 to 1.0)-keV Ar ions at ion current densities of 0.2 to 1.5 mA/sq cm for various exposure times. The resulting surface texture is in the form of needles or spires whose vertical dimensions may range from tenths to hundreds of micrometers, depending on the selection of beam energy, ion current density, and etch time. The bonding of textured surfaces is accomplished by ion-beam texturing mating pieces of either metals or fluoropolymers and applying a bonding agent which wets in and around the microscopic conelike structures. After bonding, both tensile and shear strength measurements were made on the samples. Also tested, for comparison's sake, were untextured and chemically etched fluoropolymers. The results of these measurements are presented in this paper. (Author)

A79-14951 * # Application of ion chromatography to the study of hydrolysis of some halogenated hydrocarbons at ambient temperatures. D. A. Otterson (NASA, Lewis Research Center, Cleveland, Ohio). *Dionex Corp., Symposium on Ion Chromatography, Sunnyvale, Calif., June 21, 1978, Paper, 23 p.* 10 refs.

A79-27232 * Coatings for wear and lubrication. T. Spalvins (NASA, Lewis Research Center, Cleveland, Ohio). (*International Conference on Metallurgical Coatings, San Francisco, Calif., Apr. 3-7, 1978.*) *Thin Solid Films*, vol. 53, 1978, p. 285-300. 43 refs.

In this paper we review the recent advances in the tribological uses of R.F.-sputtered and ion-plated films of solid film lubricants (laminar solids, soft metals, organic polymers) and wear-resistant refractory compounds (carbides, nitrides, silicides). The sputtering and ion-plating potentials and the corresponding coatings formed are evaluated relative to the friction coefficient, wear endurance limit and mechanical properties. The tribological and mechanical properties of each kind of film are discussed in terms of film adherence, coherence, density, grain size, morphology, internal stresses and thickness and substrate conditions such as temperature, topography, chemistry and d.c. biasing. The ion-plated metallic films in addition to improved tribological properties also have better mechanical properties such as tensile strength and fatigue life. (Author)

A79-49536 * # Electrochemical fluorination of trichloroethylene and N, N-dimethyltrifluoroacetamide. L. C. Hsu (NASA, Lewis Research Center, Cleveland, Ohio). *Electrochemical Society, Meeting, 155th, Boston, Mass., May 6-11, 1979, Paper, 12 p.* 6 refs.

The paper presents the results of experiments concerning the fluorination of trichloroethylene and N, N-dimethyltrifluoroacetamide carried out on a laboratory scale in an advanced 'Simons' type electrochemical apparatus which could be operated automatically from ambient to 50 psi pressure. It is shown that a variety of fluorine-substituted products are formed, depending upon electrolysis conditions and concentrations of reactant relative to the NaF, KF, HF electrolyte. A new reaction mechanism of electrochemical fluorination of trichloroethylene is proposed. Finally, the solvency-to-fluorine content relationship of fluorinated N, N-dimethyltrifluoroacetamide is described. M. E. P.

A79-32924 * The catalysis of nucleotide polymerization by compounds of divalent lead. H. L. Sleeper and L. E. Orgel (Salk Institute for Biological Studies, San Diego, Calif.). *Journal of Molecular Evolution*, vol. 12, Apr. 12, 1979, p. 357-364. 11 refs. Grant No. NGR-05-067-001.

The nonenzymatic, nontemplate catalysis of nucleotide polymerization by Pb(2+) ions, a possible prebiotic catalyst, is reported. Adenosine and uridine phosphoimidazoles were reacted in buffered solutions of lead salts and products were analyzed by means of paper chromatography and electrophoresis. In the presence of Pb(2+) ion at pH 8.0 and 7.0 the reaction is found to progress rapidly with excellent yields of oligomers, with optimal yields observed at pH 8.0. Little temperature dependence in the range 0 to 30 C is observed, however hydrolysis of the reaction products is minimal when the reaction is carried out at 0 C. Results show that the yield of oligomers is insensitive to mixing or the source of lead ions, indicating that naturally occurring minerals or precipitates could be a source of Pb(2+) ions under prebiotic conditions. (Author)

24 COMPOSITE MATERIALS

Includes laminates.

N79-15157* National Aeronautics and Space Administration, Lewis Research Center, Cleveland, Ohio.

DYNAMIC MECHANICAL ANALYSIS OF FIBER REINFORCED COMPOSITES

Katherine E. Reed 1979 20 p. refs. Presented at 34th Ann. Conf. of Reinforced Plastics/Composites of the Inst. of the Soc. of the Plastics Industry, Inc., New Orleans, La., 29 Jan. - 2 Feb. 1979.

(NASA-TM-79033; E-9831) Avail. NTIS HC A02/MF A01 CSCL 11D

Dynamic mechanical and thermal properties were determined for unidirectional epoxy/glass composites at various fiber orientation angles. Resonant frequency and relative logarithmic decrement were measured as functions of temperature. In low angle and longitudinal specimens a transition was observed above the resin glass transition temperature which was manifested mechanically as an additional damping peak and thermally as a change in the coefficient of thermal expansion. The new transition was attributed to a heterogeneous resin matrix induced by the fiber. The temperature span of the glass-rubber relaxation was found to broaden with decreasing orientation angle, reflecting the growth of fiber contribution and exhibiting behavior similar to that of Young's modulus. The change in resonant frequency through the glass transition was greatest for samples of intermediate fiber angle, demonstrating behavior similar to that of the longitudinal shear modulus. Author

N79-16075* National Aeronautics and Space Administration, Lewis Research Center, Cleveland, Ohio.

EFFECTS OF GRAPHITE FIBER STABILITY ON THE PROPERTIES OF PMR POLYIMIDE COMPOSITES

Peter Delvigs, William B. Alston (Army Aviation Res. and Develop. Command, Cleveland, Ohio), and Raymond D. Vannucci 1979 18 p. refs. To be presented at the 24th Natl. SAMPE Symp., San Francisco, 8-10 May 1979.

(NASA-TM-79062; E-9877; AVRADCOM-TR-78-62) Avail. NTIS HC A02/MF A01 CSCL 11D

The effect of the stability of graphite fibers on composite properties after exposure in air at 600 F was investigated. Composites were fabricated from PMR-15 and PMR-2 monomer solutions, using HTS-2 and Celion 6000 graphite fibers as the reinforcement. The effect of long-term exposure in air at 600 F on composite weight loss and mechanical properties was determined. These composites exhibited a significantly increased lifetime at that temperature compared to composites fabricated from HTS fiber sold prior to 1975. The effect of the PMR-15 and PMR-II resin compositions on long-term composite performance at 600 F is also discussed. A R H

N79-16076* National Aeronautics and Space Administration, Lewis Research Center, Cleveland, Ohio.

SOME PROPERTIES OF AN ADVANCED BORON FIBER

Donald R. Behrendt 1979 11 p. refs. Presented at the Meeting of the Am. Ceramic Soc., Merritt Island, Fla., 22-24 Jan. 1979. (NASA-TM 79065; E-9881) Avail. NTIS HC A02/MF A01 CSCL 11D

An advanced coreless boron fiber exhibits tensile strengths which are more than twice that of the normal CVD B/W fibers. The coreless fiber is made by the chemical removal of the tungsten boride core exposed by splitting the as-grown fiber. The easily splittable fiber is made by the chemical vapor deposition of boron on a larger than usual tungsten substrate. It is expected that the ease of splitting is related to residual stresses in these fibers. Measurements of the axial residual stresses in both the normal and the splittable fibers are presented and the results compared. Differences in these stresses are discussed in connection with the ease of splitting in the splittable fibers. A R H

N79-16077* National Aeronautics and Space Administration, Lewis Research Center, Cleveland, Ohio.

HIGH TEMPERATURE DYNAMIC MODULUS AND DAMPING OF ALUMINUM AND TITANIUM MATRIX COMPOSITES

J. A. DiCarlo and J. E. Maisel (Cleveland State Univ.) 1979 37 p. refs. Presented at the Symp. on Advanced Fibers and Composites for Appl. at Elevated Temp., New Orleans, 18-22 Feb. 1979, sponsored by the Met. Soc. of AIME.

(NASA-TM-79080; E-9901) Avail. NTIS HC A03/MF A01 CSCL 11D

Dynamic modulus and damping capacity property data were measured from 20 to over 500 C for unidirectional B/Al (1100), B/Al (6061), B/SiC/Al (6061), Al₂O₃/Al, SiC/Ti-6Al-4V, and SiC/Ti composites. The measurements were made under vacuum by the forced vibration of composite bars at free-free flexural resonance near 2000 Hz and at amplitudes below 0.000001. Whereas little variation was observed in the dynamic moduli of specimens with approximately the same fiber content (50 percent), the damping of B/Al composites was found at all temperatures to be significantly greater than the damping of the Al₂O₃/Al and SiC/Ti composites. For those few situations where slight deviations from theory were observed, the dynamic data were examined for information concerning microstructural changes induced by composite fabrication and thermal treatment. The 270 C damping peak observed in B/Al (6061) composites after heat treatment above 460 C appears to be the result of a change in the 6061 aluminum alloy microstructure induced by interaction with the boron fibers. The growth characteristics of the damping peak suggest its possible value for monitoring fiber strength degradation caused by excess thermal treatment during B/Al (6061) fabrication and use. S E S

N79-16918* National Aeronautics and Space Administration, Lewis Research Center, Cleveland, Ohio.

CHARACTERIZATION OF PMR POLYIMIDES: CORRELATION OF ESTER IMPURITIES WITH COMPOSITE PROPERTIES

R. W. Lauver and R. D. Vannucci 1979 12 p. refs. To be presented at the 24th Natl. SAMPE Symp., San Francisco, 8-10 May 1979.

(NASA-TM-79068; E-9884) Avail. NTIS HC A02/MF A01 CSCL 11D

The presumed relationship of chemical impurities to final composite properties was investigated for PMR-polyimide resin. Ester/acid solutions of one monomer were aged at selected temperatures and chemical changes were monitored spectroscopically. At selected intervals, graphite fiber reinforced composite panels were fabricated. Changes in resin processing characteristics and composite properties were determined. The correlation of these data are discussed as are related characterization studies of PMR-polyimide resin. A R H

N79-16919* National Aeronautics and Space Administration, Lewis Research Center, Cleveland, Ohio.

PREDICTION OF PROPERTIES OF INTRAPLY HYBRID COMPOSITES

C. C. Chamis and J. H. Sinclair 1979 19 p. refs. Presented at the 34th Ann. Conf. of the Reinforced Plastics/Composite Inst., New Orleans, 29 Jan. 1979 - 2 Feb. 1979.

(NASA-TM 79087; E-9911) Avail. NTIS HC A02/MF A01 CSCL 11D

Equations based on the mixtures rule are presented for predicting the physical, thermal, hygral, and mechanical properties of unidirectional intraply hybrid composites (UIHC) from the corresponding properties of their constituent composites. Bounds were derived for uniaxial longitudinal strengths, tension, compression, and flexure of UIHC. The equations predict shear and flexural properties which agree with experimental data from UIHC. Use of these equations in a composites mechanics computer code predicted flexural moduli which agree with experimental data from various intraply hybrid angleplied laminates (IHAL). It is indicated, briefly, how these equations can be used in conjunction with composite mechanics and structural analysis during the analysis/design process. Author

N79-16920* National Aeronautics and Space Administration, Lewis Research Center, Cleveland, Ohio.

RESIN/FIBER THERMO-OXIDATIVE INTERACTIONS IN PMR POLYIMIDE/GRAPHITE COMPOSITES

William B. Alston 1979 13 p refs To be presented at the 24th SAMPE Symp., San Francisco, 8-10 May, 1979 Prepared in part by Army Aviation Res. and Develop. Command, Cleveland, Ohio.

(NASA-TM-79093; AVRADCOM-TR-79-6; E-9917) Avail NTIS HC A02/MF A01 CSCL 11D

The amounts of resin weight loss and fiber weight loss in four PMR-polyimide graphite fiber composites were calculated from the composite weight losses and the fiber/resin ratios of the composites after long term thermo-oxidative aging in 600 F air. The accelerating effect of graphite fiber on resin weight loss, compared to neat resin weight loss, indicated the presence of a deleterious resin/fiber thermo-oxidative interaction, presumably due to fiber impurities. Similarly, the decelerating effect of the protective matrix resin on fiber weight loss, compared to bare fiber weight loss, was also demonstrated. The amount of hydrazine-indigestible resin and the amount of loose surface graphite fiber that formed during 600 deg F exposure of the composites were quantitatively determined. The indigestible residual resin was also qualitatively studied by scanning electron microscopy.

Author

N79-16921* National Aeronautics and Space Administration, Lewis Research Center, Cleveland, Ohio.

STABILITY OF PMR-POLYIMIDE MONOMER SOLUTIONS

Richard W. Lauver, William B. Alston, and Raymond D. Vannucci 1979 15 p refs Prepared in part by Army Aviation Res. and Develop. Command, Cleveland.

(NASA-TM-79063; E-9878; AVRADCOM-TR-78-63) Avail NTIS HC A02/MF A01 CSCL 11D

The stability of alcohol solutions of norborneyl capped PMR-polyimide resins was monitored during storage at ambient and subambient temperatures. Chemical changes during storage were determined spectroscopically using nuclear magnetic resonance. Resin processability and cured resin quality were determined by fabrication of unidirectional, graphite fiber composites using aged solutions and testing of selected composite properties. PMR-15 solutions exhibit nominally two weeks of useful life and PMR-2 solutions exhibit nominally two days of useful life at ambient conditions. The limiting factor is precipitation of imide reaction products from the monomer solutions. Both solutions exhibit substantially longer useful lifetimes in subambient storage. PMR-15 shows no precipitation after several months storage at subambient temperatures. PMR-2 solutions do exhibit precipitates after extended subambient storage, however, the precipitates formed under these conditions can be redissolved. The chemical implications of these observations are discussed.

LS

N79-17916* National Aeronautics and Space Administration, Lewis Research Center, Cleveland, Ohio.

METHOD OF MAKING BEARING MATERIALS Patent

Harold E. Sliney inventor (to NASA) Issued 23 Jan 1979 5 p Filed 13 Dec 1977 Division of US Patent Appl. SN-764245, filed 31 Jan 1977, which is a division of abandoned US Patent Appl. SN-616528, filed 25 Sep 1975, which is a division of US Patent Appl. SN-513611, filed 10 Oct 1974, US Patent-3, 953,343.

(NASA Case-LEW-11930-4, US Patent-4,136,211, US Patent Appl. SN-860406, US Patent Class-427-34, US Patent Class-427-122, US Patent Class-308-78, US Patent Class-308-87R, US Patent Class-308-168, US Patent Class-308-171, US Patent Class-308-DIG 8, US Patent Class-308-DIG 9, US Patent Class-427-292, US Patent Class-427-327, US Patent Class-427-328, US Patent Class-427-355, US Patent Class-427-376B, US Patent Class-427-376C, US Patent-3,953,343, US Patent Appl. SN-764245, US Patent Appl. SN-616528, US Patent Appl. SN-513611) Avail US Patent and Trademark Office CSCL 11D

A method is described for making a composite material which provides low friction surfaces for materials in rolling or sliding

contact. The composite material which is self-lubricating and oxidation resistant up to and in excess of about 930 C is comprised of a metal component which lends strength and elasticity to the structure and a fluorine salt component which provides oxidation protection to the metal but may also enhance the lubrication qualities of the composite.

Official Gazette of the U.S. Patent and Trademark Office

N79-12150* National Aeronautics and Space Administration, Lewis Research Center, Cleveland, Ohio.

STATUS REVIEW OF PMR POLYIMIDES

Tito T. Serafini 1978 8 p refs Proposed for presentation at the Symp. on Resins for Aerospace at the Am. Chem. Soc./Chem. Soc. of Japan Chem. Congr., Honolulu, 1-6 Apr. 1979.

(NASA-TM-79039; E-9841) Avail NTIS HC A02/MF A01 CSCL 11D

The current status of first and second generation PMR polyimides are reviewed. Synthesis, processing, and applications were considered, using prepreg materials based on processable, high temperature resistant polyimides.

J.A.M.

N79-12153* National Aeronautics and Space Administration, Lewis Research Center, Cleveland, Ohio.

EVALUATION OF MANUFACTURING PROCESSES FOR BORON/ALUMINUM COMPOSITES CONTAINING 0.2-MM-DIAMETER BORON FIBERS

Thomas J. Moore and Paul E. Moorhead Nov 1978 55 p

(NASA-TM-79008; E-9792) Avail NTIS HC A04/MF A01 CSCL 11D

The effects of starting materials and fabrication techniques on the properties and cost of producing boron/aluminum (B/Al) composite panels containing 0.2-mm-diameter boron fibers are evaluated. The boron fibers were obtained from a single supplier. Five kinds of B/Al tape were used to produce 105, 8-ply panels. Consolidation was accomplished by hot pressing in air or in vacuum. Nondestructive and destructive tests included room-temperature tensile tests. On the basis of an evaluation of the test results and relative cost estimates, two kinds of tape were selected for use: fugitive binder tape and dry woven tape.

GG

N79-12154* National Aeronautics and Space Administration, Lewis Research Center, Cleveland, Ohio.

FRACTURE MODES IN OFF-AXIS FIBER COMPOSITES

J. H. Sinclair and C. C. Chamis 1978 25 p refs Proposed for presentation at the 34th Ann. Conf. of the SPI Reinforced Plastics/Composites Inst., New Orleans, 29 Jan - 2 Feb 1979 (NASA-TM-79036; E-9836) Avail NTIS HC A02/MF A01 CSCL 11D

Criteria were developed for identifying, characterizing, and quantifying fracture modes in high-modulus graphite-fiber/resin unidirectional composites subjected to off-axis tensile loading. Procedures are described which use sensitivity analyses and off-axis data to determine the uniaxial strength of fiber composites. It was found that off-axis composites fail by three fracture modes which produce unique fracture surface characteristics. The stress that dominates each fracture mode and the load angle range of its dominance can be identified. Linear composite mechanics is adequate to describe quantitatively the mechanical behavior of off-axis composites. The uniaxial strengths predicted from off-axis data are comparable to those measured in uniaxial tests.

GY

N79-20186* National Aeronautics and Space Administration, Lewis Research Center, Cleveland, Ohio.

MECHANISMS OF BORON FIBER STRENGTHENING BY THERMAL TREATMENT

J. A. DiCarlo 1979 27 p refs Presented at 3d Ann. Conf. on Composites and Advanced Mater., Merritt Island, Fla., 21-24 Jan 1979; Sponsored in part by the Am. Ceram. Soc. (NASA-TM-79077; E-9894) Avail NTIS HC A03/MF A01 CSCL 11D

The fracture strain for boron on tungsten fibers was studied for improvement by heat treatment under vacuum or argon

environments. The mechanical basis for this improvement is thermally-induced axial contraction of the entire fiber, whereby strength-controlling core flaws are compressed and fiber fracture strain increased by the value of the contraction strain. By highly sensitive measurements of fiber density and volume, the physical mechanism responsible for contraction under both environments was identified as boron atom diffusion out of the fiber sheath. The fiber contracts because the average volume of the resulting microvoid was determined to be only 0.26 plus or minus 0.09 the average atomic volume of the removed atom. The basic and practical implications of these results are discussed with particular emphasis on the theory, use, and limitations of heat-induced contraction as a simple cost-effective secondary processing method. Author

N79-20187* National Aeronautics and Space Administration, Lewis Research Center, Cleveland, Ohio.

TUNGSTEN FIBER REINFORCED FeCrAlY: A FIRST GENERATION COMPOSITE TURBINE BLADE MATERIAL
D. W. Petrasek, E. A. Winsa, L. J. Westfall, and R. A. Signorelli 1979 27 p refs Presented at the 108th Ann. meeting of the Am. Inst. of Mining, Met. and Petroleum Engr., New Orleans, 18-22 Feb. 1979

(NASA-TM-79094; E-9918) Avail: NTIS HC A03/MF A01 CSCL 11D

Tungsten-fiber/FeCrAlY (W/FeCrAlY) was identified as a promising aircraft engine, first generation, turbine blade composite material. Based on available data, W/FeCrAlY should have the stress-rupture, creep, tensile, fatigue, and impact strengths required for turbine blades operating from 1250 to 1370 K. It should also have adequate oxidation, hot corrosion, and thermal cycling damage resistance as well as high thermal conductivity. Concepts for potentially low cost blade fabrication were developed. These concepts were used to design a first stage JT9D convection cooled turbine blade having a calculated 50 K use-temperature advantage over the directionally solidified superalloy blade. L.S.

N79-20188* National Aeronautics and Space Administration, Lewis Research Center, Cleveland, Ohio.

FABRICATION AND TESTING OF NONGRAPHITIC SUPERHYBRID COMPOSITES

R. F. Lark, J. H. Sinclair, and C. C. Chamis 1979 17 p refs To be presented at the 24th Natl. SAMPE Symp., San Francisco, 8-10 May 1979

(NASA-TM-79102; E-9926) HC A02/MF A01 CSCL 11D

The fabrication feasibility and the mechanical properties of adhesively-bonded boron/aluminum, titanium, nongraphitic fiber/epoxy-resin superhybrid composite laminates were studied for potential aerospace applications. The major guiding force was the elimination of a potential graphite fiber release problem in the event of a fire. Results show that nongraphitic fibers, such as S-glass and Kevlar 49, can be substituted for the graphite fibers used in superhybrid composites. However, the nongraphic superhybrids have lower stiffness properties than the graphitic superhybrids. In-plane and flexural moduli of the laminates studied can be predicted using linear laminate theory, while nonlinear laminate theory is required for strength predictions. L.P.

N79-22211* National Aeronautics and Space Administration, Lewis Research Center, Cleveland, Ohio.

DEVELOPMENT AND FABRICATION OF HIGH STRENGTH ALLOY FIBERS FOR USE IN METAL-METAL MATRIX COMPOSITES

G. W. King (Westinghouse Electric Corp., Bloomfield, N. J.) and D. W. Petrasek 1979 15 p refs Presented at the 108th Ann. Meeting of the Am. Inst. of Mining, Met. and Petroleum Engr., New Orleans, 18-22 Feb. 1979

(NASA-TM-79115; E-9951) Avail: NTIS HC A02/MF A01 CSCL 11D

Metal fiber reinforced superalloys are being considered for construction of critical components in turbine engines that operate at high temperature. The problems involved in fabricating refractory metal alloys into wire form in such a manner as to maximize their strength properties without developing excessive

structural defects are described. The fundamental principles underlying the development of such alloy fibers are also briefly discussed. The progress made to date in developing tungsten, tantalum and columbium base alloys for fiber reinforcement is reported and future prospects for alloy fiber development considered. Author

N79-28234* National Aeronautics and Space Administration, Lewis Research Center, Cleveland, Ohio.

THERMAL-CONDUCTIVITY MEASUREMENTS OF TUNGSTEN-FIBER-REINFORCED SUPERALLOY COMPOSITES USING A THERMAL-CONDUCTIVITY COMPARATOR

Leonard J. Westfall and Edward A. Winsa Jul. 1979 23 p refs

(NASA-TP-1445; E-9910) Avail: NTIS HC A02/MF A01 CSCL 11D

The thermal conductivity (TC) of tungsten-fiber-reinforced superalloys was determined for two composite systems by using a thermal conductivity standard from the National Bureau of Standards and a comparator and technique developed for that purpose. The results were compared with TC data for the nickel-base alloy MAR-M200. The technique lends itself to applications involving thin specimens, such as thin-walled turbine blades. The TC's of the composite systems were considerably higher in both the longitudinal and transverse directions than that of the monolithic superalloys used as the matrices. Author

N79-29224* National Aeronautics and Space Administration, Lewis Research Center, Cleveland, Ohio.

COMPUTER AND LABORATORY SIMULATION OF INTERACTIONS BETWEEN SPACECRAFT SURFACES AND CHARGED-PARTICLE ENVIRONMENTS

N. John Stevens 1979 39 p refs Presented at 12th Fluid and Plasma Dyn. Conf., Williamsburg, Va., 24-26 Jul. 1979; sponsored by AIAA

(NASA-TM-79219; E-111) Avail: NTIS HC A03/MF A01 CSCL 22B

Cases where the charged-particle environment acts on the spacecraft (e.g., spacecraft charging phenomena) and cases where a system on the spacecraft causes the interaction (e.g., high voltage space power systems) are considered. Both categories were studied in ground simulation facilities to understand the processes involved and to measure the pertinent parameters. Computer simulations are based on the NASA Charging Analyzer Program (NASCAP) code. Analytical models are developed in this code and verified against the experimental data. Extrapolation from the small test samples to space conditions are made with this code. Typical results from laboratory and computer simulations are presented for both types of interactions. Extrapolations from these simulations to performance in space environments are discussed. A.R.H.

N79-29240* National Aeronautics and Space Administration, Lewis Research Center, Cleveland, Ohio.

HIGH CHAR IMIDE-MODIFIED EPOXY MATRIX RESINS

Tito T. Serafini, Peter Delvigs, and Raymond D. Vannucci 1979 12 p refs Proposed for presentation at 11th Natl. SAMPE Tech Conf., Boston, 13-15 Nov. 1979

(NASA-TM-79226; E-123) Avail: NTIS HC A02/MF A01 CSCL 11D

The synthesis of a class of bis(imide-amine) curing agents for epoxy matrix resins is discussed. Glass transition temperatures and char yield data of an epoxy cured with various bis(imide-amine)s are presented. The room temperature and 350 F mechanical properties, and char yields of unidirectional graphite fiber laminates prepared with conventional epoxy and imide-modified epoxy resins are presented. A.R.H.

N79-30296* National Aeronautics and Space Administration
Lewis Research Center, Cleveland, Ohio.

FATIGUE BEHAVIOR OF SiC REINFORCED TITANIUM COMPOSITES

R. T. Bhatt and H. H. Grimes 1979 19 p refs Presented at Symp. on Fatigue of Fibrous Composite Mater., San Francisco, 22-23 May 1979, sponsored by Am. Soc. for Testing and Mater.

(NASA-TM-79223, E-118) Avail NTIS HC A02/MF A01 CSCL 11D

The low cycle axial fatigue properties of 25 and 44 fiber volume percent SiC/Ti(6Al-4V) composites were measured at room temperature and at 650 deg C. The S-N curves for the composites showed no anticipated improvement over bulk matrix behavior at room temperature. Although axial and transverse tensile strength results suggest a degradation in SiC fiber strength during composite fabrication, it appears that the poor fatigue life of the composites was caused by a reduced fatigue resistance of the reinforced Ti(6Al-4V) matrix. The reduced matrix behavior was due, to the presence of flawed and fractured fibers created near the specimen surfaces by preparation techniques and to the large residual tensile stresses that can exist in fiber reinforced matrices. The effects of fatigue testing at high temperature are discussed. A W H

N79-30323* National Aeronautics and Space Administration
Lewis Research Center, Cleveland, Ohio.

RECENT DEVELOPMENTS IN PMR POLYIMIDES AT NASA LEWIS

T. T. Serafini In NASA Langley Res. Center Graphite/Polyimide Composites Aug 1979 p 391-412 refs (For primary document see N79-30297 21-24)

Avail NTIS HC A19/MF A01 CSCL 11D

The following areas of PMR polyimide research were reviewed: (1) prepreg tack and drape; (2) cure temperature; (3) solution characterization; and (4) elevated temperature composite properties. Recent hardware applications of PMR-15 by various fabricators were also reviewed. R E S

N79-31349* National Aeronautics and Space Administration
Lewis Research Center, Cleveland, Ohio.

EVALUATION OF SILICON CARBIDE FIBER/TITANIUM COMPOSITES

R. W. Jech and R. A. Signorelli Jul 1979 28 p refs

(NASA-TM-79232, E-134) Avail NTIS HC A03/MF A01 CSCL 11D

Izod impact tensile and modulus of elasticity were determined for silicon carbide fiber/titanium composites to evaluate their potential usefulness as substitutes for titanium alloys or stainless steel in stiffness critical applications for aircraft turbine engines. Variations in processing conditions and matrix ductility were examined to produce composites having good impact strength in both the as-fabricated condition and after air exposure at elevated temperature. The impact strengths of composites containing 36 volume percent silicon carbide (SiC) fiber in an unalloyed (A-40) titanium matrix were found to be equal to unreinforced titanium 6 aluminum 4 vanadium alloy; the tensile strengths of the composites were marginally better than the unreinforced unalloyed (A-70) matrix at elevated temperature, though not at room temperature. At room temperature the modulus of elasticity of the composites was 48 percent higher than titanium or its alloys and 40 percent higher than that of stainless steel. Author

A79-15543* The effects of eccentricities on the fracture of off-axis fiber composites. C. C. Chamis and J. H. Sinclair (NASA, Lewis Research Center, Materials and Structures Div., Cleveland, Ohio). In: Reinforced Plastics/Composites Institute, Annual Conference, 33rd, Washington, D.C., February 7-10, 1978, Proceedings. (A79-15526 04-24) New York, Society of the Plastics Industry, Inc., 1978, p. 22 A 1 to 22 A 6 5 refs.

Finite element analyses were performed to investigate theoretically the effects of in-plane and out-of-plane eccentricities, bending or twisting, and thickness non-uniformity on the axial stress and

strain variations across the width of off-axis specimens. The results are compared with measured data and are also used to access the effects of these eccentricities on the fracture stress of off-axis fiber composites. Guidelines for detecting and minimizing the presence of eccentricities are described. (Author)

A79-15545* Use of an ultrasonic-acoustic technique for nondestructive evaluation of fiber composite strength. A. Vary and K. J. Bowles (NASA, Lewis Research Center, Cleveland, Ohio). In: Reinforced Plastics/Composites Institute, Annual Conference, 33rd, Washington, D.C., February 7-10, 1978, Proceedings. (A79-15526 04-24) New York, Society of the Plastics Industry, Inc., 1978, p. 24-A 1 to 24-A 5 5 refs.

This report describes the ultrasonic-acoustic technique used to measure a 'Stress Wave Factor'. In a prior study this factor was found effective in evaluating the interlaminar shear strength of fiber-reinforced composites. Details of the method used to measure the stress wave factor are described. In addition, frequency spectra of the stress waves are analyzed in order to clarify the nature of the wave phenomena involved. The stress wave factor can be measured with simple contact probes requiring only one-side access to a part. This is beneficial in nondestructive evaluations because the waves can run parallel to fiber directions and thus measure material properties in directions assumed by actual loads. Moreover, the technique can be applied where conventional through transmission techniques are impractical or where more quantitative data are required. The stress wave factor was measured for a series of graphite/polyimide composite panels and results obtained are compared with through transmission immersion ultrasonic scans. (Author)

A79-20836* Titanium/beryllium laminates. Fabrication, mechanical properties, and potential aerospace applications. C. C. Chamis and R. F. Lark (NASA, Lewis Research Center, Cleveland, Ohio). In: Selective application of materials for products and energy; Proceedings of the Twenty-third National Symposium and Exhibition, Anaheim, Calif., May 2-4, 1978. (A79-20801 07-23) Azusa, Calif., Society for the Advancement of Material and Process Engineering, 1978, p. 611-632. 5 refs.

The paper describes an investigation to assess the fabricability, mechanical properties, and possible aerospace applications of adhesively-bonded titanium/beryllium Tiber laminates. The results of the investigation indicate that structural laminates can be made which have a modulus of elasticity comparable to steel, fracture strength comparable to the yield strength of titanium, density comparable to aluminum, impact resistance comparable to titanium, and little or no notch sensitivity. These laminates can have stiffness and weight advantages over other materials, including advanced fiber composites, in some aerospace applications where buckling resistance, vibration frequencies, and weight considerations control the design. (Author)

A79-24132* Effects of moisture profiles and laminate configuration on the hygro stress in advanced composites. C. C. Chamis, R. F. Lark, and J. H. Sinclair (NASA, Lewis Research Center, Cleveland, Ohio). In: Materials synergisms, Proceedings of the Tenth National Technical Conference, Kiamesha Lake, N.Y., October 17-19, 1978. (A79-24076 08-31) Azusa, Calif., Society for the Advancement of Material and Process Engineering, 1978, p. 684-700.

A theoretical investigation was performed using a recently developed integrated theory for predicting the hygrothermomechanical response to investigate the effects of three different moisture profiles on the ply hygro stresses in angle-ply laminates. The moisture profiles were linear, parabolic and hyperbolic varying from 1 percent at the exposed ply to 10 percent in the protected ply. The angle-ply laminates were of two generic configurations. The results obtained are summarized graphically to illustrate the effects of both moisture profile and laminate configuration. (Author)

A79-26132 * # High temperature dynamic modulus and damping of aluminum and titanium matrix composites. J. A. DiCarlo (NASA, Lewis Research Center, Cleveland, Ohio) and J. E. Maisel (Cleveland State University, Cleveland, Ohio). *Metallurgical Society of AIME, Symposium on Advanced Fibers and Composites for Application at Elevated Temperatures, New Orleans, La., Feb. 18-22, 1979, Paper, 36 p. 31 refs.*

Dynamic modulus and damping capacity property data were measured from 20 to over 500 C for unidirectional B/Al (1100), B/Al (6061), B/SiC/Al (6061), Al₂O₃/Al, SiC/Ti-6Al-4V, and SiC/Ti composites. The measurements were made under vacuum by the forced vibration of composite bars at free-free flexural resonance near 2000 Hz and at strain application below 0.000001. The damping of B/Al composites was found at all temperatures to be significantly greater than the damping of the Al₂O₃/Al and SiC/Ti composites, with little variation observed in the dynamic moduli of specimens having almost the same fiber content. It is concluded that on the practical level, the finding of a damping-strength correlation supports the use of composite damping measurements for the nondestructive evaluation of boron fiber strength in as-fabricated and heat-treated B/Al (6061) composites. A.A.

A79-30396 * # Mechanisms of boron fiber strengthening by thermal treatment. J. A. DiCarlo (NASA, Lewis Research Center, Cleveland, Ohio). *American Ceramic Society, Annual Conference in Composites and Advanced Materials, 3rd, Merritt Island, Fla., Jan. 21-24, 1979, Paper, 25 p. 19 refs.*

The fracture strain for boron on tungsten fibers can be improved by heat treatment under vacuum or argon environments. The mechanical basis for this improvement is thermally-induced axial contraction of the entire fiber, whereby strength-controlling core flaws are compressed and fiber fracture strain increased by the value of the contraction strain. By highly sensitive measurements of fiber density and volume, the physical mechanisms responsible for contraction under both environments was identified as boron atom diffusion out of the fiber sheath. The fiber contracts because the average volume of the resulting microvoid was determined to be only 0.26 - or - 0.09 the average atomic volume of the removed atom. The basic and practical implications of these results are discussed with particular emphasis on the theory, use, and limitations of heat-induced contraction as a simple cost-effective secondary processing method. (Author)

A79-30397 * # Tungsten fiber reinforced FeCrAlY - A first generation composite turbine blade material. D. W. Petrusek, E. A. Winsa, L. J. Westfall, and R. A. Signorelli (NASA, Lewis Research Center, Cleveland, Ohio). *American Institute of Mining, Metallurgical and Petroleum Engineers, Annual Meeting, 108th, New Orleans, La., Feb. 18-22, 1979, Paper, 27 p. 20 refs.*

General and composite turbine blade material requirements are examined to identify a specific tungsten fiber reinforced superalloy (TFRS) having, in addition to strength, the desired combination of other material properties needed in turbine blades. Experimental data indicated that a thiated tungsten fiber reinforced FeCrAlY matrix composite should have the stress-rupture, creep, tensile, fatigue, and impact strengths required for turbine blades operating from 1250 to 1370 K. Fabrication and design concepts are developed to demonstrate the feasibility of fabricating a hollow TFRS turbine blade at reasonable cost. A.A.

A79-30399 * # Status review of PMR polyimides. T. T. Serafini (NASA, Lewis Research Center, Cleveland, Ohio). *American Chemical Society and Chemical Society of Japan, Symposium on Resins for Aerospace, Honolulu, Hawaii, Apr. 16, 1979, Paper, 6 p. 14 refs.*

In the NASA developed PMR (polymerization of monomer reactants) the reinforcing fibers are impregnated with a solution containing a mixture of monomers dissolved in a low boiling point alkyl alcohol solvent, with the monomers reacting in situ at elevated

temperatures to form a thermo-oxidatively stable polyimide matrix. The current status of first and second generation PMR polyimides is reviewed, considering synthesis and properties, processing, and applications. It is concluded that the PMR approach offers various significant advantages, especially superior high temperature properties and processing versatility, to fabricators and users of polyimide/fiber composites. A.A.

A79-31033 * # Mechanics of intraply hybrid composites - Properties, analysis and design. C. C. Chamis and J. H. Sinclair (NASA, Lewis Research Center, Materials and Structures Div., Cleveland, Ohio). In: *Reinforcing the future; Proceedings of the Thirty-fourth Annual Conference, New Orleans, La., January 30-February 2, 1979. (A79-31026 12-24)* New York, Society of the Plastics Industry, Inc., 1979, p. 20-E 1 to 20-E 8, 6 refs.

A mechanics theory is developed for predicting the physical thermal, hygral and mechanical properties (including various strengths) of unidirectional intraply hybrid composites (UIHC) based on unidirectional properties of the constituent composites. Procedures are described which can use this theory in conjunction with composite mechanics computer codes and general purpose structural analysis finite element programs for the analysis/design of structural components made from intraply hybrid angleplyed laminates (IHAL). Comparisons with limited data show that this theory predicts mechanical properties of UIHC and flexural stiffnesses of IHAL which are in good agreement with experimental data. The theory developed herein makes it possible to design and optimize structural components from IHAL based on a large class of available constituent fibers. (Author)

A79-31035 * # Fracture modes in off-axis fiber composites. J. H. Sinclair and C. C. Chamis (NASA, Lewis Research Center, Composites and Structures Branch, Cleveland, Ohio). In: *Reinforcing the future; Proceedings of the Thirty-fourth Annual Conference, New Orleans, La., January 30-February 2, 1979. (A79-31026 12-24)* New York, Society of the Plastics Industry, Inc., 1979, p. 22-A 1 to 22-A 11, 8 refs.

Criteria have been developed for identifying, characterizing, and quantifying fracture modes in high-modulus graphite-fiber/resin unidirectional composites subjected to off-axis tensile loading. Procedures are described which use sensitivity analyses and off-axis data to determine the uniaxial strength of fiber composites. It was found that off-axis composites fail by three fracture modes which produce unique fracture surface characteristics. The stress that dominates each fracture mode and the load angle range of its dominance can be identified. Linear composite mechanics is adequate to describe quantitatively the mechanical behavior of off-axis composites. The uniaxial strengths predicted from off-axis data are comparable to those measured in uniaxial tests. (Author)

A79-31040 * # Dynamic mechanical analysis of fiber reinforced composites. K. E. Reed (NASA, Lewis Research Center, Materials and Structures Div., Cleveland, Ohio). In: *Reinforcing the future; Proceedings of the Thirty-fourth Annual Conference, New Orleans, La., January 30-February 2, 1979. (A79-31026 12-24)* New York, Society of the Plastics Industry, Inc., 1979, p. 22-G 1 to 22-G 5, 12 refs.

Dynamic mechanical and thermal properties were determined for unidirectional epoxy/glass composites at various fiber orientation angles. Resonant frequency and relative logarithmic decrement were measured as functions of temperature. In low angle and longitudinal specimens a transition was observed above the resin/glass transition temperature which was manifested mechanically as an additional damping peak and thermally as a change in the coefficient of thermal expansion. The new transition was attributed to a heterogeneous resin matrix induced by the fiber. The temperature span of the glass-rubber relaxation was found to broaden with decreasing orientation angle, reflecting the growth of fiber contribution and exhibiting behavior similar to that of Young's modulus. The change in resonant frequency through the glass transition was greatest for

samples of intermediate fiber angle showing behavior similar to that of the longitudinal shear mode. (Author)

A79-43265 * Characterization of PMR polyimides - Correlation of ester impurities with composite properties. R. W. Lauver and R. D. Vannucci (NASA, Lewis Research Center, Cleveland, Ohio). In: The enigma of the eighties: Environment, economics, energy; Proceedings of the Twenty-fourth National Symposium and Exhibition, San Francisco, Calif., May 8-10, 1979, Book 1. (A79-43278 18-23) Azusa, Calif., Society for the Advancement of Material and Process Engineering, 1979, p. 522-532. 6 refs.

The presumed relationship of chemical impurities in final composite properties is the rationale for most chemical characterization studies. This study examines this relationship for PMR polyimide resin. Ester/acid solutions of one monomer were aged at selected temperatures and chemical changes were monitored spectroscopically. At selected intervals, graphite fiber reinforced composite panels were fabricated. Changes in resin processing characteristics and composite properties were determined. The correlation of these data are discussed as are related characterization studies of PMR polyimide resin. (Author)

A79-43239 * Fabrication and testing of non-graphitic superhybrid composites. R. F. Lark, J. H. Sinclair, and C. C. Chamis (NASA, Lewis Research Center, Cleveland, Ohio). In: The enigma of the eighties: Environment, economics, energy; Proceedings of the Twenty-fourth National Symposium and Exhibition, San Francisco, Calif., May 8-10, 1979, Book 1. (A79-43228 18-23) Azusa, Calif., Society for the Advancement of Material and Process Engineering, 1979, p. 776-790. 6 refs.

A study was conducted to determine the fabrication feasibility and the mechanical properties of adhesively-bonded boron aluminum/titanium and non-graphitic fiber/epoxy resin superhybrid (NGSH) composite laminates for potential aerospace applications. The major driver for this study was the elimination of a potential graphite fiber release problem in the event of a fire. The results of the study show that non-graphitic fibers, such as S-glass and Kevlar 49, may be substituted for the graphite fibers used in superhybrid (SH) composites for some applications. As is to be expected, however, the non-graphitic superhybrids have lower stiffness properties than the graphitic superhybrids, in-plane and flexural moduli of the laminates studied in this program can be predicted reasonably well using linear laminate theory while nonlinear laminate theory is required for strength predictions. (Author)

A79-43309 * Effects of graphite fiber stability on the properties of PMR polyimide composites. P. Delvigs, W. B. Alston, and R. D. Vannucci (NASA, Lewis Research Center; U.S. Army, Propulsion Laboratory, Cleveland, Ohio). In: The enigma of the eighties: Environment, economics, energy; Proceedings of the Twenty-fourth National Symposium and Exhibition, San Francisco, Calif., May 8-10, 1979, Book 2. (A79-43315 18-23) Azusa, Calif., Society for the Advancement of Material and Process Engineering, 1979, p. 1053-1068. 6 refs.

Studies were performed to investigate the effect of the stability of graphite fibers on composite properties after exposure in air at 600 F. Composites were fabricated from PMR-15 and PMR-II monomer solutions, using HTS-2 and Celion 6000 graphite fibers as the reinforcement. The effect of long-term exposure in air at 600 F on composite weight loss and mechanical properties was determined. These composites exhibited a significantly increased lifetime at 600 F compared to composites fabricated from HTS fiber sold prior to 1975. The effect of the PMR-15 and PMR-II resin compositions on long term composite performance at 600 F is also discussed. (Author)

A79-49536 * Electrochemical fluorination of trichloroethylene and N, N-dimethyltrifluoroacetamide. L.-C. Hsu (NASA, Lewis Research Center, Cleveland, Ohio). *Electrochemical Society, Meeting, 155th, Boston, Mass., May 6-11, 1979, Paper*. 12 p. 6 refs.

The paper presents the results of experiments concerning the fluorination of trichloroethylene and N, N-dimethyltrifluoroacetamide carried out on a laboratory scale in an advanced 'Simons' type electrochemical apparatus which could be operated automatically from ambient to 50 psi pressure. It is shown that a variety of fluorine-substituted products are formed, depending upon electrolysis conditions and concentrations of reactant relative to the NaF, KF, HF electrolyte. A new reaction mechanism of electrochemical fluorination of trichloroethylene is proposed. Finally, the solvency-to-fluorine content relationship of fluorinated N, N-dimethyltrifluoroacetamide is described. M.E.P.

A79-53720 * Composites emerging for aeropropulsion applications. G. M. Ault and J. C. Freche (NASA, Lewis Research Center, Cleveland, Ohio). *Astronautics and Aeronautics*, vol. 17, Oct. 1979, p. 48-59, 80, 81. 47 refs.

The paper deals with applying composites to the cold- and hot-section components of aircraft turbine engines and analyzing composite structures. The primary experience to date has been with graphite-epoxy materials. The emerging new composites based on fabricable polyimides will find application in components that can operate at temperatures higher than the 350 F allowed by the epoxy. Further major benefits would result if the fiber-reinforced polymer composites could be used for key rotating components, such as the fans of large high-bypass-ratio engines. For the very critical hot turbine components, fiber-reinforced superalloys for turbine blades are considered. V.T.

N79-16924* Nevada Engineering and Technology Corp., Long Beach, Calif.

ELEVATED TEMPERATURE PROPERTIES OF BORON/ALUMINUM COMPOSITES Final Report, 26 Jan. 1978

26 Jan. 1977

Pamela G. Sullivan Nov 1978 116 p refs

(Contract NAS3-20079)

(NASA-CR-159445) Avail NTIS HC A06/MF A01 CSCI 11D

The high temperature properties of boron/aluminum composites, fabricated by an air diffusion bonding technique utilizing vacuum-bonded monolayer tape are reported. Seventeen different combinations of matrix alloy, reinforcement diameter, reinforcement volume percent, angle-ply and matrix enhancement (i.e. titanium cladding and interleaves) were fabricated, inspected, and tested. It is shown that good to excellent mechanical properties could be obtained for air-bonded boron/aluminum composites and that these properties did not decrease significantly up to a test temperature of at least 260 C. Composites made with 8 mil B/W fiber show a much greater longitudinal strength dependence on volume percent fiber than composites made with 5.6 mil fiber. The addition of titanium caused difficulties in composite bonding and yielded composites with reduced strength. G.G.

N79-26120* Boeing Aerospace Co., Seattle, Wash.
EVALUATION OF FLAWED COMPOSITE STRUCTURAL COMPONENTS UNDER STATIC AND CYCLIC LOADING

T. R. Porter Feb 1979 255 p refs

(Contract NAS3-19709)

(NASA-CR-135403) Avail NTIS HC A12/MF A01 CSCI 11D

The effects of initial defects on the fatigue and fracture response of graphite-epoxy composite laminates are presented. The structural laminates investigated were a typical angle ply laminate, a polar/hoop wound pressure vessel laminate, and a typical engine fan blade laminate. Defects investigated were full and half penetration circular holes, full and half penetration slits, and countersink holes. The effects of the defect size and type on the static fracture strength, fatigue performance, and residual static strength are shown as well as the results of loadings on

damage propagation in composite laminates. The data obtained were used to define proof test levels as a qualification procedure in composite structure subjected to cyclic loading. A.R.H.

N79-33294* Lehigh Univ., Bethlehem, Pa. Inst. of Fracture and Solid Mechanics

OFF-AXIS IMPACT OF UNIDIRECTIONAL COMPOSITES WITH CRACKS: DYNAMIC STRESS INTENSIFICATION
Interim Report

G. C. Sih and E. P. Chen Jan. 1979 65 p refs

(Grant NSG-3179)

(NASA-CR-159537) IFSM-79-95)

Avail: NTIS

HC A04/MF A01 CSCL 11D

The dynamic response of unidirectional composites under off axis (angle loading) impact is analyzed by assuming that the composite contains an initial flaw in the matrix material. The analytical method utilizes Fourier transform for the space variable and Laplace transform for the time variable. The off axis impact is separated into two parts, one being symmetric and the other skew-symmetric with reference to the crack plane. Transient boundary conditions of normal and shear tractions are applied to a crack embedded in the matrix of the unidirectional composite. The two boundary conditions are solved independently and the results superimposed. Mathematically, these conditions reduce the problem to a system of dual integral equations which are solved in the Laplace transform plane for the transformation of the dynamic stress intensity factor. The time inversion is carried out numerically for various combinations of the material properties of the composite and the results are displayed graphically.

Author

N79-30295* General Electric Co., Cincinnati, Ohio

METAL SPAR/SUPERHYBRID SHELL COMPOSITE FAN BLADES Final Report

C. T. Salemme and G. C. Murphy Aug. 1979 135 p

(Contract NAS3-20402)

(NASA-CR-159594) Avail: NTIS HC A07/MF A01 CSCL 11D

The use of superhybrid materials in the manufacture and testing of large fan blades is analyzed. The FOD resistance of large metal spar/superhybrid fan blades is investigated. The technical effort reported was comprised of: (1) preliminary blade design, (2) detailed analysis of two selected superhybrid blade designs, (3) manufacture of two process evaluation blades and destructive evaluation, and (4) manufacture and whirlig testing of six prototype superhybrid blades.

A.W.H.

N79-31348* General Electric Co., Cincinnati, Ohio. Aircraft Engine Group

CONTAINMENT OF COMPOSITE FAN BLADES Final Report

C. L. Stotler and A. P. Coppa Jul. 1979 144 p ref

(Contract NAS3-20118)

(NASA-CR-159544 R79AEG197)

Avail: NTIS

HC A07/MF A01 CSCL 11D

A lightweight containment was developed for turbofan engine fan blades. Subscale ballistic-type tests were first run on a number of concepts. The most promising configuration was selected and further evaluated by larger scale tests in a rotating test rig. Weight savings made possible by the use of this new containment system were determined and extrapolated to a CF6-size engine. An analytical technique was also developed to predict the released blades motion when involved in the blade/casing interaction process. Initial checkout of this procedure was accomplished using several of the tests run during the program.

Author

N79-31350* Celanese Research Co., Summit, N.J.

ULTRAFINE POLYBENZIMIDAZOLE (PBI) FIBERS Final Report, Jun. 1976 - Jun. 1979

E. C. Chenevey Jun. 1979 119 p refs

(Contract NAS3-20040)

(NASA-CR-159644) Avail: NTIS HC A06/MF A01 CSCL 11D

Mats were made from ultrafine polybenzimidazole (PBI) fibers

to provide an alternate to the use of asbestos as separators in fuel cells and alkaline batteries. To minimize distortion during mat drying, a process to provide a dry fibril was developed. Two fibril types were developed: one coarse, making mats for battery separators; the other fine, making low permeability matrices for fuel cells. Eventually, it was demonstrated that suitable mat fabrication techniques yielded fuel cell separators from the coarser alkaline battery fibrils. The stability of PBI mats to 45% KOH at 123 C can be increased by heat treatment at high temperatures. Weight loss data to 1000 hours exposure show the alkali resistance of the mats to be superior to that of asbestos.

Author

N79-33258* United Technologies Research Center, East Hartford, Conn.

DEVELOPMENT OF SIALON MATERIALS Final Report, Jun. 1976 - Sep. 1979

G. K. Layden Sep. 1979 145 p refs

(Contract NAS3-19712)

(NASA-CR-159675 R79-912997-39)

Avail: NTIS

HC A07/MF A01 CSCL 11D

Cold pressing and sintering techniques were used to produce ceramic test specimens in which the major phase was either Si₃N₄ or a solid solution having the beta Si₃N₄ structure. Additional components were incorporated to promote liquid phase sintering. Glass and/or crystalline phase were consequently retained in boundaries between Si₃N₄ grains which largely determined the physical properties of the bodies. Systems investigated most extensively included R-Si-Al-O-N (R = rare earth element) Zr-Si-Al-O-N, Y-Si-Be-O-N, and R1-R2-Si-O-N. Room temperature and 1370 C modulus of rupture, 1370 C creep, and oxidation behavior are discussed in terms of phase relationships in a parent quinary, and relevant oxide systems.

Author

A79-20859* Increasing the FOD tolerance of composites.

R. C. Novak (United Technologies Research Center, East Hartford, Conn.). In: Selective application of materials for products and energy; Proceedings of the Twenty-third National Symposium and Exhibition, Anaheim, Calif., May 2-4, 1978. (A79-20801 07-23) Azusa, Calif., Society for the Advancement of Material and Process Engineering, 1978, p. 936-949, 7 refs. Contract No. NAS3-18941.

An experimental program was conducted for the purpose of increasing the foreign object damage tolerance of resin matrix composites in gas turbine engine fan blade applications. The superhybrid concept consisting of a resin matrix composite core surrounded by a sheath of boron/aluminum and titanium was found to be the most promising approach.

(Author)

25 INORGANIC AND PHYSICAL CHEMISTRY

Includes chemical analysis, e.g., chromatography; combustion theory; electrochemistry; and photochemistry.

For related information see also 77 *Thermodynamics and Statistical Physics*.

N79-12180* National Aeronautics and Space Administration, Lewis Research Center, Cleveland, Ohio.

CATALYST SURFACES FOR THE CHROMOUS/CHROMIC REDOX COUPLE Patent Application

Jose D. Giner (Giner, Inc., Waltham, Mass.) and Kathleen J. Cahill, inventors (to NASA) (Giner, Inc., Waltham, Mass.) Filed 29 Nov. 1978. 16 p. Sponsored by NASA. (NASA-Case-LEW-13148-1, US-Patent-Appl-SN 964754) Avail. NTIS HC A02/MF A01 CSCL 07D

An electricity producing cell of the reduction oxidation (REDOX) type is described. The cell comprises a container divided into anode and cathode compartments respectively, by an ion permeable membrane. An anode fluid is directed through a compartment from a source while a cathode fluid is directed through a different compartment from a different source. These fluids are aqueous HCl solutions each containing a different metallic chloride salt. In an exemplary cell the anode fluid contains chromium chloride while the cathode fluid contains iron chloride. Circulation of the anode and cathode fluids produces a difference of potential between inert, electrically conductive electrodes. NASA

N79-14172* National Aeronautics and Space Administration, Lewis Research Center, Cleveland, Ohio.

METHOD OF CROSS-LINKING POLYVINYL ALCOHOL AND OTHER WATER SOLUBLE RESINS Patent Application

D. W. Sheibley, W. H. Philipp, and L. C. Hsu, inventors (to NASA) Filed 20 Dec. 1978. 13 p. (NASA-Case-LEW-13103-1, US-Patent-Appl-SN 971596) Avail. NTIS HC A02/MF A01 CSCL 07D

A self-supporting sheet structure comprising a water soluble, non-cross-linked polymer, such as polyvinyl alcohol, is reported which is capable of being cross-linked by reaction with hydrogen atom radicals and hydroxyl molecule radicals in an aqueous solution having a pH of less than 8 and containing a dissolved salt in an amount sufficient to prevent dissolution of the non-cross-linked polymer. The aqueous solution is then irradiated with ionizing radiation to form hydrogen atom radicals and hydroxyl molecule radicals. The irradiation is continued for a time sufficient to produce a water-insoluble polymer sheet structure. The method has particular application in the production of battery separators and electrode envelopes for alkaline batteries. NASA

N79-14173* National Aeronautics and Space Administration, Lewis Research Center, Cleveland, Ohio.

CROSS-LINKED POLYVINYL ALCOHOL AND METHOD OF MAKING SAME Patent Application

Li-Chen Hsu, Dean W. Heibley, and Warren H. Philipp, inventors (to NASA) Filed 20 Dec. 1978. 12 p. (NASA-Case-LEW-13101-1, US-Patent-Appl-SN 971473) Avail. NTIS HC A02/MF A01 CSCL 07D

A polyvinyl alcohol battery separator is described which has good tensile strength, good resistance to conditions prevailing in alkaline batteries, and an electrical resistivity of less than 1 ohm/sq cm. The product is made by admixing polyvinyl alcohol, preferably in the form of a readily available aqueous solution, and a polyaldehyde polysaccharide such as inexpensive, readily available polydialdehyde starch. The admixture is formed into a sheet by casting an aqueous admixture of the resin and the cross-linking agent. The dried sheet or film is cut to size if desired and may be assembled into bag form for use in a battery. Cross-linking is effected by contacting the film, with a conventional aqueous acid catalyst solution, in an amount sufficient to prevent dissolution of the polymer in the aqueous acid solution. NASA

N79-14174* National Aeronautics and Space Administration, Lewis Research Center, Cleveland, Ohio.

IN-SITU CROSS-LINKING OF POLYVINYL ALCOHOL Patent Application

W. H. Philipp, L. C. Hsu, and D. W. Sheibley, inventors (to NASA) Filed 20 Dec. 1978. 13 p. (NASA-Case-LEW-13135-1, US-Patent-Appl-SN 971475) Avail. NTIS HC A02/MF A01 CSCL 07D

Precise control of crosslinking in the preparation of polyvinyl alcohol battery separators is achieved by incorporating the crosslinking agent in the polyvinyl alcohol and then effecting crosslinking after the polymer is shaped or fabricated into a useful configuration. Aqueous polyvinyl alcohol is admixed with an aqueous dialdehyde crosslinking agent. The pH of the solution is preferably alkaline to prevent premature crosslinking reaction. The aqueous admixture is cast into a sheet and dried to form a self-supporting film which is then immersed in an aqueous acid catalyst solution containing a dissolved salt in an amount sufficient to inhibit dissolution of the noncrosslinked polymer. The resultant crosslinked film has excellent properties, such as low electrical resistivity, rendering the film suitable for use as a separator for an alkaline battery. NASA

N79-16930* National Aeronautics and Space Administration, Lewis Research Center, Cleveland, Ohio.

EVALUATION OF THE APPLICATION OF SOME GAS CHROMATOGRAPHIC METHODS FOR THE DETERMINATION OF PROPERTIES OF SYNTHETIC FUELS

Albert C. Antoine, Jan. 1979. 46 p. refs. Presented at the Aerospace Meeting, San Diego, Calif., 27-30 Nov. 1978, sponsored by the Soc. of Automotive Engrs. (NASA-TM-79035, E-9834) Avail. NTIS HC A03/MF A01 CSCL 21B

The purpose of the investigation was to evaluate the applicability, to some synthetic fuels, of some gas chromatographic methods now under development for use with petroleum based fuels. Thirty two jet and diesel fuel samples which were prepared from oil shale and coal syncrudes were examined. The boiling range distribution of each was determined by gas chromatography, and from that data distillation properties were calculated. The calculated results gave sufficient agreement with the measured values that the equations could be useable in their present form. Bulk fuel properties were calculated for the sixteen JP-5 and Diesel No. 2 type fuels. The results show that the equations would not give useable results. Capillary column gas chromatography was used to determine the n-alkane content of the eight JP-5 type samples and the results related to the observed freezing points. The results show that the concentrations of the long straight chain molecules in the fuels exert influence on the freezing point but are not the complete controlling factor. L.S.

N79-20200* National Aeronautics and Space Administration, Lewis Research Center, Cleveland, Ohio.

PRELIMINARY EVALUATION OF THE ROLE OF K2S IN MHD HOT STREAM SEED RECOVERY Final Report

James Edward Bennett (Arkansas State Univ.) and Fred J. Kohl, Mar. 1979. 24 p. refs. (Contract EF-77-A-01-2674) (NASA-TM-79114, DOE/NASA/2674-79/1, E-9948) Avail. NTIS HC A02/MF A01 CSCL 07D

Results are presented for recent analytical and experimental studies of the role of K₂S in MHD hot stream seed recovery. The existing thermodynamic data base was found to contain large uncertainties and to be nonexistent for vapor phase K₂S. Knudsen cell mass spectrometric experiments were undertaken to determine the vapor species in equilibrium with K₂S(s). K atoms and S₂ molecules were found to be the major vapor phase species in vacuum, accounting for greater than 99 percent of the vapor phase. Combustion gas deposition studies using No. 2 Diesel fuel were also undertaken and revealed that condensed phase K₂SO₃ may potentially be an important compound in the MHD stream at near-stoichiometric combustion. Author

N79-22735* National Aeronautics and Space Administration. Lewis Research Center, Cleveland, Ohio.

METHOD AND DEVICE FOR THE DETECTION OF PHENOL AND RELATED COMPOUNDS Patent

Julian G. Schiller (Pittsburgh Univ., Pa.) and Chung C. Liu, inventors (to NASA) (Pittsburgh Univ., Pa.) Issued 20 Mar 1979 8 p Filed 25 Feb 1977 Supersedes N77-18238 (15 - 09, p 1148) Sponsored by NASA

(NASA Case-LEW-12513-1; US-Patent-4,145,255; US-Patent-Appl-SN-772167; US-Patent-Class-195-103 5R; US-Patent-Class-195-127; US-Patent-Class-204-1T; US-Patent-Class-2041-1958) Avail: US Patent and Trademark Office CSCL 07D

A method is described which permits the selective oxidation and potentiometric detection of phenol and related compounds in an electrochemical cell. An anode coated with a gel immobilized oxidative enzyme and a cathode are each placed in an electrolyte solution. The potential of the cell is measured by a potentiometer connected to the electrodes.

Official Gazette of the U. S. Patent and Trademark Office

N79-22246* National Aeronautics and Space Administration. Lewis Research Center, Cleveland, Ohio.

CONTROL OF VOLUME RESISTIVITY IN INORGANIC ORGANIC SEPARATORS

Dean W. Sheibley and Michelle A. Manzo Apr 1979 17 p refs

(NASA-TP-1439, E-9830) Avail: NTIS HC A02/MF A01 CSCL 07D

Control of resistivity in NASA inorganic-organic separators is achieved by incorporating small percentages of high surface area, fine particle silica with other ingredients in the separator coating. The volume resistivity is predictable from the surface area of filler particles in the coating. The approach is applied to two polymer-plasticizer-filler coating systems, where the filler content of each is below the generally acknowledged critical pigment volume concentration of the coating. Application of these coating systems to 0.0254 cm thick (10-mil) fuel cell grade asbestos sheet produces inexpensive, flexible, microporous separators that perform as well as the original inorganic-organic concept, the Astropower separator. Author

N79-25181* National Aeronautics and Space Administration. Lewis Research Center, Cleveland, Ohio.

IMPROVED, LOW COST INORGANIC-ORGANIC SEPARATORS FOR RECHARGEABLE SILVER-ZINC BATTERIES

Dean W. Sheibley Jun 1979 27 p refs

(NASA-TP-1476, E-9930) Avail: NTIS HC A03/MF A01 CSCL 07D

Several flexible, low cost inorganic-organic separators with performance characteristics and cycle life equal to, or better than the Lewis Research Center Astropower separator were developed. These new separators can be made on continuous-production equipment at about one-fourth the cost of the Astropower separator produced at the same way. In test cells, these new separators demonstrate cycle life improvement, acceptable operating characteristics, and uniform current density. The various separator formulas, test cell construction, and data analysis are described. A R H

N79-27279* National Aeronautics and Space Administration. Lewis Research Center, Cleveland, Ohio.

MASS SPECTROMETRIC INVESTIGATION OF THE VAPORIZATION OF SODIUM AND POTASSIUM CHROMATES: PRELIMINARY RESULTS

Carl A. Stearns, Fred J. Kohl, Robert A. Miller, and George C. Fryburg 1979 16 p refs Presented at the 8th Midwest High Temp Chem Conf., Milwaukee, 3-6 Jun 1979

(NASA-TM-79210, E-095) Avail: NTIS HC A02/MF A01

Knudsen cell mass spectrometry was used to study the vaporization of sodium and potassium chromates. For both salts, the vaporization proceeds predominately by the reactions $M2CrO4(c) = 2M(g) + 5/4O2(g) + 1/2 Cr2O3(s)$ and $M2CrO4(c) = M2CrO4(g)$ where $M = Na$ or K . The distribution of the ions $M(+)$, $O2(+)$ and $M2CrO4(+)$ in the measured mass

spectrum was found to depend on the material used for the Knudsen cell, even for materials such as platinum and gold. In the case of sodium chromate, the decomposition reaction appears to be less important than the molecular vaporization reaction. A preliminary value of 72 kcal/mole at 1141 K was measured for the heat of the molecular vaporization reaction for sodium chromate. In the case of potassium chromate, it has not been possible to conclude which mode of vaporization dominates. For potassium chromate a value of 101 kcal/mole at 1173 K was obtained for the heat of the molecular vaporization reaction.

Author

N79-28258* National Aeronautics and Space Administration. Lewis Research Center, Cleveland, Ohio.

THE ROLE OF NaCl IN FLAME CHEMISTRY, IN THE DEPOSITION PROCESS, AND IN ITS REACTIONS WITH PROTECTIVE OXIDES AS RELATED TO HOT CORROSION

Fred J. Kohl and Carl A. Stearns 1979 27 p refs Prepared for 4th Conf. on Gas Turbine Materials in a Marine Environment, Annapolis, Md., 25-28 Jun 1979

(NASA-TM-79225, E-120) Avail: NTIS HC A03/MF A01 CSCL 07D

Sodium chloride is believed to be the primary source of turbine engine contamination that contributes to hot corrosion. The behavior of NaCl-containing aerosols ingested with turbine intake air is very complex; some of the NaCl may vaporize during combustion while some may remain as particulates. The NaCl can lead to $Na2SO4$ formation by several possible routes or it can contribute to corrosion directly. Hydrogen or oxygen atom reaction with $NaCl(c)$ was shown to result in the release of $Na(g)$. Gaseous $NaCl$ in flames can be partially converted to gaseous $Na2SO4$ by homogeneous reactions. The remaining gaseous $NaCl$ and other Na-containing molecules can act as sodium carriers for condensate deposition of $Na2SO4$ on cool surfaces. A frozen boundary layer theory was developed to predict the rates of deposition. The condensed phase NaCl can be converted directly to condensed $Na2SO4$ by reaction with sulfur oxides and $O2$. Reaction of gaseous $NaCl$ with $Cr2O3$ results in the vapor phase transport of chromium by the formation of complex Cr-containing gaseous molecules. Similar gaseous complexes are formed with molybdenum. The presence of gaseous $NaCl$ was shown to affect the oxidation kinetics of Ni-Cr alloys. It also causes changes in the surface morphology of $Al2O3$ scales formed on Al-containing alloys. F O S

N79-31361* National Aeronautics and Space Administration. Lewis Research Center, Cleveland, Ohio.

THE CHEMISTRY OF SODIUM CHLORIDE INVOLVEMENT IN PROCESSES RELATED TO HOT CORROSION

Carl A. Stearns, Fred J. Kohl, and George C. Fryburg 1979 32 p refs Presented at the Conf. on Advanced Materials for Alternate Fuel Capable Directly Fired Heat Engines, Castine, Maine, 30 Jul - 3 Aug 1979

(NASA-TM-79251, E-161) Avail: NTIS HC A03/MF A01 CSCL 07D

Thermodynamic and mass transport calculations, and laboratory experiments elucidating the behavior of sodium chloride in combustion environments, in the deposition process, and in reactions with certain oxides on the surfaces of superalloys are summarized. It was found that some of the ingested salt is separated out of the air stream by the compressor. However, sodium chloride does pass from the compressor to the combustor where numerous chemical reactions take place. Here some of the salt is vaporized to yield gaseous sodium chloride molecules. Hydrogen and oxygen atoms present in the combustion products react with some sodium chloride to yield other gaseous species such as sodium, and a fraction of the salt remains as particulates. Both the gas phase and condensed sodium chloride can lead to sodium sulfate formation by various routes, all of which involve reaction with sulfur oxides and oxygen. In addition to contributing to the formation of sodium sulfate, the sodium chloride can contribute to corrosion directly. K L

A79-11542 * # Effect of inlet temperature on the performance of a catalytic reactor. D. N. Anderson (NASA, Lewis Research Center, Cleveland, Ohio). *U.S. Environmental Protection Agency, Workshop on Catalytic Combustion, 3rd, Asheville, N.C., Oct. 3, 4, 1978, Paper, 21 p.* 17 refs. Contract No. EC-77-A-31-1040.

A 12-cm-diameter by 15-cm-long catalytic reactor was tested with No. 2 diesel fuel in a combustion test rig at inlet temperatures of 700, 800, 900, and 1000 K. Other test conditions included pressures of 300,000 and 600,000 Pa, reference velocities of 10, 15, and 20 m/s, and adiabatic combustion temperatures in the range from 1100 to 1400 K. The combustion efficiency was calculated from measurements of carbon monoxide and unburned hydrocarbon emissions. Nitrogen oxide emissions and reactor pressure drop were also measured. At a reference velocity of 10 m/s, the CO and unburned hydrocarbons emissions and, therefore, the combustion efficiency were independent of inlet temperature. At an inlet temperature of 1000 K, they were independent of reference velocity. Nitrogen oxides emissions resulted from conversion of the small amount of fuel-bound nitrogen in the fuel. Up to 90% conversion was observed with no apparent effect of any of the test variables. For typical gas-turbine operating conditions, all three pollutants were below levels which would permit the most stringent proposed automotive emissions standards to be met. (Author)

A79-11547 * # Determination of the zincate diffusion coefficient and its application to alkaline battery problems. C. E. May and H. E. Kautz (NASA, Lewis Research Center, Cleveland, Ohio). *Electrochemical Society, Meeting, 154th, Pittsburgh, Pa., Oct. 15-20, 1978, Paper, 19 p.* 11 refs.

The diffusion coefficient for the zincate ion at 24 C was found to be 9.9×10^{-7} to the 7th power sq cm/sec + or - 30% in 45% potassium hydroxide and 1.4×10^{-7} to the 7th power sq cm/sec + or - 25% in 40% sodium hydroxide. Comparison of these values with literature values at different potassium hydroxide concentrations show that the Stokes-Einstein equation is obeyed. The diffusion coefficient is characteristic of the zincate ion (not the cation) and independent of its concentration. Calculations with the measured value of the diffusion coefficient show that the zinc concentration in an alkaline zincate half-cell becomes uniform throughout in tens of hours by diffusion alone. Diffusion equations are derived which are applicable to finite-size chambers. Details and discussion of the experimental method are also given. (Author)

A79-14956 * # Correlations of catalytic combustor performance parameters. D. L. Bulzan (NASA, Lewis Research Center, Cleveland, Ohio). *U.S. Environmental Protection Agency, Workshop on Catalytic Combustion, 3rd, Asheville, N.C., Oct. 3, 4, 1978, Paper, 14 p.* Contract No. EC-77-A-31-1040.

A 12-cm-diameter catalytic combustor test rig using propane fuel at an inlet temperature of 800 K, a pressure of 300,000 Pa, and reference velocities from 10 to 20 m/s was studied. Combustion efficiency at the test conditions is a function of the catalyst bed cell density, cell circumference, reactor length, and the reference velocity. The efficiency was also dependent on the adiabatic reaction temperature to the tenth power. The percentage pressure drop is proportional to the reference velocity to the 1.5 power and is also proportional to the reactor length and inversely proportional to the cell hydraulic diameter, fractional open area, and the pressure. The minimum adiabatic reaction temperature required to meet the emissions goals is proportional to the reference velocity to the 0.1 power and inversely proportional to the cell circumference, cell density, and reactor length to the 0.1 power. The parameters which are a function of a catalyst factor are reported. M. L.

A79-19480 * # Turbulence effects on flame speed and flame structure. K. O. Smith (NASA, Lewis Research Center, Cleveland, Ohio; Cornell University, Ithaca, N.Y.) and F. C. Gouldin (Cornell University, Ithaca, N.Y.). *American Institute of Aeronautics and Astronautics, Aerospace Sciences Meeting, 17th, New Orleans, La., Jan. 15-17, 1979, Paper 79-0016, 10 p.* 21 refs. Grant No. NSG 3019.

Turbulence effects on methane-air flames stabilized in grid turbulence were investigated through measurements of flame speed and mean and fluctuating flame temperature profiles. Published turbulent flame speed correlations were able to correlate the experimental flame speed data but were contradictory in indicating flame structure and combustion mechanisms. A simple, one-dimensional, wrinkled laminar flame model was used to predict characteristic flame temperature fluctuation levels. Comparison of these predictions with measured temperature fluctuations indicated that the majority of the flames studied were wrinkled laminar flames. However, a wrinkled laminar flame structure was inappropriate for the most intensely turbulent flames examined. (Author)

A79-19586 * # Experimental study of the effects of flameholder geometry on emissions and performance of lean premixed combustors. G. Roffe, K. S. Venkataramani (General Applied Sciences Laboratories, Inc., Westbury, N.Y.), and R. M. Duerr (NASA, Lewis Research Center, Cleveland, Ohio). *American Institute of Aeronautics and Astronautics, Aerospace Sciences Meeting, 17th, New Orleans, La., Jan. 15-17, 1979, Paper 79-0187, 10 p.* NASA-supported research.

Emissions of NO_x, CO and unburned hydrocarbons (UHC) are reported for a lean premixed propane-air system at inlet conditions of 800K and 1 MPa using twelve flameholder designs. The flameholders tested represent six design concepts with two values of blockage for each concept. Data were obtained at reference velocities of 35 m/s, 25 m/s and 20 m/s at combustor stations 10 cm and 30 cm downstream of the flameholders. Flameholder pressure drop was found to be a principal determinant of emissions performance. Designs producing larger pressure drops also produced less NO_x, CO and UHC emissions. The lean stability limit equivalence ratio was found to be approximately 0.35 for all designs. Flashback velocities (axial components in the flameholder passages) varied between 30 m/s and 40 m/s. A perforated plate flameholder was operated with a velocity as low as 23 m/s through the perforations at equivalence ratio 0.7 without producing flashback. (Author)

A79-21722 * # Ion chromatographic determination of sulfur in fuels. C. S. Mizisin, D. E. Kuivinen, and D. A. Otterson (NASA, Lewis Research Center, Cleveland, Ohio). *U.S. Environmental Protection Agency, National Symposium on Ion Chromatographic Analysis of Environmental Pollutants and Other Analogous Compounds, 2nd, Research Triangle Park, N.C., Oct. 11-13, 1978, Paper, 15 p.* 9 refs.

A79-25917 * # Evaluation of the application of some gas chromatographic methods for the determination of properties of synthetic fuels. A. C. Antoine (NASA, Lewis Research Center, Cleveland, Ohio). *Society of Automotive Engineers, Aerospace Meeting, San Diego, Calif., Nov. 27-30, 1978, Paper, 45 p.* 6 refs.

The purpose of the investigation was to evaluate the applicability, to some synthetic fuels, of some gas chromatographic methods now under development for use with petroleum based fuels. Thirty-two jet and diesel fuel samples which were prepared from oil shale and coal syncrudes were examined. The boiling range distribution of each was determined by gas chromatography, and from that data distillation properties were calculated. The calculated results gave sufficient agreement with the measured values that the equations could be useable in their present form. Bulk fuel properties were calculated for the 16 JP-5 and Diesel No. 2 type fuels. The results show that the equations would not give useable results. Capillary column gas chromatography was used to determine the n-alkane content of the eight JP-5 type samples and the results related to the observed freezing points. The results show that the concentrations of the long straight chain molecules in the fuels exert influence on the freezing point but are not the complete controlling factor. (Author)

A79-26374 * Burn coal cleanly in a fluidized bed - The key is in the controls. J. A. Kobak (NASA, Lewis Research Center, Cleveland, Ohio). *Instruments and Control Systems*, Jan. 1979, p. 29-32.

The fluidized-bed combustion (FBC) process produces few sulfur emissions, and can burn wood, municipal solid waste as well as every kind of coal available in the U.S. The pressurized, coal-burning fluidized-bed reactor at NASA's Lewis Research Center is described, together with a discussion of the operating results. The FBC system at Lewis, having a completely instrumented reactor, is used to test turbine blade alloys for future power plant applications. With the same type of coal and limestone used in the first testing phase covering 136 hours, it was found that all NO_x values were below the EPA standard of 0.7 lb/MBtu, whereas the maximum observed level of SO₂ was above the EPA standard of 1.3 lb/MBtu, but with the average SO₂ level, however, only 0.63 lb/MBtu. Unburned hydrocarbon and CO levels were very low, indicating combustion efficiencies of close to 99% in almost all tests. Testing is now underway using high temperature cyclones and gas turbine to eliminate erosion and corrosion effects which were observed after the initial tests on the turbine and blades. A.A.

A79-26546 * Effect of a chromium-containing fuel additive on hot corrosion. C. E. Lowell and D. L. Deadmore (NASA, Lewis Research Center, Cleveland, Ohio). *Corrosion Science*, vol. 18, 1978, p. 747-749, 751-759, 761-763. 8 refs.

Four cast superalloys (one cobalt-base and three nickel-base) were tested at 900 C for 100 h in Mach 0.3 combustion gases. 5 ppm of synthetic sea salt were added to the gases in the combustion chamber. Several types of thermal cycle and washing procedures were employed. Similar tests were made with the addition of 300 ppm of a chromium-containing fuel additive. In both sets of tests the extent of hot corrosion was evaluated by specific weight change and metal recession. In general, the chromium additive in the fuel reduced the extent of hot (salt) corrosion but did not eliminate it. The percentage reduction of hot corrosion attack was similar for all four alloys. As great a reduction of hot corrosion was achieved by reducing the number of thermal cycles during the test from 100 to 5 or 6. The effect of washing the alloys every ten cycles as opposed to the end of the test was erratic; some alloys were attacked slightly more, others somewhat less. A NiCrAlY coating was found to be more effective in reducing hot corrosion than either the fuel additive or the washing schedule. (Author)

A79-39036 * Effect of degree of fuel vaporization upon emissions for a premixed prevaporized combustion system. L. P. Cooper (NASA, Lewis Research Center, Cleveland, Ohio). *AIAA, SAE, and ASME, Joint Propulsion Conference, 15th, Las Vegas, Nev., June 18-20, 1979, AIAA Paper 79-1320* 13 p. 20 refs.

An experimental and analytical study of the combustion of partially vaporized fuel-air mixtures was performed to assess the impact of the degree of fuel vaporization upon emissions for a premixing-prevaporizing flametube combustor. Data collected showed near-linear increases in NO_x emissions with decreasing vaporization at equivalence ratios of 0.6. For equivalence ratios of 0.72, the degree of vaporization had very little impact on NO_x emissions. A simple mechanism which accounts for the combustion of liquid droplets in partially vaporized mixtures was found to agree with the measured results with fair accuracy with respect to both trends and magnitudes. (Author)

A79-46366 * Resonance-tube ignition of aluminum. B. R. Phillips (NASA, Lewis Research Center, Cleveland, Ohio) and K. J. de Witt (Toledo, University, Toledo, Ohio). *Combustion and Flame*, vol. 35, Aug. 1979, p. 249-258. 12 refs.

An experimental program was carried out to determine whether spontaneous fluid-dynamic oscillations could create a hazard in gaseous oxygen flow systems by igniting metal contaminants. The particular fluid-dynamic oscillation studied was the resonance-tube phenomenon as it was excited in a tee-shaped configuration

representative of configurations found in many industrial flow systems. Pure aluminum was chosen as the candidate material for ignition. The oscillations in the tee-shaped configuration were compared with oscillations driven by choked convergent nozzles and were found to differ markedly. The temperatures generated at the base of the resonance tube were well in excess of 1000 F for both gaseous oxygen and nitrogen. The effect of inert particulate matter introduced into the resonance tube was to increase significantly the measured temperatures. Aluminum in both powder and fiber form was readily ignited within the resonance tube at pressures less than 1200 psia. At higher pressures, the aluminum-oxygen mixture exploded. This investigation confirms the hazardous nature of resonance-tube oscillations as generated in typical piping configurations that use high-pressure oxygen. (Author)

A79-49533 * # Mass spectrometric investigation of the vaporization of sodium and potassium chromates - Preliminary results. C. A. Stearns, F. J. Kohl, R. A. Miller, and G. C. Fryburg (NASA, Lewis Research Center, Cleveland, Ohio). *Midwest High Temperature Chemistry Conference, 8th, Milwaukee, Wis., June 3-6, 1979, Paper, 14 p. 17 refs.*

A79-49534 * # The role of NaCl in flame chemistry, in the deposition process, and in its reactions with protective oxides as related to hot corrosion. F. J. Kohl, C. A. Stearns, and G. C. Fryburg (NASA, Lewis Research Center, Cleveland, Ohio). *Conference on Gas Turbine Materials in a Marine Environment, 4th, Annapolis, Md., June 25-28, 1979, Paper, 26 p. 61 refs.*

N79-10165*# General Applied Science Labs, Inc., Westbury, N. Y.

EMISSION MEASUREMENTS FOR A LEAN PREMIXED PROPANE/AIR SYSTEM AT PRESSURES UP TO 30 ATMOSPHERES Final Report

Gerald Roffe and K. S. Venkataramani Jun 1978 41 p ref (Contract NAS3-20603) (NASA-CR-159421, GASL TR-250) Avail NTIS HC A03/MF A01 CSCL 21B

The emissions of a lean premixed system of propane/air were measured in a flametube apparatus. Tests were conducted at inlet temperatures of 600K and 800K and pressures of 10 atm and 30 atm over a range of equivalence ratios. The data obtained were combined with previous data taken in the same apparatus to correlate nitrogen oxide emissions with operating conditions. Sampling probe design was found to have a pronounced effect on measured CO levels but did not influence measurements. The most effective probe tested was one which combined thermal and pressure quenching of the gas sample. A.R.H.

N79-22241*# United Technologies Research Center, East Hartford, Conn.

LEAN STABILITY AUGMENTATION STUDY Final Report John B. McVey and Jan B. Kennedy May 1979 185 p refs (Contract NAS3-20804) (NASA-CR-159536, UTRC/R79-914104-18) Avail NTIS HC A09/MF A01 CSCL 21B

An analytical conceptual design study and an experimental test program were conducted to investigate techniques and develop technology for improving the lean combustion limits of premixing, prevaporizing combustors applicable to gas turbine engine main burners. The use of hot gas pilots, catalyzed flameholder elements, and heat recirculation to augment lean stability limits was considered in the conceptual design study. Tests of flameholders embodying selected concepts were conducted at a pressure of 10 atm and over a range of entrance temperatures simulating conditions to be encountered during stratospheric cruise. The tests were performed using an axisymmetric flametube test rig having a nominal diameter of 10.2 cm. A total of sixteen test configurations were examined in which lean blowout limits, pollutant emission characteristics, and combustor performance were evaluated. The use of a piloted

perforated plate flameholder employing a pilot fuel flow rate equivalent to 4 percent of the total fuel flow at a simulated cruise condition resulted in a lean blowout equivalence ratio of less than 0.25 with a design point ($T_{sub\ zero} = 600K$, $\Phi = 0.6$) NOx emission index of less than 1.0 g/kg. Author

N79-23168* Georgia Inst. of Tech., Atlanta School of Aerospace Engineering

MEASUREMENTS OF ADMITTANCES AND CHARACTERISTIC COMBUSTION TIMES OF REACTIVE GASEOUS PROPELLANT COAXIAL INJECTORS

B. A. Janardan, B. R. Daniel, and B. T. Zinn Mar. 1979 78 p refs

(Grant NsG-3052)

(NASA-CR-159542) Avail: NTIS HC A05/MF A01 CSCL 21B

The results of an experimental investigation that was concerned with the quantitative determination of the capabilities of combustion processes associated with coaxial injectors to amplify and sustain combustor oscillations was described. The driving provided by the combustion process was determined by employing the modified standing-wave method utilizing coaxial injectors and air-acetylene mixtures. Analyses of the measured data indicate that the investigated injectors are capable of initiating and amplifying combustion instabilities under favorable conditions of injector-combustion coupling and over certain frequency ranges. These frequency ranges and the frequency at which an injector's driving capacity is maximum are observed to depend upon the equivalence ratio, the pressure drop across the injector orifices and the number of injector elements. The characteristic combustion times of coaxial injectors were determined from steady state temperature measurements. G Y

N79-25178* Case Western Reserve Univ., Cleveland, Ohio
X-RAY PHOTOELECTRON SPECTROSCOPY STUDY OF NICKEL AND NICKEL-BASE ALLOY SURFACE ALTERATIONS IN SIMULATED HOT CORROSION CONDITIONS WITH EMPHASIS ON EVENTUAL APPLICATION TO TURBINE BLADE CORROSION Final Report

Gheorghe D. Mateescu and Steven R. Smith Jun. 1979 49 p refs

(Grant NsG-3009)

(NASA-CR-159553) Avail: NTIS HC A03/MF A01 CSCL 07D

Research on the high temperature oxidation and Na₂SO₄ induced hot corrosion of some nickel base superalloys was accomplished by using ESCA to determine the surface composition of the oxidized or corroded samples. Oxidation was carried out at 900 or 1000 C in slowly flowing O₂ for samples of B-1900, NASA TRW VIA 713C and IN-738. Oxidation times ranged from 0.5 to 100 hr. Hot corrosion of B-1900 was induced applying a coating of Na₂SO₄ to peroxidized samples, the heating to 900 C in slowly flowing O₂. For oxidized samples, the predominant type of scale formed by each superalloy was determined, and a marked surface enrichment of Ti was found in each case. For corroded samples, the transfer of significant amounts of material from the oxide layer to the surface of the salt layer was observed to occur long before the onset of accelerating weight gain. Changes in surface composition were observed to coincide with the beginning of accelerating corrosion, the most striking of which was a tenfold decrease in the sulfur to sodium ratio and an increase in the Cr(VI) ratio. Author

N79-25183* Yale Univ., New Haven, Conn. High Temperature Chemical Reaction Engineering Lab

EXPERIMENTAL STUDIES OF THE FORMATION/DEPOSITION OF SODIUM SULFATE IN/ FROM COMBUSTION GASES Semiannual Report, 16 Nov. 1977 - 15 May 1978

Daniel E. Rosner 15 May 1978 14 p refs

(Grant NsG-3169)

(NASA-CR-159612 SAR 1) Avail: NTIS HC A02/MF A01 CSCL 21B

Processes related to the hot corrosion of gas turbine components were examined in two separate investigations.

Monochromatic laser light was used to probe condensation onset and condensate film growth (via interference of reflected light) on electrically heated ribbons immersed in seeded, flat flame combustion product gases. Boron trichloride is used as the seed gas in these preliminary experiments conducted to obtain precise measurements of the dew point/deposition rates. Because of the importance of gaseous Na(g) as a precursor to NaSO₄ formation, the kinetics and mechanisms of the heterogeneous reaction $H(g) + NaCl(s) \rightarrow Na(g) + HCl(g)$ was studied using atomic absorption spectroscopy combined with microwave discharge-vacuum flow reactor techniques at moderate temperatures. Preliminary results indicate the H-atom attack of solid NaCl vaporization is negligible, hence the corresponding gas phase (homogeneous) reaction no role in the observed Na(g) production. A R H

N79-31358* General Electric Co., Cincinnati, Ohio
LEAN, PREMIXED-PREVAPORIZED (LPP) COMBUSTOR CONCEPTUAL DESIGN STUDY Final Report

R. A. Dickman, W. J. Dodds, and E. E. Ekstedt May 1979 152 p refs

(Contract NAS3-21255)

(NASA-CR-159629, R79AEG376)

Avail: NTIS

HC A08/MF A01 CSCL 21B

Four combustion systems were designed and sized for the energy efficient engine. A fifth combustor was designed for the cycle and envelope of the twin-spool, high bypass ratio, high pressure ratio turbofan engine. Emission levels, combustion performance, life, and reliability assessments were made for these five combustion systems. Results of these design studies indicate that cruise NOx emission can be reduced by the use of lean, premixed-prevaporized combustion and airflow modulation. Author

N79-32303* Notre Dame Univ., Ind. Dept. of Aerospace and Mechanical Engineering

FEASIBILITY STUDY OF LIQUID POOL BURNING IN REDUCED GRAVITY Final Report, Jul. 1977 - Feb. 1979

A. Murty Kanury Sep. 1979 79 p refs

(Contract NAS3-21018)

(NASA-CR-159642, TR-79-1) Avail: NTIS HC A05/MF A01 CSCL 21B

The feasibility of conducting experiments in the Spacelab on ignition and flame spread with liquid fuel pools which are initially at a temperature lower than the fuels flash point temperature was studied. Theories were developed for the ignition and flame spread processes, and experiments were conducted to understand the factors influencing the ignition process and the spread rate. The results were employed to revise a conceptual Spacelab experiment which is expected to be feasible for a safe conduct and to be suitable for obtaining crucial data on the concerned processes. K L

N79-33288* State Univ. of New York at Stony Brook
COMBUSTION OF POROUS SOLIDS AT REDUCED GRAVITATIONAL CONDITIONS Final Report

A. L. Berlad and J. Killroy Washington NASA Oct. 1979 110 p refs

(Grant NsG-3051)

(NASA-CR-3197) Avail: NTIS HC A06/MF A01 CSCL 21B

A ground-based experimental and analytic study considered the utility and the feasibility of a space shuttle-based experimental study of the combustion of porous solids at reduced gravitational conditions. This ground-based study employed the Lewis Research Center's g = 0 (drop tower) facility. Experimental g = 1 studies were performed both at the Lewis Research Center and at State University of New York at Stony Brook. It is found that the considered space shuttle-based experimental program is expected to yield vital fundamental combustion information that is not obtainable from earth-bound studies alone. The considered space shuttle-based study is entirely feasible and a detailed approach to these experiments is presented. M M M

26 METALLIC MATERIALS

Includes physical, chemical, and mechanical properties of metals, e.g., corrosion, and metallurgy.

N79-1179* National Aeronautics and Space Administration
Lewis Research Center, Cleveland, Ohio

THERMAL BARRIER COATINGS: BURNER RIG HOT CORROSION TEST RESULTS Final Report

Philip E. Hodge, Stephen Stecura, Michael A. Gedwill, Isidor Zaplatynsky, and Stanley R. Levine. Oct. 1978. 35 p. refs.
(Contract EF 77 A 01 2593)

(NASA-TM-79005, E-9787, DOE/NASA/2593-78/3) Avail.
NTIS HC A03/MF A01 CSCL 11F

A Mach 0.3 burner rig test program was conducted to examine the sensitivity of thermal barrier coatings to Na and V contaminated combustion gases simulating potential utility gas turbine environments. Coating life of the standard ZrO₂ 12Y2O₃/Ni-16 2Cr-5.6Al-0.6Y NASA thermal barrier coating system which was developed for aircraft gas turbines was significantly reduced in such environments. Two thermal barrier coating systems, Ca₂SiO₄/Ni-16 2Cr-5.6Al-0.6Y and ZrO₂ 8Y2O₃/Ni-16 4Cr-5.1Al-0.15Y and a less insulative cermet coating system, 50 volume percent MgO-50 volume percent Ni-19 6Cr-17 1Al-0.97Y/Ni-16 2Cr-5.6Al-0.6Y, were identified as having much improved corrosion resistance compared to the standard coating. Author

N79-12201* National Aeronautics and Space Administration
Lewis Research Center, Cleveland, Ohio

THE EFFECT OF NITROGEN ION (N(+)) IMPLANTATION ON THE FRICTION AND WEAR CHARACTERISTICS OF IRON

William R. Jones, Jr. and John Ferrante. Nov. 1978. 18 p. refs.

(NASA-TM-79029, E-9824) Avail. NTIS HC A02/MF A01 CSCL 11F

The friction and wear properties of pure iron sliding against M-50 steel were not significantly altered after nitrogen implantation. The unimplanted iron exhibited an average wear rate of 1.47×10^{-3} or 0.27 M to the third power/N-M compared to 1.53×10^{-3} or 0.73 for the nitrogen implanted iron. Average friction coefficients were 0.10 (unimplanted) and 0.09 (implanted). G.G.

N79-12203* National Aeronautics and Space Administration
Lewis Research Center, Cleveland, Ohio

FRETTING WEAR OF IRON, NICKEL, AND TITANIUM UNDER VARIOUS ENVIRONMENTAL CONDITIONS

Robert C. Bill, (AVRADCOM Res. and Technol. Labs.) 1978. 30 p. refs. Proposed for presentation at the Intern. Conf. Wear of Mater., Dearborn, Mich., 16-18 Apr. 1979; sponsored by ASME, ASLE, ASM, ASTM 62, SAE, SME, Am. Chem. Soc., AIAA, and APS.

(NASA-TM-78972, AVRADCOM-TR-78-59, E-9745) Avail.
NTIS HC A03/MF A01 CSCL 11F

Fretting wear experiments were conducted on high purity iron, nickel and titanium in air under conditions of varied humidity and temperature, and in nitrogen. For iron and titanium, maximum fretting occurred at 1% and 30 percent relative humidity respectively. Nickel showed a minimum in fretting wear at about 10 percent relative humidity. With increasing temperature, all three metals initially showed reduced fretting wear, with increasing wear observed as temperatures increased beyond 200-300 C. For titanium, dramatically reduced fretting wear was observed at temperatures above 500 C, relatable to a change in oxidation kinetics. All three metals showed much less fretting wear in N₂ than the presence of moisture in N₂ having a proportionally stronger effect than in air. Author

N79-12204* National Aeronautics and Space Administration
Lewis Research Center, Cleveland, Ohio

WEAR OF SEAL MATERIALS USED IN AIRCRAFT PROPULSION SYSTEMS

Robert C. Bill and Lawrence P. Ludwig. 1978. 30 p. refs. Presented at the Mater. and Processing Congr., Philadelphia, 7-9 Nov. 1978. Prepared in cooperation with Army Aviation Research and Development Command, St. Louis, Mo.

(NASA-TM-79003, E-9789, AVRADCOM-TR-78-47) Avail.
NTIS HC A03/MF A01 CSCL 11F

The various types of seal locations in a gas turbine engine are described, and the significance of wear to each type is reviewed. Starting with positive contact shaft seals, existing material selection guidelines are reviewed, and the existing PV (contact pressure X sliding velocity) criteria for selecting seal materials are discussed, along with the theoretical background for these criteria. Examples of wear mechanisms observed to operate in positive contact seals are shown. Design features that can extend the operating capabilities of positive contact seals, including pressure balancing and incorporation of hydrodynamic lift are briefly discussed. It is concluded that, despite the benefits arising from these design features, improved positive contact seal materials from the standpoint of wear, erosion and oxidation resistance will be necessary for further improvements in seal performance and durability, and to meet stringent future challenges. Author

N79-12205* National Aeronautics and Space Administration
Lewis Research Center, Cleveland, Ohio

SHEAR RUPTURE OF A DIRECTIONALLY SOLIDIFIED EUTECTIC GAMMA/GAMMA PRIME - ALPHA (Mo) ALLOY

Fredric H. Harf. 1978. 15 p. refs. Presented at the Conf. on In-Situ Composites 3, Boston, 27 Nov. - 1 Dec. 1978; sponsored by the Mater. Res. Soc.

(NASA-TM-79038, E-9840) Avail. NTIS HC A02/MF A01 CSCL 11F

Directionally solidified Mo alloys are evaluated to determine the shear rupture strength and to possibly improve it by microstructural and heat treatment variations. Bars of the alloy containing nominally 5.7% Al and 33.5% Mo by weight with balance Ni were directionally solidified at rates between 10 and 100 mm per hour in furnaces with thermal gradients at the liquid-solid interface of 250 or 100 C per cm. A limited number of longitudinal shear rupture tests were conducted at 760 C and 207 MPa in the as-solidified and in several heat treated conditions. It is shown that shear rupture failures are partly transgranular and that resistance to failure is prompted by good fiber alignment and a matrix structure consisting mainly of gamma prime. Well aligned as-solidified specimens sustained the shear stress for an average of 81 hours. A simulated coating heat treatment appeared to increase the transformation of gamma to gamma prime and raised the average shear life of aligned specimens to 111 hours. However, heat treatments at 1245 C and especially at 1190 C appeared to be detrimental by causing partial solutioning of the gamma prime, and reducing lives to 47 and 10 hours, respectively. G.G.

N79-19145* National Aeronautics and Space Administration
Lewis Research Center, Cleveland, Ohio

HIGH TOUGHNESS-HIGH STRENGTH IRON ALLOY Patent Application

J. R. Stephens and W. R. Witzke, inventors (to NASA). 25 Jan. 1979. 11 p.

(NASA-Case-LEW-12542-3, US Patent Appl. SN 007083) Avail.
NTIS HC A02/MF A01 CSCL 11F

An improved steel alloy is described which exhibits both high toughness and high strength at cryogenic temperatures. The alloy consists essentially of about 10 to 16 percent by weight nickel, up to 1.0 percent by weight aluminum, and up to about 3 percent by weight of at least one of the following additional elements: copper, lanthanum, niobium, tantalum, titanium, vanadium, yttrium, zirconium and the rare earth metals, with the balance being essentially iron. The steel alloy is produced by a process which includes using cold rolling at room temperature and subsequent heat treatment at temperatures ranging from 500 deg to 650 C. The alloy possesses a fracture toughness ranging from 200 to 230 ksi in and yield strengths up to 230 ksi. NASA

N79-20216* National Aeronautics and Space Administration, Lewis Research Center, Cleveland, Ohio.

CRITICAL MASS FLUX THROUGH SHORT BORDA TYPE INLETS OF VARIOUS CROSS SECTIONS

R. C. Hendricks and N. P. Poulos (Lake Ridge Academy, North Ridgeville, Ohio) 1979 26 p refs To be presented at the 15th Intern. Congr. of Refrigeration, Venice, 23-29 Sep. 1979; sponsored by the Intern. Inst. of Refrigeration (NASA-TM-79017; E-9888) Avail: NTIS HC A03/MF A01 CSCL 11F

Mass flux measurements associated with choked flows through four Borda type inlet geometries: circular, square, triangular and rectangular (two-dimensional) and two sharp edged geometries taken over a very wide range of inlet stagnation conditions. The measurements indicate that: (1) the mass flux is independent of the inlet cross-section geometry and (2) the mass flux is dependent only on the inlet stagnation conditions. Also by using choked flow results found in the literature, the reduced mass flux is independent of working fluid. Two implications are drawn which remain to be verified: (1) since seal leak rates are weakly dependent on geometry but pressure distribution is strongly dependent on geometry, seal design efforts should be directed more toward controlling the dynamics, and (2) high-L/D ducts of arbitrary cross section and Borda type inlets can possess free jets. L.S.

N79-20217* National Aeronautics and Space Administration, Lewis Research Center, Cleveland, Ohio.

EVALUATION OF A BRAYTON CYCLE RECUPERATOR AFTER 21,000 HOURS OF GROUND TESTING

Thomas J. Moore Feb. 1979 28 p refs (NASA-TM-79091; E-9915) Avail: NTIS HC A03/MF A01 CSCL 11F

A metallographic examination was conducted on a Brayton cycle recuperator and associated ducting after 21,000 hours of ground testing in air. At the hot (turbine) end, the recuperator operated at a nominal temperature of 675 C. The type 347 stainless-steel recuperator performed satisfactorily in the ground test even though the primary working fluid leaked to the atmosphere periodically. The leakage path was located at plate-bar braze joints which cracked as a result of thermal stresses. The welded type 347 stainless steel ducting a type 347/Hastelloy X bellows survived the ground test with no apparent loss of ductility or integrity. Some apparent aging embrittlement was observed in the Hastelloy X ducting but the serviceability was not affected. Author

N79-20218* National Aeronautics and Space Administration, Lewis Research Center, Cleveland, Ohio.

CHARACTERIZATION OF DEFECT GROWTH STRUCTURE IN ION PLATED FILMS BY SCANNING ELECTRON MICROSCOPY

Talivaldis Spalvins 1979 12 p refs Presented at the Intern. Conf. on Met. Coatings, San Diego, Calif., 23-27 Apr. 1979; sponsored by Am. Vacuum Soc. (NASA-TM-79110; E-9528) Avail: NTIS HC A02/MF A01 CSCL 11F

Copper and gold films (0.2 to 2 microns) were ion plated onto polished 304-stainless-steel surfaces. These coatings were examined by scanning electron microscopy for coating growth defects. Three types of defects were distinguished: nodular growth, abnormal or runaway growth, and spits. The cause and origin for each type of defect was traced. Nodular growth is primarily due to inherent substrate microdefects, abnormal or runaway growth is due to external surface inclusions, and spits are due to nonuniform evaporation. All these defects have adverse effects on the coatings. They induce stresses and produce porosity in the coatings and thus weaken their mechanical properties. Friction and wear characteristics are affected by coating defects, since the large nodules are pulled out and additional wear debris is generated. Author

N79-20220* National Aeronautics and Space Administration, Lewis Research Center, Cleveland, Ohio.

ADHERENCE OF SPUTTERED TITANIUM CARBIDES

William A. Brainard and Donald R. Wheeler 1979 10 p refs Presented at the Intern. Conf. on Met. Coatings, San Diego, Calif., 23-27 Apr. 1979 (NASA-TM-79117; E-9950) Avail: NTIS HC A02/MF A01 CSCL 11F

Sputtered coatings of the refractory metal carbides are of great interest for applications where hard wear-resistant materials are desired. The usefulness of sputtered refractory carbides is often limited, in practice, by spalling or interfacial separation. In this work improvements in the adherence of refractory carbides on iron, nickel and titanium based alloys were obtained by using oxidation, reactive sputtering or sputtered interlayers to alter the coating-substrate interfacial region. X-ray photoelectron spectroscopy and argon ion etching were used to characterize the interfacial regions, and an attempt was made to correlate adherence as measured in wear tests with the chemical nature of the interface. Author

N79-21184* National Aeronautics and Space Administration, Lewis Research Center, Cleveland, Ohio.

WEAR OF ALUMINUM AND HYPOEUTECTIC ALUMINUM-SILICON ALLOYS IN BOUNDARY-LUBRICATED PIN-ON-DISK SLIDING

John Ferrante and William A. Brainard Apr. 1979 27 p refs (NASA-TP-1442; E-9809) Avail: NTIS HC A03/MF A01 CSCL 11F

The friction and wear of pure aluminum and a number of hypoeutectic aluminum-silicon alloys (with 3 to 12 wt %Si) were studied with a pin-on-disk apparatus. The contacts were lubricated with mineral oil and sliding was in the boundary-lubrication regime at 2.6 cm/sec. Surfaces were analyzed with photomicrographs, scanning electron microscopy, X-ray dispersive analysis, and diamond pyramid hardness measurements. There were two wear regimes for the alloys - high and low - whereas pure aluminum exhibited a high wear rate throughout the test period. Wear rate decreased and the transition stress from high to low wear increased with increasing hardness. There was no correlation between friction coefficient and hardness. A least squares curve fit indicated a wear-rate dependence greater than the inverse first power of hardness. The lower wear rates of the alloys may be due to the composites of silicon platelets in aluminum resulting in increased hardness and thus impairing the shear of the aluminum. Author

N79-22271* National Aeronautics and Space Administration, Lewis Research Center, Cleveland, Ohio.

PROCESS FOR MAKING A HIGH TOUGHNESS-HIGH STRENGTH ION ALLOY Patent

Joseph R. Stephens and Walter R. Witzke, inventors (to NASA) Issued 27 Mar. 1979 4 p Filed 13 Dec. 1977 Supersedes: N78-22205 (16 - 13, p. 1681) Division of US Patent Appl. SN-803822, filed 6 Jun. 1977 (NASA-Case-LEW-12542-2; US-Patent-4,146,409; US-Patent-Appl-SN-860405; US-Patent-Class-148-2; US-Patent-Class-148-12F; US-Patent-Class-148-12-4; US-Patent-Appl-SN-803822) Avail: US Patent and Trademark Office

A steel alloy is produced by a process which includes using cold rolling at room temperature and subsequent heat treatment at temperatures ranging from 500 C to 650 C. The resulting alloys exhibit excellent strength and toughness characteristics at cryogenic temperatures. This alloy consists essentially of about 10 to 16 percent by weight nickel, to about 1.0 percent by weight aluminum, and 0 to about 3 percent by weight of at least one of the following additional elements: copper, lanthanum, niobium, tantalum, titanium, vanadium, yttrium, zirconium and the rare earth metals, with the balance being essentially iron. The improved alloy possesses a fracture toughness ranging from 200 to 230 ksi sq in. and yield strengths up to 230 ksi.

Official Gazette of the U.S. Patent and Trademark Office

N79-22274* National Aeronautics and Space Administration. Lewis Research Center, Cleveland, Ohio.

THE FRICTION AND WEAR OF METALS AND BINARY ALLOYS IN CONTACT WITH AN ABRASIVE GRIT OF SINGLE-CRYSTAL SILICON CARBIDE

Kazuhisa Miyoshi and Donald H. Buckley 1979 28 p refs Proposed for presentation at the Joint Lubrication Conf., Dayton, Ohio, 16-18 Oct. 1979; cosponsored by Am. Soc. of Lubrication Engr. and ASME

(NASA-TM-79131; E-9973) Avail: NTIS HC A03/MF A01 CSCL 11F

Sliding friction experiments were conducted with various metals and iron-base binary alloys (alloying elements Ti, Cr, Mn, Ni, Rh and W) in contact with single crystal silicon carbide riders. Results indicate that the friction force in the plowing of metal and the groove height (corresponding to the wear volume of the groove) decrease linearly as the shear strength of the bulk metal increases. The coefficient of friction and groove height generally decrease, and the contact pressure increases with an increase in solute content of binary alloys. There appears to be very good correlation of the solute to iron atomic ratio with the decreasing rate of change of coefficient of friction, the decreasing rate of change of groove height and the increasing rate of change of contact pressure with increasing solute content. These rates of change increase as the solute to iron atomic radius ratio increases or decreases from unity. Author

N79-23196* National Aeronautics and Space Administration. Lewis Research Center, Cleveland, Ohio.

THE STRAINRANGE PARTITIONING BEHAVIOR OF AN ADVANCED GAS TURBINE DISK ALLOY, AF2-1DA

G. R. Halford and A. J. Nachtigall 1979 11 p refs Presented at the 15th Joint Propulsion Conf., Las Vegas, 18-20 Jun. 1979; cosponsored by AIAA, the Soc. of Automotive Engr., and ASME (NASA-TM-79179; E-046) Avail: NTIS HC A02/MF A01 CSCL 11F

The low-cycle, creep-fatigue characteristics of the advanced gas turbine disk alloy, AF2-1DA have been determined at 1400 F and are presented in terms of the method of strainrange partitioning (SRP). The mean stresses which develop in the PC and CP type SRP cycles at the lowest inelastic strainrange were observed to influence the cyclic lives to a greater extent than the creep effects and hence interfered with a conventional interpretation of the results by SRP. A procedure is proposed for dealing with the mean stress effects on life which is compatible with SRP. Author

N79-25195* National Aeronautics and Space Administration. Lewis Research Center, Cleveland, Ohio.

METAL-DIELECTRIC INTERACTIONS

Donald H. Buckley 1979 24 p refs Presented at Conf. on Electrical Insulation and Dielectric Phenomena, Whitehaven, Pa., 21-25 Oct. 1979; sponsored by NRC (NASA-TM-79151) Avail: NTIS HC A02/MF A01 CSCL 11F

Metal dielectric surface interactions and dielectric films on metal substrates were investigated. Since interfacial interaction depends so heavily on the nature of the surfaces, analytical surface tools such as Auger emission spectroscopy, X-ray photoelectron spectroscopy and field ion microscopy were used to assist in surface and interfacial characterization. The results indicate that with metals contacting certain glasses in the clean state interfacial bonding produces fractures in the glasses while when a film such as water is present, fractures occur in the metal near the interface. Friction forces were used to measure the interfacial bond strengths. Studies with metals contacting polymers using field ion microscopy revealed that strong bonding forces could develop being between a metal and polymer surface with polymer transferring to the metal surface in various ways depending upon the forces applied to the surface in contact. With the deposition of refractory carbides, silicides and borides onto metal and alloy substrates the presence of oxides at the interface or active gases in the deposition plasma were shown to alter interfacial properties and chemistry. Auger ion depth profile analysis indicated the chemical composition at the interface

and this could be related to the mechanical, friction, and wear behavior of the coating. R.E.S.

N79-29292* National Aeronautics and Space Administration. Lewis Research Center, Cleveland, Ohio.

AN EXPERIMENTAL, LOW-COST, SILICON SLURRY/ALUMINIDE HIGH-TEMPERATURE COATING FOR SUPER-ALLOYS

Stanley G. Young and Daniel L. Deadmore Jul 1979 24 p refs (NASA-TM-79178; E-045) Avail: NTIS HC A02/MF A01 CSCL 11F

A duplex silicon-slurry/aluminide coating has been developed and cyclically tested in Mach 1 combustion gases for oxidation and thermal fatigue resistance at 1093 C and in Mach 0.3 gases for hot-corrosion resistance at 900 C. The base-metal superalloys were V1A and B-1900. The coated B-1900 specimens performed much better in oxidation than similar specimens coated with aluminides and almost as well as the more-expensive Pt-Al and MCrAlY (where M is Ni and/or Co) coatings deposited by the physical vapor deposition process. The coating also provided good hot-corrosion protection. Metallographic, X-ray, and electron microprobe studies were made to characterize the coating, determine failure mechanisms, and study some of the changes due to exposure. Author

N79-29293* National Aeronautics and Space Administration. Lewis Research Center, Cleveland, Ohio.

EFFECTS OF YTTRIUM, ALUMINUM, AND CHROMIUM CONCENTRATIONS IN BOND COATINGS ON THE PERFORMANCE OF ZIRCONIA-YTRIA THERMAL BARRIERS

Stephan Stecura Jul 1979 30 p refs (NASA-TM-79206; E-091) Avail: NTIS HC A03/MF A01 CSCL 11F

A cyclic furnace study was conducted between 990 - 280 C and 1095 - 280 C to evaluate the effects of yttrium, chromium, and aluminum concentrations in nickel base alloy bond coatings and also the effect of the bond coating thickness on the performance of yttria-stabilized zirconia thermal barrier coatings. The presence and the concentration of yttrium is very critical. Without yttrium, rapid oxidation of Ni-Al, Ni-Cr, and Ni-Cr-Al bond coatings causes zirconia thermal barrier coatings to fail very rapidly. Concentrations of chromium and aluminum in Ni-Cr-Al-Y bond coating have a very significant effect on the thermal barrier coating life. This effect, however, is not as great as that due to yttrium. Furthermore, the thickness and the thickness uniformity also have a very significant effect on the life of the thermal barrier system. Author

N79-30355* National Aeronautics and Space Administration. Lewis Research Center, Cleveland, Ohio.

TRANSVERSE AND LONGITUDINAL TENSILE PROPERTIES AT 760 C OF SEVERAL OXIDE DISPERSION STRENGTHENED NICKEL-BASE ALLOYS

Albert E. Anglin, Jr. 1979 24 p refs Presented at Meeting of the Metallurgical Soc. of the Am. Inst. of Mining, Metallurgical, and Petroleum Engineers, New Orleans, La., 18-20 Feb 1979 (NASA-TM-79189; E-058) Avail: NTIS HC A02/MF A01 CSCL 11F

The transverse and longitudinal tensile properties of the oxide dispersion strengthened nickel base alloys MA-793, MA-754, MA-755E, and MA-6000E were determined at 760 C. Transverse tensile strengths were comparable to longitudinal strengths. Transverse ductility levels generally were less than two percent elongation. Both tensile and yield strengths increased with increasing strain rate over the range 0.001 to 0.05 per second. Ductility was not strain rate sensitive, but related to grain size and grain aspect ratio. The fracture mode of most alloys changed from transgranular for longitudinally oriented specimens to intergranular for transverse specimens. Transverse properties of DM MAR M-200 + Hf were also determined for comparison. Author

N79-30356* National Aeronautics and Space Administration, Lewis Research Center, Cleveland, Ohio.

THE EROSION/CORROSION OF SMALL SUPERALLOY TURBINE ROTORS OPERATING IN THE EFFLUENT OF A PFB COAL COMBUSTOR

G. R. Zellars, S. M. Benfold, A. P. Rowe, and C. E. Lowell 1979 27 p Presented at the Advanced Mater. for Alternate Fuel Capable Directly Fired Heat Engines Conf., Castine, Maine, 30 Jul. - 3 Aug. 1979; cosponsored by DOE and EPRI (NASA-TM-79227; E-125) Avail: NTIS HC A03/MF A01 CSCL 11F

Superalloy turbine rotors in a single stage turbine with 6 percent partial admittance were operated in the effluent of a pressurized fluidized bed coal combustor for up to 164 hours. Total mass flow was 300 kg/hr and average particulate loadings ranged from 600 to 2800 ppm for several coal/sorbent combinations. A 5.5 atm turbine inlet gas pressure and inlet gas temperatures from 700 to 800 C yielded absolute gas velocities at the stator exit of about 500 m/s. The angular rotation speed (40,000 rpm) of the six inch diameter rotors was equivalent to a tip speed of about 300 m/s, and average gas velocities relative to the rotating surface ranged from 260 to 330 m/s at mean radius. The rotor erosion pattern reflects heavy particle separation with severe (5 to 500 cm/yr) erosion at the leading edge, pressure side center, and suction side trailing edge at the tip. The erosion distribution pattern provides a spectrum of erosion/oxidation/deposition as a function of blade position. This spectrum includes enhanced oxidation (10 to 100 x air), mixed oxides in exposed depletion zones, sulfur rich oxides in deposition zones, and rugged areas of erosive oxide removal.

A.W.H.

N79-31372* National Aeronautics and Space Administration, Lewis Research Center, Cleveland, Ohio.

SURVEY OF ION PLATING SOURCES

Talivaldis Spalvins 1979 25 p refs Presented at 26th Natl. Vacuum Symp., N. Y., 2-5 Oct. 1979; sponsored by the Am. Vacuum Soc. (NASA-TM-79269; E-188) Avail: NTIS HC A02/MF A01 CSCL 11F

Based on the type of evaporation source, gaseous media and mode of transport, the following is discussed: resistance, electron beam, sputtering, reactive and ion beam evaporation. Ionization efficiencies and ion energies in the glow discharge determine the percentage of atoms which are ionized under typical ion plating conditions. The plating flux consists of a small number of energetic ions and a large number of energetic neutrals. The energy distribution ranges from thermal energies up to a maximum energy of the discharge. The various reaction mechanisms which contribute to the exceptionally strong adherence - formation of a graded substrate/coating interface are not fully understood, however the controlling factors are evaluated. The influence of process variables on the nucleation and growth characteristics are illustrated in terms of morphological changes which affect the mechanical and tribological properties of the coating.

M.M.M.

N79-33306* National Aeronautics and Space Administration, Lewis Research Center, Cleveland, Ohio.

SOME TEM OBSERVATIONS OF Al₂O₃ SCALES FORMED ON NiCrAl ALLOYS

J. Smialek and R. Cibala (Case Western Reserve Univ., Cleveland, Ohio) 1979 34 p refs Presented at Gordon Conf. on Corrosion, New London, N. H., 23-27 Jul. 1979 (NASA-TM-79259; E-171) Avail: NTIS HC A03/MF A01 CSCL 11F

The microstructural development of Al₂O₃ scales on NiCrAl alloys has been examined by transmission electron microscopy. Voids were observed within grains in scales formed on a pure NiCrAl alloy. Both voids and oxide grains grew measurably with oxidation time at 1100 C. The size and amount of porosity decreased towards the oxide-metal growth interface. The voids resulted from an excess number of oxygen vacancies near the oxide-metal interface. Short-circuit diffusion paths were discussed in reference to current growth stress models for oxide scales. Transient oxidation of pure, Y-doped, and Zr-doped NiCrAl was

also examined. Oriented alpha-(Al, Cr)₂O₃ and Ni(Al, Cr)₂O₄ scales often coexisted in layered structures on all three alloys. Close-packed oxygen planes and directions in the corundum and spinel layers were parallel. The close relationship between oxide layers provided a gradual transition from initial transient scales to steady state Al₂O₃ growth.

M.M.M.

A79-10420 * The hot corrosion of Co-25Cr-10Ni-5Ta-3Al-0.5Y alloy /S-57/. G. J. Santoro (NASA, Lewis Research Center, Cleveland, Ohio). *Corrosion Science*, vol. 18, 1978, p. 651-677. 29 refs.

A cobalt-base alloy, Co-25Cr-10Ni-5Ta-3Al-0.5Y (S-57), was subjected to hot corrosion in Mach 0.3 burner-rig combustion gases at maximum alloy temperatures of 900 and 1000 C. Various salt concentrations were injected into the burner: 0.5, 2.5, and 10 parts per million synthetic sea salt and 4 parts per million sodium sulfate (Na₂SO₄). The extent of corrosion was determined by measuring the maximum depth of corrosion in the alloy, and the corrosion process was studied by metallography, X-ray diffraction, scanning electron microscopy, and electron microprobe analysis. While S-57 was found to possess only moderate oxidation resistance at these temperatures, this alloy resisted significant hot corrosion attack under all but the most severe test conditions. The process of hot corrosion attack under the most severe conditions of this study was primarily sulfidation.

(Author)

A79-13100 * Some properties of low-vapor-pressure braze alloys for thermionic converters. V. L. Bair (NASA, Lewis Research Center, Cleveland, Ohio). *Institute of Electrical and Electronics Engineers, International Conference on Plasma Science, Monterey, Calif., May 15-18, 1978, Paper*. 13 p. 10 refs.

Density, dc electrical resistivity, thermal conductivity, and linear thermal expansion are measured for arc-melted rod-shaped samples of binary eutectics of Zr, Hf, Ru, Nb, Ir, Mo, Ta, Os, Re, and W selected as very-low-pressure braze fillers for thermionic converters. The first two properties are measured at 296 K for Zr-21.7 at% Ru, Zr-13 wt% W, Zr-19 wt% W, Zr-22.3 at% Nb, Nb-66.9 at% Ru, Hf-25.3 wt% Re, Zr-25.7 at% Ta, Hf-22.5 at% W, and Nb-35 wt% Mo. The last property is measured from 293 K to 2/3 melting point for specified alloys of different compositions. Resistivities of 0.000055 to 0.000181 ohm-cm are observed with the alloys having resistivities about ten times that of the less resistive constituent metal and about three times that of the more resistive constituent metal, except for Zr-19 wt% W and Nb-35 wt% Mo (greater resistivities). Thermal expansion coefficients vary from 0.000006 to 0.0000105/K. All brazes exhibit linear thermal expansion near that of their constituent metals.

S.D.

A79-14955 * Longitudinal shear behavior of several oxide dispersion strengthened alloys. T. K. Glasgow (NASA, Lewis Research Center, Cleveland, Ohio). *American Institute of Mining, Metallurgical and Petroleum Engineers, Fall Meeting, Chicago, Ill., Oct. 24-27, 1977, Paper*. 19 p. 11 refs.

Two commercial oxide dispersion strengthened (ODS) alloys, MA-753 and MA-754, and three experimental ODS alloys, MA-757E, MA-755E, and MA-6000E, were tested in shear at 760 C. Comparisons were made with other turbine-blade and vane alloys. All of the ODS alloys exhibited less shear strength than directionally solidified Mar-M 200 + Hf or than conventionally cast B-1900. The strongest ODS alloy tested, MA-755E, was comparable in both shear and tensile strength to the lamellar directionally solidified eutectic alloy gamma/gamma-prime - delta. Substantial improvements in shear resistance were found for all alloys tested when the geometry of the specimen was changed from one generating a transverse tensile stress in the shear area to one generating a transverse compressive stress. Finally, 760-C shear strength as a fraction of tensile strength was found to increase linearly with the log of the transverse tensile ductility.

(Author)

A79-16038 * Interpolation and extrapolation of creep rupture data by the Minimum Commitment Method. I - Focal-point convergence. II - Oblique translation. III - Analysis of multiheats. S. S. Manson (Case Western Reserve University, Cleveland, Ohio) and C. R. Ensign (NASA, Lewis Research Center, Cleveland, Ohio). In: Characterization of materials for service at elevated temperatures; Proceedings of the Pressure Vessel and Pipework Conference, Montreal, Canada, June 25-29, 1978. (A79-16026 04-26) New York, American Society of Mechanical Engineers, 1978, p. 299-457. 26 refs. Research supported by the Electric Power Research Institute and NASA.

The framework in which minimum-commitment analyses of creep-rupture data can be implemented is outlined. The approach is termed the focal point convergence method (FPCM) because the basic parameter A, also known as stability factor, is geometrically the (imaginary) focal point of convergence of all isothermals when extended to the very long or very short times necessary for such convergence to occur. The method can be implemented either by manual-graphical analysis or by computer code. The method is illustrated in detail for the nickel-base alloy Astroloy, as well as for steels, other nickel-base alloys, and aluminum alloys. The minimum-commitment concept is extended to the analysis of creep-rupture data where each isothermal is generated by an oblique translation of the 'master curve' when plotted on log rupture time and log stress axes. The oblique translation method uses the same types of functions in the FPCM. Approaches for treating multiheats on the basis of the FPCM are discussed in detail. (Author)

A79-19458 * An acoustic emission study of plastic deformation in polycrystalline aluminum. R. C. Bill (NASA, Lewis Research Center, Cleveland, Ohio), J. R. Frederick, and D. K. Felbeck (Michigan, University, Ann Arbor, Mich.). *Journal of Materials Science*, vol. 14, Jan. 1979, p. 25-32. 7 refs.

Acoustic emission experiments were performed on polycrystalline and single crystal 99.99% aluminum while undergoing tensile deformation. It was found that acoustic emission counts as a function of grain size showed a maximum value at a particular grain size. Furthermore, the slip area associated with this particular grain size corresponded to the threshold level of detectability of single dislocation slip events. The rate of decline in acoustic emission activity as grain size is increased beyond the peak value suggests that grain boundary associated dislocation sources are giving rise to the bulk of the detected acoustic emissions. (Author)

A79-21299 * Effects of compositional changes on the performance of a thermal barrier coating system. S. Secura (NASA, Lewis Research Center, Cleveland, Ohio). *American Ceramic Society, Annual Conference on Composites and Advanced Materials*, 3rd, Merritt Island, Fla., Jan. 21-24, 1979, Paper 32 p. 14 refs.

Systems consisting of Ni-base bond coatings containing about 16Cr, 6Al, and from 0.15 to 1.08Y (all in wt %) and zirconium oxide layers containing from 4.0 to 24.4Y₂O₃ were evaluated for suitability as thermal barrier systems for advanced aircraft gas turbine engine components. The evaluations were performed in a cyclic furnace between 990 and 280 C as well as between 1095 and 280 C on solid specimens, in a natural gas oxygen torch rig between about 1200 and 100 C on solid specimens and up to 1580 C surface temperatures on air-cooled blades and in a Mach 1.0 burner rig up to 1570 C surface temperatures on air-cooled blades. The data indicate that the best systems consist of combinations involving the Ni-16.4Cr-5.1Al-0.15Y and Ni-17.0Cr-5.4Al-0.3Y bond coatings and the 6.2Y₂O₃ and 7.9Y₂O₃ (all in wt %) stabilized zirconium oxide layers. (Author)

A79-21301 * Shear rupture of a directionally solidified eutectic gamma/gamma prime - alpha (Mo) alloy. F. H. Harf (NASA, Lewis Research Center, Cleveland, Ohio). *Materials Research Society, Conference on In Situ Composites III*, Boston, Mass., Nov. 27-Dec. 1, 1978, Paper 14 p. 8 refs.

Directionally solidified gamma/gamma prime - alpha (Mo) eutectic alloys are being evaluated for application as advanced aircraft

engine turbine blades. Their excellent high temperature strength is partly due to their directionally aligned microstructure. However, alloys with such directional structures may display low shear strength at 760 C, the operating temperature of advanced blade roots. The objective of this investigation was to determine the shear rupture strength of the gamma/gamma prime - alpha eutectic alloy and possibly to improve it by microstructural and heat-treatment variations. Bars of gamma/gamma prime - alpha alloy containing nominally 5.7% Al and 33.5% Mo by weight with balance Ni were directionally solidified at rates between 10 and 100 mm per hour. Materials were solidified in furnaces with thermal gradients at the liquid-solid interface of 250 or 100 C per cm. A limited number of longitudinal shear rupture tests were conducted at 760 C and 207 MPa in the as-solidified and in several heat-treated conditions. It was found that the shear rupture failures are partly transgranular and that resistance to failure is promoted by good fiber alignment and a matrix structure consisting mainly of gamma prime. Well-aligned as solidified specimens sustained the shear stress for an average of 81 hours, while cellular material failed in one hour or less. (Author)

A79-24262 * Influence of composition, annealing treatment, and texture on the fracture toughness of Ti-5Al-2.5Sn plate at cryogenic temperatures. R. H. Van Stone (GE Corporate Research and Development Center, Schenectady, N.Y.), J. L. Shannon, Jr., W. S. Pierce (NASA, Lewis Research Center, Strength of Materials Section, Cleveland, Ohio), and J. R. Low, Jr. (Carnegie-Mellon University, Pittsburgh, Pa.). In: Toughness and fracture behavior of titanium, Proceedings of the Symposium, Toronto, Canada, May 1-6, 1977. (A79-24256 08-26) Philadelphia, Pa., American Society for Testing and Materials, 1978, p. 154-179. 29 refs. Grant No. NGR 39-087-047.

A79-27233 * A feasibility study of a diffusion barrier between Ni-Cr-Al coatings and nickel-based eutectic alloys. S. G. Young and G. R. Zellars (NASA, Lewis Research Center, Cleveland, Ohio). (*International Conference on Metallurgical Coatings, San Francisco, Calif., Apr. 3-7, 1978*) *Thin Solid Films*, vol. 53, 1978, p. 241-250. 16 refs.

Coating systems have been proposed for potential use on eutectic alloy components in high-temperature gas turbine engines. In a study to prevent the deterioration of such systems by diffusion, a tungsten sheet 25 microns thick was placed between eutectic alloys and an Ni-Cr-Al layer. Layered test specimens were aged at 1100 C for as long as 500 h. Without the tungsten barrier the delta phase of the eutectic deteriorated by diffusion of niobium into the Ni-Cr-Al. Insertion of the tungsten barrier stopped the diffusion of niobium from the delta phase. Chromium diffusion from the Ni-Cr-Al into the gamma/gamma prime phase of the eutectic was greatly reduced by the barrier. However, the barrier thickness decreased with time, and tungsten diffused into both the Ni-Cr-Al and the eutectic. When the delta platelets were aligned parallel rather than perpendicular to the Ni-Cr-Al layer, diffusion into the eutectic was reduced. (Author)

A79-28276 * An oxide dispersion strengthened alloy for gas turbine blades. T. K. Glasgow (NASA, Lewis Research Center, Cleveland, Ohio). In: Structures, Structural Dynamics, and Materials Conference, 20th, St. Louis, Mo., April 4-6, 1979, Technical Papers on Dynamics and Loads. (A79-28251 10-39) New York, American Institute of Aeronautics and Astronautics, Inc., 1979, p. 249-255. 12 refs. (AIAA 79-0763)

The strength of the newly developed alloy MA 6000E is derived from a nickel alloy base, an elongated grain structure, naturally occurring precipitates of gamma prime, and an artificial distribution of extremely fine, stable oxide particles. Its composition is Ni-15% Cr-2% Mo-2% Ta-4% W-4.5% Al-2.5% Ti-0.15% Zr-0.05% C-0.01% B-1.1% Y₂O₃. It exhibits strength of a conventional nickel-base alloy at 1400 F, but is quite superior at 2000 F. Its shear strength is relatively low, necessitating consideration of special joining procedures. Its high cycle, low cycle, and thermal fatigue properties are

excellent. The relationship between alloy micro-structure and properties is discussed. (Author)

A79-32600 * Effects of thermomechanical processing on strength and toughness of Fe-12Ni reactive metal alloys at 77K. J. R. Stephens and W. R. Witzke (NASA, Lewis Research Center, Cleveland, Ohio). *Cryogenics*, vol. 19, Mar. 1979, p. 153-160. 10 refs.

A79-34992 * Characterization of defect growth structures in ion plated films by scanning electron microscopy. T. Spalvins (NASA, Lewis Research Center, Cleveland, Ohio). *American Vacuum Society and American Society for Metals, International Conference on Metallurgical Coatings, San Diego, Calif., Apr. 23-27, 1979, Paper*. 10 p. 9 refs.

Gold and copper films (0.2-2 micron thick) are ion plated on very smooth stainless steel 304 and mica surfaces. The deposited films are examined by SEM to identify the morphological growth of defects. Three types of coating defects are distinguished: nodular growth, abnormal or runaway growth, and spits. The potential nucleation sites for defect growth are analyzed to determine the cause of defect formation. It is found that nuclear growth is due to inherent surface microdefects, abnormal or runaway growth is due to external surface inclusions, and spits are due to nonuniform evaporation and ejection of droplets. All these defects have adverse effects on the coatings. S.D.

A79-34995 * Fretting wear of iron, nickel, and titanium under varied environmental conditions. R. C. Bill (NASA, Lewis Research Center; U.S. Army, Aviation Research and Development Command, Cleveland, Ohio). *ASME, ASLE, ASM, ASTM, SAE, SME, ACS, AIME, and APS, International Conference on Wear of Materials, Dearborn, Mich., Apr. 16-18, 1979, Paper*. 29 p. 21 refs.

Fretting wear experiments were conducted on high-purity iron, nickel and titanium in air under conditions of varied humidity and temperature, and in nitrogen. For iron and titanium, maximum fretting occurred at 10 and 30 percent relative humidity respectively. Nickel showed a minimum in fretting wear at about 10% relative humidity. With increasing temperature, all three metals initially showed reduced fretting wear, with increasing wear observed as temperatures increased beyond 200-300 C. For titanium, dramatically reduced fretting wear was observed at temperatures above 500 C, relatable to a change in oxidation kinetics. All three metals showed much less fretting wear in N₂ with the presence of moisture in N₂ having a proportionally stronger effect than in air. (Author)

A79-34997 * Adherence of sputtered titanium carbides. W. A. Brainard and D. R. Wheeler (NASA, Lewis Research Center, Cleveland, Ohio). *American Vacuum Society and American Society for Metals, International Conference on Metallurgical Coatings, San Diego, Calif., Apr. 23-27, 1979, Paper*. 8 p. 15 refs.

The study searches for interface treatment that would increase the adhesion of TiC coating to nickel and titanium base alloys. Tené 41 (19 wt percent Cr, 11 wt percent Mo, 3 wt percent Ti, balance Ni) and Ti-6Al-4V (6 wt percent Al, 4 wt percent V, balance Ti) are considered. Adhesion of the coatings is evaluated in pin-and-disk friction tests. The coatings and interface regions are examined by X-ray photoelectron spectroscopy. Results suggest that sputtered refractory compound coatings adhere best when a mixed compound of coating and substrate metals is formed in the interfacial region. The most effective type of refractory compound interface appears to depend on both substrate and coating material. A combination of metallic interlayer deposition and mixed compound interface formation may be more effective for some substrate coating combinations than either alone. S.D.

A79-38977 * The strainrange partitioning behavior of an advanced gas turbine disk alloy, AF2-1DA. G. R. Halford and A. J. Nachtigall (NASA, Lewis Research Center, Cleveland, Ohio). *AIAA, SAE, and ASME, Joint Propulsion Conference, 15th, Las Vegas, Nev., June 18-20, 1979, AIAA Paper 79-1192*. 10 p. 14 refs.

The low-cycle, creep-fatigue characteristics of the advanced gas turbine disk alloy, AF2-1DA have been determined at 1400 F and are presented in terms of the method of strainrange partitioning (SRP). The mean stresses which develop in the PC (tensile Plasticity reversed by compressive Creep) and CP (tensile Creep reversed by compressive Plasticity) type SRP cycles at the lowest inelastic strainrange were observed to influence the cyclic lives to a greater extent than the creep effects and hence interfered with a conventional interpretation of the results by SRP. A procedure is proposed for dealing with the mean stress effects on life which is compatible with SRP. (Author)

A79-39972 * A proposed physical model for the impregnated tungsten cathode based on Auger surface studies of the Ba-O-W system. R. Forman (NASA, Lewis Research Center, Cleveland, Ohio). *Applications of Surface Science*, vol. 2, 1979, p. 258-274. 15 refs.

Auger spectra and work function measurements are used to study the surface reactions between tungsten surface and adsorbed layers of barium, and barium and oxygen. The barium on an impregnated tungsten cathode seems to be an intermediate state, probably a coadsorbed barium-oxygen layer on tungsten. A slightly revised version of the previously suggested (1976) impregnated tungsten cathode model is proposed. This revised model assumes that the cathode surface during life has an adsorbed surface layer of a monolayer or less of both barium and oxygen on the surface. At end of life, steep drop in electron emission and resultant cathode failure occur. Recent NASA life test results on TWT type tubes are reported and explained by the proposed model. S.D.

A79-49531 * Transverse and longitudinal tensile properties at 760 C of several oxide dispersion strengthened nickel-base alloys. A. E. Anglin, Jr. (NASA, Lewis Research Center, Cleveland, Ohio). *American Institute of Mining, Metallurgical, and Petroleum Engineers, Annual Meeting, 108th, New Orleans, La., Feb. 18-20, 1979, Paper*. 22 p. 8 refs.

The transverse and longitudinal tensile properties of the oxide dispersion strengthened nickel-base alloys were determined at 760 C. The alloys with small amounts of gamma prime have strength levels suitable for turbine vane applications, while other highly alloyed, gamma prime strengthened superalloys have strengths typical of turbine blade materials. These alloys were produced by mechanical alloying and extrusion and the turbine blade alloys were also directionally recrystallized. Resultant grain aspect ratios varied from 1:1 to over 20:1. Longitudinal tensile strengths ranged from 285 to 1175 MPa, while longitudinal elongations were in excess of 4 percent for all alloys. Transverse tensile strengths were comparable to longitudinal strengths, but transverse ductility levels were generally less than 2 percent elongation. Tensile and yield strengths increased with increasing strain rate over the range 0.001 to 0.05 per second. Ductility in both orientations was not strain rate sensitive but could be related to grain size and grain aspect ratio. (Author)

A79-50912 * Chemically frozen multicomponent boundary layer theory of salt and/or ash deposition rates from combustion gases. D. E. Rosner, B. K. Chen (Yale University, New Haven, Conn.), G. C. Fryburg, and F. J. Kohl (NASA, Lewis Research Center, Cleveland, Ohio). *Combustion Science and Technology*, vol. 20, no. 3-4, 1979, p. 87-106, 57 refs. Grant No. NSG-3107.

There is increased interest in, and concern about, deposition and corrosion phenomena in combustion systems containing inorganic condensable vapors and particles (salts, ash). To meet the need for a computationally tractable deposition rate theory general enough to embrace multielement/component situations of current and future gas turbine and magnetogasdynamic interest, a multicomponent

chemically 'frozen' boundary layer (CFBL) deposition theory is presented and its applicability to the special case of Na₂SO₄ deposition from seeded laboratory burner combustion products is demonstrated. The coupled effects of Fick (concentration) diffusion and Soret (thermal) diffusion are included, along with explicit corrections for effects of variable properties and free stream turbulence. The present formulation is sufficiently general to include the transport of particles provided they are small enough to be formally treated as heavy molecules. Quantitative criteria developed to delineate the domain of validity of CFBL-rate theory suggest considerable practical promise for the present framework, which is characterized by relatively modest demands for new input information and computer time. (Author)

A79-52697* Analysis of solidification interface shape during continuous casting of a slab. R. Siegel (NASA, Lewis Research Center, Cleveland, Ohio). *International Journal of Heat and Mass Transfer*, vol. 21, Nov. 1978, p. 1421-1430. 11 refs.

An analysis was made of the two-dimensional interface shape of a slab ingot being cast continuously by withdrawing it from a mold. The sides of the ingot are being cooled and the upper boundary of the ingot is in contact with a pool of molten metal. The solidification interface shape was determined from the analysis of the heat flow, utilizing the condition that the solidification interface is at constant temperature and must be normal to the lines of heat flow carrying away latent heat of fusion from the interface. The analysis includes the effect of interface curvature which, for a constant rate of withdrawing the cast ingot from the mold, causes the solidification to be nonuniform along the interface. The analysis was carried out by a conformal mapping procedure. (Author)

N79-11180* TRW Inc. Cleveland, Ohio
EXPLORATORY THERMAL MECHANICAL FATIGUE RESULTS FOR RENE 80 IN ULTRAHIGH VACUUM
Final Report. 11 Jul. 1977. 11 Jul. 1978

A. A. Sheinker. Oct. 1978. 23 p. refs.
(Contract NAS3-21019)
(NASA-CR-159444 TRW-ER 8028) Avail. NTIS
HC A03/MF A01 CSCL 11F

A limited study was conducted of the use of strain range partitioning for predicting the thermal-mechanical fatigue life of cast nickel base superalloy Rene 80. The fatigue lives obtained by combined inphase thermal and mechanical strain cycling between 400 C (752 F) and 1000 C (1802 F) in an ultrahigh vacuum were considerably shorter than those represented by the four basic partitioned inelastic strain range fatigue life relationships established previously for this alloy at 871 C (1600 F) and 1000 C (1832 F) in an ultrahigh vacuum. This behavior was attributed to the drastic decrease in ductility with decreasing temperature for this alloy. These results indicated that the prediction of the thermal-mechanical fatigue life of Rene 80 by the method of strain range partitioning may be improved if based on the four basic fatigue life relationships determined at a lower temperature in the thermal-mechanical strain cycle. (Author)

N79-12202* Carnegie-Mellon Inst. of Research, Pittsburgh, Pa.

EVALUATION OF THE MECHANICAL PROPERTIES OF ELECTROSLAG REFINED Fe-12Ni ALLOYS

G. K. Bhat. Apr. 1978. 70 p. refs.
(Contract NAS3-20370)
(NASA-CR-159394) Avail. NTIS HC A04/MF A01 CSCL 11F

Three Fe-12Ni alloys, individually alloyed with small amounts of V, Ti, and Al, were manufactured through different melting techniques, with special emphasis on electroslag remelting, in order to achieve different levels of metal purity and associated costs. The relative effectiveness of these melting techniques was evaluated from tensile and slow bend fracture toughness behavior at 25 C and 196 C after tempering the test specimens at various temperatures. The best melting procedure was vacuum

induction melting (VIM) with or without electroslag remelting (ESR). VIM+ESR is the recommended procedure since ESR provides increased yield of plate product, a reduction of overall manufacturing costs and, depending on the alloy composition, improved tensile and fracture toughness properties. G.G.

N79-16948* General Electric Co., Schenectady, N. Y. Corporate Research and Development Center.

EVALUATION OF DIRECTIONALLY SOLIDIFIED EUTECTIC SUPERALLOYS FOR TURBINE BLADE APPLICATIONS

Final Report

Michael E. Henry, Melvin R. Jackson, and John L. Walter. Apr. 1978. 107 p. refs.

(Contract NAS3-19711)
(NASA-CR-135151 SRD-78-198) Avail. NTIS
HC A06/MF A01 CSCL 11F

Alloys from the following systems were selected for property evaluation: (1) gamma/gamma-Mo (Ni-base, rods of Mo); (2) gamma-beta (Ni-base, lamellae or rods of (Ni, Fe/Co Al)); and (3) gamma-gamma (Ni-base rods of Ni3Al gamma). The three alloys were subjected to longitudinal and transverse tensile and rupture tests from 750 C to 1100 C, longitudinal shear strength was measured at several temperatures, resistance to thermal cycling to 1150 C was determined, cyclic oxidation resistance was evaluated at 750 C and 1100 C, and each system was directionally solidified in an alumina shell mold turbine shape to evaluate mold/metal reactivity. The gamma/gamma-Mo system has good rupture resistance, transverse properties and processability, and is a high potential system for turbine blades. The gamma-beta system has good physical properties and oxidation resistance, and is a potential system for turbine vanes. The gamma-gamma system has good high temperature rupture resistance and requires further exploratory research. A.R.H.

N79-20221* Minnesota Univ., Minneapolis.
WHISKERS, CONES AND PYRAMIDS CREATED IN SPUTTERING BY ION BOMBARDMENT Final Report

G. K. Wehner. Mar. 1979. 47 p. refs.
(Grant NSG-3041)
(NASA-CR-159549) Avail. NTIS HC A03/MF A01 CSCL 11F

A thorough study of the role which foreign atoms play in cone formation during sputtering of metals revealed many experimental facts. Two types of cone formation were distinguished, deposit cones and seed cones. Twenty-six combinations of metals for seed cone formation were tested. The sputtering yield variations with composition for combinations which form seed cones were measured. It was demonstrated that whisker growth becomes a common occurrence when low melting point material is sputter deposited on a hot nonsputtered high melting point electrode. G.Y.

N79-20222* General Electric Co., Schenectady, N. Y.
EVALUATION OF AN ADVANCED DIRECTIONALLY SOLIDIFIED GAMMA/GAMMA'-ALPHA Mo EUTECTIC ALLOY

M. F. Henry, M. R. Jackson, M. F. X. Gigliotti, and P. B. Nelson. Jan. 1979. 67 p. refs.

(Contract NAS3-20383)
(NASA-CR-159416 SRD-78-191) Avail. NTIS
HC A04/MF A01 CSCL 11F

An attempt was made to improve on the properties of the candidate jet engine turbine blade material AG-60, a gamma/gamma prime-alpha Mo eutectic composite. Alloy 38 (AG-170) was evaluated in the greatest detail. This alloy, Ni-5.88 Al-29.74 Mo-1.65 V-1.2 C Re (weight percent), represents an improvement beyond AG-60, based on mechanical testing of the transverse and/or longitudinal orientations over a range of temperatures in tension, shear, rupture, and rupture after thermal exposure. It is likely that other alloys in the study represent a similar improvement. G.Y.

N79-24121*# AirResearch Mfg. Co., Phoenix, Ariz
**LOW-COST DIRECTIONALLY-SOLIDIFIED TURBINE
BLADES, VOLUME 1 Completion Report**

L. W. Sink, G. S. Hoppin, III, and M. Fujii Jan 1979 272 p
(Contract NAS3-20073)

(NASA-CR-159464, AFRJ Arch-21-2953-1) Avail NTIS
HC A12/MF A01 CSCI 11F

A low cost process of manufacturing high stress rupture strength directionally-solidified high pressure turbine blades was successfully developed for the TFE731-3 Turbofan Engine. The basic processing parameters were established using MAR-M 247 and employing the exothermic directional-solidification process in trial castings of turbine blades. Nickel-based alloys were evaluated as directionally-solidified cast blades. A new turbine blade, disk, and associated components were then designed using previously determined material properties. Engine tests were run and the results were analyzed and compared to the originally established goals. The results showed that the stress rupture strength of exothermically heated, directionally-solidified MAR-M 247 turbine blades exceeded program objectives and that the performance and cost reduction goals were achieved. RES

N79-25184*# Yale Univ., New Haven, Conn. High Temperature
Chemical Reaction Engineering Lab.

**EXPERIMENTAL STUDIES OF THE FORMATION/
DEPOSITION OF SODIUM SULFATE IN/FROM COMBUSTION
CASES Semiannual Report, 15 May - 15 Nov. 1978**

Daniel E. Rosner 15 Nov 1978 16 p refs
(Grant NSG-3169)

(NASA-CR-159613, SAR-2) Avail NTIS HC A02/MF A01
CSCI 21B

Interference in a reflected beam of monochromatic light from a linearly polarized helium-neon laser was used to determine the dew point and deposition rate of Na_2SO_4 on a heated platinum target. Preliminary results at different BCl_3 seed levels, except for one flow velocity and equivalence ratio (817) are presented and discussed. Alkali chloride reactions with atomic oxygen were also investigated. Readily detectable $\text{Na}^+(\text{g})$ and $\text{K}^+(\text{g})$ atoms were observed in emission at 589 nm, 766 nm, 796 nm, respectively. A R H

N79-25196*# Pittsburgh Univ., Pa. Dept. of Metallurgical
and Materials Engineering

**AN INVESTIGATION OF THE INITIATION STAGE OF HOT
CORROSION IN Ni-BASE ALLOYS Progress Report**

T. T. Huang and G. H. Meier 31 Mar 1979 44 p refs
(Grant NSG-3714)

(NASA-CR-15, 316) Avail NTIS HC A03/MF A01 CSCI
11F

The mechanisms which lead to the destruction of a normally protective scale during the initial stages of hot corrosion of 14 nickel base alloys contaminated with Na_2SO_4 and other condensed deposits were investigated. A continuous reading microbalance was used to record weight changes at temperatures between 900 C and 1000 C at 1 atmosphere pressure of slowly flowing oxygen. The reaction was initiated by raising a preheated furnace around the quartz tube in which the specimen was supported with oxygen flowing. The furnace was raised in a time period of seconds. At 900 C the system, and specimen came to thermal equilibrium in less than one minute. Oxidized specimens were studied using optical and scanning electron metallography and X-ray diffraction techniques. Transmission electron microscopy and electron diffraction spectroscopy were also used to identify the structure of carbides in some of the commercial alloys. A R H

N79-26173*# Battelle Columbus Labs., Ohio Metalworking
Section

**COMPUTER AIDED ANALYSIS AND DESIGN OF THE
SHAPE ROLLING PROCESS FOR PRODUCING TURBINE
ENGINE AIRFOILS Interim Topical Report, 1 Oct. 1976 -
31 Dec. 1977**

C. G. Lahot, N. Akgerman, and T. Altan Mar 1978 65 p
refs

(Contract NAS3-20380)

(NASA-CR-135367) Avail NTIS HC A04/MF A01 CSCI
11F

Mild steel (AISI 1018) was selected as model cold-rolling material and Ti-6Al-4V and INCONEL 718 were selected as typical hot-rolling and cold rolling alloys, respectively. The flow stress and workability of these alloys were characterized and friction factor at the roll/workpiece interface was determined at their respective working conditions by conducting ring tests. Computer-aided mathematical models for predicting metal flow and stresses, and for simulating the shape-rolling process were developed. These models utilize the upper-bound and the slab methods of analysis, and are capable of predicting the lateral spread, roll-separating force, roll torque and local stresses, strains and strain rates. This computer-aided design (CAD) system is also capable of simulating the actual rolling process and thereby designing roll-pass schedule in rolling of an airfoil or similar shape. The predictions from the CAD system were verified with respect to cold rolling of mild steel plates. The system is being applied to cold and hot isothermal rolling of an airfoil shape, and will be verified with respect to laboratory experiments under controlled conditions. Author

N79-32326*# Pratt and Whitney Aircraft Group, West Palm
Beach, Fla. Government Products Div.

**DEVELOPMENT OF SPUTTERED TECHNIQUES FOR
THRUST CHAMBERS Final Report**

J. R. Mullaly and P. A. Allard Mar 1979 96 p refs
(Contract NAS3-20377)

(NASA-CR-159637, FR-11409) Avail NTIS
HC A05/MF A01 CSCI 11F

The 0.152 cm thick sputtered and copper deposits were electron beam welded to wrought copper. Tensile specimens were machined from the weld assemblies and tested at room temperature. Tensile strength approached the strength of wrought material. Elongations up to 25% were measured. Sputtered aluminum was used to fill 0.157 cm wide by 0.127 cm deep grooves in thrust chamber spool piece liners. The liners were closed out by sputtering copper from post and hollow cathodes. Author

N79-33305*# Westinghouse Astronuclear Lab., Pittsburgh, Pa.
**INTERDIFFUSION BEHAVIOR OF TUNGSTEN OR RHENIUM
AND GROUP 5 AND 6 ELEMENTS AND ALLOYS OF
THE PERIODIC TABLE, PART 2B: APPENDICES Final
Report**

F. G. Arcella Sep 1974 261 p refs
(Contract NSG-3-13231)

(NASA-CR-1525, WANL-M-FR-74-005 Pt-2) Avail NTIS
HCA12*# CSCI 11F

The following are appended: (1) The Hartley Computer Program; (2) The Lifshin Computer Program; (3) Modification of the Culby Magic Program for Quantitative Electron Microprobe Analysis; and (4) Error and Correction Analysis. G M M

27 NONMETALLIC MATERIALS

Includes physical, chemical, and mechanical properties of plastics, elastomers, lubricants, polymers, textiles, adhesives, and ceramic materials

N79-11216* National Aeronautics and Space Administration
Lewis Research Center, Cleveland, Ohio

MODIFICATION OF THE ELECTRICAL AND OPTICAL PROPERTIES OF POLYMERS Patent Application

M. J. Mirtich and James S. Sovey, inventors (to NASA) Filed 7 Nov 1978 11 p

(NASA Case LEW-13027-1, US Patent Appl. SN 958575) Avail NTIS HC A02/MF A01 CSCL 07C

The surface of a polymer is irradiated to modify the optical and electrical properties as well as to change the surface morphology. A polymer is placed in a vacuum of about 4×10^{-5} to the minus 5th power torr. A surface of the polymer is exposed to a beam of argon ions having an energy between 500 and 1000 eV and an ion beam current density between 0.1 and 1.0 mA/sq cm. The resulting texturing of the surface causes a large decrease in spectral transmittance at all wavelengths. The surface conductivity of the polymer is also increased. The textured surface further enhances the adherence of thin films to the polymer. A polyimide (Kaptan) and a fluorinated ethylene propylene (Teflon) are surface treated in accordance with the invention.

NASA

N79-12223* National Aeronautics and Space Administration
Lewis Research Center, Cleveland, Ohio

DEVELOPMENT OF SPRAYED CERAMIC SEAL SYSTEMS FOR TURBINE GAS PATH SEALING

Robert C. Bill (AVRADCOM Res and Technol Labs), L. T. Shiembob (Pratt and Whitney Aircraft Group, East Hartford, Conn.), and O. L. Stewart (Pratt and Whitney Aircraft Group, East Hartford, Conn.) 1978 22 p refs. Presented at the Winter Ann Meeting, San Francisco, 10-15 Dec 1978, sponsored by Am Soc of Mech Engrs.

(NASA TM 79022, E-9819, AVRADCOM TR 78-52) Avail NTIS HC A02/MF A01 CSCL 11A

A ceramic seal system is reported that employs plasma sprayed graded metal/ceramic yttria stabilized zirconium oxide (YSZ). The performance characteristics of several YSZ configurations were determined through rig testing for thermal shock resistance, abrasability and erosion resistance. Results indicate that this type of sealing system offers the potential to meet operating requirements of future gas turbine engines. G G

N79-13159* National Aeronautics and Space Administration
Lewis Research Center, Cleveland, Ohio

LUBRICATION AND FAILURE MECHANISMS OF MOLYBDENUM DISULFIDE FILMS. 1: EFFECT OF ATMOSPHERE

Robert L. Fusaro, Dec 1978 29 p

(NASA TP 1343, E-9600) Avail NTIS HC A03/MF A01 CSCL 11H

Friction, wear, and wear lives of rubbed molybdenum disulfide (MoS₂) films applied to sanded 440C HT steel surfaces were evaluated in moist air, dry air, and dry argon. Optical microscope observations were made as a function of sliding distance to determine the effect of moisture and oxygen on the lubricating and failure mechanisms of MoS₂ films. In general, the lubrication process consisted of the formation of a thin, metallic colored, coalesced film of MoS₂ that flowed between the surfaces in relative motion. In air, failure was due to the transformation of the metallic colored, coalesced film to a black, powdery material. Water in the air appeared to accelerate the transformation rate. In argon, no transformation of MoS₂ was observed with the microscope, but cracking and swelling of the coalesced film occurred and resulted in the gradual deterioration of the film.

Author

N79-13159* National Aeronautics and Space Administration
Lewis Research Center, Cleveland, Ohio

LUBRICATION AND FAILURE MECHANISMS OF MOLYBDENUM DISULFIDE FILMS. 2: EFFECT OF SUBSTRATE ROUGHNESS

Robert L. Fusaro, Dec 1978 30 p refs

(NASA-TP-1379, E-9715) Avail NTIS HC A03/MF A01 CSCL 11H

An optical microscope was used to study the lubrication and failure mechanisms of rubbed MoS₂ films applied to three substrate surface finishes: polished, sanded, and sandblasted as a function of sliding distance. The lubrication mechanism was the plastic flow of thin films of MoS₂ between flat plateaus on the rider and on the metallic substrate. If the substrate was rough, flat plateaus were created during run-in and the MoS₂ flowed across them. Wear life was extended by increasing surface roughness since valleys in the roughened substrate served as reservoirs for MoS₂ and as deposit sites for wear debris. In moist air, the failure mechanism was the transformation of metallic colored MoS₂ films to a black, powdery material that was found by X-ray diffraction to be alpha iron, MoO₃, and possibly FeMoO₃. In dry argon the failure mechanism was the gradual depletion of MoS₂ from the contact region by transverse flow, and the wear debris on the track at failure was alpha iron, residual MoS₂, and possibly FeS.

Author

N79-15184* National Aeronautics and Space Administration
Lewis Research Center, Cleveland, Ohio

EFFECT OF NITROGEN-CONTAINING PLASMA ON ADHERENCE, FRICTION, AND WEAR OF RADIOFREQUENCY-SPUTTERED TITANIUM CARBIDE COATINGS

William A. Brainard and Donald R. Wheeler, Jan 1979 21 p refs

(NASA-TP-1377, E-9681) Avail NTIS HC A02/MF A01 CSCL 11D

Friction and wear experiments on 440C steel surfaces that were rf sputtered with titanium carbide when a small percentage of nitrogen was added to the plasma were conducted. Both X-ray photoelectron spectroscopy and X-ray diffraction were used to analyze the resultant coatings. Results indicate that the small partial pressure of nitrogen (approximately 0.5 percent) markedly improves the adherence, friction, and wear properties when compared with coatings applied to sputter-etched surfaces, oxidized surfaces, or in the presence of a small oxygen partial pressure. The improvements are related to the formation of an interface containing a mixture of the nitrides of titanium and iron, which are harder than their corresponding oxides. A R H

N79-15185* National Aeronautics and Space Administration
Lewis Research Center, Cleveland, Ohio

BOUNDARY LUBRICATION, THERMAL AND OXIDATIVE STABILITY OF A FLUORINATED POLYETHER AND A PERFLUOROPOLYETHER TRIAZINE

William R. Jones, Jr. and Carl E. Snyder, Jr. (AFML, Ohio) 1979 24 p refs. Proposed for presentation at Ann Meeting of the Am Soc of Lubrication Engineers, St. Louis, Mo., 30 Apr - 3 May 1979.

(NASA-TM 79064, E-9879) Avail NTIS HC A02/MF A01 CSCL 11H

Boundary lubricating characteristics, thermal stability, and oxidation-corrosion stability were determined for a fluorinated polyether and a perfluoropolyether triazine. A ball-on-disk apparatus, a tensimeter, and oxidation-corrosion apparatus were used. Results were compared to data for a polyphenyl ether and a C-ether. The polyether and triazine yielded better boundary lubricating characteristics than either the polyphenyl ether or C-ether. The polyphenyl ether had the greatest thermal stability (447 C) while the other fluids had stabilities in the range 389 to 397 C. Oxidation-corrosion results indicated the following order of stabilities: perfluoropolyether triazine greater than polyphenyl ether greater than C-ether greater than fluorinated polyether.

Author

N79-15186* National Aeronautics and Space Administration, Lewis Research Center, Cleveland, Ohio.

EFFECT OF THERMAL AGING ON THE TRIBOLOGICAL PROPERTIES OF POLYIMIDE FILMS AND POLYIMIDE-BONDED GRAPHITE FLUORIDE FILMS

Robert L. Fusaro 1979 32 p refs. Proposed for presentation at the 34th Ann. Meeting, St. Louis, 30 Apr - 3 May 1979. Sponsored by the Am. Soc. of Lubrication Engr. (NASA-TM-79045, E-9879-1) Avail: NTIS HC A03/MF A01 CSCL 07C

Weight loss, adherence, friction and wear of polyimide films and polyimide-bonded graphite fluoride films applied to stainless steel disks and to 304 stainless steel thin foils were studied. The films were exposed at temperatures of 315 D, 345 D, 370 D, or 400 C for 100 hours or more and then evaluated at temperatures of 25 D, 315 D, or 345 C in atmospheres of dry or moist air. Polyimide films were found to be brittle after thermal exposure, but polyimide-bonded graphite fluoride possessed good adherence and gave low friction and wear results. Polyimide-bonded graphite fluoride films appear to be good candidates for solid lubrication applications where long thermal soaks are prevalent. G G

N79-16984* National Aeronautics and Space Administration, Lewis Research Center, Cleveland, Ohio.

HIGH VELOCITY BURNER RIG OXIDATION AND THERMAL FATIGUE BEHAVIOR OF Si₃N₄- AND SiC BASE CERAMICS TO 1370 DEG C

William A. Sanders and James R. Johnston Nov. 1978 44 p refs. (NASA-TM-79040, E-9842) Avail: NTIS HC A03/MF A01 CSCL 11B

One SiC material and three Si₃N₄ materials including hot-pressed Si₃N₄ as a baseline were exposed in a Mach-1-gas-velocity burner rig simulating a turbine engine environment. Criteria for the materials selection were: potential for gas-turbine usage, near-net-shape fabricability, and commercial/domestic availability. Cyclic exposures of test vanes up to 250 cycles (50 hr at temperature) were at leading edge temperatures to 1370 C. Materials and batches were compared as to weight change, surface change, fluorescent penetrant inspection, and thermal fatigue behavior. Hot-pressed Si₃N₄ survived the test to 1370 C with slight weight losses. Two types of reaction-sintered Si₃N₄ displayed high weight gains and considerable weight change variability, with one material exhibiting superior thermal fatigue behavior. A siliconized SiC showed slight weight gains, but considerable batch variability in thermal fatigue. Author

N79-20240* National Aeronautics and Space Administration, Lewis Research Center, Cleveland, Ohio.

WIDE-TEMPERATURE SPECTRUM SELF-LUBRICATING COATINGS PREPARED BY PLASMA SPRAYING

Harold E. Sliney 1979 10 p refs. Presented at the Intern. Conf. on Met. Coatings, San Diego, Calif., 23-27 Apr. 1979, cosponsored by the Am. Vacuum Soc. and the Am. Soc. for Metals. (NASA-TM-79113, E-9945) Avail: NTIS HC A02/MF A01 CSCL 11H

Self-lubricating, multicomponent coatings, which lubricate over a wide range of operating conditions, are described. The coatings were successfully applied by plasma-spraying mixed powders onto superalloy substrates. They were evaluated in friction and wear experiments, and in sliding contact bearing tests. These coatings are wear resistant by virtue of their self-lubricating characteristics rather than because of extreme hardness, a further benefit is low friction. Experiments with simple pin on disk sliding specimens and oscillating plain cylindrical bearing tests were performed to evaluate the tribological properties of the coatings. It was shown that coatings of nichrome, glass and calcium fluoride are self-lubricating from about 500 to 900 C, but give high friction at the lower temperatures. The addition of silver to the coating composition improved the low temperature bearing properties and resulted in coatings which are self-lubricating from cryogenic temperatures to at least 870 C, they are therefore, wide temperature spectrum self-lubricating compositions. L S

N79-21204* National Aeronautics and Space Administration, Lewis Research Center, Cleveland, Ohio.

EFFECT OF OXYGEN-NITROGEN RATIO ON SINTERABILITY OF SIALONS

Alan Arias Apr. 1979 24 p refs. (NASA-TP-1382, E-9814) Avail: NTIS HC A02/MF A01 CSCL 11B

The effect of varying the sintering temperature and the oxygen to nitrogen ratio (O/N) on the sinterability of Sialons of the formula Si₂55Al_{0.60}N₄-0.667y was investigated for y between 0.57 and 1.92 (O/N between 0.157 and 0.706). The Sialons reached maximum density on pressureless sintering for 4 hours at about 1760 C in nitrogen. Optimum sinterability with densities up to about 98 percent of theoretical was attained with negligible X-phase in the O/N range from about 0.2 to 0.3. On sintering at approximately 1830 C the Sialons decomposed with evolution of silicon and aluminum. Author

N79-21205* National Aeronautics and Space Administration, Lewis Research Center, Cleveland, Ohio.

THERMAL STRESS ANALYSIS OF CERAMIC GAS-PATH SEAL COMPONENTS FOR AIRCRAFT TURBINES

Francis E. Kennedy and Bert C. Bill Apr. 1979 22 p refs. Prepared in cooperation with Army Aviation Res. and Develop. Command, Cleveland. (NASA-TP-1437, E-9842) Avail: NTIS HC A02/MF A01 CSCL 11B

Stress and temperature distributions were evaluated numerically for a blade-tip seal system proposed for gas turbine applications. The seal consists of an abradable ceramic layer on metallic backing with intermediate layers between the ceramic layer and metal substrate. The most severe stresses in the seal, as far as failure is concerned, are tensile stresses at the top of the ceramic layer and shear and normal stresses at the layer interfaces. All these stresses reach their maximum values during the deceleration phase of a test engine cycle. A parametric study was carried out to evaluate the influence of various design parameters on these critical stress values. The influences of material properties and geometric parameters of the ceramic, intermediate, and backing layers were investigated. After the parametric study was completed, a seal system was designed which incorporated materials with beneficial elastic and thermal properties in each layer of the seal. An analysis of the proposed seal design shows an appreciable decrease in the magnitude of the maximum critical stresses over those obtained with earlier configurations. Author

N79-23216* National Aeronautics and Space Administration, Lewis Research Center, Cleveland, Ohio.

EFFECT OF STERILIZATION IRRADIATION ON FRICTION AND WEAR OF ULTRAHIGH MOLECULAR-WEIGHT POLYETHYLENE

William R. Jones, Jr., William F. Hady, and Aldo Crugnola (Lowell Univ.) May 1979 22 p refs. (NASA Order C-8756) (NASA-TP-1462, E-9697) Avail: NTIS HC A02/MF A01 CSCL 07C

The effect of sterilization gamma irradiation on the friction and wear properties of ultrahigh molecular weight polyethylene (UHMWPE) sliding against 316L stainless steel in dry air at 23 C was determined. A pin-on-disk apparatus was used. Experimental conditions included a 1-kilogram load, a 0.061- to 0.27-meter-per-second sliding velocity, and a 32000- to 578000-meter sliding distance. Although sterilization doses of 2.5 and 5.0 megarads greatly altered the average molecular weight and the molecular weight distribution, the friction and wear properties of the polymer were not significantly changed. Author

N79-24154* National Aeronautics and Space Administration
Lewis Research Center, Cleveland, Ohio

ION BEAM SPUTTER DEPOSITION OF FLUOROPOLYMERS
Patent Application

Bruce A. Banks and James S. Sovey, inventors (to NASA) Filed
21 May 1979 8 p
(NASA-Case-LEW-13122-1; US-Patent-Appl-SN-041146) Avail
NTIS HC A02/MF A01 CSCL 07C

Ions are impinged on a fluoropolymer target which is the
sputter deposition source for a large area substrate to be coated.
A clear hydrophobic coating is produced on a substrate of selected
solid materials. NASA

N79-27306* National Aeronautics and Space Administration
Lewis Research Center, Cleveland, Ohio

**ADHESIVE MATERIAL TRANSFER IN THE EROSION OF
AN ALUMINUM ALLOY**

Joshua Salik and William A. Brainard May 1979 10 p refs
(NASA-TM-79165, E-028) Avail NTIS HC A02/MF A01
CSCL 11A

In order to study the basic mechanisms of erosion, hardened
steel balls were shot into annealed 6061 Al alloy targets at
velocity of up to 150 m/sec. The projectiles were collected and
examined by a scanning electron microscope combined with
energy-dispersive X-ray analyzer and it was found that target
material in substantial amounts is adhesively transferred to the
projectile. The transferred material forms on the projectile surface
a layer the thickness of which increases with increases in impact
velocity. Author

N79-27308* National Aeronautics and Space Administration
Lewis Research Center, Cleveland, Ohio

**AUGER SPECTROSCOPY ANALYSIS OF LUBRICATION
WITH ZINC DIALKYLDITHIOPHOSPHATE OF SEVERAL
METAL COMBINATIONS IN SLIDING CONTACT**

Donald H. Buckley Jul 1979 19 p
(NASA-TP-1489, E-9909) Avail NTIS HC A02/MF A01 CSCL
11H

Sliding friction experiments were conducted with aluminum
and other riders rubbing on disks of various elemental metals in
the presence of a thin film of zinc dialkyldithiophosphate (ZDP).
Auger emission spectroscopy was used to in situ monitor the
changes in surface chemistry with rubbing under various loads.
The metal disks examined included iron, titanium, rhodium,
tungsten, molybdenum, and copper. For equivalent films of ZDP
the film is a more effective lubricant for some metals than it is
for others. The important active element in the compound varies
with the metal lubricated and is a function of metal chemistry.
The zinc in the ZDP is susceptible to electron beam induced
desorption. Author

N79-27309* National Aeronautics and Space Administration
Lewis Research Center, Cleveland, Ohio

**MODULES OF RUPTURE AND OXIDATION RESISTANCE
OF Si2.55Al0.60072N3.52 SIALON**

Alan Arias Jul 1979 15 p refs
(NASA-TP-1490, E-9971) Avail NTIS HC A02/MF A01 CSCL
11B

A Sialon of formula $\text{Si}_{2.55}\text{Al}_{0.60072}\text{N}_{3.52}$ was made from
ball milled $\alpha\text{-Si}_3\text{N}_4$, AlN, and SiO_2 by sintering the powder
compacts at 1760 C for 4 hours in stagnant nitrogen. This
Sialon had an average modulus of rupture ranging from
404 megapascals (58.6 ksi) at room temperature to
254 megapascals (36.8 ksi) at 1400 C. Oxidation tests at
1400 C in air showed it to have a parabolic oxidation rate
constant less than or equal to 2.8×10^{-10} to the -10^{th} power sq
 $\text{g/cm}^4 \text{ hr}$, which is smaller than that of any other Si_3N_4 base
ceramic reported in the literature. Author

N79-28307* National Aeronautics and Space Administration
Lewis Research Center, Cleveland, Ohio

**CATALYTIC TRIMERIZATION OF AROMATIC NITRILES
AND TRIARYL-S-TRIAZINE RING CROSS-LINKED HIGH
TEMPERATURE RESISTANT POLYMERS AND COPOLY-
MERS MADE THEREBY** Patent

Li-Chen Hsu, inventor (to NASA) Issued 26 Jun 1979 30 p
Filed 12 May 1977 Supersedes N77-32244 (15 : 23, p 3049)
Division of US Patent Appl. SN-513613, filed 10 Oct 1974,
US-Patent-4,061,856

(NASA-Case-LEW-12053-2, US-Patent-4,159,262,
US-Patent-Appl-SN-796263, US-Patent-Class-528-126,
US-Patent-Class-260-37N, US-Patent-Class-260-42,
US-Patent-Class-260-53, US-Patent-Class-544-193,
US-Patent-Class-528-221, US-Patent-Class-528-223,
US-Patent-Class-528-229, US-Patent-Class-528-227,
US-Patent-Class-528-225, US-Patent-Class-528-127,
US-Patent-Class-528-128, US-Patent-Class-528-336,
US-Patent-Class-528-337, US-Patent-Class-528-338,
US-Patent-Class-528-342, US-Patent-Class-528-331) Avail US
Patent and Trademark Office CSCL 07C

Triazine compounds and cross-linked polymer compositions
are made by heating aromatic nitriles to a temperature in the
range of from about 100 C to about 700 C, and preferably in
the range of from about 200 C to about 350 C, in the presence
of a catalyst or mixture of catalysts selected from one or more
of the following groups: (1) organic sulfonic and sulfonic acids,
(2) organic phosphonic and phosphinic acids, and (3) metallic
acetylacetonates, at a pressure in the range of from about
atmospheric pressure to about 10,000 psi and preferably in the
range of from about 200 psi to about 750 psi. Aromatic
nitrile-modified (terminated and/or appended) imide, benzimidazole,
imidazopyrrolone, quinoxaline, and other condensation type
prepolymers or their prepolymers are made which are trimerized
with or without a filler by the aforementioned catalytic trimeriza-
tion process into triaryl-s-triazine ring containing or cross-linked
polymeric or copolymeric products useful in applications requiring
high thermal oxidative stability and high performance structural
properties at elevated temperatures.

Official Gazette of the U.S. Patent and Trademark Office

N79-28327* National Aeronautics and Space Administration
Lewis Research Center, Cleveland, Ohio

**PLASMA-SPRAYED COATINGS FOR LUBRICATION OF A
TITANIUM ALLOY IN AIR AT 430 deg C**

Harold E. Sliney and Donald H. Wisander Jul 1979 14 p
(NASA-TP-1509, E-9876) Avail NTIS HC A02/MF A01 CSCL
11H

Plasma sprayed coatings of pure silver and of composite
materials containing silver were investigated as possible self
lubricating coatings for titanium alloys in air at 430 C. Pure
silver provided low friction but was prone to severe plastic
deformation and excessive transfer except in coating thicknesses
of 0.02 mm or less. Additions of nichrome, calcium fluoride,
and glass to silver were all beneficial in reducing plastic
deformation and otherwise improving the coatings. The longest
coating wear life, low wear of Ti alloy pins in sliding contact
with the coatings, and a steady friction coefficient of 0.19 were
obtained with a four component coating of 0.17 mm thickness.
The coating composition, in weight percent is 30 nichrome-30
Ag-25 CaF₂-15 glass. Author

N79-29329* National Aeronautics and Space Administration
Lewis Research Center, Cleveland, Ohio

**INFRARED ANALYSIS OF POLYETHYLENE WEAR SPECI-
MENS USING ATTENUATED TOTAL REFLECTION SPEC-
TROSCOPY**

William H. Jones and James L. Lauer (Rensselaer Polytech. Inst.)
Jul 1979 12 p refs
(NASA-TM-79226, E-1301) Avail NTIS HC A02/MF A01 CSCL
07D

Attenuated total reflection infrared spectroscopy was used
to analyze ultrahigh molecular weight polyethylene wear test
specimens. Three different specimens were analyzed. One
specimen was gamma irradiated to a dose of 5.0 MRad, another
to a dose of 2.5 MRad, and the final specimen was unirradiated.

There was no conclusive evidence of chemical changes (i.e., unsaturation or oxidation) in the surface regions of any of the polyethylene samples. Therefore, it was concluded that the gamma irradiation sterilization procedure should not alter the boundary lubricating properties of the polyethylene. Author

N79-30378* National Aeronautics and Space Administration, Lewis Research Center, Cleveland, Ohio

STATE-OF-THE-ART OF SiAlON MATERIALS

Sunil Dutta 1979 22 p refs Presented at 49th Meeting of the Structures and Materials Panel Including a Specialist Meeting on Ceramics for Turbine Engine Applications, Cologne, Germany, 7-12 Oct 1979 sponsored by AGARD (NASA-TM-79267, E-092) Avail NTIS HC A02/MF A01 CSCL 11G

Research presented includes work on phase relations, crystal structure, synthesis, fabrication, and properties of various SiAlONs. The essential features of compositions, fabrication methods, and microstructure are reviewed. High temperature flexure strength, creep, fracture toughness, oxidation, and thermal shock resistance are discussed. These data are compared to those for some currently produced silicon nitride ceramics to assess the potential SiAlON materials for use in advanced gas turbine engines. M M M

N79-30379* National Aeronautics and Space Administration, Lewis Research Center, Cleveland, Ohio

BEND STRENGTHS OF REACTION BONDED SILICON NITRIDE PREPARED FROM DRY ATTRITION MILLED SILICON POWDER

T P Herbell and T K Glasgow 1979 14 p refs Presented at 3d Ann Conf on Composites and Advan Mater, Merritt Island, Fla 21-24 Jan 1979, sponsored by Am Ceram Soc (Contract EC 77-A-31-1040) (NASA-TM 79230, E-132, DOE/NASA/1040-79/8) Avail NTIS HC A02/MF A01 CSCL 11G

Dry attrition milled silicon powder was compacted, sintered in helium, and reaction bonded in nitrogen 4 volume percent hydrogen. Bend strengths of bars with as-nitrified surfaces averaged as high as 210 MPa at room temperature and 220 MPa at 1400 C. Bars prepared from the milled powder were stronger than those prepared from as-received powder at both room temperature and at 1400 C. Room temperature strength decreased with increased milling time and 1400 C strength increased with increased milling time. Author

N79-30380* National Aeronautics and Space Administration, Lewis Research Center, Cleveland, Ohio

ANISOTROPIC FRICTION, DEFORMATION, AND FRACTURE OF SINGLE CRYSTAL SILICON CARBIDE AT ROOM TEMPERATURE

Kazuhiro Miyoshi and Donald H Buckley Aug 1979 24 p refs (NASA TP-1525, E-9988) Avail NTIS HC A02/MF A01 CSCL 07D

Anisotropic friction, deformation, and fracture studies were conducted with $\{0001\}$, $\{10\bar{1}110\}$, and $\{11\bar{1}210\}$ silicon carbide surfaces in sliding contact with diamond. The experiments were conducted with loads of 0.1, 0.2, and 0.3 N at a sliding velocity of 3 mm/min in mineral oil or in dry argon at room temperature. The $\{10\bar{1}110\}$ direction on the basal $\{0001\}$ plane exhibits the lowest coefficient of friction and the greatest resistance to abrasion for silicon carbide. Anisotropic friction and deformation of the $\{0001\}$, $\{10\bar{1}110\}$, and $\{11\bar{1}210\}$ silicon carbide surfaces are primarily controlled by the slip system $\{10\bar{1}110\}$ $\{11\bar{1}210\}$. The anisotropic fracture during sliding on the basal plane is due to surface cracking along $\{10\bar{1}110\}$ and subsurface cracking along $\{0001\}$. The fracture during sliding on the $\{11\bar{1}210\}$ or $\{10\bar{1}110\}$ surfaces is due to surface cracking along $\{0001\}$ and $\{11\bar{1}210\}$ or $\{10\bar{1}110\}$ and to subsurface cracking along $\{10\bar{1}110\}$. Author

N79-30381* National Aeronautics and Space Administration, Lewis Research Center, Cleveland, Ohio

LUBRICATING AND WEAR MECHANISMS FOR A HEMI-SPHERE SLIDING ON POLYIMIDE-BONDED GRAPHITE FLUORIDE FILM

Robert L Fusaro Aug 1979 30 p refs (NASA-TP-1524, E-9965) Avail NTIS HC A03/MF A01 CSCL 11H

Friction, wear life, rider wear, and film wear for a 440 C high-temperature stainless-steel, hemispherically tipped rider sliding against polyimide-bonded graphite fluoride films were evaluated in a moist-air atmosphere at 25 C. Optical microscope and surface profilometry observations were made at various sliding intervals to determine how film thickness affected the lubricating and failure mechanisms of the films. Two lubrication regimes operated for the same load. In the first, the film supported the load and the lubricating mechanism consisted of the shear (plastic flow) of a thin layer of the lubricant between the metallic rider and the film surface. In the second, the film did not support the load (it was worn away) and the lubricating mechanism consisted of the shear of very thin lubricant films between flat areas generated on the rider and on sandblasted metallic asperities in the film wear track. Lubricant was supplied from the valleys between the asperities or from the sides of the wear track. With thicker films, wear life increased since a greater lubricant supply was available from the sides of the wear track. Author

N79-31391* National Aeronautics and Space Administration, Lewis Research Center, Cleveland, Ohio

MECHANICAL AND CHEMICAL EFFECTS OF ION-TEXTURING BIOMEDICAL POLYMERS

A J Weigand and M A Cenkus 1979 29 p refs Presented at 32nd Ann Conf of Engr in Med and Biol, Denver, 6-10 Oct 1979, sponsored by Alliance for Engr in Med (NASA TM 79245, E-152) Avail NTIS HC A03/MF A01 CSCL 07C

To determine whether sputter etching may provide substantial polymer surface texturing with insignificant changes in chemical and mechanical properties, an 8 cm beam diameter, electron bombardment, argon ion source was used to sputter etch (ion-texture process) nine biomedical polymers. The materials included silicone rubber, 32% carbon impregnated polyolefin, polyoxymethylene, polytetrafluoroethylene, ultrahigh molecular weight (UHMW) polyethylene, UHMW polyethylene with carbon fibers (10%), and several polyurethanes (bioelectric segmented, and cross linked). Ion textured microtensile specimens of each material except UHMW polyethylene and UHMW polyethylene with 10% carbon fibers were used to determine the effect of ion texturing on tensile properties. Scanning electron microscopy was used to determine surface morphology changes, and electron spectroscopy for chemical analysis was used to analyze the near surface chemical changes that result from ion texturing. Ion energies of 500 eV with beam current densities ranging from 0.08 to 0.19 mA/sq cm were used to ion texture the various materials. Standard microtensile specimens of seven polymers were exposed to a saline environment for 24 hours prior to and during the tensile testing. The surface chemical changes resulting from sputter etching are minimal in spite of the often significant changes in the surface morphology. A W H

N79-32359* National Aeronautics and Space Administration, Lewis Research Center, Cleveland, Ohio

EVALUATION AND AUGER ANALYSIS OF A ZINC DIALKYL-DITHIOPHOSPHATE ANTIWEAR ADDITIVE IN SEVERAL DIESTER LUBRICANTS

William A Brainard and John Ferrante Washington Oct 1979 16 p refs (NASA TP 1544, F-9944) Avail NTIS HC A02/MF A01 CSCL 11H

The wear of pure iron in sliding contact with hardened M 2 tool steel was measured for a series of synthetic diester fluids, both with and without a zinc dialkyl dithiophosphate (ZDP) antiwear additive, as test lubricants. Selected wear scars were analyzed by an Auger emission spectroscopy (AES) depth profiling technique in order to assess the surface film elemental composi-

tion. The ZDP was an effective antiwear additive for all the diesters except dibutyl oxalate and dibutyl sebacate. The high wear measured for the additive-containing oxalate was related to corrosion; the higher wear measured for the additive-containing sebacate was due to an oxygen interaction. The AES of dibutyl sebacate surfaces run in dry air and in dry nitrogen showed large differences only in the amount of oxygen present. The AES of worn surfaces where the additive was effective showed no zinc, only a little phosphorus, and large amounts of sulfur.

Author

N79-33326* National Aeronautics and Space Administration, Lewis Research Center, Cleveland, Ohio.

PLASMA-SPRAYED ZIRCONIA GAS PATH SEAL TECHNOLOGY: A STATE-OF-THE-ART REVIEW

Robert C. Bill. 1979. 17 p. refs. Presented at the Manufacturing Technol. Advisory Rev., Phoenix, Ariz., 21-25 Oct. 1979; sponsored by the Soc. of Manufacturing Engrs. (NASA-TM-79273, AVRADCOM-TR-79-47, E-9941). Avail. NTIS HC A02/MF A01 CSCL 11A

The benefits derived from application of ceramic materials to high pressure turbine gas path seal components are described and the developmental backgrounds of various approaches are reviewed. The most fully developed approaches are those employing plasma sprayed zirconium oxide as the ceramic material. Prevention of cracking and spalling of the zirconium oxide under cyclic thermal shock conditions imposed by the engine operating cycle is the most immediate problem to be solved before implementation is undertaken. Three promising approaches to improving cyclic thermal shock resistance are described and comparative rig performance of each are reviewed. Advanced concepts showing potential for performance improvements are described.

A K L

A79-11548* Effects of pressure and temperature on hot pressing a sialon. H. C. Yeh and W. J. Waters (NASA, Lewis Research Center, Cleveland, Ohio). *American Ceramic Society, Fall Meeting, Hyannis, Mass., Sept. 25-28, 1977, Paper*, 17 p. 10 refs.

The combined effects of temperature and pressure on the resulting density of a sialon (i.e., a ceramic composed of Si, Al, O, and N) are evaluated. Pressures in the 3.5-27.5 MPa range and temperatures in the 1550-1750 C range are considered. It is found that: (1) fully dense sialon bodies may be produced at lower temperatures than those usually used in the field; (2) the phase equilibrium reaction is increased by increased pressure; (3) the iso-density contour may be used to help design the desired microstructure; (4) phase changes occurring in the sample during hot pressing influenced sialon densification to a large extent; and (5) microstructures exceeding 98% theoretical density suggest that plastic deformation has contributed to densification.

S C S

A79-15534* Effects of hydrothermal exposure on a low-temperature cured epoxy. R. W. Lauver (NASA, Lewis Research Center, Cleveland, Ohio). In: *Reinforced Plastics Composites Institute, Annual Conference*, 33rd, Washington, D.C., February 7-10, 1978. Proceedings. (A79-15526 04 24) New York, Society of the Plastics Industry, Inc., 1978, p. 15 C 1 to 15 C 4.

Thermal mechanical analysis was employed to monitor the penetration, temperature of a low-temperature epoxy resin (EPON 826 D230). Both neat resin and E-glass composite samples were examined. The effects of cure temperature variation and moisture content on the apparent glass transition temperature were determined.

(Author)

A79-16659* A comparison of the lubricating mechanisms of graphite fluoride and molybdenum disulfide films. R. L. Fusaro (NASA, Lewis Research Center, Cleveland, Ohio). In: *International Conference on Solid Lubrication*, 2nd, Denver, Colo., August 15-18, 1978. Proceedings. (A79-16651 04 27) Park Ridge, Ill., American Society of Lubrication Engineers, 1978, p. 59-78. 21 refs.

A microscopic study of 440 C steel sliding surfaces lubricated by

graphite fluoride or molybdenum disulfide solid lubricant rubbed films was conducted. The sliding surfaces, along with the friction, wear, and wear life were observed as a function of the number of sliding revolutions in three different atmospheres: moist air (10,000 ppm H₂O), dry air (less than 20 ppm H₂O), or dry argon (less than 20 ppm H₂O). In general, the lubricating mechanisms of the two solid lubricants were found to be relatively similar; that is, a dynamic, thin, layer-like film (which sheared on relative motion) was formed between the two metallic surfaces. The mechanisms of failure were found to be somewhat different, however. Failure of MoS₂ films was very dependent on atmospheric degradation, while that of graphite fluoride films was more dependent on flow of the lubricant film out of the contact zone.

(Author)

A79-16666* The friction and wear properties of sputtered hard refractory compounds. W. A. Brainard (NASA, Lewis Research Center, Cleveland, Ohio). In: *International Conference on Solid Lubrication*, 2nd, Denver, Colo., August 15-18, 1978. Proceedings. (A79-16651 04 27) Park Ridge, Ill., American Society of Lubrication Engineers, 1978, p. 139-147. 17 refs.

The friction and wear properties of several refractory silicides, borides, and carbide coatings were examined. The coatings were applied to type 440C steel surfaces by radio-frequency sputtering. The friction and wear properties of the coatings were found to be related to stoichiometry and impurity content of the bulk coating as well as the degree of interfacial adherence between coating and substrate. Bulk coating stoichiometry could to large extent be controlled by the application of a negative bias voltage during deposition. Adherence was promoted by the formation of an oxidized layer at the interface. Deliberate preoxidizing of the 440C produced enhanced adherence for many compounds which is related to the formation of a mixed oxide transition region.

(Author)

A79-21022* An XPS study of the adherence of refractory carbide, silicide, and boride RF-sputtered wear-resistant coatings. W. A. Brainard and D. R. Wheeler (NASA, Lewis Research Center, Cleveland, Ohio). *Journal of Vacuum Science and Technology*, vol. 15, Nov-Dec 1978, p. 1800-1805. 15 refs.

Radio frequency sputtering was used to deposit refractory carbide, silicide, and boride coatings on 440C steel substrates. Both sputter etched and pre-oxidized substrates were used and the films were deposited with and without a substrate bias. The composition of the coatings was determined as a function of depth by X-ray photoelectron spectroscopy combined with argon ion etching. Friction and wear tests were conducted to evaluate coating adherence. In the interfacial region there was evidence that bias may produce a graded interface for some compounds. Biasing, while generally improving bulk film stoichiometry, can adversely affect adherence by removing interfacial oxide layers. Oxides of all film constituents except carbon and iron were present in all cases but the iron oxide coverage was only complete on the preoxidized substrates. The film and iron oxides were mixed in the MoSi₂ and Mo₂C films but layered in the Mo₂B₅ films. In the case of mixed oxides, preoxidation enhanced film adherence. In the layered case it did not.

(Author)

A79-21295* NASA thermal barrier coatings: Summary and update. F. S. Stepka (NASA, Lewis Research Center, Turbine Cooling Section, Cleveland, Ohio). *U.S. Navy and U.S. Air Force, Workshop on Cooling Problems in Aircraft Gas Turbines, Monterey, Calif., Sept. 27, 28, 1978, Paper*, 22 p. 25 refs. Project SQUID.

The work conducted at the NASA Lewis Research Center to evolve and evaluate a thermal barrier coating system will be discussed. A durable, two-layer, plasma-sprayed coating consisting of a ceramic layer over a metallic layer was developed that has the potential of insulating hot engine parts and thereby reducing metal temperatures and coolant flow requirements and/or permitting use of less costly and complex cooling configurations and materials. The paper summarizes the results of analytical and experimental investigations of the coatings on flat metal specimens, turbine vanes and

blades, and combustor liners. Discussed are results of investigations to determine coating adherence and durability, coating thermal, strength and fatigue properties, and chemical reactions of the coating with oxides and sulfates. Also presented are the effect of the coating on aerodynamic performance of a turbine vane, measured vane and combustor liner temperatures with and without the coating, and predicted turbine metal temperatures and coolant flow reductions potentially possible with the coating. Included also are summaries of some current research related to the coating and potential applications for the coating. (Author)

A79-21297 * # Some properties of an advanced boron fiber. D. R. Behrendt (NASA, Lewis Research Center, Cleveland, Ohio). *American Ceramic Society, Annual Conference on Composites and Advanced Materials, 3rd, Merritt Island, Fla., Jan. 21-24, 1979, Paper.* 10 p.

An advanced coreless boron fiber has exhibited tensile strengths which are more than twice that of the normal CVD B/W fibers. The coreless fiber is made by the chemical removal of the tungsten boride core exposed by splitting the as-grown fiber. The easily splittable fiber is made by the chemical vapor deposition of boron on a larger than usual tungsten substrate. It is expected that the ease of splitting is related to residual stresses in these fibers. Measurements of the axial residual stresses in both the normal and the splittable fibers are presented and the results compared. Differences in these stresses are discussed in connection with the ease of splitting in the splittable fibers. (Author)

A79-27231 * Emission and absorptance of the National Aeronautics and Space Administration ceramic thermal barrier coating. C. H. Liebert (NASA, Lewis Research Center, Cleveland, Ohio). (*International Conference on Metallurgical Coatings, San Francisco, Calif., Apr. 3-7, 1978.*) *Thin Solid Films*, vol. 53, 1978, p. 235-240. 9 refs.

The spectral emittance of a NASA developed zirconia ceramic thermal barrier coating system, consisting of a metal substrate, a layer of Ni-Cr-Al-Y bond material and a layer of yttria-stabilized zirconia ceramic material, is analyzed. The emittance, needed for evaluation of radiant heat loads on cooled coated gas turbine components, was measured over a range of temperatures that would be typical of its use on such components. Emittance data were obtained with a spectrometer, a reflectometer and a radiation pyrometer at a single bond coating thickness of 0.010 cm and at a ceramic coating thickness of 0.0076 cm. The data were transformed into the hemispherical total emittance and were correlated to the ceramic coating thickness and temperature using multiple-regression curve fitting techniques. The system was found to be highly reflective, and, consequently, capable of significantly reducing radiation heat loads on cooled gas turbine engine components. A.A.

A79-31041 * # Stability of PMR-polyimide monomer solutions. R. W. Lauver, R. D. Vannucci (NASA, Lewis Research Center, Cleveland, Ohio), and W. B. Alston (NASA, Lewis Research Center, U.S. Army, Air Mobility Research and Development Laboratory, Cleveland, Ohio). In: *Reinforcing the future, Proceedings of the Thirty-fourth Annual Conference, New Orleans, La., January 30-February 2, 1979.* (A79-31026 12-24) New York, Society of the Plastics Industry, Inc., 1979, p. 23-A 1 to 23-A 7. 7 refs.

The stability of alcohol solutions of norbornenyl capped PMR polyimide resins (both PMR-15 and PMR-11) has been monitored during storage at ambient and subambient (5 C and -18 C) temperatures. PMR-15 solutions exhibit nominally two weeks of useful life and PMR-11 solutions exhibit nominally two days of useful life at ambient conditions. The limiting factor is precipitation of imide reaction products from the monomer solutions. Both solutions exhibit substantially longer useful lifetimes in subambient storage. PMR-15 shows no precipitation after several months storage at subambient temperatures. PMR-11 solutions do exhibit precipitates after extended subambient storage (nominally three months at -18

C), however, the precipitates formed under these conditions can be redissolved. The chemical implications of these observations are discussed. (Author)

A79-31249 * Mechanisms of graphite fluoride (CF_x)_n lubrication. R. L. Fusaro (NASA, Lewis Research Center, Cleveland, Ohio). *Wear*, vol. 53, Apr. 1979, p. 303-323. 10 refs.

Friction, wear and wear life results were compared with optical microscope observations as a function of sliding distance for graphite fluoride rubbed films applied to three surface finishes - polished, sanded and sandblasted. The lubricating process consisted of the plastic flow of thin films of graphite fluoride between flat areas on the rider and on the metallic substrate. If the substrate was rough, flat areas were created during run-in, and the graphite fluoride (CF_x)_n flowed across them. Wear life was enhanced by restricting radial (or transverse) flow of the graphite fluoride from the contact region by increasing surface roughness. Valleys in the roughened substrate surface served as a reservoir for graphite fluoride and as a deposit site for wear debris. Failure resulted from the gradual depletion of graphite fluoride from the contact region with the subsequent formation of powdery metallic debris that covered both rider and disk surfaces. (Author)

A79-32149 * Friction and fracture of single-crystal silicon carbide in contact with itself and titanium. K. Miyoshi (NASA, Lewis Research Center, Cleveland, Ohio; Kanazawa University, Kanazawa, Japan) and D. H. Buckley (NASA, Lewis Research Center, Cleveland, Ohio). *ASLE Transactions*, vol. 22, Apr. 1979, p. 146-153. 12 refs.

An investigation was conducted to examine the friction properties and mechanical behavior of single-crystal silicon carbide (0001) surface sliding against itself and against polycrystalline titanium. The results indicate hexagon-shaped pits of silicon carbide and the formation of platelet hexagon-shaped wear debris of silicon carbide due to cleavages of both prismatic and basal planes as a result of silicon carbide sliding against itself. The fracturing of silicon carbide also occurs near the adhesive bond to titanium. The wear debris produced by brittle fracture plows the titanium and transfers to it. Further, the silicon carbide wear debris, which adhered and transferred to titanium, plows the silicon carbide surface and transfers back to it. (Author)

A79-32931 * Consolidation of Si₃N₄ by hot isostatic pressing. H. C. Yeh (Cleveland State University, Cleveland, Ohio) and P. F. Sikora (NASA, Lewis Research Center, Cleveland, Ohio). *American Ceramic Society Bulletin*, vol. 58, Apr. 1979, p. 444-447. 7 refs. NASA supported research.

Silicon nitride (Si₃N₄) is being considered for gas turbine engine applications because present-day metallic alloys are rapidly approaching the limits of their temperature capabilities. The present investigation was undertaken to determine the feasibility of producing a sound, dense Si₃N₄ body without additives, using conventional gas hot-isostatic-pressing techniques and an uncommon hydraulic hot-isostatic-pressing technique. These two hot-isostatic-pressing (HIP) techniques produce much higher pressure (275-413 MN/sq m) than conventional hot-pressing techniques and have the potential of producing large bodies of desirable shapes. Evaluation was based on density measurement, microscopic examination, both optical and electron, and X-ray diffraction analysis. (Author)

A79-34996 * Tests of NASA ceramic thermal barrier coating for gas turbine engines. C. H. Liebert (NASA, Lewis Research Center, Cleveland, Ohio). *American Vacuum Society and American Society for Metals, International Conference on Metallurgical Coatings, San Diego, Calif., Apr. 23-27, 1979, Paper.* 8 p. 5 refs.

A NASA ceramic thermal barrier coating (TBC) system was tested by industrial and governmental organizations for a variety of aeronautical, marine, and ground-based gas turbine engine applica-

tions. This TBC is a two-layer system with a bond coating of nickel-chromium-aluminum-yttrium (Ni-16Cr-6Al-0.6Y, in wt %) and a ceramic coating of yttria stabilized zirconia (ZrO₂-12Y₂O₃, in wt %). Tests (Liebert and Stenka, 1979) have been conducted to determine corrosion resistance, thermal protection, durability, thermal conductivity, and fatigue characteristics. The information presented covers some of the significant test results obtained on the first three items. The information also includes photographs of coated parts after tests, measurements of coating loss, amount of metal wall temperature reduction when the TBC is used, and extent of base metal corrosion. (Author)

N79-12238* Martin Marietta Corp., Denver, Colo.
CRYOGENIC PROPELLANT DENSIFICATION STUDY
Final Report, Jul. 1977 - Jul. 1978

R O Ewart and R H Dergance Nov 1978 178 p refs
 (Contract NAS3-21014)
 (NASA-CR-159438 MCR 78-586) Avail NTIS
 HC A09/MF A01 CSCL 211

Ground and vehicle system requirements are evaluated for the use of densified cryogenic propellants in advanced space transportation systems. Propellants studied were slush and triple point liquid hydrogen, triple point liquid oxygen, and slush and triple point liquid methane. Areas of study included propellant production, storage, transfer, vehicle loading and system requirements definition. A savings of approximately 8.2 x 100,000 Kg can be achieved in single stage to orbit gross lift-off weight for a payload of 29,484 Kg by utilizing densified cryogenics in place of normal boiling point propellants. G G

N79-18063* TRW Defense and Space Systems Group, Redondo Beach, Calif. Chemistry and Chemical Engineering Lab.
SYNTHESIS OF IMPROVED MOISTURE RESISTANT POLYMERS Final Report, 24 Jun. 1977 - 24 Aug. 1978

M K Orell 15 Mar 1979 45 p refs
 (Contract NAS3-21011)
 (NASA-CR-159456 TRW 31781-6016 RU 00) Avail NTIS
 HC A03/MF A01 CSCL 11C

The use of difluoromaleimide-capped prepolymers to provide improved moisture resistant polymers was investigated. Six different prepolymer formulations were prepared by two different methods. One method utilized the PMR approach to polyimides and the second method employed the normal condensation route to provide fully imidized prepolymers. Polymer specimens cured at 450 F exhibited adequate long-term stability in air at 40% F. Moisture absorption studies were conducted on one polymer formulation. Neat Polymer specimens exhibited weight gains of up to 2% (w/w) after exposure to 100% relative humidity at 344K (160 F) for 400 hours. (Author)

N79-23218* United Technologies Research Center, East Hartford, Conn.

SYNTHESIS OF IMPROVED MOISTURE RESISTANT POLYMERS Final Report

D A Scola and R H Pater 20 Dec 1978 105 p refs
 (Contract NAS3-21010)
 (NASA-CR-159510 R78-912941-15) Avail NTIS
 HC A06/MF A01 CSCL 07C

The synthesis and characterization of novel moisture resistant aliphatic polyimides are described. Several novel aliphatic imides of diversified functionalities were synthesized, purified and characterized. They include (1) N-(12-aminododecyl)-5-norbornene-2,3-dicarboximide, (2) N,N'-[[2,2,2-trifluoro-1-(trifluoromethyl)ethylidene] bis[(1,3-dioxo-5,2-isoindolinediyl)dodecamethylene]] di-5-norbornene-2,3-dicarboximide, (3) N,N'-dodecamethylenedi-5-norbornene-2,3-dicarboximide, (4) N,N'-dodecamethylenedi-5,6-epoxy-2,3-norbornanedicarboximide, and (5) N,N'-Bis[(1,2,3,4-norbornene-2,3-dicarboximidododecyl)-1,2,3,4-butanetetracarboxylic 1,2,3,4-dimide]. The structures of these compounds were established by elemental analysis, IR, NMR, and mass spectra. (Author)

N79-28315* IIT Research Inst., Chicago, Ill.
PROGRAM FOR PLASMA-SPRAYED SELF-LUBRICATING COATINGS Final Report

G C Walther Jul 1979 81 p refs
 (Contract NAS3-20827)
 (NASA-CR-3163 D6146) Avail NTIS HC A05/MF A01 CSCL 11H

A method for preparing composite powders of the three coating components was developed and a procedure that can be used in applying uniform coatings of the composite powders was demonstrated. Composite powders were prepared by adjusting particle sizes of the components and employing a small amount of monoaluminum phosphate as an inorganic binder. Quantitative microscopy (image analysis) was found to be a convenient method of characterizing the composition of the multiphase plasma-sprayed coatings. Area percentages and distribution of the components were readily obtained by this method. The adhesive strength of the coating to a nickel-chromium alloy substrate was increased by about 40 percent by a heat treatment of 20 hours at 550 C. S E S

N79-29331* United Technologies Research Center, East Hartford, Conn.

NEW HIGH TEMPERATURE CROSS LINKING MONOMERS

Daniel A Scola 20 Dec 1978 115 p refs
 (Contract NAS3-21009)
 (NASA-CR-159514 UTRC R78-912897-15) Avail NTIS
 HC A06/MF A01 CSCL 07C

Several PMR polyimide resins capable of being processed at a maximum temperature of 232 C to 288 C without sacrifice of high temperature capability were developed. Four monomethyl esters were synthesized and characterized for use in the crosslinking studies. The infrared and DSC studies of each crosslinker suggested that curing could be accomplished at 288 C. However, fabrication of dense, void free polymer specimens required a temperature of 316 C and a pressure of 0.69 MPa (100 psi). Crosslinkers were evaluated in Celion 6000/PMR polyimide composites. These composites were characterized at RT, 288 C and 316 C initially and after isothermal aging at 288 C and 316 C for several hundred hours. The results suggest that both PMR systems are promising candidates as matrices for addition type polyimide composites. It is demonstrated that alternate crosslinkers are feasible, but mechanisms to lower the crosslinking temperature must be developed to provide lower temperature processing PMR-type polyimides. K L

N79-30377* Horizons Research Inc., Cleveland, Ohio
SURVEY OF INORGANIC POLYMERS

Arthur H Garber and Eugene F McInerney Jun 1979 316 p refs
 (Contract NAS3-21369)
 (NASA-CR-159563 HRI 396) Avail NTIS HC A14/MF A01 CSCL 07C

A literature search was carried out in order to identify inorganic, metallo-organic, and hybrid inorganic-organic polymers that could serve as potential matrix resins for advanced composites. The five most promising candidates were critically reviewed and recommendations were made for the achievement of their potential in terms of performance and cost. These generic polymer classes comprise: (1) Poly(silyl) sesquioxanes; (2) Poly(silyl) arylene siloxanes; (3) Poly(silyl)enes; (4) Poly(isilicon linked ferrocenes); and (5) Poly(organo)phosphazenes. No single candidate currently possesses the necessary combination of physico-mechanical properties, thermal stability, processability, and favorable economics. The first three classes exhibit the best thermal performance. On the other hand, poly(organo)phosphazenes, the most extensively studied polymer class, exhibit the best combination of structure-property control, processability and favorable economics. K L

A79-31957 * **Static evaluation of surface coatings for compliant gas bearings in an oxidizing atmosphere to 650 C.** B. Bhushan and S. Gray (Mechanical Technology, Inc., Latham, N.Y.). In: *Metallurgical coatings 1978; Proceedings of the Fifth International Conference, San Francisco, Calif., April 3-7, 1978. Volume 1.* (A79-31951 12-23) Lausanne, Elsevier Sequoia, S.A., 1978, p. 313-331, 17 refs. Contract No. NAS3-19427.

Hard wear-resistant coatings and soft low shear strength coatings were developed for an air-lubricated compliant journal bearing for a future automotive gas turbine engine. The coatings were expected to function in either 540 or 650 C ambient. Soft lubricant coatings were generally limited in temperature. Therefore emphasis was on the hard wear-resistant coatings. The coating materials covered were TiC, B₄C, Cr₃C₂, WC, SiC, CrB₂, TiB₂, Cr₂O₃, Al₂O₃, Si₃N₄, Tribaloy 800, CaF₂, CaF₂-BaF₂ eutectic, Ni-Co, silver, CdO-graphite and proprietary compounds. The coatings on test coupons were subjected to static oven screening tests. The test consisted of exposure of material samples in an oven for 300 h at the maximum temperature (540 or 650 C) and ten temperature cycles from room temperature to the maximum service temperature. On the basis of the specimen examinations the following coatings were recommended for future wear tests: TiC (sputtered), Cr₂O₃ (sputtered), Si₃N₄ (sputtered), CdO and graphite (fused), Kaman DES (a proprietary coating), CrB₂ (plasma sprayed), Cr₃C₂ (detonation gun) and NASA PS-106 (plasma sprayed). (Author)

A79-51103 * **UV blocking filters for polymeric films.** G. J. Rayl (General Electric Co., Space Div., Valley Forge, Pa.). *American Vacuum Society, Meeting, Princeton, N.J., May 17, 1979. Paper 17* p. 5 refs. Contract No. NAS3 21264

The concept of incorporating UV screening agents in silicone resins as a means of protecting underlying solar cell covers and adhesives from UV degradation is presented. A silicone hard-coat resin incorporating a UV screening agent was selected as a suitable coating material for PFA Teflon solar cell covers. Consideration is given to fabrication procedures and techniques for introduction of the UV screening agents into silicone resins and application of these UV-inhibited coatings to the Teflons. Some preliminary environmental tests, such as thermal shock and temperature humidity, were conducted. V.T.

28 PROPELLANTS AND FUELS

Includes rocket propellants, igniters, and oxidizers, storage and handling, and aircraft fuels.

For related information see also 07 Aircraft Propulsion and Power, 20 Spacecraft Propulsion and Power, and 44 Energy Production and Conversion

N79-13196* National Aeronautics and Space Administration, Lewis Research Center, Cleveland, Ohio.

CHARACTERISTICS AND COMBUSTION OF FUTURE HYDROCARBON FUELS

R. A. Rudey and J. S. Grobman. In AGARD Aircraft Eng. Future Fuels and Energy Conserv. Sep. 1978. 23 p. refs. (For primary document see N79-13192 04-28)

Avail. NTIS HC A05/MF A01 CSCL 21D

Changes in fuel properties that are expected in future hydrocarbon fuels for aircraft are discussed along with the principal properties of 'syncrudes' and the fuels that can be derived from them. The impact that the resultant potential changes in fuel properties may have on combustion and thermal stability characteristics is illustrated and discussed in terms of ignition, soot formation, carbon deposition, flame radiation, and emissions.

J.M.S.

N79-13197* National Aeronautics and Space Administration, Lewis Research Center, Cleveland, Ohio.

IMPACT OF FUTURE FUEL PROPERTIES ON AIRCRAFT ENGINES AND FUEL SYSTEMS

R. A. Rudey and J. S. Grobman. In AGARD Aircraft Eng. Future Fuels and Energy Conserv. Sep. 1978. 29 p. refs. (For primary document see N79-13192 04-28)

Avail. NTIS HC A09/MF A01 CSCL 21D

The effect of modifications in hydrocarbon jet fuels specifications on engine performance, component durability and maintenance, and aircraft fuel system performance is discussed. Specific topics covered include: specific fuel consumption; ignition at relight limits, exhaust emissions, combustor liner temperatures, carbon deposition, gum formation in fuel nozzles, erosion and corrosion of turbine blades and vanes, deposits in fuel system heat exchangers, and pumpability and flowability of the fuel. Data that evaluate the ability of current technology aircraft to accept fuel specification changes are presented, and selected technological advances that can reduce the severity of the problems are described and discussed.

J.M.S.

N79-15199* National Aeronautics and Space Administration, Lewis Research Center, Cleveland, Ohio.

HIGH FREEZING POINT FUELS USED FOR AVIATION TURBINE ENGINES

Robert Friedman. 1979. 14 p. refs. To be presented at the 24th Ann Intern. Gas Turbine Conf., San Diego, Calif., 11-15 Mar. 1979, sponsored by ASME.

(NASA TM 79015 E 9804) Avail. NTIS HC A02/MF A01 CSCL 21D

Broadened specification aviation fuels could be produced from a greater fraction of crude source material with improvements in fuel supply and price. These fuels, particularly those with increased final boiling temperatures, would have higher freezing temperatures than current aviation turbine fuels. For the small but significant fraction of commercial flights where low fuel temperatures make higher freezing point fuel use unacceptable, adaptations to the fuel or fuel system may be made to accommodate this fuel. Several techniques are discussed. Fuel heating is the most promising concept. One simple design uses existing heat rejection from a fuel lubricating oil cooler; another uses an engine driven generator for electrical heating.

A.R.H.

N79-16136* National Aeronautics and Space Administration, Lewis Research Center, Cleveland, Ohio.

EFFECT OF BROADENED-SPECIFICATION FUELS ON AIRCRAFT ENGINES AND FUEL SYSTEMS

R. A. Rudey. 1979. 25 p. refs. To be presented at the 4th Intern. Symp. on Airbreathing Eng., Lake Buena Vista, Fla., 1-6 Apr. 1979, sponsored by AIAA.

(NASA-TM-79086 E-9898) Avail. NTIS HC A02/MF A01 CSCL 21D

A wide variety of studies on the potential effects of broadened-specification fuels on future aircraft engines and fuel systems are summarized. The compositions and characteristics of aircraft fuels that may be derived from current and future crude-oil sources are described, and the most critical properties that may affect aircraft engines and fuel systems are identified and discussed. The problems that are most likely to be encountered because of changes in selected fuel properties are explored, and the related effects on engine performance, component durability and maintenance, and aircraft fuel system performance are examined. The ability of current technology to accept possible future fuel specification changes is assessed and selected technological advances that can reduce the severity of the potential problems are illustrated.

A.R.H.

N79-20265* National Aeronautics and Space Administration, Lewis Research Center, Cleveland, Ohio.

AIRFOIL COOLING HOLE PLUGGING BY COMBUSTION GAS IMPURITIES OF THE TYPE FOUND IN COAL DERIVED FUELS

Daniel L. Deadmore and Carl E. Lowell. Feb. 1979. 14 p. refs. (Contract EF-77-A-01-2593)

(NASA-TM-79076 E-9893; DOE/NASA/2593-79/1) Avail. NTIS HC A02/MF A01 CSCL 21D

The plugging of airfoil cooling holes by typical coal-derived fuel impurities was evaluated using doped combustion gases in an atmospheric pressure burner rig. Very high specific cooling air mass flow rates reduced or eliminated plugging. The amount of flow needed was a function of the composition of the deposit. It appears that plugging of film-cooled holes may be a problem for gas turbines burning coal-derived fuels.

Author

N79-28349* National Aeronautics and Space Administration, Lewis Research Center, Cleveland, Ohio.

USE OF REFINERY COMPUTER MODEL TO PREDICT FUEL PRODUCTION

Francisco J. Flores. Jun. 1979. 25 p. refs.

(NASA TM 79203 E-088) Avail. NTIS HC A02/MF A01 CSCL 21D

Several factors (crudes, refinery operation and specifications) that affect yields and properties of broad specification jet fuel were parameterized using the refinery simulation model which can simulate different types of refineries were used to make the calculations. Results obtained from the program are used to correlate yield as a function of final boiling point, hydrogen content and freezing point for jet fuels produced in two refinery configurations, each one processing a different crude mix. Refinery performances are also compared in terms of energy consumption.

A.R.H.

N79-28350* National Aeronautics and Space Administration, Lewis Research Center, Cleveland, Ohio.

AXIAL JET MIXING OF ETHANOL IN CYLINDRICAL CONTAINERS DURING WEIGHTLESSNESS

John C. Aydelott. Jul. 1979. 43 p. refs.

(NASA TP 1487 E 9937) Avail. NTIS HC A03/MF A01 CSCL 21D

An experimental program was conducted to examine the liquid flow patterns that result from the axial jet mixing of ethanol in 10 centimeter diameter cylindrical tanks in weightlessness. A convex hemispherically ended tank and two Centaur liquid hydrogen tank models were used for the study. Four distinct liquid flow patterns were observed to be a function of the tank geometry, the liquid jet velocity, the volume of liquid in the

tank, and the location of the tube from which the liquid jet exited
Author

N79-31403* # National Aeronautics and Space Administration
Lewis Research Center, Cleveland, Ohio

THERMOPHYSICAL PROPERTY DATA: WHO NEEDS THEM?

R. C. Hendricks. 1979. 27 p. refs. Proposed for presentation at the Winter Ann. Meeting of the ASME, N. Y., 2-7 Dec 1979

(NASA-TM-79241, E-149) Avail. NTIS HC A03/MF A01 CSCL 07D

Specific examples are cited to illustrate the universal needs and demands for thermophysical property data. Applications of the principle of similarity in fluid mechanics and heat transfer and extensions of the principle to fluid mixtures are discussed. It becomes quite clear that no matter how eloquent theories (or experiments) in fluid mechanics or heat transfer are, results of their application can be no more accurate than the thermophysical properties required to transform these theories into practice - or in the case of an experiment, to reduce the data. Present day projects take place on such a scale that the need for international standards groups and mutual cooperation is evident. Author

N79-31405* # National Aeronautics and Space Administration
Lewis Research Center, Cleveland, Ohio

COMPARISON OF THE PROPERTIES OF SOME SYNTHETIC CRUDES WITH PETROLEUM CRUDES

Albert C. Antoine. Jul 1979. 31 p. refs.

(NASA-TM-79220, E-115) Avail. NTIS HC A03/MF A01 CSCL 21D

Physical properties and chemical compositions of six synthetic crudes were determined. The results were compared to those of typical petroleum crudes with the interest being the feasibility of making jet fuels from oil shale and coal syncrudes. The specific gravity, viscosity, and pour point were measured, showing that these crudes would be described as heavier rather than lighter crudes. The boiling range distribution of the crudes was determined by distillation and by gas chromatography. In addition, gel permeation chromatograms were obtained, giving a unique molecular weight distribution profile for each crude. Analyses for carbon, hydrogen, nitrogen, and sulfur concentrations were performed, as well as for hydrocarbon group type and trace element concentrations. It was found that the range in concentration of vanadium, an element whose presence in turbine fuels is of major concern, was lower than that of petroleum crudes. Sodium and potassium, other elements of concern, were present in comparatively high concentrations. Author

A79-10824 * # Alternative aircraft fuels. J. P. Longwell (MIT, Cambridge, Mass.) and J. Grobman (NASA, Lewis Research Center, Cleveland, Ohio). *American Society of Mechanical Engineers Gas Turbine Conference and Products Show, London, England, Apr. 9-13, 1978, Paper, 21 p.* 11 refs.

In connection with the anticipated impossibility to provide on a long term basis liquid fuels derived from petroleum, an investigation has been conducted with the objective to assess the suitability of jet fuels made from oil shale and coal and to develop a data base which will allow optimization of future fuel characteristics, taking energy efficiency of manufacture and the tradeoffs in aircraft and engine design into account. The properties of future aviation fuels are examined and proposed solutions to problems of alternative fuels are discussed. Attention is given to the refining of jet fuel to current specifications, the control of fuel thermal stability, and combustor technology for use of broad specification fuels. The first solution is to continue to develop the necessary technology at the refinery to produce specification jet fuels regardless of the crude source. G. R.

A79-11599 * # Characteristics and combustion of future hydrocarbon fuels. R. A. Rudey and J. S. Grobman (NASA, Lewis Research Center, Cleveland, Ohio). *NATO, AGARD, Lecture Series on Energy Conservation in Aircraft Propulsion, Munich, West Germany, Oct. 26, 27, 1978, Paper, 25 p.* 19 refs.

Dwindling supply of high-quality crude is beginning to manifest itself in the form of crude oils containing higher percentages of aromatic compounds, sulfur, nitrogen, and trace constituents. In the present paper, problems which have arisen with regard to the hydrogen content in jet fuels derived from these crude oil sources are discussed, with particular reference to the effects of varying the fuel properties on the combustion and thermal stability characteristics of a fuel. The importance of knowing how severe the effects of variations in hydrogen content, fuel-bound-nitrogen content, and boiling range are on such combustion phenomena as soot and carbon formation, emissions, and ignition is pointed out. V. P.

A79-12378 * # Alternative aviation turbine fuels. J. Grobman (NASA, Lewis Research Center, Advanced Technology Section, Cleveland, Ohio). In: *National Conference on Energy Conservation in General Aviation, 1st, Kalamazoo, Mich., October 10, 11, 1977, Proceedings (A79-12376 02-07) Kalamazoo, Mich., Western Michigan University, 1977, p. 40-59, 11 refs.*

The efficient utilization of fossil fuels by future jet aircraft may necessitate the broadening of current aviation turbine fuel specifications. The most significant changes in specifications would be an increased aromatics content and a higher final boiling point in order to minimize refinery energy consumption and costs. These changes would increase the freezing point and might lower the thermal stability of the fuel and could cause increased pollutant emissions, increased smoke and carbon formation, increased combustor liner temperatures, and poorer ignition characteristics. This paper discusses the effects that broadened specification fuels may have on present-day jet aircraft and engine components and the technology required to use fuels with broadened specifications. (Author)

A79-30555 * # High-freezing-point fuels used for aviation turbine engines. R. Friedman (NASA, Lewis Research Center, Cleveland, Ohio). *American Society of Mechanical Engineers Gas Turbine Conference and Exhibit and Solar Energy Conference, San Diego, Calif., Mar. 12-15, 1979, Paper 79-GT-141, 12 p.* 21 refs.

Broadened-specification aviation fuels could be produced from a greater fraction of crude source material with improvements in fuel supply and price. These fuels, particularly those with increased final boiling temperatures, would have higher freezing temperatures than current aviation turbine fuels. The higher-freezing-point fuels can be substituted in the majority of present commercial flights, since temperature data indicate that in-flight fuel temperatures are relatively mild. For the small but significant fraction of commercial flights where low fuel temperatures make higher freezing-point fuel use unacceptable, adaptations to the fuel or fuel system may be made to accommodate this fuel. Several techniques are discussed. Fuel heating is the most promising concept. One simple system design uses existing heat rejection from the fuel-lubricating oil cooler, another uses an engine-driven generator for electrical heating. Both systems offer advantages that outweigh the obvious penalties. (Author)

A79-38980 * # Analysis of the impact of the use of broad specification fuels on combustors for commercial aircraft gas turbine engines. E. J. Szelata (United Technologies Research Center, East Hartford, Conn.), R. P. Lehmann (United Technologies Corp., Pratt and Whitney Aircraft Group, East Hartford, Conn.), and A. L. Smith (NASA, Lewis Research Center, Cleveland, Ohio). *AIAA, SAE, and ASME Joint Propulsion Conference, 15th, Las Vegas, Nev., June 18-20, 1979, AIAA Paper 79-1155, 11 p.* 16 refs.

An analytical study was conducted to assess the impact of the use of broad specification fuels with reduced hydrogen content on the design, performance, durability, emissions, and operational characteristics of combustors for commercial aircraft gas turbine

engines. The study was directed at defining necessary design revisions to combustors designed for use of Jet A when such are operated on ERBS (Experimental Referee Broad Specification Fuel) which has a nominal hydrogen content of 12.8 percent as opposed to 13.7 percent in current Jet A. The results indicate that improvements in combustor liner coating, and/or materials, and methods of fuel atomization will be required if the hydrogen content of aircraft gas turbine fuel is decreased. (Author)

N79-10226*# Southwest Research Inst., San Antonio, Tex. WORKBOOK FOR ESTIMATING EFFECTS OF ACCIDENTAL EXPLOSIONS IN PROPELLANT GROUND HANDLING AND TRANSPORT SYSTEMS Final Report

W E Baker, J J Kulesz, R E Ricker, P S Westine, V B Parr, L M Vargas, and P K Moseley Aug 1978 274 p refs (Contract NAS3-20497) (NASA CR 3023 Rept 02-4778) Avail NTIS HC A12/MF A01 CSCL 21D

A workbook is presented to supplement an earlier NASA publication which was intended to provide the designer and safety engineer with rapid methods for predicting damage and hazards from explosions of liquid propellant and compressed gas vessels used in ground storage, transport and handling. Information is presented in the form of graphs and tables. How easy calculation, using only desk or handheld calculators. Topics covered in various chapters are: (1) estimates of explosive yield, (2) characteristics of pressure waves, (3) effects of pressure waves, (4) characteristics of fragments, and (5) effects of fragments and related topics. (Author)

N79-20266*# General Applied Science Labs., Inc., Westbury, N Y

PREMIX FUELS STUDY APPLICABLE TO DUCT BURNER CONDITIONS FOR A VARIABLE CYCLE ENGINE Final Report

K S Venkataramani Dec 1978 44 p refs (Contract NAS3-20603) (NASA-CR-159513, TR-251) Avail NTIS HC A03/MF A01 CSCL 21D

Emission levels and performance of a premixing Jet-A/air duct burner were measured at reference conditions representative of take-off and cruise for a variable cycle engine. In a parametric variation sequence of tests, data were obtained at inlet temperatures of 400, 500 and 600K at equivalence ratios varying from 0.9 to the lean stability limit. Ignition was achieved at all the reference conditions although the CO levels were very high. Significant nonuniformity across the combustor was observed for the emissions at the take-off condition. At a reference Mach number of 0.117 and an inlet temperature of 600K, corresponding to a simulated cruise condition, the NO_x emission level was approximately 1 gm/kg-fuel. (LS)

N79-20267*# Exxon Research and Engineering Co., Linden, N J. HIGH PERFORMANCE, HIGH DENSITY HYDROCARBON FUELS

J W Frankenfeld, T W Hastings, M Lieberman, and W F Taylor Oct 1978 239 p refs (Contract NAS3-20394) (NASA-CR-159480, EXXON/GRUS 1KWD 78) Avail NTIS HC A11/MF A01 CSCL 21D

The fuels were selected from 77 original candidates on the basis of estimated merit index and cost effectiveness. The ten candidates consisted of 3 pure compounds, 4 chemical plant streams and 3 refinery streams. Critical physical and chemical properties of the candidate fuels were measured including heat of combustion, density, and viscosity as a function of temperature, freezing points, vapor pressure, boiling point, thermal stability. The best all-around candidate was found to be a chemical plant olefin stream rich in dicyclopentadiene. This material has a high merit index and is available at low cost. Possible problem areas were identified as low temperature flow properties and thermal stability. An economic analysis was carried out to determine the production costs of top candidates. The chemical plant and refinery streams were all less than 44 cent/kg while the pure

compounds were greater than 44 cent/kg. A literature survey was conducted on the state of the art of advanced hydrocarbon fuel technology as applied to high energy propellants. Several areas for additional research were identified. (LS)

N79-24172*# Boeing Commercial Airplane Co., Seattle, Wash. DESIGN AND EVALUATION OF AIRCRAFT HEAT SOURCE SYSTEMS FOR USE WITH HIGH-FREEZING POINT FUELS Final Report

A J Pasion NASA May 1979 53 p refs (Contract NAS3-20815) (NASA-CR-159568, D6-48097) Avail NTIS HC A03/MF A01 CSCL 21D

The objectives were the design, performance and economic analyses of practical aircraft fuel heating systems that would permit the use of high freezing-point fuels on long-range aircraft. Two hypothetical hydrocarbon fuels with freezing points of -29 C and -18 C were used to represent the variation from current day jet fuels. A Boeing 747-200 with JT9D-7/7A engines was used as the baseline aircraft. A 9300 Km mission was used as the mission length from which the heat requirements to maintain the fuel above its freezing point was based. (JAM)

N79-26221*# General Electric Co., Evendale, Ohio. EXPERIMENTAL CLEAN COMBUSTOR PROGRAM: DIESEL NO. 2 FUEL ADDENDUM, PHASE 3 Final Report

C C Gleason and D W Bahr May 1979 66 p refs (Contract NAS3-19736) (NASA-CR-135413, R79AEG367) Avail NTIS HC A04/MF A01 CSCL 21D

A CF6-50 engine equipped with an advanced, low emission, double annular combustor was operated 4.8 hours with No. 2 diesel fuel. Fourteen steady-state operating conditions ranging from idle to full power were investigated. Engine/combustor performance and exhaust emissions were obtained and compared to JF-5 fueled test results. With one exception, fuel effects were very small and in agreement with previously obtained combustor test rig results. At high power operating condition, the two fuels produced virtually the same peak metal temperatures and exhaust emission levels. At low power operating conditions, where only the pilot stage was fueled, smoke levels tended to be significantly higher with No. 2 diesel fuel. Additional development of this combustor concept is needed in the areas of exit temperature distribution, engine fuel control, and exhaust emission levels before it can be considered for production engine use. (JAM)

N79-29355*# Lockheed-California Co., Burbank. EXPERIMENTAL STUDY OF LOW TEMPERATURE BEHAVIOR OF AVIATION TURBINE FUELS IN A WING TANK MODEL Final Report

Francis J Stockemer 1979 112 p refs (Contract NAS3-20814) (NASA-CR-159515) Avail NTIS HC A06/MF A01 CSCL 21D

An experimental investigation was performed to study aircraft fuels at low temperatures near the freezing point. The objective was an improved understanding of the flowability and pumpability of the fuels under conditions encountered during cold weather flight of a long range commercial aircraft. The test tank simulated a section of an outer wing tank and was chilled on the upper and lower surfaces. Fuels included commercial Jet A and Diesel D-2, JP-5 from oil shale, and Jet A, intermediate freeze point, and D-2 fuels derived from selected paraffinic and naphthenic crudes. A pour point depressant was tested. (MMM)

N75 25382* TRW, Inc., Cleveland, Ohio
AUTOMATED PLASMA SPRAY (APS) PROCESS FEASIBILITY STUDY: PLASMA SPRAY PROCESS DEVELOPMENT AND EVALUATION Interim Report
C. W. Fetheroff, T. Derkacs, and I. M. Matay May 1979 117 p
refs
(Contract NAS3-20112)
(NASA-CR-159579, TRW-ER-8019-1) Avail NTIS
HC A06/MF A01 CSCL 13H

An automated plasma spray (APS) process was developed to apply two layer (NiCrAlY and ZrO₂-12Y₂O₃) thermal-barrier coatings to aircraft gas turbine engine blade airfoils. The APS process hardware consists of four subsystems: a mechanical blade positioner incorporating two interlaced six-degree-of-freedom assemblies; a noncoherent optical metrology subsystem; a microprocessor-based adaptive system controller; and commercial plasma spray equipment. Over fifty JT9D first stage turbine blades specimens were coated with the APS process in preliminary checkout and evaluation studies. The best of the preliminary specimens achieved an overall coating thickness uniformity of \pm or \pm 53 micrometers, much better than is achievable manually. Factors limiting this performance were identified and process modifications were initiated accordingly. Comparative evaluations of coating thickness uniformity for manually sprayed and APS coated specimens were initiated. One of the preliminary evaluation specimens was subjected to a torch test and metallographic evaluation.

M M M

31 ENGINEERING (GENERAL)

Includes vacuum technology; control engineering; display engineering; and cryogenics

N79-21225* National Aeronautics and Space Administration, Lewis Research Center, Cleveland, Ohio.

LOW HEAT LEAK CONNECTOR FOR CRYOGENIC SYSTEM **Patent**

Philip D. Stelts, inventors (to NASA) (Air Products and Chemical Inc., Philadelphia) Issued 2 Nov 1965 6 p Filed 1 Oct 1964 Sponsored by NASA

(NASA Case XLE-02367-1, US-Patent-3,215,313)

US-Patent-Appl-SN 400857, US-Patent-Class-222-131) Avail US Patent and Trademark Office CSCL 20L

Heat leak from the surrounding atmosphere during fluid transfer from a spaced shell-insulated vessel for storing liquefied gas having an upper gaseous phase, is minimized by forming a relatively wide, shallow blister on the wall of the vessel at the point of transfer line connection. The shell and the opposed walls of the blister have aligned openings whose common axis passes centrally through the blister and is normal to the surfaces of the vessel and shell. A fluid transfer line conduit passing through the shell opening is in fluid-tight connection with the shell and blister wall. The fluid transfer line confines the fluid in a continuous stream. The blister is filled with a heat insulating material which provides a thermal break between the central wall portions of the blister. A connector at the bottom of the vessel comprises a tube extending between the openings in the blister which projects a short distance within the body of liquefied gas and terminates in a reverse bend to prevent backflow of liquid through the pipe. A R H

N79-23257*# National Aeronautics and Space Administration, Lewis Research Center, Cleveland, Ohio.

IDENTIFICATION AND DUAL ADAPTIVE CONTROL OF A TURBOJET ENGINE

Walter Merrill and Gary Leininger (Toledo Univ.) 1979 10 p refs. Proposed for presentation at the 5th IFAC Symp. on Identification and System Parameter Estimation, Darmstadt, West Ger., 24-28 Sep. 1979

(NASA-TM-79145, E 10000) Avail NTIS HC A02/MF A01 CSCL 21E

The objective of this paper is to utilize the design methods of modern control theory to realize a dual-adaptive feedback control unit for a highly nonlinear single spool airbreathing turbojet engine. Using a very detailed and accurate simulation of the nonlinear engine as the data source, linear operating point models of unspecified dimension are identified. Feedback control laws are designed at each operating point for a prespecified set of sampling rates using sampled-data output regulator theory. The control system sampling rate is determined by an adaptive sampling algorithm in correspondence with turbojet engine performance. The result is a dual adaptive control law that is functionally dependent upon the sampling rate selected and environmental operating conditions. Simulation transients demonstrate the utility of the dual-adaptive design to improve on-board computer utilization while maintaining acceptable levels of engine performance. Author

A79-19816 * Some flow phenomena in a constant area duct with a Borda type inlet including the critical region. R. C. Hendricks and P. J. Simoneau (NASA, Lewis Research Center, Cleveland, Ohio) *American Society of Mechanical Engineers, Winter Annual Meeting, San Francisco, Calif., Dec. 10-15, 1973, Paper 78-WA-HT-37* 7 p 13 refs. Members \$1.50, nonmembers \$3.00

Mass limiting flow characteristics for a 55 L/D tube with a Borda type inlet have been assessed over large ranges of temperature and pressure using fluid nitrogen. Under certain conditions, separation and pressure drop at the inlet was sufficiently strong to permit partial vaporization and the remaining fluid flowed through the tube as if it were a free jet. An empirical relation was determined which defines conditions under which this type of flow can occur. A flow

coefficient is presented which enables one to estimate flow rates over the experimental range. A flow rate stagnation pressure map for selected stagnation isotherms and pressure profiles document these flow phenomena. (Author)

N79-30415*# Boeing Engineering and Construction, Seattle, Wash.

MOD-2 FAILURE MODE AND EFFECTS ANALYSIS

Robert Lynette and Robert Poore Jul 1979 302 p Sponsored by NASA

(Contract DEN3-2, DE-AI01-79ET20485)

(NASA-CR-159632) Avail NTIS HC A14/MF A01 CSCL 13L

The results of a failure mode and effects analysis of the Mod-2 wind turbine are presented. Author

32 COMMUNICATIONS

Includes land and global communications, communications theory, and optical communications.

For related information see also 04 *Aircraft Communications and Navigation* and 17 *Spacecraft Communications, Command and Tracking*

N79-14275* National Aeronautics and Space Administration, Lewis Research Center, Cleveland, Ohio.

DESIGN OF A VIDEO TELECONFERENCE FACILITY FOR A SYNCHRONOUS SATELLITE COMMUNICATIONS LINK
Michael D. Richardson Jan. 1979 20 p. refs.
(NASA-TP-1376, E-9202) Avail. NTIS HC A02/MF A01 CSCL 17B

The system requirements, design tradeoffs, and final design of a video teleconference facility are discussed, including proper lighting, graphics transmission, and picture aesthetics. Methods currently accepted in the television broadcast industry are used in the design. The unique problems associated with using an audio channel with a synchronous satellite communications link are discussed, and a final audio system design is presented.

Author

N79-16169* National Aeronautics and Space Administration, Lewis Research Center, Cleveland, Ohio.

TELECOMMUNICATION SERVICE MARKETS THROUGH THE YEAR 2000 IN RELATION TO MILLIMETER WAVE SATELLITE SYSTEMS

Steven M. Stevenson 1979 13 p. Presented at the Intern. Telecommunication Exposition, Dallas, 26 Feb. - 2 Mar. 1979 (NASA-TM-79099) Avail. NTIS HC A02/MF A01 CSCL 17B

NASA is currently conducting a series of millimeter wave satellite system market studies to develop 30/20 GHz satellite system concepts that have commercial potential. Four contractual efforts were undertaken: two parallel and independent system studies and two parallel and independent market studies. The marketing efforts are focused on forecasting the total domestic demand for long haul telecommunications services for the 1980-2000 period. Work completed to date and reported in this paper include projections of geographical distribution of traffic, traffic volume as a function of urban area size, and user identification and forecasted demand.

Author

N79-17072* National Aeronautics and Space Administration, Lewis Research Center, Cleveland, Ohio.

DETERMINING POTENTIAL 30/20 GHz DOMESTIC SATELLITE SYSTEM CONCEPTS AND ESTABLISHMENT OF A SUITABLE EXPERIMENTAL CONFIGURATION

Grady H. Stevens and Godfrey Anzic 1979 19 p. refs. Presented at the Intern. Telecommun. Exposition, Dallas, 26 Feb. 1976 - 2 Mar. 1979

(NASA-TM-79092, E-9916) Avail. NTIS HC A02/MF A01 CSCL 17B

NASA is conducting a series of millimeter wave satellite communication systems and market studies to: (1) determine potential domestic 30/20 GHz satellite concepts and market potential, and (2) establish the requirements for a suitable technology verification payload which, although intended to be modest in capacity, would sufficiently demonstrate key technologies and experimentally address key operational issues. Preliminary results and critical issues of the current contracted effort are described. Also included is a description of a NASA-developed multibeam satellite payload configuration which may be representative of concepts utilized in a technology flight verification program.

F.O.S.

N79-20300* National Aeronautics and Space Administration, Lewis Research Center, Cleveland, Ohio.

RESULTS OF THIN ROUTE SATELLITE COMMUNICATION SYSTEM ANALYSES INCLUDING ESTIMATED SERVICE COSTS

David L. Wright 1979 12 p. ref. Presented at the Intern. Telecommun. Exposition, Dallas, 26 Feb. - 2 Mar. 1979. Prepared

in cooperation with Fairchild Space and Electronics Co., Germantown, Md.

(Contract NAS3-20364)

(NASA-TM-79098, E-9922) Avail. NTIS HC A02/MF A01 CSCL 17B

A variety of cost and performance tradeoffs are addressed and the preliminary design of a communications satellite system capable of meeting isolated rural users' needs is presented. Small inexpensive rural earth stations are linked via the satellite to a nation wide network of large earth stations which are, in turn, interconnected to the switching exchanges of the conventional telephone network. Optimum earth station EIRP and G/T and satellite transponder power are defined as a function of a wide variety of system options.

G.Y.

N79-23313* National Aeronautics and Space Administration, Lewis Research Center, Cleveland, Ohio.

VHF DOWNLINK COMMUNICATION SYSTEM FOR SLAR DATA

R. J. Schertler, T. L. Chase, R. A. Mueller, I. Kramarchuk, R. J. Jirberg, and R. T. Gedney 1979 10 p. refs. Presented at the 13th Intern. Symp. on Remote Sensing of Environment, Ann Arbor, Mich., 23-27 Apr. 1979, sponsored by Michigan Univ. (NASA-TM-79164, E-025) Avail. NTIS HC A02/MF A01 CSCL 17I

A real time VHF downlink communication system is described for transmitting side-looking airborne radar (SLAR) data directly from an aircraft to a portable ground/shipboard receiving station. Use of this receiving station aboard the U.S. Coast Guard icebreaker Mackinaw for generating real-time photographic quality radar images is discussed. The system was developed and demonstrated in conjunction with the U.S. Coast Guard and NOAA National Weather Service as part of the Project Icewarn all weather ice information system for the Great Lakes Winter Navigation Program.

Author

N79-27351* National Aeronautics and Space Administration, Lewis Research Center, Cleveland, Ohio.

SATELLITE COMMUNICATIONS FOR DISASTER RELIEF OPERATIONS

Joseph N. Sivo 1979 20 p. refs. Proposed for presentation at Intern. Astron. Federation Munich, 17-23 Sep. 1979

(NASA-TM-79198, E-078) Avail. NTIS HC A02/MF A01 CSCL 17B

The use of existing and planned communication satellite systems to provide assistance in the implementation of disaster relief operations on a global basis was discussed along with satellite communications system implications and their potential impact on field operations in disaster situations. Consideration are given to the utilization of both INTELSAT and MARISAT systems operating at frequencies ranging from 1.5 to 4 GHz and to the size and type of ground terminals necessary for satellite access. Estimates of communication requirements for a global system are given. Some discussion of cost estimates for satellite services to support operations are included. Studies of communication satellites for both pre and post disaster applications conducted for NOAA are included as well as recent experiments conducted in conjunction with the Office of Foreign Disaster Assistance of the Agency for International Development.

M.M.M.

N79-33379* National Aeronautics and Space Administration, Lewis Research Center, Cleveland, Ohio.

CARRIER INTERFERENCE RATIOS FOR FREQUENCY SHARING BETWEEN SATELLITE SYSTEMS TRANSMITTING FREQUENCY MODULATED AND DIGITAL TELEVISION SIGNALS

Scott P. Barnes 1979 8 p. refs. To be presented at the Natl. Telecommun. Conf., Washington, D. C., 26-28 Nov. 1979, sponsored by IEEE.

(NASA-TM-79265, E-180) Avail. NTIS HC A02/MF A01 CSCL 17B

Results are presented of subjective and quantitative tests describing the results of interference to a particular digital television system from a frequency modulated (FMT) television

system, and for interference to an FM television system from a digital television system. M M M

A79-14948 * # 20/30 GHz satellite systems technology needs assessment. G. Stevens and D. Wright (NASA, Lewis Research Center, Cleveland, Ohio). *Instrument Society of America, International Telemetry Conference, Los Angeles, Calif., Nov. 14-16, 1978, Paper. 12 p. 8 refs.*

The paper surveys the system and market work done at NASA-Lewis with regard to exploring the potential of the 20/30 GHz bands for domestic satellite communications. The 20/30 GHz bands appear attractive economically and, with certain technology advances, appear to offer a virtually unlimited spectrum resource. This attractiveness is especially relevant to high density trunking where there is sufficient traffic to justify dual station site diversity. Ongoing system and market studies actively involve satellite system suppliers and carriers as well as the government in a cooperative, mutually beneficial effort. It is considered that this is the approach most likely to result in a spectrum-efficient acceptable-risk high-capacity 30/30 GHz satellite system which is relevant to anticipated markets. B.J.

A79-27397 * # Determining potential 30/20 GHz domestic satellite system concepts and establishment of a suitable experimental configuration. G. H. Stevens and G. Anzic (NASA, Lewis Research Center, Cleveland, Ohio). *International Telecommunication Exposition, Dallas, Tex., Feb. 26-Mar. 2, 1979, Paper. 19 p. 6 refs.*

Issues and results in a NASA study of the potential concepts and markets for a multibeam 30/20 GHz domestic satellite system in the 1990s are presented. Issues considered include the reduction of signal attenuation due to rain, beam-beam interference isolation in the multibeam system, the method of access/modulation (FDMA, TDMA or hybrid) and the market for reduced reliability and wideband services. A hypothetical demonstration payload configuration which would attempt to resolve these issues is illustrated. The communications payload would employ a system of seven contiguous coverage spots in order to demonstrate a typical cell in a contiguous beam system having extensive frequency reuse, as in a direct-to-user system, and a single spot, typical of a trunking system, to determine signal isolation. The payload could be carried on several existing buses and is illustrated on an MMS bus. A.L.W.

A79-27398 * # Telecommunication service markets through the year 2000 in relation to millimeter wave satellite systems. S. M. Stevenson (NASA, Lewis Research Center, Cleveland, Ohio). *International Telecommunication Exposition, Dallas, Tex., Feb. 26-Mar. 2, 1979, Paper. 12 p.*

NASA is currently conducting a series of millimeter wave satellite system and market studies to develop 30/20 GHz satellite system concepts that have commercial potential for the period 1980-2000. The results of the market studies to-date focusing on the overall demand forecasts and distributions by geographic location, distance, and user category are discussed. Tables are presented indicating baseline market forecast voice and video services, data service category, impacted baseline forecast, and traffic/distance distribution voice services. It is concluded that the total market and system activity will be influential in determining the potential role of millimeter wave systems in the overall transmission needs of the nation, and the amount of the total forecasted traffic suitable for millimeter wave systems. A.A.

A79-29784 * Millimeter wave communication satellite concepts. L. D. Holland, N. B. Hilsen, R. W. Wallace (Georgia Institute of Technology, Atlanta, Ga.), and G. Stevens (NASA, Lewis Research Center, Cleveland, Ohio). In: *Canadian Communications and Power Conference, Montreal, Canada, October 18-20, 1978, Proceedings. (A79-29776 11 32)* New York, Institute of Electrical and Electronics Engineers, Inc., 1978, p. 93-95. 5 refs. Contract No.

NAS3-20110.

Methodology has been developed for identifying viable and appropriate technologies for future NASA millimeter wave research as based upon the technical requirements of potential space communication services. Applicability of the methodology has been verified through its use with two conceptual communications systems. The subsystem cost and weight models are the appropriate level of detail for this study. Application of the methodology to the detailed design of a satellite system would require further model refinement. B.J.

A79-30394 * # Global disaster satellite communications system for disaster assessment and relief coordination. B. E. LeRoy (NASA, Lewis Research Center, Cleveland, Ohio). *International Telecommunication Exposition, Dallas, Tex., Feb. 26-Mar. 2, 1979, Paper. 10 p. 6 refs.*

Global communication requirements for disaster assistance are analyzed in the light of operationally feasible satellite system concepts and associated system parameters. Present and planned commercially available systems are considered, together with an assessment of the associated global disaster communication yearly service costs. It is concluded that a likely number of transportable terminals required for long distance relief communications activities would be less than 10, with the transportation costs not expected to exceed 25% of the annual systems' cost. Consequently, no sound economic justification is seen for ground terminal development for the global disaster communications system. A.A.

A79-30395 * # Results of thin-route satellite communication system analyses including estimated service costs. D. L. Wright (NASA, Lewis Research Center, Cleveland, Ohio). *International Telecommunications Exposition, Dallas, Tex., Feb. 26-Mar. 2, 1979, Paper. 10 p. Contract No. NAS3-20364.*

Ways for determining optimum satellite and terrestrial system architectures and parameters for providing the most economical telephone service to remote areas of the U.S. are explored. Several configurations for an isolated rural telephone system, covering all the states plus Alaska, employing satellites is considered. Both direct-to-the user and community-type of systems are evaluated using UHF and Ku-band RF equipment for the rural/satellite links. The effect of multiple spot beams, outage, signal quality, modulation method, satellite accessing, forward error correction, and the number of users are also evaluated. The total cost for a 5-minute call from an isolated rural user to a TELCO user was shown to be as low as \$1.30 for a system with 1.8 X 10 to the sixth rural users. A.A.

N79-12273*# Fairchild Space and Electronics Co. Germantown, Md.

COMMUNICATIONS SYSTEMS TECHNOLOGY ASSESSMENT STUDY. VOLUME 2: RESULTS Final Report

R. L. Kelley, R. K. Khatri, J. D. Kiesling, and J. A. Weiss. Oct 1977. 352 p.

(Contract NAS3-20364)

(NASA-CR 135224) Avail. NTIS HC A16/MF A01 CSCL 17B

The cost and technology characteristics are examined for providing special satellite services at UHF, 2.5 GHz, and 14/12 GHz. Considered are primarily health, educational, informational and emergency disaster type services. The total cost of each configuration including space segment, earth station, installation operation and maintenance was optimized to reduce the user's total annual cost and establish preferred equipment performance parameters. Technology expected to be available between now and 1985 is identified and comparisons made between selected alternatives. A key element of the study is a survey of earth station equipment updating past work in the field, providing new insight into technology, and evaluating production and test methods that can reduce costs in large production runs. Various satellite configurations were examined. The cost impact of rain attenuation at Ku band was evaluated. The factors affecting the

ultimate capacity achievable with the available orbital arc and available bandwidth were analyzed. G G

N79-17071* Dayton Univ. Research Inst., Ohio.
A CROSS IMPACT METHODOLOGY FOR THE ASSESSMENT OF US TELECOMMUNICATIONS SYSTEM WITH APPLICATION TO FIBER OPTICS DEVELOPMENT: EXECUTIVE SUMMARY Final Report

Joseph P. Martino, Ralph C. Lenz, Jr., and Kuei-Lin Chen. Jan. 1979. 36 p.
(Contract NAS3-20365)
(NASA-CR-135209, UDR-TR-79-17) Avail. NTIS HC A03/MF A01 CSCL 17B

A cross impact model of the U.S. telecommunications system was developed. For this model, it was necessary to prepare forecasts of the major segments of the telecommunications system, such as satellites, telephone, TV, CATV, radio broadcasting, etc. In addition, forecasts were prepared of the traffic generated by a variety of new or expanded services, such as electronic check clearing and point of sale electronic funds transfer. Finally, the interactions among the forecasts were estimated (the cross impacts). Both the forecasts and the cross impacts were used as inputs to the cross impact model, which could then be used to stimulate the future growth of the entire U.S. telecommunications system. By varying the inputs, technology changes or policy decisions with regard to any segment of the system could be evaluated in the context of the remainder of the system. To illustrate the operation of the model, a specific study was made of the deployment of fiber optics, through the telecommunications system. Author

N79-18159* Dayton Univ. Research Inst., Ohio.
A CROSS IMPACT METHODOLOGY FOR THE ASSESSMENT OF US TELECOMMUNICATIONS SYSTEM WITH APPLICATION TO FIBER OPTICS DEVELOPMENT, VOLUME 1 Final Report

Joseph P. Martino, Ralph C. Lenz, Jr., Kuei-Lin Chen, Peter Kahut, Robert Sekely, and John Weiler. Jan. 1979. 220 p.
(Contract NAS3-20365)
(NASA-CR-159511, UDR-TR-79-18-Vol-1) Avail. NTIS HC A10/MF A01 CSCL 17B

A cross impact model of the U.S. telecommunications system was developed. It was necessary to prepare forecasts of the major segments of the telecommunications system, such as satellites, telephone, TV, CATV, radio broadcasting, etc. In addition, forecasts were prepared of the traffic generated by a variety of new or expanded services, such as electronic check clearing and point of sale electronic funds transfer. Finally, the interactions among the forecasts were estimated (the cross impact). Both the forecasts and the cross impacts were used as inputs to the cross impact model, which could then be used to stimulate the future growth of the entire U.S. telecommunications system. By varying the inputs, technology changes or policy decisions with regard to any segment of the system could be evaluated in the context of the remainder of the system. To illustrate the operation of the model, a specific study was made of the deployment of fiber optics throughout the telecommunications system. Author

N79-18160* Dayton Univ. Research Inst., Ohio.
A CROSS IMPACT METHODOLOGY FOR THE ASSESSMENT OF US TELECOMMUNICATIONS SYSTEM WITH APPLICATION TO FIBER OPTICS DEVELOPMENT, VOLUME 2 Final Report

Joseph P. Martino, Ralph C. Lenz, Jr., Kuei-Lin Chen, Peter Kahut, Robert Sekely, and John Weiler. Jan. 1979. 258 p. refs.
(Contract NAS3-20365)
(NASA-CR-159511, UDR-TR-79-19-Vol-2) Avail. NTIS HC A12/MF A01 CSCL 17B

The appendices for the cross impact methodology are presented. These include: user's guide, telecommunication events, cross impacts, projection of historical trends, and projection of trends in satellite communications. F O S

N79-33373* Hughes Aircraft Co., Los Angeles, Calif. Space and Communications Group.

THE 18 AND 30 GHz FIXED SERVICE COMMUNICATIONS SATELLITE SYSTEM STUDY: EXECUTIVE SUMMARY Final Report

Leonard M. Bronstein. Sep. 1979. 11 p.
(Contract NAS3-21367)
(NASA-CR-159627-1, HAC-REF-E1992-1, SCG-90275R) Avail. NTIS HC A02/MF A01 CSCL 17B

The use of the 18 and 30 GHz bands for fixed service satellite communications is examined. Primary objectives were to determine if satellite communication systems using this allocation (27.5 to 30.0 GHz uplink; 17.7 to 20.2 GHz downlink) can be cost competitive with alternate means of communication, and to determine what technological developments would be required to make these systems competitive. To meet these objectives, the cost and performance to be expected of 18 and 30 GHz hardware in the 1985 to 1990 era was assessed, selected trunking and direct to user concepts were optimized, and the cost of these systems was estimated. Finally, the technology developments required to make the most promising of the concepts competitive were identified. M M M.

N79-33374* Hughes Aircraft Co., Los Angeles, Calif. Space and Communications Group.

THE 18 AND 30 GHz FIXED SERVICE COMMUNICATIONS SATELLITE SYSTEM STUDY Final Report

Leonard M. Bronstein. Sep. 1979. 297 p. refs.
(Contract NAS3-21367)
(NASA-CR-159627-2, HAC-REF-E1992-2, SCG-90272R) Avail. NTIS HC A13/MF A01 CSCL 17B

The use of the 18 and 30 GHz bands for fixed service satellite communications is examined. The cost and performance expected of 18 and 30 GHz hardware is assessed, selected trunking and direct to user concepts are optimized, and the cost of these systems are estimated. The effect of rain attenuation on the technical and economic viability of the system and methods circumventing the problem are discussed. Technology developments are investigated and cost estimates of these developments are presented. A W H.

A79-33793 * On the distribution of computation for sequential decoding using the stack algorithm. R. Johannesson (Lund, Universitet, Lund, Sweden). *IEEE Transactions on Information Theory*, vol. IT-25, May 1979, p. 323-331. 18 refs. Research supported by the American-Swedish Foundation and L. M. Ericsson Telephone Co., Grant No. NGL 5025.

A method is developed for estimating the computational distribution for the stack algorithm for sequential decoding, that is, the probability that the computation required to decode the first branch of the tree is greater than or equal to N, for small N. The analysis relies heavily on the theory of multitype branching processes. A step in the analysis is the determination of the distribution of the minimum of the cumulative metrics along the transmitted path in the code tree. This is used to obtain the distribution of the number of computations made by the decoder in order to decode the first branch in the tree, and this random variable serves as an approximation of the average number of computations per decoded branch. At information rates below the cutoff rate, the calculated computational performance is virtually identical to that obtained by time-consuming simulations. P T H.

33 ELECTRONICS AND ELECTRICAL ENGINEERING

Includes test equipment and maintainability, components, e.g., tunnel diodes and transistors, microminiaturization, and integrated circuitry.

For related information see also 60 *Computer Operations and Hardware* and 76 *Solid-State Physics*.

N79-14309* National Aeronautics and Space Administration, Lewis Research Center, Cleveland, Ohio.

SPACE SHUTTLE ACTIVE-POGO-SUPPRESSOR CONTROL DESIGN USING LINEAR QUADRATIC REGULATOR TECHNIQUES

Bruce Lehtinen and Carl F. Lorenz. Jan. 1979. 83 p. refs. (NASA-TP-1217, E-9578) Avail. NTIS HC A05/MF A01 CSCL 09C

Two methods of active pogo suppression (stabilization) for the space shuttle vehicle were studied analytically. The basis for both approaches was the linear quadratic regulator, state space technique. The first approach minimized root-mean-square pump inlet pressure by using either full-state feedback, partial-state feedback, or output feedback with a Kalman filter. The second approach increased the modal damping associated with the critical structural modes by using either full-state feedback or reconstructed state feedback. A number of implementable controls were found by both approaches. The designs were analyzed with respect to sensitivity, complexity, and controller energy requirements, as well as controller performance. Practical controllers resulting from the two design approaches tended to use pressure and flow as feedback variables for the minimum-rms method and structural accelerations or velocities for the modal control method. Both approaches are suitable for the design of active pogo-suppression controllers. Author

N79-17139* National Aeronautics and Space Administration, Lewis Research Center, Cleveland, Ohio.

EFFICIENCY ENHANCEMENT OF OCTAVE-BANDWIDTH TRAVELING WAVE TUBES BY USE OF MULTISTAGE DEPRESSED COLLECTORS

Peter Ramins and Thomas A. Fox. Feb. 1979. 29 p. refs. (NASA-TP-1416, E-9749) Avail. NTIS HC A03/MF A01 CSCL 09A

Small, three- and five-stage depressed collectors were evaluated in conjunction with a 4.8- to 9.6-GHz TWT of 325- to 675-W power output and a beam of 0.5 microperv. The multistage depressed collector (MDC) performed well even though its design had been optimized for a TWT of identical design but considerably less output power. Despite large, fixed losses, significant efficiency enhancement was demonstrated with both the three- and five-stage depressed collectors. At saturated rf power output, the improvement in the overall efficiency ranged from a factor of 2.5 to 3.0 for the three-stage collector and a factor of 3.0 to 3.5 for the five-stage collector. At saturation, three-stage collector efficiencies of 77 to 80 percent and five-stage collector efficiencies of 81 to 84 percent were obtained across the frequency band. An overall efficiency of 37.0 to 44.3 percent across the frequency band of 4.8 to 9.6 GHz was demonstrated with the use of harmonic injection. For operation below saturation, even larger relative improvements in the overall TWT efficiency were demonstrated. Collector performance was relatively insensitive to the degree of regulation of the collector power supply. LS

N79-20316* National Aeronautics and Space Administration, Lewis Research Center, Cleveland, Ohio.

TWT DESIGN REQUIREMENTS FOR 30/20 GHz DIGITAL COMMUNICATIONS SATELLITE

N. Stankiewicz and G. Anzic. 1979. 13 p. Presented at the 17th Aerospace Sci. Meeting, New Orleans, 15-17 Jan. 1979, sponsored by AIAA. (NASA-TM-79119, E-9952) Avail. NTIS HC A02/MF A01 CSCL 09A

The rapid growth of communication traffic (voice, data, and video) requires the development of additional frequency bands before the 1990's. The frequencies currently in use for satellite communications at 6/4 GHz are crowded and demands for 14/12 GHz systems are increasing. Projections are that these bands will be filled to capacity by the late 1980's. The next higher frequency band allocated for satellite communications is at 30/20 GHz. For interrelated reasons of efficiency, power level, and system reliability criteria, a candidate for the downlink amplifier in a 30/20 GHz communications satellite is a dual mode traveling wave tube (TWT) equipped with a highly efficient depressed collector. A summary is given of the analyses which determine the TWT design requirements. The overall efficiency of such a tube is then inferred from a parametric study and from experimental data on multistaged depressed collectors. The expected TWT efficiency at 4 dB below output saturation is 24 percent in the high mode and 22 percent in the low mode. LS

N79-22375* National Aeronautics and Space Administration, Lewis Research Center, Cleveland, Ohio.

ANALYTICAL PREDICTION WITH MULTIDIMENSIONAL COMPUTER PROGRAMS AND EXPERIMENTAL VERIFICATION OF THE PERFORMANCE, AT A VARIETY OF OPERATING CONDITIONS, OF TWO TRAVELING WAVE TUBES WITH DEPRESSED COLLECTORS

James A. Dayton, Jr., Henry G. Kosmahl, Peter Ramins, and Norbert Stankiewicz. May 1979. 28 p. refs. (NASA-TP-1449, E-9728) Avail. NTIS HC A03/MF A01 CSCL 09A

Experimental and analytical results are compared for two high performance, octave bandwidth TWTs that use depressed collectors (MDCs) to improve the efficiency. The computations were carried out with advanced, multidimensional computer programs that are described here in detail. These programs model the electron beam as a series of either disks or rings of charge and follow their multidimensional trajectories from the RF input of the ideal TWT, through the slow wave structure, through the magnetic refocusing system, to their points of impact in the depressed collector. Traveling wave tube performance, collector efficiency, and collector current distribution were computed and the results compared with measurements for a number of TWT-MDC systems. Power conservation and correct accounting of TWT and collector losses were observed. For the TWTs operating at saturation, very good agreement was obtained between the computed and measured collector efficiencies. For a TWT operating 3 and 6 dB below saturation, excellent agreement between computed and measured collector efficiencies was obtained in some cases but only fair agreement in others. However, deviations can largely be explained by small differences in the computed and actual spent beam energy distributions. The analytical tools used here appear to be sufficiently refined to design efficient collectors for this class of TWT. However, for maximum efficiency, some experimental optimization (e.g., collector voltages and aperture sizes) will most likely be required. Author

N79-23348* National Aeronautics and Space Administration, Lewis Research Center, Cleveland, Ohio.

DESCRIPTION OF A 2.3 kW POWER TRANSFORMER FOR SPACE APPLICATIONS

Irving Hansen. 1979. 12 p. refs. Presented at the Aerospace High Voltage Workshop, Anaheim, Calif., 26-27 Feb. 1979, sponsored in part by Intern. Electron. Packaging Soc., Aerospace Electron. Systems Soc., and IEEE. (NASA-TM-79138, E-9976) Avail. NTIS HC A02/MF A01 CSCL 09C

The principle features and special testing of a high voltage high power transformer designed and developed for space application are described. The transformer is operated in a series resonant inverter supplying beam power to a 30 cm mercury ion thruster. Electrical requirements include operation of 2.3 kV/continuous power output, primary currents to 35 amps rms, and frequencies up to 20 kHz. High efficiency was obtained through detailed considerations of the tradeoffs available in core materials, wire selection, coil configurations and thermal control. A number of novel heat removal techniques are discussed which

control the winding temperature using only the available
conductive cooling L.S.

N79-26316* National Aeronautics and Space Administration
Lewis Research Center, Cleveland, Ohio
**PERFORMANCE OF A 14.9-kW LAMINATED-FRAME dc
SERIES MOTOR WITH CHOPPER CONTROLLER**

John R. Schwaib Jun 1979 41 p refs Prepared for DOE
(Contract EC-77 A-31-1044)
(NASA-TM-79177; DOE/NASA/1044-79/2) Avail NTIS
HC A03/MF A01 CSCL 09A

Traction motor using two types of excitation: ripple free dc
from a motor generator set for baseline data and chopped dc
as supplied by a battery and chopper controller was tested. For
the same average values of input voltage and current, the power
output was independent of the type of excitation. At the same
speeds, motor efficiency at low power output (corresponding to
low duty cycle of the controller) was 5 to 10 percentage points
less on chopped dc than on ripple-free dc. This illustrates that
for chopped waveforms, it is incorrect to calculate input power
as the product of average voltage and average current. Locked-
rotor torque, no load losses, and magnetic saturation data were
so determined. S.E.S.

N79-27400* National Aeronautics and Space Administration
Lewis Research Center, Cleveland, Ohio

**DESIGN OF HIGH-PERFORMANCE CONFINED-FLOW GUNS
FOR PERIODIC PERMANENT-MAGNET-FOCUSED TUBES**
N. Stankiewicz Jun 1979 17 p refs
(NASA-TP-1485; E-9729) Avail NTIS HC A02/MF A01 CSCL
09C

An approach to the design of high perveance, low compression
guns is described in which confinement is used to stabilize the
beam for subsequent periodic permanent-magnet focusing. The
computed results for two cases are presented. A magnetic
boundary value problem was solved for the scalar potential from
which the axial magnetic field was computed. A solution was
found by iterating between Poisson's equation and the electron
trajectory calculations. Magnetic field values were varied in
magnitude until a laminar beam with minimum scalloping was
produced. R.E.S.

N79-28420* National Aeronautics and Space Administration
Lewis Research Center, Cleveland, Ohio

**EFFICIENCY ENHANCEMENT OF DUAL-MODE TRAVELING
WAVE TUBES AT SATURATION AND IN THE LINEAR
RANGE BY USE OF SPENT-BEAM REFocusing AND
MULTISTAGE DEPRESSED COLLECTORS**

Peter Ramins and Thomas A. Fox Jul 1979 26 p refs
(NASA-TP-1486; E-9912) Avail NTIS HC A03/MF A01 CSCL
09C

An axisymmetric, multistage depressed collector of fixed
geometric design was evaluated in conjunction with an octave-
bandwidth, dual-mode TWT. The TWT was operated over a wide
range of conditions to simulate different applications. The collector
was operated in three-, four-, and five-stage configurations, and
its performance was optimized (within the constraint of fixed
geometric design) over the range of TWT operating conditions
covered. For operation of the dual-mode TWT at and near
saturation, the collectors increased the TWT overall efficiency
by a factor of 2 1/2 to 3 1/2. Collector performance was
relatively constant for both the high and low TWT modes and
for operation of the TWT across an octave bandwidth. For operation
of the TWT in the linear, low-distortion range, collector ef-
ficiencies of 90 percent and greater were obtained, leading to a
five- to twelvefold increase in the TWT overall efficiency for the
range of operating conditions covered and reasonably high (greater
than 25 percent) overall efficiencies well below saturation.

Author

N79-31499* National Aeronautics and Space Administration
Lewis Research Center, Cleveland, Ohio

**ANALYTICAL CORE LOSS CALCULATIONS FOR MAGNETIC
MATERIALS USED IN HIGH-FREQUENCY HIGH-POWER
CONVERTER APPLICATIONS** Ph.D. Thesis - Toledo Univ.
James E. Triner Aug 1979 103 p refs
(NASA-TM-79234; E-9993) Avail NTIS HC A06/MF A01
CSCL 09A

The basic magnetic properties under various operating
conditions encountered in the state-of-the-art DC-AC/DC
converters are examined. Using a novel core excitation circuit,
the basic B-H and loss characteristics of various core materials
may be observed as a function of circuit configuration, frequency
of operation, input voltage, and pulse-width modulation conditions.
From this empirical data, a mathematical loss characteristics
equation is developed to analytically predict the specific core
loss of several magnetic materials under various waveform
excitation conditions. G.Y.

N79-32463* National Aeronautics and Space Administration
Lewis Research Center, Cleveland, Ohio

**MULTISTAGE DEPRESSED COLLECTOR FOR DUAL-MODE
OPERATION** Patent Application

H. G. Kosmahl, inventor (to NASA) Filed 7 Sep 1979 14 p
(NASA-Case-LFW 13282-1; US Patent Appl-SN-073579) Avail:
NTIS HC A02/MF A01 CSCL 09C

A depressed collector which captures the spent electrons of
a microwave transmitting tube at high efficiency in both high
and low power modes of operation is provided. The end electrode
has a spike extending toward the entrance electrode. Intermediate
electrodes and the entrance electrode have central apertures
increasing in size in a downstream direction. These electrodes
capture most high power mode spent electrons. A low power
mode electrode is positioned between the last intermediate
electrode and the end electrode to capture low power spent
electrons. This electrode has a central aperture preferably smaller
but no larger than that of the last intermediate electrode. An
auxiliary low power mode electrode with a central aperture larger
than that of the low power mode electrode may be axially
positioned between the end electrode and the low power mode
electrode. The electrodes are all at voltages provided by a voltage
divider connected between a negative potential and a common
ground return. NASA

N79-32467* National Aeronautics and Space Administration
Lewis Research Center, Cleveland, Ohio

**OPTICALLY ISOLATED LOGARITHMIC MICROAMMETER
CAPABLE OF FLOATING TO 5 KILOVOLTS**

John C. Sturman and John C. DeLaat Washington Oct 1979
22 p refs
(NASA-TP-1527; E-9934) Avail NTIS HC A02/MF A01 CSCL
09C

A logarithmic current-measuring instrument was developed
to measure plasma coupling currents at a common mode voltage
of 5 kilovolts. Positive or negative currents can be measured
from 10 to the -9th power to 0.01 ampere direct current. Optical
isolation is used to control input switching and to provide data
referenced to ground potential. Analog meter readouts as well
as zero to five volt outputs are provided for peripheral data
collection. Six independent channels are provided. Three measure
positive currents, and three measure negative currents. Although
designed for vacuum operation, it can be used equally well in
air to measure low currents at high common mode voltages.

K.L.

A79-15305* Design study of superconducting magnets for a
combustion magnetohydrodynamic (MHD) generator. R. J. Thome,
J. W. Ayers, T. M. Hryciak (Magnetic Corporation of America,
Waltham, Mass.), and J. A. Burkhardt (NASA, Lewis Research Center,
Cleveland, Ohio). In: Advances in cryogenic engineering, Volume 23.
Proceedings of the Conference, Boulder, Colo., August 2-5, 1977.
(A79-15301-04-31) New York: Plenum Press, 1978, p. 28-36.
Contract No. NAS3-19865.

Results are presented for a trade-off and preliminary design
study on concepts of a superconducting magnet system for a

combustion MHD generator test facility. The main objective is to gain insight into the magnitude of the project in terms of physical characteristics and cost. The net result of a first-phase evaluation of attractive design alternatives is to concentrate subsequent efforts on (1) a racetrack coil geometry with an operating temperature of 4.2 K, (2) a racetrack coil geometry with an operating temperature of 2.0 K, and (3) a rectangular saddle coil geometry with an operating temperature of 4.2 K. All three systems are to produce 8 T, and use NbTi superconductor and iron for field enhancement. Design characteristics of the three systems are described. It is shown that the racetrack and rectangular saddle coil geometries seem most suitable for this application, the former because of its simplicity and the latter because of its efficient use of material. Advantages of the rectangular saddle over the two other systems are stressed. S.D.

A79-10881 * Generalized computer-aided discrete time domain modeling and analysis of dc-dc converters. F. C. Lee, R. P. Iwens, Y. Yu (TRW Defense and Space Systems Group, Redondo Beach, Calif.), and J. E. Triner (NASA, Lewis Research Center, Cleveland, Ohio). In: Power Electronics Specialists Conference, Palo Alto, Calif., June 14-16, 1977, Record. (A79 10876 01 33) New York, Institute of Electrical and Electronics Engineers, Inc., 1977, p. 58-69. 13 refs. Contract No. NAS3-19690.

A generalized discrete time domain modeling and analysis technique is presented for all types of switching regulators using any type of duty-cycle controller, and operating in both continuous and discontinuous inductor current. State space techniques are employed to derive an equivalent nonlinear discrete time model that describes the converter exactly. The system is linearized about its equilibrium state to obtain a linear discrete time model for small signal performance evaluations, such as stability, audiosusceptibility and transient response. The analysis makes extensive use of the digital computer as an analytical tool. It is universal, exact and easy to use. (Author)

A79-10885 * Power converter design optimization. Y. Yu, F. C. Y. Lee (TRW Defense and Space Systems Group, Redondo Beach, Calif.), and J. E. Triner (NASA, Lewis Research Center, Cleveland, Ohio). In: Power Electronics Specialists Conference, Palo Alto, Calif., June 14-16, 1977, Record. (A79 10876 01 33) New York, Institute of Electrical and Electronics Engineers, Inc., 1977, p. 104-112. 11 refs. Contract No. NAS3-19690.

Utilizing the demonstrated capability of nonlinear programming algorithms, a practical design optimization approach for power converters is established to conceive a design to meet all power-converter performance requirements and concurrently optimize a defined quantity such as weight or losses. In addition, to facilitate a cost-effective design, the computer-aided approach provides a means to readily assess (1) the weight-efficiency tradeoff, (2) impacts of converter requirements and component characteristics on a given design, and (3) optimum power system configurations. (Author)

A79-10896 * The solid state remote power controller - Its status, use and perspective. G. R. Sundberg (NASA, Lewis Research Center, Cleveland, Ohio) and W. W. Billings (Westinghouse Electric Corp., Aerospace Electrical Div., Lima, Ohio). In: Power Electronics Specialists Conference, Palo Alto, Calif., June 14-16, 1977, Record. (A79 10876 01 33) New York, Institute of Electrical and Electronics Engineers, Inc., 1977, p. 244-253. 16 refs.

Remote power controllers (RPCs) are solid state devices that combine in one unit the capability to perform all the needed functions of load switching, overload protection, and a direct indication of whether the load is on or off. They provide total system protection of equipment and wires. RPCs are designed to be located near the load and communicate control and status information remotely via low level signals of a few milliwatts. The design and operation of the RPC are considered, taking into account the operation of an RPC, the RPC power switch and drive circuits, control and trip circuits, fail-safe devices, and RPC overcurrent

protection. Attention is given to the RPC development status, RPC applications, and RPC perspectives. G.R.

A79-25116 * Comments on measuring the overall and the depressed collector efficiency in TWT's and klystron amplifiers. H. G. Kosmahl (NASA, Lewis Research Center, Cleveland, Ohio). *IEEE Transactions on Electron Devices*, vol. ED-26, Feb. 1979, p. 156.

Kosmahl and Ramins (1977), who reported results achieved with broadband, high-performance TWT's, augmented with multi-stage depressed collectors for higher overall efficiency, have pointed out the necessity for accurately measuring and correctly defining the various power terms involved. In view of the now wide-spread use of depressed collectors and reported results, the definitions of tube and collector efficiency are restated and comments are provided on the sensitivity of these terms to various sources of experimental and definitional errors in order to permit a uniform evaluation of collector performance. G.R.

A79-34001 * Description of A 2.3 kW power transformer for space applications. I. Hansen (NASA, Lewis Research Center, Cleveland, Ohio). *International Electronics Packaging Society Aerospace Electronic Systems Society, and IEEE, Aerospace High Voltage Workshop, Anaheim, Calif., Feb. 26, 27, 1979, Paper*. 10 p.

The paper describes the principal features and special testing of a high-frequency high-power low-specific-weight (0.57 kg/kW) 2.3-kW electronic power transformer developed for space applications. The transformer is operated in a series resonant inverter supplying beam power to a 30-cm mercury ion thruster. High efficiency (above 98.5%) is obtained through careful detailed design. A number of unique heat removal techniques are discussed which control the winding temperature using only the available conductive cooling. S.D.

A79-42024 * Comment on the mechanism of operation of the impregnated tungsten cathode. R. Forman (NASA, Lewis Research Center, Cleveland, Ohio). *Journal of Applied Physics*, vol. 50, Mar. 1979, p. 1546, 1547. 9 refs.

Recent life-test measurements, over 20,000-30,000 h, on impregnated tungsten cathodes in tubes employing an open-type electron-gun structure, show emission current degradation with time. This is in contrast to those recently published by Rittner on B-type cathodes, run in close-spaced diodes, taken some years ago. These more recent life-test results are consistent with the model suggested by Forman and disputed by Rittner that the barium coverage on an impregnated cathode is less than a monolayer for most of its life and decreases with time. (Author)

A79-49526 * Fundamental mechanisms that influence the estimate of heat transfer to gas turbine blades. R. W. Graham (NASA, Lewis Research Center, Fundamental Heat Transfer Section, Cleveland, Ohio). *American Society of Mechanical Engineers and American Institute of Chemical Engineers, National Heat Transfer Conference, San Diego, Calif., Aug. 5-8, 1979, Paper*. 11 p. 32 refs.

Heat transfer problems in aircraft gas turbines required for improved prediction of turbine blade or vane gas side heat transfer are examined. Estimates of the heat transfer from the gas to vanes or rotating blades are uncertain due to the complexity of the heat transfer processes, since the gas flow is three dimensional with complex secondary viscous flow patterns that interact with the endwalls and blade surfaces. In addition, upstream disturbances, stagnation flow, curvature effects, and flow acceleration complicate the thermal transport mechanisms in the boundary layers. The thermal state and flow characteristics of the hot gases that enter the turbine blade row, analytical methods for calculating the gas side heat transfer to turbine blades, and flow phenomena such as stagnation, curvature effects, acceleration, secondary flows, and transition that influences local heat transfer rates are discussed. A T

A79-49535 * # Condensation on a noncollapsing vapor bubble in a subcooled liquid. K. J. Baumeister and R. J. Simoneau (NASA, Lewis Research Center, Cleveland, Ohio). *National Heat Transfer Conference, 18th, San Diego, Calif., Aug. 5-8, 1979, Paper.* 15 p. 13 refs.

An experimental procedure is presented by which an estimate can be made of the condensation coefficient on a noncollapsing stationary vapor bubble in subcooled liquid nitrogen. The present experimental study utilizes film boiling from a thin wire to generate vapor bubbles which remain fixed to the wire at their base. A balance was established between the evaporation in the thin annular region along the wire and the condensation in the vapor bubbles. (Author)

N79-14325* # Textron Bell Aerospace Co., Buffalo, N. Y.
A THREE-DIMENSIONAL TURBULENT COMPRESSIBLE FLOW MODEL FOR EJECTOR AND FLUTED MIXERS
W. L. Rushmore and S. W. Zelazny Dec. 1978 133 p refs
Sponsored by NASA
(NASA-CR-159467) Avail. NTIS HC A07/MF A01 CSCL 20D

A three dimensional finite element computer code was developed to analyze ejector and axisymmetric fluted mixer systems whose flow fields are not significantly influenced by streamwise diffusion effects. A two equation turbulence model was used to make comparisons between theory and data for various flow fields which are components of the ejector system, i.e., (1) turbulent boundary layer in a duct; (2) rectangular nozzle (free jet); (3) axisymmetric nozzle (free jet); (4) hypermixing nozzle (free jet); and (5) plane wall jet. Likewise, comparisons of the code with analytical results and/or other numerical solutions were made for components of the axisymmetric fluted mixer system. These included: (1) developing pipe flow; (2) developing flow in an annular pipe; (3) developing flow in an axisymmetric pipe with conical center body and no fluting and (4) developing fluted pipe flow. Finally, two demonstration cases are presented which show the code's ability to analyze both the ejector and axisymmetric fluted mixers. Author

N79-20317* # Hughes Aircraft Co., Culver City, Calif. Technology Support Div
LIGHTWEIGHT MULTIPLE OUTPUT CONVERTER DEVELOPMENT
Jack J. Kisch and R. M. Martinelli Dec. 1978 75 p refs
(Contract NAS3-21045)
(NASA-CR-159526) P78-683R) Avail. NTIS
HC A04/MF A01 CSCL 09C

A high frequency, multiple output power conditioner was developed and breadboarded using an eight-stage capacitor diode voltage multiplier to provide +1200 Vdc and a three-stage for -350 Vdc. In addition, two rectifier bridges were capacitively coupled to the eight-stage multiplier to obtain 0.5 and 0.65 a dc constant current outputs referenced to +1200 Vdc. Total power was 120 watts with an overall efficiency of 85 percent at the 80 kHz operating frequency. All outputs were regulated to three percent or better, with complete short circuit protection. The power conditioner component weight and efficiency were compared to the equivalent four outputs of the 10 kHz conditioner for the Bion engine. Weight reduction for the four outputs was 557 grams, extrapolated in the same ratio to all nine outputs, it would be 1100 to 1400 grams. Author

N79-21273* # Westinghouse Research and Development Center, Pittsburgh, Pa.
DEVELOPMENT AND FABRICATION OF IMPROVED POWER TRANSISTOR SWITCHES Final Report
P. L. Hower and C. K. Chu Jan. 1979 86 p refs
(Contract NAS3-18916)
(NASA-CR-159524) Avail. NTIS HC A05/MF A01 CSCL 09A

A new class of high voltage power transistors was achieved by adapting present interdigitated thyristor processing techniques to the fabrication of npn Si transistors. Present devices are 2.3 cm in diameter and have V sub CEO (sus) in the range of

400 to 600V. V sub CEO (sus) = 450V devices were made with an (h sub FEI) sub C) product of 900A at V sub CE = 2.5V. The electrical performance obtained was consistent with the predictions of an optimum design theory specifically developed for power switching transistors. The device design, wafer processing, and assembly techniques are described. Experimental measurements of the dc characteristics, forward SOA, and switching times are included. A new method of characterizing the switching performance of power transistors is proposed.

J. A. M.

N79-25312* # TRW Defense and Space Systems Group, Redondo Beach, Calif.

EFFECTS OF ARCING DUE TO SPACECRAFT CHARGING ON SPACECRAFT SURVIVAL Final Report, May - Nov. 1978

A. Rosen, N. L. Sanders, J. M. Ellen, Jr., and G. T. Inouye
14 Nov. 1978 172 p refs
(Contract NAS3-21363)
(NASA-CR-159593) TRW 33631-6006 RU-00) Avail. NTIS
HC A08/MF A01 CSCL 09C

A quantitative assessment of the hazard associated with spacecraft charging and arcing on spacecraft systems is presented. A literature survey on arc discharge thresholds and characteristics was done and gaps in the data and requirements for additional experiments were identified. Calculations of coupling of arc discharges into typical spacecraft systems were made and the susceptibility of typical spacecraft to disruption by arc discharges was investigated. Design guidelines and recommended practices to reduce or eliminate the threat of malfunction and failures due to spacecraft charging/arcing were summarized. R. E. S.

N79-27397* # Systems Science and Software, La Jolla, Calif.
EXTENSION, VALIDATION AND APPLICATION OF THE NASCAP CODE Final Report, 9 Sep. 1977 - 11 Jan. 1979
I. Katz, J. J. Cassidy, III, M. J. Mandell, G. W. Schnuelle, P. G. Steen, D. E. Parks, M. Rotenberg, and J. H. Alexander Jan. 1979 326 p refs
(Contract NAS3-21050)
(NASA-CR-159595) SSS R-79-3904) Avail. NTIS
HC A15/MF A01 CSCL 09C

Numerous extensions were made in the NASCAP code. They fall into three categories: a greater range of definable objects, a more sophisticated computational model, and simplified code structure and usage. An important validation of NASCAP was performed using a new two dimensional computer code (TWOD). An interactive code (MATCHG) was written to compare material parameter inputs with charging results. The first major application of NASCAP was performed on the SCATHA satellite. Shadowing and charging calculation were completed. NASCAP was installed at the Air Force Geophysics Laboratory, where researchers plan to use it to interpret SCATHA data. R. E. S.

N79-27398* # Systems Science and Software, La Jolla, Calif.
NASCAP USER'S MANUAL 1978 Contractor Report, Sep. 1977 - Sep. 1978
J. J. Cassidy, III Aug. 1978 257 p refs
(Contract NAS3-21050)
(NASA-CR-159417) SSS R-78-3739) Avail. NTIS
HC A12/MF A01 CSCL 09C

NASCAP simulates the charging process for a complex object in either tenuous plasma (geosynchronous orbit) or ground test (electron gun source) environment. Program control words, the structure of user input files, and various user options available are described in this computer programmer's user manual. R. E. S.

N79-28418* Science Applications, Inc., Vienna, Va. Radiation and Electromagnetics Div.

FIRST PRINCIPLES NUMERICAL MODEL OF AVALANCHE-INDUCED ARC DISCHARGES IN ELECTRON-IRRADIATED DIELECTRICS. Final Report, Jul. 1978 - Feb. 1979

B. L. Beers, V. W. Pirie, H. C. Hwang, H. W. Bloomberg, D. L. Lin, M. J. Schmidt, and D. J. Strickland. Mar. 1979. 203 p. refs.

(Contract NAS3-21378)

(NASA CR-159560, SAI-102-79-002)

Avail. NTIS

HC A10/MF A01 CSDL 09C

The model consists of four phases: single electron dynamics, single electron avalanche, negative streamer development, and tree formation. Numerical algorithms and computer code implementations are presented for the first three phases. An approach to developing a code description of fourth phase is discussed. Numerical results are presented for a crude material model of Teflon. (Author)

A79-10880 * A general unified approach to modelling switching dc-to-dc converters in discontinuous conduction mode. S. Cuk and R. D. Middlebrook (California Institute of Technology, Pasadena, Calif.). In: Power Electronics Specialists Conference, Palo Alto, Calif., June 14-16, 1977, Record. (A79-10876 01-33) New York, Institute of Electrical and Electronics Engineers, Inc., 1977, p. 36-57. 13 refs. Contracts No. NAS3-19690, No. NAS3-20102, No. MIPR-N 0095377MP09018.

A method for modelling switching converters in the discontinuous conduction mode is developed, whose starting point is the unified state-space representation, and whose end result is a complete linear circuit model which correctly represents all essential features, namely, the input, output, and transfer properties (static dc as well as dynamic ac small signal). While the method is generally applicable to any switching converter operating in the discontinuous conduction mode, it is extensively illustrated for the three common power stages (buck, boost, and buck-boost). The results for these converters are then easily tabulated owing to the fixed equivalent circuit topology of their canonical circuit model. (Author)

A79-10888 * A new optimum topology switching dc-to-dc converter. S. Cuk and R. D. Middlebrook (California Institute of Technology, Pasadena, Calif.). In: Power Electronics Specialists Conference, Palo Alto, Calif., June 14-16, 1977, Record. (A79-10876 01-33) New York, Institute of Electrical and Electronics Engineers, Inc., 1977, p. 160-179. 10 refs. Contracts No. NAS3-19690, No. NAS3-20102, No. MIPR-N 0095377MP09018.

A novel switching dc-to-dc converter is presented, which has the same general conversion property (increase or decrease of the input dc voltage) as does the conventional buck-boost converter, and which offers through its new optimum topology higher efficiency, lower output voltage ripple, reduced EMI, smaller size and weight, and excellent dynamic response. One of its most significant advantages is that both input and output current are not pulsating but are continuous (essentially dc with small superimposed switching current ripple), thus resulting in a close approximation to the ideal physically nonrealizable dc-to-dc transformer. The converter retains the simplest possible structure with the minimum number of components which, when interconnected in its optimum topology, yield the maximum performance. (Author)

A79-48653 * Input filter design for switching regulators. F. C. Lee (Virginia Polytechnic Institute and State University, Blacksburg, Va.) and Y. Yu (TRW Defense and Space Systems Group, Redondo Beach, Calif.). In: NAECON 1979, Proceedings of the National Aerospace and Electronics Conference, Dayton, Ohio, May 15-17, 1979, Volume 2. (A79-48590 21-01) New York, Institute of Electrical and Electronics Engineers, Inc., 1979, p. 704-711. 7 refs. Contract No. NAS3-20102.

A small signal average model is derived to study analytically the complex interaction among input filter, output filter and control loop, which frequently causes degradation of switch regulator

performance. Analytically based design guidelines are formulated, and key design parameters are identified. It is shown that minimization of the forward transfer characteristics and the output impedance of the input filter at filter resonance are key to designing an input filter for a switching regulator with given output filter parameters and specified line and load conditions. (Author)

A79-49397 * Analysis of a parallel-arrayed power regulating system. B. K. Colburn (Texas A & M University, College Station, Tex.), H. M. Horton (M & S Computing, Inc., Huntsville, Ala.), and M. A. Honnell (Auburn University, Auburn, Ala.). *IEEE Transactions on Industrial Electronics and Control Instrumentation*, vol. IECI-26, Aug. 1979, p. 134-141. 9 refs. Contract No. NAS8-26752.

A power regulation system incorporating n-parallel power supplies employing PWM switching regulators is studied. Analysis of individual unit operation and coupled-system parameter sensitivity is considered from an operations viewpoint. A detailed example is included to illustrate parallel system operation for 18 such units powered by solar-cell banks. (Author)

A79-49398 * Modeling of switching regulator power stages with and without zero-inductor-current dwell time. F. C. Y. Lee (Virginia Polytechnic Institute and State University, Blacksburg, Va.) and Y. Yu (TRW Defense and Space Systems Group, Redondo Beach, Calif.). *IEEE Transactions on Industrial Electronics and Control Instrumentation*, vol. IECI-26, Aug. 1979, p. 142-150. 10 refs. Contract No. NAS3-1960.

State-space techniques are employed to derive accurate models for the three basic switching converter power stages: buck, boost, and buck/boost operating with and without zero-inductor-current dwell time. A generalized procedure is developed which treats the continuous inductor-current mode without dwell time as a special case of the discontinuous-current mode when the dwell time vanishes. Abrupt changes of system behavior, including a reduction of the system order when the dwell time appears, are shown both analytically and experimentally. Merits resulting from the present modeling technique in comparison with existing modeling techniques are illustrated. (Author)

34 FLUID MECHANICS AND HEAT TRANSFER

Includes boundary layers, hydrodynamics, fluidics, mass transfer, and ablation cooling

For related information see also 02 *Aerodynamics and 77 Thermodynamics and Statistical Physics*

N79-10339* National Aeronautics and Space Administration
Lewis Research Center, Cleveland, Ohio

TRAVELING WAVE TUBE CIRCUIT Patent

Denis J. Connolly, inventor (to NASA) Issued 3 Oct 1978
4 p. Filed 15 Feb 1977 Supersedes N77-17360 (15 - 08, p 1025)

(NASA-Case-LEW-12013-1, US Patent-4,118,671)

US Patent Appl-SN-768795, US Patent Class-330-42

US Patent Class-315-35, US Patent Class-315-36

US Patent Class-301-82) Avail US Patent Office CSCL 09A

A traveling wave tube (TWT) has a slow wave structure (SWS) which is severed into two or more sections. A signal path connects the end of an SWS section to the beginning of the following SWS section. The signal path comprises an impedance matching coupler (IMC), followed by an isolator, a variable phase shifter, and a second IMC. The aggregate band pass characteristic of the components in the signal path is chosen to reject, or strongly attenuate, all frequencies outside the desired operating frequency range of the TWT and yet pass, with minimal attenuation in the forward direction, all frequencies within the desired operating frequency range. The isolator is chosen to reject, or strongly attenuate, waves, of all frequencies, which propagate in the backward direction. The aggregate phase shift characteristic of the components in the signal path is chosen to apply signal power to the beginning of the following SWS section with the phase angle yielding maximum efficiency.

Official Gazette of the U.S. Patent Office

N79-12361* National Aeronautics and Space Administration
Lewis Research Center, Cleveland, Ohio

DECAY OF HOMOGENEOUS TURBULENCE FROM A GIVEN STATE AT HIGHER REYNOLDS NUMBER

R. G. Deissler, Nov 1978, 15 p. refs. Presented at the 31st Ann. Meeting of the Am. Phys. Soc. Div. of Fluid Dyn., Los Angeles, 19-21 Nov 1978

(NASA-TM-79011, E-9796) Avail NTIS HC A02/MF A01 CSCL 20D

The turbulence equations are closed by specification of initial conditions (using either a Taylor or an exponential series) and by a modified Kovasznay-type closure. Good results for large times are obtained only for the initial conditions closure used with four or more terms of an exponential series. The evolution of all of the initially specified spectra can be calculated rather well from the theory. From a fundamental standpoint the method thus seems to be satisfactory. Author

N79-12362* National Aeronautics and Space Administration
Lewis Research Center, Cleveland, Ohio

ATOMIZATION OF WATER JETS AND SHEETS IN AXIAL AND SWIRLING AIRFLOWS

Robert D. Ingebo [1977], 12 p. refs. Proposed for presentation at the 24th Ann. Intern. Gas Turbine Conf., San Diego, Calif., 11-15 Mar 1979, sponsored by the Am. Soc. of Mech. Engr. (NASA-TM-79043, E-9847) Avail NTIS HC A02/MF A01 CSCL 20D

Axial and swirling airflows were used to break up water jets and sheets into sprays of droplets to determine the overall effects of orifice diameter, weight flow of air, and the use of an air swirler on fineness of atomization as characterized by mean drop size. A scanning radiometer was used to determine the mean drop diameter of each spray. Swirling airflows were produced with an axial combustor, 70 deg blade angle, air swirling. Water jets were injected axially upstream, axially downstream, and cross stream into the airflow. In addition, pressure atomizing fuel nozzles which produced a sheet and ligament type of breakup

were investigated. Increasing the weight flow rate of air or the use of an air swirling markedly reduced the spray mean drop size. G.G.

N79-13288* National Aeronautics and Space Administration
Lewis Research Center, Cleveland, Ohio

HEAT EXCHANGER Patent

Daniel E. Sokolowski, inventor (to NASA) Issued 22 Aug 1978
6 p. Filed 19 Mar 1975 Supersedes N75-19579 (13 - 11, p 1244)

(NASA-Case-LEW-12252-1, US Patent-4,107,919)

US Patent Appl-SN-559847, US Patent Class-165-169,

US Patent Class-60-267, US Patent Class-239-127.1) Avail US Patent and Trademark Office CSCL 20D

A heat exchanger, as exemplified by a rocket combustion chamber, is constructed by stacking thin metal rings having micro-sized openings therein at selective locations to form cooling passages defined by an inner wall, an outer wall and fins. Suitable manifolds are provided at each end of the rocket chamber. In addition to the cooling channel openings, coolant feed openings may be formed in each of rings. The coolant feed openings may be nested or positioned within generally U-shaped cooling channel openings. Compression on the stacked rings may be maintained by welds or the like or by bolts extending through the stacked rings.

Official Gazette of the U.S. Patent and Trademark Office

N79-13289* National Aeronautics and Space Administration
Lewis Research Center, Cleveland, Ohio

HEAT EXCHANGER AND METHOD OF MAKING Patent

Anthony Fortini and John M. Kazaroff, inventors (to NASA) Issued 22 Aug 1978, 5 p. Filed 19 Mar 1975 Supersedes N75 19580 (13 - 11, p 1244)

(NASA-Case-LEW-12441-1, US Patent-4,108,241)

US Patent Appl-SN-559846, US Patent Class-165-146,

US Patent Class-165-169, US Patent Class-60-267,

US Patent Class-239-127.1) Avail US Patent and Trademark Office CSCL 20D

A heat exchanger of increased effectiveness is disclosed. A porous metal matrix is disposed in a metal chamber or between walls through which a heat-transfer fluid is directed. The porous metal matrix has internal bonds and is bonded to the chamber in order to remove all thermal contact resistance within the composite structure. Utilization of the invention in a rocket chamber is disclosed as a specific use. Also disclosed is a method of constructing the heat exchanger.

Official Gazette of the U.S. Patent and Trademark Office

N79-15267* National Aeronautics and Space Administration
Lewis Research Center, Cleveland, Ohio

SOME HEAT TRANSFER AND HYDRODYNAMIC PROBLEMS ASSOCIATED WITH SUPERCONDUCTING CABLES (SPTL)

Robert C. Hendricks, David E. Daney (NBS, Boulder, Colo.), V. M. Yeroshenko (Khrzhizhanovsky Power Inst., Moscow), Ye. V. Kuznetsov (Khrzhizhanovsky Power Inst., Moscow) and O. A. Shevchenko (Khrzhizhanovsky Power Inst., Moscow), 1978, 28 p. refs. Presented at the US USSR Comm. for Superconducting Power Transmission, Upton, N. Y., 5-6 Oct 1978

(NASA-TM-79023, DOE/NASA/O207-78/1) Avail NTIS HC A03/MF A01 CSCL 20D

To study some effects of thermogravitation on (CIK SPTL) systems, a heated tube experiment was set up at Khrzhizhanovsky Power Engineering Institute, Moscow, U.S.S.R. Heat transfer data were taken with fluid helium flowing through a 2.85 m, 19 mm diameter uniformly heated horizontal tube. Temperatures were measured on the top and bottom of the tube at six axial locations with three other circumferential measurements made at (X/L) = 57. Typical temperature profiles show significant variations both axially and circumferentially. The data are grouped using reduced Nusselt number (NuR) and the bulk expansion parameter for each axial location. The average data for 0.26 less than or equal to X/L less than or equal to 0.76 follow a power law relation with the average expansion parameter.

System instabilities are noted and discussed. Future work including heat transfer in coaxial cylinders is discussed. Author

N79-18288* National Aeronautics and Space Administration
Lewis Research Center, Cleveland, Ohio

TACT 1: A COMPUTER PROGRAM FOR THE TRANSIENT THERMAL ANALYSIS OF A COOLED TURBINE BLADE OR VANE EQUIPPED WITH A COOLANT INSERT. 2. PROGRAMMERS MANUAL

Raymond E. Gaugler. Jan. 1979. 164 p. refs.
(NASA-TP-1391, E-9767) Avail NTIS HC A08/MF A01 CSCL 20D

A computer program to calculate transient and steady state temperatures, pressures, and coolant flows in a cooled axial flow turbine blade or vane with an impingement insert is described. Coolant-side heat transfer coefficients are calculated internally in the program, with the user specifying either impingement or convection heat transfer at each internal flow station. Spent impingement air flows in a chordwise direction and is discharged through the trailing edge and through film cooling holes. The ability of the program to handle film cooling is limited by the internal flow model. Input to the program includes a description of the blade geometry, coolant supply conditions, outside thermal boundary conditions, and wheel speed. The blade wall can have two layers of different materials, such as a ceramic thermal barrier coating over a metallic substrate. Program output includes the temperature at each node, the coolant pressures and flow rates, and the coolant-side heat transfer coefficients. Author

N78-20341* National Aeronautics and Space Administration
Lewis Research Center, Cleveland, Ohio

FLOW FRICTION OF THE TURBULENT COOLANT FLOW IN CRYOGENIC POROUS CABLES

Robert C. Hendricks, V. M. Yeroshenko (Khrizhchanovsky Power Eng. Inst.), L. I. Zaichik (Khrizhchanovsky Power Eng. Inst.), and L. S. Yanovsky (Khrizhchanovsky Power Eng. Inst.) 1979. 18 p. refs. Proposed for presentation at the 15th Intern. Congr. on Refrigeration, Venice, 23-29 Sep. 1979, sponsored by Intern. Inst. of Refrigeration. Prepared for DOE
(NASA-TM-79052; DOE/NASA/O207-79/1) Avail NTIS HC A02/MF A01 CSCL 20D

Considered are cryogenic power transmission cables with porous cores. Calculations of the turbulent coolant flow with injection or suction through the porous wall are presented within the framework of a two-layer model. Universal velocity profiles were obtained for the viscous sublayer and flow core. Integrating the velocity profile, the law of flow friction in the pipe with injection has been derived for the case when there is a tangential injection velocity component. The effect of tangential velocity on the relative law of flow friction is analyzed. The applicability of the Prandtl model to the problem under study is discussed. It is shown that the error due to the acceptance of the model increases with the injection parameter and at lower Reynolds numbers, under these circumstances, the influence of convective terms in the turbulent energy equation or the mechanism of turbulent transport should be taken into account. Author

N79-20336* National Aeronautics and Space Administration
Lewis Research Center, Cleveland, Ohio

CLOSED LOOP SPRAY COOLING APPARATUS. Patent

Donald L. Alger, William B. Schwab, and Edward R. Furman (inventors to NASA). Issued 27 Feb. 1979. 4 p. Filed 31 Aug. 1977. Supersedes N77-32434 (15-23 p. 3075). Division of US Patent Appl. SN 672220, filed 31 Mar. 1976. US Patent 4,068,495

(NASA Case LEW 11981-2, US Patent 4,141,224)
US Patent Appl. SN 829315, US Patent Class 52-514H
US Patent Class 62-268, US Patent Class 62-376
US Patent Class 750-352, US Patent Class 313-72
US Patent Class 313-35, US Patent Appl. SN 672220
US Patent 4,068,455; Avail. US Patent and Trademark Office
CSCL 20D

A closed loop apparatus for jet spraying coolant against the back of a radiation target is described. The coolant is circulated

through a closed loop with a bubble of inert gas being maintained around the spray. Mesh material is disposed between the bubble and the surface of the liquid coolant which is below the bubble at a predetermined level. In a second arrangement no inert gas is used, the bubble consists of vapor produced when the coolant is sprayed against the target.

Official Gazette of the U.S. Patent and Trademark Office

N79-20337* National Aeronautics and Space Administration
Lewis Research Center, Cleveland, Ohio

SOME EFFECTS OF CYCLIC INDUCED DEFORMATION IN ROCKET THRUST CHAMBERS

N. P. Hannum and R. J. Quentmeyer. 1979. 15 p. refs. To be presented at the Conf. on Advanced Technol. for Future Space Systems, Hampton, Va., 8-11 May 1979, sponsored by AIAA
(NASA-TM-79112, E-9939) Avail NTIS HC A02/MF A01 CSCL 20D

A test program to investigate the deformation process observed in the hot gas wall of rocket thrust chambers was conducted using three different liner materials. Five thrust chambers were cycled to failure using hydrogen and oxygen as propellants at a chamber pressure of 4.14 MN/m² (600 psia). The deformation was observed nondestructively at midline points and destructively after failure occurred. The cyclic life results are presented with an accompanying discussion about the types of failure encountered. Data indicating the deformation of the thrust chamber liner as cycles are accumulated are presented for each of the test thrust chambers. Author

N79-20338* National Aeronautics and Space Administration
Lewis Research Center, Cleveland, Ohio

ON THE EQUIVALENCE BETWEEN SEMIEMPIRICAL FRACTURE ANALYSES AND R-CURVES

Thomas W. Orange. 1979. 34 p. refs. Presented at the 12th Natl. Symp. on Fracture Mech., St. Louis, 21-23 May 1978, sponsored by the Am. Soc. For Testing Mater.
(NASA-TM-79127, E-9963) Avail NTIS HC A03/MF A01 CSCL 20D

The relationship between several semiempirical fracture analyses (SEFA) and the R-curve concept of fracture mechanics is examined. The conditions for equivalence between a SEFA and an R-curve are derived. A hypothetical material is employed to study the relationship analytically. Equivalent R-curves are developed for real materials using data from the literature. For each SEFA there is an equivalent R-curve whose magnitude and shape are determined by the SEFA formulation and its empirical parameters. If the R-curve is indeed unique then the various empirical parameters cannot be constant, and vice versa. However, for one SEFA the differences are small enough that they may be within the range of normal data scatter for real materials. J.M.S.

N79-20346* National Aeronautics and Space Administration
Lewis Research Center, Cleveland, Ohio

FUNDAMENTAL MECHANISMS THAT INFLUENCE THE ESTIMATE OF HEAT TRANSFER TO GAS TURBINE BLADES

R. W. Graham. 1979. 13 p. refs. To be presented at the Natl. Heat Transfer Conf., San Diego, Calif., 5-8 Aug. 1979, cosponsored by ASME and the Am. Inst. of Chem. Engr.
(NASA-TM-79128, E-9966) Avail NTIS HC A02/MF A01 CSCL 21E

Estimates of the heat transfer from the gas to stationary (vanes) or rotating blades poses a major uncertainty due to the complexity of the heat transfer processes. The gas flow through these blade rows is three dimensional with complex secondary viscous flow patterns that interact with the endwalls and blade surfaces. In addition upstream disturbances, stagnation flow, curvature effects, and flow acceleration complicate the thermal transport mechanisms in the boundary layers. Some of these fundamental heat transfer effects are discussed. The chief purpose of the discussion is to acquaint those in the heat transfer community not directly involved in gas turbines, of the seriousness

of the problem and to recommend some basic research that would improve the capability for predicting gas-side heat transfer on turbine blades and vanes. L.S.

N79-21313* National Aeronautics and Space Administration, Lewis Research Center, Cleveland, Ohio.

A HEAT EXCHANGER AND METHOD OF MAKING Patent Application

A. Fortini and John M. Kazaroff, inventors (to NASA) Filed 30 Nov 1977 14 p.

(NASA Case-LEW-12441-2; US Patent-Appl-SN-856462) Avail. NTIS HC A02/MF A01 CSCL 20D

A heat exchanger of increased effectiveness is described. A porous metal matrix is disposed in a metal chamber or between walls through which a heat-transfer fluid is directed. The porous metal matrix has internal bonds and is bonded to the chamber in order to remove all thermal contact resistance within the composite structure. A specific use is to provide a method of making a rocket chamber with maximum heat transfer at the throat area where inner wall temperatures are the highest.

NASA

N79 22415* National Aeronautics and Space Administration, Lewis Research Center, Cleveland, Ohio.

INTRODUCTION: THERMAL RADIATION IN INDUSTRIAL FLAMES

R. Siegel, *In* Von Karman Inst. for Fluid Dyn. Thermal Radiation in Ind. Flames, 1971, 72 p., refs. (For primary document see N79 22413 13-34)

Avail. NTIS HC A14/MF A01 CSCL 20D

The following topics are addressed: (1) emissive characteristics of a blackbody; (2) definition of properties for nonblack surfaces; (3) fundamentals of radiation in absorbing, emitting, and scattering media; (4) radiation in the presence of other modes of energy transfer; and (5) propagation in isotropic medium (the complex refractive index). G.Y.

N79 22426* National Aeronautics and Space Administration, Lewis Research Center, Cleveland, Ohio.

TITANIUM ALLOY, METALLIC FLUID HEAT PIPES FOR SPACE SERVICE

James F. Morris, Mar. 1979, 15 p., refs.

(NASA TM 79132, E 9974) Avail. NTIS HC A02/MF A01 CSCL 20D

Reactivities of titanium limit its long-term terrestrial use for unprotected heat pipe envelopes to about 870 K (1100 F). But this external thermochemical limitation disappears when considerations shift to space applications. In such hard-vacuum utilization much higher operating temperatures are possible. Primary restrictions in space environment result from vaporization, thermal creep, and internal compatibilities. Unfortunately, a respected heat pipe reference indicates that titanium is compatible only with cesium from the alkali metal working fluid family. This problem and others are subjects of the present paper which advocates titanium alloy, metallic fluid heat pipes for long-lived, weight-effective space service between 500 and 1300 K (440 and 1880 F). Author

N79 22427* National Aeronautics and Space Administration, Lewis Research Center, Cleveland, Ohio.

REVIEW AND STATUS OF LIQUID COOLING TECHNOLOGY FOR GAS TURBINES

G. James VanFossen, Jr. and Francis S. Stepka, Washington, Apr. 1979, 31 p., refs.

(NASA TP-1038, E 9517, AVFADCOM TR 78-21) Avail. NTIS HC A03/MF A01 CSCL 20D

A review was conducted of liquid-cooled turbine technology. Selected liquid-cooled systems and methods are presented along with an assessment of the current technology status and requirements. A comprehensive bibliography is presented. Author

N79-233F3* National Aeronautics and Space Administration, Lewis Research Center, Cleveland, Ohio.

A HEAT EXCHANGER AND METHOD OF MAKING Patent Application

A. Fortini and John M. Kazaroff, inventors (to NASA) Filed 23 Apr. 1979, 14 p.

(NASA Case-LEW-12441-3; US Patent-Appl-SN-C32307) Avail. NTIS HC A02/MF A01 CSCL 20D

A heat exchanger of increased effectiveness is disclosed. A porous metal matrix is disposed in a metal chamber or between walls through which a heat-transfer fluid is directed. The porous metal matrix has internal bonds and is bonded to the chamber in order to remove all thermal contact resistance within the composite structure. Utilization of the invention in a rocket chamber is disclosed as a specific use. Also disclosed is a method of constructing the heat exchanger. NASA

N79-23384* National Aeronautics and Space Administration, Lewis Research Center, Cleveland, Ohio.

MEASUREMENTS OF MIXED CONVECTIVE HEAT TRANSFER TO LOW TEMPERATURE HELIUM IN A HORIZONTAL CHANNEL

V. M. Yeroshenko (Khrzhizhanovskiy Power Eng. Inst.), Ye. V. Kuznetsov (Khrzhizhanovskiy Power Eng. Inst.), O. A. Shevchenko (Khrzhizhanovskiy Power Eng. Inst.), Robert C. Hendricks, and D. E. Daney (NBS, Boulder, Colo.), 1979, 16 p., refs. Proposed for presentation at the 15th Intern. Congr. on Refrigeration, Venice, 23-29 Sep. 1979; sponsored in part by the Intern. Inst. of Refrigeration. Sponsored by NASA. Prepared for DOE.

(NASA-TM-79158, DOE/NASA/0207-79/3, E-014) Avail. NTIS HC A02/MF A01 CSCL 20D

A horizontal 2.85 m long, 19 mm i.d. stainless steel heated circular channel was employed to measure coefficients of heat transfer to low temperature helium flow. Experimental parameters range from 5.5 to 15 K, from 0.12 to 0.3 MPa at heat fluxes up to 1000 W/m² square and Reynolds numbers from 9,000 to 20,000. A significantly nonuniform distribution of heat transfer coefficients over the tube periphery is observed. Difference between temperatures on the upper and lower surfaces of the stainless steel channel wall was found to reach 9 K. It was noted that the highest temperature on the wall outer surface is displaced from its uppermost point. Measurements of local flow temperatures revealed vortical structure of the flow. The displacement of the point with the highest temperature is attributable to the effect of vortices. The relationships for calculating local and averaged coefficients of heat transfer are proposed. Author

N79-27460* National Aeronautics and Space Administration, Lewis Research Center, Cleveland, Ohio.

SOME FLOW CHARACTERISTICS OF CONVENTIONAL AND TAPERED HIGH PRESSURE DROP SIMULATED SEALS

R. C. Hendricks, 1979, 18 p., refs. To be presented at the Joint Lubrication Conf., Dayton, Ohio, 16-18 Oct. 1979; sponsored by Am. Soc. of Lubrication Engrs. and ASME.

(NASA TM 79192, E 064) Avail. NTIS HC A02/MF A01 CSCL 20D

The leak rates through shaft seals with large pressure drops were simulated using gaseous hydrogen or nitrogen flowing through an annulus with a nonrotating centerbody. The flows were choked. For concentric or eccentric position of the rotor and parallel or convergent tapered flow passages, data and analysis revealed that mass flux or leak rate can be determined from a relation whose normalizing parameters depend on the thermodynamic critical constants of the working fluid and an average flow area expressed in terms of the inlet and exit cross-sectional areas. Using these normalized relations, the flow data for parallel and three convergent tapered shaft seal configurations are in good agreement. Generalization to any simple gas or gas mixture is implied and demonstrated. Author

N79-27461* National Aeronautics and Space Administration, Lewis Research Center, Cleveland, Ohio

CONDENSATION ON A NONCOLLAPSING VAPOR BUBBLE IN A SUBCOOLED LIQUID

Kenneth J. Baumeister and Robert J. Simoneau. 1979. 17 p. refs. Prepared for 18th Natl. Heat Transfer Conf., San Diego, Calif., 5 & Aug. 1979.

(NASA TM-79212, E-098) Avail. NTIS HC A02/MF A01 CSCL 20D

An experimental procedure is presented by which an estimate can be made of the condensation coefficient on a noncollapsing stationary vapor bubble in subcooled liquid nitrogen. Film boiling from a thin wire was used to generate vapor bubbles which remain fixed to the wire at their base. A balance was established between the evaporation in the thin annular region along the wire and the condensation in the vapor bubbles. J M S

N79-29467* National Aeronautics and Space Administration, Lewis Research Center, Cleveland, Ohio

CONTOURED TANK OUTLETS FOR DRAINING OF CYLINDRICAL TANKS IN LOW GRAVITY ENVIRONMENT

Eugene P. Symons. Jul. 1979. 45 p.

(NASA TP-1492, E-9969) Avail. NTIS HC A03/MF A01 CSCL 20D

An analysis is presented for defining the outlet contour of a hemispherical-bottomed cylindrical tank that will prevent vapor ingestion when the tank is drained. The analysis was used to design two small-scale tanks that were fabricated and then tested in a low gravity environment. The draining performance of the tanks was compared with that for a tank with a conventional outlet having a constant circular cross-sectional area under identical conditions. Even when drained at off-design conditions, the contoured tank had less liquid residuals at vapor ingestion than the conventional outlet tank. Effects of outflow rate, gravitational environment, and fluid properties on the outlet contour are discussed. Two potential applications of outlet contouring are also presented and discussed. K L

N79-29468* National Aeronautics and Space Administration, Lewis Research Center, Cleveland, Ohio

TWO PHASE CHOKED FLOW OF CRYOGENIC FLUIDS IN CONVERGING DIVERGING NOZZLES

Robert J. Simoneau and Robert C. Hendricks. Jul. 1979. 83 p. refs.

(NASA TP-1484, E-9659) Avail. NTIS HC A05/MF A01 CSCL 20D

Data are presented for the two phase choked flow of three cryogenic fluids: nitrogen, methane, and hydrogen, in four converging-diverging nozzles. The data cover a range of inlet stagnation conditions, all single phase, from well below to well above the thermodynamic critical conditions. In almost all cases the nozzle throat conditions were two phase. The results indicate that the choked flow rates were not very sensitive to nozzle geometry. However, the axial pressure profiles, especially the throat pressure and the point of vaporization, were very sensitive to both nozzle geometry and operating conditions. A modified Henry-Fauske model correlated all the choked flow rate data to within ± 10 percent. Neither the equilibrium model nor the Henry-Fauske model predicted throat pressures well over the whole range of data. Above the thermodynamic critical temperature the homogeneous equilibrium model was preferred for both flow rate and pressure ratio. The data of the three fluids could be normalized by the principle of corresponding states. K L

N79-30615* National Aeronautics and Space Administration, Lewis Research Center, Cleveland, Ohio

APPLICATION OF THE PRINCIPLE OF SIMILARITY FLUID MECHANICS

R. C. Hendricks and I. V. Sengers (Md. Univ., College Park). 1979. 49 p. refs.

(NASA TM-79258, E-170) Avail. NTIS HC A03/MF A01 CSCL 20D

The principle of similarity applied to fluid mechanics is described and illustrated. The concept of transforming the

conservation equations by combining similarity principles for thermophysical properties with those for fluid flow is examined. The usefulness of the procedure is illustrated by applying such a transformation to calculate two phase critical mass flow through a nozzle. A W H

N79-30516* National Aeronautics and Space Administration, Lewis Research Center, Cleveland, Ohio

DESCRIPTION AND ORBIT DATA OF VARIABLE-CONDUCTANCE HEAT PIPE SYSTEM FOR THE COMMUNICATIONS TECHNOLOGY SATELLITE

Louis Gedeon. Aug. 1979. 23 p. refs.

(NASA-TP-1465, E-9880) Avail. NTIS HC A02/MF A01 CSCL 20D

A variable-conductance heat pipe system (VCHPS) with methanol as the working fluid and a nitrogen and helium mixture as the control gas was used for the thermal control of a 200 W RF traveling wave tube of the Communication Technology Satellite. Three stainless steel heat pipes (one redundant) and an aluminum radiator were designed to transfer 196 watts for an evaporator temperature of 50 C. The system has operated for three years with no noticeable change in performance. On four occasions the heat pipes apparently depried. A short time after reducing the tube power, the heat pipes reprimed and the system continued to operate normally. The description, qualification testing, and orbit data of the VCHPS are presented. K L

N79-31526* National Aeronautics and Space Administration, Lewis Research Center, Cleveland, Ohio

FREE JET PHENOMENA IN A 90 DEGREE SHARP EDGE INLET GEOMETRY

R. C. Hendricks. 1979. 30 p. refs. Presented at Intern. Cryogenic Engr. Conf. and the Intern. Cryogenic Materials Conf., Madison, Wis., 21-24 Aug. 1979, sponsored by NBS.

(NASA TM-79229, E-131) Avail. NTIS HC A03/MF A01 CSCL 20D

Under certain conditions, inlets with a sharp edge or geometric corner were shown to exhibit sufficiently strong separation effects to permit the working fluid to flow through the duct as if it were a free jet. Mass limiting flow data and associated pressure profiles for tubes of 53, 64, 73, and 105 length/diameter with a 90 deg sharp edge or orifice type inlet were taken and compared to Borda type inlet data to determine bounds of the free jet phenomena. For smooth tubes the limits appear to be one dimensional and dependent only on inlet stagnation conditions. Similar free jet effects were found for fluid hydrogen indicating that fluid jetting may common to all fluids flowing through 90 deg sharp edge inlet geometries. Author

N79-31527* National Aeronautics and Space Administration, Lewis Research Center, Cleveland, Ohio

A REDUCED VOLUMETRIC EXPANSION FACTOR PLOT

R. C. Hendricks. 1979. 29 p. refs. Presented at Cryogenic Engr. Conf. and the Intern. Cryogenic Materials Conf., Madison, Wis., 21-24 Aug. 1979.

(NASA TM-79240, E-148) Avail. NTIS HC A03/MF A01 CSCL 20D

A reduced volumetric expansion factor plot was constructed for simple fluids which is suitable for engineering computations in heat transfer. Volumetric expansion factors were found useful in correlating heat transfer data over a wide range of operating conditions, including liquids, gases and the near critical region. G Y

A79-10002* Decay of homogeneous turbulence from a given state at higher Reynolds number. R. G. Deissler (NASA, Lewis Research Center, Cleveland, Ohio). *American Physical Society Annual Meeting, 31st, Los Angeles, Calif., Nov. 19-21, 1978, Paper 14 p.* 8 refs.

The turbulence equations are closed by specification of initial conditions (using either a Taylor or an exponential series) and by a modified Kuvshinov type closure. Good results for large times are obtained only for the initial conditions closure used with four or

more terms of an exponential series. The evolution of all of the initially specified spectra can be calculated rather well from the theory. From a fundamental standpoint the method thus seems to be satisfactory. (Author)

A79-22424 * Comparison of a correlation term-discard closure for decaying homogeneous turbulence with experiment. R. G. Deissler (NASA, Lewis Research Center, Cleveland, Ohio). *Physics of Fluids*, vol. 22, Jan. 1979, p. 185, 186. 11 refs.

Turbulence decay is calculated by using experimental initial conditions and discarding quadruple-correlation terms in the correlation equations. Agreement with experiment is good only for moderately small times, but there are no perceptible negative spectral energies even at large times. (Author)

A79-30556 * # Atomization of water jets and sheets in axial and swirling airflows. R. D. Ingebo (NASA, Lewis Research Center, Cleveland, Ohio). *American Society of Mechanical Engineers, Gas Turbine Conference and Exhibit and Solar Energy Conference, San Diego, Calif., Mar. 12-15, 1979, Paper 79-GT-170*. 10 p.

Axial and swirling airflows were used to break up water jets and sheets into sprays of droplets to determine the overall effects of orifice diameter, weight flow of air, and the use of an air swirler on fineness of atomization as characterized by mean drop size. A scanning radiometer was used to determine the mean drop diameter of each spray. Swirling airflows were produced with an axial combustor, 70 deg blade angle, air swirling. Water jets were injected axially upstream, axially downstream and cross stream into the airflow. In addition, pressure atomizing fuel nozzles which produced a sheet and ligament type of breakup were investigated. Increasing the weight flow rate of air or the use of an air swirling markedly reduced the spray mean drop size. Test conditions included a water flow rate of 68.0 liter per hour and airflow rates (per unit area) of 3.7 to 25.7 g per square cm per sec, at 293 K and inlet air static pressures of 1.01×10 to the 5th to 1.90×10 to the 5th N/sq m. (Author)

A79-37140 * Scattering and distortion of the unsteady motion on transversely sheared mean flows. M. E. Goldstein (NASA, Lewis Research Center, Cleveland, Ohio). *Journal of Fluid Mechanics*, vol. 91, Apr. 27, 1979, p. 601-632. 20 refs.

It is shown that the pressure and velocity fluctuations of the unsteady motion on a transversely sheared mean flow can be expressed entirely in terms of the derivatives of two potential functions. One of these is a connected quantity that can be specified as a boundary condition and is related to a transverse component of the upstream velocity field. The other can be determined by solving an inhomogeneous wave equation whose source term is also a connected quantity that can be specified as a boundary condition in any given problem. The general theory is used to study the interaction of an unsteady flow with a semi-infinite plate embedded in a shear layer. The acoustic field produced by this interaction is calculated in the limits of low and high frequency. The results are compared with experimental one third octave sound pressure level radiation patterns. The agreement is found to be excellent, especially in the low frequency range, where the mean flow and convective effects are shown to have a strong influence on the directivity of the sound. (Author)

A79-45463 * Turbulence generated by the interaction of entropy fluctuations with non-uniform mean flows. M. E. Goldstein (NASA, Lewis Research Center, Cleveland, Ohio). *Journal of Fluid Mechanics*, vol. 93, July 26, 1979, p. 209-224. 20 refs.

The turbulence generated by random entropy fluctuations in an accelerating stream is analyzed. The results are obtained by using rapid distortion theory together with a high frequency solution of a previously developed wave equation that governs the small amplitude unsteady vortical and entropic motion on steady potential flows (Goldstein, 1978). Simple results are obtained for the case of

symmetric contraction, expansion or combination of the two. It is shown that the energy of the entropy generated turbulence increases more rapidly with the contraction ratio of a subsonic flow than that of any imposed upstream turbulence. This result indicates that the entropy-generated turbulence may be more significant than the hydrodynamically generated turbulence in the turbine stages of aircraft engines. S.D.

A79-45526 * # Fundamental mechanisms that influence the estimate of heat transfer to gas turbine blades. R. W. Graham (NASA, Lewis Research Center, Fundamental Heat Transfer Section, Cleveland, Ohio). *American Society of Mechanical Engineers and American Institute of Chemical Engineers, National Heat Transfer Conference, San Diego, Calif., Aug. 5-8, 1979, Paper*. 11 p. 32 refs.

Heat transfer problems in aircraft gas turbines required for improved prediction of turbine blade or vane gas side heat transfer are examined. Estimates of the heat transfer from the gas to vanes or rotating blades are uncertain due to the complexity of the heat transfer processes, since the gas flow is three dimensional with complex secondary viscous flow patterns that interact with the endwalls and blade surfaces. In addition, upstream disturbances, stagnation flow, curvature effects, and flow acceleration complicate the thermal transport mechanisms in the boundary layers. The thermal state and flow characteristics of the hot gases that enter the turbine blade row, analytical methods for calculating the gas side heat transfer to turbine blades, and flow phenomena such as stagnation, curvature effects, acceleration, secondary flows, and transition that influences local heat transfer rates are discussed. A.T.

A79-49535 * # Condensation on a noncollapsing vapor bubble in a subcooled liquid. K. J. Baumeister and R. J. Simonau (NASA, Lewis Research Center, Cleveland, Ohio). *National Heat Transfer Conference 18th, San Diego, Calif., Aug. 5-8, 1979, Paper*. 5 p. 13 refs.

An experimental procedure is presented by which an estimate can be made of the condensation coefficient on a noncollapsing stationary vapor bubble in subcooled liquid nitrogen. The present experimental study utilizes film boiling from a thin wire to generate vapor bubbles which remain fixed to the wire at their base. A balance was established between the evaporation in the thin annular region along the wire and the condensation in the vapor bubbles. (Author)

N79-12356* # United Technologies Research Center East Hartford, Conn.

DEVELOPMENT OF A THREE DIMENSIONAL TURBULENT DUCT FLOW ANALYSIS Final Report

P. R. Eiseman, R. Levy, H. McDonald, and W. R. Briley. Nov. 1978. 117 p. refs.

(Contract NAS3 19856)

(NASA CR 3029) Avail. NTIS HC A06/MF A01 CSCL 20D

A method for computing three dimensional turbulent subsonic flow in curved ducts is described. An approximate set of governing equations is given for viscous flows which have a primary flow direction. The derivation is coordinate invariant and the resulting equations are expressed in terms of tensors. General tube-like coordinates were developed for a general class of geometries applicable to many internal flow problems. The coordinates are then particularized to pipes having superelliptic cross sections whose shape can vary continuously between a circle and a near rectangle. The analysis is applied to a series of relevant aerodynamic problems including transition from nearly square to round pipes and flow through a pipe with an S shaped bend. Author

N79-22428* # Stanford Univ., Calif.
FULL COVERAGE FILM COOLING. 3 DIMENSIONAL MEASUREMENTS OF TURBULENCE STRUCTURE AND PREDICTION OF RECOVERY REGION HYDRODYNAMICS
Final Report
 S. Yavuzkurt, R. J. Moffat, and W. M. Kays. Mar. 1979. 188 p. refs.

(Contract NAS3-14336)
(NASA-CR-3104; SU-HMT-27) Avail: NTIS HC A09/MF A01
CSCL 20D

Hydrodynamic measurements were made with a triaxial hot-wire in the full-coverage region and the recovery region following an array of injection holes inclined downstream, at 30 degrees to the surface. The data were taken under isothermal conditions at ambient temperature and pressure for two blowing ratios: $M = 0.9$ and $M = 0.4$. Profiles of the three main velocity components and the six Reynolds stresses were obtained at several spanwise positions at each of the five locations down the test plate. A one-equation model of turbulence (using turbulent kinetic energy with an algebraic mixing length) was used in a two-dimensional computer program to predict the mean velocity and turbulent kinetic energy profiles in the recovery region. A new real-time hotwire scheme was developed to make measurements in the three-dimensional turbulent boundary layer over the full-coverage surface. Author

N79-22429* Stanford Univ., Calif.

HEAT TRANSFER TO A FULL-COVERAGE, FILM-COOLED SURFACE WITH COMPOUND-ANGLE (30 DEG AND 45 DEG) HOLE INJECTION Final Report

H. K. Kim, R. J. Moffat, and W. M. Kays Feb. 1979 159 p
refs

(Contract NAS3-14336)
(NASA-CR-3103; SU-HMT-28) Avail: NTIS HC A08/MF A01
CSCL 20D

An experimental study of heat transfer was conducted on a turbulent boundary layer with full-coverage film cooling through an array of holes inclined at 30 deg to the surface and 45 deg to the flow direction (compound-angle injection). Heat transfer coefficients were measured over a range of injectant flows ($M = 0$ to $M = 1.5$) and Reynolds numbers at velocities between 9.8 and 16.8 m/s. Data are presented for injectant temperature equal to the wall temperature and injectant temperature equal to the stream temperature. Compound-angle injection gives better thermal protection than in-line, slant-hole injection, but the beneficial effect is minimal in the first six rows of holes. For a value of $M = 0.37$ the heat transfer coefficient with compound-angle injection was the same as for the slant-angle injection after six rows, but was only one-half the slant-hole value after 11 rows. The data for compound-angle injection show the same general features as for slant-angle and normal injection. Recovery is rapid after the last row of holes, with the heat

N79-22434* TRW Defense and Space Systems Group, Redondo Beach, Calif.

CTS-TYPE VARIABLE CONDUCTANCE HEAT PIPES FOR SEP FM/FPU Final Report, Oct. 1977 - Dec. 1978

D. Antoniuk and E. E. Luedke Dec. 1978 45 p
(Contract NAS3-21130)
(NASA-CR-159550; TRW-30979-6003-RU-00) Avail: NTIS
HC A03/MF A01 CSCL 20D

The development effort for, and the fabrication and testing of, six CTS-type variable conductance heat pipes is described. The heat pipes are constructed of stainless steel, use methanol as a working fluid, and a nitrogen/helium mixture as the control gas. The wicking structure consists of interior wall grooves, a metal-felt diametral slab wick, and two wire-mesh arteries. The heat pipes are used to cool two Functional Model/Power Processing Units in a Solar Electric Propulsion prototype BIMOD thruster subsystem assembly. The Power Processing Units convert the electric power from a spacecraft solar array system to the voltages required to operate the electric thrusters which are part of the BIMOD assembly. G.Y.

N79-25349* TRW Defense and Space Systems Group, Redondo Beach, Calif.

HEAT PIPE LIFE AND PROCESSING STUDY Final Report
David Antoniuk and Edward Luedke Apr. 1979 94 p

(Contract NAS3-21200)
(NASA-CR-159581; TRW-32937-6001-TU-00) Avail: NTIS
HC A05/MF A01 CSCL 20D

The merit of adding water to the reflux charge in chemically and solvent cleaned aluminum/slab wick/ammonia heat pipes was evaluated. The effect of gas in the performance of three heat pipe thermal control systems was found significant in simple heat pipes, less significant in a modified simple heat pipe model with a short wickless pipe section. Use of gas data for the worst and best heat pipes of the matrix in a variable conductance heat pipe model showed a 3 C increase in the source temperature at full on condition after 20 and 246 years, respectively. Author

N79-28456* Detroit Diesel Allison, Indianapolis, Ind.
LASER ANEMOMETER MEASUREMENTS AT THE EXIT OF A T63-C20 COMBUSTOR Final Report, Sep. 1978 - Apr. 1979

D. B. Zimmerman Apr. 1979 44 p refs Sponsored in part by Army Research and Develop. Command, Cleveland
(Contract NAS3-21267; DA Proj. 1L1-62209-AH-76)
(NASA-CR-159623; DDA-RN-79-4) Avail: NTIS
HC A03/MF A01 CSCL 20D

An experimental study of the flow downstream of a T63-C20 gas turbine engine combustor was performed. Laser anemometer measurements of the mean and fluctuating velocities were made in a combustion rig across an annulus simulating the inlet to turbine. A window design suitable for similar measurements in a gas turbine engine was made based on the results of this experiment. Insufficient numbers of naturally-occurring scattering particles were present in the flow. Hollow phenolic particles added to the flow provided adequate signal strength for measurement. For each of the simulated engine operating conditions of flight idle, 30% power and 90% power, both with and without the addition of fuel, the mean velocities and turbulent intensities were uniform across the annulus. The turbulent intensity was substantially unaffected by the addition of fuel but was apparently only dependent on the inlet flow condition at a given power point. Little or no swirl was present in the flow at the annulus. Author

N79-30514* Cincinnati Univ., Ohio Dept. of Aerospace Engineering and Applied Mechanics

A CALCULATION PROCEDURE FOR VISCOUS FLOW IN TURBOMACHINES, VOLUME 1

I. Khalil and W. Tabakoff Jul. 1979 97 p refs
(Contract NAS3-21609; DA Proj. 1L1-61102-AH-45)
(NASA-CR-159635) Avail: NTIS HC A05/MF A01 CSCL
20D

A method for analyzing the nonadiabatic viscous flow through turbomachine rotors is presented. The field analysis is based upon the numerical integration of the full incompressible stream function vorticity form of the Navier-Stokes equations, together with the energy equation over the rotor blade-to-blade stream channels. The numerical code used to solve the governing equations employs a nonorthogonal boundary fitted coordinate system that suits the most complicated blade geometries. A numerical scheme is used to carry out the necessary integration of the elliptic governing equations. The flow characteristics within the rotor of a radial inflow turbine are investigated over a wide range of operating conditions. The calculated results are compared to existing experimental data. The flow in a radial compressor is analyzed in order to study the behavior of viscous flow in diffusing cascades. The results are compared qualitatively to known experimental trends. The solution obtained provides insight into the flow phenomena in this type of turbomachine. It is concluded that the method of analysis is quite general and gives a good representation of the actual flow behavior within turbomachine passages. K.L.

N79-33432* General Dynamics/Convair, San Diego, Calif.
STUDY OF LIQUID AND VAPOR FLOW INTO A CENTAUR
CAPILLARY DEVICE

M. H. Blatt and J. A. Risberg Sep 1979 161 p refs
(Contract NAS3-20092)

(NASA-CR-159657; GDC-NAS-79-001) Avail: NTIS
HC A08/MF A01 CSCL 20D

The following areas of liquid and vapor flow were analyzed and experimentally evaluated: 1) the refilling of capillary devices with settled liquid, and 2) vapor flow across wetted screens. These investigations resulted in: 1) the development of a versatile computer program that was successfully correlated with test data and used to predict Centaur D-1S LO2 and LH2 start basket refilling; 2) the development of a semi-empirical model that was only partially correlated with data due to difficulties in obtaining repeatable test results. Also, a comparison was made to determine the best propellant management system for the Centaur D-1S vehicle. The comparison identified the baseline Centaur D-1S system (using pressurization, boost pumps and propellant settling) as the best candidate based on payload weight penalty. However, other comparison criteria and advanced mission condition were identified where pressure fed systems, thermally subcooled boost pumps and capillary devices would be selected as attractive alternatives.

RE S

A79-32912* Filtering of non-linear instabilities. P. K. Khosla and S. G. Rubin (New York, Polytechnic Institute, Farmingdale, N.Y.). *Journal of Engineering Mathematics*, vol. 13, Apr. 1979, p. 127-141, 10 refs. Grant No. NSG-1244.

For Courant numbers larger than one and cell Reynolds numbers larger than two, oscillations and in some cases instabilities are typically found with implicit numerical solutions of the fluid dynamics equations. This behavior has sometimes been associated with the loss of diagonal dominance of the coefficient matrix. It is shown here that these problems can in fact be related to the choice of the spatial differences, with the resulting instability related to aliasing or nonlinear interaction. Appropriate 'filtering' can reduce the intensity of these oscillations and in some cases possibly eliminate the instability. These filtering procedures are equivalent to a weighted average of conservation and non-conservation differencing. The entire spectrum of filtered equations retains a three-point character as well as second-order spatial accuracy. Burgers equation has been considered as a model. Several filters are examined in detail, and smooth solutions have been obtained for extremely large cell Reynolds numbers.

(Author)

A79-42890* Heat transfer from a row of jets impinging on concave semi-cylindrical surface. P. Hrycak (New Jersey Institute of Technology, Newark, N.J.). In: International Heat Transfer Conference, 6th, Toronto, Canada, August 7-11, 1978, General Papers, Volume 2 (A79-42886 15-34) Washington, D.C., Hemisphere Publishing Corp., 1978, p. 67-72, 27 refs. Grant No. NGR-31-009-004; Contract No. NAS3-11175.

Heat transfer from impinging jets has been analyzed. Based on similarities of the boundary conditions of the related flow fields, analogies between heat transfer from impinging jets at the stagnation point and in the wall jet region have been shown for several flow geometries. Calculation of heat transfer in the stagnation region and in the wall jet region, based on available theory and the parameters, obtained from direct measurements, have been carried out, for the single, round, impinging jets. It has been shown that heat transfer from a row of round jets impinging on flat and concave surfaces can be comprehensively described through analysis of impinging jets of simpler geometries. Finally, experimental results for the local and average heat transfer effects are presented and discussed. Comparisons are made with theory and results of other investigators, with fairly satisfactory agreement.

(Author)

35 INSTRUMENTATION AND PHOTOGRAPHY

Includes remote sensors, measuring instruments and gages, detectors, cameras and photographic supplies, and holography

For aerial photography see 43 *Earth Resources*. For related information see also 06 *Aircraft Instrumentation*, and 19 *Spacecraft Instrumentation*.

N79-12414* National Aeronautics and Space Administration, Lewis Research Center, Cleveland, Ohio

AN ELECTRO OPTIC, HIGH VOLTAGE, TRANSIENT PROBE

Stephan J. Posta and Charles J. Michels, Oct 1978, 13 p, refs

(NASA TM 79019, E-9588) Avail NTIS HC A02/MF A01 CSCL 14B

A newly developed electro optic voltage transducer is described. It is capable of measuring 30 ns rise time, floating or single ended, 0 to 20 kV transients in a high noise environment such as a fast discharge laser or energetic switch system. The voltage transient is detected by a specially developed resistor in series with a light emitting diode. The light output (proportional to voltage) is transmitted remotely via a fiber optic cable to a detector and recorder. Typical signals and comparison with commercial probe system signals are described. *A. Ithor*

N79-14345* National Aeronautics and Space Administration, Lewis Research Center, Cleveland, Ohio

INDICATED MEAN-EFFECTIVE PRESSURE INSTRUMENT

William J. Rice, inventor (to NASA), Issued 5 Sep 1978, 5 p, Filed 29 Sep 1977, Supersedes N77-32461 (15 - 23, p 3080)

(NASA Case-LEW-12661-1, US Patent-4,111,041, US Patent-Appl-SN-837796, US Patent-Class-73-115) Avail US Patent and Trademark Office CSCL 14B

An apparatus for measuring indicated mean effective pressure (IMEP) of an internal combustion piston or rotary engine or of an external combustion engine such as a Stirling engine is disclosed. An optical shaft encoder measures crankshaft angle of the engine. Changes in volume with respect to changes in crank angle of one or more cylinders ($dV/d\theta$) is determined either empirically or algebraically from engine geometry and stored in a memory. As the crank angle changes, $dV/d\theta$ is read from the memory and multiplied by chamber or cylinder pressure. The product ($P dV/d\theta$) is then added to the total previously accumulated in the cycle. Each time θ changes by an amount equal to 2π , the process is repeated. At the end of each engine cycle, the total is equal to the IMEP value for that cycle. *Official Gazette of the U.S. Patent and Trademark Office*

N79-14346* National Aeronautics and Space Administration, Lewis Research Center, Cleveland, Ohio

THERMOCOUPLES OF MOLYBDENUM AND IRIUM ALLOYS FOR MORE STABLE VACUUM-HIGH TEMPERATURE PERFORMANCE Patent

James F. Morris, inventor (to NASA), Issued 5 Sep 1978, 5 p, Filed 21 Nov 1977, Continuation-in-part of abandoned US Patent Appl. SN-667929, filed 18 Mar 1973

(NASA Case-LEW-12174-2, US Patent-4,111,718, US Patent-Appl-SN-853679, US Patent-Class-136-236, US Patent-Class-136-202, US Patent-Appl-SN-667929) Avail US Patent and Trademark Office CSCL 14B

Thermocouples providing stability and performance reliability in systems involving high temperatures and vacuums by employing a bimetallic thermocouple sensor are described. Each metal of the sensor is selected from a group of metals comprising molybdenum and iridium and alloys containing only those two metals. The molybdenum-iridium thermocouple sensor alloys provide bare metal thermocouple sensors having advantageous vapor pressure compatibility and performance characteristics.

The compatibility and physical characteristics of the thermocouple sensor alloys result in improved emf, temperature properties and thermocouple hot junction performance.

Official Gazette of the U.S. Patent and Trademark Office

N79-17192* National Aeronautics and Space Administration, Lewis Research Center, Cleveland, Ohio

FINE PARTICULATE CAPTURE DEVICE Patent

Victor S. Peterson and Robert D. Siewert, inventors (to NASA), Issued 16 Jan 1979, 4 p, Filed 8 Nov 1973, Supersedes N74-13199 (12 - 4, p 0420)

(NASA Case-LEW-11583-1, US Patent-4,134,744, US Patent-Appl-SN-414042, US Patent-Class-55-118, US Patent-Class-55-122, US Patent-Class-55-127, US Patent-Class-55-155, US Patent-Class-55-241, US Patent-Class-55-242, US Patent-Class-55-360, US Patent-Class-55-407) Avail US Patent and Trademark Office CSCL 14B

To capture fine particulate matter in a gas such as air, a dielectric fluid is directed to the center of whichever face of a rotating disc is exposed to the air flow. The disc is comprised of two or more segments which bear opposite electrostatic potentials. As the dielectric fluid is centrifuged towards the periphery of the rotating disc, the fluid becomes charged to the same potential as the segment over which it is passing. Particulate matter is attracted to the charged segment and is captured by the fluid. The fluid then carries the captured particulate matter to a collection device such as a toroidal container disposed around the periphery of the disc. A grounded electrically-conductive ring may be disposed at the outer periphery of the disc to neutralize the captured particles and the fluid before they enter the container.

Official Gazette of the U.S. Patent and Trademark Office

N79-17195* National Aeronautics and Space Administration, Lewis Research Center, Cleveland, Ohio

HOLOGRAPHY THROUGH OPTICALLY ACTIVE WINDOWS

Arthur J. Decker, Feb 1979, 18 p, refs
(NASA TP-1414, E-9808) Avail NTIS HC A02/MF A01 CSCL 14E

By using two orthogonally polarized reference beams, holograms can be recorded through stressed windows and the reconstructed virtual image will show no stress pattern. As shown analytically, the stress-pattern-free hologram is recordable for any polarization state of the object illumination. Hence, the more efficient nondepolarizing diffuser can be used in performing holography through stressed windows if two reference beams are used. Results are presented for a pair of machined polysulfone windows intended for use in a holographic flow-visualization setup in a single-stage compressor test rig. *Author*

N79-22448* National Aeronautics and Space Administration, Lewis Research Center, Cleveland, Ohio

MEASURING UNSTEADY PRESSURE ON ROTATING COMPRESSOR BLADES

David R. Englund, Howard P. Grant (Pratt and Whitney Aircraft, East Hartford, Conn.), and George A. Lanati (Pratt and Whitney Aircraft, East Hartford, Conn.), 1979, 28 p, refs. Presented at the 25th Intern. Instrumentation Symp., Anaheim, Calif., 7-10 May 1979, sponsored by the Instr. Soc. of Am.
(NASA TM-79159, E-015) Avail NTIS HC A03/MF A01 CSCL 14B

Miniature semiconductor strain gage pressure transducers mounted in several arrangements were studied. Both surface mountings and recessed flush mountings were tested. Test parameters included mounting arrangement, blade material, temperature, local strain in the acceleration normal to the transducer diaphragm, centripetal acceleration, and pressure. Test results show no failures of transducers or mountings and indicate an uncertainty of unsteady pressure measurement of approximately ± 6 percent ± 0.1 kPa for a typical application. Two configurations were used on a rotating fan flutter program. Examples of transducer data and correction factors are presented. *Author*

N79-27480* National Aeronautics and Space Administration, Lewis Research Center, Cleveland, Ohio.
EVALUATION OF MINIATURE SINGLE-WIRE SHEATHED THERMOCOUPLES FOR TURBINE BLADE TEMPERATURE MEASUREMENT
 Raymond Hollanda Jun. 1979 20 p refs
 (NASA-TM-79173; E-068) Avail. NTIS HC A02/MF A01 CSCL 09A

Chromel Alumel thermocouples were used, with sheath diameters of 0.15 and 0.25 mm. Tests were conducted at temperatures ranging from 750 to 1250 K. Both steady state and thermal cycling tests were performed for times up to 200 hours. Initial testing was performed in a low velocity gas stream for long time periods using a Meker-type burner. Additional testing was done in a high velocity gas stream for short time periods using a hot gas tunnel and also in a J75 jet engine. A total of eleven 0.15 mm diameter thermocouples and six 0.25 mm diameter thermocouples were tested. Drift rates up to 2.5% in 10 hours were observed. Photomicrographs show that this design is near the limit of miniaturization based on present manufacturing capabilities. Results indicate that the effects of miniaturization on reliability and accuracy must be considered when choosing thermocouples for a particular application. S.E.S.

A79-10800* Pressure instrumentation for gas turbine engines - A review of measurement technology. E. C. Armentrout (NASA, Lewis Research Center, Cleveland, Ohio) and J. C. Kicks (Kulite Semiconductor Products, Inc., Bridgfield, N.J.). *American Society of Mechanical Engineers, Gas Turbine Conference and Products Show, London, England, Apr. 9-13, 1978, Paper 78-GT-148*, 11 p. 50 refs. Members, \$1.50; nonmembers, \$3.00.

Many types and designs of pressure measuring instrumentation are used during the development and testing of gas turbine engines. This paper provides an overview of more commonly available pressure transducers and their characteristics. Probe designs for use in both steady state and dynamic pressure measurement systems are reviewed. Techniques used to qualify instrument probes and the methods used to calibrate pressure transducers during engine testing are described. (Author)

A79-10992* Auger spectroscopy analysis in adhesion, friction and wear studies. D. H. Buckley (NASA, Lewis Research Center, Cleveland, Ohio). *International Advances in Nondestructive Testing*, vol. 5, 1977, p. 303-320, 18 refs.

The paper reviews the current use of Auger electron spectroscopy in adhesion, friction, wear and lubrication studies. Conventional Auger spectroscopy is adopted to complement LEED studies of the adhesion of metal single crystals. In addition, Auger cylindrical mirror analysis is applied to the study of changes in surface chemistry during dynamic friction and wear experiments on polycrystalline metals and alloys. Important conclusions are that (1) segregation of alloying elements to the surface of metals can alter adhesion behavior, (2) hydrocarbons are adsorbed readily to clean iron surfaces at 23 C, (3) transfer from one surface to another for dissimilar materials in contact can be followed in sliding or rubbing friction studies, and (4) the friction process can enhance surface activity for metals with hydrocarbons. S.D.

A79-15067* Global sensing of gaseous and aerosol trace species using automated instrumentation on 747 airliners. P. J. Perkins and L. C. Papathakos (NASA, Lewis Research Center, Cleveland, Ohio). In: *Joint Conference on Sensing of Environmental Pollutants*, 4th, New Orleans, La., November 6-11, 1977, Proceedings. (A79-15023/4-45) Washington, D.C., American Chemical Society, 1978, p. 307-312, 8 refs.

The Global Atmospheric Sampling Program (GASP) is collecting and analyzing data on gaseous and aerosol trace contaminants in the upper troposphere and lower stratosphere. Measurements are obtained from automated systems installed on four 747 airliners flying global air routes. Improved instruments and analysis techniques are providing an expanding data base for trace species including ozone,

carbon monoxide, water vapor, condensation nuclei, and mass concentration of sulfates and nitrates. Simultaneous measurements of several trace species obtained frequently can be used to identify the source of the air mass as being typically tropospheric or stratospheric. B.J.

A79-20742* Improved apparatus for trapped radical and other studies down to 1.5 K. J. A. Woollam and K. Sugawara (NASA, Lewis Research Center, Cleveland, Ohio). *Review of Scientific Instruments*, vol. 49, Dec. 1978, p. 1745.

A Dewar system and associated equipment for electron paramagnetic resonance (EPR) studies of trapped free radicals and other optical or irradiation experiments are described. The apparatus is capable of reaching a temperature of 1.5 K and transporting on the order of 20 W per K temperature gradient. Its principal advantages are for use at pumped cryogen temperatures and for experiments with large heat inputs. Two versions of the apparatus are discussed, one of which is designed for EPR in a rectangular cavity operating in a TE(102) mode and another in which EPR is performed in a cylindrical microwave cavity. F.G.M.

N79-12418* Pratt and Whitney Aircraft, East Hartford, Conn. Commercial Products Div.

INSTRUMENTATION FOR MEASURING THE DYNAMIC PRESSURE ON ROTATING COMPRESSOR BLADES
Final Report

H. P. Grant and George A. Lanati Sep 1978 182 p
 (Contract NAS3-20296)

(NASA CR 159466, PWA-5558-12) Avail. NTIS
 HC A09/MF A01 CSCL 14B

To establish the capability for measurement of oscillatory pressure on rotating blades, miniature fast response semiconductor strain gage pressure transducers (2mm x 0.33mm) were mounted in several configurations on thin titanium and steel compressor blades and subjected to pressure cycles from 1 to 310 kPa during static tests and spin tests. Static test conditions included 20 C to 150 C, 0 to 3000 tensile microstrain, -1000 to +1000 bending microstrain and + or - 650G vibration. The spin test conditions included 20 C to 82 C at 0 to 90,000G. Durability was excellent. Pressure transducer sensitivity changed by only a few percent over this range of environmental conditions. Noise signal due to oscillatory acceleration normal to the diaphragm was acceptable (0.33Pa/G). Noise signal due to oscillatory strain was acceptable (0.5 Pa/microstrain) when the transducer was mounted on a 0.05mm rubber pad, with a total buildup of 0.38mm on the measure surface. Back mounting or partial recessing to eliminate buildup, increased the strain effect to 1.2 Pa/microstrain. Flush mounting within the blade to eliminate buildup reduced the strain effect, but required development of a special transducer shape. This transducer was not available in time for spin tests. Unpredictable zero drift + or - 14 kPa ruled out the use of these mounting arrangements for accurate steady state (D.C.) measurements on rotating blades. The two best configurations fully developed and spin tested were then successfully applied in the NAS3-20606 rotating fan flutter program for quantitative measurement of oscillatory pressure amplitudes. Author

N79-19314* Pratt and Whitney Aircraft, East Hartford, Conn. Commercial Products Div.

STRAIN GAGE SYSTEM EVALUATION PROGRAM
Final Report

G. W. Dolleris, H. J. Mazur, and E. Kokoszka, Jr. Dec. 1978 126 p

(Contract NAS3-20298)
 (NASA CR 159486, PWA-5615-3) Avail. NTIS
 HC A07/MF A01 CSCL 14B

A program was conducted to determine the reliability of various strain gage systems when applied to rotating compressor blades in an aircraft gas turbine engine. A survey of current technology strain gage systems was conducted to provide a basis for selecting candidate systems for evaluation. Testing and evaluation was conducted in an F 100 engine. Sixty strain gage systems of seven different designs were installed on the first

and third stages of an F 100 engine fan. Nineteen strain gage failures occurred during 62 hours of engine operation, for a survival rate of 68 percent. Of the failures, 16 occurred at blade-to-disk leadwire jumps (84 percent), two at a leadwire splice (11 percent), and one at a gage splice (5 percent). Effects of erosion, temperature, G-loading, and stress levels are discussed. Results of a post-test analysis of the individual components of each strain gage system are presented. M.M.

N79-21329* National Aeronautics and Space Administration, Lewis Research Center, Cleveland, Ohio.

SIMULATED ELECTRONIC HETERODYNE RECORDING AND PROCESSING OF PULSED-LASER HOLOGRAMS

Arthur J. Decker Apr 1979 40 p refs

(NASA-TP 1444, E-9813) Avail: NTIS HC A03/MF A01 CSCL 14E

The electronic recording of pulsed-laser holograms is proposed. The polarization sensitivity of each resolution element of the detector is controlled independently to add an arbitrary phase to the image waves. This method which can be used to simulate heterodyne recording and to process three-dimensional optical images, is based on a similar method for heterodyne recording and processing of continuous wave holograms. A.R.H.

N79-26384* Mathematical Sciences Northwest, Inc., Bellevue, Wash.

DESIGN INVESTIGATION OF SOLAR POWERED LASERS FOR SPACE APPLICATIONS Final Report

R. Taussig, C. Bruzzone, D. Quimby, L. Nelson, W. Christiansen, S. Neice, P. Cassidy, and A. Pindroh May 1979 184 p refs (Contract NAS3-21134)

(NASA CR 159554, MSNW 79-1087/1090-1) Avail: NTIS HC A09/MF A01 CSCL 20E

The feasibility of solar powered lasers for continuous operation in space power transmission was investigated. Laser power transmission in space over distances of 10 to 100 thousand kilometers appears possible. A variety of lasers was considered, including solar-powered GDLs and EDLs, and solar-pumped lasers. An indirect solar-pumped laser was investigated which uses a solar-heated black body cavity to pump the laser. Efficiencies in the range of 10 to 20 percent are projected for these indirect optically pumped lasers. G.Y.

N79-27478* Creare, Inc., Hanover, NH.

DESIGN, DEVELOPMENT, AND TEST OF A LASER VELOCIMETER FOR A SMALL 8:1 PRESSURE RATIO CENTRIFUGAL COMPRESSOR Final Report

Francis X. Dolan and Peter W. Runstadler, Jr. Mar 1979 206 p refs

(Contract NAS3-17860)

(NASA CR 134781, Creare TN-289)

Avail: NTIS

HC A10/MF A01 CSCL 14E

The instrument was designed as a diagnostic tool for the basic fluid dynamics of the inducer, impeller, and diffuser regions of this type compressor. The LV instrumentation was optimized to measure instantaneous velocities up to approximately 500 m/s, measured in absolute coordinates within the rotating compressor impeller and in the two dimensional radial plane of the diffuser. Some measurements were made within the diffuser and the impeller inlet flows; however, attempts to make detailed measurements of the velocity field were not successful. Difficulties in maintaining high seed particle rates within the probe volume and the improper operation of the blade gating optics may explain the lack of success. Recommendations are made to further pursue these problems. At 100% speed the stage attained a total static pressure ratio of 7.5:1 at 75% total static efficiency. Flow range from choke to surge was 6.8% of choking mass flow rate. Performance was lower than the design intent of 8:1 pressure ratio at 77% efficiency and 12% flow range. Detailed measurements of the stage components are presented which show the reasons for the stage performance deficiencies. S.E.S.

A79-38738* Fiber optic sensors for military, industrial and commercial applications. K. A. James, W. H. Quick, and V. H. Strahan (Rockwell International Corp., Electronics Research Center, Anaheim, Calif.). In: ITC/USA/'78, Proceedings of the International Telemetry Conference, Los Angeles, Calif., November 14-16, 1978. (A79-38676 16-32) Pittsburgh, Pa., Instrument Society of America, 1978, p. 777-782. Contract No. NAS3-21005.

Four examples of specific fiber optic sensor system designs, each of which demonstrates a different optical modulation format, are described. The birefringent temperature transducer illustrates direct digital signal modulation. The temperature/pressure dependent semiconductor filter illustrates high-pass optical wavelength signal encoding. The coupled polarized-mode transducer shows how a solid-state sensor can produce narrow-bandpass optical wavelength signal encoding. The luminescent temperature sensor illustrates a way to construct a solid state sensor in order to produce pulse width modulation of an optical signal. B.J.

36 LASERS AND MASERS

Includes parametric amplifiers.

A79-19078 * Gain measurements of the Ca-Xe charge exchange system. C. J. Michels and D. L. Chubb (NASA, Lewis Research Center, Cleveland, Ohio). *Journal of Applied Physics*, vol. 49, Oct. 1978, p. 5084-5092. 16 refs.

Charge-exchange-pumped $\text{Ca}(+)$ was studied for possible positive laser gain at 370.6 and 315.9 nm using an Xe MPD arc as the $\text{Xe}(+)$ source. The present paper describes the MPD arc, the calcium injection system, the diagnostics for gain, and spontaneous emission measurements and results. No positive gain measurements were observed. A small Xe-Ca charge exchange cross section compared to He-metal laser systems charge exchange cross sections is the most probable reason why the result was negative. B.J.

N79-21334*# Lockheed Missiles and Space Co., Palo Alto, Calif. Research Lab

LASER POWER CONVERSION SYSTEM ANALYSIS, VOLUME 1 Final Report, 26 Sep. 1977 - 26 Sep. 1978

W. S. Jones, L. L. Morgan, J. B. Forsyth, and J. P. Skratt 15 Mar. 1979 109 p refs

(Contract NAS3-21137)

(NASA-CR-159523-Vol. 1 LMSC-D673466-Vol. 1) Avail NTIS HC A06/MF A01 CSCL 20E

The orbit-to-orbit laser energy conversion system analysis established a mission model of satellites with various orbital parameters and average electrical power requirements ranging from 1 to 300 kW. The system analysis evaluated various conversion techniques, power system deployment parameters, power system electrical supplies and other critical supplies and other critical subsystems relative to various combinations of the mission model. The analysis shows that the laser power system would not be competitive with current satellite power systems from weight, cost and development risk standpoints. Author

N79-21335*# Lockheed Missiles and Space Co., Palo Alto, Calif. Research Lab

LASER POWER CONVERSION SYSTEM ANALYSIS, VOLUME 2 Final Report, 26 Sep. 1977 - 26 Sep. 1978

W. S. Jones, L. L. Morgan, J. B. Forsyth, and J. P. Skratt 15 Mar. 1979 112 p refs

(Contract NAS3-21137)

(NASA-CR-159523-Vol. 2 LMSC-D673466-Vol. 2) Avail NTIS HC A06/MF A01 CSCL 20E

The orbit-to-ground laser power conversion system analysis investigated the feasibility and cost effectiveness of converting solar energy into laser energy in space, and transmitting the laser energy to earth for conversion to electrical energy. The analysis included space laser systems with electrical outputs on the ground ranging from 100 to 10,000 MW. The space laser power system was shown to be feasible and a viable alternate to the microwave solar power satellite. The narrow laser beam provides many options and alternatives not attainable with a microwave beam. Author

N79-21337*# Lockheed Missiles and Space Co., Sunnyvale, Calif. Research Lab

LASER ROCKET SYSTEM ANALYSIS Final Report, 27 Sep. 1978 - 27 Sep. 1978

W. S. Jones, J. B. Forsyth, and J. P. Skratt 15 Mar. 1979 198 p refs

(Contract NAS3-20372)

(NASA-CR-159521 LMSC-D564671A) Avail NTIS HC A09/MF A01 CSCL 20E

The laser rocket systems investigated in this study were for orbital transportation using space-based, ground-based and airborne laser transmitters. The propulsion unit of these systems utilizes a continuous wave (CW) laser beam focused into a thrust chamber which initiates a plasma in the hydrogen propellant, thus heating the propellant and providing thrust through a

suitably designed nozzle and expansion skirt. The specific impulse is limited only by the ability to adequately cool the thruster and the amount of laser energy entering the engine. The results of the study showed that, with advanced technology, laser rocket systems with either a space- or ground-based laser transmitter could reduce the national budget allocated to space transportation by 10 to 345 billion dollars over a 10-year life cycle when compared to advanced chemical propulsion systems (LO2-LH2) of equal capability. The variation in savings depends upon the projected mission model. LS

N79-32538*# Rockwell International Corp., Anaheim, Calif. **HIGH POWER PHASE LOCKED LASER OSCILLATORS Final Report**

C. L. Hayes, C. L. Telk, J. Soohoo, and W. C. Davis May 1979 103 p refs

(Contract NAS3-20376)

(NASA-CR-159630 C76-1555/501)

Avail NTIS

HC A06/MF A01 CSCL 20E

The feasibility of mechanizing an adaptive array of independent laser oscillators for generation of a high power coherent output was experimentally investigated. Tests were structured to evaluate component/system requirements for delivery of energy to a low-earth orbit satellite. Initial experiments addressed the control issues of phase locking unstable resonators at low power levels. A successful phase lock demonstration formed the basis for the design and fabrication of the high power, water-cooled, control mirror subsequently installed in the NASA LeRC high power laser. Tests were performed to characterize the operational limits of the laser system and included quantitative assessment of the frequency stability, noise sources, and optical properties of the beam. Author

A79-32981 * Simmer-enhanced flashlamp-pumped dye laser.

T. K. Yee, T. K. Gustafson (California, University, Berkeley, Calif.), and B. Fan (IBM Thomas J. Watson Research Center, Yorktown Heights, N.Y.). *Applied Optics*, vol. 18, Apr. 15, 1979, p. 1131, 1132. Grants No. DAHCO4-75-C-0095; No. NSG-2151.

It has been demonstrated experimentally that by enhancing the simmer current in the flash lamps before the energy discharge, the lamp inductance is reduced and the dye laser efficiency is thus remarkably improved. This technique has advantages over the prepulsing technique for conditioning flash lamps: the electronic circuit for the simmer enhancement is simple, inexpensive and reliable, and accurate timing is not required. Furthermore, the simmer enhancement consumes much less power, thus minimizing the attendant thermal effects and improving overall laser efficiency. B.J.

A79-38202 * Solar pumped lasers for space power trans-

mission. R. Taussig, C. Bruzzone, L. Nelson, D. Quimby (Mathematical Sciences Northwest, Inc., Bellevue, Wash.), and W. Christiansen (Washington, University, Seattle, Wash.) *American Institute of Aeronautics and Astronautics, Terrestrial Energy Systems Conference, Orlando, Fla., June 4-6, 1979, Paper 79-1015* 18 p. 40 refs. Contract No. NAS3-21134.

Multi-Megawatt CW solar pumped lasers appear to be technologically feasible for space power transmission in the 1990s time frame. A new concept for a solar pumped laser is presented which utilizes an intermediate black body cavity to provide a uniform optical pumping environment for the laser, either CO or CO₂. Reradiation losses are minimized with resulting high efficiency operation. A 1 MW output laser may weigh as little as 8000 kg including solar collector, black body cavity, laser cavity and ducts, pumps, power systems and waste heat radiator. The efficiency of such a system will be on the order of 10 to 20%. Details of the new concept, laser design, comparison to competing solar powered lasers and applications to a laser solar power satellite (SPS) concept are presented. (Author)

37 MECHANICAL ENGINEERING

Includes auxiliary systems (non-power), machine elements and processes, and mechanical equipment.

N79-10418* National Aeronautics and Space Administration
Lewis Research Center, Cleveland, Ohio

CANTILEVER MOUNTED RESILIENT PAD GAS BEARING Patent

Izhak Etsion, inventor (to NASA) (NAS-NRC, Washington, D.C.)
Issued 11 Jul 1978 6 p Filed 28 Apr 1977 Supersedes
N77 24496 (15 15 p 1998) Sponsored by NASA
(NASA Case LEW 12569-1, US Patent 4,099,799,
US Patent Appl-SN-792069, US Patent Class 308-5R,
US Patent Class 308-9, US Patent Class 308-121,
US Patent Class 308-160, US Patent Class 308-163,
US Patent Class 308-172, US Patent Class 308 DIG 1) Avail
US Patent Office CSCL 11A

A gas lubricated bearing is described, employing at least one pad mounted on a rectangular cantilever beam to produce a lubricating wedge between the face of the pad and a moving surface. The load-carrying and stiffness characteristics of the pad are related to the dimensions and modulus of elasticity of the beam. The bearing is applicable to a wide variety of types of hydrodynamic bearings. Official Gazette of the U.S. Patent Office

N79-10424* National Aeronautics and Space Administration
Lewis Research Center, Cleveland, Ohio

COMPRESSIBLE FLOW ACROSS NARROW PASSAGES; COMPARISON OF THEORY AND EXPERIMENT FOR FACE SEALS

Gordon P. Allen, Donald W. Wisander, and William F. Hady
Nov 1978 19 p refs
(NASA TP 1346, E 9120) Avail NTIS HC A02/MF AC1 CSCL 11A

Computer calculation for determining compressible flow across radial face seals were compared with measured results obtained in a seal simulator rig at pressure ratios to 0.9 (ambient pressure/seal pressure). In general, the measured and calculated leakages across the seal rim agreed within 3 percent. The resultant loss coefficient, dependent upon the pressure ratio, ranged from 0.47 to 0.58. The calculated pressures were within 2.5 N/cm² of the measured values. G G

N79-10425* National Aeronautics and Space Administration
Lewis Research Center, Cleveland, Ohio

ANISOTROPIC FRICTION AND WEAR OF SINGLE-CRYSTAL

Kazuhisa Miyoshi (Kanazawa Univ., Japan) and Donald H. Buckley
Oct 1978 23 p refs
(NASA TP 1339, E 9673) Avail NTIS HC A02/MF A01 CSCL 20L

Sliding friction experiments were conducted with manganese zinc ferrite (100), (110), (111), and (211) planes in contact with themselves. Mating the highest atomic density directions (110) of matched crystallographic planes resulted in the lowest coefficients of friction. Mating matched (same) high atomic density planes and matched (same) crystallographic directions resulted in low coefficients of friction. Mating dissimilar crystallographic planes, however, did not give significantly different friction results from those with matched planes. Sliding caused cracking and the formation of hexagonal and rectangular platelet wear debris on ferrite surfaces, primarily from cleavage of the (110) planes. Author

N79-10426* National Aeronautics and Space Administration
Lewis Research Center, Cleveland, Ohio

FREE PISTON REGENERATIVE HOT GAS HYDRAULIC ENGINE Patent Application

Donald G. Baremand, inventor (to NASA) Filed 12 Oct 1978
21 p

(NASA Case LEW 12274-1, US Patent Appl-SN-950876) Avail
NTIS HC A02/MF A01 CSCL 13I

A free piston, regenerative, hydraulic engine is described, including displacer piston which is driven by a high pressure or low pressure gas. Actuation of the displacer piston circulates the working fluid through a heater, a regenerator, and a cooler. This invention includes an inertial mass, such as a piston or a hydraulic fluid column to effectively store and supply energy during portions of the cycle. Power is transmitted from the working fluid to a hydraulic fluid across a diaphragm or lightweight piston to achieve a hydraulic power output. The displacer piston may be driven pneumatically, hydraulically, or electromagnetically. The displacer piston and the inertial mass may be positioned on the same side of the diaphragm member or may be separated by the diaphragm member. NASA

N79-11403* National Aeronautics and Space Administration
Lewis Research Center, Cleveland, Ohio

FUEL DELIVERY SYSTEM INCLUDING HEAT EXCHANGER MEANS Patent

George A. Coffinberry, inventor (to NASA) (G.E., Cincinnati, Ohio)
Issued 8 Aug 1978 6 p Filed 29 Nov 1976 Sponsored by NASA

(NASA Case LEW 12793-1, US Patent 4,104,873,
US Patent Appl-SN 745766, US Patent Class 60-39 28R,
US Patent Class 60-39 08, US Patent Class 60-39 66) Avail
US Patent Office CSCL 13I

A fuel delivery system is presented wherein first and second heat exchanger means are each adapted to provide the transfer of heat between the fuel and a second fluid such as lubricating oil associated with the gas turbine engine. Valve means are included which are operative in a first mode to provide for flow of the second fluid through both first and second heat exchanger means and further operative in a second mode for bypassing the second fluid around the second heat exchanger means.

Official Gazette of the U.S. Patent Office

N79-12445* National Aeronautics and Space Administration
Lewis Research Center, Cleveland, Ohio

SELF-STABILIZING RADIAL FACE SEAL Patent Application

I. Etsion, inventor (to NASA) (Technion Research and Development Foundation, Haifa, Israel) Filed 17 Nov 1978 15 p Sponsored by NASA

(NASA Case LEW 12991-1, US Patent Appl-SN 961832) Avail
NTIS HC A02/MF A01 CSCL 11A

A self-stabilizing radial face seal is reported that consists of a primary seal ring juxtapositioned to a seal seat. The seal seat is provided with a porous ring-like circumferential structure which allows for the fluid pressure in the system to reach equilibrium. A cavity behind the porous ring provides a constant pressure reservoir. NASA

N79-13369* National Aeronautics and Space Administration
Lewis Research Center, Cleveland, Ohio

PERFORMANCE OF A NASVYTIS MULTIROLLER TRACTION DRIVE

Stuart H. Loewenthal, Neil E. Anderson (AVRADCOM Res. and Technol. Labs.), and Algirdas L. Nasvytis (Transmission Res., Inc.)
Nov 1978 36 p refs
(NASA TP 1378, E-9632, AVRADCOM TR-78-36) Avail NTIS
HC A03/MF A01 CSCL 13I

Tests were conducted to determine the operational and performance characteristics of a high-speed, 14.7-to-1 fixed-ratio Nasvytis Multiroller Traction Drive at speeds to 73,000 rpm and power levels to 127 kW (170 hp). The test drive was arranged in a single-stage planetary configuration with two rows of stepped planet rollers contained between concentric sun and ring rollers. It was lubricated with a traction fluid. Two drives were tested concurrently in a back-to-back arrangement. They exhibited good performance and operated smoothly, with a nominal peak efficiency of 95 percent. Variations of the design traction coefficient imposed by the automatic roller-loading device

of 0.039, 0.048, and 0.057 seemed to have relatively little effect on any of the operating variables. Author

N79-14386* National Aeronautics and Space Administration, Lewis Research Center, Cleveland, Ohio.
FRICITION AND TRANSFER OF COPPER, SILVER, AND GOLD TO IRON IN THE PRESENCE OF VARIOUS ADSORBED SURFACE FILMS

Donald H. Buckley Jan 1979 19 p refs
(NASA-TP-1392, E-9684) Avail: NTIS HC A02/MF A01 CSCL 20K

Sliding friction experiments were conducted with the noble metals copper, silver, and gold and two binary alloys of these metals contacting iron in the presence of various adsorbates including oxygen, methyl mercaptan, and methyl chloride. A pin on disk specimen configuration was used with a load of 100 grams, sliding velocity of 60 mm/min, at 25 C with the surfaces saturated with the adsorbates. Auger emission spectroscopy was used to monitor surface films. Results of the experiments indicate that friction and transfer characteristics are highly specific with respect to both the noble metal and surface film present. With all three metals and films transfer of the noble metal to iron occurred very rapidly. With all metals and films transfer of the noble metal to iron continuously increased with repeated passes except for silver and copper sliding on iron sulfide.

Author

N79-14387* National Aeronautics and Space Administration, Lewis Research Center, Cleveland, Ohio.

FRICITION AND WEAR CHARACTERISTICS OF IRON-CHROMIUM ALLOYS IN CONTACT WITH THEMSELVES AND SILICON CARBIDE

Kazuhisa Miyoshi and Donald H. Buckley Jan 1979 23 p refs
(NASA-TP-1387, E-9670) Avail: NTIS HC A02/MF A01 CSCL 20K

Sliding friction experiments were conducted with various iron-chromium alloys in contact with (1) themselves, (2) single crystal silicon carbide disks, and (3) single crystal abrasive grit of silicon carbide. Results indicate the coefficients of friction for the alloys sliding against themselves are between those for pure iron and pure chromium, and are only slightly different with 1, 5, 9, 14, and 19 weight percent chromium in iron. The wear is due, primarily, to shearing, or tearing fracture, of the cohesive bonds in the bulk metal and plowing of the bulk by lumps of wear debris. There are only slight differences in the coefficients of friction for the various alloys when sliding on silicon carbide. The coefficient of friction for the alloys are higher than those for pure iron and pure chromium. Alloy hardening observed in the alloys plays a dominant role in controlling the abrasive friction and wear behavior of the alloys. Author

N79-14389* National Aeronautics and Space Administration, Lewis Research Center, Cleveland, Ohio.

EVALUATION OF CBS 600 CARBURIZED STEEL AS A GEAR MATERIAL

Dennis P. Townsend, Richard J. Parker, and Erwin V. Zaritsky Jan 1979 27 p refs
(NASA-TP-1390, E-9651) Avail: NTIS HC A03/MF A01 CSCL 131

Gear endurance tests were conducted with one lot of consumable-electrode vacuum-melted (CVM) AISI 9310 gears and one lot of air-melt CBS 600 gears. The gears were 8 pitch with a pitch diameter of 8.89 centimeters (3.5 in.). Bench-type rolling element fatigue tests were also conducted with one lot of CVM AISI 9310, three lots of CVM CBS 600, and one of air-melt CBS 600 material. The rolling element bars were 0.952 centimeter (0.375 in.) in diameter. The CBS 600 material exhibited pitting fatigue lives in both rolling element specimens and gears at least equivalent to that of CVM AISI 9310. Tooth fracture failure occurred with the CBS 600 gears after overrunning a fatigue spall, but it did not occur with the CVM AISI 9310 gears. Tooth fracture in the CBS 600 was attributed to

excessive carbon content in the case, excessive case depth, and a higher than normal core hardness. Author

N79-17227* National Aeronautics and Space Administration, Lewis Research Center, Cleveland, Ohio.

FRICITION AND WEAR WITH A SINGLE-CRYSTAL ABRASIVE GRIT OF SILICON CARBIDE IN CONTACT WITH IRON-BASE BINARY ALLOYS IN OIL: EFFECTS OF ALLOYING ELEMENT AND ITS CONTENT

Kazuhisa Miyoshi (Kanazawa Univ., Japan) and Donald H. Buckley Feb. 1979 19 p
(NASA-TP-1394, E-9765) Avail: NTIS HC A02/MF A01 CSCL 20K

Sliding friction experiments were conducted with various iron-base binary alloys (alloying elements were Ti, Cr, Mn, Ni, Rh, and W) in contact with a rider of 0.025-millimeter-radius, single-crystal silicon carbide in mineral oil. Results indicate that atomic size and content of alloying element play a dominant role in controlling the abrasive-wear and friction properties of iron-base binary alloys. The coefficient of friction and groove height (wear volume) general alloy decrease, and the contact pressure increases in solute content. There appears to be very good correlation of the solute to iron atomic radius ratio with the decreasing rate of coefficient of friction, the decreasing rate of groove height (wear volume), and the increasing rate of contact pressure with increasing solute content C. Those rates increase as the solute to iron atomic radius ratio increases from unity.

LS

N79-18318* National Aeronautics and Space Administration, Lewis Research Center, Cleveland, Ohio.

COMPOSITE SEAL FOR TURBOMACHINERY Patent

Robert C. Bill and Lawrence P. Ludwig, inventors (to NASA) Issued 23 Jan 1979 5 p. Filed 27 May 1977 Supersedes N77-24498 (15 15 p 1999)
(NASA Case LEW-12131-1 US Patent 4,135,851, US Patent Appl-SN 801290, US Patent Class 415 174 US Patent Class 415 200) Avail: US Patent and Trademark Office CSCL 11A

A gas path seal suitable for use with a turbine engine or compressor is provided. A shroud wearable or abradable by the abrasion of the rotor blades of the turbine or compressor protects the rotor blades. A compliant backing surrounds the shroud. The backing may be made of corrugated sheets or the like with adjacent layers having offset corrugations, with axes of the folds parallel to the rotor axis. The sheets may be bonded together at points of contact by brazing, welding or the like. In another embodiment a compliant material is covered with a thin ductile layer. A mounting fixture surrounds the backing.

Official Gazette of the U.S. Patent and Trademark Office

N79-18323* National Aeronautics and Space Administration, Lewis Research Center, Cleveland, Ohio.

OPERATING CHARACTERISTICS OF A LARGE BORE ROLLER BEARING TO SPEEDS OF 3 TIMES 10 TO THE 6TH POWER DN

Fredrick T. Schuller Feb. 1979 32 p refs
(NASA-TP-1413, E-9657) Avail: NTIS HC A03/MF A01 CSCL 131

A 118 millimeter bore roller bearing was studied parametrically at speeds from 10,000 to 25,500 rpm. The bearing had a round outer ring (not preloaded) and provisions were made for lubrication and cooling through the inner ring. In some tests the outer ring was also cooled. The bearing ran successfully at 300,000 DN with very small evidence of cage slip. Load, which was varied from 2200 to 8900 newtons (500 to 2000 lb), had no effect on bearing temperature or cage slip over the speed range tested. Bearing temperature varied inversely with cage slip for all test conditions. Cooling the outer ring decreased its temperature but increased the inner ring temperature. Heat rejected to the lubricant (power loss within the bearing) increased with both shaft speed and total oil flow rate to the inner ring. Author

N79-22475* National Aeronautics and Space Administration
Lewis Research Center, Cleveland, Ohio.

SHAFT SEAL ASSEMBLY FOR HIGH SPEED AND HIGH PRESSURE APPLICATIONS Patent

William F. Hadt and Lawrence P. Ludwig, inventors (to NASA)
Issued 20 Mar. 1979 7 p. Filed 8 Jul. 1977 Supersedes
N77-27404 (15 - 18, p. 2390)

(NASA-Case-LEW-11873-1; US-Patent-4,145,058;

US-Patent-Appl-SN-814006; US-Patent-Class-277-62;

US-Patent-Class-277-96 1) Avail: US Patent and Trademark
Office CSCL 11A

A seal assembly is provided for reducing the escape of fluids from between a housing and a shaft rotably mounted in the housing. The seal assembly comprises a pair of seal rings resiliently connected to each other and disposed in side-by-side relationship. In each seal ring, both the internal bore surface and the radial face which faces away from the other seal ring are provided with a plurality of equi-spaced recesses. The seal faces referred to are located adjacent a seating surface of the housing. Under normal operating conditions, the seal assembly is stationary with respect to the housing, and the recesses generate life, keep the assembly spaced from the rotating shaft and allow slip therebetween. The seal assembly can seize on the shaft, and slip will then occur between the radial faces and the housing.

Official Gazette of the U.S. Patent and Trademark Office

N79-22518* National Aeronautics and Space Administration
Lewis Research Center, Cleveland, Ohio

OPERATING CHARACTERISTICS OF A CANTILEVER-MOUNTED RESILIENT-PAD GAS LUBRICATED THRUST BEARING

Zoltan N. Nemeth, Washington, Apr. 1979 30 p. refs.
(NASA-TP-1438 E 9815) Avail: NTIS HC A03/MF A01 CSCL 131

A resilient-pad gas thrust bearing consisting of pads mounted on cantilever beams was tested to determine its operating characteristic. The bearing was run at a thrust load of 74 newtons to a speed of 17000 rpm. The pad film thickness and bearing friction torque were measured and compared with theory. The measured film thickness was less than that predicted by theory. The bearing friction torque was greater than that predicted by theory.

Author

N79-22519* National Aeronautics and Space Administration
Lewis Research Center, Cleveland, Ohio

COMPARISON OF ANALYSIS AND EXPERIMENT FOR SELF-ACTING SEALS FOR LIQUID-OXYGEN TURBOPUMPS

Gordon P. Allen, Apr. 1979 15 p. refs.
(NASA-TP-1443 E 9806) Avail: NTIS HC A02/MF A01 CSCL 131

Two LOX turbopump applications were analyzed over ranges of pressure differential and speed. Predictions were compared with test results. A small seal was analyzed up to 161 in/sec and 310 N/sq cm differential and a larger seal up to 147 m/sec and 448 N/sq cm. Tests confirmed analytical predictions of operation without rubbing contact. The seals evidently operated with mostly liquid in the pads and mostly gas across the dam although the best prediction of trends was based on assuming gas throughout the entire seal.

Author

N79-23430* National Aeronautics and Space Administration
Lewis Research Center, Cleveland, Ohio

TWO-DIMENSIONAL RANDOM SURFACE MODEL FOR ASPERITY CONTACT IN ELASTOHYDRODYNAMIC LUBRICATION

John J. Coy (Army Aviation Res. and Develop. Command, Cleveland) and Steven M. Sidik, 1979 31 p. refs. Presented at the Intern. Conf. on Metrology and Properties of Eng. Surfaces, Leicester, England, 18-20 Apr. 1979.

(NASA-TM-79006, AVRADCOM-TR-78-48 E 9265 1) Avail: NTIS HC A03/MF A01 CSCL 11H

Relations for the asperity contact time function during elastohydrodynamic lubrication of a ball bearing are presented.

The analysis is based on a two-dimensional random surface model, and actual profile traces of the bearing surfaces are used as statistical sample records. The results of the analysis show that transition from 90 percent contact to 1 percent contact occurs within a dimensionless film thickness range of approximately four to five. This thickness ratio is several times larger than reported in the literature where one-dimensional random surface models were used. It is shown that low-pass filtering of the statistical records will bring agreement between the present results and those in the literature.

Author

N79-24350* National Aeronautics and Space Administration
Lewis Research Center, Cleveland, Ohio

DIAGNOSTICS OF WEAR IN AERONAUTICAL SYSTEMS

L. D. Wedeven, 1979 5 p. refs. Presented at the 15th State-of-the-Art Symp. on Corrosion and Wear, Washington, D. C., 4-6 Jun. 1979, sponsored by the Am. Chem. Soc. (NASA-TM-79185, E-052) Avail: NTIS HC A02/MF A01 CSCL 20K

Maintenance costs associated with the transmissions and drive train greatly increase the maintenance burden and failure risk. Detection measurements fall under two general categories of vibration and particle detectors. The latter are more amenable to checking wear. Wear debris analysis can supply a great deal of information such as particle concentration, rate of change in concentration, composition, particle size and shape, principal metals, etc. It is not economically feasible to monitor all variables. At least one role of the lubrication and wear specialist is to provide guidance in selecting the most appropriate variables to monitor.

RES

N79-28554* National Aeronautics and Space Administration
Lewis Research Center, Cleveland, Ohio

ELASTOHYDRODYNAMIC FILM THICKNESS MEASUREMENTS OF ARTIFICIALLY PRODUCED NONSMOOTH SURFACES

C. Cusano (Illinois Univ., Urbana) and L. D. Wedeven, 1979 47 p. refs. Proposed for presentation at Joint Lubrication Conf., Dayton, Ohio, 16-18 Oct. 1979, sponsored by Am. Soc. of Lubrication Engr. and the ASME.

(NASA-TM-79214, E-9977) Avail: NTIS HC A03/MF A01 CSCL 11H

Optical interferometry is used to measure the elastohydrodynamic (EHD) film thickness associated with artificially produced nonsmooth surfaces. The nonsmooth surfaces are produced by modifying the surfaces of highly polished balls with irregularities in the form of multiple grooves and dents. By closely spacing these irregularities it is possible not only to produce depressions on the surface of the balls but also to generate pseudo asperities. The average roughness wavelength of this artificially-produced, nonsmooth, surface approximates the average fundamental roughness wavelength found on surfaces of some mechanical elements operating under concentrated contact. By comparing the measured film thickness profiles to the stylus traces of the irregularities, it was possible to observe the local deformations associated with micro-EHD pressure generation. In both pure rolling and pure sliding conditions the artificially-produced asperities are deformed and complete separation exists between them and the mating surface. Such findings demonstrate the importance of local surface topography and resulting micro-EHD effects on the film thickness between rough surfaces in concentrated contact. Sliding data are presented which demonstrate a severe constriction caused by the irregularities at the exit of the Hertzian region.

Author

N79-31604* National Aeronautics and Space Administration
Lewis Research Center, Cleveland, Ohio

EVALUATION OF HIGH CONTACT RATIO SPUR GEARS WITH PROFILE MODIFICATION

Dennis P. Townsend, Berl B. Baber (Southwest Research Inst., San Antonio, Tex.) and Andrew Nagy (Southwest Research Inst., San Antonio, Tex.), Sep. 1979 24 p. refs.

(NASA-TP-1458, E-9949) Avail: NTIS HC A02/MF A01 CSCL 131

Scoring tests, surface fatigue tests, and single tooth bending

fatigue tests were conducted with four sets of spur gears of standard design and three sets of spur gears of new-tooth-form design. The new-tooth-form and standard gears scored at approximately the same gear bulk temperature of 409 K (277 F). The scoring load for the new-tooth-form gears was 22 percent less than that for the standard gears. The pitting fatigue lives of the standard and new-tooth-form gears were statistically equal for equal Hertz stress, while the surface fatigue life of the new-tooth-form gears was approximately five times that of the standard gears at the same load. The standard gears failed at a 17 percent higher bending stress than the new-tooth-form gears when stress was calculated by the AGMA method. However, the difference is not statistically significant. The standard gears failed at a tooth load 1.9 times that for the new-tooth-form gears.

Author

N79-31605* National Aeronautics and Space Administration, Lewis Research Center, Cleveland, Ohio.
FERROGRAPHIC ANALYSIS OF WEAR DEBRIS FROM FULL SCALE BEARING FATIGUE TESTS
 William R. Jones, Jr. and Stuart H. Loewenthal. Sep. 1979. 19 p. refs.
 (NASA-TP-1511, E-9827) Avail. NTIS HC A02/MF A01 CSCL 131

The Ferrograph was used to determine the types and quantities of wear particles generated during full scale bearing fatigue tests. Deep groove ball bearings made from steel were used. A tetraester lubricant was used in a recirculating lubricant system containing a 49 micrometers absolute filter. Test conditions include a maximum Hertz stress of 2.4 GPa, a shaft speed of 15,000 rpm, and a lubricant supply temperature of 74 C (165 F). Four fatigue failures were detected by accelerometers in this test set. In general, the Ferrograph was more sensitive (up to 23 hr) in detecting spall initiation than either accelerometers or the normal spectrographic oil analysis. Four particle types were observed: normal rubbing wear: particles, spheres, nonferrous particles, and severe wear (spall) fragments.

Author

N79-32552* National Aeronautics and Space Administration, Lewis Research Center, Cleveland, Ohio.
COMPARISON OF PREDICTED AND MEASURED ELASTOHYDRODYNAMIC FILM THICKNESS IN A 20-MILLIMETER-BORE BALL BEARING
 John J. Coy, Rama S. R. Gorla (Cleveland State Univ., Ohio), and Dennis P. Townsend. Oct. 1979. 29 p. refs.
 (NASA-TP-1542, AVRADCOM-TR-79-20, E-9992) Avail. NTIS HC A03/MF A01 CSCL 131

Elastohydrodynamic film thicknesses were measured for a 20-mm bore ball bearing using the capacitance technique. The bearing was thrust loaded to 90, 445, and 778 N (20, 100, and 175 lb). The corresponding maximum contact stress on the inner race was 1.28, 2.09, and 2.45 GPa (185,000, 303,000, and 356,000 psi). Test speeds ranged from 400 to 15,000 rpm. Measurements were taken with four different lubricants: (1) synthetic paraffinic, (2) synthetic paraffinic with additives, (3) synthetic type II aircraft oil, and (4) synthetic cycloaliphatic hydrocarbon traction fluid. The test bearing was mist lubricated. Test temperatures were 27, 65, and 121 C (80, 150, and 250 F). The measured results for the various test parameters were compared to theoretical predictions from computer programs. Also the data were plotted on dimensionless coordinates and compared to several classical isothermal theories.

Author

N79-33475* National Aeronautics and Space Administration, Lewis Research Center, Cleveland, Ohio.
TRACTION DRIVE PERFORMANCE PREDICTION FOR THE JOHNSON AND TEVAARWERK TRACTION MODEL
 Joseph L. Tevaarwerk. Washington. Oct. 1979. 41 p. refs.
 (NASA TP-1530, E-033) Avail. NTIS HC A03/MF A01 CSCL 131

The fluid rheology model is used to investigate the traction behavior for typical traction drive contacts. The aspect ratio of the contact and the invariably present spin are investigated. Contacts with a low aspect ratio predict a superior performance

in that they show less slip for the same degree of traction. Spin always has a diminishing effect on the traction at the same slip. At sufficiently high spin the model may be simplified to a limiting shear stress model. The conventional rigid plastic analysis applies here equally well.

K. L.

N79-33476* National Aeronautics and Space Administration, Lewis Research Center, Cleveland, Ohio.
CORRELATION OF ASPERITY CONTACT-TIME FRACTION WITH ELASTOHYDRODYNAMIC FILM THICKNESS IN A 20-MILLIMETER-BORE BALL BEARING
 John J. Coy. Washington. Oct. 1979. 21 p. refs.
 (NASA-TP-1547, AVRADCOM-TR-79-26) Avail. NTIS HC A02/MF A01 CSCL 131

Elastohydrodynamic film thicknesses and asperity contact-time fractions were measured for a 20 mm bore ball bearing by using the capacitance and conductance techniques. The bearing was thrust loaded to 90, 445, and 778 N. The corresponding maximum stresses on the inner race were 1.28, 2.09, and 2.45 GPa. The test speed ranged from 400 to 15,000 rpm. The test bearing was mist lubricated with a MIL-L-23699A turbine oil. The temperature was 27 C. The experimental results were correlated to give the percent film (no-contact-time fraction) as a function of measured film thickness. Measurements were made for three test series that represented the test bearing in various conditions of run-in. The measurements show that the percent film changes with bearing run-in time. The experimental results agreed well with theoretical predictions based on surface trace analysis for a new bearing. For the run-in state, they agreed with previously reported experimental results. The results show that asperity contact existed at a film thickness-roughness ratio λ of 6.0 or less for a new bearing. After run-in, no asperity contact occurred at a λ of 3.5 or greater.

Author

N79-33477* National Aeronautics and Space Administration, Lewis Research Center, Cleveland, Ohio.
NASA GEAR RESEARCH AND ITS PROBABLE EFFECT ON ROTORCRAFT TRANSMISSION DESIGN
 Erwin V. Zaretsky, Dennis P. Townsend, and John J. Coy. 1979. 19 p. refs. Presented at the Meeting on Helicopter Propulsion Systems, Williamsburg, Va., 6-8 Nov. 1979, sponsored by Am. Helicopter Soc.
 (NASA TM 79292, E-235) Avail. NTIS HC A02/MF A01 CSCL 131

The results of the NASA gear research is reviewed as well as those programs which are presently being undertaken. Research programs studying pitting fatigue, gear steels and processing, life prediction methods, gear design and dynamics, elastohydrodynamic lubrication, lubrication methods and gear noise are presented. The impact of advanced gear research technology on rotorcraft transmission design is discussed.

M. M.

A79-10038* Liquid-cooling technology for gas turbines: Review and status. G. J. Van Fossen, Jr. (NASA, Lewis Research Center, Cleveland, Ohio, U.S. Army, Propulsion Laboratory, St. Louis, Mo.) and F. S. Stepka (NASA, Lewis Research Center, Cleveland, Ohio). In: Intersociety Energy Conversion Engineering Conference, 13th, San Diego, Calif., August 20-25, 1978, Proceedings, Volume 1. (A79-10001, 01-44) Warrendale, Pa.: Society of Automotive Engineers, Inc., 1978, p. 262-271. 40 refs.

After a brief review of past efforts involving the forced convection cooling of gas turbines, the paper surveys the state of the art of the liquid cooling of gas turbines. Emphasis is placed on thermosyphon methods of cooling, including those utilizing closed, open, and closed-loop thermosyphons, other methods, including sweat, spray, and stator cooling, are also discussed. The more significant research efforts, design data, correlations, and analytical methods are mentioned and voids in technology are summarized.

B. J.

A79-11545 * # The practical impact of elastohydrodynamic lubrication. W. J. Anderson (NASA, Lewis Research Center, Cleveland, Ohio). *Leeds-Lyon Symposium on Tribology, 5th, Leeds, England, Sept. 19-22, 1978, Paper*. 13 p. 55 refs.

Elastohydrodynamic lubrication has had its most significant impact on, among all the types of concentrated contact mechanisms, rolling element bearings. EHL technology, through its inclusion in computer codes, now provides us with more effective methods for optimizing bearing design and for predicting bearing life, power loss, temperature and dynamic behavior. Bearing life prediction has advanced to a much more sophisticated level as compared to the calculation of fatigue life based on Lundberg Palmgren theory. Application of elastohydrodynamics to gearing has, more or less, been limited to the calculation of pitch point film thicknesses. Techniques for calculating film thicknesses over the entire range of tooth meshes for arbitrarily shaped gear teeth (noninvolute, spur, helical, etc.) need to be developed. Elastomer seals with both unidirectional and reciprocating motion offer a fruitful application for the elastohydrodynamics of low modulus materials. (Author)

A79-12850 * # Ceramics for the advanced automotive gas turbine engine - A look at a single shaft design. S. M. Nosek (NASA, Lewis Research Center, Cleveland, Ohio). In: *Ceramics for high performance applications II, Proceedings of the Fifth Army Materials Technology Conference, Newport, R.I., March 21-25, 1977* (A79 12804 02-37) Chestnut Hill, Mass., Brook Hill Publishing Co., 1978, p. 959-972.

A single-shaft regenerative design with a single-stage radial turbine is analyzed in terms of achievable fuel economy for the cases of both limited and unlimited turbine tip speed and regenerator inlet temperature. The 100 hp engine for a 3500 lb automobile is designed to use gasoline. Fuel economy data and operating parameters are presented for different values of turbine inlet temperatures, and turbine stress estimates and ceramic design stress estimates are discussed. M.L.

A79-12851 * # Ceramic applications in the advanced Stirling automotive engine. W. A. Tomazic and J. E. Carrelli (NASA, Lewis Research Center, Cleveland, Ohio). In: *Ceramics for high performance applications II, Proceedings of the Fifth Army Materials Technology Conference, Newport, R.I., March 21-25, 1977* (A79 12804 02-37) Chestnut Hill, Mass., Brook Hill Publishing Co., 1978, p. 973-987.

The requirements of the ideal Stirling cycle, as well as basic types of practical engines are described. Advantages, disadvantages, and problem areas of these Stirling engines are discussed. The potential for ceramic components is also considered. Currently ceramics are used in only two areas, the air preheater and insulating tiles between the burner and the heater head. For the advanced Stirling engine to achieve high efficiency and low cost, the principal components are expected to be made from ceramic materials, including the heater head, air preheater, regenerator, the burner and the power piston. Supporting research and technology programs for ceramic component development are briefly described. (Author)

A79-14797 * # Ion beam sputtering of fluoropolymers. J. S. Sovey (NASA, Lewis Research Center, Cleveland, Ohio). *American Vacuum Society, National Vacuum Symposium, 25th, San Francisco, Calif., Nov. 28-Dec. 1, 1978, Paper*. 14 p. 17 refs.

Etching and deposition of fluoropolymers are of considerable industrial interest for applications dealing with adhesion, chemical inertness, hydrophobicity, and dielectric properties. This paper describes ion beam sputter processing rates as well as pertinent characteristics of etched targets and films. An argon ion beam source was used to sputter etch and deposit the fluoropolymers PTFE, FEP, and CTFE. Ion beam energy, current density, and target temperature were varied to examine effects on etch and deposition rates. The ion etched fluoropolymers yield cone or spire-like surface structures, which vary depending upon the type of polymer, ion beam power density, etch time, and target temperature. Also presented are

sputter target and film characteristics which were documented by spectral transmittance measurements, X-ray diffraction, ESCA, and SEM photomicrographs. (Author)

A79-14950 * # Proposed design procedure for transmission shafting under fatigue loading. S. H. Loewenthal (NASA, Lewis Research Center, Cleveland, Ohio). *Illinois Institute of Technology, Annual Meeting of the National Conference on Power Transmission, 5th, Philadelphia, Pa., Nov. 7-9, 1978, Paper*. 10 p. 13 refs.

The B106 American National Standards Committee is currently preparing a new standard for the design of transmission shafting. A design procedure, proposed for use in the new standard, for computing the diameter of rotating solid steel shafts under combined cyclic bending and steady torsion is presented. The formula is based on an elliptical variation of endurance strength with torque exhibited by combined stress fatigue data. Fatigue factors are cited to correct specimen bending endurance strength data for use in the shaft formula. A design example illustrates how the method is to be applied. (Author)

A79-16663 * # Sputtering technology in solid film lubrication. T. Spalvins (NASA, Lewis Research Center, Cleveland, Ohio). In: *International Conference on Solid Lubrication, 2nd, Denver, Colo., August 15-18, 1978, Proceedings* (A79-16651 04-27) Park Ridge, Ill., American Society of Lubrication Engineers, 1978, p. 109-117. 13 refs.

Current and potential sputtering technology is reviewed as it applies primarily to the deposition of MoS₂, though such lubricants as WS₂ and PTFE are also considered. It is shown by electron microscopy and surface sensitive analytical techniques that the lubricating properties of sputtered MoS₂ films are directly influenced by the sputtering parameters selected (i.e., power density, pressure, sputter etching, dc-biasing, etc.), substrate temperature, chemistry, topography, and environmental conditions during the friction test. Electron micrographs and diffractograms of sputtered MoS₂ films clearly show the resultant changes in film morphology which affect film adherence and frictional properties. B.J.

A79-16664 * # Application of ESCA to the determination of stoichiometry in sputtered coatings and interface regions. D. R. Wheeler (NASA, Lewis Research Center, Cleveland, Ohio). In: *International Conference on Solid Lubrication, 2nd, Denver, Colo., August 15-18, 1978, Proceedings* (A79-16651 04-27) Park Ridge, Ill., American Society of Lubrication Engineers, 1978, p. 118-127. 21 refs.

X-ray Photoelectron Spectroscopy (XPS) was used to characterize radiofrequency sputter deposited films of several refractory compounds. Both the bulk film properties such as purity and stoichiometry and the character of the interfacial region between the film and substrate were examined. The materials were CrB₂, MoS₂, Mo₂C, and Mo₂B₅ deposited on 440C steel. It was found that oxygen from the sputtering target was the primary impurity in all cases. Biasing improves the film purity. The effect of biasing on film stoichiometry is different for each compound. Comparison of the interfacial composition with friction data suggests that adhesion of these films is improved if a region of mixed film and iron oxides can be formed. (Author)

A79-16678 * # Graphite-fiber-reinforced polyimide liners of various compositions in plain spherical bearings. H. E. Sliney and T. P. Jacobson (NASA, Lewis Research Center, Cleveland, Ohio). In: *International Conference on Solid Lubrication, 2nd, Denver, Colo., August 15-18, 1978, Proceedings* (A79-16651 04-27) Park Ridge, Ill., American Society of Lubrication Engineers, 1978, p. 258-267. 20 refs.

Composites made of graphite-fiber reinforced polyimide (GFRPI) with a fiber-resin ratio (by weight) of about 1 were evaluated as molded outer-race liners in plain spherical bearings. Several compositions were examined: two types of polyimide

(addition and condensation polymers), two types of graphite fiber (high and low modulus) and four powder additives (CdO, CdI₂, (CF₃)₂Sn, and MoS₂). Friction and wear were measured during oscillation at 25, 200, and 315 C. It is shown that all compositions provided good lubrication in dry air, that neither type of polyimide or graphite fiber nor the additives gave a clear advantage, and that wear rates were always higher during run-in, before conditions stabilized. It is concluded that GFRPI composites are self-lubricating under all but the most extreme moisture-free conditions at 25 C. The additives are helpful only with very high loads or extremely dry environments. S.D.

A79-20700 * **Energy conservation through sealing technology.** W. K. Stair (Tennessee University, Knoxville, Tenn.) and L. P. Ludwig (NASA, Lewis Research Center, Cleveland, Ohio). (*American Society of Mechanical Engineers, Annual Meeting, 33rd, Dearborn, Mich., Apr. 17-20, 1978. Lubrication Engineering*, vol. 34, Nov. 1978, p. 618-624, 12 refs.

Improvements in fluid film sealing resulting from a proposed research program could lead to an annual energy saving, on a national basis, equivalent to about 37 million bbl of oil or 0.3% of the total U.S. energy consumption. Further, the application of known sealing technology can result in an annual saving of an additional 10 million bbl of oil. The energy saving would be accomplished by reduction in process heat energy loss, reduction of frictional energy generated, and minimization of energy required to operate ancillary equipment associated with the seal system. In addition to energy saving, cost effectiveness is further enhanced by reduction in maintenance and minimization of equipment for collecting leakage and for meeting environmental pollution standards. (Author)

A79-23229 * **Elastohydrodynamic lubrication of elliptical contacts for materials of low elastic modulus. II - Starved conjunction.** B. J. Hamrock (NASA, Lewis Research Center, Cleveland, Ohio) and D. Dowson (Leeds University, Leeds, England). (*American Society of Mechanical Engineers and American Society of Lubrication Engineers, Joint Lubrication Conference, Minneapolis, Minn., Oct. 24-26, 1978, ASME Paper 78-Lub-1* 7 p. 12 refs. Members, \$1.50, nonmembers, \$3.00.

The study evaluates the effect of lubricant starvation on minimum film thickness in starved elliptical elastohydrodynamic conjunctions for materials of low elastic modulus. Lubricant starvation is studied simply by moving the inlet boundary closer to the center of the conjunction. A simple expression is presented for the dimensionless inlet boundary distance; this inlet boundary distance defines whether a fully flooded or a starved condition exists in the conjunction. A formula for the minimum film thickness under the starvation condition is derived. Contour plots of the pressure and film thickness in and around the contact are presented for both the fully flooded and starved lubrication conditions. It is shown that the inlet pressure contours become less circular and that the film thickness decreases substantially with increasing starvation severity. S.D.

A79-23235 * **Stiffness of straight and tapered annular gas path seals.** D. P. Fleming (NASA, Lewis Research Center, Cleveland, Ohio). (*American Society of Mechanical Engineers and American Society of Lubrication Engineers, Joint Lubrication Conference, Minneapolis, Minn., Oct. 24-26, 1978, ASME Paper 78-Lub-18* 6 p. 18 refs. Members, \$1.50, nonmembers, \$3.00.

Radial stiffness of annular (ring type) gas path seals is calculated for both constant clearance designs and tapered designs for which the inlet clearance is larger than the outlet clearance. Under some conditions a constant clearance seal can have a negative stiffness; this undesirable property can be completely eliminated by use of tapered seals. Leakage rates are only moderately higher in tapered seals. (Author)

A79-23237 * **Effect of geometry on hydrodynamic film thickness.** D. E. Brew (U.S. Army, Air Mobility Research and Development Laboratory, Cleveland, Ohio), B. J. Hamrock (NASA, Lewis Research Center, Cleveland, Ohio), and C. M. Taylor (Leeds University, Leeds, England). (*American Society of Mechanical Engineers and American Society of Lubrication Engineers, Joint Lubrication Conference, Minneapolis, Minn., Oct. 24-26, 1978, ASME Paper 78-Lub-24* 7 p. 18 refs. Members, \$1.50, nonmembers, \$3.00.

The influence of geometry on the isothermal hydrodynamic film separating two rigid solids was investigated. Pressure-viscosity effects were not considered. The minimum film thickness is derived for fully flooded conjunctions by using the Reynolds boundary conditions. It was found that the minimum film thickness had the same speed, viscosity, and load dependence as Kapitza's classical solution. However, the incorporation of Reynolds boundary conditions resulted in an additional geometry effect. Solutions using the parabolic film approximation are compared with those using the exact expression for the film in the analysis. Contour plots are shown that indicate in detail the pressure developed between the solids. (Author)

A79-23246 * **Filtration effects on ball bearing life and condition in a contaminated lubricant.** S. H. Loewenthal (NASA, Lewis Research Center, Cleveland, Ohio) and D. W. Moyer (Tribon Bearing Co., Cleveland, Ohio). (*American Society of Mechanical Engineers and American Society of Lubrication Engineers, Joint Lubrication Conference, Minneapolis, Minn., Oct. 24-26, 1978, ASME Paper 78-Lub-34* 6 p. 20 refs. Members, \$1.50, nonmembers, \$3.00.

Ball bearings were fatigue tested with a noncontaminated MIL-L-23699 lubricant and with a contaminated MIL-L-23699 lubricant under four levels of filtration. The test filters had absolute particle removal ratings of 3, 30, 49, and 105 microns. Aircraft turbine engine contaminants were injected into the filter's supply line at a constant rate of 125 milligrams per bearing hour. Bearing life and running track condition generally improved with finer filtration. The experimental lives of 3- and 30-micron filter bearings were statistically equivalent, approaching those obtained with the noncontaminated lubricant bearings. Compared to these bearings, the lives of the 49-micron bearings were statistically lower. The 105-micron bearings experienced gross wear. The degree of surface distress, weight loss, and probable failure mode were dependent on filtration level, with finer filtration being clearly beneficial. (Author)

A79-23251 * **Some loads limits and self-lubricating properties of plain spherical bearings with molded graphite fiber-reinforced polyimide liners to 320 C.** H. E. Siney (NASA, Lewis Research Center, Cleveland, Ohio). (*American Society of Lubrication Engineers and American Society of Mechanical Engineers, Joint Lubrication Conference, Minneapolis, Minn., Oct. 24-26, 1978, ASLE Preprint 78-LC-5C-2* 5 p. 7 refs.

A79-23267 * **Elastohydrodynamic film thickness measurements of artificially produced surface dents and grooves.** I. D. Wedeven (NASA, Lewis Research Center, Cleveland, Ohio) and C. Cusano (Illinois University, Urbana, Ill.). (*American Society of Lubrication Engineers and American Society of Mechanical Engineers, Joint Lubrication Conference, Minneapolis, Minn., Oct. 24-26, 1978, ASLE Preprint 78-LC-1A-1* 12 p. 32 refs.

Elastohydrodynamic (EHD) film thickness measurements using optical interferometry have been made of artificially produced dents and grooves under rolling and sliding conditions. These measurements are compared to stylus traces of the dent and groove profiles to determine the local deformation associated with micro-EHD pressure generation. The surface geometry associated with the dents and grooves is seen to become intimately involved in the lubrication process itself, creating local pressure variations that substantially deform the local surface geometry, particularly under sliding conditions. The rolling results have implications concerning surface

initiated fatigue and the sliding results show clearly the EHD surface interactions that must occur prior to scuffing failure. (Author)

A79-24035 * # Analysis/design of strip reinforced random composites /strip hybrids/. C. G. Chamis and J. H. Sinclair (NASA, Lewis Research Center, Cleveland, Ohio). *American Society of Mechanical Engineers, Winter Annual Meeting, San Francisco, Calif., Dec. 10-15, 1978, Paper 22* p. 6 refs.

Results are described which were obtained by applying advanced analysis methods and composite mechanics to a strip-reinforced random composite square panel with fixed ends. This was done in order to illustrate the use of these methods for the a priori assessment of the composite panel when subjected to complex loading conditions. The panel was assumed to be of E-Glass/Random Composite. The strips were assumed to be of three advanced unidirectional composites to cover a range of low, intermediate, and high modulus stiffness. The panels were assumed to be subjected to complex loading to assess their adequacy as load-carrying members in auto body, aircraft engine nacelle, and windmill blade applications. The results show that strip hybrid panels can be several times more structurally efficient than the random composite base materials. Some of the results are presented in graphical form and procedures are described for use of these graphs as guides for preliminary design of strip hybrids. (Author)

A79-24121 * The use of ion beam cleaning to obtain high quality cold welds with minimal deformation. B. L. Sater and T. J. Moore (NASA, Lewis Research Center, Cleveland, Ohio). In *Materials synergisms, Proceedings of the Tenth National Technical Conference, Kiamesha Lake, N.Y., October 17-19, 1978* (A79-24076 OR 31) Azusa, Calif., Society for the Advancement of Material and Process Engineering, 1978, p. 548-560, 9 refs.

This paper describes a variation of cold welding which utilizes an ion beam to clean mating surfaces prior to joining in a vacuum environment. High quality solid state welds were produced with minimal deformation. Due to experimental fixture limitation in applying pressure work has been limited to a few low yield strength materials. (Author)

A79-25103 * Use of a nitrogen-argon plasma to improve adherence of sputtered titanium carbide coatings on steel. W. A. Brainard and D. R. Wheeler (NASA, Lewis Research Center, Cleveland, Ohio). *Journal of Vacuum Science and Technology*, vol. 16, Jan.-Feb. 1979, p. 31-36, 12 refs.

Friction and wear experiments on 440-C steel surfaces that had been RF sputtered with titanium carbide when a small percentage of nitrogen was added to the plasma were conducted. X-ray photoelectron spectroscopy and X-ray diffraction were used to analyze the resultant coatings. Results indicate that a small partial pressure of nitrogen (about 0.5%) markedly improves the adherence, friction, and wear properties when compared with coatings applied on sputter-etched oxidized surfaces or in the presence of a small oxygen partial pressure. The improvements are related to the formation of an interface containing a mixture of the nitrides of titanium and steel, which are harder than their corresponding oxides. (Author)

A79-30398 * # Industrial potential, uses, and performance of sputtered and ion plated films. T. Spalvins (NASA, Lewis Research Center, Cleveland, Ohio). *Society of Vacuum Coaters, Annual Technical Conference 22nd, New Orleans, La., Mar. 28-30, 1979, Paper 14* p. 16 refs.

The sputtering and ion plating technology is reviewed in terms of potential, uses, and performance. Sputtering is not regulated by classical thermodynamics and Gibbs phase rule relationships, thus eliminating the restrictions for materials combinations and consequently making possible tailoring of coatings in any preferred chemical combination. The future of sputtered and ion plated films

for industrial applications is expected to depend primarily on greater comprehension of materials selection, and the utilization of the proper deposition parameters. A.A.

A79-31368 * Initial comparison of single cylinder Stirling engine computer model predictions with test results. R. C. Tew, Jr., L. G. Thieme, and D. Miao (NASA, Lewis Research Center, Cleveland, Ohio). *Society of Automotive Engineers, Congress and Exposition, Detroit, Mich., Feb. 26-Mar. 2, 1979, Paper 790327*, 18 p. 15 refs.

A NASA developed digital computer code for a Stirling engine, modelling the performance of a single cylinder rhombic drive ground performance unit (GPU), is presented and its predictions are compared to test results. The GPU engine incorporates eight regenerator/cooler units and the engine working space is modeled by thirteen control volumes. The model calculates indicated power and efficiency for a given engine speed, mean pressure, heater and expansion space metal temperatures and cooler water inlet temperature and flow rate. Comparison of predicted and observed powers implies that the reference pressure drop calculations underestimate actual pressure drop possibly due to oil contamination in the regenerator/cooler units, methane contamination in the working gas or the underestimation of mechanical loss. For a working gas of hydrogen, the predicted values of brake power are from 0 to 6% higher than experimental values, and brake efficiency is 6 to 16% higher, while for helium the predicted brake power and efficiency are 2 to 15% higher than the experimental. A.L.W.

A79-32414 * # Elastomer mounted rotors - An alternative for smoother running turbomachinery. J. A. Tecza, S. W. Jones, A. J. Smalley (Mechanical Technology Inc., Latham, N.Y.), R. E. Cunningham (NASA, Lewis Research Center, Cleveland, Ohio), and M. S. Darlow. *American Society of Mechanical Engineers, Gas Turbine Conference and Exhibit and Solar Energy Conference, San Diego, Calif., Mar. 12-15, 1979, Paper 79-GT-149* 6 p. 25 refs. Members, \$1.50, nonmembers, \$3.00. NASA sponsored research.

This paper describes the design of elastomeric bearing supports for a rotor built to simulate the power turbine of an advanced gas turbine engine which traverses two bending critical speeds. The elastomer dampers were constructed so as to minimize rotor dynamic response at the critical speeds. Results are presented of unbalance response tests performed with two different elastomer materials. These results showed that the resonances on the elastomer mounted rotor were well damped for both elastomer materials and showed little response to the unbalance weights used for response testing. Additional tests were performed using solid steel supports at either end (hard-mounted), which resulted in drastically increased sensitivity and nonlinear response, and with steel supports in one end of the rotor and the elastomer at the other, which yielded results which were between the soft and hard mounted cases. It is concluded that elastomeric supports are a viable alternative to other methods of mounting flexible rotors, that damping was well in excess of predictions and that elastomeric supports are tolerant of small rotor misalignments. (Author)

A79-34993 * Wide temperature spectrum self lubricating coatings prepared by plasma spraying. H. E. Shively (NASA, Lewis Research Center, Cleveland, Ohio). *American Vacuum Society and American Society for Metals, International Conference on Metallurgical Coatings, San Diego, Calif., Apr. 24-27, 1979, Paper 8* p. 1 refs.

Self lubricating multicomponent coatings which operate over a wide range of operating temperatures and pressures. The coatings have been successfully applied by plasma spraying on steel powder metal superalloy substrates. They have been evaluated in friction and wear experiments and in sliding contact bearing tests. These coatings are wear resistant by virtue of their self lubricating characteristics rather than because of extreme hardness. A further benefit is low friction. Experiments with reciprocating pin-on-disc testing specimens and with rotating pin-on-disc testing for tribology performance have substantiated the superior behavior of these coatings. It was shown that coatings

of nichrome, glass and calcium fluoride are self lubricating from about 500 to 900 C, but give high friction at the lower temperatures. The addition of silver to the coating composition improved the low temperature bearing properties and resulted in coatings which are self lubricating from cryogenic temperatures to at least 870 C, they are therefore "wide temperature spectrum," self lubricating compositions (Author)

A79-39805 * **Diagnostics of wear in aeronautical systems.** L. D. Wedeven (NASA, Lewis Research Center, Cleveland, Ohio). *American Chemical Society, State-of-the-Art Symposium on Corrosion and Wear, 15th, Washington, D.C., June 4-6, 1979, Paper, 4 n. 17 refs.*

The use of appropriate diagnostic tools for aircraft oil wetted components is reviewed, noting that it can reduce direct operating costs through reduced unscheduled maintenance, particularly in helicopter engine and transmission systems where bearing failures are a significant cost factor. Engine and transmission wear modes are described, and diagnostic methods for oil and wet particle analysis, the spectrometric oil analysis program, chip detectors, ferrography, in-line oil monitor and radioactive isotope tagging are discussed, noting that they are effective over a limited range of particle sizes but complement each other if used in parallel. Fine filtration can potentially increase time between overhauls, but reduces the effectiveness of conventional oil monitoring techniques so that alternative diagnostic techniques must be used. It is concluded that the development of a diagnostic system should be parallel and integral with the development of a mechanical system. (Author)

A79-39811 * **Two-dimensional random surface model for asperity-contact in elastohydrodynamic lubrication.** J. J. Coy (U.S. Army, Propulsion Laboratory, Cleveland, Ohio) and S. M. Sidik (NASA, Lewis Research Center, Cleveland, Ohio). *International Conference on Metrology and Properties of Engineering Surfaces, Leicester, England, Apr 18-20, 1979, Paper, 27 p. 23 refs.*

Relations for the asperity contact time fraction during elastohydrodynamic lubrication of a ball bearing are presented. The analysis is based on a two-dimensional random surface model, and actual profile traces of the bearing surfaces are used as statistical sample records. The results of the analysis show that transition from 90 percent contact to 1 percent contact occurs within a dimensionless film thickness range of approximately four to five. This thickness ratio is several times larger than reported in the literature where two-dimensional random surface models were used. It is shown that low pass filtering of the statistical records will bring agreement between the present results and those in the literature. (Author)

N79-10423* Avco Lycoming Div., Stratford, Conn. **TRANSMISSION SEAL DEVELOPMENT Final Report, 1 Jul 1976 - 30 Apr 1977**
Michael Brien Oct 1977 41 p. refs. Sponsored in part by USAAMRDC
(Contract NAS3 20045)
(NASA CR 135372) (LYC 77-65) Avail NTIS
HC A03/MF A01 CSCL 11A

An experimental evaluation was performed on a high speed 172.9 m/s (14,349 ft/min) transmission seal of the synergistic type. During testing of the seal, oil leakage occurred at positive bearing cavity pressures. Modifications were made in an attempt to eliminate the leakage but none were completely successful. Leakage appears to be the result of questionable positioning of the sealing elements resulting in inadequate shaft contact by the oil side sealing element. This condition may be related to the non-symmetrical shape of the elastomeric retainer and to dimensional changes caused by swelling of the elastomeric retainer from exposure to the sealed fluid. Indications of a speed dependent leakage characteristic were also observed. (Author)

N79-11406* Ford Motor Co., Dearborn, Mich. **AUTOMOTIVE STIRLING ENGINE DEVELOPMENT PROGRAM Quarterly Technical Progress Report, Apr 1978 Jun 1978**
Jun 1978 96 p. Sponsored by NASA
(Contract EC-77 C-02 4396)
(NASA CR 159436) (CONS/4396-3) Avail NTIS
HC A05/MF A01 CSCL 13F

The third quarter (April-June, 1978) effort of the Ford/DOE Automotive Stirling Engine Development Program is reported, specifically Task 1 of that effort which is Fuel Economy Assessment. At the end of this quarter the total fourth generation fuel economy projection was 26.12 MPG (gasoline) with a confidence level of 44%. This represents an improvement of 66.4% over the baseline M.H. fuel economy of 15.7 MPG. The confidence level for the original 20.6 MPG goal has been increased from 53% to 57%. Engine 3X17 has accumulated a total of 213 hours of variable speed running. A summary of the individual sub tasks of Task 1 are given. The sub tasks are grouped into two categories. Category 1 consists of those sub tasks which are directly related to fuel economy and Category 2 consists of those sub tasks which are not directly related to fuel economy but are an integral part of the Task 1 effort. (G Y)

N79-11407* AiResearch Mfg. Co., Phoenix, Ariz. **MINI BRAYTON ROTATING FOIL BEARING DEVELOPMENT Progress Report, 1 Jan 1978 - 30 Jan 1978**
F. X. Dobler and L. J. Miller Oct 1978 150 p. refs.
(Contract NAS3 18517)
(NASA CR 159442) (AiResearch 31 2936) Avail NTIS
HC A07/MF A01 CSCL 13E

The analysis revealed the failure agent to be a combination of poor teflon coating adhesion, a decrease in bearing sway space and, possibly, lack of flushing flow through the bearing. A change in Teflon coating vendors provided substantially improved coating quality and surface finish. The sway space was increased and the cooling bleed flow was adjusted to flush the bearing. These changes were included in a test conducted in the WHL from 6 April to 22 May 1978 which resulted in the completion of 1006.9 hours of operation at temperature and load. Post test inspection revealed the bearings to be in excellent condition and capable of completing a much longer test. (L S)

N79-11408* AiResearch Mfg. Co., Phoenix, Ariz. **ANALYSIS, DESIGN, FABRICATION AND TESTING OF THE MINI BRAYTON ROTATING UNIT (MINI BRU) VOLUME 1. TEXT AND TABLES Final Report, Apr 1974 - Jun 1978**
F. X. Dobler et al. Oct 1978 215 p. refs. 2 Vol.
(Contract NAS3 18517)
(NASA CR 159441 Vol 1) (AiResearch 31 2935-1) Avail NTIS
HC A10/MF A01 CSCL 13I

A 500 to 2100 watt power output Mini Brayton Rotating Unit (Mini BRU) was analyzed, designed, fabricated and tested. Performance and test data for the various components is included. Components tested include the 2.12 in. diameter compressor, the 2.86 in. diameter turbine, the 6000 alternator and the cantilevered foil type journal and thrust bearings. Also included are results on the fabrication of a 6.103 turbine plenum nozzle assembly and on offgassing of the organic materials in the alternator stator. (Author)

N79-11409* AiResearch Mfg. Co., Phoenix, Ariz. **ANALYSIS, DESIGN, FABRICATION AND TESTING OF THE MINI BRAYTON ROTATING UNIT (MINI BRU) VOLUME 2. FIGURES AND DRAWINGS Final Report**
F. X. Dobler Oct 1978 448 p. 2 Vol.
(Contract NAS3 18517)
(NASA CR 159441 Vol 2) (AiResearch 31 2935-2) Avail NTIS
HC A19/MF A01 CSCL 13I

This volume contains the figures and drawings reference in Volume 1. (Author)

N79-14386* Battelle Columbus Labs., Ohio
DETERMINATION OF LUBRICANT SELECTION BASED ON ELASTOHYDRODYNAMIC FILM THICKNESS AND TRACTION MEASUREMENT Final Report
 T. A. Dow and J. W. Kannel Jan 1979 113 p refs Sponsored in part by Army Aviation Research and Development Command, St. Louis
 (NASA-CR-159428) Avail NTIS HC A06/MF A01 CSCL 11H

The project was conducted to aid in the development of an elastohydrodynamic specification for military lubricants. Experiments were conducted with a rolling disk apparatus designed to simulate a bearing or gear type contact. Measurements included lubricant film thickness, lubricant breakdown and traction for a range of loads, speeds, temperatures, and surface roughnesses. Several lubricants were used in the investigations including a traction fluid, two synthetic paraffinic lubricants and several lubricants conforming to MIL-L 7808 and 23699 specifications. Recommendations regarding an EHD specification are included.

Author

N79-17219* SKF Industries, Inc., King of Prussia, Pa.
AIRCRAFT ENGINE SUMP FIRE MITIGATION, PHASE 2 Final Report
 J. W. Rosenlieb Apr 1978 142 p refs
 (Contract NAS3-19436)
 (NASA-CR-135379) AL78T0071 Avail NTIS
 HC A07/MF A01 CSCL 21B

The effect of changes in the input parameters (air leakage flow rate and temperature and lubricating oil inlet flow rate and temperature) over a specified range on the flammability conditions within an aircraft engine bearing sump was investigated. An analytical study was performed to determine the effect of various parameters on the generation rate of oil vapor from oil droplets in a hot air stream flowing in a cylindrical tube. The ignition of the vapor-air mixture by an ignition source was considered. The experimental investigation demonstrated that fires would be ignited by a spark ignitor over the full range of air and oil flow rates and air temperatures evaluated. However, no fires could be ignited when the oil inlet temperature was maintained below 417 K (290 F). The severity of the fires ignited were found to be directly proportional to the hot air flow rate. Reasonably good correlation was found between the mixture temperature in the sump at the ignitor location and the flammability limits as defined by flammability theory, thus a fairly reliable experimental method of determining flammable conditions within a sump was demonstrated. The computerized mathematical model shows that oil droplet size and air temperature have the greatest influence on the generation rate of oil vapor.

A R H

N79-17221* Rockwell International Corp., Canoga Park, Calif.
SMALL, HIGH PRESSURE, LIQUID OXYGEN TURBOPUMP Final Report
 A. Csomor Oct 1978 156 p refs
 (Contract NAS3-17800)
 (NASA-CR-159509) R1/RD78-2781 Avail NTIS
 HC A08/MF A01 CSCL 13I

A small, high pressure LOX turbopump was designed, fabricated, and tested. The pump was of a single-stage, centrifugal type; power to the pump was supplied by a single-stage, partial-admission axial-impulse turbine. Design conditions included an operating speed of 7330 rad/sec (70,000 rpm), pump discharge pressure of 2977 N/sq cm (4318 psia) and a pump flowrate of 16.4 kg/s (36.21 lb/sec). The turbine was propelled by LOX/LH2 combustion products at 1041 K (1974 R) inlet temperature, and at a design pressure ratio of 1.424. Test data obtained with the turbopump are presented and mechanical performance is discussed.

Author

N79-17222* SKF Industries, Inc., King of Prussia, Pa.
HIGH SPEED CYLINDRICAL ROLLER BEARING ANALYSIS, SKF COMPUTER PROGRAM CYBEAN, VOLUME 1: ANALYSIS Final Report
 R. J. Kleckner and J. Pirvics Jul 1978 108 p refs 2 Vol
 (Contract NAS3-20068)
 (NASA-CR-159460) AL78P-022-Vol-1) Avail NTIS
 HC A06/MF A01 CSCL 13I

The CYBEAN (CYlindrical BEaring ANALysis) program was created to detail radially loaded, aligned and misaligned cylindrical roller bearing performance under a variety of operating conditions. The models and associated mathematics used within CYBEAN are described. The user is referred to the material for formulation assumptions and algorithm detail.

L S

N79-17223* SKF Industries, Inc., King of Prussia, Pa.
 Technology Services Div.
HIGH SPEED CYLINDRICAL ROLLER BEARING ANALYSIS, SKF COMPUTER PROGRAM CYBEAN, VOLUME 2: USER'S MANUAL Final Report
 R. J. Kleckner and J. Pirvics Jul 1978 141 p refs 2 Vol
 (Contract NAS3-20068)
 (NASA-CR-159461) AL78P023-Vol-2) Avail NTIS
 HC A07/MF A01 CSCL 13I

The CYBEAN (CYlindrical BEaring ANALysis) was created to detail radially loaded, aligned and misaligned cylindrical roller bearing performance under a variety of operating conditions. Emphasis was placed on detailing the effects of high speed, preload and system thermal coupling. Roller tilt, skew, radial, circumferential and axial displacement as well as flange contact were considered. Variable housing and flexible out-of-round outer ring geometries, and both steady state and time transient temperature calculations were enabled. The complete range of elastohydrodynamic contact considerations, employing full and partial film conditions were treated in the computation of raceway and flange contacts. Input and output architectures containing guidelines for use and a sample execution are detailed.

L S

N79-17226* Israel Inst. of Tech., Haifa
HYDRODYNAMIC EFFECTS IN A MISALIGNED RADIAL FACE SEAL Final Report
 I. Etsion Jul 1977 38 p refs
 (Grant NSG-7317)
 (NASA-CR-135228) Avail NTIS HC A03/MF A01 CSCL 11A

Hydrodynamic effects in a flat seal having an angular misalignment are analyzed, taking into account the radial variation in seal clearance. An analytical solution for axial force, restoring moment, and transverse moment is presented that covers the whole range from zero to full angular misalignment. Both low pressure seals with cavitating flow and high pressure seals with full fluid film are considered. Strong coupling is demonstrated between angular misalignment and transverse moment which leads the misalignment vector by 90 degrees. This transverse moment, which is entirely due to hydrodynamic effects, is a significant factor in the seal operating mechanism.

Author

N79-17228* Mechanical Technology, Inc., Latham, N. Y.
EXPERIMENTS ON MULTIPLANE BALANCING USING A LASER FOR MATERIAL REMOVAL Final Report
 Russell S. Demuth Feb 1979 45 p
 (Contract NAS3-18520)
 (NASA-CR-3105) MTI-78TR69) Avail NTIS
 HC A03/MF A01 CSCL 20E

The modifications of a flexible rotor system for two-plane laser balancing is described. Experimental testing of the laser material removal method for balancing through the first bending critical speed was demonstrated. The testing optical configuration, and a neodymium glass laser system were assembled and calibrated for static and rotating material removal rates. The laser control computer program was combined with the influence coefficient balancing process, resulting in a completely automated data acquisition, laser and balancing system. The laser system

rotor was balanced through the first bending critical speed using the laser material removal procedure to apply trial weights and correction weights without stopping the rotor. G Y

N79-23429* Shaker Research Corp., Ballston Lake, N. Y.
EXPERIMENTAL AND ANALYTICAL TOOLS FOR EVALUATION OF STIRLING ENGINE ROD SEAL BEHAVIOR Interim Report

A. I. Krauter and H. S. Cheng (Northwestern Univ.) Feb. 1979
 124 p refs
 (Contracts DEN-3-22; ED-77-A-31-1040)
 (NASA-CR-159543; SRC-78TP-39) Avail NTIS
 HC A06/MF A01 CSCL 11A

The first year of a two year experimental and analytical program is reported. The program is directed at the elastohydrodynamic behavior of sliding elastomeric rod seals for the Stirling engine. During the year, experimental and analytical tools were developed for evaluating seal leakage, seal friction, and the fluid film thickness at the seal/cylinder interface. G Y

N79-24373* Mechanical Technology, Inc., Latham, N. Y.
DEVELOPMENT OF PROCEDURES FOR CALCULATING STIFFNESS AND DAMPING OF ELASTOMERS IN ENGINEERING APPLICATIONS. PART 5: ELASTOMER PERFORMANCE LIMITS AND THE DESIGN AND TEST OF AN ELASTOMER DAMPER

J. A. Tecza, M. S. Darlow, and A. J. Smalley Feb. 1979
 144 p refs
 (Contract NAS3-18546)
 (NASA CR 159552; Rept-79TR30 Pt 5) Avail NTIS
 HC A07/MF A01 CSCL 20K

Tests were performed on elastomer specimens of the material polybutadiene to determine the performance limitations imposed by strain, temperature, and frequency. Three specimens were tested: a shear specimen, a compression specimen, and a second compression specimen in which thermocouples were embedded in the elastomer buttons. Stiffness and damping were determined from all tests, and internal temperatures were recorded for the instrumented compression specimen. Measured results are presented together with comparisons between predictions of a thermo-viscoelastic analysis and the measured results. Dampers of polybutadiene and Viton were designed, built, and tested. Vibration measurements were made and sensitivity of vibration to change in unbalance was also determined. Values for log decrement were extracted from the synchronous response curves. Comparisons were made between measured sensitivity to unbalance and log decrement and predicted values for these quantities. R E S

N79-25392* Mechanical Technology, Inc., Latham, N. Y.
T700 POWER TURBINE ROTOR MULTIPLANE/MULTISPEED BALANCING DEMONSTRATION

G. Burgess and R. Rio Feb. 1979 40 p refs
 (Contract NAS3-18520)
 (NASA CR 159586; MIT 79 TR 29) Avail NTIS
 HC A03/MF A01 CSCL 20E

Research was conducted to demonstrate the ability of influence coefficient based multispeed balancing to control rotor vibration through bending criticals. Rotor dynamic analyses were conducted of the General Electric T700 power turbine rotor. The information was used to generate expected rotor behavior for optimal considerations in designing a balance rig and a balance technique. The rotor was successfully balanced 9500 rpm. Uncontrollable coupling behavior prevented observations through the 16 000 rpm service speed. The balance technique is practical and with additional refinement it can meet production standards. Author

N79-25395* Oak Ridge National Lab., Tenn.
USER'S MANUAL FOR PRESTO: A COMPUTER CODE FOR THE PERFORMANCE OF REGENERATIVE STEAM TURBINE CYCLES

L. C. Fuller and T. K. Stovall Jun. 1979 93 p refs
 (NASA Order C-10669-D; Contracts W-7405-eng-26; DOE-40-666-77)
 (NASA-CR-159540; ORNL-5547) Avail NTIS
 HC A05/MF A01 CSCL 13I

Standard turbine cycles for baseload power plants and cycles with such additional features as process steam extraction and induction and feedwater heating by external heat sources may be modeled. Peaking and high back pressure cycles are also included. The code's methodology is to use the expansion line efficiencies, exhaust loss, leakages, mechanical losses, and generator losses to calculate the heat rate and generator output. A general description of the code is given as well as the instructions for input data preparation. Appended are two complete example cases. R E S

N79-31602* Pratt and Whitney Aircraft Group, East Hartford, Conn. Commercial Products Div.

DEVELOPMENT OF A PLASMA SPRAYED CERAMIC GAS PATH SEAL FOR HIGH PRESSURE TURBINE APPLICATIONS Final Report, 12 Sep. 1978 - 12 Apr. 1979

L. T. Shiembob and J. F. Hyland Sep. 1979 43 p
 (Contract NAS3-21390)
 (NASA-CR-159669; PWA-5633-11) Avail NTIS
 HC A03/MF A01 CSCL 11A

Development of the plasma sprayed graded, layered ZrO₂/CoCrAlY seal system for gas turbine engine blade tip seal application up to 1589 K (2400 F) surface temperature was continued. Methods of improvement of the cyclic thermal shock resistance of the sprayed zirconia seal system were investigated. The most promising method, reduction of the ceramic thickness and metallic substrate stiffness were selected based upon potential and feasibility. Specimens were fabricated and experimentally evaluated to: (1) substantiate the capacity of the geometry changes to reduce operating stresses in the sprayed structure; and (2) define the abrasability, erosion, thermal shock and physical property characteristic for the sprayed ceramic seal system. Thermal stress analysis was performed and correlated with thermal shock test results. Author

N79-31603* Mechanical Technology, Inc., Latham, N. Y.
DESIGN AND APPLICATION OF A TEST RIG FOR SUPERCRITICAL POWER TRANSMISSION SHAFTS Final Report

M. Darlow and A. Smalley Washington, NASA Aug. 1979
 168 p refs
 (Contract NAS3-16824)
 (NASA CR 3155; MTI-78TR41) Avail NTIS
 HC A08/MF A01 CSCL 13I

The design, assembly, operational check-out and application of a test facility for testing supercritical power transmission shafts under realistic conditions of size, speed and torque are described. Alternative balancing methods and alternative damping mechanisms are demonstrated and compared. The influence of torque upon the unbalance distribution is studied, and its effect on synchronous vibrations is investigated. The feasibility of operating supercritical power transmission shafting is demonstrated, but the need for careful control, by balancing and damping, of synchronous and nonsynchronous vibrations is made clear. The facility was demonstrated to be valuable for shaft system development programs and studies for both advanced and current production hardware. G Y

N79-32651* Avco Lycoming Div., Stratford, Conn.
DEVELOPMENT OF SPIRAL GROOVE SELF-ACTING SEALS FOR HELICOPTER ENGINES Final Report, 10 Jun. 1977 - 31 Dec. 1978

Michael O'Brien Jun. 1979 62 p. Sponsored in part by Army Res. and Technol. Labs.
 (Contract NAS3-20795)
 (NASA CR 159622; LYC-79-25) Avail NTIS
 HC A04/MF A01 CSCL 11A

A spiral-groove, self-acting face seal was rig tested at advanced gas turbine operating conditions to determine wear and leakage rates. The spiral-groove, self-acting geometry was located in the rotating seal seat. Seal component wear induced by start-stop operation was measured after subjecting the test seal to 176 start-stop cycles. Wear occurring during normal operation was documented throughout a 75-hour endurance test. Seal air leakage was also measured. During endurance operation, the seal was subjected to operating conditions bounded by the values surface speed - 244 m/s (800 ft/sec), air pressure - 148 N/sq cm abs (215 psia), and air temperature - 622 K (660 F). The post-test condition of the seal components was documented. Wear data is presented in tabular form, while seal air leakage is presented graphically, as a function of pressure and speed. F.O.S.

A79-12848 * **Ceramic blade attachments.** G. S. Calvert and W. D. Carruthers (United Technologies Corp., Pratt and Whitney Aircraft Group, West Palm Beach, Fla.). In: *Ceramics for high performance applications - II*, Proceedings of the Fifth Army Materials Technology Conference, Newport, R.I., March 21-25, 1977. (A79 12804 02-37) Chestnut Hill, Mass., Brook Hill Publishing Co., 1978, p. 839-860. Contract No. NAS3-19715.

Studies under way on two concepts for producing a turbine rotor with ceramic blades and superalloy disks are discussed. One concept employs hot pressed silicon nitride blades and a compliant interlayer at the blade root end fitting whereas the second concept relies on a superplastic plastic forging technique to attach ceramic blades to the metal disk. This latter concept has been hot spin tested at 2250 F and 45,000 RPM for 50 hours in a vacuum spin pit. The fully bladed (30 blades) rotor survived this major test. (Author)

A79-16011 * **Design and test of a squeeze-film damper for a flexible power transmission shaft.** M. S. Darlow and A. J. Smalley (Mechanical Technology, Inc., Latham, N.Y.). In: *Topics in fluid film bearing and rotor bearing system design and optimization*; Proceedings of the Design Engineering Conference, Chicago, Ill., April 17-20, 1978. (A79 16010 04-37) New York, American Society of Mechanical Engineers, 1978, p. 43-54, 7 refs. Contract No. NAS3-16824.

For a flexible shaft designed to pass through a number of bending critical speeds, a squeeze-film damper has been designed and tested. The damper properties were selected to provide control of all critical speeds, while meeting additional constraints of high power transmission requirements and damper simplicity. The damper was fabricated and installed and its ability to control flexible shaft vibrations was demonstrated by the comparison of vibration amplitudes both with and without the damper. (Author)

A79 23252 * **Development of surface coatings for air-lubricated, compliant journal bearings to 650 C.** B. Bhushan and S. Gray (Mechanical Technology, Inc., Latham, N.Y.). *American Society of Lubrication Engineers and American Society of Mechanical Engineers, Joint Lubrication Conference, Minneapolis, Minn., Oct. 24-26, 1978, ASLE Preprint 78-LC-3C.1*, 11 p. Contract No. NAS3-19427.

Surface coatings for an air lubricated, compliant journal for an automotive gas turbine engine were tested to find those capable of withstanding temperatures of either 540 C (1000 F) or 650 C (1200 F). Also, the coatings have to be capable of surviving the start-stop sliding contact cycles prior to rotor lift off and at touchdown. Selected coating combinations were tested in start-stop tests at 14 kPa (2 psi) loading for 2000 cycles at room and maximum temperatures. Specific coating recommendations are: Cdo and graphite on foil versus chrome carbide on journal up to 370 C (700 F); NASA PS 120 (Tribaloy 400, silver, and CaF₂) on journal versus uncoated foil up to 540 C (1000 F), and chemically adherent Cr₂O₃ on journal and foil up to 650 C (1200 F). The chemically adherent Cr₂O₃ coating system was further tested successfully at 35 kPa (5 psi) loading for 2000 start-stop cycles. (Author)

A79-26985 * **Proof test criteria for thin walled pressure vessels.** R. W. Finger (Boeing Aerospace Co., Seattle, Wash.). In: *Application of fracture mechanics to design*. (A79-26980 10-37) New York, Plenum Press, 1979, p. 83-110, 6 refs. Contract No. NAS3-18906.

A proof test criterion for assuring minimum service life requirements for aerospace pressure vessels is provided. The criteria proposed are based on the results of several experimental programs conducted on surface flaw specimens fabricated from 2219 aluminum base and weld metal. A description is presented of the stable crack growth behavior of surface flaws during loading. Conclusions derived from an experimental program are discussed. It is found that significant stable crack growth under increasing load can occur prior to failure. However, significant variability in results can be anticipated even when carefully controlled laboratory procedures are employed. G.R.

A79-32351 * # **Laser balancing demonstration on a high-speed flexible rotor.** R. S. DeMuth, R. A. Rio (Mechanical Technology, Inc., Latham, N.Y.), and D. P. Fleming (NASA, Lewis Research Center, Seals and Rotor Dynamics Section, Cleveland, Ohio). *American Society of Mechanical Engineers, Gas Turbine Conference and Exhibit and Solar Energy Conference, San Diego, Calif., Mar. 12-15, 1979, Paper 79-GT-56*, 6 p. 6 refs. Members, \$1.50; nonmembers, \$3.00. Contract No. NAS3-18520.

This paper describes a flexible rotor system used for two-plane laser balancing and an experimental demonstration of the laser material removal method for balancing. A laboratory test rotor was modified to accept balancing corrections using a laser metal removal method while the rotor is at operating speed. The laser setup hardware required to balance the rotor using two correction planes is described. The test rig optical configuration and a neodymium glass laser were assembled and calibrated for material removal rates. Rotor amplitudes before and after balancing, trial and correction weights, rotor speed during operation of laser, and balancing time were documented. The rotor was balanced through the first bending critical speed using the laser material removal procedure to apply trial weights and correction weights without stopping the rotor. (Author)

A79-32412 * # **Nonsynchronous vibrations observed in a supercritical power transmission shaft.** M. S. Darlow and E. S. Zorzi (Mechanical Technology, Inc., Latham, N.Y.). *American Society of Mechanical Engineers, Gas Turbine Conference and Exhibit and Solar Energy Conference, San Diego, Calif., Mar. 12-15, 1979, Paper 79-GT-146*, 9 p. 6 refs. Members, \$1.50; nonmembers, \$3.00. Contract No. NAS3-16824.

A flexible shaft is prone to a number of vibration phenomena which occur at frequencies other than synchronous with rotational speed. Nonsynchronous vibrations from several sources were observed while running a test rig designed to simulate the operation of a supercritical power transmission shaft. The test rig was run first with very light external damping and then with a higher level of external damping, for comparison. As a result, the effect of external damping on the nonsynchronous vibrations of the test rig was observed. All of these nonsynchronous vibrations were of significant amplitude. Their presence in the vibration spectra for a supercritical power transmission shaft at various speeds in the operating range indicates that very careful attention to all of the vibration spectra should be made in any supercritical power transmission shafting. This paper presents a review of the analysis performed and a comparison with experimental data. A thorough discussion of the observed nonsynchronous whirl is also provided. (Author)

A79-32423 * # An introduction to a unified approach to flexible rotor balancing. A. G. Parkinson (University College, London, England), A. J. Smalley, R. H. Badgley (Mechanical Technology, Inc., Latham, N.Y.), and M. S. Darlow. *American Society of Mechanical Engineers, Gas Turbine Conference and Exhibit and Solar Energy Conference, San Diego, Calif., Mar. 12-15, 1979, Paper 79-GT-161*. 14 p. 10 refs. Members, \$1.50; nonmembers, \$3.00. Contract No. NAS3-16824.

Two types of technique for flexible-rotor balancing are examined: the influence coefficient method, and the modal balancing method. Briefly, the influence coefficient method seeks those correction masses in a predetermined set of planes which will minimize measured vibration (readings) at a series of sensors and speeds, as predicted by influence coefficients relating vibration readings to mass additions; the influence coefficients are normally determined by a series of trial mass tests. The modal balancing method seeks to balance the rotor, one mode at a time, with a set of masses specifically selected not to disturb previously balanced lower modes, the sensitivity to this combination of masses is determined empirically by a series of trial mass tests. The two approaches are compared in supercritical-shaft balancing tests, and some common features are stressed for ultimate incorporation into a unified approach toward flexible-rotor balancing. S.D.

38 QUALITY ASSURANCE AND RELIABILITY

Includes product sampling procedures and techniques; and quality control.

N79-29630* National Aeronautics and Space Administration. Lewis Research Center, Cleveland, Ohio.

A REVIEW OF ISSUES AND STRATEGIES IN NONDESTRUCTIVE EVALUATION OF FIBER REINFORCED STRUCTURAL COMPOSITES

Alex Vary 1979 14 p refs Proposed for presentation at 11th Natl. SAMPE Tech. Conf., Boston, 13-15 Nov. 1979 (NASA-TM-79246; E-153) Avail: NTIS HC A02/MF A01 CSCL 14D

Techniques for quantitative assessment of the mechanical strength and integrity of fiber composites during manufacture and service and following repair operations are presented. Problems and approaches are discussed relative to acceptance criteria, calibrating standards, and methods for nondestructive evaluation of composites in strength-critical applications. Acousto-ultrasonic techniques provide the methods of choice in this area. M.M.M.

A79-39809 * Computer signal processing for ultrasonic attenuation and velocity measurements for material property characterizations. A. Vary (NASA, Lewis Research Center, Cleveland, Ohio). *American Society for Nondestructive Testing and Southwest Research Institute, Symposium on Nondestructive Evaluation*, 12th, San Antonio, Tex., Apr. 24-26, 1979, Paper. 18 p. 8 refs.

This report deals with instrumentation and computer programming concepts that have been developed for ultrasonic materials characterization. Methods that facilitate velocity and attenuation measurements are described. The apparatus described is based on a broadband, buffered contact probe using a pulse-echo approach for simultaneously measuring velocity and attenuation. Instrumentation, specimen condition, and signal acquisition and acceptance criteria are discussed. Typical results with some representative materials are presented. (Author)

N79-21410* Martin Marietta Aerospace, Denver, Colo. DEFINITION OF MUTUALLY OPTIMUM NDI AND PROOF TEST CRITERIA FOR 2219 ALUMINUM PRESSURE VESSELS. VOLUME 1: METHODS

Fred R. Schwartzberg, Richard G. King, and Paul H. Todd, Jr. Feb. 1979 138 p refs 3 Vol. (Contract NAS3-17790) (NASA-CR-135445) Avail: NTIS HC A07/MF A01 CSCL 14D

The requirements for proof testing and nondestructive inspection of aluminum pressure vessels were discussed. The following conclusions are (1) lack-of-fusion weld defects are sufficiently tight in the as-welded condition to be considered undetectable; (2) proof-level loads are required to fully open lack-of-fusion weld defects; (3) significant crack opening occurs at subproof levels so that an inspection enhancement loading treatment designed to avoid catastrophic failure is feasible; (4) currently used proof levels for 2219 pressure vessels are adequate for postproof inspection; (5) quantification of defect size and location using collimated ultrasonic pitch-catch techniques appears sufficiently feasible for tankage to warrant developmental work; (6) for short-time single-cycle pressure-vessel applications, postproof inspection is desirable; and (7) for long-term multiple-cycle pressure-vessel applications, postproof inspection is essential for life assurance. Author

N79-21411* Martin Marietta Aerospace, Denver, Colo. DEFINITION OF MUTUALLY OPTIMUM NDI AND PROOF TEST CRITERIA FOR 2219 ALUMINUM PRESSURE VESSELS. VOLUME 2: OPTIMIZATION AND FRACTURE STUDIES

Fred R. Schwartzberg, Charles Toth, Jr., Richard G. King, and Paul H. Todd, Jr. Feb. 1979 183 p refs 3 Vol. (Contract NAS3-17790) (NASA-CR-135446) Avail: NTIS HC A09/MF A01 CSCL 14D

Certain behavioral aspects associated with fracture and crack extension that cannot be studied using other techniques were evaluated with the ultrasonic method. Characterization of collimated beam techniques showed that significant beam width reduction could be accomplished. Techniques for collimation are given. The crack-opening displacement-gage correction-factor study showed that displacement resulting from crack opening and that from plasticity could be readily differentiated. Crack closure studies using both ultrasonic and crack-opening displacement measurements showed an opening and closing behavior associated with load-unload curves. The results of this work were in general agreement with the closure concepts of Elber. Ultrasonic measurements used to study the nature of flaw extension characteristics associated with failure of the ligament between the flaw front and back surface showed that penetration could occur by an abrupt fracturing after subcritical growth or by continuous growth. Author

N79-21412* Martin Marietta Aerospace, Denver, Colo. DEFINITION OF MUTUALLY OPTIMUM NDI AND PROOF TEST CRITERIA FOR 2219 ALUMINUM PRESSURE VESSELS. VOLUME 3: APPLICATIONS TO RAIL DEFECT EVALUATION

Fred R. Schwartzberg, Charles Toth, Jr., Richard G. King, and Paul H. Todd, Jr. Feb. 1979 35 p 3 Vol. (Contract NAS3-17790) (NASA-CR-135447) Avail: NTIS HC A03/MF A01 CSCL 14D

The technique for inspection of railroad rails containing transverse fissure defects was discussed. Both pulse-echo and pitch-catch inspection techniques were used. The pulse-echo technique results suggest that a multiple-scan approach using varying angles of inclination, three-surface scanning, and dual-direction traversing may offer promise of characterization of transverse defects. Because each scan is likely to produce a reflection indicating only a portion of the defect, summing of the individual reflections must be used to obtain a reasonably complete characterization of the defect. The ability of the collimated pitch-catch technique to detect relatively small amounts of flaw growth was shown. The method has a problem in characterizing the portions of the defect near the top surface or web intersection. The work performed was a preliminary evaluation of the prospects for automated mapping of rail flaws. Author

39 STRUCTURAL MECHANICS

Includes structural element design and weight analysis; fatigue; and thermal stress.

For applications see 05 Aircraft Design, Testing and Performance and 18 Spacecraft Design, Testing and Performance.

N79-10480* National Aeronautics and Space Administration. Lewis Research Center, Cleveland, Ohio.

STRAINRANGE PARTITIONING BEHAVIOR OF THE NICKEL-BASE SUPERALLOYS, RENE 80 AND IN-100

G. R. Halford and A. J. Nachtigall. In AGARD Characterization of Low Cycle High Temp. Fatigue by the Strainrange Partitioning Method. Aug. 1978. 14 p. refs. (For primary document see N79-10477 01-39)

Avail: NTIS HC A15/MF A01 CSDL 20K

A study was made to assess the ability of the method of strainrange partitioning (SRP) to both correlate and predict high temperature, low cycle fatigue lives of nickel-base superalloys for gas turbine applications. Baseline data from strain-controlled, low cycle fatigue tests were expressed in terms of the PP, PC, CP, and CC partitioned inelastic strainrange versus life relationships for coated and uncoated Rene 80 at 1000 C, Gatorized (creep-formed) IN 100 at 760 C, and cast IN 100 at 925 C. The SRP is shown to correlate the cyclic lives of the baseline tests to within factors of nearly two. The partitioned strainrange versus life relationships for uncoated Rene 80 and cast IN 100 were also determined from the ductility normalized-strainrange partitioning equations. These were used to predict the cyclic lives of the baseline tests. Predicted and observed cyclic lives agreed to within factors of nearly three. J.A.M.

N79-11433* National Aeronautics and Space Administration. Lewis Research Center, Cleveland, Ohio.

THERMAL-STRUCTURAL MISSION ANALYSES OF AIR-COOLED GAS TURBINE BLADES

Albert Kaufman and Raymond E. Gaugler. 1978. 13 p. refs. Proposed for presentation at the Intern. Gas Turbine Conf., San Diego, Calif., 11-15 Mar. 1979.

(NASA-TM-78963; E-9720) Avail: NTIS HC A02/MF A01 CSDL 21E

Cyclic temperature and stress-strain states in cooled turbine blades were calculated for a simulated mission of an advanced technology aircraft engine. TACT1 (three dimensional heat transfer) and MARC (nonlinear structural analysis) computer programs were used to analyze impingement cooled airfoils, with and without leading-edge film cooling. Creep was the predominant damage mode, particularly around film cooling holes. Radially angled holes exhibited less creep than holes normal to surface. Beam-type analyses of all-impingement cooled airfoils gave fair agreement with MARC results for initial creep. Author

N79-15326* National Aeronautics and Space Administration. Lewis Research Center, Cleveland, Ohio.

CELFE/NASTRAN CODE FOR THE ANALYSIS OF STRUCTURES SUBJECTED TO HIGH VELOCITY IMPACT

C. C. Chamis. 1978. 25 p. refs. Presented at 7th NASTRAN User's Colloq., Huntsville, Ala., 4-6 Oct. 1978.

(NASA-TM-79048; E-9857) Avail: NTIS HC A02/MF A01 CSDL 20K

CELFE (Coupled Eulerian Lagrangian Finite Element)/NASTRAN Code three-dimensional finite element code has the capability for analyzing of structures subjected to high velocity impact. The local response is predicted by CELFE and, for large problems, the far-field impact response is predicted by NASTRAN. The coupling of the CELFE code with NASTRAN (CELFE/NASTRAN code) and the application of the code to selected three-dimensional high velocity impact problems are described. Author

N79-15326* National Aeronautics and Space Administration. Lewis Research Center, Cleveland, Ohio.

CODSTRAN: COMPOSITE DURABILITY STRUCTURAL ANALYSIS

C. C. Chamis and G. T. Smith. 17 Nov. 1978. 14 p. refs. Presented at the 4th Conf. on Fibrous Composites in Struct. Design, San Diego, Calif., 14-17 Nov. 1978. (NASA-TM-79070; E-9837) Avail: NTIS HC A02/MF A01 CSDL 20K

CODSTRAN (COMposite Durability STRuctural ANalysis) is an integrated computer program being developed for the prediction of defect growth and fracture of composite structures subjected to service loads and environments. CODSTRAN is briefly described with respect to organization, capabilities and present status. Application of CODSTRAN current capability to a flat composite laminate with a center slit which was subjected to axial tension loading predicted defect growth which is in good agreement with C-scan ultrasonic test records. Author

N79-16300* National Aeronautics and Space Administration. Lewis Research Center, Cleveland, Ohio.

EXPERIMENTAL EVALUATION OF THE EFFECT OF INLET DISTORTION ON COMPRESSOR BLADE VIBRATIONS

J. F. Lubomski. 1979. 17 p. refs. Presented at the Intern. Gas Turbine Conf., San Diego, Calif., 12-15 Mar. 1979; sponsored by Am. Soc. of Mechanical Engineers.

(NASA-TM-79066; E-9882) Avail: NTIS HC A02/MF A01 CSDL 20K

Compressor rotor strain gage data from an engine test conducted with an inlet screen distortion were reduced and analyzed. These data are compared to data obtained from the same engine without inlet pressure distortion to determine the net effect of the distortion on the vibratory response of the compressor blades. The results obtained are presented. Author

N79-17263* National Aeronautics and Space Administration. Lewis Research Center, Cleveland, Ohio.

CHARACTERISTICS OF AEROELASTIC INSTABILITIES IN TURBOMACHINERY - NASA FULL SCALE ENGINE TEST RESULTS

Joseph F. Lubomski. 1979. 21 p. refs. To be presented at the 4th Intern. Symp. on Air Breathing Eng., Lake Buena Vista, Fla., 1-6 Apr. 1979; sponsored by AIAA.

(NASA-TM-79085; E-9908) Avail: NTIS HC A02/MF A01 CSDL 20K

Several aeromechanical programs were conducted in the NASA/USAF Joint Engine System Research Programs. The scope of these programs, the instrumentation, data acquisition and reduction, and the test results are discussed. Data pertinent to four different instabilities were acquired: two types of stall flutter, choke flutter and a system mode instability. The data indicates that each instability has its own unique characteristics. These characteristics are described. G.Y.

N79-19415* National Aeronautics and Space Administration. Lewis Research Center, Cleveland, Ohio.

MEASUREMENT OF TRANSIENT STRAIN AND SURFACE TEMPERATURE ON SIMULATED TURBINE BLADES USING NONCONTACTING TECHNIQUES

Frederick D. Calfo and Frank G. Pollack. Aug. 1978. 18 p. refs.

(NASA-TM-78982; C-9180) Avail: NTIS HC A02/MF A01 CSDL 20K

Noncontacting techniques were used to measure strain and temperature in thermally cycled simulated turbine blades. An electro-optical extensometer was used to measure the displacement between parallel targets mounted on the leading edge of the blades throughout a complete heating and cooling cycle. An infrared photographic pyrometry method was used to measure blade steady state surface temperature. The blade was cyclically heated and cooled by moving it into and out of a Mach 1 hot-gas stream. Transient leading edge strain and steady state surface temperature distributions are presented for blades of three different configurations. Author

N79-20380* National Aeronautics and Space Administration, Lewis Research Center, Cleveland, Ohio.

INVESTIGATION OF WING SHIELDING EFFECTS ON CTOL ENGINE NOISE

Harry E. Bloomer 1979 34 p refs Presented at the 5th Annual Aeroacoustics Conf., Seattle, 12-14 Mar. 1979; sponsored by AIAA

(NASA-TM-79078; E-9895) Avail: NTIS HC A03/MF A01 CSCL 20K

A full scale engine wing shielding investigation was conducted at the Lewis Research Center using a 97,900-N (22,000 lb) thrust turbofan engine and a simulated wing section sized around a conventional-take-off type four-engine narrow body airplane. Sound data were obtained for the wing placed at seven positions in a plane parallel to the engine axis, and were compared to data obtained without the wing at both take off and approach power. In addition, the engine was operated with and without extensive acoustic treatment, including a sonic inlet in order to evaluate wing shielding effectiveness with a highly suppressed engine. The wing shielding effectiveness was also calibrated using a 3.8 cm diam air nozzle as a second source. Results indicated that even though about 10 dB broad band shielding was achieved, the equivalent flyover noise reduction was less than 3.0 EPNdB for most configurations. Author

N79-20381* National Aeronautics and Space Administration, Lewis Research Center, Cleveland, Ohio.

SOME ASPECTS OF A FREE JET PHENOMENA TO 106 L/D IN A CONSTANT AREA DUCT

R. C. Hendricks 1979 41 p refs Proposed for presentation at the 15th Intern. Congr. of Refrig., Venice, 23-29 Sep. 1979; sponsored in part by the Intern. Inst. of Refrig.

(NASA-TM-79050; E-9867) Avail: NTIS HC A03/MF A01 CSCL 20K

Under certain conditions, inlets with a Borda type geometry were shown to exhibit sufficiently strong separation effects to permit the working fluid to flow through the duct as if it were a free jet. Mass limiting flow data and associated pressure profiles for tubes of 14, 53, 64, 73, and 105 L/D with a Borda type inlet were taken to determine bounds of the free jet phenomena. For a given tube roughness, the limits appear to be one dimensional and dependent only on inlet stagnation conditions. For smooth tubes the upper L/D boundary is related by $P_{sub} R$ roughly equal to CT to the 17th power and sub R, C roughly equal to 0.0017 (L/D) to the 2.5 power where $F_{sub} R = P/P_{sub}$ c is reduced pressure and $T_{sub} R = T/T_{sub}$ c is reduced temperature. The lower bound appears to be saturation conditions at the inlet. Similar free jet effects were found for fluid hydrogen indicating that fluid jetting may be common to all fluids. While limited data on surface roughness show a decrease in the upper L/D limit, nevertheless fluid jetting still occurred. LS.

N79-20388* National Aeronautics and Space Administration, Lewis Research Center, Cleveland, Ohio.

ANALYSIS OF HIGH VELOCITY IMPACT ON HYBRID COMPOSITE FAN BLADES

C. C. Chamis and J. H. Sinclair 1979 17 p refs Presented at the 20th Structures, Structural Dyn. and Mater. Conf., St. Louis, Mo., 4-6 Apr. 1979; cosponsored by AIAA, ASME, ASCE, and AHS

(NASA-TM-79133; E-9979) Avail: NTIS HC A02/MF A01 CSCL 21E

Recent developments in the analysis of high velocity impact of composite blades are described, using a computerized capability which consists of coupling a composites mechanics code with the direct-time integration features of NASTRAN. The application of the capability to determine the linear dynamic response of an interply hybrid composite aircraft engine fan blade is described in detail. The results also show that the impact stresses reach sufficiently high magnitudes to cause failures in the impact region at early times of the impact event. G.Y.

N79-24389* National Aeronautics and Space Administration, Lewis Research Center, Cleveland, Ohio.

COMPUTER SIGNAL PROCESSING FOR ULTRASONIC ATTENUATION AND VELOCITY MEASUREMENTS FOR MATERIAL PROPERTY CHARACTERIZATIONS

Alex Vary 1979 19 p refs Presented at the 12th Symp on Nondestructive Evaluation, San Antonio, Tex., 24-26 Apr. 1979; cosponsored by the Am. Soc. for Nondestructive Testing and the Southwest Res. Inst.

(NASA-TM-79180; E-048) Avail: NTIS HC A02/MF A01 CSCL 14D

Instrumentation and computer programming concepts that were developed for ultrasonic materials characterization are described. Methods that facilitate velocity and attenuation measurements are outlined. The apparatus described is based on a broadband, buffered contact probe using a pulse-echo approach for simultaneously measuring velocity and attenuation. Instrumentation, specimen condition, and signal acquisition and acceptance criteria are discussed. Typical results with some representative materials are presented. LS.

N79-22585* National Aeronautics and Space Administration, Lewis Research Center, Cleveland, Ohio.

EFFECT OF GRAIN ORIENTATION AND COATING ON THERMAL FATIGUE RESISTANCE OF A DIRECTIONALLY SOLIDIFIED SUPERALLOY (MAR-M 247)

P. T. Bizon, R. L. Dreshfield, and F. D. Calfo Apr. 1979 24 p refs

(NASA-TM-79129; E-9968) Avail: NTIS HC A02/MF A01 CSCL 20K

The effect of off-axis directionally solidified (DS) grain growth on thermal fatigue life of Mar-M 247 alloy was evaluated. Uncoated conventionally cast as well as DS wedge bars were cycled in a burner rig between 1070 C and room temperature. The longitudinal axis and leading edge of the specimen coincided. As the angle between the specimen longitudinal axis and growth axis increased, the thermal fatigue life decreased for both the uncoated and aluminide-coated bars. Life increases of about 50 cycles for the DS conditions were attributed to coating. The decrease in thermal fatigue life with increasing angle is primarily attributed to the increase in modulus of elasticity with increasing angle and not to the intersection of DS grain boundaries with the specimen leading edge. The thermal fatigue cracks were observed to be transgranular in the DS material. Limited tensile and stress-rupture properties of conventionally cast and off-axis DS Mar-M 247 alloy are also presented. LS.

N79-31619* National Aeronautics and Space Administration, Lewis Research Center, Cleveland, Ohio.

STRAINRANGE PARTITIONING LIFE PREDICTIONS OF THE LONG TIME METAL PROPERTIES COUNCIL CREEP-FATIGUE TESTS

J. F. Saltzman and G. R. Halford 1979 34 p refs Proposed for presentation at the Winter Ann. Meeting, N. Y., 2-7 Dec. 1979; sponsored by Am. Soc. of Mech. Engr.

(NASA-TM-79260; E-174) Avail: NTIS HC A03/MF A01 CSCL 20K

The method of strainrange partitioning is used to predict the cyclic lives of the Metal Properties Council's long time creep-fatigue interspersed tests of several steel alloys. Comparisons are made with predictions based upon the time- and cycle-fraction approach. The method of strainrange partitioning is shown to give consistently more accurate predictions of cyclic life than is given by the time- and cycle-fraction approach. Author

A79-10823 * Synthesis of blade flutter vibratory patterns using stationary transducers. A. Korkov and J. Dicus (NASA, Lewis Research Center, Cleveland, Ohio). *American Society of Mechanical Engineers, Gas Turbine Conference and Products Show, London, England, Apr. 9-13, 1978, Paper. 25 p.* 9 refs.

Flutter frequency was determined and rotor vibratory amplitude and phase distributions during flutter were reconstructed from stationary aerodynamic type measurements. A previously reported

optical method for measuring blade-tip displacement during flutter was extended by means of digital analysis. Displacement amplitudes and phase angle were determined based on this method. For selected blades, spectral results were also obtained from strain gage measurements. The results from these three types of measurement were compared and critically evaluated. (Author)

A79-11543 * # Acoustic emission testing of composite vessels under sustained loading. R. F. Lark and P. E. Moorhead (NASA, Lewis Research Center, Cleveland, Ohio). *American Society for Testing and Materials, Symposium on Nondestructive Evaluation and Flaw Criticality for Composite Materials*, Philadelphia, Pa., Oct. 10, 11, 1978, Paper. 24 p. 8 refs.

Acoustic emission (AE) tests have been conducted on small-diameter Kevlar 49/epoxy pressure vessels subjected to long-term sustained load-to-failure tests. Single-cycle burst tests were used as a basis for determining the test pressure in the sustained-loading tests. AE data from two vessel locations were compared. The data suggest that AE from vessel wall-mounted transducers is quite different for identical vessels subjected to the same pressure loading. AE from boss-mounted transducers yielded relatively consistent values. These values were not a function of time for vessel failure. The development of an AE test procedure for predicting the residual service life or integrity of composite vessels is discussed. S.C.S.

A79-14954 * # Review of the Agard S&M panel evaluation program of the NASA-Lewis 'SRP' approach to high-temperature LCF life prediction. M. H. Hirschberg (NASA, Lewis Research Center, Cleveland, Ohio). *NATO, AGARD, Meeting, 52nd, Cleveland, Ohio, Oct. 23-27, 1978, Paper*. 10 p. 26 refs.

Twenty laboratories in six countries participated in this program, each testing its own materials of interest under its own laboratory conditions. In this way the results obtained provided validation of the Strainrange Partitioning (SRP) method for a wide range of materials and insured maximum usefulness to each of the participating laboratories. The first, very necessary step in the evaluation of any life prediction approach - assessing the ability of the method to predict life of simple laboratory specimens subjected to complex loading, was thereby taken. The culmination of this program was the Specialists Meeting that was held in Aalborg, Denmark in April of 1978. At that meeting the various investigators shared their findings, thus providing the basis for an in-depth evaluation of the SRP method. While the results were variable from laboratory to laboratory, most investigators agreed that the SRP method was a significant step toward life prediction in the presence of high temperature and cyclic stresses. (Author)

A79-15588 * # Mode I analysis of a cracked circular disk subject to a couple and a force. B. Gross (NASA, Lewis Research Center, Cleveland, Ohio). In: *Developments in theoretical and applied mechanics*. Volume 9 - Proceedings of the Ninth South-eastern Conference, Nashville, Tenn., May 4, 5, 1978. (A79-15576 04-31) Nashville, Tenn., Vanderbilt University, 1978, p. 195-203. 8 refs.

Mode I stress intensity coefficients were obtained for an edge-cracked disk (round compact specimen). Results for this plane elastostatic problem, obtained by a boundary collocation analysis are presented for A/D ratios of 0.35 to 1, where A is the crack length and D is the disk diameter. The results presented are for two complementary types of loading. By superposition of these results the stress intensity factor for any practical load line location of a pin-loaded round compact specimen can be obtained. (Author)

A79-21298 * # CELFE/NASTRAN Code for the analysis of structures subjected to high velocity impact. C. C. Chamis (NASA, Lewis Research Center, Cleveland, Ohio). *NASA Marshall Space Flight Center, NASTRAN User's Colloquium*, 7th, Huntsville, Ala., Oct. 4-6, 1978, Paper. 24 p. Contract No. NAS7-18908.

The CELFE (Coupled Eulerian Lagrangian Finite Element)/NASTRAN Code three-dimensional finite element code has the capability for analyzing of structures subjected to high velocity impact. The local response is predicted by CELFE and, for large problems, the far-field impact response is predicted by NASTRAN. The coupling of the CELFE code with NASTRAN (CELFE/NASTRAN code) and the application of the code to selected three-dimensional high velocity impact problems are described. (Author)

A79-21831 * Mode I analysis of a face cracked plate subjected to rotationally constrained end displacements. B. Gross (NASA, Lewis Research Center, Cleveland, Ohio). *International Journal of Fracture*, vol. 14, Dec. 1978, p. 623-631. 6 refs.

A79-29027 * # Analysis of high velocity impact on hybrid composite fan blades. J. C. Chamis and J. H. Sinclair (NASA, Lewis Research Center, Composites and Structures Branch, Cleveland, Ohio). In: *Structures, Structural Dynamics, and Materials Conference*, 20th, St. Louis, Mo., April 4-6, 1979, Technical Papers on Structures and Materials. (A79-29002 11-39) New York, American Institute of Aeronautics and Astronautics, Inc., 1979, p. 249-257. 6 refs. (AIAA 79-0783)

This paper describes recent developments in the analysis of high velocity impact of composite blades using a computerized capability which consists of coupling a composites mechanics code with the direct-time integration features of NASTRAN. The application of the capability to determine the linear dynamic response of an intraply hybrid composite aircraft engine fan blade is described in detail. The predicted results agree with measured data. The results also show that the impact stresses reach sufficiently high magnitudes to cause failures in the impact region at early times of the impact event. (Author)

A79-30558 * # Experimental evaluation of the effect of inlet distortion on compressor blade vibrations. J. F. Lubomski (NASA, Lewis Research Center, Cleveland, Ohio). *American Society of Mechanical Engineers, Gas Turbine Conference and Exhibit and Solar Energy Conference*, San Diego, Calif., Mar. 12-15, 1979, Paper. 15 p. 7 refs.

Compressor rotor strain gage data from an engine test conducted with an inlet screen distortion were reduced and analyzed. The data were compared to results obtained from the same engine without inlet pressure distortion to determine the net effect of the distortion on the vibratory response of the compressor blades. The effect of the distortion was found to be most prominent in the first three compressor stages, with the rotor speed establishing the period of the complex wave and, consequently, the frequencies of all the higher engine order excitations. At certain speeds it was observed that the complex pressure wave had the frequency content to excite a number of modes simultaneously, although the overall magnitudes were small and well within allowable stress limits. A.A.

A79-37292 * # CODSTRAN - Composite durability structural analysis. C. C. Chamis and G. T. Smith (NASA, Lewis Research Center, Cleveland, Ohio). *Conference on Fibrous Composites in Structural Design*, 4th, San Diego, Calif., Nov. 14-17, 1978, Paper. 13 p. 13 refs.

CODSTRAN (COmposite Durability STRucture ANALysis) a NASA Lewis Center computer program for the prediction of defect growth and fracture of composite structures when subjected to service loads is presented. Organization, capabilities and present status are discussed. Organizational aspects include executive, input, output, analysis and composite mechanics modules. Capabilities include: durability assessment of large structures and complex structural parts from composites, structural response due to static, cyclic, transient impact and thermal loads, and criteria for static, cyclic, and dynamic fracture. At the present state of development some of CODSTRAN's analysis capabilities include composite

mechanics, static failures, and lamination residual stresses. An application in which CODSTRAN is used to predict the defect growth in a flat specimen, with a center through-slit under tension is studied. When completed, CODSTRAN will account for geometry and material nonlinearities, environmental effects as well as static, cyclic and dynamic fracture. M.E.P.

A79-39812 * # Mode I crack surface displacements for a round compact specimen subject to a couple and force. B. Gross (NASA, Lewis Research Center, Cleveland, Ohio). *American Society for Testing and Materials, National Symposium on Fracture Mechanics, 12th, St. Louis, Mo., May 21-23, 1979, Paper.* 10 p. 5 refs.

Mode I displacement coefficients along the crack surface are presented for a radially cracked round compact specimen, treated as a plane elastostatic problem, subjected to two types of loading; a uniform tensile stress and a nominal bending stress distribution across the net section. By superposition the resultant displacement coefficient or the corresponding influence coefficient can be obtained for any practical load location. Load line displacements are presented for A/D ratios ranging from 0.40 to 0.95, where A is the crack length measured from the crack mouth to the crack tip and D is the specimen diameter. Through a linear extrapolation procedure crack mouth displacements are also obtained. Experimental evidence shows that the results of this study are valid over the range of A/D ratios analyzed for a practical pin loaded round compact specimen. (Author)

A79-39813 * # On the equivalence between semiempirical fracture analyses and R-curves. T. W. Orange (NASA, Lewis Research Center, Cleveland, Ohio). *American Society for Testing and Materials, National Symposium on Fracture Mechanics, 12th, St. Louis, Mo., May 21-23, 1979, Paper.* 32 p. 10 refs.

The relationships between several semiempirical fracture analyses (Brockrath and Glassco, 1974; Newman, 1973; Kuhn, 1968; Orange, 1971; Feddersen, 1971) and the R-curve concept of fracture mechanics are examined. Some characteristics of the R-curve concept when applied to finite-width specimens are reviewed, and conditions for equivalence between a semiempirical analysis (SEFA) and an R-curve are derived. The relationship between R-curves and SEFAs is studied for a hypothetical material. It is shown that for each SEFA there is an equivalent R-curve, the magnitude and shape of which are determined by the SEFA formulation and parameters, and which predicts precisely the same relationship between fracture stress and original crack length. A given SEFA correlates residual strength data closely if its equivalent R-curve closely matches the actual R-curve of the material studied. The SEFA given by Newman is found to yield best results for the hypothetical case considered. Equivalent R-curves for real materials are developed using data from the literature. C.K.D.

N79-10479 * # TRW, Inc., Cleveland, Ohio. Materials Technology Lab.

A STRAINRANGE PARTITIONING ANALYSIS OF LOW CYCLE FATIGUE OF COATED AND UNCOATED RENE 80 C. S. Kontovich and A. A. Sheinker. In *AGARD Characterization of Low Cycle High Temp. Fatigue by the Strainrange Partitioning Method* Aug. 1978 23 p refs. Sponsored in part by Army Air Mobility Res. and Develop. Lab. (For primary document see N79-10477 01-39)

(Contract NAS3-17830)

Avail: NTIS HC A15/MF A01 CSCL 20K

A strainrange partitioning analysis was conducted on ultrahigh vacuum, strain-controlled, low-cycle fatigue behavior of uncoated and aluminide coated Rene 80 nickel-base superalloy at 1000 C (1832 F) and 871 C (1600 F). The results indicated little effect of coating or temperature on the fatigue resistance. There was, however, a significant effect on fatigue life when creep was introduced into the strain cycles. The effect of this creep component was analyzed in terms of the method of strainrange partitioning. Author

N79-13486 * # Battelle Columbus Labs., Ohio.
STRESS ANALYSIS FOR STRUCTURES WITH SURFACE CRACKS Final Report
J. C. Bell Aug. 1978 182 p refs
(Contract NAS3-21020)
(NASA-CR-159400) Avail: NTIS HC A08/MF A01 CSCL 20K

Two basic forms of analysis, one treating stresses around arbitrarily loaded circular cracks, the other treating stresses due to loads arbitrarily distributed on the surface of a half space, are united by a boundary-point least squares method to obtain analyses for stresses from surface cracks in plates or bars. Calculations were for enough cases to show how effects from the crack vary with the depth-to-length ratio, the fractional penetration ratio, the obliquity of the load, and to some extent the fractional open ratio. The results include plots showing stress intensity factors, stress component distributions near the crack, and crack opening displacement patterns. Favorable comparisons are shown with two kinds of independent experiments, but the main method for confirming the results is by wide checking of overall satisfaction of boundary conditions, so that external confirmation is not essential. Principles involved in designing analyses which promote dependability of the results are proposed and illustrated. A.R.H.

N79-13488 * # Battelle Columbus Labs., Ohio.
USER'S MANUAL FOR FRAC3D: SUPPLEMENT TO REPORT ON STRESS ANALYSIS FOR STRUCTURES WITH SURFACE CRACKS
J. C. Bell, A. T. Hopper, and P. A. Hayes Aug. 1978 125 p refs
(Contract NAS3-21020)
(NASA-CR-159401) Avail: NTIS HC A08/MF A01 CSCL 20K

The FRAC3D computer program, designed for use in analyzing stresses in structures (including plates, bars, or blocks) which may contain part-circular surface cracks or embedded circular cracks is described. Instructions are provided for preparing input, including that for the supporting programs LATTICE and MATSOL as well as for FRAC3D. The course of a substantial illustrative calculation is shown with both input and output. The formulas underlying the calculations are summarized and related to the subroutines in which they are used. Many issues of strategy in using this program for analyzing stresses around surface cracks are elucidated. A.R.H.

N79-18343 * # Massachusetts Inst. of Tech., Cambridge. Aeroelastic and Structures Research Lab.
USER'S GUIDE TO COMPUTER PROGRAMS JET 5A AND CIVM-JET 5B TO CALCULATE THE LARGE ELASTIC-PLASTIC DYNAMICALLY-INDUCED DEFORMATIONS OF MULTILAYER PARTIAL AND/OR COMPLETE STRUCTURAL RINGS

Richard W. H. Wu, Thomas R. Stagliano, Emmett A. Witmer, and Robert L. Spilker Nov. 1978 381 p refs
(Grant NGR-22-009-339)
(NASA-CR-159484, ASRL-TR-154-10) Avail: NTIS HC A17/MF A01 CSCL 20K

These structural ring deflections lie essentially in one plane and, hence, are called two-dimensional (2-d). The structural rings may be complete or partial; the former may be regarded as representing a fragment containment ring while the latter may be viewed as a 2-d fragment-deflector structure. These two types of rings may be either free or supported in various ways (pinned-fixed, locally clamped, elastic-foundation supported, mounting-bracket supported, etc.). The initial geometry of each ring may be circular or arbitrarily curved, uniform-thickness or variable-thickness rings may be analyzed. Strain-hardening and strain-rate effects of initially-isotropic material are taken into account. An approximate analysis utilizing kinetic energy and momentum conservation relations is used to predict the after-impact velocities of each fragment and of the impact-affected region of the ring; this procedure is termed the collision-imparted velocity method (CIVM) and is used in the CIVM-JET 5 B program. This imparted-velocity information is used in conjunction with a finite-element structural response computation code to predict

the transient, large-deflection, elastic-plastic responses of the ring. Similarly, the equations of motion of each fragment are solved in small steps in time. Provisions are made in the CIVM-JET 5B code to analyze structural ring response to impact attack by from 1 to 3 fragments, each with its own size, mass, translational velocity components, and rotational velocity. The effects of friction between each fragment and the impacted ring are included.

F.O.S.

N78-18414* California Univ. at Los Angeles.
NONLINEAR EQUATIONS OF EQUILIBRIUM FOR ELASTIC HELICOPTER OR WIND TURBINE BLADES UNDERGOING MODERATE DEFORMATION Final Report
 Avin Rosen and Peretz P. Friedmann Dec. 1978 104 p refs
 (Grant NaG-3082; Contract E(49-26)-1028)
 (NASA-CR-159478; UCLA-ENG-7718;
 DOE/NASA/3082-78/1) Avail: NTIS HC A06/MF A01 CSCL 20K

A set of nonlinear equations of equilibrium for an elastic wind turbine or helicopter blades are presented. These equations are derived for the case of small strains and moderate rotations (slopes). The derivation includes several assumptions which are carefully stated. For the convenience of potential users the equations are developed with respect to two different systems of coordinates, the undeformed and the deformed coordinates of the blade. Furthermore, the loads acting on the blade are given in a general form so as to make them suitable for a variety of applications. The equations obtained in the study are compared with those obtained in previous studies. L.S.

N78-20382* California Univ. at Los Angeles.
NONLINEAR EQUATIONS OF EQUILIBRIUM FOR ELASTIC HELICOPTER OR WIND TURBINE BLADES UNDERGOING MODERATE DEFORMATION Final Report
 Avin Rosen and Peretz P. Friedmann Dec. 1978 105 p refs
 Prepared for DOE
 (Grant NaG-3082; Contract E(49-26)-1028)
 (NASA-CR-159478; DOE/NASA/3082-78/1;
 UCLA-ENG-7718) Avail: NTIS HC A06/MF A01 CSCL 20K

The equations are derived for the case of small strains and moderate rotations (slopes). For the convenience of potential users the equations are developed with respect to two different systems of coordinates, the undeformed and the deformed coordinates of the blade. The loads acting on the blade are given in a general form so as to make them suitable for a variety of applications. Author

N78-28429* Syracuse Univ., N. Y. George Sachs Fracture and Fatigue Research Lab.

A LITERATURE REVIEW ON FATIGUE AND CREEP INTERACTION

Wen-Ching Chen [1978] 41 p refs
 (Grant NGR-33-022-157)
 (NASA-CR-135305; MTS-HWL-4116-776) Avail: NTIS HC A03/MF A01 CSCL 20K

Life-time prediction methods, which are based on a number of empirical and phenomenological relationships, are presented. Three aspects are reviewed: effects of testing parameters on high temperature fatigue, life-time prediction, and high temperature fatigue crack growth. M.M.M.

N78-31627* Lehigh Univ., Bethlehem, Pa. Inst. of Fracture and Solid Mechanics

NORMAL AND RADIAL IMPACT OF COMPOSITES WITH EMBEDDED PENNY-SHAPED CRACKS Interim Report

G. C. Sih Feb. 1979 54 p refs
 (Grant NaG-3179)
 (NASA-CR-159538; IFSM-79-99) Avail: NTIS HC A04/MF A01

A method is developed for the dynamic stress analysis of a layered composite containing an embedded penny-shaped crack and subjected to normal and radial impact. The material properties

of the layers are chosen such that the crack lies in a layer of matrix material while the surrounding material possesses the average elastic properties of a two-phase medium consisting of a large number of fibers embedded in the matrix. Quantitatively, the time-dependent stresses near the crack border can be described by the dynamic stress intensity factors. Their magnitude depends on time, on the material properties of the composite and on the relative size of the crack compared to the composite local geometry. Results obtained show that, for the same material properties and geometry of the composite, the dynamic stress intensity factors for an embedded (penny-shaped) crack reach their peak values within a shorter period of time and with a lower magnitude than the corresponding dynamic stress intensity factors for a through-crack. Author

A79-27938* Stresses from arbitrary loads on a circular crack. J. C. Bell (Battelle Columbus Laboratories, Columbus, Ohio). *International Journal of Fracture*, vol. 15, Feb. 1979, p. 85-104, 18 refs. Research supported by the Battelle Memorial Institute and Bell Aerospace Co.; Contracts No. F33615-72-C-1739; No. NAS3-17760.

An inclusive theory is developed for stresses and displacements due to arbitrarily distributed normal and tangential loads acting on a circular crack in an infinite body. The representation chosen for the boundary conditions leads to solutions expressed as series of Bessel-function integrals of a class quite susceptible to further analysis and to rapid evaluation on modern computers. The load coefficients which appear in all the solution series bear intelligible interpretation, and stress intensity factors are related to them by simple formulas. The inclusiveness and tractability of the solutions qualify this theory to be a useful part of analyses for cracks in finite bodies in which the effective crack loads can assume many patterns. (Author)

43 EARTH RESOURCES

Includes remote sensing of earth resources by aircraft and spacecraft, photogrammetry, and aerial photography. For instrumentation see 35 Instrumentation and Photography.

N78-13472* National Aeronautics and Space Administration, Lewis Research Center, Cleveland, Ohio.
APPLICATION OF MULTISPECTRAL SCANNER DATA TO THE STUDY OF AN ABANDONED SURFACE COAL MINE
Ernie W. Spiez Nov. 1978 80 p refs Original contains color illustrations
(NASA-TM-78912; E-9647) Avail: NTIS HC A05/MF A01 CSCL 081

The utility of aircraft multispectral scanner data for describing the land cover features of an abandoned contour-mined coal mine is considered. The data were obtained with an 11 band multispectral scanner at an altitude of 1.2 kilometers. Supervised, maximum-likelihood statistical classifications of the data were made to establish land-cover classes and also to describe in more detail the barren surface features as they may pertain to the reclamation or restoration of the area. The scanner data for the surface-water areas were studied to establish the variability and range of the spectral signatures. Both day and night thermal images of the area are presented. The results of the study show that a high degree of statistical separation can be obtained from the multispectral scanner data for the various land-cover features. G.G.

N78-22589* National Aeronautics and Space Administration, Lewis Research Center, Cleveland, Ohio.
A COMPARISON OF MEASURED AND CALCULATED UPWELLING RADIANCE OVER WATER AS A FUNCTION OF SENSOR ALTITUDE
Thom A. Coney and Jack A. Salzman 1979 19 p refs Presented at the 13th Intern. Symp. on Remote Sensing of Environment, Ann Arbor, Mich., 23-27 Apr. 1979, sponsored by Mich. Univ. (NASA-TM-79147; E-003) Avail: NTIS HC A02/MF A01 CSCL 08H

A comparison is made between remote sensing data measured over water at altitudes ranging from 30 m to 15.2 km and data calculated for corresponding altitudes using surface measurements and an atmospheric radiative transfer model. Data were acquired on June 22, 1978 in Lake Erie, a cloudless, calm, near haze free day. Suspended solids and chlorophyll concentrations were 0.59 ± 0.002 mg/l and 2.42 ± 0.003 micrograms/l respectively throughout the duration of the experiment. Remote sensor data were acquired by two multispectral scanners each having 10 bands between 410 nm and 1040 nm. Calculated and measured nadir radiances for altitudes of 152 m and 12.5 km agree to within 16% and 14% respectively. The variation in measured radiance with look angle was poorly simulated by the model. It was concluded that an accurate assessment of the source of error will require the inclusion in the analysis of the contributions made by the sea state and specular sky reflectance. Author

N78-22590* National Aeronautics and Space Administration, Lewis Research Center, Cleveland, Ohio.
FEASIBILITY OF DETERMINING FLAT ROOF HEAT LOSSES USING AERIAL THERMOGRAPHY
Robert L. Bowman and John R. Jack 1979 17 p refs Presented at the 13th Intern. Symp. on Remote Sensing of Environment, Ann Arbor, Mich., 23-27 Apr. 1979, sponsored by Mich. Univ. (NASA-TM-79152; E-9981) Avail: NTIS HC A02/MF A01 CSCL 13B

The utility of aerial thermography for determining rooftop heat losses was investigated experimentally using several completely instrumented test roofs with known thermal resistances. Actual rooftop heat losses were obtained both from in-situ instrumentation and aerial thermography obtained from overflights at an altitude of 305 m. In general, the remotely determined roof surface temperatures agreed very well with those obtained

from ground measurements. The roof heat losses calculated using the remotely determined roof temperature agreed to within 17% of those calculated from $1/R \Delta T$ using ground measurements. However, this agreement may be fortuitous since the convective component of the heat loss is sensitive to small changes in roof temperature and to the average heat transfer coefficient used, whereas the radiative component is less sensitive. This, at this time, it is felt that an acceptable quantitative determination of roof heat losses using aerial thermography is only feasible when the convective term is accurately known or minimized. The sensitivity of the heat loss determination to environmental conditions was also evaluated. The analysis showed that the most reliable quantitative heat loss determinations can probably be obtained from aerial thermography taken under conditions of total cloud cover with low wind speeds and at low ambient temperatures. Author

A79-36537* Radar image processing of real aperture SLAR data for the detection and identification of iceberg and ship targets. J. G. Marthaler (U.S. Coast Guard, Office of Research and Development, Washington, D.C.) and J. E. Heighway (NASA, Lewis Research Center, Applications Div., Cleveland, Ohio). In: Canadian Symposium on Remote Sensing, 5th, Victoria, British Columbia, Canada, August 28-31, 1978. Proceedings. (A79-36486 15-43) Ottawa, Canadian Aeronautics and Space Institute, 1979, p. 483-494.

An iceberg detection and identification system consisting of a moderate resolution Side Looking Airborne Radar (SLAR) interfaced with a Radar Image Processor (RIP) based on a ROLM 1664 computer with a 32K core memory updatable to 64K is described. The system can be operated in high- or low-resolution sampling modes. Specifically designed algorithms are applied to digitized signal returns to provide automatic target detection and location, geometrically correct video image display and data recording. The real aperture Motorola AN/APR-94D SLAR operates in the X-band and is tunable between 9.10 and 9.40 GHz; its output power is 45 kW peak with a pulse repetition rate of 750 pulses per hour. Schematic diagrams of the system are provided, together with preliminary test data. C.K.D.

A79-51095* Feasibility of determining flat roof heat losses using aerial thermography. R. L. Bowman and J. R. Jack (NASA, Lewis Research Center, Cleveland, Ohio). University of Michigan, International Symposium on Remote Sensing of Environment, 13th, Ann Arbor, Mich., Apr. 23-27, 1979, Paper. 15 p. 8 refs.

The utility of aerial thermography for determining rooftop heat losses is investigated. Actual rooftop heat losses were obtained both from in-situ instrumentation of test roofs with known thermal resistances and aerial thermography obtained from overflights at an altitude of 305 m. It is found that the roof heat losses calculated using the remotely determined roof temperature agreed to within 17% of those calculated from ground measurements. However it is noted that an acceptable quantitative determination of roof heat losses using aerial thermography is only feasible when the convective term is accurately known or minimized. In addition, the sensitivity of the heat loss determination to environmental conditions is also evaluated. Finally, the analysis shows that the most reliable determinations can probably be obtained under conditions of total cloud cover with low wind speeds and at low ambient temperatures. M.E.P.

N78-12524* Environmental Research Inst. of Michigan, Ann Arbor, Infrared and Optics Div.
ATMOSPHERIC TRANSFORMATION OF MULTISPECTRAL REMOTE SENSOR DATA Final Report, 2 Nov. 1978 - 1 Oct. 1977
Robert E. Turner, Principal investigator Nov. 1977 128 p refs ERTS
(Contract NAS3-20483)
(E79-10006, NASA CR-135338, ERIM-126100-3-F) Avail: NTIS HC A07/MF A01 CSCL 20F

The author has identified the following significant results:

The effects of earth's atmosphere were accounted for, and a simple algorithm, based upon a radiative transfer model, was developed to determine the radiance at earth's surface free of atmospheric effects. Actual multispectral remote sensor data for Lake Erie and associated optical thickness data were used to demonstrate the effectiveness of the atmospheric transformation algorithm. The basic transformation was general in nature and could be applied to the large scale processing of multispectral aircraft or satellite remote sensor data.

44 ENERGY PRODUCTION AND CONVERSION

Includes specific energy conversion systems, e.g., fuel cells and batteries, global sources of energy, fossil fuels, geophysical conversion, hydroelectric power, and wind power.

For related information see also 07 Aircraft Propulsion and Power, 20 Spacecraft Propulsion and Power, 28 Propellants and Fuels, and 85 Urban Technology and Transportation.

N79-11467* National Aeronautics and Space Administration Lewis Research Center, Cleveland, Ohio **SOLAR CELLS HAVING INTEGRAL COLLECTOR GRID** Patent

John C. Evans, Jr., inventor (to NASA). Issued 1 Aug. 1978. 7 p. Filed 6 Jun. 1977. Supersedes N77 24593 (15, 15, p. 2011).

(NASA Case LEW 12819-1; US Patent 4,104,084; US Patent Appl. SN 803823; US Patent Class 136-89CC; US Patent Class 136-89SJ; US Patent Class 357-15; US Patent Class 357-16; US Patent Class 357-30; US Patent Class 357-65; US Patent Class 357-67). Avail. US Patent Office. CSCL 10A.

A heterojunction or Schottky barrier photovoltaic device is described, comprising a conductive base metal layer. A back surface field region was formed at the interface between the device and the base metal layer, a transparent, conductive mixed metal oxide layer in integral contact with the n-type layer of the heterojunction or Schottky barrier device. A metal alloy grid network was included. An insulating layer prevented electrical contact between the conductive metal base layer and the transparent, conductive metal oxide layer.

Official Gazette of the U.S. Patent Office

N79-11468* National Aeronautics and Space Administration Lewis Research Center, Cleveland, Ohio

APPLICATION OF SEMICONDUCTOR DIFFUSANTS TO SOLAR CELLS BY SCREEN PRINTING Patent

John C. Evans, Jr., Henry W. Brandhorst, Jr., George A. Mazari, and Larry R. Scudder, inventors (to NASA). Issued 1 Aug. 1978. 5 p. Filed 20 May 1977. Supersedes N77 24589 (15, 15, p. 2010).

(NASA Case LEW 12775-1; US Patent 4,104,091; US Patent Appl. SN 799026; US Patent Class 148-188; US Patent Class 29-572; US Patent Class 136-89; US Patent Class 427-75). Avail. US Patent Office. CSCL 10A.

Diffusants were applied onto semiconductor solar cell substrates using screen printing techniques. The method was applicable to square and rectangular cells and can be used to apply dopants of opposite types to the front and back of the substrate. Then, simultaneous diffusion of both dopants can be performed with a single furnace pass.

Official Gazette of the U.S. Patent Office

N79-11472* National Aeronautics and Space Administration Lewis Research Center, Cleveland, Ohio

SOLAR CELL COLLECTOR AND METHOD FOR PRODUCING SAME Patent

John C. Evans, Jr., inventor (to NASA). Issued 24 Oct. 1978. 5 p. Filed 21 Oct. 1977. Division of US Patent Appl. SN 770869. Filed 22 Feb. 1977. US Patent 4,082,569.

(NASA Case LEW 12552-2; US Patent 4,122,214; US Patent Appl. SN 844346; US Patent Class 427-75; US Patent Class 427-84; US Patent Class 427-123; US Patent Class 427-126; US Patent Class 427-261; US Patent Class 427-343; US Patent Class 427-398A; US Patent Class 427-399; US Patent Class 29-572; US Patent 4,082,569; US Patent Appl. SN 770869). Avail. US Patent Office. CSCL 10A.

A transparent, conductive collector layer containing conductive metal channels is formed as a layer on a photovoltaic substrate by coating a photovoltaic substrate with a conductive mixed

metal layer. A heat sink having portions protruding from one of its surfaces is attached. These protruding portions define a continuous pattern in combination with recessed regions among them such that they are in contact with the conductive layer of the photovoltaic substrate. Heating the substrate while simultaneously oxidizing the portions of the conductive layer exposed to a gaseous oxidizing substance forced into the recessed regions of the heat sink, creates a transparent metal oxide layer on the substrate. A continuous pattern of highly conductive metal channels is contained in the metal oxide layer.

Official Gazette of the U.S. Patent Office

N79-11477* National Aeronautics and Space Administration Lewis Research Center, Cleveland, Ohio

OPTIMUM DRY-COOLING SUB-SYSTEMS FOR A SOLAR AIR CONDITIONER

James L. S. Chen and David Namkoong. Oct. 1978. 41 p. refs.

(NASA TM 79007; E 9788). Avail. NTIS. HC A03/MF A01. CSCL 10A.

Dry-cooling sub-systems for residential solar-powered Rankine compression air conditioners were economically optimized and compared with the cost of a wet-cooling tower. Results in terms of yearly incremental busbar cost due to the use of dry-cooling were presented for Philadelphia and Miami. With input data corresponding to local weather, energy rate and capital costs, condenser surface designs and performance, the computerized optimization program yields design specifications of the sub-system which has the lowest annual incremental cost. Author.

N79-11478* National Aeronautics and Space Administration Lewis Research Center, Cleveland, Ohio

PRELIMINARY SUMMARY OF THE ETF CONCEPTUAL STUDIES

George R. Seikel, Robert W. Bercaw, C. Victor Pearson (Argonne Natl. Lab.) and William R. Owens (Gilbert Assoc., Inc.). 1978. 20 p. refs. Presented at the 4th US-USSR Colloq. on MHD Elec. Power Generation, Washington, D. C. 5-6 Oct. 1978. (Contract EF 77 A 01 2674).

(NASA TM 78999; E 9783; DOE/NASA/2674 78/1). Avail. NTIS. HC A02/MF A01. CSCL 10A.

Power plant studies have shown the attractiveness of MHD topped steam power plants for baseload utility applications. To realize these advantages, a three-phase development program was initiated. In the first phase, the engineering data and experience were developed for the design and construction of a pilot plant, the Engineering Test Facility (ETF). Results of the ETF studies are reviewed. These three parallel independent studies were conducted by industrial teams led by the AVCO Everet Research Laboratory, the General Electric Corporation, and the Westinghouse Corporation. A preliminary analysis and the status of the critical evaluation of these results are presented. L.S.

N79-11479* National Aeronautics and Space Administration Lewis Research Center, Cleveland, Ohio

SUPPLY OF REACTANTS FOR REDOX BULK ENERGY STORAGE SYSTEMS Final Report

Randall F. Gahn. Sep. 1978. 12 p. refs.

(Contract E(49-28) 1002). (NASA TM 78995; E 9779; DOE/NASA/1002 78/1). Avail. NTIS. HC A02/MF A01. CSCL 10A.

World resources, reserves, production and costs of reactant materials, iron, chromium, titanium and bromine for proposed redox cell bulk energy storage systems are reviewed. Supplying required materials for multimegawatt hour systems appears to be feasible even at current production levels. Iron and chromium ores are the most abundant and lowest cost of four reactants. Chromium is not a domestic reserve but redox system installations would represent a small fraction of U.S. imports. Vast quantities of bromine are available, but present production is low and therefore cost is high. Titanium is currently available at reasonable cost, with ample reserves available for the next fifty years.

S.B.S.

N79-11480* National Aeronautics and Space Administration
Lewis Research Center, Cleveland, Ohio

CORRELATIONS OF CATALYTIC COMBUSTOR PERFORMANCE PARAMETERS

Daniel L. Bulzani. Oct 1978. 15 p. refs. Presented at the 3d Workshop on Catalytic Combustion, Asheville, N.C., 2-4 Oct 1978, sponsored by EPA.

(Contract EC 77-A 31-1040)

(NASA TM 79014 E 9803 DOE/NASA/1040-78/4) Avail
NTIS HC A02/MF A01 CSCL 10A

Correlations for combustion efficiency, percentage drop and the minimum required adiabatic reaction temperature necessary to meet emissions goals of 136 g CO/kg fuel and 164 g HC/kg fuel are presented. Combustion efficiency was found to be a function of the cell density, cell circumference, reactor length, reference velocity, and adiabatic reaction temperature. The percentage pressure drop at an adiabatic reaction temperature of 1450 K was found to be proportional to the reference velocity to the 1.5 power and to the reactor length. It is inversely proportional to the pressure, cell hydraulic diameter, and fractional open area. The minimum required adiabatic reaction temperature was found to increase with reference velocity and decrease with cell circumference, cell density, and reactor length. A catalyst factor was introduced into the correlations to account for differences between catalysts. Combustion efficiency, the percentage pressure drop, and the minimum required adiabatic reaction temperature were found to be a function of the catalyst factor. This data was from a 12 cm diameter test rig with noble metal reactors using propane fuel at an inlet temperature of 800 K. S B S

N79-11481* National Aeronautics and Space Administration
Lewis Research Center, Cleveland, Ohio

THERMAL STORAGE FOR INDUSTRIAL PROCESS AND REJECT HEAT

R. A. Duschka and W. J. Masica. 1978. 14 p. refs. Presented at the 2d Conf. on Waste Heat Management and Util., Miami Beach, Fla., 4-6 Dec 1978.

(Contract EC 77-A 31-1034)

(NASA TM 78994 E 9777 DOE/NASA/1034-78/3) Avail
NTIS HC A02/MF A01 CSCL 10A

Industrial production uses about 40 percent of the total energy consumed in the United States. The major share of this is derived from fossil fuel. Potential savings of scarce fuel is possible through the use of thermal energy storage (TES) of reject or process heat for subsequent use. Three especially significant industries where high temperature TES appears attractive—paper and pulp, iron and steel, and cement—are discussed. Potential annual fuel savings, with large scale implementation of near term TES systems for these three industries, is nearly 9,000,000 bbl of oil. S B S

N79-12548* National Aeronautics and Space Administration
Lewis Research Center, Cleveland, Ohio

MICROPROCESSOR CONTROL OF A WIND TURBINE GENERATOR

Arthur J. Gnecco and Gary T. Whithead. 1978. 17 p. Presented at the Conf. on Ind. Appl. of Microprocessors, Philadelphia, 20-22 Mar. 1978, sponsored by IEEE.

(Contract E(49-26)-1028)

(NASA TM 79021 E 9818 DOE/NASA/1028-78/20) Avail
NTIS HC A02/MF A01 CSCL 10B

A microprocessor based system was used to control the unattended operation of a wind turbine generator. The turbine and its microcomputer system are fully described with special emphasis on the wide variety of tasks performed by the microprocessor for the safe and efficient operation of the turbine. The flexibility, cost, and reliability of the microprocessor were major factors in its selection. A A

N79-14528* National Aeronautics and Space Administration
Lewis Research Center, Cleveland, Ohio

BACK WALL SOLAR CELL PATENT

Henry W. Brandhorst, Jr., inventor (to NASA). Issued 26 Dec 1978. 5 p. Filed 24 Apr. 1978. Supersedes N78-25556 (16-

16, p. 2137). Continuation-in-part of abandoned US Patent Appl. SN-760771, filed 19 Jan. 1977.

(NASA Case-LEW-12236-2; US Patent-4,131,486;

US Patent-Appl-SN-899123; US Patent-Class-136-89SJ;

US Patent-Class-357-30; US Patent-Appl-SN-760771) Avail
US Patent and Trademark Office CSCL 10A

A solar cell is disclosed which comprises a first semiconductor material of one conductivity type with one face having the same conductivity type but more heavily doped to form a field region arranged to receive the radiant energy to be converted to electrical energy, and a layer of a second semiconductor material, preferably highly doped, of opposite conductivity type on the first semiconductor material adjacent the first semiconductor material at an interface remote from the heavily doped field region. Instead of the opposite conductivity layer, a metallic Schottky diode layer may be used, in which case no additional back contact is needed. A contact, such as a gridded contact, previous to the radiant energy may be applied to the heavily doped field region of the more heavily doped, same conductivity material for its contact. Official Gazette of the U.S. Patent and Trademark Office

N79-14538* National Aeronautics and Space Administration
Lewis Research Center, Cleveland, Ohio

CATALYST SURFACES FOR THE CHROMOUS/CHROMIC REDOX COUPLE Patent Application

Jose D. Giner (Giner, Inc., Waltham, Mass.) and Kathleen J. Cahill, inventors (to NASA) (Giner, Inc., Waltham, Mass.) Filed 29 Nov. 1978. 13 p. Sponsored by NASA.

(NASA Case-LEW-13148-1; US Patent-Appl-SN-964754) Avail
NTIS HC A02/MF A01 CSCL 10A

An electricity-producing cell of the reduction-oxidation (REDOX) type is presented. The cell comprises a container divided into anode and cathode compartments by an ion permeable membrane. The novelty of the invention appears to lie in the provision of selected catalytic coatings with lead on the anode electrode of a REDOX cell to greatly increase current density. NASA

N79-15403* National Aeronautics and Space Administration
Lewis Research Center, Cleveland, Ohio

COMPARISON OF FUEL CELL AND DIESEL INTEGRATED ENERGY SYSTEMS AND A CONVENTIONAL SYSTEM FOR A 500-UNIT APARTMENT

Stephen N. Simons and William L. Maag. Nov. 1978. 26 p. refs.

(NASA TM-79037 E 9835) Avail NTIS HC A03/MF A01 CSCL 10B

The electrical and thermal energy utilization efficiencies of a 500 unit apartment complex are analyzed and compared for each of three energy supply systems. Two on site integrated energy systems, one powered by diesel engines and the other by phosphoric acid fuel cells were compared with a conventional system which uses purchased electricity and on site boilers for heating. All fuels consumed on-site are clean, synthetic fuels (distillate fuel oil or pipeline quality gas) derived from coal. Purchased electricity was generated from coal at a central station utility. The relative energy consumption and economics of the three systems are analyzed and compared. Author

N79-15410* National Aeronautics and Space Administration
Lewis Research Center, Cleveland, Ohio

BENEFITS OF SOLAR/FOSSIL HYBRID GAS TURBINE SYSTEMS

Harvey S. Bloomfield. 1978. 18 p. refs. Proposed for Presentation at the Gas Turbine Conf. and Solar Energy Conf., San Diego, Calif., 12-15 Mar. 1979, sponsored by Am. Soc. of Mech. Engrs.

(NASA TM 79083 E 9905) Avail NTIS HC A02/MF A01 CSCL 10A

The potential benefits of solar/fossil hybrid gas turbine power systems were assessed. Both retrofit and new systems were considered from the aspects of cost of electricity, fuel conservation, operational mode, technology requirements, and fuels flexibility. Hybrid retrofit (repowering) of existing combustion (simple Brayton cycle) turbines can provide near term fuel savings

and solar experience, while new and advanced recuperated or combined cycle systems may be an attractive fuel saving and economically competitive vehicle to transition from today's gas and oil-fired powerplants to other more abundant fuels. Author

N79-15411* National Aeronautics and Space Administration, Lewis Research Center, Cleveland, Ohio.

PHOTOVOLTAIC POWER SYSTEMS FOR RURAL AREAS OF DEVELOPING COUNTRIES

Louis Rosenblum, William J. Bifano, Gerald F. Hein, and Anthony F. Ratajczak 1979 19 p refs Presented at the Intern. Seminar on Solar Energy, Tokyo, 5-10 Feb. 1979, sponsored by the United Nations and Govt. of Japan (NASA-TM-79097, E-9921) Avail: NTIS HC A02/MF A01 CSCL 10A

Systems technology, reliability, and present and projected costs of photovoltaic systems are discussed using data derived from NASA, Lewis Research Center experience with photovoltaic systems deployed with a variety of users. Operating systems in two villages, one in Upper Volta and the other in southwestern Arizona are described. Energy cost comparisons are presented for photovoltaic systems versus alternative energy sources. Based on present system technology, reliability, and costs, photovoltaics provides a realistic energy option for developing nations.

A.R.H.

N79-16355* National Aeronautics and Space Administration, Lewis Research Center, Cleveland, Ohio.

POWER TRAIN ANALYSIS FOR THE DOE/NASA 100-kW WIND TURBINE GENERATOR Final Report

Robert C. Seidel, Harold Gold, and Leon M. Wenzel Oct. 1978 57 p refs Prepared for DOE (Contract E(49-26)-1028) (NASA-TM-78997, DOE/NASA/1026-78/19, E-9413) Avail: NTIS HC A04/MF A01 CSCL 10A

Progress in explaining variations of power experienced in the on-line operation of a 100 kW experimental wind turbine generator is reported. Data are presented that show the oscillations tend to be characteristic of a wind-driven synchronous generator because of low torsional damping in the power train, resonances of its large structure, and excitation by unsteady and nonuniform wind flow. The report includes dynamic analysis of the drive-train torsion, the generator, passive driveline damping, and active pitch control as well as correlation with experimental recordings. The analysis assumes one machine on an infinite bus with constant generator-field excitation. Author

N79-16356* National Aeronautics and Space Administration, Lewis Research Center, Cleveland, Ohio.

BASELINE PERFORMANCE OF THE GPU 3 STIRLING ENGINE

Lanny G. Thienie and Roy C. Tew, Jr. Nov. 1978 14 p refs Presented at the Highway Vehicle Systems Contractors Coordination Meeting, Dearborn, Michigan, 17-20 Oct. 1978 (Contract EC 77-A 31-1040) (NASA-TM-79038, E-9838, DOE/NASA/1040-78/5) Avail: NTIS HC A02/MF A01 CSCL 10B

A 10 horsepower single-cylinder rhombic-drive Stirling engine was converted to a research configuration to obtain data for validation of Stirling computer simulations. The engine was originally built by General Motors Research Laboratories for the U.S. Army in 1965 as part of a 3 kW engine-generator set, designated the GPU 3 (Ground Power Unit). This report presents test results for a range of heater gas temperatures, mean compression-space pressures, and engine speeds with both helium and hydrogen as the working fluids. Also shown are initial data comparisons with computer simulation predictions. Author

N79-16357* National Aeronautics and Space Administration, Lewis Research Center, Cleveland, Ohio.

AN OPERATING 200-kW HORIZONTAL AXIS WIND TURBINE

Charles L. Hunnicutt (Lockheed Aircraft Service Co., Ontario, Calif.), Bradford Linscott, and Robert A. Wolf 1978 25 p Presented at 23rd Natl. SAMPE Symp. and Exhibition, Anaheim, Calif., 2-4 May 1978 (Contract E(49-26)-1004) (NASA-TM-79034, E-9833) Avail: NTIS HC A02/MF A01 CSCL 10B

The Mod-OA wind turbine blades were rotated for the first time on November 30, 1977, establishing the Mod-OA as the first wind-driven generator in 35 years to be continually tied into an electrical power system which services a community. Tower-mounted equipment and blade structural design and fabrication are discussed. J.M.S.

N79-17313* National Aeronautics and Space Administration, Lewis Research Center, Cleveland, Ohio.

FORMULATED PLASTIC SEPARATORS FOR SOLUBLE ELECTRODE CELLS Patent

Dean W. Sheibley, inventor (to NASA) Issued 9 Jan. 1979 8 p Filed 10 Mar. 1977 Supersedes N77-18560 (15 - 09, p 1194) (NASA-Case-LEW-12358-1; US-Patent-4,133,941; US-Patent-Appl-SN-776146; US Patent-Class-429-33; US-Patent-Class-429-101) Avail: US Patent and Trademark Office CSCL 10A

The fabrication and milling of membranes comprising a hydrochloric acid-insoluble sheet of a mixture of a rubber and a powdered ion transport material are described. The sheet can be present as a coating upon a flexible and porous substrate. These membranes can be used in oxidation-reduction electrical accumulator cells wherein the reduction of one member of a couple is accompanied by the oxidation of the other member of the couple on the other side of the cell and this must be accompanied by a change in chloride ion concentration in both sides.

Official Gazette of the U.S. Patent and Trademark Office

N79-17333* National Aeronautics and Space Administration, Lewis Research Center, Cleveland, Ohio.

A 200-kW WIND TURBINE GENERATOR CONCEPTUAL DESIGN STUDY

Jan. 1979 111 p refs (Contract E(49-26)-1028) (NASA-TM-79032, DOE/NASA/1028-79/1) Avail: NTIS HC A06/MF A01 CSCL 10B

A conceptual design study was conducted to define a 200 kW wind turbine power system configuration for remote applications. The goal was to attain an energy cost of 1 to 2 cents per kilowatt-hour at a 14 mph site (mean average wind velocity at an altitude of 30 ft). The costs of the Clayton, New Mexico, Mod-OA (200-kW) were used to identify the components, subsystems, and other factors that were high in cost and thus candidates for cost reduction. Efforts devoted to developing component and subsystem concepts and ideas resulted in a machine concept that is considerably simpler, lighter in weight, and lower in cost than the present Mod-OA wind turbines. In this report are described the various innovations that contributed to the lower cost and lighter weight design as well as the method used to calculate the cost of energy. Author

N79-17334* National Aeronautics and Space Administration, Lewis Research Center, Cleveland, Ohio.

EFFECT OF THERMAL BARRIER COATINGS ON THE PERFORMANCE OF STEAM AND WATER COOLED GAS TURBINE/STEAM TURBINE COMBINED CYCLE SYSTEM Final Report

Joseph J. Nairiger Dec. 1978 37 p refs (Contract EF 77 A 01 2593) (NASA-TM-79057, E-9807, DOE/NASA/2593-78/4) Avail: NTIS HC A03/MF A01 CSCL 10B

An analytical study was made of the performance of air, steam, and water-cooled gas turbine/steam turbine combined-cycle systems with and without thermal-barrier coatings. For steam cooling, thermal barrier coatings permit an increase in the turbine inlet temperature from 1205 C (2200 F), resulting in an efficiency improvement of 1.9 percentage points. The maximum specific power improvement with thermal barriers is 32.4 percent, when the turbine inlet temperature is increased from 1425 C (2600 F) to 1675 C (3050 F) and the airfoil temperature is kept the same. For water cooling, the maximum efficiency improvement is 2.2 percentage points at a turbine inlet temperature of 1683 C (3062 F) and the maximum specific power improvement is 36.6 percent by increasing the turbine inlet temperature from 1425 C (2600 F) to 1730 C (3150 F) and keeping the airfoil temperatures the same. These improvements are greater than that obtained with combined cycles using air cooling at a turbine inlet temperature of 1205 C (2200 F). The large temperature differences across the thermal barriers at these high temperatures, however, indicate that thermal stresses may present obstacles to the use of coatings at high turbine inlet temperatures. Author

N79-17335* National Aeronautics and Space Administration, Lewis Research Center, Cleveland, Ohio

EVALUATION OF THE ECAS OPEN CYCLE MHD POWER PLANT DESIGN Final Report

George R. Seikel, Peter J. Staiger, and Carlson C. P. Pian Nov. 1978 27 p refs Prepared for DOE

(Contract E1-77 A-01-2674)

(NASA-TM-79012; E-9799; DOE/NASA/2674-78/2) Avail: NTIS HC A03/MF A01 CSCL 10B

The Energy Conversion Alternatives Study (ECAS) MHD/steam power plant is described. The NASA critical evaluation of the design is summarized. Performance of the MHD plant is compared to that of the other type ECAS plant designs on the basis of efficiency and the 30-year leveled cost of electricity. Techniques to improve the plant design and the potential performance of lower technology plants requiring shorter development time and lower development cost are then discussed. Author

N79-17336* National Aeronautics and Space Administration, Lewis Research Center, Cleveland, Ohio

PHOTOVOLTAIC TESTS AND APPLICATIONS PROJECT Final Progress Report, Apr. 1976 - Jun. 1977

Nov 1978 90 p refs

(Contract E(49-26)-1022)

(NASA-TM-79018; E-9811; DOE/NASA/1022-78/42) Avail: NTIS HC A05/MF A01 CSCL 10A

The activities and accomplishments of the Photovoltaic Tests and Applications Project during the period April 1976 through June 1977 are summarized. Results of efforts to identify potential near-term photovoltaic applications and users are discussed, including the outcome of an extensive survey of Federal government agencies. The status of application experiments is presented. Various general engineering efforts are reported, including the design and construction of a photovoltaic Systems Test Facility. Efforts to develop a high efficiency 10 kVA self-commutated inverter and controller specifically designed for photovoltaic systems are also discussed. The results of a wide variety of activities in the area of photovoltaic measurements and standards are related. Documents generated by the Project during the reporting period are listed in an Appendix. G.Y.

N79-18444* National Aeronautics and Space Administration, Lewis Research Center, Cleveland, Ohio

METHOD FOR FABRICATING SOLAR CELLS HAVING INTEGRATED COLLECTOR GRIDS Patent

John C. Evans Jr., inventor (to NASA) Issued 23 Jan. 1979 6 p Filed 23 Dec. 1977 Supersedes N78 25558 (16 - 16, p. 2138) Division of US Patent Appl. SN 803823, filed 6 Jun. 1977 US Patent 4,104,084

(NASA Case LEW 12819.2 US Patent 4,135,290

US Patent Appl. SN 863770 US Patent Class 29 572

US Patent Class 29 578 US Patent Class 29 591

US-Patent-Class-148-63, US-Patent-4,104,084.

US-Patent-Appl-SN-803823) Avail US Patent and Trademark Office CSCL 10A

The photovoltaic devices of the invention are heterojunction or Schottky barrier devices which possess an integral mixed metal oxide coating in which is embedded a metallic network which functions as an efficient collector of electrons set in motion by the photovoltaic process. The metal grid system is formed from the metal elements of the transparent, conductive mixed metal oxide coating which is in contact with the oxide coating which constitutes the barrier of the devices with the semiconductor substrate.

Official Gazette of the U.S. Patent and Trademark Office

N79-18455* National Aeronautics and Space Administration, Lewis Research Center, Cleveland, Ohio

ATOMIC HYDROGEN STORAGE METHOD AND APPARATUS Patent Application

John A. Woolam, inventor (to NASA) Filed 6 Feb. 1979 10 p

(NASA Case LEW-12081.3, US Patent Appl. SN-009887) Avail: NTIS HC A02/MF A01 CSCL 10B

Atomic hydrogen, for use as a fuel or an explosive is stored in the presence of a strong magnetic field in exfoliated layered compounds such as molybdenum disulfide or an elemental layer material such as graphite. The compound is maintained at liquid helium temperatures and the atomic hydrogen is collected on the surfaces of the layered compound which are exposed during delamination (exfoliation). The strong magnetic field and the low temperature combine to prevent the atoms of hydrogen from combining to form molecules. NASA

N79-20484* National Aeronautics and Space Administration, Lewis Research Center, Cleveland, Ohio

UTILITY OPERATIONAL EXPERIENCE ON THE NASA/DOE MOD-OA 200-kW WIND TURBINE

J. C. Glasgow and W. H. Robbins 1979 30 p refs Presented at the 6th Energy Technol. Conf., Washington, D. C., 26-28 Feb. 1979; sponsored by Am. Gas Assoc. - Gas. Res. Inst., Elec. Power Res. Inst., and Thomas Alva Edison Found. (Contract E(49-26)-1004)

(NASA-TM-79084; E9907; DOE/NASA/1004-79/1) Avail: NTIS HC A03/MF A01 CSCL 10B

The Mod-OA 200 wind turbine was designed and fabricated as part of the Federal Wind Energy Program. Early wind turbine operation and performance data were obtained while gaining initial experience in the operation of large, horizontal axis wind turbines in typical utility environments. The Mod-OA wind turbine was turned over to the Town of Clayton Light and Water Plant, Clayton, NM, for utility operation; and on December 31, 1978, the machine had completed ten months of utility operation. The machine is described and the recent operational experience at Clayton, NM is documented. J.M.S.

N79-20485* National Aeronautics and Space Administration, Lewis Research Center, Cleveland, Ohio

THERMAL STORAGE TECHNOLOGIES FOR SOLAR INDUSTRIAL PROCESS HEAT APPLICATIONS

Larry H. Gordon 1979 19 p refs

(Contract EC-77-A-31-1034)

(NASA-TM-79130; DOE/NASA/1034-79/2; E-9970) Avail: NTIS HC A02/MF A01 CSCL 10A

The state-of-the-art of thermal storage subsystems for the intermediate and high temperature (100 C to 600 C) solar industrial process heat generation is presented. Primary emphasis is focused on buffering and diurnal storage as well as total energy transport. In addition, advanced thermal storage concepts which appear promising for future solar industrial process heat applications are discussed. J.M.S.

N79-20620* National Aeronautics and Space Administration, Lewis Research Center, Cleveland, Ohio.

DECAY OF THE ZINCATE CONCENTRATION GRADIENT AT AN ALKALINE ZINC CATHODE AFTER CHARGING

Harold E. Kautz and Charles E. May 1979 21 p refs To be presented at the Meeting of the Electrochem. Soc., Los Angeles, 14-19 Oct. 1979

(NASA-TM-79106; E-9931) Avail: NTIS HC A02/MF A01 CSCL 10C

The transport of the zincate ion to the alkaline zinc cathode was studied by observing the decay of the zincate concentration gradient at a horizontal zinc cathode after charging. This decay was found to approximate first order kinetics as expected from a proposed boundary layer model. The concentrations were calculated from polarization voltage. The decay half life was shown to be a linear function of the thickness of porous zinc deposit on the cathode indicating a very rapid transport of zincate through porous zinc metal. The rapid transport is attributed to an electrochemical mechanism. From the linear dependence of the half life on the thickness the boundary layer thickness was found to be about 0.010 cm when the cathode was at the bottom of the cell. No significant dependence of the boundary layer thickness on the viscosity of electrolyte was observed. The data also indicated a relatively sharp transition between the diffusion and convection transport regions. When the cathode was at the top of the cell, the boundary layer thickness was found to be roughly 0.080 cm. The diffusion of zincate ion through asbestos submerged in alkaline electrolyte was shown to be comparable with that predicted from the bulk diffusion coefficient of the zincate ion in alkali.

J.M.S.

N79-21549* National Aeronautics and Space Administration, Lewis Research Center, Cleveland, Ohio.

EVALUATION OF MOSTAS COMPUTER CODE FOR PREDICTING DYNAMIC LOADS IN TWO BLADED WIND TURBINES

K. R. V. Kaza (Toledo Univ.), D. C. Janetzke, and T. L. Sullivan 1979 21 p refs Presented at AIAA/ASCE/AHS 20th Structures, Structural Dynamics and Mater. Conf., St. Louis, Mo., 4-6 Apr. 1979

(Contract E(49-26)-1028)

(NASA-TM-79101; DOE/NASA/1028-72/2; E-9925) Avail: NTIS HC A02/MF A01 CSCL 10B

Calculated dynamic blade loads were compared with measured loads over a range of yaw stiffnesses of the DOE/NASA Mod-O wind turbine to evaluate the performance of two versions of the MOSTAS computer code. The first version uses a time-averaged coefficient approximation in conjunction with a multi-blade coordinate transformation for two bladed rotors to solve the equations of motion by standard eigenanalysis. The second version accounts for periodic coefficients while solving the equations by a time history integration. A hypothetical three-degree of freedom dynamic model was investigated. The exact equations of motion of this model were solved using the Floquet-Lipunov method. The equations with time-averaged coefficients were solved by standard eigenanalysis.

L.P.

N79-21550* National Aeronautics and Space Administration, Lewis Research Center, Cleveland, Ohio.

THE ROLE OF THERMAL ENERGY STORAGE IN INDUSTRIAL ENERGY CONSERVATION

Rudolph A. Duscha and William J. Masica 1979 13 p refs Presented at a Conf. on Ind. Energy Conserv. Technol. and Exhibition, Houston, Tex., 22-25 Apr. 1979; sponsored by DOE and the Texas Ind. Comm.

(Contract EC-77-A-31-1034)

(NASA-TM-79122; DOE/NASA/1034-79/1; E-9957) Avail: NTIS HC A02/MF A01 CSCL 10C

Thermal Energy Storage for Industrial Applications is a major thrust of the Department of Energy's Thermal Energy Storage Program. Utilizing Thermal Energy Storage (TES) with process or reject heat recovery systems is shown to be extremely beneficial for several applications. Recent system studies resulting from contracts awarded by the Department of Energy (DOE) identified four especially significant industries where TES appears attractive - food processing, paper and pulp, iron and steel, and cement.

Potential annual fuel savings with large scale implementation of near term TES systems for these industries is over 9,000,000 bbl of oil. This savings is due to recuperation and storage in the food processing industry, direct fuel substitution in the paper and pulp industry and reduction in electric utility peak fuel use through inplant production of electricity from utilization of reject heat in the steel and cement industries.

Author

N79-21576* National Aeronautics and Space Administration, Lewis Research Center, Cleveland, Ohio.

LEWIS RESEARCH CENTER PROGRAM

D. G. Soltis In NASA, Goddard Space Flight Center The 1977 Goddard Space Flight Center Battery Workshop 1977 p 133-136 (For primary document see N79-21565 12-44) Avail: NTIS HC A25/MF A01 CSCL 10C

As part of the NASA lightweight battery program, the Lewis Research Center has a number of programs that are being reviewed. A brief and general discussion of these programs is presented.

G.Y.

N79-22623* National Aeronautics and Space Administration, Lewis Research Center, Cleveland, Ohio.

PRELIMINARY COMPARISON OF THEORY AND EXPERIMENT FOR A CONICAL, PRESSURIZED-FLUIDIZED-BED COAL COMBUSTOR

R. W. Patch Mar 1979 E6 p refs

(NASA-TM-79137; E-9985) Avail: NTIS HC A04/MF A01 CSCL 10A

A published model was used for a comparison of theory with an actual combustor burning caking bituminous coal and using limestone to reduce sulfur dioxide emission. Theoretical bed pressure drop was in good agreement with experiment. The burnable carbon elutriated was not in agreement with experiment, at least partly because the exhaust port was apparently below the transport c. engaging height. The observed nitrogen oxides emission rate was about half the theoretical value. There was order-of-magnitude agreement of sulfur dioxide emission rates.

Author

N79-22624* National Aeronautics and Space Administration, Lewis Research Center, Cleveland, Ohio.

ANALYSIS OF A FUEL CELL ON-SITE INTEGRATED ENERGY SYSTEM FOR A RESIDENTIAL COMPLEX

Stephen N. Simons and William L. Maag (Solar Energy Products Co., Avon Lake, Ohio) 1979 11 p refs Proposed for presentation at the Terrest. Energy Systems Conf., Orlando, Fla., 4-6 Jun. 1979; sponsored by AIAA

(NASA-TM-79161; E-9918) Avail: NTIS HC A02/MF A01 CSCL 10B

Declining supplies of domestic oil and gas and the increased cost of energy resulted in a renewed emphasis in utilizing available resources in the most efficient manner possible. This, in turn, brought about a reassessment of a number of methods for converting fossil fuels to end uses at the highest practical efficiency. One of these is the on-site integrated energy system (OS/IES). This system provides electric power from an on-site power plant and recovers heat from the power plant that would normally be rejected to the environment. An OS/IES is potentially useful in any application that requires both electricity and heat. Several OS/IES are analyzed for a residential complex. The paper is divided into two sections; the first compares three energy supply systems; the second compares various designs for fuel cell OS/IES.

LS

N79-22626* National Aeronautics and Space Administration, Lewis Research Center, Cleveland, Ohio.

EFFECT OF STEAM ADDITION ON CYCLE PERFORMANCE OF SIMPLE AND RECUPERATED GAS TURBINES

Robert J. Boyle Apr 1979 52 p refs

(NASA-TP-1440; E-9795) Avail: NTIS HC A1/MF A01 CSCL 10B

Results are presented for the cycle efficiency and specific power of simple and recuperated gas turbine cycles in which

steam is generated and used to increase turbine flow. Calculations showed significant improvements in cycle efficiency and specific power by adding steam. The calculations were made using component efficiencies and loss assumptions typical of stationary powerplants. These results are presented for a range of operating temperatures and pressures. Relative heat exchanger size and the water use rate are also examined. Author

N79-24442* National Aeronautics and Space Administration, Lewis Research Center, Cleveland, Ohio.

REDOX FLOW CELL ENERGY STORAGE SYSTEMS

Lawrence H. Thaller 1979 11 p refs

(Contract E(49-28)-1002)

(NASA-TM-79143; DOE/NASA/1002-79/3; E-9996; Avail: NTIS HC A02/MF A01 CSCL 10A)

NASA-Redox systems are electrochemical storage devices that use two fully soluble Redox couples, anode and cathode fluids, as active electrode materials separated by a highly selective ion exchange membrane. The reactants are contained in large storage tanks and pumped through a stack of Redox flow cells where the electrochemical reactions (reduction and oxidation) take place at porous carbon felt electrodes. A string or stack of these power producing cells is connected in series in a bipolar manner. Redox energy storage systems promise to be inexpensive and possess many features that provide for flexible design, long life, high reliability and minimal operation and maintenance costs. These features include independent sizing of power and storage capacity requirements and inclusion within the cell stack of a cell that monitors the state of charge of the system as a whole, and a rebalance cell which permits continuous correction to be made for minor side reactions that would tend to result in the anode fluid and cathode fluids becoming electrochemically out of balance. These system features are described and discussed.

LS

N79-24443* National Aeronautics and Space Administration, Lewis Research Center, Cleveland, Ohio.

DESCRIPTION OF PHOTOVOLTAIC VILLAGE POWER SYSTEMS IN THE UNITED STATES AND AFRICA

A. F. Ratajczak and W. J. Brann 1979 13 p refs. Presented at the Photovoltaic Solar Energy Conf., Berlin, 23-26 Apr. 1979 (Contract DE-A101-79ET20485)

(NASA-TM-79149; DOE/NASA/20435-79/1; E-005) Avail: NTIS HC A02/MF A01 CSCL 10B

Photovoltaic power systems in remote villages in the United States and Africa are described. These projects were undertaken to demonstrate that existing photovoltaic system technology is capable of providing electrical power for basic domestic services for the millions of small, remote communities in both developed and developing countries. One system is located in the Papago Indian Village of Schuchuli in southwest Arizona (U.S.) and became operational 16 December 1978. The other system is located in Tangaye, a rural village in Upper Volta, Africa. It became operational 1 March 1979. The Schuchuli system has a 3.5 kW (peak) solar array which provides electric power for village water pumping, a refrigerator for each family, lights in the village buildings, and a community washing machine and sewing machine. The 1.8 kW (peak) Tangaye system provides power for community water pumping, flour milling and lights in the milling building. These are both stand-alone systems (i.e., no back-up power source) which are being operated and maintained by local personnel. Both systems are instrumented. Systems operations are being monitored by NASA to measure design adequacy and to refine designs for future systems. J. M. S.

N79-24444* National Aeronautics and Space Administration, Lewis Research Center, Cleveland, Ohio.

BENEFITS OF ADVANCED TECHNOLOGY IN INDUSTRIAL COGENERATION

G. J. Barna and R. K. Burns 1979 29 p. Presented at EPRI Workshop on Cogeneration, San Antonio, Tex., 1-4 Apr. 1979 (Contract EC 77-A-31-1062)

(NASA-TM-79160; DOE/NASA/1062-79/1; E-016) Avail: NTIS HC A03/MF A01 CSCL 10B

This broad study is aimed at identifying the most attractive

advanced energy conversion systems for industrial cogeneration for the 1985 to 2000 time period and assessing the advantages of advanced technology systems compared to using today's commercially available technology. Energy conversion systems being studied include those using steam turbines, open cycle gas turbines, combined cycles, diesel engines, Stirling engines, closed cycle gas turbines, phosphoric acid and molten carbonate fuel cells and thermionics. Specific cases using today's commercially available technology are being included to serve as a baseline for assessing the advantages of advanced technology.

LS

N79-24445* National Aeronautics and Space Administration, Lewis Research Center, Cleveland, Ohio.

REDOX FLOW CELL DEVELOPMENT AND DEMONSTRATION PROJECT, CALENDAR YEAR 1977

Jan. 1979 53 p refs

(Contract E(49-28)-1002)

(NASA-TM-79067; DOE/NASA/1002-78/2; E-9883) Avail: NTIS HC A04/MF A01 CSCL 10A

Research and development on the redox flow cell conducted from January 1, 1977 to December 31, 1977, are described in this report. The major focus of the effort during 1977 was the key technology issues that directly influence the fundamental feasibility of the overall redox concept. These issues were the development of a suitable ion exchange membrane for the system, the screening and study of candidate redox couples to achieve optimum cell performance, and the carrying out of systems analysis and modeling to develop system performance goals and cost estimates.

LS

N79-24446* National Aeronautics and Space Administration, Lewis Research Center, Cleveland, Ohio.

PERFORMANCE OPTIMIZATION OF AN MHD GENERATOR WITH PHYSICAL CONSTRAINTS

C. C. P. Pian, G. R. Seikel, and J. Marlin Smith 1979 12 p refs. Proposed for presentation at 14th Intersoc. Energy Conversion Eng. Conf., Boston, 5-10 Aug. 1979

(Contract EF-77-A-01-2674)

(NASA-TM-79172; DOE/NASA/2674-79/5; E-036) Avail: NTIS HC A02/MF A01 CSCL 10B

A method to optimize the Faraday MHD generator performance under a prescribed set of electrical and magnet constraints is described. The results of generator performance calculations using this technique are presented for a very large MHD/steam plant. The differences between the maximum power and maximum net power generators are described. The sensitivity of the generator performance to the various operational parameters are presented.

Author

N79-25481* National Aeronautics and Space Administration, Lewis Research Center, Cleveland, Ohio.

IN SITU SELF CROSS-LINKING OF POLYVINYL ALCOHOL BATTERY SEPARATORS Patent

Warren H. Philipp, Li-Chen Hsu, and Dean W. Sheibley inventors (to NASA) Issued 15 May 1979 5 p. Filed 19 Apr. 1978 Supersedes N78-22157 (16-13, p. 1674)

(NASA Case-LEW-12972-1; US Patent-4,154,912)

US Patent-Appl-SN-897829 US Patent-Class-526-7;

US Patent-Class-429-253 US Patent-Class-526-9) Avail: US Patent and Trademark Office CSCL 10C

A battery separator was produced from a polyvinyl alcohol sheet structure which was subjected to an in situ, self crosslinking process by selective oxidation of the 1,2 diol units present in the polyvinyl alcohol sheet structure. The 1,2 diol units were cleaved to form aldehyde end groups which subsequently crosslink through acetalization of the 1,3 diol units of the polyvinyl alcohol. Selective oxidation was achieved using a solution of a suitable oxidizing agent such as periodic acid or lead tetraacetate.

Official Gazette of the U.S. Patent and Trademark Office

N79-25492* National Aeronautics and Space Administration, Lewis Research Center, Cleveland, Ohio.

DOE PHOTOVOLTAIC TESTS AND APPLICATIONS PROJECT

Ron Cull and Tony Ratajczak. In OAO Corp. Proc. of the US DOE Photovoltaics Technol. Develop. and Appl. Program Rev. 1978 p 1-166 - 1-179 (For primary document see N79-25485 16-44)

Avail NTIS HC A15/MF A01 CSCL 10A

The installation date, system and location, and solar arrays are tabulated S.E.S.

N79-25498* National Aeronautics and Space Administration, Lewis Research Center, Cleveland, Ohio.

GAS-TURBINE CRITICAL RESEARCH AND ADVANCED TECHNOLOGY SUPPORT PROJECT Annual Report, FY 1978

John S. Clark, Carl E. Lowell, Richard W. Niedzwiecki, and Joseph J. Nainiger Jun. 1979 46 p refs

(Contract EF-77-A-01-2593)

(NASA-TM-79139, DOE/NASA/2593-79/6, E-9986) Avail: NTIS HC A03/MF A01 CSCL 10B

The technical progress made during the first 15 months of a planned 40-month project to provide a critical-technology data base for utility gas-turbine systems capable of burning coal-derived fuels is summarized. Tasks were included in the following areas: (1) combustion, to study the combustion of coal-derived fuels and conversion of fuel-bound nitrogen to NO_x; (2) materials, to understand and prevent hot corrosion; and (3) system studies, to integrate and guide the other technologies. Significant progress was made G.Y.

N79-25499* National Aeronautics and Space Administration, Lewis Research Center, Cleveland, Ohio.

MHD PERFORMANCE CALCULATIONS WITH OXYGEN ENRICHMENT

C. C. P. Pian, P. J. Staiger, and G. R. Seikel 1979 32 p refs Presented at 18th Symp. on Engineering Aspects of Magnetohydrodynamics, Butte, Montana, 18-20 Jun. 1979

(Contract EF-77-A-01-2674)

(NASA-TM-79140, DOE/NASA/2674-79/4, E-9987) Avail: NTIS HC A03/MF A01 CSCL 10A

The impact of oxygen enrichment of the combustion air on the generator and overall plant performance was studied for the ECAS-scale MHD/steam plants. A channel optimization technique is described and the results of generator performance calculations using this technique are presented. Performance maps were generated to assess the impact of various generator parameters. Directly and separately preheated plant performance with varying O₂ enrichment was calculated. The optimal level of enrichment was a function of plant type and preheat temperature. The sensitivity of overall plant performance to critical channel assumptions and oxygen plant performance characteristics was also examined Author

N79-25500* National Aeronautics and Space Administration, Lewis Research Center, Cleveland, Ohio.

COMMERCIAL PHOSPHORIC ACID FUEL CELL SYSTEM TECHNOLOGY DEVELOPMENT

Paul R. Prokopius, Marvin Warshaw, Stephen N. Simons, and Robert B. King 1979 9 p refs Proposed for presentation at the 14th Intersociety Energy Conversion Engr. Conf., Boston, Mass., 5-10 Aug. 1979

(Contract DE-AL-03-79ET11272)

(NASA-TM-79169, DOE/NASA/11272-79/1, E-034) Avail: NTIS HC A02/MF A01 CSCL 10C

Reducing cost and increasing reliability were the technology drivers in both the electric utility and on-site integrated energy system applications. The longstanding barrier to the attainment of these goals was materials. Differences in approaches and their technological features, including electrodes, matrices, intercell cooling, bipolar/separator plates, electrolyte management, fuel selection, and system design philosophy were discussed. Author

N79-25501* National Aeronautics and Space Administration, Lewis Research Center, Cleveland, Ohio.

SOCIAL AND ECONOMIC IMPACT OF SOLAR ELECTRICITY AT SCHUCHULI VILLAGE

William J. Bifano, Anthony F. Ratajczak, Donald M. Behr (Arizona State Univ., Tempe), and Billy G. Garrett (Arizona State Univ., Tempe) 1979 18 p refs Presented at the Seminar on Solar Technol. in Rural Settings: Assessments of Field Experiences, Atlanta, Ga., 1-2 Jun. 1979; sponsored by United Nations Univ.

(Contract DE-AL-01-79ET20485)

(NASA-TM-79194, DOE/NASA/20485-79/3, E-071) Avail: NTIS HC A02/MF A01 CSCL 10A

Schuchuli, a small remote village on the Papago Indian Reservation in southwest Arizona, is 27 kilometers (17 miles) from the nearest available utility power. Its lack of conventional power is due to the prohibitive cost of supplying a small electrical load with a long-distance distribution line. Furthermore, alternate energy sources are expensive and place a burden on the resources of the villagers. On December 16, 1978, as part of a federally funded project, a solar cell power system was put into operation at Schuchuli. The system powers the village water pump, lighting for homes and other village buildings, family refrigerators and a communal washing machine and sewing machine. J.A.M.

N79-26474* National Aeronautics and Space Administration, Lewis Research Center, Cleveland, Ohio.

ELECTROCHEMICAL CELL FOR REBALANCING REDOX FLOW SYSTEM Patent

Lawrence H. Thaller, inventor (to NASA) Issued 26 Jun. 1979 5 p Filed 9 Jun. 1978 Supersedes N78-25554 (16 - 16 p 2137)

(NASA-Case-LEW-13150-1, US-Patent-4,159,366)

US-Patent-Appl-SN-914260; US-Patent-Class-429-15,

US-Patent-Class-429-101) Avail: US Patent and Trademark Office CSCL 10C

An electrically rechargeable REDOX cell or battery system including one of more rebalancing cells is described. Each rebalancing cell is divided into two chambers by an ion permeable membrane. The first chamber is fed with gaseous hydrogen and a cathode fluid which is circulated through the cathode chamber of the REDOX cell is also passed through the second chamber of the rebalancing cell. Electrochemical reactions take place on the surface of inert electrodes in the first and second chambers to rebalance the electrochemical capacity of the anode and cathode fluids of the REDOX system.

Official Gazette of the U.S. Patent and Trademark Office

N79-26476* National Aeronautics and Space Administration, Lewis Research Center, Cleveland, Ohio.

HANDBOOK OF DATA ON SELECTED ENGINE COMPONENTS FOR SOLAR THERMAL APPLICATIONS

Jun. 1979 240 p refs Prepared for DOE

(Contract EX-76-A-29-1060)

(NASA-TM-79027, E-9822, DOE/NASA/1060-78, 1) Avail: NTIS HC A11/MF A01 CSCL 10B

A data base on developed and commercially available power conversion system components for Rankine and Brayton cycle engines, which have potential application to solar thermal power-generating systems is presented. The status of the Stirling engine is discussed. For individual titles, see N79-26477 through N79-26484 S.E.S.

N79-26477* National Aeronautics and Space Administration, Lewis Research Center, Cleveland, Ohio.

SOLAR THERMAL POWER-CONVERSION SYSTEM

Harvey S. Bloomfield. In its Handbook of Data on Selected Eng. Components for Solar Thermal Appl. Jun. 1979 p 3-12 (For primary document see N79-26476 17-44)

Avail: NTIS HC A11/MF A01 CSCL 10B

The structure, applications, and operating concepts of solar thermal power conversion system are described S.E.S.

N79-26478* National Aeronautics and Space Administration. Lewis Research Center, Cleveland, Ohio.

RANKINE-CYCLE COMPONENT CHARACTERISTICS

Thaddeus S. Mroz and M. Murray Bailey. In *its Handbook of Data on Selected Eng. Components for Solar Thermal Appl.* Jun. 1979 p 13-83 (For primary document see N79-26476 17-44)
Avail: NTIS HC A11/MF A01 CSCL 10B

The performance and cost data for the major components of steam and organic Rankine cycle power conversion systems are presented. Rankine cycle components discussed include: (1) steam and organic turbines; (2) reciprocating engines; (3) surface condensers; and (4) boiler feed and condensate pumps. Component designs, component development status, operating characteristics, availability, cost, and component experience factors are described. S.E.S.

N79-26479* National Aeronautics and Space Administration. Lewis Research Center, Cleveland, Ohio.

BRAYTON-CYCLE COMPONENT CHARACTERISTICS

Thaddeus S. Mroz, Jack A. Heller, and Harvey S. Bloomfield. In *its Handbook of Data on Selected Eng. Components for Solar Thermal Appl.* Jun. 1979 p 85-126 (For primary document see N79-26476 17-44)

Avail: NTIS HC A11/MF A01 CSCL 10B

The gas turbine engine which operates on the Brayton cycle principle is described. The two basic types of Brayton gas turbine engine were developed and are presented in use: the closed cycle engine and open cycle engine. S.E.S.

N79-26480* National Aeronautics and Space Administration. Lewis Research Center, Cleveland, Ohio.

STIRLING ENGINE CHARACTERISTICS

Harry M. Cameron. In *its Handbook of Data on Selected Eng. Components for Solar Thermal Appl.* Jun. 1979 p 127-157 (For primary document see N79-26476 17-44)

Avail: NTIS HC A11/MF A01 CSCL 10B

The Stirling engine is described for the following factors: (1) excellent fuel economy; (2) low exhaust emissions; (3) multifuel capability; (4) flat torque curve; and (5) low noise level. The Stirling cycle, free piston engines, and the seals and hydrogen containment are discussed. S.E.S.

N79-26481* National Aeronautics and Space Administration. Lewis Research Center, Cleveland, Ohio.

SPEED REDUCERS-INCREASERS

Thaddeus S. Mroz. In *its Handbook of Data on Selected Eng. Components for Solar Thermal Appl.* Jun. 1979 p 159-173 (For primary document see N79-26476 17-44)

Avail: NTIS HC A11/MF A01 CSCL 10B

Prime movers such as steam-organic engines, gas turbines, Stirling engines, and piston engines were designed for peak efficiency at specific operating parameters. Gear systems are used to reduce or increase the output speed of the prime mover to the speed requirement of the driven machine, at the operational load. The configurations of gear systems discussed include: (1) Horizontal parallel-shaft offset; (2) Horizontal parallel-shaft in line; (3) Horizontal right angle; (4) Vertical right angle; and (5) Epicyclic. S.E.S.

N79-26482* National Aeronautics and Space Administration. Lewis Research Center, Cleveland, Ohio.

COMMERCIAL SYNCHRONOUS ALTERNATING CURRENT GENERATORS

James H. Dunn. In *its Handbook of Data on Selected Eng. Components for Solar Thermal Appl.* Jun. 1979 p 175-186 (For primary document see N79-26476 17-44)

Avail: NTIS HC A11/MF A01 CSCL 10B

Different types of generator and generator system are discussed. Variable speed and constant frequency systems are described. The flux switch alternator in alternating current generators used for induction hardening was examined for industrial utilization. S.E.S.

N79-26483* National Aeronautics and Space Administration. Lewis Research Center, Cleveland, Ohio.

POWER-CONVERSION SYSTEM COMPONENT SUMMARY

Thaddeus S. Mroz, M. Murray Bailey, Jack A. Heller, Harvey S. Bloomfield, Robert J. Stochl, and Robert E. Hyland. In *its Handbook of Data on Selected Eng. Components for Solar Thermal Appl.* Jun. 1979 p 187-190 (For primary document see N79-26476 17-44)

Avail: NTIS HC A11/MF A01 CSCL 10B

Commercial components applicable to Rankine cycle, Brayton cycle, and Stirling cycle solar thermal power generating systems were surveyed. The solar thermal power generating systems and their components are described. Data on these components are presented and include development status, availability, cost, operating constraints, operating characteristics, and experience factors. S.E.S.

N79-26484* National Aeronautics and Space Administration. Lewis Research Center, Cleveland, Ohio.

CANDIDATE POWER-CONVERSION SYSTEM CYCLES, APPENDIX A

Robert J. Stochl. In *its Handbook of Data on Selected Eng. Components for Solar Thermal Appl.* Jun. 1979 p 191-209 (For primary document see N79-26476 17-44)

Avail: NTIS HC A11/MF A01 CSCL 10B

The Rankine cycle, Brayton cycle, and Stirling cycle are described for solar thermal applications. The basic cycle configuration, its operation, and the basic relations for calculating cycle efficiencies and work outputs are presented. The system modifications used to increase performance over that of the basic cycle are discussed. S.E.S.

N79-26502* National Aeronautics and Space Administration. Lewis Research Center, Cleveland, Ohio.

THE USE OF WIND DATA WITH AN OPERATIONAL WIND TURBINE IN A RESEARCH AND DEVELOPMENT ENVIRONMENT

Hazrold E. Neustadter. 1979 13 p refs. Presented at the Am. Meteorological Soc., Portland, Oreg., 19-21 Jun. 1979 (Contract E(49-26)-1004)

(NASA-TM-73832, DOE/NASA/1004-79/16, E-9419) Avail: NTIS HC A02/MF A01 CSCL 10A

The status of the use of wind information is presented in four areas, namely: operational control, design verification, power performance analysis, and lifetime estimation. Attention is given to some of the identified wind information needs and the steps taken to meet these needs. M.M.M.

N79-26503* National Aeronautics and Space Administration. Lewis Research Center, Cleveland, Ohio.

A METHOD FOR CORRELATING PERFORMANCE DATA OF A TERRESTRIAL SOLAR CELL ARRAY

Frederick F. Simon. May 1979 45 p refs. Prepared for DOE (NASA-TM-79163, DOE/NASA/20485-79/2, E-023) Avail: NTIS HC A03/MF A01 CSCL 10A

An analytical method was proposed for characterizing array power output, in the region of maximum power, as a function of environmental variables. The correlation provided a way of evaluating the output of an array under environmental conditions that differ from those encountered during testing. Power data obtained at one location was used to predict array performance at other locations. R.E.S.

N79-26504* National Aeronautics and Space Administration. Lewis Research Center, Cleveland, Ohio.

LARGE HORIZONTAL AXIS WIND TURBINE DEVELOPMENT

William H. Robbins and Ronald L. Thomas. 1979 16 p refs. Presented at the Wind Energy Innovative Systems Conf., Colo. Springs, Colo., 23-25 May 1979, sponsored by Solar Energy Res. Inst. (Contract E(49-26)-1059)

(NASA-TM-79174, DOE/NASA/1059-79/2; E-039) Avail: NTIS HC A02/MF A01 CSCL 10A

An overview of the NASA activities concerning ongoing wind systems oriented toward utility application is presented. First-generation technology large wind turbines were designed and are in operation at selected utility sites. In order to make a significant energy impact, costs of 2 to 3 cents per kilowatt hour must be achieved. The federal program continues to fund the development by industry of wind turbines which can meet the cost goals of 2 to 3 cents per kilowatt hour. Lower costs are achieved through the incorporation of new technology and innovative system design to reduce weight and increase energy capture. M.M.M.

N79-26506* National Aeronautics and Space Administration, Lewis Research Center, Cleveland, Ohio
RECENT ADVANCES IN REDOX FLOW CELL STORAGE SYSTEMS

Lawrence H. Thaller 1979 10 p. refs. Presented at the 14th Intersoc. Energy Conversion Eng. Conf., Boston, 5-10 Aug. 1979. Prepared for DOE (Contract EC-77-A-31-1002)

(NASA-TM-79186, DOE/NASA/1002-79/4; E-053) Avail: NTIS HC A02/MF A01 CSCL 10C

Several features which were conceived and incorporated into complete redox systems that greatly enhanced its ability to be kept in proper charge balance, to be capable of internal voltage regulation, and in general be treated as a true multicell electrochemical system rather than an assembly of single cells that were wired together, were discussed. The technology status as it relates to the two application areas of solar photovoltaic/wind and distributed energy storage for electric utility applications was addressed. The cost and life advantages of redox systems were also covered. R.E.S.

N79-27663* National Aeronautics and Space Administration, Lewis Research Center, Cleveland, Ohio

ENERGY STATE FORMULATION OF LUMPED VOLUME DYNAMIC EQUATIONS WITH APPLICATION TO A SIMPLIFIED FREE PISTON STIRLING ENGINE

Carl J. Daniele and Carl F. Lorenzo 1979 20 p. refs. Presented at the Soc. for Computer Simulation, Pittsburgh, 21-22 May 1979

(NASA-TM-79197, E-075) Avail: NTIS HC A02/MF A01 CSCL 10B

Lumped volume dynamic equations are derived using an energy state formulation. This technique requires that kinetic and potential energy state functions be written for the physical system being investigated. To account for losses in the system, a Rayleigh dissipation function is formed. Using these functions, a Lagrangian is formed and using Lagrange's equation, the equations of motion for the system are derived. The results of the application of this technique to a lumped volume are used to derive a model for the free piston Stirling engine. The model was simplified and programmed on an analog computer. Results are given comparing the model response with experimental data. Author

N79-27664* National Aeronautics and Space Administration, Lewis Research Center, Cleveland, Ohio

REDUCTION OF PARTICULATE CARRYOVER FROM A PRESSURIZED FLUIDIZED BED

R. W. Patch 1979 22 p. refs. Presented at 2d Symp. on the Transfer and Utilization of Particulate Control Technol., Denver, Colo., 23-27 Jul. 1979

(NASA-TM-79216, E-106) Avail: NTIS HC A02/MF A01 CSCL 10B

A bench scale fluidized bed combustor was constructed with a conical shape so that the enlarged upper part of the combustor would also serve as a granular bed filter. The combustor was fed coal and limestone. Ninety-nine tests of about four hours each were conducted over a range of conditions. Coal-to-air ratio varied from 0.033 to 0.098 (all lean). Limestone-to-coal ratio varied from 0.06 to 0.36. Bed depth varied from 3.66 to

8.07 feet. Temperature varied from 1447 to 1905 F. Pressure varied from 40 to 82 psia. Heat transfer area had the range zero to 2.72 ft squared. Two cone angles were used. The average particulate carry over of 2.5 grains/SCF was appreciably less than cylindrical fluidized bed combustors. The carry over was correlated by multiple regression analysis to yield the dependence on bed depth and hence the collection efficiency, which was 20%. A comparison with a model indicated that the exhaust port may be below the transport disengaging height for most of the tests, indicating that further reduction in carry over and increase in collection efficiency could be affected by increasing the freeboard and height of the exhaust port above the bed. Author

N79-27665* National Aeronautics and Space Administration, Lewis Research Center, Cleveland, Ohio

ENERGY AND COST SAVING RESULTS FOR ADVANCED TECHNOLOGY SYSTEMS FROM THE COGENERATION TECHNOLOGY ALTERNATIVES STUDY (CTAS)

G. D. Sagerman, G. J. Barne, and R. K. Burns 1979 22 p. Presented at AIAA Terrestrial Energy System Conf., Orlando, Fla., 4-6 Jun. 1979

(Contract EC-77-A-31-1062)

(NASA-TM-79213, DOE/NASA/1062-79/2; AIAA-78-1000) Avail: NTIS HC A02/MF A01 CSCL 10A

An overview of the organization and methodology of the Cogeneration Technology Alternatives Study is presented. The objectives of the study were to identify the most attractive advanced energy conversion systems for industrial cogeneration applications in the future and to assess the advantages of advanced technology systems compared to those systems commercially available today. Advanced systems studied include steam turbines, open and closed cycle gas turbines, combined cycles, diesel engines, Stirling engines, phosphoric acid and molten carbonate fuel cells and thermionics. Steam turbines, open cycle gas turbines, combined cycles, and diesel engines were also analyzed in versions typical of today's commercially available technology to provide a base against which to measure the advanced systems. Cogeneration applications in the major energy consuming manufacturing industries were considered. Results of the study in terms of plant level energy savings, annual energy cost savings and economic attractiveness are presented for the various energy conversion systems considered. R.E.S.

N79-28672* National Aeronautics and Space Administration, Lewis Research Center, Cleveland, Ohio

LIGHTWEIGHT POROUS PLASTIC PLAQUE

Margaret Reid In NASA Goddard Space Flight Center 11th Ann. Battery Workshop 1975 p. 31-42 (For primary document see N79-28669 19-44)

Avail: NTIS HC A23/MF A01 CSCL 10C

The porosity and platability of various materials were investigated to determine a suitable substrate for nickel-plated electrodes. Immersion, ultrasonics, and flow-through plating techniques were tried using nonproprietary formulations, and proprietary phosphide and boride baths. Modifications to the selected material include variations in formulation and treatment, carbon loading to increase conductivity, and the incorporation of a grid. Problems to be solved relate to determining conductivities and porosities as a function of amount of nickel plated on the plastics, loading, charge and discharge curves of electrodes at different current densities, cell performance, and long term degradation of electrodes. A.R.H.

N79-28725* National Aeronautics and Space Administration, Lewis Research Center, Cleveland, Ohio

SAFETY CONSIDERATIONS IN THE DESIGN AND OPERATION OF LARGE WIND TURBINES Final Report

Dwight H. Reilly Jun. 1979 38 p. refs. Sponsored in part by DOE

(Contract DE-AI01-79ET20305)

(NASA-TM-79193, E-067, DOE/NASA/20305-79/3) Avail: NTIS HC A03/MF A01 CSCL 10B

The engineering and safety techniques used to assure the reliable and safe operation of large wind turbine generators utilizing

the Mod 2 Wind Turbine System Program as an example is described. The techniques involve a careful definition of the wind turbine's natural and operating environments, use of proven structural design criteria and analysis techniques, an evaluation of potential failure modes and hazards, and use of a fail safe and redundant component engineering philosophy. The role of an effective quality assurance program, tailored to specific hardware criticality, and the checkout and validation program developed to assure system integrity are described. Author

N79-28726* National Aeronautics and Space Administration, Lewis Research Center, Cleveland, Ohio.
STIRLING ENGINES FOR AUTOMOBILES
 Donald G Beremand 1979 15 p refs Proposed for presentation at Intern. Conf. on Energy Use Management, Los Angeles, Calif., 22-26 Oct. 1979. Sponsored in part by DOE (Contract EC-77-A-31-1040) (NASA-TM-79222; E-116) Avail. NTIS HC A02/MF A01 CSCL 10B

The results of recent and ongoing automobile Stirling engine development efforts are reviewed and technology status and requirements are identified. Key technology needs include those for low cost, high temperature (1300 - 1500 F) metal alloys for heater heads, and reliable long-life, low-leakage shaft seals. Various fuel economy projections for Stirling powered automobiles are reviewed and assessed. Author

N79-28727* National Aeronautics and Space Administration, Lewis Research Center, Cleveland, Ohio.
DESIGN, FABRICATION, AND INITIAL TEST OF A FIXTURE FOR REDUCING THE NATURAL FREQUENCY OF THE MOD-O WIND TURBINE TOWER
 J R Winemiller, T L Sullivan, R L Sizemore, and S T Yee Jul. 1979 21 p Prepared for DOE (Contract EX 76-1-01 1028) (NASA-TM-79200; C-081; DOE/NASA/1028-79/24) Avail. NTIS HC A02/MF A01 CSCL 10B

It was desired to observe the behavior of a two bladed wind turbine where the tower first bending natural frequency is less than twice the rotor speed. The system then passes through resonance when accelerating to operating speed. The frequency of the original Mod-O tower was reduced by placing it on a spring fixture. The fixture is adjustable to provide a range of tower bending frequencies. Fixture design details are given and behavior during initial operation is described. Author

N79-28728* National Aeronautics and Space Administration, Lewis Research Center, Cleveland, Ohio.
EFFECT OF POSITIVE PULSE CHARGE WAVEFORMS ON CYCLE LIFE OF NICKEL ZINC CELLS Final Report
 John J Smithrick Jul. 1979 14 p refs Sponsored in part by DOE (Contract EC-77-A-31-1044) (NASA-TM-79215; E-100; DOE/NASA/1044-79/3) Avail. NTIS HC A02/MF A01 CSCL 10C

Five amp-hour nickel-zinc cells were life cycled to evaluate four different charge methods. Three of the four waveforms investigated were 120 Hz full wave rectified sinusoidal (FWRS), 120 Hz silicon controlled rectified (SCR), and 1 kHz square wave (SW). The fourth, a constant current method, was used as a baseline of comparison. Three sealed Ni-Zn cells connected in series were cycled. Each series string was charged at an average c/20 rate, and discharged at a c/2.5 rate to a 75% rated depth. Author

N79-29599* National Aeronautics and Space Administration, Lewis Research Center, Cleveland, Ohio.
DYNAMIC ANALYSIS OF A PHOTOVOLTAIC POWER SYSTEM WITH BATTERY STORAGE CAPABILITY Final Report
 Walter C Merrill, Ronald J Blaha, and Roy L Pickrell Jul. 1979 47 p ref (DE-A101-79ET20485)

(NASA-TM-79209; E-094; DOE/NASA/20485-79/4) Avail. NTIS HC A03/MF A01 CSCL 10C

A photovoltaic power system with a battery storage capability is analyzed. A dual battery current control concept is proposed, which enables the battery to either supply or accept power depending upon system environment and load conditions. A simulation of the power system, including the battery current control, is developed and evaluated. The evaluation demonstrates the viability of the battery control concept of switch the battery from a charge to discharge mode and back as required by load and environmental conditions. An acceptable system operation is demonstrated over the entire insolation range. Additionally, system sensitivity, bandwidth, and damping characteristics of the battery control are shown to be acceptable for a projected hardware implementation. Author

N79-29600* National Aeronautics and Space Administration, Lewis Research Center, Cleveland, Ohio.
THE ALKALINE ZINC ELECTRODE AS A MIXED POTENTIAL SYSTEM
 William L Fielder Jul. 1979 22 p refs (NASA-TM-79235; E-141) Avail. NTIS HC A02/MF A01 CSCL 10C

Cathodic and anodic processes for the alkaline zinc electrode in 0.01 molar zincate electrolyte (9 molar hydroxide) were investigated. Cyclic voltammograms and current-voltage curves were obtained by supplying pulses through a potentiostat to a zinc rotating disk electrode. The data are interpreted by treating the system as one with a mixed potential; the processes are termed The zincate and corrosion reactions. The relative proportions of the two processes vary with the supplied potential. For the cathodic region, the cathodic corrosion process predominates at higher potentials while both processes occur simultaneously at a lower potential (i.e., 50 mV). For the anodic region, the anodic zincate process predominates at higher potentials while the anodic corrosion process is dominant at lower potential (i.e., 50 mV) if H₂ is present. Author

N79-30719* National Aeronautics and Space Administration, Lewis Research Center, Cleveland, Ohio.
WIND TURBINES FOR ELECTRIC UTILITIES: DEVELOPMENT STATUS AND ECONOMICS
 J R Ramler and R M Donovan 1979 21 p refs Presented at Terrest. Energy Systems Conf., Orlando, Fla., 4-6 Jun. 1979; sponsored by AIAA (Contract E(49-26)-1028) (NASA-TM-79170; E-035; DOE/NASA/1028-79/23) Avail. NTIS HC A02/MF A01 CSCL 10B

The technology and economics of the large, horizontal-axis wind turbines currently in the Federal Wind Energy Program are presented. Wind turbine technology advancements made in the last several years are discussed. It is shown that, based on current projections of the costs of these machines when produced in quantity, they should be attractive for utility application. The cost of electricity (COE) produced at the busbar is shown to be a strong function of the mean wind speed at the installation site. The breakeven COE as a fuel saver is discussed and the COE range that would be generally attractive to utilities is indicated. Author

N79-30720* National Aeronautics and Space Administration, Lewis Research Center, Cleveland, Ohio.
PERFORMANCE CHARACTERISTICS OF A SLAGGING GASIFIER FOR MHD COMBUSTOR SYSTEMS Final Report
 Kenneth O Smith Jun. 1979 49 p refs Sponsored in part by DOE (Contract EF-77-A-01-2674) (NASA-TM-79195; E-072; DOE/NASA/2674-79/6) Avail. NTIS HC A03/MF A01 CSCL 10A

The performance of a two stage, coal combustor concept for magnetohydrodynamic (MHD) systems was investigated analytically. The two stage MHD combustor is comprised of an entrained flow, slagging gasifier as the first stage, and a gas

phase reactor as the second stage. The first stage was modeled by assuming instantaneous coal devolatilization, and volatiles combustion and char gasification by CO₂ and H₂O in plug flow. The second stage combustor was modeled assuming adiabatic instantaneous gas phase reactions. Of primary interest was the dependence of char gasification efficiency on first stage particle residence time. The influence of first stage stoichiometry, heat loss, coal moisture, coal size distribution, and degree of coal devolatilization on gasifier performance and second stage exhaust temperature was determined. Performance predictions indicate that particle residence times on the order of 500 msec would be required to achieve gasification efficiencies in the range of 90 to 95 percent. The use of a finer coal size distribution significantly reduces the required gasifier residence time for acceptable levels of fuel use efficiency. Residence time requirements are also decreased by increased levels of coal devolatilization. Combustor design efforts should maximize devolatilization by minimizing mixing times associated with coal injection. K L

N79-31781* National Aeronautics and Space Administration, Lewis Research Center, Cleveland, Ohio
DISCHARGE CHARACTERISTICS OF 300 AMPERE-HOUR Ni-Zn TRACTION CELLS
 John G. Ewashinka Aug 1979 11 p
 (NASA-TM-79244, E-151) Avail NTIS HC A13/MF A01 CSCL 10C

Preliminary tests were performed on 300 ampere-hour nickel-zinc cells containing the Lewis improved inorganic-organic (I/O) separator. These cells also have other design features included to optimize performance and cycle life. The tests carried out were formation tests and characteristic discharge tests. Information obtained include case temperature and maximum power delivered. A R H

N79-32640* National Aeronautics and Space Administration, Lewis Research Center, Cleveland, Ohio
SOLAR CELL HIGH EFFICIENCY AND RADIATION DAMAGE, 1979
 Aug 1979 250 p refs Conf held at Cleveland 13-14 Jun 1979
 (NASA-CP-2097, D-133) Avail NTIS HC A13/MF A01 CSCL 10A

Progress in the effort to increase the end-of-life efficiency of solar cells for space use is assessed. Silicon solar cell efficiency, radiation effects, and gallium arsenide cells are emphasized. For individual titles see N79-32641 through N79-32673.

N79-32641* National Aeronautics and Space Administration, Lewis Research Center, Cleveland, Ohio
THE NASA LEWIS RESEARCH CENTER PROGRAM IN SPACE SOLAR CELL RESEARCH AND TECHNOLOGY
 Henry W. Brandhorst, Jr. In its Solar Cell High Efficiency and Radiation Damage, 1979 Aug 1979 p 1-4 (For primary document see N79-32640 23-44)
 Avail NTIS HC A13/MF A01 CSCL 10A

Progress in space solar cell research and technology is reported. An 18 percent-AMO-efficient silicon solar cell, reduction in the radiation damage suffered by silicon solar cells in space, and high efficiency wrap-around contact and thin (50 micrometer) coplanar back contact silicon cells are among the topics discussed. Reduction in the cost of silicon cells for space use, cost effective GaAs solar cells, the feasibility of 30 percent AMO solar energy conversion, and reliable encapsulants for space blankets are also considered. J M S

N79-32648* Spire Corp., Bedford, Mass.
APPLICATIONS OF ION IMPLANTATION TO HIGH PERFORMANCE, RADIATION TOLERANT SILICON SOLAR CELLS
 Allen R. Kirkpatrick, John A. Minnucci, and Keith W. Matthei. In NASA Lewis Res. Center: Solar Cell High Efficiency and Radiation Damage, 1979 Aug 1979 p 51-59 refs (For primary document see N79-32640 23-44)

(Contracts NAS3-20823, NAS3-21276)
 Avail NTIS HC A13/MF A01 CSCL 10A

Progress in the development of ion implanted silicon solar cells is reported. Effective back surface preparation by implantation, junction processing to achieve high open circuit voltages in low-resistivity cells, and radiation tolerance cells are among the topics studied. J M S

N79-32649* National Aeronautics and Space Administration, Lewis Research Center, Cleveland, Ohio
OPEN-CIRCUIT VOLTAGE IMPROVEMENTS IN LOW-RESISTIVITY SOLAR CELLS
 Michael P. Godlewski, Thomas M. Klucher, George A. Mazaris, and Victor G. Weizer. In its Solar Cell High Efficiency and Radiation Damage, 1979 Aug 1979 p 61-70 refs (For primary document see N79-32640 23-44)
 Avail NTIS HC A13/MF A01 CSCL 10A

Mechanisms limiting the open-circuit voltage in 0.1 ohm-cm solar cells were investigated. It was found that a rather complicated multistep diffusion process could produce cells with significantly improved voltages. The voltage capabilities of various laboratory cells were compared independent of their absorption and collection efficiencies. This was accomplished by comparing the cells on the basis of their saturation currents or, equivalently, comparing their voltage outputs at a constant current-density level. The results show that for both the Lewis diffused emitter cell and the Spire ion-implanted emitter cell the base component of the saturation current is voltage controlling. The evidence for the University of Florida cells, although not very conclusive, suggests emitter control of the voltage in this device. The data suggest further that the critical voltage-limiting parameter for the Lewis cell is the electron mobility in the cell base. R E S

N79-32650* National Aeronautics and Space Administration, Lewis Research Center, Cleveland, Ohio
MODELING OF THIN, BACK-WALL SILICON SOLAR CELLS
 Cosmo R. Baraona. In its Solar Cell High Efficiency and Radiation Damage, 1979 Aug 1979 p 73-78 refs (For primary document see N79-32640 23-44)
 Avail NTIS HC A13/MF A01 CSCL 10A

The performance of silicon solar cells with p-n junctions on the nonilluminated surface (i.e., upside-down or back-wall cells) was calculated. These structures consisted of a uniformly shaped p-type substrate layer, a p(+)-type field layer on the front (illuminated) surface, and a shallow, n-type junction on the back (nonilluminated) surface. A four-layer solar cell model was used to calculate efficiency, open-circuit voltage, and short-circuit current. The effect on performance of p-layer thickness and resistivity was determined. The diffusion length was varied to simulate the effect of radiation damage. The results show that peak initial efficiencies greater than 15 percent are possible for cell thicknesses of 100 micrometers or less. After 10 years of radiation damage in geosynchronous orbit, thin (25 to 50 micrometers thick) cells made from 10 to 100 ohm-cm material show the smallest decrease (approximately 10 percent) in performance. Author

N79-32653* General Electric Co., Schenectady, N. Y.
HIGH EFFICIENCY CELL GEOMETRY
 R. N. Hall. In NASA Lewis Res. Center: Solar Cell High Efficiency and Radiation Damage, 1979 Aug 1979 p 97-100 (For primary document see N79-32640 23-44)
 Avail NTIS HC A13/MF A01 CSCL 10A

A new silicon solar cell is described which has an array of small-area conduction paths to transport current directly through the wafer to metal electrodes on the back. This design eliminates grid shadowing and many of the other losses inherent in conventional cells. Early experimental units without texturing or antireflection coatings show 13.3% efficiency under air-mass-one illumination. insolation. Author

N79-32658* National Aeronautics and Space Administration
Lewis Research Center, Cleveland, Ohio.

RADIATION DAMAGE IN HIGH-VOLTAGE SILICON SOLAR CELLS

Irving Weinberg, Clifford K. Swartz, and Victor G. Weizer. *In its Solar Cell High Efficiency and Radiation Damage*. 1979 Aug 1979 p 137-143 refs (For primary document see N79-32640 23-44)

Avail NTIS HC A13/MF A01 CSCL 10A

Three types of open circuit high voltage solar cells were tested to determine their performance after exposure to 1 MeV electron irradiations. The cells with a relatively deep n-type emitter were more susceptible to radiation damage than other high open circuit high voltage cells. The use of diffused or ion implanted junctions leads to open circuit high voltage cell designs that are less susceptible to radiation damage. These latter two types of cells show degradations that are typical of the 0.1 ohm-cm material from which they are fabricated. Furthermore, exposure to ionizing radiation causes oxide degradation and decreased cell performance in cells that depend on a charged oxide to achieve significant cell properties. Hence, the combination of a charged oxide and a relatively deep n-type emitter is not recommended for incorporation into a cell designed for use in the particulate radiation environment of space. M M M

N79-32660* National Aeronautics and Space Administration
Lewis Research Center, Cleveland, Ohio.

REVERSE ANNEALING IN RADIATION-DAMAGED, SILICON SOLAR CELLS

Irving Weinberg and Clifford K. Swartz. *In its Solar Cell High Efficiency and Radiation Damage*. 1979 Aug 1979 p 161-171 refs (For primary document see N79-32640 23-44)

Avail NTIS HC A13/MF A01 CSCL 10A

In order to understand the results in terms of properties of the radiation induced defects, a combination of diffusion length measurements and defect data obtained from Deep Level Transient Spectroscopy were used. The results indicate that the defect at $E_{\text{sub}} \approx 0.30$ eV is responsible for the observed reverse annealing. The defect was identified as a boron-oxygen vacancy complex. This identification is a guide to processing efforts aimed at increasing the concentration of these radiation induced defects. M M M

N79-32665* National Aeronautics and Space Administration
Lewis Research Center, Cleveland, Ohio.

TEMPERATURE AND INTENSITY DEPENDENCE OF THE PERFORMANCE OF AN ELECTRON IRRADIATED (AlGa)As/GaAs SOLAR CELL

Clifford K. Swartz and Russell E. Hurt, Jr. *In its Solar Cell High Frequency and Radiation Damage*. 1979 Aug 1979 p 217-226 refs (For primary document see N79-32640 23-44)

Avail NTIS HC A13/MF A01 CSCL 10A

The performance of a Hughes, liquid phase epitaxial, 2 centimeter by 2 centimeter, (AlGa)As/GaAs solar cell was measured before and after irradiations with 1 MeV electrons to fluences of 1×10 to the 16th power electrons/sq cm. The temperature dependence of performance was measured over the temperature range 135 to 415 K at each fluence level. In addition, temperature dependences were measured at five intensity levels from 137 to 257 mW/sq cm before irradiation and after a fluence of 1×10 to the 16th power electrons/sq cm. For the intermediate fluences, performance was measured as a function of intensity at 298 K only. G Y

N79-32666* Lincoln Lab, Mass Inst of Tech, Lexington
SHALLOW HOMOJUNCTION GaAs SOLAR CELLS

John C. C. Fan. *In NASA Lewis Res Center Solar Cell High Frequency and Radiation Damage*. 1979 Aug 1979 p 227-233 refs. Sponsored in part by AF (For primary document see N79-32640 23-44)

Avail NTIS HC A13/MF A01 CSCL 10A

Single-crystal GaAs shallow homojunction solar cells on GaAs or Ge substrates without Ga sub $1 \times$ Al sub x As window layers, that have conversion efficiencies exceeding 20% at AM1

(17% at AM0). Using a simple theoretical model, good fits were obtained between computer calculations and experimental data for external quantum efficiency and conversion efficiency of cells with different values of n+ layer thickness. The calculations not only yield values for material properties of the GaAs layers composing the cells but will also permit the optimization of cell designs for space and terrestrial applications. Preliminary measurements indicate that the shallow-homojunction cells are resistant to electron irradiation. In the best test so far, bombardment with 1×10 to the 16th power/sq cm fluence of 1 MeV electrons reduced the short-circuit current by only about 6%.

G Y

N79-32669* Hughes Research Labs., Malibu, Calif.
SUMMARY OF GaAs SOLAR CELL PERFORMANCE AND RADIATION DAMAGE WORKSHOP

G. S. Kamath. *In NASA Lewis Res Center Solar Cell High Efficiency and Radiation Damage*. 1979 Aug 1979 p 253-254 (For primary document see N79-32640 23-44)

Avail NTIS HC A13/MF A01 CSCL 10A

The workshop considered the GaAs solar cell capability and promise in several steps: (1) maximum efficiency; (2) space application; (3) major technology problems (AR coating optimization, contacts); (4) radiation resistance; (5) cost and availability; and (6) alternatives. The workshop believes that GaAs solar cells are fast approaching the fulfillment of their potential as candidates for space cells. A maximum efficiency of 20 to 31 percent AMO can be reasonably expected from GaAs based cells, and this may go a little higher with concentration. The use of concentration in space needs to be more carefully evaluated.

G Y

N79-33572* National Aeronautics and Space Administration
Lewis Research Center, Cleveland, Ohio.

ANNEALING OF RADIATION DAMAGE IN 0.1- AND 2-OHM-CENTIMETER SILICON SOLAR CELLS

Irving Weinberg and Clifford K. Swartz. Oct 1979 13 p refs (NASA-TP-1559, E-9997) Avail NTIS HC A02/MF A01 CSCL 10A

Isochronal and isothermal annealing studies were conducted on 0.1 and 2 ohm centimeter n(+)/p silicon cells after irradiation by 1 MeV electrons at fluences of 10 to the 14th power, 5 times 10 to the 14th power, and 10 to the 15th power per square centimeter. For the 0.1 ohm centimeter cells, reverse annealing was not observed in the isochronal data. However, reverse annealing was observed between approximately 200 and 325 C in the isochronal data of the 2 ohm centimeter cells. Isothermal annealing of 0.1 ohm centimeter cells at 500 C restored pre-irradiation maximum power $P_{\text{sub max}}$ within 20 minutes at fluence = 10 to the 14th power, in 180 minutes at fluence = 5 times 10 to the 14th power and to 92 percent of pre-irradiation $P_{\text{sub max}}$ in 180 minutes for fluence = 10 to the 15th power. Annealing at 450 C was found inadequate to restore 0.1 ohm centimeter cell performance within reasonable times for all fluence levels. By comparison, at 450 C, the $P_{\text{sub max}}$ of 2 ohm centimeter cells was restored within 45 minutes, for the two highest fluence levels, while for the lowest fluence, restoration was completed within 15 minutes. Spectral response data indicate that, for both resistivities, degradation occurs predominantly in the cells p-type base region. Author

A79 10084 * Rapid, efficient charging of lead acid and nickel zinc traction cells. J. J. Smithrick (NASA, Lewis Research Center, Cleveland, Ohio). In: Intersociety Energy Conversion Engineering Conference, 13th, San Diego, Calif., August 20-25, 1978. Proceedings, Volume 1. (A79 10001 01 44) Warrendale, Pa. Society of Automotive Engineers, Inc., 1978. p. 672-676. 6 refs. NASA supported research, Contract No. EC 77 A 31 1011.

Lead acid and nickel-zinc traction cells were rapidly and efficiently charged using a high rate tapered dc charge (HRTDC) method which could possibly be used for on-the-road service recharge of electric vehicles. The HRTDC method takes advantage of initial high cell charge acceptance and uses cell gassing rate and temperature as an indicator of charging efficiency. On the average,

300 amp-hour nickel-zinc traction cells were given a HRTDC to 78% of rated amp-hour capacity within 53 minutes at an amp-hour efficiency of 92% and an energy efficiency of 52%. Three-hundred amp-hour lead-acid traction cells were charged to 69% of rated amp-hour capacity within 46 minutes at an amp-hour efficiency of 91% with an energy efficiency of 64%. B.J.

A79-10097 * **Response of lead-acid batteries to chopper-controlled discharge.** R. L. Cataldo (NASA, Lewis Research Center, Cleveland, Ohio). In: Intersociety Energy Conversion Engineering Conference, 13th, San Diego, Calif., August 20-25, 1978, Proceedings, Volume 1. (A79-10001 01-44) Warrendale, Pa., Society of Automotive Engineers, Inc., 1978, p. 764-768.

The results of tests on an electric vehicle battery, using a simulated electric vehicle chopper-speed controller, show energy output losses up to 25 percent compared to constant current discharges at the same average current of 100 A. However, an energy output increase of 22 percent is noticed at the 200 A average level and 44 percent increase at the 300 A level using pulse discharging. Because of these complex results, electric vehicle battery/speed controller interactions must be considered in vehicle design. (Author)

A79-10101 * **Thermal energy storage for industrial waste heat recovery.** H. W. Hoffman, R. J. Kedi (Oak Ridge National Laboratory, Oak Ridge, Tenn.), and R. A. Duscha (NASA, Lewis Research Center, Cleveland, Ohio). In: Intersociety Energy Conversion Engineering Conference, 13th, San Diego, Calif., August 20-25, 1978, Proceedings, Volume 2. (A79-10001 01-44) Warrendale, Pa., Society of Automotive Engineers, Inc., 1978, p. 910-916. NASA-supported research. Contract No. W-7405-eng-26.

Thermal energy storage systems designed for energy conservation through the recovery, storage, and reuse of industrial process waste heat are reviewed. Consideration is given to systems developed for primary aluminum, cement, the food processing industry, paper and pulp, and primary iron and steel. Projected waste-heat recovery and energy savings are listed for each category. S.C.S.

A79-10108 * **Storage systems for solar thermal power.** J. E. Calogeras and L. H. Gordon (NASA, Lewis Research Center, Cleveland, Ohio). In: Intersociety Energy Conversion Engineering Conference, 13th, San Diego, Calif., August 20-25, 1978, Proceedings, Volume 2. (A79-10001 01-44) Warrendale, Pa., Society of Automotive Engineers, Inc., 1978, p. 970-976. 11 refs.

A major constraint to the evolution of solar thermal power systems is the need to provide continuous operation during periods of solar outage. A number of high temperature thermal energy storage technologies which have the potential to meet this need are currently under development. The development status is reviewed of some thermal energy storage technologies specifically oriented towards providing diurnal heat storage for solar central power systems and solar total energy systems. These technologies include sensible heat storage in caverns and latent heat storage using both active and passive heat exchange processes. In addition, selected thermal storage concepts which appear promising to a variety of advanced solar thermal system applications are discussed. (Author)

A79-10113 * **Lithium and potassium heat pipes for thermionic converters.** G. Miskolczy (Thermo Electron Corp., Waltham, Mass.) and E. Kroeger (NASA, Lewis Research Center, Cleveland, Ohio). In: Intersociety Energy Conversion Engineering Conference, 13th, San Diego, Calif., August 20-25, 1978, Proceedings, Volume 2. (A79-10001 01-44) Warrendale, Pa., Society of Automotive Engineers, Inc., 1978, p. 1035-1039. 5 refs. Contract No. NAS3-20270.

A prototypic heat pipe system for an out-of-core thermionic reactor has been built and tested. The emitter of the concentric thermionic converter consists of the condenser of a tungsten heat pipe utilizing a lithium working fluid. The evaporator section of the emitter heat pipe is radiation heated to simulate the thermal input

from the nuclear reactor. The emitter heat pipe thermal transport is matched to the thermionic converter input requirement. The collector heat pipe of niobium, 1%-zirconium alloy uses potassium as the working fluid. The thermionic collector is coupled to the heat pipe by a tapered conical joint designed to minimize the temperature drop. The area ratio of the evaporator to condenser is 16:1, which increases the radiation area. The composite wick structure consists of seven arteries and cylindrical wraps. The collector heat flux matches the design requirements of the thermionic converter. (Author)

A79-10234 * **Design and operating experience on the U.S. Department of Energy Experimental Mod-O 100 kW Wind Turbine.** J. C. Glasgow and A. G. Birchenough (NASA, Lewis Research Center, Cleveland, Ohio). In: Intersociety Energy Conversion Engineering Conference, 13th, San Diego, Calif., August 20-25, 1978, Proceedings, Volume 3. (A79-10001 01-44) Warrendale, Pa., Society of Automotive Engineers, Inc., 1978, p. 2052-2059. 5 refs.

The Mod-O 100 kW Experimental Wind Turbine was designed and fabricated by NASA, as part of the Federal Wind Energy Program, to assess technology requirements and engineering problems of large wind turbines. The machine became operational in October 1975 and has demonstrated successful operation in all of its design modes. During the course of its operations the machine has generated a wealth of experimental data and has served as a prototype developmental test bed for the Mod-OA operational wind turbines which are currently used on utility networks. This paper describes the mechanical and control systems as they evolved in operational tests and describes some of the experience with various systems in the downwind rotor configuration. (Author)

A79-10235 * **DOE/NASA Mod-OA wind turbine performance.** T. R. Richards and H. E. Neustadter (NASA, Lewis Research Center, Cleveland, Ohio). In: Intersociety Energy Conversion Engineering Conference, 13th, San Diego, Calif., August 20-25, 1978, Proceedings, Volume 3. (A79-10001 01-44) Warrendale, Pa., Society of Automotive Engineers, Inc., 1978, p. 2060-2063. 11 refs.

The NASA Lewis Research Center has designed, built, and is operating a 200-kW wind turbine (designated the Mod-OA 1) at Clayton, New Mexico. This paper compares the measured power-vs-speed performance of the Mod-OA 1 with predictions made using the PROP code. It is found that the actual performance closely matches predictions. B.J.

A79-10241 * **SIMWEST - A simulation model for wind energy storage systems.** R. W. Edsinger, A. W. Warren (Boeing Computer Services, Inc., Seattle, Wash.), L. H. Gordon (NASA, Lewis Research Center, Cleveland, Ohio), and G. C. Chang (U.S. Department of Energy, Washington, D.C.). In: Intersociety Energy Conversion Engineering Conference, 13th, San Diego, Calif., August 20-25, 1978, Proceedings, Volume 3. (A79-10001 01-44) Warrendale, Pa., Society of Automotive Engineers, Inc., 1978, p. 2108-2114.

This paper describes a comprehensive and efficient computer program for the modeling of wind energy systems with storage. The level of detail of SIMWEST (Simulation Model for Wind Energy Storage) is consistent with evaluating the economic feasibility as well as the general performance of wind energy systems with energy storage options. The software package consists of two basic programs and a library of system, environmental, and control components. The first program is a precompiler which allows the library components to be put together in building block form. The second program performs the technoeconomic system analysis with the required input/output, and the integration of system dynamics. An example of the application of the SIMWEST program to a current 100 kW wind energy storage system is given. (Author)

A79-11824 * Factors affecting the open-circuit voltage and electrode kinetics of some iron/titanium/redox flow cells. M. A. Reid and R. F. Gahn (NASA, Lewis Research Center, Cleveland, Ohio). In: Symposium on Electrode Materials and Processes for Energy Conversion and Storage, Philadelphia, Pa., May 9-12, 1977, Proceedings. (A79-11776 02-25) Princeton, N.J., Electrochemical Society, Inc., 1977, p. 732-749. 10 refs. Contract No. E(49-28)-1002.

The effect of acid concentration on the performance of the iron-titanium redox flow cell was studied. When the acidity was increased, open-circuit voltages decreased on the titanium side but load voltages increased due to decreased polarization. The best load voltage occurs when there is high acidity on the titanium side coupled with low acidity on the iron side, but such cells show voltage losses with repeated cycling because of the diffusion of acid through the membrane. No membrane tested has been found capable of maintaining the differences in acidity. Chelating agents show some promise in reducing polarization at the Ti electrode and thus improving energy efficiency. M.L.

A79-13098 * # Diminide thermionic energy conversion with lanthanum-hexaboride electrodes. E. W. Kroeger, V. L. Bair, and J. F. Morris (NASA, Lewis Research Center, Cleveland, Ohio). *Institute of Electrical and Electronics Engineers, International Conference on Plasma Science, Monterey, Calif., May 15-18, 1978, Paper*. 17 p. 41 refs.

This paper presents thermionic conversion data obtained from a variable-gap cesium diminide with a hot-pressed, sintered lanthanum-hexaboride emitter and an arc-melted lanthanum-hexaboride collector. Performance curves cover a range of temperatures: emitter 1500 to 1700 K, collector 750 to 1000 K, and cesium reservoir 370 to 510 K. Calculated values of emitter and collector work functions and barrier index are also given. (Author)

A79-13099 * # Optimize out-of-core thermionic energy conversion for nuclear electric propulsion. J. F. Morris (NASA, Lewis Research Center, Thermionics and Heat Pipe Section, Cleveland, Ohio). *Institute of Electrical and Electronics Engineers, International Conference on Plasma Science, Monterey, Calif., May 15-18, 1978, Paper*. 14 p. 14 refs.

Thermionic energy conversion (TEC) potentialities for nuclear electric propulsion (NEP) are examined. Considering current designs, their limitations, and risks raises critical questions about the use of TEC for NEP. Apparently a reactor cooled by hotter than 1675 K heat pipes has good potentialities. TEC with higher temperatures and greater power densities than the currently proposed 1650 K, 5-to-6 W/sq cm version offers substantial gains. Other approaches to high-temperature electric isolation appear also promising. A high-power-density, high-temperature TEC for NEP appears, therefore, attainable. It is recommended to optimize out-of-core thermionic energy conversion for nuclear electric propulsion. Although current TEC designs for NEP seem unnecessary compared with Brayton versions, large gains are apparently possible with increased temperatures and greater power densities. G.R.

A79-13867 * # NASA Lewis Research Center photovoltaic application experiments. A. Ratajczak, W. Bifano, J. Maritz, and P. O'Donnell (NASA, Lewis Research Center, Cleveland, Ohio). *American Institute of Aeronautics and Astronautics and Arizona Solar Energy Research Commission, Conference on Solar Energy Technology Status, Phoenix, Ariz., Nov. 27-29, 1978, AIAA Paper 78-1768*. 9 p.

The NASA Lewis Research Center has installed 16 geographically dispersed terrestrial photovoltaic systems as part of the DOE National Photovoltaic Program. Four additional experiments are in progress. Currently, operating systems are powering refrigerators, a highway warning sign, forest lookout towers, remote weather stations, a water chiller and insect survey traps. Experiments in progress include the world's first village power system, an air pollution monitor and seismic sensors. Under a separate activity,

funded by the U.S. Agency for International Development, a PV-powered water pump and grain grinder is being prepared for an African village. System descriptions and status are included in this report. (Author)

A79-14947 * # Fuel cell on-site integrated energy system parametric analysis of a residential complex. S. N. Simons (NASA, Lewis Research Center, Cleveland, Ohio). *U.S. Department of Energy, Fuel Cell Workshop, Sarasota, Fla., Nov. 14-17, 1977, Paper*. 24 p. 7 refs.

The use of phosphoric acid fuel cell powerplant to provide all the electricity required by an 81-unit garden apartment complex is studied. Byproduct heat is recovered and provides some of the heat required by the complex. The onsite integrated energy system contains energy conversion equipment including combinations of compression and absorption chillers, heat pumps, electric resistance heaters, and thermal storage. The annual fuel requirement for several onsite integrated energy systems as well as the fuel cell breakeven cost for one specific system were calculated. It is found that electrical efficiency cannot be traded off against thermal efficiency without paying a penalty in system efficiency. M.L.

A79-15574 * Control of wind turbine generators connected to power systems. H. H. Hwang, H. V. Mozeico (Hawaii, University, Honolulu, Hawaii), and L. J. Gilbert (NASA, Lewis Research Center, Cleveland, Ohio). In: Power system control and protection, New York, Academic Press, Inc., 1978, p. 239-259. 16 refs. Research supported by the Hawaii Natural Energy Institute and NASA.

A unique simulation model based on a Mode-O wind turbine is developed for simulating both speed and power control. An analytical representation for a wind turbine that employs blade pitch angle feedback control is presented, and a mathematical model is formulated. For Mode-O serving as a practical case study, results of a computer simulation of the model as applied to the problems of synchronization and dynamic stability are provided. It is shown that the speed and output of a wind turbine can be satisfactorily controlled within reasonable limits by employing the existing blade pitch control system under specified conditions. For power control, an additional excitation control is required so that the terminal voltage, output power factor, and armature current can be held within narrow limits. As a result, the variation of torque angle is limited even if speed control is not implemented simultaneously with power control. Design features of the ERDA/NASA 100-kW Mode-O wind turbine are included. S.D.

A79-15881 * Large wind turbine generators. R. L. Thomas and R. M. Donovan (NASA, Lewis Research Center, Cleveland, Ohio). In: Energy technology V: Challenges to technology. Proceedings of the Fifth Conference, Washington, D.C., February 27-March 1, 1978. (A79-15879 04-44) Washington, D.C., Government Institutes, Inc., 1978, p. 64-82. 17 refs.

The large wind turbine portion of the Federal Wind Energy Program consists of two major project efforts: (1) the Mod-0 test bed project for supporting research technology, and (2) the large experimental wind turbines for electric utility applications. The Mod-0 has met its primary objective of providing the entire wind energy program with early operations and performance data. The large experimental wind turbines to be tested in utility applications include three of the Mod-0A (200 kW) type, one Mod-1 (2000 kW), and possibly several of the Mod-2 (2500 kW) designs. This paper presents a description of these wind turbine systems, their programmatic status, and a summary of their potential costs. B.J.

A79-20828 * **Wind-turbine-generator rotor-blade concepts with low-cost potential.** T. L. Sullivan, T. P. Cahill (NASA, Lewis Research Center, Cleveland, Ohio), D. G. Critfee, Jr. (NASA, Lewis Research Center, Cleveland, Ohio; United Technologies Corp., Hamilton Standard Div., Windsor Locks, Conn.), and H. W. Gewehr (NASA, Lewis Research Center, Cleveland, Ohio; Kaman Aerospace Corp., Bloomfield, Conn.). In: Selective application of materials for products and energy; Proceedings of the Twenty-third National Symposium and Exhibition, Anaheim, Calif., May 2-4, 1978. (A79-20801 07-23) Azusa, Calif., Society for the Advancement of Material and Process Engineering, 1978, p. 428-456.

Four processes for producing blades are examined. Two use filament winding techniques and two involve filling a mold or form to produce all or part of a blade. The processes are described and a comparison is made of costs, material properties, designs and free vibration characteristics. Conclusions are made regarding the feasibility of each process to produce low-cost, structurally adequate blades.

(Author)

A79-20829 * **An operating 200 kW horizontal axis wind turbine.** C. L. Hunnicutt (Lockheed Aircraft Service Co., Ontario, Calif.), B. Linscott, and R. A. Wolf (NASA, Lewis Research Center, Cleveland, Ohio). In: Selective application of materials for products and energy; Proceedings of the Twenty-third National Symposium and Exhibition, Anaheim, Calif., May 2-4, 1978. (A79-20801 07-23) Azusa, Calif., Society for the Advancement of Material and Process Engineering, 1978, p. 457-478.

Output from the 200 kilowatt machine will be enough to meet the power requirements of about 60 families. The experimental wind turbine generator (WTG) is a two-bladed, horizontal axis, rotor system driving a synchronous electric generator through a step-up gear box located within a nacelle. The nacelle is mounted on top of a 100-foot tower with the rotor located downwind from the tower. The 200 kilowatt rated power output of the wind turbine is achieved at a turbine rotor speed of 40 rpm and a rated wind speed of 18.3 mph. The rated wind speed is defined as the lowest wind speed at which full power is achieved. Attention is given to operational details, aspects of blade design, blade fabrication, the use of strain gages, questions of aeroelastic stability, and an early analysis of test data.

G.R.

A79-21300 * **Thermal storage for industrial process and reject heat.** R. A. Duschka and W. J. Masica (NASA, Lewis Research Center, Cleveland, Ohio). *U.S. Department of Energy, Conference on Waste Heat Management and Utilization, 2nd, Miami Beach, Fla., Dec. 4-6, 1978, Paper, 12 p. 7 refs.* Contract No. EC-77 A-31-1034.

Industrial production uses about 40% of the total energy consumed in the United States. The major share of this is derived from fossil fuel. Potential savings of scarce fuel is possible through the use of thermal energy storage (TES) of reject or process heat for subsequent use. Results of study contracts awarded by the Department of Energy (DOE) and managed by the NASA Lewis Research Center have identified three especially significant industries where high temperature TES appears attractive: paper and pulp, iron and steel, and cement. Potential annual fuel savings with large scale implementation of near-term TES systems for these three industries is nearly 9 million bbl of oil.

(Author)

A79-21302 * **Microprocessor control of a wind turbine generator.** A. J. Gnecco and G. T. Whitehead (NASA, Lewis Research Center, Cleveland, Ohio). *Institute of Electrical and Electronics Engineers, Conference on Industrial Applications of Microprocessors, Philadelphia, Pa. Mar. 20-22, 1978, Paper, 15 p.* Contract No. E(49-26) 1028.

This paper describes a microprocessor based system used to control the unattended operation of a wind turbine generator. The turbine and its microcomputer system are fully described with special emphasis on the wide variety of tasks performed by the microprocessor for the safe and efficient operation of the turbine.

The flexibility, cost and reliability of the microprocessor were major factors in its selection.

(Author)

A79-26131 * **Photovoltaic power systems for rural areas of developing countries.** L. Rosenblum, W. J. Bifano, G. F. Hein, and A. F. Ratajczak (NASA, Lewis Research Center, Cleveland, Ohio). *United Nations, International Seminar on Solar Energy, Tokyo, Japan, Feb. 5-10, 1979, Paper, 18 p. 9 refs.*

Photovoltaic (PV) applications for rural areas of underdeveloped countries are discussed in relation to PV system technology, reliability, and present and projected cost. The information presented is derived mainly from NASA, Lewis Research Center experience with PV systems deployed with a variety of users for applications relevant to LDCs. A detailed description of two village power systems is included. Energy cost comparisons are presented for PV systems versus alternative energy sources. It is concluded, based on present PV system technology, reliability and cost that photovoltaics provides a realistic energy option for LDCs in both the near and far-term.

(Author)

A79-30554 * **Benefits of solar/fossil hybrid gas turbine systems.** H. S. Bloomfield (NASA, Lewis Research Center, Cleveland, Ohio). *American Society of Mechanical Engineers, Gas Turbine Conference and Exhibit and Solar Energy Conference, San Diego, Calif., Mar. 12-15, 1979, Paper 79-GT-35, 16 p.*

The potential benefits of solar/fossil hybrid gas turbine power systems were assessed. Both retrofit and new systems were considered from the aspects of cost of electricity, fuel conservation, operational mode, technology requirements, and fuels flexibility. Hybrid retrofit (repowering) of existing combustion (simple Brayton cycle) turbines can provide near-term fuel savings and solar experience, while new and advanced recuperated or combined cycle systems may be an attractive fuel saving and economically competitive vehicle to transition from today's gas and oil-fired powerplants to other more abundant fuels.

(Author)

A79-38191 * **Redox flow cell energy storage systems.** L. H. Thaller (NASA, Lewis Research Center, Solar and Electrochemistry Div., Cleveland, Ohio). *American Institute of Aeronautics and Astronautics, Terrestrial Energy Systems Conference, Orlando, Fla., June 4-6, 1979, Paper 79-0989, 9 p. 7 refs.* Contract No. E(49-28) 1002.

The redox flow cell energy storage system being developed by NASA for use in remote power systems and distributed storage installations for electric utilities is presented. The system under consideration is an electrochemical storage device which utilizes the oxidation and reduction of two fully soluble redox couples (acidified chloride solutions of chromium and iron) at active electrode materials separated by a highly selective ion exchange membrane. The reactants are contained in large storage tanks and pumped through a stack of redox flow cells where the electrochemical reactions take place at porous carbon felt electrodes. Redox equipment has allowed the incorporation of state of charge readout, stack voltage control and system capacity maintenance (re-balance) devices to regulate cells in a stack jointly. A 200 W, 12 V system with a capacity of about 400 Wh has been constructed, and a 2 kW, 10kWh system is planned.

A L W

A79-38192 * **Analysis of a fuel cell on site integrated energy system for a residential complex.** S. N. Simons (NASA, Lewis Research Center, Fuel Cell Projects Office, Cleveland, Ohio) and W. L. Maag (Solar Energy Products Co., Avon Lake, Ohio). *American Institute of Aeronautics and Astronautics, Terrestrial Energy Systems Conference, Orlando, Fla., June 4-6, 1979, Paper 79-0990, 10 p. 8 refs.*

The energy use and costs of the on site integrated energy system (OSIES) which provides electric power from an on site power plant and recovers heat that would normally be rejected to the environ-

ment is compared to a conventional system purchasing electricity from a utility and a phosphoric acid fuel cell powered system. The analysis showed that for a 500-unit apartment complex a fuel OS/IES would be about 10% more energy conservative in terms of total coal consumption than a diesel OS/IES system or a conventional system. The fuel cell OS/IES capital costs could be 30 to 55% greater than the diesel OS/IES capital costs for the same life cycle costs. The life cycle cost of a fuel cell OS/IES would be lower than that for a conventional system as long as the cost of electricity is greater than \$0.05 to \$0.065/kWh. An analysis of several parametric combinations of fuel cell power plant and state-of-art energy recovery systems and annual fuel requirement calculations for four locations were made. It was shown that OS/IES component choices are a major factor in fuel consumption, with the least efficient system using 25% more fuel than the most efficient. Central air conditioning and heat pumps result in minimum fuel consumption while individual air conditioning units increase it, and in general the fuel cell of highest electrical efficiency has the lowest fuel consumption.

A.T.

A79-38885 * # Wind turbines for electric utilities - Development status and economics. J. R. Ramler and R. M. Donovan (NASA, Lewis Research Center, Cleveland, Ohio). *American Institute of Aeronautics and Astronautics, Terrestrial Energy Systems Conference, Orlando, Fla., June 4-6, 1979, Paper 79-0965*. 19 p. 15 refs.

The technology and economics of the large, horizontal-axis wind turbines currently in the Federal Wind Energy Program are presented. Wind turbine technology advancements made in the last several years are discussed. It is shown that, based on current projections of the costs of these machines when produced in quantity, they should be attractive for utility application. The cost of electricity (COE) produced at the turbine is shown to be a strong function of the mean wind speed at the installation site. The breakeven COE as a 'fuel saver' is discussed and the COE range that would be generally attractive to utilities is indicated. (Author)

A79-40398 * # Ultraviolet irradiation at elevated temperatures and thermal cycling in vacuum of FEP-A covered silicon solar cells. J. D. Broder and S. J. Marsik (NASA, Lewis Research Center, Cleveland, Ohio). In: *Photovoltaic Specialists Conference, 13th, Washington, D.C., June 5-8, 1978, Conference Record*. (A79-40881 17 44) New York, Institute of Electrical and Electronics Engineers, Inc., 1978, p. 122-126. 9 refs.

Silicon solar cells covered with FEP-A were irradiated in vacuum with ultraviolet light and then subjected to thermal cycling. These accelerated laboratory conditions are believed to be equivalent to those experienced by FEP-A covered cells on the ATS-6 spacecraft and the results indicate a probable mechanism for the faster degradation of the FEP-A covered cells. Heat bonded FEP-A covers apparently embrittle when exposed to four months of space UV radiation at elevated temperatures, and crack when subjected to thermal cycling during the eclipse period. Low energy proton radiation can then penetrate to the junction of the cell causing degradation of the open circuit voltage and maximum power to occur. An alternate method of application of FEP-A, such as with adhesives, may prevent such cracking. V.T.

A79-41022 * # Endurance testing of first generation /Block I/ commercial solar cell modules. E. Anagnostou and A. F. Forestieri (NASA, Lewis Research Center, Cleveland, Ohio). In: *Photovoltaic Specialists Conference, 13th, Washington, D.C., June 5-8, 1978, Conference Record*. (A79-40881 17 44) New York, Institute of Electrical and Electronics Engineers, Inc., 1978, p. 843-846. Contract No. E(49-26) 1022

NASA LeRC has conducted outdoor endurance tests on modules commercially produced as part of the 46 kW purchase of first generation (Block I) modules by the JPL Low Cost Silicon Solar Array Project. Block I modules from four manufacturers were installed at commercial testing sites in Florida, Puerto Rico and Arizona and at noncommercial sites in Cleveland, Ohio. The

conditions endured by these modules included hot and dry, hot and humid, tropical rain forest, sea-air, urban industrial and urban clean; exposures were for periods up to one year. Test results are presented and discussed. B.J.

A79-41023 * # Variation of solar cell sensitivity and solar radiation on tilted surfaces. T. M. Klucher (NASA, Lewis Research Center, Cleveland, Ohio). In: *Photovoltaic Specialists Conference, 13th, Washington, D.C., June 5-8, 1978, Conference Record*. (A79-40881 17 44) New York, Institute of Electrical and Electronics Engineers, Inc., 1978, p. 847-852. Contract No. E(49-26) 1022.

An empirical study was performed (1) to evaluate the validity of various insolation models used to compute solar radiation incident on tilted surfaces from global data measured on horizontal surfaces and (2) to determine the variation of solar cell sensitivity to solar radiation over a wide range of atmospheric condition. Evaluation of the insolation data indicates that the isotropic sky model of Liu and Jordan underestimates the amount of solar radiation falling on tilted surfaces by as much as 10%. An anisotropic-clear-sky model proposed by Temps and Coulson was also evaluated and found to be deficient under cloudy conditions. A new model, formulated herein, reduced the deviations between measured and predicted insolation to less than 3%. Evaluation of solar cell sensitivity data indicates small change (2-3%) in sensitivity from winter to summer for tilted cells. The feasibility of using such global data as a means for calibrating terrestrial solar cells as done by Treble is discussed. (Author)

A79-41047 * # An inverter/controller subsystem optimized for photovoltaic applications. R. L. Pickrell, W. C. Merrill (NASA, Lewis Research Center, Cleveland, Ohio), and G. O'Sullivan (Abacus Controls, Inc., Somerville, N.J.). In: *Photovoltaic Specialists Conference, 13th, Washington, D.C., June 5-8, 1978, Conference Record*. (A79-40881 17 44) New York, Institute of Electrical and Electronics Engineers, Inc., 1978, p. 984-991. 5 refs.

Conversion of solar array dc power to ac power stimulated the specification, design, and simulation testing of an inverter/controller subsystem tailored to the photovoltaic power source characteristics. This paper discusses the optimization of the inverter/controller design as part of an overall Photovoltaic Power System (PPS) designed for maximum energy extraction from the solar array. The special design requirements for the inverter/controller include: (1) a power system controller (PSC) to control continuously the solar array operating point at the maximum power level based on variable solar insolation and cell temperatures; and (2) an inverter designed for high efficiency at rated load and low losses at light loadings to conserve energy. It must be capable of operating connected to the utility line at a level set by an external controller (PSC). (Author)

A79-41089 * # Design and fabrication of a photovoltaic power system for the Papago Indian Village of Schuchuli/Gunsight/, Arizona. W. J. Bifano, A. F. Ratajczak, and W. J. Ice (NASA, Lewis Research Center, Cleveland, Ohio). In: *Photovoltaic Specialists Conference, 13th, Washington, D.C., June 5-8, 1978, Conference Record*. (A79-40881 17 44) New York, Institute of Electrical and Electronics Engineers, Inc., 1978, p. 1262-1267.

A79-41091 * # Description and status of NASA/LeRC/DOE photovoltaic applications systems experiments. A. F. Ratajczak (NASA, Lewis Research Center, Cleveland, Ohio). In: *Photovoltaic Specialists Conference, 13th, Washington, D.C., June 5-8, 1978, Conference Record*. (A79-40881 17 44) New York, Institute of Electrical and Electronics Engineers, Inc., 1978, p. 1272-1277. Contract No. E(49-26) 1022.

In its role of supporting the DOE Photovoltaic Program, the NASA Lewis Research Center has designed, fabricated and installed 16 geographically dispersed photovoltaic systems. These systems are powering a refrigerator, highway warning sign, forest lookout towers, remote weather stations, a water chiller at a visitor center, and insect

survey traps. Each of these systems is described in terms of load requirements, solar array and battery size, and instrumentation and controls. Operational experience is described and present status is given for each system. The P/V power systems have proven to be highly reliable with almost no problems with modules and very few problems overall. (Author)

A79-41098 * # Photon degradation effects in terrestrial solar cells. V. G. Weizer, H. W. Brandhorst, J. D. Broder, R. E. Hart, and J. H. Lamneck (NASA, Lewis Research Center, Cleveland, Ohio). In: Photovoltaic Specialists Conference, 13th, Washington, D.C., June 5-8, 1973, Conference Record. (A79-40881 17-44) New York, Institute of Electrical and Electronics Engineers, Inc., 1978, p. 1327-1332. 1C refs.

A certain type of photon degradation effect has been observed experimentally in n(+)/p solar cells. It is found that this effect is caused by a recombination center, the formation of which requires the simultaneous presence of a lattice defect and a silver atom or complex of atoms. The center is electrically active in its equilibrium state; the energy level of the inactive center is located in the band gap, 0.37 eV below the conduction band. Conversion to an active recombination center can be brought about either by raising the minority carrier quasi-Fermi level to coincide with the position of the latent center level in the band gap or by the direct excitation of electrons from the valence band to the latent center level. Photon degradation can be prevented either by preventing the introduction of silver through the use of a clean diffusion system and clean initial material or by eliminating lattice damage through sufficient surface material removal prior to diffusion while at the same time restricting diffusion temperatures to 875 C or below. B.J.

A79-42545 * Photon-degradation effects in terrestrial silicon solar cells. V. G. Weizer, H. W. Brandhorst, J. D. Broder, R. E. Hart, and J. H. Lamneck (NASA, Lewis Research Center, Cleveland, Ohio). *Journal of Applied Physics*, vol. 50 June 1979, p. 4443-4449. 10 refs. Contract No. EX 76-A-29 1002.

The effect of instability in terrestrial solar cells and identification of mechanisms involved are presented. The effect is similar to photon-induced degradation in radiation-damaged space solar cells, with reduction in cell output in n(+)/p cells upon exposure to illumination or upon the application of a sufficiently high forward bias. It was found that the photon-degradation effect is caused by a recombination center identified as a complex of a lattice defect and a silver atom or cluster of atoms. The center is electrically inactive in its ground state but can be activated by raising the minority-carrier quasi-Fermi level to coincide with the position of the latent-center level in the band gap, or by direct excitation of electrons from the valence band to the latent-center level. Photon degradation can be prevented by avoiding the introduction of silver through the use of a clean diffusion system and clean initial material, or by eliminating lattice damage by sufficient surface material removal prior to diffusion and restricting diffusion temperatures to 875 C or below. A.T.

A79-44225 * # Energy and cost savings results for advanced technology systems from the Cogeneration Technology Alternatives Study (CTAS). G. D. Sagerman, G. J. Barna, and R. K. Burns (NASA, Lewis Research Center, Cleveland, Ohio). *American Institute of Aeronautics and Astronautics, Terrestrial Energy Systems Conference, Orlando, Fla June 4-6, 1979, Paper 79-1000*. 20 p. Contract No. EC-77-A 31 1062.

The Cogeneration Technology Alternatives Study (CTAS), a program undertaken to identify the most attractive advanced energy conversion systems for industrial cogeneration applications in the 1985-2000 time period, is described, and preliminary results are presented. Two cogeneration options are included in the analysis: a topping application, in which fuel is input to the energy conversion system which generates electricity and waste heat from the conversion system is used to provide heat to the process, and a bottoming application, in which fuel is burned to provide high temperature

process heat and waste heat from the process is used as thermal input to the energy conversion system which generates energy. Steam turbines, open and closed cycle gas turbines, combined cycles, diesel engines, Stirling engines, phosphoric acid and molten carbonate fuel cells and thermionics are examined. Expected plant level energy savings, annual energy cost savings, and other results of the economic analysis are given, and the sensitivity of these results to the assumptions concerning fuel prices, price of purchased electricity and the potential effects of regional energy use characteristics is discussed. C.K.D.

A79-46527 * # Large horizontal axis wind turbine development. W. H. Robbins and R. L. Thomas (NASA, Lewis Research Center, Cleveland, Ohio). In: Workshop on Economic and Operational Requirements and Status of Large Scale Wind Systems, Monterey, Calif., March 28-30, 1979, Proceedings. (A79-46526 20-44) Santa Cruz, Calif., Altas Corp., 1979, p. 50-70; Discussion, p. 71, 72.

The paper presents an overview of the NASA activities in large horizontal axis wind turbine development. First generation technology large wind turbines (Mod-0A, Mod-1) have been designed and are in operation at selected utility sites. Second generation machines (Mod-2) are scheduled to begin operations on a utility site in 1980. These machines are estimated to generate electricity at less than 4 cents/kWh when manufactured in modest production rates. Meanwhile, plans are being made to continue developing wind turbines which can meet the cost goals of 2 to 3 cents/kWh. V.T.

A79-46537 * # Utility operational experience on the NASA/DOE Mod-0A 200 kW Wind Turbine. J. C. Glasgow and W. H. Robbins (NASA, Lewis Research Center, Cleveland, Ohio). In: Workshop on Economic and Operational Requirements and Status of Large Scale Wind Systems, Monterey, Calif., March 28-30, 1979, Proceedings. (A79-46526 20-44) Santa Cruz, Calif., Altas Corp., 1979, p. 215-245; Discussion, p. 246-247. 6 refs.

The Mod-0A 200 kW Wind Turbine was designed and fabricated by the Lewis Research Center of the NASA under the direction of the U.S. Department of Energy. The project is a part of the Federal Wind Energy Program and is designed to obtain early wind turbine operation and performance data while gaining initial experience in the operation of large, horizontal axis wind turbines in typical utility environments. On March 6, 1978, the Mod-0A wind turbine was turned over to the Town of Clayton Light and Water Plant, Clayton, NM, for utility operation and on December 31, 1978 the machine had completed ten months of utility operation. This paper describes the machine and documents the recent operational experience at Clayton, NM. (Author)

A79-46547 * # Lewis Research Center studies of multiple large wind turbine generators on a utility network. L. J. Gilbert (NASA, Lewis Research Center, Cleveland, Ohio) and D. M. Triesenberg (Purdue University, West Lafayette, Ind.). In: Workshop on Economic and Operational Requirements and Status of Large Scale Wind Systems, Monterey, Calif., March 28-30, 1979, Proceedings. (A79-46526 20-44) Santa Cruz, Calif., Altas Corp., 1979, p. 388-402. 5 refs.

A NASA-Lewis program to study the anticipated performance of a wind turbine generator farm on an electric utility network is surveyed. The paper describes the approach of the Lewis Wind Energy Project Office to developing analysis capabilities in the area of wind turbine generator-utility network computer simulations. Attention is given to areas such as, the Lewis Purdue hybrid simulation, an independent stability study, DOE multiunit plant study, and the WEST simulator. Also covered are the Lewis mod-2 simulation including analog simulation of a two wind turbine system and comparison with Boeing simulation results, and gust response of a two machine model. Finally future work to be done is noted and it is concluded that the study shows little interaction between the generators and between the generators and the bus. M.E.P.

A79-47651 * # **A mobile apparatus for solar collector testing.** G. B. Hotchkiss (Texas Instruments, Inc., Dallas, Tex.), F. F. Simon (NASA, Lewis Research Center, Cleveland, Ohio), and L. C. Burmeister (Kansas, University, Lawrence, Kan.). *American Society of Mechanical Engineers, Design Engineering Conference and Show, Chicago, Ill., May 7-10, 1979, Paper 79-DE-5.* 6 p. 14 refs. Grant No. NSG 3087.

The design, construction, and operation of a mobile apparatus for solar collector testing (MASCOT) is described. The MASCOT is a self-contained test unit costing about \$10,000 whose only external requirement for operation is electrical power and which is capable of testing two water-cooled flat-plate solar collectors simultaneously. The MASCOT is small enough and light enough to be transported to any geographical site for outdoor tests at the location of collector usage. It has been used in both indoor solar simulator tests and outdoor tests. (Author)

A79-49527 * # **Reduction of particulate carryover from a pressurized fluidized bed.** R. W. Patch (NASA, Lewis Research Center, Cleveland, Ohio). *Symposium on the Transfer and Utilization of Particulate Control Technology, 2nd, Denver, Colo., July 23-27, 1979. Paper.* 20 p.

A bench-scale pressurized fluidized bed combustor (PFBC) constructed with a conical shape to reduce the particulate carryover is examined. The combustor was fed coal and limestone with the coal to air ratio varying from 0.033 to 0.098 (air lean) and the coal to limestone ratio varying from 0.06 to 0.36. Two cone angles were used and it is shown that the average particulate carryover of 2.5 grains/SCF is appreciably less than cylindrical fluidized bed combustors. In addition the carryover was correlated by multiple regression analysis to yield the dependence on bed depth and hence the collection efficiency, which was 20%. Finally, a comparison with a model indicated that the exhaust port may be below the transport disengaging height for most of the tests showing that further improvements could be achieved by increasing the freeboard height of the exhaust port above the bed. M.E.P.

A79-51809 * # **Commercial phosphoric acid fuel cell system technology development.** P. R. Prokopius, M. Warshaw, S. N. Simons, and R. B. King (NASA, Lewis Research Center, Fuel Cell Projects Office, Cleveland, Ohio). In: *Intersociety Energy Conversion Engineering Conference, 14th, Boston, Mass., August 5-10, 1979. Proceedings, Volume 1.* (A79-51726 23-44) Washington, D.C., American Chemical Society, 1979, p. 538-543. 6 refs.

A review of the current commercial phosphoric acid fuel cell system technology development efforts is presented. In both the electric utility and on-site integrated energy system applications, reducing cost and increasing reliability are the technology drivers at this time. The longstanding barrier to the attainment of these goals, which manifests itself in a number of ways, has been materials. The differences in approach among the three major participants (United Technologies Corporation (UTC), Westinghouse Electric Corporation/Energy Research Corporation (ERC), and Engelhard Industries) and their unique technological features, including electrodes, matrices, intercell cooling, bipolar separator plates, electrolyte management, fuel selection and system design philosophy are discussed. (Author)

A79-51837 * # **Recent advances in Redox flow cell storage systems.** L. H. Thaller (NASA, Lewis Research Center, Cleveland, Ohio). In: *Intersociety Energy Conversion Engineering Conference, 14th, Boston, Mass., August 5-10, 1979. Proceedings, Volume 1.* (A79-51726 23-44) Washington, D.C., American Chemical Society, 1979, p. 715-719. 8 refs.

Attention is given to recent data pertaining to flow cell storage system-related features as well as the state of Redox membrane technology. In addition, the state of the technology as it relates to the two application areas of storage for photovoltaic/wind and distributed energy storage for electrical utility applications is addressed. Also covered are the cost and life advantages of Redox

systems as well as a discussion of such cells as the open circuit voltage cell, the rebalance cell, and the trim cell. Finally, it is concluded that the main thrust of membrane development will be to reduce the interaction between the dilute complex of iron in the ferric state since this is the major factor in membrane area resistivity. M.E.P.

A79-53491 * **Evaluation of models to predict insolation on tilted surfaces.** T. M. Klucher (NASA, Lewis Research Center, Cleveland, Ohio). *Solar Energy*, vol. 23, no. 2, 1979, p. 111-114. 8 refs.

An empirical study was performed to evaluate the validity of various insolation models which employ either an isotropic or an anisotropic distribution approximation for sky light when predicting insolation on tilted surfaces. Data sets of measured hourly insolation values were obtained over a 6-month period using pyranometers which received diffuse and total solar radiation on a horizontal plane and total radiation on surfaces tilted toward the equator at 37 degrees and 60 degrees angles above the horizon. Data on the horizontal surfaces were used in the insolation models to predict insolation on the tilted surface; comparisons of measured vs calculated insolation on the tilted surface were examined to test the validity of the sky light approximations. It was found that the Liu-Jordan isotropic distribution model provides a good fit to empirical data under overcast skies but underestimates the amount of solar radiation incident on tilted surfaces under clear and partly cloudy conditions. (Author)

N79-10625*# **United Technologies Corp., Windsor Locks, Conn. DESIGN, FABRICATION, AND TEST OF A COMPOSITE MATERIAL WIND TURBINE ROTOR BLADE. Final Report** D. G. Griffie, Jr., R. E. Gustafson, and E. R. More. Nov 1977. 185 p. refs. (Contracts NAS3-19773, E(49-26)-1028) (NASA-CR-135389, DOE/NASA/9773-78/1, HSER-7383) Avail. NTIS HC A09/MF A01 CSCL 10A

The aerodynamic design, structural design, fabrication, and structural testing is described for a 60 foot long filament wound, fiberglass/epoxy resin matrix wind turbine rotor blade for a 125 foot diameter, 100 kW wind energy conversion system. One blade was fabricated which met all aerodynamic shape requirements and was structurally capable of operating under all specified design conditions. The feasibility of filament winding large rotor blades was demonstrated. Author

N79-10626*# **AiResearch Mfg Co, Phoenix, Ariz. MINI-BRU/BIPS 1300 W. DYNAMIC POWER CONVERSION SYSTEM DEVELOPMENT: EXECUTIVE SUMMARY** Sep 1978. 25 p. refs. (Contract NAS3-18517) (NASA-CR-159440, AiResearch-31 2937) Avail. NTIS HC A02/MF A01 CSCL 10B

The status of the Brayton Isotope Power System (BIPS) is summarized. A 1200 watt sub-e ground development unit was built and tested in a 0.000010 torr vacuum environment. Performance mapping and 1000 hours of proof of concept system testing were completed. Specific components, primarily turbocompressor/alternator and recuperator performed according to predictions, thus achieving the design goal of 25 percent net power conversion efficiency. The system was fabricated from superalloy (Hastelloy-X and Waspaloy) thus placing it entirely within current state-of-the-art technology. The system could be flyable in the early 1980's pending flight qualification. J.M.S.

N79-11473* Rocket Research Corp., Redmond, Wash
APPLICATIONS OF THERMAL ENERGY STORAGE TO PROCESS HEAT AND WASTE HEAT RECOVERY IN THE IRON AND STEEL INDUSTRY Final Report, Sep. 1977 - Sep. 1978

Lincoln B. Katter and Daniel J. Peterson Oct. 1978 136 p
refs. Sponsored by NASA
(Contracts EC-77-C-1-5081, EC-77-A-31-1034)
(NASA CR-159397, RRC-78-R-607, CONS/5081-1 Avail NTIS HC A07/MF A01 CSCL 10A

The system identified operates from the primary arc furnace evacuation system as a heat source. Energy from the fume stream is stored as sensible energy in a solid medium (packed bed). A steam-driven turbine is arranged to generate power for peak shaving. A parametric design approach is presented since the overall system design, at optimum payback is strongly dependent upon the nature of the electric pricing structure. The scope of the project was limited to consideration of available technology so that industry wide application could be achieved by 1985. A search of the literature, coupled with interviews with representatives of major steel producers, served as the means whereby the techniques and technologies indicated for the specific site are extrapolated to the industry as a whole and to the 1985 time frame. The conclusion of the study is that by 1985, a national yearly savings of 1.9 million barrels of oil could be realized through recovery of waste heat from primary arc furnace fume gases on an industry-wide basis. Economic studies indicate that the proposed system has a plant payback time of approximately 5 years. LS

N79-11476* AirResearch Mfg. Co., Torrance, Calif
DESIGN AND FABRICATION OF THE MINI-BRAYTON RECUPERATOR (MBR) Final Report, Mar. 1974 - Jul. 1978

J. J. Killackey, R. Graves, and G. Mosinskis Apr. 1978 99 p
refs.
(Contract NAS3-18029)
(NASA CR-159429, AirResearch 78-14972) Avail NTIS HC A05/MF A01 CSCL 10B

Development of a recuperator for a 2.0 kW closed Brayton space power system is described. The plate fin heat exchanger is fabricated entirely from Hastelloy X and is designed for 10 years continuous operation at 1000 K (1300 F) with a Xenon/helium working fluid. Special design provisions assure uniform flow distribution crucial for meeting 0.975 temperature effectiveness. Low cycle fatigue, resulting from repeated startup and shutdown cycles, was identified as the most critical structural design problem. It is predicted that the unit has a minimum fatigue life of 220 cycles. This is in excess of the BIPS requirement of 100 cycles. Heat transfer performance and thermal cycle testing with air, using a prototype unit, verified that all design objectives can be met. Author

N79-12550* Martin Marietta Corp., Denver, Colo
DEVELOPMENT OF SINGLE-CELL PROTECTORS FOR SEALED SILVER-ZINC CELLS Final Report

John W. Lear, Richard L. Donovan, and Mathew S. Imamura Nov. 1978 68 p
refs.
(Contract NAS3-19432)
(NASA CR-159407, MCR-78-571) Avail NTIS HC A04/MF A01 CSCL 10C

Three design approaches to cell-level protection were developed, fabricated, and tested. These systems are referred to as the single-cell protector (SCP), multiplexed cell protector (MCP). To evaluate the systems 18-cell battery packs without cell level control were subjected to cycle life test. A total of five batteries were subjected to simulate synchronous orbit cycling at 40% depth of discharge at 22C. Batteries without cell-level protection failed between 345 and 255 cycles. Cell failure in the cell level protected batteries occurred between 412 and 540. It was determined that the cell-level monitoring and protection is necessary to attain the long cycle life of a AgZn battery. The best method of providing control and protection of the AgZn cells depends on the specific application and capability of the user. Author

N79-12553* United Technologies Corp., East Hartford, Conn.
Power Systems Div.

DEVELOPMENT OF ADVANCED FUEL CELL SYSTEM Final Report, 26 Feb. - 31 Dec. 1976

B. Gitlow, A. F. Meyer, W. F. Bell, and R. E. Martin 6 Jun. 1978 74 p
refs.
(Contract NAS3-19778)
(NASA CR-159443, FCR-0398) Avail NTIS HC A04/MF A01 CSCL 10A

An experimental program was conducted continuing the development effort to improve the weight, life, and performance characteristics of hydrogen-oxygen alkaline fuel cells for advanced power systems. These advanced technology cells operate with passive water removal which contributes to a lower system weight and extended operating life. Endurance evaluation of two single cells and two, two-cell plaques was continued. Three new test articles were fabricated and tested. A single cell completed 7036 hours of endurance testing. This cell incorporated a Fybex matrix, hybrid-frame, PPF anode, and a 90 Au/10 Pt cathode. This configuration was developed to extend cell life. Two cell plaques with dedicated flow fields and manifolds for all fluids did not exhibit the cell-to-cell electrolyte transfer that limited the operating life of earlier multicell plaques. Author

N79-12554* General Electric Co., Philadelphia, Pa. Space Div.

MINI-BRAYTON HEAT SOURCE ASSEMBLY DEVELOPMENT Final Report, 27 Jun. 1974 - 1 Oct. 1978

D. Wein and W. F. Zimmerman 1 Nov. 1978 306 p
refs.
(Contract NAS3-18541)
(NASA CR-159447, Doc 78SDS4252) Avail NTIS HC A14/MF A01 CSCL 10A

The work accomplished on the Mini Brayton Heat Source Assembly program is summarized. Required technologies to design, fabricate and assemble components for a high temperature Heat Source Assembly (HSA) which would generate and transfer the thermal energy for a spaceborne Brayton Isotope Power System (BIPS) were developed. BB

N79-13480* Naval Weapons Support Center, Crane, Ind.
BLOCK 2 SOLAR CELL MODULE ENVIRONMENTAL TEST PROGRAM

Kevin L. Holloway Oct. 1978 56 p
refs.
(NASA Order C-1892 D, Contract E(49-26)-1022)
(NASA CR-153393, DOE/NASA/1892-78/1, WQEC/C-78-224) Avail NTIS HC A04/MF A01 CSCL 10A

Environmental tests were performed on 76 solar cell modules produced by four different manufacturers. The following tests were performed: (1) 28 day temperature and humidity, (2) rain and icing, (3) salt fog, (4) sand and dust, (5) vacuum/steam/pressure, (6) fungus, (7) temperature/altitude, and (8) thermal shock. Environmental testing of the solar cell modules produced cracked cells, cracked encapsulant and encapsulant delaminations on various modules. In addition, there was some minor cell and frame corrosion. GY

N79-13496* General Electric Co., Santa Barbara, Calif
TEMPO

CONCEPTUAL DESIGN OF THERMAL ENERGY STORAGE SYSTEMS FOR NEAR TERM ELECTRIC UTILITY APPLICATIONS VOLUME 1: SCREENING OF CONCEPTS

W. Hausz, B. J. Berkowitz, and R. C. Hare Oct. 1978 266 p
Sponsored in part by Electric Power Research Inst. 2 Vol.
(Contracts DEN-3-12, EC-77-A-31-1034)
(NASA CR-159411 Vol. 1, GE78TMP-60 Vol. 1, DOE/NASA/0012-78/1-Vol. 1, EPRI-RP1092-1-Vol. 1) Avail NTIS HC A12/MF A01 CSCL 10C

Over forty thermal energy storage (TES) concepts gathered from the literature and personal contacts were studied for their suitability for the electric utility application of storing energy off-peak discharge during peak hours. Twelve selections were derived from the concepts for screening, they used as storage media high temperature water (HTW), hot oil, molten salts, and packed beds of solids such as rock. HTW required pressure containment by prestressed cast iron or concrete vessels, or lined

underground cavities. Both steam generation from storage and feedwater heating from storage were studied. Four choices were made for further study during the project. Economic comparison by electric utility standard cost practices, and near-term availability (low technical risk) were principal criteria but suitability for utility use, conservation potential, and environmental hazards were considered. Author

N79-13497* General Electric Co. Santa Barbara, Calif. TEMPO.

CONCEPTUAL DESIGN OF THERMAL ENERGY STORAGE SYSTEMS FOR NEAR TERM ELECTRIC UTILITY APPLICATIONS. VOLUME 2: APPENDICES - SCREENING OF CONCEPTS

W Hausz, B J Berkowitz, and R. C. Hare Oct 1978 144 p refs. Sponsored in part by Electric Power Research Inst. 2 Vol

(Contracts DEN-3-12; EC-77-A-31-1034)

(NASA-CR-159411-Vol-2; GE78TMP-60-Vol-2;

DOE/NASA/0012-78/1 Vol-2; EPRI-RP1082-1-Vol-2) Avail NTIS HC A07/MF A01 CSCL 10C

Volume 2 of this 2 volume report is represented. This volume contains three appendices: (1) bibliography and cross references; (2) taxonomy - proponents and sources; and (3) concept definitions. G.Y.

N79-16374* Energy Research Corp., Bethel, Conn. **FABRICATION AND TESTING OF SILVER-HYDROGEN CELLS**

M G Klein Nov 1978 48 p

(Contract NAS3-19780)

(NASA-CR-159431) Avail NTIS HC A03/MF A01 CSCL 10B

The development and life testing of single electrode and multi electrode stacks to optimize the individual components and characterize the performance of a silver hydrogen battery system are described. A NASA developed inorganic separator material was used as the main separator within the cells. Single electrode test cells were cycled at 75% of nominal capacity out through approximately 1 000 cycles in a number of cases where deterioration in performance was observed. This deterioration appears to be a decay in usable capacity of the silver electrode, but the exact mechanism is still unidentified. Twenty ampere-hour boilerplate test cells consisting of a stack of ten silver electrodes and twenty hydrogen electrodes were cycled also at 75% depth of discharge. The oldest stack achieved 522 stable cycles to the end of the program. Weight analysis of light weight cells showed that 50 ampere-hour cells with improved components could be capable of as much as 40 watt hours per pound.

A.R.H.

N79-16375* Energy Research Corp., Bethel, Conn. **FABRICATION AND TESTING OF SILVER-HYDROGEN CELLS**

Daniel J. DeBicari and Allen Charkey Dec 1978 26 p

(Contract NAS3-20805)

(NASA-CR-159490) Avail NTIS HC A03/MF A01 CSCL 10B

Silver electrodes containing various additives were fabricated and tested in single electrode cells in order to improve the electrochemical utilization of sintered silver cathodes in Ag-H₂ aerospace batteries. A standard stack arrangement was used which featured a NASA-developed organic-inorganic separator. All cells were cycled in a regime designed to remove 75% of the cells nominal capacity based on 3.3 gms/AHr Ag utilization. In cases where performance degradation was observed, the main feature mode appeared to be corrosion of either the expanded silver current collector or the connection between the silver electrode and the electrode tab. Promising silver electrodes from single electrode studies were used in the construction of 35 AHr Ag-H₂ cells. Two such cells were constructed and installed in heavy walled pressure vessels for testing. Based on the data obtained from all cells tested during the program, four lightweight 35 AHr cells were fabricated. During acceptance testing these

cells yielded an average gravimetric energy density of 30 WHr/lb A.R.H.

N79-17330* EIC, Inc., Newton, Mass.

FEASIBILITY STUDY FOR A SECONDARY Na/S BATTERY

Final Report, 1 Oct. 1977 - 30 Sep. 1978

K. M. Abraham, R. Schiff, and S. B. Brummer Jan. 1979 65 p

refs

(Contract NAS3-21028)

(NASA-CR-159469) Avail NTIS HC A04/MF A01 CSCL 10C

The feasibility of a moderate temperature Na battery was studied. This battery is to operate at a temperature in the range of 100-150 C. Two kinds of cathode were investigated: (1) a soluble S cathode consisting of a solution of Na₂Sn in an organic solvent and (2) an insoluble S cathode consisting of a transition metal dichalcogenide in contact with a Na⁺/ion conducting electrolyte. Four amide solvents, dimethyl acetamide, diethyl acetamide, N-methyl acetamide and acetamide, were investigated as possible solvents for the soluble S cathode. Results of stability and electrochemical studies using these solvents are presented. The dialkyl substituted amides were found to be superior. Although the alcohol 1,3-cyclohexanediol was found to be stable in the presence of Na₂Sn at 130 C, its Na₂Sn solutions did not appear to have suitable electrochemical properties. J.M.S.

N79-19448* RCA Labs., Princeton, N. J.

EPITAXIAL SOLAR-CELL FABRICATION. PHASE 2

Final Report, 11 Nov. 1974 - 10 Jun. 1977

R. V. Daeillo, P. H. Robinson and H. Kressel Nov. 1977 75 p

refs

(Contract NAS3-19401)

(NASA-CR-135350; PRRL-77-CR-45)

Avail NTIS

HC A04/MF A01 CSCL 10A

Dichlorosilane (SiH₂Cl₂) was used as the silicon source material in all of the epitaxial growths. Both n/p/p(+) and p/n/n(+) structures were studied. Correlations were made between the measured profiles and the solar cell parameters, especially cell open-circuit voltage. It was found that in order to obtain consistently high open-circuit voltage, the epitaxial techniques used to grow the surface layer must be altered to obtain very abrupt doping profiles in the vicinity of the junction. With these techniques, it was possible to grow reproducibly both p/n/n(+) and n/p/p(+) solar cell structures having open-circuit voltages in the 610- to 630-mV range, with fill factors in excess of 0.80 and AM-1 efficiencies of about 13%. Combinations and comparisons of epitaxial and diffused surface layers were also made. Using such surface layers, we found that the blue response of epitaxial cells could be improved, resulting in AM-1 short-circuit current densities of about 30 mA/cm sq. The best cells fabricated in this manner had AM-1 efficiency of 14.1%.

L.S.

N79-19451* Technical Marketing Associates, Inc., Concord, Mass.

MARKET DEFINITION STUDIES FOR PHOTOVOLTAIC HIGHWAY APPLICATIONS

Dec 1978 121 p

(Contracts DEN-3-40; DE-A101-79ET204R5)

(NASA-CR-159477; DOE/NASA/0040-78/1) Avail NTIS

HC A06/MF A01 CSCL 10A

Prospects for solar electric power in applications related to highways within the continental United States are examined. Principal prospective users are found to be the highway departments of the various states. Economic analysis is employed to demonstrate that suitable applications can occur when powering apparatus such as signs, crossing signals, or instruments which consume less than 100 watts on the average, provided they are located at least one-half mile from existing utility power. Such applications are projected to occur two or three times per state per year. Attitudes of highway officials toward possible use of solar power are sampled and described. Although falling photovoltaic cell prices are expected to have little effect on sales potential here, methods for federal stimulation of this market are discussed. G.Y.

N79-19454* Comstock and Wescott, Inc., Cambridge, Mass.
DEVELOPMENT OF A PHASE-CHANGE THERMAL STORAGE SYSTEM USING MODIFIED ANHYDROUS SODIUM HYDROXIDE FOR SOLAR ELECTRIC POWER GENERATION

Barry M. Cohen, Richard E. Rice, and Peter E. Rowny Dec. 1978 252 p refs Prepared for DOE
(Contracts NAS3-20615; EC-77-A-31-1034)
(NASA-CR-159465, DOE/NASA/0615-79/1) Avail: NTIS HC A12/MF A01 CSCL 10A

A thermal storage system for use in solar power electricity generation was investigated analytically and experimentally. The thermal storage medium is principally anhydrous NaOH with 8% NaNO₃ and 0.2% MnO₂. Heat is charged into storage at 584 K and discharged from storage at 582 K by Therminol-66. Physical and thermophysical properties of the storage medium were measured. A mathematical simulation and computer program describing the operation of the system were developed. A 1/10 scale model of a system capable of storing and delivering 3.1 x 10 to the 6th power kJ of heat was designed, built, and tested. Tests included steady state charging, discharging, idling, and charge-discharge conditions simulating a solar daily cycle. Experimental data and computer-predicted results are correlated. A reference design including cost estimates of the full-size system was developed. Author

N79-20487* West Virginia Univ., Morgantown.
SIMULATION OF FLUIDIZED BED COAL COMBUSTORS
Final Report

Renga Rajan Feb 1979 215 p refs
(Grant NSG-3134)
(NASA-CR-159529) Avail: NTIS HC A10/MF A01 CSCL 10B

The many deficiencies of previous work on simulation of fluidized bed combustion (FBC) processes are presented. An attempt is made to reduce these deficiencies, and to formulate a comprehensive FBC model taking into account the following elements: (1) devolatilization of coal and the subsequent combustion of volatiles and residual char; (2) sulfur dioxide capture by limestone; (3) NO_x release and reduction of NO_x by char; (4) attrition and elutriation of char and limestone; (5) bubble hydrodynamics; (6) solids mixing; (7) heat transfer between gas and solid, and solid and heat exchange surfaces; and (8) freeboard reactions. G Y

N79-20487* Technical Report Services, Rocky River, Ohio.
EVALUATION OF URETHANE FOR FEASIBILITY OF USE IN WIND TURBINE BLADE DESIGN **Final Report**

Seymour Lieblein, Robert S. Ross (Concept Development Inst., Hudson, Ohio), and Demeter G. Fertis (Akron Univ.) Apr 1979 156 p
(NASA Order C-7653, Contract E(49-26)-1028)
(NASA-CR-159530, DOE/NASA/7653-79/1, TRS-101) Avail: NTIS HC A08/MF A01 CSCL 10B

A preliminary evaluation was conducted of the use of cast urethane as a possible material for low cost blades for wind turbines. Specimen test data are presented for ultimate tensile strength, elastic modulus, flexural strain, creep, and fatigue properties of a number of urethane formulations. Data are also included for a large-scale urethane blade section composed of cast symmetrical half-profiles tested as a cantilever beam. Based on these results, an analysis was conducted of a full-scale blade design of cast urethane that meets the design specifications of the rotor blades for the NASA/DOE experimental 100-kW MOD-0 wind turbine. Because of the low value of elastic modulus for urethane (around 457 000 psi), the design loads would have to be carried by metal reinforcement. Considerations for further evaluation are noted. Author

N79-21554* Honeywell, Inc., Minneapolis, Minn.
ACTIVE HEAT EXCHANGE SYSTEM DEVELOPMENT FOR LATENT HEAT THERMAL ENERGY STORAGE

R. T. LeFrois, G. R. Knowles, A. K. Mathur, and J. Budimir

Feb. 1979 122 p refs

(Contracts DEN-3-38, EC-77-A-31-1034)
(NASA-CR-159479, HI-78336, DOE/NASA/0038-79/1) Avail: NTIS HC A06/MF A01 CSCL 10A

Active heat exchange concepts for use with thermal energy storage systems in the temperature range of 250 C to 350 C, using the heat of fusion of molten salts for storing thermal energy are described. Salt mixtures that freeze and melt in appropriate ranges are identified and are evaluated for physico-chemical, economic, corrosive and safety characteristics. Eight active heat exchange concepts for heat transfer during solidification are conceived and conceptual; designed for use with selected storage media. The concepts are analyzed for their scalability, maintenance, safety, technological development and costs. A model for estimating and scaling storage system costs is developed and is used for economic evaluation of salt mixtures and heat exchange concepts for a large scale application. The importance of comparing salts and heat exchange concepts on a total system cost basis, rather than the component cost basis alone, is pointed out. The heat exchange concepts were sized and compared for 6.5 MPa/281 C steam conditions and a 1000 MW(t) heat rate for six hours. A cost sensitivity analysis for other design conditions is also carried out. L.P.

N79-26506* General Electric Co., Philadelphia, Pa. Space Div.

AN INVESTIGATION OF THE ADHESIVE BONDING OF TEFLON SOLAR CELL COVERS

George J. Rayl 30 Apr 1979 42 p refs
(Contract NAS3-21264)
(NASA-CR-159565, DOC-79SDS4218) Avail: NTIS HC A03/MF A01 CSCL 10A

The concept of introducing organic agents into silicone resins to stabilize these materials against the ravages of ultraviolet radiation is presented. A screening of coating materials, cover materials and ultraviolet screening agents is described. Fabrication processes were developed for the application of thin 25 micrometer coatings to Teflon. Temperature shock and temperature-humidity tests were conducted. Author

N79-29603* Owens-Illinois, Inc., Toledo, Ohio.
ALTERNATE METHODS OF APPLYING DIFFUSANTS TO SILICON SOLAR CELLS **Final Report, Jan. 1977 - Jan. 1978**

Thomas W. Brock and Marshall B. Field (Pantek International, Lewistown, Pa.) Aug 1979 23 p refs
(Contract NAS3-20579)
(NASA-CR-159508) Avail: NTIS HC A02/MF A01 CSCL 10A

Low-melting phosphate and borate glasses were screen printed on silicon wafers and heated to form n and p junctions. Data on surface appearance, sheet resistance and junction depth are presented. Similar data are reported for vapor phase transport from sintered aluminum metaphosphate and boron-containing glass-ceramic solid sources. Simultaneous diffusion of an Ni(+) layer with screen-printed glass and a pl(-) layer with screen-printed Al alloy paste was attempted. No pl(-) back surface field formation was achieved. Some good cells were produced but the heating in an endless-belt furnace caused a large scatter in sheet resistance and junction depth for three separate lots of wafers. Author

N79-29604* Energy Research Corp., Danbury, Conn.
TECHNOLOGY DEVELOPMENT FOR PHOSPHORIC ACID FUEL CELL POWERPLANT, PHASE 2 **Quarterly Report**

Larry Christner Mar 1979 50 p refs Prepared for NASA and DOE
(Contract DEN3-67)
(NASA-CR-159572, DOE/NASA/0067-79/1) Avail: NTIS HC A03/MF A01 CSCL 10B

Component development has resulted in routine molding of 12 in by 17 in bipolar plates with 80 percent acceptance. A 5 C per hour post-cure heating cycle for these plates was found to give blister free materials. Lowering the resin in a bipolar plate content from 32 percent to 22 percent decreases the

resistivity more than 50 percent. Evaluation of the corrosion resistance of Novolak and Resol resins at 185 C in phosphoric acid indicates a slow etch. Aresol modified phenolics, however, decompose rapidly. Estimates of acid loss by the use of analytical expressions known as Margule, van Laar, and Wilson equations were not satisfactory. Experimental evaluation of the P4O10 vapor concentration of 103 wt percent acid at 191 C provided a value of 2 ppm. This value is based on a single experiment. Author

N79-30801* Boeing Engineering and Construction, Seattle, Wash.

APPLICATIONS OF THERMAL ENERGY STORAGE TO PROCESS HEAT STORAGE AND RECOVERY IN THE PAPER AND PULP INDUSTRY Final Report, Sep. 1977 - May 1978

J. H. Carr, P. J. Hurley, and P. J. Martin Sep 1978 244 p refs Sponsored by NASA

(Contracts EC-77-A-31-1034; EC-77-C-01-5082)

(NASA-CR-159398; CONS-5082-1) Avail: NTIS HC A11/MF A01 CSCL 10C

Applications of Thermal Energy Storage (TES) in a paper and pulp mill power house were studied as one approach to the transfer of steam production from fossil fuel boilers to waste fuel (hog fuel) briquers. Data from specific mills were analyzed, and various TES concepts evaluated for application in the process steam supply system. Constant pressure and variable pressure steam accumulators were found to be the most attractive storage concepts for this application. DOE

N79-31784* United Technologies Corp., South Windsor, Conn. Power Systems Div.

STRIP CELL TEST AND EVALUATION PROGRAM Final Report, 15 Jun. 1976 - 30 Apr. 1977

B. Gitlow, W. F. Bell, and R. E. Martin 27 Oct 1978 76 p refs

(Contract NAS3-20042)

(NASA-CR-159652; FCR 0945) Avail: NTIS HC A05/MF A01 CSCL 10B

The performance characteristics of alkaline fuel cells to be used for space power systems were tested. Endurance tests were conducted on the cells during energy conversion operations. A feature of the cells fabricated and tested was the capability to evaporate the product water formed during the energy conversion reaction directly to space vacuum. A fuel cell powerplant incorporating these cells does not require a condenser and a hydrogen recirculating pump-water separator, to remove the product water. This simplified the fuel cell powerplant system, reduced the systems weight, and reduced the systems parasitic power. AWH

N79-32646* Comsat Labs., Clarksburg, Md.

LIMITING PROCESS IN SHALLOW JUNCTION SOLAR CELLS

A. Meulenbergh and E. Rittner /in NASA Lewis Res. Center Solar Cell High Efficiency and Radiation Damage, 1979 Aug. 1979 p 35-36 Submitted for publication (For primary document see N79-32640 23-44)

Avail: NTIS HC A13/MF A01 CSCL 10A

In extending the violet and nonreflective cell technology to lower resistivities, several processes limiting output power were encountered. The most important was the dark diffusion current due to recombination at the front grid contacts. After removal of this problem by reduction of the silicon metal contact area (to 0.14 percent of the total area), the electric field enhanced junction recombination current $J_{sub r}$ was the main limitation. Alteration of the diffusion profile to reduce the junction field is shown to be an effective means of influencing $J_{sub r}$. The remaining problems are the bulk recombination in the n^+ layer and the surface recombination at the oxide-silicon interface, both of these problems are aggravated by band narrowing resulting from heavy doping in the diffused layer. Experimental evidence for the main limitations is shown, where increased diffusion temperature is seen to reduce both the influence of the front grid contacts and the junction electric field by increasing the

junction depth. The potential for further significant improvement in efficiency appears to be high. J.M.S.

N79-32647* Florida Univ., Gainesville. Dept. of Electrical Engineering

DESIGN OF HIGH EFFICIENCY HLE SOLAR CELLS FOR SPACE AND TERRESTRIAL APPLICATIONS

A. Neugroschel and F. A. Lindholm /in NASA Lewis Res. Center Solar Cell High Efficiency and Radiation Damage, 1979 Aug. 1979 p 37-50 refs (For primary document see N79-32640 23-44)

(Grant NSG-3018)

Avail: NTIS HC A13/MF A01 CSCL 10A

A first-order analysis of HLE cells is presented for both beginning-of-life and end-of-life conditions. Based on this analysis and on experimentally observed values for material parameters. Design approaches for both space and terrestrial cells are presented. The approaches result in specification of doping levels, junction depths, and surface conditions. The proposed structures are projected to have both high $V_{sub OC}$ and high $J_{sub SC}$. J.M.S.

N79-32652* Solarex Corp., Rockville, Md.

THIN CELLS FOR SPACE

G. Storti, J. Wohlgemuth, and C. Wrigley /in NASA Lewis Res. Center Solar Cell High Efficiency and Radiation Damage, 1979 Aug. 1979 p 87-95 refs (For primary document see N79-32640 23-44)

(Contracts NAS3-21250; JPL-954883)

Avail: NTIS HC A13/MF A01 CSCL 10A

Research and pilot line production efforts directed towards the fabrication of high efficiency ultrathin silicon solar cells (50 micrometers) are reported. Conventional ultrathin cells with air-mass-zero (AM0) efficiencies exceeding 14% and coplanar back contact cells with AM0 efficiencies up to 11.7% were developed. The primary mechanisms limiting efficiency were determined in both types of cells, and they are discussed within the context of further improving efficiency. Results of pilot line production of conventional ultrathin cells are also presented. Average AM0 efficiencies of 12% were readily achieved for 2000 cell production runs. RES

N79-32654* Optical Coating Lab., Inc., City of Industry, Calif.
SILICON SOLAR CELLS FOR SPACE USE: PRESENT PERFORMANCE AND TRENDS

P. A. Iles, F. T. Ho, and S. Khemthong /in NASA Lewis Res. Center Solar Cell High Efficiency and Radiation Damage, 1979 Aug. 1979 p 101-104 (For primary document see N79-32640 23-44)

Avail: NTIS HC A13/MF A01 CSCL 10A

A technology assessment of present performance levels and current fabrication methods and designs is presented. RES

N79-32662* State Univ. of New York at Albany. Inst. for the Study of Defects in Solids

HIGH-ENERGY ELECTRON-INDUCED DAMAGE PRODUCTION AT ROOM TEMPERATURE IN ALUMINUM-DOPED SILICON

J. W. Corbett, L.-J. Cheng, A. Jaworowski, J. P. Karins, Y. H. Lee, L. Lindstrom (Foersvaret Forskningsanstalt, Stockholm, Sweden), P. M. Mooney (Vassar Coll.), G. Oehrten, and K. L. Wang (GE Co., Schenectady, N. Y.) /in NASA Lewis Res. Center Solar Cell High Efficiency and Radiation Damage, 1979 Aug. 1979 p 185-196 refs (For primary document see N79-32640 23-44)

Avail: NTIS HC A13/MF A01 CSCL 10A

DLTS and EPR measurements are reported on aluminum-doped silicon that was irradiated at room temperature with high-energy electrons. Comparisons are made to comparable experiments on boron-doped silicon. Many of the same defects observed in boron-doped silicon are also observed in aluminum-doped silicon, but several others were not observed, including the aluminum interstitial and aluminum-associated defects.

Damage production modeling, including the dependence on aluminum concentration, is presented. M M M

test-circuit design is presented and experimental results are discussed. S.C.S.

N79-33560*# General Electric Co. Schenectady, N. Y.
CONCEPTUAL DESIGN OF THERMAL ENERGY STORAGE SYSTEMS FOR NEAR TERM ELECTRIC UTILITY APPLICATIONS Final Report

E. W. Hall, W. Hausz, R. Anand, N. LaMarche, J. Oplinger, and M. Katzer Jul 1979 359 p refs Sponsored by NASA Prepared for DOE

(Contracts DEN3-12, EC-77-A-21-1034-2, EPRI Proj. RP1082-1)

(NASA-CR-159577, GE79ET0101, DOE/NASA/0012-79/2) Avail NTIS HC A16/MF A01 CSCL 10B

Potential concepts for near term electric utility applications were identified. The most promising ones for conceptual design were evaluated for their economic feasibility and cost benefits. The screening process resulted in selecting two coal-fired and two nuclear plants for detailed conceptual design. The coal plants utilized peaking turbines and the nuclear plants varied the feedwater extraction to change power output. It was shown that the performance and costs of even the best of these systems could not compete in near term utility applications with cycling coal plants and typical gas turbines available for peaking power. Lower electricity costs, greater flexibility of operation, and other benefits can be provided by cycling coal plants for greater than 1500 hours of peaking or by gas turbines for less than 1500 hours if oil is available and its cost does not increase significantly.

R E S

N79-33581*# United Technologies Corp. South Windsor, Conn.
Power Systems Div

ADVANCED TECHNOLOGY LIGHT WEIGHT FUEL CELL PROGRAM Final Report, 9 May 1977 - 16 Jun. 1978

R. E. Martin 16 Jun 1978 73 p refs

(Contracts NAS3 20621, NAS3 20604)

(NASA-CR-159653, FCR-1017)

Avail NTIS

HC A04/MF A01 CSCL 10A

A high performance hydrogen-oxygen alkaline fuel cell was investigated. Cell performance goals include 0.9 volts at a current density of 1000 amperes per sq ft for 3000 hours at a cell temperature up to 300 F and reactant pressure up to 250 psia. Subscale research cells were tested in the evaluation of five anode and five cathode catalyst configurations. Fuel cell matrices were fabricated from NASA supplied polybenzimidazole (PBI) powder. A cell edge frame and PBI matrix samples were corrosion tested in 42 wt% KOH at 250 F (121 C). A total of 13,828 hours of research cell testing at 250 F was completed. In addition 494 hours of testing at temperatures up to 300 F and reactant pressures up to 250 psia with 27 hours of operation at or above 0.9 V/c at 1000 ASF was completed. A supported platinum-on-carbon catalyst configuration demonstrated stable operation at high temperature. A new cell edge frame structure showed low weight loss during corrosion testing, an indication of the material stability and long life potential. J M S

A79-10106* NaOH-based high temperature heat-of-fusion thermal energy storage device. B. M. Cohen and R. E. Rice (Comstock and Wescott, Inc., Cambridge, Mass.). In: Intersociety Energy Conversion Engineering Conference, 13th, San Diego, Calif., August 20-25, 1978, Proceedings, Volume 2. (A79-10001 01-44) Warrendale, Pa. Society of Automotive Engineers, Inc., 1978, p. 941-947. Research supported by the U.S. Department of Energy; Contract No. NAS3-20615.

A material called Thermkeep, developed as a low-cost method for the storage of thermal energy for solar electric power generating systems is discussed. The storage device consists of an insulated cylinder containing Thermkeep in which coiled tubular heat exchangers are immersed. A one-tenth scale model of the design contains 25 heat-exchanger tubes and 1500 kg of Thermkeep. Its instrumentation includes thermocouples to measure internal Thermkeep temperatures, vessel surface, heated shroud surface, and pressure gauges to indicate heat-exchanger pressure drops. The

A79-17321* Phase change thermal storage for a solar total energy system. R. E. Rice and B. M. Cohen (Comstock and Wescott, Inc., Cambridge, Mass.). In: Sun: Mankind's future source of energy; Proceedings of the International Solar Energy Congress, New Delhi, India, January 16-21, 1978, Volume 1. (A79-17276 05-44) Elmsford, N.Y., Pergamon Press, Inc., 1978, p. 511-515. Research supported by the U.S. Department of Energy; Contract No. NAS3-20615.

An analytical and experimental program is being conducted on a one-tenth scale model of a high-temperature (584 K) phase-change thermal energy storage system for installation in a solar total energy test facility at Albuquerque, New Mexico, U.S.A. The thermal storage medium is anhydrous sodium hydroxide with 8% sodium nitrate. The program will produce data on the dynamic response of the system to repeated cycles of charging and discharging simulating those of the test facility. Data will be correlated with a mathematical model which will then be used in the design of the full-scale system.

(Author)

A79-20825* Background and system description of the Mod 1 wind turbine generator. E. H. Ernst (General Electric Co., Valley Forge, Pa.). In: Selective application of materials for products and energy; Proceedings of the Twenty-third National Symposium and Exhibition, Anaheim, Calif., May 2-4, 1978. (A79-20801 07-23) Azusa, Calif., Society for the Advancement of Material and Process Engineering, 1978, p. 403-408. Contract No. NAS3-20058.

The Mod-1 wind turbine considered is a large utility-class machine, operating in the high wind regime, which has the potential for generation of utility grade power at costs competitive with other alternative energy sources. A Mod-1 wind turbine generator (WTG) description is presented, taking into account the two variable-pitch steel blades of the rotor, the drive train, power generation/control, the Nacelle structure, and the yaw drive. The major surface elements of the WTG are the ground enclosure, the back up battery system, the step-up transformer, elements of the data system, cabling, area lighting, and tower foundation. The final system weight (rotor, Nacelle, and tower) is expected to be about 650,000 pounds. The WTG will be capable of delivering 1800 kW to the utility grid in a wind-speed above 25 mph.

G. R.

A79-20826* Wind turbine generator application places unique demands on tower design and materials. J. P. Kita (General Electric Co., Space Div., Valley Forge, Pa.). In: Selective application of materials for products and energy; Proceedings of the Twenty-third National Symposium and Exhibition, Anaheim, Calif., May 2-4, 1978. (A79-20801 07-23) Azusa, Calif., Society for the Advancement of Material and Process Engineering, 1978, p. 409-416. Contract No. NAS3-20058.

The most relevant contractual tower design requirements and goal for the Mod-1 tower are related to steel truss tower construction, cost-effective state-of-the-art design, a design life of 30 years, and maximum wind conditions of 120 mph at 30 feet elevation. The Mod-1 tower design approach was an iterative process. Static design loads were calculated and member sizes and overall geometry chosen with the use of finite element computer techniques. Initial tower dynamic characteristics were then combined with the dynamic properties of the other wind turbine components, and a series of complex dynamic computer programs were run to establish a dynamic load set and then a second tower design.

G. R.

A79-20827 * **Fatigue impact on Mod-1 wind turbine design.** C. V. Stahle, Jr. (General Electric Co., Space Div., Valley Forge, Pa.). In: Selective application of materials for products and energy; Proceedings of the Twenty-third National Symposium and Exhibition, Anaheim, Calif., May 2-4, 1978. (A79-20801 07-23) Azusa, Calif., Society for the Advancement of Material and Process Engineering, 1978, p. 417-427. Contract No. NAS3-20058.

Fatigue is a key consideration in the design of a long-life Wind Turbine Generator (WTG) system. This paper discusses the fatigue aspects of the large Mod-1 horizontal-axis WTG design starting with the characterization of the environment and proceeding through the design. Major sources of fatigue loading are discussed and methods of limiting fatigue loading are described. NASTRAN finite element models are used to determine dynamic loading and internal cyclic stresses. Recent developments in determining the allowable fatigue stress consistent with present construction codes are discussed relative to their application to WTG structural design. (Author)

A79-27400 * # **The application of hydraulics in the 2,000 kW wind turbine generator.** S. Onufreiczuk (General Electric Co., Space Div., Valley Forge, Pa.). *National Conference on Fluid Power and Power Transmission, Philadelphia, Pa., Nov. 7, 1978, Paper. 16 p.* Contract No. NAS3-20058.

A 2000 kW turbine generator using hydraulic power in two of its control systems is being built under the management of NASA Lewis Research Center. The hydraulic systems providing the control torques and forces for the yaw and blade pitch control systems are discussed. The yaw-drive-system hydraulic supply provides the power for positioning the nacelle so that the rotary axis is kept in line with the direction of the prevailing wind, as well as pressure to the yaw and high speed shaft brakes. The pitch-change-mechanism hydraulic system provides the actuation to the pitch change mechanism and permits feathering of the blades during an emergency situation. It operates in conjunction with the overall windmill computer system, with the feather control permitting slewing control flow to pass from the servo valve to the actuators without restriction. A.A.

A79-51780 * **Control and stabilization of the DOE/NASA Mod-1 two megawatt wind turbine generator.** R. S. Barton (General Electric Co., King of Prussia, Pa.), C. E. J. Bowler, and R. J. Piwko (General Electric Co., Electric Utility Systems Engineering Dept., Schenectady, N.Y.). In: Intersociety Energy Conversion Engineering Conference, 14th, Boston, Mass., August 5-10, 1979, Proceedings, Volume 1. (A79-51726 23-44) Washington, D.C., American Chemical Society, 1979, p. 325-330. 5 refs. Research supported by the U.S. Department of Energy. Contract No. NAS3-20058.

This paper describes the controls design, performance simulation process and specialized dynamic considerations for the DOE/NASA Mod-1 wind turbine generator (WTG). It shows controls, structural and utility interface considerations of the wind turbine generator and shows how a wind turbine generator can be integrated with a synchronous power system. Differences with respect to fossil or hydro generation and their implications are vital to long-term WTG reliability and availability and acceptance by utilities and consumers. The paper describes the control performance requirements to provide stable pitch and excitation control with drivetrain torsional dynamics, and the control of power swing stability and utility feeder voltage due to wind gusts. (Author)

45 ENVIRONMENT POLLUTION

Includes air, noise, thermal and water pollution, environment monitoring, and contamination control

N79-12686* National Aeronautics and Space Administration
Lewis Research Center, Cleveland, Ohio

APPLICATION OF ION CHROMATOGRAPHY TO THE STUDY OF HYDROLYSIS OF SOME HALOGENATED HYDROCARBONS AT AMBIENT TEMPERATURES

Dumas A. Otterson 1978 24 p. refs. Presented at Symp. on Ion Chromatography, Sunnyvale, Calif., 21 Jun 1978. Sponsored by the Dionex Corp.
(NASA-TM-79020, E-9817) Avail NTIS HC A02/MF A01 CSDL 07D

The application of ion chromatography to the study of very slow rates of hydrolysis of some halogenated hydrocarbons was investigated. The halide concentrations in the aqueous phase of mixtures of a carbonate buffer (pH = 10.3) and either chloroform (CHCl₃) or fluorotrichloromethane (CFC13) after aging for various lengths of time at room temperature, were determined by ion chromatography. Hydrolysis of CHCl₃ caused the Cl⁻ concentration to increase by about 1500 ppb per day. On the other hand neither the F⁻ or Cl⁻ concentration in the CFC13 mixture increased by as much as 1 ppb per day. The magnitude of errors in the determination of halides prevented any firm conclusions regarding hydrolysis in this mixture. However, these results were used to show how ion chromatography could expedite identification of the hydrolyzing substance as well as investigations of hydrolysis mechanisms. Author

N79-15448* National Aeronautics and Space Administration
Lewis Research Center, Cleveland, Ohio

NASA GLOBAL ATMOSPHERIC SAMPLING PROGRAM (GASP) DATA REPORT FOR TAPE VLO009

J. D. Holdeman, Thomas J. Dudzinski, Ted W. Nyland, and Marvin W. Tiefermann Dec 1978 37 p. refs.
(NASA-TM-79058, E-9872, Rept 8) Avail NTIS HC A03/MF A01 CSDL 04A

The GASP atmospheric trace constituent data cover atmospheric ozone, carbon monoxide, condensation nuclei, clouds, and related meteorological and flight information obtained during October 28-31, 1977. Reported herein are flight routes and dates, instrumentation, data processing procedures, and data tape specifications. G G

N79-15450* National Aeronautics and Space Administration
Lewis Research Center, Cleveland, Ohio

NASA GLOBAL ATMOSPHERIC SAMPLING PROGRAM (GASP) DATA REPORT FOR TAPES VLO010 AND VLO012

J. D. Holdeman, Thomas J. Dudzinski, Marvin W. Tiefermann, and Ted W. Nyland Jan 1979 77 p. refs.
(NASA-TM-79061, E-9874) Avail NTIS HC A05/MF A01 CSDL 13B

The GASP atmospheric trace constituent data currently available are considered. Included on tapes are in-situ measurements of atmospheric ozone, carbon monoxide, water vapor, and clouds, data from laboratory analysis of filters exposed in flight, and related flight and meteorological data. Measurements of ozone levels within the first class cabin of these aircraft are also reported. In addition to the GASP data, tropopause pressures obtained from time and space interpolation of NMC archived data for the dates of the flights are included. Reported herein are the flight routes and dates, instrumentation, data processing procedures, data tape specifications, and analyses of the cabin ozone measurements. G G

N79-17358* National Aeronautics and Space Administration
Lewis Research Center, Cleveland, Ohio

ION CHROMATOGRAPHIC DETERMINATION OF SULFUR IN FUELS

Constance S. Mizisin, David E. Kuivinen, and Dumas A. Otterson 1978 16 p. refs. Presented at the 2nd Natl. Symp. on Ion

Chromatographic Analysis of Environ. Pollutants and other Analogous Compounds, Research Triangle Park, N. C., 11-13 Oct 1978, sponsored by EPA
(NASA-TM-78971, E-9743) Avail NTIS HC A02/MF A01 CSDL 13B

The sulfur content of fuels was determined using an ion chromatograph to measure the sulfate produced by a modified Parr bomb oxidation. Standard Reference Materials from the National Bureau of Standards, of approximately 0.2 + or - 0.004% sulfur, were analyzed resulting in a standard deviation no greater than 0.008. The ion chromatographic method can be applied to conventional fuels as well as shale-oil derived fuels. Other acid forming elements such as fluorine, chlorine and nitrogen could be determined at the same time, provided that these elements have reached a suitable ionic state during the oxidation of the fuel. G Y

N79-17359* National Aeronautics and Space Administration
Lewis Research Center, Cleveland, Ohio

NASA GLOBAL ATMOSPHERIC SAMPLING PROGRAM (GASP) DATA REPORT FOR TAPES VLO007 AND VLO008

J. D. Holdeman, Daniel J. Gauntner, Francis M. Humenik, and Daniel Briehl Nov 1977 58 p. refs.
(NASA-TM-73784, E-9348) Avail NTIS HC A04/MF A01 CSDL 13B

The Global Atmospheric Sampling Program (GASP) is obtaining measurements of atmospheric trace constituents in the upper troposphere and lower stratosphere using fully automated air sampling systems on board the NASA CV-990 research aircraft and four commercial B-747 aircraft in routine airline service. In-situ measurements of atmospheric ozone and water vapor, data from laboratory analysis of filters exposed in flight, and related flight and meteorological data obtained from September 1976 through January 1977 are reported. These data are now available on GASP tapes VLO007 & VLO008 from the National Climatic Center, Asheville, North Carolina. In addition to the GASP data, tropopause pressure fields obtained from NMC archives for the dates of the GASP flights are included on the data tape. Flight routes and dates, instrumentation, data processing procedures, and data tape specifications are described. Author

N79-18479* National Aeronautics and Space Administration
Lewis Research Center, Cleveland, Ohio

CONDENSATION NUCLEI (AITKEN PARTICLE) MEASUREMENT SYSTEM USED IN NASA GLOBAL ATMOSPHERIC SAMPLING PROGRAM

Ted W. Nyland Feb 1979 28 p. refs.
(NASA-TP-1415, E-9816) Avail NTIS HC A03/MF A01 CSDL 13B

The condensation nuclei (Aitken particle) measuring system used in the NASA Global Atmospheric Sampling Program is described. Included in the paper is a description of the condensation nuclei monitor sensor, the pressurization system, and the Pollack counter calibration system used to support the CN measurement. The monitor has a measurement range to 1000 CN/cm³ and a noise level equivalent to 5 CN/cm³ at flight altitudes between 6 and 13 km. Author

N79-20627* National Aeronautics and Space Administration
Lewis Research Center, Cleveland, Ohio

INDUSTRIAL POTENTIAL, USES, AND PERFORMANCE OF SPUTTERED AND ION PLATED FILMS

Talivaldis Spalvins 1979 16 p. refs. Presented at the 22nd Ann. Tech. Conf. of the Soc. of Vacuum Coaters, New Orleans, 28-30 Mar 1979
(NASA-TM-79107, E-9932) Avail NTIS HC A02/MF A01 CSDL 20A

The sputtering and ion plating technology is reviewed in terms of their potential, uses and performance. It offers the greatest flexibility in coating preparation, since coatings can be tailored in any preferred chemical combination, and graded type interfaces (ceramic to metal seals) can be formed. Sputtered and ion plated film characteristics such as the degree of adherence, coherence and morphological growth which contribute to film performance and reliability are described and illustrated.

as used in practice. It is concluded that the potential future of sputtered and ion plated films for industrial applications will depend primarily upon greater comprehension of materials selection, possible elimination of restrictions for coating/substrate combinations and the awareness of utilizing the proper deposition parameters. Author

N79-20628* National Aeronautics and Space Administration, Lewis Research Center, Cleveland, Ohio.

EFFECTS OF AIR INJECTION ON A TURBOCHARGED TELEDYNE CONTINENTAL MOTORS TSIO-380-C ENGINE
Donald V. Cosgrove and Erwin E. Kempke 1979 37 p refs
Presented at the Business Aircraft Meeting, Wichita, Kans., 3-6 Apr. 1979; sponsored by the Soc. of Automotive Engrs. (NASA-TM-79121, E-9955) Avail. NTIS HC A03/MF A01

A turbocharged fuel injected aircraft engine was operated over a range of test conditions that included that EPA five-mode emissions cycle and fuel air ratio variations for individual modes while injecting air into the exhaust gas. Air injection resulted in a decrease of hydrocarbons and carbon monoxide while exceeding the maximum recommended turbine inlet temperature of 1650 F at the full rich mixture of the engine. Leanout tests indicated that the EPA standards could be met through the combined use of fuel management and air injection. Author

N79-22664* National Aeronautics and Space Administration, Lewis Research Center, Cleveland, Ohio.

OZONE MEASUREMENT SYSTEM FOR NASA GLOBAL AIR SAMPLING PROGRAM

Marvin W. Tiefermann May 1979 21 p refs
(NASA-TP-1451, E-9829) Avail. NTIS HC A02/MF A01 CSCL 13B

The ozone measurement system used in the NASA Global Air Sampling Program is described. The system uses a commercially available ozone concentration monitor that was modified and repackaged so as to operate unattended in an aircraft environment. The modifications required for aircraft use are described along with the calibration techniques, the measurement of ozone loss in the sample lines, and the operating procedures that were developed for use in the program. Based on calibrations with JPL's 5-meter ultraviolet photometer, all previously published GASP ozone data are biased high by 9 percent. A system error analysis showed that the total system measurement random error is from 3 to 8 percent of reading (depending on the pump diaphragm material) or 3-ppbv, whichever are greater. Author

N79-31841* National Aeronautics and Space Administration, Lewis Research Center, Cleveland, Ohio.

CARBON MONOXIDE MEASUREMENT IN THE GLOBAL ATMOSPHERIC SAMPLING PROGRAM

Thomas J. Dudzinski Sep. 1979 26 p refs
(NASA-TP-1526, E-9972) Avail. NTIS HC A03/MF A01 CSCL 13B

The carbon monoxide measurement system used in the NASA Global Atmospheric Sampling Program (GASP) is described. The system used a modified version of a commercially available infrared absorption analyzer. The modifications increased the sensitivity of the analyzer to 1 ppmv full scale, with a limit of detectability of 0.02 ppmv. Packaging was modified for automatic, unattended operation in an aircraft environment. The GASP system is described along with analyzer operation, calibration procedures, and measurement errors. Uncertainty of the CO measurement over a 2-year period ranged from ± 3 to ± 13 percent of reading plus an error due to random fluctuation of the output signal ± 3 to ± 15 ppbv. Author

A79-15079* Pattern recognition methods and air pollution source identification. H. F. Leibeck and R. B. King (NASA, Lewis Research Center, Cleveland, Ohio). In: Joint Conference on Sensing of Environmental Pollutants, 4th, New Orleans, La., November 6-11, 1977, Proceedings. (A79-15023 04-45) Washington, D.C., American Chemical Society, 1978, p. 434-437, 9 refs.

Directional air samplers, used for resolving suspended particulate matter on the basis of time and wind direction were used to assess the feasibility of characterizing and identifying emission source types in urban multisource environments. Filters were evaluated for 16 elements and X-ray fluorescence methods yielded elemental concentrations for direction, day, and the interaction of direction and day. Large numbers of samples are necessary to compensate for large day-to-day variations caused by wind perturbations and/or source changes. S.C.S.

A79-31332* Measurements of carbon monoxide, condensation nuclei, and ozone on a B 747SP aircraft flight around the world. D. J. Gauntner, T. Nyland, M. Tiefermann, and T. Dudzinski (NASA, Lewis Research Center, Cleveland, Ohio). *Geophysical Research Letters*, vol. 6, Mar. 1979, p. 167-170, 10 refs.

Measurements of carbon monoxide, condensation nuclei, and ozone concentrations were obtained during a 54 hour polar flight around the world by an automated instrument package carried by a B-747SP commercial aircraft. These and other data were obtained as part of the NASA Global Atmospheric Sampling Program. All data exhibited longitudinal and hemispheric differences. Analysis of the data indicate increased concentrations of carbon monoxide and condensation nuclei at flight levels in the troposphere over tropical land masses. A background concentration for condensation nuclei was found to be 200 per cu cm for tropical tropospheric maritime air. (Author)

A79-38942* Experimental evidence of interhemispheric transport from airborne carbon monoxide measurements. R. E. Newell (MIT, Cambridge, Mass.) and D. J. Gauntner (NASA, Lewis Research Center, Cleveland, Ohio). *Journal of Applied Meteorology*, vol. 18, May 1979, p. 696-699, 9 refs. Research supported by the U.S. Department of Energy.

During the period 28-30 October 1977, a Pan American 747 SP aircraft flew around the world with an automated instrument package that included measurements of atmospheric CO made every 4 sec. The flight path extended from San Francisco, over the North Pole to London, south to Capetown, over the South Pole to Auckland, and back to San Francisco. The data collected show large changes with longitude, which are interpreted as direct evidence of interhemispheric mixing. Possible sources for CO are discussed. S.D.

A79-49494* Sulfate and nitrate mixing ratios in the vicinity of the tropopause. E. A. Lezberg, F. M. Humenik, and D. A. Otterson (NASA, Lewis Research Center, Cleveland, Ohio). *Atmospheric Environment*, vol. 13, no. 9, 1979, p. 1299-1304, 18 refs.

Measurements of sulfate and nitrate in filter samples made during the Global Atmospheric Sampling Program (GASP) from aircraft flying near the tropopause over a period of 28 months beginning in early 1976 are presented. Sulfate and nitrate mixing ratios show a peak near or just above the tropopause during the winter-spring seasons. No peak is evident for sulfate during the summer-fall seasons. The sulfate mixing ratios show a constant average level in 1977-78 of 0.12 ± 0.04 ppbm above the tropopause and 0.05 ± 0.04 ppbm below the tropopause with higher levels in the spring. Nitrate levels are similar but exhibit greater variability. Correlations between sulfate and nitrate ($r = 0.78$) and between sulfate and nitrate, on ozone ($r = 0.80, 0.78$) suggest a predominately stratospheric source for these species. (Author)

N79-27716* State Univ. of New York at Albany Atmospheric Sciences Research Center.

A SUMMARY OF RESEARCH ON THE NASA-GLOBAL ATMOSPHERIC SAMPLING PROGRAM PERFORMED BY THE ATMOSPHERIC SCIENCES RESEARCH CENTER Final Report

Phillip D. Falconer and Robert W. Pratt Jun. 1979 59 p refs (Grant NsG-3138) (NASA-CR-159614) Avail: NTIS HC A04/MF A01 CSCI 138

The annual variations of ozone near the tropopause are derived from aircraft exhibit year-to-year differences which are not explicitly accounted for by the simple, classical ozone transport theory. Phenomena such as tropopause lifting, interannual variations in the rates of stratospheric-tropospheric exchange and meridional mixing, contribute differently to the distribution of ozone in this altitude region. Ozone encounter climatologies have been represented by global maps which show the probability of exceeding ambient ozone levels of 200, 300, and 400 ppbV along flight routes during the year. Continuous ozone records obtained from the GASP system revealed the presence of gravity waves whose wavelength is of the order 20 km. The GASP data cannot, however, be utilized for the evaluation of horizontal fluxes of such quantities as ozone, sensible heat, and zonal momentum; the data are too sparsely and irregularly distributed for the computation of stable correlations. Multiple species data from the unique circumglobal flight of a Pan American airliner on 28-30 October 1977 are discussed with particular regard to the apparent interhemispheric differences in tropospheric species concentrations, variation between the Arctic and Antarctic stratospheres, to possible covariations between species, and to potential source regions for various constituents. J M S

46 GEOPHYSICS

Includes aeronomy; upper and lower atmosphere studies; ionospheric and magnetospheric physics; and geomagnetism.

For space radiation see 93 Space Radiation

A79-15068 * **An analysis of the first two years of GASP data.** J. D. Holdeman (NASA, Lewis Research Center, Combustion and Pollution Research Branch, Cleveland, Ohio), G. D. Nastrom (Control Data Corp., Minneapolis, Minn.), and P. D. Falconer (New York State University, Albany, N.Y.). In: Joint Conference on Sensing of Environmental Pollutants, 4th, New Orleans, La., November 6-11, 1977, Proceedings. (A79-15023 04 45) Washington, D.C., American Chemical Society, 1978, p. 313-317, 21 refs.

Distributions of mean ozone levels from the first two years of data from the NASA Global Atmospheric Sampling Program (GASP) show spatial and temporal variations in agreement with previous measurements. The standard deviations of these distributions reflect the large natural variability of ozone levels in the altitude range of the GASP measurements. Monthly mean levels of ozone below the tropopause show an annual cycle with a spring maximum which is believed to result from transport from the stratosphere. Correlations of ozone with independent meteorological parameters, and meteorological parameters obtained by the GASP systems show that this transport occurs primarily through cyclogenesis at mid-latitudes. The GASP water vapor data, analyzed with respect to the location of the tropopause, correlates well with the simultaneously obtained ozone and cloud data. (Author)

A79-44810 * **Ozone in the upper troposphere from Gasp measurements.** G. D. Nastrom (Control Data Corp., Minneapolis, Minn.). *Journal of Geophysical Research*, vol. 84, July 20, 1979, p. 3683-3688, 24 refs. Contract No. NAS3-21249.

Several aspects of tropospheric ozone variations are examined by using ozone measurements made from commercial airliners (Gasp data). Through visual inspection of the autocorrelation function it is shown that the east-west variations of ozone have a predominant wavelength near 2400 km, while temperature and wind have predominant wavelengths near 3300 km. Distance-lagged correlation functions of ozone with temperature and wind show a definite periodicity with wavelengths near 2400 km. Attention is given to the tropical tropospheric ozone values above 100 parts per billion by volume, which appear to be associated with meridional transport from middle latitudes, and in some cases, relatively large tropical ozone values are coincident with clouds. M.E.P.

47 METEOROLOGY AND CLIMATOLOGY

Includes weather forecasting and modification

N79-17418* National Aeronautics and Space Administration
Lewis Research Center, Cleveland, Ohio

AIRCRAFT ICING

Porter J. Perkins. In: Tenn. Univ. Space Inst. Proc. of the 2nd Ann. Workshop on Meteorol. and Environ. Inputs to Aviation Systems. Mar. 1978. p. 85-99. refs. (For primary document see N79-17413 08-47)

Avail. NTIS HC A12/MF A01 CSCL 04B

A representative of the NASA Lewis Research Center presented a discussion which concentrated on the meteorology of icing and its measurements. Other areas addressed were test facilities, ice protection systems, and the effects of ice on performance. G Y

N79-20572* National Aeronautics and Space Administration
Lewis Research Center, Cleveland, Ohio

MODE I CRACK SURFACE DISPLACEMENTS FOR A ROUND COMPACT SPECIMEN SUBJECT TO A COUPLE AND FORCE

Bernard Gross. 1979. 13 p. refs. Presented at the 12th Natl. Symp. on Fracture Mech., St. Louis, 21-23 May 1979; sponsored in part by the Am. Soc. for Testing and Mater.

(NASA-TM-79096, E-9920). Avail. NTIS HC A02/MF A01 CSCL 04B

Mode I displacement coefficients along the crack surface are presented for a radially cracked round compact specimen, treated as a plane elastostatic problem, subjected to two types of loading: a uniform tensile stress and a nominal bending stress distribution across the net section. By superposition the resultant displacement coefficient or the corresponding influence coefficient can be obtained for any practical load location. Load line displacements are presented for A/D ratios ranging from 0.40 to 0.95, where A is the crack length measured from the crack mouth to the crack tip and D is the specimen diameter. Through a linear extrapolation procedure crack mouth displacements are also obtained. Experimental evidence shows that the results are valid over the range of A/D ratios analyzed for a practical pin loaded round compact specimen. J M S

N79-20521* National Aeronautics and Space Administration
Lewis Research Center, Cleveland, Ohio

COMMERCIAL AIRCRAFT DERIVED HIGH RESOLUTION WIND AND TEMPERATURE DATA FROM THE TROPICS FOR FGGE: IMPLICATIONS FOR NASA

R. Steinberg. In: NASA. Goddard Space Flight Center. 3d NASA Weather and Climate Program Sci. Rev. 1977. p. 265-270. (For primary document see N79-20575 11-47)

Avail. NTIS HC A14/MF A01 CSCL 04B

Two programs involving over 100 commercial aircraft were initiated to provide global high resolution in-situ windfield and temperature data during the FGGE. The concepts developed for these programs could have important implications for both meteorology and aviation in the near term. G Y

A79-17180 * Ground-to-space optical power transfer. G. E. Meyers, C. L. Hayes, J. F. Scofield (Rockwell International Electronics Research Center, Anaheim, Calif.) and R. M. Stubbs (NASA, Lewis Research Center, Cleveland, Ohio). In: Adaptive optical components. Proceedings of the Seminar, Washington, D.C., March 30, 31, 1978. (A79-17170 05-35) Bellingham, Wash.: Society of Photo Optical Instrumentation Engineers, 1978. p. 108-117. 17 refs. Contract No. NAS3-18937

Using laser radiation as the energy input to a rocket, it is possible to consider the transfer of large payloads economically between low initial orbits and higher energy orbits. In this paper we will discuss the results of an investigation to use a ground based High

Energy Laser (HEL) coupled to an adaptive antenna to transmit multi-megawatts of power to a satellite in low-earth orbit. Our investigation included diffraction effects, atmospheric transmission efficiency, adaptive compensation for atmospheric turbulence effects, including the servo bandwidth requirements for this correction, and the adaptive compensation for thermal blooming. For these evaluations we developed vertical profile models of atmospheric absorption, strength of optical turbulence (CN2), wind, temperature, and other parameters necessary to calculate system performance. Our atmospheric investigations were performed for CO₂, 12C18O₂ isotope, CO and DF wavelengths. For all of these considerations, output antenna locations of both sea level and mountain top (3.5 km above sea level) were used. Several adaptive system concepts were evaluated with a multiple source phased array concept being selected. This system uses an adaption technique of phase locking independent laser oscillators. When both system losses and atmospheric effects were assessed, the results predicted an overall power transfer efficiency of slightly greater than 50%. (Author)

48 OCEANOGRAPHY

Includes biological, dynamic and physical oceanography;
and marine resources

A79-51095 * # A comparison of measured and calculated upwelling radiance over water as a function of sensor altitude. T. A. Coney and J. A. Salzman (NASA, Lewis Research Center, Cleveland, Ohio), *University of Michigan, International Symposium on Remote Sensing of Environment, 13th, Ann Arbor, Mich., Apr. 23-27, 1979, Paper*. 17 p. 7 refs.

The present paper compares remote sensing data measured over water at altitudes ranging from 30 m to 15.2 km to data calculated for corresponding altitudes using surface measurements and an atmospheric radiative transfer model. The data were acquired on June 22, 1978 in Lake Erie and it was found that suspended solids and chlorophyll concentrations were 0.59 ± 0.02 mg/liter and 2.42 ± 0.03 micro gram/liter respectively throughout the duration of the experiment. Calculated and measured nadir radiances for altitudes of 152 m and 12.5 km agree to within 16% and 14% respectively. It is noted that the model offered a poor simulation of the variation in measured radiance with look angle. Finally, it is concluded that an accurate assessment of the source of error will require the inclusion in the analysis of the contributions made by the sea state and specular sky reflectance. M.E.P.

53 BEHAVIORAL SCIENCES

Includes psychological factors; individual and group behavior, crew training and evaluation; and psychiatric research.

N79-25753* # National Aeronautics and Space Administration. Lewis Research Center, Cleveland, Ohio.

OVERALL LOUDNESS OF STEADY SOUNDS ACCORDING TO THEORY AND EXPERIMENT

Walton L. Howes. Oct. 1979. 150 p. refs.
(NASA-RP-1001; E-8342) Avail. NTIS MF A01, HC SOD CSCL 05J

A mathematical theory for calculating the loudness of any steady sound from information on its spectrum is constructed from physical principles and psychological and physiological information on mammalian auditory systems. The theory involves filtering, channeling, squaring, half-wave rectification, and time average of the signal. The theory accounts for critical bands for loudness, audibility of sounds consisting of subliminal components, audible beats, periodicity pitch, and pitch of the residue. These and other psychoacoustic phenomena are explained in terms of electrical activity in the peripheral nervous system. Simple approximations for loudness are derived from the more exact formulas. Loudness predictions are compared with a wide variety of published loudness judgement data with considerable success.

Author

54 MAN/SYSTEM TECHNOLOGY AND LIFE SUPPORT

Includes human engineering, biotechnology, and space suits and protective clothing

A79-11544 * # Digital enhancement of computerized axial tomograms. E. Roberts, Jr. (NASA, Lewis Research Center, Cleveland, Ohio). *IEEE, NIH, and Stanford University, Annual Computers in Cardiology Conference, 5th, Stanford, Calif., Sept. 12-14, 1978, Paper*. 5 p.

A systematic evaluation has been conducted of certain digital image enhancement techniques performed in image space. Three types of images have been used, computer generated phantoms, tomograms of a synthetic phantom, and axial tomograms of human anatomy containing images of lesions, artificially introduced into the tomograms. Several types of smoothing, sharpening, and histogram modification have been explored. It has been concluded that the most useful enhancement techniques are a selective smoothing of singular picture elements, combined with contrast manipulation. The most useful tool in applying these techniques is the gray-scale histogram. (Author)

60 COMPUTER OPERATIONS AND HARDWARE

Includes computer graphics and data processing
For components see 33 *Electronics and Electrical
Engineering*

N79-20782* National Aeronautics and Space Administration.
Lewis Research Center, Cleveland, Ohio.

LEWIS HYBRID COMPUTING SYSTEM, USFAS MANUAL
William M. Bruton and David S. Cwynar. Apr. 1979. 91 p.
(NASA-TM-79111; E-9938) Avail: NTIS HC A05/MF A01
CSCL 098

The Lewis Research Center's Hybrid Simulation Lab contains a collection of analog, digital, and hybrid (combined analog and digital) computing equipment suitable for the dynamic simulation and analysis of complex systems. This report is intended as a guide to users of these computing systems. The report describes the available equipment and outlines procedures for its use. Particular is given to the operation of the PACER 100 digital processor. System software to accomplish the usual digital tasks such as compiling, editing, etc. and Lewis-developed special purpose software are described. Author

N79-28881* National Aeronautics and Space Administration.
Lewis Research Center, Cleveland, Ohio.

INTRAOCULAR PRESSURE REDUCTION AND REGULATION SYSTEM

Edward F. Baehr, James E. Burnett, Sanford F. Felder, and William J. McGannon. 1979. 14 p. Presented at Symp. on Glaucoma Surgery, Detroit, 17-18 May 1979.
(NASA-TM-79187; E-038) Avail: NTIS HC A02/MF A01 CSCL 06E

An intraocular pressure reduction and regulation system is described and data are presented covering performance in (1) reducing intraocular pressure to a preselected value, (2) maintaining a set minimum intraocular pressure, and (3) reducing the dynamic increases in intraocular pressure resulting from external loads applied to the eye. Author

61 COMPUTER PROGRAMMING AND SOFTWARE

Includes computer programs, routines, and algorithms.

N79-21798* National Aeronautics and Space Administration, Lewis Research Center, Cleveland, Ohio.
INTERACTIVE DEBUG PROGRAM FOR EVALUATION AND MODIFICATION OF ASSEMBLY-LANGUAGE SOFTWARE
Jale J. Arpasi Apr 1979 82 p refs
(NASA-TP-1441; E-9219) Avail: NTIS HC A05/MF A01 CSCL 09B

An assembly-language debug program written for the Honeywell HDC-601 and DDP-516/316 computers is described. Names and relative addressing to improve operator-machine interaction are used. Features include versatile display, on-line assembly, and improved program execution and analysis. The program is discussed from both a programmer's and an operator's standpoint. Functional diagrams are included to describe the program, and each command is illustrated. S.E.S.

N79-23688* National Aeronautics and Space Administration, Lewis Research Center, Cleveland, Ohio.
WETAIR: A COMPUTER CODE FOR CALCULATING THERMODYNAMIC AND TRANSPORT PROPERTIES OF AIR-WATER MIXTURES
Theodore E. Fessler May 1979 16 p refs
(NASA-TP-1466; E-9801) Avail: NTIS HC A02/MF A01 CSCL 09B

A computer program subroutine, WETAIR, was developed to calculate the thermodynamic and transport properties of air-water mixtures. It determines the thermodynamic state from assigned values of temperature and density, pressure and density, temperature and pressure, pressure and entropy, or pressure and enthalpy. The WETAIR calculates the properties of dry air and water (steam) by interpolating to obtain values from property tables. Then it uses simple mixing laws to calculate the properties of air-water mixtures. Properties of mixtures with water contents below 40 percent (by mass) can be calculated at temperatures from 273.2 to 1497 K and pressures to 450 MN/sq m. Dry air properties can be calculated at temperatures as low as 150 K. Water properties can be calculated at temperatures to 1747 K and pressures to 100 MN/sq m. The WETAIR is available in both SFTAN and FORTRAN. J.M.S.

N79-29832* Lockheed Missiles and Space Co., Huntsville, Ala. Research and Engineering Center.
CELFE: COUPLED EULERIAN-LAGRANGIAN FINITE ELEMENT PROGRAM FOR HIGH VELOCITY IMPACT. PART 1: THEORY AND FORMULATION. Final Report, Jun. 1975 - Sep. 1977
C. H. Lee Jan 1978 168 p
(Contract NAS3-18908)
(NASA-CR-159395; LMSC-HREC-TR-D497204-Pt-1) Avail: NTIS HC A08/MF A01 CSCL 09B

A 3-D finite element program capable of simulating the dynamic behavior in the vicinity of the impact point, together with predicting the dynamic response in the remaining part of the structural component subjected to high velocity impact is discussed. The finite algorithm is formulated in a general moving coordinate system. In the vicinity of the impact point contained by a moving failure front, the relative velocity of the coordinate system will approach the material particle velocity. The dynamic behavior inside the region is described by Eulerian formulation based on a hydroelasto-viscoplastic model. The failure front which can be regarded as the boundary of the impact zone is described by a transition layer. The layer changes the representation from the Eulerian mode to the Lagrangian mode outside the failure front by varying the relative velocity of the coordinate system to zero. The dynamic response in the remaining part of the structure described by the Lagrangian formulation is treated using advanced structural analysis. An interfacing algorithm for coupling CELFE with NASTRAN is constructed to provide computational capabilities for large structures. A.R.H.

N79-29833* Lockheed Missiles and Space Co., Huntsville, Ala. Research and Engineering Center.
CELFE: COUPLED EULERIAN-LAGRANGIAN FINITE ELEMENT PROGRAM FOR HIGH VELOCITY IMPACT. PART 2: PROGRAM USER'S MANUAL. Final Report, Jun. 1975 - Sep. 1977
C. H. Lee Jan 1978 270 p
(Contract NAS3-18908)
(NASA-CR-159396; LMSC-HREC-TR-D497204-Pt-2) Avail: NTIS HC A12/MF A01 CSCL 09B

The CELFE computer program and user's manual, together with the execution of the CELFE/NASTRAN system, are described. The execution procedure and the transfer of data between the CELFE and NASTRAN programs are controlled through the use of DATA files in the Univac 1100 system. Five data files are used to control the runstream and data transfer, and three files are used to hold the programs. These files are contained on a single tape. Changes in NASTRAN routines required by the present analysis are also discussed in this report. All the program listings, except the last two files (where the absolute and relocatable elements are stored), are included in the appendixes. Author

N79-33881* Boeing Computer Services, Inc., Seattle, Wash. Energy Technology Applications Div.
AN EXPANDED SYSTEM SIMULATION MODEL FOR SOLAR ENERGY STORAGE (TECHNICAL REPORT), VOLUME 1. Final Report
A. W. Warren Aug 1979 107 p refs 2 Vol.
(Contracts DEN3-42; EX-76-A-31-1026)
(NASA-CR-159601; DOE/NASA/0042-79/1-Vol-1; BCS-40159-1) Avail: NTIS HC A06/MF A01 CSCL 09B

The simulation model for wind energy storage (SIMWEST) program now includes wind and/or photovoltaic systems utilizing any combination of five types of storage (pumped hydro, battery, thermal, flywheel and pneumatic) and is available for the UNIVAC 1100 series and the CDC 6000 series computers. The level of detail is consistent with a role of evaluating the economic feasibility as well as the general performance of wind and/or photovoltaic energy systems. The software package consists of two basic programs and a library of system, environmental, and load components. The first program is a precompiler which generates computer models (in FORTRAN) of complex wind and/or photovoltaic source/storage/application systems, from user specifications using the respective library components. The second program provides the techno-economic system analysis with the respective I/O, the integration of system dynamics, and the iteration for conveyance of variables. A.R.H.

N79-33882* Boeing Computer Services, Inc., Seattle, Wash. Energy Technology Applications Div.
AN EXPANDED SYSTEM SIMULATION MODEL FOR SOLAR ENERGY STORAGE (UNIVAC OPERATION MANUAL REVISIONS), VOLUME 2. Final Report
A. W. Warren Aug 1979 198 p refs 2 Vol.
(Contracts DEN3-42; EX-76-A-31-1026)
(NASA-CR-159602; DOE/NASA/0042-79/2-Vol-2; BCS-40180-2-Rev) Avail: NTIS HC A09/MF A01 CSCL 09B

Additions or revisions of components of the SIMWEST program are provided for insertion into the manual used with the UNIVAC 1100 series computer. A.R.H.

N79-33883* Boeing Computer Services, Inc., Seattle, Wash. Energy Technology Applications Div.
SIMWEST: A SIMULATION MODEL FOR WIND AND PHOTOVOLTAIC ENERGY STORAGE SYSTEMS (CDC USER'S MANUAL), VOLUME 1. Final Report
A. W. Warren and A. W. Esinger Aug 1979 486 p refs 2 Vol.
(Contracts DEN3-42; EX-76-A-31-1026)
(NASA-CR-159607; DOE/NASA/0042-79/3-Vol-1; BCS-40262-1) Avail: NTIS HC A21/MF A01 CSCL 09B

Procedures are given for using the SIMWEST program on CDC 6000 series computers. This expanded software package includes wind and/or photovoltaic systems utilizing any combination of five types of storage (pumped hydro, battery, thermal, flywheel, and pneumatic). A.R.H.

N79-33884* Boeing Computer Services, Inc., Seattle, Wash.
Energy Technology Applications Div.
**SIMWEST: A SIMULATION MODEL FOR WIND AND
PHOTOVOLTAIC ENERGY STORAGE SYSTEMS (CDC
PROGRAM DESCRIPTIONS), VOLUME 2 Final Report**
A. W. Warren, R. W. Edsinger and J. D. Burroughs Aug. 1979
247 p 2 Vol.
(Contracts DEN3-42, EX-76-A-31-1026)
(NASA-CR-159608; DOE/NASA/0042-79; *Vol-2;
BCS-40262-2) Avail. NTIS HC A11/MF A01 CSCL 09B
The computer programs for the CDC version of SIMWEST
(1979 revision) are described. Macro flow charts and source
code listings for each major program entity are presented. A. R. H.

64 NUMERICAL ANALYSIS

Includes iteration, difference equations, and numerical approximation.

N79-28970* National Aeronautics and Space Administration. Lewis Research Center, Cleveland, Ohio.

NUMBERS OF CENTER POINTS APPROPRIATE TO BLOCKED RESPONSE SURFACE EXPERIMENTS

Arthur G. Holms. 1979. 34 p. refs. Presented at 139th Ann. Meeting of the Am. Statistical Assoc., Washington, D. C., 13-16 Aug. 1979.

(NASA-TM-79201 E-082) Avail. NTIS HC A03/MF A01 CSCI 12A

Tables are given for the numbers of center points to be used with blocked sequential designs of composite response surface experiments as used in empirical optimum seeking. The star point radii for exact orthogonal blocking is presented. The center point options varied from a lower limit of one to an upper limit equal to the numbers proposed by Box and Hunter for approximate rotatability and uniform variance, and exact orthogonal blocking. Some operating characteristics of the proposed options are described. S E S

A79-40494 * Acceleration of linear and logarithmic convergence. D. A. Smith and W. F. Ford (NASA, Lewis Research Center, Computer Services Div., Cleveland, Ohio). *SIAM Journal on Numerical Analysis*, vol. 16, Apr. 1979, p. 223-240. 39 refs. Grant No. N5G-3160.

Eleven different methods for accelerating convergence of sequences and series have been tested and compared on a wide range of test problems, including both linearly and logarithmically convergent series, monotone and alternating series. All but one of these methods are already in the literature, and they include both linear and nonlinear methods. The only methods found to accelerate convergence across the board were the u and v transforms of Levin and the theta algorithm of Brezinski. The paper gives detailed comparisons of all the tested methods on the basis of number of correct digits in the answer as a function of number of terms of the series used. A theorem of Germain-Bonne states that methods of a certain form which are exact on geometric series will accelerate linear convergence. The theorem applies to theta sub 2, and we have extended it to apply to Levin's transforms. No corresponding theorem is known for logarithmic convergence, but u , v , and theta are exact on certain large classes of logarithmic series, and all tested methods lacking this property failed to accelerate some logarithmically convergent series.

(Author)

65 STATISTICS AND PROBABILITY

Includes data sampling and smoothing, Monte Carlo method, and stochastic processes.

N79-23735* National Aeronautics and Space Administration, Lewis Research Center, Cleveland, Ohio.

MAXIMUM LIKELIHOOD ESTIMATION FOR LIFE DISTRIBUTIONS WITH COMPETING FAILURE MODES

Steven M. Sidik. 1979. 41 p. refs. Presented at the Ann. Meeting of the Am. Statist. Assoc., Washington, D. C., 13-16 Aug. 1979.

(NASA TM-79126, E-9962) Avail. NTIS HC A03/MF A01 CSCL 14D

Systems which are placed on test at time zero, function for a period and die at some random time were studied. Failure may be due to one of several causes or modes. The parameters of the life distribution may depend upon the levels of various stress variables the item is subject to. Maximum likelihood estimation methods are discussed. Specific methods are reported for the smallest extreme value distributions of life. Monte Carlo results indicate the methods to be promising. Under appropriate conditions, the location parameters are nearly unbiased, the scale parameter is slightly biased, and the asymptotic covariances are rapidly approached. S.E.S.

A79-49528 * Maximum likelihood estimation for life distributions with competing failure modes. S. M. Sidik (NASA, Lewis Research Center, Cleveland, Ohio). *American Statistical Association, Annual Meeting, 39th, Washington, D.C., Aug. 13-16, 1979, Paper*. 37 p. 13 refs.

The general model for the competing failure modes assuming that location parameters for each mode are expressible as linear functions of the stress variables and the failure modes act independently is presented. The general form of the likelihood function and the likelihood equations are derived for the extreme value distributions, and solving these equations using nonlinear least squares techniques provides an estimate of the asymptotic covariance matrix of the estimators. Monte Carlo results indicate that, under appropriate conditions, the location parameters are nearly unbiased, the scale parameter is slightly biased, and the asymptotic covariances are rapidly approached. A.T.

A79-49529 * Numbers of center points appropriate to blocked response surface experiments. A. G. Holms (NASA, Lewis Research Center, Cleveland, Ohio). *American Statistical Association, Annual Meeting, 139th, Washington, D.C., Aug. 13-16, 1979, Paper*. 33 p. 16 refs.

Tables are given for the numbers of center points to be used with blocked sequential designs of composite response surface experiments as used in empirical optimum seeking. The tables also give the star point radii for exact orthogonal blocking. The center point options vary from a lower limit of one to an upper limit equal to the numbers proposed by Box and Hunter for approximate rotatability and uniform variance, and exact orthogonal blocking. Some operating characteristics of the proposed options are described.

(Author)

66 SYSTEMS ANALYSIS

Includes mathematical modeling; network analysis; and operations research.

N79-29938* # National Aeronautics and Space Administration, Lewis Research Center, Cleveland, Ohio

COMPUTERIZED SYSTEMS ANALYSIS AND OPTIMIZATION OF AIRCRAFT ENGINE PERFORMANCE, WEIGHT, AND LIFE CYCLE COSTS

Laurence H. Fishbach. 1979. 22 p. refs. Presented at Flight Mech. Panel Symp. on the Use of Computers as a Design Tool, Munich, 3-6 Sep. 1979, sponsored by AGARD (NASA TM-79221, E-112). Avail. NTIS HC A02/MF A01 CSCL 12B

The computational techniques utilized to determine the optimum propulsion systems for future aircraft applications and to identify system tradeoffs and technology requirements are described. The characteristics and use of the following computer codes are discussed: (1) NNEP - a very general cycle analysis code that can assemble an arbitrary matrix fans, turbines, ducts, shafts, etc., into a complete gas turbine engine and compute on- and off-design thermodynamic performance; (2) WATE - a preliminary design procedure for calculating engine weight using the component characteristics determined by NNEP; (3) POD DRG - a table look-up program to calculate wave and friction drag of nacelles; (4) LIFCYC - a computer code developed to calculate life cycle costs of engines based on the output from WATE; and (5) INSTAL - a computer code developed to calculate installation effects, inlet performance and inlet weight. Examples are given to illustrate how these computer techniques can be applied to analyze and optimize propulsion system fuel consumption, weight, and cost for representative types of aircraft and missions.

J M S

70 PHYSICS (GENERAL)

For geophysics see 46 *Geophysics* For astrophysics
see 90 *Astrophysics* For solar physics see 92 *Solar physics*

A79-50938 * Effects of bulk and surface conductivity on the potential developed by dielectrics exposed to electron beams. M. Rotenberg (Systems, Science and Software, California, University, La Jolla, Calif.), M. J. Mandell, and D. E. Parks (Systems, Science and Software, La Jolla, Calif.). *Journal of Applied Physics*, vol. 50, Sept. 1979, p. 5823-5825, 7 refs. Contract No. NAS3-21050.

The charging and discharging of a dielectric material which has bulk and surface conductivities is discussed. Two model problems are solved. In the first problem, a semi-infinite dielectric plane, attached to an infinite grounded conducting substrate and exposed to a monoenergetic electron beam, is analyzed. Bulk and surface conductivities and secondary emission characteristics are taken into account as parameters. In the second problem the dielectric is charged but the electron beam is shut off so only the bulk and surface conductivities enter the calculation. The principal result of the latter calculation is to show that steep tangential gradients develop in the presence of a surface conductivity during decay, and that for asymptotic times the temporal behavior, for a fixed position, is proportional to the square root of t rather than exponential, as expected in the presence of a bulk conductivity. (Author)

71 ACOUSTICS

Includes sound generation, transmission and attenuation

For noise pollution see 45 Environment Pollution

N79-14871* National Aeronautics and Space Administration, Lewis Research Center, Cleveland, Ohio.

SOUND-SUPPRESSING STRUCTURE WITH THERMAL RELIEF Patent

Dudley O. Nash (GE, Cincinnati) and Joseph Holowach, inventors (to NASA) Issued 15 Aug 1978 5 p Filed 2 Jul 1976 Sponsored by NASA

(NASA-Case-LFW-12658-1; US-Patent-4,106,587;

US-Patent-Appl-SN-702115; US-Patent-Class-181-213;

US-Patent-Class-181-222; US-Patent-Class-181-190;

US-Patent-Class-181-293) Avail: US Patent and Trademark Office CSCL 20A

Sound-suppressing structure comprising stacked acoustic panels wherein the inner high frequency panel is mounted for thermal expansion with respect to the outer low frequency panel is discussed. Slip joints eliminate the potential for thermal stresses, and a thermal expansion gap between the panels provides for additional relative thermal growth while reducing heat convection into the low frequency panel.

Official Gazette of the U.S. Patent and Trademark Office

N79-15757* National Aeronautics and Space Administration, Lewis Research Center, Cleveland, Ohio

FEASIBILITY OF WING SHIELDING OF THE AIRPLANE INTERIOR FROM THE SHOCK NOISE GENERATED BY SUPERSONIC TIP SPEED PROPELLERS

James H. Dittmar Dec 1978 25 p refs

(NASA-TM-79042; E-9845) Avail: NTIS HC A02/MF A01 CSCL 20A

A high tip speed turboprop is being considered as a future energy conservative airplane. The high tip speed of the propeller, combined with the speed of the airplane, results in supersonic relative flow on the propeller tips. These supersonic blade sections could generate noise that is a cabin environment problem. The feasibility of using wing shielding to lessen the impact of this supersonic propeller noise was investigated. An analytical model is chosen which considers that shock waves are associated with the propeller tip flow and indicates how they would be prevented from impinging on the airplane fuselage. An example calculation is performed where a swept wing is used to shield the fuselage from significant portions of the propeller shock waves. A R H

N79-15758* National Aeronautics and Space Administration, Lewis Research Center, Cleveland, Ohio

ONE NOISE OF THREE SUPERSONIC HELICAL TIP SPEED PROPELLERS IN A WIND TUNNEL AT 0.8 MACH NUMBER

James H. Dittmar, Bernard J. Blaha, and Robert J. Jeracki Dec 1978 22 p refs

(NASA-TM-79046; E-9854) Avail: NTIS HC A02/MF A01 CSCL 20A

Three supersonic helical tip speed propellers were tested in the NASA Lewis 8- by 6-foot wind tunnel. Noise data were obtained while these propellers were operating at a simulated cruise condition. The walls of this tunnel were not acoustically treated and therefore this was not an ideal location for taking noise data, but it was thought that the differences in noise among the three propellers would be meaningful. The straight bladed propeller which did not incorporate sweep was the noisiest with the aerodynamically swept propeller only slightly quieter. However, the acoustically swept propeller was significantly quieter than the straight propeller, thereby indicating the merit of this design technique. Author

N79-15759* National Aeronautics and Space Administration, Lewis Research Center, Cleveland, Ohio

OPTIMIZED MULTISECTIONED ACOUSTIC LINERS

Kenneth J. Baumeister 1979 17 p refs Presented at the 17th Aerospace Sci. Meeting, New Orleans, 15-17 Jan 1979, sponsored by AIAA

(NASA-TM-79028; E-9823) Avail: NTIS HC A02/MF A01 CSCL 20A

New calculations show that segmenting is most efficient at high frequencies with relatively long duct lengths where the attenuation is low for both uniform and segmented liners. Statistical considerations indicate little advantage in using optimized liners with more than two segments while the bandwidth of an optimized two-segment liner is shown to be nearly equal to that of a uniform liner. Multielement liner calculations show a large degradation in performance due to changes in assumed input modal structure. Computer programs are used to generate theoretical attenuations for a number of liner configurations for liners in a rectangular duct with no mean flow. Overall, the use of optimized multisectioned liners fails to offer sufficient advantage over a uniform liner to warrant their use except in low frequency single mode application. Author

N79-15756* National Aeronautics and Space Administration, Lewis Research Center, Cleveland, Ohio

MODAL PROPAGATION ANGLES IN A CYLINDRICAL DUCT WITH FLOW AND THEIR RELATION TO SOUND RADIATION

Edward J. Rice, Marcus F. Heidmann, and Thomas G. Sofrin (Pratt and Whitney Aircraft, East Hartford, Conn.) Jan 1979 12 p refs Presented at 17th Aerospace Sci. Meeting, New Orleans, La. 15-17 Jan 1979, sponsored by AIAA

(NASA-TM-79030; E-9826) Avail: NTIS HC A02/MF A01 CSCL 20A

The main emphasis is upon the propagation angle with respect to the duct axis and its relation to the far-field acoustic radiation pattern. When the steady flow Mach number is accounted for in the duct, the propagation angle in the duct is shown to be coincident with the angle of the principal lobe of far-field radiation obtained using the Wiener-Hopf technique. Different Mach numbers are allowed within the duct and in the external field. For static tests with a steady flow in an inlet but with no external Mach number the far-field radiation pattern is shifted considerably toward the inlet axis when compared to zero Mach number radiation theory. As the external Mach number is increased the noise radiation pattern is shifted away from the inlet axis. The theory is developed using approximations for sound propagation in circular ducts. An exact analysis using Henkel function solutions for the zero Mach number case is given to provide a check of the simpler approximate theory. Author

N79-16644* National Aeronautics and Space Administration, Lewis Research Center, Cleveland, Ohio

THREE DIMENSIONAL FINITE ELEMENT ELASTIC ANALYSIS OF A THERMALLY CYCLED SINGLE EDGE WEDGE GEOMETRY SPECIMEN

Peter T. Bizon, Richard J. Hill (AFAPL), Bruce P. Williams, Sandra K. Draks (AFAPL), and Jeffrey L. Kladden (AFAPL) Jan 1979 53 p refs

(NASA-TM-79026; E-9861) Avail: NTIS HC A04/MF A01 CSCL 20A

An elastic stress analysis was performed on a wedge specimen (prismatic bar with single wedge cross section) subjected to thermal cycles in fluidized beds. Seven different combinations consisting of three alloys (NASA TAZ 8A, 316 stainless steel, and A 286) and four thermal cycling conditions were analyzed. The analyses were performed as a joint effort of two laboratories using different models and computer programs (NASTRAN and ISO3DQ). Stress, strain, and temperature results are presented. Author

N79-16645* National Aeronautics and Space Administration
Lewis Research Center, Cleveland, Ohio
**FULL SCALE ENGINE TESTS OF BULK ABSORBER
ACOUSTIC INLET TREATMENT**
L J Heidelberg and L Homyak 1979 16 p refs Presented
at the 5th Aeroacoustics Conf., Seattle, 12-14 Mar 1979,
sponsored by AIAA
(NASA TM 79079, E-9899) Avail NTIS HC A02/MF A01
CSCL 20A

Three different densities of Kevlar bulk absorber fan inlet
treatment were tested on a YF 102 turbofan engine. This bulk
absorber material may have potential for flight application. Farfield
noise measurements were made and the attenuation properties
of the three treatment densities were compared. In addition, the
best bulk treatment was compared to the best single degree of
freedom, SDOF (honeycomb and perforated cover sheet) treatment
from another investigation. Although the density was varied over
a large range (3 to 1) the effect on attenuation was small. The
highest density treatment, 118 lb/cubic ft, had a somewhat
broader attenuation bandwidth. The comparison of the best bulk
and SDOF treatments showed the bulk to have a much greater
attenuation bandwidth. At the design frequency both types of
treatment had almost equal performance. Author

N79-16646* National Aeronautics and Space Administration
Lewis Research Center, Cleveland, Ohio
**MODAL PROPAGATION ANGLES IN DUCTS WITH SOFT
WALLS AND THEIR CONNECTION WITH SUPPRESSOR
PERFORMANCE**
Edward J Rice 1979 16 p refs Presented at the 5th
Aeroacoustics Conf., Seattle, 12-14 Mar 1979, sponsored by
AIAA
(NASA TM 79081, E 9902) Avail NTIS HC A02/MF A01
CSCL 20A

The angles of propagation of the wave fronts associated
with duct modes are derived for a cylindrical duct with soft
walls (acoustic suppressors) and a uniform steady flow. The angle
of propagation with respect to the radial coordinate (angle of
incidence on the wall) is shown to be a better correlating parameter
for the optimum wall impedance of spinning modes than the
previously used mode cutoff ratio. Both the angle of incidence
upon the duct wall and the propagation angle with respect to
the duct axis are required to describe the attenuation of a
propagating mode. Using the modal propagation angles, a
geometric acoustics approach to suppressor acoustic performance
was developed. Results from this approximate method were
compared to exact modal propagation calculations to check the
accuracy of the approximate method. The results are favorable
except in the immediate vicinity of the modal optimum impedance
where the approximate method yields about one half of the exact
maximum attenuation. Author

N79-16647* National Aeronautics and Space Administration
Lewis Research Center, Cleveland, Ohio
**EFFECTS OF INFLOW DISTORTION PROFILES ON FAN
TONE NOISE CALCULATED USING A 3 D THEORY**
Hiroshi Kobayashi and John F. Groeneweg 1979 18 p refs
Presented at the 5th Aeroacoustics Conf., Seattle, Wash.,
12-14 Mar 1979, sponsored by AIAA
(NASA TM 79082, E 9904) Avail NTIS HC A02/MF A01
CSCL 20A

Calculations of the fan tone acoustic power and modal
structure generated by complex distortions in axial inflow velocity
are presented. The model used treats the motor as a rotating
three dimensional cascade and calculates the acoustic field from
the distortion produced dipole distribution on the blades including
noncompact source effects. Radial and circumferential distortion
shapes are synthesized from Fourier Bessel components represent-
ing individual distortion modes. The relation between individual
distortion modes and the generated acoustic modes is examined
for particular distortion cases. Comparisons between theoretical
and experimental results for distortions produced by wakes from
upstream radial rods show that the analysis is a good predictor
of acoustic power dependence on disturbance strength. Author

N79-17659* National Aeronautics and Space Administration
Lewis Research Center, Cleveland, Ohio
**COMPUTATION OF ATMOSPHERIC ATTENUATION OF
SOUND FOR FRACTIONAL OCTAVE BANDS**
Francis J Montegani Feb 1979 32 p refs
(NASA-TP 1412, E-9763) Avail NTIS HC A03/MF A01 CSCL
20A

Correct methods of accounting for atmospheric attenuation
in band data requiring consideration of the integrated effect across
the bands of the specific distance involved are discussed. Computer
programs are provided that are understandable, efficient, and
simple to use. It is hoped that this will facilitate more widespread
use of correct computational methods, especially where routine
computer processing of data is employed. J.M.S.

N79-20819* National Aeronautics and Space Administration
Lewis Research Center, Cleveland, Ohio
**EXPERIMENTAL STUDY OF COAXIAL NOZZLE EXHAUST
NOISE**
Jack H Goodykoontz and James R Stone 1979 29 p refs
Presented at 5th Aeroacoustics Conf., Seattle, Wash., 12-14 Mar.
1979, sponsored by AIAA
(NASA TM 79090, E-9914) Avail NTIS HC A03/MF A01
CSCL 20A

Experimental results are presented for static acoustic model
tests of various geometrical configurations of coaxial nozzles
operating over a range of flow conditions. The geometrical
configurations consisted of nozzles with coplanar and non-coplanar
exit planes and various exhaust area ratios. Primary and secondary
nozzle flows were varied independently over a range of nozzle
pressure ratios from 1.4 to 3.0 and gas temperatures from 280
to 1100 K. Acoustic data are presented for the conventional
mode of coaxial nozzle operation as well as for the inverted
velocity profile mode. Comparisons are presented to show the
effect of configuration and flow changes on the acoustic
characteristics of the nozzles. Author

N79-20830* National Aeronautics and Space Administration
Lewis Research Center, Cleveland, Ohio
**EFFECTS OF GEOMETRIC AND FLOW FIELD VARIABLES
ON INVERTED-VELOCITY-PROFILE COAXIAL JET NOISE**
James R Stone 1979 30 p refs Presented at the 5th
Aeroacoustics Conf., Seattle, 12-14 Mar 1979, sponsored by
AIAA
(NASA TM 79095, E 9919) Avail NTIS HC A03/MF A01
CSCL 20A

Relationships between the noise generation characteristics
and the flow field characteristics for inverted-velocity profile
coaxial jets are discussed. Noise measurements were made at
four different sideline distances in order to determine the
apparent noise source locations and flow field characteristics
were determined from jet plume pressure/temperature surveys.
These relationships are based on a published NASA Lewis
prediction model, the basic assumptions of which are shown to
be consistent with the experimental data reported herein.
Improvements to the noise prediction procedure, on the basis of
the present study, are included, which increase the accuracy of
the high frequency noise prediction. A.R.H.

N79-24770* National Aeronautics and Space Administration
Lewis Research Center, Cleveland, Ohio
**AN IMPROVED METHOD FOR PREDICTING THE EFFECTS
OF FLIGHT ON JET MIXING NOISE**
James R Stone 1979 28 p refs Presented at the 97th
Meeting of the Acoustical Soc. of America, Cambridge, Mass.,
11-15 Jun 1979
(NASA TM 79155, E 0111) Avail NTIS HC A02/MF A01 CSCL
20A

The NASA method (1976) for predicting the effects of flight
on jet mixing noise was improved. The earlier method agreed
reasonably well with experimental flight data for jet velocities
up to about 520 m/sec (approximately 1700 ft/sec). The poorer
agreement at high jet velocities appeared to be due primarily to
the manner in which supersonic convection effects were
formulated. The purely empirical supersonic convection formula-

of the earlier method was replaced by one based on theoretical considerations. Other improvements of an empirical nature included were based on model-jet/free-jet simulated flight tests. The revised prediction method is presented and compared with experimental data obtained from the Bertin Aerotrain with a J85 engine, the DC-10 airplane with JT9D engines, and the DC-9 airplane with refanned JT8D engines. It is shown that the new method agrees better with the data base than a recently proposed SAE method. A R H

N79-26840*# National Aeronautics and Space Administration
Lewis Research Center, Cleveland, Ohio
TONE NOISE OF THREE SUPERSONIC HELICAL TIP SPEED PROPELLERS IN A WIND TUNNEL

James H. Dittmar, Robert J. Jeracki, and Bernard J. Blaha. 1979. 66 p. refs. Presented at 97th Meeting of the Acoustical Soc. of Am., Cambridge, Mass., 11-15 Jun. 1979. (NASA-TM-79167, E-030) Avail NTIS HC A04/MF A01 CSDL 20A

Three supersonic helical tip speed propellers were tested in the NASA Lewis 8- by 6-foot wind tunnel. This is a perforated-wall wind tunnel but it does not have acoustic damping material on its walls. The propellers were tested at tunnel through flow Mach numbers of 0.6, 0.7, 0.75, 0.8, and 0.85 with different rotational speeds and blade setting angles. The three propellers, which had approximately the same aerodynamic performance, incorporated different plan forms and different amounts of sweep and yielded different near field noise levels. The acoustically designed propeller had 45 deg of tip sweep and was significantly quieter at $M = 0.8$ cruise than the straight bladed propeller. The intermediate 30 deg tip sweep propeller, which was swept for aerodynamic purposes, exhibited noise that was between the other two propellers. Noise trends with varying helical tip Mach number and blade loading were also observed. Author

N79-26841*# National Aeronautics and Space Administration
Lewis Research Center, Cleveland, Ohio
ASSESSMENT AT FULL SCALE OF NOZZLE/WING GEOMETRY EFFECTS ON OTW AERO ACOUSTIC CHARACTERISTICS

D. Groesbeck and U. vonGlahn. 1979. 31 p. refs. (NASA TM 79168, E-031) Avail NTIS HC A03/MF A01 CSDL 20A

The effects on acoustic characteristics of nozzle type and location on a wing for STOL engine over the wing configurations are assessed at full scale on the basis of model-scale data. Three types of nozzle configurations are evaluated: a circular nozzle with external deflector mounted above the wing; a slot nozzle with external deflector mounted on the wing; and a slot nozzle mounted on the wing. Nozzle exhaust plane locations with respect to the wing leading edge are varied from 10 to 46 percent chord (flaps retracted) with flap angles of 20 (takeoff altitude) and 60 (approach attitude). Perceived noise levels (PNL) are calculated as a function of flyover distance at 152 m altitude. From these plots, static EPNL values, defined as flyover relative noise levels, are calculated and plotted as a function of lift and thrust ratios. From such plots the acoustic benefits attributable to variations in nozzle/deflector/wing geometry at full scale are assessed for equal aerodynamic performance. Author

N79-27930*# National Aeronautics and Space Administration
Lewis Research Center, Cleveland, Ohio
TRAILING EDGE NOISE DATA WITH COMPARISON TO THEORY

W. Olsen and D. Boldman. 1979. 30 p. refs. Presented at 12th Fluid and Plasma Dynamics Conf., Williamsburg, Va., 23-25 Jul. 1979, sponsored by AIAA. (NASA TM 79208, E-093, AIAA 79-1524) Avail NTIS HC A03/MF A01 CSDL 20A

The noise emission generated by the passage of a turbulent airstream over the trailing edge of a semi-infinite plate was measured over a large range of airstream velocity and plate geometry. The experiment was designed to validate trailing edge noise theories. The results show that the peak of the radiation

pattern moves from an upstream to a downstream direction as the velocity increases. The measured radiation pattern of the noise was in excellent agreement with that predicted by the recent theory of Goldstein. As predicted, the pattern shape was independent of the nature of the turbulence producing the noise. Author

N79-31002*# National Aeronautics and Space Administration
Lewis Research Center, Cleveland, Ohio
DISPERSION OF SOUND IN A COMBUSTION DUCT BY FUEL DROPLETS AND SOOT PARTICLES

J. H. Miles and D. D. Raftopoulos (Toledo Univ., Ohio). 1979. 29 p. refs. Presented at 98th Meeting of the Acoustical Soc. of Am., Salt Lake City, 26-30 Nov. 1979. (NASA-TM-79236, E-142) Avail NTIS HC A03/MF A01 CSDL 20A

Dispersion and attenuation of acoustic plane wave disturbances propagating in a ducted combustion system are studied. The dispersion and attenuation are caused by fuel droplet and soot emissions from a jet engine combustor. The attenuation and dispersion are due to heat transfer and mass transfer and viscous drag forces between the emissions and the ambient gas. Theoretical calculations show sound propagation at speeds below the isentropic speed of sound at low frequencies. Experimental results are in good agreement with the theory. Author

A79-19581*# Optimized multisectioned acoustic liners. K. J. Baumeister (NASA, Lewis Research Center, Cleveland, Ohio). *American Institute of Aeronautics and Astronautics, Aerospace Sciences Meeting, 17th, New Orleans, La., Jan. 15-17, 1979, Paper 79-0182*. 10 p. 24 refs.

A critical examination is presented of the use of optimized axially segmented acoustic liners to increase the attenuation of a liner. New calculations show that segmenting is most efficient at high frequencies with relatively long duct lengths where the attenuation is low for both uniform and segmented liners. Statistical considerations indicate little advantage in using optimized liners with more than two segments while the bandwidth of an optimized two-segment liner is shown to be nearly equal to that of a uniform liner. Multielement liner calculations show a large degradation in performance due to changes in assumed input modal structure. Finally, in order to substantiate previous and future analytical results, in-house (finite difference) and contractor (mode matching) programs are used to generate theoretical attenuations for a number of liner configurations for liners in a rectangular duct with no mean flow. Overall, the use of optimized multisectioned liners (sometimes called phased liners) fails to offer sufficient advantage over a uniform liner to warrant their use except in low frequency single mode application. (Author)

A79-19582*# Modal propagation angles in a cylindrical duct with flow and their relation to sound radiation. E. J. Rice, M. F. Heidmann (NASA, Lewis Research Center, Cleveland, Ohio), and T. G. Seifrin (United Technologies Corp., Pratt and Whitney Aircraft Group, East Hartford, Conn.). *American Institute of Aeronautics and Astronautics, Aerospace Sciences Meeting, 17th, New Orleans, La., Jan. 15-17, 1979, Paper 79-0183*. 11 p. 19 refs.

The angles of propagation for the wave front making up a duct mode are presented with the Mach number in the duct. Approximate equations are derived to provide simple utilitarian expressions. These expressions are valid only near the outer wall which is the most important region since the bulk of the acoustic intensity is located there. Exact solutions using Hankel functions are given in an appendix. These data corroborate the approximate solution accuracy near the outer wall. The axial propagation angle is used to infer information about the far field radiation pattern. The resultant axial angle of propagation in the duct is shown to agree exactly with the peak of the principal lobe to far field radiation obtained from formal radiation calculations when the Mach number is uniform everywhere. The obtained solution is extended to cover the case of different

Mach numbers inside and outside the duct for which exact calculations have not been available for engine inlet configurations.
G.R.

A79-25946 * Numerical spatial marching techniques in duct acoustics. K. J. Baumeister (NASA, Lewis Research Center, Cleveland, Ohio). *Acoustical Society of America, Journal*, vol. 65, Feb. 1979, p. 297-306. 23 refs.

Direct calculation of the internal structure of a ducted noise source from farfield pressure measurements is regarded as an initial value problem, where the pressure and pressure gradient (farfield impedance) are assumed to be known along a line in the farfield. If pressure and impedance are known at the boundary of the farfield, the pressure can be uniquely determined in the vicinity of the inlet and inside the inlet ducting. A marching procedure is developed which, with this information obtained from measurements, enables a description of a ducted noise source. The technique uses a finite difference representation of the homogeneous Helmholtz equation.
P.T.H.

A79-26880 * Modal propagation angles in ducts with soft walls and their connection with suppressor performance. E. J. Rice (NASA, Lewis Research Center, Acoustics Section, Cleveland, Ohio). *American Institute of Aeronautics and Astronautics, Aeroacoustics Conference, 5th, Seattle, Wash., Mar. 12-14, 1979, Paper 79-0624*. 10 p. 8 refs.

The angles of propagation of the wave fronts associated with duct modes are derived for a cylindrical duct with soft walls (acoustic suppressors) and a uniform steady flow. The angle of propagation with respect to the radial coordinate (angle of incidence on the wall) is shown to be a better correlating parameter for the optimum wall impedance of spinning modes than the previously used mode cutoff ratio. Both the angle of incidence upon the duct wall and the propagation angle with respect to the duct axis are required to describe the attenuation of a propagating mode. Using the modal propagation angles, a geometric acoustics approach to suppressor acoustic performance was developed. Results from this approximate method were compared to exact modal propagation calculations to check the accuracy of the approximate method. The results are favorable except in the immediate vicinity of the modal optimum impedance where the approximate method yields about one-half of the exact maximum attenuation.
(Author)

A79-26911 * Effects of inflow distortion profiles on fan tone noise calculated using a 3-D theory. H. Kobayashi (NASA, Lewis Research Center, Cleveland, Ohio; National Aerospace Laboratory, Tokyo, Japan) and J. F. Groeneweg (NASA, Lewis Research Center, Turbomachinery Noise Section, Cleveland, Ohio). *American Institute of Aeronautics and Astronautics, Aeroacoustics Conference, 5th, Seattle, Wash., Mar. 12-14, 1979, Paper 79-0577*. 11 p. 12 refs.

Calculations of the fan tone acoustic power and modal structure generated by complex distortions in axial inflow velocity are presented. The model used treats the rotor as a rotating three-dimensional cascade and calculates the acoustic field from the distortion-produced dipole distribution on the blades including noncompact source effects. Radial and circumferential distortion shapes are synthesized from Fourier-Bessel components representing individual distortion modes. The relation between individual distortion modes and the generated acoustic modes is examined for particular distortion cases. Comparisons between theoretical and experimental results for distortions produced by wakes from upstream radial rods show that the analysis is a good predictor of acoustic power dependence on disturbance strength.
(Author)

A79-26963 * Experimental study of coaxial nozzle exhaust noise. J. H. Goodykoontz and J. R. Stone (NASA, Lewis Research Center, Jet Acoustics Branch, Cleveland, Ohio). *American Institute of Aeronautics and Astronautics, Aeroacoustics Conference, 5th, Seattle, Wash., Mar. 12-14, 1979, Paper 79-0631*. 29 p. 11 refs.

Experimental results are presented for static acoustic model tests of various geometrical configurations of coaxial nozzles operating over a range of flow conditions. The geometrical configurations consisted of nozzles with coplanar and non-coplanar exit planes and various exhaust area ratios. Primary and secondary nozzle flows were varied independently over a range of nozzle pressure ratios from 1.4 to 3.0 and gas temperatures from 280 to 1100 K. Acoustic data are presented for the conventional mode of coaxial nozzle operation as well as for the inverted velocity profile mode. Comparisons are presented to show the effect of configuration and flow changes on the acoustic characteristics of the nozzles.
(Author)

A79-32126 * Effects of geometric and flow-field variables on inverted-velocity-profile coaxial jet noise and source distributions. J. R. Stone, J. H. Goodykoontz, and O. A. Gutierrez (NASA, Lewis Research Center, Jet Acoustics Branch, Cleveland, Ohio). *American Institute of Aeronautics and Astronautics, Aeroacoustics Conference, 5th, Seattle, Wash., Mar. 12-14, 1979, Paper 79-0635*. 27 p. 18 refs.

This paper presents relationships between the noise generation characteristics and the flow-field characteristics for inverted-velocity-profile coaxial jets. Noise measurements were made at four different sideline distances in order to determine the apparent noise source locations, and flow-field characteristics were determined from jet plume pressure/temperature surveys. These relationships are based on a published NASA Lewis prediction model, the basic assumptions of which are shown to be consistent with the experimental data reported herein. Improvements to the noise prediction procedure, on the basis of the present study, are included, which increase the accuracy of the high-frequency noise prediction.
(Author)

A79-39801 * Tone noise of three supersonic helical tip speed propellers in a wind tunnel. J. H. Dittmar, R. J. Jeracki, and B. J. Blaha (NASA, Lewis Research Center, Cleveland, Ohio). *Acoustical Society of America, Meeting, 97th, Cambridge, Mass., June 11-15, 1979, Paper 62* p. 7 refs.

Three eight bladed supersonic helical tip speed propellers were tested in the NASA Lewis Wind Tunnel at through flow Mach numbers of 0.6, 0.7, 0.75, 0.8, and 0.85. Such propellers are being considered as propulsors for a future energy conservative aircraft. The three propellers of equal performance, incorporate different plan forms and different amounts of sweep in order to investigate their noise generation, which could cause a cabin environment problem. The acoustically designed propeller SR-3 had 45 deg of tip sweep and was significantly quieter at Mach 0.8 cruise than the straight bladed propeller, SR-2. An intermediate 30 deg tip sweep propeller, SR-1m exhibited a noise level between the other two. Enhanced pressure-time traces indicated that SR-2 and SR-1m exhibited shock-like pressure traces at Mach 0.8 cruise while the SR-3 did not. Noise trends with varying helical tip Mach number and blade loading were also observed.
M.E.P.

A79-39802 * Assessment at full scale of nozzle/wing geometry effects on OTW aeroacoustic characteristics. D. Groesbeck and U. von Gihm (NASA, Lewis Research Center, Cleveland, Ohio). *Acoustical Society of America, Meeting, 97th, Cambridge, Mass., June 11-15, 1979, Paper 29* p. 5 refs.

The effects on acoustic characteristics of nozzle type and location on a wing for STOL engine over-the-wing configurations are assessed at full scale on the basis of model scale data. Three types of nozzle configurations are evaluated: a circular nozzle with external deflector mounted above the wing, a slot nozzle with external deflector mounted on the wing and a slot nozzle mounted on the wing. Nozzle exhaust plane locations with respect to the wing leading edge are varied from 10 to 46 percent chord (flaps retracted) with

flap angles of 20 deg (take-off attitude) and 60 deg (approach attitude). Perceived noise levels (PNL) are calculated as a function of flyover distance at 152 m altitude. From these plots, static EPNL values, defined as flyover relative noise levels, are calculated and plotted as a function of lift and thrust ratios. From such plots the acoustic benefits attributable to variations in nozzle/deflector/wing geometry at full scale are assessed for equal aerodynamic performance. (Author)

A79-39803 * # **An improved method for predicting the effects of flight on jet mixing noise.** J. R. Stone (NASA, Lewis Research Center, Cleveland, Ohio). *Acoustical Society of America, Meeting, 97th, Cambridge, Mass., June 11-15, 1979, Paper, 26 p.* 20 refs.

A method for predicting the effects of flight on jet mixing noise has been developed on the basis of the jet noise theory of Ffowcs-Williams (1963) and data derived from model-jet/free-jet simulated flight tests. Predicted and experimental values are compared for the J85 turbojet engine on the Bertin Aerobrain, the low-bypass refanned JT8D engine on a DC-9, and the high-bypass JT9D engine on a DC-10. Over the jet velocity range from 280 to 680 m/sec, the predictions show a standard deviation of 1.5 dB.

J.M.B.

A79-39975 * # **Loudness of steady sounds - A new theory.** W. L. Howes (NASA, Lewis Research Center, Cleveland, Ohio). *Acustica*, vol. 41, no. 5, 1979, p. 277-320. 87 refs.

A new mathematical theory for calculating the loudness of steady sounds from power summation and frequency interaction, based on psychoacoustic and physiological information, assumes that loudness is a subjective measure of the electrical energy transmitted along the auditory nerve to the central nervous system. The auditory system consists of the mechanical part modeled by a bandpass filter with a transfer function dependent on the sound pressure, and the electrical part where the signal is transformed into a half-wave reproduction represented by the electrical power in impulsive discharges transmitted along neurons comprising the auditory nerve. In the electrical part the neurons are distributed among artificial parallel channels with frequency bandwidths equal to 'critical bandwidths for loudness', within which loudness is constant for constant sound pressure. The total energy transmitted to the central nervous system is the sum of the energy transmitted in all channels, and the loudness is proportional to the square root of the total filtered sound energy distributed over all channels. The theory explains many psychoacoustic phenomena such as audible beats resulting from closely spaced tones, interaction of sound stimuli which affect the same neurons affecting loudness, and of individually subliminal sounds becoming audible if they lie within the same critical band. (Author)

A.T.

A79-46707 * # **A statistical theory of sound radiation from a two-dimensional lined duct.** Y. C. Cho (NASA, Lewis Research Center, Cleveland, Ohio, Joint Institute for Advancement of Flight Sciences, Hampton, Va.) and W. R. Watson (NASA, Langley Research Center, Hampton, Va.). *American Institute of Aeronautics and Astronautics, Fluid and Plasma Dynamics Conference, 12th, Williamsburg, Va., July 23-25, 1979, Paper 79-1521.* 5 p. 7 refs.

A statistical theory coupled with a finite element theory is employed for investigation of sound radiation from a two-dimensional lined duct. The analysis does not utilize duct modes, and can be applied to a non-uniform duct with variable wall liner properties. Numerical results are presented for various shapes of the incident wave. The results are in good agreement with the Wiener-Hopf calculation for cases where the latter can be made. (Author)

A79-47340 * # **Trailing edge noise data with comparison to theory.** W. Olsen and D. Boldman (NASA, Lewis Research Center, Cleveland, Ohio). *American Institute of Aeronautics and Astronautics, Fluid and Plasma Dynamics Conference, 12th, Williamsburg, Va., July 23-25, 1979, Paper 79-1524.* 28 p. 20 refs.

The noise emission generated by the passage of a turbulent airstream over the trailing edge of a semiinfinite plate was measured over a large range of airstream velocity and plate geometry. The experiment was designed to validate trailing-edge noise theories. The results show that the peak of a radiation pattern moves from an upstream to a downstream direction as the velocity increases. The measured radiation pattern of the noise was in agreement with that predicted by a recent fundamental theory for leading- and trailing-edge noise. Although large changes in the character of the turbulent flow near the trailing edge effect the level and spectra of trailing-edge noise, the shape of the pattern is still accurately predicted by this theory. (V.T.)

N79-10842*# Lockheed-Georgia Co. Marietta
DUCT WALL IMPEDANCE CONTROL AS AN ADVANCED CONCEPT FOR ACOUSTIC SUPPRESSION ENHANCEMENT Final Report

Peter D. Dean: Oct 1978 115 p refs

(Contract NAS3-20071)

(NASA CR-159425, LG78ER0243)

Avail NTIS

HC A65/MF A01 CSCL 20A

A systems concept procedure is described for the optimization of acoustic duct liner design for both uniform and multisegment types. The concept was implemented by the use of a double reverberant chamber flow duct facility coupled with sophisticated computer control and acoustic analysis systems. The optimization procedure for liner insertion loss was based on the concept of variable liner impedance produced by bias air flow through a multilayer resonant cavity liner. A multiple microphone technique for in situ wall impedance measurements was used and successfully adapted to produce automated measurements for all liner configurations tested. The complete validation of the systems concept was prevented by the inability to optimize the insertion loss using bias flow induced wall impedance changes. This inability appeared to be a direct function of the presence of a higher order energy carrying modes which were not influenced significantly by the wall impedance changes. (A.R.H.)

N79-14873*# Lockheed-Georgia Co. Marietta
THE FREE JET AS A SIMULATOR OF FORWARD VELOCITY EFFECTS ON JET NOISE Final Report

K. K. Ahuja, B. J. Tester, and H. K. Tanna: Oct 1978 324 p refs

(Contract NAS3-20050)

(NASA CR-3056, LG78ER0065)

Avail NTIS

HC A14/MF A01 CSCL 20A

A thorough theoretical and experimental study of the effects of the free-jet shear layer on the transmission of sound from a model jet placed within the free jet to the far-field receiver located outside the free-jet flow was conducted. The validity and accuracy of the free-jet flight simulation technique for forward velocity effects on jet noise was evaluated. Transformation charts and a systematic computational procedure for converting measurements from a free-jet simulation to the corresponding results from a wind-tunnel simulation, and, finally, to the flight case were provided. The effects of simulated forward flight on jet mixing noise, internal noise and shock-associated noise from model-scale unheated and heated jets were established experimentally in a free-jet facility. It was illustrated that the existing anomalies between full-scale flight data and model-scale flight simulation data projected to the flight case, could well be due to the contamination of flight data by engine internal noise. (Author)

Author

N79-14875* General Electric Co., Schenectady, N. Y. Corporate Research and Development.

BASIC RESEARCH IN FAN SOURCE NOISE: INLET DISTORTION AND TURBULENCE NOISE Final Report, 16 Sep. 1976 - 16 Apr. 1978

R. A. Kantola and R. E. Warren Dec 1978 161 p refs (Contract NAS3-17853)

(NASA-CR-159451) SRD-78-186 Avail: NTIS HC A08/MF A01 CSCL 20A

A widely recognized problem in jet engine fan noise is the discrepancy between inflight and static tests. This discrepancy consists of blade passing frequency tones, caused by ingested turbulence that appear in the static tests but not in flight. To reduce the ingested distortions and turbulence in an anechoic chamber, a reverse cone inlet is used to guide the air into the fan. This inlet also has provisions for boundary layer suction and is used in conjunction with a turbulence control structure (TCS) to condition the air impinging on the fan. The program was very successful in reducing the ingested turbulence, to the point where reductions in the acoustic power at blade passing frequency are as high as 18 db for subsonic tip speeds. Even with this large subsonic tone suppression, the supersonic tip speed tonal content remains largely unchanged, indicating that the TCS did not appreciably attenuate the noise but effects the generation via turbulence reduction. Turbulence mapping of the inlet confirmed that the tone reductions are due to a reduction in turbulence, as the low frequency power spectra of the streamwise and transverse turbulence were reduced by up to ten times and 100 times, respectively. F O S

N79-17656* General Electric Co., Cincinnati, Ohio Aircraft Engine Group

EXPERIMENTAL CLEAN COMBUSTOR PROGRAM, PHASE 3: NOISE MEASUREMENT ADDENDUM Final Report

V. L. Doyle Dec 1978 139 p refs

(Contract NAS3-19736)

(NASA-CR-159456) R78AEG319 Avail: NTIS HC A07/MF A01 CSCL 20A

The acoustic characteristics of the double annular combustor in a CF6-50 high bypass turbofan engine were investigated. Internal fluctuating pressure measurements were made in the combustor region and in the core exhaust. The transmission loss at the turbine and nozzle was determined from the measurements and compared to previous component results and prediction theory. The primary noise source location in the combustor was investigated. Spectral comparisons of test rig results were made with the engine results. The measured overall power level was compared with component and engine correlating parameters. A R H

N79-25845* Virginia Polytechnic Inst and State Univ., Blacksburg

AN ANALYTICAL AND EXPERIMENTAL STUDY OF SOUND PROPAGATION AND ATTENUATION IN VARIABLE-AREA DUCTS Final Report

A. H. Nayfeh, J. F. Kaiser, R. L. Marshall, and L. J. Hurst Oct 1976 134 p refs (Contract NAS3-18553)

(NASA-CR-135392) Avail: NTIS HC A07/MF A01 CSCL 20A

The performance of sound suppression techniques in ducts that produce refraction effects due to axial velocity gradients was evaluated. A computer code based on the method of multiple scales was used to calculate the influence of axial variations due to slow changes in the cross-sectional area as well as transverse gradients due to the wall boundary layers. An attempt was made to verify the analytical model through direct comparison of experimental and computational results and the analytical determination of the influence of axial gradients on optimum liner properties. However, the analytical studies were unable to examine the influence of non-parallel ducts on the optimum liner conditions. For liner properties not close to optimum, the analytical predictions and the experimental measurements were compared. The circumferential variations of pressure amplitudes and phases at several axial positions were examined in straight and variable-area ducts, hard-wall and lined sections with and without

a mean flow. Reasonable agreement between the theoretical and experimental results was obtained. A R H

N79-26884* General Electric Co., Cincinnati, Ohio Aircraft Engine Group

ACOUSTIC AND AERODYNAMIC PERFORMANCE INVESTIGATION OF INVERTED VELOCITY PROFILE COANNULAR PLUG NOZZLES, COMPREHENSIVE DATA REPORT, VOLUME 1 Final Report

P. R. Knott, J. T. Blozy, and P. S. Staid May 1979 713 p 3 Vol

(Contract NAS3-19777)

(NASA-CR-159575-Vol-1, R79AEG166-Vol-1) Avail: NTIS HC A99/MF A01 CSCL 20A

Volume 1 of a three volume report is presented. Volume 1 contains a description of the acoustic configurations, test facilities, data reduction techniques, test conditions, and detailed test results from the hot, static acoustic tests. G Y

N79-26885* General Electric Co., Cincinnati, Ohio Aircraft Engine Group

ACOUSTIC AND AERODYNAMIC PERFORMANCE INVESTIGATION OF INVERTED VELOCITY PROFILE COANNULAR PLUG NOZZLES, COMPREHENSIVE DATA REPORT, VOLUME 2 Final Report

P. R. Knott, J. T. Blozy, and P. S. Staid May 1979 523 p 3 Vol

(Contract NAS3-19777)

(NASA-CR-159575-Vol-2, R79AEG166-Vol-2) Avail: NTIS HC A22/MF A01 CSCL 20A

Volume 2 of a three volume report is presented. Volume 2 presents acoustic data comparisons in graphic form. G Y

N79-26886* General Electric Co., Cincinnati, Ohio Aircraft Engine Group

ACOUSTIC AND AERODYNAMIC PERFORMANCE INVESTIGATION OF INVERTED VELOCITY PROFILE COANNULAR PLUG NOZZLES, COMPREHENSIVE DATA REPORT, VOLUME 3 Final Report

P. R. Knott, J. T. Blozy, and P. S. Staid May 1979 291 p 3 Vol

(Contract NAS3-19777)

(NASA-CR-159575-Vol-3, R79AEG166-Vol-3) Avail: NTIS HC A13/MF A01 CSCL 20A

Volume 3 of a three volume report is presented. Volume 3 contains the detailed aerodynamic test results plus the concept screening and model design report. G Y

N79-27933* Lockheed Georgia Co., Marietta

STUDIES OF THE ACOUSTIC TRANSMISSION CHARACTERISTICS OF COAXIAL NOZZLES WITH INVERTED VELOCITY PROFILES: COMPREHENSIVE DATA REPORT Final Report

P. D. Datta, M. Salikuddin, K. K. Ahuja, H. E. Plumblee, and P. Mungur May 1979 182 p ref

(Contract NAS3-20797)

(NASA-CR-159628) Avail: NTIS HC A09/MF A01 CSCL 20A

The efficiency of internal noise radiation through a coannular exhaust nozzle with an inverted velocity profile was studied. A preliminary investigation was first undertaken (1) to define the test parameters which influence the internal noise radiation, (2) to develop a test methodology which could realistically be used to examine the effects of the test parameters, and (3) to validate this methodology. The result was the choice of an acoustic impulse as the internal noise source in the jet nozzles. Noise transmission characteristics of a coannular nozzle system were then investigated. In particular, the effects of fan convergence angle, core extension length to annulus height ratio and flow Mach numbers and temperatures were studied. Relevant spectral data only is presented in the form of normalized nozzle transfer function versus nondimensional frequency. A R H

N79-32066* # Hersh Acoustical Engineering, Chatsworth, Calif. EFFECT OF GRAZING FLOW ON THE ACOUSTIC IMPEDANCE OF HELMHOLTZ RESONATORS CONSISTING OF SINGLE AND CLUSTERED ORIFICES Final Report

Alan S. Hersh and Bruce Walker Aug 1979 183 p refs (Contract NAS3-19745)

(NASA-CR-3177) Avail: NTIS HC A09/MF A01 CSDL 20A

A semiempirical fluid mechanical model is derived for the acoustic behavior of thin-walled single orifice Helmholtz resonators in a grazing flow environment. The incident and cavity sound fields are connected in terms of an orifice discharge coefficient whose values are determined experimentally using the two-microphone method. Measurements show that at high grazing flow speeds, acoustical resistance is almost linearly proportional to the grazing flow speed and almost independent of incident sound pressure. The corresponding values of reactance are much smaller and tend towards zero. For thicker-walled orifice plates, resistance and reactance were observed to be less sensitive to grazing flow as the ratio of plate thickness to orifice diameter increased. Loud tones were observed to radiate from a single orifice Helmholtz resonator due to interaction between the grazing flow shear layer and the resonator cavity. Measurements showed that the tones radiated at a Strouhal number equal to 0.26. The effects of grazing flow on the impedance of Helmholtz resonators consisting of clusters of orifices was also studied. In general, both resistance and reaction were found to be virtually independent of orifice relative spacing and number. These findings are valid with and without grazing flow. Author

A79-26890* # An impulse test technique with application to acoustic measurements. M. Salikuddin, P. D. Dean, H. E. Plumblee, Jr., and K. K. Ahuja (Lockheed-Georgia Co., Marietta, Ga.). *American Institute of Aeronautics and Astronautics, Aeroacoustics Conference, 5th, Seattle, Wash., Mar. 12-14, 1979, Paper 79-0679*. 12 p. 13 refs. Research sponsored by the Lockheed Independent Research and Development Program; Contract No. NAS3-20797.

A method has been presented for measuring the acoustic properties of an absorbent material and a duct/nozzle system (with or without airflow) using a high voltage spark discharge as an impulse source of sound. The cross-spectra of the incident, reflected and transmitted acoustic pressure transients are analyzed by way of a FFT digital processor in the form of complex transfer functions. These transfer functions have a direct relationship to the termination impedance and radiation directivity. The impulse method has been justified by comparisons, with data obtained from existing methods (both experimental and theoretical), that show excellent agreement. Reflection coefficients and radiation impedances of various duct-nozzle systems and their associated far-field directivities are also presented as some of the applications of the impulse technique.

(Author)

A79-26910* # Acoustic behavior of a fibrous bulk material. A. S. Hersh and B. Walker (Hersh Acoustical Engineering, Chatsworth, Calif.). *American Institute of Aeronautics and Astronautics, Aeroacoustics Conference, 5th, Seattle, Wash., Mar. 12-14, 1979, Paper 79-0599*. 11 p. Contract No. NAS3-19745.

A semiempirical model is presented describing the acoustic behavior of Kevlar 29, a bulk absorbing material. The model is based on an approximate solution to the one-dimensional equations representing conservation of fluctuating mass, momentum and energy. By treating the material as a momentum sink, theoretical expressions of the material complex propagation constants and characteristic impedance were derived in terms of a single constant. Evaluating the constant at a single frequency for a particular specimen, excellent agreement between prediction and measurement was achieved for a large range of sound frequencies and material porosities and thicknesses. Results show that Kevlar 29 absorbs sound efficiently even at low frequencies. This is explained in terms of a frequency dependent material phase speed. (Author)

A79-28923* # Noise from struts and splitters in turbofan exit ducts. M. R. Fink (United Technologies Research Center, East Hartford, Conn.). *American Institute of Aeronautics and Astronautics, Aeroacoustics Conference, 5th, Seattle, Wash., Mar. 12-14, 1979, Paper 79-0637*. 10 p. 13 refs. Contract No. NAS3-17863.

An analytical method for calculating noise radiation from isolated airfoils in turbulent flow was combined with a method for calculating transmission of sound through a subsonic exit duct and with an empirical far field directivity shape. This combination provides a method for predicting engine internally generated noise from radial struts and stators and annular splitter rings. Calculated sound power spectra, directivity, and acoustic pressure spectra are compared with data. These data were for noise caused by a fan exit duct splitter ring, large-chord stator blades, and turbine exit struts. However, the lack of turbulence intensity and scale length measurements for these flow ducts prevented an absolute validation of the prediction method. (Author)

A79-26936* # Effects of simulated forward flight on jet noise, shock noise and internal noise. K. K. Ahuja, H. K. Tanna, and B. J. Tester (Lockheed-Georgia Co., Marietta, Ga.). *American Institute of Aeronautics and Astronautics, Aeroacoustics Conference, 5th, Seattle, Wash., Mar. 12-14, 1979, Paper 79-0615*. 11 p. 12 refs. Contract No. NAS3-20050.

Inflight simulation experiments are conducted in an anechoic free-jet facility to examine the flight effects on various combinations of jet noise, shock noise and internal noise. The jet mixing noise component reduces with forward velocity at all angles and frequencies. When jet mixing noise is contaminated with internal noise, forward motion provides a noise reduction in the rear arc and a noise increase in the forward arc, with little change at 90 deg. The results are similar for shock-containing jets. It is found that the existing anomalies between full-scale flight data and model-scale flight simulation data could well be due to the contamination of the flight data by internal noise. (Author)

A79-28964* # A jet exhaust noise prediction procedure for inverted velocity profile coannular nozzles. R. S. Larson (United Technologies Corp., Pratt and Whitney Aircraft Group, East Hartford, Conn.). *American Institute of Aeronautics and Astronautics, Aeroacoustics Conference, 5th, Seattle, Wash., Mar. 12-14, 1979, Paper 79-0633*. 21 p. 26 refs. Contract No. NAS3-20061.

Acoustic model tests have demonstrated that significant noise suppression can be obtained from inverted velocity profile coannular nozzles. An acoustic prediction procedure was developed for inverted velocity profile coannular nozzles that can be used to predict SPL spectra as a function of nozzle geometry and flow conditions. In the development of this prediction procedure, the noise spectrum at a given angle was decomposed into four noise components: a low frequency mixing noise component, a high frequency mixing noise component, an outer stream shock noise component, and an inner stream shock noise component. The physics of the inverted velocity flow field development was used to formulate noise generation models. Scaling laws for each noise component were defined based on these models. Comparisons of predictions from this procedure with experimental data were conducted to verify the prediction procedure. (Author)

72 ATOMIC AND MOLECULAR PHYSICS

Includes atomic structure and molecular spectra.

N79-18711* Minnesota Univ., Minneapolis. Dept. of Electrical Engineering.

INVESTIGATIONS OF NEGATIVE AND POSITIVE CESIUM ION SPECIES Final Report

L. M. Chanin Sep 1978 35 p refs

(Grant NsG-3094)

(NASA-CR-159446) Avail: NTIS HC A03/MF A01 CSCL 20H

A direct test of the hypothesis of negative ion creation at the collector of a diode operating under conditions similar to a cesium thermionic converter. The experimental technique involves using direct ion sampling through the collector electrode with mass analysis using a quadrupole mass analyzer. Similar measurements are undertaken on positive ions extracted through the emitter electrode. Measurements were made on a variety of gases including pure cesium, helium-cesium mixtures and cesium-hydrogen as well as cesium-xenon mixtures. The gas additive was used primarily to aid in understanding the negative ion formation processes. Measurements were conducted using emitter (cathode) temperatures up to about 1000 F. The major negative ion identified through the collector was $\text{Cs}(-)$ with minor negative ion peaks tentatively identified as $\text{H}(-)$, $\text{H}_2(-)$, $\text{H}_3(-)$, $\text{He}(-)$ and a mass 66. Positive ions detected were believed to be $\text{Cs}(+)$, $\text{Cs}_2(+)$ and $\text{Cs}_3(+)$. L.S.

N79-19826* Colorado State Univ., Fort Collins. Dept. of Physics.

INDUSTRIAL ION SOURCE TECHNOLOGY Annual Report

Harold R. Kaufman and Raymond S. Robinson Dec 1978 70 p refs

(Grant NsG-3086)

(NASA-CR-159534) Avail: NTIS HC A04/MF A01 CSCL 20H

An analytical model was developed to describe the development of a coned surface texture with ion bombardment and simultaneous deposition of an impurity. A mathematical model of sputter deposition rate from a beveled target was developed in conjunction with the texturing models to provide an important input to that model. The establishment of a general procedure that will allow the treatment of many different sputtering configurations is outlined. Calculation of cross sections for energetic binary collisions was extended to Ar, Kr, and Xe with total cross sections for viscosity and diffusion calculated for the interaction energy range from 1eV to 1000eV. Physical sputtering and reactive ion etching experiments provided experimental data on the operating limits of a broad beam ion source using CF₄ as a working gas to produce reactive species in a sputtering beam. Magnetic clustering effects are observed when Al is seeded with Fe and sputtered with Ar(\pm) ions. Silicon was textured at a micron scale by using a substrate temperature of 600 C. L.S.

73 NUCLEAR AND HIGH-ENERGY PHYSICS

Includes elementary and nuclear particles, and reactor theory.

For space radiation see 93 *Space Radiation*.

N79-12884* TRW Defense and Space Systems Group, Redondo Beach, Calif.

ION BEAM TECHNOLOGY APPLICATIONS STUDY Final Report

J. M. Sellen, Jr. 1 Nov 1978 36 p

(Contract NAS3-21027)

(NASA-CR-159437 TRW-32100-6009-R1J-00) Avail NTIS HC A03/MF A01 CSCL 20H

Specific perceptions and possible ion beam technology applications were obtained as a result of a literature search and contact interviews with various institutions and individuals which took place over a 5-month period. The use of broad beam electron bombardment ion sources is assessed for materials deposition, removal, and alteration. Special techniques examined include: (1) cleaning, cutting, and texturing for surface treatment; (2) crosslinking of polymers, stress relief in deposited layers and the creation of defect states in crystalline material by ion impact; and (3) ion implantation during epitaxial growth and the deposition of neutral materials sputtered by the ion beam. The aspects, advantages, and disadvantages of ion beam technology and the competitive role of alternative technologies are discussed. A R H

N79-27975* Rockwell International Corp., Anaheim, Calif. Electronics Research Center

ANALYSIS AND PRELIMINARY DESIGN OF OPTICAL SENSORS FOR PROPULSION CONTROL Final Report

K. A. James, W. H. Quick, and V. H. Strahan 23 Jan 1979 90 p refs

(Contract NAS3-21005)

(NASA-CR-159519 C79-386/501) Avail NTIS HC A05/MF A01 CSCL 20F

A fiber-optic sensor concept screening study was performed. Twenty sensor subsystems were identified and evaluated. Two concepts selected for further study were the Fabry Perot fiber optic temperature sensor and the pulse width modulated phosphorescent temperature sensor. Various designs suitable for a Fabry Perot temperature sensor to be used as a remote fiber optic transducer were investigated. As a result, a particular design was selected and constructed. Tests on this device show that spectral peaks are produced from visible white light, and the change in wavelength of the spectral peaks produced by a change in temperature is consistent with theory and is 36 nm/C for the first order peak. A literature search to determine a suitable phosphor for implementing the pulse width modulated fiber optic temperature sensor was conducted. The search indicated that such a device could be made to function for temperatures up to approximately 200 C. Materials like ZnCdS and ZnSe activated with copper will be particularly applicable to temperature sensing in the cryogenic to room temperature region. While this sensing concept is probably not applicable to jet engines, the simplicity and potential reliability make the concept highly desirable for other applications. A R H

75 PLASMA PHYSICS

Includes magnetohydrodynamics and plasma fusion.
For ionospheric plasmas see 46 Geophysics. For space plasmas see 90 Astrophysics.

N79-10694* National Aeronautics and Space Administration, Lewis Research Center, Cleveland, Ohio.

HYDROGEN HOLLOW CATHODE ION SOURCE Patent Application

M. Mirtich, J. Sovey, and R. Roman, inventors (to NASA) 23 Oct. 1978 8 p.

(NASA-Case LEW-12940-1; US-Patent-Appl-SN-953391) Avail. NTIS HC A02/MF A01 CSCL 201

A hydrogen source is disclosed which includes a chamber having at one end a cathode which provides electrons and through which hydrogen gas flows into the chamber. Screen and accelerator grids are provided at the other end of the chamber. A baffle plate is placed between the cathode and the grids, and a cylindrical baffle is disposed coaxially with the cathode at the one end of the chamber. The cylindrical baffle is of greater diameter than the baffle plate to provide discharge impedance and also to protect the cathode from ion flux. An anode electrode draws the electrons away from the cathode. The hollow cathode includes a tubular insert of tungsten impregnated with a low work function material to provide ample electrons. A heater is provided around the hollow cathode to initiate electron emission from the low work function material. The source provides hydrogen or deuterium ions at a beam current density exceeding 0.1 amperes (A)/sq. cm and has a discharge current which can exceed 100A for duty cycles of several minutes. NASA

N79-12908* National Aeronautics and Space Administration, Lewis Research Center, Cleveland, Ohio.

ADHESIVE BONDING OF ION BEAM TEXTURED METALS AND FLUOROPOLYMERS

Michael J. Mirtich and James S. Sovey 1978 14 p. refs. Presented at the 25th Natl. Vacuum Symp., San Francisco, 28 Nov. - 1 Dec. 1978. Sponsored by the Am. Vacuum Soc. (NASA-TM 79004, E-9790) Avail. NTIS HC A02/MF A01 CSCL 201

An electron bombardment argon ion source was used to ion etch various metals and fluoropolymers. The metal and fluoropolymers were exposed to (0.5 to 1.0) keV Ar ions at ion current densities of (0.2 to 1.5) mA/sq. cm for various exposure times. The resulting surface texture is in the form of needles or spires whose vertical dimensions may range from tenths to hundreds of micrometers, depending on the selection of beam energy, ion current density, and etch time. The bonding of textured surfaces is accomplished by ion beam texturing mating pieces of either metals or fluoropolymers and applying a bonding agent which wets in and around the microscopic cone-like structures. After bonding, both tensile and shear strength measurements were made on the samples. Also tested, for comparison's sake, were untextured and chemically etched fluoropolymers. The results of these measurements are presented. Author

N79-19867* National Aeronautics and Space Administration, Lewis Research Center, Cleveland, Ohio.

ION CONFINEMENT AND TRANSPORT IN A TOROIDAL PLASMA WITH EXTERNALLY IMPOSED RADIAL ELECTRIC FIELDS

J. Reece Roth, Walter M. Krawczonek, Edward J. Powers (Texas Univ., Austin), Young C. Kim (Texas Univ., Austin), and Hae Y. Hong (Texas Univ., Austin) Mar. 1979 86 p. refs. (NASA TP 1411, E-9754) Avail. NTIS HC A05/MF A01 CSCL 201

Strong electric fields were imposed along the minor radius of the toroidal plasma by biasing it with electrodes maintained at kilovolt potentials. Coherent, low frequency disturbances characteristic of various magnetohydrodynamic instabilities were absent in the high-density, well-confined regime. High, direct current radial electric fields with magnitudes up to 135 volts per centimeter penetrated inward to at least one-half the plasma

radius. When the electric field pointed radially toward, the ion transport was inward against a strong local density gradient; and the plasma density and confinement time were significantly enhanced. The radial transport along the electric field appeared to be consistent with fluctuation-induced transport. With negative electrode polarity the particle confinement was consistent with a balance of two processes: a radial infusion of ions, in those sectors of the plasma not containing electrodes, that resulted from the radially inward fields; and ion losses to the electrodes, each of the which acted as a sink and drew ions out of the plasma. A simple model of particle confinement was proposed in which the particle confinement time is proportional to the plasma volume. The scaling predicted by this model was consistent with experimental measurements. L.S.

N79-20964* National Aeronautics and Space Administration, Lewis Research Center, Cleveland, Ohio.

ION BEAM PROBING OF ELECTROSTATIC FIELDS

Hans Persson Feb. 1979 66 p. refs.

(NASA-TM-X-79120, E-9953) Avail. NTIS HC A04/MF A01 CSCL 201

The determination of a cylindrically symmetric, time-independent electrostatic potential V in a magnetic field B with the same symmetry by measurements of the deflection of a primary beam of ions is analyzed and substantiated by examples. Special attention is given to the requirements on canonical angular momentum and total energy set by an arbitrary, nonmonotone V , to scaling laws obtained by normalization, and to the analogy with ionospheric sounding. The inversion procedure with the Abel analysis of an equivalent problem with a one-dimensional fictitious potential is used in a numerical experiment with application to the NASA Lewis Modified Penning Discharge. The determination of V from a study of secondary beams of ions with increased charge produced by hot plasma electrons is also analyzed, both from a general point of view and with application to the NASA Lewis SUMMA experiment. Simple formulas and geometrical constructions are given for the minimum energy necessary to reach the axis, the whole plasma, and any point in the magnetic field. The common, simplifying assumption that V is a small perturbation is critically and constructively analyzed; an iteration scheme for successively correcting the orbits and points of ionization for the electrostatic potential is suggested. J.M.S.

N79-22897* National Aeronautics and Space Administration, Lewis Research Center, Cleveland, Ohio.

PRELIMINARY RESULTS IN THE NASA LEWIS H2-O2 COMBUSTION MHD EXPERIMENT

J. Marlin Smith 1979 11 p. refs. To be presented at the 18th Symp. on the Eng. Aspects of Magnetohydrodyn., Butte, Mont., 18-20 Jun. 1979.

(NASA-TM-79135, E-9983) Avail. NTIS HC A02/MF A01 CSCL 201

MHD (magnetohydrodynamic) power generation experiments were carried out in the NASA Lewis Research Center cesium-seeded H₂-O₂ combustion facility. This facility uses a neon-cooled cryomagnat capable of producing magnetic fields in excess of 5 tesla. The effects of power takeoff location, generator loading, B-field strength, and electrode breakdown on generator performance are discussed. The experimental data is compared to a theory based on one dimensional flow with heat transfer, friction, and voltage drops. G.Y.

A79-14953* Microwave radiation measurements near the electron plasma frequency of the NASA Lewis Bumpy Torus plasma. R. Mallavarpu and J. R. Roth (NASA, Lewis Research Center, Cleveland, Ohio). *American Physical Society, Meeting, Colorado Springs, Colo., Oct. 30-Nov. 3, 1978, Paper 20 p. 12 refs.*

Microwave emission near the electron plasma frequency of the NASA Lewis Bumpy Torus plasma has been observed, and its relation to the average electron density and the dc toroidal magnetic field was examined. The emission was detected using a spectrum analyzer and a 50-ohm miniature coaxial probe. The radiation appeared as a broad amplitude peak that shifted in frequency as the

plasma parameters were varied. The observed radiation scanned an average plasma density ranging from 20 billion to 800 billion per cu cm. A linear relation was observed between the density calculated from the emission frequency and the average plasma density measured with a microwave interferometer. With the aid of a relative density profile measurement of the plasma, it was determined that the emissions occurred from the outer periphery of the plasma.

(Author)

A79-15597 * # Hartmann flow with temperature-dependent physical properties. G. T. Linn (NASA, Lewis Research Center, Cleveland, Ohio) and J. S. Walker (Illinois, University, Urbana, Ill.). In: Developments in theoretical and applied mechanics. Volume 9. Proceedings of the Ninth Southeastern Conference, Nashville, Tenn., Mar. 4-5, 1978. (A79-15576 04-31) Nashville, Tenn., Vanderbilt University, 1978, p. 393-401. 6 refs. NSF Grant No. ENG-74-23778.

Attention is given to the steady, fully developed, one-dimensional flow of a liquid metal in which thermal conductivity, electrical conductivity, and viscosity are functions of temperature. It is found that the properties are decreasing functions of temperature and the first differences between temperature-dependent and constant properties are discussed.

S.C.S.

A79-26184 * # Velocity, temperature, and electrical conductivity profiles in hydrogen-oxygen MHD duct flows. M. S. Greywall (Wichita State University, Wichita, Kan.) and C. C. P. Pian (NASA, Lewis Research Center, Cleveland, Ohio). In: Fluids engineering in advanced energy systems; Proceedings of the Winter Annual Meeting, San Francisco, Calif., December 10-15, 1978. (A79-26176 09-44) New York, American Society of Mechanical Engineers, 1978, p. 111-120. 8 refs. Contract No. EF-77-A-01-2647; Grant No. NsG 3186.

This paper presents results of two-dimensional duct flow computations for radial distributions of velocity, temperature, and electrical conductivity. Calculations were carried out for the flow conditions representative of NASA Lewis hydrogen-oxygen combustion driven MHD duct. Results are presented for two sets of computations: (1) profiles of developing flow in a smooth duct, and (2) profiles of fully developed pipe flow with a specified streamwise shear stress distribution. The predicted temperature and electrical conductivity profiles for the developing flows compared well with available experimental data.

(Author)

A79-39807 * # Preliminary results in the NASA Lewis H2-O2 combustion MHD experiment. J. M. Smith (NASA, Lewis Research Center, Cleveland, Ohio). *Montana Energy and MHD Research and Development Institute, Montana College of Mineral Science and Technology, and Montana State University, Symposium on the Engineering Aspects of Magnetohydrodynamics, 18th, Butte, Mont., June 19-20, 1979, Paper 9*.

MHD power generation experiments have been carried out in the NASA Lewis Research Center cesium-seeded H2-O2 combustion facility. This facility uses a neon-cooled cryomagnet capable of producing magnetic fields in excess of 5 tesla. The effects of power takeoff location, generator loading, B field strength, and electrode breakdown on generator performance are discussed. The experimental data is compared to a theory based on one-dimensional flow with heat transfer, friction, and voltage drops.

(Author)

A79-41768 * # Trajectories of charged particles in radial electric and uniform axial magnetic fields. G. W. Englert (NASA, Lewis Research Center, Cleveland, Ohio). *IEEE Transactions on Plasma Science*, vol. PS-7, June 1979, p. 72-80. 21 refs.

Trajectories of charged particles were determined over a wide range of parameters characterizing motion in cylindrical low pressure gas discharges and plasma heating devices which have steady radial electric fields perpendicular to uniform steady magnetic fields. Consideration was given to radial distributions characteristic of fields measured in a modified Penning discharge, in two NASA Lewis

burnout-type plasma heating devices, and that estimated for the Ixion device. Numerical calculations of trajectories for such devices showed that differences between cyclotron frequency and qB/m and between azimuthal drift and a guiding center approximation are appreciable.

B.J.

A79-51995 * # Performance optimization of an MHD generator with physical constraints. C. C. P. Pian, G. R. Seikel, and J. M. Smith (NASA, Lewis Research Center, Cleveland, Ohio). In: *Inter-society Energy Conversion Engineering Conference, 14th, Boston, Mass., August 5-10, 1979, Proceedings, Volume 2* (A79-51726 23-44) Washington, D.C., American Chemical Society, 1979, p. 1939-1944. 7 refs.

A technique has been described which optimizes the power out of a Faraday MHD generator operating under a prescribed set of electrical and magnetic constraints. The method does not rely on complicated numerical optimization techniques. Instead the magnetic field and the electrical loading are adjusted at each streamwise location such that the resultant generator design operates at the most limiting of the cited stress levels. The simplicity of the procedure makes it ideal for optimizing generator designs for system analysis studies of power plants. The resultant locally optimum channel designs are, however, not necessarily the global optimum designs. The results of generator performance calculations are presented for an approximately 2000 MWe size plant. The difference between the maximum power generator design and the optimal design which maximizes net MHD power are described. The sensitivity of the generator performance to the various operational parameters are also presented.

(Author)

A79-53867 * Method for decomposing observed line shapes resulting from multiple causes. Application to plasma charge-exchange neutral spectra. R. W. Patch (NASA, Lewis Research Center, Cleveland, Ohio). *Journal of Quantitative Spectroscopy and Radiative Transfer*, vol. 22, Sept. 1979, p. 273-286. 24 refs.

A method is given for decomposing the widths of observed spectral lines resulting from unresolved line splitting, additive kinetic processes of different types, instrumental broadening (slit function), Doppler broadening, etc. all superimposed. The second moments are used as measures of the various widths involved. The method is not applicable if dispersion type (Lorentz) broadening occurs. Application is made to plasma charge-exchange neutral spectra of hydrogen, deuterium, and helium.

(Author)

N79-26943 # Colorado State Univ. Fort Collins Dept. of Physics

PHYSICAL PROCESSES IN DIRECTED ION BEAM SPUTTERING Ph.D. Thesis

Raymond S. Robinson Mar 1979 153 p refs

(Grant NsG 3086)

(NASA CR-159567) Avail NTIS HC A08/MF A01 CSCL 201

The general operation of a discharge chamber for the production of ions is described. A model is presented for the magnetic containment of both primary and secondary or Maxwellian electrons in the discharge plasma. Cross sections were calculated for energy and momentum transfer in binary collisions between like pairs of Ar, Kr, and Xe atoms in the energy range from about 1 eV to 1000 eV. These calculations were made from available pair interaction potentials using a classical model. Experimental data from the literature were fit to a theoretical expression for the Ar⁺ resonance charge exchange cross section over the same energy range. A model was developed that describes the processes of conical texturing of a surface due to simultaneous directed ion beam etching and sputter deposition of an impurity material. This model accurately predicts both a minimum temperature for texturing to take place and the variation of cone density with temperature. It also provides the correct order of magnitude of cone separation. It was predicted from the model and subsequently verified experimentally that a high sputter yield material could serve as a seed for coning of

a lower sputter yield substrate. Seeding geometries and seed deposition rates were studied to obtain an important input to the theoretical texturing model.

A.R.H.

76 SOLID-STATE PHYSICS

Includes superconductivity.
For related information, see also 33 Electronics and Electrical Engineering and 36 Lasers and Masers.

N79-13886* National Aeronautics and Space Administration, Lewis Research Center, Cleveland, Ohio.

IONIZED DOPANT CONCENTRATIONS AT THE HEAVILY DOPED SURFACE OF A SILICON SOLAR CELL

Irving W. Berg, Jacob D. Broder, George A. Mazaris, Jr., and Lan Hsu. Dec. 1978. 19 p. refs.
(Grant NSG-3014)

(NASA-TP-1347; E-9629) Avail: NTIS HC A02/MF A01 CSCI 10B

Data are combined with concentrations obtained by a bulk measurement method using successive layer removal with measurements of Hall effect and resistivity. From the MOS (metal-oxide-semiconductor) measurements it is found that the ionized dopant concentration N has the value $(1.4 \pm 0.1) \times 10^{10}$ to the 20^{th} power/cm at distances between 100 and 220 nm from the $n(+)$ surface. The bulk measurement technique yields average values of N over layers whose thickness is 2000 nm. Results show that, at the higher concentrations encountered at the $n(+)$ surface, the MOS C-V technique, when combined with a bulk measurement method, can be used to evaluate the effects of materials preparation methodologies on the surface and near surface concentrations of silicon cells.

Author

N79-16699* National Aeronautics and Space Administration, Lewis Research Center, Cleveland, Ohio.

FRICTION AND WEAR OF SINGLE-CRYSTAL MANGANESE-ZINC FERRITE

Kazuhisa Miyoshi and Donald H. Buckley. 1979. 19 p. refs. To be presented at the Intern. Conf. on Wear of Mater., Dearborn, Mich., 16-18 Apr. 1979, sponsored by ASME, ASLE, ASM, ASTM 62, SAE, SME, Am. Chem. Soc., AIME, and APS. (NASA-TM-78580; E-9673-1) Avail: NTIS HC A02/MF A01 CSCI 20B

Sliding friction experiments were conducted with single crystal manganese-zinc ferrite in contact with itself and with transition metals. Results indicate mating highest atomic density directions (110) on matched crystallographic planes exhibit the lowest coefficient of friction, indicating that direction is important in the friction behavior of ferrite. Matched parallel high atomic density planes and crystallographic directions at the interface exhibit low coefficients of friction. The coefficients of friction for ferrite in contact with various metals are related to the relative chemical activity of these metals. The more active the metal, the higher the coefficient of friction. Cracking and the formation of hexagonal- and rectangular-shaped platelet wear debris due to cleavages of (110) planes are observed on the ferrite surfaces as a result of sliding.

Author

N79-21910* National Aeronautics and Space Administration, Lewis Research Center, Cleveland, Ohio.

METHOD FOR THE PREPARATION OF INORGANIC SINGLE CRYSTAL AND POLYCRYSTALLINE ELECTRONIC MATERIALS Patent

Warren O. Groves, inventor (to NASA) (Monsanto Co., St. Louis, Mo.) Issued 25 Feb. 1969. 3 p. Filed 5 Feb. 1965. Sponsored by NASA.

(NASA Case-XLE 02545-1; US-Patent-3,429,756; US-Patent-Appl-SN-430748; US-Patent-Class-156-17) Avail: US Patent and Trademark Office CSCI 20B

Large area, semiconductor crystals selected from group 3-5 compounds and alloys are provided for semiconductor device fabrication by the use of a selective etching operation which completely removes the substrate on which the desired crystal was deposited. The substrate, selected from the same group as the single crystal, has a higher solution rate than the crystal, single crystal which is essentially unaffected by the etching solution. The preparation of gallium phosphide single crystals

using a gallium arsenide substrate and a concentrated nitric acid etching solution is described. A.R.H.

A79-10417* Optical, spin-resonance, and magnetoresistance studies of tetrathiatetracene/2-iodine/3 - The nature of the ground state. R. B. Somoano, S. P. S. Yen, V. Hadek, S. K. Khanna (California Institute of Technology, Jet Propulsion Laboratory, Pasadena, Calif.), M. Novotny (Stanford University, Stanford, Calif.), T. Datta, A. M. Hermann (Tulane University, New Orleans, La.), and J. A. Woollam (NASA, Lewis Research Center, Cleveland, Ohio). *Physical Review B - Solid State, 3rd Series*, vol. 17, Apr. 1, 1978, p. 2853-2857. 19 refs. Contract No. NAS7-100.

A recent investigation in which Isett and Perez-Albuern (1977) found that (tetrathiatetracene)2(iodine)3 is a stable organic metal down to 3.3 K is of considerable interest. In view of the diversity of suggestions made regarding this compound, measurements, were made of its electrical, magnetic, and optical properties. The results obtained indicate a metallic state at high temperatures, but also support a nonmetallic state at temperatures below 30 K. At 20-30 K, a metal-to-insulator phase transition occurs. This is indicated by the onset of a large and positive magnetoresistance, the leveling off in the temperature dependence of the ESR linewidth, and by recent derivative analysis of the electrical conductivity in this region. The investigated compound represents an interesting one-dimensional electronic system in which it may be possible to study the combined effects of disorder and interchain coupling on charge transport processes.

G.R.

A79-20219* Superconducting properties of evaporated copper molybdenum sulfide films. J. A. Woollam (NASA, Lewis Research Center, Cleveland, Ohio), K. C. Chi, R. O. Dillon, R. F. Bunshah (California, University, Los Angeles, Calif.), and S. A. Alterovitz. *Journal of Applied Physics*, vol. 49, Dec. 1978, p. 6027-6030. 20 refs.

Films of copper molybdenum sulfide were produced by coevaporation. Those that were superconducting contained only the ternary compound and free molybdenum. The range of copper content in the ternary compound was as large as that in polycrystalline material, that is, it includes either phase alone, or a mixture of the two phases of this material. This is in contrast with sputtered materials where copper concentration has been limited to a narrower range. The upper critical field and the critical current were measured as functions of external magnetic field, and found to be similar to those of sputtered copper molybdenum sulfide, when the comparison was made for samples having the same amount of copper.

(Author)

A79-20529* Properties and performance of fine-filament

bronze-process Nb₃Sn conductors. M. S. Walker, J. M. Cutro, B. A. Zeitlin, G. M. Dzeryansky, R. E. Schwall (Intermagneutics General Corp., Guilderland, N.Y.), C. E. Oberly (USAF, Wright-Patterson AFB, Ohio), J. C. Ho (Wichita State University, Wichita, Kan.), and J. A. Woollam (NASA, Lewis Research Center, Cleveland, Ohio). (*Applied Superconductivity Conference, Pittsburgh, Pa., Sept. 25-28, 1978*). *IEEE Transactions on Magnetics*, vol. MAG-15, Jan. 1979, p. 80-82. 8 refs. USAF-supported research.

Fine-filament bronze-process Nb₃Sn superconductors were fabricated to fulfill stringent requirements on critical current under tension in a one-inch bend diameter, current density, stability, and conductor losses. A large fraction of niobium filaments was incorporated in a bronze matrix, and a cable containing 4453 2-micron diameter filaments in each of six strands provided a current density of 85,000 A/sq cm at 10 to the 11th ohm-cm, 10 T, and 4.2 K. The next step was to incorporate copper stabilizer in a conductor with 20,538 filaments. These conductors, fabricated so that bend strains of about 1% would be experienced by the filaments in the one-inch bend, stably carried currents in the 200-500 A range. A quench current of 540 A in a 5-cm bend corresponds to 158,000 A/sq cm in the bronze and filament area, believed to be the highest critical current density reported for multifilamentary Nb₃Sn. P.T.H.

A79-20539 * Critical current density in wire drawn and hydrostatically extruded Nb-Ti superconductors. S. A. Alterovitz, J. A. Woollam (NASA, Lewis Research Center, Cleveland, Ohio), and E. W. Collings (Battelle Memorial Institute, Columbus, Ohio). (*Applied Superconductivity Conference, Pittsburgh, Pa., Sept. 25-29, 1978*) *IEEE Transactions on Magnetics*, vol. MAG-15, Jan. 1979, p. 404, 405, 6 refs. Contract No. W-7405-eng-92. DOE Task 64.

Critical current studies have been made on copper-clad Nb-Ti composite wire prepared under area reductions of 100:1 and 10,000:1 by hydrostatic extrusion (HE), wire drawing and HE plus drawing. Comparative evaluation of the thermomechanical processing equivalent of HE was performed. (Author)

A79-21157 * Hall effect and magnetoresistivity in the ternary molybdenum sulfides. J. A. Woollam (NASA, Lewis Research Center, Cleveland, Ohio), E. J. Haugland (NASA, Lewis Research Center, Case Western Reserve University, Cleveland, Ohio), and S. A. Alterovitz. *Physics Letters*, vol. 68A, Sept. 18, 1978, p. 122-124, 7 refs.

The Hall coefficient and magnetoresistance of sputtered films of $\text{Cu}(x)\text{Mo}_6\text{S}_8$ and PbMo_6S_8 have been measured, as well as the magnetoresistance in sintered samples of the same materials. Assuming a single band model, net carrier densities and mean mobilities are determined. (Author)

A79-23633 * Anomalous galvanomagnetic properties of graphite in strong magnetic fields. K. Sugihara (Matsushita Electric Industrial Co., Ltd., Osaka, Japan) and J. A. Woollam (NASA, Lewis Research Center, Cleveland, Ohio). *Physical Society of Japan, Journal*, vol. 45, Dec. 1978, p. 1891-1898, 19 refs.

A79-26375 * Critical current and scaling laws in evaporated two-phase $\text{Cu}_2.5\text{Mo}_6\text{S}_8$. S. A. Alterovitz and J. A. Woollam (NASA, Lewis Research Center, Cleveland, Ohio). *Journal of Low Temperature Physics*, vol. 32, no. 5-6, 1978, p. 839-851, 23 refs.

A79-27229 * Normal state properties of the ternary molybdenum sulfides. J. A. Woollam (NASA, Lewis Research Center, Cleveland, Ohio) and S. A. Alterovitz. *Solid State Communications*, vol. 27, no. 6, 1978, p. 669-671, 11 refs.

By making a large number of normal state and superconducting properties measurements, all on the same ternary molybdenum sulfide samples, we obtain values for Fermi surface and superconducting parameters. From these we conclude that sputtered ternary molybdenum sulfides are not completely in the dirty superconductor limit, and that they are d-band metals with a high electron carrier density. (Author)

A79-27230 * Low temperature normal state resistance of ternary molybdenum sulfides. J. A. Woollam (NASA, Lewis Research Center, Cleveland, Ohio) and S. A. Alterovitz. *Solid State Communications*, vol. 27, no. 5, 1978, p. 571-574, 27 refs.

A79-28300 * Comparison of projected critical currents in PbMo_6S_8 and Nb_3Ge . S. A. Alterovitz (NASA, Lewis Research Center, Cleveland, Ohio) and J. A. Woollam. *Cryogenics*, vol. 19, Mar. 1979, p. 157-169, 18 refs. NSF supported research.

Critical current densities, J_c , of sputtered Chevrel phase PbMo_6S_8 films have been measured as a function of field to 19 T at several temperatures. The pinning forces were found to obey a scaling law. Assuming an effective upper critical field $B_{c2} = 45$ T, an effective critical temperature $T_c = 13$ K, together with empirical estimates of numerical factors in the scaling law, the upper limits for critical current density J_c in PbMo_6S_8 are estimated. Comparisons

are made with estimates of J_c for Nb_3Ge at 4.2 K. A crossover of J_c vs. B is found for B of the order of 25 to 30 T. Below this point, Nb_3Ge is projected to have a higher critical current density. Thus practical use of Chevrel materials in high field magnets only appears to be competitive with Nb_3Ge for fields above 25 to 30 T. (Author)

A79-31973 * Reactively evaporated films of copper molybdenum sulfide. K. C. Chi, R. O. Dillon, R. F. Bunshah (California University, Los Angeles, Calif.), S. Alterovitz, and J. A. Woollam (NASA, Lewis Research Center, Cleveland, Ohio). In: *Metallurgical coatings 1978; Proceedings of the Fifth International Conference, San Francisco, Calif., April 3-7, 1978, Volume 2*. (A79-31951 12-23) Lausanne, Elsevier Sequoia, S. A., 1978, p. 259-262, 12 refs.

Films of superconducting Chevrel-phase copper molybdenum sulfide $\text{Cu}_x\text{Mo}_6\text{S}_8$ were deposited on sapphire substrates by reactive evaporation using H_2S as the reacting gas. Two superconducting temperatures (10.0 K and 5.0 K) of the films were found, corresponding to two different phases with different copper concentrations. All films were superconducting above 4.2 K and contained Chevrel-phase compound as well as free molybdenum. The critical current was measured as a function of applied field. One sample was found to deviate from the scaling law found for co-evaporated or sputtered samples, which possibly indicates a different pinning mechanism or inhomogeneity of the sample. (Author)

A79-34994 * # Friction and wear of single-crystal manganese-zinc ferrite. K. Miyoshi and D. H. Buckley (NASA, Lewis Research Center, Cleveland, Ohio). *ASME, ASLE, ASM, ASTM, SAE, SME, ACS, AIME, and APS, International Conference on Wear of Materials, Dearborn, Mich., Apr. 16-18, 1979, Paper*, 17 p, 12 refs.

Sliding friction experiments were conducted with single-crystal manganese-zinc ferrite in contact with itself and with transition metals. Results indicate mating highest atomic density directions (110 line type) in matched crystallographic planes exhibit the lowest coefficient of friction indicating that direction is important in the friction behavior of ferrite. Matched parallel high atomic density planes and crystallographic directions at the interface exhibit low coefficients of friction. The coefficients of friction for ferrite in contact with various metals are related to the relative chemical activity of these metals. The more active the metal, the higher the coefficient of friction. Cracking and the formation of hexagonal- and rectangular-shaped, platelet wear debris due to cleavages are observed on the ferrite surfaces as a result of sliding. (Author)

A79-3840 * The magnetocaloric effect in dysprosium. S. M. Benford (NASA, Lewis Research Center, Cleveland, Ohio). (*American Institute of Physics and Institute of Electrical and Electronics Engineers, Annual Conference on Magnetism and Magnetic Materials, 24th, Cleveland, Ohio, Nov. 14-18, 1978*) *Journal of Applied Physics*, vol. 50, Mar. 1979, pt. 2, p. 186B-1870, 12 refs.

The magnetocaloric effect in polycrystalline Dy was measured in the 84-280 K range in measuring fields from 1 to 7 T. These adiabatic temperature changes reflect structural changes in Dy with applied field and temperature, and include the first magnetocaloric data for a helical antiferromagnet. Above the Neel point (172 K) a field increase always caused heating; below the Neel point fields less than about 2 T cause cooling for some values of initial temperature. The largest temperature increase with a 7 T field occurs at the Neel point and at fields below 2 T near the Curie point. For refrigeration purposes the optimal working region for a Dy cooling element is field dependent. B.J.

A79-50231 * Indirect measurements of Fermi surface parameters of some chevrel phase materials. J. A. Woollam (NASA, Lewis Research Center, Cleveland, Ohio) and S. A. Alterovitz. *Journal of Magnetism and Magnetic Materials*, vol. 11, Apr. 1979, p. 177-181, 27 refs.

A series of measurements of normal state and superconducting properties were made in zero and in high magnetic fields. When these results are combined with a complete set of theoretical expressions, a number of Fermi surface parameters are found. (Author)

A79-50233 * Thermal expansion of some nickel and cobalt spinels and their solid solutions. I. Zaplatynsky (NASA, Lewis Research Center, Cleveland, Ohio). *British Ceramic Society, Transactions and Journal*, vol. 78, no. 1, 1979, p. 1-3. 15 refs.

N79-11921*# Case Western Reserve Univ., Cleveland, Ohio Engineering Design Center

ADAPTATION OF ION BEAM TECHNOLOGY TO MICRO-FABRICATION OF SOLID STATE DEVICES AND TRANSDUCERS

James A. Topich, Nov 1978, 40 p, refs

(Grant NsG 3131)

(NASA CR 159439) Avail NTIS HC A03/MF A01 CSCL 20L

A number of areas were investigated to determine the potential uses of ion beam techniques in the construction of solid state devices and transducers and the packaging of implantable electronics for biomedical applications. The five areas investigated during the past year were: (1) diode-like devices fabricated on textured silicon; (2) a photolithographic technique for patterning ion beam sputtered PVC (polyvinyl chloride); (3) use of sputtered Teflon as a protective coating for implantable pressure sensors; (4) the sputtering of Macor to seal implantable hybrid circuits; and (5) the use of sputtered Teflon to immobilize enzymes. G Y

A79-44548 * Nb₃Ge as a potential candidate material for 15- to 25-T magnets. M. R. Daniel, A. I. Braginski, C. W. Roland, J. R. Gavalier, and A. T. Santhanam (Westinghouse Research and Development Center, Pittsburgh, Pa.). In: *Advances in cryogenic engineering*, Volume 24 - Proceedings of the Second International Cryogenic Materials Conference, Boulder, Colo., August 2-5, 1977. (A79-44526 19-26) New York, Plenum Press, 1978, p. 459-464. 8 refs. Contracts No. NAS3 20233; No. F44620-70-C-0042.

The critical temperature, upper critical field and structure of Nb₃Ge materials produced by sputtering onto sapphire or by chemical vapor deposition on sapphire or Hastelloy were determined. In the case of the samples formed by deposition, several dopants, including Nb₅Ge₃, NbN and NbC were used. A variety of deposition temperatures were studied. Highest upper critical field values were obtained in samples deposited in the 750 to 850 C range. The degree of flux pinning exhibited a correlation with grain size. The presence of an impurity dopant had a depressant effect on the critical temperature and upper critical field. C K D.

77 THERMODYNAMICS AND STATISTICAL PHYSICS

Includes quantum mechanics; and Bose and Fermi statistics

For related information see also 25 *Inorganic and Physical Chemistry* and 34 *Fluid Mechanics and Heat Transfer*

A79-41731 * **Electronic properties of PbMo6S8 and CuxMo6S8.** J. A. Woollam (NASA, Lewis Research Center, Cleveland, Ohio) and S. A. Alterovitz (NASA, Lewis Research Center, Cleveland, Ohio; Tel Aviv University, Tel Aviv, Israel). *Physical Review B - Solid State, 3rd Series*, vol. 19, Jan. 15, 1979, p. 749-761. 42 refs.

Normal-state properties of sputtered, evaporated, and sintered PbMo6S8 and CuxMo6S8 (where x is between 1.6 and 2.5) samples are reported. These include the temperature dependence of resistivity, magnetoresistance and Hall effect. When combined with superconducting properties (measured on the same samples) and theory, a number of Fermi-surface and superconducting parameters are derived. Fits to the temperature dependence of the resistivity are compared with similar fits for A-15 structure superconductors.

(Author)

A79-49532 * # **Energy-state formulation of lumped volume dynamic equations with application to a simplified free piston Stirling engine.** C. J. Daniele and C. F. Lorenzo (NASA, Lewis Research Center, Cleveland, Ohio). *International Conference on Energy and the Environment, 6th, Pittsburgh, Pa., May 21-24, 1979, Paper*. 28 p. 8 refs.

Lumped volume dynamic equations are derived using an energy-state formulation. This technique requires that kinetic and potential energy state functions be written for the physical system being investigated. To account for losses in the system, a Rayleigh dissipation function is also formed. Using these functions, a Lagrangian is formed and using Lagrange's equation, the equations of motion for the system are derived. The results of the application of this technique to a lumped volume are used to derive a model for the free-piston Stirling engine. The model was simplified and programmed on an analog computer. Results are given comparing the model response with experimental data.

(Author)

85 URBAN TECHNOLOGY AND TRANSPORTATION

Includes applications of space technology to urban problems, technology transfer, technology assessment, and surface and mass transportation.

For related information see 03 Air Transportation and Safety, 16 Space Transportation, and 44 Energy Production and Conversion.

N79-11955* National Aeronautics and Space Administration Lewis Research Center, Cleveland, Ohio

FUEL CELL ON-SITE INTEGRATED ENERGY SYSTEM PARAMETRIC ANALYSIS OF A RESIDENTIAL COMPLEX
Stephen N. Simons [1977] 25 p. refs. Presented at the Fuel Cell Workshop, Sarasota, Fla. 14-17 Nov. 1977. sponsored by DOE.

(NASA TM 78996, E 9780) Avail. NTIS HC A02/MF A01 CSCL 10B

A parametric energy use analysis was performed for a large apartment complex served by a fuel cell on site integrated energy system (OS/IES). The variables parameterized include operating characteristics for four phosphoric acid fuel cells, eight OS/IES energy recovery systems, and four climatic locations. The annual fuel consumption for selected parametric combinations are presented and a breakeven economic analysis is presented for one parametric combination. The results show fuel cell electrical efficiency and system component choice have the greatest effect on annual fuel consumption, fuel cell thermal efficiency and geographic location have less of an effect. Author.

N79-16721* National Aeronautics and Space Administration Lewis Research Center, Cleveland, Ohio

INITIAL COMPARISON OF SINGLE CYLINDER STIRLING ENGINE COMPUTER MODEL PREDICTIONS WITH TEST RESULTS

Roy C. Tew, Jr., Lanny G. Thieme, and David Miao. 1979. 37 p. refs. Presented at the Intern. Congr. and Exposition, Detroit, 26 Feb. 1979 - 4 Mar. 1979. sponsored by the Soc. of Automotive Engrs.

(Contract EC 77-A-1-1040)

(NASA TM 79044, DOE/NASA/1040-78/30, E 9848) Avail. NTIS HC A03/MF A01 CSCL 10B

A Stirling engine digital computer model developed at NASA Lewis Research Center was configured to predict the performance of the GPU-3 single cylinder rhombic drive engine. Revisions to the basic equations and assumptions are discussed. Model predictions with the early results of the Lewis Research Center GPU-3 tests are compared. A R H

N79-27023* National Aeronautics and Space Administration Lewis Research Center, Cleveland, Ohio

LOW-POWER BASELINE TEST RESULTS FOR THE GPU-3 STIRLING ENGINE Final Report

Lanny G. Thieme, Jr. Apr. 1979. 68 p. refs. Document includes microfiche supplement. Supplement is available from NTIS. (Contract EC 77-A-31-1040)

(NASA TM 79103, E 9927, DOE/NASA/1040-79/6) Avail. NTIS HC E04/MF A01 CSCL 10B

A 7.5 kW (10 hp) Stirling engine was converted to a research configuration in order to obtain data for validating Stirling cycle computer simulations. Test results for a range of heater tube gas temperatures, mean compression-space pressures, and engine speeds with both helium and hydrogen as the working fluid are summarized. An instrumentation system to determine indicated work is described and preliminary results are presented. G Y

A79-37293* A cycle timer for testing electric vehicles. R. F. Soltis (NASA, Lewis Research Center, Cleveland, Ohio). *Electric Vehicle Council, International Electric Vehicle Symposium, 5th, Philadelphia, Pa., Oct. 2-5, 1978, Paper*. 10 p. Contract No. EC-77-A-31-1011.

The paper presents a cycle timer which enables the accurate following and repetition of SAE driving schedules of stop and go cycles, for electric vehicles, by reducing the human factor. The system which consists of a programmable read-only memory (PROM) stores each of these cycles, which are detailed, on its own plug-in card. The actual vehicle speed, and the PROM indicated desired speed are displayed on a dual scale meter allowing the driver to match them. A speed change is preceded by a half second buzzer warning and a new cycle by a one second warning. The PROM controls the recycle start time as well as the buzzer activation. A 5 volt regulator providing logic power, and a 12 volt dc-dc converter providing analog and memory power are described. M.E.P.

N79-12968* Booz Allen and Hamilton, Inc., Cleveland, Ohio Design and Development

PRELIMINARY POWER TRAIN DESIGN FOR A STATE-OF-THE-ART ELECTRIC VEHICLE (EXECUTIVE SUMMARY)
[1978] 119 p.

(Contract NAS3-20595)

(NASA-CR-157625) Avail. NTIS HC A09/MF A01 CSCL 13F

The preliminary design of a state-of-the-art electric power train is part of a national effort to reap the potential benefit of useful urban electric passenger vehicles. Outlined in a detailed presentation are: (1) assessment of the state-of-the-art in electric vehicle technology, (2) state-of-the-art power train design, (3) improved power train, and (4) summary and recommendations. G Y

N79-12969* Ford Motor Co., Dearborn, Mich.
EVALUATION OF ADVANCED REGENERATOR SYSTEMS
J. A. Cook, C. A. Fucinari, J. N. Lingscheit, and C. J. Rahnke. Aug. 1978. 39 p. refs.

(Contract DEN3-8)

(NASA-CR-159422, DOE/NASA/0008-78/4) Avail. NTIS HC A03/MF A01 CSCL 13F

The major considerations are discussed which will affect the selection of a ceramic regenerative heat exchanger for an improved 100 HP automotive gas turbine engine. The regenerator considered for this application is about 36 cm in diameter. Regenerator comparisons are made on the basis of material, method of fabrication, cost, and performance. A regenerator inlet temperature of 1000 C is assumed for performance comparisons, and laboratory test results are discussed for material comparisons at 1100 and 1200 C. Engine test results using the Ford 707 industrial gas turbine engine are also discussed. Author.

N79-29110* Mechanical Technology, Inc., Latham, N. Y.
CONCEPTUAL DESIGN STUDY OF AN AUTOMOTIVE STIRLING REFERENCE ENGINE SYSTEM

Jun. 1979. 31 p. Prepared for NASA and DOT.

(Contracts DEN3-32, EC 77-A-31-10040)

(NASA-CR-159605, MTI 79ASE53RE1A)

DOE/NASA 0032-79-11 Avail. NTIS HC A03/MF A01 CSCL 13F

The studies that were made, the methodology that was used, and the results which support the concluded recommendation of a four cylinder double acting square U design with external regenerators are described. Optimization of this design concept resulted in a calculated fuel economy of 36.3 mpg for a 3200 pound vehicle compared to the program goal of 30.0 mpg, and acceleration time of 13.1 seconds compared to the program goal of 15.0 seconds. The engine will meet or exceed the program emission goals of HC - 0.41 gram/mile, CO - 3.4 gram/mile, and nitrogen oxide - 0.4 gram/mile. A R H

N79-31087* # Detroit Diesel Allison, Indianapolis, Ind.
CONCEPTUAL DESIGN STUDY OF AN IMPROVED GAS TURBINE (IGT) POWERTRAIN Report, Mar. - Nov. 1978
 R A Johnson Jul 1979 241 p refs Revised
 (Contract DEN3-28)
 (NASA CR 159604 DDA EDR 9719 DOE/NASA/0028-79/1)
 Avail NTIS HC A11/MF A01 CSCL 13F

Design concepts for an improved automotive gas turbine powertrain are discussed. Twenty percent fuel economy improvement (over 1976), competitive costs (initial and life cycle), high reliability/life, low emissions, and noise/safety compliance were among the factors considered. The powertrain selected consists of a two shaft gas turbine engine with variable geometry aerodynamic components and a single disk rotating regenerator. The regenerator disk, gasifier turbine rotor, and several hot section flowpath parts are ceramic. The powertrain utilizes a conventional automatic transmission. The closest competitor was a single shaft turbine engine matched to a continuously variable transmission (CVT). Both candidate powertrain systems were found to be similar in many respects, however, the CVT represented a significant increase in development cost, technical risk, and production start up costs over the conventional automatic transmission. Installation of the gas turbine powertrain was investigated for a transverse mounted, front wheel drive vehicle.

K L

N79-31088* # Ford Motor Co., Dearborn, Mich.
CONCEPTUAL DESIGN STUDY OF IMPROVED AUTOMOTIVES GAS TURBINE POWERTRAIN Final Report
 May 1979 215 p refs. Prepared in cooperation with AiResearch Mfg. Co., Phoenix, Ariz.
 (Contracts DEN3-37 EC 77 A 31 1040)
 (NASA CR 159580 DOE/NASA/0037-79/1) Avail NTIS HC A10/MF A01 CSCL 13F

Twenty two candidate engine concepts and nineteen transmission concepts. Screening of these concepts, predominantly for fuel economy, cost and technical risk, resulted in a recommended powertrain consisting of a single shaft engine, with a ceramic radial turbine rotor, connected through a differential split power transmission utilizing a variable stator torque converter and a four speed automatic gearbox. Vehicle fuel economy and performance projections, preliminary design analyses and installation studies in a were completed. A cost comparison with the conventional spark ignited gasoline engine showed that the turbine engine would be more expensive initially, however, lifetime cost of ownership is in favor of the gas turbine. A powertrain research and development plan was constructed to gain information on timing and costs to achieve the required level of technology and demonstrate the engine in a vehicle by the year 1983.

A R H

N79-32129* # Detroit Diesel Allison, Indianapolis, Ind.
SINGLE SHAFT AUTOMOTIVE GAS TURBINE ENGINE CHARACTERIZATION TEST Final Report
 R A Johnson Sep 1979 103 p Prepared for NASA and DOE
 (Contracts DEN3-4 EC 77 A 31 1040)
 (NASA CR 159654 DDA EDR 9790 DOE/NASA/0004-79/1)
 Avail NTIS HC A06/MF A01 CSCL 13F

An automotive gas turbine incorporating a single stage centrifugal compressor and a single stage radial inflow turbine is described. Among the engine's features is the use of wide range variable geometry at the inlet guide vanes, the compressor diffuser vanes, and the turbine inlet vanes to achieve improved part load fuel economy. The engine was tested to determine its performance in both the variable geometry and equivalent fixed geometry modes. Testing was conducted without the originally designed recuperator. Test results were compared with the predicted performance of the nonrecuperative engine based on existing component rig test maps. Agreement between test results and the computer model was achieved.

A W H

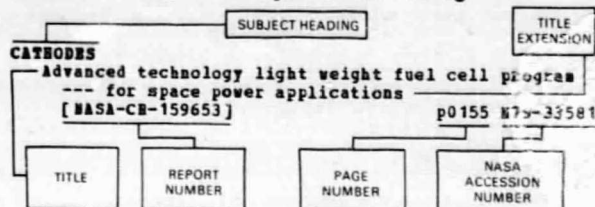
99 GENERAL

A79-21277 * # **Engineering in the 21st century.** J. F. McCarthy, Jr. (NASA, Lewis Research Center, Cleveland, Ohio). *American Astronautical Society, Anniversary Conference, 25th, Houston, Tex., Oct. 30-Nov. 2, 1978, Paper 78-192*, 14 p. 11 refs.

A description is presented of the nature of the aerospace technology system that might be expected by the 21st century from a reasonable evolution of the current resources and capabilities. An aerospace employment outlook is provided. The years 1977 and 1978 seem to be marking the beginning of a period of stability and moderate growth in the aerospace industry. Aerospace research and development employment increased to 70,000 in 1977 and is now occupying a near-constant 18% share of the total research and development work force. The changing job environment is considered along with the future of aerospace education. It is found that one trend is toward a more interdisciplinary education. Most trend setters in engineering education recognize that the really challenging engineering problems invariably require the judicious exercise of several disciplines for their solution. Some future trends in aerospace technology are discussed. By the year 2000 space technology will have achieved major advances in four areas, including management of information, transportation, space structures, and energy. G. R.

SUBJECT INDEX

Typical Subject Index Listing



The title is used to provide a description of the subject matter. When the title is insufficiently descriptive of the document content, a title extension is added, separated from the title by three hyphens. The STAR or IAA accession number is included in each entry to assist the user in locating the abstract in the abstract section. If applicable, a report number is also included as an aid in identifying the document. The page and accession numbers are located beneath and to the right of the title. Under any one subject heading the accession numbers are arranged in sequence with the IAA accession numbers appearing first.

A

ABLATION

Laser balancing demonstration on a high-speed flexible rotor
[ASME PAPER 79-GT-56] p0123 A79-32351

ABRASION

Friction and wear with a single-crystal abrasive grit of silicon carbide in contact with iron base binary alloys in oil: Effects of alloying element and its content
[NASA-TF-1394] p0114 A79-17227

ABSORBERS (MATERIALS)

An impulse test technique with application to acoustic measurements --- for engine noise absorbers
[AIAA PAPER 79-0679] p0178 A79-26890
Full-scale engine tests of bulk absorber acoustic inlet treatment
[NASA-TM-79079] p0173 A79-16645

ABSORPTANCE

Emittance and absorptance of the National Aeronautics and Space Administration ceramic thermal barrier coating --- for gas turbine engine components
p0086 A79-27231

AC GENERATORS

Commercial synchronous alternating-current generators
p0140 A79-26482

ACCELERATED LIFE TESTS

Comment on the mechanism of operation of the impregnated tungsten cathode
p0099 A79-42024
Some practical observations on the accelerated testing of Nickel-Cadmium Cells
p0058 A79-51911

ACCRETION

U DEPOSITION

ACCUMULATORS

NT SOLAR COLLECTORS

Efficiency enhancement of octave-bandwidth traveling wave tubes by use of multistage depressed collectors
[NASA-TF-1416] p0057 A79-17139
Method for fabricating solar cells having integrated collector grids
[NASA-CASE-LEW-12819-2] p0136 A79-18444
Efficiency enhancement of dual-mode traveling wave tubes at saturation and in the linear range by use of spent-beam refocusing and multistage depressed collectors
[NASA-TF-1486] p0058 A79-28420

Multistage depressed collector for dual node operation --- for travelling wave tubes
[NASA-CASE-LEW-13282-1] p0098 A79-32463

ACCURACY

Fundamental mechanisms that influence the estimate of heat transfer to gas turbine blades
[NASA-TM-79128] p0103 A79-20346

ACETYL COMPOUNDS

Electrochemical fluorination of trichloroethylene and N, N-dimethyltrifluoroacetamide
[NASA-TM-79188] p0059 A79-27242

ACIDITY

Factors affecting the open-circuit voltage and electrode kinetics of some iron/titanium/redox flow cells
p0146 A79-11824

ACIDS

NT PHOSPHORIC ACID

ACOUSTIC ATTENUATION

NT SHOCK WAVE ATTENUATION

Optimized multisectioned acoustic liners
[AIAA PAPER 79-0182] p0174 A79-19581
Full-scale engine tests of bulk absorber acoustic inlet treatment
[AIAA PAPER 79-0600] p0026 A79-26881
Acoustic behavior of a fibrous bulk material --- Kevlar 29 sound absorber
[AIAA PAPER 79-0599] p0178 A79-26910
Duct wall impedance control as an advanced concept for acoustic suppression enhancement --- engine noise reduction
[NASA-CR-159425] p0176 A79-10842
Optimized multisectioned acoustic liners
[NASA-TM-79028] p0172 A79-15759
Dispersion of sound in a combustion duct by fuel droplets and soot particles
[NASA-TM-79236] p0174 A79-31002

ACOUSTIC COMBUSTION

U COMBUSTION STABILITY

ACOUSTIC DUCTS

Modal propagation angles in a cylindrical duct with flow and their relation to sound radiation
[AIAA PAPER 79-0183] p0174 A79-19582
Numerical spatial marching techniques in duct acoustics --- noise source calculation from far field pressure measurements
p0175 A79-25946

Modal propagation angles in ducts with soft walls and their connection with suppressor performance
[AIAA PAPER 79-0624] p0175 A79-26880
Duct wall impedance control as an advanced concept for acoustic suppression enhancement --- engine noise reduction
[NASA-CR-159425] p0176 A79-10842
An analytical and experimental study of sound propagation and attenuation in variable-area ducts --- reducing aircraft engine noise
[NASA-CR-135392] p0177 A79-25845

ACOUSTIC EMISSION

Acoustic emission testing of composite vessels under sustained loading
p0128 A79-11543
An acoustic emission study of plastic deformation in polycrystalline aluminum
p0077 A79-19458

Experimental clean combustor program, phase 3: Noise measurement addendum --- CF6-50 high bypass turbofan engine noise
[NASA-CR-159458] p0177 A79-17656
Trailing edge noise data with comparison to theory
[NASA-TM-79208] p0174 A79-27930

ACOUSTIC IMPEDANCE

Investigation of wing shielding effects on C70L engine noise
[AIAA PAPER 79-0669] p0011 A79-28970

ACOUSTIC MEASUREMENTS

SUBJECT INDEX

Effect of grazing flow on the acoustic impedance of Helmholtz resonators consisting of single and clustered orifices
[NASA-CR-3177] p0178 N79-32056

ACOUSTIC MEASUREMENTS
NT NOISE MEASUREMENT
An impulse test technique with application to acoustic measurements --- for engine noise absorbers
[AIAA PAPER 79-0679] p0178 A79-26890

Experimental study of coaxial nozzle exhaust noise --- acoustic measurements
[NASA-TM-79090] p0173 N79-20829

Acoustic and aerodynamic performance investigation of inverted velocity profile conannular plug nozzles, comprehensive data report, volume 1
[NASA-CR-159575-VOL-1] p0177 N79-26884

Acoustic and aerodynamic performance investigation of inverted velocity profile conannular plug nozzles, comprehensive data report, volume 2
[NASA-CR-159575-VOL-2] p0177 N79-26885

Acoustic and aerodynamic performance investigation of inverted velocity profile conannular plug nozzles, comprehensive data report, volume 3
[NASA-CR-159575-VOL-3] p0177 N79-26886

Studies of the acoustic transmission characteristics of coaxial nozzles with inverted velocity profiles: Comprehensive data report --- nozzle transfer functions
[NASA-CR-159628] p0177 N79-27933

ACOUSTIC PROPAGATION
Modal propagation angles in ducts with soft walls and their connection with suppressor performance
[NASA-TM-79081] p0173 N79-16646

Theory of low frequency noise transmission through turbines
[NASA-CR-159457] p0033 N79-20117

ACOUSTIC PROPERTIES
NT ACOUSTIC IMPEDANCE
NT ACOUSTIC VELOCITY
Aerodynamic and acoustic effects of eliminating core swirl from a full scale 1.6 stage pressure ratio fan (QF-5A)
[NASA-TM-78991] p0002 N79-11001

Aerodynamic performance of scarf inlets --- including acoustic advantages
[NASA-TM-79055] p0003 N79-14998

ACOUSTIC RADIATION
U SOUND WAVES
ACOUSTIC VELOCITY
Aerodynamic and acoustic investigation of inverted velocity profile conannular exhaust nozzle models and development of aerodynamic and acoustic prediction procedures, comprehensive data report, volume 1
[NASA-CR-159515] p0034 N79-30185

Aerodynamic and acoustic investigation of inverted velocity profile conannular exhaust nozzle models and development of aerodynamic and acoustic prediction procedures, comprehensive data report, volume 2
[NASA-CR-159516] p0034 N79-30186

ACOUSTIC VIBRATIONS
U SOUND WAVES
ACOUSTICS
NT AEROACOUSTICS
NT PSYCHOACOUSTICS
Loudness of steady sounds - A new theory
p0176 A79-39975

Full-scale engine tests of bulk absorber acoustic inlet treatment
[NASA-TM-79079] p0173 N79-16645

Overall loudness of steady sounds according to theory and experiment
[NASA-RP-1001] p0163 N79-25753

ACQUISITION
NT DATA ACQUISITION
ACTINIDE SERIES
NT PLUTONIUM 238
ACTUATOR DISKS
Analysis of supersonic stall bending flutter in axial-flow compressor by actuator disk theory
[NASA-TF-1345] p0003 N79-13003

ADAPTIVE CONTROL
Identification and dual adaptive control of a turbojet engine
[NASA-TM-79145] p0093 N79-23257

High power phase locked laser oscillators
[NASA-CR-159630] p0112 N79-32538

ADAPTIVE CONTROL SYSTEMS
U ADAPTIVE CONTROL
ADAPTIVE OPTICS
Ground-to-space optical power transfer --- using laser propulsion for orbit transfer
p0161 A79-17180

ADDITIVES
NT OIL ADDITIVES
Effect of a chromium-containing fuel additive on hot corrosion
p0071 A79-26546

Ionized dopant concentrations at the heavily doped surface of a silicon solar cell
[NASA-TP-1347] p0184 N79-13886

Evaluation and auger analysis of a zinc-dialkyl-dithiophosphate antiwear additive in several diester lubricants
[NASA-TP-1544] p0084 N79-32359

ADHERENCE
U ADHESION TESTS
ADHESION
An XPS study of the adherence of refractory carbide, silicide, and boride RF-sputtered wear-resistant coatings --- X-ray Photoelectron Spectroscopy of steel surfaces
p0085 A79-21022

Effect of nitrogen-containing plasma on adherence, friction, and wear of radiofrequency-sputtered titanium carbide coatings
[NASA-TP-1377] p0081 N79-15184

Adherence of sputtered titanium carbides
[NASA-TM-79117] p0074 N79-20220

Improved adherence of sputtered titanium carbide coatings on nickel- and titanium-base alloys
[NASA-TP-1450] p0059 N79-22194

Adhesive material transfer in the erosion of an aluminum alloy
[NASA-TM-79165] p0083 N79-27306

ADHESION TESTS
Auger spectroscopy analysis in adhesion, friction and wear studies
p0110 A79-10992

Use of a nitrogen-argon plasma to improve adherence of sputtered titanium carbide coatings on steel
p0119 A79-25103

Adherence of sputtered titanium carbides
p0078 A79-34997

ADHESIVE BONDING
Adhesive bonding of ion beam textured metals and fluoropolymers
p0060 A79-14798

Titanium/beryllium laminates - Fabrication, mechanical properties, and potential aerospace applications
p0064 A79-20836

Adhesive bonding of ion beam textured metals and fluoropolymers
[NASA-TM-79004] p0181 N79-12909

An investigation of the adhesive bonding of Teflon solar cell covers
[NASA-CR-159565] p0153 N79-26506

ADIABATIC CONDITIONS
The magnetocaloric effect in dysprosium
p0185 A79-38402

AERIAL IMAGERY
U AERIAL PHOTOGRAPHY
AERIAL PHOTOGRAPHY
Feasibility of determining flat roof heat losses using aerial thermography
p0131 A79-51095

Feasibility of determining flat roof heat losses using aerial thermography
[NASA-TM-79152] p0131 N79-22590

AEROACOUSTICS
Measured and predicted noise of the AVCO-Lycoming YF-102 turbofan engine
[AIAA PAPER 79-0641] p0026 A79-26877

Modal propagation angles in ducts with soft walls and their connection with suppressor performance
[AIAA PAPER 79-0624] p0175 A79-26880

Noise from struts and splitters in turbofan exit ducts
[AIAA PAPER 79-0637] p0178 A79-26923

Reduction of rotor-turbulence interaction noise in static fan noise testing
[AIAA PAPER 79-0656] p0036 A79-26925

Effects of simulated forward flight on jet noise, shock noise and internal noise

SUBJECT INDEX

AERONAUTICAL ENGINEERING

- [AIAA PAPER 79-0615] p0178 A79-26936
- Analysis of radiation patterns of interaction tones generated by inlet rods in the JT15D engine
- [AIAA PAPER 79-0581] p0027 A79-26944
- Investigation of wing shielding effects on CTOL engine noise
- [AIAA PAPER 79-0669] p0011 A79-28970
- Assessment at full scale of nozzle/wing geometry effects on OTW aeroacoustic characteristics --- Over The Wing STOL engine configurations
- p0175 A79-39802
- An improved method for predicting the effects of flight on jet mixing noise
- p0176 A79-39803
- Trailing edge noise data with comparison to theory
- [AIAA PAPER 79-1524] p0176 A79-47340
- Aerodynamic performance of scarf inlets --- including acoustic advantages
- [NASA-T-79-55] p0003 A79-14998
- Assessment of full scale of nozzle/wing geometry effects on OTW aero-acoustic characteristics --- short takeoff aircraft noise
- [NASA-TM-79168] p0174 A79-25841
- Dispersion of sound in a combustion duct by fuel droplets and soot particles
- [NASA-TM-79236] p0174 A79-31002
- Aerodynamic and acoustic investigation of inverted velocity profile coannular exhaust nozzle models and development of aerodynamic and acoustic prediction procedures
- [NASA-CR-3168] p0035 A79-31212
- AERODYNAMIC AXIS**
- U AERODYNAMIC BALANCE
- AERODYNAMIC BALANCE**
- T700 power turbine rotor multiplane/multispeed balancing demonstration
- [NASA-CR-159586] p0122 A79-25392
- AERODYNAMIC BRAKES**
- NT TRAILING-EDGE FLAPS
- AERODYNAMIC CENTER**
- U AERODYNAMIC BALANCE
- AERODYNAMIC CHARACTERISTICS**
- NT AERODYNAMIC BALANCE
- NT JET LIFT
- NT LIFT
- Aerodynamic performance of scarf inlets
- [AIAA PAPER 79-0380] p0005 A79-23510
- Aerodynamic performance of a 1.35-pressure-ratio axial-flow fan stage
- [NASA-TP-1299] p0002 A79-10022
- Determining and improving labyrinth seal performance in current and advanced high performance gas turbines
- p0031 A79-11068
- Aerodynamic performance of scarf inlets --- including acoustic advantages
- [NASA-TM-79055] p0003 A79-14998
- Effect of lip and centerbody geometry on aerodynamic performance of inlets for tilting-nacelle VTOL aircraft
- [NASA-TM-79056] p0003 A79-14999
- The use of wind data with an operational wind turbine in a research and development environment
- [NASA-TM-73832] p0140 A79-26502
- Acoustic and aerodynamic performance investigation of inverted velocity profile coannular plug nozzles, comprehensive data report, volume 1
- [NASA-CR-159575-VOL-1] p0177 A79-26884
- Acoustic and aerodynamic performance investigation of inverted velocity profile coannular plug nozzles, comprehensive data report, volume 2
- [NASA-CR-159575-VOL-2] p0177 A79-26885
- Acoustic and aerodynamic performance investigation of inverted velocity profile coannular plug nozzles, comprehensive data report, volume 3
- [NASA-CR-159575-VOL-3] p0177 A79-26886
- Aerodynamic and acoustic investigation of inverted velocity profile coannular exhaust nozzle models and development of aerodynamic and acoustic prediction procedures
- [NASA-CR-3168] p0035 A79-31212
- AERODYNAMIC CHORDS**
- U AIRFOIL PROFILES
- AERODYNAMIC COEFFICIENTS**
- Aerodynamic and acoustic investigation of inverted velocity profile coannular exhaust nozzle models and development of aerodynamic and acoustic prediction procedures, comprehensive data report, volume 1
- [NASA-CR-159515] p0034 A79-30185
- Aerodynamic and acoustic investigation of inverted velocity profile coannular exhaust nozzle models and development of aerodynamic and acoustic prediction procedures, comprehensive data report, volume 2
- [NASA-CR-159516] p0034 A79-30186
- AERODYNAMIC CONFIGURATIONS**
- NT WING NACELLE CONFIGURATIONS
- Effect of lip and centerbody geometry on aerodynamic performance of inlets for tilting-nacelle VTOL aircraft
- [AIAA PAPER 79-0381] p0025 A79-23509
- Design, fabrication, and test of a composite material wind turbine rotor blade
- [NASA-CR-135389] p0150 A79-10525
- Rotor redesign for a highly loaded 1800 ft/sec tip speed fan. 1: Aerodynamic and mechanical design report
- [NASA-CR-159596] p0034 A79-26055
- Performance of two-stage fan with a first-stage rotor redesigned to account for the presence of a part-span damper
- [NASA-TP-1483] p0024 A79-30191
- AERODYNAMIC FORCES**
- NT AERODYNAMIC LOADS
- NT GUST LOADS
- NT JET LIFT
- NT LIFT
- NT WING LOADING
- AERODYNAMIC LIFT**
- U LIFT
- AERODYNAMIC LOADS**
- NT GUST LOADS
- Effect of flight loads on turbofan engine performance deterioration
- p0027 A79-30559
- Wing aerodynamic loading caused by jet-induced lift associated with STOL-OTW configurations
- [AIAA PAPER 79-1664] p0006 A79-47346
- Supersonic unstalled flutter --- aerodynamic loading of thin airfoils induced by cascade motion
- [NASA-TM-79001] p0002 A79-11000
- Supersonic unstalled flutter
- p0023 A79-27181
- AERODYNAMIC NOISE**
- Experimental study of coaxial nozzle exhaust noise
- [AIAA PAPER 79-0631] p0175 A79-28963
- A jet exhaust noise prediction procedure for inverted velocity profile coannular nozzles
- [AIAA PAPER 79-0633] p0178 A79-28964
- Tone noise of three supersonic helical tip speed propellers in a wind tunnel
- p0175 A79-39801
- Trailing edge noise data with comparison to theory
- [AIAA PAPER 79-1524] p0176 A79-47340
- Aerodynamic and acoustic effects of eliminating core swirl from a full scale 1.6 stage pressure ratio fan (GF-5A)
- [NASA-TM-78991] p0002 A79-11001
- An improved method for predicting the effects of flight on jet mixing noise
- [NASA-TM-79155] p0173 A79-24770
- Trailing edge noise data with comparison to theory
- [NASA-TM-79208] p0174 A79-27930
- AERODYNAMICS**
- NT ROTOR AERODYNAMICS
- Preliminary results in the NASA Lewis H2-O2 combustion MHD experiment
- p0162 A79-39807
- AEROELASTICITY**
- Characteristics of aeroelastic instabilities in turbomachinery - NASA full scale engine test results
- [AIAA 79-7011] p0027 A79-29386
- Wind tunnel tests of a blade subjected to midchord torsional oscillation at high subsonic stall flutter conditions
- [NASA-TM-78998] p0002 A79-12016
- Characteristics of aeroelastic instabilities in turbomachinery - NASA full scale engine test results
- [NASA-TM-79085] p0126 A79-17263
- Nonlinear equations of equilibrium for elastic helicopter or wind turbine blades undergoing moderate deformation
- [NASA-CR-159478] p0130 A79-19414
- AERONAUTICAL ENGINEERING**
- Diagnostics of wear in aeronautical systems

AERONAUTICAL SATELLITES

SUBJECT INDEX

- [NASA-TN-79185] p0115 W79-24350
- AERONAUTICAL SATELLITES**
- Automated meteorological data from commercial aircraft via satellite - Present experience and future implications p0010 A79-17092
- AEROPHYSICS**
- U ATMOSPHERIC PHYSICS**
- AEROSOLS**
- Global sensing of gaseous and aerosol trace species using automated instrumentation on 747 airliners p0110 A79-15067
- AEROSPACE ENGINEERING**
- NT AERONAUTICAL ENGINEERING**
- AEROSPACE ENVIRONMENTS**
- Large space system - Charged particle environment interaction technology --- effects on high voltage solar array performance [AIAA 79-0913] p0055 A79-34775
- UV blocking filters for polymeric films p0088 A79-51103
- Space environmental interactions with spacecraft surfaces [NASA-TN-79016] p0046 W79-15150
- Large space system: Charged particle environment interaction technology [NASA-TN-79156] p0046 W79-22188
- Titanium-alloy, metallic-fluid heat pipes for space service [NASA-TN-79132] p0104 W79-22426
- Spacecraft Charging Technology, 1978 [NASA-CP-2071] p0047 W79-24001
- The capabilities of the NASA charging analyzer program p0047 W79-24011
- Geosynchronous satellite operating anomalies caused by interaction with the local spacecraft environment p0050 W79-24049
- AEROSPACE INDUSTRY**
- Engineering in the 21st century --- aerospace technology prospects [AAS PAPER 78-192] p0190 A79-21277
- AFTERBURNERS**
- U AFTERBURNING**
- AFTERBURNING**
- Test verification of a turbofan partial swirl afterburner [AIAA PAPER 79-1199] p0029 A79-38981
- Operating condition and geometry effects on low-frequency afterburner combustion instability in a turbofan at altitude [NASA-TP-1475] p0022 W79-25022
- AGE HARDENING**
- U PRECIPITATION HARDENING**
- AIR BEARINGS**
- U GAS BEARINGS**
- AIR BREATHING ENGINES**
- NT DUCTED FAN ENGINES**
- NT GAS TURBINE ENGINES**
- NT J-85 ENGINE**
- NT JET ENGINES**
- NT T-53 ENGINE**
- NT TURBOFAN ENGINES**
- NT TURBOJET ENGINES**
- NT TURBOPROP ENGINES**
- Multivariable control altitude demonstration on the F100 turbofan engine [NASA-TN-79183] p0022 W79-25015
- AIR CONDITIONING EQUIPMENT**
- Optimum dry-cooling sub-systems for a solar air conditioner [NASA-TN-79007] p0133 W79-11477
- AIR COOLING**
- The NASA high pressure facility and turbine test rig p0038 A79-21296
- Thermal-structural mission analyses of air-cooled gas turbine blades [ASME PAPER 79-GT-19] p0027 A79-30553
- Thermal-structural mission analyses of air-cooled gas turbine blades [NASA-TN-78963] p0126 W79-11433
- Internally coated air-cooled gas turbine blading [NASA-CN-159574] p0034 W79-25018
- AIR CURRENTS**
- NT MERIDIONAL FLOW**
- AIR FLOW**
- NT MERIDIONAL FLOW**
- Atomization of water jets and sheets in axial and swirling airflows [ASME PAPER 79-GT-170] p0106 A79-30556
- Atomization of water jets and sheets in axial and swirling airflows [NASA-TN-79043] p0102 W79-12362
- Modeling of premixing-prevaporizing fuel-air mixing passages p0019 W79-24998
- Aerodynamic performance of axial-flow fan stage operated at nine inlet guide vane angles --- to be used on vertical lift aircraft [NASA-TP-1510] p0024 W79-31214
- AIR INLETS**
- U AIR INTAKES**
- AIR INTAKES**
- NT ENGINE INLETS**
- NT SUPERSONIC INLETS**
- Experimental investigation of a 0.15-scale model of an underfuselage normal-shock inlet [NASA-CN-3049] p0006 W79-12014
- Self stabilizing sonic inlet [NASA-CASE-LEW-11890-1] p0011 W79-24976
- A throat-bypass stability-bleed system using relief valves to increase the transient stability of a mixed-compression inlet --- YF-12 aircraft inlet tests in the Lewis 10 by 10 ft supersonic wind tunnel [NASA-TP-1083] p0023 W79-28176
- AIR POLLUTION**
- NT GLOBAL AIR POLLUTION**
- Wide range operation of advanced low NOx aircraft gas turbine combustors [ASME PAPER 78-GT-128] p0024 A79-10792
- Pattern recognition methods and air pollution source identification --- based on wind direction p0158 A79-15079
- Reduction of particulate carryover from a pressurized fluidized bed p0150 A79-49527
- Reduction of particulate carryover from a pressurized fluidized bed p0150 A79-49527
- Correlations of catalytic combustor performance parameters [NASA-TN-79014] p0134 W79-11480
- The advanced low-emissions catalytic-combustor program. Phase 1: Description and status [NASA-TN-79049] p0015 W79-15047
- Ozone measurement system for NASA global air sampling program [NASA-TP-1451] p0158 W79-22654
- Experimental Clean Combustor Program (ECCP), phase 3 --- commercial aircraft turbofan engine tests with double annular combustor [NASA-CN-135384] p0035 W79-31207
- AIR QUALITY**
- NASA Global Atmospheric Sampling Program (GASP) data report for tape VL0009 [NASA-TN-79058] p0157 W79-15448
- NASA Global Atmospheric Sampling Program (GASP) data report for tapes VL0010 and VL0012 [NASA-TN-79061] p0157 W79-15450
- NASA Global Atmospheric Sampling Program (GASP) data report for tapes VL0007 and VL0008 [NASA-TN-73784] p0157 W79-17359
- AIR SAMPLING**
- Pattern recognition methods and air pollution source identification --- based on wind direction p0158 A79-15079
- Experimental evidence of interhemispheric transport from airborne carbon monoxide measurements p0158 A79-38942
- Sulfate and nitrate mixing ratios in the vicinity of the tropopause p0158 A79-49494
- Airborne atmospheric sampling system p0012 A79-50333
- AIR SEA INTERACTIONS**
- U AIR WATER INTERACTIONS**
- AIR WATER INTERACTIONS**
- WETAIR: A computer code for calculating thermodynamic and transport properties of air-water mixtures [NASA-XP-1466] p0166 W79-23688
- AIRBORNE EQUIPMENT**
- NT AIRBORNE/SPACEBORNE COMPUTERS**

SUBJECT INDEX

AIRCRAFT EQUIPMENT

- An airborne meteorological data collection system using satellite relay /ASDAR/ p0010 A79-14949
- Experimental evidence of interhemispheric transport from airborne carbon monoxide measurements p0158 A79-38942
- AIRBORNE SURVEILLANCE RADAR**
Radar image processing of real aperture SAR data for the detection and identification of iceberg and ship targets p0131 A79-36537
- AIRBORNE/SPACEBORNE COMPUTERS**
Computer aided control of a mechanical arm A79-50334
- AIRCRAFT ANTENNAS**
UHF coplanar-slot antenna for aircraft-to-satellite data communications [NASA-TN-79239] p0010 A79-31185
- AIRCRAFT BRAKES**
NT TRAILING-EDGE FLAPS
- AIRCRAFT CABINS**
U AIRCRAFT COMPARTMENTS
- AIRCRAFT COMMUNICATION**
Automated meteorological data from commercial aircraft via satellite - Present experience and future implications p0010 A79-17092
- UHF coplanar-slot antenna for aircraft-to-satellite data communications [NASA-TN-79239] p0010 A79-31185
- AIRCRAFT COMPARTMENTS**
Simultaneous measurements of ozone outside and inside cabins of two B-747 airliners and a Gates Learjet business jet p0008 A79-27571
- Feasibility of wing shielding of the airplane interior from the shock noise generated by supersonic tip speed propellers [NASA-TN-79042] p0172 A79-15757
- Ozone contamination in aircraft cabins: Objectives and approach p0008 A79-21022
- Ozone Contamination in Aircraft Cabins: Summary of recommendations p0008 A79-21026
- Ozone Contamination in Aircraft Cabins: Post workshop review of recommendations p0008 A79-21027
- Ozone Contamination in Aircraft Cabins: Appendix B: Overview papers. In-flight measurements p0008 A79-21029
- Procedures for estimating the frequency of commercial airline flights encountering high cabin ozone levels [NASA-TF-1560] p0008 A79-33171
- AIRCRAFT CONSTRUCTION**
U AIRCRAFT STRUCTURES
- AIRCRAFT DESIGN**
NT HELICOPTER DESIGN
Recent applications of theoretical analysis to V/STOL inlet design p0006 A79-49530
- The M-15-aircraft (samolot M-15) [NASA-TN-75586] p0013 A79-12063
- AIRCRAFT ENGINES**
NT HELICOPTER ENGINES
NT T-55 ENGINE
NT T-63 ENGINE
NT TF-30 ENGINE
NT VARIABLE CYCLE ENGINES
Wide range operation of advanced low NOx aircraft gas turbine combustors [ASME PAPER 78-GT-128] p0024 A79-10792
- Impact of future fuel properties on aircraft engines and fuel systems p0024 A79-11600
- Fuel conservative aircraft engine technology p0025 A79-20078
- NASA research on general aviation power plants [AIAA PAPER 79-0561] p0026 A79-25870
- Effect of broadened-specification fuels on aircraft engines and fuel systems [AIAA 79-7008] p0027 A79-29383
- Thermal-structural missile analyses of air-cooled gas turbine blades [ASME PAPER 79-GT-19] p0027 A79-30553
- Effect of flight loads on turbofan engine performance deterioration p0027 A79-30559
- The GATE studies - Assessing the potential of future small general aviation turbine engines p0027 A79-30560
- Preliminary CCGAT program test results --- Quiet, Clean General Aviation Turbofan [SAE PAPER 790596] p0028 A79-36729
- Concepts for reducing exhaust emissions and fuel consumption of the aircraft piston engine [SAE PAPER 790605] p0036 A79-36737
- A review of Curtiss-Wright rotary engine developments with respect to general aviation potential [SAE PAPER 790621] p0036 A79-36749
- Wind tunnel performance of four energy efficient propellers designed for Mach 0.8 cruise [SAE PAPER 790573] p0028 A79-36759
- Effects of air injection on a turbocharged Teledyne Continental Motors TS10-360-C engine [SAE PAPER 790607] p0028 A79-36760
- Application of digital controls on the quiet clean short haul experimental engines [AIAA PAPER 79-1203] p0029 A79-38984
- Energy efficient aircraft engines [AIAA PAPER 79-1861] p0030 A79-47918
- Fundamental mechanisms that influence the estimate of heat transfer to gas turbine blades p0099 A79-49526
- An overview of NASA research on positive displacement type general aviation engines [AIAA PAPER 79-1824] p0038 A79-53750
- Evaluation of the cyclic behavior of aircraft turbine disk alloys [NASA-CN-159409] p0030 A79-10058
- Energy efficient engine preliminary design and integration study [NASA-CN-135396] p0012 A79-12084
- Impact of future fuel properties on aircraft engines and fuel systems p0089 A79-13197
- Computer simulation of an aircraft engine fuel injection system [NASA-CN-157641] p0016 A79-15052
- The rotary combustion engine: A candidate for general aviation --- conferences [NASA-CN-2067] p0016 A79-15961
- Effect of broadened-specification fuels on aircraft engines and fuel systems [NASA-TN-79086] p0089 A79-16136
- Generation of linear dynamic models from a digital nonlinear simulation [NASA-TF-1388] p0001 A79-16796
- Aircraft engine sump fire mitigation, phase 2 [NASA-CN-135379] p0121 A79-17219
- Effects of air injection on a turbocharged Teledyne Continental Motors TS10-360-C engine [NASA-TN-79121] p0158 A79-20528
- Premixed Prevaporized Combustor Technology Forum [NASA-CN-2078] p0019 A79-24994
- Lean, premixed, prevaporized combustor conceptual design study p0021 A79-25013
- Lean, premixed, prevaporized combustor conceptual design study p0022 A79-25014
- An analytical and experimental study of sound propagation and attenuation in variable-area ducts --- reducing aircraft engine noise [NASA-CN-135392] p0177 A79-25845
- Energy efficient aircraft engines [NASA-TN-79208] p0022 A79-27141
- Advanced General Aviation Turbine Engine (GATE) study [NASA-CN-159624] p0039 A79-29189
- Computerized systems analysis and optimization of aircraft engine performance, weight, and life cycle costs [NASA-TN-79221] p0170 A79-29938
- Energy efficient engine flight propulsion system preliminary analysis and design report [NASA-CN-159487] p0035 A79-30189
- An overview of NASA research on positive displacement type general aviation engines [NASA-TN-79254] p0024 A79-31210
- AIRCRAFT EQUIPMENT**
The solid state remote power controller - Its status, use and perspective --- for aircraft and spacecraft p0099 A79-10896

AIRCRAFT FUEL SYSTEMS

Effect of broadened-specification fuels on aircraft engines and fuel systems [NASA-TM-79006] p0089 N79-16136

AIRCRAFT FUELS

Alternative aircraft fuels p0090 A79-10824

Characteristics and combustion of future hydrocarbon fuels p0090 A79-11599

Alternative aviation turbine fuels p0090 A79-12370

High-freezing-point fuels used for aviation turbine engines [ASME PAPER 79-GT-141] p0090 A79-30555

Analytical evaluation of the impact of broad specification fuels on high bypass turbofan engine combustors [NASA-CR-159454] p0031 N79-13050

Effect of broadened-specification fuels on aircraft engines and fuel systems [NASA-TM-79006] p0089 N79-16136

Lean, premixed, prevaporized combustion for aircraft gas turbine engines [NASA-TM-79148] p0018 N79-23964

Lean, premixed, prevaporized combustion for aircraft gas turbine engines [NASA-TM-79148] p0018 N79-23964

Design and evaluation of aircraft heat source systems for use with high-freezing point fuels [NASA-CR-159568] p0091 N79-24172

Autoignition of fuels p0020 N79-25001

Experimental study of low temperature behavior of aviation turbine fuels in a wing tank model [NASA-CR-159615] p0091 N79-29355

AIRCRAFT HAZARDS

Aircraft cabin ozone measurements on B747-100 and B747-SP aircraft: Correlations with atmospheric ozone and ozone encounter statistics [NASA-TM-79060] p0008 N79-15013

Aircraft icing [NASA-CR-2086] p0004 N79-23912

Executive summary of Aircraft Icing Specialists Workshop p0004 N79-23914

AIRCRAFT INSTRUMENTS

NT FLIGHT RECORDERS

An airborne meteorological data collection system using satellite relay /ASDAR/ p0010 A79-14949

AIRCRAFT NOISE

NT JET AIRCRAFT NOISE

NT SONIC BOOMS

Assessment at full scale of nozzle/wing geometry effects on OTW aeroacoustic characteristics --- Over The Wing STOL engine configurations p0175 A79-39802

AIRCRAFT PARTS

Wear of seal materials used in aircraft propulsion systems [NASA-TM-79003] p0073 N79-12204

Fundamentals of Gas Turbine combustion [NASA-CR-2087] p0022 N79-25016

AIRCRAFT PERFORMANCE

Effect of lip and centerbody geometry on aerodynamic performance of inlets for tilting-nacelle VTOL aircraft [AIAA PAPER 79-0381] p0025 A79-21509

AIRCRAFT POWER SOURCES

U AIRCRAFT ENGINES

AIRCRAFT SAFETY

Rotor fragment protection program: Statistics on aircraft gas turbine engine rotor failures that occurred in US commercial aviation during 1976 [NASA-CR-159474] p0032 N79-18977

AIRCRAFT SPECIFICATIONS

Effect of broadened-specification fuels on aircraft engines and fuel systems [AIAA 79-7008] p0027 A79-29383

AIRCRAFT STRUCTURES

NT AIRFRAMES

NT CENTERBODIES

Composites emerging for aeropropulsion applications p0066 A79-53720

AIRFOIL CHARACTERISTICS

U AIRFOILS

AIRFOIL PROFILES

Study of blade aspect ratio on a compressor front

stage aerodynamic and mechanical design report [NASA-CR-159555] p0034 N79-23085

Rotor redesign for a highly loaded 1800 ft/sec tip speed fan. 1: Aerodynamic and mechanical design report [NASA-CR-159596] p0034 N79-26055

AIRFOIL SECTIONS

U AIRFOIL PROFILES

AIRFOIL THICKNESS

U AIRFOIL PROFILES

AIRFOILS

NT PROPELLER BLADES

NT ROTARY WINGS

NT THIN AIRFOILS

NT TIP DRIVEN SECTIONS

NT TRAILING-EDGE FLAPS

NT WINGS

Computer-aided analysis and design of the shape rolling process for producing turbine engine airfoils [NASA-CR-159455] p0012 N79-12087

Airfoil cooling hole plugging by combustion gas impurities of the type found in coal derived fuels [NASA-TM-79076] p0089 N79-20265

Computer-aided analysis and design of the shape rolling process for producing turbine engine airfoils [NASA-CR-135367] p0080 N79-26175

Supersonic unstalled flutter p0023 N79-27181

AIRFRAMES

Aerospace Transparent Materials and Enclosures (12th) [AD-A065049] p0018 N79-23066

AIRLINE OPERATIONS

Aircraft cabin ozone measurements on B747-100 and B747-SP aircraft: Correlations with atmospheric ozone and ozone encounter statistics [NASA-TM-79060] p0008 N79-15013

AITKEN NUCLEI

Condensation-nuclei (Aitken Particle) measurement system used in NASA global atmospheric sampling program [NASA-TP-1415] p0157 N79-18479

ALARMS

U WARNING SYSTEMS

ALCOHOLS

NT ETHYL ALCOHOL

NT PHENOLS

NT POLYVINYL ALCOHOL

ALGEBRA

NT NONLINEAR EQUATIONS

ALGORITHMS

On the distribution of computation for sequential decoding using the stack algorithm p0096 A79-33793

Atmospheric transformation of multispectral remote sensor data --- Great Lakes [E79-10006] p0131 N79-12524

ALIPHATIC COMPOUNDS

NT ACETYL COMPOUNDS

NT CHLOROETHYLENE

NT DIALLYL COMPOUNDS

NT ETHYL ALCOHOL

NT METHYL COMPOUNDS

NT PROPANE

NT URETHANES

ALKALI HALIDES

NT SODIUM CHLORIDES

ALKALI METALS

NT LIQUID LITHIUM

NT POTASSIUM

ALKALIES

NT POTASSIUM HYDROXIDES

NT SODIUM HYDROXIDES

An investigation of the initiation stage of hot corrosion in Ni-base alloys [NASA-CR-159616] p0080 N79-25196

The alkaline zinc electrode as a mixed potential system [NASA-TM-79235] p0142 N79-29600

ALKALINE BATTERIES

Determination of the zincate diffusion coefficient and its application to alkaline battery problems p0070 A79-11547

Cross-linked polyvinyl alcohol and method of making same --- separator for alkaline batteries [NASA-CASE-LEW-13101-1] p0068 N79-14173

- Decay of the zincate concentration gradient at an alkaline zinc cathode after charging
[NASA-TM-79106] p0137 N79-20520
- Control of volume resistivity in inorganic organic separators
[NASA-TP-1439] p0069 N79-22246
- Ultrafine polybenzimidazole (PBI) fibers --- separators for alkaline batteries and fuel cells
[NASA-CR-159644] p0067 N79-31350
- Strip cell test and evaluation program
[NASA-CR-159652] p0154 N79-31784
- ALKANES
NT PROPANE
- ALLOYS
NT ALUMINUM ALLOYS
NT BINARY ALLOYS
NT BRONZES
NT CAST ALLOYS
NT CHROMIUM ALLOYS
NT COBALT ALLOYS
NT EUTECTIC ALLOYS
NT HEAT RESISTANT ALLOYS
NT HIGH STRENGTH ALLOYS
NT HIGH STRENGTH STEELS
NT IRON ALLOYS
NT MANGANESE ALLOYS
NT MOLYBDENUM ALLOYS
NT NICKEL ALLOYS
NT NICKEL STEELS
NT RARE EARTH ALLOYS
NT REFRACTORY METAL ALLOYS
NT RENE 41
NT RHENIUM ALLOYS
NT STAINLESS STEELS
NT STEELS
NT TITANIUM ALLOYS
NT TUNGSTEN ALLOYS
NT ZINC ALLOYS
Longitudinal shear behavior of several oxide dispersion strengthened alloys p0076 A79-14955
Effects of yttrium, aluminum, and chromium concentrations in bond coatings on the performance of zirconia-yttria thermal barriers
[NASA-TM-79206] p0075 N79-29293
- ALTERNATING CURRENT GENERATORS
U AC GENERATORS
ALTERNATORS (GENERATORS)
U AC GENERATORS
- ALTITUDE TESTS
Multivariable control altitude demonstration on the F100 turbofan engine
[AIAA PAPER 79-1204] p0029 A79-39814
Turbine engine altitude chamber and flight testing with liquid hydrogen
[NASA-TM-79196] p0022 N79-27140
- ALUMINA
U ALUMINUM OXIDES
- ALUMINIZING
U ALUMINUM COATINGS
- ALUMINUM
An acoustic emission study of plastic deformation in polycrystalline aluminum p0077 A79-19458
Resonance-tube ignition of aluminum p0071 A79-46366
Evaluation of manufacturing processes for boron/aluminum composites containing 0.2-m-diameter boron fibers
[NASA-TM-79008] p0062 N79-12153
High temperature dynamic modulus and damping of aluminum and titanium matrix composites
[NASA-TM-79080] p0061 N79-16077
Wear of aluminum and hypoeutectic aluminum-silicon alloys in boundary-lubricated pin-on disk sliding
[NASA-TP-1442] p0074 N79-21184
Fabrication of J79 boron/aluminum compressor blades
[NASA-CR-159566] p0034 N79-23970
High-energy electron-induced damage production at room temperature in aluminum-doped silicon p0154 N79-32662
- ALUMINUM ALLOYS
Shear rupture of a directionally solidified eutectic gamma/gamma-prime - alpha /Mo/ alloy --- for aircraft engine turbine blades p0077 A79-21301
Adhesive material transfer in the erosion of an aluminum alloy
[NASA-TM-79165] p0083 N79-27306
- Some TEM observations of Al₂O₃ scales formed on NiCrAl alloys
[NASA-TM-79259] p0076 N79-33306
- ALUMINUM BORON COMPOSITES
High temperature dynamic modulus and damping of aluminum and titanium matrix composites p0065 A79-26132
Fabrication and testing of non-graphitic superhybrid composites p0066 A79-43289
Elevated temperature properties of boron/aluminum composites
[NASA-CR-159445] p0066 N79-16924
- ALUMINUM COATINGS
Internally coated air-cooled gas turbine blading
[NASA-CR-159574] p0034 N79-25018
An experimental, low-cost, silicon slurry/aluminate high-temperature coating for superalloys
[NASA-TM-79178] p0075 N79-29292
- ALUMINUM COMPOUNDS
NT ALUMINUM OXIDES
NT ALUMINUM SILICATES
ALUMINUM OXIDES
Some TEM observations of Al₂O₃ scales formed on NiCrAl alloys
[NASA-TM-79259] p0076 N79-33306
- ALUMINUM SILICATES
Ceramic applications in the advanced Stirling automotive engine p0117 A79-12851
- AMBIENT TEMPERATURE
Application of ion chromatography to the study of hydrolysis of some halogenated hydrocarbons at ambient temperatures p0060 A79-14951
- AMBIT
U FIELD THEORY (PHYSICS)
- AMIDES
NT POLYIMIDES
Electrochemical fluorination of trichloroethylene and N, N-dimethyltrifluoroacetamide p0060 A79-49536
Electrochemical fluorination of trichloroethylene and N, N-dimethyltrifluoroacetamide p0060 A79-49536
Electrochemical fluorination of trichloroethylene and N, N-dimethyltrifluoroacetamide
[NASA-TM-79188] p0059 N79-27242
- AMINES
High char imide-modified epoxy matrix resins --- for graphite-epoxy composites
[NASA-TM-79226] p0063 N79-29240
Curing agent for polyepoxides and epoxy resins and composites cured therewith
[NASA-CASE-LEN-13226-1] p0059 N79-31345
- AMMETERS
NT MICROMILLIAMMETERS
- AMPERAGE
U ELECTRIC CURRENT
- AMPLIFICATION
NT POWER GAIN
- AMPLIFIERS
NT MICROWAVE AMPLIFIERS
- ANALOG COMPUTERS
NT UNIVAC 1100 SERIES COMPUTERS
Energy-state formulation of lumped volume dynamic equations with application to a simplified free piston Stirling engine p0187 A79-49532
- ANALYSIS (MATHEMATICS)
NT BURGER EQUATION
NT FINITE DIFFERENCE THEORY
NT FINITE ELEMENT METHOD
NT INTERPOLATION
NT LOGARITHMS
NT MONTE CARLO METHOD
NT NONLINEAR EQUATIONS
NT NUMERICAL ANALYSIS
NT NUMERICAL INTEGRATION
NT SERIES (MATHEMATICS)
Analytical core loss calculations for magnetic materials used in high frequency high power converter applications
[NASA-TM-79234] p0098 N79-31499
- ANALYTIC GEOMETRY
NT ELLIPSES
- ANALYZERS
NT ENGINE ANALYZERS

ANATOMY

NT EYE (ANATOMY)

NT HUMAN BODY

ANEMOMETRY

U VELOCITY MEASUREMENT

ANGLES (GEOMETRY)

NT GRAZING INCIDENCE

Modal propagation angles in a cylindrical duct
with flow and their relation to sound radiation
[AIAA PAPER 79-0183] p0174 A79-19582

Modal propagation angles in ducts with soft walls
and their connection with suppressor performance
[AIAA PAPER 79-0624] p0175 A79-26880

ANGULAR DISTRIBUTION

Modal propagation angles in a cylindrical duct
with flow and their relation to sound radiation
[NASA-TM-79030] p0172 A79-15756

Modal propagation angles in ducts with soft walls
and their connection with suppressor performance
[NASA-TM-79081] p0173 A79-16646

ANISOTROPY

Anisotropic friction and wear of single-crystal
manganese-zinc ferrite in contact with itself
[NASA-TP-1339] p0113 A79-10425

Anisotropic friction, deformation, and fracture of
single-crystal silicon carbide at room temperature
[NASA-TP-1525] p0084 A79-30380

ANNEALING

Influence of composition, annealing treatment, and
texture on the fracture toughness of
Ti-5Al-2.5Sn plate at cryogenic temperatures
p0077 A79-24262

Reverse annealing in radiation-damaged, silicon
solar cells
p0144 A79-32660

Annealing of radiation damage in 0.1- and
2-ohm-centimeter Silicon solar cells
[NASA-TP-1559] p0144 A79-33572

ANNULAR FLOW

An experimental investigation of forced mixing of
a turbulent boundary layer in an annular diffuser
--- for boundary layer control
[NASA-TM-79171] p0004 A79-23920

ANNULAR NOZZLES

A jet exhaust noise prediction procedure for
inverted velocity profile coannular nozzles
[AIAA PAPER 79-0633] p0178 A79-28964

Performance of a vortex-controlled diffuser in an
annular swirl-can combustor at inlet Mach
numbers up to 0.53
[NASA-TP-1452] p0017 A79-22099

Acoustic and aerodynamic performance investigation
of inverted velocity profile coannular plug
nozzles, comprehensive data report, volume 1
[NASA-CR-159575-VOL-1] p0177 A79-26884

Acoustic and aerodynamic performance investigation
of inverted velocity profile coannular plug
nozzles, comprehensive data report, volume 2
[NASA-CR-159575-VOL-2] p0177 A79-26885

Acoustic and aerodynamic performance investigation
of inverted velocity profile coannular plug
nozzles, comprehensive data report, volume 3
[NASA-CR-159575-VOL-3] p0177 A79-26886

Aerodynamic and acoustic investigation of inverted
velocity profile coannular exhaust nozzle models
and development of aerodynamic and acoustic
prediction procedures
[NASA-CR-3168] p0035 A79-31212

ANNULI

Stiffness of straight and tapered annular gas path
seals
[ASME PAPER 78-LUB-18] p0118 A79-23235

ANODES

Advanced technology light weight fuel cell program
--- for space power applications
[NASA-CR-159653] p0155 A79-33581

ANOMALIES

Thermal anomalies of the transmitter experiment
package on the communications technology satellite
[NASA-TP-1410] p0044 A79-21120

Geosynchronous satellite operating anomalies
caused by interaction with the local spacecraft
environment
p0050 A79-24049

ANTENNAS

NT AIRCRAFT ANTENNAS

NT RADIO ANTENNAS

NT SLOT ANTENNAS

ANTIFRICTION BEARINGS

NT BALL BEARINGS

NT ROLLER BEARINGS

Some load limits and self-lubricating properties
of plain spherical bearings with molded graphite
fiber-reinforced polyimide liners to 320 C
[ASLE PREPRINT 78-LC-5C-2] p0118 A79-23251

Method of making bearing materials ---
self-lubricating, oxidation resistant composites
for high temperature applications
[NASA-CASE-LEW-11930-4] p0062 A79-17916

ANTIREFLECTION COATINGS

A brief survey of the solar cell state-of-the-art
p0052 A79-10130

APPLICATION

U UTILIZATION

APPLICATIONS PROGRAMS (COMPUTERS)

Extension, validation and application of the
NASCAP code
[NASA-CR-159595] p0100 A79-27397

APPROXIMATION

NT FINITE DIFFERENCE THEORY

NT FINITE ELEMENT METHOD

AQUEOUS SOLUTIONS

Method of cross-linking polyvinyl alcohol and
other water soluble resins
[NASA-CASE-LEW-13103-1] p0068 A79-14172

ARC DISCHARGES

Effects of arcing due to spacecraft charging on
spacecraft survival
[NASA-CR-159593] p0100 A79-25312

First principles numerical model of
avalanche-induced arc discharges in
electron-irradiated dielectrics
[NASA-CR-159560] p0101 A79-28418

ARC HEATING

Applications of thermal energy storage to process
heat and waste heat recovery in the iron and
steel industry
[NASA-CR-159397] p0151 A79-11473

ARGON

Inert gas ion source program
[NASA-CR-159423] p0056 A79-10120

ARIP (IMPACT PREDICTION)

U COMPUTERIZED SIMULATION

ARRAYS

NT SOLAR ARRAYS

ARSENIC COMPOUNDS

NT GALLIUM ARSENIDES

ARSENIDES

NT GALLIUM ARSENIDES

ARTIFICIAL SATELLITES

NT AERONAUTICAL SATELLITES

NT ATS 5

NT ATS 6

NT COMMUNICATION SATELLITES

NT COMMUNICATIONS TECHNOLOGY SATELLITE

NT NOAA SATELLITES

NT ORBITAL SPACE STATIONS

NT SYNCHRONOUS SATELLITES

Laser power conversion system analysis, volume 1
[NASA-CR-159523-VOL-1] p0112 A79-21334

ASHES

Chemically frozen multicomponent boundary layer
theory of salt and/or ash deposition rates from
combustion gases
p0078 A79-50912

ASPECT RATIO

NT LOW ASPECT RATIO

Effects of diffusion factor, aspect ratio and
solidity on overall performance of 14 compressor
middle stages --- the effects of varying both
diffusion through the rotor and compressor
blades and blade aspect ratio
[NASA-TP-1523] p0038 A79-33210

ASPIRATION

U VACUUM

ASSEMBLY LANGUAGE

Interactive debug program for evaluation and
modification of assembly-language software
[NASA-TP-1441] p0166 A79-21798

ASSESSMENTS

NT TECHNOLOGY ASSESSMENT

ASTROLOY (TRADEMARK)

Interpolation and extrapolation of creep rupture
data by the Minimum Commitment Method. I -
Focal-point convergence. II - Oblique
translation. III - Analysis of multiheats
p0077 A79-16038

ASTRONOMICAL OBSERVATORIES
 NT HEAD
 ATLAS LAUNCH VEHICLES
 Atlas 5013 tank corrosion test
 [NASA-CR-158760] p0050 N79-27234
 ATMOSPHERIC ABSORPTION
 U ATMOSPHERIC ATTENUATION
 ATMOSPHERIC ATTENUATION
 Computation of atmospheric attenuation of sound
 for fractional-octave bands
 [NASA-TP-1412] p0173 N79-17659
 ATMOSPHERIC CHEMISTRY
 Experimental evidence of interhemispheric
 transport from airborne carbon monoxide
 measurements p0156 A79-38942
 ATMOSPHERIC COMPOSITION
 NT ATMOSPHERIC MOISTURE
 An analysis of the first two years of GASP data
 --- Global Atmospheric Sampling Program p0160 A79-15068
 Simultaneous measurements of ozone outside and
 inside cabins of two B-747 airliners and a Gates
 Learjet business jet p0008 A79-27571
 Measurements of carbon monoxide, condensation
 nuclei, and ozone on a B 747SP aircraft flight
 around the world p0158 A79-31332
 NASA Global Atmospheric Sampling Program (GASP)
 data report for tapes VL0010 and VL0012
 [NASA-TN-79061] p0157 N79-15450
 ATMOSPHERIC EFFECTS
 Lubrication and failure mechanisms of molybdenum
 disulfide films. 1: Effect of atmosphere
 [NASA-TP-1343] p0081 N79-13158
 ATMOSPHERIC IMPUNITIES
 U AIR POLLUTION
 ATMOSPHERIC MODELS
 NT DYNAMIC MODELS
 ATMOSPHERIC MOISTURE
 Fretting wear of iron, nickel, and titanium under
 varied environmental conditions
 [NASA-TN-78972] p0073 N79-12203
 ATMOSPHERIC PHYSICS
 High power phase locked laser oscillators
 [NASA-CR-159630] p0112 N79-32538
 ATMOSPHERIC RADIATION
 NT SKY RADIATION
 ATMOSPHERIC TEMPERATURE
 Fretting wear of iron, nickel, and titanium under
 varied environmental conditions
 [NASA-TN-78972] p0073 N79-12203
 ATMOSPHERIC TURBULENCE
 Experimental clean combustor program: Phase 3:
 Turbulence measurement addendum
 [NASA-CR-135422] p0031 N79-12088
 ATOMIZATION
 U ATOMIZING
 ATOMIZING
 Atomization of water jets and sheets in axial and
 swirling airflows
 [ASME PAPER 79-GT-170] p0106 A79-30556
 Atomization of water jets and sheets in axial and
 swirling airflows
 [NASA-TN-79043] p0102 N79-12362
 Modeling of premixing-prevaporizing fuel-air
 mixing passages p0019 N79-24998
 Performance of a multiple venturi fuel-air
 preparation system --- fuel injection for gas
 turbines p0020 N79-25000
 ATOMS
 NT HYDROGEN ATOMS
 ATS
 NT ATS 5
 NT ATS 6
 ATS 5
 Summary of the two year NASA program for active
 control of ATS-5/6 environmental charging ---
 with a thermionic electron source and a plasma
 source p0047 N79-24006
 ATS 6
 Summary of the two year NASA program for active
 control of ATS-5/6 environmental charging ---
 with a thermionic electron source and a plasma
 source
 Operations of the ATS-6 ion engine p0047 N79-24006
 Characteristics of differential charging of ATS-6
 p0049 N79-24007
 p0049 N79-24008
 ATTACK AIRCRAFT
 NT F-15 AIRCRAFT
 NT F-102 AIRCRAFT
 NT YF-12 AIRCRAFT
 ATTENUATION
 NT ACOUSTIC ATTENUATION
 NT ATMOSPHERIC ATTENUATION
 NT SHOCK WAVE ATTENUATION
 NT WAVE ATTENUATION
 ATTITUDE (INCLINATION)
 NT YAW
 Variation of solar cell sensitivity and solar
 radiation on tilted surfaces p0148 A79-41023
 ATTENTION (MATERIALS)
 U COMBUSTION
 AUDITORY PERCEPTION
 Loudness of steady sounds - A new theory
 p0176 A79-39975
 Overall loudness of steady sounds according to
 theory and experiment
 [NASA-RP-1001] p0163 N79-25753
 AUDITORY STIMULI
 Overall loudness of steady sounds according to
 theory and experiment
 [NASA-RP-1001] p0163 N79-25753
 AUGER SPECTROSCOPY
 Auger spectroscopy analysis in adhesion, friction
 and wear studies p0110 A79-10992
 Auger spectroscopy analysis of lubrication with
 zinc dialkyldithiophosphate of several metal
 combinations in sliding contact
 [NASA-TP-1489] p0083 N79-27308
 Evaluation and auger analysis of a
 zinc-dialkyl-dithiophosphate antiwear additive
 in several diester lubricants
 [NASA-TP-1544] p0084 N79-32359
 AUGMENTATION
 NT THRUST AUGMENTATION
 Lean stability augmentation study p0021 N79-25007
 AUTOMATIC CONTROL
 NT ADAPTIVE CONTROL
 NT DYNAMIC CONTROL
 NT FEEDBACK CONTROL
 NT NUMERICAL CONTROL
 NT OFF-ON CONTROL
 NT OPTIMAL CONTROL
 Microprocessor control of a wind turbine generator
 [NASA-TN-79021] p0134 N79-12548
 AUTOMATIC PATTERN RECOGNITION
 U PATTERN RECOGNITION
 AUTOMATIC ROCKET IMPACT PREDICTORS
 U COMPUTERIZED SIMULATION
 AUTOMOBILE ENGINES
 Effect of inlet temperature on the performance of
 a catalytic reactor p0070 A79-11542
 Ceramics for the advanced automotive gas turbine
 engine - A look at a single shaft design
 p0117 A79-12850
 Ceramic applications in the advanced Stirling
 automotive engine p0117 A79-12851
 Correlations of catalytic combustor performance
 parameters p0070 A79-14956
 Initial comparison of single cylinder Stirling
 engine computer model predictions with test
 results
 [SAE PAPER 790327] p0119 A79-31368
 Cold-air performance of free power turbine
 designed for 112-kilowatt automotive gas-turbine
 engine. 2: Effects of variable
 stator-vane-chord setting angle on turbine
 performance p0017 N79-17859
 Evaluation of ceramics for stator application:
 Gas turbine engine report
 [NASA-CR-159533] p0033 N79-21075
 Conceptual design study of an automotive Stirling
 reference engine system
 [NASA-CR-159605] p0188 N79-29110

- Conceptual design study of an Improved Gas Turbine
[IGT] powertrain
[NASA-CR-159604] p0189 N79-31087
- Conceptual design study of improved automotive
gas turbine powertrain
[NASA-CR-159580] p0189 N79-31088
- Single shaft automotive gas turbine engine
characterization test
[NASA-CR-159654] p0189 N79-32129
- AUTOMOBILE FUELS**
Automotive Stirling engine development program
[NASA-CR-159436] p0120 N79-11406
- AUTOMOBILES**
Stirling engines for automobiles
[NASA-TN-79222] p0142 N79-28726
- AUXILIARY POWER SOURCES**
NT SPACE POWER REACTORS
- AUXILIARY PROPULSION**
Liquid oxygen/liquid hydrogen boost/vane pump for
the advanced orbit transfer vehicles auxiliary
propulsion system
[NASA-CR-159640] p0057 N79-31341
- AVAILANCES**
First principles numerical model of
avalanche-induced arc discharges in
electron-irradiated dielectrics
[NASA-CR-159560] p0101 N79-28418
- AVIONICS**
Experimental evidence of interhemispheric
transport from airborne carbon monoxide
measurements
p0158 A79-38942
- AXIAL COMPRESSORS**
U TURBOCOMPRESSORS
- AXIAL FLOW**
Unsteady flow in a supersonic cascade with
subsonic leading-edge locus
p0005 A79-16047
- Atomization of water jets and sheets in axial and
swirling airflows
[ASME PAPER 79-GT-170] p0106 A79-30556
- Aerodynamic performance of a 1.35-pressure-ratio
axial-flow fan stage
[NASA-TP-1299] p0002 N79-10022
- AXIAL FLOW COMPRESSORS**
U TURBOCOMPRESSORS
- AXIAL FLOW PUMPS**
NT TURBINE PUMPS
- AXIAL FLOW TURBINES**
Effect of rotor tip clearance and configuration on
overall performance of a 12.77-centimeter tip
diameter axial-flow turbine
[ASME PAPER 79-GT-42] p0027 A79-30521
- Cold-air performance of free power turbine
designed for 112-kilowatt automotive gas-turbine
engine. 2: Effects of variable
stator-vane-chord setting angle on turbine
performance
[NASA-TN-78993] p0017 N79-17859
- TACT 1: A computer program for the transient
thermal analysis of a cooled turbine blade or
vane equipped with a coolant insert. 2.
Programmers manual
[NASA-TP-1391] p0103 N79-18288
- Aerodynamic performance of 1.38-pressure-ratio,
variable-pitch fan stage
[NASA-TP-1502] p0024 N79-31213
- Aerodynamic performance of axial-flow fan stage
operated at nine inlet guide vane angles --- to
be used on vertical lift aircraft
[NASA-TP-1510] p0024 N79-31214
- Flow in nonrotating passages of radial inflow
turbines
[NASA-CR-159679] p0035 N79-32212
- AXISYMMETRIC FLOW**
NT ANNULAR FLOW
- AXLES**
U SHAFTS (MACHINE ELEMENTS)
- AZINES**
Catalytic trimerization of aromatic nitriles and
triaryl-s-triazine ring cross-linked high
temperature resistant polymers and copolymers
made thereby
[NASA-CASE-LEW-12053-2] p0083 N79-28307
- B**
- BALANCING**
Laser balancing demonstration on a high-speed
flexible rotor
[ASME PAPER 79-GT-56] p0123 A79-32351
- An introduction to a unified approach to flexible
rotor balancing
[ASME PAPER 79-GT-161] p0124 A79-32423
- Experiments on multiplane balancing using a laser
for material removal
[NASA-CR-3105] p0121 N79-17228
- BALL BEARINGS**
The practical impact of elastohydrodynamic
lubrication
p0117 A79-11545
- Graphite-fiber-reinforced polyimide liners of
various compositions in plain spherical bearings
p0117 A79-16678
- Filtration effects on ball bearing life and
condition in a contaminated lubricant
[ASME PAPER 78-LUB-34] p0118 A79-23246
- Elastohydrodynamic film thickness measurements of
artificially produced surface dents and grooves
--- on fatigue failure of bearings
[ASLE PREPRINT 78-LC-1A-1] p0118 A79-23267
- Two-dimensional random surface model for
asperity-contact in elastohydrodynamic lubrication
p0120 A79-39811
- Two-dimensional random surface model for
asperity-contact in elastohydrodynamic lubrication
[NASA-TN-79006] p0115 N79-23430
- Ferrographic analysis of wear debris from
full-scale bearing fatigue tests
[NASA-TP-1511] p0116 N79-31605
- Comparison of predicted and measured
elastohydrodynamic film thickness in a
20-millimeter-bore ball bearing
[NASA-TP-1542] p0116 N79-32552
- Correlation of asperity contact-time fraction with
elastohydrodynamic film thickness in a
20-millimeter-bore ball bearing
[NASA-TP-1547] p0116 N79-33476
- BANDPASS FILTERS**
Reynolds number, scale and frequency content
effects on F-15 inlet instantaneous distortion
[AIAA PAPER 79-0104] p0005 A79-19533
- BANDWIDTH**
NT SPECTRAL LINE WIDTH
- BANG-BANG CONTROL**
U OFF-ON CONTROL
- BARRIER APPROXIMATION**
U BARRIER LAYERS
- U ELECTRICAL PROPERTIES**
U SURFACE PROPERTIES
- BARIUM**
A proposed physical model for the impregnated
tungsten cathode based on Auger surface studies
of the Ba-O-W system
p0078 A79-39972
- BARRIER LAYERS**
NASA thermal barrier coatings: Summary and update
[NASA-TN-79053] p0015 N79-15048
- BATTERIES**
U ELECTRIC BATTERIES
- BATTERY CHARGERS**
Effect of positive pulse charge waveforms on cycle
life of nickel-zinc cells
[NASA-TN-79215] p0142 N79-28728
- BATTERY SEPARATORS**
U SEPARATORS
- BEAM CURRENTS**
Physical processes in directed ion beam sputtering
[NASA-CR-159567] p0182 N79-26943
- BEAM WAVEGUIDES**
Definition of mutually optimum NDI and proof test
criteria for 2219 aluminum pressure vessels.
Volume 3: Applications to rail defect evaluation
[NASA-CR-135447] p0125 N79-21412
- BEAMS (RADIATION)**
NT ELECTRON BEAMS
NT ION BEAMS
NT PARTICLE BEAMS
NT PHOTON BEAMS
- BEAMS (SUPPORTS)**
NT CANTILEVER BEAMS
- BEAMSHAPING**
U COLLIMATION
- BEARINGS**
NT ANTI-FRICTION BEARINGS
NT BALL BEARINGS
NT FOIL BEARINGS
NT GAS BEARINGS

- NT JOURNAL BEARINGS
NT ROLLER BEARINGS
NT THRUST BEARINGS
BEARING FATIGUE
Proposed design procedure for transmission
shafting under fatigue loading p0117 A79-14950
Bend strengths of reaction bonded silicon nitride
prepared from dry attrition milled silicon powder
[NASA-TM-79230] p0084 N79-30379
BERYLLIUM
Titanium/beryllium laminates - Fabrication,
mechanical properties, and potential aerospace
applications p0064 A79-20836
BIBLIOGRAPHIES
Conceptual design of thermal energy storage
systems for near term electric utility
applications. Volume 2: Appendices - screening
of concepts [NASA-CR-159411-VOL-2] p0152 N79-13497
BINARY ALLOYS
Some properties of low-vapor-pressure braze alloys
for thermionic converters p0076 A79-13103
Thermal expansion of some nickel and cobalt
spinels and their solid solutions p0186 A79-50233
The friction and wear of metals and binary alloys
in contact with an abrasive grit of
single-crystal silicon carbide [NASA-TM-79131] p0075 N79-22274
BINARY CODES
On the distribution of computation for sequential
decoding using the stack algorithm p0096 A79-33793
BINARY MIXTURES
NT EUTECTIC ALLOYS
BINARY SYSTEMS (DIGITAL)
U DIGITAL SYSTEMS
BINARY SYSTEMS (MATERIALS)
NT BINARY ALLOYS
NT EUTECTIC ALLOYS
BIOMEDICAL DATA
Intraocular pressure reduction and regulation system
[NASA-TM-79187] p0165 N79-28881
BIOTECHNOLOGY
Mechanical and chemical effects of ion-texturing
biomedical polymers [NASA-TM-79245] p0084 N79-31391
BIPROPELLANTS
U LIQUID ROCKET PROPELLANTS
BIT SYNCHRONIZATION
Multiple speed expandable bit synchronizer
[NASA-TM-79262] p0010 N79-33185
BITSERIAL CODE
Multiple speed expandable bit synchronizer
[NASA-TM-79262] p0010 N79-33185
BLACK BODY RADIATION
Introduction: Thermal Radiation in Industrial
Flames p0104 N79-22415
BLADE TIPS
Synthesis of blade flutter vibratory patterns
using stationary transducers p0127 A79-10823
Effect of rotor tip clearance and configuration on
overall performance of a 12.77-centimeter tip
diameter axial-flow turbine [ASME PAPER 79-GT-42] p0027 A79-30521
Effect of rotor tip clearance and configuration on
overall performance of a 12.77-centimeter tip
diameter axial-flow turbine [NASA-TM-79025] p0002 N79-12015
Containment of composite fan blades [NASA-CR-158168] p0032 N79-18978
JT8D revised high-pressure turbine cooling and
other outer air seal program [NASA-CR-159551] p0033 N79-21076
Tone noise of three supersonic helical tip speed
propellers in a wind tunnel [NASA-TM-79167] p0174 N79-25840
Development of a plasma sprayed ceramic gas path
seal for high pressure turbine applications [NASA-CR-159669] p0122 N79-31602
BLADDES
Wind tunnel tests of a blade subjected to midchord
torsional oscillation at high subsonic stall
flutter conditions
- [NASA-TM-78998] p0002 N79-12016
BLENDS
U MIXTURES
BLOCKING
Effects of flameholder blockage on emissions and
performance of lean premixed-prevaporized
combustors p0021 N79-25006
BLOWING
Performance of a V/STOL tilt nacelle inlet with
blowing boundary layer control [AIAA PAPER 79-1163] p0006 A79-47347
BLOWOUTS
Modelling turbulent flame ignition and blowout
p0021 N79-25008
BODIES OF REVOLUTION
NT CONICAL BODIES
NT CYLINDRICAL BODIES
BORING AIRCRAFT
NT BORING 747 AIRCRAFT
BORING 747 AIRCRAFT
Simultaneous measurements of ozone outside and
inside cabins of two E-747 airliners and a Gates
Learjet business jet p0008 A79-27571
Aircraft cabin ozone measurements on B747-100 and
B747-SP aircraft: Correlations with atmospheric
ozone and ozone encounter statistics [NASA-TM-79060] p0008 N79-15013
BOILING
NT FILM BOILING
BONDING
NT ADHESIVE BONDING
NT CERAMIC BONDING
NT METAL BONDING
NT METAL-METAL BONDING
BORON
Some properties of an advanced boron fiber
p0086 A79-21297
Mechanism of boron fiber strengthening by thermal
treatment p0065 A79-30396
Some properties of an advanced boron fiber
high strength, splittable fibers [NASA-TM-79065] p0061 N79-16076
Fabrication of J79 boron/aluminum compressor blades
[NASA-CR-159566] p0034 N79-23970
Reverse annealing in radiation-damaged, silicon
solar cells p0144 N79-32660
BORON REINFORCED MATERIALS
Evaluation of manufacturing processes for
boron/aluminum composites containing
0.2-mm-diameter boron fibers [NASA-TM-79008] p0062 N79-12153
Mechanisms of boron fiber strengthening by thermal
treatment [NASA-TM-79077] p0062 N79-20186
BOUNDARIES
NT GRAIN BOUNDARIES
BOUNDARY LAYER CONTROL
Performance of a V/STOL tilt nacelle inlet with
blowing boundary layer control [AIAA PAPER 79-1163] p0006 A79-47347
An experimental investigation of forced mixing of
a turbulent boundary layer in an annular diffuser
--- for boundary layer control [NASA-TM-79171] p0004 N79-23920
Performance of a V/STOL tilt nacelle inlet with
blowing boundary layer control [NASA-TM-79176] p0004 N79-27093
BOUNDARY LAYER EQUATIONS
Chemically frozen multicomponent boundary layer
theory of salt and/or ash deposition rates from
combustion gases p0078 A79-50912
BOUNDARY LAYER FLOW
NT BOUNDARY LAYER SEPARATION
NT SECONDARY FLOW
BOUNDARY LAYER NOISE
U AERODYNAMIC NOISE
U BOUNDARY LAYERS
BOUNDARY LAYER SEPARATION
Self stabilizing sonic inlet [NASA-CASE-LW-11890-1] p0011 N79-24976
BOUNDARY LAYERS
NT TURBULENT BOUNDARY LAYER
Full-coverage film cooling: 3-dimensional
measurements of turbulence structure and

BOUNDARY LUBRICATION

SUBJECT INDEX

prediction of recovery region hydrodynamics
[NASA-CR-3104] p0106 N79-22428

Heat transfer to a full-coverage, film-cooled
surface with compound-angle (30 deg and 45 deg)
hole injection
[NASA-CR-3103] p0107 N79-22429

BOUNDARY LUBRICATION
Boundary lubrication, thermal and oxidative
stability of a fluorinated polyether and a
perfluoropolyether triazine
[NASA-TM-79064] p0081 N79-15165

Wear of aluminum and hypoeutectic aluminum-silicon
alloys in boundary-lubricated pin-on disk sliding
[NASA-TP-1442] p0074 N79-21184

BOW SHOCK WAVES
U SHOCK WAVES

BRAKES (FOR ARRESTING MOTION)
NT TRAILING-EDGE FLAPS

BRAYTON CYCLE
Mini-BRU/BIPS 1300 watt (sub) e dynamic power
conversion system development: Executive summary
[NASA-CR-159440] p0150 N79-10526

Mini-BRU/BIPS foil bearing development
[NASA-CR-159442] p0130 N79-11407

Analysis, design, fabrication and testing of the
Mini-Brayton rotating unit (Mini-BRU). Volume
1: Text and tables
[NASA-CR-159441-VOL-1] p0120 N79-11408

Analysis, design, fabrication and testing of the
Mini-Brayton rotating unit (Mini-BRU). Volume
2: Figures and drawings
[NASA-CR-159441-VOL-2] p0120 N79-11409

Design and fabrication of the Mini-Brayton
Recuperator (MBR)
[NASA-CR-159429] p0151 N79-11476

Mini-Brayton heat source assembly development
[NASA-CR-159447] p0151 N79-12554

Benefits of solar/fossil hybrid gas turbine systems
[NASA-TM-79083] p0134 N79-15410

Evaluation of a Brayton cycle recuperator after
21,000 hours of ground testing
[NASA-TM-79091] p0074 N79-20217

Brayton-cycle component characteristics
p0140 N79-26479

Candidate power-conversion system cycles, appendix A
p0140 N79-26484

BRAZING
Some properties of low-vapor-pressure braze alloys
for thermionic converters
p0076 A79-13100

BREAKAWAY
U BOUNDARY LAYER SEPARATION

BROADCASTING
Communications technology satellite: United
States experiments and disaster communications
applications
[NASA-TM-79109] p0044 N79-23999

BROMINE
Supply of reactants for Redox bulk energy storage
systems
[NASA-TM-78995] p0133 N79-11479

BRONZES
Properties and performance of fine-filament
bronze-process Nb3Sn conductors
p0184 A79-20529

BUBBLES
Condensation on a noncollapsing vapor bubble in a
subcooled liquid
[NASA-TM-79212] p0105 N79-27461

BUILDING MATERIALS
U CONSTRUCTION MATERIALS

BUILDING STRUCTURES
U BUILDINGS

BUILDINGS
Fuel cell on-site integrated energy system
parametric analysis of a residential complex
p0146 A79-14947

Feasibility of determining flat roof heat losses
using aerial thermography
p0131 A79-51095

Comparison of fuel-cell and diesel integrated
energy systems and a conventional system for a
500-unit apartment
[NASA-TM-79037] p0134 N79-15403

BULK MODULUS
Full-scale engine tests of bulk absorber acoustic
inlet treatment
[NASA-TM-79079] p0173 N79-16645

BURGER EQUATION
Filtering of non-linear instabilities --- from
finite difference solution of fluid dynamics
equations
p0108 A79-32912

BURNERS
Progress on Variable Cycle Engines
[AIAA PAPER 79-1312] p0036 A79-40759

BURNING
U COMBUSTION
BURNING PROCESS
U COMBUSTION

BUYERFLY VALVES
NT DAMPERS (VALVES)

BYPASSES
A throat-bypass stability-bleed system using
relief valves to increase the transient
stability of a mixed-compression inlet --- YF-12
aircraft inlet tests in the Lewis 10 by 10 ft
supersonic wind tunnel
[NASA-TP-1083] p0023 N79-28176

C

C BAND
Global disaster satellite communications system
for disaster assessment and relief coordination
p0095 A79-30394

CABIN ATMOSPHERES
Simultaneous measurements of ozone outside and
inside cabins of two B-747 airliners and a Gates
Learjet business jet
p0008 A79-27571

Aircraft cabin ozone measurements on B747-100 and
B747-SP aircraft: Correlations with atmospheric
ozone and ozone encounter statistics
[NASA-TM-79060] p0008 N79-15013

CADMIUM NICKEL BATTERIES
U NICKEL CADMIUM BATTERIES

CALCULUS
NT SERIES (MATHEMATICS)

CALIBRATING
An in-place recalibration technique to extend the
temperature capability of capacitance-sensing,
rotor-blade-tip-clearance measurement systems
[SAE PAPER 781003] p0026 A79-25885

Condensation-nuclei (Aitken Particle) measurement
system used in NASA global atmospheric sampling
program
[NASA-TP-1415] p0157 N79-18479

CAMS
Cam-operated pitch-change apparatus
[NASA-CASE-LEW-13050-1] p0014 N79-14095

CANOPIES
Aerospace Transparent Materials and Enclosures
(12th)
[AD-A065049] p0018 N79-23066

CANTILEVER BEAMS
Cantilever mounted resilient pad gas bearing
[NASA-CASE-LEW-12569-1] p0113 N79-10418

Operating characteristics of a cantilever-mounted
resilient-pad gas-lubricated thrust bearing
[NASA-TP-1438] p0115 N79-22518

CANTILEVER MEMBERS
NT CANTILEVER BEAMS
CANTILEVER WINGS
U WINGS

CAPILLARY CIRCULATION
U CAPILLARY FLOW
CAPILLARY FLOW
Study of liquid and vapor flow into a Centaur
capillary device
[NASA-CR-159657] p0108 N79-33432

CAPTIVE TESTS
NT STATIC TESTS

CARBAMATES (TRADENAME)
NT URETHANES

CARBIDES
NT SILICON CARBIDES
NT TITANIUM CARBIDES

CARBON COMPOUNDS
NT FLUOROPOLYMERS
NT HALOCARBONS
NT SILICON CARBIDES
NT TITANIUM CARBIDES
Mechanisms of graphite fluoride /CFx/n lubrication
p0086 A79-31249

CARBON FIBER REINFORCED PLASTICS
Some loads limits and self-lubricating properties

- of plain spherical bearings with molded graphite fiber-reinforced polyimide liners to 320 C [ASLE PREPRINT 78-LC-5C-2] p0118 A79-23251
- Stability of PNR-polyimide monomer solutions p0086 A79-31041
- Effects of graphite fiber stability on the properties of PNR polyimide composites p0066 A79-43309
- Effects of graphite fiber stability on the properties of PNR polyimide composites [NASA-TM-79062] p0061 A79-16075
- Stability of PNR-polyimide monomer solutions [NASA-TM-79063] p0062 A79-16921
- Curing agent for polyepoxides and epoxy resins and composites cured therewith [NASA-CASE-LEN-13226-1] p0059 A79-31345
- CARBON FIBERS**
- Resin/fiber thermo-oxidative interactions in PNR polyimide/graphite composites [NASA-TM-79093] p0062 A79-16920
- Polyimide prepreg material having improved tack retention --- polyimide-graphite fiber composites [NASA-CASE-LEN-12933-1] p0059 A79-24061
- CARBON MONOXIDE**
- Measurements of carbon monoxide, condensation nuclei, and ozone on a B 747SP aircraft flight around the world p0158 A79-31332
- Experimental evidence of interhemispheric transport from airborne carbon monoxide measurements p0158 A79-38942
- Carbon monoxide measurement in the global atmospheric sampling program [NASA-TP-1526] p0158 A79-31841
- CARBONACEOUS ROCKS**
- NT COAL**
- CARBURIZING**
- Evaluation of CDS 600 carburized steel as a gear material [NASA-TP-1390] p0114 A79-14389
- CARRIER FREQUENCIES**
- Carrier: Interference ratios for frequency sharing between satellite systems transmitting frequency modulated and digital television signals [NASA-TM-79265] p0094 A79-33379
- CARRIER MOBILITY**
- Normal state properties of the ternary molybdenum sulfides p0185 A79-27229
- CARRIER ROCKETS**
- U LAUNCH VEHICLES**
- CARTOGRAPHY**
- U MAPPING**
- CASCADE FLOW**
- Supersonic unstalled flutter p0004 A79-12599
- Unsteady flow in a supersonic cascade with subsonic leading-edge locus p0005 A79-16047
- High speed smoke flow visualization for the determination of cascade shock losses [AIAA PAPER 79-0042] p0005 A79-19495
- Axial-flow compressor turning angle and loss by inviscid-viscous interaction blade-to-blade computation [ASME PAPER 79-GT-5] p0006 A79-30504
- Low-turbulence high-speed wind tunnel for the determination of cascade shock losses [ASME PAPER 79-GT-129] p0039 A79-32398
- Supersonic unstalled flutter --- aerodynamic loading of thin airfoils induced by cascade motion [NASA-TM-79001] p0002 A79-11000
- Supersonic unstalled flutter p0023 A79-27181
- CASCADES (FLUID DYNAMICS)**
- U FLUID DYNAMICS**
- CASES (CONTAINERS)**
- NT ROCKET ENGINE CASES**
- CAST ALLOYS**
- Analysis of solidification interface shape during continuous casting of a slab p0079 A79-52697
- CATALYSIS**
- The catalysis of nucleotide polymerization by compounds of divalent lead --- prebiotic synthesis p0060 A79-32924
- Correlations of catalytic combustor performance parameters
- [NASA-TM-79014] p0134 A79-11480
- The advanced low-emissions catalytic-combustor program. Phase I: Description and status [NASA-TM-79049] p0012 A79-15047
- CATALYSTS**
- NT ELECTROCATALYSTS**
- Advanced low emissions catalytic combustor program at General Electric p0021 A79-25011
- Advanced low emissions catalytic combustor program at Pratt and Whitney p0021 A79-25012
- Advanced technology light weight fuel cell program --- for space power applications [NASA-CR-159653] p0155 A79-33581
- CATALYTIC ACTIVITY**
- Effect of inlet temperature on the performance of a catalytic reactor p0070 A79-11542
- Correlations of catalytic combustor performance parameters p0070 A79-14956
- The Advanced Low-Emissions Catalytic Combustor Program: Phase I - Description and status --- for aircraft gas turbine engines [ASME PAPER 79-GT-192] p0027 A79-30557
- CATHODES**
- NT HOLLOW CATHODES**
- NT THERMIONIC CATHODES**
- A proposed physical model for the impregnated tungsten cathode based on Auger surface studies of the Ba-O-W system p0078 A79-39972
- Feasibility study for a secondary Na/S battery [NASA-CR-159469] p0152 A79-17330
- Advanced technology light weight fuel cell program --- for space power applications [NASA-CR-159653] p0155 A79-33581
- CATIONS**
- NT METAL IONS**
- CAUSTICS**
- U ALKALIES**
- CAVITY RESONATORS**
- Effect of grazing flow on the acoustic impedance of Helmholtz resonators consisting of single and clustered orifices [NASA-CR-3177] p0178 A79-32056
- CDC COMPUTERS**
- SIMWEST: A simulation model for wind and photovoltaic energy storage systems (CDC user's manual), volume 1 [NASA-CR-159607] p0166 A79-33883
- SIMWEST: A simulation model for wind and photovoltaic energy storage systems (cdc program descriptions), volume 2 [NASA-CR-159608] p0167 A79-33884
- CENTAUR LAUNCH VEHICLE**
- Study of liquid and vapor flow into a Centaur capillary device [NASA-CR-159657] p0108 A79-33432
- CENTAUR VEHICLE**
- U CENTAUR LAUNCH VEHICLE**
- CENTERBODIES**
- Effect of l/p and centerbody geometry on aerodynamic performance of inlets for tilting-manoeuvre VTOL aircraft [AIAA PAPER 79-0381] p0025 A79-23509
- CENTRIFUGAL COMPRESSORS**
- Design, development and test of a laser velocimeter for a small 6:1 pressure ratio centrifugal compressor [NASA-CR-134781] p0111 A79-27478
- CENTRIFUGAL PUMPS**
- Small, high-pressure, liquid oxygen turbopump [NASA-CR-159509] p0121 A79-17221
- CERAMAL PROTECTIVE COATINGS**
- U PROTECTIVE COATINGS**
- CERAMIC BONDING**
- Ceramic blade attachments --- for turbine rotors p0123 A79-12848
- Thermal stress analysis of ceramic gas-path seal components for aircraft turbines [NASA-TP-1437] p0082 A79-21205
- CERAMIC COATINGS**
- Effects of compositional changes on the performance of a thermal barrier coating system --- for aircraft gas turbine engines p0077 A79-21299

- Use of a nitrogen-argon plasma to improve adherence of sputtered titanium carbide coatings on steel p0119 A79-25103
- Emission and absorptance of the National Aeronautics and Space Administration ceramic thermal barrier coating --- for gas turbine engine components p0086 A79-27231
- Coatings for wear and lubrication p0060 A79-27232
- Industrial potential, uses, and performance of sputtered and ion plated films p0119 A79-30398
- Tests of NASA ceramic thermal barrier coating for gas-turbine engines p0086 A79-34996
- Development of sprayed ceramic seal systems for turbine gas path sealing [NASA-TM-79022] p0081 A79-12223
- Low-cycle fatigue of thermal-barrier coatings at 982 deg C [NASA-TP-1322] p0014 A79-13046
- CERAMICS**
- Effects of pressure and temperature on hot pressing a sialon --- Si-Al-O-N ceramics p0085 A79-11548
- Ceramic blade attachments --- for turbine rotors p0123 A79-12848
- Ceramics for the advanced automotive gas turbine engine - A look at a single shaft design p0117 A79-12850
- Ceramic applications in the advanced Stirling automotive engine p0117 A79-12851
- NASA thermal barrier coatings - Summary and update p0085 A79-21295
- Thermal barrier coatings: Burner rig hot corrosion test results [NASA-TM-79005] p0073 A79-11179
- Evaluation of advanced regenerator systems [NASA-CR-159422] p0188 A79-12969
- Ceramic coating effect on liner metal temperatures of film-cooled annular combustor [NASA-TP-1323] p0015 A79-14098
- NASA thermal barrier coatings: Summary and update [NASA-TM-79053] p0015 A79-15048
- High velocity burner rig oxidation and thermal fatigue behavior of Si3N4- and SiC base ceramics to 1370 deg C [NASA-TM-79040] p0082 A79-16984
- Effect of thermal barrier coatings on the performance of steam and water-cooled gas turbine/steam turbine combined cycle system [NASA-TM-79057] p0135 A79-17334
- Design, fabrication and spin testing of ceramic blade metal disk attachment [NASA-CR-159532] p0032 A79-17857
- Tests of NASA ceramic thermal barrier coating for gas-turbine engines [NASA-TM-79116] p0017 A79-20118
- Evaluation of ceramics for stator application: Gas turbine engine report [NASA-CR-159533] p0033 A79-21075
- Effect of oxygen-nitrogen ratio on sinterability of Sialons [NASA-TP-1382] p0082 A79-21204
- Industry tests of NASA ceramic thermal barrier coating --- for gas turbine engine applications [NASA-TP-1425] p0022 A79-25023
- Modules of rupture and oxidation resistance of Si2.55Al1.60O.72N3.52 sialon [NASA-TP-1490] p0083 A79-27309
- State-of-the-art of SialON materials --- conferences [NASA-TM-79207] p0084 A79-30378
- Development of SialON materials [NASA-CR-159675] p0067 A79-33258
- CESIUM ION**
- Investigations of negative and positive cesium ion species [NASA-CR-159446] p0175 A79-18711
- CFRP**
- U CARBON FIBER REINFORCED PLASTICS
- CHALCOGENIDES**
- NT ALUMINUM OXIDES
- NT CARBON MONOXIDE
- NT COPPER SULFIDES
- NT LEAD SULFIDES
- NT MOLYBDENUM DISULFIDES
- NT MOLYBDENUM SULFIDES
- NT NICKEL OXIDES
- NT NITRIC OXIDE
- NT NITROGEN OXIDES
- NT OXIDES
- NT SULFIDES
- NT YTTRIUM OXIDES
- NT ZIRCONIUM OXIDES
- CHANNEL FLOW**
- Measurements of mixed convective heat transfer to low temperature helium in a horizontal channel [NASA-TM-79158] p0104 A79-23384
- CHAPMAN SHEAR LAYER**
- U SHEAR LAYERS
- CHAPMAN-JOUGET FLAME**
- U FLAME PROPAGATION
- CHARACTERISTIC METHOD**
- U METHOD OF CHARACTERISTICS
- CHARACTERIZATION**
- Status of materials characterization studies p0048 A79-24030
- CHARGE DISTRIBUTION**
- Area scaling investigations of charging phenomena -- discharge pulse characteristics of Teflon thermal control tape p0048 A79-24032
- CHARGE EXCHANGE**
- Gain measurements of the Ca-Fe charge exchange system --- for UV lasers p0112 A79-19078
- Method for decomposing observed line shapes resulting from multiple causes - Application to plasma charge-exchange-neutral spectra p0182 A79-53667
- Charging rates of metal-dielectric structures --- with implications for spacecraft p0048 A79-24033
- CHARGED PARTICLES**
- NT ELECTRON PLASMA
- NT HELIUM PLASMA
- NT HIGH TEMPERATURE PLASMAS
- NT HYDROGEN PLASMA
- NT METAL IONS
- NT PLASMAS (PHYSICS)
- NT TOROIDAL PLASMAS
- Space environmental interactions with spacecraft surfaces [AIAA PAPER 79-0386] p0049 A79-23511
- Large space system - Charged particle environment interaction technology --- effects on high voltage solar array performance [AIAA 79-0513] p0055 A79-34775
- NASCAP modelling of high-voltage power system interactions with space charged-particle environments --- particle impact on solar satellite surfaces p0051 A79-39806
- Trajectories of charged particles in radial electric and uniform axial magnetic fields p0182 A79-41788
- Space environmental interactions with spacecraft surfaces [NASA-TM-79016] p0046 A79-15150
- Large space system: Charged particle environment interaction technology [NASA-TM-79156] p0046 A79-22188
- Interactions between spacecraft and the charged-particle environment p0047 A79-24021
- Plasma Interaction Experiment (PIX) flight results p0047 A79-24022
- Effect of parasitic plasma currents on solar-array power output p0047 A79-24025
- Potential mapping with charged-particle beams p0049 A79-24038
- CHARGING**
- Rapid, efficient charging of lead-acid and nickel-zinc traction cells --- for electric vehicles p0144 A79-10084
- Effects of bulk and surface conductivity on the potential developed by dielectrics exposed to electron beams p0171 A79-50538
- CHECKOUT EQUIPMENT**
- U TEST EQUIPMENT
- CHEMICAL ANALYSIS**
- NT GAS ANALYSIS

NT CZOMCHETRY

NT VOLUMETRIC ANALYSIS

Ion chromatographic determination of sulfur in fuels
p007C A79-21222

Evaluation of the application of some gas chromatographic methods for the determination of properties of synthetic fuels
[NASA-TM-79035] p0068 A79-16930

CHEMICAL ATTACK

The role of NaCl in flame chemistry, in the deposition process, and in its reactions with protective oxides as related to hot corrosion
p0071 A79-49534

CHEMICAL COMPOSITION

Alternative aviation turbine fuels
p0090 A79-12378

Effects of compositional changes on the performance of a thermal barrier coating system --- for aircraft gas turbine engines
p0077 A79-21299

Effect of broadened-specification fuels on aircraft engines and fuel systems
[AIAA 79-7008] p0027 A79-29383

CHEMICAL EFFECTS

Mechanical and chemical effects of ion-texturing biomedical polymers
[NASA-TM-79245] p0084 A79-31391

CHEMICAL ELEMENTS

NT ALUMINUM

NT ARGON

NT BARIUM

NT BERYLLIUM

NT BORON

NT BROMINE

NT CHROMIUM

NT COPPER

NT DYSPROSIUM

NT GOLD

NT HELIUM

NT HYDROGEN

NT HYDROGEN ATOMS

NT HYDROGEN IONS

NT HYDROGEN PLASMA

NT IODINE

NT IRON

NT ISOTOPES

NT LIQUID HYDROGEN

NT LIQUID LITHIUM

NT LIQUID NITROGEN

NT MANGANESE

NT MERCURY (METAL)

NT MOLYBDENUM

NT NITROGEN

NT NITROGEN IONS

NT OXYGEN

NT PLUTONIUM 238

NT POTASSIUM

NT RARE GASES

NT REFRACTORY METALS

NT SILICON

NT SILVER

NT SULFUR

NT TITANIUM

NT TRACE ELEMENTS

NT TUNGSTEN

NT XENON

NT ZINC

CHEMICAL EVOLUTION

The catalysis of nucleotide polymerization by compounds of divalent lead --- prebiotic synthesis
p0060 A79-32924

CHEMICAL EXPLOSIONS

NT GAS EXPLOSIONS

Workbook for estimating effects of accidental explosions in propellant ground handling and transport systems
[NASA-CR-3023] p0091 A79-10226

CHEMICAL FUELS

NT AIRCRAFT FUELS

NT AUTOMOBILE FUELS

NT DIESEL FUELS

NT GASOLINE

NT HIGH ENERGY FUELS

NT HYDROCARBON FUELS

NT JET ENGINE FUELS

NT JP-5 JET FUEL

NT SYNTHETIC FUELS

CHEMICAL KINETICS

U REACTION KINETICS

CHEMICAL PROPERTIES

NT ACIDITY

Characterization of PMR polyimides: Correlation of ester impurities with composite properties
[NASA-TM-79068] p0061 A79-16918

CHEMICAL PROPULSION

NT HYBRID PROPULSION

Space propulsion technology overview
[AIAA 79-0860] p0054 A79-34704

Low-thrust chemical orbit transfer propulsion
[AIAA PAPER 79-1182] p0055 A79-39815

Low-thrust chemical orbit transfer propulsion
[NASA-TM-79190] p0043 A79-25129

CHEMICAL REACTIONS

NT ELECTROCHEMICAL OXIDATION

NT FLUORINATION

NT HYDROLYSIS

NT NITRIDING

NT OXIDATION

NT OXIDATION-REDUCTION REACTIONS

NT REDUCTION (CHEMISTRY)

A study of various synthetic routes to produce a halogen-labeled traction fluid
[NASA-TM-79024] p0059 A79-11119

Synthesis of improved moisture resistant polymers
[NASA-CR-159456] p0087 A79-18053

Synthesis of improved moisture resistant polymers
[NASA-CR-159510] p0087 A79-23218

The role of NaCl in flame chemistry, in the deposition process, and in its reactions with protective oxides as related to hot corrosion
[NASA-TM-79225] p0069 A79-28258

CHEMICAL REACTORS

Effect of inlet temperature on the performance of a catalytic reactor
p0070 A79-11542

CHEMICAL TESTS

NT CHEMICAL ANALYSIS

NT GAS ANALYSIS

NT CZOMCHETRY

NT SALT SPRAY TESTS

NT VOLUMETRIC ANALYSIS

CHEMONUCLEAR PROPULSION

U CHEMICAL PROPULSION

CHILLING

U COOLING

CHLORIDES

NT SODIUM CHLORIDES

CHLORINE COMPOUNDS

NT SODIUM CHLORIDES

CHLOROTHYLENE

Electrochemical fluorination of trichloroethylene and N, N-dimethyltrifluoroacetamide
p0060 A79-49536

Electrochemical fluorination of trichloroethylene and N, N-dimethyltrifluoroacetamide
p0060 A79-49536

Electrochemical fluorination of trichloroethylene and N, N-dimethyltrifluoroacetamide
[NASA-TM-79188] p0059 A79-27242

CHOKES (RESTRICTIONS)

Two-phase choked flow of cryogenic fluids in converging-diverging nozzles
[NASA-TF-1484] p0105 A79-29468

CHOPPERS (ELECTRIC)

U ELECTRIC CHOPPERS

CHROMATES

NT POTASSIUM CHROMATES

CHROMATOGRAPHY

NT GAS CHROMATOGRAPHY

Application of ion chromatography to the study of hydrolysis of some halogenated hydrocarbons at ambient temperatures
p0060 A79-14951

Ion chromatographic determination of sulfur in fuels
p0070 A79-21222

Application of ion chromatography to the study of hydrolysis of some halogenated hydrocarbons at ambient temperatures
[NASA-TM-79020] p0157 A79-12586

Ion chromatographic determination of sulfur in fuels
[NASA-TM-78971] p0157 A79-17358

CHROMIUM

U CHROMIUM

CHROMIUM

Effect of a chromium-containing fuel additive on hot corrosion
p0071 A79-26546

- Supply of reactants for Redox bulk energy storage systems
[NASA-TM-78995] p0133 W79-11479
- CHROMIUM ALLOYS**
NT ASTROLOY (TRADEMARK)
NT BENE 41
 Friction and wear characteristics of iron-chromium alloys in contact with themselves and silicon carbide
[NASA-TP-1387] p0114 W79-14387
 Some TEM observations of Al₂O₃ scales formed on NiCrAl alloys
[NASA-TM-79259] p0076 W79-33306
- CHROMIUM COMPOUNDS**
NT POTASSIUM CHROMATES
 Mass spectrometric investigation of the vaporization of sodium and potassium chromates: Preliminary results
[NASA-TM-79210] p0069 W79-27279
- CHUGGING**
U COMBUSTION STABILITY
- CIRCUIT BOARDS**
 Traveling wave tube circuit
[NASA-CASE-LFP-12013-1] p0102 W79-10339
- CIRCUIT PROTECTION**
 A brief survey of the solar cell state-of-the-art
p0052 W79-10130
- CIRCUIT RELIABILITY**
 Slower-enhanced flashlamp-pumped dye laser
p0112 W79-32981
- CIRCUITS**
NT EQUIVALENT CIRCUITS
NT POWER SUPPLY CIRCUITS
NT SWITCHING CIRCUITS
- CIRCULAR PLATES**
 Mode I analysis of a cracked circular disk subject to a couple and a force
p0128 W79-15588
 Mode I crack surface displacements for a round compact specimen subject to a couple and force
p0129 W79-39812
- CLARK I AIRFOIL**
U AIRFOIL PROFILES
- CLEAN ENERGY**
 Burn coal cleanly in a fluidized bed - The key is in the controls
p0071 W79-26374
 An operating 200-kw horizontal axis wind turbine
[NASA-TM-79034] p0135 W79-16357
- CLEARANCES**
 Effect of rotor tip clearance and configuration on overall performance of a 12.77-centimeter tip diameter axial-flow turbine
[ASME PAPER 79-GT-42] p0027 W79-30521
 Effect of rotor tip clearance and configuration on overall performance of a 12.77-centimeter tip diameter axial-flow turbine
[NASA-TM-79025] p0002 W79-12015
- CLOGGING**
U CLOGGING
- CLOSED CICLES**
 Stirling engine characteristics
p0140 W79-26480
- CLOSED LOOP SYSTEMS**
U FEEDBACK CONTROL
- CLOSURE LAW**
 Decay of homogeneous turbulence from a given state at higher Reynolds number
p0105 W79-14952
 Comparison of a correlation term-discard closure for decaying homogeneous turbulence with experiment
p0106 W79-22424
- COAL**
 Application of multispectral scanner data to the study of an abandoned surface coal mine
[NASA-TM-78912] p0131 W79-13472
 The erosion/corrosion of small superalloy turbine rotors operating in the effluent of a PFB coal combustor
[NASA-TM-79227] p0076 W79-30356
- COAL GASIFICATION**
 Performance characteristics of a slagging gasifier for BHD combustor systems
[NASA-TM-79195] p0142 W79-30720
- COAL UTILISATION**
 Alternative aircraft fuels
p0090 W79-10824
- Burn coal cleanly in a fluidized bed - The key is in the controls
p0071 W79-26374
- Reduction of particulate carryover from a pressurized fluidized bed
p0150 W79-49527
- Reduction of particulate carryover from a pressurized fluidized bed
p0150 W79-49527
- Preliminary comparison of theory and experiment for a conical, pressurized-fluidized-bed coal combustor
[NASA-TM-79137] p0137 W79-22623
- COATING**
 Ion beam sputter deposition of fluoropolymers
[NASA-CASE-LEW-13122-1] p0083 W79-24154
 Automated Plasma Spray (APS) process feasibility study: Plasma spray process development and evaluation
[NASA-CN-159579] p0092 W79-29382
- COATINGS**
NT ALUMINUM COATINGS
NT ANTIREFLECTION COATINGS
NT CERAMIC COATINGS
NT INORGANIC COATINGS
NT METAL COATINGS
NT NICKEL COATINGS
NT PROTECTIVE COATINGS
NT SPRAYED COATINGS
NT THERMAL CONTROL COATINGS
 Thermal barrier coatings: Burner rig hot corrosion test results
[NASA-TM-79005] p0073 W79-11179
 Effect of nitrogen-containing plasma on adherence, friction, and wear of radiofrequency-sputtered titanium carbide coatings
[NASA-TP-1377] p0081 W79-15184
 Characterization of defect growth structure in ion plated films by scanning electron microscopy
[NASA-TM-79110] p0074 W79-20218
 Industrial potential, uses, and performance of sputtered and ion plated films
[NASA-TM-79107] p0157 W79-20527
- COAXIAL NOZZLES**
 Progress on Variable Cycle Engines
[AIAA PAPER 79-1312] p0036 W79-40759
 Studies of the acoustic transmission characteristics of coaxial nozzles with inverted velocity profiles: Comprehensive data report
--- nozzle transfer functions
[NASA-CN-159628] p0177 W79-27933
- COBALT ALLOYS**
NT ASTROLOY (TRADEMARK)
NT BENE 41
 The hot corrosion of Co-25Cr-10Ni-5Ta-3Al-0.5Ti alloy /S-57/
p0076 W79-10420
 Thermal expansion of some nickel and cobalt spinels and their solid solutions
p0186 W79-50233
- CODING**
NT DECODING
 Comparison of NASCAP predictions with experimental data
p0047 W79-24013
- COEFFICIENT OF FRICTION**
 Anisotropic friction and wear of single-crystal manganese-zinc ferrite in contact with itself
[NASA-TP-1339] p0113 W79-10425
 Lubrication and failure mechanisms of molybdenum disulfide films. 1: Effect of atmosphere
[NASA-TP-1343] p0081 W79-13158
 Lubricating and wear mechanisms for a hemisphere sliding on polyimide-bonded graphite fluoride film
[NASA-TP-1524] p0084 W79-30381
- COEFFICIENTS**
NT AERODYNAMIC COEFFICIENTS
NT COEFFICIENT OF FRICTION
NT DIFFUSION COEFFICIENT
NT HEAT TRANSFER COEFFICIENTS
NT STRUCTURAL INFLUENCE COEFFICIENTS
- COLD FLOW TESTS**
 Cold-air performance of free power turbine designed for 112-kilowatt automotive gas-turbine engine. 2: Effects of variable stator-vane-chord setting angle on turbine performance
[NASA-TM-78993] p0017 W79-17859

- COLD PRESSING**
Development of SiAlON materials
[NASA-CR-159675] p0067 879-33258
- COLD STRENGTH**
Influence of composition, annealing treatment, and texture on the fracture toughness of Ti-5Al-2.5Sn plate at cryogenic temperatures p0077 879-24262
- COLD SURFACES**
Condensation on a noncollapsing vapor bubble in a subcooled liquid p0100 879-49535
- COLD WALLS**
U COLD SURFACES
- COLD WELDING**
The use of ion beam cleaning to obtain high quality cold welds with minimal deformation p0119 879-24121
- COLLECTORS**
U ACCUMULATORS
- COLLIMATION**
Definition of mutually optimum NDI and proof test criteria for 2219 aluminum pressure vessels. Volume 2: Optimization and fracture studies [NASA-CR-135446] p0125 879-21411
- COLLISION PARAMETERS**
Physical processes in directed ion beam sputtering [NASA-CR-159567] p0182 879-26943
- COLLISION WARNING DEVICES**
U WARNING SYSTEMS
- COLLOCATION**
Mode I analysis of a face cracked plate subjected to rotationally constrained end displacements p0128 879-21831
- COLLOIDS**
U AEROSOLS
- COLOR**
U WATER COLOR
- COMBUSTIBILITY**
U FLAMMABILITY
- COMBUSTION**
U AFTERBURNING
U FUEL COMBUSTION
U HYDROCARBON COMBUSTION
U METAL COMBUSTION
Definition of smolder experiments for Spacelab [NASA-CR-159528] p0040 879-20161
Preliminary results in the NASA Lewis H2-O2 combustion MHD experiment [NASA-TM-79135] p0181 879-22897
Gas-turbine critical research and advanced technology support project [NASA-TM-79139] p0139 879-25498
Laser anemometer measurements at the exit of a T63-C20 combustor [NASA-CR-159623] p0107 879-28456
- COMBUSTION CHAMBERS**
Wide range operation of advanced low NOx aircraft gas turbine combustors [ASME PAPER 78-GT-128] p0024 879-10792
Correlation of combustor acoustic power levels inferred from internal fluctuating pressure measurements p0025 879-14796
Correlations of catalytic combustor performance parameters p0070 879-14956
Experimental study of the effects of flameholder geometry on emissions and performance of lean premixed combustors [AIAA PAPER 79-0187] p0070 879-19586
The NASA high pressure facility and turbine test rig p0038 879-21296
The Advanced Low-Emissions Catalytic-Combustor Program: Phase I - Description and status --- for aircraft gas turbine engines [ASME PAPER 79-GT-192] p0027 879-30557
Some effects of cyclic induced deformation in rocket thrust chambers [AIAA 79-0911] p0054 879-34736
Analysis of the impact of the use of broad specification fuels on combustors for commercial aircraft gas turbine engines [AIAA PAPER 79-1195] p0090 879-38980
Lean stability augmentation for premixing, prevaporizing combustors [AIAA PAPER 79-1319] p0036 879-39035
Effect of degree of fuel vaporization upon emissions for a premixed prevaporized combustion system [AIAA PAPER 79-1320] p0071 879-39036
Reduction of particulate carryover from a pressurized fluidized bed p0150 879-49527
Reduction of particulate carryover from a pressurized fluidized bed p0150 879-49527
Correlations of catalytic combustor performance parameters [NASA-TM-79014] p0134 879-11480
Experimental clean combustor program: Phase 3: Turbulence measurement addendum [NASA-CR-135422] p0031 879-12088
Heat exchanger --- rocket combustion chambers and cooling systems [NASA-CASE-LBW-12252-1] p0102 879-13288
Ceramic coating effect on liner metal temperatures of film-cooled annular combustor [NASA-TF-1323] p0015 879-14098
The advanced low-emissions catalytic-combustor program. Phase 1: Description and status [NASA-TM-79049] p0015 879-15047
Experimental clean combustor program, phase 3: Noise measurement addendum --- CF6-50 high bypass turbofan engine noise [NASA-CR-159458] p0177 879-17656
Parametric performance of a turbojet engine combustor using jet A and A diesel fuel [NASA-TM-79089] p0017 879-20114
Simulation of fluidized bed coal combustors [NASA-CR-159529] p0153 879-20487
Performance of a vortex-controlled diffuser in an annular swirl-can combustor at inlet Mach numbers up to 0.53 [NASA-TF-1452] p0017 879-22099
Lean stability augmentation study --- on gas turbine combustion chambers [NASA-CR-159536] p0071 879-22244
Preliminary comparison of theory and experiment for a conical, pressurized-fluidized-bed coal combustor [NASA-TM-79137] p0137 879-22623
Effect of degree of fuel vaporization upon emissions for a premixed prevaporized combustion system --- for gas turbine engines [NASA-TM-79154] p0012 879-23965
Premixed Prevaporized Combustor Technology Forum [NASA-CF-2078] p0019 879-24994
Effect of fuel sprays on emissions p0020 879-24999
Performance of a multiple venturi fuel-air preparation system --- fuel injection for gas turbines p0020 879-25000
Effects of flameholder geometry on emissions and performance of lean premixed combustors p0021 879-25005
Effects of flameholder blockage on emissions and performance of lean premixed-prevaporized combustors p0021 879-25006
Modelling turbulent flame ignition and blowout p0021 879-25008
Advanced low emissions catalytic combustor program at General Electric p0021 879-25011
Advanced low emissions catalytic combustor program at Pratt and Whitney p0021 879-25012
Lean, premixed, prevaporized combustor conceptual design study p0021 879-25013
Lean, premixed, prevaporized combustor conceptual design study p0022 879-25014
Fundamentals of Gas Turbine combustion [NASA-CF-2087] p0022 879-25016
Experimental clean combustor program: Diesel no. 2 fuel addendum, phase 3 [NASA-CR-135413] p0091 879-26221
Reduction of particulate carryover from a pressurized fluidized bed [NASA-TM-79216] p0141 879-27664
Laser anemometer measurements at the exit of a T63-C20 combustor [NASA-CR-159623] p0107 879-28456
Performance characteristics of a slagging gasifier for MHD combustor systems

- [NASA-TM-79195] p0142 W79-30720
Experimental Clean Combustor Program (ECCP), phase 3
--- commercial aircraft turbofan engine tests
with double annular combustor
[NASA-CR-135384] p0035 W79-31207
Lean, Premixed-Prevaporized (LPP) combustor
conceptual design study
[NASA-CR-159629] p0072 W79-31358
Lean, premixed, prevaporized fuel combustor
conceptual design study
[NASA-CR-159647] p0035 W79-32211
- COMBUSTION EFFICIENCY**
Lean, premixed, prevaporized combustion for
aircraft gas turbine engines
[AIAA PAPER 79-1318] p0029 W79-39034
Lean stability augmentation for premixing,
prevaporizing combustors
[AIAA PAPER 79-1319] p0036 W79-39035
Analytical evaluation of the impact of broad
specification fuels on high bypass turbofan
engine combustors
[NASA-CR-159454] p0031 W79-13050
Lean, premixed, prevaporized combustion for
aircraft gas turbine engines
[NASA-TM-79148] p0018 W79-23964
Lean, premixed, prevaporized combustion for
aircraft gas turbine engines
[NASA-TM-79148] p0018 W79-23964
Lean Stability augmentation study
p0021 W79-25007
Performance characteristics of a slagging gasifier
for MHD combustor systems
[NASA-TM-79195] p0142 W79-30720
- COMBUSTION INSTABILITY**
U COMBUSTION STABILITY
COMBUSTION PHYSICS
Lean combustion limits of a confined
premixed-prevaporized propane jet
[AIAA PAPER 79-0538] p0026 W79-25856
Chemically frozen multicomponent boundary layer
theory of salt and/or ash deposition rates from
combustion gases
p0078 W79-50912
Characteristics and combustion of future
hydrocarbon fuels
p0089 W79-13196
Premix fuels study applicable to duct burner
conditions for a variable cycle engine
[NASA-CR-159513] p0091 W79-20266
Lean stability augmentation study --- on gas
turbine combustion chambers
[NASA-CR-159536] p0071 W79-22244
Fuel spray data with LDV --- solar laser
morphokinetic capabilities in combustion
research
p0015 W79-24997
- COMBUSTION PRODUCTS**
The hot corrosion of Co-25Cr-10Ni-5Ta-3Al-0.5Y
alloy /S-57/
p0076 W79-10420
Lean stability augmentation for premixing,
prevaporizing combustors
[AIAA PAPER 79-1319] p0036 W79-39035
Effect of degree of fuel vaporization upon
emissions for a premixed prevaporized combustion
system
[AIAA PAPER 79-1320] p0071 W79-39036
The role of NaCl in flame chemistry, in the
deposition process, and in its reactions with
protective oxides as related to hot corrosion
p0071 W79-49534
Effect of fuel sprays on emissions
p0020 W79-24999
Effect of fuel/air nonuniformity on nitric oxide
emissions
p0020 W79-25004
Effects of flameholder geometry on emissions and
performance of lean premixed combustors
p0021 W79-25005
Experimental studies of the formation/deposition
of sodium sulfate in/from combustion gases ---
hot corrosion in gas turbine engines
[NASA-CR-159612] p0072 W79-25183
Experimental studies of the formation/deposition
of sodium sulfate in/from combustion gases ---
hot corrosion
[NASA-CR-159613] p0080 W79-25184
High char inside-modified epoxy matrix resins ---
for graphite-epoxy composites
- [NASA-TM-79226] p0063 W79-29240
Dispersion of sound in a combustion duct by fuel
droplets and soot particles
[NASA-TM-79236] p0174 W79-31002
- COMBUSTION STABILITY**
Correlation of combustor acoustic power levels
inferred from internal fluctuating pressure
measurements
p0025 W79-14796
Turbulence effects on flame speed and flame
structure
[AIAA PAPER 79-0016] p0070 W79-19480
The Advanced Low-Emissions Catalytic-Combustor
Program: Phase I - Description and status ---
for aircraft gas turbine engines
[ASME PAPER 79-GT-192] p0027 W79-30557
Test verification of a turbofan partial swirl
afterburner
[AIAA PAPER 79-1199] p0029 W79-38981
Measurements of admittances and characteristic
combustion times of reactive gaseous propellant
coaxial injectors
[NASA-CR-159542] p0072 W79-23168
Lean Stability augmentation study
p0021 W79-25007
Operating condition and geometry effects on
low-frequency afterburner combustion instability
in a turbofan at altitude
[NASA-TF-1475] p0022 W79-25022
- COMBUSTION WAVES**
U FLAME PROPAGATION
COMBUSTORS
U COMBUSTION CHAMBERS
COMMERCIAL AIRCRAFT
NT BOEING 747 AIRCRAFT
NT LEAR JET AIRCRAFT
Automated meteorological data from commercial
aircraft via satellite - Present experience and
future implications
p0010 W79-17092
Simultaneous measurements of ozone outside and
inside cabins of two B-747 airliners and a Gates
Learjet business jet
p0008 W79-27571
Analytical evaluation of the impact of broad
specification fuels on high bypass turbofan
engine combustors
[NASA-CR-159454] p0031 W79-13050
Rotor fragment protection program: Statistics on
aircraft gas turbine engine rotor failures that
occurred in US commercial aviation during 1976
[NASA-CR-159474] p0032 W79-18977
Commercial aircraft derived high resolution wind
and temperature data from the tropics for FGGE:
Implications for NASA
p0161 W79-20621
Experimental Clean Combustor Program (ECCP), phase 3
--- commercial aircraft turbofan engine tests
with double annular combustor
[NASA-CR-135384] p0035 W79-31207
Procedures for estimating the frequency of
commercial airline flights encountering high
cabin ozone levels
[NASA-TF-1560] p0008 W79-33171
- COMMERCIAL AVIATION**
U COMMERCIAL AIRCRAFT
COMMERCIAL ENERGY
Commercial synchronous alternating-current
generators
p0140 W79-26482
- COMBINATION**
Bond strengths of reaction bonded silicon nitride
prepared from dry attrition milled silicon powder
[NASA-TM-79230] p0084 W79-30379
- COMMUNICATING**
NT AIRCRAFT COMMUNICATION
NT NASCOM NETWORK
NT POINT TO POINT COMMUNICATIONS
COMMUNICATION CABLES
NT BEAM WAVEGUIDES
COMMUNICATION NETWORKS
NT NASCOM NETWORK
Global disaster satellite communications system
for disaster assessment and relief coordination
p0095 W79-30394
Results of thin-route satellite communication
system analyses including estimated service costs
p0095 W79-30395

- Results of thin-route satellite communication system analyses including estimated service costs [NASA-TM-79098] p0094 N79-20300
- The 18 and 30 GHz fixed service communications satellite system study --- to determine the cost and performance characteristics [NASA-CR-159627-2] p0096 N79-33374
- COMMUNICATION SATELLITES**
- NT AERONAUTICAL SATELLITES
- NT COMMUNICATIONS TECHNOLOGY SATELLITE
- Automated meteorological data from commercial aircraft via satellite - Present experience and future implications p0010 A79-17092
- Telecommunication service markets through the year 2000 in relation to millimeter wave satellite systems p0095 A79-27398
- Millimeter wave communication satellite concepts p0095 A79-29784
- Global disaster satellite communications system for disaster assessment and relief coordination p0095 A79-30394
- Results of thin-route satellite communication system analyses including estimated service costs p0093 A79-30395
- Design of a video teleconference facility for a synchronous satellite communications link [NASA-TP-1376] p0094 N79-14275
- Telecommunication service markets through the year 2000 in relation to millimeter wave satellite systems [NASA-TM-79099] p0094 N79-16169
- Determining potential 30/20 GHz domestic satellite system concepts and establishment of a suitable experimental configuration [NASA-TM-79092] p0094 N79-17072
- Results of thin-route satellite communication system analyses including estimated service costs [NASA-TM-79098] p0094 N79-20300
- TWT design requirements for 30/20 GHz digital communications' satellite [NASA-TM-79119] p0097 N79-20316
- Millimeter wave satellite concepts. Volume 1: Executive summary [NASA-CR-159504] p0041 N79-26101
- Millimeter wave satellite concepts. Volume 2: Technical report [NASA-CR-159503] p0041 N79-26102
- Satellite communications for disaster relief operations [NASA-TM-79198] p0094 N79-27351
- The 18 and 30 GHz fixed service communication satellite system study: Executive summary [NASA-CR-159627-1] p0096 N79-33373
- COMMUNICATION SYSTEMS**
- U TELECOMMUNICATION
- COMMUNICATIONS TECHNOLOGY SATELLITE**
- Thermal anomalies of the transmitter experiment package on the communications technology satellite [NASA-TP-1410] p0044 N79-21120
- Communications technology satellite: United States experiments and disaster communications applications [NASA-TM-79109] p0044 N79-23999
- Description and orbit data of variable-conductance heat-pipe system for the communications technology satellite [NASA-TP-1465] p0105 N79-30516
- Life characteristics assessment of the communications technology satellite transmitter experiment package [NASA-TM-79181] p0044 N79-31264
- COMPARATORS**
- Thermal-conductivity measurements of tungsten-fiber-reinforced superalloy composites using a thermal-conductivity comparator [NASA-TP-1445] p0063 N79-28234
- COMPARTMENTS**
- NT AIRCRAFT COMPARTMENTS
- NT PRESSURE CHAMBERS
- NT TEST CHAMBERS
- COMPLEX VARIABLES**
- NT LOGARITHMS
- COMPLIANCE (ELASTICITY)**
- U MODULUS OF ELASTICITY
- COMPONENT RELIABILITY**
- Determining and improving labyrinth seal performance in current and advanced high performance gas turbines p0031 N79-11068
- COMPOSITE MATERIALS**
- NT ALUMINUM BORON COMPOSITES
- NT BORON REINFORCED MATERIALS
- NT CARBON FIBER REINFORCED PLASTICS
- NT FIBER COMPOSITES
- NT GLASS FIBER REINFORCED PLASTICS
- NT GRAPHITE-EPOXY COMPOSITE MATERIALS
- NT LAMINATES
- NT METAL MATRIX COMPOSITES
- NT POLYMER MATRIX COMPOSITE MATERIALS
- Titanium/beryllium laminates - Fabrication, mechanical properties, and potential aerospace applications p0064 A79-20836
- Recent developments at CNEBA in the field of structural analysis methods [CNEBA, TP NO. 1979-79] A79-49537
- Design, fabrication, and test of a composite material wind turbine rotor blade [NASA-CR-135389] p0150 N79-10525
- Status review of PBR polyimides [NASA-TM-79039] p0062 N79-12150
- Fracture modes in off-axis fiber composites [NASA-TM-79036] p0062 N79-12154
- Dynamic mechanical analysis of fiber reinforced composites [NASA-TM-79033] p0061 N79-15157
- Characterization of PBR polyimides: Correlation of ester impurities with composite properties [NASA-TM-79068] p0061 N79-16918
- Prediction of properties of intraply hybrid composites [NASA-TM-79087] p0061 N79-16919
- Resin/fiber thermo-oxidative interactions in PBR polyimide/graphite composites [NASA-TM-79093] p0062 N79-16920
- Method of making bearing materials --- self-lubricating, oxidation resistant composites for high temperature applications [NASA-CASE-LEW-11930-4] p0062 N79-17916
- Composite seal for turbomachinery --- backings for turbine engine shrouds [NASA-CASE-LEW-12131-1] p0114 N79-18318
- Containment of composite fan blades [NASA-CR-158168] p0032 N79-18978
- Tungsten fiber reinforced FeCrAl: A first generation composite turbine blade material [NASA-TM-79094] p0063 N79-20187
- Analysis of high velocity impact on hybrid composite fan blades [NASA-TM-79133] p0127 N79-20398
- Polyimide prepreg material having improved tack retention --- polyimide-graphite fiber composites [NASA-CASE-LEW-12933-1] p0059 N79-24061
- Thermal-conductivity measurements of tungsten-fiber-reinforced superalloy composites using a thermal-conductivity comparator [NASA-TP-1445] p0063 N79-28234
- A review of issues and strategies in nondestructive evaluation of fiber reinforced structural composites [NASA-TM-79246] p0125 N79-29530
- Off-axis impact of unidirectional composites with cracks: Dynamic stress intensification [NASA-CR-159537] p0067 N79-30294
- Containment of composite fan blades [NASA-CR-159544] p0067 N79-31348
- Normal and radial impact of composites with embedded penny-shaped cracks [NASA-CR-159538] p0130 N79-31627
- COMPOSITE STRUCTURES**
- NT LAMINATES
- Acoustic emission testing of composite vessels under sustained loading p0128 A79-11543
- Analysis/design of strip reinforced random composites /strip hybrids/ p0119 A79-24035
- Analysis of high velocity impact on hybrid composite fan blades [AIAA 79-0783] p0128 A79-29027
- CODSTHAN - Composite durability structural analysis p0128 A79-37292
- Characterization of PBR polyimides - Correlation of ester impurities with composite properties p0066 A79-43265

- CCDSTRAN: Composite durability structural analysis**
[NASA-TN-79070] p0126 N79-15326
- Test results for electron beam charging of flexible insulators and composites --- solar array substrates, honeycomb panels, and thin dielectric films**
p0048 N79-24031
- Evaluation of flawed composite structural components under static and cyclic loading --- fatigue life of graphite-epoxy composite materials**
[NASA-CR-135403] p0066 N79-26120
- Metal spar/superhybrid shell composite fan blades --- for application to turbofan engines**
[NASA-CR-159594] p0067 N79-30295
- COMPOSITE WRAPPING**
Effect of low-stiffness closeout overwrap on rocket thrust-chamber life
[NASA-TP-1456] p0053 N79-23132
- COMPOSITES**
U COMPOSITE MATERIALS
- COMPOSITION (PROPERTY)**
NT ATMOSPHERIC COMPOSITION
NT ATMOSPHERIC MOISTURE
NT CHEMICAL COMPOSITION
NT CONCENTRATION (COMPOSITION)
NT MOISTURE CONTENT
- COMPRESSED GAS**
Workbook for estimating effects of accidental explosions in propellant ground handling and transport systems
[NASA-CR-3023] p0091 N79-10226
- COMPRESSIBILITY EFFECTS**
Turbulence generated by the interaction of entropy fluctuations with non-uniform mean flows
p0106 A79-45468
- COMPRESSIBLE FLOW**
NT TRANSONIC FLOW
An efficient user-oriented method for calculating compressible flow about three-dimensional inlets
[AIAA PAPER 79-0081] p0005 A79-19524
- Compressible flow across narrow passages:**
Comparison of theory and experiment for face seals
[NASA-TI-1346] p0113 N79-10424
- A three-dimensional turbulent compressible flow model for ejector and fluted mixers**
[NASA-CR-159467] p0100 N79-14325
- COMPRESSION LOADS**
NT IMPACT LOADS
- COMPRESSOR BLADES**
Axial-flow compressor turning angle and loss by inviscid-viscous interaction blade-to-blade computation
[ASME PAPER 79-GT-5] p0006 A79-30504
- Experimental evaluation of the effect of inlet distortion on compressor blade vibrations**
p0128 A79-30558
- Instrumentation for measuring the dynamic pressure on rotating compressor blades**
[NASA-CR-159466] p0110 N79-12418
- Experimental evaluation of the effect of inlet distortion on compressor blade vibrations**
[NASA-TN-79066] p0126 N79-16300
- Interactive multi-mode blade impact analysis**
[NASA-CR-159462] p0032 N79-17858
- Fabrication of J79 boron/aluminum compressor blades**
[NASA-CR-159566] p0034 N79-23970
- Aerodynamic performance of 1.38-pressure-ratio, variable-pitch fan stage**
[NASA-TP-1502] p0024 N79-31213
- Effects of diffusion factor, aspect ratio and solidity on overall performance of 14 compressor middle stages --- the effects of varying both diffusion through the rotor and compressor blades and blade aspect ratio**
[NASA-TP-1523] p0038 N79-33210
- COMPRESSOR EFFICIENCY**
Statistical study of supersonic compressors
p0039 N79-21060
- COMPRESSOR ROTORS**
An off-design correlation of part span damper losses through transonic axial fan rotors
[ASME PAPER 79-GT-6] p0028 A79-32329
- Effect of casing treatment on performance of a two-stage high-pressure-ratio fan**
[NASA-TP-1409] p0017 N79-16852
- Measuring unsteady pressure on rotating compressor blades**
[NASA-TN-79159] p0109 N79-22448
- Rotor redesign for a highly loaded 1800 ft/sec tip speed fan. 1: Aerodynamic and mechanical design report**
[NASA-CR-159596] p0034 N79-26055
- Effect of rotor meridional velocity ratio on response to inlet radial and circumferential distortion**
[NASA-TP-1278] p0023 N79-28177
- Performance of two-stage fan with a first-stage rotor redesigned to account for the presence of a part-span damper**
[NASA-TP-1483] p0024 N79-30191
- Effects of diffusion factor, aspect ratio and solidity on overall performance of 14 compressor middle stages --- the effects of varying both diffusion through the rotor and compressor blades and blade aspect ratio**
[NASA-TP-1523] p0038 N79-33210
- COMPRESSORS**
NT CENTRIFUGAL COMPRESSORS
NT SUPERCHARGERS
NT SUPERSONIC COMPRESSORS
NT TRANSONIC COMPRESSORS
NT TURBOCOMPRESSORS
- Causes of high pressure compressor deterioration in service**
[AIAA PAPER 79-1234] p0036 A79-40483
- Strain gage system evaluation program**
[NASA-CR-159486] p0110 N79-19314
- Design problems of small turbomachinery**
p0046 N79-22097
- Study of blade aspect ratio on a compressor front stage aerodynamic and mechanical design report**
[NASA-CR-159555] p0034 N79-23085
- Turbulence characteristics of compressor discharge flows --- T9D engine tests**
p0019 N79-24995
- Turbulence measurements in the compressor exit flow of a General Electric CP6-50 engine**
p0019 N79-24996
- COMPUTER GRAPHICS**
Digital enhancement of computerized axial tomograms
p0164 A79-11544
- COMPUTER METHODS**
U COMPUTER PROGRAMS
- COMPUTER PROGRAMMING**
Computer signal processing for ultrasonic attenuation and velocity measurements for material property characterizations
p0125 A79-39809
- Computer signal processing for ultrasonic attenuation and velocity measurements for material property characterizations**
[NASA-TN-79180] p0127 N79-24359
- COMPUTER PROGRAMS**
NT NASTRAN
NT SUBROUTINE LIBRARIES (COMPUTERS)
- SINWEST - A simulation model for wind energy storage systems**
p0145 A79-10241
- A computer program for the calculation of the flow field in supersonic mixed-compression inlets at angle of attack using the three-dimensional method of characteristics with discrete shock wave fitting**
[NASA-TN-78947] p0002 N79-10023
- User's manual for FRAC3D: Supplement to report on stress analysis for structures with surface cracks**
[NASA-CR-159401] p0129 N79-13406
- CODSTRAN: Composite durability structural analysis**
[NASA-TN-79070] p0126 N79-15326
- Three-dimensional finite-element elastic analysis of a thermally cycled single-edge wedge geometry specimen**
[NASA-TN-79026] p0172 N79-16644
- Computation of atmospheric attenuation of sound for fractional-octave bands**
[NASA-TP-1412] p0173 N79-17659
- Interactive multi-mode blade impact analysis**
[NASA-CR-159462] p0032 N79-17858
- TACT 1: A computer program for the transient thermal analysis of a cooled turbine blade or vane equipped with a coolant insert. 2. Programmers manual**
[NASA-TP-1391] p0103 N79-18288
- Evaluation of HOSTAS computer code for predicting dynamic loads in two bladed wind turbines**
[NASA-TN-79101] p0137 N79-21549

- Interactive debug program for evaluation and modification of assembly-language software
[NASA-TF-1441] p0166 W79-21798
- Analytical prediction with multidimensional computer programs and experimental verification of the performance, at a variety of operating conditions, of two traveling wave tubes with depressed collectors
[NASA-TF-1449] p0097 W79-22375
- WETAIR: A computer code for calculating thermodynamic and transport properties of air-water mixtures
[NASA-TF-1466] p0166 W79-23688
- Modeling of premixing-prevaporizing fuel-air mixing passages
p0019 W79-24998
- User's manual for PRESTO: A computer code for the performance of regenerative steam turbine cycles
[NASA-CR-159540] p0122 W79-25395
- Computer programs for calculating two-dimensional potential flow through deflected nozzles
[NASA-TN-79144] p0004 W79-26019
- NASCAP user's manual, 1978
[NASA-CR-159417] p0100 W79-27398
- Use of refinery computer model to predict fuel production
[NASA-TN-79203] p0085 W79-28349
- CELFE: Coupled Eulerian-Lagrangian Finite Element program for high velocity impact. Part 1: Theory and formulation --- hydroelasto-viscoplastic model
[NASA-CR-159395] p0166 W79-29832
- CELFE: Coupled Eulerian-Lagrangian Finite Element program for high velocity impact. Part 2: Program user's manual
[NASA-CR-159396] p0166 W79-29833
- COMPUTER SIMULATION**
U COMPUTERIZED SIMULATION
COMPUTER SYSTEMS PROGRAMS
NT SUBROUTINE LIBRARIES (COMPUTERS)
COMPUTER TECHNIQUES
The application of hydraulics in the 2,000 kW wind turbine generator
p0156 A79-27400
- Computerized systems analysis and optimization of aircraft engine performance, weight, and life cycle costs
[NASA-TN-79221] p0170 W79-29938
- COMPUTERIZED CONTROL**
U NUMERICAL CONTROL
COMPUTERIZED DESIGN
Power converter design optimization
p0099 A79-10885
- Recent applications of theoretical analysis to V/STOL inlet design
p0006 A79-49530
- Computer-aided analysis and design of the shape rolling process for producing turbine engine airfoils
[NASA-CR-159455] p0012 W79-12087
- Computer-aided analysis and design of the shape rolling process for producing turbine engine airfoils
[NASA-CR-135367] p0080 W79-26175
- COMPUTERIZED SIMULATION**
NT DIGITAL SIMULATION
SINWEST - A simulation model for wind energy storage systems
p0145 A79-10241
- Generalized computer-aided discrete time domain modeling and analysis of dc-dc converters
p0099 A79-10881
- Phase change thermal storage for a solar total energy system
p0155 A79-17321
- Evaluation of MOSTAS computer code for predicting dynamic loads in two-bladed wind turbines
[AIAA 79-0733] p0005 A79-29007
- Analysis of high velocity impact on hybrid composite fan blades
[AIAA 79-0783] p0128 A79-29027
- CODSTRAIN - Composite durability structural analysis
p0128 A79-37292
- NASCAP modelling of high-voltage power system interactions with space charged-particle environments --- particle impact on solar satellite surfaces
p0051 A79-39806
- Maximum likelihood estimation for life distributions with competing failure modes
p0169 A79-49528
- A method to estimate weight and dimensions of large and small gas turbine engines
[NASA-CR-159481] p0015 W79-15046
- Computer simulation of an aircraft engine fuel injection system
[NASA-CR-157641] p0016 W79-15052
- High speed cylindrical roller bearing analysis, SKF computer program CYBEAN. Volume 1: Analysis
[NASA-CR-159460] p0121 W79-17222
- Simulation of fluidized bed coal combustors
[NASA-CR-159529] p0153 W79-20487
- Lewis hybrid computing system, users manual
[NASA-TN-79111] p0165 W79-20752
- Combined pressure and temperature distortion effects on internal flow of a turbofan engine
[NASA-TN-79136] p0012 W79-23963
- Low-power baseline test results for the GPU 3 Stirling engine
[NASA-TN-79103] p0188 W79-27023
- Computer and laboratory simulation of interactions between spacecraft surfaces and charged-particle environments
[NASA-TN-79219] p0063 W79-29224
- NASCAP modelling of environmental-charging-induced discharges in satellites
[NASA-TN-79247] p0048 W79-31265
- An expanded system simulation model for solar energy storage (technical report), volume 1
[NASA-CR-159601] p0166 W79-33881
- An expanded system simulation model for solar energy storage (UNIVAC operation manual revisions), volume 2
[NASA-CR-159602] p0166 W79-33882
- SINWEST: A simulation model for wind and photovoltaic energy storage systems (CDC user's manual), volume 1
[NASA-CR-159607] p0166 W79-33883
- SINWEST: A simulation model for wind and photovoltaic energy storage systems (cdc program descriptions), volume 2
[NASA-CR-159608] p0167 W79-33884
- COMPUTERS**
NT AIRBORNE/SPACEBORNE COMPUTERS
NT ANALOG COMPUTERS
NT CDC COMPUTERS
NT HONEYWELL COMPUTERS
NT HYBRID COMPUTERS
NT UNIVAC 1100 SERIES COMPUTERS
- CONCENTRATION (COMPOSITION)**
NT ATMOSPHERIC MOISTURE
NT MOISTURE CONTENT
Ionized dopant concentrations at the heavily doped surface of a silicon solar cell
[NASA-TF-1347] p0184 W79-13886
- Ozone measurement system for NASA global air sampling program
[NASA-TF-1451] p0158 W79-22654
- CONDENSATION**
Condensation on a noncollapsing vapor bubble in a subcooled liquid
p0100 A79-49535
- CONDENSING**
Condensation-nuclei (Aitken Particle) measurement system used in NASA global atmospheric sampling program
[NASA-TF-1415] p0157 W79-18479
- Condensation on a noncollapsing vapor bubble in a subcooled liquid
[NASA-TN-79212] p0105 W79-27461
- CONDITIONS**
NT ADIABATIC CONDITIONS
NT FLIGHT CONDITIONS
- CONDUCTORS**
NT ION EXCHANGE MEMBRANE ELECTROLYTES
NT SUPERCONDUCTORS
- CONES**
NT CONICAL BODIES
- CONFERENCES**
Future Orbital Power Systems Technology Requirements
[NASA-CF-2058] p0052 W79-10122
- Preliminary CCGAT program test results
[NASA-TN-79013] p0016 W79-15051
- The rotary combustion engine: A candidate for general aviation --- conferences
[NASA-CF-2067] p0016 W79-15961

Aircraft icing
[NASA-CP-2086] p0004 N79-23912
Spacecraft Charging Technology, 1978
[NASA-CP-2071] p0047 N79-24001
Premixed Prevaporized Combustor Technology Forum
[NASA-CP-2078] p0015 N79-24994
Review of the AGARD S and M panel evaluation
program of the NASA-Lewis SRP approach to
high-temperature ICF life prediction p0023 N79-27179
Characteristics of primary electric propulsion
systems --- conferences
[NASA-TM-79255] p0053 N79-30290
State-of-the-art of SiAlON materials --- conferences
[NASA-TM-79207] p0084 N79-30378
Survey of ion plating sources --- conferences
[NASA-TM-79269] p0076 N79-31372
Solar Cell High Efficiency and Radiation Damage,
1979
[NASA-CP-2097] p0143 N79-32640

CONFLUENCE
U CONVERGENCE
CONICAL BODIES
Preliminary comparison of theory and experiment
for a conical, pressurized-fluidized-bed coal
combustor
[NASA-TM-79137] p0137 N79-22623

CONICS
NT ELLIPSES
CONNECTORS
Low heat leak connector for cryogenic system
[NASA-CASE-XLE-02367-1] p0093 N79-21225

CONOIDS
U CONICAL BODIES
CONSERVATION
NT ENERGY CONSERVATION
CONSERVATION EQUATIONS
Application of the principle of similarity fluid
mechanics
[NASA-TM-79258] p0105 N79-30515

CONSTANT SPEED PROPELLERS
U VARIABLE PITCH PROPELLERS
CONSTRAINTS
NT METEOROLOGICAL PARAMETERS
CONSTRUCTION MATERIALS
Titanium/beryllium laminates - Fabrication,
mechanical properties, and potential aerospace
applications p0064 A79-20836

CONSUMABLES (SPACECRAFT)
NT WORKING FLUIDS
CONSUMPTION
NT FUEL CONSUMPTION
CONTACT POTENTIALS
Evaluation of high-contact-ratio spur gears with
profile modification
[NASA-TF-1458] p0115 N79-31604

CONTAINMENT
Containment of composite fan blades
[NASA-CR-158168] p0032 N79-18978
Containment of composite fan blades
[NASA-CR-159544] p0067 N79-31340

CONTAMINANTS
NT TRACE CONTAMINANTS
NASA Global Atmospheric Sampling Program (GASP)
data report for tape VL0009
[NASA-TM-79058] p0157 N79-15448

CONTAMINATION
Filtration effects on ball bearing life and
condition in a contaminated lubricant
[ASME PAPER 78-LUB-34] p0118 A79-23246
Ozone contamination in aircraft cabins:
Objectives and approach p0008 N79-21022
Ozone Contamination in Aircraft Cabins: Summary
of recommendations p0008 N79-21026
Ozone Contamination in Aircraft Cabins: Post
workshop review of recommendations p0008 N79-21027
Ozone Contamination in Aircraft Cabins: Appendix
B: Overview papers. In-flight measurements
p0008 N79-21029

CONTINUOUS WAVE LASERS
Solar-pumped lasers for space power transmission
[AIAA PAPER 79-1015] p0112 A79-38202

CONTROL DEVICES
U CONTROL EQUIPMENT

CONTROL EQUIPMENT

Design and operating experience on the U.S.
Department of Energy Experimental Mod-O 100 kW
Wind Turbine p0145 A79-10234
The solid state remote power controller - Its
status, use and perspective --- for aircraft and
spacecraft p0099 A79-10896
Evaluation of two inflow control devices for
flight simulation of fan noise using a JT15D
engine
[AIAA PAPER 79-0654] p0026 A79-26926
Evaluation of two inflow control devices for
flight simulation of fan noise using a JT15D
engine
[NASA-TM-79072] p0017 N79-15969

CONTROL SIMULATION
Control of wind turbine generators connected to
power systems p0146 A79-15574

CONTROL SURFACES
NT GUIDE VANES
NT TRAILING-EDGE FLAPS
CONTROL THEORY
Generation of linear dynamic models from a digital
nonlinear simulation
[NASA-TF-1388] p0001 N79-16796

CONTROLLED ATMOSPHERES
NT CABIN ATMOSPHERES
CONTROLLERS
NT SERVOMECHANISMS
An inverter/controller subsystem optimized for
photovoltaic applications p0148 A79-41047

CONVECTION
Modal propagation angles in ducts with soft walls
and their connection with suppressor performance
[NASA-TM-79081] p0173 N79-16646

CONVECTIVE HEAT TRANSFER
Convective heat flux in a laser-heated thruster
p0057 A79-22396

CONVERGENCE
Acceleration of linear and logarithmic convergence
p0168 A79-40494

CONVERGENT-DIVERGENT NOZZLES
Two-phase choked flow of cryogenic fluids in
converging-diverging nozzles
[NASA-TF-1484] p0105 N79-29468

CONVERTERPLANES
U V-STOL AIRCRAFT
COOLING
NT AIR COOLING
NT FILM COOLING
NT LIQUID COOLING
TACT 1: A computer program for the transient
thermal analysis of a cooled turbine blade or
vane equipped with a coolant insert. 2.
Programmers manual
[NASA-TF-1391] p0103 N79-18288

COOLING SYSTEMS
Liquid-cooling technology for gas turbines -
Review and status p0116 A79-10038
Optimum dry-cooling sub-systems for a solar air
conditioner
[NASA-TM-79007] p0133 N79-11477
Heat exchanger --- rocket combustion chambers and
cooling systems
[NASA-CASE-LEW-12252-1] p0102 N79-13288
Effect of thermal barrier coatings on the
performance of steam and water-cooled gas
turbine/steam turbine combined cycle system
[NASA-TM-79057] p0135 N79-17334
Closed loop spray cooling apparatus
[NASA-CASE-LEW-11981-2] p0103 N79-20336

COPPER
Characterization of defect growth structures in
ion plated films by scanning electron microscopy
p0078 A79-34992
Effect of low-stiffness closeout overwrap on
rocket thrust-chamber life
[NASA-TF-1456] p0053 N79-23132
Development of sputtered techniques for thrust
chambers
[NASA-CR-159637] p0080 N79-32326

COPPER ALLOYS
NT BRONZES

COPPER COMPOUNDS

NT COPPER SULFIDES

COPPER SULFIDES

Superconducting properties of evaporated copper molybdenum sulfide films

p0184 A79-20219

Critical current and scaling laws in evaporated two-phase Cu₂S/MoS₈

p0185 A79-26375

Reactively evaporated films of copper molybdenum sulfide

p0185 A79-31973

Electronic properties of PbMoS₈ and CuMoS₈ --- for superconductivity

p0187 A79-41731

CORE FLOW

Aerodynamic and acoustic effects of eliminating core swirl from a full scale 1.6 stage pressure ratio fan (QF-5A)

[NASA-TM-78991]

p0002 N79-11001

CORPUSCULAR RADIATION

NT ELECTRON BEAMS

CORRELATION

NT DATA CORRELATION

NT SIGNAL ANALYSIS

An off-design correlation of part span damper losses through transonic axial fan rotors

[ASME PAPER 79-GT-6]

p0028 A79-32329

CORRELATION FUNCTIONS

U CORRELATION

CORROSION

NT PRETTING CORROSION

NT HOT CORROSION

NT SCALE (CORROSION)

Chemically frozen multicomponent boundary layer theory of salt and/or ash deposition rates from combustion gases

p0078 A79-50912

The role of NaCl in flame chemistry, in the deposition process, and in its reactions with protective oxides as related to hot corrosion

[NASA-TM-79225]

p0069 N79-28258

The chemistry of sodium chloride involvement in processes related to hot corrosion --- in gas turbine engines

[NASA-TM-79251]

p0069 N79-31361

CORROSION PREVENTION

Effect of a chromium-containing fuel additive on hot corrosion

p0071 A79-26546

Internally coated air-cooled gas turbine blading

[NASA-CR-159574]

p0034 N79-25018

Gas-turbine critical research and advanced technology support project

[NASA-TM-79139]

p0139 N79-25496

CORROSION RESISTANCE

NT OXIDATION RESISTANCE

Thermal barrier coatings: Burner rig hot corrosion test results

[NASA-TM-79005]

p0073 N79-11179

Technology development for phosphoric acid fuel cell powerplant, phase 2

[NASA-CR-159572]

p0153 N79-29604

CORROSION TESTS

NT SALT SPRAY TESTS

The hot corrosion of Co-25Cr-10Ni-5Ta-3Al-0.5Y alloy /S-57/

p0076 A79-10420

Atlas 5013 tank corrosion test

[NASA-CR-158760]

p0050 N79-27234

CORUNDUM

U ALUMINUM OXIDES

COSMIC GASES

NT NEUTRAL GASES

COST ANALYSIS

Diagnostics of wear in aeronautical systems

p0120 A79-39805

Energy and cost savings results for advanced technology systems from the Cogeneration Technology Alternatives Study /CTAS/

[AIAA PAPER 79-1000]

p0149 A79-44225

Communications systems technology assessment study. Volume 2: Results

[NASA-CR-135224]

p0095 N79-12273

Results of thin-route satellite communication system analyses including estimated service costs

[NASA-TM-79998]

p0094 N79-20300

Rankine-cycle component characteristics

p0140 N79-26478

Wind turbines for electric utilities: Development status and economics

[NASA-TM-79170]

p0142 N79-30719

The 18 and 30 GHz fixed service communications

satellite system study --- to determine the cost

and performance characteristics

[NASA-CR-159627-2]

p0096 N79-33374

COST EFFECTIVENESS

Space propulsion technology overview

[AIAA 79-0860]

p0054 A79-34704

Analysis of a fuel cell on-site integrated energy

system for a residential complex

[AIAA PAPER 79-0990]

p0147 A79-38192

COST ESTIMATES

Wind turbines for electric utilities - Development status and economics

[AIAA PAPER 79-0965]

p0148 A79-38888

Laser power conversion system analysis, volume 1

[NASA-CR-159523-VOL-1]

p0112 N79-21334

COSTS

NT LOW COST

COULOMB POTENTIAL

The decrease in effective photocurrents due to saddle points in electrostatic potentials near differentially charged spacecraft

p0049 A79-30140

COUPLED MODES

Mode I analysis of a cracked circular disk subject to a couple and a force

p0128 A79-15588

COWELL METHOD

U NUMERICAL INTEGRATION

CRACK FORMATION

U CRACK INITIATION

CRACK INITIATION

On the equivalence between semiempirical fracture analyses and R-curves

[NASA-TM-79127]

p0103 N79-20338

CRACK PROPAGATION

On the equivalence between semiempirical fracture analyses and R-curves

p0129 A79-39813

CODSTRAN: Composite durability structural analysis

[NASA-TM-79070]

p0126 N79-15326

On the equivalence between semiempirical fracture analyses and R-curves

[NASA-TM-79127]

p0103 N79-20338

Mode I crack surface displacements for a round compact specimen subject to a couple and force

[NASA-TM-79096]

p0161 N79-20572

Definition of mutually optimum NDI and proof test criteria for 2219 aluminum pressure vessels.

Volume 1: Methods

[NASA-CR-135445]

p0125 N79-21410

Definition of mutually optimum NDI and proof test criteria for 2219 aluminum pressure vessels.

Volume 2: Optimization and fracture studies

[NASA-CR-135446]

p0125 N79-21411

Off-axis impact of unidirectional composites with cracks: Dynamic stress intensification

[NASA-CR-159537]

p0067 N79-30294

CRACKING (FRACTURING)

Mode I analysis of a cracked circular disk subject to a couple and a force

p0128 A79-15588

Mode I crack surface displacements for a round compact specimen subject to a couple and force

p0129 A79-39812

CRACKS

NT SURFACE CRACKS

Stresses from arbitrary loads on a circular crack

[NASA-TM-79070]

p0130 A79-27938

Normal and radial impact of composites with embedded penny-shaped cracks

[NASA-CR-159538]

p0130 N79-31627

CRAZING

U SURFACE CRACKS

CREEP ANALYSIS

Thermal-structural mission analyses of air-cooled gas turbine blades

[NASA-TM-78963]

p0126 N79-11433

CREEP PROPERTIES

The strainrange partitioning behavior of an advanced gas turbine disk alloy, AP2-1DA

[AIAA PAPER 79-1192]

p0078 A79-38977

A literature review on fatigue and creep interaction

[NASA-CR-135305]

p0130 N79-26429

CREEP RUPTURE STRENGTH

Interpolation and extrapolation of creep rupture

- data by the Minimum Commitment Method. I - Focal-point convergence. II - Oblique translation. III - Analysis of multiheats
p0077 A79-16038
- Modules of rupture and oxidation resistance of S12.55Al0.600.72N3.52 sialon [NASA-TF-1490] p0083 N79-27309
- CREEP TESTS**
Strainrange partitioning life predictions of the long time metal properties council creep-fatigue tests [NASA-TM-79260] p0127 N79-31619
- CRESTATIONS**
U TRAVELING WAVE TUBES
- CREVICES**
J CRACKS
- CRITERIA**
NT STRUCTURAL DESIGN CRITERIA
- CRITICAL NACH NUMBER**
U CRITICAL VELOCITY
- CRITICAL REYNOLDS NUMBER**
U CRITICAL VELOCITY
U REYNOLDS NUMBER
- CRITICAL SPEED**
U CRITICAL VELOCITY
- CRITICAL TEMPERATURE**
Nb3Ge as a potential candidate material for 15- to 25-T magnets p0186 A79-44548
- CRITICAL VELOCITY**
Nonsynchronous vibrations observed in a supercritical power transmission shaft [ASME PAPER 79-GT-146] p0123 A79-32412
An introduction to a unified approach to flexible rotor balancing [ASME PAPER 79-GT-161] p0124 A79-32423
- CROSSLINKING**
Method of cross-linking polyvinyl alcohol and other water soluble resins [NASA-CASE-LEW-13103-1] p0068 E79-14172
Cross-linked polyvinyl alcohol and method of making same --- separator for alkaline batteries [NASA-CASE-LEW-13101-1] p0068 N79-14173
Three methods for in situ cross-linking of polyvinyl alcohol films for application as ion-conducting membranes in potassium hydroxide electrolyte --- battery separators [NASA-TF-1407] p0059 N79-21128
In situ self cross-linking of polyvinyl alcohol battery separators [NASA-CASE-LEW-12972-1] p0138 N79-25481
Catalytic trimerization of aromatic nitriles and triaryl-s-triazine ring cross-linked high temperature resistant polymers and copolymers made thereby [NASA-CASE-LEW-12053-2] p0083 N79-28307
New high temperature cross linking monomers --- for polymer matrix composite materials [NASA-CR-159514] p0087 N79-29331
- CRUDE OIL**
Use of refinery computer model to predict fuel production [NASA-TM-79203] p0089 N79-28349
Comparison of the properties of some synthetic crudes with petroleum crudes [NASA-TM-79220] p0090 N79-31405
- CRYOGENIC EQUIPMENT**
Improved apparatus for trapped radical and other studies down to 1.5 K --- microwave cavity cryogenic equipment for electron paramagnetic resonance experiments p0110 A79-20742
Flow friction of the turbulent coolant flow in cryogenic porous cables [NASA-TM-79052] p0103 N79-20341
- CRYOGENIC FLUID STORAGE**
Low heat leak connector for cryogenic system [NASA-CASE-XLE-02367-1] p0093 N79-21225
- CRYOGENIC FLUIDS**
NT LIQUID HYDROGEN
NT LIQUID NITROGEN
NT LIQUID OXYGEN
Two-phase choked flow of cryogenic fluids in converging-diverging nozzles [NASA-TF-1884] p0105 N79-29468
- CRYOGENIC MAGNETS**
Design study of superconducting magnets for a combustion magnetohydrodynamic /MHD/ generator p0098 A79-15305
- Preliminary results in the NASA Lewis H2-O2 combustion MHD experiment p0182 A79-39807
- CRYOGENIC ROCKET PROPELLANTS**
Cryogenic propellant densification study [NASA-CR-159438] p0087 N79-12238
Liquid oxygen/liquid hydrogen boost/vane pump for the advanced orbit transfer vehicles auxiliary propulsion system [NASA-CR-159648] p0057 N79-31341
- CRYOGENICS**
Effects of thermomechanical processing on strength and toughness of Fe-12Ni reactive metal alloys at 77K p0078 A79-32600
Free jet phenomena in a 90 degree-sharp edge inlet geometry [NASA-TM-79229] p0105 N79-31526
- CRYSTAL DEFECTS**
NT EDGE DISLOCATIONS
Photon-degradation effects in terrestrial silicon solar cells p0149 A79-42545
- CRYSTAL DISLOCATIONS**
NT EDGE DISLOCATIONS
- CRYSTAL GROWTH**
NT DIRECTIONAL SOLIDIFICATION (CRYSTALS)
NT EPITAXY
- CRYSTAL STRUCTURE**
State-of-the-art of SIALON materials --- conferences [NASA-TM-79207] p0084 N79-30378
- CRYSTAL SURFACES**
Anisotropic friction, deformation, and fracture of single-crystal silicon carbide at room temperature [NASA-TF-1525] p0084 N79-30380
- CRYSTALLIZATION**
NT DIRECTIONAL SOLIDIFICATION (CRYSTALS)
- CRYSTALLOGRAPHY**
Optical, spin-resonance, and magnetoresistance studies of tetrathiatetracene/2-iodide/3 - The nature of the ground state p0184 A79-10417
- CRYSTALS**
NT DOPED CRYSTALS
NT POLYCRYSTALS
NT SINGLE CRYSTALS
- CURING**
Curing agent for polyepoxides and epoxy resins and composites cured therewith [NASA-CASE-LEW-13226-1] p0059 N79-31345
- CURRENT DENSITY**
Critical current density in wire drawn and hydrostatically extruded Nb-Ti superconductors p0185 A79-20539
Critical current and scaling laws in evaporated two-phase Cu2.5Mo6S8 p0185 A79-26375
Comparison of projected critical currents in PbMo6S8 and Nb3Ge p0185 A79-28300
Nb3Ge as a potential candidate material for 15- to 25-T magnets p0186 A79-44548
Improved, low cost inorganic-organic separators for rechargeable silver-zinc batteries [NASA-TF-1476] p0069 N79-25181
- CYCLES**
NT BRAYTON CYCLE
NT RANKINE CYCLE
NT STELLING CYCLE
NT STRESS CYCLES
NT THERMODYNAMIC CYCLES
- CYCLIC LOADS**
Proposed design procedure for transmission shafting under fatigue loading p0117 A79-14950
Review of the Agard S6M panel evaluation program of the NASA-Lewis 'SRP' approach to high-temperature LCF life prediction --- Strainrange Partitioning for Low Cycle Fatigue p0128 A79-14954
Evaluation of flawed composite structural components under static and cyclic loading --- fatigue life of graphite-epoxy composite materials [NASA-CR-135403] p0066 N79-26120
- CYLINDRICAL AFTERBODIES**
U CYLINDRICAL BODIES
- CYLINDRICAL BODIES**
Modal propagation angles in a cylindrical duct

with flow and their relation to sound radiation
[NASA-TN-79030] p0172 N79-15756

CYLINDRICAL CHAMBERS
Structural analysis of cylindrical thrust
chambers, volume 1
[NASA-CN-159522] p0057 N79-19073

CYLINDRICAL TANKS
Axial jet mixing of ethanol in cylindrical
containers during weightlessness
[NASA-TP-1487] p0090 N79-28350

Contoured tank outlets for draining of cylindrical
tanks in low-gravity environment --- Lewis
Research Center Zero Gravity Facility
[NASA-TP-1412] p0105 N79-29467

CYLINDROIDS
U CYLINDRICAL BODIES

D

DARMO (DATA ANALYSIS)
U DATA REDUCTION
U DATA TRANSMISSION

DAMAGE
NT IMPACT DAMAGE
NT RADIATION DAMAGE

DAMPERS
Performance of two-stage fan with larger dampers
on first-stage rotor
[NASA-TP-1399] p0018 N79-23967

DAMPERS (VALVES)
An off-design correlation of part span damper
losses through transonic axial fan rotors
[ASME PAPER 79-GT-6] p0028 A79-32329

DAMPING
NT VIBRATION DAMPING
High temperature dynamic modulus and damping of
aluminum and titanium matrix composites
[NASA-TN-79080] p0061 N79-16077

Power train analysis for the DOE/NASA 100-kW wind
turbine generator
[NASA-TN-78997] p0135 N79-16355

Development of procedures for calculating
stiffness and damping of elastomers in
engineering applications. Part 5: Elastomer
performance limits and the design and test of an
elastomer damper
[NASA-CN-159552] p0122 N79-24373

DAMPING FACTOR
U DAMPING

DAMPING IN PITCH
U DAMPING

DAMPING IN ROLL
U DAMPING

DAMPING IN YAW
U DAMPING
U YAW

DAMPNESS
U MOISTURE CONTENT

DART TURBOPROP ENGINES
U TURBOPROP ENGINES

DATA ACQUISITION
The NASA high pressure facility and turbine test rig
p0038 A79-21296

Turbojet blade vibration data acquisition design
and feasibility testing
[NASA-CN-159505] p0032 N79-18976

Fuel spray data with LDV --- solar laser
morphokinetic capabilities in combustion
research
p0019 N79-24997

DATA ADAPTIVE EVALUATOR/MONITOR
U DATA REDUCTION
U DATA TRANSMISSION

DATA ANALYSIS
U DATA REDUCTION

DATA BASES
Handbook of data on selected engine components for
solar thermal applications
[NASA-TN-79027] p0139 N79-26476

DATA COLLECTION PLATFORMS
An airborne meteorological data collection system
using satellite relay /ASDAR/
p0010 A79-14949

DATA CONVERTERS
Multiple speed expandable bit synchronizer
[NASA-TN-79262] p0010 N79-33185

DATA CORRELATION
NT SIGNAL ANALYSIS

A reduced volumetric expansion factor plot
[NASA-TN-79240] p0105 N79-31527

DATA LINKS
Design of a video teleconference facility for a
synchronous satellite communications link
[NASA-TP-1376] p0094 N79-14275

DATA PROCESSING
NT DATA CORRELATION
NT DATA REDUCTION
NT SIGNAL ANALYSIS
NT SIGNAL PROCESSING

DATA PROCESSING EQUIPMENT
NT AIRBORNE/SPACEBORNE COMPUTERS
NT ANALOG COMPUTERS
NT CDC COMPUTERS
NT HONEYWELL COMPUTERS
NT HYBRID COMPUTERS
NT MICROPROCESSORS
NT UNIVAC 1100 SERIES COMPUTERS

DATA REDUCTION
Interpolation and extrapolation of creep rupture
data by the Minimum Commitment Method. I -
Focal-point convergence. II - Oblique
translation. III - Analysis of multiheats
p0077 A79-16038

DATA TRANSMISSION
Automated meteorological data from commercial
aircraft via satellite - Present experience and
future implications
p0010 A79-17092

DE LAVAL NOZZLES
U CONVERGENT-DIVERGENT NOZZLES

DEADWEIGHT
U STATIC LOADS

DECAY
NT ACOUSTIC EMISSION
NT ELECTRON EMISSION
NT EMISSION
NT MICROWAVE EMISSION
NT PHOTOELECTRIC EMISSION
NT SECONDARY EMISSION
NT SPONTANEOUS EMISSION
NT THERMIONIC EMISSION

Decay of homogeneous turbulence from a given state
at higher Reynolds number
[NASA-TN-79011] p0102 N79-12361

DECODERS
Multiple speed expandable bit synchronizer
[NASA-TN-79262] p0010 N79-33185

DECODING
On the distribution of computation for sequential
decoding using the stack algorithm
p0096 A79-33793

DEFECTS
NT CRYSTAL DEFECTS
NT EDGE DISLOCATIONS
NT SURFACE DEFECTS

Evaluation of flawed composite structural
components under static and cyclic loading ---
fatigue life of graphite-epoxy composite materials
[NASA-CN-135403] p0066 N79-26120

DEFORMATION
NT ELASTIC DEFORMATION
NT PLASTIC DEFORMATION

User's guide to computer programs JET 5A and
CIVM-JET 5B to calculate the large
elastic-plastic dynamically-induced deformations
of multilayer partial and/or complete structural
rings
[NASA-CN-159484] p0129 N79-18343

Some effects of cyclic induced deformation in
rocket thrust chambers
[NASA-TN-79112] p0103 N79-20337

Computer-aided analysis and design of the shape
rolling process for producing turbine engine
airfoils
[NASA-CN-135367] p0080 N79-26175

DEGRADATION
NT THERMAL DEGRADATION

Effects of moisture profiles and laminate
configuration on the hygro stress in advanced
composites
p0064 A79-24132

DELTA DAGGER AIRCRAFT
U F-102 AIRCRAFT

DENSIFICATION
Cryogenic propellant densification study
[NASA-CN-159438] p0087 N79-12238

DENSITY (MASS/VOLUME)

High performance, high density hydrocarbon fuels
[NASA-CR-159480] p0091 N79-20267

DENSITY (RATE/AREA)

U FLUX DENSITY

DEPENDENCE

NT TEMPERATURE DEPENDENCE

DEPOSITION

NT ELECTRODEPOSITION

NT VAPOR DEPOSITION

Experimental studies of the formation/deposition
of sodium sulfate in/from combustion gases ---
hot corrosion in gas turbine engines
[NASA-CR-159612] p0072 N79-25183

Experimental studies of the formation/deposition
of sodium sulfate in/from combustion gases ---
hot corrosion
[NASA-CR-159613] p0080 N79-25184

DESIGN ANALYSIS

Design and test of a squeeze-film damper for a
flexible power transmission shaft p0123 A79-16011

An approach to optimum subsonic inlet design
[NASA-TN-79051] p0002 N79-12020

A 200-MW wind turbine generator conceptual design
study [NASA-TN-79032] p0135 N79-17333

Evaluation of the ECAS open cycle MHD power plant
design [NASA-TN-79012] p0136 N79-17335

Design, fabrication and spin testing of ceramic
blade metal disk attachment [NASA-CR-159532] p0032 N79-17857

TWT design requirements for 30/20 GHz digital
communications' satellite [NASA-TN-79119] p0097 N79-20316

Lean, premixed, prevaporized combustor conceptual
design study p0021 N79-25013

Lean, premixed, prevaporized combustor conceptual
design study p0022 N79-25014

Metal spar/superhybrid shell composite fan blades
--- for application to turbofan engines
[NASA-CR-159594] p0067 N79-30295

Design of high efficiency HLE solar cells for
space and terrestrial applications p0154 N79-32647

DESIGN OF EXPERIMENTS

U EXPERIMENTAL DESIGN

DETECTION

NT RADAR DETECTION

DEVELOPING NATIONS

Photovoltaic power systems for rural areas of
developing countries p0147 A79-26131

Photovoltaic power systems for rural areas of
developing countries [NASA-TN-79097] p0135 N79-15411

DEWAR SYSTEMS

U CRYOGENIC EQUIPMENT

DIAGNOSIS

Diagnostics of wear in aeronautical systems
[NASA-TN-79185] p0115 N79-24350

DIAGRAMS

NT S-N DIAGRAMS

DIALYL COMPOUNDS

Evaluation and auger analysis of a
zinc-dialkyl-dithiophosphate antiwear additive
in several diester lubricants [NASA-TN-1544] p0084 N79-32359

DIELECTRIC MATERIALS

U DIELECTRICS

DIELECTRIC PROPERTIES

Effects of bulk and surface conductivity on the
potential developed by dielectrics exposed to
electron beams p0171 N79-50938

Fine particulate capture device
[NASA-CASE-LEW-11583-1] p0100 N79-17192

Stable dielectric charge distributions from field
enhancement of secondary emission p0045 N79-24046

DIELECTRICS

Laboratory studies of electrical properties of
insulating materials --- thermal insulation of
spacecraft dielectrics p0044 A79-20877

Charging rates of metal-dielectric structures ---
with implications for spacecraft p0048 N79-24033

Metal-dielectric interactions
[NASA-TN-79151] p0075 N79-25195

First principles numerical model of
avalanche-induced arc discharges in
electron-irradiated dielectrics
[NASA-CR-159560] p0101 N79-28418

DIESEL ENGINES

Comparison of fuel-cell and diesel integrated
energy systems and a conventional system for a
500-unit apartment [NASA-TN-79037] p0134 N79-15403

An overview of NASA research on positive
displacement type general aviation engines
[NASA-TN-79254] p0024 N79-31210

DIESEL JETLS

Parametric performance of a turbojet engine
combustor using jet A and A diesel fuel
[NASA-TN-79089] p0017 N79-20114

Experimental clean combustor program: Diesel no. 2
fuel addendum, phase 3 [NASA-CR-135413] p0091 N79-26221

DIFFERENTIAL ANALYZERS

U ANALOG COMPUTERS

DIFFERENTIAL EQUATIONS

NT BURGER EQUATION

DIFFUSERS

Application of semiconductor diffusants to solar
cells by screen printing [NASA-CASE-LEW-12775-1] p0133 N79-11468

Performance of a vortex-controlled diffuser in an
annular swirl-can combustor at inlet Mach
numbers up to 0.53 [NASA-TN-1452] p0017 N79-22099

An experimental investigation of forced mixing of
a turbulent boundary layer in an annular diffuser
--- for boundary layer control [NASA-TN-79171] p0004 N79-23920

DIFFUSION

NT IONIC DIFFUSION

NT TURBULENT DIFFUSION

Effects of diffusion factor, aspect ratio and
solidity on overall performance of 14 compressor
middle stages --- the effects of varying both
diffusion through the rotor and compressor
blades and blade aspect ratio [NASA-TN-1523] p0038 N79-33210

DIFFUSION COEFFICIENT

Determination of the zincate diffusion coefficient
and its application to alkaline battery problems
p0070 A79-11547

A feasibility study of a diffusion barrier between
Ni-Cr-Al coatings and nickel-based eutectic alloys
p0077 A79-27233

DIFFUSION EFFECT

U DIFFUSION

DIGITAL COMPUTERS

NT HOVEYWELL COMPUTERS

NT UNIVAC 1100 SERIES COMPUTERS

DIGITAL DATA

Multiple speed expandable bit synchronizer
[NASA-TN-79262] p0010 N79-33185

DIGITAL RADAR SYSTEMS

Radar image processing of real aperture SAR data
for the detection and identification of iceberg
and ship targets p0131 A79-36537

DIGITAL SIMULATION

Control of wind turbine generators connected to
power systems p0146 A79-15574

Initial comparison of single cylinder Stirling
engine computer model predictions with test
results [NASA-TN-79044] p0188 N79-16721

Generation of linear dynamic models from a digital
nonlinear simulation [NASA-TN-1388] p0001 N79-16796

DIGITAL SYSTEMS

NT DIGITAL RADAR SYSTEMS

Application of digital controls on the quiet clean
short haul experimental engines [AIAA PAPER 79-1203] p0029 A79-38984

Analysis and preliminary design of an optical
digital tip clearance sensor for propulsion
control [NASA-CR-159434] p0031 N79-15053

- TWT design requirements for 30/20 GHz digital communications' satellite
[NASA-TM-79119] p0097 N79-20316
- DIGITAL TECHNIQUES**
Digital enhancement of computerized axial tomograms
p0164 A79-11544
- DIGITAL TELEVISION**
Carrier: Interference ratios for frequency sharing between satellite systems transmitting frequency modulated and digital television signals
[NASA-TM-79265] p0094 N79-33379
- DIGITAL TRANSDUCERS**
Fiber optic sensors for military, industrial and commercial applications
p0111 A79-38738
- DILATOMETERS**
U EXTENSOMETERS
- DIMENSIONAL STABILITY**
NT STRUCTURAL STABILITY
- DIMENSIONLESS NUMBERS**
NT REYNOLDS NUMBER
- DIMENSIONS**
NT FILM THICKNESS
- DIODES**
NT SCHOTTKY DIODES
- DIRECT POWER GENERATORS**
NT ALKALINE BATTERIES
NT FUEL CELLS
NT HYDROGEN OXYGEN FUEL CELLS
NT MAGNETOHYDRODYNAMIC GENERATORS
NT NICKEL ZINC BATTERIES
NT SOLAR CELLS
NT THERMIONIC CONVERTERS
Mini-BRU/BIPS 1300 watt (sub) dynamic power conversion system development: Executive summary
[NASA-CR-159440] p0150 N79-10526
- DIRECTIONAL ANTENNAS**
NT SLOT ANTENNAS
- DIRECTIONAL SOLIDIFICATION (CRYSTALS)**
Shear rupture of a directionally solidified eutectic gamma/gamma-prime - alpha /Mo/ alloy --- for aircraft engine turbine blades
p0077 A79-21301
Analysis of solidification interface shape during continuous casting of a slab
p0079 A79-52697
Shear rupture of a directionally solidified eutectic gamma/gamma prime - alpha (Mo) alloy
[NASA-TM-79118] p0073 N79-12205
Evaluation of directionally solidified eutectic superalloys for turbine blade applications
[NASA-CR-135151] p0079 N79-16948
- DISASTERS**
Global disaster satellite communications system for disaster assessment and relief coordination
p0095 A79-30394
Global disaster satellite communications system for disaster assessment and relief coordination
[NASA-TM-79105] p0044 N79-20176
Communications technology satellite: United States experiments and disaster communications applications
[NASA-TM-79109] p0044 N79-23999
Satellite communications for disaster relief operations
[NASA-TM-79198] p0054 N79-27351
- DISKS (SHAPES)**
NT ACTUATOR DISKS
NT ROTATING DISKS
Mode I analysis of a cracked circular disk subject to a couple and a force
p0128 A79-15588
Design, fabrication and spin testing of ceramic blade metal disk attachment
[NASA-CR-159532] p0032 N79-17857
- DISLOCATIONS (MATERIALS)**
NT EDGE DISLOCATIONS
- DISPERSION PRECIPITATION HARDENING**
U PRECIPITATION HARDENING
- DISPERSIONS**
NT AEROSOLS
NT LIQUID-GAS MIXTURES
- DISPLACEMENT MEASUREMENT**
Mode I crack surface displacements for a round compact specimen subject to a couple and force
p0125 A79-39812
Measurement of transient strain and surface temperature on simulated turbine blades using noncontacting techniques
- [NASA-TM-78982] p0126 N79-19415
Definition of mutually optimum NDI and proof test criteria for 2219 aluminum pressure vessels. Volume 2: Optimization and fracture studies
[NASA-CR-135446] p0125 N79-21411
- DISSIPATION**
NT ENERGY DISSIPATION
- DISTORTION**
NT FLOW DISTORTION
Combined pressure and temperature distortion effects on internal flow of a turbofan engine
[NASA-TM-79136] p0012 N79-23963
Effect of steady-state pressure distortion on flow characteristics entering a turbofan engine
[NASA-TM-79134] p0019 N79-23969
- DISTRIBUTION (PROPERTY)**
NT ANGULAR DISTRIBUTION
NT CHARGE DISTRIBUTION
NT FLOW DISTRIBUTION
NT FREQUENCY DISTRIBUTION
NT HOLE DISTRIBUTION (MECHANICS)
NT LOAD DISTRIBUTION (FORCES)
NT MASS DISTRIBUTION
NT PRESSURE DISTRIBUTION
NT RADIAL DISTRIBUTION
NT STRESS CONCENTRATION
NT TEMPERATURE DISTRIBUTION
NT VELOCITY DISTRIBUTION
- DOCUMENTS**
NT BIBLIOGRAPHIES
NT MANUALS
NT USER MANUALS (COMPUTER PROGRAMS)
- DOMESTIC ENERGY**
Design and operating experience on the U.S. Department of Energy Experimental Mod-O 100 kW Wind Turbine
p0145 A79-10234
Photovoltaic power systems for rural areas of developing countries
p0147 A79-26131
- DOMESTIC SATELLITE COMMUNICATIONS SYSTEMS**
20/30 GHz satellite systems technology needs assessment --- for domestic communications
p0095 A79-14948
Determining potential 30/20 GHz domestic satellite system concepts and establishment of a suitable experimental configuration
p0095 A79-27397
- DOPED CRYSTALS**
Reverse annealing in radiation-damaged, silicon solar cells
p0144 N79-32660
High-energy electron-induced damage production at room temperature in aluminum-doped silicon
p0154 N79-32662
- DOPING (ADDITIVES)**
U ADDITIVES
- DRAW BALANCE**
U AERODYNAMIC BALANCE
- DRAW COEFFICIENT**
U AERODYNAMIC COEFFICIENTS
- DRAW DEVICES**
NT TRAILING-EDGE FLAPS
- DRAINAGE**
Contoured tank outlets for draining of cylindrical tanks in low-gravity environment --- Lewis Research Center Zero Gravity Facility
[NASA-TF-1492] p0105 N79-29467
- DRAINING**
U DRAINAGE
- DRILLING**
NT LASER DRILLING
- DROPS (LIQUIDS)**
Dispersion of sound in a combustion duct by fuel droplets and soot particles
[NASA-TM-79235] p0174 N79-1002
- DRY CELLS**
NT NICKEL ZINC BATTERIES
- DUAL MODE PROPULSION**
U HYBRID PROPULSION
- DUCTED BODIES**
A statistical theory of sound radiation from a two-dimensional lined duct
[AIAA PAPER 79-1521] p0176 A79-46707
- DUCTED FAN ENGINES**
Noise from struts and splitters in turbofan exit ducts
[AIAA PAPER 79-0637] p0178 A79-26923

DOCTED FANS

Energy efficient aircraft engines
[AIAA PAPER 79-1861] p0030 A79-47918
Cam-operated pitch-change apparatus
[NASA-CASE-LEW-13050-1] p0014 A79-14095
Theoretical fan velocity distortions
due to inlets
and nozzles --- in V/STOL aircraft
[NASA-TN-79150] p0003 A79-23911

DOCTED FLOW

Modal propagation angles in a cylindrical duct
with flow and their relation to sound radiation
[AIAA PAPER 79-0183] p0174 A79-19562
Some flow phenomena in a constant area duct with a
Borda type inlet including the critical region
[ASME PAPER 78-WA/HT-37] p0093 A79-19816
Velocity, temperature, and electrical conductivity
profiles in hydrogen-oxygen MHD duct flows
p0182 A79-26184
Modal propagation angles in ducts with soft walls
and their connection with suppressor performance
[AIAA PAPER 79-0624] p0175 A79-26860
Development of a three-dimensional turbulent duct
flow analysis
[NASA-CR-3029] p0106 A79-12366
Some aspects of a free jet phenomena to 105 L/D in
a constant area duct
[NASA-TN-79050] p0127 A79-20391
An analytical and experimental study of sound
propagation and attenuation in variable-area ducts
--- reducing aircraft engine noise
[NASA-CR-135392] p0177 A79-25845

DUCTS

NT ACOUSTIC DUCTS

DURABILITY

COMPOSITE - Composite durability structural analysis
p0128 A79-37292

DYE LASERS

Sismer-enhanced flashlamp-pumped dye laser
p0112 A79-32981

DYNAMIC CHARACTERISTICS

NT COMBUSTION STABILITY

NT FLOW CHARACTERISTICS

NT FLOW DISTRIBUTION

NT FLOW STABILITY

NT JET LIFT

NT LIFT

DYNAMIC CONTROL

Control and stabilization of the DGE/NASA Mod-1
two megawatt wind turbine generator
p0156 A79-51780

DYNAMIC LOADS

NT AERODYNAMIC LOADS

NT CYCLIC LOADS

NT GUST LOADS

NT IMPACT LOADS

NT ROLLING CONTACT LOADS

NT TRANSIENT LOADS

NT WING LOADING

Fatigue impact on Mod-1 wind turbine design
p0156 A79-20827
Evaluation of MOSTAS computer code for predicting
dynamic loads in two-bladed wind turbines
[AIAA 79-0733] p0005 A79-29007
Evaluation of MOSTAS computer code for predicting
dynamic loads in two bladed wind turbines
[NASA-TN-79101] p0137 A79-21549

DYNAMIC MODELS

Generation of linear dynamic models from a digital
nonlinear simulation
[NASA-TF-1398] p0001 A79-16796

DYNAMIC MODULUS OF ELASTICITY

High temperature dynamic modulus and damping of
aluminum and titanium matrix composites
p0065 A79-26132
High temperature dynamic modulus and damping of
aluminum and titanium matrix composites
[NASA-TN-79080] p0061 A79-16077

DYNAMIC RESPONSE

Study of 153 engine vibration
[NASA-CR-135449] p0030 A79-10061
Cam-operated pitch-change apparatus
[NASA-CASE-LEW-13050-1] p0014 A79-14095
Predicting dynamic performance limits for
servosystems with saturating nonlinearities
[NASA-TP-1488] p0038 A79-28186
Off-axis impact of unidirectional composites with
cracks: Dynamic stress intensification
[NASA-CR-159537] p0067 A79-30294

DYNAMIC STABILITY

NT COMBUSTION STABILITY

NT FLOW STABILITY

DYNAMIC STRUCTURAL ANALYSIS

Evaluation of MOSTAS computer code for predicting
dynamic loads in two-bladed wind turbines
[AIAA 79-0733] p0005 A79-29007
Analysis of high velocity impact on hybrid
composite fan blades
[AIAA 79-0783] p0128 A79-29027
Dynamic mechanical analysis of fiber reinforced
composites
p0065 A79-31040
Dynamic mechanical analysis of fiber reinforced
composites
[NASA-TN-79033] p0061 A79-15157
CELFE/NASTHAN code for the analysis of structures
subjected to high velocity impact
[NASA-TN-79048] p0126 A79-15325
Structural analysis of cylindrical thrust
chambers, volume 1
[NASA-CR-159522] p0057 A79-19073
Nonlinear equations of equilibrium for elastic
helicopter or wind turbine blades undergoing
moderate deformation
[NASA-CR-159478] p0130 A79-19414

DYSPROSIUM

The magnetocaloric effect in dysprosium
p0185 A79-38402

E

EARTH ATMOSPHERE

NT MAGNETOSPHERE

NT TROPOPAUSE

NT TROFOSPHERE

Atmospheric transformation of multispectral remote
sensor data --- Great Lakes
[E79-10006] p0131 A79-12524

EARTH RESOURCES

NT COAL

NT CRUDE OIL

NT FOSSIL FUELS

NT ICEBERGS

EARTH SATELLITES

NT AERONAUTICAL SATELLITES

NT AIS 5

NT AIS 6

NT COMMUNICATION SATELLITES

NT COMMUNICATIONS TECHNOLOGY SATELLITE

NT NOAA SATELLITES

NT SYNCHRONOUS SATELLITES

EARTH SURFACE

Atmospheric transformation of multispectral remote
sensor data --- Great Lakes
[E79-10006] p0131 A79-12524

ECCENTRICITY

The effects of eccentricities on the fracture of
off-axis fiber composites
p0064 A79-15543

ECONOMIC ANALYSIS

An economic analysis of a commercial approach to
the design and fabrication of a space power system
[AIAA 79-0914] p0055 A79-34737
An economical approach to space power systems
p0052 A79-10139
An economic analysis of a commercial approach to
the design and fabrication of a space power system
[NASA-TN-79153] p0053 A79-22193
Social and economic impact of solar electricity at
Schuchuli Village
[NASA-TN-79194] p0139 A79-25501
ECONOMIC FACTORS
New opportunities for future small civil turbine
engines - Overviewing the GATE studies
[SAE PAPER 790619] p0028 A79-36747
Wind turbines for electric utilities - Development
status and economics
[AIAA PAPER 79-0965] p0148 A79-38888

EDDIES

NT VORTICES

EDDY DIFFUSION

NT TURBULENT DIFFUSION

EDGE DISLOCATIONS

An acoustic emission study of plastic deformation
in polycrystalline aluminum
p0077 A79-19458

EDGES

NT LEADING EDGES

- NT TRAILING EDGES
Insulator edge voltage gradient effects in spacecraft charging phenomena p0088 A79-30139
- EFFECTIVENESS
NT COST EFFECTIVENESS
NT SYSTEM EFFECTIVENESS
- EFFECTORS
U CONTROL EQUIPMENT
- EFFICIENCY
NT COMBUSTION EFFICIENCY
NT COMPRESSOR EFFICIENCY
NT ENERGY CONVERSION EFFICIENCY
NT NOZZLE EFFICIENCY
NT POWER EFFICIENCY
NT PROPELLER EFFICIENCY
NT PROPELLER EFFICIENCY
NT TRANSMISSION EFFICIENCY
- EJECTORS
A three-dimensional turbulent compressible flow model for ejector and fluted mixers [NASA-CN-159467] p0160 W79-14325
- ELASTIC DEFORMATION
Three-dimensional finite-element elastic analysis of a thermally cycled single-edge wedge geometry specimen [NASA-TN-79026] p0172 W79-16644
- ELASTIC MODULUS
U MODULUS OF ELASTICITY
- ELASTIC PROPERTIES
NT AEROELASTICITY
NT DYNAMIC MODULUS OF ELASTICITY
NT MODULUS OF ELASTICITY
- ELASTIC STABILITY
U DAMPING
- ELASTIC WAVES
NT AERODYNAMIC NOISE
NT AIRCRAFT NOISE
NT ENGINE NOISE
NT JET AIRCRAFT NOISE
NT NOISE (SOUND)
NT SHOCK WAVES
NT SONIC BOOMS
NT SOUND WAVES
NT STRESS WAVES
- ELASTODYNAMICS
NT ELASTIC HYDRODYNAMICS
Normal and radial impact of composites with embedded penny-shaped cracks [NASA-CN-159536] p0130 W79-31627
- ELASTOHYDRODYNAMICS
The practical impact of elastohydrodynamic lubrication p0117 A79-11545
Elastohydrodynamic lubrication of elliptical contacts for materials of low elastic modulus. II - Starved conjunction [ASME PAPER 78-LUB-1] p0118 A79-23229
Effect of geometry on hydrodynamic film thickness [ASME PAPER 78-LUB-24] p0118 A79-23237
Elastohydrodynamic film thickness measurements of artificially produced surface dents and grooves --- on fatigue failure of bearings [ASME PREPRINT 78-IC-1A-1] p0118 A79-23267
Two-dimensional random surface model for asperity-contact in elastohydrodynamic lubrication p0120 A79-39811
Determination of lubricant selection based on elastohydrodynamic film thickness and traction measurement [NASA-CN-159428] p0121 W79-14385
Two-dimensional random surface model for asperity-contact in elastohydrodynamic lubrication [NASA-TN-79006] p0115 W79-23430
Elastohydrodynamic film thickness measurements of artificially produced nonsmooth surfaces [NASA-TN-79214] p0115 W79-28554
Comparison of predicted and measured elastohydrodynamic film thickness in a 20-millimeter-bore ball bearing [NASA-TF-1542] p0116 W79-32552
Correlation of asperity contact-time fraction with elastohydrodynamic film thickness in a 20-millimeter-bore ball bearing [NASA-TF-1547] p0116 W79-33476
- ELASTOMERS
Elastomer mounted rotors - An alternative for smoother running turbomachinery [ASME PAPER 79-GT-149] p0115 A79-32414
- Development of procedures for calculating stiffness and damping of elastomers in engineering applications. Part 5: Elastomer performance limits and the design and test of an elastomer dumper [NASA-CN-159552] p0122 W79-24373
- ELASTOSTATICS
Mode I crack surface displacements for a round compact specimen subject to a couple and force [NASA-TN-79096] p0161 W79-20572
- ELECTRIC BATTERIES
NT ALKALINE BATTERIES
NT LEAD ACID BATTERIES
NT NICKEL CADMIUM BATTERIES
NT NICKEL ZINC BATTERIES
NT SILVER ZINC BATTERIES
NT SODIUM SULFUR BATTERIES
NT STORAGE BATTERIES
Technology status: Batteries and fuel cells p0052 W79-10132
Supply of reactants for Redox bulk energy storage systems [NASA-TN-78995] p0133 W79-11479
Lewis Research Center program p0137 W79-21576
- ELECTRIC CHARGE
NT ELECTROSTATIC CHARGE
Charging rates of metal-dielectric structures --- with implications for spacecraft p0048 W79-24033
- ELECTRIC CHOPPERS
Performance of a 14.9-kV laminated-frame dc series motor with chopper controller [NASA-TN-79177] p0098 W79-26316
- ELECTRIC CURRENT
NT ARC DISCHARGES
NT BEAM CURRENTS
NT ELECTRIC DISCHARGES
The decrease in effective photocurrents due to saddle points in electrostatic potentials near differentially charged spacecraft p0049 A79-30140
Effect of parasitic plasma currents on solar-array power output p0047 W79-24025
- ELECTRIC DISCHARGES
NT ARC DISCHARGES
Response of lead-acid batteries to chopper-controlled discharge --- for electric vehicles p0145 A79-10097
Insulator edge voltage gradient effects in spacecraft charging phenomena p0048 A79-30139
Effects of bulk and surface conductivity on the potential developed by dielectrics exposed to electron beams p0171 A79-50938
Area scaling investigations of charging phenomena --- discharge pulse characteristics of Teflon thermal control tape p0048 W79-24032
NASCAP modelling of environmental-charging-induced discharges in satellites [NASA-TN-79247] p0048 W79-31265
Discharge characteristics of 300 ampere-hour Ni-Zn traction cells [NASA-TN-79244] p0143 W79-31781
- ELECTRIC ENERGY STORAGE
Electrochemical cell for rebalancing REDOX flow system [NASA-CASE-LEW-13150-1] p0139 W79-26474
Dynamic analysis of a photovoltaic power system with battery storage capability [NASA-TN-79209] p0142 W79-29599
- ELECTRIC EQUIPMENT TESTS
Description of a 2.3 kW power transformer for space applications p0099 A79-34991
Development of single-cell protectors for sealed silver-zinc cells [NASA-CN-159407] p0151 W79-12550
Photovoltaic tests and applications project [NASA-TN-79018] p0136 W79-17336
- ELECTRIC FIELDS
Ion confinement and transport in a toroidal plasma with externally imposed radial electric fields [NASA-TF-1411] p0181 W79-19867

- Potential mapping with charged-particle beams
p0049 N79-24038
- Stable dielectric charge distributions from field
enhancement of secondary mission
p0049 N79-24046
- ELECTRIC GENERATORS**
- NT AC GENERATORS
- NT ALKALINE BATTERIES
- NT DIRECT POWER GENERATORS
- NT FUEL CELLS
- NT HYDROGEN OXYGEN FUEL CELLS
- NT MAGNETOHYDRODYNAMIC GENERATORS
- NT NICKEL ZINC BATTERIES
- NT SOLAR CELLS
- NT SOLAR GENERATORS
- NT THERMIONIC CONVERTERS
- NT TURBOGENERATORS
- Photovoltaic power systems for rural areas of
developing countries
p0147 A79-26131
- Analysis of a fuel cell on-site integrated energy
system for a residential complex
[AIAA PAPER 79-0990]
p0147 A79-38192
- Future Orbital Power Systems Technology Requirements
[NASA-CR-2058]
p0052 N79-10122
- Development of a phase-change thermal storage
system using modified anhydrous sodium hydroxide
for solar electric power generation
[NASA-CR-159465]
p0153 N79-19454
- Description of photovoltaic village power systems
in the United States and Africa
[NASA-TN-79149]
p0138 N79-24443
- Solar thermal power-conversion system
p0139 N79-26477
- Commercial synchronous alternating-current
generators
p0140 N79-26482
- Power-conversion system component summation
p0140 N79-26483
- Candidate power-conversion system cycles, appendix A
p0140 N79-24484
- ELECTRIC MOTOR VEHICLES**
- Rapid, efficient charging of lead-acid and
nickel-zinc traction cells --- for electric
vehicles
p0144 A79-10084
- Response of lead-acid batteries to
chopper-controlled discharge --- for electric
vehicles
p0145 A79-10097
- A cycle timer for testing electric vehicles
p0188 A79-37293
- Preliminary power train design for a
state-of-the-art electric vehicle (executive
summary)
[NASA-CR-157625]
p0188 N79-12968
- ELECTRIC MOTORS**
- Performance of a 14.9-kW laminated-frame dc series
motor with chopper controller
[NASA-TN-79177]
p0058 N79-26316
- ELECTRIC NETWORKS**
- Lewis Research Center studies of multiple large
wind turbine generators on a utility network
p0149 A79-46547
- ELECTRIC POTENTIAL**
- NT CONTACT POTENTIALS
- NT COLLOID POTENTIAL
- Insulator edge voltage gradient effects in
spacecraft charging phenomena
[NASA-TN-78988]
p0046 N79-11109
- Operations of the A1S-6 ion engine
p0049 N79-24007
- Characteristics of differential charging of A1S-6
p0049 N79-24008
- Potential mapping with charged-particle beams
p0049 N79-24038
- The alkaline zinc electrode as a mixed potential
system
[NASA-TN-79235]
p0142 N79-29600
- Open-circuit voltage improvements in
low-resistivity solar cells
p0143 N79-32649
- ELECTRIC POWER CONVERSION**
- U ELECTRIC GENERATORS
- ELECTRIC POWER PLANTS**
- Fuel cell on-site integrated energy system
parametric analysis of a residential complex
p0146 A79-14947
- Large wind turbine generators --- NASA program
status and potential costs
p0146 A79-15881
- Benefits of solar/fossil hybrid gas turbine systems
[ASME PAPER 79-GT-38]
p0147 A79-30554
- Evaluation of the ECAS open cycle MHD power plant
design
[NASA-TN-79012]
p0136 N79-17335
- Analysis of a fuel cell on-site integrated energy
system for a residential complex
[NASA-TN-79161]
p0137 N79-22624
- Conceptual design of thermal energy storage
systems for near term electric utility
applications
[NASA-CR-159577]
p0155 N79-33560
- ELECTRIC POWER SUPPLIES**
- NT SPACECRAFT POWER SUPPLIES
- Design and fabrication of a photovoltaic power
system for the Papago Indian Village of
Schuchuli /Gunsight/, Arizona
p0148 A79-41089
- Analysis of a parallel-arrayed power regulating
system
p0101 A79-49397
- Applications of thermal energy storage to process
heat and waste heat recovery in the iron and
steel industry
[NASA-CR-159397]
p0151 N79-11473
- Comparison of fuel-cell and diesel integrated
energy systems and a conventional system for a
500-unit apartment
[NASA-TN-79037]
p0134 N79-15403
- Description of a 2.3 kW power transformer for
space applications
[NASA-TN-79138]
p0097 N79-23348
- ELECTRIC PROPULSION**
- NT ION PROPULSION
- NT SOLAR ELECTRIC PROPULSION
- Space propulsion technology overview
[AIAA 79-0860]
p0054 A79-34704
- Primary electric propulsion for future space
missions
[AIAA 79-0881]
p0055 A79-34773
- Inert gas ion source program
[NASA-CR-159423]
p0056 N79-10120
- Primary electric propulsion for future space
missions
[NASA-TN-79141]
p0052 N79-22190
- ELECTRIC ROCKET ENGINES**
- NT ELECTROSTATIC ENGINES
- NT ION ENGINES
- NT MERCURY ION ENGINES
- ELECTRICAL BREAKDOWN**
- U ELECTRICAL FAULTS
- ELECTRICAL CONDUCTIVITY**
- U ELECTRICAL RESISTIVITY
- ELECTRICAL FAULTS**
- Preliminary results in the NASA Lewis H2-O2
combustion MHD experiment
p0182 A79-39807
- ELECTRICAL IMPEDANCE**
- NT ELECTRICAL RESISTANCE
- ELECTRICAL INSULATION**
- Insulator edge voltage gradient effects in
spacecraft charging phenomena
p0048 A79-30139
- Status of materials characterization studies
p0048 N79-24030
- ELECTRICAL MEASUREMENT**
- An electro-optic, high-voltage, transient probe
[NASA-TN-79019]
p0109 N79-12414
- ELECTRICAL PROPERTIES**
- NT CARRIER MOBILITY
- NT CHARGE DISTRIBUTION
- NT DIELECTRIC PROPERTIES
- NT ELECTRICAL RESISTANCE
- NT ELECTRICAL RESISTIVITY
- NT MAGNETORESISTIVITY
- NT SUPERCONDUCTIVITY
- Properties and performance of fine-filament
bronze-process Nb3Sn conductors
p0184 A79-20529
- Laboratory studies of electrical properties of
insulating materials --- thermal insulation of
spacecraft dielectrics
p0044 A79-20677
- Modification of the electrical and optical
properties of polymers --- ion irradiation
[NASA-CASE-LEW-13027-1]
p0081 N79-11216

- ELECTRICAL RESISTANCE**
Low temperature normal state resistance of ternary molybdenum sulfides p0185 A79-27230
- ELECTRICAL RESISTIVITY**
NT MAGNETORESISTIVITY
NT SUPERCONDUCTIVITY
Velocity, temperature, and electrical conductivity profiles in hydrogen-oxygen MHD duct flows p0182 A79-26184
Electronic properties of PbMoS8 and CuMoS8 --- for superconductivity p0187 A79-41731
Effects of bulk and surface conductivity on the potential developed by dielectrics exposed to electron beams p0171 A79-50938
Control of volume resistivity in inorganic organic separators [NASA-TF-1439] p0065 A79-22246
Technology development for phosphoric acid fuel cell powerplant, phase 2 [NASA-CR-159572] p0153 A79-29604
- ELECTRICITY**
Laser power conversion system analysis, volume 1 [NASA-CR-159523-VOL-1] p0112 A79-21334
Laser power conversion system analysis, volume 2 [NASA-CR-159523-VOL-2] p0112 A79-21335
Social and economic impact of solar electricity at Schuchuli Village [NASA-TM-79194] p0139 A79-25501
- ELECTROCATALYSTS**
Catalyst surfaces for the chromous/chromic redox couple [NASA-CASE-LEW-13148-1] p0134 A79-14538
- ELECTROCHEMICAL CELLS**
NT ALKALINE BATTERIES
NT ELECTRIC BATTERIES
NT FUEL CELLS
NT HYDROGEN OXYGEN FUEL CELLS
NT LEAD ACID BATTERIES
NT NICKEL CADMIUM BATTERIES
NT NICKEL ZINC BATTERIES
NT SILVER ZINC BATTERIES
NT SODIUM SULFUR BATTERIES
NT STORAGE BATTERIES
Factors affecting the open-circuit voltage and electrode kinetics of some iron/titanium/redox flow cells p0146 A79-11824
Redox flow cell energy storage systems [AIAA PAPER 79-0989] p0147 A79-38191
Recent advances in Redox flow cell storage systems p0150 A79-51837
Catalyst surfaces for the chromous/chromic redox couple [NASA-CASE-LEW-13148-1] p0134 A79-14538
Comparison of fuel-cell and diesel integrated energy systems and a conventional system for a 500-unit apartment [NASA-TM-79037] p0134 A79-15403
Method and device for the detection of phenol and related compounds --- in an electrochemical cell [NASA-CASE-LEW-12513-1] p0069 A79-22235
Electrochemical cell for rebalancing REDOX flow system [NASA-CASE-LEW-13150-1] p0139 A79-26474
Effect of positive pulse charge waveforms on cycle life of nickel-zinc cells [NASA-TM-79215] p0142 A79-28728
The alkaline zinc electrode as a mixed potential system [NASA-TM-79235] p0142 A79-29600
- ELECTROCHEMICAL OXIDATION**
Method and device for the detection of phenol and related compounds --- in an electrochemical cell [NASA-CASE-LEW-12513-1] p0069 A79-22235
- ELECTROCHEMISTRY**
Electrochemical fluorination of trichloroethylene and N, N-dimethyltrifluoroacetamide p0060 A79-49536
Electrochemical fluorination of trichloroethylene and N, N-dimethyltrifluoroacetamide p0060 A79-49536
Redox flow cell development and demonstration project, calendar year 1977 [NASA-TM-79067] p0138 A79-24445
Electrochemical fluorination of trichloroethylene and N, N-dimethyltrifluoroacetamide
- [NASA-TM-79188] p0059 A79-27242
- ELECTROCONDUCTIVITY**
Hartmann flow with temperature-dependent physical properties --- magnetohydrodynamics of liquid metal p0182 A79-15597
- ELECTRODE FILM BARRIERS**
Formulated plastic separators for soluble electrode cells --- rubber-ion transport membranes [NASA-CASE-LEW-12358-1] p0135 A79-17313
- ELECTRODEPOSITION**
Method and device for the detection of phenol and related compounds --- in an electrochemical cell [NASA-CASE-LEW-12513-1] p0069 A79-22235
- ELECTRODES**
NT ANODES
NT CATHODES
NT HOLLOW CATHODES
NT SOLID ELECTRODES
NT THERMIONIC CATHODES
NT TUBE GRIDS
Factors affecting the open-circuit voltage and electrode kinetics of some iron/titanium/redox flow cells p0146 A79-11824
Some properties of low-vapor-pressure braze alloys for thermionic converters p0076 A79-13100
Decay of the zincate concentration gradient at an alkaline zinc cathode after charging [NASA-TM-79106] p0137 A79-20520
- ELECTROGENERATORS**
U ELECTRIC GENERATORS
ELECTROHYDRAULIC CONTROL
U HYDRAULIC CONTROL
ELECTROLYTES
NT ION EXCHANGE MEMBRANE ELECTROLYTES
ELECTROLYTIC CELLS
Development of single-cell protectors for sealed silver-zinc cells [NASA-CR-159407] p0151 A79-12550
Catalyst surfaces for the chromous/chromic redox couple [NASA-CASE-LEW-13148-1] p0134 A79-14538
Fabrication and testing of silver-hydrogen cells [NASA-CR-159431] p0152 A79-16374
Fabrication and testing of silver-hydrogen cells [NASA-CR-159490] p0152 A79-16375
- ELECTROMAGNETIC CONTROL**
U REMOTE CONTROL
ELECTROMAGNETIC FIELDS
NT FAR FIELDS
ELECTROMAGNETIC INTERACTIONS
NT PLASMA-ELECTROMAGNETIC INTERACTION
ELECTROMAGNETIC INTERFERENCE
Carrier: Interference ratios for frequency sharing between satellite systems transmitting frequency modulated and digital television signals [NASA-TM-79265] p0094 A79-33379
- ELECTROMAGNETIC PROPERTIES**
NT ABSORPTANCE
NT DIELECTRIC PROPERTIES
NT ELECTRICAL PROPERTIES
NT OPTICAL PROPERTIES
NT PHOTOELECTRIC EMISSION
NT RADIANCE
NT TRANSPARENCY
NT WATER COLOR
ELECTROMAGNETIC PROPULSION
NT MASS DRIVERS (PAYLOAD DELIVERY)
ELECTROMAGNETIC RADIATION
NT BLACK BODY RADIATION
NT MICROWAVE EMISSION
NT MILLIMETER WAVES
NT PHOTON BEAMS
NT SKY RADIATION
NT THERMAL RADIATION
NT ULTRAVIOLET RADIATION
ELECTROMAGNETIC SPECTRA
NT LINE SPECTRA
ELECTROMAGNETIC WAVE FILTERS
NT BANDPASS FILTERS
NT OPTICAL FILTERS
ELECTROMAGNETIC WAVE TRANSMISSION
NT LIGHT TRANSMISSION
NT MICROWAVE TRANSMISSION
ELECTROMAGNETS
NT HIGH FIELD MAGNETS
NT SUPERCONDUCTING MAGNETS

ELECTRON BEAMS

Effects of bulk and surface conductivity on the potential developed by dielectrics exposed to electron beams

p0171 A79-50938

Efficiency enhancement of octave-bandwidth traveling wave tubes by use of multistage depressed collectors

[NASA-TF-1416] p0097 A79-17139

ELECTRON BOMBARDMENT

Ion beam technology applications study --- ion impact, implantation, and surface finishing

[NASA-CR-159437] p0180 A79-12884

Whiskers, cones and pyramids created in sputtering by ion bombardment

[NASA-CR-159549] p0079 A79-20221

Characteristics of primary electric propulsion systems --- conferences

[NASA-TN-79255] p0053 A79-30290

Mechanical and chemical effects of ion-texturing biomedical polymers

[NASA-TN-79245] p0084 A79-31391

ELECTRON CAPTURE

Multistage depressed collector for dual node operation --- for travelling wave tubes

[NASA-CASE-LEW-13282-1] p0098 A79-32463

ELECTRON EMISSION

NT PHOTOELECTRIC EMISSION

NT SECONDARY EMISSION

Comment on the mechanism of operation of the impregnated tungsten cathode

p0099 A79-42024

ELECTRON FLUX DENSITY

Temperature and intensity dependence of the performance of an electron-irradiated (AlGa)As/GaAs solar cell

p0144 A79-32665

ELECTRON GUNS

Comment on the mechanism of operation of the impregnated tungsten cathode

p0099 A79-42024

Design of high-perveance confined-flow guns for periodic-permanent-magnet-focused tubes

[NASA-TF-1485] p0098 A79-27400

ELECTRON INTENSITY

U ELECTRON FLUX DENSITY

ELECTRON IRRADIATION

Test results for electron beam charging of flexible insulators and composites --- solar array substrates, honeycomb panels, and thin dielectric films

p0048 A79-24031

First principles numerical model of avalanche-induced arc discharges in electron-irradiated dielectrics

[NASA-CR-159560] p0101 A79-28418

High-energy electron-induced damage production at room temperature in aluminum-doped silicon

p0154 A79-32662

Temperature and intensity dependence of the performance of an electron-irradiated (AlGa)As/GaAs solar cell

p0144 A79-32665

ELECTRON MICROSCOPES

Mini-BRO/HIPS foil bearing development

[NASA-CR-159442] p0120 A79-11407

ELECTRON MICROSCOPY

U ELECTRON MICROSCOPES

Characterization of defect growth structure in ion plated films by scanning electron microscopy

[NASA-TN-79110] p0074 A79-20218

Some TEM observations of Al₂O₃ scales formed on NiCrAl alloys

[NASA-TN-79259] p0076 A79-33306

ELECTRON PARAMAGNETIC RESONANCE

Improved apparatus for trapped radical and other studies down to 1.5 K --- microwave cavity cryogenic equipment for electron paramagnetic resonance experiments

p0110 A79-20742

ELECTRON PHONON INTERACTIONS

Indirect measurements of Fermi surface parameters of some chevre phase materials

p0185 A79-50231

ELECTRON PLASMA

Microwave radiation measurements near the electron plasma frequency of the NASA Lewis Bumpy Torus plasma

p0181 A79-14953

ELECTRON RADIATION

NT ELECTRON BEAMS

ELECTRON RECOMBINATION

Photon-degradation effects in terrestrial silicon solar cells

p0149 A79-42545

ELECTRON SPIN RESONANCE

U ELECTRON PARAMAGNETIC RESONANCE

ELECTRON TRANSITIONS

Friction and transfer of copper, silver, and gold to iron in the presence of various adsorbed surface films

[NASA-TF-1392] p0114 A79-14386

ELECTRON TUBES

NT KLISTRONS

NT TRAVELING WAVE TUBES

ELECTRONIC CONTROL

The application of hydraulics in the 2,000 kW wind turbine generator

p0156 A79-27400

A summary of NASA/Air Force full scale engine research programs using the F100 engine

[NASA-TN-79267] p0024 A79-30188

ELECTRONIC EQUIPMENT

NT ELECTRONIC FILTERS

NT ELECTRONIC MODULES

NT ELECTRONIC RECORDING SYSTEMS

NT ELECTRONIC TRANSDUCERS

NT METAL OXIDE SEMICONDUCTORS

NT PHOTOVOLTAIC CELLS

NT SEMICONDUCTOR DEVICES

NT SOLID STATE DEVICES

NT THYRISTORS

NT TRANSISTORS

Multistage depressed collector for dual node operation --- for travelling wave tubes

[NASA-CASE-LEW-13282-1] p0098 A79-32463

ELECTRONIC FILTERS

Input filter design for switching regulators

p0101 A79-48653

ELECTRONIC MODULES

Block 2 solar cell module environmental test program

[NASA-CR-159393] p0151 A79-13490

ELECTRONIC RECORDING SYSTEMS

Simulated electronic heterodyne recording and processing of pulsed-laser holograms

[NASA-TF-1444] p0111 A79-21329

ELECTRONIC SWITCHES

U SWITCHING CIRCUITS

ELECTRONIC TRANSDUCERS

Fiber optic sensors for military, industrial and commercial applications

p0111 A79-38738

ELECTROSTATIC EFFECT

U ELECTRIC CURRENT

ELECTROSLAG REFINING

Evaluation of the mechanical properties of electroslog refined Fe-12Ni alloys

[NASA-CR-159394] p0079 A79-12202

ELECTROSTATIC CHARGE

Jupiter probe charging study

[NASA-TF-1263] p0046 A79-15149

Characteristics of differential charging of AIS-6

p0049 A79-24008

NASCAP modelling of environmental-charging-induced discharges in satellites

[NASA-TN-79247] p0048 A79-31265

ELECTROSTATIC ENGINES

Mercury ion thruster research, 1978

[NASA-CR-159485] p0056 A79-16913

Inert gas thrusters

[NASA-CR-159527] p0057 A79-26110

ELECTROSTATIC FIELDS

U ELECTRIC FIELDS

ELECTROSTATIC PLASMA

U PLASMAS (PHYSICS)

ELECTROSTATIC PRECIPITATORS

Fine particulate capture device

[NASA-CASE-LEW-11583-1] p0109 A79-17192

ELECTROSTATIC PROPULSION

NT ION PROPULSION

ELECTROSTATICS

The decrease in effective photocurrents due to saddle points in electrostatic potentials near differentially charged spacecraft

p0049 A79-30140

ELEMENTARY PARTICLE INTERACTIONS

NT ELECTRON CAPTURE

ELLIPSES

Elastohydrodynamic lubrication of elliptical contacts for materials of low elastic modulus.
II - Starved conjunction
[ASME PAPER 78-LUB-1] p0118 A79-23229

ELLIPTICAL ORBITS

NT TRANSFER ORBITS

EMANATION

U EMISSION

EMISSION

NT ACOUSTIC EMISSION

NT ELECTRON EMISSION

NT MICROWAVE EMISSION

NT PHOTOELECTRIC EMISSION

NT SECONDARY EMISSION

NT SPONTANEOUS EMISSION

NT THERMIONIC EMISSION

Correlations of catalytic combustor performance parameters
[NASA-TN-79014] p0134 A79-11480
Effects of flameholder blockage on emissions and performance of lean premixed-prevaporized combustors p0021 A79-25006

EMISSIONITY

Introduction: Thermal Radiation in Industrial Flames p0104 A79-22415

EMIITTANCE

Emission and absorptance of the National Aeronautics and Space Administration ceramic thermal barrier coating --- for gas turbine engine components p0086 A79-27231

EMITTERS

NT THERMIONIC CATHODES

NT THERMIONIC EMITTERS

ENCLOSURES

Aerospace Transparent Materials and Enclosures (12th)
[AD-A065049] p0018 A79-23066

ENCODING

U CODING

ENERGETIC PARTICLES

NT PLASMAS (PHYSICS)

ENERGY CONSERVATION

Fuel conservative aircraft engine technology p0025 A79-20078
Energy conservation through sealing technology p0118 A79-20700
Analysis of a fuel cell on-site integrated energy system for a residential complex [AIAA PAPER 79-0990] p0147 A79-38192
Feasibility of determining flat roof heat losses using aerial thermography p0131 A79-51095

Fuel cell on-site integrated energy system parametric analysis of a residential complex [NASA-TN-78996] p0188 A79-11955

Energy efficient engine preliminary design and integration study [NASA-CR-135396] p0012 A79-12084

Energy efficient engine: Propulsion system-aircraft integration evaluation [NASA-CR-159488] p0032 A79-16850

Wind tunnel performance of four energy efficient propellers designed for Mach 0.8 cruise --- Lewis 8x6 foot wind tunnel studies for noise reduction in high speed turboprop aircraft [NASA-TN-79124] p0003 A79-20069

The role of thermal energy storage in industrial energy conservation [NASA-TN-79122] p0137 A79-21550

Energy and cost saving results for advanced technology systems from the Cogeneration Technology Alternatives Study (CTAS) [NASA-TN-79213] p0141 A79-27665

Energy efficient engine flight propulsion system preliminary analysis and design report [NASA-CR-159487] p0035 A79-30189

ENERGY CONVERSION

NT SATELLITE SOLAR ENERGY CONVERSION

NT SOLAR ENERGY CONVERSION

Disinclide thermionic energy conversion with lanthanum-hexaboride electrodes p0146 A79-13098
Energy and cost savings results for advanced technology systems from the Cogeneration Technology Alternatives Study /CTAS/

[AIAA PAPER 79-1000] p0149 A79-44225
Results from Symposium on Future Orbital power systems technology requirements [NASA-TN-79125] p0053 A79-22191

Benefits of advanced technology in industrial cogeneration [NASA-TN-79160] p0138 A79-24444

Energy-state formulation of lumped volume dynamic equations with application to a simplified free piston Stirling engine [NASA-TN-79197] p0141 A79-27663

Energy and cost saving results for advanced technology systems from the Cogeneration Technology Alternatives Study (CTAS) [NASA-TN-79213] p0141 A79-27665

Strip cell test and evaluation program [NASA-CR-159652] p0154 A79-31784

ENERGY CONVERSION EFFICIENCY

Status of wraparound contact solar cells and arrays --- for spacecraft electric propulsion p0054 A79-10014

Rapid, efficient charging of lead-acid and nickel-zinc traction cells --- for electric vehicles p0144 A79-10084

Response of lead-acid batteries to chopper-controlled discharge --- for electric vehicles p0145 A79-10097

DOE/NASA Mod-0A wind turbine performance p0145 A79-10235

Simmer-enhanced flashlamp-pumped dye laser p0112 A79-32581

Redox flow cell energy storage systems [AIAA PAPER 79-0989] p0147 A79-38191

Analysis of a fuel cell on-site integrated energy system for a residential complex [AIAA PAPER 79-0990] p0147 A79-38192

Fundamental mechanisms that influence the estimate of heat transfer to gas turbine blades p0099 A79-49526

Energy efficient aircraft engines [NASA-TN-79204] p0022 A79-27141

Solar Cell High Efficiency and Radiation Damage, 1979 [NASA-CR-20977] p0143 A79-32640

The NASA Lewis Research Center program in space solar cell research and technology --- efficient silicon solar cell development program p0143 A79-32641

Limiting process in shallow junction solar cells p0154 A79-32646

Design of high efficiency HLE solar cells for space and terrestrial applications p0154 A79-32647

Applications of ion implantation to high performance, radiation tolerant silicon solar cells p0143 A79-32648

Open-circuit voltage improvements in low-resistivity solar cells p0143 A79-32649

Modeling of thin, back-wall silicon solar cells p0143 A79-32650

Thin cells for space p0154 A79-32652

High efficiency cell geometry p0143 A79-32653

ENERGY CONVERTERS

U DIRECT POWER GENERATORS

ENERGY DENSITY

U FLUX DENSITY

ENERGY DISSIPATION

Energy-state formulation of lumped volume dynamic equations with application to a simplified free piston Stirling engine p0187 A79-49532

ENERGY EXCHANGE

U ENERGY TRANSFER

ENERGY LEVELS

NT GROUND STATE

ENERGY LOSSES

U ENERGY DISSIPATION

ENERGY POLICY

Applications of thermal energy storage to process heat and waste heat recovery in the iron and steel industry [NASA-CR-159397] p0151 A79-11473

- Thermal storage for industrial process and reject heat
[NASA-TM-78994] p0134 N79-11481
- Microprocessor control of a wind turbine generator
[NASA-TM-79021] p0134 N79-12548
- Application of multispectral scanner data to the study of an abandoned surface coal mine
[NASA-TM-78912] p0131 N79-13472
- Comparison of fuel-cell and diesel integrated energy systems and a conventional system for a 500-unit apartment
[NASA-TM-79037] p0134 N79-15403
- Thermal storage technologies for solar industrial process heat applications
[NASA-TM-79130] p0136 N79-20498
- Redox flow cell energy storage systems
[NASA-TM-79143] p0138 N79-24442
- Benefits of advanced technology in industrial cogeneration
[NASA-TM-79160] p0138 N79-24444
- Redox flow cell development and demonstration project, calendar year 1977
[NASA-TM-79067] p0138 N79-24445
- Energy and cost saving results for advanced technology systems from the Cogeneration Technology Alternatives Study (CTAS)
[NASA-TM-79213] p0141 N79-27665
- Dynamic analysis of a photovoltaic power system with battery storage capability
[NASA-TM-79209] p0142 N79-29599
- Conceptual design study of an Improved Gas Turbine (IGT) powertrain
[NASA-CR-159604] p0189 N79-31087
- ENERGY REQUIREMENTS**
- Fuel cell on-site integrated energy system parametric analysis of a residential complex
p0146 A79-14947
- An economical approach to space power systems
p0052 N79-10139
- ENERGY SPECTRA**
- Decay of homogeneous turbulence from a given state at higher Reynolds number
p0105 A79-14952
- ENERGY STORAGE**
- HT ELECTRIC ENERGY STORAGE**
- HT HEAT STORAGE**
- NaOH-based high temperature heat-of-fusion thermal energy storage device
p0155 A79-10106
- Storage systems for solar thermal power
p0145 A79-10108
- SINWEST - A simulation model for wind energy storage systems
p0145 A79-10241
- Redox flow cell energy storage systems
[AIAA PAPER 79-0989] p0147 A79-38191
- Commercial phosphoric acid fuel cell system technology development
p0150 A79-51809
- The role of fuel cells in NASA's space power systems
p0056 A79-51810
- Recent advances in Redox flow cell storage systems
p0150 A79-51837
- Applications of thermal energy storage to process heat and waste heat recovery in the iron and steel industry
[NASA-CR-159397] p0151 N79-11473
- Supply of reactants for Redox bulk energy storage systems
[NASA-TM-78995] p0133 N79-11479
- Atomic hydrogen storage method and apparatus
[NASA-CASE-LEW-12081-3] p0136 N79-18455
- Thermal storage technologies for solar industrial process heat applications
[NASA-TM-79130] p0136 N79-20498
- Redox flow cell energy storage systems
[NASA-TM-79143] p0138 N79-24442
- Recent advances in redox flow cell storage systems
[NASA-TM-79186] p0141 N79-26505
- Technology development for phosphoric acid fuel cell powerplant, phase 2
[NASA-CR-159572] p0153 N79-29604
- Applications of thermal energy storage to process heat storage and recovery in the paper and pulp industry
[NASA-CR-159398] p0154 N79-30801
- Strip cell test and evaluation program
[NASA-CR-159652] p0154 N79-31784
- Conceptual design of thermal energy storage systems for near term electric utility applications
[NASA-CR-159577] p0155 N79-33560
- An expanded system simulation model for solar energy storage (technical report), volume 1
[NASA-CR-159601] p0166 N79-33881
- An expanded system simulation model for solar energy storage (UNIVAC operation manual revisions), volume 2
[NASA-CR-159602] p0166 N79-33882
- SINWEST: A simulation model for wind and photovoltaic energy storage systems (CDC user's manual), volume 1
[NASA-CR-159607] p0166 N79-33883
- SINWEST: A simulation model for wind and photovoltaic energy storage systems (cdc program descriptions), volume 2
[NASA-CR-159608] p0167 N79-33884
- ENERGY STORAGE DEVICES**
- U ENERGY STORAGE**
- ENERGY TECHNOLOGY**
- Design and fabrication of a photovoltaic power system for the Papago Indian Village of Schuchuli /Gunsight/, Arizona
p0148 A79-41089
- Description and status of NASA-LeRC/DOE photovoltaic applications systems experiments
p0148 A79-41091
- Energy and cost savings results for advanced technology systems from the Cogeneration Technology Alternatives Study /CTAS/
[AIAA PAPER 79-1000] p0149 A79-44225
- Back wall solar cell
[NASA-CASE-LEW-12236-2] p0134 N79-14528
- An operating 200-kW horizontal axis wind turbine
[NASA-TM-79034] p0135 N79-16357
- Utility operational experience on the NASA/DOE MCD-0A 200-kW wind turbine
[NASA-TM-79084] p0136 N79-20494
- Active heat exchange system development for latent heat thermal energy storage
[NASA-CR-159479] p0153 N79-21554
- Benefits of advanced technology in industrial cogeneration
[NASA-TM-79160] p0138 N79-24444
- Energy and cost saving results for advanced technology systems from the Cogeneration Technology Alternatives Study (CTAS)
[NASA-TM-79213] p0141 N79-27665
- Conceptual design of thermal energy storage systems for near term electric utility applications
[NASA-CR-159577] p0155 N79-33560
- ENERGY TRANSFER**
- Laser power conversion system analysis, volume 1
[NASA-CR-159523-VOL-1] p0112 N79-21334
- Laser power conversion system analysis, volume 2
[NASA-CR-159523-VOL-2] p0112 N79-21335
- ENGINE ANALYZERS**
- Indicated mean-effective pressure instrument
[NASA-CASE-LEW-12661-1] p0109 N79-14345
- ENGINE CONTROL**
- HT TURBOJET ENGINE CONTROL**
- Application of digital controls on the quiet clean short haul experimental engines
[AIAA PAPER 79-1203] p0029 A79-38984
- Generation of linear dynamic models from a digital nonlinear simulation
[NASA-TF-1388] p0001 N79-16796
- Speed reducers-increasers
p0140 N79-26481
- Analysis and preliminary design of optical sensors for propulsion control --- temperature sensors
[NASA-CR-159519] p0180 N79-27975
- ENGINE DESIGN**
- HT ROCKET ENGINE DESIGN**
- Ceramics for the advanced automotive gas turbine engine - A look at a single shaft design
p0117 A79-12850
- Fuel conservative aircraft engine technology
p0025 A79-20078
- NASA research on general aviation power plants
[AIAA PAPER 79-0561] p0026 A79-25870
- Elastomer mounted rotors - An alternative for smoother running turbomachinery
[ASME PAPER 79-GT-149] p0119 A79-32414
- Preliminary CIGAT program test results --- Quiet, Clean General Aviation Turbopfan

- [SAE PAPER 790596] p0028 A79-36729
Wind tunnel performance of four energy efficient
propellers designed for Mach 0.8 cruise
[SAE PAPER 790573] p0028 A79-36759
Lean, premixed, prevaporized combustion for
aircraft gas turbine engines
[AIAA PAPER 79-1318] p0029 A79-39034
Materials and structural aspects of advanced
gas-turbine helicopter engines p0029 A79-39804
Progress on Variable Cycle Engines
[AIAA PAPER 79-1312] p0036 A79-40759
Energy efficient aircraft engines
[AIAA PAPER 79-1861] p0030 A79-47918
Fundamental mechanisms that influence the estimate
of heat transfer to gas turbine blades p0099 A79-49526
Energy-state formulation of lumped volume dynamic
equations with application to a simplified free
piston Stirling engine p0187 A79-49532
QCSSE - The key to future short-haul air transport
--- Quiet, Clean, Short-Haul Experimental Engine
program p0030 A79-50208
An overview of NASA research on positive
displacement type general aviation engines
[AIAA PAPER 79-1824] p0038 A79-53750
Energy efficient engine preliminary design and
integration study p0012 A79-12084
Cold-air performance of free power turbine
designed for 112-kilowatt automotive gas-turbine
engine 3: Effect of stator vane end clearances
on performance p0014 A79-13049
Analytical evaluation of the impact of broad
specification fuels on high bypass turbofan
engine combustors p0031 A79-13050
Advanced electrostatic ion thruster for space
propulsion p0056 A79-14153
The rotary combustion engine: A candidate for
general aviation --- conferences p0016 A79-15961
New opportunities for future small civil turbine
engines: Overviewing the GATE studies p0017 A79-16849
Advanced engine study for mixed-mode
orbit-transfer vehicles p0057 A79-19074
Variable cycle engine technology program planning
and definition study p0034 A79-23084
Advanced low emissions catalytic combustor program
at General Electric p0021 A79-25011
Advanced low emissions catalytic combustor program
at Pratt and Whitney p0021 A79-25012
Lean, premixed, prevaporized combustor conceptual
design study p0021 A79-25013
Lean, premixed, prevaporized combustor conceptual
design study p0022 A79-25014
Design study and performance analysis of a
high-speed multistage variable-geometry fan for
a variable cycle engine p0034 A79-25020
The 30-centimeter ion thrust subsystem design manual
[NASA-TM-79191] p0053 A79-25131
Conceptual design study of an automotive Stirling
reference engine system p0188 A79-29110
Advanced General Aviation Turbine Engine (GATE)
study p0035 A79-29189
A summary of NASA/Air Force full scale engine
research programs using the F100 engine p0024 A79-30188
Energy efficient engine flight propulsion system
preliminary analysis and design report p0035 A79-30189
[NASA-CR-159487]
Conceptual design study of an Improved Gas Turbine
(IGT) powertrain p0189 A79-31087
[NASA-CR-159604]
Conceptual design study of improved automobiles
gas turbine powertrain p0189 A79-31088
Single shaft automotive gas turbine engine
characterization test p0189 A79-32129
Lean, premixed, prevaporized fuel combustor
conceptual design study p0035 A79-32211
[NASA-CR-159647]
ENGINE FAILURE
Effects of steady-state pressure distortion on the
stall margin of a J85-21 turbojet engine p0018 A79-23968
[NASA-TN-79123]
ENGINE INLETS
Effect of lip and centerbody geometry on
aerodynamic performance of inlets for
tilting-nacelle VTOL aircraft p0025 A79-23509
[AIAA PAPER 79-0381]
Aerodynamic performance of scarf inlets p0005 A79-23510
[AIAA PAPER 79-0380]
Full-scale engine tests of bulk absorber acoustic
inlet treatment p0026 A79-26881
[AIAA PAPER 79-0600]
Experimental evaluation of the effect of inlet
distortion on compressor blade vibrations p0128 A79-30558
An approach to optimum subsonic inlet design
[NASA-TN-79051] p0002 A79-12020
Theoretical study of VTOL tilt-nacelle
axisymmetric inlet geometries p0003 A79-14996
[NASA-TF-1380]
Aerodynamic performance of scarf inlets ---
including acoustic advantages p0003 A79-14598
[NASA-TN-79055]
Effect of lip and centerbody geometry on
aerodynamic performance of inlets for
tilting-nacelle VTOL aircraft p0003 A79-14999
[NASA-TN-79056]
Analysis of radiation patterns of interaction
tones generated by inlet rods in the JT15D engine p0016 A79-15960
[NASA-TN-79074]
Self stabilizing sonic inlet p0011 A79-24976
[NASA-CASE-LEW-11890-1]
Recent applications of theoretical analysis to
V/SIGL inlet design p0004 A79-29143
[NASA-TN-79211]
ENGINE MONITORING INSTRUMENTS
Diagnostics of wear in aeronautical systems p0120 A79-39805
ENGINE NOISE
Correlation of combustor acoustic power levels
inferred from internal fluctuating pressure
measurements p0025 A79-14796
Full-scale engine tests of bulk absorber acoustic
inlet treatment p0026 A79-26881
[AIAA PAPER 79-0600]
An impulse test technique with application to
acoustic measurements --- for engine noise
absorbers p0178 A79-26890
[AIAA PAPER 79-0679]
Evaluation of two inflow control devices for
flight simulation of fan noise using a JT15D
engine p0026 A79-26926
[AIAA PAPER 79-0654]
Effects of simulated forward flight on jet noise,
shock noise and internal noise p0178 A79-26936
[AIAA PAPER 79-0615]
Investigation of wing shielding effects on CTOL
engine noise p0011 A79-28970
[AIAA PAPER 79-0669]
Duct wall impedance control as an advanced concept
for acoustic suppression enhancement --- engine
noise reduction p0176 A79-10842
[NASA-CR-159425]
Basic research in fan source noise: Inlet
distortion and turbulence noise p0177 A79-14875
[NASA-CR-159451]
Measured and predicted noise of the Avco-Lycoming
YF-102 turbofan noise p0016 A79-15957
[NASA-TN-79069]
Analysis of radiation patterns of interaction
tones generated by inlet rods in the JT15D engine p0016 A79-15960
[NASA-TN-79074]
Experimental clean combustor program, phase 3:
Noise measurement addendum --- CF6-50 high
bypass turbofan engine noise p0177 A79-17656
[NASA-CR-159458]

- Theory of low frequency noise transmission through turbines
[NASA-CR-159457] p0033 N79-20117
- Investigation of wing shielding effects on CTOL engine noise
[NASA-TM-79078] p0127 N79-20390
- Dispersion of sound in a combustion duct by fuel droplets and soot particles
[NASA-TM-79236] p0174 N79-31002
- ENGINE PARTS**
- Ceramic applications in the advanced Stirling automotive engine
p0117 A79-12851
- NASA thermal barrier coatings - Summary and update
p0085 A79-21295
- Composites emerging for aeropropulsion applications
p0066 A79-53720
- Gas path sealing in turbine engines
p0013 N79-11057
- Materials and structural aspects of advanced gas-turbine helicopter engines
[NASA-TM-79100] p0001 N79-20008
- Handbook of data on selected engine components for solar thermal applications
[NASA-TM-79027] p0139 N79-26476
- Brayton-cycle component characteristics
p0140 N79-26479
- Development of spiral-groove self-acting seals for helicopter engines
[NASA-CR-159622] p0122 N79-32551
- ENGINE TESTING LABORATORIES**
- The NASA high pressure facility and turbine test rig
p0038 A79-21296
- NASA CF6 jet engine diagnostics program:
Long-term CF6-6D low-pressure turbine deterioration
[NASA-CR-159618] p0039 N79-29191
- A summary of NASA/Air Force full scale engine research programs using the F100 engine
[NASA-TM-79267] p0024 N79-30188
- ENGINE TESTS**
- NT COLD FLOW TESTS**
- NT SPACE ELECTRIC ROCKET TESTS**
- Effect of forward velocity and crosswind on the reverse-thrust performance of a variable-pitch fan engine
[AIAA PAPER 79-0105] p0025 A79-23512
- Characteristics of aeroelastic instabilities in turbomachinery - NASA full scale engine test results
[AIAA 79-7011] p0027 A79-29386
- Initial comparison of single cylinder Stirling engine computer model predictions with test results
[SAE PAPER 790327] p0119 A79-31368
- Some effects of cyclic induced deformation in rocket thrust chambers
[AIAA 79-0911] p0054 A79-34736
- A review of Curtiss-Wright rotary engine developments with respect to general aviation potential
[SAE PAPER 790621] p0036 A79-36749
- Test verification of a turbofan partial swirl afterburner
[AIAA PAPER 79-1199] p0029 A79-38981
- Multivariable control altitude demonstration on the F100 turbofan engine
[AIAA PAPER 79-1204] p0029 A79-39814
- A summary of NASA/Air Force Full Scale Engine Research programs using the F100 engine
[AIAA PAPER 79-1308] p0030 A79-40488
- Progress on Variable Cycle Engines
[AIAA PAPER 79-1312] p0036 A79-40759
- Baseline performance of the GPU 3 Stirling engine
[NASA-TM-79038] p0135 N79-16356
- Full-scale engine tests of bulk absorber acoustic inlet treatment
[NASA-TM-79079] p0173 N79-16645
- Initial comparison of single cylinder Stirling engine computer model predictions with test results
[NASA-TM-79044] p0188 N79-16721
- Characteristics of aeroelastic instabilities in turbomachinery - NASA full scale engine test results
[NASA-TM-79085] p0126 N79-17263
- JT8D and JT9D jet engine performance improvement program. Task 1: Feasibility analysis
[NASA-CR-159449] p0033 N79-20116
- Turbulence characteristics of compressor discharge flows --- JT9D engine tests
p0019 N79-24995
- Turbulence measurements in the compressor exit flow of a General Electric CF6-50 engine
p0019 N79-24996
- Low-power baseline test results for the GPU 3 Stirling engine
[NASA-TM-79103] p0188 N79-27023
- NASA CF6 jet engine diagnostics program:
Long-term CF6-6D low-pressure turbine deterioration
[NASA-CR-159618] p0039 N79-29191
- A summary of NASA/Air Force full scale engine research programs using the F100 engine
[NASA-TM-79267] p0024 N79-30188
- Experimental Clean Combustor Program (ECCP), phase 3 --- commercial aircraft turbofan engine tests with double annular combustor
[NASA-CR-135384] p0035 N79-31207
- Aerodynamic performance of axial-flow fan stage operated at nine inlet guide vane angles --- to be used on vertical lift aircraft
[NASA-TP-1510] p0024 N79-31214
- Single shaft automotive gas turbine engine characterization test
[NASA-CR-159654] p0189 N79-32129
- CF6 jet engine performance improvement program. Short core exhaust nozzle performance improvement concept --- specific fuel consumption reduction
[NASA-CR-159564] p0038 N79-33206
- SERT 2 1979 extended flight thruster system performance
[NASA-TM-79256] p0054 N79-33252
- Preliminary results of the mission profile life test of a 30 cm Hg bombardment thruster
[NASA-TM-79261] p0054 N79-33254
- Neutralization tests on the SERT 2 spacecraft
[NASA-TM-79271] p0054 N79-33255
- ENGINEERING DEVELOPMENT**
- U PRODUCT DEVELOPMENT**
- ENGINES**
- NT AIR BREATHING ENGINES**
- NT DIESEL ENGINES**
- NT DUCTED FAN ENGINES**
- NT ELECTROSTATIC ENGINES**
- NT GAS TURBINE ENGINES**
- NT HELICOPTER ENGINES**
- NT HYDROGEN OXYGEN ENGINES**
- NT INTERNAL COMBUSTION ENGINES**
- NT ION ENGINES**
- NT J-85 ENGINE**
- NT JET ENGINES**
- NT LIQUID PROPELLANT ROCKET ENGINES**
- NT MERCURY ION ENGINES**
- NT PISTON ENGINES**
- NT ROCKET ENGINES**
- NT T-53 ENGINE**
- NT T-55 ENGINE**
- NT T-63 ENGINE**
- NT TP-30 ENGINE**
- NT TURBINE ENGINES**
- NT TURBOFAN ENGINES**
- NT TURBOJET ENGINES**
- NT TURBOPROP ENGINES**
- NT VARIABLE CYCLE ENGINES**
- NT WANKEL ENGINES**
- Variable cycle engine technology program planning and definition study
[NASA-CR-159539] p0034 N79-23084
- Experimental and analytical tools for evaluation of Stirling engine rod seal behavior
[NASA-CR-159543] p0122 N79-23429
- Advanced General Aviation Turbine Engine (GATE) concepts
[NASA-CR-159603] p0034 N79-25017
- Low-power baseline test results for the GPU 3 Stirling engine
[NASA-TM-79103] p0188 N79-27023
- Stirling engines for automobiles
[NASA-TM-79222] p0142 N79-28726
- ENHANCEMENT**
- U AUGMENTATION**
- ENTROPY**
- Turbulence generated by the interaction of entropy fluctuations with non-uniform mean flows
p0106 A79-45468

ENVIRONMENT EFFECTS

Effects of moisture profiles and laminate configuration on the hygro stress in advanced composites

p0064 A79-24132

ENVIRONMENT MODELS

Spacecraft charging modeling development and validation study

p0050 M79-24051

ENVIRONMENT POLLUTION

NT AIR POLLUTION

NT GLOBAL AIR POLLUTION

ENVIRONMENT SIMULATION

NT SPACE ENVIRONMENT SIMULATION

ENVIRONMENT SIMULATORS

Computer and laboratory simulation of interactions between spacecraft surfaces and charged-particle environments
[NASA-TN-79219]

p0063 M79-29224

ENVIRONMENTAL CHAMBERS

U TEST CHAMBERS

ENVIRONMENTAL CHEMISTRY

NT ATMOSPHERIC CHEMISTRY

ENVIRONMENTAL QUALITY

NT AIR QUALITY

NT WATER QUALITY

ENVIRONMENTAL TEMPERATURE

U AMBIENT TEMPERATURE

ENVIRONMENTAL TESTS

NT CORROSION TESTS

NT HIGH TEMPERATURE TESTS

NT LOW TEMPERATURE TESTS

NT SALT SPRAY TESTS

Pretting wear of iron, nickel, and titanium under varied environmental conditions

p0078 A79-34995

Endurance testing of first generation /Block I/ commercial solar cell modules

p0148 A79-41022

Block 2 solar cell module environmental test program
[NASA-CR-159393]

p0151 M79-13490

DCE photovoltaic tests and applications project

p0139 M79-25492

Experimental study of low temperature behavior of aviation turbine fuels in a wing tank mode

p0091 M79-29355

ENVIRONMENTS

NT AEROSPACE ENVIRONMENTS

NT MAGNETOSPHERE

NT SPACECRAFT ENVIRONMENTS

EPITAXY

Epitaxial solar-cell fabrication, phase 2

p0152 M79-19448

Method for the preparation of inorganic single crystal and polycrystalline electronic materials
[NASA-CASE-XLE-02545-1]

p0184 M79-21910

EPOXY RESINS

Effects of hydrothermal exposure on a low-temperature cured epoxy

p0085 A79-15534

Dynamic mechanical analysis of fiber reinforced composites

p0061 M79-15157

High char imide-modified epoxy matrix resins --- for graphite-epoxy composites

p0063 M79-29240

Curing agent for polyepoxides and epoxy resins and composites cured therewith
[NASA-CASE-LFW-13226-1]

p0059 M79-31345

EQUATIONS OF MOTION

NT EULER EQUATIONS OF MOTION

NT NAVIER-STOKES EQUATION

EQUILIBRIUM EQUATIONS

Nonlinear equations of equilibrium for elastic helicopter or wind turbine blades undergoing moderate deformation
[NASA-CR-159478]

p0130 M79-19414

EQUIVALENT CIRCUITS

A general unified approach to modelling switching dc-to-dc converters in discontinuous conduction mode

p0101 A79-10880

Generalized computer-aided discrete time domain modeling and analysis of dc-dc converters

p0099 A79-10881

EROSION

Adhesive material transfer in the erosion of an aluminum alloy
[NASA-TN-79165]

p0083 M79-27306

ERROR BAND

U ACCURACY

ESTERS

NT URETHANES

Characterization of PBR polyimides - Correlation of ester impurities with composite properties
p0066 A79-43265

Characterization of PBR polyimides: Correlation of ester impurities with composite properties
[NASA-TN-79068]

p0061 M79-16918

ESTIMATES

NT COST ESTIMATES

Fundamental mechanisms that influence the estimate of heat transfer to gas turbine blades
[NASA-TN-79128]

p0103 M79-20346

ETCHING

Ion beam sputtering of fluoropolymers

p0117 A79-14797

Adhesive bonding of ion beam textured metals and fluoropolymers

p0181 M79-12909

Mechanical and chemical effects of ion-texturing biomedical polymers

p0084 M79-31391

ETHYL ALCOHOL

Axial jet mixing of ethanol in cylindrical containers during weightlessness
[NASA-TF-1487]

p0090 M79-28350

ETHYLENE COMPOUNDS

NT CHLOROETHYLENE

EUCLIDEAN GEOMETRY

NT ANGLES (GEOMETRY)

NT ELLIPSES

EULER EQUATIONS OF MOTION

CELFE: Coupled Eulerian-Lagrangian Finite Element program for high velocity impact. Part 1: Theory and formulation --- hydroelasto-viscoplastic model

p0166 M79-29832

CELFE: Coupled Eulerian-Lagrangian Finite Element program for high velocity impact. Part 2: Program user's manual

p0166 M79-29833

EULER-LAGRANGE EQUATION

CELFE/NASTRAN Code for the analysis of structures subjected to high velocity impact

p0128 A79-21298

CELFE/NASTRAN code for the analysis of structures subjected to high velocity impact
[NASA-TN-79048]

p0126 M79-15325

CELFE: Coupled Eulerian-Lagrangian Finite Element program for high velocity impact. Part 1: Theory and formulation --- hydroelasto-viscoplastic model

p0166 M79-29832

CELFE: Coupled Eulerian-Lagrangian Finite Element program for high velocity impact. Part 2: Program user's manual

p0166 M79-29833

EUTECTIC ALLOYS

Some properties of low-vapor-pressure braze alloys for thermionic converters

p0076 A79-13100

Shear rupture of a directionally solidified eutectic gamma/gamma'-prime - alpha /Mo/ alloy --- for aircraft engine turbine blades

p0077 A79-21301

A feasibility study of a diffusion barrier between Ni-Cr-Al coatings and nickel-based eutectic alloys

p0077 A79-27233

Evaluation of directionally solidified eutectic superalloys for turbine blade applications
[NASA-CR-135151]

p0079 M79-16948

Evaluation of an advanced directionally solidified gamma/gamma'-alpha Mo eutectic alloy
[NASA-CR-159416]

p0079 M79-20222

Wear of aluminum and hypoeutectic aluminum-silicon alloys in boundary-lubricated pin-on disk sliding
[NASA-TF-1442]

p0074 M79-21184

EUTECTICS

NT EUTECTIC ALLOYS

EVAPORATION

Reactively evaporated films of copper molybdenum sulfide

p0185 A79-31973

EVAPORATIVE COOLING

NT FILM COOLING

EVOLUTION (DEVELOPMENT)

NT CHEMICAL EVOLUTION

EXCHANGING

NT CHARGE EXCHANGE

NT ION EXCHANGING

EXECUTIVE AIRCRAFT

U GENERAL AVIATION AIRCRAFT

EXHAUST FLOW SIMULATION

NT FLIGHT SIMULATION

EXHAUST GASES

Experimental study of the effects of flameholder geometry on emissions and performance of lean premixed combustors

[AIAA PAPER 79-0187] p0070 A79-19586

Concepts for reducing exhaust emissions and fuel consumption of the aircraft piston engine

[SAE PAPER 790605] p0036 A79-36737

Reduction of particulate carryover from a pressurized fluidized bed

p0150 A79-49527

Reduction of particulate carryover from a pressurized fluidized bed

p0150 A79-49527

Emission measurements for a lean premixed propane/air system at pressures up to 30 atmospheres

[NASA-CR-159421] p0071 A79-10165

Effect of swirler-mounted mixing venturi on emissions of flame-tube combustor using jet A fuel

[NASA-TP-1393] p0015 A79-14099

Effects of air injection on a turbocharged Teledyne Continental Motors TSIO-360-C engine

[NASA-TM-79121] p0158 A79-20528

Effect of degree of fuel vaporization upon emissions for a premixed prevaporized combustion system --- for gas turbine engines

[NASA-TM-79154] p0012 A79-23965

An improved method for predicting the effects of flight on jet mixing noise

[NASA-TM-79155] p0173 A79-24770

Effect of fuel sprays on emissions

p0020 A79-24999

Emissions measurements for a lean premixed propane/air system at pressures up to 30 atmospheres

p0020 A79-25002

Effect of degree of fuel vaporization on emissions for a premixed-prevaporized combustor system

[NASA-TM-79154] p0012 A79-23965

Effect of fuel/air nonuniformity on nitric oxide emissions

p0020 A79-25004

Lean, Premixed-Prevaporized (LPP) combustor conceptual design study

[NASA-CR-159629] p0072 A79-31358

Lean, premixed, prevaporized fuel combustor conceptual design study

[NASA-CR-159647] p0035 A79-32211

EXHAUST JETS

U EXHAUST GASES

EXHAUST NOZZLES

NT CONVERGENT-DIVERGENT NOZZLES

NT PLUG NOZZLES

Noise from struts and splitters in turbofan exit ducts

[AIAA PAPER 79-0637] p0176 A79-26923

Effect of shocks on film cooling of a full scale turbojet exhaust nozzle having an external expansion surface

[AIAA PAPER 79-1170] p0026 A79-38969

Variable area exhaust nozzle

[NASA-CASE-LEW-12378-1] p0014 A79-14097

Experimental study of coaxial nozzle exhaust noise --- acoustic measurements

[NASA-TM-79090] p0173 A79-20829

Studies of the acoustic transmission characteristics of coaxial nozzles with inverted velocity profiles: Comprehensive data report

--- nozzle transfer functions

[NASA-CR-159628] p0177 A79-27933

Aerodynamic and acoustic investigation of inverted velocity profile coannular exhaust nozzle models and development of aerodynamic and acoustic prediction procedures, comprehensive data report, volume 1

[NASA-CR-159515] p0034 A79-30185

Aerodynamic and acoustic investigation of inverted velocity profile coannular exhaust nozzle models and development of aerodynamic and acoustic prediction procedures, comprehensive data report, volume 2

[NASA-CR-159516] p0034 A79-30186

Aerodynamic and acoustic investigation of inverted velocity profile coannular exhaust nozzle models and development of aerodynamic and acoustic prediction procedures

[NASA-CR-3168] p0035 A79-31212

CF6 jet engine performance improvement program. Short core exhaust nozzle performance improvement concept --- specific fuel consumption reduction

[NASA-CR-159564] p0038 A79-33206

EXHAUST VELOCITY

Effects of geometric and flow-field variables on inverted-velocity-profile coaxial jet noise --- nozzle geometry

[NASA-TM-79095] p0173 A79-20830

EXPANDABLE STRUCTURES

Effect of shocks on film cooling of a full scale turbojet exhaust nozzle having an external expansion surface

[NASA-TM-79157] p0018 A79-23966

Effect of shocks on film cooling of a full scale turbojet exhaust nozzle having an external expansion surface

[NASA-TM-79157] p0018 A79-23966

EXPANSION

NT THERMAL EXPANSION

EXPERIMENTAL DESIGN

Numbers of center points appropriate to blocked response surface experiments

Definition of smolder experiments for Spacelab

[NASA-CR-159528] p0040 A79-20161

Numbers of center points appropriate to blocked response surface experiments

[NASA-TM-79201] p0168 A79-28970

EXPLOSIONS

NT CHEMICAL EXPLOSIONS

NT GAS EXPLOSIONS

EXPONENTIAL FUNCTIONS

NT LOGARITHMS

EXTENSOMETERS

Measurement of transient strain and surface temperature on simulated turbine blades using noncontacting techniques

[NASA-TM-78982] p0126 A79-19415

EXTRAPOLATION

Interpolation and extrapolation of creep rupture data by the Minimum Commitment Method. I - Focal-point convergence. II - Oblique translation. III - Analysis of multiheats

p0077 A79-16038

EXTRATERRESTRIAL MATTER

NT NEUTRAL GASES

EXTREMELY HIGH FREQUENCIES

The 18 and 30 GHz fixed service communication satellite system study: Executive summary

[NASA-CR-159627-1] p0096 A79-31373

EXTRUDING

Critical current density in wire drawn and hydrostatically extruded Nb-Ti superconductors

p0185 A79-20539

EYE (ANATOMY)

Intraocular pressure reduction and regulation system

[NASA-TM-79187] p0165 A79-28881

F

F-15 AIRCRAFT

Reynolds number, scale and frequency content effects on F-15 inlet instantaneous distortion

[AIAA PAPER 79-0104] p0005 A79-15533

F-102 AIRCRAFT

Measured and predicted noise of the AVCO-Lycoming YF-102 turbofan engine

[AIAA PAPER 79-0641] p0026 A79-26877

FABRICATION

Wind-turbine-generator rotor-blade concepts with low-cost potential

p0147 A79-20828

An operating 200 kW horizontal axis wind turbine

p0147 A79-20829

An economic analysis of a commercial approach to the design and fabrication of a space power system

[AIAA 79-0914] p0055 A79-34737

Fabrication and testing of non-graphitic superhybrid composites

p0066 A79-43289

- A brief survey of the solar cell state-of-the-art
p0052 N79-10130
- Adaptation of ion beam technology to microfabrication of solid state devices and transducers
[NASA-CR-159439] p0186 N79-11921
- Fabrication and testing of silver-hydrogen cells
[NASA-CR-159431] p0152 N79-16374
- Fabrication and testing of silver-hydrogen cells
[NASA-CR-159490] p0152 N79-16375
- Method for fabricating solar cells having integrated collector grits
[NASA-CASE-LEW-12819-2] p0136 N79-18444
- Fabrication and testing of nongraphitic superhybrid composites
[NASA-TM-79102] p0063 N79-20188
- Development of a plasma sprayed ceramic gas path seal for high pressure turbine applications
[NASA-CR-159669] p0122 N79-31602
- Shallow-homojunction GaAs solar cells
p0144 N79-32666
- FABRY-PEROT LASERS**
U LASERS
- FAILURE**
NT ENGINE FAILURE
NT STRUCTURAL FAILURE
- FAILURE ANALYSIS**
Some effects of cyclic induced deformation in rocket thrust chambers
[AIAA 79-0911] p0054 A79-34736
- Some practical observations on the accelerated testing of Nickel-Cadmium Cells
p0056 A79-51911
- Lubrication and failure mechanisms of molybdenum disulfide films. 1: Effect of atmosphere
[NASA-TP-1343] p0081 N79-13158
- Lubrication and failure mechanisms of molybdenum disulfide films. 2: Effect of substrate roughness
[NASA-TP-1379] p0081 N79-13159
- MOD-2 failure mode and effects analysis
[NASA-CR-159632] p0093 N79-30415
- FAILURE MODES**
Filtration effects on ball bearing life and condition in a contaminated lubricant
[ASME PAPER 78-LUB-34] p0118 A79-23246
- Maximum likelihood estimation for life distributions with competing failure modes
p0165 A79-49528
- Maximum likelihood estimation for life distributions with competing failure modes
[NASA-TM-79126] p0165 N79-23735
- MOD-2 failure mode and effects analysis
[NASA-CR-159632] p0093 N79-30415
- FAVLIPT DEVICES**
U LIPT FANS
- FANS**
Reduction of rotor-turbulence interaction noise in static fan noise testing
[AIAA PAPER 79-0656] p0036 A79-26925
- Performance of two-stage fan with larger dampers on first-stage rotor
[NASA-TP-1399] p0018 N79-23967
- Performance of two-stage fan having low-aspect-ratio first-stage rotor blading
[NASA-TP-1493] p0023 N79-27143
- FAR FIELDS**
Modal propagation angles in a cylindrical duct with flow and their relation to sound radiation
[AIAA PAPER 79-0183] p0174 A79-19582
- Numerical spatial marching techniques in duct acoustics --- noise source calculation from far field pressure measurements
p0175 A79-25946
- FATIGUE (MATERIALS)**
NT BENDING FATIGUE
NT METAL FATIGUE
NT STRUCTURAL STRAIN
NT THERMAL FATIGUE
- A strainrange partitioning analysis of low cycle fatigue of coated and uncoated Rene 80
p0129 N79-10479
- Exploratory thermal-mechanical fatigue results for Rene 80 in ultrahigh vacuum
[NASA-CR-159444] p0079 N79-11180
- Evaluation of CBS 600 carburized steel as a gear material
[NASA-TP-1390] p0114 N79-14389
- The strainrange partitioning behavior of an advanced gas turbine disk alloy, AF2-1CA
[NASA-TM-79179] p0075 N79-23196
- A literature review on fatigue and creep interaction
[NASA-CR-135305] p0130 N79-26429
- Strainrange partitioning life predictions of the long time metal properties council creep-fatigue tests
[NASA-TM-79260] p0127 N79-31619
- FATIGUE DIAGRAMS**
U S-N DIAGRAMS
- FATIGUE LIFE**
Proposed design procedure for transmission shafting under fatigue loading
p0117 A79-14950
- Review of the Agard S6M panel evaluation program of the NASA-Lewis 'SEP' approach to high-temperature LCF life prediction --- Strainrange Partitioning for Low Cycle Fatigue
p0128 A79-14954
- Filtration effects on ball bearing life and condition in a contaminated lubricant
[ASME PAPER 78-LUB-34] p0118 A79-23246
- The strainrange partitioning behavior of an advanced gas turbine disk alloy, AF2-1CA
[AIAA PAPER 79-1192] p0078 A79-38977
- Exploratory thermal-mechanical fatigue results for Rene 80 in ultrahigh vacuum
[NASA-CR-159444] p0079 N79-11180
- Low-cycle fatigue of thermal-barrier coatings at 982 deg C
[NASA-TF-1322] p0014 N79-13046
- Effect of low-stiffness closeout overwrap on rocket thrust-chamber life
[NASA-TF-1456] p0053 N79-23132
- Evaluation of flawed composite structural components under static and cyclic loading --- fatigue life of graphite-epoxy composite materials
[NASA-CR-135403] p0066 N79-26120
- Review of the AGARD S and M panel evaluation program of the NASA-Lewis SEP approach to high-temperature LCF life prediction
p0023 N79-27179
- FATIGUE TESTS**
Fatigue impact on Mod-1 wind turbine design
p0156 A79-20827
- Effects of thermomechanical processing on strength and toughness of Fe-12Ni reactive metal alloys at 77K
p0078 A79-32600
- Exploratory thermal-mechanical fatigue results for Rene 80 in ultrahigh vacuum
[NASA-CR-159444] p0079 N79-11180
- Some effects of cyclic induced deformation in rocket thrust chambers
[NASA-TM-79112] p0103 N79-20337
- Fatigue behavior of SiC reinforced titanium composites
[NASA-TM-79223] p0064 N79-30296
- Evaluation of high-contact-ratio spur gears with profile modification
[NASA-TP-1458] p0115 N79-31604
- Ferrographic analysis of wear debris from full-scale bearing fatigue tests
[NASA-TF-1511] p0116 N79-31605
- Strip cell test and evaluation program
[NASA-CR-159652] p0154 N79-31784
- FAULT MECHANICS**
U FRACTURE MECHANICS
- FEASIBILITY ANALYSIS**
Feasibility of determining flat roof heat losses using aerial thermography
p0131 A79-51095
- Preliminary summary of the ETF conceptual studies
[NASA-TM-78999] p0133 N79-11478
- JT8D and JT9D jet engine performance improvement program. Task 1: Feasibility analysis
[NASA-CR-159449] p0033 N79-20116
- Evaluation of urethane for feasibility of use in wind turbine blade design
[NASA-CR-159530] p0153 N79-20497
- Combustion of porous solids at reduced gravitational conditions
[NASA-CR-3197] p0072 N79-33288
- FEED SYSTEMS**
Study of liquid and vapor flow into a Centaur capillary device
[NASA-CR-159657] p0108 N79-33432

FEEDBACK CONTROL

Bilinear tangent yaw guidance
[AIAA 79-1730] p0045 A79-45374
Multivariable control altitude demonstration on
the F100 turbofan engine
[NASA-TN-79183] p0022 N79-25015

FERRI SURFACES

Normal state properties of the ternary molybdenum
sulfides p0185 A79-27229
Indirect measurements of Feral surface parameters
of some chevrel phase materials p0185 A79-50231

FERRITES

Friction and wear of single-crystal manganese-zinc
ferrite p0185 A79-34994
Anisotropic friction and wear of single-crystal
manganese-zinc ferrite in contact with itself
[NASA-TF-1339] p0113 N79-10425
Friction and wear of single-crystal manganese-zinc
ferrite p0184 N79 16699
[NASA-TN-78980]

FIBER COMPOSITES

NT CARBON FIBER REINFORCED PLASTICS
NT GLASS FIBER REINFORCED PLASTICS
The effects of eccentricities on the fracture of
off-axis fiber composites p0064 A79-15543
Use of an ultrasonic-acoustic technique for
nondestructive evaluation of fiber composite
strength p0064 A79-15545
Analysis of high velocity impact on hybrid
composite fan blades p0128 A79-29027
[AIAA 79-0783]
Status review of FRB polyimides --- Polymerization
of Monomer Reactants p0065 A79-30399
Mechanics of intraply hybrid composites -
Properties, analysis and design p0065 A79-31033
Fracture modes in off-axis fiber composites
p0065 A 9-31035
Dynamic mechanical analysis of fiber reinforced
composites p0065 A79-31040
Evaluation of silicon carbide fiber/titanium
composites p0064 N79-31349
[NASA-TN-79232]

FIBER OPTICS

Fiber optic sensors for military, industrial and
commercial applications p0111 A79-38738
A cross impact methodology for the assessment of
US telecommunications system with application to
fiber optics development: Executive summary
[NASA-CR-135209] p0096 N79-17071
A cross impact methodology for the assessment of
US telecommunications system with application to
fiber optics development, volume 1
[NASA-CR-135208] p0096 N79-18159
A cross impact methodology for the assessment of
US telecommunications system with application to
fiber optics development, volume 2
[NASA-CR-159511-VOL-2] p0096 N79-18160
Analysis and preliminary design of optical sensors
for propulsion control --- temperature sensors
[NASA-CR-159519] p0180 N79-27975

FIBER STRENGTH

Some properties of an advanced boron fiber
p0086 A79-21297
Mechanisms of boron fiber strengthening by thermal
treatment p0065 A79-30396
Some properties of an advanced boron fiber ---
high strength, splittable fibers p0061 N79-16076
[NASA-TN-79065]
Mechanisms of boron fiber strengthening by thermal
treatment p0062 N79-20186
[NASA-TN-79077]

FIBERGLASS

U GLASS FIBERS

FIBERS

NT CARBON FIBERS
NT GLASS FIBERS
NT METAL FIBERS
NT REINFORCING FIBERS
NT SYNTHETIC FIBERS

Some properties of an advanced boron fiber ---
high strength, splittable fibers p0061 N79-16076
[NASA-TN-79065]

FIBROUS MATERIALS

U FIBERS

FIDELITY

U ACCURACY

FIELD THEORY (PHYSICS)

Anomalous galvanomagnetic properties of graphite
in strong magnetic fields p0185 A79-23633

FIGHTER AIRCRAFT

NT F-15 AIRCRAFT

NT F-102 AIRCRAFT

NT YF-12 AIRCRAFT

FILAMENT WINDING

Acoustic emission testing of composite vessels
under sustained loading p0128 A79-11543
Wind-turbine-generator rotor-blade concepts with
low-cost potential p0147 A79-20828

FILAMENT WOUND CONSTRUCTION

U FILAMENT WINDING

FILM BOILING

Condensation on a noncollapsing vapor bubble in a
subcooled liquid p0100 A79-49535

FILM COOLING

Effect of shocks on film cooling of a full scale
turbojet exhaust nozzle having an external
expansion surface p0028 A79-38969
[AIAA PAPER 79-1170]
Ceramic coating effect on liner metal temperatures
of film-cooled annular combustor p0015 N79-14098
[NASA-TF-1323]
Airfoil cooling hole plugging by combustion gas
impurities of the type found in coal derived fuels
[NASA-TN-79076] p0089 N79-20265
Full-coverage film cooling: 3-dimensional
measurements of turbulence structure and
prediction of recovery region hydrodynamics
[NASA-CR-3104] p0106 N79-22428
Heat transfer to a full-coverage, film-cooled
surface with compound-angle (30 deg and 45 deg)
hole injection p0107 N79-22429
[NASA-CR-3103]
Effect of shocks on film cooling of a full scale
turbojet exhaust nozzle having an external
expansion surface p0018 N79-23966
[NASA-TN-79157]
Effect of shocks on film cooling of a full scale
turbojet exhaust nozzle having an external
expansion surface p0018 N79-23966
[NASA-TN-79157]
Flow visualization of discrete-hole film cooling
with spanwise injection over a cylinder
[NASA-TF-1491] p0023 N79-27142

FILM THICKNESS

Elastohydrodynamic lubrication of elliptical
contacts for materials of low elastic modulus.
II - Starved conjunction p0118 A79-23229
[ASME PAPER 78-LUB-1]
Effect of geometry on hydrodynamic film thickness
[ASME PAPER 78-LUB-24] p0118 A79-23237
Elastohydrodynamic film thickness measurements of
artificially produced surface dents and grooves
--- on fatigue failure of bearings p0118 A79-23267
[ASLE PREPRINT 78-LC-1a-1]
Determination of lubricant selection based on
elastohydrodynamic film thickness and traction
measurement p0121 N79-14385
[NASA-CR-159428]
Experimental and analytical tools for evaluation
of Stirling engine rod seal behavior p0122 N79-23429
[NASA-CR-159543]
Elastohydrodynamic film thickness measurements of
artificially produced nonsmooth surfaces p0115 N79-28554
[NASA-TN-79214]
Comparison of predicted and measured
elastohydrodynamic film thickness in a
20-millimeter-bore ball bearing p0116 N79-32552
[NASA-TF-1542]
Correlation of asperity contact-time fraction with
elastohydrodynamic film thickness in a
20-millimeter-bore ball bearing p0116 N79-33474
[NASA-TF-1547]

FILTRATION

NT SPATIAL FILTERING

FINITE DIFFERENCE THEORY

Numerical spatial marching techniques in duct acoustics --- noise source calculation from far field pressure measurements

p0175 A79-25946

Filtering of non-linear instabilities --- from finite difference solution of fluid dynamics equations

p0108 A79-32912

FINITE ELEMENT METHOD

CELFE/NASTRAN Code for the analysis of structures subjected to high velocity impact

p0128 A79-21298

Recent developments at ONERA in the field of

structural analysis methods

[ONERA, TP NO. 1979-79]

A79-49537

A three-dimensional turbulent compressible flow model for ejector and fluted mixers

p0100 W79-14325

CELFE/NASTRAN code for the analysis of structures subjected to high velocity impact

p0126 W79-15325

Applications of velocity potential function to acoustic duct propagation and radiation from inlets using finite element theory

p0016 W79-15959

Three-dimensional finite-element elastic analysis of a thermally cycled single-edge wedge geometry specimen

p0172 W79-16644

Structural analysis of cylindrical thrust

chambers, volume 1

[NASA-CN-159522]

p0057 W79-19073

Comparison of NASCAP predictions with experimental data

p0047 W79-24013

CELFE: Coupled Eulerian-Lagrangian Finite Element program for high velocity impact. Part 1:

Theory and formulation ---

hydroelasto-viscoplastic model

p0166 W79-29832

CELFE: Coupled Eulerian-Lagrangian Finite Element program for high velocity impact. Part 2:

Program user's manual

[NASA-CN-159396]

p0166 W79-29833

FIRE PREVENTION

Aircraft engine sump fire mitigation, phase 2

[NASA-CN-135379]

p0121 W79-17219

FISH TAILING

U TAW

FLAME FRONTS

U FLAME PROPAGATION

FLAME HOLDERS

Experimental study of the effects of flameholder geometry on emissions and performance of lean

premixed combustors

[AIAA PAPER 79-0187]

p0070 A79-19586

Lean stability augmentation for premixing,

prevaporizing combustors

[AIAA PAPER 79-1319]

p0036 A79-39035

Effect of degree of fuel vaporization upon

emissions for a premixed prevaporized combustion

system

[AIAA PAPER 79-1320]

p0071 A79-39036

Effects of flameholder geometry on emissions and

performance of lean premixed combustors

p0021 W79-25005

Effects of flameholder blockage on emissions and

performance of lean premixed-prevaporized

combustors

p0021 W79-25006

Lean Stability augmentation study

p0021 W79-25007

FLAME INTERACTION

U CHEMICAL REACTIONS

U FLAME PROPAGATION

FLAME PROPAGATION

Turbulence effects on flame speed and flame

structure

[AIAA PAPER 79-0016]

p0070 A79-19480

Modelling turbulent flame ignition and blowout

p0021 W79-25008

The role of NaCl in flame chemistry, in the

deposition process, and in its reactions with

protective oxides as related to hot corrosion

[NASA-TN-79225]

p0065 W79-28258

FLAME SPECTROSCOPY

The role of NaCl in flame chemistry, in the

deposition process, and in its reactions with

protective oxides as related to hot corrosion

p0071 A79-49534

FLAMES

NT PREMIXED FLAMES

Introduction: Thermal Radiation in Industrial

Flames

p0104 W79-22415

FLAMMABILITY

Aircraft engine sump fire mitigation, phase 2

[NASA-CN-135379]

p0121 W79-17219

FLAPS (CONTROL SURFACES)

NT TRAILING-EDGE FLAPS

FLASH LAMPS

Simmer-enhanced flashlamp-pumped dye laser

p0112 A79-32981

FLASH TUBES

U FLASH LAMPS

FLAT PLATES

Scattering and distortion of the unsteady motion

on transversely sheared mean flows

p0106 A79-37140

FLAW DETECTION

U NONDESTRUCTIVE TESTS

FLAWS

U DEFECTS

FLEXIBLE BODIES

Design and test of a squeeze-film damper for a

flexible power transmission shaft

p0123 A79-16011

Laser balancing demonstration on a high-speed

flexible rotor

[ASME PAPER 79-GT-56]

p0121 A79-32351

An introduction to a unified approach to flexible

rotor balancing

[ASME PAPER 79-GT-161]

p0124 A79-32423

FLIGHT CHARACTERISTICS

The M-15-aircraft (samolot M-15)

[NASA-TN-75586]

p0013 W79-12063

FLIGHT COMPUTERS

U AIRBORNE/SPACEBORNE COMPUTERS

FLIGHT CONDITIONS

An improved method for predicting the effects of

flight on jet mixing noise

p0176 A79-39803

FLIGHT CONTROL

Bilinear tangent yaw guidance

[AIAA 79-1730]

p0045 A79-45374

FLIGHT PERFORMANCE

U FLIGHT CHARACTERISTICS

FLIGHT RECORDERS

Ozone Contamination in Aircraft Cabins. Appendix

B: Overview papers. In-flight measurements

p0008 W79-21029

FLIGHT SIMULATION

Evaluation of two inflow control devices for

flight simulation of fan noise using a JT15D

engine

[AIAA PAPER 79-0654]

p0026 A79-26926

Effects of simulated forward flight on jet noise,

short noise and internal noise

[AIAA PAPER 79-0615]

p0178 A79-26936

Evaluation of two inflow control devices for

flight simulation of fan noise using a JT15D

engine

[NASA-TN-79072]

p0017 W79-15969

Effects of steady-state pressure distortion on the

stall margin of a J85-21 turbojet engine

[NASA-TN-79123]

p0018 W79-23968

An improved method for predicting the effects of

flight on jet mixing noise

[NASA-TN-79155]

p0173 W79-24770

FLIGHT TESTS

Plasma Interaction Experiments (PIX) flight results

with liquid hydrogen

[NASA-TN-79196]

p0022 W79-27140

FLOW CHARACTERISTICS

NT FLOW DISTRIBUTION

NT FLOW STABILITY

Some flow phenomena in a constant area duct with a

Borda type inlet including the critical region

[ASME PAPER 78-WA/HT-37]

p0093 A79-19816

Effect of steady-state pressure distortion on flow

characteristics entering a turbofan engine

[NASA-TN-79134]

p0019 W79-23969

Turbulence characteristics of compressor discharge

flows --- JT9D engine tests

p0019 W79-24995

- Turbulence measurements in the compressor exit flow of a General Electric CP6-50 engine
p0019 N79-24996
- Design of high-perveance confined-flow guns for periodic-permanent-magnet-focused tubes
[NASA-TN-1485] p0058 N79-27400
- Some flow characteristics of conventional and tapered high pressure drop simulated seals
[NASA-TN-79192] p0104 N79-27460
- FLOW DISTORTIONS**
- Unsteady vortical and entropic distortions of potential flows round arbitrary obstacles
p0005 A79-19452
- Reynolds number scale and frequency content effects on inlet instantaneous distortion
[AIAA PAPER 79-0104] p0005 A79-19533
- Effects of inflow distortion profiles on fan tone noise calculated using a 3-D theory
[AIAA PAPER 79-0577] p0175 A79-26911
- Combined pressure and temperature distortion effects on internal flow of a turbofan engine
[AIAA PAPER 79-1309] p0025 A79-29031
- Theoretical fan velocity distortions due to inlets and nozzles
p0006 A79-29810
- Turbulence generated by the interaction of entropy fluctuations with non-uniform mean flows
p0108 A79-45468
- Experimental evaluation of the effect of inlet distortion on compressor flow coefficients
[NASA-TN-79066] p0126 N79-16300
- Effects of inflow distortion profiles on fan tone noise calculated using a 3-D theory
[NASA-TN-79082] p0173 N79-16647
- Effects of steady-state pressure distortion on the stall margin of a J85-21 turbojet engine
[NASA-TN-79123] p0018 N79-23968
- Effect of rotor meridional velocity ratio on response to inlet radial and circumferential distortion
[NASA-TP-1278] p0023 N79-28177
- FLOW DISTRIBUTION**
- An efficient user-oriented method for calculating compressible flow about three-dimensional inlets
[AIAA PAPER 79-0081] p0005 A79-19524
- Calculation of the three-dimensional flow field in supersonic inlets at angle of attack using a bicharacteristic method with discrete shock wave fitting
[AIAA PAPER 79-0379] p0025 A79-19696
- Effects of geometric and flow-field variables on inverted-velocity-profile coaxial jet noise and source distributions
[AIAA PAPER 79-0635] p0175 A79-32126
- A computer program for the calculation of the flow field in supersonic mixed-compression inlets at angle of attack using the three-dimensional method of characteristics with discrete shock wave fitting
[NASA-TN-78947] p0002 N79-10023
- Effects of geometric and flow-field variables on inverted-velocity-profile coaxial jet noise --- nozzle geometry
[NASA-TN-79095] p0173 N79-20930
- Effect of grazing flow on the acoustic impedance of Helmholtz resonators consisting of single and clustered orifices
[NASA-CN-3177] p0178 N79-32056
- Flow in nonrotating passages of radial inflow turbines
[NASA-CN-15479] p0035 N79-32212
- FLOW EQUATIONS**
- Filtering of non-linear instabilities --- from finite difference solution of fluid dynamics equations
p0108 A79-32912
- FLOW FIELDS**
- U FLOW DISTRIBUTION**
- FLOW GEOMETRY**
- Trailing edge noise data with comparison to theory
[NASA-TN-79208] p0174 N79-27930
- Effect of steady-state temperature distortion and combined distortion on inlet flow to a turbofan engine
[NASA-TN-79237] p0023 N79-30187
- Free jet phenomena in a 90 degree-sharp edge inlet geometry
[NASA-TN-79229] p0105 N79-3152
- FLOW MEASUREMENT**
- Study of mean- and turbulent-velocity fields in a large-scale turbine-vane passage
[NASA-CN-3067] p0032 N79-16853
- FLOW PATTERNS**
- U FLOW DISTRIBUTION**
- FLOW REGULATORS**
- NT FUEL FLOW REGULATORS
- FLOW RESISTANCE**
- Flow friction of the turbulent coolant flow in cryogenic porous cables
[NASA-TN-79052] p0103 N79-20341
- FLOW SEPARATION**
- U BOUNDARY LAYER SEPARATION**
- FLOW STABILITY**
- Filtering of non-linear instabilities --- from finite difference solution of fluid dynamics equations
p0108 A79-32912
- Hydrodynamic effects in a misaligned radial face seal
[NASA-CN-135228] p0121 N79-17226
- Performance of a vortex-controlled diffuser in an annular swirl-can combustor at inlet Mach numbers up to 0.53
[NASA-TP-1452] p0017 N79-22099
- A throat-bypass stability-bleed system using relief valves to increase the transient stability of a mixed-compression inlet --- YF-12 aircraft inlet tests in the Lewis 10 by 10 ft supersonic wind tunnel
[NASA-TP-1083] p0023 N79-28176
- FLOW VISUALIZATION**
- NT NUMERICAL FLOW VISUALIZATION
- High speed smoke flow visualization for the determination of cascade shock losses
[AIAA PAPER 79-0042] p0005 A79-19495
- Low-turbulence high-speed wind tunnel for the determination of cascade shock losses
[ASME PAPER 79-GT-129] p0039 A79-32398
- Holography through optically active windows
[NASA-TP-1414] p0109 N79-17195
- Flow visualization of discrete-hole film cooling with spanwise injection over a cylinder
[NASA-TP-1491] p0023 N79-27142
- FLUID DYNAMICS**
- NT AERODYNAMICS
- NT ELASTICHYDRODYNAMICS
- NT HYDRODYNAMICS
- NT MAGNETOHYDRODYNAMICS
- NT ROTOR AERODYNAMICS
- Filtering of non-linear instabilities --- from finite difference solution of fluid dynamics equations
p0108 A79-32912
- Application of the principle of similarity fluid mechanics
[NASA-TN-79258] p0105 N79-30515
- FLUID FILMS**
- Design and test of a squeeze-film damper for a flexible power transmission shaft
p0123 A79-16011
- Energy conservation through sealing technology
p0118 A79-20700
- Effect of geometry on hydrodynamic film thickness
[ASME PAPER 78-LUB-24] p0118 A79-23237
- FLUID FILTERS**
- Filtration effects on ball bearing life and condition in a contaminated lubricant
[ASME PAPER 78-LUB-34] p0118 A79-23246
- Filtering of non-linear instabilities --- from finite difference solution of fluid dynamics equations
p0108 A79-32912
- FLUID FLOW**
- NT AIR FLOW
- NT ANNULAR FLOW
- NT AXIAL FLOW
- NT BOUNDARY LAYER SEPARATION
- NT CAPILLARY FLOW
- NT CASCADE FLOW
- NT CHANNEL FLOW
- NT COMPRESSIBLE FLOW
- NT CREEP FLOW
- NT DUCTED FLOW
- NT GAS FLOW
- NT HARTMANN FLOW
- NT INCOMPRESSIBLE FLOW
- NT INLET FLOW

- NT INVISCID FLOW
 NT JET FLOW
 NT JET MIXING FLOW
 NT MAGNETOHYDRODYNAMIC FLOW
 NT MASS FLOW
 NT MERIDIONAL FLOW
 NT NONUNIFORM FLOW
 NT NOZZLE FLOW
 NT ONE DIMENSIONAL FLOW
 NT OUTLET FLOW
 NT POTENTIAL FLOW
 NT SECONDARY FLOW
 NT STEADY FLOW
 NT STEAM FLOW
 NT SUBSONIC FLOW
 NT SUPERSONIC FLOW
 NT THREE DIMENSIONAL FLOW
 NT TRANSONIC FLOW
 NT TURBULENT FLOW
 NT TWO DIMENSIONAL FLOW
 NT TWO PHASE FLOW
 NT UNSTEADY FLOW
 NT VISCOUS FLOW
 NT WALL FLOW
 NT WATER FLOW
 Compressible flow across narrow passages:
 Comparison of theory and experiment for face seals
 [NASA-TM-1346] p0113 N79-10424
 Self-stabilizing radial face seal
 [NASA-CASE-LEW-12991-1] p0113 N79-12445
- FLUID INJECTION**
 NT GAS INJECTION
 NT WATER INJECTION
 Effect of steam addition on cycle performance of
 simple and recuperated gas turbines
 [NASA-TM-1440] p0137 N79-22626
- FLUID JETS**
 NT FREE JETS
 Atomization of water jets and sheets in axial and
 swirling airflows
 [NASA-TM-79043] p0102 N79-12362
- FLUID MECHANICS**
 NT AERODYNAMICS
 NT ELASTIC HYDRODYNAMICS
 NT FLUID DYNAMICS
 NT HYDRODYNAMICS
 NT MAGNETOHYDRODYNAMICS
 NT ROTOR AERODYNAMICS
 Thermophysical property data: Who needs them?
 [NASA-TM-79241] p0090 N79-31403
- FLUID PRESSURE**
 Self-stabilizing radial face seal
 [NASA-CASE-LEW-12991-1] p0113 N79-12445
- FLUID TRANSMISSION LINES**
 Transmission seal development
 [NASA-CR-135372] p0120 N79-10423
 Low heat leak connector for cryogenic systems
 [NASA-CASE-XLE-02367-1] p0093 N79-21225
- FLUIDIZED BED PROCESSORS**
 Burn coal cleanly in a fluidized bed - The key is
 in the controls
 p0071 N79-26374
 Reduction of particulate carryover from a
 pressurized fluidized bed
 p0150 N79-49527
 Reduction of particulate carryover from a
 pressurized fluidized bed
 p0150 N79-49527
 Three-dimensional finite-element elastic analysis
 of a thermally cycled single-edge wedge geometry
 specimen
 [NASA-TM-79026] p0172 N79-16644
 Simulation of fluidized bed coal combustors
 [NASA-CR-159529] p0153 N79-20487
 Preliminary comparison of theory and experiment
 for a conical, pressurized-fluidized-bed coal
 combustor
 [NASA-TM-79137] p0137 N79-22623
 Reduction of particulate carryover from a
 pressurized fluidized bed
 [NASA-TM-79216] p0141 N79-27664
- FLUORIDES**
 A comparison of the lubricating mechanisms of
 graphite fluoride and molybdenum disulfide films
 p0085 N79-16659
 Mechanisms of graphite fluoride /CF_x/n lubrication
 p0086 N79-31249
 Effect of thermal aging on the tribological
 properties of polyimide films and
 polyimide-bonded graphite fluoride films
 [NASA-TM-79045] p0082 N79-15186
- FLUORINATION**
 Electrochemical fluorination of trichloroethylene
 and N, N-dimethyltrifluoroacetamide
 p0060 A79-49536
 Electrochemical fluorination of trichloroethylene
 and N, N-dimethyltrifluoroacetamide
 p0060 A79-49536
 Electrochemical fluorination of trichloroethylene
 and N, N-dimethyltrifluoroacetamide
 [NASA-TM-79188] p0059 N79-27242
- FLUORINE COMPOUNDS**
 NT FLUORIDES
 NT FLUORO COMPOUNDS
 NT FLUOROPOLYMERS
FLUORINE ORGANIC COMPOUNDS
 NT FLUOROPOLYMERS
FLUORO COMPOUNDS
 NT FLUOROPOLYMERS
 Electrochemical fluorination of trichloroethylene
 and N, N-dimethyltrifluoroacetamide
 [NASA-TM-79188] p0059 N79-27242
- FLUOROPOLYMERS**
 NT TEFLON (TETRAFLUOROETHYLENE)
 Ion beam sputtering of fluoropolymers
 p0117 A79-14797
 Adhesive bonding of ion beam textured metals and
 fluoropolymers
 p0060 A79-14798
 Adhesive bonding of ion beam textured metals and
 fluoropolymers
 [NASA-TM-79004] p0181 N79-12909
 Ion beam sputter deposition of fluoropolymers
 [NASA-CASE-LEW-13122-1] p0083 N79-24154
- FLUTTER**
 NT SUPERSONIC FLUTTER
 NT TRANSONIC FLUTTER
FLUTTER ANALYSIS
 Synthesis of blade flutter vibratory patterns
 using stationary transducers
 p0127 A79-10823
 Supersonic unstalled flutter
 p0004 A79-12599
 Characteristics of aeroelastic instabilities in
 turboachinery - NASA full scale engine test
 results
 [AIAA 79-7011] p0027 A79-29386
 A summary of NASA/Air Force Full Scale Engine
 Research programs using the F100 engine
 [AIAA PAPER 79-1308] p0030 A79-40488
 Supersonic unstalled flutter --- aerodynamic
 loading of thin airfoils induced by cascade motion
 [NASA-TM-79001] p0002 N79-11000
 A summary of NASA/Air Force full scale engine
 research programs using the F100 engine
 [NASA-TM-79267] p0024 N79-30188
- FLUX (RATE PER UNIT AREA)**
 U FLUX DENSITY
FLUX DENSITY
 NT CURRENT DENSITY
 NT ELECTRON FLUX DENSITY
 NT RADIANCE
 Critical mass flux through short Borda type inlets
 of various cross sections
 [NASA-TM-79017] p0074 N79-20216
- FLUX MAPPING**
 U FLUX DENSITY
 U MAPPING
FLUX PINNING
 Comparison of projected critical currents in
 Pb0.65Sb and Nb3Ge
 p0185 A79-28300
- FLUXMETERS**
 U MEASURING INSTRUMENTS
FLYING QUALITIES
 U FLIGHT CHARACTERISTICS
FOCUSING
 Efficiency enhancement of dual-mode traveling wave
 tubes at saturation and in the linear range by
 use of spent-beam refocusing and multistage
 depressed collectors
 [NASA-TM-1486] p0098 N79-28420
- FOIL BEARINGS**
 Mini-BRO/BIPS foil bearing development
 [NASA-CR-159442] p0120 N79-11407
- POKKER BOND TESTERS**
 U ADHESION TESTS

FORCE FIELDS

U FIELD THEORY (PHYSICS)

FORCED OSCILLATION

U FORCED VIBRATION

FORCED VIBRATION

Experimental evaluation of the effect of inlet distortion on compressor blade vibrations
[NASA-TN-79066] p0126 N79-16300

FORCED VIBRATORY MOTION EQUATIONS

U FORCED VIBRATION

FORECASTING

NT PERFORMANCE PREDICTION

NT PREDICTION ANALYSIS TECHNIQUES

NT TECHNOLOGICAL FORECASTING

FOREIGN POLICY

NT INTERNATIONAL COOPERATION

FORMING TECHNIQUES

NT EXTRUDING

NT METAL DRAWING

NT ROLL FORMING

FOSSIL FUELS

NT COAL

NT CRUDE OIL

Benefits of solar/fossil hybrid gas turbine systems
[ASME PAPER 79-G1-38] p0147 A79-30554

FRACTURE MECHANICS

The effects of eccentricities on the fracture of off-axis fiber composites p0064 A79-15543

Mode I analysis of a cracked circular disk subject to a couple and a force p0128 A79-15588

Stresses from arbitrary loads on a circular crack p0130 A79-27938

Fracture modes in off-axis fiber composites p0065 A79-31035

Friction and fracture of single-crystal silicon carbide in contact with itself and titanium p0086 A79-32149

CODSTRAN - Composite durability structural analysis p0128 A79-37292

On the equivalence between semiempirical fracture analyses and R-curves p0129 A79-39813

Fracture modes in off-axis fiber composites [NASA-TN-79036] p0062 N79-12154

On the equivalence between semiempirical fracture analyses and R-curves [NASA-TN-79127] p0103 N79-20338

Mode I crack surface displacements for a round compact specimen subject to a couple and force [NASA-TN-79096] p0161 A79-20572

Definition of actually optimum NDI and proof test criteria for 2219 aluminum pressure vessels. Volume 1: Methods [NASA-CR-135445] p0125 N79-21410

FRACTURE RESISTANCE

U FRACTURE STRENGTH

FRACTURE STRENGTH

Mode I analysis of a face cracked plate subjected to rotationally constrained end displacements p0128 A79-12831

Influence of composition, annealing treatment, and texture on the fracture toughness of Ti-5Al-2.5Sn plate at cryogenic temperatures p0077 A79-24262

Proof test criteria for thin walled pressure vessels p0123 A79-26985

Mechanisms of boron fiber strengthening by thermal treatment p0065 A79-30396

Mode I crack surface displacements for a round compact specimen subject to a couple and force p0129 A79-39812

Process for making a high toughness-high strength ion alloy [NASA-CASE-LEW-12542-2] p0074 N79-22271

Bond strengths of reaction bonded silicon nitride prepared from dry attrition milled silicon powder [NASA-TN-79230] p0084 N79-30379

FRACTURE TOUGHNESS

U FRACTURE STRENGTH

FRACTURES (MATERIALS)

Stress analysis for structures with surface cracks [NASA-CR-159400] p0125 N79-13405

User's manual for FRAC3D: Supplement to report on stress analysis for structures with surface cracks [NASA-CR-159401] p0129 N79-13406

Anisotropic friction, deformation, and fracture of single-crystal silicon carbide at room temperature [NASA-TF-1525] p0084 N79-30380

FRAMES

NT AIRFRAMES

FRAUNHOFER REGION

U FAR FIELDS

FREE JETS

The free jet as a simulator of forward velocity effects on jet noise [NASA-CR-3056] p0176 N79-14673

Some aspects of a free jet phenomena to 105 L/D in a constant area duct [NASA-TN-79050] p0127 N79-20391

Free jet phenomena in a 90 degree-sharp edge inlet geometry [NASA-TN-79229] p0105 N79-31526

FREE RADICALS

Improved apparatus for trapped radical and other studies down to 1.5 K --- microwave cavity cryogenic equipment for electron paramagnetic resonance experiments p0110 A79-20742

FREEZING

Design and evaluation of aircraft heat source systems for use with high-freezing point fuels [NASA-CR-159568] p0091 N79-24172

FREEZING POINTS

U MELTING POINTS

FREQUENCIES

NT C BAND

NT CARRIER FREQUENCIES

NT EXTREMELY HIGH FREQUENCIES

NT LOW FREQUENCIES

NT PLASMA FREQUENCIES

NT RADIO FREQUENCIES

NT RESONANT FREQUENCIES

NT SUPERHIGH FREQUENCIES

NT ULTRAHIGH FREQUENCIES

Analysis of radiation patterns of interaction tones generated by inlet rods in the J115E engine [NASA-TN-79074] p0016 N79-15960

FREQUENCY BANDS

U FREQUENCIES

FREQUENCY CONTROL

Cam-operated pitch-change apparatus [NASA-CASE-LEW-13050-1] p0014 N79-14095

FREQUENCY DISTRIBUTION

Reynolds number, scale and frequency content effects on F-15 inlet instantaneous distortion [AIAA PAPER 79-0104] p0005 A79-19533

FREQUENCY MODULATION

Carrier: Interference ratios for frequency sharing between satellite systems transmitting frequency modulated and digital television signals [NASA-TN-79265] p0094 N79-33379

FREQUENCY REGULATION

U FREQUENCY CONTROL

FRETTING CORROSION

Fretting wear of iron, nickel, and titanium under varied environmental conditions p0078 A79-34995

Fretting wear of iron, nickel, and titanium under varied environmental conditions [NASA-TN-78972] p0073 N79-12203

FRICTION

NT FLOW RESISTANCE

NT SLIDING FRICTION

The friction and wear properties of sputtered hard refractory compounds p0085 A79-16666

Effect of nitrogen-containing plasma on adherence, friction, and wear of radiofrequency-sputtered titanium carbide coatings [NASA-TF-1377] p0081 N79-15184

Friction and wear of single-crystal manganese-zinc ferrite [NASA-TN-78980] p0184 N79-16699

FRICTION COEFFICIENT

U COEFFICIENT OF FRICTION

FRICTION MEASUREMENT

Auger spectroscopy analysis in adhesion, friction and wear studies p0110 A79-10992

Use of a nitrogen-argon plasma to improve adherence of sputtered titanium carbide coatings on steel p0119 A79-25103

Determination of lubricant selection based on elastohydrodynamic film thickness and traction measurement
[NASA-CR-159428] p0121 N79-14385

FRICTION REDUCTION

Surface chemistry of iron sliding in air and nitrogen lubricated with hexadecane and hexadecane containing dibenzyl-dithiolide
[NASA-TF-1545] p0059 N79-31346

FUEL CELL CATALYSTS

U ELECTROCATALYSTS

FUEL CELLS

HT HYDROGEN OXYGEN FUEL CELLS

Fuel cell on-site integrated energy system parametric analysis of a residential complex
p0146 A79-14947

Commercial phosphoric acid fuel cell system technology development
p0150 A79-51809

The role of fuel cells in NASA's space power systems
p0056 N79-51810

Technology status: Batteries and fuel cell
p0052 N79-10132

Fuel cell on-site integrated energy system parametric analysis of a residential complex
[NASA-TM-7899] p0188 N79-11955

Analysis of a fuel cell on-site integrated energy system for a residential complex
[NASA-TM-79161] p0137 N79-22624

The role of fuel cells in NASA's space power systems
[NASA-TM-79182] p0053 N79-23133

Commercial phosphoric acid fuel cell system technology development
[NASA-TM-79169] p0139 N79-25500

Recent advances in redox flow cell storage systems
[NASA-TM-79186] p0141 N79-26505

Technology development for phosphoric acid fuel cell powerplant, phase 2
[NASA-CR-159572] p0153 N79-29604

Ultrafine polybenzimidazole (PBI) fibers --- separators for alkaline batteries and fuel cells
[NASA-CR-159644] p0067 N79-31350

Advanced technology light weight fuel cell program --- for space power applications
[NASA-CR-159653] p0155 N79-33581

FUEL COMBUSTION

Characteristics and combustion of future hydrocarbon fuels
p0090 A79-11599

Impact of future fuel properties on aircraft engines and fuel systems
p0024 A79-11600

Effect of a chromium-containing fuel additive on hot corrosion
p0071 A79-26546

Effect of degree of fuel vaporization upon emissions for a premixed prevaporized combustion system
[AIAA PAPER 79-1320] p0071 A79-39036

Preliminary results in the NASA Lewis H2-C2 combustion MHD experiment
p0182 A79-39807

Characteristics and combustion of future hydrocarbon fuels
p0085 N79-13196

Effect of swirler-mounted mixing venturi on emissions of flame-tube combustor using jet A fuel
[NASA-TF-1393] p0015 N79-14099

Airfoil cooling hole plugging by combustion gas impurities of the type found in coal derived fuels
[NASA-TM-79076] p0089 N79-20265

Premix fuels study applicable to duct burner conditions for a variable cycle engine
[NASA-CR-159513] p0091 N79-20266

Premixed Prevaporized Combustor Technology Forum
[NASA-CR-2078] p0019 N79-24994

Effect of fuel sprays on emissions
p0020 N79-24999

Autoignition of fuels
p0020 N79-25001

Effect of degree of fuel vaporization on emissions for a premixed-prevaporized combustor system
p0020 N79-25003

Effect of fuel/air nonuniformity on nitric oxide emissions
p0020 N79-25004

Feasibility study of liquid pool burning in reduced gravity
[NASA-CR-159642] p0072 N79-32303

FUEL CONSUMPTION

Fuel conservative aircraft engine technology
p0025 A79-20078

Concepts for reducing exhaust emissions and fuel consumption of the aircraft piston engine
[SAE PAPER 790605] p0036 A79-36737

Analysis of a fuel cell on-site integrated energy system for a residential complex
[AIAA PAPER 79-0990] p0147 A79-38192

Energy efficient aircraft engines
[AIAA PAPER 79-1861] p0030 A79-47918

Automotive Stirling engine development program
[NASA-CR-159436] p0120 N79-11406

Energy efficient engine preliminary design and integration study
[NASA-CR-135396] p0012 N79-12084

Energy efficient engine: Propulsion system-aircraft integration evaluation
[NASA-CR-159488] p0032 N79-16850

Wind tunnel performance of four energy efficient propellers designed for Mach 0.8 cruise --- Lewis 8x6 foot wind tunnel studies for noise reduction in high speed turboprop aircraft
[NASA-TM-79124] p0003 N79-20069

Energy efficient aircraft engines
[NASA-TM-79204] p0022 N79-27141

CF6 jet engine performance improvement program. Short core exhaust nozzle performance improvement concept --- specific fuel consumption reduction
[NASA-CR-159564] p0038 N79-33206

FUEL FLOW REGULATORS

Lean stability augmentation for premixing, prevaporizing combustors
[AIAA PAPER 79-1319] p0036 A79-39035

FUEL INJECTION

Effect of swirl-mounted mixing venturi on emissions of flame-tube combustor using jet A fuel
[NASA-TF-1393] p0015 N79-14099

Computer simulation of an aircraft engine fuel injection system
[NASA-CR-157641] p0016 N79-15052

Effects of air injection on a turbocharged Teledyne Continental Motors TS10-360-C engine
[NASA-TM-79121] p0158 N79-20528

Measurements of admittances and characteristic combustion times of reactive gaseous propellant coaxial injectors
[NASA-CR-159542] p0072 N79-23168

Performance of a multiple venturi fuel-air preparation system --- fuel injection for gas turbines
p0020 N79-25000

FUEL PUMPS

Liquid oxygen/liquid hydrogen boost/vane pump for the advanced orbit transfer vehicles auxiliary propulsion system
[NASA-CR-159648] p0057 N79-31341

FUEL SPRAYS

Fuel spray data with LDV --- solar laser morphokinometer capabilities in combustion research
p0019 N79-24997

Modeling of premixing-prevaporizing fuel-air mixing passages
p0019 N79-24998

Effect of fuel sprays on emissions
p0020 N79-24999

FUEL SYSTEMS

HT AIRCRAFT FUEL SYSTEMS

Impact of future fuel properties on aircraft engines and fuel systems
p0024 A79-11600

Effect of broadened-specification fuels on aircraft engines and fuel systems
[AIAA 79-7608] p0027 A79-29383

Fuel delivery system including heat exchanger means
[NASA-CASE-LEW-12793-1] p0113 N79-11403

Impact of future fuel properties on aircraft engines and fuel systems
p0089 N79-13197

FUEL TANKS

Inflight fuel tank temperature survey data
[NASA-CR-159569] p0009 N79-23940

Atlas 5013 tank corrosion test
[NASA-CR-158760] p0050 N79-27234

FUEL TESTS

Evaluation of the application of some gas chromatographic methods for the determination of

properties of synthetic fuels p0070 A79-25917

FUEL-AIR RATIO

Effects of air injection on a turbocharged
Teledyne Continental Motors TSIO-360-C engine
[NASA-TM-79121] p0158 A79-20528

Lean, premixed, prevaporized combustion for
aircraft gas turbine engines
[NASA-TM-79148] p0018 A79-23964

Lean, premixed, prevaporized combustion for
aircraft gas turbine engines
[NASA-TM-79148] p0018 A79-23964

Effect of degree of fuel vaporization upon
emissions for a premixed prevaporized combustion
system --- for gas turbine engines
[NASA-TM-79154] p0012 A79-23965

Performance of a multiple venturi fuel-air
preparation system --- fuel injection for gas
turbines p0020 A79-25000

Emissions measurements for a lean premixed
propane/air system at pressures up to 30
atmospheres p0020 A79-25002

Effect of fuel/air nonuniformity on nitric oxide
emissions p0020 A79-25004

Lean Stability augmentation study p0021 A79-25007

Lean, premixed, prevaporized fuel combustor
conceptual design study
[NASA-CR-159647] p0035 A79-32211

FUELS

NT AIRCRAFT FUELS

NT AUTOMOBILE FUELS

NT COAL

NT CRYOGENIC ROCKET PROPELLANTS

NT DIESEL FUELS

NT FOSSIL FUELS

NT GASOLINE

NT HIGH ENERGY FUELS

NT HYDROCARBON FUELS

NT JET ENGINE FUELS

NT JP-5 JET FUEL

NT LIQUID ROCKET PROPELLANTS

NT SYNTHETIC FUELS

Ion chromatographic determination of sulfur in fuels
[NASA-TM-78971] p0157 A79-17358

FULL SCALE TESTS

Full-scale engine tests of bulk absorber acoustic
inlet treatment
[AIAA PAPER 79-0600] p0026 A79-26881

Assessment at full scale of nozzle/wing geometry
effects on OTW aeroacoustic characteristics ---
Over The Wing STCL engine configurations p0175 A79-39802

A summary of NASA/Air Force Full Scale Engine
Research programs using the F100 engine
[AIAA PAPER 79-1308] p0030 A79-40488

FUNCTIONS (MATHEMATICS)

NT LOGARITHMS

NT PROBABILITY DISTRIBUTION FUNCTIONS

NT TIME FUNCTIONS

NT TRANSFER FUNCTIONS

FUSION WELDING

NT BRAZING

G

GAGES

U MEASURING INSTRUMENTS

GALLIUM ARSENIDES

Shallow-homojunction GaAs solar cells p0144 A79-32666

GALLIUM COMPOUNDS

NT GALLIUM ARSENIDES

GALVANIC CELLS

U ELECTROLYTIC CELLS

GALVANOMAGNETIC EFFECTS

Anomalous galvanomagnetic properties of graphite
in strong magnetic fields p0185 A79-23633

GALVANOMAGNETISM

U GALVANOMAGNETIC EFFECTS

GARP

U GLOBAL ATMOSPHERIC RESEARCH PROGRAM

GAS ANALYSIS

NT GROMMETHY

Emission measurements for a lean premixed
propane/air system at pressures up to 30
atmospheres [NASA-CR-159421] p0071 A79-10165

GAS BEARINGS

Development of surface coatings for
air-lubricated, compliant journal bearings to
650 C [ASLE PREPRINT 78-LC-3C-1] p0123 A79-23252

Static evaluation of surface coatings for
compliant gas bearings in an oxidizing
atmosphere to 650 C p0088 A79-31957

Cantilever mounted resilient pad gas
bearing [NASA-CASE-LEW-12569-1] p0113 A79-10418

Operating characteristics of a cantilever-mounted
resilient-pad gas-lubricated thrust bearing
[NASA-TF-1438] p0115 A79-22518

GAS CHROMATOGRAPHY

Evaluation of the application of some gas
chromatographic methods for the determination of
properties of synthetic fuels p0070 A79-25917

Evaluation of the application of some gas
chromatographic methods for the determination of
properties of synthetic fuels [NASA-TF-79035] p0068 A79-16930

GAS DYNAMICS

NT AERODYNAMICS

NT ROTOR AERODYNAMICS

GAS EXPLOSIONS

Resonance-tube ignition of aluminum p0071 A79-46366

GAS FLOW

NT AIR FLOW

NT ERIDICNAL FLOW

Stiffness of straight and tapered annular gas path
seals [ASME PAPER 78-LUB-18] p0118 A79-23235

Gas path sealing in turbine engines p0013 A79-11057

Thermal stress analysis of ceramic gas-path seal
components for aircraft turbines [NASA-TF-1437] p0082 A79-21205

GAS GENERATOR ENGINES

U ENGINES

GAS INJECTION

Effects of air injection on a turbocharged
Teledyne Continental Motors TSIO-360-C engine
[SAE PAPER 790607] p0028 A79-36760

GAS IONIZATION

Hydrogen hollow cathode ion source
[NASA-CASE-LEW-12940-1] p0181 A79-10894

GAS LASERS

NT ULTRAVIOLET LASERS

Gain measurements of the Ca-Ie charge exchange
system --- for UV lasers p0112 A79-19078

GAS LIQUEFACTION

U CONDENSING

GAS LUBRICANTS

Cantilever mounted resilient pad gas
bearing [NASA-CASE-LEW-12569-1] p0113 A79-10418

GAS LUBRICATED BEARINGS

U GAS BEARINGS

GAS MIXTURES

Emission measurements for a lean premixed
propane/air system at pressures up to 30
atmospheres [NASA-CR-159421] p0071 A79-10165

Lean, premixed, prevaporized combustion for
aircraft gas turbine engines [NASA-TM-79148] p0018 A79-23964

Lean, premixed, prevaporized combustion for
aircraft gas turbine engines [NASA-TM-79148] p0018 A79-23964

Effect of degree of fuel vaporization upon
emissions for a premixed prevaporized combustion
system --- for gas turbine engines [NASA-TM-79154] p0012 A79-23965

Emissions measurements for a lean premixed
propane/air system at pressures up to 30
atmospheres p0020 A79-25002

Effect of degree of fuel vaporization on emissions
for a premixed-prevaporized combustor system p0020 A79-25003

Effect of fuel/air nonuniformity on nitric oxide
emissions

- Lean, premixed, prevaporized fuel combustor
conceptual design study
[NASA-CR-155647] p0020 N79-25004
- GAS PHASES**
U VAPOR PHASES
GAS SPECTROSCOPY
NT FLAME SPECTROSCOPY
GAS TEMPERATURE
Predicted inlet gas temperatures for tungsten
fiber reinforced superalloy turbine blades
p0025 A79-17029
- GAS TURBINE ENGINES**
NT DUCTED FAN ENGINES
NT J-85 ENGINE
NT JET ENGINES
NT T-53 ENGINE
NT T-55 ENGINE
NT T-63 ENGINE
NT TF-30 ENGINE
NT TURBOFAN ENGINES
NT TURBOJET ENGINES
NT TURBOPROP ENGINES
Liquid-cooling technology for gas turbines -
Review and status p0116 A79-10038
- Wide range operation of advanced low NOx aircraft
gas turbine combustors
[ASME PAPER 78-GT-128] p0024 A79-10792
- Pressure instrumentation for gas turbine engines -
A review of measurement technology
[ASME PAPER 78-GT-148] p0110 A79-10800
- Effect of inlet temperature on the performance of
a catalytic reactor p0070 A79-11542
- Alternative aviation turbine fuels p0090 A79-12378
- Ceramics for the advanced automotive gas turbine
engine - A look at a single shaft design
p0117 A79-12850
- The NASA high pressure facility and turbine test rig
p0038 A79-21296
- Emission and absorptance of the National
Aeronautics and Space Administration ceramic
thermal barrier coating --- for gas turbine
engine components p0086 A79-27231
- A feasibility study of a diffusion barrier between
Ni-Cr-Al coatings and nickel-based eutectic alloys
p0077 A79-27233
- An oxide dispersion strengthened alloy for gas
turbine blades
[AIAA 79-0763] p0077 A79-28276
- Thermal-structural mission analyses of air-cooled
gas turbine blades
[ASME PAPER 79-GT-19] p0027 A79-30553
- The Advanced Low-Emissions Catalytic-Combustor
Program: Phase I - Description and status ---
for aircraft gas turbine engines
[ASME PAPER 79-GT-192] p0027 A79-30557
- Consolidation of Si3N4 by hot isostatic pressing
p0086 A79-32931
- Tests of NASA ceramic thermal barrier coating for
gas-turbine engines p0086 A79-34996
- Effects of air injection on a turbocharged
Teledyne Continental Motors TSIO-360-C engine
[SAE PAPER 790607] p0028 A79-36760
- Analysis of the impact of the use of broad
specification fuels on combustors for commercial
aircraft gas turbine engines
[AIAA PAPER 79-1195] p0090 A79-38980
- Lean, premixed, prevaporized combustion for
aircraft gas turbine engines
[AIAA PAPER 79-1318] p0029 A79-39034
- Lean stability augmentation for premixing,
prevaporizing combustors
[AIAA PAPER 79-1319] p0036 A79-39035
- Materials and structural aspects of advanced
gas-turbine helicopter engines p0029 A79-39804
- Causes of high pressure compressor deterioration
in service
[AIAA PAPER 79-1234] p0036 A79-40483
- Fundamental mechanisms that influence the estimate
of heat transfer to gas turbine blades
p0099 A79-49526
- The role of NaCl in flame chemistry, in the
deposition process, and in its reactions with
protective oxides as related to hot corrosion
p0071 A79-49534
- Study of 153 engine vibration
[NASA-CR-135449] p0030 N79-10061
- Gas path sealing in turbine engines p0013 N79-11057
- Self-acting shaft seals --- gas turbine engines
p0013 N79-11070
- Thermal-structural mission analyses of air-cooled
gas turbine blades
[NASA-TM-78963] p0126 N79-11433
- Correlations of catalytic combustor performance
parameters
[NASA-TM-79014] p0134 N79-11480
- Experimental clean combustor program: Phase 3:
Turbulence measurement addendum
[NASA-CR-135422] p0031 N79-12088
- Development of sprayed ceramic seal systems for
turbine gas path sealing
[NASA-TM-79022] p0081 N79-12223
- Cold-air performance of free power turbine
designed for 112-kilowatt automotive gas-turbine
engine 3: Effect of stator vane end clearances
on performance
[NASA-TM-78956] p0014 N79-13049
- Analytical evaluation of the impact of broad
specification fuels on high bypass turbofan
engine combustors
[NASA-CR-159454] p0031 N79-13050
- Integrated gas turbine engine-nacelle
[NASA-CASE-LEW-12389-3] p0014 N79-14096
- Variable area exhaust nozzle
[NASA-CASE-LEW-12378-1] p0014 N79-14097
- A method to estimate weight and dimensions of
large and small gas turbine engines
[NASA-CR-159481] p0015 N79-15046
- Study of mean- and turbulent-velocity fields in a
large-scale turbine-vane passage
[NASA-CR-3067] p0032 N79-16853
- Effect of thermal barrier coatings on the
performance of steam and water-cooled gas
turbine/steam turbine combined cycle system
[NASA-TM-79057] p0135 N79-17334
- Cold-air performance of free power turbine
designed for 112-kilowatt automotive gas-turbine
engine. 2: Effects of variable
stator-vane-chord setting angle on turbine
performance
[NASA-TM-78993] p0017 N79-17859
- Rotor fragment protection program: Statistics on
aircraft gas turbine engine rotor failures that
occurred in US commercial aviation during 1976
[NASA-CR-159474] p0032 N79-18977
- Strain gage system evaluation program
[NASA-CR-159486] p0110 N79-19314
- Materials and structural aspects of advanced
gas-turbine helicopter engines
[NASA-TM-79100] p0001 N79-20008
- Tests of NASA ceramic thermal barrier coating for
gas-turbine engines
[NASA-TM-79116] p0017 N79-20118
- An oxide dispersion strengthened alloy for gas
turbine blades
[NASA-TM-79088] p0052 N79-20180
- Study of an advanced General Aviation Turbine
Engine (GATE)
[NASA-CR-159558] p0033 N79-21073
- Evaluation of ceramics for stator application:
Gas turbine engine report
[NASA-CR-159533] p0033 N79-21075
- Lean stability augmentation study --- on gas
turbine combustion chambers
[NASA-CR-159536] p0071 N79-22244
- Lean, premixed, prevaporized combustion for
aircraft gas turbine engines
[NASA-TM-79148] p0018 N79-23964
- Lean, premixed, prevaporized combustion for
aircraft gas turbine engines
[NASA-TM-79148] p0018 N79-23964
- Effect of degree of fuel vaporization upon
emissions for a premixed prevaporized combustion
system --- for gas turbine engines
[NASA-TM-79154] p0012 N79-23965
- Premixed Prevaporized Combustor Technology Forum
[NASA-CP-2078] p0019 N79-24994
- Turbulence characteristics of compressor discharge
flows --- JT9D engine tests p0019 N79-24995

- Turbulence measurements in the compressor exit
flow of a General Electric CF6-50 engine
[NASA-CR-159604] p0019 N79-24996
- Advanced low emissions catalytic combustor program
at General Electric
[NASA-TP-1425] p0021 N79-25011
- Internally coated air-cooled gas turbine blading
[NASA-CR-159574] p0034 N79-25018
- Industry tests of NASA ceramic thermal barrier
coating --- for gas turbine engine applications
[NASA-TP-1425] p0022 N79-25013
- Experimental studies of the formation/deposition
of sodium sulfate in/from combustion gases ---
hot corrosion in gas turbine engines
[NASA-CR-159612] p0072 N79-25183
- Brayton-cycle component characteristics
[NASA-TP-1425] p0140 N79-26479
- Laser anemometer measurements at the exit of a
T63-C20 combustor
[NASA-CR-159623] p0107 N79-28456
- Advanced General Aviation Turbine Engine (GATE)
study
[NASA-CR-159624] p0039 N79-29189
- An experimental, low-cost, silicon
slurry/aluminate high-temperature coating for
superalloys
[NASA-TM-79178] p0075 N79-29292
- State-of-the-art of SiAlON materials --- conferences
[NASA-TM-79207] p0084 N79-30378
- Conceptual design study of improved automotive
gas turbine powertrain
[NASA-CR-159580] p0189 N79-31088
- Lean, Premixed-Evaporized (LPE) combustor
conceptual design study
[NASA-CR-159629] p0072 N79-31358
- The chemistry of sodium chloride involvement in
processes related to hot corrosion --- in gas
turbine engines
[NASA-TM-79251] p0069 N79-31361
- Single shaft automotive gas turbine engine
characterization test
[NASA-CR-159654] p0189 N79-32129
- Lean, premixed, prevaporized fuel combustor
conceptual design study
[NASA-CR-159647] p0035 N79-32211
- GAS TURBINES**
- Benefits of solar/fossil hybrid gas turbine systems
[ASME PAPER 79-GT-38] p0147 A79-30554
- Apparatus and method for reducing thermal stress
in a turbine rotor
[NASA-CASE-LEW-12232-1] p0013 N79-10057
- Determining and improving labyrinth seal
performance in current and advanced high
performance gas turbines
[NASA-TP-1425] p0031 N79-11068
- Wear of seal materials used in aircraft propulsion
systems
[NASA-TM-79003] p0073 N79-12204
- Benefits of solar/fossil hybrid gas turbine systems
[NASA-TM-79083] p0134 N79-15410
- High velocity burner rig oxidation and thermal
fatigue behavior of Si3N4- and SiC base ceramics
to 1370 deg C
[NASA-TM-79040] p0082 N79-16984
- Fundamental mechanisms that influence the estimate
of heat transfer to gas turbine blades
[NASA-TM-79128] p0103 N79-20346
- Review and status of liquid-cooling technology for
gas turbines
[NASA-RP-1038] p0104 N79-22427
- Effect of steam addition on cycle performance of
simple and recuperated gas turbines
[NASA-TP-1440] p0137 N79-22626
- The strainrange partitioning behavior of an
advanced gas turbine disk alloy, AP2-1DA
[NASA-TM-79179] p0075 N79-23196
- Effect of fuel sprays on emissions
[NASA-TP-1425] p0020 N79-24999
- Performance of a multiple venturi fuel-air
preparation system --- fuel injection for gas
turbines
[NASA-TP-1425] p0020 N79-25000
- Fundamentals of Gas Turbine combustion
[NASA-CP-2087] p0022 N79-25016
- Gas-turbine critical research and advanced
technology support project
[NASA-TM-79139] p0139 N79-25498
- Conceptual design study of an Improved Gas Turbine
(IGT) powertrain
[NASA-CR-159604] p0189 N79-31087
- Development of SiAlON materials
[NASA-CR-159675] p0067 N79-33258
- Plasma-sprayed zirconia gas path seal technology:
A state-of-the-art review
[NASA-TM-79273] p0085 N79-33325
- GAS WELDING**
- NT BRAZING**
- GAS-LIQUID INTERACTIONS**
- NT AIR WATER INTERACTIONS**
- GAS-METAL INTERACTIONS**
- Survey of ion plating sources --- conferences
[NASA-TM-79269] p0076 N79-31372
- GAS-SOLID INTERACTIONS**
- NT GAS-METAL INTERACTIONS**
- GASEOUS CAVITATION**
- U GAS FLOW**
- GASEOUS ROCKET PROPELLANTS**
- Measurements of admittances and characteristic
combustion times of reactive gaseous propellant
coaxial injectors
[NASA-CR-159542] p0072 N79-23166
- GASES**
- NT ARGON**
- NT CARBON MONOXIDE**
- NT CHARGED PARTICLES**
- NT COMPRESSED GAS**
- NT EXHAUST GASES**
- NT GAS MIXTURES**
- NT HELIUM**
- NT HYDROGEN**
- NT HYDROGEN ATOMS**
- NT HYDROGEN IONS**
- NT HYDROGEN PLASMA**
- NT LIQUID HYDROGEN**
- NT LIQUID NITROGEN**
- NT LIQUID OXYGEN**
- NT NEUTRAL GASES**
- NT NITROGEN**
- NT NITROGEN IONS**
- NT OXYGEN**
- NT OZONE**
- NT RARE GASES**
- NT VACUUM**
- GASIFICATION**
- NT COAL GASIFICATION**
- GASOLINE**
- Automotive Stirling engine development program
[NASA-CR-159436] p0120 N79-11406
- GASP**
- U GLOBAL AIR SAMPLING PROGRAM**
- GEAR TEETH**
- Evaluation of high-contact-ratio spur gears with
profile modification
[NASA-TP-1458] p0115 N79-31604
- GEARS**
- The practical impact of elastohydrodynamic
lubrication
[NASA-TP-1458] p0117 A79-11545
- Evaluation of CBS 600 carburized steel as a gear
material
[NASA-TP-1390] p0114 N79-14389
- Speed reducers-increasers
[NASA-TP-1458] p0140 N79-26481
- Evaluation of high-contact-ratio spur gears with
profile modification
[NASA-TP-1458] p0115 N79-31604
- GENERAL AVIATION AIRCRAFT**
- NASA research on general aviation power plants
[AIAA PAPER 79-0561] p0026 A79-25870
- The GATE studies - Assessing the potential of
future small general aviation turbine engines
[NASA-TP-1440] p0027 A79-30560
- Preliminary QCGAT program test results --- Quiet,
Clean General Aviation Turbofan
[SAE PAPER 790596] p0028 A79-36729
- Concepts for reducing exhaust emissions and fuel
consumption of the aircraft piston engine
[SAE PAPER 790605] p0036 A79-36737
- New opportunities for future small civil turbine
engines - Overlooking the GATE studies
[SAE PAPER 790619] p0028 A79-36747
- A review of Curtiss-Wright rotary engine
developments with respect to general aviation
potential
[SAE PAPER 790621] p0036 A79-36749
- An overview of NASA research on positive
displacement type general aviation engines
[AIAA PAPER 79-1824] p0038 A79-53750

- NASA research on general aviation power plants
[NASA-TM-79031] p0014 N79-12086
- Preliminary QCGAT program test results
[NASA-TM-79013] p0016 N79-15051
- The gate studies: Assessing the potential of
future small general aviation turbine engines
[NASA-TM-79075] p0016 N79-15958
- The rotary combustion engine: A candidate for
general aviation --- conferences
[NASA-CP-2067] p0016 N79-15961
- New opportunities for future small civil turbine
engines: Overviewing the GATE studies
[NASA-TM-79073] p0017 N79-16849
- Study of an advanced General Aviation Turbine
Engine (GATE)
[NASA-CR-159558] p0033 N79-21073
- Advanced General Aviation Turbine Engine (GATE)
concepts
[NASA-CR-159603] p0034 N79-25017
- Advanced General Aviation Turbine Engine (GATE)
study
[NASA-CR-159624] p0039 N79-29189
- An overview of NASA research on positive
displacement type general aviation engines
[NASA-TM-79254] p0024 N79-31210
- GENERAL DYNAMICS AIRCRAFT**
NT F-102 AIRCRAFT
- GEOMAGNETIC EFFECTS**
U MAGNETIC EFFECTS
- GEOMAGNETIC STORMS**
U MAGNETIC STORMS
- GEOMETRICAL HYDROMAGNETICS**
U MAGNETOHYDRODYNAMICS
- GEOMETRY**
NT ANGLES (GEOMETRY)
NT ELLIPSES
NT FLOW GEOMETRY
NT NOZZLE GEOMETRY
NT TANK GEOMETRY
NT TOPOLOGY
Effect of geometry on hydrodynamic film thickness
[ASME PAPER 78-LUB-24] p0118 A79-23237
Effects of flameholder geometry on emissions and
performance of lean premixed combustors
p0021 N79-25005
- GEOSTATIONARY SATELLITES**
U SYNCHRONOUS SATELLITES
- GEOSYNCHRONOUS ORBITS**
Geosynchronous satellite operating anomalies
caused by interaction with the local spacecraft
environment
p0050 N79-24049
- GRADIENT ARC HEATERS**
U ARC HEATING
- GERMANIUM COMPOUNDS**
Nb₃Ge as a potential candidate material for 15-
25-T magnets
p0186 A79-44548
- GLASS**
NT GLASS FIBERS
- GLASS FIBER REINFORCED PLASTICS**
Analysis/design of strip reinforced random
composites /strip hybrids/
p0119 A79-24035
Dynamic mechanical analysis of fiber reinforced
composites
p0065 A79-31040
- GLASS FIBERS**
Fabrication and testing of non-graphitic
superhybrid composites
p0066 A79-43289
- GLOBAL AIR POLLUTION**
Global sensing of gaseous and aerosol trace
species using automated instrumentation on 747
airliners
p0110 A79-15067
Sulfate and nitrate mixing ratios in the vicinity
of the tropopause
p0158 A79-49494
Airborne atmospheric sampling system
p0012 A79-50333
- GLOBAL AIR SAMPLING PROGRAM**
Global sensing of gaseous and aerosol trace
species using automated instrumentation on 747
airliners
p0110 A79-15067
An analysis of the first two years of GASF data
--- Global Atmospheric Sampling Program
p0160 A79-15068
- NASA Global Atmospheric Sampling Program (GASF)
data report for tape VL0009
[NASA-TM-79058] p0157 N79-15448
- NASA Global Atmospheric Sampling Program (GASF)
data report for tapes VL0010 and VL0012
[NASA-TM-79061] p0157 N79-15450
- NASA Global Atmospheric Sampling Program (GASF)
data report for tapes VL0007 and VL0008
[NASA-TM-73784] p0157 N79-17359
- Ozone measurement system for NASA global air
sampling program
[NASA-TP-1451] p0158 N79-22654
- A summary of research on the NASA-Global
Atmospheric Sampling Program performed by the
Atmospheric Sciences Research Center --- ozone
transport theory
[NASA-CR-159614] p0159 N79-27716
- Carbon monoxide measurement in the global
atmospheric sampling program
[NASA-TP-1526] p0158 N79-31841
- GLOBAL ATMOSPHERIC RESEARCH PROGRAM**
Condensation-nuclei (Aitken Particle) measurement
system used in NASA global atmospheric sampling
program
[NASA-TP-1415] p0157 N79-18479
- GOLD**
Characterization of defect growth structures in
ion plated films by scanning electron microscopy
p0078 A79-34992
- GRADIENTS**
NT POTENTIAL GRADIENTS
NT PRESSURE GRADIENTS
Insulator edge voltage gradient effects in
spacecraft charging phenomena
[NASA-TM-78988] p0046 N79-11109
- GRADUATION**
U CALIBRATING
- GRAIN BOUNDARIES**
Effect of grain orientation and coating on thermal
fatigue resistance of a directionally solidified
superalloy (MAR-M 247)
[NASA-TM-79129] p0127 N79-22565
- GRAPHITE**
A comparison of the lubricating mechanisms of
graphite fluoride and molybdenum disulfide films
p0085 A79-16659
Graphite-fiber-reinforced polyimide liners of
various compositions in plain spherical bearings
p0117 A79-16678
Anomalous galvanomagnetic properties of graphite
in strong magnetic fields
p0185 A79-23633
Mechanisms of graphite fluoride /CF_x/n lubrication
p0086 A79-31249
Effect of thermal aging on the tribological
properties of polyimide films and
polyimide-bonded graphite fluoride films
[NASA-TM-79045] p0082 N79-15186
Polyimide prepreg material having improved tack
retention --- polyimide-graphite fiber composites
[NASA-CASE-LEW-12933-1] p0059 N79-24061
Lubricating and wear mechanisms for a hemisphere
sliding on polyimide-bonded graphite fluoride film
[NASA-TP-1524] p0084 N79-30381
- GRAPHITE-EPOXY COMPOSITE MATERIALS**
Impact behavior of filament-wound graphite/epoxy
fan blades --- foreign object damage to turbofan
engines
p0025 A79-20880
Analysis/design of strip reinforced random
composites /strip hybrids/
p0119 A79-24035
Fracture modes in off-axis fiber composites
p0065 A79-31035
Fabrication and testing of nongraphitic
superhybrid composites
[NASA-TM-79102] p0063 N79-20188
Evaluation of flawed composite structural
components under static and cyclic loading ---
fatigue life of graphite-epoxy composite materials
[NASA-CR-135403] p0066 N79-26120
High char inside-modified epoxy matrix resins ---
for graphite-epoxy composites
[NASA-TM-79226] p0063 N79-29240
- GRAVITATION**
NT REDUCED GRAVITY
- GRAVITY GRADIENT SATELLITES**
NT ATS 5
NT ATS 6

GRAZING INCIDENCE

Effect of grazing flow on the acoustic impedance of Helmholtz resonators consisting of single and clustered orifices

[NASA-CR-3177] p0178 W79-32056

GREAT LAKES (NORTH AMERICA)

NT LAKE ERIE

Atmospheric transformation of multispectral remote sensor data --- Great Lakes

[E79-10006] p0131 W79-12524

GROUND STATE

Optical, spin-resonance, and magnetoresistance studies of /tetrathiatetracene/2/iodide/3 - The nature of the ground state

p0184 A79-10417

GROUND TESTS

NT COLD FLOW TESTS

Evaluation of a Brayton cycle recuperator after 21,000 hours of ground testing

[NASA-TM-79091] p0074 W79-20217

Spacecraft charging modeling development and validation study

p0050 W79-24051

Sputtering in mercury ion thrusters

[NASA-TM-79266] p0054 W79-31343

Combustion of porous solids at reduced gravitational conditions

[NASA-CR-3197] p0072 W79-33288

GROWTH

NT DIRECTIONAL SOLIDIFICATION (CRYSTALS)

NT EPITAXY

GUIDANCE (MOTION)

NT SATELLITE GUIDANCE

GUIDE VANES

Study of mean- and turbulent-velocity fields in a large-scale turbine-vane passage

[NASA-CR-3067] p0032 W79-16853

Aerodynamic performance of axial-flow fan stage operated at nine inlet guide vane angles --- to be used on vertical lift aircraft

[NASA-TF-1510] p0024 W79-31214

GUST LOADS

Scattering and distortion of the unsteady motion on transversely sheared mean flows

p0106 A79-37140

H

HALIDES

NT FLUORIDES

NT SODIUM CHLORIDES

HALL COEFFICIENT

U HALL EFFECT

HALL CURRENTS

U ELECTRIC CURRENT

U HALL EFFECT

HALL EFFECT

Hall effect and magnetoresistivity in the ternary molybdenum sulfides

p0185 A79-21157

HALL GENERATORS

Preliminary results in the NASA Lewis H2-O2 combustion MHD experiment

p0182 A79-39807

HALOCARBONS

Application of ion chromatography to the study of hydrolysis of some halogenated hydrocarbons at ambient temperatures

p0060 A79-14951

A study of various synthetic routes to produce a halogen-labeled traction fluid

[NASA-TM-79024] p0059 W79-11119

Application of ion chromatography to the study of hydrolysis of some halogenated hydrocarbons at ambient temperatures

[NASA-TM-79020] p0157 W79-12586

HALOGEN COMPOUNDS

NT FLUORO COMPOUNDS

NT FLUOROPOLYMERS

NT HALOCARBONS

NT SODIUM CHLORIDES

HALOGENATION

NT FLUORINATION

HALOGENS

NT BROMINE

HANDBOOKS

NT USER MANUALS (COMPUTER PROGRAMS)

HARDENING (MATERIALS)

NT CARBURIZING

NT HOT PRESSING

NT NITRIDING

NT PRECIPITATION HARDENING

NT SILICONIZING

NT STRAIN HARDENING

HARTMANN FLOW

Hartmann flow with temperature-dependent physical properties --- magnetohydrodynamics of liquid metal

p0182 A79-15597

HAZARDS

NT AIRCRAFT HAZARDS

HEAD

Bilinear tangent yaw guidance

[AIAA 78-1730] p0045 A79-45374

HEAT DISSIPATION

U COOLING

HEAT DISSIPATION CHILLING

U COOLING

HEAT EFFECTS

U TEMPERATURE EFFECTS

HEAT EQUATIONS

U THERMODYNAMICS

HEAT EXCHANGERS

Fuel delivery system including heat exchanger means

[NASA-CASE-LEW-12793-1] p0113 W79-11403

Design and fabrication of the Mini-Brayton

recuperator (HBR)

[NASA-CR-159429] p0151 W79-11476

Evaluation of advanced regenerator systems

[NASA-CR-159422] p0188 W79-12969

Heat exchanger --- rocket combustion chambers and

cooling systems

[NASA-CASE-LEW-12252-1] p0102 W79-13288

Heat exchanger and method of making --- bonding

rocket chambers with a porous metal matrix

[NASA-CASE-LEW-12441-1] p0102 W79-13289

Development of a phase-change thermal storage

system using modified anhydrous sodium hydroxide

for solar electric power generation

[NASA-CR-159465] p0153 W79-19454

A heat exchanger and method of making --- rocket

lining

[NASA-CASE-LEW-12441-2] p0104 W79-21313

Active heat exchange system development for latent

heat thermal energy storage

[NASA-CR-159479] p0153 W79-21554

A heat exchanger and method of making

[NASA-CASE-LEW-12441-3] p0104 W79-23383

HEAT FLOW

U HEAT TRANSMISSION

HEAT PIPES

Lithium and potassium heat pipes for thermionic

converters

p0145 A79-10113

Titanium-alloy, metallic-fluid heat pipes for

space service

[NASA-TM-79132] p0104 W79-22426

CIS-type variable conductance heat pipes for SEF

FM/FPD

[NASA-CR-159550] p0107 W79-22434

Heat pipe life and processing study

[NASA-CR-159581] p0107 W79-25349

Description and orbit data of variable-conductance

heat-pipe system for the communications

technology satellite

[NASA-TF-1465] p0105 W79-30516

HEAT REGULATION

U TEMPERATURE CONTROL

HEAT RESISTANCE

U THERMAL RESISTANCE

HEAT RESISTANT ALLOYS

NT MOLYBDENUM ALLOYS

NT REFRACTORY METAL ALLOYS

NT RENE 41

NT RHENIUM ALLOYS

NT TUNGSTEN ALLOYS

The hot corrosion of Co-25Cr-10Ni-5Ta-3Al-0.5Y alloy /S-57/

p0076 A79-10420

Interpolation and extrapolation of creep rupture data by the Minimum Commitment Method. I -

Focal-point convergence. II - Oblique

translation. III - Analysis of multibeats

p0077 A79-16038

Predicted inlet gas temperatures for tungsten

fiber reinforced superalloy turbine blades

p0025 A79-17029

- Effect of a chromium-containing fuel additive on hot corrosion p0071 A79-26546
- A feasibility study of a diffusion barrier between Ni-Cr-Al coatings and nickel-based eutectic alloys p0077 A79-27233
- Tungsten fiber reinforced FeCrAlY - A first generation composite turbine blade material p0065 A79-30397
- Strainrange partitioning behavior of the nickel-base superalloys, Rene 80 and IN-100 p0126 W79-10480
- Exploratory thermal-mechanical fatigue results for Rene' 80 in ultrahigh vacuum p0079 W79-11180
- Evaluation of directionally solidified eutectic superalloys for turbine blade applications [NASA-CR-135151] p0079 W79-16948
- An oxide dispersion strengthened alloy for gas turbine blades p0752 W79-20180
- Tungsten fiber reinforced FeCrAlY: A first generation composite turbine blade material [NASA-TM-79094] p0061 W79-20187
- Effect of grain orientation and coating on thermal fatigue resistance of a directionally solidified superalloy (MAR-M 247) p0127 W79-22565
- The strainrange partitioning behavior of an advanced gas turbine disk alloy, AF2-12A [NASA-TM-79179] p0075 W79-23196
- Thermal-conductivity measurements of tungsten-fiber-reinforced superalloy composites using a thermal-conductivity comparator [NASA-TF-1445] p0063 W79-28234
- An experimental, low-cost, silicon slurry/aluminide high-temperature coating for superalloys [NASA-TM-79178] p0075 W79-29292
- HEAT SHIELDING**
- Automated Plasma Spray (APS) process feasibility study: Plasma spray process development and evaluation [NASA-CR-159579] p0092 W79-29382
- HEAT SOURCES**
- Design and evaluation of aircraft heat source systems for use with high-freezing point fuels [NASA-CR-159568] p0091 W79-24172
- HEAT STORAGE**
- Thermal energy storage for industrial waste heat recovery p0145 A79-10101
- NaOH-based high temperature heat-of-fusion thermal energy storage device p0155 A79-10106
- Storage systems for solar thermal power p0145 A79-10108
- Phase change thermal storage for a solar total energy system p0155 A79-17321
- Thermal storage for industrial process and reject heat p0147 A79-21300
- Thermal storage for industrial process and reject heat [NASA-TM-78994] p0134 W79-11481
- Conceptual design of thermal energy storage systems for near term electric utility applications. Volume 1: Screening of concepts [NASA-CR-159411-VOL-1] p0151 W79-13496
- Conceptual design of thermal energy storage systems for near term electric utility applications. Volume 2: Appendices - screening of concepts [NASA-CR-159411-VOL-2] p0152 W79-13497
- The role of thermal energy storage in industrial energy conservation [NASA-TM-79122] p0137 W79-21550
- Active heat exchange system development for latent heat thermal energy storage [NASA-CR-159479] p0153 W79-21554
- Applications of thermal energy storage to process heat storage and recovery in the paper and pulp industry [NASA-CR-159398] p0154 W79-30801
- Conceptual design of thermal energy storage systems for near term electric utility applications [NASA-CR-159577] p0155 W79-33560
- HEAT TESTS**
- U HIGH TEMPERATURE TESTS**
- HEAT TRANSFER**
- NT CONVECTIVE HEAT TRANSFER**
- Heat transfer from a row of jets impinging on concave semi-cylindrical surface p0108 A79-42890
- Fundamental mechanisms that influence the estimate of heat transfer to gas turbine blades p0099 A79-49526
- The NASA high pressure facility and turbine test rig [NASA-TM-79054] p0015 W79-15050
- Some heat transfer and hydrodynamic problems associated with superconducting cables (SFTL) [NASA-TM-79023] p0102 W79-15267
- Critical mass flux through short Borda type inlets of various cross sections p0074 W79-20216
- Fundamental mechanisms that influence the estimate of heat transfer to gas turbine blades [NASA-TM-79128] p0103 W79-20346
- Some aspects of a free jet phenomena to 105 L/D in a constant area duct [NASA-TM-79050] p0127 W79-20391
- Review and status of liquid-cooling technology for gas turbines [NASA-RF-1038] p0104 W79-22427
- Full-coverage film cooling: 3-dimensional measurements of turbulence structure and prediction of recovery region hydrodynamics [NASA-CR-3104] p0106 W79-22428
- Heat transfer to a full-coverage, film-cooled surface with compound-angle (30 deg and 45 deg) hole injection [NASA-CR-3103] p0107 W79-22429
- Applications of thermal energy storage to process heat storage and recovery in the paper and pulp industry [NASA-CR-159398] p0154 W79-30801
- A reduced volumetric expansion factor plot [NASA-TM-79240] p0105 W79-31527
- HEAT TRANSFER COEFFICIENTS**
- Measurements of mixed convective heat transfer to low temperature helium in a horizontal channel [NASA-TM-79158] p0104 W79-23384
- HEAT TRANSMISSION**
- NT CONVECTIVE HEAT TRANSFER**
- NT HEAT TRANSFER**
- Feasibility of determining flat roof heat losses using aerial thermography [NASA-TM-79152] p0131 W79-22590
- HEAT TREATMENT**
- NT ANNEALING**
- NT NITRIDING**
- Mechanisms of boron fiber strengthening by thermal treatment p0065 A79-30396
- Shear rupture of a directionally solidified eutectic gamma/gamma prime - alpha (Mo) alloy [NASA-TM-79118] p0073 W79-12205
- Mechanisms of boron fiber strengthening by thermal treatment [NASA-TM-79077] p0062 W79-20186
- HEATING**
- NT ARC HEATING**
- NT LASER HEATING**
- HEAVY ELEMENTS**
- NT PLUTONIUM 238**
- HEP (HIGH ENERGY FUELS)**
- U HIGH ENRGY FUELS**
- HELICOPTER DESIGN**
- Materials and structural aspects of advanced gas-turbine helicopter engines [NASA-TM-79100] p0001 W79-20008
- HELICOPTER ENGINES**
- Materials and structural aspects of advanced gas-turbine helicopter engines p0029 A79-39804
- Diagnostics of wear in aeronautical systems p0120 A79-39805
- Development of spiral-groove self-acting seals for helicopter engines [NASA-CR-159622] p0122 W79-32551
- HELICOPTER ROTORS**
- U ROTARY WINGS**
- HELIUM**
- Some heat transfer and hydrodynamic problems associated with superconducting cables (SFTL) [NASA-TM-79023] p0102 W79-15267

Measurements of mixed convective heat transfer to low temperature helium in a horizontal channel
[NASA-TM-79158] p0104 A79-23384

HELIUM PLASMA

Method for decomposing observed line shapes resulting from multiple causes - Application to plasma charge-exchange-neutral spectra
p0182 A79-53867

HELIX TUBES

U TRAVELING WAVE TUBES

HELMHOLTZ EQUATIONS

Numerical spatial marching techniques in duct acoustics --- noise source calculation from far field pressure measurements
p0175 A79-25946

HERMES SATELLITE

U COMMUNICATIONS TECHNOLOGY SATELLITE

HETEROCYCLIC COMPOUNDS

NT AZINES

HETERODYNING

NT OPTICAL HETERODYNING

HIGH ENERGY ASTRONOMY OBSERVATORIES

U HEAO

HIGH ENERGY FUELS

High performance, high density hydrocarbon fuels
[NASA-CR-159480] p0091 A79-20267

HIGH FIELD MAGNETS

Comparison of projected critical currents in PbMoS8 and Nb3Ge
p0185 A79-28300

HIGH MELTING COMPOUNDS

U REFRACTORY MATERIALS

HIGH PRESSURE

The NASA high pressure facility and turbine test rig
[NASA-TM-79054] p0015 A79-15050

Small, high-pressure, liquid oxygen turbopump
[NASA-CR-159509] p0121 A79-17221

JT8D revised high-pressure turbine cooling and other outer air seal program
[NASA-CR-159551] p0033 A79-21076

Shaft seal assembly for high speed and high pressure applications
[NASA-CASE-LEW-11873-1] p0115 A79-22475

Performance of two-stage fan with larger dampers on first-stage rotor
[NASA-TF-1399] p0018 A79-23967

Some flow characteristics of conventional and tapered high pressure drop simulated seals
[NASA-TM-79192] p0104 A79-27460

Design, development, and test of a laser velocimeter for a small 8:1 pressure ratio centrifugal compressor
[NASA-CR-134781] p0111 A79-27478

HIGH SPEED

High speed cylindrical roller bearing analysis, SKF computer program CYBEAN. Volume 1: Analysis
[NASA-CR-159460] p0121 A79-17222

High speed cylindrical roller bearing analysis, SKF computer program CYBEAN. Volume 2: User's manual
[NASA-CR-159461] p0121 A79-17223

Shaft seal assembly for high speed and high pressure applications
[NASA-CASE-LEW-11873-1] p0115 A79-22475

HIGH SPEED FLIGHT

U HIGH SPEED

HIGH STRENGTH

Some properties of an advanced boron fiber --- high strength, splittable fibers
[NASA-TM-79065] p0061 A79-16076

HIGH STRENGTH ALLOYS

NT ASTEROLOY (TRADEMARK)

NT HIGH STRENGTH STEELS

An oxide dispersion strengthened alloy for gas turbine blades
[AIAA 79-0763] p0077 A79-28276

High toughness-high strength iron alloy
[NASA-CASE-LEW-12542-3] p0073 A79-19145

Development and fabrication of high strength alloy fibers for use in metal-metal matrix composites
[NASA-TM-79115] p0063 A79-22211

HIGH STRENGTH STEELS

Wind turbine generator application places unique demands on tower design and materials
p0155 A79-20826

Process for making a high toughness-high strength iron alloy
[NASA-CASE-LEW-12542-2] p0074 A79-22271

HIGH TEMPERATURE

Review of the Agard S6M panel evaluation program of the NASA-Lewis 'SRP' approach to high-temperature LCP life prediction --- Strainrange Partitioning for Low Cycle Fatigue
p0128 A79-14954

Thermocouples of molybdenum and iridium alloys for more stable vacuum-high temperature performance
[NASA-CASE-LEW-12174-2] p0109 A79-14346

A literature review on fatigue and creep interaction
[NASA-CR-135305] p0130 A79-26429

Review of the AGARD S and M panel evaluation program of the NASA-Lewis SRP approach to high-temperature LCP life prediction
p0023 A79-27179

HIGH TEMPERATURE ALLOYS

U HEAT RESISTANT ALLOYS

HIGH TEMPERATURE LUBRICANTS

Coatings for wear and lubrication
p0060 A79-27232

Wide-temperature-spectrum self-lubricating coatings prepared by plasma spraying
p0119 A79-34993

Method of making bearing materials --- self-lubricating, oxidation resistant composites for high temperature applications
[NASA-CASE-LEW-11930-4] p0062 A79-17916

Design problems of small turbomachinery
p0046 A79-22097

HIGH TEMPERATURE MATERIALS

U REFRACTORY MATERIALS

HIGH TEMPERATURE PLASMAS

Trajectories of charged particles in radial electric and uniform axial magnetic fields
p0182 A79-41788

HIGH TEMPERATURE TESTS

The hot corrosion of Co-25Cr-10Ni-5Ta-3Al-0.5Y alloy /S-57/
p0076 A79-10420

Effects of pressure and temperature on hot pressing a sialon --- Si-Al-O-N ceramics
p0085 A79-11548

Static evaluation of surface coatings for compliant gas bearings in an oxidizing atmosphere to 650 C
p0088 A79-31957

Elevated temperature properties of boron/alumina composites
[NASA-CR-159445] p0066 A79-16924

Evaluation of directionally solidified eutectic superalloys for turbine blade applications
[NASA-CR-138451] p0079 A79-16948

Transverse and longitudinal tensile properties at 760 C of several oxide dispersion strengthened nickel-base alloys
[NASA-TM-79189] p0075 A79-30355

HIGH VOLTAGES

Large space system - Charged particle environment interaction technology --- effects on high voltage solar array performance
[AIAA 79-0913] p0055 A79-34775

NASCAP modelling of high-voltage power system interactions with space charged-particle environments
[NASA-TM-79146] p0046 A79-24000

High voltage surface-charged environment test results from space flight and ground simulation experiments
[NASA-TM-79184] p0043 A79-27235

Optically isolated logarithmic nanometer capable of floating to 5 kilovolts
[NASA-TF-1527] p0099 A79-32467

Radiation damage in high-voltage silicon solar cells
p0144 A79-32658

HINGED ROTOR BLADES

U ROTARY WINGS

HISTORIES

Executive summary of Aircraft Icing Specialists Workshop
p0004 A79-23914

BOHANNAN TRAJECTORIES

U TRANSFER ORBITS

BOHANNAN TRANSFER ORBITS

U TRANSFER ORBITS

HOLDERS

NT FLAME HOLDERS

HOLE DISTRIBUTION (MECHANICS)

Airfoil cooling hole plugging by combustion gas impurities of the type found in coal derived fuels

- [NASA-TN-79076] p0089 N79-20265
- HOLLOW CATHODES**
- Hydrogen hollow cathode ion source
- [NASA-CASE-LEW-12940-1] p0181 N79-10894
- Mercury ion thruster research, 1978
- [NASA-CR-159485] p0056 N79-16913
- HOLOGRAPHY**
- Holography through optically active windows
- [NASA-TF-1414] p0109 N79-17195
- Simulated electronic heterodyne recording and processing of pulsed-laser holograms
- [NASA-TF-1444] p0111 N79-21329
- HOMOGENEOUS TURBULENCE**
- Decay of homogeneous turbulence from a given state at higher Reynolds number p0105 A79-14952
- Comparison of a correlation term-discard closure for decaying homogeneous turbulence with experiment p0106 A79-22424
- HONEYWELL COMPUTERS**
- Interactive debug program for evaluation and modification of assembly-language software
- [NASA-TF-1441] p0166 N79-21798
- HOT CORROSION**
- NT TEMPERATURE DEPENDENCE**
- The role of NaCl in flame chemistry, in the deposition process, and in its reactions with protective oxides as related to hot corrosion p0071 A79-49534
- X-ray photoelectron spectroscopy study of nickel and nickel-base alloy surface alterations in simulated hot corrosion conditions with emphasis on eventual application to turbine blade corrosion
- [NASA-CR-159553] p0072 N79-25178
- Experimental studies of the formation/deposition of sodium sulfate in/from combustion gases --- hot corrosion in gas turbine engines
- [NASA-CR-159612] p0072 N79-25183
- Experimental studies of the formation/deposition of sodium sulfate in/from combustion gases --- hot corrosion
- [NASA-CR-159613] p0080 N79-25184
- An investigation of the initiation stage of hot corrosion in Ni-base alloys
- [NASA-CR-159616] p0080 N79-25196
- HOT CYCLE PROPULSION SYSTEM**
- U TIP DRIVEN ROTORS
- HOT EXTRUDING**
- U EXTRUDING
- HOT JET EXHAUST**
- U JET EXHAUST
- HOT JETS**
- U JET FLOW
- HOT PLASMAS**
- U HIGH TEMPERATURE PLASMAS
- HOT PRESSING**
- Effects of pressure and temperature on hot pressing a sialon --- Si-Al-O-N ceramics p0085 A79-11548
- Consolidation of Si₃N₄ by hot isostatic pressing p0086 A79-32931
- HOT-WIRE TURBULENCE METERS**
- U TURBULENCE METERS
- HUMAN BODY**
- Digital enhancement of computerized axial tomograms p0164 A79-11544
- HYBRID COMPUTERS**
- Lewis hybrid computing system, users manual
- [NASA-TN-79111] p0165 N79-20752
- HYBRID PROPULSION**
- Advanced engine study for mixed-mode orbit-transfer vehicles
- [NASA-CR-159491] p0057 N79-19074
- HYBRID STRUCTURES**
- Analysis/design of strip reinforced random composites /strip hybrids/ p0119 A79-24035
- Fabrication and testing of non-graphitic superhybrid composites p0066 A79-43289
- Prediction of properties of intraply hybrid composites
- [NASA-TN-79087] p0061 N79-16919
- HYDRAULIC ACTUATORS**
- U HYDRAULIC EQUIPMENT
- HYDRAULIC CONTROL**
- The application of hydraulics in the 2,000 kW wind turbine generator
- HYDRAULIC EQUIPMENT**
- Consolidation of Si₃N₄ by hot isostatic pressing p0156 A79-27400
- Free-piston regenerative hot gas hydraulic engine
- [NASA-CASE-LEW-12274-1] p0086 A79-32931
- p0113 N79-10426
- HYDRAULIC HEATING SOURCES**
- U HEAT SOURCES
- U HYDRAULIC EQUIPMENT
- HYDRAULIC PUMPS**
- U HYDRAULIC EQUIPMENT
- HYDRAULIC SYSTEMS**
- U HYDRAULIC EQUIPMENT
- HYDRAULIC VALVES**
- U HYDRAULIC EQUIPMENT
- HYDROAEROMECHANICS**
- U AERODYNAMICS
- HYDROCARBON COMBUSTION**
- Correlations of catalytic combustor performance parameters p0070 A79-14956
- Turbulence effects on flame speed and flame structure
- [AIAA PAPER 79-0016] p0070 A79-19480
- Experimental study of the effects of flameholder geometry on emissions and performance of lean premixed combustors
- [AIAA PAPER 79-0187] p0070 A79-19586
- Burn coal cleanly in a fluidized bed - The key is in the controls p0071 A79-26374
- HYDROCARBON FUELS**
- NT DIESEL FUELS
- NT FOSSIL FUELS
- NT GASOLINE
- NT JET ENGINE FUELS
- NT JP-5 JET FUEL
- Characteristics and combustion of future hydrocarbon fuels p0090 A79-11599
- Impact of future fuel properties on aircraft engines and fuel systems p0024 A79-11600
- Ion chromatographic determination of sulfur in fuels p0070 A79-21222
- Characteristics and combustion of future hydrocarbon fuels p0089 N79-13136
- Impact of future fuel properties on aircraft engines and fuel systems p0089 N79-13197
- High performance, high density hydrocarbon fuels
- [NASA-CR-159480] p0091 N79-20267
- Autoignition of fuels p0020 N79-25001
- HYDROCARBONS**
- NT PROPANE
- HYDRODYNAMIC STABILITY**
- U FLOW STABILITY
- HYDRODYNAMICS**
- NT ELASTIC HYDRODYNAMICS
- NT MAGNETIC HYDRODYNAMICS
- Some heat transfer and hydrodynamic problems associated with superconducting cables (SPTL)
- [NASA-TN-79023] p0102 N79-15267
- Hydrodynamic effects in a misaligned radial face seal
- [NASA-CR-13522e] p0121 N79-17226
- Critical mass flux through short Borda type inlets of various cross sections
- [NASA-TN-79017] p0074 N79-20216
- Some aspects of a free jet phenomena to 105 L/D in a constant area duct
- [NASA-TN-79050] p0127 N79-20391
- Full-coverage film cooling: 3-dimensional measurements of turbulence structure and prediction of recovery region hydrodynamics
- [NASA-CR-3104] p0106 N79-22428
- Heat transfer to a full-coverage, film-cooled surface with compound-angle (30 deg and 45 deg) hole injection
- [NASA-CR-3103] p0107 N79-22429
- Measurements of mixed convective heat transfer to low temperature helium in a horizontal channel
- [NASA-TN-79158] p0104 N79-23384
- HYDROGEN**
- NT HYDROGEN ATOMS
- NT HYDROGEN IONS
- NT HYDROGEN PLASMA

- NT LIQUID HYDROGEN
Fabrication and testing of silver-hydrogen cells
[NASA-CR-159490] p0152 N79-16375
- HYDROGEN ATOMS
Atomic hydrogen storage method and apparatus
[NASA-CASE-LEW-12081-3] p0136 N79-18455
- HYDROGEN IONS
Hydrogen hollow cathode ion source
[NASA-CASE-LEW-12940-1] p0181 N79-10894
- HYDROGEN OXYGEN ENGINES
Velocity, temperature, and electrical conductivity
profiles in hydrogen-oxygen MHD duct flows
p0182 A79-26184
Unconventional nozzle tradeoff study --- space tug
propulsion
[NASA-CR-159520] p0057 N79-28224
- HYDROGEN OXYGEN FUEL CELLS
Development of advanced fuel cell system
[NASA-CR-159443] p0151 N79-12553
Strip cell test and evaluation program
[NASA-CR-159652] p0154 N79-31784
- HYDROGEN PLASMA
Method for decomposing observed line shapes
resulting from multiple causes - Application to
plasma charge-exchange-neutral spectra
p0182 A79-53867
- H⁺ HYDROGEN RECOMBINATIONS
Hydrogen recombination in sealed nickel-cadmium
aerospace cells
p0057 A79-51907
- HYDROGEN-BASED ENERGY
Fabrication and testing of silver-hydrogen cells
[NASA-CR-159431] p0152 N79-16374
- HYDROLYSIS
Application of ion chromatography to the study of
hydrolysis of some halogenated hydrocarbons at
ambient temperatures
p0060 A79-14951
Application of ion chromatography to the study of
hydrolysis of some halogenated hydrocarbons at
ambient temperatures
[NASA-TN-79020] p0157 N79-12586
- HYDROMAGNETIC FLOW
U MAGNETOHYDRODYNAMIC FLOW
- HYDROMAGNETICS
U MAGNETOHYDRODYNAMICS
- HYDROMAGNETISM
U MAGNETOHYDRODYNAMICS
- HYDROMECHANICS
NT ELASTOHYDRODYNAMICS
NT HYDRODYNAMICS
NT MAGNETOHYDRODYNAMICS
- HYDROSTATIC PRESSURE
Critical current density in wire drawn and
hydrostatically extruded Nb-Ti superconductors
p0185 A79-20539
- HYDROX ENGINES
U HYDROGEN OXYGEN ENGINES
- HYDROXIDES
NT POTASSIUM HYDROXIDES
NT SODIUM HYDROXIDES
- HYDROXYL COMPOUNDS
NT ETHYL ALCOHOL
NT PHENOLS
NT POLYVINYL ALCOHOL
- HYGIAL PROPERTIES
U MOISTURE CONTENT
- HYPERVELOCITY IMPACT
Analysis of high velocity impact on hybrid
composite fan blades
[AIAA 79-0783] p0128 A79-29027
Analysis of high velocity impact on hybrid
composite fan blades
[NASA-TN-79133] p0127 N79-20398
CELFE: Coupled Eulerian-Lagrangian Finite Element
program for high velocity impact. Part 1:
Theory and formulation ---
hydroelasto-viscoplastic model
[NASA-CR-159395] p0166 N79-29832
CELFE: Coupled Eulerian-Lagrangian Finite Element
program for high velocity impact. Part 2:
Program user's manual
[NASA-CR-159396] p0166 N79-29833
- ICE
NT ICEBERGS
- ICE FORMATION
Aircraft Icing
p0161 N79-17418
Aircraft icing
[NASA-CP-2086] p0004 N79-23912
Executive summary of Aircraft Icing Specialists
Workshop
p0004 N79-23914
- ICE MAPPING
VHF downlink communication system for SLAR data
p0045 A79-51097
VHF downlink communication system for SLAR data
[NASA-TN-79164] p0094 N79-23313
- ICEBERGS
Radar image processing of real aperture SLAR data
for the detection and identification of iceberg
and ship targets
p0131 A79-36537
- ICING
U ICE FORMATION
- IGNITION
Resonance-tube ignition of aluminum
p0071 A79-46366
Autoignition of fuels
p0020 N79-25001
Modelling turbulent flame ignition and blow-out
p0021 N79-25008
- IMAGE ENHANCEMENT
Digital enhancement of computerized axial tomograms
p0164 A79-11544
- IMAGE PROCESSING
Radar image processing of real aperture SLAR data
for the detection and identification of iceberg
and ship targets
p0131 A79-36537
- IMAGERY
NT AERIAL PHOTOGRAPHY
NT HOLOGRAPHY
NT RADAR IMAGERY
NT TOMOGRAPHY
- IMAGING TECHNIQUES
NT IMAGE ENHANCEMENT
NT RADAR IMAGERY
Holography through optically active windows
[NASA-TF-1414] p0109 N79-17195
- IMIDES
High clear inside-modified epoxy matrix resins ---
for graphite-epoxy composites
[NASA-TN-79226] p0063 N79-29240
Curing agent for polyepoxides and epoxy resins and
composites cured therewith
[NASA-CASE-LEW-13226-1] p0059 N79-31345
- IMPACT
NT HYPERVELOCITY IMPACT
NT ION IMPACT
- IMPACT DAMAGE
Increasing the FOD tolerance of composites --- gas
turbine engine blade foreign object damage
p0067 A79-20859
Impact behavior of filament-wound graphite/epoxy
fan blades --- foreign object damage to turbofan
engines
p0025 A79-20880
- IMPACT LOADS
CELFE/NASTRAN Code for the analysis of structures
subjected to high velocity impact
p0128 A79-21298
Analysis of high velocity impact on hybrid
composite fan blades
[AIAA 79-0783] p0128 A79-29027
Off-axis impact of unidirectional composites with
cracks: Dynamic stress intensification
[NASA-CR-159537] p0067 N79-30294
Normal and radial impact of composites with
embedded penny-shaped cracks
[NASA-CR-159538] p0130 N79-31627
- IMPACT PRESSURES
U IMPACT LOADS
- IMPACT RESISTANCE
Containment of composite fan blades
[NASA-CR-158168] p0032 N79-18978
- IMPACT SENSITIVITY
U IMPACT RESISTANCE
- IMPACT STRENGTH
CELFE/NASTRAN code for the analysis of structures
subjected to high velocity impact
[NASA-TN-79048] p0126 N79-15325
- IMPACT TESTS
Interactive multi-mode blade impact analysis

- [NASA-CR-159462] p0032 N79-17858
 Containment of composite fan blades
 [NASA-CR-158168] p0032 N79-18978
 Analysis of high velocity impact on hybrid
 composite fan blades
 [NASA-TM-79133] p0127 N79-20398
- IMPACT TOLERANCES**
 Increasing the FOD tolerance of composites --- gas
 turbine engine blade foreign object damage
 p0067 A79-20859
- IMPEDANCE**
 NT ACOUSTIC IMPEDANCE
 NT ELECTRICAL RESISTANCE
- IMPELLER BLADES**
 U ROTOR BLADES (TURBOMACHINERY)
- IMPERFECTIONS**
 U DEFECTS
- IMPINGEMENT**
 NT JET IMPINGEMENT
 TACT 1: A computer program for the transient
 thermal analysis of a cooled turbine blade or
 vane equipped with a coolant insert. 2.
 Programmers manual
 [NASA-TF-1391] p0103 N79-18288
- IMPLANTATION**
 NT ION IMPLANTATION
- IMPREGNATING**
 Comment on the mechanism of operation of the
 impregnated tungsten cathode
 p0099 A79-42024
- IMPURITIES**
 Characterization of PMR polyimides - Correlation
 of ester impurities with composite properties
 p0066 A79-43265
 Characterization of PMR polyimides: Correlation
 of ester impurities with composite properties
 [NASA-TM-79068] p0061 N79-16918
 Airfoil cooling hole plugging by combustion gas
 impurities of the type found in coal derived fuels
 [NASA-TM-79076] p0089 N79-20265
- IN-FLIGHT MONITORING**
 NASA Global Atmospheric Sampling Program (GASP),
 data report for tape VL0009
 [NASA-TM-79058] p0157 N79-15448
 Inflight fuel tank temperature survey data
 [NASA-CR-159569] p0009 N79-23940
- INCIDENCE**
 NT GRAZING INCIDENCE
- INCOMPRESSIBLE FLOW**
 Flow in nonrotating passages of radial inflow
 turbines
 [NASA-CR-159679] p0035 N79-32212
- INDUCED FLUID FLOW**
 U FLUID FLOW
- INDUCTION SYSTEMS**
 U INTAKE SYSTEMS
- INDUSTRIAL ENERGY**
 Thermal storage for industrial process and reject
 heat
 p0147 A79-21300
 Energy and cost savings results for advanced
 technology systems from the Cogeneration
 Technology Alternatives Study /CIAS/
 [AIAA PAPER 79-1000] p0149 A79-44225
 Applications of thermal energy storage to process
 heat and waste heat recovery in the iron and
 steel industry
 [NASA-CR-159397] p0151 N79-11473
 Thermal storage for industrial process and reject
 heat
 [NASA-TM-78994] p0134 N79-11481
 Thermal storage technologies for solar industrial
 process heat applications
 [NASA-TM-79130] p0136 N79-20498
 The role of thermal energy storage in industrial
 energy conservation
 [NASA-TM-79122] p0137 N79-21550
 Benefits of advanced technology in industrial
 cogeneration
 [NASA-TM-79160] p0138 N79-24444
 Applications of thermal energy storage to process
 heat storage and recovery in the paper and pulp
 industry
 [NASA-CR-159398] p0154 N79-30801
- INDUSTRIAL WASTES**
 Thermal energy storage for industrial waste heat
 recovery
 p0145 A79-10101
- INDUSTRIES**
 NT AEROSPACE INDUSTRY
 Industrial ion source technology
 [NASA-CR-159534] p0179 N79-19828
- INERT GASES**
 U RARE GASES
- INFLUENCE COEFFICIENT**
 NT STRUCTURAL INFLUENCE COEFFICIENTS
- INFORMATION SYSTEMS**
 Global disaster satellite communications system
 for disaster assessment and relief coordination
 [NASA-TM-79105] p0044 N79-20176
- INFORMATION TRANSMISSION**
 U DATA TRANSMISSION
- INFRARED INSTRUMENTS**
 Infrared suppressor effect on T63 turboshaft
 engine performance
 [NASA-TM-78970] p0013 N79-11043
- INFRARED SPECTROSCOPY**
 Infrared analysis of polyethylene wear specimens
 using attenuated total reflection spectroscopy
 --- effects of radiation on the surface
 properties of materials for total joint prostheses
 [NASA-TM-79228] p0083 N79-29329
- INHIBITORS**
 NT WEAR INHIBITORS
- INJECTION**
 NT FLUID INJECTION
 NT FUEL INJECTION
 NT GAS INJECTION
 NT WATER INJECTION
 INJECTION CARBURIZERS
 U FUEL INJECTION
- INJECTORS**
 Measurements of admittances and characteristic
 combustion times of reactive gaseous propellant
 coaxial injectors
 [NASA-CR-159542] p0072 N79-23168
- INLET FLOW**
 Effect of inlet temperature on the performance of
 a catalytic reactor
 p0070 A79-11542
 Predicted inlet gas temperatures for tungsten
 fiber reinforced superalloy turbine blades
 p0025 A79-17029
 An efficient user-oriented method for calculating
 compressible flow about three-dimensional inlets
 [AIAA PAPER 79-0081] p0005 A79-19524
 Reynolds number, scale and frequency content
 effects on F-15 inlet instantaneous distortion
 [AIAA PAPER 79-0104] p0005 A79-19533
 Calculation of the three-dimensional flow field in
 supersonic inlets at angle of attack using a
 bicharacteristic method with discrete shock wave
 fitting
 [AIAA PAPER 79-0379] p0025 A79-19698
 Some flow phenomena in a constant area duct with a
 Borda type inlet including the critical region
 [ASME PAPER 78-WA/HT-37] p0093 A79-19816
 Aerodynamic performance of scarf inlets
 [AIAA PAPER 79-0380] p0005 A79-23510
 Effects of inflow distortion profiles on fan tone
 noise calculated using a 3-D theory
 [AIAA PAPER 79-0577] p0175 A79-26911
 Evaluation of two inflow control devices for
 flight simulation of fan noise using a JT15D
 engine
 [AIAA PAPER 79-0654] p0026 A79-26326
 Combined pressure and temperature distortion
 effects on internal flow of a turbofan engine
 [AIAA PAPER 79-1309] p0029 A79-39031
 Performance of a V/STOL tilt nacelle inlet with
 blowing boundary layer control
 [AIAA PAPER 79-1163] p0006 A79-47347
 Recent applications of theoretical analysis to
 V/STOL inlet design
 p0006 A79-49530
 Experimental investigation of a 0.15-scale model
 of an underfuselage normal-shock inlet
 [NASA-CR-3049] p0006 N79-12014
 An approach to optimum subsonic inlet design
 [NASA-TM-79051] p0002 N79-12020
 Basic research in fan source noise: Inlet
 distortion and turbulence noise
 [NASA-CR-159451] p0177 N79-14875
 Theoretical study of VTOL tilt-nacelle
 axisymmetric inlet geometries
 [NASA-TF-1380] p0003 N79-14996

- Experimental evaluation of the effect of inlet distortion on compressor blade vibrations
[NASA-TM-79066] p0126 N79-16300
- Effects of inflow distortion profiles on fan tone noise calculated using a 3-D theory
[NASA-TM-79082] p0173 N79-16647
- Critical mass flux through short Borda type inlets of various cross sections
[NASA-TM-79017] p0074 N79-20216
- Effect of steady-state pressure distortion on flow characteristics entering a turbofan engine
[NASA-TM-79134] p0019 N79-23969
- Self stabilizing sonic inlet
[NASA-CASE-LEW-11890-1] p0011 N79-24976
- Performance of a V/STOL tilt nacelle inlet with blowing boundary layer control
[NASA-TM-79176] p0004 N79-27093
- Effect of rotor meridional velocity ratio on response to inlet radial and circumferential distortion
[NASA-TF-1278] p0023 N79-28177
- Recent applications of theoretical analysis to V/STOL inlet design
[NASA-TM-79211] p0004 N79-29143
- Effect of steady-state temperature distortion and combined distortion on inlet flow to a turbofan engine
[NASA-TM-79237] p0023 N79-30187
- Free jet phenomena in a 90 degree-sharp edge inlet geometry
[NASA-TM-79229] p0105 N79-31526
- Flow in nonrotating passages of radial inflow turbines
[NASA-CR-159679] p0035 N79-32212
- INLET NOZZLES**
- Analysis of radiation patterns of interaction tones generated by inlet rods in the JT15D engine
[AIAA PAPER 79-0581] p0027 A79-26944
- An approach to optimum subsonic inlet design
[ASME PAPER 79-GT-51] p0006 A79-30527
- Theoretical fan velocity distortions due to inlets and nozzles
p0006 A79-39810
- Theoretical fan velocity distortions due to inlets and nozzles --- in V/STOL aircraft
[NASA-TM-79150] p0003 N79-23911
- INLETS (DEVICES)**
- U INTAKE SYSTEMS**
- INORGANIC COATINGS**
- NT CERAMIC COATINGS**
- Control of volume resistivity in inorganic organic separators
[NASA-TF-1439] p0069 N79-22246
- INORGANIC COMPOUNDS**
- Method for the preparation of inorganic single crystal and polycrystalline electronic materials
[NASA-CASE-XLE-02545-1] p0184 N79-21910
- Improved, low cost inorganic-organic separators for rechargeable silver-zinc batteries
[NASA-TF-1476] p0069 N79-25181
- Survey of inorganic polymers --- for composite matrix resins
[NASA-CR-159563] p0087 N79-30377
- INORGANIC NITRATES**
- NT SODIUM NITRATES**
- INORGANIC SULFIDES**
- NT COPPER SULFIDES**
- NT LEAD SULFIDES**
- NT MOLYBDENUM DISULFIDES**
- NT MOLYBDENUM SULFIDES**
- INSECTICIDES**
- NT URETHANES**
- INSENSITIVITY**
- U SENSITIVITY**
- INSOLATION**
- Variation of solar cell sensitivity and solar radiation on tilted surfaces
p0148 A79-41023
- Evaluation of models to predict insolation on tilted surfaces
p0150 A79-53491
- INSULATION**
- NT ELECTRICAL INSULATION**
- NT THERMAL INSULATION**
- INSULATORS**
- Insulator edge voltage gradient effects in spacecraft charging phenomena
[NASA-TM-78988] p0046 N79-11109
- Test results for electron beam charging of flexible insulators and composites --- solar array substrates, honeycomb panels, and thin dielectric films
p0048 N79-24031
- INTAKE SYSTEMS**
- NT AIR INTAKES**
- NT ENGINE INLETS**
- NT SUPERSONIC INLETS**
- An approach to optimum subsonic inlet design
[NASA-TM-79051] p0002 N79-12020
- Applications of velocity potential function to acoustic duct propagation and radiation from inlets using finite element theory
[NASA-TM-79071] p0016 N79-15959
- Full-scale engine tests of bulk absorber acoustic inlet treatment
[NASA-TM-79079] p0173 N79-16645
- Theoretical fan velocity distortions due to inlets and nozzles --- in V/STOL aircraft
[NASA-TM-79150] p0003 N79-23911
- INTERACTIVE GRAPHICS**
- U COMPUTER GRAPHICS**
- INTERCONNECTION**
- U JOINING**
- INTERFACES**
- NT SOLID-SOLID INTERFACES**
- INTERNAL COMBUSTION ENGINES**
- NT DIESEL ENGINES**
- NT DUCTED FAN ENGINES**
- NT GAS TURBINE ENGINES**
- NT HELICOPTER ENGINES**
- NT J-85 ENGINE**
- NT JET ENGINES**
- NT T-53 ENGINE**
- NT T-55 ENGINE**
- NT T-63 ENGINE**
- NT TF-30 ENGINE**
- NT TURBOFAN ENGINES**
- NT TURBOJET ENGINES**
- NT TURBOPROP ENGINES**
- NT WANKEL ENGINES**
- Indicated mean-effective pressure instrument
[NASA-CASE-LEW-12661-1] p0109 N79-14345
- Computer simulation of an aircraft engine fuel injection system
[NASA-CR-157641] p0016 N79-15052
- INTERNAL PRESSURE**
- Combined pressure and temperature distortion effects on internal flow of a turbofan engine
[AIAA PAPER 79-1309] p0029 A79-39031
- INTERNAL STRESS**
- U RESIDUAL STRESS**
- INTERNATIONAL COOPERATION**
- Communications technology satellite: United States experiments and disaster communications applications
[NASA-TM-79109] p0044 N79-23999
- Review of the AGARD S and M panel evaluation program of the NASA-Lewis SRP approach to high-temperature LCF life prediction
p0023 N79-27179
- Satellite communications for disaster relief operations
[NASA-TM-79198] p0094 N79-27351
- INTERNATIONAL RELATIONS**
- NT INTERNATIONAL COOPERATION**
- INTERPLANETARY PROPULSION**
- U ROCKET ENGINES**
- INTERPLANETARY SPACECRAFT**
- NT JUPITER PROBES**
- INTERPOLATION**
- Interpolation and extrapolation of creep rupture data by the Minimum Commitment Method. I - Focal-point convergence. II - Oblique translation. III - Analysis of multiheats
p0077 A79-16038
- INTERSTELLAR GAS**
- NT NEUTRAL GASES**
- INTRAOCULAR PRESSURE**
- Intraocular pressure reduction and regulation system
[NASA-TM-79187] p0165 N79-28881
- INVERSIONS**
- NT TEMPERATURE INVERSIONS**
- INVERTED CONVERTERS (DC TO AC)**
- Analytical core loss calculations for magnetic materials used in high frequency high power converter applications
[NASA-TM-79234] p0098 N79-31499

INVERTERS

An inverter/controller subsystem optimized for photovoltaic applications
p0146 A79-41047

INVISCID FLOW

Axial-flow compressor turning angle and loss by inviscid-viscous interaction blade-to-blade computation
[ASME PAPER 79-GT-5] p0006 A79-30504

ION ACCELERATORS

Increased capabilities of the 30-cm diameter Hg ion thruster
[AIAA 79-0910] p0055 A79-34774

ION BEAMS

Ion beam sputtering of fluoropolymers
p0117 A79-14797

Adhesive bonding of ion beam textured metals and fluoropolymers
p0060 A79-14798

The use of ion beam cleaning to obtain high quality cold welds with minimal deformation
p0119 A79-24121

Adaptation of ion beam technology to microfabrication of solid state devices and transducers
[NASA-CR-159439] p0186 A79-11921

Ion beam technology applications study --- ion impact, implantation, and surface finishing
[NASA-CR-159437] p0180 A79-12884

Adhesive bonding of ion beam textured metals and fluoropolymers
[NASA-TM-79004] p0181 A79-12909

Industrial ion source technology
[NASA-CR-159534] p0179 A79-19828

Ion beam probing of electrostatic fields
[NASA-TM-79120] p0181 A79-20864

Ion beam sputter deposition of fluoropolymers
[NASA-CASE-LEW-13122-1] p0083 A79-24154

Physical processes in directed ion beam sputtering
[NASA-CR-159567] p0182 A79-26943

Neutralization tests on the SERT 2 spacecraft
[NASA-TM-79271] p0054 A79-33255

ION CHAMBERS**U IONIZATION CHAMBERS****ION CURRENTS****NT ION BEAMS**

Industrial potential, uses, and performance of sputtered and ion plated films
[NASA-TM-79107] p0157 A79-20527

ION ENGINES**NT MERCURY ION ENGINES**

Operations of the ATS-6 ion engine
p0049 A79-24007

SERT 2 1979 extended flight thruster system performance
[NASA-TM-79256] p0054 A79-33252

Neutralization tests on the SERT 2 spacecraft
[NASA-TM-79271] p0054 A79-33255

ION EXCHANGE MEMBRANE ELECTROLYTES

Formulated plastic separators for soluble electrode cells --- rubber-ion transport membranes
[NASA-CASE-LEW-12358-1] p0135 A79-17313

Three methods for in situ cross-linking of polyvinyl alcohol films for application as ion-conducting membranes in potassium hydroxide electrolyte --- battery separators
[NASA-TF-1407] p0059 A79-21128

ION EXCHANGING

Application of ion chromatography to the study of hydrolysis of some halogenated hydrocarbons at ambient temperatures
p0060 A79-14951

Ion chromatographic determination of sulfur in fuels
p0070 A79-21222

ION IMPACT

Ion beam technology applications study --- ion impact, implantation, and surface finishing
[NASA-CR-159437] p0180 A79-12884

ION IMPLANTATION

The effect of nitrogen ion (N⁺) implantation on the friction and wear characteristics of iron
[NASA-TM-79029] p0073 A79-12201

Ion beam technology applications study --- ion impact, implantation, and surface finishing
[NASA-CR-159437] p0180 A79-12884

Applications of ion implantation to high performance, radiation tolerant silicon solar cells
p0143 A79-32648

ION IRRADIATION

Modification of the electrical and optical properties of polymers --- ion irradiation
[NASA-CASE-LEW-13027-1] p0081 A79-11216

ION PLATING

Industrial potential, uses, and performance of sputtered and ion plated films
p0119 A79-30398

Characterization of defect growth structure in ion plated films by scanning electron microscopy
[NASA-TM-79110] p0074 A79-20218

Survey of ion plating sources --- conferences
[NASA-TM-79269] p0076 A79-31372

ION PROPULSION

Primary electric propulsion for future space missions
[AIAA 79-08.1] p0055 A79-34773

Advanced electrostatic ion thruster for space propulsion
[NASA-CR-159406] p0056 A79-14153

Prediction of plasma properties in mercury ion thrusters
[NASA-CR-159448] p0056 A79-15152

Closed loop solar array-ion thruster system with power control circuitry
[NASA-CASE-LEW-12780-1] p0052 A79-20179

Increased capabilities of the 30-cm diameter Hg ion thruster
[NASA-TM-79142] p0053 A79-22192

The 30-centimeter ion thrust subsystem design manual
[NASA-TM-79191] p0053 A79-25131

Characteristics of primary electric propulsion systems --- conferences
[NASA-TM-79255] p0053 A79-30290

SERT 2 1979 extended flight thruster system performance
[NASA-TM-79256] p0054 A79-33252

Reduced power processor requirements for the 30-cm diameter Hg ion thruster
[NASA-TM-79257] p0054 A79-33253

Preliminary results of the mission profile life test of a 30 cm Hg bombardment thruster
[NASA-TM-79261] p0054 A79-33254

Neutralization tests on the SERT 2 spacecraft
[NASA-TM-79271] p0054 A79-33255

ION SOURCES

Inert gas ion source program
[NASA-CR-159423] p0056 A79-10120

Hydrogen hollow cathode ion source
[NASA-CASE-LEW-12940-1] p0181 A79-10894

IONIC CONDUCTIVITY**U ION CURRENTS****IONIC DIFFUSION**

Determination of the zincate diffusion coefficient and its application to alkaline battery problems
p0070 A79-11547

IONIC MOBILITY

Ion confinement and transport in a toroidal plasma with externally imposed radial electric fields
[NASA-TF-1411] p0181 A79-19867

Decay of the zincate concentration gradient at an alkaline zinc cathode after charging
[NASA-TM-79106] p0137 A79-20520

IONIC PROPELLANTS**U ION ENGINES****IONIZATION****NT GAS IONIZATION****IONIZATION CHAMBERS**

Preliminary results of the mission profile life test of a 30 cm Hg bombardment thruster
[NASA-TM-79261] p0054 A79-33254

IONIZATION COUNTERS**U IONIZATION CHAMBERS****IONIZED GASES****NT CHARGED PARTICLES****NT ELECTRON PLASMA****NT PLASMAS (PHYSICS)****NT TOROIDAL PLASMAS****IONIZED PLASMAS****U PLASMAS (PHYSICS)****IONIZING RADIATION****NT ULTRAVIOLET RADIATION**

Radiation damage in high-voltage silicon solar cells
p0144 A79-32658

IONS**NT CESIUM ION****NT HYDROGEN IONS****NT METAL IONS****NT NITROGEN IONS**

Ion chromatographic determination of sulfur in fuels
[NASA-TM-78971] p0157 N79-17358
Whiskers, cones and pyramids created in sputtering
by ion bombardment
[NASA-CR-159549] p0079 N79-20221

IP (IMPACT PREDICTION)
U COMPUTERIZED SIMULATION

IRIDIUM
Thermocouples of molybdenum and iridium alloys for
more stable vacuum-high temperature performance
[NASA-CASE-LEW-12174-2] p0119 N79-14346

IRON
Supply of reactants for Redox bulk energy storage
systems
[NASA-TM-78995] p0133 N79-11479
The effect of nitrogen ion (N⁺) implantation on
the friction and wear characteristics of iron
[NASA-TM-79029] p0073 N79-12201
Friction and transfer of copper, silver, and gold
to iron in the presence of various adsorbed
surface films
[NASA-TP-1392] p0114 N79-14386
Surface chemistry of iron sliding in air and
nitrogen lubricated with hexadecane and
hexadecane containing dibenzyl-dithiolsulfide
[NASA-TF-1545] p0059 N79-31346

IRON ALLOYS
NT HIGH STRENGTH STEELS
NT NICKEL STEELS
NT STAINLESS STEELS
NT STEELS
Tungsten fiber reinforced FeCrAlY - A first
generation composite turbine blade material
p0065 A79-30397
Evaluation of the mechanical properties of
electroslag refined Fe-12Ni alloys
[NASA-CR-159394] p0079 N79-12202
Friction and wear characteristics of iron-chromium
alloys in contact with themselves and silicon
carbide
[NASA-TF-1387] p0114 N79-14387
Friction and wear with a single-crystal abrasive
grit of silicon carbide in contact with iron
base binary alloys in oil: Effects of alloying
element and its content
[NASA-TP-1394] p0114 N79-17227
High toughness-high strength iron alloy
[NASA-CASE-LEW-12542-3] p0073 N79-19145
Process for making a high toughness-high strength
iron alloy
[NASA-CASE-LEW-12542-2] p0074 N79-22271

IRON COMPOUNDS
NT FERRITES

IRRADIATION
NT ELECTRON IRRADIATION
NT ION IRRADIATION
Effect of sterilization irradiation on friction
and wear of ultrahigh-molecular-weight
polyethylene
[NASA-TP-1462] p0082 N79-23216

IRROTATIONAL FLOW
U POTENTIAL FLOW

ISING MODEL
U MATHEMATICAL MODELS

ISOLATORS
NT VIBRATION ISOLATORS

ISOSTATIC PRESSURE
Consolidation of Si₃N₄ by hot isostatic pressing
p0086 A79-32931

ISOTHERMAL LAYERS
Effect of geometry on hydrodynamic film thickness
[ASME PAPER 78-LUB-24] p0118 A79-23237

ISOTOPES
NT PLUTONIUM 238
Mini-BRO/BIPS 1300 watt (sub) dynamic power
conversion system development: Executive summary
[NASA-CR-159440] p0150 N79-10526

J
J-85 ENGINE
Effects of steady-state pressure distortion on the
stall margin of a J85-21 turbojet engine
[NASA-TM-79123] p0018 N79-23968

JEeps
U AUTOMOBILES

JET AIRCRAFT
NT BOEING 747 AIRCRAFT
NT F-15 AIRCRAFT

NT F-102 AIRCRAFT
NT LEAR JET AIRCRAFT
NT TURBOPROP AIRCRAFT
JET AIRCRAFT NOISE
Measured and predicted noise of the AVCO-Lycoming
TF-102 turbofan engine
[AIAA PAPER 79-0641] p0026 A79-26877
Effects of inflow distortion profiles on fan tone
noise calculated using a 3-D theory
[AIAA PAPER 79-0577] p0175 A79-26911
Noise from struts and splitters in turbofan exit
ducts
[AIAA PAPER 79-0637] p0178 A79-26923
Effects of simulated forward flight on jet noise,
shock noise and internal noise
[AIAA PAPER 79-0615] p0178 A79-26936
Analysis of radiation patterns of interaction
tones generated by inlet rods in the JT15D engine
[AIAA PAPER 79-0581] p0027 A79-26944
Effects of geometric and flow-field variables on
inverted-velocity-profile coaxial jet noise and
source distributions
[AIAA PAPER 79-0635] p0175 A79-32126
An improved method for predicting the effects of
flight on jet mixing noise
p0176 A79-39803
QCSEE - The key to future short-haul air transport
--- Quiet, Clean, Short-Haul Experimental Engine
program
p0030 A79-50208
The free jet as a simulator of forward velocity
effects on jet noise
[NASA-CR-3056] p0176 N79-14873
Basic research in fan source noise: Inlet
distortion and turbulence noise
[NASA-CR-159451] p0177 N79-14875
Effects of geometric and flow-field variables on
inverted-velocity-profile coaxial jet noise ---
nozzle geometry
[NASA-TM-79095] p0173 N79-20830
An improved method for predicting the effects of
flight on jet mixing noise
[NASA-TM-79155] p0173 N79-24770
Assessment at full scale of nozzle/wing geometry
effects on OTW aero-acoustic characteristics ---
short takeoff aircraft noise
[NASA-TM-79168] p0174 N79-25341

JET DAMPING
U DAMPING

JET ENGINE CELLS
NT JF-5 JET FUEL
Alternative aircraft fuels
p0090 A79-10824
Alternative aviation turbine fuels
p0090 A79-12378
Effect of broadened-specification fuels on
aircraft engines and fuel systems
[AIAA 79-7008] p0027 A79-29383
High-freezing-point fuels used for aviation
turbine engines
[ASME PAPER 79-GT-141] p0090 A79-30555
Analysis of the impact of the use of broad
specification fuels on combustors for commercial
aircraft gas turbine engines
[AIAA PAPER 79-1195] p0090 A79-38980
Characteristics and combustion of future
hydrocarbon fuels
p0089 N79-13196
Impact of future fuel properties on aircraft
engines and fuel systems
p0089 N79-13197
High freezing point fuels used for aviation
turbine engines
[NASA-TM-79015] p0089 N79-15199
Effect of broadened-specification fuels on
aircraft engines and fuel systems
[NASA-TM-79086] p0089 N79-16136
Parametric performance of a turbojet engine
combustor using jet A and A diesel fuel
[NASA-TM-79089] p0017 N79-20114
Use of refinery computer model to predict fuel
production
[NASA-TM-79203] p0089 N79-28349
Comparison of the properties of some synthetic
crudes with petroleum crudes
[NASA-TM-79220] p0090 N79-31405

JET ENGINES
NT DUCTED FAN ENGINES
NT J-85 ENGINE

- NT T-53 ENGINE
 NT T-63 ENGINE
 NT TP-30 ENGINE
 NT TURBOFAN ENGINES
 NT TURBOJET ENGINES
 NT TURBOFROF ENGINES
 JT8D and JT9D jet engine performance improvement program. Task 1: Feasibility analysis
 [NASA-CR-159449] p0033 879-20116
 CP6 jet engine performance improvement program.
 Task 1: Feasibility analysis
 [NASA-CR-159450] p0033 879-21074
 Design study and performance analysis of a high-speed multistage variable-geometry fan for a variable cycle engine
 [NASA-CR-159545] p0034 879-25020
 Dispersion of sound in a combustion duct by fuel droplets and soot particles
 [NASA-TN-79236] p0174 873-31002
JET EXHAUST
 A jet exhaust noise prediction procedure for inverted velocity profile conannular nozzles
 [AIAA PAPER 79-0633] p0178 879-28964
 The Advanced Low-Emissions Catalytic-Combustor Program: Phase I - Description and status --- for aircraft gas turbine engines
 [ASME PAPER 79-GT-192] p0027 879-30557
JET FLAMES
 U FLAMES
 U JET FLOW
JET FLOW
 Lean combustion limits of a confined premixed-prevaporized propane jet
 [AIAA PAPER 79-0538] p0026 879-25856
 Atomization of water jets and sheets in axial and swirling airflows
 [ASME PAPER 79-GT-170] p0106 879-30556
JET FUELS
 U JET ENGINE FUELS
JET IMPINGEMENT
 Heat transfer from a row of jets impinging on concave semi-cylindrical surface
 p0108 879-42890
JET LIFT
 Wing aerodynamic loading caused by jet-induced lift associated with STOL-OTW configurations
 [NASA-TN-79218] p0004 879-28146
JET MIXING FLOW
 An improved method for predicting the effects of flight on jet mixing noise
 p0176 879-39803
 An improved method for predicting the effects of flight on jet mixing noise
 [NASA-TN-79155] p0173 879-24770
JET NOISE
 U JET AIRCRAFT NOISE
JETTAVATORS
 U GUIDE VANES
JITTER
 U VIBRATION
JOINING
 Integrated gas turbine engine-nacelle
 [NASA-CASE-LEW-12389-3] p0014 879-14096
JOURNAL BEARINGS
 Development of surface coatings for air-lubricated, compliant journal bearings to 650 C
 [ASLE PREPRINT 78-LC-3C-1] p0123 879-23252
 Static evaluation of surface coatings for compliant gas bearings in an oxidizing atmosphere to 650 C
 p0088 879-31957
JOURNALS (SHAFTS)
 U SHAFTS (MACHINE ELEMENTS)
JP-5 JET FUEL
 Evaluation of the application of some gas chromatographic methods for the determination of properties of synthetic fuels
 p0070 879-25917
JUPITER PROBES
 Jupiter probe charging study
 [NASA-TP-1263] p0046 879-15149
- KEVLAR (TRADEMARK)**
 Full-scale engine tests of bulk absorber acoustic inlet treatment
 [AIAA PAPER 79-0600] p0026 879-26881
 Acoustic behavior of a fibrous bulk material --- Kevlar 29 sound absorber
 [AIAA PAPER 79-0599] p0178 879-26910
 Fabrication and testing of non-graphitic superhybrid composites
 p0066 879-43289
KINETIC FRICTION
 NT SLIDING FRICTION
KINETIC THEORY
 NT TRANSPORT THEORY
KINETICS
 NT REACTION KINETICS
KIRCHHOFF-HUTGENS PRINCIPLE
 U WAVE PROPAGATION
KLYSTRONS
 Comments on measuring the overall and the depressed collector efficiency in TWT's and klystron amplifiers
 p0099 879-25118
KNUDSEN CELLS
 U KNUDSEN GAGES
KNUDSEN GAGES
 Mass spectrometric investigation of the vaporization of sodium and potassium chromates - Preliminary results
 p0071 879-49533
- KU BAND**
 U SUPERHIGH FREQUENCIES
- L**
L BAND
 U ULTRAHIGH FREQUENCIES
LABORATORIES
 NT ENGINE TESTING LABORATORIES
LAGRANGE EQUATIONS OF MOTION
 U EULER-LAGRANGE EQUATION
LAKE ERIE
 Atmospheric transformation of multispectral remote sensor data --- Great Lakes
 [E79-10006] p0131 879-12524
LAKES
 NT GREAT LAKES (NORTH AMERICA)
 NT LAKE ERIE
LAMINAR FLAMES
 U FLAMES
LAMINAR FLOW
 NT HARTMANN FLOW
LAMINAR FLOW CONTROL
 U BOUNDARY LAYER CONTROL
LAMINAR JETS
 U JET FLOW
LAMINAR MIXING
 An experimental investigation of forced mixing of a turbulent boundary layer in an annular diffuser --- for boundary layer control
 [NASA-TN-79171] p0004 879-23520
LAMINATED MATERIALS
 U LAMINATES
LAMINATES
 Titanium/beryllium laminates - Fabrication, mechanical properties, and potential aerospace applications
 p0064 879-20836
 Effects of moisture profiles and laminate configuration on the hygro stress in advanced composites
 p0064 879-24132
 Fabrication and testing of nongraphitic superhybrid composites
 [NASA-TN-79102] p0063 879-20188
LABORATIONS
 U LAMINATES
LANGUAGES
 NT ASSEMBLY LANGUAGE
LARGE SPACE STRUCTURES
 Space environmental interactions with spacecraft surfaces
 [AIAA PAPER 79-0386] p0049 879-23511
 Large space system - Charged particle environment interaction technology --- effects on high voltage solar array performance
 [AIAA 79-0913] p0055 879-34775
 Low-thrust chemical orbit transfer propulsion
 [AIAA PAPER 79-1182] p0055 879-39815
- K**
K BAND
 U EXTREMELY HIGH FREQUENCIES
KA BAND
 U EXTREMELY HIGH FREQUENCIES

LASER APPLICATIONS

Solar-pumped lasers for space power transmission
[AIAA PAPER 79-1015] p0112 A79-38202
An electro-optic, high-voltage, transient probe
[NASA-TM-79019] p0109 A79-12414
Experiments on multiplane balancing using a laser
for material removal
[NASA-CR-31005] p0121 A79-17228
Laser rocket system analysis
[NASA-CR-159521] p0112 A79-21337
Fuel spray data with LDV --- solar laser
morphokinometer capabilities in combustion
research p0019 A79-24997

LASER DOPPLER VELOCIMETERS

Design, development, and test of a laser
velocimeter for a small 8:1 pressure ratio
centrifugal compressor
[NASA-CR-134781] p0111 A79-27478
Laser anemometer measurements at the exit of a
T67-C20 combustor
[NASA-CR-159623] p0107 A79-28456

LASER DRILLING

Laser balancing demonstration on a high-speed
flexible rotor
[ASME PAPER 79-GT-56] p0123 A79-32351

LASER HEATING

Convective heat flux in a laser-heated thruster
p0057 A79-22396

LASER OUTPUTS

Ground-to-space optical power transfer --- using
laser propulsion for orbit transfer p0167 A79-17180

LASERS

NT CONTINUOUS WAVE LASERS
NT DYE LASERS
NT GAS LASERS
NT PULSED LASERS
NT ULTRAVIOLET LASERS
Laser power conversion system analysis, volume 1
[NASA-CR-159523-VOL-1] p0112 A79-21334
Laser power conversion system analysis, volume 2
[NASA-CR-159523-VOL-2] p0112 A79-21335
Design investigation of solar powered lasers for
space applications
[NASA-CR-159554] p0111 A79-26384
High power phase locked laser oscillators
[NASA-CR-159630] p0112 A79-32538

LATTICE IMPERFECTIONS

U CRYSTAL DEFECTS

LAUNCH VEHICLES

NT ATLAS LAUNCH VEHICLES
NT CENTAUR LAUNCH VEHICLE
Plasma Interaction Experiment (PIX) flight results
p0047 A79-24022

LAUNCHING

NT LUNAR LAUNCH
NT SPACECRAFT LAUNCHING

LAWS

NT CLOSURE LAW
NT SCALING LAWS

LEAD ACID BATTERIES

Rapid, efficient charging of lead-acid and
nickel-zinc traction cells --- for electric
vehicles p0144 A79-10084
Response of lead-acid batteries to
chopper-controlled discharge --- for electric
vehicles p0145 A79-10097

LEAD COMPOUNDS

NT LEAD SULFIDES
The catalysis of nucleotide polymerization by
compounds of divalent lead --- prebiotic synthesis
p0060 A79-32924

LEAD SULFIDES

Electronic properties of PbMo6S8 and CuMo6S8 ---
for superconductivity p0187 A79-41731

LEADING EDGES

Unsteady flow in a supersonic cascade with
subsonic leading-edge locus p0005 A79-16047

LEAKAGE

Transmission seal development
[NASA-CR-135372] p0120 A79-10423
Compressible flow across narrow passages:
Comparison of theory and experiment for face seals
[NASA-TF-1346] p0113 A79-10424

Thermal stress analysis of ceramic gas-path seal
components for aircraft turbines
[NASA-TF-1437] p0082 A79-21205
Low heat leak connector for cryogenic systems
[NASA-CASR-XLE-02367-1] p0093 A79-21225
Experimental and analytical tools for evaluation
of Stirling engine rod seal behavior
[NASA-CR-159543] p0122 A79-23429
LEAR JET AIRCRAFT
Simultaneous measurements of ozone outside and
inside cabins of two E-747 airliners and a Gates
Learjet business jet p0008 A79-27571

LEGENDRE CODE

U COMPUTER PROGRAMMING

LEVEL (QUANTITY)

NT GROUND STATE

LIFE (BIOLOGY)

U LIFE SCIENCES

LIFE (DURABILITY)

NT FATIGUE LIFE

NT SERVICE LIFE

NT STORAGE STABILITY

Some effects of cyclic induced deformation in
rocket thrust chambers
[NASA-TM-79112] p0103 A79-20337
Heat pipe life and processing study
[NASA-CR-159581] p0107 A79-25349
Strainrange partitioning life predictions of the
long time metal properties council creep-fatigue
tests
[NASA-TM-79260] p0127 A79-31619
Preliminary results of the mission profile life
test of a 30 cm Hg bombardment thruster
[NASA-TM-79261] p0054 A79-33254

LIFE CYCLE COSTS

Advanced General Aviation Turbine Engine (GATE)
concepts
[NASA-CR-159603] p0034 A79-25017
Computerized systems analysis and optimization of
aircraft engine performance, weight, and life
cycle costs
[NASA-TM-79221] p0170 A79-29938

LIFE SCIENCES

Maximum likelihood estimation for life
distributions with competing failure modes
[NASA-TM-79126] p0169 A79-23735

LIFETIME (DURABILITY)

U LIFE (DURABILITY)

LIFT

NT JET LIFT

Wing aerodynamic loading caused by jet-induced
lift associated with STOL-OTW configurations
[AIAA PAPER 79-1664] p0006 A79-47346

LIFT COEFFICIENTS

U AERODYNAMIC COEFFICIENTS

U LIFT

LIFT DISTRIBUTION

U LIFT

LIFT FANS

Aerodynamic performance of 1.38-pressure-ratio,
variable-pitch fan stage
[NASA-TF-1502] p0024 A79-31213
Aerodynamic performance of axial-flow fan stage
operated at nine inlet guide vane angles --- to
be used on vertical lift aircraft
[NASA-TF-1510] p0024 A79-31214

LIFT FORCES

U LIFT

LIGHT (VISIBLE RADIATION)

NT SKY RADIATION

LIGHT ALLOYS

NT ALUMINUM ALLOYS

LIGHT TRANSMISSION

High power phase locked laser oscillators
[NASA-CR-159630] p0112 A79-32538

LIGHTING EQUIPMENT

NT FLASH LAMPS

Market definition studies for photovoltaic highway
applications
[NASA-CR-159477] p0152 A79-19451

LINE SPECTRA

Method for decomposing observed line shapes
resulting from multiple causes - Application to
plasma charge-exchange-neutral spectra p0182 A79-53867

LINERS

U LININGS

LINING PROCESSES

Optimized multisectioned acoustic liners
[NASA-TM-79028] p0172 N79-15759

LININGS

NT SOCKET LININGS

Optimized multisectioned acoustic liners
[AIAA PAPER 79-0182] p0174 A79-19581

Some loads limits and self-lubricating properties
of plain spherical bearings with molded graphite
fiber-reinforced polyimide liners to 320 C
[ASLE PREPRINT 78-LC-5C-2] p0118 A79-23251

A statistical theory of sound radiation from a
two-dimensional lined duct
[AIAA PAPER 79-1521] p0176 A79-46707

Duct wall impedance control as an advanced concept
for acoustic suppression enhancement --- engine
noise reduction
[NASA-CN-159425] p0176 N79-10842

An analytical and experimental study of sound
propagation and attenuation in variable-area ducts
--- reducing aircraft engine noise
[NASA-CN-135392] p0177 N79-25845

LINKING

U JOINING

LIQUEFIED GASES

NT LIQUID HYDROGEN

NT LIQUID NITROGEN

NT LIQUID OXYGEN

LIQUID COOLING

NT FILM COOLING

Liquid-cooling technology for gas turbines -
Review and status
p0116 A79-10038

Review and status of liquid-cooling technology for
gas turbines
[NASA-RP-1038] p0104 N79-22427

LIQUID DROPS

U DROPS (LIQUIDS)

LIQUID FLOW

NT WATER FLOW

LIQUID HYDROGEN

Turbine engine altitude chamber and flight testing
with liquid hydrogen
[NASA-TM-79196] p0022 N79-27140

Liquid oxygen/liquid hydrogen boost/vane pump for
the advanced orbit transfer vehicles auxiliary
propulsion system
[NASA-CN-159648] p0057 N79-31341

LIQUID INJECTION

NT WATER INJECTION

LIQUID LITHIUM

Lithium and potassium heat pipes for thermionic
converters
p0145 A79-10113

LIQUID MERCURY

U MERCURY (METAL)

LIQUID METALS

NT LIQUID LITHIUM

NT MERCURY (METAL)

Hartmann flow with temperature-dependent physical
properties --- magnetohydrodynamics of liquid
metal
p0182 A79-15597

Analysis of solidification interface shape during
continuous casting of a slab
p0079 A79-52697

LIQUID NITROGEN

Condensation on a noncollapsing vapor bubble in a
subcooled liquid
p0100 A79-49535

Condensation on a noncollapsing vapor bubble in a
subcooled liquid
[NASA-TM-79212] p0105 N79-27461

LIQUID OXYGEN

Comparison of analysis and experiment for
self-acting seals for liquid-oxygen turbopumps
[NASA-TF-1443] p0115 N79-22519

Liquid oxygen/liquid hydrogen boost/vane pump for
the advanced orbit transfer vehicles auxiliary
propulsion system
[NASA-CN-159648] p0057 N79-31341

LIQUID PROPELLANT ROCKET ENGINES

NT HYDROGEN OXYGEN ENGINES

Plug cluster engine concept for in-space missions
[AIAA PAPER 79-1179] p0055 A79-38972

LIQUID ROCKET PROPELLANTS

NT CRYOGENIC ROCKET PROPELLANTS

Axial jet mixing of ethanol in cylindrical
containers during weightlessness

[NASA-TF-1487] p0090 N79-28350
Study of liquid and vapor flow into a Centaur
capillary device
[NASA-CN-159657] p0108 N79-33432

LIQUID SURFACES

Feasibility study of liquid pool burning in
reduced gravity
[NASA-CN-159642] p0072 N79-32303

LIQUID-GAS MIXTURES

NT AEROSOLS

METALM: A computer code for calculating
thermodynamic and transport properties of
air-water mixtures
[NASA-TF-1466] p0166 N79-23688

LIQUIDS

NT CRYOGENIC FLUIDS

NT CRYOGENIC ROCKET PROPELLANTS

NT LIQUID HYDROGEN

NT LIQUID LITHIUM

NT LIQUID METALS

NT LIQUID NITROGEN

NT LIQUID OXYGEN

NT LIQUID ROCKET PROPELLANTS

NT MERCURY (METAL)

LITHIUM

NT LIQUID LITHIUM

LITHOSPHERE

NT EARTH SURFACE

LOAD DISTRIBUTION (FORCES)

Stresses from arbitrary loads on a circular crack
p0130 A79-27938

LOAD FACTORS

U LOADS (FORCES)

LOAD TESTS

Mode I analysis of a cracked circular disk subject
to a couple and a force
p0128 A79-15588

Some loads limits and self-lubricating properties
of plain spherical bearings with molded graphite
fiber-reinforced polyimide liners to 320 C
[ASLE PREPRINT 78-LC-5C-2] p0118 A79-23251

Review of the AGARD S and M panel evaluation
program of the NASA-Lewis SEP approach to
high-temperature LCF life prediction
p0023 N79-27179

LOADING FORCES

U LOADS (FORCES)

LOADING WAVES

U LOADS (FORCES)

LOADS (FORCES)

NT AERODYNAMIC LOADS

NT CYCLIC LOADS

NT DYNAMIC LOADS

NT GUST LOADS

NT IMPACT LOADS

NT ROLLING CONTACT LOADS

NT STATIC LOADS

NT TRANSIENT LOADS

NT WING LOADING

CODSTRAN - Composite durability structural analysis
p0128 A79-37292

Mode I crack surface displacements for a round
compact specimen subject to a couple and force
p0129 A79-39812

Mode I crack surface displacements for a round
compact specimen subject to a couple and force
[NASA-TM-79096] p0161 N79-20572

LOGARITHMS

Acceleration of linear and logarithmic convergence
p0168 A79-40494

LOGIC DESIGN

Multivariable control altitude demonstration on
the F100 turbofan engine
[AIAA PAPER 79-1204] p0029 A79-39814

LONG TERM EFFECTS

Effects of graphite fiber stability on the
properties of PMR polyimide composites
p0066 A79-43309

LOOPS

Closed loop spray cooling apparatus
[NASA-CASE-LEW-11981-2] p0103 N79-20336

LOSSES

Low-turbulence high-speed wind tunnel for the
determination of cascade shock losses
[ASME PAPER 79-GT-129] p0039 A79-32398

LOUDNESS

Loudness of steady sounds - A new theory
p0176 A79-39975

- Overall loudness of steady sounds according to theory and experiment
[NASA-RF-1001] p0163 N79-25753
- LOW ALLOY STEELS**
U HIGH STRENGTH STEELS
- LOW ASPECT RATIO**
Study of blade aspect ratio on a compressor front stage aerodynamic and mechanical design report
[NASA-CR-159555] p0034 N79-23085
Performance of two-stage fan having low-aspect-ratio first-stage rotor blading
[NASA-TF-1493] p0023 N79-27143
- LOW COST**
Wind-turbine-generator rotor-blade concepts with low-cost potential p0147 A79-20828
- LOW FREQUENCIES**
Theory of low frequency noise transmission through turbines
[NASA-CR-159457] p0033 N79-20117
- LOW GRAVITY**
U REDUCED GRAVITY
- LOW PRESSURE**
NASA CP6 jet engine diagnostics program: Long-term CP6-6D low-pressure turbine deterioration
[NASA-CR-159618] p0039 N79-29191
- LOW TEMPERATURE**
Atomic hydrogen storage method and apparatus
[NASA-CASE-LEW-12081-3] p0136 N79-18455
Measurements of mixed convective heat transfer to low temperature helium in a horizontal channel
[NASA-TM-79158] p0104 N79-23384
Experimental study of low temperature behavior of aviation turbine fuels in a wing tank model
[NASA-CR-159615] p0091 N79-29355
- LOW TEMPERATURE TESTS**
Influence of composition, annealing treatment, and texture on the fracture toughness of Ti-5Al-2.5Sn plate at cryogenic temperatures p0077 A79-24262
Low temperature normal state resistance of ternary molybdenum sulfides p0185 A79-27230
Effects of thermomechanical processing on strength and toughness of Fe-12Ni reactive metal alloys at 77K p0078 A79-32600
- LOW THRUST PROPULSION**
NT ION PROPULSION
NT SOLAR ELECTRIC PROPULSION
NT SOLAR PROPULSION
Space propulsion technology overview
[AIAA 79-0860] p0054 A79-34704
Low-thrust chemical orbit transfer propulsion
[AIAA PAPER 79-1182] p0055 A79-39815
Low-thrust chemical orbit transfer propulsion
[NASA-TM-79190] p0043 N79-25129
- LOW TURBULENCE**
Low-turbulence high-speed wind tunnel for the determination of cascade shock losses
[ASME PAPER 79-GT-129] p0039 A79-32398
- LOWER ATMOSPHERE**
NT TROPOSPHERE
- LOX (OXYGEN)**
U LIQUID OXYGEN
- LOX-HYDROGEN ENGINES**
U HYDROGEN OXYGEN ENGINES
- LUBRICANT TESTS**
A comparison of the lubricating mechanisms of graphite fluoride and molybdenum disulfide films
p0085 A79-16659
Filtration effects on ball bearing life and condition in a contaminated lubricant
[ASME PAPER 78-LUB-34] p0118 A79-23246
Mechanisms of graphite fluoride /CF_x/n lubrication
p0086 A79-31249
Evaluation and auger analysis of a zinc-dialkyl-dithiophosphate antiwear additive in several diester lubricants
[NASA-TF-1544] p0084 A79-32359
- LUBRICANTS**
NT GAS LUBRICANTS
NT HIGH TEMPERATURE LUBRICANTS
NT LUBRICATING OILS
NT SOLID LUBRICANTS
Effect of geometry on hydrodynamic film thickness
[ASME PAPER 78-LUB-24] p0118 A79-23237
- A study of various synthetic routes to produce a halogen-labeled traction fluid
[NASA-TM-79024] p0059 N79-11119
- Lubrication and failure mechanisms of molybdenum disulfide films. 1: Effect of atmosphere
[NASA-TF-1343] p0081 N79-13158
- Lubrication and failure mechanisms of molybdenum disulfide films. 2: Effect of substrate roughness
[NASA-TF-1379] p0081 N79-13159
- Determination of lubricant selection based on elastohydrodynamic film thickness and traction measurement
[NASA-CR-159428] p0121 N79-14385
- LUBRICATING OILS**
Diagnostics of wear in aeronautical systems p0120 A79-39805
- LUBRICATION**
NT BOUNDARY LUBRICATION
NT SELF LUBRICATION
The practical impact of elastohydrodynamic lubrication p0117 A79-11545
Elastohydrodynamic lubrication of elliptical contacts for materials of low elastic modulus. II - Starved conjunction
[ASME PAPER 78-LUB-1] p0118 A79-23229
Elastohydrodynamic film thickness measurements of artificially produced surface dents and grooves --- on fatigue failure of bearings
[ASLE PREPRINT 78-LC-1A-1] p0118 A79-23267
Two-dimensional random surface model for asperity-contact in elastohydrodynamic lubrication p0120 A79-39811
Two-dimensional random surface model for asperity-contact in elastohydrodynamic lubrication
[NASA-TM-79006] p0115 N79-23430
Auger spectroscopy analysis of lubrication with zinc dialkyl-dithiophosphate of several metal combinations in sliding contact
[NASA-TF-1489] p0083 N79-27308
Elastohydrodynamic film thickness measurements of artificially produced nonsmooth surfaces
[NASA-TM-79214] p0115 N79-28554
Lubricating and wear mechanisms for a hemisphere sliding on polyimide-bonded graphite fluoride film
[NASA-TF-1524] p0084 N79-30381
Comparison of predicted and measured elastohydrodynamic film thickness in a 20-millimeter-bore ball bearing
[NASA-TF-1542] p0116 N79-32552
Correlation of asperity contact-time fraction with elastohydrodynamic film thickness in a 20-millimeter-bore ball bearing
[NASA-TF-1547] p0116 N79-33476
- LUBER BANDS**
U PLASTIC DEFORMATION
- LUMINAIRES**
NT FLASH LAMPS
- LUNAR LAUNCH**
Mass drivers. 3: Engineering p0040 N79-32232

M

MACHINE LIFE

U SERVICE LIFE

MACHINING

Laser balancing demonstration on a high-speed

flexible rotor

[ASME PAPER 79-GT-56] p0123 A79-32351

MAGNETIC DISTURBANCES

NT MAGNETIC SIGNS

MAGNETIC EFFECTS

Anomalous galvanomagnetic properties of graphite in strong magnetic fields p0185 A79-23633

MAGNETIC FIELD CONFIGURATIONS

Physical processes in directed ion beam sputtering
[NASA-CR-159567] p0182 A79-26943

MAGNETIC FIELDS

The magnetocaloric effect in dysprosium p0185 A79-38402

Trajectories of charged particles in radial electric and uniform axial magnetic fields p0182 A79-41788

Indirect measurements of Ferri surface parameters of some chevrel phase materials p0185 A79-50231

- Atomic hydrogen storage method and apparatus
[NASA-CASE-LEW-12081-3] p0136 N79-18455
Design of high-pervance confined-flow guns for
periodic-permanent-magnet-focused tubes
[NASA-TF-1485] p0098 N79-27400
- MAGNETIC MATERIALS**
Analytical core loss calculations for magnetic
materials used in high frequency high power
converter applications
[NASA-TM-79234] p0098 N79-31499
- MAGNETIC METALS**
U MAGNETIC MATERIALS
U METALS
- MAGNETIC PROPERTIES**
NT MAGNETIC EFFECTS
NT MAGNETORESISTIVITY
The magnetocaloric effect in dysprosium
p0185 A79-38402
Analytical core loss calculations for magnetic
materials used in high frequency high power
converter applications
[NASA-TM-79234] p0098 N79-31499
- MAGNETIC RESONANCE**
NT ELECTRON PARAMAGNETIC RESONANCE
- MAGNETIC STORMS**
Charging analysis of the SCATHA satellite
p0049 N79-24012
- MAGNETIC SUBSTORMS**
U MAGNETIC STORMS
- MAGNETOACTIVITY**
NT MAGNETORESISTIVITY
- MAGNETOGASDYNAMICS**
U MAGNETOHYDRODYNAMICS
- MAGNETOHYDRODYNAMIC FLOW**
Hartmann flow with temperature-dependent physical
properties --- magnetohydrodynamics of liquid
metal
p0182 A79-15597
Velocity, temperature, and electrical conductivity
profiles in hydrogen-oxygen MHD duct flows
p0182 A79-26184
- MAGNETOHYDRODYNAMIC GENERATORS**
Design study of superconducting magnets for a
combustion magnetohydrodynamic /MHD/ generator
p0098 A79-15305
Preliminary results in the NASA Lewis H2-O2
combustion MHD experiment
p0182 A79-39807
Performance optimization of an MHD generator with
physical constraints
p0182 A79-51995
Evaluation of the ECAS open cycle MHD power plant
design
[NASA-TM-79012] p0136 N79-17335
Performance optimization of an MHD generator with
physical constraints
[NASA-TM-79172] p0138 N79-24446
MHD performance calculations with oxygen enrichment
[NASA-TM-79140] p0139 N79-25499
Performance characteristics of a slagging gasifier
for MHD combustor systems
[NASA-TM-79195] p0142 N79-30720
- MAGNETOHYDRODYNAMICS**
Trajectories of charged particles in radial
electric and uniform axial magnetic fields
p0182 A79-41743
Preliminary evaluation of the role of K2S in MHD
hot stream seed recovery
[NASA-TM-79114] p0068 N79-20200
Preliminary results in the NASA Lewis H2-O2
combustion MHD experiment
[NASA-TM-79135] p0181 N79-22897
- MAGNETOIONIC PLASMA**
U PLASMAS (PHYSICS)
- MAGNETOPLASMA DYNAMICS**
U MAGNETOHYDRODYNAMICS
- MAGNETOPLASMAS**
U PLASMAS (PHYSICS)
- MAGNETORESISTIVITY**
Optical, spin-resonance, and magnetoresistance
studies of /tetrathiatetracene/2/iodide/3 - The
nature of the ground state
p0184 A79-10417
Hall effect and magnetoresistivity in the ternary
molybdenum sulfides
p0185 A79-21157
Electronic properties of PbMo6S8 and CuMo6S8 ---
for superconductivity
p0187 A79-41731
- MAGNETOSPHERE**
Spacecraft charging modeling development and
validation study
p0050 N79-24051
- MAGNETS**
NT CRYOGENIC MAGNETS
NT HIGH FIELD MAGNETS
NT SUPERCONDUCTING MAGNETS
- MAN MACHINE SYSTEMS**
Computer aided control of a mechanical arm
A79-50334
- MANAGEMENT**
NT PROJECT MANAGEMENT
NT SAFETY MANAGEMENT
- MANAGEMENT PLANNING**
NT PROJECT PLANNING
- MANEUVERS**
NT ORBITAL MANEUVERS
- MANGANESE**
Friction and wear of single-crystal manganese-zinc
ferrite
p0185 A79-34994
- MANGANESE ALLOYS**
Anisotropic friction and wear of single-crystal
manganese-zinc ferrite in contact with itself
[NASA-TF-1339] p0113 N79-10425
- MANGANESE COMPOUNDS**
Friction and wear of single-crystal manganese-zinc
ferrite
[NASA-TM-78980] p0184 N79-16699
- MANIPULATION**
U MANIPULATORS
- MANIPULATORS**
Computer aided control of a mechanical arm
A79-50334
- MANNED ORBITAL SPACE STATIONS**
U ORBITAL SPACE STATIONS
- MANNED SPACECRAFT**
NT ORBITAL SPACE STATIONS
NT SPACE SHUTTLES
- MANUALS**
NT USER MANUALS (COMPUTER PROGRAMS)
The 30-centimeter ion thrust subsystem design manual
[NASA-TM-79191] p0053 N79-25131
- MANUFACTURING**
Evaluation of manufacturing processes for
boron/aluminum composites containing
0.2-mm-diameter boron fibers
[NASA-TM-79008] p0062 N79-12153
A heat exchanger and method of making
[NASA-CASE-LEW-12441-3] p0104 N79-23383
- MAPPING**
NT ICE MAPPING
NT PHOTOMAPPING
NT THERMAL MAPPING
Definition of mutually optimum NDI and proof test
criteria for 2219 aluminum pressure vessels.
Volume 3: Applications to rail defect evaluation
[NASA-CR-135447] p0125 N79-21412
Potential mapping with charged-particle beams
p0049 N79-24038
- MARKET RESEARCH**
20/30 GHz satellite systems technology needs
assessment --- for domestic communications
p0095 A79-14948
Telecommunication service markets through the year
2000 in relation to millimeter wave satellite
systems
p0095 A79-27398
Telecommunication service markets through the year
2000 in relation to millimeter wave satellite
systems
[NASA-TM-79099] p0094 N79-16169
Determining potential 30/20 GHz domestic satellite
system concepts and establishment of a suitable
experimental configuration
[NASA-TM-79092] p0094 N79-17072
Market definition studies for photovoltaic highway
applications
[NASA-CR-159477] p0152 N79-19451
- MASS DISTRIBUTION**
An introduction to a unified approach to flexible
rotor balancing
[ASME PAPER 79-GT-161] p0124 A79-32423
- MASS DRIVERS (PAYLOAD DELIVERY)**
Mass drivers. 3: Engineering
p0040 N79-32232
- MASS FILTERS**
U FLUID FILTERS

MASS FLOW

Critical mass flux through short Borda type inlets
of various cross sections
[NASA-TM-79017] p0074 N79-20216

MASS RATIOS

Effect of oxygen-nitrogen ratio on sinterability
of Sialons
[NASA-TP-1382] p0082 N79-21204

MASS SPECTROMETRY

U MASS SPECTROSCOPY

MASS SPECTROSCOPY

Mass spectrometric investigation of the
vaporization of sodium and potassium chromates -
Preliminary results
p0071 A79-49533

Preliminary evaluation of the role of K₂S in HHD
hot stream seed recovery
[NASA-TM-79114] p0068 N79-20200

Mass spectrometric investigation of the
vaporization of sodium and potassium chromates:
Preliminary results
[NASA-TM-79210] p0069 N79-27279

MATERIAL ABSORPTION

Acoustic behavior of a fibrous bulk material ---
Kevlar 29 sound absorber
[AIAA PAPER 79-0599] p0178 A79-26910

MATERIAL REMOVAL (MACHINING)

U MACHINING

MATERIALS RECOVERY

Experiments on multiplane balancing using a laser
for material removal
[NASA-CR-3105] p0121 N79-17228

MATERIALS TESTS

Laboratory studies of electrical properties of
insulating materials --- thermal insulation of
spacecraft dielectrics
p0044 A79-20877

Computer signal processing for ultrasonic
attenuation and velocity measurements for
material property characterizations
p0125 A79-39809

Numbers of center points appropriate to blocked
response surface experiments
p0169 A79-49529

MATHEMATICAL LOGIC

NT ALGORITHMS

Overall loudness of steady sounds according to
theory and experiment
[NASA-RP-1001] p0163 N79-25753

MATHEMATICAL MODELS

NT DIGITAL SIMULATION

Control of wind turbine generators connected to
power systems
p0146 A79-15574

Mode I analysis of a face cracked plate subjected
to rotationally constrained end displacements
p0128 A79-21831

Acoustic behavior of a fibrous bulk material ---
Kevlar 29 sound absorber
[AIAA PAPER 79-0599] p0178 A79-26910

Modeling of switching regulator power stages with
and without zero-inductor-current dwell time
p0101 A79-49398

High speed cylindrical roller bearing analysis,
SKF computer program CYBEAN. Volume 1: Analysis
[NASA-CR-159460] p0121 N79-17222

Simulation of fluidized bed coal combustors
[NASA-CR-159529] p0153 N79-20487

Simulated electronic heterodyne recording and
processing of pulsed-laser holograms
[NASA-TP-1444] p0111 N79-21329

Modelling turbulent flame ignition and blowout
p0021 N79-25008

A thermal control approach for a solar electric
propulsion thrust subsystem
[NASA-TM-79175] p0043 N79-27236

First principles numerical model of
avalanche-induced arc discharges in
electron-irradiated dielectrics
[NASA-CR-159560] p0101 N79-28418

Application of the principle of similarity fluid
mechanics
[NASA-TM-79258] p0105 N79-30515

Modeling of thin, back-wall silicon solar cells
p0143 N79-32650

MATHEMATICAL PROGRAMMING

NT NONLINEAR PROGRAMMING

MAXIMUM LIKELIHOOD ESTIMATES

Maximum likelihood estimation for life

distributions with competing failure modes
p0169 A79-49528

Maximum likelihood estimation for life
distributions with competing failure modes
[NASA-TM-79126] p0169 N79-23735

MEAN TIME BETWEEN FAILURES

U MTBF

MEASURE AND INTEGRATION

NT NUMERICAL INTEGRATION

MEASURING INSTRUMENTS

NT COMPARATORS

NT ENGINE ANALYZERS

NT ENGINE MONITORING INSTRUMENTS

NT EXTENSOMETERS

NT FLIGHT RECORDERS

NT INFRARED INSTRUMENTS

NT KNUDSEN GAGES

NT LASER DOPPLER VELOCIMETERS

NT METEOROLOGICAL INSTRUMENTS

NT MICRONILLIAMMETERS

NT MULTISPECTRAL BAND SCANNERS

NT OPTICAL MEASURING INSTRUMENTS

NT PLASMA PROBES

NT STRAIN GAGES

NT TEMPERATURE MEASURING INSTRUMENTS

NT TEMPERATURE PROBES

NT TIMING DEVICES

NT TURBULENCE METERS

An in-place recalibration technique to extend the
temperature capability of capacitance-sensing,
rotor-blade-tip-clearance measurement systems
[SAE PAPER 781003] p0026 A79-25885

Condensation-nuclei (Aitken Particle) measurement
system used in NASA global atmospheric sampling
program
[NASA-TP-1415] p0157 N79-18479

Carbon monoxide measurement in the global
atmospheric sampling program
[NASA-TP-1526] p0158 N79-31841

MECHANICAL DRIVES

NT TRANSMISSIONS (MACHINE ELEMENTS)

Performance of a Wasvylis multiroller traction drive
[NASA-TP-1378] p0113 N79-13369

The rotary combustion engine: A candidate for
general aviation --- conferences
[NASA-CR-2067] p0016 N79-15961

Power train analysis for the DOE/NASA 100-kW wind
turbine generator
[NASA-TM-78997] p0135 N79-16355

Speed reducers-increasers
p0140 N79-26481

Traction drive performance prediction for the
Johnson and Tevaarwerk traction model
[NASA-TP-1530] p0116 N79-33475

NASA gear research and its probable effect on
rotorcraft transmission design
[NASA-TM-79292] p0116 N79-33477

MECHANICAL ENGINEERING

Shaft seal assembly for high speed and high
pressure applications
[NASA-CASE-LEN-11873-1] p0115 N79-22475

A heat exchanger and method of making
[NASA-CASE-LEN-12441-3] p0104 N79-23383

MECHANICAL MEASUREMENT

NT DISPLACEMENT MEASUREMENT

NT FLOW MEASUREMENT

NT FRICTION MEASUREMENT

NT PRESSURE MEASUREMENTS

NT STRESS MEASUREMENT

NT THRUST MEASUREMENT

NT VELOCITY MEASUREMENT

NT VIBRATION MEASUREMENT

MECHANICAL PROPERTIES

NT AEROELASTICITY

NT BULK MODULUS

NT COLD STRENGTH

NT CREEP PROPERTIES

NT CREEP RUPTURE STRENGTH

NT DYNAMIC MODULUS OF ELASTICITY

NT FATIGUE LIFE

NT FIBER STRENGTH

NT FRACTURE STRENGTH

NT HIGH STRENGTH

NT IMPACT STRENGTH

NT MODULUS OF ELASTICITY

NT SHEAR PROPERTIES

NT SHEAR STRENGTH

NT STIFFNESS

NT STRESS CYCLES

NT STRUCTURAL STABILITY
 NT TENSILE PROPERTIES
 NT TENSILE STRENGTH
 NT THERMAL RESISTANCE
 NT TOUGHNESS
 NT YIELD STRENGTH

An operating 200 kW horizontal axis wind turbine
 p0147 A79-20829
 Mechanics of intraply hybrid composites -
 Properties, analysis and design p0065 A79-31033

Dynamic mechanical analysis of fiber reinforced
 composites p0065 A79-31040

Effects of graphite fiber stability on the
 properties of PMR polyimide composites p0066 A79-43309

Fracture modes in off-axis fiber composites
 [NASA-TM-79036] p0062 A79-12154

Evaluation of the mechanical properties of
 electrosag refined Fe-12Ni alloys p0079 A79-12202

Effects of graphite fiber stability on the
 properties of PMR polyimide composites
 [NASA-TM-79062] p0061 A79-16075

Fabrication and testing of silver-hydrogen cells
 [NASA-CN-159490] p0152 A79-16375

Prediction of properties of intraply hybrid
 composites p0061 A79-16919

Elevated temperature properties of boron/aluminum
 composites p0066 A79-16924

Evaluation of an advanced directionally solidified
 gamma/gamma'-alpha Mo eutectic alloy p0079 A79-20222

Effect of grain orientation and coating on thermal
 fatigue resistance of a directionally solidified
 superalloy (MAR-M 247) p0127 A79-22565

Survey of ion plating sources --- conferences
 [NASA-TM-79269] p0076 A79-31372

MECHANICAL RESONANCE

U RESONANT VIBRATION

MEDICAL EQUIPMENT

NT PROSTHETIC DEVICES

MEETINGS

U CONFERENCES

MEISSNER EFFECT

U SUPERCONDUCTIVITY

MELTING POINTS

High freezing point fuels used for aviation
 turbine engines p0085 A79-15199

MELTS (CRYSTAL GROWTH)

Analysis of solidification interface shape during
 continuous casting of a slab p0079 A79-52697

MEMBRANE ANALOGY

U STRUCTURAL ANALYSIS

MEMBRANE THEORY

U STRUCTURAL ANALYSIS

MEMBRANES

NT ION EXCHANGE MEMBRANE ELECTROLYTES

MERCURY (METAL)

Prediction of plasma properties in mercury ion
 thrusters p0056 A79-15152

Increased capabilities of the 30-cm diameter Hg
 ion thruster p0053 A79-22192

MERCURY ION ENGINES

Increased capabilities of the 30-cm diameter Hg
 ion thruster p0055 A79-34774

Description of A 2.3 kW power transformer for
 space applications p0099 A79-34991

Mercury ion thruster research, 1978
 [NASA-CN-159485] p0056 A79-16913

Sputtering in mercury ion thrusters
 [NASA-TM-79266] p0054 A79-31343

Reduced power processor requirements for the 30-cm
 diameter Hg ion thruster p0054 A79-33253

Preliminary results of the mission profile life
 test of a 30 cm Hg bombardment thruster p0054 A79-33254

MERIDIONAL FLOW

Effect of rotor meridional velocity ratio on
 response to inlet radial and circumferential
 distortion p0023 A79-28177

METAL BONDING

NT METAL-METAL BONDING

Adhesive bonding of ion beam textured metals and
 fluoropolymers p0060 A79-14798

Heat exchanger and method of making --- bonding
 rocket chambers with a porous metal matrix
 [NASA-CASE-LEW-12441-1] p0102 A79-13289

A heat exchanger and method of making --- rocket
 lining p0104 A79-21313

METAL COATINGS

NT ALUMINUM COATINGS

NT NICKEL COATINGS

A feasibility study of a diffusion barrier between
 Ni-Cr-Al coatings and nickel-based eutectic alloys
 p0077 A79-27233

Industrial potential, uses, and performance of
 sputtered and ion plated films p0119 A79-30398

Characterization of defect growth structures in
 ion plated films by scanning electron microscopy
 p0078 A79-34992

A strainrange partitioning analysis of low cycle
 fatigue of coated and uncoated Rene 80 p0129 A79-10479

NASA thermal barrier coatings: Summary and update
 [NASA-TM-79053] p0015 A79-15048

Lightweight porous plastic plaque --- nickel
 cadmium batteries p0141 A79-28672

METAL COMBUSTION

Resonance-tube ignition of aluminum
 p0071 A79-46366

METAL COMPOSITION

U CORROSION

METAL DRAWING

Critical current density in wire drawn and
 hydrostatically extruded Nb-Ti superconductors
 p0195 A79-20539

METAL FATIGUE

Effects of thermomechanical processing on strength
 and toughness of Fe-12Ni reactive metal alloys
 at 77K p0078 A79-32600

Fretting wear of iron, nickel, and titanium under
 varied environmental conditions p0073 A79-12203

Fatigue behavior of SiC reinforced titanium
 composites p0064 A79-30296

METAL FIBERS

Tungsten fiber reinforced FeCrAlY - A first
 generation composite turbine blade material
 p0065 A79-30397

METAL FILMS

Comparison of projected critical currents in
 PbMo6S8 and Nb3Ge p0185 A79-28300

METAL FORMING

U METAL WORKING

METAL HALIDES

NT SODIUM CHLORIDES

METAL IONS

The catalysis of nucleotide polymerization by
 compounds of divalent lead --- prebiotic synthesis
 p0060 A79-32924

METAL MATRIX COMPOSITES

Predicted inlet gas temperatures for tungsten
 fiber reinforced superalloy turbine blades
 p0025 A79-17029

High temperature dynamic modulus and damping of
 aluminum and titanium matrix composites
 p0065 A79-26132

Tungsten fiber reinforced FeCrAlY - A first
 generation composite turbine blade material
 p0065 A79-30397

Composites emerging for aeropropulsion applications
 p0066 A79-53720

Heat exchanger and method of making --- bonding
 rocket chambers with a porous metal matrix
 [NASA-CASE-LEW-12441-1] p0102 A79-13289

High temperature dynamic modulus and damping of
 aluminum and titanium matrix composites

- [NASA-TM-79080] p0061 N79-16077
Fabrication and testing of nongraphitic
superhybrid composites
- [NASA-TM-79102] p0063 N79-20188
Development and fabrication of high strength alloy
fibers for use in metal-metal matrix composites
- [NASA-TM-79115] p0063 N79-22211
A review of issues and strategies in
nondestructive evaluation of fiber reinforced
structural composites
- [NASA-TM-79246] p0125 N79-29530
Fatigue behavior of SiC reinforced titanium
composites
- [NASA-TM-79223] p0064 N79-30296
Evaluation of silicon carbide fiber/titanium
composites
- [NASA-TM-79232] p0064 N79-31349
METAL OXIDE SEMICONDUCTORS
Ionized dopant concentrations at the heavily doped
surface of a silicon solar cell
- [NASA-TP-1347] p0184 N79-13886
METAL OXIDES
NT ALUMINUM OXIDES
NT NICKEL OXIDES
NT YTTRIUM OXIDES
NT ZIRCONIUM OXIDES
METAL PARTICLES
NT METAL POWDER
METAL PLATES
Influence of composition, annealing treatment, and
texture on the fracture toughness of
Ti-5Al-2.5Sn plate at cryogenic temperatures
- p0077 A79-24262
Charging rates of metal-dielectric structures ---
with implications for spacecraft
- p0048 N79-24033
METAL POWDER
Bend strengths of reaction bonded silicon nitride
prepared from dry attrition milled silicon powder
- [NASA-TM-79230] p0084 N79-30379
METAL SURFACES
Fretting wear of iron, nickel, and titanium under
varied environmental conditions
- p0078 A79-34995
NASCAP modelling of high-voltage power system
interactions with space charged-particle
environments --- particle impact on solar
satellite surfaces
- p0051 A79-39806
Mode I crack surface displacements for a round
compact specimen subject to a couple and force
- p0129 A79-39812
Adhesive bonding of ion beam textured metals and
fluoropolymers
- [NASA-TM-79004] p0181 N79-12909
Friction and transfer of copper, silver, and gold
to iron in the presence of various adsorbed
surface films
- [NASA-TP-1392] p0114 N79-14386
Metal-dielectric interactions
- [NASA-TM-79151] p0075 N79-25195
Adhesive material transfer in the erosion of an
aluminum alloy
- [NASA-TM-79165] p0083 N79-27306
METAL WORKING
NT METAL DRAWING
Computer-aided analysis and design of the shape
rolling process for producing turbine engine
airfoils
- [NASA-CR-135367] p0080 N79-26175
METAL-GAS SYSTEMS
A proposed physical model for the impregnated
tungsten cathode based on Auger surface studies
of the Ba-O-W system
- p0078 A79-39972
METAL-METAL BONDING
The use of ion beam cleaning to obtain high
quality cold welds with minimal deformation
- p0119 A79-24121
METALLOIDS
NT BORON
NT SILICON
METALS
NT ALUMINUM
NT ALUMINUM COATINGS
NT BARIUM
NT BERYLLIUM
NT CHROMIUM
NT DYSPROSIUM
- NT GOLD
NT IRIIDIUM
NT IRON
NT LIQUID LITHIUM
NT LIQUID METALS
NT MANGANESE
NT MERCURY (METAL)
NT METAL COATINGS
NT METAL FILMS
NT METAL MATRIX COMPOSITES
NT METAL POWDER
NT MOLYBDENUM
NT NICKEL COATINGS
NT NIOBLE METALS
NT PLUTONIUM 238
NT POTASSIUM
NT REFRACTORY METALS
NT SILVER
NT TITANIUM
NT TUNGSTEN
NT ZINC
Solar cells having integral collector grids
- [NASA-CASE-LEW-12819-1] p0133 N79-11467
Whiskers, cones and pyramids created in sputtering
by ion bombardment
- [NASA-CR-159549] p0079 N79-20221
The friction and wear of metals and binary alloys
in contact with an abrasive grit of
single-crystal silicon carbide
- [NASA-TM-79131] p0075 N79-22274
METEORITE COMPRESSION TESTS
U MECHANICAL PROPERTIES
METEOROLOGICAL FLIGHT
Airborne atmospheric sampling system
- p0012 A79-50333
METEOROLOGICAL INSTRUMENTS
Aircraft icing
- p0161 N79-17418
METEOROLOGICAL PARAMETERS
An airborne meteorological data collection system
using satellite relay /ASDAR/
- p0010 A79-14949
Automated meteorological data from commercial
aircraft via satellite - Present experience and
future implications
- p0010 A79-17092
Aircraft icing
- p0161 N79-17418
METEOROLOGICAL SATELLITES
NT NOAA SATELLITES
METERS
U MEASURING INSTRUMENTS
METHOD OF CHARACTERISTICS
Calculation of the three-dimensional flow field in
supersonic inlets at angle of attack using a
bicharacteristic method with discrete shock wave
fitting
- [AIAA PAPER 79-0379] p0025 A79-19698
METHYL COMPOUNDS
Electrochemical fluorination of trichloroethylene
and N, N-dimethyltrifluoroacetamide
- p0060 A79-49536
Electrochemical fluorination of trichloroethylene
and N, N-dimethyltrifluoroacetamide
- p0060 A79-49536
MICROCIRCUITS
U MICROELECTRONICS
MICROELECTRONICS
Adaptation of ion beam technology to
microfabrication of solid state devices and
transducers
- [NASA-CR-159439] p0186 N79-11921
MICROMILLIMETERS
Optically isolated logarithmic nanometer capable
of floating to 5 kilovolts
- [NASA-TP-1527] p0098 N79-32467
MICROPROCESSORS
Microprocessor control of a wind turbine generator
- p0147 A79-21302
Microprocessor control of a wind turbine generator
- [NASA-TM-79021] p0134 N79-12548
Automated Plasma Spray (APS) process feasibility
study: Plasma spray process development and
evaluation
- [NASA-CR-159579] p0092 N79-29382
MICROSCOPES
NT ELECTRON MICROSCOPES
MICROSCOPY
NT ELECTRON MICROSCOPY

MICROSTRUCTURE

Transverse and longitudinal tensile properties at 760 C of several oxide dispersion strengthened nickel-base alloys

p0078 A79-49531

An investigation of the initiation stage of hot corrosion in Ni-base alloys

[NASA-CR-159616] p0080 N79-25146

MICROWAVE AMPLIFIERS

Comments on measuring the overall and the depressed collector efficiency in TWT's and klystron amplifiers

p0099 A79-25118

MICROWAVE ANTENNAS

NT SLOT ANTENNAS

MICROWAVE EMISSION

Microwave radiation measurements near the electron plasma frequency of the NASA Lewis Bumpy Torus plasma

p0181 A79-14953

MICROWAVE EQUIPMENT

NT KLYSTRONS

NT MICROWAVE AMPLIFIERS

NT SLOT ANTENNAS

NT TRAVELING WAVE TUBES

Improved apparatus for trapped radical and other studies down to 1.5 K --- microwave cavity cryogenic equipment for electron paramagnetic resonance experiments

p0110 A79-20742

MICROWAVE FREQUENCIES

NT C BAND

NT EXTREMELY HIGH FREQUENCIES

NT SUPERHIGH FREQUENCIES

MICROWAVE TRANSMISSION

20/30 GHz satellite systems technology needs assessment --- for domestic communications

p0095 A79-14948

Millimeter wave communication satellite concepts

p0095 A79-29784

MICROWAVE TUBES

NT KLYSTRONS

NT TRAVELING WAVE TUBES

MICROWAVES

NT MICROWAVE EMISSION

NT MILLIMETER WAVES

MICROWEIGHING

U WEIGHT MEASUREMENT

MILLIMETERS

NT MICROMILLIMETERS

MILLIMETER WAVES

Determining potential 30/70 GHz domestic satellite system concepts and establishment of a suitable experimental configuration

p0095 A79-27397

Telecommunication service markets through the year 2000 in relation to millimeter wave satellite systems

p0095 A79-27398

Millimeter wave communication satellite concepts

p0095 A79-29784

Millimeter wave satellite concepts. Volume 1:

Executive summary

[NASA-CR-159504]

p0041 N79-26101

Millimeter wave satellite concepts. Volume 2:

Technical report

[NASA-CR-159503]

p0041 N79-26102

MINERALS

NT GRAPHITE

NT SPINEL

MINIINIZATION

U OPTIMIZATION

MINING

NT STRIP MINING

MISALIGNMENT

Hydrodynamic effects in a misaligned radial face seal

[NASA-CR-135228]

p0121 N79-17226

MISORIENTATION

U MISALIGNMENT

MISSILE DETECTION

NT RADAR DETECTION

MISSILE ENGINE CASES

U ROCKET ENGINE CASES

MISSILE STABILIZATION

U STABILIZATION

MIXING

NT LAMINAR MIXING

Lean stability augmentation study --- on gas turbine combustion chambers

[NASA-CR-159536]

p0071 N79-22244

Modeling of premixing-prevaporizing fuel-air mixing passages

p0019 N79-24998

Axial jet mixing of ethanol in cylindrical containers during weightlessness

[NASA-TP-1487]

p0090 N79-28350

MIXTURES

NT AEROSOLS

NT AQUEOUS SOLUTIONS

NT EUTECTIC ALLOYS

NT GAS MIXTURES

NT LIQUID-GAS MIXTURES

NT METAL MATRIX COMPOSITES

NT SOLID SOLUTIONS

Thermophysical property data: Who needs them?

[NASA-TS-79241]

p0090 N79-31403

MOBILITY

NT IONIC MOBILITY

MODAL RESPONSE

An introduction to a unified approach to flexible rotor balancing

[ASME PAPER 79-GT-161]

p0124 A79-32423

MODE SHAPES

U MODAL RESPONSE

MODELS

NT DIGITAL SIMULATION

NT DYNAMIC MODELS

NT ENVIRONMENT MODELS

NT MATHEMATICAL MODELS

NT SCALE MODELS

MODES

NT COUPLED MODES

NT FAILURE MODES

NT PROPAGATION MODES

MODULATION

NT FREQUENCY MODULATION

NT PHASE MODULATION

NT PULSE DURATION MODULATION

MODULES

NT ELECTRONIC MODULES

NT SERVICE MODULES

NT SPACECRAFT MODULES

MODULUS OF ELASTICITY

NT DYNAMIC MODULUS OF ELASTICITY

Effect of grain orientation and coating on thermal fatigue resistance of a directionally solidified superalloy (MAR-M 247)

[NASA-TM-79129]

p0127 N79-22565

Evaluation of silicon carbide fiber/titanium composites

[NASA-TM-79232]

p0064 N79-31349

MORE CIRCLES

U FRACTURE MECHANICS

MOISTURE

Effects of hydrothermal exposure on a low-temperature cured epoxy

p0085 A79-15534

Synthesis of improved moisture resistant polymers

[NASA-CR-159510]

p0087 N79-23218

MOISTURE CONTENT

NT ATMOSPHERIC MOISTURE

Effects of moisture profiles and laminate configuration on the hygro stress in advanced composites

p0064 A79-24132

Synthesis of improved moisture resistant polymers

[NASA-CR-159456]

p0087 N79-18013

MOLDS

Wind-turbine-generator rotor-blade concepts with low-cost potential

p0147 A79-20828

MOLYBDENUM

Thermocouples of molybdenum and iridium alloys for more stable vacuum-high temperature performance

[NASA-CASE-LEW-12174-2]

p0109 N79-14346

MOLYBDENUM ALLOYS

NT BENE 41

Shear rupture of a directionally solidified eutectic gamma/gamma-prime - alpha /Mo/ alloy --- for aircraft engine turbine blades

p0077 A79-21301

Shear rupture of a directionally solidified eutectic gamma/gamma-prime - alpha (Mo) alloy

[NASA-TM-79118]

p0073 N79-12205

MOLYBDENUM COMPOUNDS

NT MOLYBDENUM DISULFIDES

MOLYBDENUM DISULFIDES

- A comparison of the lubricating mechanisms of graphite fluoride and molybdenum disulfide films p0085 A79-16659
- Sputtering technology in solid film lubrication p0117 A79-16663
- Lubrication and failure mechanisms of molybdenum disulfide films. 1: Effect of atmosphere [NASA-TP-1343] p0081 N79-13158
- Lubrication and failure mechanisms of molybdenum disulfide films. 2: Effect of substrate roughness [NASA-TP-1379] p0081 N79-13159

MOLYBDENUM SULFIDES

- NT MOLYBDENUM DISULFIDES
- Superconducting properties of evaporated copper molybdenum sulfide films p0184 A79-20219
- Hall effect and magnetoresistivity in the ternary molybdenum sulfides p0185 A79-21157
- Critical current and scaling laws in evaporated two-phase Cu₂S-Mo₆S₈ p0185 A79-26375
- Normal state properties of the ternary molybdenum sulfides p0185 A79-27229
- Low temperature normal state resistance of ternary molybdenum sulfides p0185 A79-27230
- Comparison of projected critical currents in PbMo₆S₈ and Nb₂Ge p0185 A79-28300
- Reactively evaporated films of copper molybdenum sulfide p0185 A79-31973
- Electronic properties of PbMo₆S₈ and Cu₂Mo₆S₈ --- for superconductivity p0187 A79-41731
- Indirect measurements of Fermi surface parameters of some chevron phase materials p0185 A79-50231

MONOCRYSTALS

U SINGLE CRYSTALS

MONOMERS

- Status review of PMR polyimides --- Polymerization of Monomer Reactants p0065 A79-30199
- Stability of PMR-polyimide monomer solutions p0086 A79-31041
- Characterization of PMR polyimides - Correlation of ester impurities with composite properties p0086 A79-43265
- Effects of graphite fiber stability on the properties of PMR polyimide composites p0066 A79-43309
- New high temperature cross linking monomers --- for polymer matrix composite materials [NASA-CN-159514] p0087 N79-29331

MONOPLANES

NT F-102 AIRCRAFT

MONTE CARLO METHOD

- Maximum likelihood estimation for life distributions with competing failure modes p0169 A79-49528

MORPHOLOGY

- Mechanical and chemical effects of ion-texturing biomedical polymers [NASA-TM-79245] p0084 A79-31391

MOS (SEMICONDUCTORS)

U METAL OXIDE SEMICONDUCTORS

MOSS (SPACE STATIONS)

U ORBITAL SPACE STATIONS

MOTION STABILITY

NT FLOW STABILITY

MOTOR VEHICLES

NT AUTOMOBILES

NT ELECTRIC MOTOR VEHICLES

MOTORS

NT ELECTRIC MOTORS

MOUNTS

U SUPPORTS

MTRF

- Causes of high pressure compressor deterioration in service [AIAA PAPER 79-1234] p0036 A79-40483

MULTILAYER STRUCTURES

U LAMINATES

MULTIPHASE FLOW

NT TWO PHASE FLOW

MULTILINERS

- Lightweight multiple output converter development [NASA-CN-159526] p0100 N79-20317

MULTISPECTRAL BAND SCANNERS

- Atmospheric transformation of multispectral remote sensor data --- Great Lakes [E79-10006] p0131 N79-12524
- Application of multispectral scanner data to the study of an abandoned surface coal mine [NASA-TM-78912] p0131 N79-13472

MULTISPECTRAL PHOTOGRAPHY

- Atmospheric transformation of multispectral remote sensor data --- Great Lakes [E79-10006] p0131 N79-12524

MULTISTAGE COMPRESSORS

U TURBOCOMPRESSORS

MULTISTAGE ROCKET VEHICLES

NT ATLAS LAUNCH VEHICLES

N

N-P JUNCTIONS

U P-N JUNCTIONS

NACELLES

- Effect of lip and centerbody geometry on aerodynamic performance of inlets for tilting-nacelle VTOL aircraft* [AIAA PAPER 79-0381] p0025 A79-23509
- Theoretical fan velocity distortions due to inlets and nozzles p0006 A79-39810
- Performance of a V/STOL tilt-nacelle inlet with blowing boundary layer control [AIAA PAPER 79-1163] p0006 A79-47347
- Recent applications of theoretical analysis to V/STOL inlet design p0006 A79-49530
- Integrated gas turbine engine-nacelle [NASA-CASE-LEW-12389-3] p0014 N79-14096
- Theoretical study of VTOL tilt-nacelle axisymmetric inlet geometries [NASA-TP-1380] p0003 N79-14996
- Effect of lip and centerbody geometry on aerodynamic performance of inlets for tilting-nacelle VTOL aircraft [NASA-TM-79056] p0003 N79-14999
- Recent applications of theoretical analysis to V/STOL inlet design [NASA-TM-75211] p0004 N79-29143

NASA COMMUNICATION NETWORK

U NASCOM NETWORK

NASA PROGRAMS

NT GLOBAL ATMOSPHERIC RESEARCH PROGRAM

NT QUIET ENGINE PROGRAM

- Large wind turbine generators --- NASA program status and potential costs p0146 A79-15881
- Engineering in the 21st century --- aerospace technology prospects [AAS PAPER 78-192] p0190 A79-21277
- The NASA high pressure facility and turbine test rig p0038 A79-21296
- NASA research on general aviation power plants [AIAA PAPER 79-0561] p0026 A79-25670
- Prop-ran propulsion - Its status and potential [SAE PAPER 780995] p0026 A79-25680
- Telecommunication service networks through the year 2000 in relation to millimeter wave satellite systems p0095 A79-27398
- Large horizontal axis wind turbine development p0149 A79-46527
- Utility operational experience on the NASA/DOE Mod-GA 200 kW Wind Turbine p0149 A79-46537
- Lewis Research Center studies of multiple large wind turbine generators on a utility network p0149 A79-46547
- Control and stabilization of the DOE/NASA Mod-1 two megawatt wind turbine generator p0156 A79-51780
- The role of fuel cells in NASA's space power systems p0056 A79-51810
- An overview of NASA research on positive displacement type general aviation engines [AIAA PAPER 79-1824] p0038 A79-53750

- NASA research on general aviation power plants
[NASA-TM-79031] p0014 W79-12086
- Preliminary GCGAT program test results
[NASA-TM-79013] p0016 W79-15051
- NASA Global Atmospheric Sampling Program (GASP)
data report for tapes VL0007 and VL0008
[NASA-TM-73784] p0157 W79-17359
- Tests of NASA ceramic thermal barrier coating for
gas-turbine engines
[NASA-TM-79116] p0017 W79-20118
- Definition of smolder experiments for Spacelab
[NASA-CR-159528] p0040 W79-20161
- Ozone contamination in aircraft cabins:
Objectives and approach p0008 W79-21022
- Ozone Contamination in Aircraft Cabins: Summary
of recommendations p0008 W79-21026
- Ozone Contamination in Aircraft Cabins: Post
workshop review of recommendations p0008 W79-21027
- Ozone Contamination in Aircraft Cabins. Appendix
B: Overview papers. In-flight measurements p0008 W79-21029
- Lewis Research Center program p0137 W79-21576
- The role of fuel cells in NASA's space power systems
[NASA-TM-79182] p0053 W79-23133
- Extension, validation and application of the
NASCAP code p0100 W79-27397
- NASA gear research and its probable effect on
rotorcraft transmission design [NASA-TM-79292] p0116 W79-33477
- NASA STRUCTURAL ANALYSIS PROGRAM**
- NASTRAN**
- NASCON NETWORK**
- Determining potential 30/20 GHz domestic satellite
system concepts and establishment of a suitable
experimental configuration p0095 W79-27397
- NASTRAN**
- CELFE/NASTRAN Code for the analysis of structures
subjected to high velocity impact p0128 W79-21298
- CELFE/NASTRAN code for the analysis of structures
subjected to high velocity impact [NASA-TM-79048] p0126 W79-15325
- Analysis of high velocity impact on hybrid
composite fan blades [NASA-TM-79133] p0127 W79-20398
- NATIONS**
- NT DEVELOPING NATIONS**
- NATURAL FREQUENCIES**
- C RESONANT FREQUENCIES**
- NAVIER-STOKES EQUATION**
- Development of a three-dimensional turbulent duct
flow analysis [NASA-CR-3029] p0106 W79-12366
- NETWORK ANALYSIS**
- A general unified approach to modelling switching
dc-to-dc converters in discontinuous conduction
mode p0101 W79-10880
- Generalized computer-aided discrete time domain
modeling and analysis of dc-dc converters p0099 W79-10881
- Analysis of a parallel-arrayed power regulating
system p0101 W79-49397
- NETWORK SYNTHESIS**
- A new optimum topology switching dc-to-dc converter
p0101 W79-10888
- NEUTRAL GASES**
- Method for decomposing observed line shapes
resulting from multiple causes - Application to
plasma charge-exchange-neutral spectra p0182 W79-53867
- NEUTRALIZERS**
- Neutralization tests on the SLEET 2 spacecraft
[NASA-TM-79271] p0054 W79-33255
- NICKEL ALLOYS**
- NT ASTROLOY (TRADEMARK)**
- NT BENE 41**
- Shear rupture of a directionally solidified
eutectic gamma/gamma-prime - alpha /Mo/ alloy
--- for aircraft engine turbine blades p0077 W79-21301
- A feasibility study of a diffusion barrier between
Ni-Cr-Al coatings and nickel-based eutectic alloys
p0077 W79-27233
- Adherence of sputtered titanium carbides
p0078 W79-34997
- Transverse and longitudinal tensile properties at
760 C of several oxide dispersion strengthened
nickel-base alloys p0078 W79-49531
- Thermal expansion of some nickel and cobalt
spinel and their solid solutions p0186 W79-50233
- Strainrange partitioning behavior of the
nickel-base superalloys, BENE 80 and IN-102 p0126 W79-10480
- An oxide dispersion strengthened alloy for gas
turbine blades [NASA-TM-79088] p0052 W79-20180
- Effect of grain orientation and coating on thermal
fatigue resistance of a directionally solidified
superalloy (MAR-M 247) [NASA-TM-79129] p0127 W79-22565
- The strainrange partitioning behavior of an
advanced gas turbine disk alloy, AF2-1DA [NASA-TM-79179] p0075 W79-23196
- Low-cost directionally-solidified turbine blades,
volume 1 [NASA-CR-159464] p0080 W79-24121
- X-ray photoelectron spectroscopy study of nickel
and nickel-base alloy surface alterations in
simulated hot corrosion conditions with emphasis
on eventual application to turbine blade corrosion
[NASA-CR-159553] p0072 W79-25178
- An investigation of the initiation stage of hot
corrosion in Ni-base alloys [NASA-CR-159616] p0080 W79-25196
- Transverse and longitudinal tensile properties at
760 C of several oxide dispersion strengthened
nickel-base alloys [NASA-TM-79189] p0075 W79-30355
- Some TEM observations of Al2O3 scales formed on
NiCrAl alloys [NASA-TM-79259] p0076 W79-33306
- NICKEL CADMIUM BATTERIES**
- Hydrogen recombination in sealed nickel-cadmium
aerospace cells p0057 W79-51907
- Some practical observations on the accelerated
testing of Nickel-Cadmium Cells p0058 W79-51911
- Lightweight porous plastic plaque --- nickel
cadmium batteries p0141 W79-28672
- NICKEL COATINGS**
- Internally coated air-cooled gas turbine blading
[NASA-CR-159574] p0034 W79-25018
- NICKEL COMPOUNDS**
- NT NICKEL OXIDES**
- NICKEL OXYIDES**
- Transverse and longitudinal tensile properties at
760 C of several oxide dispersion strengthened
nickel-base alloys p0078 W79-49531
- NICKEL PLATE**
- Lightweight porous plastic plaque --- nickel
cadmium batteries p0141 W79-28672
- NICKEL STEELS**
- Effects of thermomechanical processing on strength
and toughness of Fe-12Ni reactive metal alloys
at 77K p0078 W79-32600
- Evaluation of the mechanical properties of
electroslag refined Fe-12Ni alloys [NASA-CR-159394] p0079 W79-12202
- NICKEL ZINC BATTERIES**
- Rapid, efficient charging of lead-acid and
nickel-zinc traction cells --- for electric
vehicles p0144 W79-10084
- Effect of positive pulse charge waveforms on cycle
life of nickel-zinc cells [NASA-TM-79215] p0142 W79-28728
- Discharge characteristics of 300 ampere-hour Ni-Zn
traction cells [NASA-TM-79244] p0143 W79-31781
- NIOBIUM COMPOUNDS**
- NT NIOBIUM STANNIDES**

Nb3Ge as a potential candidate material for 15- to 25-T magnets p0186 A79-44548

NIIOBIUM STANNIDES
Properties and performance of fine-filament bronze-process Nb3Sn conductors p0184 A79-20529

NITRATES
NT SODIUM NITRATES
Sulfate and nitrate mixing ratios in the vicinity of the tropopause p0158 A79-49494

NITRIC OXIDE
Effect of fuel/air nonuniformity on nitric oxide emissions p0020 N79-25004

NITRIDES
NT SILICON NITRIDES

NITRIDING
Bend strengths of reaction bonded silicon nitride prepared from dry attrition milled silicon powder [NASA-TM-79230] p0084 N79-30379

NITROGEN
NT LIQUID NITROGEN
NT NITROGEN IONS
Effect of nitrogen-containing plasma on adherence, friction, and wear of radiofrequency-sputtered titanium carbide coatings [NASA-TP-1377] p0081 N79-15184
Effect of oxygen-nitrogen ratio on sinterability of Sialons [NASA-TP-1382] p0082 N79-21204
Surface chemistry of iron sliding in air and nitrogen lubricated with hexadecane and hexadecane containing dibenzyl-dithiolide [NASA-TP-1545] p0059 N79-31346

NITROGEN COMPOUNDS
NT AMIDES
NT IMIDES
NT NITRATES
NT NITRIC OXIDE
NT NITROGEN OXIDES
NT POLYIMIDES
NT SILICON NITRIDES
NT SODIUM NITRATES

NITROGEN IONS
The effect of nitrogen ion (N+) implantation on the friction and wear characteristics of iron [NASA-TM-79029] p0073 N79-12201

NITROGEN OXIDES
NT NITRIC OXIDE
Wide range operation of advanced low NOx aircraft gas turbine combustors [ASME PAPER 78-6T-128] p0024 A79-10792
Emission measurements for a lean premixed propane/air system at pressures up to 30 atmospheres [NASA-CR-159421] p0071 N79-10165
Premix fuels study applicable to duct burner conditions for a variable cycle engine [NASA-CR-159513] p0091 N79-20266
Lean, Premixed-Prevaporized (LPP) combustor conceptual design study [NASA-CR-159629] p0072 N79-31358

NOAA SATELLITES
VHF downline communication system for SLAS data [NASA-TM-79164] p0094 N79-23313

NOBLE GASES
U RARE GASES

NOBLE METALS
N GOLD
NT SILVER
Friction and transfer of copper, silver, and gold to iron in the presence of various adsorbed surface films [NASA-TF-1392] p0114 N79-14386

NOISE (SOUND)
NT AERODYNAMIC NOISE
NT AIRCRAFT NOISE
NT ENGINE NOISE
NT JET AIRCRAFT NOISE
NT SONIC BOOMS
Applications of velocity potential function to acoustic duct propagation and radiation from inlets using finite element theory [NASA-TM-79071] p0016 N79-15959
Overall loudness of steady sounds according to theory and experiment [NASA-RP-1001] p0163 N79-25753

NOISE ATTENUATION
U NOISE REDUCTION
NOISE ELIMINATION
U NOISE REDUCTION
NOISE GENERATORS
Numerical spatial marching techniques in duct acoustics --- noise source calculation from far field pressure measurements p0175 A79-25946
Analysis of radiation patterns of interaction tones generated by inlet rods in the JT15D engine [AIAA PAPER 79-0581] p0027 A79-26944
Effects of geometric and flow-field variables on inverted-velocity-profile coaxial jet noise and source distributions [AIAA PAPER 79-0635] p0175 A79-32126
Effects of geometric and flow-field variables on inverted-velocity-profile coaxial jet noise --- nozzle geometry [NASA-TM-79095] p0173 N79-20830

NOISE HAZARDS
U NOISE (SOUND)

NOISE INTENSITY
Tone noise of three supersonic helical tip speed propellers in a wind tunnel [NASA-TM-79167] p0174 N79-25840

NOISE MEASUREMENT
Measured and predicted noise of the AVCO-Lycoming YF-102 turbofan engine [AIAA PAPER 79-0641] p0026 A79-26877
Full-scale engine tests of bulk absorber acoustic inlet treatment [AIAA PAPER 79-0600] p0026 A79-26881
Reduction of rotor-turbulence interaction noise in static fan noise testing [AIAA PAPER 79-0656] p0036 A79-26925
Tone noise of three supersonic helical tip speed propellers in a wind tunnel at 0.8 Mach number [NASA-TM-79046] p0172 N79-15758
Effects of inflow distortion profiles on fan tone noise calculated using a 3-D theory [NASA-TM-79082] p0173 N79-16647
Experimental clean combustor program, phase 3: Noise measurement addendum --- CF6-50 high bypass turbofan engine noise [NASA-CR-159458] p0177 N79-17656

NOISE PROPAGATION
QCSEE - The key to future short-haul air transport --- Quiet, Clean, Short-Haul Experimental Engine program p0030 A79-50208
Studies of the acoustic transmission characteristics of coaxial nozzles with inverted velocity profiles: Comprehensive data report --- nozzle transfer functions [NASA-CR-159628] p0177 N79-27933

NOISE REDUCTION
Correlation of combustor acoustic power levels inferred from internal fluctuating pressure measurements p0025 A79-14796
Optimized multisectioned acoustic liners [AIAA PAPER 79-0182] p0174 A79-19581
Modal propagation angles in ducts with soft walls and their connection with suppressor performance [AIAA PAPER 79-0624] p0175 A79-26880
An impulse test technique with application to acoustic measurements --- for engine noise absorbers [AIAA PAPER 79-0679] p0178 A79-26890
Reduction of rotor-turbulence interaction noise in static fan noise testing [AIAA PAPER 79-0656] p0036 A79-26925
Effects of simulated forward flight on jet noise, shock noise and internal noise [AIAA PAPER 79-0615] p0178 A79-26936
Experimental study of coaxial nozzle exhaust noise [AIAA PAPER 79-0631] p0175 A79-28963
A jet exhaust noise prediction procedure for inverted velocity profile annular nozzles [AIAA PAPER 79-0633] p0178 A79-28964
Investigation of wing shielding effects on C1CL engine noise [AIAA PAPER 79-0669] p0011 A79-28970
Preliminary QCGAT program test results --- Quiet, Clean General Aviation Turbofan [SAE PAPER 790596] p0028 A79-36729
Duct wall impedance control as an advanced concept for acoustic suppression enhancement --- engine

- noise reduction
[NASA-CR-159425] p0176 N79-10842
- Sound-suppressing structure with thermal relief
[NASA-CASE-LEW-12658-1] p0172 N79-14871
- Feasibility of wing shielding of the airplane interior from the shock noise generated by supersonic tip speed propellers
[NASA-TM-79042] p0172 N79-15757
- Evaluation of two inflow control devices for flight simulation of fan noise using a JT15D engine
[NASA-TM-79072] p0017 N79-15969
- Full-scale engine tests of bulk absorber acoustic inlet treatment
[NASA-TM-79079] p0173 N79-16645
- Modal propagation angles in ducts with soft walls and their connection with suppressor performance
[NASA-TM-79081] p0173 N79-16646
- Wind tunnel performance of four energy efficient propellers designed for Mach 0.8 cruise --- Lewis 8x6 foot wind tunnel studies for noise reduction in high speed turboprop aircraft
[NASA-TM-79124] p0003 N79-20069
- Theory of low frequency noise transmission through turbines
[NASA-CR-159457] p0033 N79-20117
- Investigation of wing shielding effects on CTOL engine noise
[NASA-TM-79073] p0127 N79-20390
- Experimental study of coaxial nozzle exhaust noise --- acoustic measurements
[NASA-TM-79090] p0173 N79-20829
- An analytical and experimental study of sound propagation and attenuation in variable-area ducts --- reducing aircraft engine noise
[NASA-CR-135392] p0177 N79-25845
- NOISE SPECTRA**
Trailing edge noise data with comparison to theory
[NASA-TM-79208] p0174 N79-27930
- NOISE SUPPRESSORS**
U NOISE REDUCTION
- NONADIABATIC PROCESSES**
U HEAT TRANSFER
- NONCONDUCTORS**
U ELECTRICAL INSULATION
- NONDESTRUCTIVE TESTS**
Use of an ultrasonic-acoustic technique for nondestructive evaluation of fiber composite strength
p0064 A79-15545
- Definition of mutually optimum NDI and proof test criteria for 2219 aluminum pressure vessels.
Volume 1: Methods
[NASA-CR-135445] p0125 N79-21410
- Definition of mutually optimum NDI and proof test criteria for 2219 aluminum pressure vessels.
Volume 3: Applications to rail defect evaluation
[NASA-CR-135447] p0125 N79-21412
- A review of issues and strategies in nondestructive evaluation of fiber reinforced structural composites
[NASA-TM-79246] p0125 N79-29530
- NONISOTROPY**
U ANISOTROPY
- NONLINEAR EQUATIONS**
Nonlinear equations of equilibrium for elastic helicopter or wind turbine blades undergoing moderate deformation
[NASA-CR-159478] p0130 N79-19414
- NONLINEAR PROGRAMMING**
Power converter design optimization
p0099 A79-10885
- NONLINEAR SYSTEMS**
Predicting dynamic performance limits for servosystems with saturating nonlinearities
[ASA-TF-1488] p0038 N79-28186
- NONUNIFORM FLOW**
Turbulence generated by the interaction of entropy fluctuations with non-uniform mean flows
p0106 A79-45468
- NONVISCOUS FLOW**
U TURBULENT FLOW
- NOTATION**
U CODING
- NOXIOUS MATERIALS**
U CONTAMINANTS
- NOZZLE COEFFICIENT**
U NOZZLE FLOW
- NOZZLE DESIGN**
An approach to optimum subsonic inlet design
[ASME PAPER 79-GT-51] p0006 A79-30527
- Variable area exhaust nozzle
[NASA-CASE-LEW-12378-1] p0014 N79-14097
- Unconventional nozzle tradeoff study --- space tug propulsion
[NASA-CR-159520] p0057 N79-28224
- NOZZLE EFFICIENCY**
Aerodynamic performance of scarf inlets
[AIAA PAPER 79-0380] p0005 A79-23510
- NOZZLE FLOW**
Experimental study of coaxial nozzle exhaust noise
[AIAA PAPER 79-0631] p0175 A79-28963
- Progress on Variable Cycle Engines
[AIAA PAPER 79-1312] p0036 A79-40759
- Computer programs for calculating two-dimensional potential flow through deflected nozzles
[NASA-TM-79144] p0004 N79-26019
- Application of the principle of similarity fluid mechanics
[NASA-TM-79258] p0105 N79-30515
- NOZZLE GEOMETRY**
Experimental study of coaxial nozzle exhaust noise
[AIAA PAPER 79-0631] p0175 A79-28963
- Assessment at full scale of nozzle/wing geometry effects on OTW aeroacoustic characteristics --- Over The Wing STOL engine configurations
p0175 A79-39802
- Experimental study of coaxial nozzle exhaust noise --- acoustic measurements
[NASA-TM-79090] p0173 N79-20829
- Effects of geometric and flow-field variables on inverted-velocity-profile coaxial jet noise --- nozzle geometry
[NASA-TM-79095] p0173 N79-20830
- Theoretical fan velocity distortions due to inlets and nozzles --- in V/STOL aircraft
[NASA-TM-79150] p0003 N79-23911
- Assessment at full scale of nozzle/wing geometry effects on OTW aero-acoustic characteristics --- short takeoff aircraft noise
[NASA-TM-79108] p0174 N79-25841
- Computer programs for calculating two-dimensional potential flow through deflected nozzles
[NASA-TM-79144] p0004 N79-26019
- Aerodynamic and acoustic investigation of inverted velocity profile conannular exhaust nozzle models and development of aerodynamic and acoustic prediction procedures
[NASA-CR-3168] p0035 N79-31212
- CF6 jet engine performance improvement program.
Short core exhaust nozzle performance improvement concept --- specific fuel consumption reduction
[NASA-CR-159564] p0038 N79-33206
- NUCLEAR AUXILIARY POWER UNITS**
NT SPACE POWER REACTORS
- NUCLEAR CAPTURE**
NT ELECTRON CAPTURE
- NUCLEAR ELECTRIC POWER GENERATION**
NT SPACE POWER REACTORS
- NUCLEAR ELECTRIC PROPULSION**
Optimize out-of-core thermionic energy conversion for nuclear electric propulsion
p0146 A79-13099
- NUCLEAR INTERACTIONS**
NT ELECTRON CAPTURE
- NUCLEAR POWER REACTORS**
NT SPACE POWER REACTORS
- NUCLEAR PROPULSION**
NT NUCLEAR ELECTRIC PROPULSION
- NUCLEAR REACTIONS**
NT ELECTRON CAPTURE
- NUCLEAR REACTORS**
NT SPACE POWER REACTORS
- NUCLEOTIDES**
The catalysis of nucleotide polymerization by compounds of divalent lead --- prebiotic synthesis
p0060 A79-32924
- NUCLIDES**
NT ISOTOPIES
NT PLUTONIUM 238
- NUMERICAL ANALYSIS**
NT FINITE DIFFERENCE THEORY
NT FINITE ELEMENT METHOD
NT INTERPOLATION
NT MONTE CARLO METHOD
NT NUMERICAL INTEGRATION

Stress analysis for structures with surface cracks
[NASA-CR-159400] p0129 N79-13405

NUMERICAL CONTROL
Microprocessor control of a wind turbine generator
p0147 A79-21302

Laser balancing demonstration on a high-speed
flexible rotor
[ASME PAPER 79-GT-56] p0123 A79-32351

Application of digital controls on the quiet clean
short haul experimental engines
[AIAA PAPER 79-1203] p0029 A79-38984

Multivariable control altitude demonstration on
the F100 turbofan engine
[AIAA PAPER 79-1204] p0029 A79-39814

Experiments on multiplane balancing using a laser
for material removal
[NASA-CR-3105] p0121 N79-17228

NUMERICAL FLOW VISUALIZATION
An efficient user-oriented method for calculating
compressible flow about three-dimensional inlets
[AIAA PAPER 79-0001] p0005 A79-19524

NUMERICAL INTEGRATION
A calculation procedure for viscous flow in
turbomachines, volume 1
[NASA-CR-159635] p0107 N79-30514

O

O RING SEALS
Stiffness of straight and tapered annular gas path
seals
[ASME PAPER 78-LUB-18] p0118 A79-23235

Self-stabilizing radial face seal
[NASA-CASE-LEW-12991-1] p0113 N79-12445

OBSERVATION AIRCRAFT
Commercial aircraft derived high resolution wind
and temperature data from the tropics for FGGE:
Implications for NASA p0161 N79-20621

OBSERVATORIES

NT HEAD

OBSTRUCTING

U BLOCKING

OFF-ON CONTROL

A general unified approach to modelling switching
dc-to-dc converters in discontinuous conduction
mode p0101 A79-10880

Generalized computer-aided discrete time domain
modeling and analysis of dc-dc converters
p0099 A79-10881

A new optimum topology switching dc-to-dc converter
p0101 A79-10888

OIL ADDITIVES

Auger spectroscopy analysis of lubrication with
zinc dialkyldithiophosphate of several metal
combinations in sliding contact
[NASA-TF-1489] p0083 N79-27308

OILS

NT CRUDE OIL
NT LUBRICATING OILS
NT SHALE OIL

ONBOARD COMPUTERS

U AIRBORNE/SPACEBORNE COMPUTERS

ONBOARD EQUIPMENT

NT AIRBORNE EQUIPMENT
NT AIRBORNE/SPACEBORNE COMPUTERS
NT AIRCRAFT EQUIPMENT

ONE DIMENSIONAL FLOW

Hartmann flow with temperature-dependent physical
properties --- magnetohydrodynamics of liquid
metal p0182 A79-15597

Application of the principle of similarity fluid
mechanics
[NASA-TM-79258] p0105 N79-30515

ORISOTROPY

U ANISOTROPY

OPERATIONS RESEARCH

Utility operational experience on the NASA/DOE
MOD-0A 200-kW wind turbine
[NASA-TM-79084] p0136 N79-20494

OPTICAL ABSORPTION

U LIGHT TRANSMISSION

OPTICAL ACTIVITY

Holography through optically active windows
[NASA-TP-1414] p0109 N79-17195

OPTICAL EQUIPMENT

NT LASER DOPPLER VELOCIMETERS

NT MULTISPECTRAL BAND SCANNERS**NT OPTICAL MEASURING INSTRUMENTS****OPTICAL FILTERS**

UV blocking filters for polymeric films
p0088 A79-51103

OPTICAL HETERODYNING

Simulated electronic heterodyne recording and
processing of pulsed-laser holograms
[NASA-TF-1444] p0111 N79-21329

OPTICAL MASERS

U LASERS

OPTICAL MEASUREMENT

Gain measurements of the Ca-Fe charge exchange
system --- for UV lasers p0112 A79-19078

OPTICAL MEASURING INSTRUMENTS**NT MULTISPECTRAL BAND SCANNERS**

Fiber optic sensors for military, industrial and
commercial applications p0111 A79-38738

Analysis and preliminary design of an optical
digital tip clearance sensor for propulsion
control
[NASA-CR-159434] p0031 N79-15053

Fuel spray data with LDV --- solar laser
morphokinometer capabilities in combustion
research p0019 N79-24997

Optically isolated logarithmic nanometer capable
of floating to 5 kilovolts
[NASA-TF-1527] p0098 N79-32467

OPTICAL PROPERTIES

NT ABSORPTANCE

NT PHOTOELECTRIC EMISSION

NT RADIANCE

NT TRANSPARENCY

NT WATER COLORS

Optical, spin-resonance, and magnetoresistance
studies of /tetrathiatetracene/2/iodide/3 - The
nature of the ground state p0184 A79-10417

Modification of the electrical and optical
properties of polymers --- ion irradiation
[NASA-CASE-LEW-13027-1] p0081 N79-11216

OPTICAL PUMPING

Simmer-enhanced flashlamp-pumped dye laser
p0112 A79-32881

Solar-pumped lasers for space power transmission
[AIAA PAPER 79-1015] p0112 A79-38202

OPTICAL SCANNERS**NT MULTISPECTRAL BAND SCANNERS****OPTICAL SENSORS****U OPTICAL MEASURING INSTRUMENTS****OPTIMUM CONTROL**

Duct wall impedance control as an advanced concept
for acoustic suppression enhancement --- engine
noise reduction p0176 N79-10842

Generation of linear dynamic models from a digital
nonlinear simulation
[NASA-TF-1388] p0001 N79-16796

OPTIMIZATION**NT OPTIMAL CONTROL**

Power converter design optimization
p0099 A79-10885

A new optimum topology switching dc-to-dc converter
p0101 A79-10888

Optimize cut-of-core thermionic energy conversion
for nuclear electric propulsion p0146 A79-13099

Performance optimization of an MHD generator with
physical constraints p0182 A79-51995

Performance optimization of an MHD generator with
physical constraints
[NASA-TM-79172] p0138 N79-24446

OPTIMUM CONTROL**U OPTIMAL CONTROL****ORBIT TRANSFER VEHICLES**

Plug cluster engine concept for in-space missions
[AIAA PAPER 79-1179] p0055 A79-38972

Advanced engine study for mixed-mode
orbit-transfer vehicles
[NASA-CR-159491] p0057 N79-19074

Space propulsion technology overview
[NASA-TM-79104] p0042 N79-20171

Liquid oxygen/liquid hydrogen boost/vane pump for
the advanced orbit transfer vehicles auxiliary
propulsion system

- [NASA-CR-159648] p0057 N79-31341
ORBITAL MANEUVERS
 Laser rocket system analysis
 [NASA-CR-159521] p0112 N79-21337
ORBITAL SPACE STATIONS
 An economic analysis of a commercial approach to the design and fabrication of a space power system
 [NASA-TN-79153] p0053 N79-22193
ORBITAL TRANSFER
 U TRANSFER ORBITS
ORBITING SATELLITES
 U ARTIFICIAL SATELLITES
ORBITS
 NT GEOSYNCHRONOUS ORBITS
 NT TRANSFER ORBITS
ORGANIC CHARGE TRANSFER SALTS
 Optical, spin-resonance, and magnetoresistance studies of tetrathiatetracene/2-iodide/3 - The nature of the ground state
 p0184 A79-10417
ORGANIC COMPOUNDS
 NT NUCLEOTIDES
 NT ORGANIC CHARGE TRANSFER SALTS
 Control of volume resistivity in inorganic organic separators
 [NASA-TF-1439] p0069 N79-22246
 Improved, low cost inorganic-organic separators for rechargeable silver-zinc batteries
 [NASA-TF-1476] p0069 N79-25181
ORGANIC LASERS
 NT DYE LASERS
ORIFICES
 Effect of grazing flow on the acoustic impedance of Helmholtz resonators consisting of single and clustered orifices
 [NASA-CR-3177] p0178 N79-32056
OSCILLATIONS
 NT PRESSURE OSCILLATIONS
OSCILLATORS
 High power phase locked laser oscillators
 [NASA-CR-159630] p0112 N79-32538
OTV
 U ORBIT TRANSFER VEHICLES
OUTLET FLOW
 Turbulence measurements in the compressor exit flow of a General Electric CF6-50 engine
 p0019 N79-24996
 Contoured tank outlets for draining of cylindrical tanks in low-gravity environment --- Lewis Research Center Zero Gravity Facility
 [NASA-TF-1492] p0105 N79-29467
OUTPUT
 NT LASER OUTPUTS
OXIDATION
 NT ELECTROCHEMICAL OXIDATION
 Boundary lubrication, thermal and oxidative stability of a fluorinated polyether and a perfluoropolyether triazine
 [NASA-TM-79064] p0081 N79-15185
 Resin/fiber thermo-oxidative interactions in FRP polyimide/graphite composites
 [NASA-TM-79093] p0062 N79-16920
 High velocity burner rig oxidation and thermal fatigue behavior of Si3N4- and SiC base ceramics to 1370 deg C
 [NASA-TM-79040] p0082 N79-16984
 Redox flow cell energy storage systems
 [NASA-TM-79143] p0138 N79-24442
 Redox flow cell development and demonstration project, calendar year 1977
 [NASA-TM-79067] p0138 N79-24445
 X-ray photoelectron spectroscopy study of nickel and nickel-base alloy surface alterations in simulated hot corrosion conditions with emphasis on eventual application to turbine blade corrosion
 [NASA-CR-159553] p0072 N79-25178
 An investigation of the initiation stage of hot corrosion in Ni-base alloys
 [NASA-CR-159616] p0080 N79-25196
 Effects of yttrium, aluminum, and chromium concentrations in bond coatings on the performance of zirconia-yttria thermal barriers
 [NASA-TM-79206] p0075 N79-29293
 The erosion/corrosion of small superalloy turbine rotors operating in the effluent of a PFB coal combustor
 [NASA-TM-79227] p0076 N79-30356
OXIDATION RESISTANCE
 Method of making bearing materials ---
 self-lubricating, oxidation resistant composites for high temperature applications
 [NASA-CASE-LEW-11930-4] p0062 N79-17916
 Modules of rupture and oxidation resistance of Si2.55Al0.600.72N3.52 sialon
 [NASA-TF-1490] p0083 N79-27309
 The erosion/corrosion of small superalloy turbine rotors operating in the effluent of a PFB coal combustor
 [NASA-TM-79227] p0076 N79-30356
OXIDATION-REDUCTION REACTIONS
 Redox flow cell energy storage systems
 [AIAA PAPER 79-0989] p0147 A79-38191
 Recent advances in Redox flow cell storage systems
 p0150 A79-51837
 Supply of reactants for Redox bulk energy storage systems
 [NASA-TM-78995] p0133 N79-11479
 Catalyst surfaces for the chromous/chromic redox couple
 [NASA-CASE-LEW-13148-1] p0134 N79-14538
 Electrochemical cell for rebalancing REDOX flow system
 [NASA-CASE-LEW-13150-1] p0139 N79-26474
 Recent advances in redox flow cell storage systems
 [NASA-TM-79186] p0141 N79-26505
OXIDE FILMS
 The role of NaCl in flame chemistry, in the deposition process, and in its reactions with protective oxides as related to hot corrosion
 p0071 A79-49534
OXIDES
 NT ALUMINUM OXIDES
 NT CARBON MONOXIDE
 NT NICKEL OXIDES
 NT NITRIC OXIDE
 NT NITROGEN OXIDES
 NT YTTRIUM OXIDES
 NT ZIRCONIUM OXIDES
 Longitudinal shear behavior of several oxide dispersion strengthened alloys
 p0076 A79-14955
 An oxide dispersion strengthened alloy for gas turbine blades
 [NASA-TM-79088] p0052 N79-20180
OXIDIZERS
 NT LIQUID OXYGEN
OXYGEN
 NT LIQUID OXYGEN
 NT OZONE
 A proposed physical model for the impregnated tungsten cathode based on Auger surface studies of the Ba-O-W system
 p0078 A79-39972
 Resonance-tube ignition of aluminum
 p0071 A79-46366
 Effect of oxygen-nitrogen ratio on sinterability of Sialons
 [NASA-TF-1382] p0082 N79-21204
 MHD performance calculations with oxygen enrichment
 [NASA-TM-79140] p0139 N79-25499
 Surface chemistry of iron sliding in air and nitrogen lubricated with hexadecane and hexadecane containing dibenzyl-dithiolide
 [NASA-TF-1545] p0059 N79-31346
OZONE
 An analysis of the first two years of GASP data --- Global Atmospheric Sampling Program
 p0160 A79-15066
 Ozone in the upper troposphere from Gasp measurements
 p0160 A79-44810
 Aircraft cabin ozone measurements on B747-100 and B747-SP aircraft: Correlations with atmospheric ozone and ozone encounter statistics
 [NASA-TM-79060] p0008 N79-15013
 The advanced low-emissions catalytic-combustor program. Phase 1: Description and status
 [NASA-TM-79049] p0015 N79-15047
 Ozone contamination in aircraft cabins: Objectives and approach
 p0008 N79-21022
 Ozone Contamination in Aircraft Cabins: Summary of recommendations
 p0008 N79-21026
 Ozone Contamination in Aircraft Cabins: Post workshop review of recommendations
 p0008 N79-21027

Ozone Contamination in Aircraft Cabins. Appendix
B: Overview papers. In-flight measurements
p0008 N79-21029

Ozone measurement system for NASA global air
sampling program
[NASA-TP-1451] p0158 N79-22654

A summary of research on the NASA-Global
Atmospheric Sampling Program performed by the
Atmospheric Sciences Research Center --- ozone
transport theory
[NASA-CR-159614] p0159 N79-27716

Procedures for estimating the frequency of
commercial airline flights encountering high
cabin ozone levels
[NASA-TF-1560] p0008 N79-33171

OZONOMETRY
Simultaneous measurements of ozone outside and
inside cabins of two D-747 airliners and a Gates
Learjet business jet
p0008 A79-27571

Measurements of carbon monoxide, condensation
nuclei, and ozone on a B 747SP aircraft flight
around the world
p0158 A79-31332

P

P-N JUNCTIONS

Photon degradation effects in terrestrial solar
cells
p0145 A79-41098

Back wall solar cell
[NASA-CASE-LEW-12236-2] p0134 N79-14528

Alternate methods of applying diffusants to
silicon solar cells --- screen printing of
thick-film paste materials and vapor phase
transport from solid sources
[NASA-CR-159508] p0153 N79-29603

Modeling of thin, back-wall silicon solar cells
p0143 N79-32650

High efficiency cell geometry
p0143 N79-32653

PACKAGING

Status of wraparound contact solar cells and arrays
--- for spacecraft electric propulsion
p0054 A79-10014

PARALLEL FLOW

NT THREE DIMENSIONAL FLOW

PARAMAGNETIC RESONANCE

NT ELECTRON PARAMAGNETIC RESONANCE

PARTIAL DIFFERENTIAL EQUATIONS

NT BURGER EQUATION

PARTICLE ACCELERATORS

NT ION ACCELERATORS

PARTICLE BEAMS

NT ELECTRON BEAMS

NT ION BEAMS

Potential mapping with charged-particle beams
p0045 N79-24058

PARTICLE DIFFUSION

NT IONIC DIFFUSION

PARTICLE EMISSION

NT ELECTRON EMISSION

NT PHOTOELECTRIC EMISSION

NT SECONDARY EMISSION

NT THERMIONIC EMISSION

PARTICLE FLUX DENSITY

NT ELECTRON FLUX DENSITY

PARTICLE INTERACTIONS

NT ELECTRON CAPTURE

Spacecraft Charging Technology, 1978
[NASA-CP-2071] p0047 N79-24001

Interactions between spacecraft and the
charged-particle environment
p0047 N79-24021

PARTICLE TRAJECTORIES

Trajectories of charged particles in radial
electric and uniform axial magnetic fields
p0182 A79-41788

PARTICLES

NT AEROSOLS

NT CHARGED PARTICLES

NT DROPS (LIQUIDS)

NT ELECTRON BEAMS

NT ELECTRON PLASMA

NT HELIUM PLASMA

NT HIGH TEMPERATURE PLASMAS

NT HYDROGEN PLASMA

NT METAL IONS

NT PLASMAS (PHYSICS)

NT TOROIDAL PLASMAS

PARTICULATE FILTERS

U FLUID FILTERS

PARTICULATE SAMPLING

Pattern recognition methods and air pollution
source identification --- based on wind direction
p0158 A79-15079

Fine particulate capture device
[NASA-CASE-LEW-11583-1] p0109 N79-17192

PARTITIONS

A strainrange partitioning analysis of low cycle
fatigue of coated and uncoated Rene 80
p0129 N79-10479

PARTITIONS (STRUCTURES)

Strainrange partitioning behavior of the
nickel-base superalloys, Rene 80 and IN-100
p0126 N79-10480

PASSENGER AIRCRAFT

NT BOEING 747 AIRCRAFT

PASSIVATION

U PASSIVITY

PASSIVITY

Heat pipe life and processing study
[NASA-CR-159581] p0107 N79-25349

PATTERN RECOGNITION

Pattern recognition methods and air pollution
source identification --- based on wind direction
p0158 A79-15079

PAYLOADS

NT SPACE SHUTTLE PAYLOADS

Determining potential 30/20 GHz domestic satellite
system concepts and establishment of a suitable
experimental configuration
p0095 A79-27397

Effect of flight loads on turbofan engine
performance deterioration
[NASA-TM-79041] p0013 N79-12085

Determining potential 30/20 GHz domestic satellite
system concepts and establishment of a suitable
experimental configuration
[NASA-TM-79092] p0094 N79-17072

PDM (MODULATION)

U PULSE DURATION MODULATION

PERCEPTION

NT AUDITORY PERCEPTION

PERFORMANCE

Summary of GaAs Solar Cell Performance and
Radiation Damage Workshop
p0144 N79-32669

PERFORMANCE PREDICTION

NT PREDICTION ANALYSIS TECHNIQUES

Initial comparison of single cylinder Stirling
engine computer model predictions with test
results
[SAE PAPER 790327] p0119 A79-31368

Wind turbines for electric utilities - Development
status and economics
[AIAA PAPER 79-0965] p0148 A79-38888

An improved method for predicting the effects of
flight on jet mixing noise
p0176 A79-39803

Modeling of switching regulator power stages with
and without zero-inductor-current dwell time
p0101 A79-49398

Performance optimization of an MHD generator with
physical constraints
p0182 A79-51995

Evaluation of models to predict insolation on
tilted surfaces
p0150 A79-53491

Prediction of plasma properties in mercury ion
thrusters
[NASA-CR-159448] p0056 N79-15152

Initial comparison of single cylinder Stirling
engine computer model predictions with test
results
[NASA-TM-79044] p0188 N79-16721

Simulation of fluidized bed coal combustors
[NASA-CR-159529] p0153 N79-20487

Analytical prediction with multidimensional
computer programs and experimental verification
of the performance, at a variety of operating
conditions, of two traveling wave tubes with
depressed collectors
[NASA-TF-1449] p0097 N79-22375

Performance characteristics of a slagging gasifier
for MHD combustor systems
[NASA-TM-79195] p0142 N79-30720

Traction drive performance prediction for the Johnson and Tevaarwerk traction model
[NASA-TP-1530] p0116 N79-33475

PERFORMANCE TESTS

Wind tunnel performance of four energy efficient propellers designed for Mach 0.8 cruise
[SAE PAPER 790573] p0028 A79-36759

Test verification of a turbofan partial swirl afterburner
[AIAA PAPER 79-1199] p0029 A79-38981

Effect of degree of fuel vaporization upon emissions for a premixed prevaporized combustion system
[AIAA PAPER 79-1320] p0071 A79-39036

Utility operational experience on the NASA/DOE Mod-0A 200 kW Wind Turbine
p0149 A79-46537

Trailing edge noise data with comparison to theory
[AIAA PAPER 79-1524] p0176 A79-47340

A mobile apparatus for solar collector testing
[ASME PAPER 79-DE-5] p0150 A79-47651

Definition study of a Variable Cycle Experimental Engine (VCEE) and associated test program and test plan
[NASA-CR-159419] p0031 N79-11042

Analysis, design, fabrication and testing of the mini-Brayton rotating unit (Mini-BRU). Volume 1: Text and tables
[NASA-CR-159441-VOL-1] p0120 N79-11408

Analysis, design, fabrication and testing of the mini-Brayton rotating unit (Mini-BRU). Volume 2: Figures and drawings
[NASA-CR-159441-VOL-2] p0120 N79-11409

Definition study for variable cycle engine testbed engine and associated test program
[NASA-CR-159459] p0031 N79-13048

Parametric performance of a turbojet engine combustor using jet A and A diesel fuel
[NASA-TM-79089] p0017 N79-20114

JT8D and JT9D jet engine performance improvement program. Task 1: Feasibility analysis
[NASA-CR-159449] p0033 N79-20116

CF6 jet engine performance improvement program. Task 1: Feasibility analysis
[NASA-CR-159450] p0033 N79-21074

Performance of a 14.9-kW laminated-frame dc series motor with chopper controller
[NASA-TM-79177] p0098 N79-26316

Rankine-cycle component characteristics
p0140 N79-26478

Low-power baseline test results for the GPO 3 Stirling engine
[NASA-TM-79103] p0188 N79-27023

NASA CF6 jet engine diagnostics program: Long-term CF6-6D low-pressure turbine deterioration
[NASA-CR-159618] p0035 N79-29191

Aerodynamic performance of axial-flow fan stage operated at nine inlet guide vane angles --- to be used on vertical lift aircraft
[NASA-TP-1510] p0024 N79-31214

Radiation damage in high-voltage silicon solar cells
p0144 N79-32658

Effects of diffusion factor, aspect ratio and solidity on overall performance of 14 compressor middle stages --- the effects of varying both diffusion through the rotor and compressor blades and blade aspect ratio
[NASA-TP-1523] p0038 N79-33210

The 18 and 30 GHz fixed service communications satellite system study --- to determine the cost and performance characteristics
[NASA-CR-159627-2] p0096 N79-33374

PERFUSION

U DIFFUSION

PETROLEUM

U CRUDE OIL

PETROLEUM PRODUCTS

NT DIESEL FUELS

NT GASOLINE

NT LUBRICATING OILS

PHASE LOCKED SYSTEMS

High power phase locked laser oscillators
[NASA-CR-159630] p0112 N79-32538

PHASE MODULATION

Closed Loop solar array-ion thruster system with power control circuitry
[NASA-CASE-LEW-12780-1] p0052 N79-20179

PHASE TRANSFORMATIONS

NT EVAPORATION

NT FILM BOILING

NT FREEZING

NT VAPORIZING

Phase change thermal storage for a solar total energy system
p0155 A79-17321

Development of a phase-change thermal storage system using modified anhydrous sodium hydroxide for solar electric power generation
[NASA-CR-159465] p0153 N79-19454

PHENOLIC RESINS

Technology development for phosphoric acid fuel cell powerplant, phase 2
[NASA-CR-159572] p0153 N79-29604

PHENOLS

Method and device for the detection of phenol and related compounds --- in an electrochemical cell
[NASA-CASE-LEW-12513-1] p0069 N79-22235

PHOSPHATES

NT NUCLEOTIDES

PHOSPHORIC ACID

Fuel cell on-site integrated energy system parametric analysis of a residential complex
p0146 A79-14947

Commercial phosphoric acid fuel cell system technology development
p0150 A79-51809

Commercial phosphoric acid fuel cell system technology development
[NASA-TM-79169] p0139 N79-25500

Technology development for phosphoric acid fuel cell powerplant, phase 2
[NASA-CR-159572] p0153 N79-29604

PHOSPHORUS COMPOUNDS

NT NUCLEOTIDES

NT PHOSPHORIC ACID

The catalysis of nucleotide polymerization by compounds of divalent lead --- prebiotic synthesis
p0060 A79-23924

PHOTOCURRENTS

U ELECTRIC CURRENT

U PHOTOELECTRIC EMISSION

PHOTOELECTRIC CELLS

NT PHOTOVOLTAIC CELLS

PHOTOELECTRIC EMISSION

The decrease in effective photocurrents due to saddle points in electrostatic potentials near differentially charged spacecraft
p0049 A79-30140

PHOTOELECTRON SPECTROSCOPY

Application of ESCA to the determination of stoichiometry in sputtered coatings and interface regions --- X-ray photoelectron spectroscopy
p0117 A79-16664

An XPS study of the adherence of refractory carbide, silicide, and boride RF-sputtered wear-resistant coatings --- X-ray Photoelectron Spectroscopy of steel surfaces
p0085 A79-21022

X-ray photoelectron spectroscopy study of nickel and nickel-base alloy surface alterations in simulated hot corrosion conditions with emphasis on eventual application to turbine blade corrosion
[NASA-CR-159553] p0072 N79-25178

PHOTOREMISSION

U PHOTOELECTRIC EMISSION

PHOTOREMISSIVITY

U EMISSIVITY

U PHOTOELECTRIC EMISSION

PHOTOGRAPHY

NT AERIAL PHOTOGRAPHY

NT HOLOGRAPHY

NT MULTISPECTRAL PHOTOGRAPHY

PHOTONAPPING

A comparison of measured and calculated upwelling radiance over water as a function of sensor altitude
p0162 A79-51096

PHOTON BEAMS

Photon degradation effects in terrestrial solar cells
p0149 A79-41098

PHOTOTHERMOTROPISM

U ANISOTROPY

U TEMPERATURE EFFECTS

PHOTOVOLTAIC CELLS

An inverter/controller subsystem optimized for photovoltaic applications p0148 A79-41047

Solar cells having integral collector grids [NASA-CASE-LEW-12819-1] p0133 N79-11467

Photovoltaic tests and applications project [NASA-TM-79018] p0136 N79-17336

Market definition studies for photovoltaic highway applications [NASA-CR-159477] p0152 N79-19451

Description of photovoltaic village power systems in the United States and Africa [NASA-TM-79149] p0138 N79-24443

Dynamic analysis of a photovoltaic power system with battery storage capability [NASA-TM-79209] p0142 N79-29599

PHOTOVOLTAIC CONVERSION

NASA Lewis Research Center photovoltaic application experiments [AIAA PAPER 78-1768] p0146 A79-13867

Photovoltaic power systems for rural areas of developing countries p0147 A79-26131

Endurance testing of first generation /Block I/ commercial solar cell modules p0148 A79-41022

Design and fabrication of a photovoltaic power system for the Papago Indian Village of Schuchuli /Gunsight/, Arizona p0148 A79-41089

Description and status of NASA-LeRC/DOE photovoltaic applications systems experiments p0148 A79-41091

Photovoltaic power systems for rural areas of developing countries [NASA-TM-79097] p0135 N79-15411

Description of photovoltaic village power systems in the United States and Africa [NASA-TM-79149] p0138 N79-24443

DOE photovoltaic tests and applications project p0139 N79-25492

An expanded system simulation model for solar energy storage (technical report), volume 1 [NASA-CR-159601] p0166 N79-33881

SIMNESI: A simulation model for wind and photovoltaic energy storage systems (cdc program descriptions), volume 2 [NASA-CR-159608] p0167 N79-33884

PHUGOID OSCILLATIONS

OSCILLATORS

PHYSICAL CHEMISTRY

Improved apparatus for trapped radical and other studies down to 1.5 K --- microwave cavity cryogenic equipment for electron paramagnetic resonance experiments p0110 A79-20742

PHYSICAL FACTORS

Performance optimization of an MHD generator with physical constraints p0182 A79-51995

PHYSIOLOGICAL FACTORS

NT PHYSICAL FACTORS

PINCH EFFECT

NT PLASMA PINCH

PISTON ENGINES

NT DIESEL ENGINES

Concepts for reducing exhaust emissions and fuel consumption of the aircraft piston engine [SAE PAPER 790605] p0036 A79-36737

Stirling engine characteristics p0140 N79-26480

Energy-state formulation of lumped volume dynamic equations with application to a simplified free piston Stirling engine [NASA-TM-79197] p0141 N79-27663

PISTONS

Free-piston regenerative hot gas hydraulic engine [NASA-CASE-LEW-12274-1] p0113 N79-10426

PLANIGRAPHY

U TOMOGRAPHY

PLANNING

NT PROJECT PLANNING

PLASMA CONFINEMENT

U PLASMA CONTROL

PLASMA CONTROL

Ion confinement and transport in a toroidal plasma with externally imposed radial electric fields [NASA-TP-1411] p0181 N79-19867

PLASMA DIAGNOSTICS

Microwave radiation measurements near the electron plasma frequency of the NASA Lewis Bumpy Torus plasma p0181 A79-14953

Ion beam probing of electrostatic fields [NASA-TM-79120] p0181 N79-20864

PLASMA FLOW

U MAGNETOHYDRODYNAMIC FLOW

PLASMA FREQUENCIES

Microwave radiation measurements near the electron plasma frequency of the NASA Lewis Bumpy Torus plasma p0181 A79-14953

PLASMA INTERACTIONS

NT PLASMA-ELECTROMAGNETIC INTERACTION

Space environmental interactions with spacecraft surfaces [AIAA PAPER 79-0386] p0049 A79-23511

Spacecraft Charging Technology, 1978 [NASA-CP-2071] p0047 N79-24001

Plasma Interaction Experiment (PIX) flight results p0047 N79-24022

Effect of parasitic plasma currents on solar-array power output p0047 N79-24025

High voltage surface-charged environment test results from space flight and ground simulation experiments [NASA-TM-79184] p0043 N79-27235

PLASMA LOSS

Analytical core loss calculations for magnetic materials used in high frequency high power converter applications [NASA-TM-79234] p0098 N79-31499

PLASMA PHYSICS

Prediction of plasma properties in mercury ion thrusters [NASA-CR-159448] p0056 N79-15152

Physical processes in directed ion beam sputtering [NASA-CR-159567] p0182 N79-26943

PLASMA PINCH

Microwave radiation measurements near the electron plasma frequency of the NASA Lewis Bumpy Torus plasma p0181 A79-14953

PLASMA POTENTIALS

Neutralization tests on the SERT 2 spacecraft [NASA-TM-79271] p0054 N79-33255

PLASMA PROBES

Ion beam probing of electrostatic fields [NASA-TM-79120] p0181 N79-20864

PLASMA RADIATION

Microwave radiation measurements near the electron plasma frequency of the NASA Lewis Bumpy Torus plasma p0181 A79-14953

PLASMA RINGS

U TOROIDAL PLASMAS

PLASMA SPECTRA

Method for decomposing observed line shapes resulting from multiple causes - Application to plasma charge-exchange-neutral spectra p0182 A79-53867

PLASMA SPRAYING

Use of a nitrogen-argon plasma to improve adherence of sputtered titanium carbide coatings on steel p0119 A79-25103

Wide-temperature-spectrum self-lubricating coatings prepared by plasma spraying p0119 A79-34993

Development of sprayed ceramic seal systems for turbine gas path sealing [NASA-TM-79022] p0081 N79-12223

NASA thermal barrier coatings: Summary and update [NASA-TM-79053] p0015 N79-15048

Wide-temperature-spectrum self-lubricating coatings prepared by plasma spraying [NASA-TM-79113] p0082 N79-20240

Program for plasma-sprayed self-lubricating coatings [NASA-CR-3163] p0087 N79-28315

Plasma-sprayed coatings for lubrication of a titanium alloy in air at 430 deg C [NASA-TP-1509] p0083 N79-29327

Automated Plasma Spray (APS) process feasibility study: Plasma spray process development and evaluation [NASA-CR-159579] p0092 N79-29382

- Development of a plasma sprayed ceramic gas path seal for high pressure turbine applications [NASA-CR-159669] p0122 N79-31602
- Plasma-sprayed zirconia gas path seal technology: A state-of-the-art review [NASA-TM-79273] p0085 N79-33325
- PLASMA THEORY**
 - U PLASMA PHYSICS**
 - PLASMA-ELECTROMAGNETIC INTERACTION**
 - NASCAP modelling of high-voltage power system interactions with space charged-particle environments [NASA-TM-79146] p0046 N79-24000
 - Computer and laboratory simulation of interactions between spacecraft surfaces and charged-particle environments [NASA-TM-79219] p0063 N79-29224
 - PLASMA-PARTICLE INTERACTIONS**
 - Neutralization tests on the SERT 2 spacecraft [NASA-TM-79271] p0054 N79-33255
 - PLASMAS (PHYSICS)**
 - NT ELECTRON PLASMA
 - NT HELIUM PLASMA
 - NT HIGH TEMPERATURE PLASMAS
 - NT HYDROGEN PLASMA
 - Preliminary results in the NASA Lewis H2-C2 combustion MHD experiment [NASA-TM-79135] p0181 N79-22897
 - Summary of the two year NASA program for active control of ATS-5/6 environmental charging --- with a thermionic electron source and a plasma source p0047 N79-24006
 - Operations of the ATS-6 ion engine p0049 N79-24007
- PLASMOIDS**
 - U PLASMAS (PHYSICS)**
- PLASTIC DEFORMATION**
 - An acoustic emission study of plastic deformation in polycrystalline aluminum p0077 A79-19458
 - Anisotropic friction, deformation, and fracture of single-crystal silicon carbide at room temperature [NASA-TP-1525] p0084 N79-30380
- PLASTIC FILMS**
 - U POLYMERIC FILMS**
- PLASTIC MATERIALS**
 - U PLASTICS**
- PLASTIC YIELDING**
 - U PLASTIC DEFORMATION**
- PLASTICS**
 - NT CARBON FIBER REINFORCED PLASTICS
 - NT EPOXY RESINS
 - NT PHENOLIC RESINS
 - NT POLYETHER RESINS
 - NT POLYETHYLENES
 - NT POLYVINYL ALCOHOL
 - NT TEFLON (TRADEMARK)
 - Lightweight porous plastic plaque --- nickel cadmium batteries p0141 N79-28672
- PLATE (METAL)**
 - U METAL PLATES**
- PLATES (STRUCTURAL MEMBERS)**
 - NT CIRCULAR PLATES
- PLATING**
 - NT ION PLATING
 - NT NICKEL PLATE
 - Industrial potential, uses, and performance of sputtered and ion plated films [NASA-TM-79107] p0157 N79-20527
- PLUG NOZZLES**
 - Plug cluster engine concept for in-space missions [AIAA PAPER 79-1179] p0055 A79-38972
 - Effect of shocks on film cooling of a full scale turbojet exhaust nozzle having an external expansion surface [NASA-TM-79157] p0018 N79-23966
 - Effect of shocks on film cooling of a full scale turbojet exhaust nozzle having an external expansion surface [NASA-TM-79157] p0018 N79-23966
 - Acoustic and aerodynamic performance investigation of inverted velocity profile coannular plug nozzles, comprehensive data report, volume 1 [NASA-CR-159575-VOL-1] p0177 N79-26884
 - Acoustic and aerodynamic performance investigation of inverted velocity profile coannular plug nozzles, comprehensive data report, volume 2 [NASA-CR-159575-VOL-2] p0177 N79-26885
- acoustic and aerodynamic performance investigation of inverted velocity profile coannular plug nozzles, comprehensive data report, volume 3 [NASA-CR-159575-VOL-3] p0177 N79-26886
- Unconventional nozzle tradeoff study --- space tug propulsion [NASA-CR-159520] p0057 N79-28224
- PLUGGING**
 - Airfoil cooling hole plugging by combustion gas impurities of the type found in coal derived fuels [NASA-TM-79076] p0089 N79-20265
- PLUMBANE**
 - U LEAD COMPOUNDS**
- PLUMES**
 - Effects of geometric and flow-field variables on inverted-velocity-profile coaxial jet noise and source distributions [AIAA PAPER 79-0635] p0175 A79-32126
- PLUTONIUM**
 - NT PLUTONIUM 238
 - PLUTONIUM ISOTOPES**
 - NT PLUTONIUM 238
 - PLUTONIUM 238**
 - Mini-Brayton heat source assembly development [NASA-CR-159447] p0151 N79-12554
- POGO EFFECTS**
 - Space shuttle active-pogo-suppressor control design using linear quadratic regulator techniques [NASA-TP-1217] p0097 N79-14309
- POINT TO POINT COMMUNICATIONS**
 - NT NASCOM NETWORK
 - Millimeter wave communication satellite concepts p0095 A79-29784
- POISONS**
 - NT URETHANES
- POLARIZATION (WAVES)**
 - Efficiency enhancement of octave-bandwidth traveling wave tubes by use of multistage depressed collectors [NASA-TP-1416] p0097 N79-17139
- POLARIZATION CHARTS**
 - U POLARIZATION (WAVES)**
- POLICIES**
 - NT ENERGY POLICY
- POLLUTANTS**
 - U CONTAMINANTS**
- POLLUTION**
 - NT AIR POLLUTION
 - NT GLOBAL AIR POLLUTION
- POLLUTION CONTROL**
 - Wide range operation of advanced low NOx aircraft gas turbine combustors [ASME PAPER 78-GT-128] p0024 A79-10792
 - Correlations of catalytic combustor performance parameters p0070 A79-14956
 - The Advanced Low-Emissions Catalytic-Combustor Program: Phase I - Description and status --- for aircraft gas turbine engines [ASME PAPER 79-GT-192] p0027 A79-30557
 - Concepts for reducing exhaust emissions and fuel consumption of the aircraft piston engine [SAE PAPER 790605] p0036 A79-36737
 - Lean, premixed, prevaporized combustion for aircraft gas turbine engines [AIAA PAPER 79-1318] p0029 A79-39034
 - Reduction of particulate carryover from a pressurized fluidized bed p0150 A79-49527
 - Reduction of particulate carryover from a pressurized fluidized bed p0150 A79-49527
 - Advanced low emissions catalytic combustor program at General Electric p0021 N79-25011
 - Advanced low emissions catalytic combustor program at Pratt and Whitney p0021 N79-25012
 - Lean, premixed, prevaporized combustor conceptual design study p0021 N79-25013
 - Lean, premixed, prevaporized combustor conceptual design study p0022 N79-25014
 - Experimental Clean Combustor Program (ECCP), phase 3 --- commercial aircraft turbofan engine tests with double annular combustor [NASA-CR-135384] p0035 N79-31207

POLLUTION MONITORING

Global sensing of gaseous and aerosol trace species using automated instrumentation on 747 airliners p0110 A79-15067

Pattern recognition methods and air pollution source identification --- based on wind direction p0158 A79-15079

Measurements of carbon monoxide, condensation nuclei, and ozone on a B 747SP aircraft flight around the world p0158 A79-31332

Airborne atmospheric sampling system p0012 A79-50333

Condensation-nuclei (Aitken Particle) measurement system used in NASA global atmospheric sampling program [NASA-TP-1415] p0157 N79-18479

A summary of research on the NASA-Global Atmospheric Sampling Program performed by the Atmospheric Sciences Research Center --- ozone transport theory [NASA-CR-159614] p0159 N79-27716

Carbon monoxide measurement in the global atmospheric sampling program [NASA-TP-1526] p0158 N79-31841

POLYAMIDE RESINS

NT KEVLAR (TRADEMARK)

POLYBENZIMIDAZOLE

Ultrafine polybenzimidazole (PBI) fibers --- separators for alkaline batteries and fuel cells [NASA-CR-159644] p0067 N79-31350

POLYCRYSTALS

An acoustic emission study of plastic deformation in polycrystalline aluminum p0077 A79-19458

Method for the preparation of inorganic single crystal and polycrystalline electronic materials [NASA-CASE-XLE-02545-1] p0184 N79-21910

POLYETHER RESINS

Boundary lubrication, thermal and oxidative stability of a fluorinated polyether and a perfluoropolyether triazine [NASA-TM-79064] p0081 N79-15185

POLYETHYLENES

Effect of sterilization irradiation on friction and wear of ultrahigh-molecular-weight polyethylene [NASA-TP-1462] p0082 N79-23216

Infrared analysis of polyethylene wear specimens using attenuated total reflection spectroscopy --- effects of radiation on the surface properties of materials for total joint prostheses [NASA-TM-79228] p0083 N79-29329

POLYIMIDE RESINS

Stability of PMR-polyimide monomer solutions p0086 A79-31041

Characterization of PMR polyimides - Correlation of ester impurities with composite properties p0066 A79-43265

Effects of graphite fiber stability on the properties of PMR polyimide composites p0066 A79-43309

Composites emerging for aer propulsion applications p0066 A79-53720

Effects of graphite fiber stability on the properties of PMR polyimide composites [NASA-TM-79062] p0061 N79-16075

Characterization of PMR polyimides: Correlation of ester impurities with composite properties [NASA-TM-79068] p0061 N79-16918

Resin/fiber thermo-oxidative interactions in PMR polyimide/graphite composites [NASA-TM-79093] p0062 N79-16520

Stability of PMR-polyimide monomer solutions [NASA-TM-79063] p0062 N79-16921

Polyimide prepreg material having improved tack retention --- polyimide-graphite fiber composites [NASA-CASE-LEW-12933-1] p0059 N79-24061

POLYIMIDES

Graphite-fiber-reinforced polyimide liners of various compositions in plain spherical bearings p0117 A79-16678

Some loads limits and self-lubricating properties of plain spherical bearings with molded graphite fiber-reinforced polyimide liners to 320 C [ASLE PREPRINT 78-LC-5C-2] p0118 A79-23251

Status review of PMR polyimides --- Polymerization of Monomer Reactants p0065 A79-30399

Status review of PMR polyimides [NASA-TM-79039] p0062 N79-12150

Effect of thermal aging on the tribological properties of polyimide films and polyimide-bonded graphite fluoride films [NASA-TM-79045] p0082 N79-15186

Synthesis of improved moisture resistant polymers [NASA-CR-159510] p0087 N79-23218

Recent developments in PMR polyimides at NASA Lewis p0064 N79-30323

POLYMER CHEMISTRY

Synthesis of improved moisture resistant polymers [NASA-CR-159456] p0087 N79-18053

In situ self cross-linking of polyvinyl alcohol battery separators [NASA-CASE-LEW-12972-1] p0138 N79-25401

POLYMER MATRIX COMPOSITE MATERIALS

Graphite-fiber-reinforced polyimide liners of various compositions in plain spherical bearings p0117 A79-16678

Increasing the FOD tolerance of composites --- gas turbine engine blade foreign object damage p0067 A79-20859

Status review of PMR polyimides --- Polymerization of Monomer Reactants p0065 A79-30399

Composites emerging for aer propulsion applications p0066 A79-53720

New high temperature cross linking monomers --- for polymer matrix composite materials [NASA-CR-159514] p0087 N79-29331

Survey of inorganic polymers --- for composite matrix resins [NASA-CR-159563] p0087 N79-30377

POLYMERIC FILMS

UV blocking filters for polymeric films p0086 A79-51103

Cross-linked polyvinyl alcohol and method of making same --- separator for alkaline batteries [NASA-CASE-LEW-13101-1] p0068 N79-14173

Three methods for in situ cross-linking of polyvinyl alcohol films for application as ion-conducting membranes in potassium hydroxide electrolyte --- battery separators [NASA-TP-1407] p0059 N79-21128

POLYMERIZATION

The catalysis of nucleotide polymerization by compounds of divalent lead --- prebiotic synthesis p0060 A79-32924

Synthesis of improved moisture resistant polymers [NASA-CR-159510] p0087 N79-23218

Catalytic trimerization of aromatic nitriles and triaryl-s-triazine ring cross-linked high temperature resistant polymers and copolymers made thereby [NASA-CASE-LEW-12053-2] p0083 N79-28307

New high temperature cross linking monomers --- for polymer matrix composite materials [NASA-CR-159514] p0087 N79-29331

Survey of inorganic polymers --- for composite matrix resins [NASA-CR-159563] p0087 N79-30377

POLYMERS

Modification of the electrical and optical properties of polymers --- ion irradiation [NASA-CASE-LEW-13027-1] p0081 N79-11216

A review of issues and strategies in nondestructive evaluation of fiber reinforced structural composites [NASA-TM-79246] p0125 N79-29530

POLYVINYL ALCOHOL

Method of cross-linking polyvinyl alcohol and other water soluble resins [NASA-CASE-LEW-13103-1] p0068 N79-14172

Cross-linked polyvinyl alcohol and method of making same --- separator for alkaline batteries [NASA-CASE-LEW-13101-1] p0068 N79-14173

Three methods for in situ cross-linking of polyvinyl alcohol films for application as ion-conducting membranes in potassium hydroxide electrolyte --- battery separators [NASA-TP-1407] p0059 N79-21128

In situ self cross-linking of polyvinyl alcohol battery separators [NASA-CASE-LEW-12972-1] p0138 N79-25481

POROUS MATERIALS

Heat exchanger and method of making --- bonding rocket chambers with a porous metal matrix

- [NASA-CASE-LEW-12441-1] p0102 N79-13289
 A heat exchanger and method of making --- rocket lining
 [NASA-CASE-LEW-12441-2] p0104 N79-21313
 Lightweight porous plastic plaque --- nickel cadmium batteries p0141 N79-28672
 Combustion of porous solids at reduced gravitational conditions [NASA-CR-3197] p0072 N79-33288
- POSITIONING DEVICES (MACHINERY)**
 NT CAMS
- POTASSIUM**
 Lithium and potassium heat pipes for thermionic converters p0145 A79-10113
- POTASSIUM CHROMATES**
 Mass spectrometric investigation of the vaporization of sodium and potassium chromates - Preliminary results p0071 A79-49533
 Mass spectrometric investigation of the vaporization of sodium and potassium chromates: Preliminary results [NASA-TM-79210] p0065 N79-27279
- POTASSIUM COMPOUNDS**
 NT POTASSIUM CHROMATES
 NT POTASSIUM HYDROXIDES
 Preliminary evaluation of the role of K2S in MHD hot stream seed recovery [NASA-TM-79114] p0068 N79-20200
- POTASSIUM HYDROXIDES**
 Three methods for in situ cross-linking of polyvinyl alcohol films for application as ion-conducting membranes in potassium hydroxide electrolyte --- battery separators [NASA-TP-1407] p0059 N79-21128
- POTENTIAL ENERGY**
 NT CONTACT POTENTIALS
 NT COULOMB POTENTIAL
 NT ELECTRIC POTENTIAL
 NT PLASMA POTENTIALS
- POTENTIAL FIELDS**
 Effects of bulk and surface conductivity on the potential developed by dielectrics exposed to electron beams p0171 A79-50938
- POTENTIAL FLOW**
 Unsteady vortical and entropic distortions of potential flows round arbitrary obstacles p0005 A79-19452
 Computer programs for calculating two-dimensional potential flow through deflected nozzles [NASA-TM-79144] p0004 N79-26019
- POTENTIAL GRADIENTS**
 Insulator edge voltage gradient effects in spacecraft charging phenomena p0048 A79-30139
- POWDER (PARTICLES)**
 NT METAL POWDER
- POWDERED METALS**
 U METAL POWDER
- POWER CONDITIONING**
 Control of wind turbine generators connected to power systems p0146 A79-15574
 Description of A 2.3 kW power transformer for space applications p0099 A79-34991
 Analysis of a parallel-arrayed power regulating system p0101 A79-49397
 Lightweight multiple output converter development [NASA-CR-159526] p0100 N79-20317
 Primary electric propulsion for future space missions [NASA-TM-79141] p0052 N79-22190
 Effect of parasitic plasma currents on solar-array power output p0047 N79-24025
 A method for correlating performance data of a terrestrial solar cell array [NASA-TM-79163] p0140 N79-26503
 Reduced power processor requirements for the 30-cm diameter Hg ion thruster [NASA-TM-79257] p0054 N79-33253
- POWER EFFICIENCY**
 Power converter design optimization p0099 A79-10885
- Comments on measuring the overall and the depressed collector efficiency in TWT's and klystron amplifiers p0099 A79-25118
 MHD performance calculations with oxygen enrichment [NASA-TM-79140] p0139 N79-25499
- POWER GAIN**
 Gain measurements of the Ca-Xe charge exchange system --- for UV lasers p0112 A79-19078
- POWER GENERATORS**
 U ELECTRIC GENERATORS
- POWER LINES**
 Flow friction of the turbulent coolant flow in cryogenic porous cables [NASA-TM-79052] p0103 N79-20341
- POWER PLANTS**
 Preliminary summary of the ETF conceptual studies [NASA-TM-78999] p0133 N79-11478
- POWER PROCESSING SYSTEMS**
 U POWER CONDITIONING
- POWER SUPPLY CIRCUITS**
 The solid state remote power controller - Its status, use and perspective --- for aircraft and spacecraft p0099 A79-10896
 Closed loop solar array-ion thruster system with power control circuitry [NASA-CASE-LEW-12780-1] p0052 N79-20179
- POWER TRANSMISSION**
 Design and test of a squeeze-film damper for a flexible power transmission shaft p0123 A79-16011
 Ground-to-space optical power transfer --- using laser propulsion for orbit transfer p0161 A79-17180
 Nonsynchronous vibrations observed in a supercritical power transmission shaft [ASME PAPER 79-GT-146] p0123 A79-32412
- PRECIOUS METALS**
 U NOBLE METALS
- PRECIPITATION HARDENING**
 Longitudinal shear behavior of several oxide dispersion strengthened alloys p0076 A79-14955
 An oxide dispersion strengthened alloy for gas turbine blades [AIAA 79-0763] p0077 A79-28276
 Transverse and longitudinal tensile properties at 760 C of several oxide dispersion strengthened nickel-base alloys p0078 A79-49531
 Transverse and longitudinal tensile properties at 760 C of several oxide dispersion strengthened nickel-base alloys [NASA-TM-79189] p0075 N79-30355
- PRECIPITATORS**
 NT ELECTROSTATIC PRECIPITATORS
- PREDICTION ANALYSIS TECHNIQUES**
 A jet exhaust noise prediction procedure for inverted velocity profile coaxial nozzles [AIAA PAPER 79-0633] p0178 A79-28964
 Prediction of properties of intraply hybrid composites [NASA-TM-79087] p0061 N79-16919
 An improved method for predicting the effects of flight on jet mixing noise [NASA-TM-79155] p0173 N79-24770
 Use of refinery computer model to predict fuel production [NASA-TM-79203] p008 N79-28349
- PREDICTIONS**
 NT PERFORMANCE PREDICTION
- PREMIXED FLAMES**
 Turbulence effects on flame speed and flame structure [AIAA PAPER 79-0016] p0070 A79-19480
 Experimental study of the effects of flameholder geometry on emissions and performance of lean premixed combustors [AIAA PAPER 79-0187] p0070 A79-19586
 Lean combustion limits of a confined premixed-prevaporized propane jet [AIAA PAPER 79-0538] p0026 A79-25856
 Emission measurements for a lean premixed propane/air system at pressures up to 30 atmospheres [NASA-CR-159421] p0071 N79-10165

- Premix fuels study applicable to duct burner conditions for a variable cycle engine
[NASA-CR-159513] p0091 N79-20266
- Premixed Prevaporized Combustor Technology Forum
[NASA-CP-2078] p0019 N79-24994
- Emissions measurements for a lean premixed propane/air system at pressures up to 30 atmospheres
p0020 N79-25002
- Effect of degree of fuel vaporization on emissions for a premixed-prevaporized combustor system
p0020 N79-25003
- PREPOLYMERS**
- NT TRIMERS**
- Polyimide prepreg material having improved tack retention --- polyimide-graphite fiber composites
[NASA-CASE-LEW-12933-1] p0059 N79-24061
- PREPRINTING**
- U SINTERING**
- PRESSURE**
- NT DENSIFICATION**
- NT FLUID PRESSURE**
- NT HIGH PRESSURE**
- NT HYDROSTATIC PRESSURE**
- NT IMPACT LOADS**
- NT INTERNAL PRESSURE**
- NT INTRAOCULAR PRESSURE**
- NT ISOSTATIC PRESSURE**
- NT LOW PRESSURE**
- NT STATIC PRESSURE**
- NT VACUUM**
- PRESSURE CHAMBERS**
- Definition of mutually optimum NDI and proof test criteria for 2219 aluminum pressure vessels.
Volume 1: Methods
[NASA-CR-135445] p0125 N79-21410
- Preliminary comparison of theory and experiment for a conical, pressurized-fluidized-bed coal combustor
[NASA-TM-79137] p0137 N79-22623
- Reduction of particulate carryover from a pressurized fluidized bed
[NASA-TM-79216] p0141 N79-27664
- PRESSURE DISTRIBUTION**
- Aerodynamic performance of a 1.35-pressure-ratio axial-flow fan stage
[NASA-TF-1299] p0002 N79-10022
- Combined pressure and temperature distortion effects on internal flow of a turbofan engine
[NASA-TM-79136] p0012 N79-23963
- Some flow characteristics of conventional and tapered high pressure drop simulated seals
[NASA-TM-79192] p0104 N79-27460
- PRESSURE EFFECTS**
- Combined pressure and temperature distortion effects on internal flow of a turbofan engine
[AIAA PAPER 79-1309] p0029 A79-39031
- Effect of steady-state pressure distortion on flow characteristics entering a turbofan engine
[NASA-TM-79134] p0019 N79-23969
- Effect of steady-state temperature distortion and combined distortion on inlet flow to a turbofan engine
[NASA-TM-79237] p0023 N79-30187
- PRESSURE FIELDS**
- U PRESSURE DISTRIBUTION**
- PRESSURE GAGES**
- NT KNUDSEN GAGES**
- PRESSURE GRADIENTS**
- Measuring unsteady pressure on rotating compressor blades
[NASA-TM-79159] p0109 N79-22448
- PRESSURE MEASUREMENTS**
- Pressure instrumentation for gas turbine engines - A review of measurement technology
[ASME PAPER 78-GT-148] p0110 A79-10800
- Correlation of combustor acoustic power levels inferred from internal fluctuating pressure measurements
p0025 A79-14796
- Numerical spatial marching techniques in duct acoustics --- noise source calculation from far field pressure measurements
p0175 A79-25946
- Instrumentation for measuring the dynamic pressure on rotating compressor blades
[NASA-CR-159466] p0110 N79-12418
- Indicated mean-effective pressure instrument
[NASA-CASE-LEW-12661-1] p0109 N79-14345
- Aerodynamic performance of 1.38-pressure-ratio, variable-pitch fan stage
[NASA-TP-1502] p0024 N79-31213
- PRESSURE OSCILLATIONS**
- Instrumentation for measuring the dynamic pressure on rotating compressor blades
[NASA-CR-159466] p0110 N79-12418
- Effects of steady-state pressure distortion on the stall margin of a J85-21 turbojet engine
[NASA-TM-79123] p0018 N79-23968
- PRESSURE PROBES**
- U PRESSURE SENSORS**
- PRESSURE RECOVERY**
- Experimental investigation of a 0.15-scale model of an underfuselage normal-shock inlet
[NASA-CR-3049] p0006 N79-12014
- PRESSURE SENSORS**
- Pressure instrumentation for gas turbine engines - A review of measurement technology
[ASME PAPER 78-GT-148] p0110 A79-10800
- Synthesis of blade flutter vibratory patterns using stationary transducers
p0127 A79-10823
- Instrumentation for measuring the dynamic pressure on rotating compressor blades
[NASA-CR-159466] p0110 N79-12418
- PRESSURE TRANSDUCERS**
- U PRESSURE SENSORS**
- PRESSURE VESSELS**
- Acoustic emission testing of composite vessels under sustained loading
p0128 A79-11543
- Proof test criteria for thin walled pressure vessels
p0123 A79-26985
- PREVENTION**
- NT CORROSION PREVENTION**
- NT FIRE PREVENTION**
- PRIMARY BATTERIES**
- NT ALKALINE BATTERIES**
- NT NICKEL ZINC BATTERIES**
- NT SODIUM SULFUR BATTERIES**
- PRINTING**
- Application of semiconductor diffusants to solar cells by screen printing
[NASA-CASE-LEW-12775-1] p0133 N79-11468
- Alternate methods of applying diffusants to silicon solar cells --- screen printing of thick-film paste materials and vapor phase transport from solid sources
[NASA-CR-159508] p0153 N79-29603
- PRIVATE AIRCRAFT**
- U GENERAL AVIATION AIRCRAFT**
- PROBABILITY**
- U PROBABILITY THEORY**
- PROBABILITY DISTRIBUTION FUNCTIONS**
- On the distribution of computation for sequential decoding using the stack algorithm
p0096 A79-33793
- PROBABILITY THEORY**
- Numbers of center points appropriate to blocked response surface experiments
p0169 A79-49529
- Numbers of center points appropriate to blocked response surface experiments
[NASA-TM-79201] p0168 N79-28970
- PROCEDURES**
- NT FINITE ELEMENT METHOD**
- PROCESS CONTROL (INDUSTRY)**
- Burn coal cleanly in a fluidized bed - The key is in the controls
p0071 A79-26374
- Recent developments in FME polyimides at NASA Lewis
p0064 N79-30323
- PRODUCT DEVELOPMENT**
- Wind turbines for electric utilities - Development status and economics
[AIAA PAPER 79-0965] p0148 A79-38888
- Large horizontal axis wind turbine development
p0149 A79-46527
- Recent developments in FME polyimides at NASA Lewis
p0064 N79-30323
- PRODUCTION ENGINEERING**
- Solar cell collector and method for producing same
[NASA-CASE-LEW-12552-2] p0133 N79-11472
- PRODUCTION METHODS**
- U PRODUCTION ENGINEERING**
- PRODUCTIVITY**
- Use of refinery computer model to predict fuel production

[NASA-TM-79203] p0089 N79-28349
PROGRAM MANAGEMENT
 U PROJECT MANAGEMENT
PROGRAM VERIFICATION (COMPUTERS)
 Initial comparison of single cylinder Stirling engine computer model predictions with test results
 [NASA-TM-79044] p0188 N79-16721
PROGRAMMING LANGUAGES
 NT ASSEMBLY LANGUAGE
PROGRAMS
 NT GLOBAL ATMOSPHERIC RESEARCH PROGRAM
 NT NASA PROGRAMS
 NT QUIET ENGINE PROGRAM
PROJECT MANAGEMENT
 Definition study of a Variable Cycle Experimental Engine (VCEE) and associated test program and test plan
 [NASA-CR-159419] p0031 N79-11042
 DOE photovoltaic tests and applications project
 p0139 N79-25492
PROJECT PLANNING
 An economical approach to space power systems
 p0052 N79-10139
 National Aeronautics and Space Administration plans for space communication technology
 [NASA-TM-79217] p0053 N79-28220
PROPAGATION (EXTENSION)
 NT CRACK PROPAGATION
 NT FLAME PROPAGATION
PROPAGATION MODES
 Modal propagation angles in a cylindrical duct with flow and their relation to sound radiation
 [AIAA PAPER 79-0183] p0174 A79-19582
 Modal propagation angles in ducts with soft walls and their connection with suppressor performance
 [AIAA PAPER 79-0624] p0175 A79-26880
PROPAGATION VELOCITY
 Turbulence effects on flame speed and flame structure
 [AIAA PAPER 79-0016] p0070 A79-19480
PROPANE
 Experimental study of the effects of flameholder geometry on emissions and performance of lean premixed combustors
 [AIAA PAPER 79-0187] p0070 A79-19586
 Lean combustion limits of a confined premixed-prevaporized propane jet
 [AIAA PAPER 79-0538] p0026 A79-25856
 Emission measurements for a lean premixed propane/air system at pressures up to 30 atmospheres
 [NASA-CR-159421] p0071 N79-10165
 Emissions measurements for a lean premixed propane/air system at pressures up to 30 atmospheres
 p0020 N79-25002
PROPELLANT TANKS
 Contoured tank outlets for draining of cylindrical tanks in low-gravity environment --- Lewis Research Center Zero Gravity Facility
 [NASA-TP-1492] p0105 N79-29467
PROPELLANTS
 NT CRYOGENIC ROCKET PROPELLANTS
 NT GASEOUS ROCKET PROPELLANTS
 NT LIQUID ROCKET PROPELLANTS
 Workbook for estimating effects of accidental explosions in propellant ground handling and transport systems
 [NASA-CR-3023] p0091 N79-10226
PROPELLER BLADES
 Tone noise of three supersonic helical tip speed propellers in a wind tunnel
 p0175 A79-39801
 Feasibility of wing shielding of the airplane interior from the shock noise generated by supersonic tip speed propellers
 [NASA-TM-79042] p0172 N79-15757
 Tone noise of three supersonic helical tip speed propellers in a wind tunnel at 0.8 Mach number
 [NASA-TM-79046] p0172 N79-15758
 Tone noise of three supersonic helical tip speed propellers in a wind tunnel
 [NASA-TM-79167] p0174 N79-25840
PROPELLER EFFICIENCY
 Wind tunnel performance of four energy efficient propellers designed for Mach 0.8 cruise
 [SAE PAPER 790573] p0028 A79-36759

Wind tunnel performance of four energy efficient propellers designed for Mach 0.8 cruise --- Lewis 8x6 foot wind tunnel studies for noise reduction in high speed turboprop aircraft
 [NASA-TM-79124] p0003 N79-20069
PROPELLER FANS
 Prop-fan propulsion - Its status and potential
 [SAE PAPER 780995] p0026 A79-25880
 Design study and performance analysis of a high-speed multistage variable-geometry fan for a variable cycle engine
 [NASA-CR-159545] p0034 N79-25020
PROPELLERS
 NT PROPELLER FANS
 NT VARIABLE PITCH PROPELLERS
PROPULSION
 NT AUXILIARY PROPULSION
 NT CHEMICAL PROPULSION
 NT ELECTRIC PROPULSION
 NT HYBRID PROPULSION
 NT ION PROPULSION
 NT LOW THRUST PROPULSION
 NT MASS DRIVERS (PAYLOAD DELIVERY)
 NT NUCLEAR ELECTRIC PROPULSION
 NT SOLAR ELECTRIC PROPULSION
 NT SOLAR PROPULSION
 NT SPACECRAFT PROPULSION
 Advanced General Aviation Turbine Engine (GATE) concepts
 [NASA-CR-159603] p0034 N79-25017
PROPULSION SYSTEM CONFIGURATIONS
 Impact of future fuel properties on aircraft engines and fuel systems
 p0024 A79-11600
 Convective heat flux in a laser-heated thruster
 p0057 A79-22396
 Prop-fan propulsion - Its status and potential
 [SAE PAPER 780995] p0026 A79-25880
 The GATE studies - Assessing the potential of future small general aviation turbine engines
 p0027 A79-30560
 Theoretical fan velocity distortions due to inlets and nozzles
 p0006 A79-39810
 NASA research on general aviation power plants
 [NASA-TM-79031] p0014 A79-12086
 Primary electric propulsion for future space missions
 [NASA-TM-79141] p0052 N79-22190
 Variable cycle engine technology program planning and definition study
 [NASA-CR-159539] p0034 N79-23084
PROPULSION SYSTEM PERFORMANCE
 Optimize out-of-core thermionic energy conversion for nuclear electric propulsion
 p0146 A79-13099
 Effect of forward velocity and crosswind on the reverse-thrust performance of a variable-pitch fan engine
 [AIAA PAPER 79-0105] p0025 A79-23512
 Effect of rotor tip clearance and configuration on overall performance of a 12.77-centimeter tip diameter axial-flow turbine
 [ASME PAPER 79-GT-42] p0027 A79-30521
 Effect of flight loads on turbofan engine performance deterioration
 p0127 A79-30559
 Effect of flight loads on turbofan engine performance deterioration
 [NASA-TM-79041] p0013 N79-12085
 Effect of forward velocity and crosswind on the reverse-thrust performance of a variable-pitch fan engine
 [NASA-TM-79059] p0015 N79-15049
 Analysis and preliminary design of an optical digital tip clearance sensor for propulsion control
 [NASA-CR-159434] p0031 N79-15053
 Energy efficient engine: Propulsion system-aircraft integration evaluation
 [NASA-CR-159488] p0032 N79-16850
 Space propulsion technology overview
 [NASA-TM-79104] p0042 N79-20171
 Design study and performance analysis of a high-speed multistage variable-geometry fan for a variable cycle engine
 [NASA-CR-159545] p0034 N79-25020
 Computerized systems analysis and optimization of aircraft engine performance, weight, and life

cycle costs
[NASA-TM-79221] p0170 N79-29938

PROPULSIVE EFFICIENCY

NT PROPELLER EFFICIENCY

Prop-fan propulsion - Its status and potential
[SAE PAPER 780995] p0026 A79-25880

Preliminary results of the mission profile life
test of a 30 cm Hg bombardment thruster
[NASA-TM-79261] p0054 N79-33254

PROSTHETIC DEVICES

Infrared analysis of polyethylene wear specimens
using attenuated total reflection spectroscopy
--- effects of radiation on the surface
properties of materials for total joint prostheses
[NASA-TM-79228] p0083 N79-29329

PROTECTION

NT CIRCUIT PROTECTION

NT CORROSION PREVENTION

NT THERMAL PROTECTION

PROTECTIVE COATINGS

NT CERAMIC COATINGS

The friction and wear properties of sputtered hard
refractory compounds p0085 A79-16666

An XPS study of the adherence of refractory
carbide, silicide, and boride RF-sputtered
wear-resistant coatings --- X-ray Photoelectron
Spectroscopy of steel surfaces p0085 A79-21022

Development of surface coatings for
air-lubricated, compliant journal bearings to
650 C [ASLE PREPRINT 78-LC-3C-1] p0123 A79-23252

Static evaluation of surface coatings for
compliant gas bearings in an oxidizing
atmosphere to 650 C p0088 A79-31957

Tests of NASA ceramic thermal barrier coating for
gas-turbine engines p0086 A79-34996

Development of sputtering process to deposit
stoichiometric zirconia coatings for the inside
wall of regeneratively cooled rocket thrust
chambers [NASA-CR-159412] p0056 N79-11115

Ceramic coating effect on liner metal temperatures
of film-cooled annular combustor [NASA-TF-1323] p0015 N79-14098

An experimental, low-cost, silicon
slurry/aluminate high-temperature coating for
superalloys [NASA-TM-79178] p0075 N79-29292

PROTECTORS

Development of single-cell protectors for sealed
silver-zinc cells [NASA-CR-159407] p0151 N79-12550

PROTEINS

NT NUCLEOTIDES

PSYCHOACOUSTICS

Loudness of steady sounds - A new theory
p0176 A79-39975

PSYCHOLOGY

NT PSYCHOACOUSTICS

PSYCHOPHYSICS

NT PSYCHOACOUSTICS

PULSATING FLOW

U UNSTEADY FLOW

PULSE DURATION MODULATION

Analysis of a parallel-arrayed power regulating
system p0101 A79-49397

PULSE MODULATION

NT PULSE DURATION MODULATION

PULSE TIME MODULATION

NT PULSE DURATION MODULATION

PULSE WIDTH MODULATION

U PULSE DURATION MODULATION

PULSED LASERS

NT ULTRAVIOLET LASERS

Simulated electronic heterodyne recording and
processing of pulsed-laser holograms
[NASA-TF-1444] p0111 N79-21329

PUMPS

NT CENTRIFUGAL PUMPS

NT FUEL PUMPS

NT TURBINE PUMPS

PWM (MODULATION)

U PULSE DURATION MODULATION

PYRAZINES

NT AZINES

PYROGRAPHALLOY

U COMPOSITE MATERIALS

U REFRACTORY MATERIALS

PYROMETRY

U TEMPERATURE MEASUREMENT

Q

QUALITY

NT AIR QUALITY

NT WATER QUALITY

QUALITY CONTROL

Determination of lubricant selection based on
elastohydrodynamic film thickness and traction
measurement [NASA-CR-159428] p0121 N79-14385

QUIET ENGINE PROGRAM

Effect of forward velocity and crosswind on the
reverse-thrust performance of a variable-pitch
fan engine [AIAA PAPER 79-0105] p0025 A79-23512

Measured and predicted noise of the AVCO-Lycoming
YF-102 turbofan engine [AIAA PAPER 79-0641] p0026 A79-26877

Preliminary QCGAT program test results --- Quiet,
Clean General Aviation Turbofan [SAE PAPER 790596] p0028 A79-36729

QCSSE - The key to future short-haul air transport
--- Quiet, Clean, Short-Haul Experimental Engine
program p0030 A79-50208

R

RADAR

NT AIRBORNE SURVEILLANCE RADAR

NT SATELLITE-BORNE RADAR

NT SIDE-LOOKING RADAR

RADAR DETECTION

Radar image processing of real aperture SLAR data
for the detection and identification of iceberg
and ship targets p0131 A79-36537

RADAR IMAGERY

VHF downlink communication system for SLAR data
p0045 A79-51097

RADAR MAPS

NT RADAR IMAGERY

RADIAL DISTRIBUTION

Normal and radial impact of composites with
embedded penny-shaped cracks [NASA-CR-159538] p0130 N79-31627

RADIANCE

A comparison of measured and calculated upwelling
radiance over water as a function of sensor
altitude [NASA-TM-79147] p0131 N79-22589

RADIANT FLUX DENSITY

NT ELECTRON FLUX DENSITY

NT RADIANCE

RADIATION ABSORPTION

NT ATMOSPHERIC ATTENUATION

RADIATION DAMAGE

Photon degradation effects in terrestrial solar
cells p0149 A79-41098

Photon-degradation effects in terrestrial silicon
solar cells p0149 A79-42545

Radiation damage in high-voltage silicon solar cells
p0144 N79-32658

High-energy electron-induced damage production at
room temperature in aluminum-doped silicon
p0154 N79-32662

Summary of GAs Solar Cell Performance and
Radiation Damage Workshop p0144 N79-32669

Annealing of radiation damage in 0.1- and
2-cm-centimeter Silicon solar cells
[NASA-TF-1559] p0144 N79-33572

RADIATION EFFECTS

NT RADIATION DAMAGE

Infrared analysis of polyethylene wear specimens
using attenuated total reflection spectroscopy
--- effects of radiation on the surface
properties of materials for total joint prostheses
[NASA-TM-79228] p0083 N79-29329

RADIATION MEASURING INSTRUMENTS

NT INFRARED INSTRUMENTS

RADIATION RESISTANCE

U RADIATION TOLERANCE

RADIATION SPECTRA

NT LINE SPECTRA

RADIATION TOLERANCE

Solar Cell High Efficiency and Radiation Damage,

1979

[NASA-CF-2097]

p0143 N79-32640

Applications of ion implantation to high performance, radiation tolerant silicon solar cells

p0143 N79-32648

RADICALS

NT FREE RADICALS

RADIO ANTENNAS

UHF coplanar-slot antenna for aircraft-to-satellite data communications

[NASA-TM-79239]

p0010 N79-31185

RADIO BROADCASTING

U BROADCASTING

RADIO COMMUNICATION

NT RADIO RELAY SYSTEMS

NT TELEPHONE

UHF coplanar-slot antenna for aircraft-to-satellite data communications

[NASA-TM-79239]

p0010 N79-31185

RADIO EQUIPMENT

NT RADIO ANTENNAS

NT VERY HIGH FREQUENCY RADIO EQUIPMENT

RADIO FREQUENCIES

NT C BAND

NT EXTREMELY HIGH FREQUENCIES

NT LOW FREQUENCIES

NT SUPERHIGH FREQUENCIES

NT ULTRAHIGH FREQUENCIES

The 18 and 30 GHz fixed service communications satellite system study --- to determine the cost and performance characteristics

[NASA-CR-159627-2]

p0096 N79-33374

RADIO RELAY SYSTEMS

An airborne meteorological data collection system using satellite relay /ASDAR/

p0010 A79-14949

RADIO TRANSMISSION

NT MICROWAVE TRANSMISSION

RADIO WAVES

NT MICROWAVE EMISSION

NT MILLIMETER WAVES

RADIOACTIVE ISOTOPES

NT PLUTONIUM 238

RADIOGRAPHY

NT TOMOGRAPHY

RADIOSENSITIVITY

U RADIATION TOLERANCE

RAILS

Definition of mutually optimum NDI and proof test criteria for 2219 aluminum pressure vessels.

Volume 3: Applications to rail defect evaluation

[NASA-CR-135447]

p0125 N79-21412

RANDOM DISTRIBUTIONS

U STATISTICAL DISTRIBUTIONS

RANDOM LOADS

NT GUST LOADS

RANKINE CYCLE

Rankine-cycle component characteristics

p0140 N79-26478

Candidate power-conversion system cycles, appendix A

p0140 N79-26484

RARE EARTH ALLOYS

The magnetocaloric effect in dysprosium

p0185 A79-38402

RARE EARTH ELEMENTS

NT DYSPROSIUM

RARE GASES

NT ARGON

NT HELIUM

NT XENON

Inert gas thrusters

[NASA-CR-159527]

p0057 N79-26110

REFINED GASES

NT NEUTRAL GASES

RATE METERS

U MEASURING INSTRUMENTS

RATES (PER TIME)

NT ACOUSTIC VELOCITY

NT COLLISION PARAMETERS

NT CRITICAL VELOCITY

NT CURRENT DENSITY

NT ELECTRON FLUX DENSITY

NT EXHAUST VELOCITY

NT FLUX DENSITY

NT HIGH SPEED

NT PROPAGATION VELOCITY

NT RADIANCE

NT ROTOR SPEED

NT STRAIN RATE

NT SUBSONIC SPEED

NT SUPERSONIC SPEEDS

NT TIP SPEED

NT WIND VELOCITY

RATIOS

NT ASPECT RATIO

NT FUEL-AIR RATIO

NT LOW ASPECT RATIO

NT MASS RATIOS

NT REYNOLDS NUMBER

NT THICKNESS RATIO

RAYLEIGH EQUATIONS

Energy-state formulation of lumped volume dynamic equations with application to a simplified free piston Stirling engine

p0187 A79-49532

REACTION JETS

U JET FLOW

REACTION KINETICS

Experimental studies of the formation/deposition of sodium sulfate in/from combustion gases --- hot corrosion in gas turbine engines

[NASA-CR-159612]

p0072 N79-25183

Experimental studies of the formation/deposition of sodium sulfate in/from combustion gases --- hot corrosion

[NASA-CR-159613]

p0080 N79-25184

REAL VARIABLES

NT BURGER EQUATION

NT NONLINEAR EQUATIONS

NT NUMERICAL INTEGRATION

NT SERIES (MATHEMATICS)

RECIPROCATING ENGINES

U PISTON ENGINES

RECLAMATION

NT MATERIALS RECOVERY

RECOGNITION

NT PATTERN RECOGNITION

RECOMBINATION REACTIONS

NT ELECTRON RECOMBINATION

NT HYDROGEN RECOMBINATIONS

RECOMMENDATIONS

Ozone Contamination in Aircraft Cabins: Post workshop review of recommendations

p0008 N79-21027

RECORDING INSTRUMENTS

NT FLIGHT RECORDERS

RECOVERABLE SPACECRAFT

NT SPACE SHUTTLES

RECTIFIERS

NT THYRISTORS

REGENERATORS

U REGENERATORS

REDUCED GRAVITY

Feasibility study of liquid pool burning in reduced gravity

[NASA-CR-159642]

p0072 N79-32303

REDUCTION (CHEMISTRY)

Redox flow cell energy storage systems

[NASA-TM-79143]

p0138 N79-24442

Redox flow cell development and demonstration project, calendar year 1977

[NASA-TM-79067]

p0138 N79-24445

REFINING

NT ELECTROSLAG REFINING

Use of refinery computer model to predict fuel production

[NASA-TM-79203]

p0089 N79-28349

REFRACTORY MATERIALS

NT CHROMIUM

NT IRIIDIUM

NT MOLYBDENUM

NT MOLYBDENUM ALLOYS

NT REFRACTORY METAL ALLOYS

NT REFRACTORY METALS

NT RENE 41

NT RHENIUM ALLOYS

NT TUNGSTEN

NT TUNGSTEN ALLOYS

- Effects of pressure and temperature on hot pressing a sialon --- Si-Al-O-N ceramics
p0085 A79-11548
- The friction and wear properties of sputtered hard refractory compounds
p0085 A79-16666
- An XPS study of the adherence of refractory carbide, silicide, and boride xF-sputtered wear-resistant coatings --- X-ray Photoelectron Spectroscopy of steel surfaces
p0085 A79-21022
- Stability of PHE-polyimide monomer solutions [NASA-TM-79063]
p0062 N79-16921
- Materials and structural aspects of advanced gas-turbine helicopter engines [NASA-TM-79100]
p0001 N79-20008
- Catalytic trimerization of aromatic nitriles and triaryl-s-triazine ring cross-linked high temperature resistant polymers and copolymers made thereby
[NASA-CASE-LEW-12053-2]
p0083 N79-28307
- REFRACTORY METAL ALLOYS**
- NT MOLYBDENUM ALLOYS**
- NT RENE 41**
- NT RHENIUM ALLOYS**
- NT TUNGSTEN ALLOYS**
- The strainrange partitioning behavior of an advanced gas turbine disk alloy, AP2-1DA [AIAA PAPER 79-1192]
p0078 A79-38977
- Transverse and longitudinal tensile properties at 760 C of several oxide dispersion strengthened nickel-base alloys [NASA-TM-79189]
p0075 N79-30355
- Interdiffusion behavior of tungsten or rhenium and group 5 and 6 elements and alloys of the periodic table. Part 2b: Appendices [NASA-CR-134526]
p0080 N79-33305
- REFRACTORY METALS**
- NT CHROMIUM**
- NT IODIUM**
- NT MOLYBDENUM**
- NT TUNGSTEN**
- Development and fabrication of high strength alloy fibers for use in metal-metal matrix composites [NASA-TM-79115]
p0063 N79-22211
- REFRASIL (TRADEMARK)**
- U FIBERS**
- REGENERATION (ENGINEERING)**
- Free-piston regenerative hot gas hydraulic engine [NASA-CASE-LEW-12274-1]
p0113 N79-10426
- User's manual for PRESTO: A computer code for the performance of regenerative steam turbine cycles [NASA-CR-159540]
p0122 N79-25395
- REGENERATIVE CYCLES**
- U REGENERATION (ENGINEERING)**
- REGENERATORS**
- Design and fabrication of the Mini-Brayton Regenerator (MBR) [NASA-CR-159429]
p0151 N79-11476
- Operation of advanced regenerator systems [NASA-CR-159422]
p0188 N79-12969
- Evaluation of a Brayton cycle recuperator after 21,000 hours of ground testing [NASA-TM-79091]
p0074 N79-20217
- REGIONS**
- NT REMOTE REGIONS**
- REGULATORS**
- NT FREQUENCY CONTROL**
- NT FUEL FLOW REGULATORS**
- NT VOLTAGE REGULATORS**
- REIGNITION**
- U IGNITION**
- REINFORCED MATERIALS**
- U COMPOSITE MATERIALS**
- REINFORCED PLASTICS**
- NT CLASS FIBER REINFORCED PLASTICS**
- REINFORCING FIBERS**
- NT CARBON FIBERS**
- Some properties of an advanced boron fiber
p0086 A79-21297
- Analysis/design of strip reinforced random composites /strip hybrids/
p015 A79-24035
- Mechanisms of boron fiber strengthening by thermal treatment
p0065 A79-30396
- Dynamic mechanical analysis of fiber reinforced composites [NASA-TM-79033]
p0061 N79-15157
- Prediction of properties of intraply hybrid composites [NASA-TM-79087]
p0061 N79-16919
- Tungsten fiber reinforced FeCrAlY: A first generation composite turbine blade material [NASA-TM-79094]
p0063 N79-20187
- Development and fabrication of high strength alloy fibers for use in metal-metal matrix composites [NASA-TM-79115]
p0063 N79-22211
- Thermal-conductivity measurements of tungsten-fiber-reinforced superalloy composites using a thermal-conductivity comparator [NASA-TP-1445]
p0063 N79-28234
- A review of issues and strategies in nondestructive evaluation of fiber reinforced structural composites [NASA-TM-79246]
p0125 N79-29530
- Fatigue behavior of SiC reinforced titanium composites [NASA-TM-79223]
p0064 N79-30296
- RELIABILITY**
- NT CIRCUIT RELIABILITY**
- NT COMPONENT RELIABILITY**
- Safety considerations in the design and operation of large wind turbines [NASA-TM-79193]
p0141 N79-28725
- RELIABILITY ANALYSIS**
- Proof test criteria for thin walled pressure vessels
p0123 A79-26985
- Causes of high pressure compressor deterioration in service [AIAA PAPER 79-1234]
p0036 A79-40483
- Evaluation of ceramics for stator applications: Gas turbine engine report [NASA-CR-159533]
p0033 N79-21075
- RELIABILITY CONTROL**
- U QUALITY CONTROL**
- REMOTE CONTROL**
- The solid state remote power controller - Its status, use and perspective --- for aircraft and spacecraft
p0099 A79-10896
- REMOTE REGIONS**
- NASA Lewis Research Center photovoltaic application experiments [AIAA PAPER 78-1768]
p0146 A79-13867
- REMOTE SENSORS**
- Application of multispectral scanner data to the study of an abandoned surface coal mine [NASA-TM-76912]
p0131 N79-13472
- A comparison of measured and calculated upwelling radiance over water as a function of sensor altitude [NASA-TM-79147]
p0111 N79-22583
- Analysis and preliminary design of optical sensors for propulsion control --- temperature sensors [NASA-CR-159519]
p0130 N79-27975
- RENE 41**
- Improved adherence of sputtered titanium carbide coatings on nickel- and titanium-base alloys [NASA-TP-1450]
p0059 N79-22194
- RESEARCH**
- NT MARKET RESEARCH**
- NT NONLINEAR PROGRAMMING**
- NT OPERATIONS RESEARCH**
- RESEARCH AND DEVELOPMENT**
- Engineering in the 21st century --- aerospace technology prospects [AAS PAPER 78-192]
p0190 A79-21277
- NASA research on general aviation power plants [AIAA PAPER 79-0561]
p0026 A79-25870
- Determining potential 30/20 GHz domestic satellite system concepts and establishment of a suitable experimental configuration
p0095 A79-27397
- A review of Curtiss-Wright rotary engine developments with respect to general aviation potential [SAE PAPER 790621]
p0036 A79-36749
- A summary of NASA/Air Force Full Scale Engine Research programs using the F100 engine [AIAA PAPER 79-1308]
p0030 A79-40488
- An overview of NASA research on positive displacement type general aviation engines [AIAA PAPER 79-1824]
p0038 A79-53150
- RESEARCH FACILITIES**
- Lewis Research Center program
p0137 N79-21576

- Preliminary results in the NASA Lewis H2-O2 combustion MHD experiment
[NASA-TM-79135] p0181 N79-22897
- RESIDENTIAL AREAS**
Fuel cell on-site integrated energy system
parametric analysis of a residential complex p0146 A79-14947
Analysis of a fuel cell on-site integrated energy system for a residential complex
[NASA-TM-79161] p0137 N79-22624
- RESIDUAL STRESS**
Some properties of an advanced boron fiber p0086 A79-21297
- RESINS**
NT EPOXY RESINS
NT KEVLAR (TRADEMARK)
NT PHENOLIC RESINS
NT POLYETHER RESINS
NT POLYIMIDE RESINS
Method of cross-linking polyvinyl alcohol and other water soluble resins
[NASA-CASE-LEW-13103-1] p0068 N79-14172
- RESISTIVITY**
U ELECTRICAL RESISTIVITY
- RESONANCE**
NT ELECTRON PARAMAGNETIC RESONANCE
NT RESONANT VIBRATION
NT SPIN RESONANCE
- RESONANT CAVITIES**
U CAVITY RESONATORS
- RESONANT FREQUENCIES**
Design, fabrication, and initial test of a fixture for reducing the natural frequency of the Mod-0 wind turbine tower
[NASA-TM-79200] p0142 N79-28727
- RESONANT VIBRATION**
Experimental evaluation of the effect of inlet distortion on compressor blade vibrations
[NASA-TM-79066] p0126 N79-16300
- RESONATORS**
NT CAVITY RESONATORS
- RESOURCES**
NT COAL
NT CRUDE OIL
NT FOSSIL FUELS
NT ICEBERGS
- RESPONSES**
NT DYNAMIC RESPONSE
NT MODAL RESPONSE
- REUSABLE SPACECRAFT**
NT SPACE SHUTTLES
- REVERSING**
Reverse annealing in radiation-damaged, silicon solar cells p0144 N79-32660
- REYNOLDS NUMBER**
Decay of homogeneous turbulence from a given state at higher Reynolds number p0105 A79-14952
Reynolds number, scale and frequency content effects on F-15 inlet instantaneous distortion
[AIAA PAPER 79-0104] p0005 A79-19533
Decay of homogeneous turbulence from a given state at higher Reynolds number
[NASA-TM-79011] p0102 N79-12361
- RHENIUM ALLOYS**
Interdiffusion behavior of tungsten or rhenium and group 5 and 6 elements and alloys of the periodic table. Part 3b: Appendices
[NASA-CR-134526] p0080 N79-33305
- RHEOLOGY**
Traction drive performance prediction for the Johnson and Tevaarwerk traction model
[NASA-TP-1530] p0116 N79-33475
- RICHARDSON-POSSHAM EQUATION**
- TEMPERATURE EFFECTS
U THERMIONIC EMISSIONS
- RIPG STRUCTURES**
User's guide to computer programs JET 5A and CIVM-JET 5B to calculate the large elastic-plastic dynamically-induced deformations of multilayer partial and/or complete structural rings
[NASA-CR-139484] p0129 N79-18343
- ROCKET CHAMBERS**
U THROST CHAMBERS
- ROCKET ENGINE CASES**
Development of sputtering process to deposit stoichiometric zirconia coatings for the inside wall of regeneratively cooled rocket thrust chambers
[NASA-CR-159412] p0056 N79-11115
- ROCKET ENGINE DESIGN**
Optimize out-of-core thermionic energy conversion for nuclear electric propulsion p0146 A79-13099
Plug cluster engine concept for in-space missions
[AIAA PAPER 79-1179] p0055 A79-38972
- ROCKET ENGINES**
NT ELECTROSTATIC ENGINES
NT HYDROGEN OXYGEN ENGINES
NT ION ENGINES
NT LIQUID PROPELLANT ROCKET ENGINES
NT MERCURY ION ENGINES
Convective heat flux in a laser-heated thruster p0057 A79-22396
Some effects of cyclic induced deformation in rocket thrust chambers
[AIAA 79-0911] p0054 A79-34736
Advanced electrostatic ion thruster for space propulsion
[NASA-CR-159406] p0056 N79-14153
Increased capabilities of the 30-cm diameter Hg ion thruster
[NASA-TM-79142] p0053 N79-22192
- ROCKET LAUNCHING**
NT LUNAR LAUNCH
- ROCKET LININGS**
A heat exchanger and method of making --- rocket lining
[NASA-CASE-LEW-12441-2] p0104 N79-21313
Effect of low-stiffness closeout overwrap on rocket thrust-chamber life
[NASA-TP-1456] p0053 N79-23132
- ROCKET MOTOR CASES**
U ROCKET ENGINE CASES
- ROCKET PROPELLANT TANKS**
U PROPELLANT TANKS
- ROCKET PROPELLANTS**
NT CRYOGENIC ROCKET PROPELLANTS
NT GASEOUS ROCKET PROPELLANTS
NT LIQUID ROCKET PROPELLANTS
- ROCKET VEHICLES**
NT ATLAS LAUNCH VEHICLES
NT CENTAUR LAUNCH VEHICLE
- ROCKS**
NT COAL
- RODS**
Analysis of radiation patterns of interaction tones generated by inlet rods in the JT15D engine
[NASA-TM-79074] p0016 N79-15960
- ROLL FORMING**
Computer-aided analysis and design of the shape rolling process for producing turbine engine airfoils
[NASA-CR-135367] p0080 N79-26175
- ROLLER BEARINGS**
The practical impact of elastohydrodynamic lubrication p0117 A79-11545
High speed cylindrical roller bearing analysis, SKF computer program CYBEAN. Volume 1: Analysis
[NASA-CR-159460] p0121 N79-17222
High speed cylindrical roller bearing analysis, SKF computer program CYBEAN. Volume 2: User's manual
[NASA-CR-159461] p0121 N79-17223
Operating characteristics of a large-bore roller bearing to speeds of 3 times 10 to the 6th power DN
[NASA-TP-1413] p0114 N79-18323
- ROLLING**
Computer-aided analysis and design of the shape rolling process for producing turbine engine airfoils
[NASA-CR-159455] p0012 N79-12087
- ROLLING CONTACT LOADS**
Elastohydrodynamic film thickness measurements of artificially produced surface dents and grooves --- on fatigue failure of bearings
[ASLE PREPRINT 78-1C-1A-1] p0118 A79-23267
Operating characteristics of a large-bore roller bearing to speeds of 3 times 10 to the 6th power DN
[NASA-TP-1413] p0114 N79-18323
- ROLLUP SOLAR ARRAYS**
U SOLAR ARRAYS

ROOFS

Feasibility of determining flat roof heat losses using aerial thermography
[NASA-TM-79152] p0131 N79-22590

ROOM TEMPERATURE

High-energy electron-induced damage production at room temperature in aluminum-doped silicon
p0154 N79-32662

ROTARY DRIVES

U MECHANICAL DRIVES

ROTARY WING AIRCRAFT

NASA gear research and its probable effect on rotorcraft transmission design
[NASA-TM-79293] p0116 N79-33477

ROTARY WINGS

NT TIP DRIVEN ROTORS

Nonlinear equations of equilibrium for elastic helicopter or wind turbine blades undergoing moderate deformation
[NASA-CR-159478] p0130 N79-19414

ROTATING BODIES

NT COMPRESSOR ROTORS

NT ROTARY WINGS

NT ROTATING DISKS

NT ROTORS

NT TIP DRIVEN ROTORS

NT TURBINE WHEELS

ROTATING DISKS

The strain rate partitioning behavior of an advanced gas turbine disk alloy, AF2-1DA
[NASA-TM-79179] p0075 N79-23196

ROTATING GENERATORS

NT AC GENERATORS

NT TURBOGENERATORS

ROTATING SHAFTS

NT SHAFTS (MACHINE ELEMENTS)

NT TURBOSHAFTS

Proposed design procedure for transmission shafting under fatigue loading
p0117 A79-14950

Design and test of a squeeze-film damper for a flexible power transmission shaft
p0123 A79-16011

Nonsynchronous vibrations observed in a supercritical power transmission shaft
[ASME PAPER 79-GT-146] p0123 A79-32412

An introduction to a unified approach to flexible rotor balancing
[ASME PAPER 79-GT-161] p0124 A79-32423

Self-acting shaft seals --- gas turbine engines
p0013 N79-11070

Commercial synchronous alternating-current generators
p0140 N79-26482

ROTATIONAL FLOW

U FLUID FLOW

U VORTICES

ROTOR AERODYNAMICS

An off-design correlation of part span damper losses through transonic axial fan rotors
[ASME PAPER 79-GT-6] p0028 A79-32329

Effect of casing treatment on performance of a two-stage high-pressure-ratio fan
[NASA-TF-1409] p0017 N79-16852

T700 power turbine rotor multiplane/multispeed balancing demonstration
[NASA-CR-159586] p0122 N79-25392

Effect of rotor meridional velocity ratio on response to inlet radial and circumferential distortion
[NASA-TF-1278] p0023 N79-28177

Performance of two-stage fan with a first-stage rotor redesigned to account for the presence of a part-span damper
[NASA-TF-1483] p0024 N79-30191

ROTOR BLADES

An in-place recalibration technique to extend the temperature capability of capacitance-sensing, rotor-blade-tip-clearance measurement systems
[SAE PAPER 781003] p0026 A79-25885

Apparatus and method for reducing thermal stress in a turbine rotor
[NASA-CASE-LEW-12232-1] p0013 N79-10057

ROTOR BLADES (TURBOMACHINERY)

Ceramic blade attachments --- for turbine rotors
p0123 A79-12848

Wind-turbine-generator rotor-blade concepts with low-cost potential
p0147 A79-20828

An operating 200 kW horizontal axis wind turbine
p0147 A79-20829

Analysis of high velocity impact on hybrid composite fan blades
[AIAA 79-0783] p0128 A79-29027

Characteristics of aeroelastic instabilities in turbomachinery - NASA full scale engine test results
[AIAA 79-7011] p0027 A79-29386

Effect of rotor tip clearance and configuration on overall performance of a 12.77-centimeter tip diameter axial-flow turbine
[ASME PAPER 79-GT-42] p0027 A79-30521

Experimental evaluation of the effect of inlet distortion on compressor blade vibrations
p0128 A79-30558

Causes of high pressure compressor deterioration in service
[AIAA PAPER 79-1234] p0036 A79-40483

Design, fabrication, and test of a composite material wind turbine rotor blade
[NASA-CR-135389] p0150 N79-10525

Effect of rotor tip clearance and configuration on overall performance of a 12.77-centimeter tip diameter axial-flow turbine
[NASA-TM-79025] p0002 N79-12015

Effect of casing treatment on performance of a two-stage high-pressure-ratio fan
[NASA-TF-1409] p0017 N79-16852

Strain gage system evaluation program
[NASA-CR-159486] p0110 N79-19314

Evaluation of urethane for feasibility of use in wind turbine blade design
[NASA-CR-159530] p0153 N79-20497

Performance of two-stage fan having low-aspect-ratio first-stage rotor blading
[NASA-TF-1493] p0023 N79-27143

Supersonic unstalled flutter
p0023 N79-27181

Performance of two-stage fan with a first-stage rotor redesigned to account for the presence of a part-span damper
[NASA-TF-1483] p0024 N79-30191

Metal spar/superhybrid shell composite fan blades --- for application to turboprop engines
[NASA-CR-159594] p0067 N79-30295

Aerodynamic performance of 1.38-pressure-ratio, variable-pitch fan stage
[NASA-TF-1502] p0024 N79-31213

ROTOR DISKS

U TURBINE WHEELS

ROTOR HUBS

U ROTORS

ROTOR SPEED

T700 power turbine rotor multiplane/multispeed balancing demonstration
[NASA-CR-159586] p0122 N79-25392

ROTORCRAFT

U ROTARY WING AIRCRAFT

ROTORCRAFT

NT COMPRESSOR ROTORS

NT ROTARY WINGS

NT TIP DRIVEN ROTORS

NT TURBINE WHEELS

Laser balancing demonstration on a high-speed flexible rotor
[ASME PAPER 79-GT-56] p0123 A79-32351

Elastomer mounted rotors - An alternative for smoother running turbomachinery
[ASME PAPER 79-GT-149] p0119 A79-32414

Rotor fragment protection program: Statistics on aircraft gas turbine engine rotor failures that occurred in US commercial aviation during 1976
[NASA-CR-159474] p0032 N79-18977

ROTORCRAFT

U ROTARY WING AIRCRAFT

ROTORCRAFT

NT COMPRESSOR ROTORS

NT ROTARY WINGS

NT TIP DRIVEN ROTORS

NT TURBINE WHEELS

Formulated plastic separators for soluble electrode cells --- rubber-ion transport membranes
[NASA-CASE-LEW-12358-1] p0135 N79-17313

ROTORCRAFT

U DRAINAGE

RURAL AREAS

Photovoltaic power systems for rural areas of developing countries
p0147 A79-26131

Photovoltaic power systems for rural areas of developing countries

[NASA-TM-79097]

p0135 N79-15411

S

S BAND

U SUPERHIGH FREQUENCIES

U ULTRAHIGH FREQUENCIES

S-N DIAGRAMS

The strainrange partitioning behavior of an

advanced gas turbine disk alloy, AP2-1EA

[AIAA PAPER 79-1192]

p0078 A79-38977

SAFETY

NT AIRCRAFT SAFETY

Safety considerations in the design and operation

of large wind turbines

[NASA-TM-79193]

p0141 N79-28725

SAFETY MANAGEMENT

Effects of arcing due to spacecraft charging on

spacecraft survival

[NASA-CR-159593]

p0100 N79-25312

SALT SPRAY TESTS

Effect of a chromium-containing fuel additive on

hot corrosion

p0071 A79-26546

SALTS

Chemically frozen multicomponent boundary layer

theory of salt and/or ash deposition rates from

combustion gases

p0078 A79-50912

SAMPLING

NT AIR SAMPLING

NT PARTICULATE SAMPLING

SATELLITE COMMUNICATIONS

U SPACECRAFT COMMUNICATION

SATELLITE CONFIGURATIONS

Determining potential 30/20 GHz domestic satellite

system concepts and establishment of a suitable

experimental configuration

p0095 A79-27397

SATELLITE GROUND SUPPORT

Ground-to-space optical power transfer --- using

laser propulsion for orbit transfer

p0161 A79-17180

SATELLITE GUIDANCE

Nonlinear tangent yaw guidance

[AIAA 79-1730]

p0045 A79-45374

SATELLITE LAUNCHING

U SPACECRAFT LAUNCHING

SATELLITE NETWORKS

Results of thin-route satellite communication

system analyses including estimated service costs

p0095 A79-30395

SATELLITE ORBITS

NT GEOSYNCHRONOUS ORBITS

SATELLITE POWER TRANSMISSION (TO EARTH)

Solar-pumped lasers for space power transmission

[AIAA PAPER 79-1015]

p0112 A79-18202

SATELLITE SOLAR ENERGY CONVERSION

The NASA Lewis Research Center program in space

solar cell research and technology --- efficiency

silicon solar cell development program

p0143 A79-32641

SATELLITE SOLAR POWER STATIONS

Solar-pumped lasers for space power transmission

[AIAA PAPER 79-1015]

p0112 A79-18202

NASCAP modelling of high-voltage power system

interactions with space charged-particle

environments --- particle impact on solar

satellite surfaces

p0051 A79-39806

Results from Symposium on Future Orbital power

system technology requirements

[NASA-TN-79125]

p0053 N79-22191

An economic analysis of a commercial approach to

the design and fabrication of a space power system

[NASA-TM-79153]

p0053 N79-22193

SATELLITE TRACKING

High power phase locked laser oscillators

[NASA-CR-159630]

p0112 N79-32538

SATELLITE TRANSMISSIONS

An airborne meteorological data collection system

using satellite relay /ASDAR/

p0010 A79-14949

Thermal anomalies of the transmitter experiment

package on the communications technology satellite

[NASA-TP-1410]

p0044 N79-21120

Communications technology satellite: United

States experiments and disaster communications

applications

[NASA-TM-79109]

p0044 N79-23999

Life characteristics assessment of the

communications technology satellite transmitter

experiment package

[NASA-TM-79181]

p0044 N79-31264

SATELLITE-BORNE RADAR

VHF downline communication system for SLAR data

[NASA-TM-79164]

p0094 N79-23313

SATELLITES

NT AERONAUTICAL SATELLITES

NT ARTIFICIAL SATELLITES

NT ATS 5

NT ATS 6

NT COMMUNICATION SATELLITES

NT COMMUNICATIONS TECHNOLOGY SATELLITE

NT NOAA SATELLITES

NT ORBITAL SPACE STATIONS

NT SYNCHRONOUS SATELLITES

SCALE (CORROSION)

An investigation of the initiation stage of hot

corrosion in Ni-base alloys

[NASA-CR-159616]

p0080 N79-25196

Some TEM observations of Al₂O₃ scales formed on

NiCrAl alloys

[NASA-TM-79259]

p0076 N79-33006

SCALE MODELS

Experimental investigation of a 0.15-scale model

of an underfuselage normal-shock inlet

[NASA-CR-1049]

p0006 N79-12014

SCALING LAWS

Critical current and scaling laws in evaporated

two-phase Cu₂S_{0.6}S_{0.4}

p0185 A79-26375

Area scaling investigations of charging phenomena

--- discharge pulse characteristics of Teflon

thermal control tape

p0048 N79-24032

SCANNERS

NT MULTISPECTRAL BAND SCANNERS

SCANS (GEOLOGY)

U EROSION

SCHEDULING

NT PREDICTION ANALYSIS TECHNIQUES

SCHOTTKY BARRIER DIODES

U SCHOTTKY DIODES

SCHOTTKY DIODES

Solar cells having integral collector grids

[NASA-CASE-LEW-12819-1]

p0133 N79-11467

Back wall solar cell

[NASA-CASE-LEW-12236-2]

p0134 N79-14528

SCIENTIFIC SATELLITES

NT ATS 5

NT ATS 6

SEA ICE

NT ICEBERGS

SEA TROUT

A comparison of measured and calculated upwelling

radiance over water as a function of sensor

altitude

p0162 A79-51096

SEALANTS

U SEALERS

SEALERS

Gas path sealing in turbine engines

p0013 N79-11057

Experimental and analytical tools for evaluation

of Stirling engine rod seal behavior

[NASA-CR-159543]

p0122 N79-23429

SEALING

NT SELF SEALING

Energy conservation through sealing technology

p0118 A79-20700

SEALS (STOPPERS)

NT O-RING SEALS

The practical impact of elastohydrodynamic

lubrication

p0117 A79-11545

Transmission seal development

[NASA-CR-135372]

p0120 N79-10423

Compressible flow across narrow passages:

Comparison of theory and experiment for face seals

[NASA-TP-1346]

p0113 N79-10424

Gas path sealing in turbine engines

p0013 N79-11057

Determining and improving labyrinth seal

performance in current and advanced high

performance gas turbines

p0031 N79-11068

- Self-acting shaft seals --- gas turbine engines
p0013 N79-11070
- Wear of seal materials used in aircraft propulsion systems
[NASA-TM-79003] p0073 N79-12204
- Development of sprayed ceramic seal systems for turbine gas path sealing
[NASA-TM-79022] p0081 N79-12223
- Hydrodynamic effects in a misaligned radial face seal
[NASA-CR-135228] p0121 N79-17226
- Composite seal for turbomachinery --- backings for turbine engine shrouds
[NASA-CASP-LEW-12131-1] p0114 N79-18318
- Shaft seal assembly for high speed and high pressure applications
[NASA-CASE-LEW-11873-1] p0115 N79-22475
- Comparison of analysis and experiment for self-acting seals for liquid-oxygen turbopumps
[NASA-TP-1443] p0115 N79-22519
- Experimental and analytical tools for evaluation of Stirling engine rod seal behavior
[NASA-CR-159543] p0122 N79-23429
- Some flow characteristics of conventional and tapered high pressure drop simulated seals
[NASA-TM-79192] p0104 N79-27460
- Development of a plasma sprayed ceramic gas path seal for high pressure turbine applications
[NASA-CR-159669] p0122 N79-31602
- Development of spiral-groove self-acting seals for helicopter engines
[NASA-CR-159622] p0122 N79-32551
- Plasma-sprayed zirconia gas path seal technology: A state-of-the-art review
[NASA-TM-79273] p0085 N79-33325
- SECONDARY BATTERIES**
U STORAGE BATTERIES
- SECONDARY EMISSION**
Stable dielectric charge distributions from field enhancement of secondary emission
p0049 N79-24046
- SECONDARY FLOW**
Study of mean- and turbulent-velocity fields in a large-scale turbine-vane passage
[NASA-CR-3067] p0032 N79-16853
- SECULAR PERTURBATION**
U LONG TERM EFFECTS
- SEDIMENTARY ROCKS**
NT COAL
- SELF INDUCED VIBRATION**
NT SUPERSONIC FLUTTER
NT TRANSONIC FLUTTER
- SELF LUBRICATING MATERIALS**
Graphite-fiber-reinforced polyimide liners of various compositions in plain spherical bearings
p0117 N79-16678
- Wide-temperature-spectrum self-lubricating coatings prepared by plasma spraying
p0119 N79-34993
- Wide-temperature-spectrum self-lubricating coatings prepared by plasma spraying
[NASA-TM-79113] p0082 N79-20240
- Program for plasma-sprayed self-lubricating coatings
[NASA-CR-3163] p0087 N79-28315
- Plasma-sprayed coatings for lubrication of a titanium alloy in air at 430 deg C
[NASA-TP-1509] p0083 N79-29327
- SELF LUBRICATION**
Some loads limits and self-lubricating properties of plain spherical bearings with molded graphite fiber-reinforced polyimide liners to 320 C
[ASLE PREPRINT 78-LC-5C-2] p0118 N79-23251
- Method of making bearing materials --- self-lubricating, oxidation resistant composites for high temperature applications
[NASA-CASE-LEW-11930-4] p0062 N79-17916
- SELF REGULATING**
U AUTOMATIC CONTROL
- SELF SEALING**
Self-stabilizing radial face seal
[NASA-CASE-LEW-12991-1] p0113 N79-12445
- SEMICONDUCTING FILMS**
Preliminary evaluation of glass resin materials for solar cell cover use --- on spacecraft
p0055 N79-40984
- SEMICONDUCTOR DEVICES**
NT METAL OXIDE SEMICONDUCTORS
NT PHOTOVOLTAIC CELLS
NT SCHOTTKY DIODES
- NT THYRISTORS
- NT TRANSISTORS
Measuring unsteady pressure on rotating compressor blades
[NASA-TM-79159] p0109 N79-22448
- SEMICONDUCTOR DIODES**
NT SCHOTTKY DIODES
- SEMICONDUCTOR JUNCTIONS**
NT P-N JUNCTIONS
NT SILICON JUNCTIONS
Limiting process in shallow junction solar cells
p0154 N79-32646
- Shallow-homojunction GaAs solar cells
p0144 N79-32666
- SEMICONDUCTORS (MATERIALS)**
NT METAL OXIDE SEMICONDUCTORS
Application of semiconductor diffusants to solar cells by screen printing
[NASA-CASE-LEW-12775-1] p0133 N79-11468
- Method for the preparation of inorganic single crystal and polycrystalline electronic materials
[NASA-CASE-XLE-02545-1] p0184 N79-21910
- SENDERS**
U TRANSMITTERS
- SENSE ORGANS**
NT EYE (ANATOMY)
- SENSIBILITY**
U SENSITIVITY
- SENSITIVITY**
NT IMPACT RESISTANCE
NT RADIATION TOLERANCE
Variation of solar cell sensitivity and solar radiation on tilted surfaces
p0148 N79-41023
- SENSORY PERCEPTION**
NT AUDITORY PERCEPTION
- SEPARATED FLOW**
NT BOUNDARY LAYER SEPARATION
- SEPARATORS**
NT ELECTROSTATIC PRECIPITATORS
NT FLUID FILTERS
Cross-linked polyvinyl alcohol and method of making same --- separator for alkaline batteries
[NASA-CASE-LEW-13101-1] p0068 N79-14173
- Formulated plastic separators for soluble electrode cells --- rubber-ion transport membranes
[NASA-CASE-LEW-12358-1] p0135 N79-17313
- Three methods for in situ cross-linking of polyvinyl alcohol films for application as ion-conducting membranes in potassium hydroxide electrolyte --- battery separators
[NASA-TP-1407] p0059 N79-21128
- Control of volume resistivity in inorganic organic separators
[NASA-TP-1439] p0069 N79-22246
- Improved, low cost inorganic-organic separators for rechargeable silver-zinc batteries
[NASA-TP-1476] p0069 N79-25181
- In situ self cross-linking of polyvinyl alcohol battery separators
[NASA-CASE-LEW-12972-1] p0138 N79-25481
- Ultrafine polybenzimidazole (FBI) fibers --- separators for alkaline batteries and fuel cells
[NASA-CR-159644] p0067 N79-31350
- SEQUENTIAL ANALYSIS**
On the distribution of computation for sequential decoding using the stack algorithm
p0096 N79-33793
- SERIES (MATHEMATICS)**
Acceleration of linear and logarithmic convergence
p0168 N79-40494
- SERT (ROCKET TESTS)**
U SPACE ELECTRIC ROCKET TESTS
- SERT 2 SPACECRAFT**
SERT 2 1979 extended flight thruster system performance
[NASA-TM-79256] p0054 N79-33252
- Neutralization tests on the SERT 2 spacecraft
[NASA-TM-79271] p0054 N79-33255
- SERVICE LIFE**
Proof test criteria for thin walled pressure vessels in service
[AIAA PAPER 79-1234] p0036 N79-40483
- Endurance testing of first generation /Block I/ commercial solar cell modules
p0148 N79-41022

- Maximum likelihood estimation for life distributions with competing failure modes
p0169 A79-49528
- Development of advanced fuel cell system
[NASA-CR-159443] p0151 A79-12553
- Effect of positive pulse charge waveforms on cycle life of nickel-zinc cells
[NASA-TM-79215] p0142 A79-28728
- SERVICE MODULES**
Computer aided control of a mechanical arm
A79-50334
- SERVO MECHANISMS**
Predicting dynamic performance limits for servosystems with saturating nonlinearities
[NASA-TN-1488] p0038 A79-28186
- SHAFTS (MACHINE ELEMENTS)**
NT TURBO SHAFTS
Shaft seal assembly for high speed and high pressure applications
[NASA-CASE-LEW-11873-1] p0115 A79-22475
Design and application of a test rig for supercritical power transmission shafts
[NASA-CR-3155] p0122 A79-31603
- SHALE OIL**
Alternative aircraft fuels
p0090 A79-10824
- SHEAR LAYERS**
Scattering and distortion of the unsteady motion on transversely sheared mean flows
p0106 A79-37140
- SHEAR PROPERTIES**
NT SHEAR STRENGTH
Shear rupture of a directionally solidified eutectic gamma/gamma-prime - alpha /Mo/ alloy --- for aircraft engine turbine blades
p0077 A79-21301
- SHEAR STRENGTH**
Longitudinal shear behavior of several oxide dispersion strengthened alloys
p0076 A79-14955
Use of an ultrasonic-acoustic technique for nondestructive evaluation of fiber composite strength
p0064 A79-15545
Shear rupture of a directionally solidified eutectic gamma/gamma-prime - alpha (Mo) alloy
[NASA-TM-79118] p0073 A79-12205
- SHEAR STRESS**
NT TORSIONAL STRESS
- SHELLS (STRUCTURAL FORMS)**
NT THIN WALLED SHELLS
Metal spar/superhybrid shell composite fan blades --- for application to turbofan engines
[NASA-CR-159594] p0067 A79-30295
- SHIELDING**
NT HEAT SHIELDING
Feasibility of wing shielding of the airplane interior from the shock noise generated by supersonic tip speed propellers
[NASA-TM-79042] p0172 A79-15757
- SRIPS**
Radar image processing of real aperture SLAR data for the detection and identification of iceberg and ship targets
p0131 A79-36537
VHF downlink communication system for SLAR data
[NASA-TM-79164] p0094 A79-23313
- SHOCK DIFFUSERS**
U SHOCK WAVE ATTENUATION
- SHOCK RESISTANCE**
NT IMPACT RESISTANCE
- SHOCK TESTS**
Effect of shocks on film cooling of a full scale turbojet exhaust nozzle having an external expansion surface
[NASA-TM-79157] p0010 A79-23966
Effect of shocks on film cooling of a full scale turbojet exhaust nozzle having an external expansion surface
[NASA-TM-79157] p0018 A79-23966
- SHOCK WAVE ATTENUATION**
High speed smoke flow visualization for the determination of cascade shock losses
[AIAA PAPER 79-0042] p0005 A79-19495
Feasibility of wing shielding of the airplane interior from the shock noise generated by supersonic tip speed propellers
[NASA-TM-79042] p0172 A79-15757
- SHOCK WAVES**
NT SONIC BOOMS
Calculation of the three-dimensional flow field in supersonic inlets at angle of attack using a bicharacteristic method with discrete shock wave fitting
[AIAA PAPER 79-0379] p0025 A79-19698
Low-turbulence high-speed wind tunnel for the determination of cascade shock losses
[ASME PAPER 79-GT-129] p0039 A79-32398
Effect of shocks on film cooling of a full scale turbojet exhaust nozzle having an external expansion surface
[AIAA PAPER 79-1170] p0028 A79-38969
- SHORT HAUL AIRCRAFT**
Application of digital controls on the quiet clean short haul experimental engines
[AIAA PAPER 79-1203] p0029 A79-38984
QCSEE - The key to future short-haul air transport --- Quiet, Clean, Short-Haul Experimental Engine program
p0030 A79-50208
- SHORT TAKEOFF AIRCRAFT**
Assessment at full scale of nozzle/wing geometry effects on OTW aeroacoustic characteristics --- Over The Wing STOL engine configurations
p0175 A79-39802
Wing aerodynamic loading caused by jet-induced lift associated with STOL-OTW configurations
[AIAA PAPER 79-1664] p0006 A79-47346
Assessment at full scale of nozzle/wing geometry effects on OTW aero-acoustic characteristics --- short takeoff aircraft noise
[NASA-TM-79168] p0174 A79-25841
Wing aerodynamic loading caused by jet-induced lift associated with STOL-OTW configurations
[NASA-TM-79218] p0004 A79-28146
- SHORT WAVE RADIATION**
NT MICROWAVE EMISSION
NT MILLIMETER WAVES
- SHROUDED BODIES**
U SHROUDS
SHROUDED TURBINES
Composite seal for turbomachinery --- backings for turbine engine shrouds
[NASA-CASE-LEW-12131-1] p0114 A79-18318
- SHROUDS**
Composite seal for turbomachinery --- backings for turbine engine shrouds
[NASA-CASE-LEW-12131-1] p0114 A79-18318
- SHUMTS**
U BYPASSES
- SIC (COEFFICIENT)**
U STRUCTURAL INFLUENCE COEFFICIENTS
- SIDE-LOOKING RADAR**
NT RADAR IMAGERY
Radar image processing of real aperture SLAR data for the detection and identification of iceberg and ship targets
p0131 A79-36537
VHF downlink communication system for SLAR data
p0045 A79-51097
- SIGNAL ANALYSIS**
Computer signal processing for ultrasonic attenuation and velocity measurements for material property characterizations
p0125 A79-39809
- SIGNAL PROCESSING**
On the distribution of computation for sequential decoding using the stack algorithm
p0096 A79-33793
Computer signal processing for ultrasonic attenuation and velocity measurements for material property characterizations
p0125 A79-39809
Computer signal processing for ultrasonic attenuation and velocity measurements for material property characterizations
[NASA-TM-79180] p0127 A79-24359
- SIGNAL TRANSMISSION**
NT DATA TRANSMISSION
NT MICROWAVE TRANSMISSION
NT SATELLITE TRANSMISSION
- SILICATES**
NT ALUMINUM SILICATES
- SILICON**
Wear of aluminum and hypoeutectic aluminum-silicon alloys in boundary-lubricated pin-on disk sliding
[NASA-TN-1442] p0074 A79-21184

- The NASA Lewis Research Center program in space solar cell research and technology --- efficient silicon solar cell development program
p0143 N79-32641
- Limiting process in shallow junction solar cells
p0154 N79-32646
- Design of high efficiency HLE solar cells for space and terrestrial applications
p0154 N79-32647
- Applications of ion implantation to high performance, radiation tolerant silicon solar cells
p0143 N79-32648
- SILICON CARBIDES**
- High temperature dynamic modulus and damping of aluminum and titanium matrix composites
p0065 A79-26132
- Friction and fracture of single-crystal silicon carbide in contact with itself and titanium
p0086 A79-32149
- High velocity burner rig oxidation and thermal fatigue behavior of Si₃N₄- and SiC base ceramics to 1370 deg C
[NASA-TM-79040] p0082 N79-16984
- Friction and wear with a single-crystal abrasive grit of silicon carbide in contact with iron base binary alloys in oil: Effects of alloying element and its content
[NASA-TF-1394] p0114 N79-17227
- The friction and wear of metals and binary alloys in contact with an abrasive grit of single-crystal silicon carbide
[NASA-TM-79131] p0075 N79-22274
- Fatigue behavior of SiC reinforced titanium composites
[NASA-TM-79223] p0064 N79-30296
- Anisotropic friction, deformation, and fracture of single-crystal silicon carbide at room temperature
[NASA-TF-1525] p0084 N79-30380
- Evaluation of silicon carbide fiber/titanium composites
[NASA-TM-79232] p0064 N79-31349
- SILICON COMPOUNDS**
- NT ALUMINUM SILICATES
- NT SILICON CARBIDES
- NT SILICON NITRIDES
- Effect of oxygen-nitrogen ratio on sinterability of Sialons
[NASA-TF-1382] p0082 N79-21204
- Modules of rupture and oxidation resistance of Si₂55Al_{0.600}72N_{3.52} sialon
[NASA-TF-1490] p0083 N79-27309
- SILICON JUNCTIONS**
- Photon-degradation effects in terrestrial silicon solar cells
p0149 A79-42545
- SILICON NITRIDES**
- Ceramic blade attachments --- for turbine rotors
p0123 A79-12848
- Ceramics for the advanced automotive gas turbine engine - A look at a single shaft design
p0117 A79-12850
- Consolidation of Si₃N₄ by hot isostatic pressing
p0086 A79-32931
- High velocity burner rig oxidation and thermal fatigue behavior of Si₃N₄- and SiC base ceramics to 1370 deg C
[NASA-TM-79040] p0082 N79-16984
- State-of-the-art of SiAlON materials --- conferences
[NASA-TM-79207] p0084 N79-30378
- Bond strengths of reaction bonded silicon nitride prepared from dry attrition milled silicon powder
[NASA-TM-79230] p0084 N79-30379
- Development of SiAlON materials
[NASA-CR-159675] p0067 N79-33258
- SILICON POLYMERS**
- Mechanical and chemical effects of γ -texturing biomedical polymers
[NASA-TM-79245] p0084 N79-31391
- SILICON SOLAR CELLS**
- U SOLAR CELLS
- SILICONIZING**
- An experimental, low-cost, silicon slurry/aluminide high-temperature coating for superalloys
[NASA-TM-79178] p0075 N79-29292
- SILVER**
- Fabrication and testing of silver-hydrogen cells
[NASA-CR-159431] p0152 N79-16374
- Fabrication and testing of silver-hydrogen cells
[NASA-CR-159490] p0152 N79-16375
- SILVER OXIDE ZINC BATTERIES**
- U SILVER ZINC BATTERIES
- SILVER ZINC BATTERIES**
- Development of single-cell protectors for sealed silver-zinc cells
[NASA-CR-159407] p0151 N79-12550
- Improved, low cost inorganic-organic separators for rechargeable silver-zinc batteries
[NASA-TF-1476] p0069 N79-25181
- SIMILARITY THEOREM**
- Application of the principle of similarity fluid mechanics
[NASA-TM-79258] p0105 N79-30515
- Thermophysical property data: Who needs them?
[NASA-TM-79241] p0090 N79-31403
- SIMULATION**
- NT COMPUTERIZED SIMULATION
- NT CONTROL SIMULATION
- NT DIGITAL SIMULATION
- NT FLIGHT SIMULATION
- NT SPACE ENVIRONMENT SIMULATION
- SIMULATORS**
- NT CONTROL SIMULATION
- NT ENVIRONMENT SIMULATORS
- SINGLE CRYSTALS**
- Friction and fracture of single-crystal silicon carbide in contact with itself and titanium
p0086 A79-32149
- Friction and wear of single-crystal manganese-zinc ferrite
p0185 A79-34994
- Anisotropic friction and wear of single-crystal manganese-zinc ferrite in contact with itself
[NASA-TF-1339] p0113 N79-10425
- Friction and wear of single-crystal manganese-zinc ferrite
[NASA-TM-78980] p0184 N79-16699
- Method for the preparation of inorganic single crystal and polycrystalline electronic materials
[NASA-CASE-XLE-02545-1] p0184 N79-21910
- SINTERING**
- Effect of oxygen-nitrogen ratio on sinterability of Sialons
[NASA-TF-1382] p0082 N79-21204
- Development of SialON materials
[NASA-CR-159675] p0067 N79-33258
- SKY RADIATION**
- Evaluation of models to predict insolation on tilted surfaces
p0150 A79-53491
- SLAGS**
- Performance characteristics of a slagging gasifier for MHD combustor systems
[NASA-TM-79195] p0142 N79-30720
- SLIDING FRICTION**
- A comparison of the lubricating mechanisms of graphite fluoride and molybdenum disulfide films
p0085 A79-16659
- Development of surface coatings for air-lubricated, compliant journal bearings to 650 C
[ASLE PREPRINT 78-LC-3C-1] p0123 A79-23252
- Elastohydrodynamic film thickness measurements of artificially produced surface dents and grooves --- on fatigue failure of bearings
[ASLE PREPRINT 78-LC-1A-1] p0118 A79-23267
- Friction and fracture of single-crystal silicon carbide in contact with itself and titanium
p0086 A79-32149
- Friction and wear of single-crystal manganese-zinc ferrite
p0185 A79-34994
- The effect of nitrogen ion (N⁺) implantation on the friction and wear characteristics of iron
[NASA-TM-79029] p0073 N79-12201
- Friction and transfer of copper, silver, and gold to iron in the presence of various adsorbed surface films
[NASA-TF-1392] p0114 N79-14386
- Friction and wear characteristics of iron-chromium alloys in contact with themselves and silicon carbide
[NASA-TF-1387] p0114 N79-14387
- Friction and wear with a single-crystal abrasive grit of silicon carbide in contact with iron base binary alloys in oil: Effects of alloying element and its content

SUBJECT INDEX

SOLAR CELLS

[NASA-TP-1394] p0114 N79-17227
The friction and wear of metals and binary alloys
in contact with an abrasive grit of
single-crystal silicon carbide
[NASA-TN-79131] p0075 N79-22274
Effect of sterilization irradiation on friction
and wear of ultrahigh-molecular-weight
polyethylene
[NASA-TF-1462] p0082 N79-23216
Anisotropic friction, deformation, and fracture of
single-crystal silicon carbide at room temperature
[NASA-TP-1525] p0084 N79-30380
Lubricating and wear mechanisms for a hemisphere
sliding on polyimide-bonded graphite fluoride film
[NASA-TP-1524] p0084 N79-30381
Surface chemistry of iron sliding in air and
nitrogen lubricated with hexadecane and
hexadecane containing dibenzyl-dithiolide
[NASA-TF-1545] p0059 N79-31346
Evaluation and auger analysis of a
zinc-dialkyl-dithiophosphate antiwear additive
in several diester lubricants
[NASA-TP-1544] p0084 N79-32359

SLIP BANDS
U EDGE DISLOCATIONS

SLOT ANTENNAS
UHF coplanar-slot antenna for
aircraft-to-satellite data communications
[NASA-TN-79239] p0010 N79-31185

SLOTTED ANTENNAS
U SLOT ANTENNAS

SM-65 MISSILE
U ATLAS LAUNCH VEHICLES

SODIUM CHLORIDES
The role of NaCl in flame chemistry, in the
deposition process, and in its reactions with
protective oxides as related to hot corrosion
p0071 N79-49534
The role of NaCl in flame chemistry, in the
deposition process, and in its reactions with
protective oxides as related to hot corrosion
[NASA-TN-79225] p0069 N79-28258
The chemistry of sodium chloride involvement in
processes related to hot corrosion --- in gas
turbine engines
[NASA-TN-79251] p0069 N79-31361

SODIUM COMPOUNDS
NT SODIUM CHLORIDES
NT SODIUM HYDROXIDES
NT SODIUM NITRATES
NT SODIUM SULFATES
Mass spectrometric investigation of the
vaporization of sodium and potassium chromates -
Preliminary results
p0071 N79-49533
Mass spectrometric investigation of the
vaporization of sodium and potassium chromates:
Preliminary results
[NASA-TN-79210] p0069 N79-27279

SODIUM HYDROXIDES
NaOH-based high temperature heat-of-fusion thermal
energy storage device
p0155 N79-10106
Phase change thermal storage for a solar total
energy system
p0155 N79-17321
Development of a phase-change thermal storage
system using modified anhydrous sodium hydroxide
for solar electric power generation
[NASA-CR-159465] p0153 N79-19454

SODIUM NITRATES
Phase change thermal storage for a solar total
energy system
p0155 N79-17321

SODIUM SULFATES
The role of NaCl in flame chemistry, in the
deposition process, and in its reactions with
protective oxides as related to hot corrosion
p0071 N79-49534
Experimental studies of the formation/deposition
of sodium sulfate in/from combustion gases ---
hot corrosion in gas turbine engines
[NASA-CR-159612] p0072 N79-25183
Experimental studies of the formation/deposition
of sodium sulfate in/from combustion gases ---
hot corrosion
[NASA-CR-159613] p0080 N79-25184

SODIUM SULFUR BATTERIES
Feasibility study for a secondary Na/S battery

[NASA-CR-159469] p0152 N79-17330
SOFTWARE (COMPUTERS)
U COMPUTER PROGRAMS

SOLAR ARRAYS
Status of wraparound contact solar cells and arrays
--- for spacecraft electric propulsion
p0054 N79-10014
Large space system - Charged particle environment
interaction technology --- effects on high
voltage solar array performance
[AIAA 79-0913] p0055 N79-34775
An inverter/controller subsystem optimized for
photovoltaic applications
p0148 N79-41047
Evaluation of models to predict insolation on
tilted surfaces
p0150 N79-53491
Closed Loop solar array-ion thruster system with
power control circuitry
[NASA-CASE-LEW-12780-1] p0052 N79-20179
Effect of parasitic plasma currents on solar-array
power output
p0047 N79-24025
Test results for electron beam charging of
flexible insulators and composites --- solar
array substrates, honeycomb panels, and thin
dielectric films
p0048 N79-24031
A method for correlating performance data of a
terrestrial solar cell array
[NASA-TN-79163] p0140 N79-26503
Silicon solar cells for space use: Present
performance and trends
p0154 N79-32654
Reduced power processor requirements for the 30-cm
diameter Bg ion thruster
[NASA-TN-79257] p0054 N79-33253

SOLAR CELLS
Status of wraparound contact solar cells and arrays
--- for spacecraft electric propulsion
p0054 N79-10014
Ultraviolet irradiation at elevated temperatures
and thermal cycling in vacuum of PEP-A covered
silicon solar cells
p0148 N79-40898
Preliminary evaluation of glass resin materials
for solar cell cover use --- on spacecraft
p0055 N79-40984
Endurance testing of first generation /Block I/
commercial solar cell modules
p0148 N79-41022
Variation of solar cell sensitivity and solar
radiation on tilted surfaces
p0148 N79-41023
Design and fabrication of a photovoltaic power
system for the Papago Indian Village of
Schuchuli /Gunsight/, Arizona
p0148 N79-41089
Description and status of NASA-LeRC/DOE
photovoltaic applications systems experiments
p0148 N79-41091
Photon degradation effects in terrestrial solar
cells
p0149 N79-41098
Photon-degradation effects in terrestrial silicon
solar cells
p0149 N79-42545
UV blocking filters for polymeric films
p0088 N79-51103
A brief survey of the solar cell state-of-the-art
p0052 N79-10130
Application of semiconductor diffusants to solar
cells by screen printing
[NASA-CASE-LEW-12775-1] p0133 N79-11468
Block 2 solar cell module environmental test program
[NASA-CR-159393] p0151 N79-13490
Ionized dopant concentrations at the heavily doped
surface of a silicon solar cell
[NASA-TF-1347] p0184 N79-13886
Back wall solar cell
[NASA-CASE-LEW-12236-2] p0134 N79-14528
Method for fabricating solar cells having
integrated collector grits
[NASA-CASE-LEW-12819-2] p0136 N79-18444
Epitaxial solar-cell fabrication, phase 2
[NASA-CR-135350] p0152 N79-19448
Market definition studies for photovoltaic highway
applications
[NASA-CR-159477] p0152 N79-19451

- An investigation of the adhesive bonding of Teflon solar cell covers
[NASA-CR-159565] p0153 W79-26506
- High voltage surface-charged environment test results from space flight and ground simulation experiments
[NASA-TN-79184] p0043 W79-27235
- Alternate methods of applying diffusants to silicon solar cells --- screen printing of thick-film paste materials and vapor phase transport from solid sources
[NASA-CR-159508] p0153 W79-29603
- Solar Cell High Efficiency and Radiation Damage, 1979
[NASA-CR-2097] p0143 W79-32640
- The NASA Lewis Research Center program in space solar cell research and technology --- efficient silicon solar cell development program
p0143 W79-32641
- Limiting process in shallow junction solar cells
p0154 W79-32646
- Design of high efficiency HLE solar cells for space and terrestrial applications
p0154 W79-32647
- Applications of ion implantation to high performance, radiation tolerant silicon solar cells
p0143 W79-32648
- Open-circuit voltage improvements in low-resistivity solar cells
p0143 W79-32649
- Modeling of thin, back-wall silicon solar cells
p0143 W79-32650
- Thin cells for space
p0154 W79-32652
- High efficiency cell geometry
p0143 W79-32653
- Silicon solar cells for space use: Present performance and trends
p0154 W79-32654
- Radiation damage in high-voltage silicon solar cells
p0144 W79-32658
- Reverse annealing in radiation-damaged, silicon solar cells
p0144 W79-32660
- High-energy electron-induced damage production at room temperature in aluminum-doped silicon
p0154 W79-32662
- Temperature and intensity dependence of the performance of an electron-irradiated (AlGa)As/GaAs solar cell
p0144 W79-32665
- Shallow-homojunction GaAs solar cells
p0144 W79-32666
- Summary of GaAs Solar Cell Performance and Radiation Damage Workshop
p0144 W79-32669
- Annealing of radiation damage in 0.1- and 2-ohm-centimeter Silicon solar cells
[NASA-TF-1559] p0144 W79-33572
- SOLAR COLLECTORS**
- NaOH-based high temperature heat-of-fusion thermal energy storage device
p0155 A79-10106
- A mobile apparatus for solar collector testing
[ASME PAPER 79-DE-5] p0150 A79-47651
- Solar cells having integral collector grids
[NASA-CASE-LEW-12819-1] p0133 W79-11467
- Solar cell collector and method for producing same
[NASA-CASE-LEW-12552-2] p0133 W79-11472
- Design investigation of solar powered lasers for space applications
[NASA-CR-159554] p0111 W79-26384
- SOLAR CONVERTERS**
- U SOLAR GENERATORS**
- SOLAR ELECTRIC PROPULSION**
- Status of wraparound contact solar cells and arrays --- for spacecraft electric propulsion
p0054 A79-10014
- Increased capabilities of the 30-cm diameter Hg ion thruster
[AIAA 79-0910] p0055 A79-34774
- Description of a 2.3 kW power transformer for space applications
p0099 A79-34991
- Closed Loop solar array-ion thruster system with power control circuitry
[NASA-CASE-LEW-12780-1] p0052 W79-20179
- CTS-type variable conductance heat pipes for SEP FH/PPU
[NASA-CR-159550] p0107 W79-22434
- A thermal control approach for a solar electric propulsion thrust subsystem
[NASA-TN-79175] p0043 W79-27236
- SOLAR ENERGY**
- Storage systems for solar thermal power
p0145 A79-10108
- Optimum dry-cooling sub-systems for a solar air conditioner
[NASA-TN-79007] p0133 W79-11477
- Social and economic impact of solar electricity at Schuchuli Village
[NASA-TN-79194] p0139 W79-25501
- An expanded system simulation model for solar energy storage (technical report), volume 1
[NASA-CR-159601] p0166 W79-33881
- SOLAR ENERGY CONVERSION**
- NASA Lewis Research Center photovoltaic application experiments
[AIAA PAPER 78-1768] p0146 A79-13867
- Phase change thermal storage for a solar total energy system
p0155 A79-17321
- Photovoltaic power systems for arid areas of developing countries
p0147 A79-26131
- Benefits of solar/fossil hybrid gas turbine systems
[ASME PAPER 79-GT-38] p0147 A79-30554
- Solar-pumped lasers for space power transmission
[AIAA PAPER 79-1015] p0112 A79-38202
- An inverter/controller subsystem optimized for photovoltaic applications
p0148 A79-41047
- Design and fabrication of a photovoltaic power system for the Papago Indian Village of Schuchuli /Gunsight/, Arizona
p0148 A79-41089
- Description and status of NASA-LeRC/DOE photovoltaic applications systems experiments
p0148 A79-41091
- Benefits of solar/fossil hybrid gas turbine systems
[NASA-TN-79083] p0134 W79-15410
- Photovoltaic tests and applications project
[NASA-TN-79018] p0136 W79-17336
- Laser power conversion system analysis, volume 1
[NASA-CR-159523-VOL-1] p0112 W79-21334
- Laser power conversion system analysis, volume 2
[NASA-CR-159523-VOL-2] p0112 W79-21335
- Description of photovoltaic village power systems in the United States and Africa
[NASA-TN-79149] p0138 W79-24443
- Handbook of data on selected engine components for solar thermal applications
[NASA-TN-79027] p0139 W79-26476
- Solar thermal power-conversion system
p0139 W79-26477
- Power-conversion system component summation
p0140 W79-26483
- Reduced power processor requirements for the 30-cm diameter Hg ion thruster
[NASA-TN-79257] p0054 W79-33253
- An expanded system simulation model for solar energy storage (UNIVAC operation manual revisions), volume 2
[NASA-CR-159602] p0166 W79-33882
- SINWEST: A simulation model for wind and photovoltaic energy storage systems (GLC user's manual), volume 1
[NASA-CR-159607] p0166 W79-33883
- SOLAR GENERATORS**
- NT SOLAR CELLS**
- Development of a phase-change thermal storage system using modified anhydrous sodium hydroxide for solar electric power generation
[NASA-CR-159465] p0153 W79-19454
- Thermal storage technologies for solar industrial process heat applications
[NASA-TN-79130] p0136 W79-20498
- Design investigation of solar powered lasers for space applications
[NASA-CR-159554] p0111 W79-26384
- A method for correlating performance data of a terrestrial solar cell array
[NASA-TN-79163] p0140 W79-26503
- SOLAR POWER GENERATION**
- U SOLAR GENERATORS**

SOLAR POWER SOURCES**U SOLAR GENERATORS****SOLAR PROPULSION****NT SOLAR ELECTRIC PROPULSION**

Design investigation of solar powered lasers for space applications
[NASA-CR-159554] p0111 N79-26384

SOLID ELECTRODES

The alkaline zinc electrode as a mixed potential system
[NASA-TN-79235] p0142 N79-29600

SOLID LUBRICANTS

A comparison of the lubricating mechanisms of graphite fluoride and molybdenum disulfide films
p0085 A79-16659

Sputtering technology in solid film lubrication
p0117 A79-16663

Application of ESCA to the determination of stoichiometry in sputtered coatings and interface regions --- X-ray photoelectron spectroscopy
p0117 A79-16664

Coatings for wear and lubrication
p0060 A79-27232

Mechanisms of graphite fluoride /CF₂/n lubrication
p0046 A79-31249

Effect of thermal aging on the tribological properties of polyimide films and polyimide-bonded graphite fluoride films
[NASA-TN-79045] p0082 N79-15186

Method of making bearing materials --- self-lubricating, oxidation resistant composites for high temperature applications
[NASA-CASE-LEW-11930-4] p0062 N79-17916

Wide-temperature-spectrum self-lubricating coatings prepared by plasma spraying
[NASA-TN-79113] p0082 N79-20240

Program for plasma-sprayed self-lubricating coatings
[NASA-CR-3163] p0087 N79-28315

Lubricating and wear mechanisms for a hemisphere sliding on polyimide-bonded graphite fluoride film
[NASA-TN-1524] p0084 N79-30381

SOLID SOLUTIONS

Thermal expansion of some nickel and cobalt spinels and their solid solutions
p0186 A79-50233

SOLID STATE DEVICES**NT METAL OXIDE SEMICONDUCTORS****NT PHOTOVOLTAIC CELLS****NT SEMICONDUCTOR DEVICES****NT THYRISTORS****NT TRANSISTORS**

The solid state remote power controller - Its status, use and perspective --- for aircraft and spacecraft
p0099 A79-10896

Adaptation of ion beam technology to microfabrication of solid state devices and transducers
[NASA-CR-159439] p0186 N79-11921

SOLID SURFACES**NT CRYSTAL SURFACES****SOLID-SOLID INTERFACES**

Adherence of sputtered titanium carbides
p0078 A79-34997

SOLIDIFICATION

Evaluation of an advanced directionally solidified gamma/gamma'-alpha Mo eutectic alloy
[NASA-CR-159416] p0079 N79-20222

Low-cost directionally-solidified turbine blades, volume 1
[NASA-CR-159464] p0080 N79-24121

SOLUTIONS**NT AQUEOUS SOLUTIONS****NT GAS MIXTURES****NT SOLID SOLUTIONS****SONIC BOOMS**

Effects of simulated forward flight on jet noise, shock noise and internal noise
[AIAA PAPER 79-0615] p0178 A79-26936

SONIC FLOW**U TRANSONIC FLOW****SONIC SPEED****U ACOUSTIC VELOCITY****SORTIE CAN****U SPACELAB****SORTIE LAB****U SPACELAB****SOUND****U ACOUSTICS****SOUND ABSORPTION****U SOUND TRANSMISSION****SOUND BARRIER****U ACOUSTIC VELOCITY****SOUND FIELDS**

Effects of inflow distortion profiles on fan tone noise calculated using a 3-D theory
[AIAA PAPER 79-C577] p0175 A79-26911

Scattering and distortion of the unsteady motion on transversely sheared mean flows
p0106 A79-37140

SOUND MEASUREMENT**U ACOUSTIC MEASUREMENTS****SOUND PERCEPTION****U AUDITORY PERCEPTION****SOUND PROPAGATION**

Modal propagation angles in a cylindrical duct with flow and their relation to sound radiation
[AIAA PAPER 79-0183] p0174 A79-19582

Analysis of radiation patterns of interaction tones generated by inlet rods in the JT15D engine
[AIAA PAPER 79-0581] p0027 A79-26944

Computation of atmospheric attenuation of sound for fractional-octave bands
[NASA-TP-1412] p0173 N79-17659

An analytical and experimental study of sound propagation and attenuation in variable-area ducts --- reducing aircraft engine noise
[NASA-CR-135392] p0177 N79-25845

SOUND TRANSMISSION

Acoustic behavior of a fibrous bulk material --- Kevlar 29 sound absorber
[AIAA PAPER 79-0599] p0178 A79-26910

Effect of grazing flow on the acoustic impedance of Helmholtz resonators consisting of single and clustered orifices
[NASA-CR-3177] p0178 N79-32056

SOUND VELOCITY**U ACOUSTIC VELOCITY****SOUND WAVES****NT AERODYNAMIC NOISE****NT AIRCRAFT NOISE****NT ENGINE NOISE****NT JET AIRCRAFT NOISE****NT NOISE (SCOUND)****NT SONIC BOOMS**

A statistical theory of sound radiation from a two-dimensional lined duct
[AIAA PAPER 79-1521] p0176 A79-46707

Modal propagation angles in a cylindrical duct with flow and their relation to sound radiation
[NASA-TN-79030] p0172 N79-15756

Analysis of radiation patterns of interaction tones generated by inlet rods in the JT15D engine
[NASA-TN-79074] p0016 N79-15960

SPACE COMMUNICATION**NT SPACECRAFT COMMUNICATION**

Communications systems technology assessment study, Volume 2: Results
[NASA-CR-135224] p0095 N79-12273

National Aeronautics and Space Administration plans for space communication technology
[NASA-TN-79217] p0053 N79-28220

SPACE ELECTRIC ROCKET TESTS

SERT 2 1979 extended flight thruster system performance
[NASA-TN-79256] p0054 N79-33252

SPACE ENVIRONMENT**U AEROSPACE ENVIRONMENTS****SPACE ENVIRONMENT SIMULATION**

Laboratory studies of electrical properties of insulating materials --- thermal insulation of spacecraft dielectrics
p0044 A79-20877

Large space system - Charged particle environment interaction technology --- effects on high voltage solar array performance
[AIAA 79-0913] p0055 A79-34775

SPACE MISSIONS

Advanced electrostatic ion thruster for space propulsion
[NASA-CR-159406] p0056 N79-14153

Large space system: Charged particle environment interaction technology
[NASA-TN-79156] p0046 N79-22188

Primary electric propulsion for future space missions

SPACE POWER REACTORS

SUBJECT INDEX

- [NASA-TM-79141] p0052 N79-22190
- SPACE POWER REACTORS**
- Mini-Brayton heat source assembly development [NASA-CR-159447] p0131 N79-12554
- The role of fuel cells in NASA's space power systems [NASA-TM-79182] p0053 N79-23133
- SPACE PROBES**
- NT JUPITER PROBES
- SPACE SHUTTLE PAYLOADS**
- NT SPACELAB
- Plug cluster engine concept for in-space missions [AIAA PAPER 79-1179] p0055 A79-38972
- SPACE SHUTTLES**
- Space shuttle active-pogo-suppressor control design using linear quadratic regulator techniques [NASA-TF-1217] p0097 N79-14309
- Space propulsion technology overview [NASA-TM-79104] p0042 N79-20171
- SPACE STATIONS**
- NT ORBITAL SPACE STATIONS
- SPACE TRANSPORTATION**
- NT SPACE TRANSPORTATION SYSTEM
- SPACE TRANSPORTATION SYSTEM**
- NT SPACE SHUTTLES
- Cryogenic propellant densification study [NASA-CR-159438] p0087 N79-12238
- Characteristics of primary electric propulsion systems --- conferences [NASA-TM-79255] p0053 N79-30290
- SPACE TUGS**
- Unconventional nozzle tradeoff study --- space tug propulsion [NASA-CR-159520] p0057 N79-28224
- SPACECRAFT CHARGING**
- Insulator edge voltage gradient effects in spacecraft charging phenomena p0048 A79-30139
- The decrease in effective photocurrents due to saddle points in electrostatic potentials near differentially charged spacecraft p0049 A79-30140
- NASCAP modelling of high-voltage power system interactions with space charged-particle environments --- particle impact on solar satellite surfaces p0051 A79-39806
- Insulator edge voltage gradient effects in spacecraft charging phenomena [NASA-TM-78988] p0046 N79-11109
- Jupiter probe charging study [NASA-TP-1263] p0046 N79-15149
- Space environmental interactions with spacecraft surfaces [NASA-TM-79016] p0046 N79-15150
- Spacecraft Charging Technology, 1978 [NASA-CP-2071] p0047 N79-24001
- Summary of the two year NASA program for active control of ATS-5/6 environmental charging --- with a thermionic electron source and a plasma source p0047 N79-24006
- Operations of the ATS-6 ion engine p0049 N79-24007
- Characteristics of differential charging of ATS-6 p0049 N79-24008
- The capabilities of the NASA charging analyzer program p0047 N79-24011
- Charging analysis of the SCATPA satellite p0049 N79-24012
- Comparison of NASCAP predictions with experimental data p0047 N79-24013
- Interactions between spacecraft and the charged-particle environment p0047 N79-24021
- Plasma Interaction Experiment (PIX) flight results p0047 N79-24022
- Status of materials characterization studies p0048 N79-24030
- Test results for electron beam charging of flexible insulators and composites --- solar array substrates, honeycomb panels, and thin dielectric films p0048 N79-24031
- Area scaling investigations of charging phenomena --- discharge pulse characteristics of Teflon thermal control tape p0048 N79-24032
- Charging rates of metal-dielectric structures --- with implications for spacecraft p0048 N79-24033
- Potential mapping with charged-particle beams p0049 N79-24038
- Stable dielectric charge distributions from field enhancement of secondary mission p0049 N79-24046
- Geosynchronous satellite operating anomalies caused by interaction with the local spacecraft environment p0050 N79-24049
- Spacecraft charging modeling development and validation study p0050 N79-24051
- Effects of arcing due to spacecraft charging on spacecraft survival [NASA-CR-159593] p0100 N79-25312
- Extension, validation and application of the NASCAP code [NASA-CR-159595] p0100 N79-27397
- NASCAP user's manual, 1978 [NASA-CR-159417] p0100 N79-27398
- Computer and laboratory simulation of interactions between spacecraft surfaces and charged-particle environments [NASA-TM-79219] p0063 N79-29224
- NASCAP modelling of environmental-charging-induced discharges in satellites [NASA-TM-79247] p0048 N79-31265
- SPACECRAFT COMMUNICATIONS**
- Global disaster satellite communications system for disaster assessment and relief coordination p0095 A79-30394
- Communications systems technology assessment study. Volume 2: Results [NASA-CR-135224] p0095 N79-12273
- Global disaster satellite communications system for disaster assessment and relief coordination [NASA-TM-79105] p0044 N79-20176
- UHF coplanar-slot antenna for aircraft-to-satellite data communications [NASA-TM-79239] p0010 N79-31185
- The 18 and 30 GHz fixed service communication satellite system study: Executive summary [NASA-CR-159627-1] p0096 N79-33373
- The 18 and 30 GHz fixed service communications satellite system study --- to determine the cost and performance characteristics [NASA-CR-159627-2] p0096 N79-33374
- SPACECRAFT COMPONENTS**
- NT SERVICE MODULES
- NT SPACECRAFT MODULES
- Characteristics of differential charging of ATS-6 p0049 N79-24008
- SPACECRAFT CONFIGURATIONS**
- NT SATELLITE CONFIGURATIONS
- Plug cluster engine concept for in-space missions [AIAA PAPER 79-1179] p0055 A79-38972
- Determining potential 30/20 GHz domestic satellite system concepts and establishment of a suitable experimental configuration [NASA-TM-79092] p0094 N79-17072
- SPACECRAFT CONSTRUCTION MATERIALS**
- Laboratory studies of electrical properties of insulating materials --- thermal insulation of spacecraft dielectrics p0044 A79-20877
- SPACECRAFT DESIGN**
- An economic analysis of a commercial approach to the design and fabrication of a space power system [AIAA 79-0914] p0055 A79-34737
- Jupiter probe charging study [NASA-TP-1263] p0046 N79-15149
- SPACECRAFT ENVIRONMENTS**
- Space environmental interactions with spacecraft surfaces [AIAA PAPER 79-0386] p0049 A79-23511
- Spacecraft Charging Technology, 1978 [NASA-CP-2071] p0047 N79-24001
- Summary of the two year NASA program for active control of ATS-5/6 environmental charging --- with a thermionic electron source and a plasma source p0047 N79-24006
- SPACECRAFT GUIDANCE**
- NT SATELLITE GUIDANCE
- SPACECRAFT LAUNCHING**
- Bilinear tangent yaw guidance

- [AIAA 79-1730] p0045 A79-45374
SPACECRAFT MANEUVERS
 NT ORBITAL MANEUVERS
SPACECRAFT MODULES
 Computer aided control of a mechanical arm A79-50334
- SPACECRAFT ORBITS**
 NT GEOSYNCHRONOUS ORBITS
 NT TRANSFER ORBITS
SPACECRAFT POWER SUPPLIES
 The solid state remote power controller - Its status, use and perspective --- for aircraft and spacecraft p0099 A79-10896
 An economic analysis of a commercial approach to the design and fabrication of a space power system [AIAA 79-0914] p0055 A79-34737
 Large space system - Charged particle environment interaction technology --- effects on high voltage solar array performance [AIAA 79-0913] p0055 A79-34775
 Preliminary evaluation of glass resin materials for solar cell cover use --- on spacecraft p0055 A79-40984
 The role of fuel cells in NASA's space power systems p0056 A79-51810
 Future Orbital Power Systems Technology Requirements [NASA-CP-2058] p0052 A79-10122
 An economical approach to space power systems p0052 A79-10139
 Design and fabrication of the Mini-Brayton Recuperator (MBR) [NASA-CR-159429] p0151 A79-11476
 Results from Symposium on Future Orbital power systems technology requirements [NASA-TM-79125] p0053 A79-22191
 An economic analysis of a commercial approach to the design and fabrication of a space power system [NASA-TM-79153] p0053 A79-22193
 Description of a 2.3 kW power transformer for space applications [NASA-TM-79138] p0097 A79-23348
 NASCAP modelling of high-voltage power system interactions with space charged-particle environments [NASA-TM-79146] p0046 A79-24000
 Strip cell test and evaluation program [NASA-CR-159652] p0154 A79-31784
 Reduced power processor requirements for the 30-cm diameter Bq ion thruster [NASA-TM-79257] p0054 A79-33253
 Advanced technology light weight fuel cell program --- for space power applications [NASA-CR-159653] p0155 A79-33581
- SPACECRAFT PROPULSION**
 NT ION PROPULSION
 NT MASS DRIVERS (PAYLOAD DELIVERY)
 NT SOLAR ELECTRIC PROPULSION
 NT SOLAR PROPULSION
 Optimize out-of-core thermionic energy conversion for nuclear electric propulsion p0146 A79-13099
 Ground-to-space optical power transfer --- using laser propulsion for orbit transfer p0161 A79-17180
 Convective heat flux in a laser-heated thruster p0057 A79-22396
 Space propulsion technology overview [AIAA 79-0860] p0054 A79-34704
 Some effects of cyclic induced deformation in rock thrust chambers [AIAA 79-0911] p0054 A79-34736
 Primary electric propulsion for future space missions [AIAA 79-0881] p0055 A79-34773
 Advanced engine study for mixed-mode orbit-transfer vehicles [NASA-CR-159491] p0057 A79-19074
 Laser rocket system analysis [NASA-CR-159521] p0112 A79-21337
 Primary electric propulsion for future space missions [NASA-TM-79141] p0052 A79-22190
 Inert gas thrusters [NASA-CR-159527] p0057 A79-26110
 A thermal control approach for a solar electric propulsion thrust subsystem [NASA-TM-79175] p0043 A79-27236
- SPACECRAFT STRUCTURES**
 Recent developments at ONERA in the field of structural analysis methods [ONERA, TP NO. 1979-79] A79-45537
 Hydrogen recombination in sealed nickel-cadmium aerospace cells p0057 A79-51907
 Interactions between spacecraft and the charged-particle environment p0047 A79-24021
- SPACECRAFT TRACKING**
 NT SATELLITE TRACKING
SPACELAB
 Definition of solder experiments for Spacelab [NASA-CR-159528] p0040 A79-20161
 Combustion of porous solids at reduced gravitational conditions [NASA-CR-3197] p0072 A79-33288
- SPANNING BLOWING**
 NT BLOWING
SPATIAL FILTERING
 Simulated electronic heterodyne recording and processing of pulsed-laser holograms [NASA-TM-1444] p0111 A79-21329
- SPATIAL ORIENTATION**
 U ATTITUDE (INCLINATION)
SPECIFICATIONS
 NT AIRCRAFT SPECIFICATIONS
 Effect of broadened-specification fuels on aircraft engines and fuel systems [NASA-TM-79086] p0089 A79-16136
- SPECTRA**
 NT ENERGY SPECTRA
 NT LINE SPECTRA
 NT NOISE SPECTRA
 NT PLASMA SPECTRA
SPECTRAL ANALYSIS
 U SPECTRUM ANALYSIS
SPECTRAL LINE WIDTH
 Method for decomposing observed line shapes resulting from multiple causes - Application to plasma charge-exchange-neutral spectra p0182 A79-53867
- SPECTRAL LINES**
 U LINE SPECTRA
SPECTROSCOPIC ANALYSIS
 NT FLAME SPECTROSCOPY
SPECTROSCOPY
 NT AUGER SPECTROSCOPY
 NT FLAME SPECTROSCOPY
 NT INFRARED SPECTROSCOPY
 NT MASS SPECTROSCOPY
 NT PHOTOELECTRON SPECTROSCOPY
 NT X RAY SPECTROSCOPY
SPECTRUM ANALYSIS
 NT FLAME SPECTROSCOPY
 Synthesis of blade flutter vibratory patterns using stationary transducers p0127 A79-10823
 Decay of homogeneous turbulence from a given state at higher Reynolds number p0105 A79-14952
- SPEED CONTROL**
 Response of lead-acid batteries to chopper-controlled discharge --- for electric vehicles p0145 A79-10097
 DOE/NASA Mod-CA wind turbine performance p0145 A79-10235
 Control of wind turbine generators connected to power systems p0146 A79-15574
 Speed reducers-increasers p0140 A79-26481
- SPEED REGULATION**
 U SPEED CONTROL
SPIN
 NT ELECTRON CAPTURE
SPIN RESONANCE
 Optical, spin-resonance, and magnetoresistance studies of tetrathiatetracene/2-iodide/3 - The nature of the ground state p0184 A79-10417
- SPIN TESTS**
 Design, fabrication and spin testing of ceramic blade metal disk attachment [NASA-CR-159532] p0032 A79-17857
- SPIN-ORBIT INTERACTIONS**
 NT ELECTRON CAPTURE

- SPINEL**
Thermal expansion of some nickel and cobalt spinels and their solid solutions p0186 A79-50233
- SPLITTING**
Some properties of an advanced boron fiber --- high strength, splittable fibers [NASA-TN-79065] p0061 A79-16076
- SPONTANEOUS EMISSION**
Gain measurements of the Ca-Te charge exchange system --- for UV lasers p0112 A79-19078
- SPRAYED COATINGS**
Effects of compositional changes on the performance of a thermal barrier coating system --- for aircraft gas turbine engines p0077 A79-21299
Coatings for wear and lubrication p0060 A79-27232
Wide-temperature-spectrum self-lubricating coatings prepared by plasma spraying p0119 A79-34993
Wide-temperature-spectrum self-lubricating coatings prepared by plasma spraying [NASA-TN-79113] p0082 A79-20240
Plasma-sprayed coatings for lubrication of a titanium alloy in air at 430 deg C [NASA-TP-1509] p0083 A79-29327
- SPRAYED PROTECTIVE COATINGS**
U PROTECTIVE COATINGS
U SPRAYED COATINGS
- SPRAYING**
U PLASMA SPRAYING
Closed loop spray cooling apparatus [NASA-CASE-LEW-11981-2] p0103 A79-20336
- SPUTTERING**
Ion beam sputtering of fluoropolymers p0117 A79-14797
Sputtering technology in solid film lubrication p0117 A79-16663
Application of ESCA to the determination of stoichiometry in sputtered coatings and interface regions --- X-ray photoelectron spectroscopy p0117 A79-16664
The friction and wear properties of sputtered hard refractory compounds p0085 A79-16666
An XPS study of the adherence of refractory carbide, silicide, and boride RF-sputtered wear-resistant coatings --- X-ray Photoelectron Spectroscopy of steel surfaces p0085 A79-21022
The use of ion beam cleaning to obtain high quality cold welds with minimal deformation p0119 A79-24121
Use of a nitrogen-argon plasma to improve adherence of sputtered titanium carbide coatings on steel p0119 A79-25103
Industrial potential, uses, and performance of sputtered and ion plated films p0119 A79-30398
Adherence of sputtered titanium carbides p0078 A79-34997
Development of sputtering process to deposit stoichiometric zirconia coatings for the inside wall of regeneratively cooled rocket thrust chambers [NASA-CR-159412] p0J56 A79-11115
Effect of nitrogen-containing plasma on adherence, friction, and wear of radiofrequency-sputtered titanium carbide coatings [NASA-TP-1377] p0081 A79-15184
Industrial ion source technology [NASA-CR-159534] p0179 A79-19828
Adherence of sputtered titanium carbides [NASA-TN-79117] p0074 A79-20220
Whiskers, cones and pyramids created in sputtering by ion bombardment [NASA-CR-159549] p0079 A79-20221
Industrial potential, uses, and performance of sputtered and ion plated films [NASA-TN-79107] p0157 A79-20527
A heat exchanger and method of making --- rocket lining [NASA-CASE-LEW-12441-2] p0104 A79-21313
Improved adherence of sputtered titanium carbide coatings on nickel- and titanium-base alloys
- [NASA-TP-1450] p0059 A79-22194
Ion beam sputter deposition of fluoropolymers [NASA-CASE-LEW-13122-1] p0083 A79-24154
Physical processes in directed ion beam sputtering [NASA-CR-159567] p0182 A79-26943
Sputtering in mercury ion thrusters [NASA-TN-79266] p0054 A79-31343
Mechanical and chemical effects of ion-texturing biomedical polymers [NASA-TN-79245] p0084 A79-31391
Development of sputtered techniques for thrust chambers [NASA-CR-159637] p0080 A79-32326
- STABILITY**
U COMBUSTION STABILITY
U FLOW STABILITY
U STORAGE STABILITY
U STRUCTURAL STABILITY
U THERMAL STABILITY
- STABILIZATION**
Control and stabilization of the DOE/NASA Mod-1 two megawatt wind turbine generator p0156 A79-51780
- STACKING FAULTS**
U CRYSTAL DEFECTS
- STAINLESS STEELS**
CTS-type variable conductance heat pipes for SFP PH/PPU [NASA-CR-159550] p0107 A79-22434
- STANDS**
U SUPPORTS
- STANNIDES**
U NIOBIUM STANNIDES
- STATIC LOADS**
Acoustic emission testing of composite vessels under sustained loading p0128 A79-11543
Evaluation of flawed composite structural components under static and cyclic loading --- fatigue life of graphite-epoxy composite materials [NASA-CR-135403] p0066 A79-26120
- STATIC PRESSURE**
U HYDROSTATIC PRESSURE
Effect of steady-state pressure distortion on flow characteristics entering a turbofan engine [NASA-TN-79134] p0019 A79-23969
- STATIC STABILITY**
U STRUCTURAL STABILITY
- STATIC TESTS**
Reduction of rotor-turbulence interaction noise in static fan noise testing [AJAA PAPER 79-0656] p0036 A79-26925
Experimental study of coaxial nozzle exhaust noise [AIAA PAPER 79-0631] p0175 A79-28963
Static evaluation of surface coatings for compliant gas bearings in an oxidizing atmosphere to 650 C p0088 A79-31957
Status of materials characterization studies p0048 A79-24030
- STATICS**
U ELECTROSTATICS
- STATIONS**
U ORBITAL SPACE STATIONS
- STATISTICAL ANALYSIS**
U PROBABILITY DISTRIBUTION FUNCTIONS
U SEQUENTIAL ANALYSIS
A statistical theory of sound radiation from a two-dimensional lined duct [AIAA PAPER 79-1521] p0176 A79-46707
Numbers of center points appropriate to blocked response surface experiments p0169 A79-49529
Statistical study of supersonic compressors p0039 A79-21064
Two-dimensional random surface model for asperity-contact in elastohydrodynamic lubrication [NASA-TN-79006] p0115 A79-23430
Numbers of center points appropriate to blocked response surface experiments [NASA-TN-79201] p0168 A79-28970
- STATISTICAL DISTRIBUTIONS**
U PROBABILITY DISTRIBUTION FUNCTIONS
Maximum likelihood estimation for life distributions with competing failure modes p0169 A79-49528
- STATISTICAL PROBABILITY**
U PROBABILITY THEORY

STATOR BLADES

Cold-air performance of free power turbine designed for 112-kilowatt automotive gas-turbine engine. 3: Effect of stator vane end clearances on performance
[NASA-TM-78956] p0014 W79-13049
Effect of casing treatment on performance of a two-stage high-pressure-ratio fan
[NASA-TP-1409] p0017 W79-16852

STATORS

Cold-air performance of free power turbine designed for 112-kilowatt automotive gas-turbine engine. 2: Effects of variable stator-vane-chord setting angle on turbine performance
[NASA-TM-78993] p0017 W79-17859
Evaluation of ceramics for stator application: Gas turbine engine report
[NASA-CR-159533] p0033 W79-21075

STEADY FLOW

NT HARTMANN FLOW

Modal propagation angles in a cylindrical duct with flow and their relation to sound radiation
[NASA-TM-79030] p0172 W79-15756

STEAM FLOW

Effect of steam addition on cycle performance of simple and recuperated gas turbines
[NASA-TP-1440] p0137 W79-22626

STEAM TURBINES

User's manual for PRESTO: A computer code for the performance of regenerative steam turbine cycles
[NASA-CR-159540] p0122 W79-25395

STEEL STRUCTURES

Wind turbine generator application places unique demands on tower design and materials
p0155 A79-20826

STEELS

NT HIGH STRENGTH STEELS

NT NICKEL STEELS

NT STAINLESS STEELS

Use of a nitrogen-argon plasma to improve adherence of sputtered titanium carbide coatings on steel
p0119 A79-25103

Evaluation of CBS 600 carburized steel as a gear material
[NASA-TP-1390] p0114 W79-14389

Strain-range partitioning life predictions of the long time metal properties council creep-fatigue tests
[NASA-TM-79260] p0127 W79-31619

STEEL GRADIENT AIRCRAFT

U V/STOL AIRCRAFT

STERILIZATION

Effect of sterilization irradiation on friction and wear of ultrahigh-molecular-weight polyethylene
[NASA-TP-1462] p0082 W79-23216

STERILIZATION EFFECTS

NT CHEMICAL EFFECTS

NT THERMAL DEGRADATION

STIFFNESS

Stiffness of straight and tapered annular gas path seals
[ASME PAPER 78-LUB-18] p0118 A79-23235

Development of procedures for calculating stiffness and damping of elastomers in engineering applications. Part 5: Elastomer performance limits and the design and test of an elastomer damper
[NASA-CR-159552] p0122 W79-24373

STIMULATED EMISSION DEVICES

NT CONTINUOUS WAVE LASERS

NT DYE LASERS

NT GAS LASERS

NT LASERS

NT PULSED LASERS

NT ULTRAVIOLET LASERS

STIMULATION

NT AUDIOTORY STIMULI

STIRLING CYCLE

Ceramic applications in the advanced Stirling automotive engine
p0117 W79-12851
Initial comparison of single cylinder Stirling engine computer model predictions with test results
[SAE PAPER 790327] p0119 A79-21368

Energy-state formulation of lumped volume dynamic equations with application to a simplified free piston Stirling engine
p0187 A79-49532

Baseline performance of the GPU 3 Stirling engine
[NASA-TM-79038] p0135 W79-16356

Initial comparison of single cylinder Stirling engine computer model predictions with test results
[NASA-TM-79044] p0188 W79-16721

Stirling engine characteristics
p0140 W79-26480

Candidate power-conversion system cycles, appendix A
p0140 W79-26484

Low-power baseline test results for the GPU 3 Stirling engine
[NASA-TM-79103] p0188 W79-27023

Energy-state formulation of lumped volume dynamic equations with application to a simplified free piston Stirling engine
[NASA-TM-79197] p0141 W79-27663

Stirling engines for automobiles
[NASA-TM-79222] p0142 W79-28726

Conceptual design study of an automotive Stirling reference engine system
[NASA-CR-159605] p0188 W79-29110

STOICHIOMETRY

Application of ESCA to the determination of stoichiometry in sputtered coatings and interface regions --- X-ray photoelectron spectroscopy
p0117 A79-16664

STOL AIRCRAFT

U SHORT TAKEOFF AIRCRAFT

STORABLE PROPELLANTS

NT AIRCRAFT FUELS

STORAGE BATTERIES

NT LEAD ACID BATTERIES

NT NICKEL CADMIUM BATTERIES

NT NICKEL ZINC BATTERIES

NT SILVER ZINC BATTERIES

Determination of the zincate diffusion coefficient and its application to alkaline battery problems
p0070 A79-11547

Factors affecting the open-circuit voltage and electrode kinetics of some iron/titanium/redox flow cells
p0146 A79-11824

Fabrication and testing of silver-hydrogen cells
[NASA-CR-159431] p0152 W79-16374

Fabrication and testing of silver-hydrogen cells
[NASA-CR-159490] p0152 W79-16375

Formulated plastic separators for soluble electrode cells --- rubber-ion transport membranes
[NASA-CR-159469] p0152 W79-17330

Feasibility study for a secondary Na/S battery
[NASA-CR-159469] p0152 W79-17330

Redox flow cell energy storage systems
[NASA-TM-79143] p0138 W79-24442

Redox flow cell development and demonstration project, calendar year 1977
[NASA-TM-79067] p0138 W79-24445

Dynamic analysis of a photovoltaic power system with battery storage capability
[NASA-TM-79209] p0142 W79-29599

STORAGE STABILITY

Stability of PMR-polyimide monomers
p0086 A79-31041

STORMS

NT MAGNETIC STORMS

STRAIN AGING

U PRECIPITATION HARDENING

STRAIN DISTRIBUTION

U STRESS CONCENTRATION

STRAIN FATIGUE

U FATIGUE (MATERIALS)

STRAIN GAGES

Instrumentation for measuring the dynamic pressure on rotating compressor blades
[NASA-CR-159466] p0110 W79-17418

Strain gage system evaluation program
[NASA-CR-159486] p0110 W79-19314

Measuring unsteady pressure on rotating compressor blades
[NASA-TM-79159] p0109 W79-22448

STRAIN HARDENING

Mechanisms of boron fiber strengthening by thermal treatment
[NASA-TM-79077] p0062 W79-20186

STRAIN RATE

STRAIN RATE

- A strainrange partitioning analysis of low cycle fatigue of coated and uncoated Rene 80
 - p0129 N79-10479
- Strainrange partitioning behavior of the nickel-base superalloys, Rene 80 and IN-100
 - p0126 N79-10480
- Strainrange partitioning life predictions of the long time metal properties council creep-fatigue tests
 - [NASA-TN-79260] p0127 N79-31619

STRAIN SOFTENING

U PLASTIC DEFORMATION

STRATOSPHERE

- A summary of research on the NASA-Global Atmospheric Sampling Program performed by the Atmospheric Sciences Research Center --- ozone transport theory
 - [NASA-CR-159614] p0159 N79-27716

STREAMLINING

- Unsteady vortical and entropic distortions of potential flows round arbitrary obstacles
 - p0005 A79-19452

STRENGTH OF MATERIALS

U MECHANICAL PROPERTIES

STRESS ANALYSIS

- Fatigue impact on Mod-1 wind turbine design
 - p0156 A79-20827
- Stresses from arbitrary loads on a circular crack
 - p0130 A79-27938
- The strainrange partitioning behavior of an advanced gas turbine disk alloy, AF2-1DA
 - [AIAA PAPER 79-1192] p0078 A79-38977
- Stress analysis for structures with surface cracks
 - [NASA-CR-159400] p0129 N79-13405
- User's manual for FRAC3D: Supplement to report on stress analysis for structures with surface cracks
 - [NASA-CR-159401] p0129 N79-13406
- Three-dimensional finite-element elastic analysis of a thermally cycled single-edge wedge geometry specimen
 - [NASA-TN-79026] p0172 N79-16644
- Off-axis impact of unidirectional composites with cracks: Dynamic stress intensification
 - [NASA-CR-159537] p0067 N79-30294
- Normal and radial impact of composites with embedded penny-shaped cracks
 - [NASA-CR-159538] p0130 N79-31627

STRESS CALCULATIONS

U STRESS ANALYSIS

STRESS CONCENTRATION

- The effects of eccentricities on the fracture of off-axis fiber composites
 - p0064 A79-15543
- Mode I analysis of a face cracked plate subjected to rotationally constrained end displacements
 - p0128 A79-21831
- On the equivalence between semiempirical fracture analyses and R-curves
 - p0129 A79-39813
- Measurement of transient strain and surface temperature on simulated turbine blades using noncontacting techniques
 - [NASA-TN-78982] p0126 N79-19415
- On the equivalence between semiempirical fracture analyses and R-curves
 - [NASA-TN-79127] p0103 N79-20338

STRESS CYCLES

- Some effects of cyclic induced deformation in rocket thrust chambers
 - [NASA-TN-79112] p0103 N79-20337
- The strainrange partitioning behavior of an advanced gas turbine disk alloy, AF2-1DA
 - [NASA-TN-79179] p0075 N79-23196

STRESS DISTRIBUTION

U STRESS CONCENTRATION

STRESS MEASUREMENT

- Strain gage system evaluation program
 - [NASA-CR-159486] p0110 N79-19314

STRESS RUPTURE STRENGTH

U CREEP RUPTURE STRENGTH

STRESS WAVES

- Use of an ultrasonic-acoustic technique for nondestructive evaluation of fiber composite strength
 - p0064 A79-15545

STRESS-STRAIN DISTRIBUTION

U STRESS CONCENTRATION

SUBJECT INDEX

STRESSES

N1 RESIDUAL STRESS

N1 THERMAL STRESSES

N1 TORSIONAL STRESS

STRIP MINING

- Application of multispectral scanner data to the study of an abandoned surface coal mine
 - [NASA-TN-78912] p0131 N79-13472

STRUCTURAL ANALYSIS

N1 DYNAMIC STRUCTURAL ANALYSIS

N1 FLUTTER ANALYSIS

- Review of the Agard S6M panel evaluation program of the NASA-Lewis 'SRP' approach to high-temperature LCF life prediction --- Strainrange Partitioning for Low Cycle Fatigue
 - p0128 A79-14154

- CELFR/NASTRAN Code for the analysis of structures subjected to high velocity impact
 - p0128 A79-21298

- Thermal-structural mission analyses of air-cooled gas turbine blades
 - [ASME PAPER 79-GT-19] p0027 A79-30553

- Recent developments at ONERA in the field of structural analysis methods
 - [ONERA, TP NO. 1979-79] A79-49537

- Thermal-structural mission analyses of air-cooled gas turbine blades
 - [NASA-TN-78963] p0126 N79-11433

- Stress analysis for structures with surface cracks
 - [NASA-CR-159400] p0129 N79-13405

- User's manual for FRAC3D: Supplement to report on stress analysis for structures with surface cracks
 - [NASA-CR-159401] p0129 N79-13406

- CODSTHAN: Composite durability structural analysis
 - [NASA-TN-79070] p0126 N79-15326

- Three-dimensional finite-element elastic analysis of a thermally cycled single-edge wedge geometry specimen
 - [NASA-TN-79026] p0172 N79-16644

- Design, fabrication, and initial test of a fixture for reducing the natural frequency of the Mod-0 wind turbine tower
 - [NASA-TN-79200] p0142 N79-28727

STRUCTURAL DESIGN

- Wind turbine generator application places unique demands on tower design and materials
 - p0155 A79-20826

- Fatigue impact on Mod-1 wind turbine design
 - p0156 A79-20827

- An operating 200 kW horizontal axis wind turbine
 - p0147 A79-20829

- Analysis/design of strip reinforced random composites /strip hybrids/
 - p0119 A79-24035

- Mechanics of intraply hybrid composites - Properties, analysis and design
 - p0065 A79-31033

- Materials and structural aspects of advanced gas-turbine helicopter engines
 - [NASA-TN-79100] p0031 N79-20008

- Design problems of small turbomachinery
 - p0046 N79-22097

- Design, fabrication, and initial test of a fixture for reducing the natural frequency of the Mod-C wind turbine tower
 - [NASA-TN-79200] p0142 N79-28727

- Design and application of a test rig for super-critical power transmission shafts
 - [NASA-CR-3155] p0122 N79-31603

STRUCTURAL DESIGN CRITERIA

- Proposed design procedure for transmission shafting under fatigue loading
 - p0117 A79-14950

- Preliminary summary of the ETF conceptual studies
 - [NASA-TN-78999] p0133 N79-11478

- Safety considerations in the design and operation of large wind turbines
 - [NASA-TN-79193] p0141 N79-28725

STRUCTURAL DYNAMICS

U DYNAMIC STRUCTURAL ANALYSIS

STRUCTURAL FAILURE

- Structural analysis of cylindrical thrust chambers, volume 1
 - [NASA-CR-159522] p0057 N79-19073

STRUCTURAL FATIGUE

U FATIGUE (MATERIALS)

STRUCTURAL INFLUENCE COEFFICIENTS

- An introduction to a unified approach to flexible rotor balancing

- [ASME PAPER 79-GT-161] p0124 A79-32423
- STRUCTURAL MATERIALS**
 U CONSTRUCTION MATERIALS
- STRUCTURAL MEMBERS**
 NT CANTILEVER BEAMS
 NT CIRCULAR PLATES
 NT FLAT PLATES
 NT STRUTS
 NT TRUSSES
- STRUCTURAL RIGIDITY**
 U STRUCTURAL STABILITY
- STRUCTURAL STABILITY**
 Effects of graphite fiber stability on the properties of PBR polyimide composites p0066 A79-43309
- STRUCTURAL STRAIN**
 Review of the Agard S68 panel evaluation program of the NASA-Lewis 'SRP' approach to high-temperature LCF life prediction --- Strainrange Partitioning for Low Cycle Fatigue p0128 A79-14954
- STRUCTURAL VIBRATION**
 NT SUPERSONIC FLUTTER
 NT TRANSONIC FLUTTER
 Experimental evaluation of the effect of inlet distortion on compressor blade vibrations p0128 A79-30558
 Nonsynchronous vibrations observed in a supercritical power transmission shaft [ASME PAPER 79-GT-146] p0123 A79-32412
 Space shuttle active-pogo-suppressor control design using linear quadratic regulator techniques [NASA-TN-1217] p0097 A79-14309
- STRUCTURAL WEIGHT**
 Computerized systems analysis and optimization of aircraft engine performance, weight, and life cycle costs [NASA-TN-79221] p0170 A79-29938
- STRUTS**
 Noise from struts and splitters in turbofan exit ducts [AIAA PAPER 79-0637] p0178 A79-26923
- STS**
 U SPACE TRANSPORTATION SYSTEM
- SUBGRAVITY**
 U REDUCED GRAVITY
- SUBROUTINE LIBRARIES (COMPUTERS)**
 An expanded system simulation model for solar energy storage (technical report), volume 1 [NASA-CN-159601] p0166 A79-33881
- SUBSONIC AIRCRAFT**
 Advanced low emissions catalytic combustor program at Pratt and Whitney p0021 A79-25012
- SUBSONIC FLOW**
 Unsteady flow in a supersonic cascade with subsonic leading-edge locus p0005 A79-16047
 An approach to optimum subsonic inlet design [ASME PAPER 79-GT-51] p0006 A79-30527
 Turbulence generated by the interaction of entropy fluctuations with non-uniform mean flows p0106 A79-45468
- SUBSONIC SPEED**
 Self stabilizing sonic inlet [NASA-CASE-LEN-11890-1] p0011 A79-24976
- SUCTION**
 Performance of a vortex-controlled diffuser in an annular swirl-can combustor at inlet Mach numbers up to 0.53 [NASA-TN-1452] p0017 A79-22099
- SULFATES**
 NT SODIUM SULFATES
 Sulfate and nitrate mixing ratios in the vicinity of the tropopause p0158 A79-49494
- SULFIDES**
 NT COPPER SULFIDES
 NT LEAD SULFIDES
 NT MOLYBDENUM DISULFIDES
 NT MOLYBDENUM SULFIDES
 Preliminary evaluation of the role of K2S in HHD hot stream seed recovery [NASA-TN-79114] p0068 A79-20200
- SULFUR**
 Ion chromatographic determination of sulfur in fuels p0070 A79-21222
 Ion chromatographic determination of sulfur in fuels [NASA-TN-78971] p0157 A79-17358
- SULFUR COMPOUNDS**
 NT COPPER SULFIDES
 NT LEAD SULFIDES
 NT MOLYBDENUM DISULFIDES
 NT MOLYBDENUM SULFIDES
 NT SODIUM SULFATES
 NT SULFATES
 NT SULFIDES
- SUPERALLOYS**
 U HEAT RESISTANT ALLOYS
- SUPERCARGERS**
 Effects of air injection on a turbocharged Teledyne Continental Motors TSIO-360-C engine [SAE PAPER 790607] p0028 A79-36760
 Effects of air injection on a turbocharged Teledyne Continental Motors TSIO-360-C engine [NASA-TN-79121] p0158 A79-20528
- SUPERCARGING**
 U SUPERCARGERS
- SUPERCONDUCTING MAGNETS**
 Design study of superconducting magnets for a combustion magnetohydrodynamic /MHD/ generator p0098 A79-15305
 Comparison of projected critical currents in PbMo6S8 and Nb3Ge p0185 A79-28300
 Nb3Ge as a potential candidate material for 15- to 25-T magnets p0186 A79-44548
- SUPERCONDUCTIVITY**
 Normal state properties of the ternary molybdenum sulfides p0185 A79-27229
 Indirect measurements of Fermi surface parameters of some chevron phase materials p0185 A79-50231
- SUPERCONDUCTORS**
 Superconducting properties of evaporated copper molybdenum sulfide films p0184 A79-20219
 Properties and performance of fine-filament bronze-process Nb3Sn conductors p0184 A79-20529
 Critical current density in wire drawn and hydrostatically extruded Nb-Ti superconductors p0185 A79-20539
 Hall effect and magnetoresistivity in the ternary molybdenum sulfides p0185 A79-21157
 Critical current and scaling laws in evaporated two-phase Cu2.5Mo6S8 p0185 A79-26375
 Low temperature normal state resistance of ternary molybdenum sulfides p0185 A79-27230
 Reactively evaporated films of copper molybdenum sulfide p0185 A79-31973
 Electronic properties of PbMo6S8 and CuMo6S8 --- for superconductivity p0187 A79-41731
 Nb3Ge as a potential candidate material for 15- to 25-T magnets p0186 A79-44548
 Some heat transfer and hydrodynamic problems associated with superconducting cables (SFTL) [NASA-TN-79023] p0102 A79-15267
- SUPERHIGH FREQUENCIES**
 20/30 GHz satellite systems technology needs assessment --- for domestic communications p0095 A79-14948
- SUPERNATURAL MATERIALS**
 NT GRAPHITE-EPOXY COMPOSITE MATERIALS
- SUPERMAGNETS**
 U HIGH FIELD MAGNETS
- SUPERSONIC AIRCRAFT**
 NT F-15 AIRCRAFT
 NT F-102 AIRCRAFT
- SUPERSONIC COMPRESSORS**
 Supersonic unstalled flutter p0004 A79-12599
 Statistical study of supersonic compressors p0039 A79-21064
- SUPERSONIC FLOW**
 Unsteady flow in a supersonic cascade with subsonic leading-edge locus p0005 A79-16047
 Unsteady vortical and entropic distortions of potential flows round arbitrary obstacles

High speed smoke flow visualization for the
determination of cascade shock losses
[AIAA PAPER 79-0042] p0005 A79-19495

SUPERSONIC FLOW INLETS
U SUPERSONIC INLETS
SUPERSONIC FLUTTER
Supersonic unstalled flutter p0004 A79-12599

Supersonic unstalled flutter --- aerodynamic
loading of thin airfoils induced by cascade motion
[NASA-TN-79001] p0002 A79-11000

Analysis of supersonic stall bending flutter in
axial-flow compressor by actuator disk theory
[NASA-TF-1345] p0003 A79-13003

Supersonic unstalled flutter p0023 A79-27181

SUPERSONIC INLETS
Calculation of the three-dimensional flow field in
supersonic inlets at angle of attack using a
bicharacteristic method with discrete shock wave
fitting
[AIAA PAPER 79-0379] p0025 A79-19698

A computer program for the calculation of the flow
field in supersonic mixed-compression inlets at
angle of attack using the three-dimensional
method of characteristics with discrete shock
wave fitting
[NASA-TN-78947] p0002 A79-10023

Experimental investigation of a 0.15-scale model
of an underfuselage normal-shock inlet
[NASA-CR-3049] p0006 A79-12014

A throat-bypass stability-bleed system using
relief valves to increase the transient
stability of a mixed-compression inlet --- IF-12
aircraft inlet tests in the Lewis 10 by 10 ft
supersonic wind tunnel
[NASA-TF-1083] p0023 A79-28176

SUPERSONIC SPEEDS
Feasibility of wing shielding of the airplane
interior from the shock noise generated by
supersonic tip speed propellers
[NASA-TN-79047] p0172 A79-15757

Tone noise of three supersonic helical tip speed
propellers in a wind tunnel at 0.8 Mach number
[NASA-TN-79046] p0172 A79-15758

Tone noise of three supersonic helical tip speed
propellers in a wind tunnel
[NASA-TN-79167] p0174 A79-25840

SUPERSONIC WIND TUNNELS
Low-turbulence high-speed wind tunnel for the
determination of cascade shock losses
[ASME PAPER 79-GT-129] p0039 A79-32398

SUPPORTS
Elastomer mounted rotors - An alternative for
smoother running turbomachinery
[ASME PAPER 79-GT-149] p0119 A79-32414

SUPPRESSORS
Infrared suppressor effect on T63 turboshaft
engine performance
[NASA-TN-78970] p0013 A79-11043

SURFACE CRACKS
Mode I analysis of a face cracked plate subjected
to rotationally constrained end displacements
p0128 A79-21831

Stress analysis for structures with surface cracks
[NASA-CR-159400] p0129 A79-13405

User's manual for FRAC3D: Supplement to report on
stress analysis for structures with surface cracks
[NASA-CR-159401] p0129 A79-13406

SURFACE DEFECTS
Elastohydrodynamic film thickness measurements of
artificially produced surface dents and grooves
--- on fatigue failure of bearings
[ASLE PREPRINT 78-LC-1A-1] p0118 A79-23267

Characterization of defect growth structures in
ion plated films by scanning electron microscopy
p0078 A79-34992

Characterization of defect growth structure in ion
plated films by scanning electron microscopy
[NASA-TN-79110] p0074 A79-20218

SURFACE FINISHING
The use of ion beam cleaning to obtain high
quality cold welds with minimal deformation
p0119 A79-24121

Modification of the electrical and optical
properties of polymers --- ion irradiation
[NASA-CASE-LEW-13027-1] p0081 A79-11216

Ion beam technology applications study --- ion
impact, implantation, and surface finishing
[NASA-CR-159437] p0180 A79-12884

Improved adherence of sputtered titanium carbide
coatings on nickel- and titanium-base alloys
[NASA-TF-1450] p0059 A79-22194

Effect of grain orientation and coating on thermal
fatigue resistance of a directionally solidified
superalloy (NAN-M 247)
[NASA-TN-79129] p0127 A79-22565

SURFACE INTERACTIONS
U SURFACE REACTIONS
SURFACE PROPERTIES
W1 ADHESION
W1 COEFFICIENT OF FRICTION
W1 SURFACE CRACKS
W1 SURFACE DEFECTS
W1 SURFACE ROUGHNESS
W1 SURFACE TEMPERATURE
Effects of bulk and surface conductivity on the
potential developed by dielectrics exposed to
electron beams p0171 A79-50930

Friction and wear with a single-crystal abrasive
grit of silicon carbide in contact with iron
base binary alloys in oil: Effects of alloying
element and its content
[NASA-TF-1394] p0114 A79-17227

Status of materials characterization studies
p0048 A79-24030

Computer and laboratory simulation of interactions
between spacecraft surfaces and charged-particle
environments
[NASA-TN-79219] p0063 A79-29224

Infrared analysis of polyethylene wear specimens
using attenuated total reflection spectroscopy
--- effects of radiation on the surface
properties of materials for total joint prostheses
[NASA-TN-79228] p0083 A79-29329

Evaluation of high-contact-ratio spur gears with
profile modification
[NASA-TF-1458] p0115 A79-31604

SURFACE REACTIONS
Adhesive bonding of ion beam textured metals and
fluoropolymers p0060 A79-14798

A proposed physical model for the impregnated
tungsten cathode based on Auger surface studies
of the Ba-C-W system p0078 A79-39972

Space environmental interactions with spacecraft
surfaces
[NASA-TN-79016] p0046 A79-15150

Interactions between spacecraft and the
charged-particle environment p0047 A79-24021

Plasma Interaction Experiment (PIX) flight results
p0047 A79-24022

Metal-dielectric interactions
[NASA-TN-79151] p0075 A79-25195

Adhesive material transfer in the erosion of an
aluminum alloy
[NASA-TN-79165] p0083 A79-27306

Surface chemistry of iron sliding in air and
nitrogen lubricated with hexadecane and
hexadecane containing dibenzyl-dithiolide
[NASA-TF-1545] p0059 A79-31346

SURFACE ROUGHNESS
Two-dimensional random surface model for
asperity-contact in elastohydrodynamic lubrication
p0120 A79-39811

Lubrication and failure mechanisms of molybdenum
disulfide films. 2: Effect of substrate
roughness
[NASA-TF-1379] p0081 A79-13159

Elastohydrodynamic film thickness measurements of
artificially produced nonsmooth surfaces
[NASA-TN-79214] p0115 A79-28554

SURFACE ROUGHNESS EFFECTS
Elastohydrodynamic film thickness measurements of
artificially produced surface dents and grooves
--- on fatigue failure of bearings
[ASLE PREPRINT 78-LC-1A-1] p0118 A79-23267

SURFACE TEMPERATURE
Measurement of transient strain and surface
temperature on simulated turbine blades using
noncontacting techniques
[NASA-TN-78982] p0126 A79-19415

- SURFACE TREATMENT**
 U SURFACE FINISHING
SURFACE VEHICLES
 NT AUTOMOBILES
 NT ELECTRIC MOTOR VEHICLES
SURFACE WATER
 Atmospheric transformation of multispectral remote sensor data --- Great Lakes [E79-10006] p0131 N79-12524
- SURGES**
 An electro-optic, high-voltage, transient probe [NASA-TN-79019] p0109 N79-12414
- SURVEILLANCE RADAR**
 NT AIRBORNE SURVEILLANCE RADAR
- SWIRLING**
 Atomization of water jets and sheets in axial and swirling airflows [ASME PAPER 79-GT-170] p0106 A79-30556
 Test verification of a turbofan partial swirl afterburner [AIAA PAPER 79-1199] p0029 A79-38581
- SWITCHES**
 NT SWITCHING CIRCUITS
SWITCHING CIRCUITS
 1 general unified approach to modelling switching dc-to-dc converters in discontinuous conduction mode p0101 A79-10880
 A new optimum topology switching dc-to-dc converter p0101 A79-10888
 Input filter design for switching regulators p0101 A79-48653
 Analysis of a parallel-arrayed power regulating system p0101 A79-49397
 Modeling of switching regulator power stages with and without zero-inductor-current dwell time p0101 A79-49398
- SWITCHING ELEMENTS**
 U SWITCHING CIRCUITS
- SYMMETRICAL BODIES**
 NT CONICAL BODIES
 NT CYLINDRICAL BODIES
- SYNCHRONISE**
 NT BIT SYNCHRONIZATION
- SYNCHRONOUS SATELLITES**
 Insulator edge voltage gradient effects in spacecraft charging phenomena p0048 A79-30139
 NASCAP modelling of environmental-charging-induced discharges in satellites [NASA-TN-79247] p0048 N79-31265
- SYNCON 4 SATELLITE**
 NT ARTIFICIAL SATELLITES
- SYNTHETIC FIBERS**
 NT GLASS FIBERS
 Ultrafine polybenzimidazole (PBI) fibers --- separators for alkaline batteries and dfuel cells [NASA-CR-159644] p0067 N79-31350
- SYNTHETIC FUELS**
 Characteristics and combustion of future hydrocarbon fuels p0090 A79-11599
 Evaluation of the application of some gas chromatographic methods for the determination of properties of synthetic fuels p0070 A79-25917
 Evaluation of the application of some gas chromatographic methods for the determination of properties of synthetic fuels [NASA-TN-79035] p0068 N79-16930
 Comparison of the properties of some synthetic crudes with petroleum crudes [NASA-TN-79220] p0090 N79-31405
- SYNTHETIC RESINS**
 NT EPOXY RESINS
 NT Kevlar (TRADEMARK)
 NT PHENOLIC RESINS
 NT POLYETHER RESINS
- SYNTHETIC RUBBERS**
 NT ELASTOMERS
- SYSTEM EFFECTIVENESS**
 Spacecraft charging modeling development and validation study p0050 N79-24051
- SYSTEMS ANALYSIS**
 Energy-state formulation of lumped volume dynamic equations with application to a simplified free piston Stirling engine
- Fuel cell on-site integrated energy system parametric analysis of a residential complex [NASA-TN-78996] p0188 N79-11955
 Results of thin-route satellite communication system analyses including estimated service costs [NASA-TN-79098] p0294 N79-20300
 Characteristics of primary electric propulsion systems --- conferences [NASA-TN-79255] p0053 N79-30290
 The 18 and 30 GHz fixed service communication satellite system study: Executive summary [NASA-CR-159527-1] p0096 N79-33373
- SYSTEMS DESIGN**
 U SYSTEMS ENGINEERING
SYSTEMS ENGINEERING
 Design and operating experience on the U.S. Department of Energy Experimental Rod-0 100 kW Wind Turbine p0145 L79-10234
 20/30 GHz satellite systems technology needs assessment --- for domestic communications p0095 A79-14948
 Fiber optic sensors for military, industrial and commercial applications p0111 A79-38738
 Analysis, design, fabrication and testing of the mini-Brayton rotating unit (Mini-BRU). Volume 1: Text and tables [NASA-CR-159441-VOL-1] p0120 N79-11408
 Preliminary power train design for a state-of-the-art electric vehicle (executive summary) [NASA-CR-157625] p0188 N79-12968
 Conceptual design of thermal energy storage systems for near term electric utility applications. Volume 1: Screening of concepts [NASA-CR-159411-VOL-1] p0151 N79-13496
 Conceptual design of thermal energy storage systems for near term electric utility applications. Volume 2: Appendices - screening of concepts [NASA-CR-159411-VOL-2] p0152 N79-13497
 Turbojet blade vibration data acquisition design and feasibility testing [NASA-CR-159505] p0032 N79-18976
 Active heat exchange system development for latent heat thermal energy storage [NASA-CR-159479] p0153 N79-21554
 Large space system: Charged particle environment interaction technology [NASA-TN-79156] p0046 N79-22188
 The 30-centimeter ion thrust subsystem design manual [NASA-TN-79191] p0053 N79-25131
 Development of a plasma sprayed ceramic gas path seal for high pressure turbine applications [NASA-CR-159669] p0122 N79-31602
 Mass drivers. 3: Engineering p0040 N79-32232

T

- T-53 ENGINE**
 Study of T53 engine vibration [NASA-CR-135449] p0030 N79-10061
- T-55 ENGINE**
 Effect of forward velocity and crosswind on the reverse-thrust performance of a variable-pitch fan engine [AIAA PAPER 79-0105] p0025 A79-23512
- T-63 ENGINE**
 Infrared suppressor effect on T63 turboshaft engine performance [NASA-TN-78970] p0113 N79-11043
- TACKINESS**
 Polyimide prepreg material having improved tack retention --- polyimide-graphite fiber composites [NASA-CASE-LEW-12933-1] p0059 N79-24061
- TAILLESS AIRCRAFT**
 NT F-102 AIRCRAFT
- TANK GEOMETRY**
 Contoured tank outlets for draining of cylindrical tanks in low-gravity environment --- Lewis Research Center Zero Gravity Facility [NASA-TN-1492] p0105 N79-29467
- TANKS (CONTAINERS)**
 NT CYLINDRICAL TANKS
 NT FUEL TANKS
 NT PROPELLANT TANKS

TARE (DATA REDUCTION)

TARE (DATA REDUCTION)

U DATA REDUCTION

TECHNOLOGICAL FORECASTING

Engineering in the 21st century --- aerospace technology prospects
[AAS PAPER 78-192] p0190 A79-21277
New opportunities for future small civil turbine engines: Overviews of the GATE studies
[NASA-TM-79073] p0017 N79-16849
Space propulsion technology overview
[NASA-TM-79104] p0043 N79-21711

TECHNOLOGIES

NT BICTECHNOLOGY

NT ENERGY TECHNOLOGY

TECHNOLOGY ASSESSMENT

Liquid-cooling technology for gas turbines - Review and status
p0116 A79-10038
Pressure instrumentation for gas turbine engines - A review of measurement technology
[ASME PAPER 78-GT-148] p0110 A79-10800
Prop-fan propulsion - Its status and potential
[SAE PAPER 780995] p0026 A79-25880
The Advanced Low-Emissions Catalytic-Combustor Program: Phase I - Description and status --- for aircraft gas turbine engines
[ASME PAPER 79-GT-19-] p0027 A79-30557
Space propulsion technology overview
[AIAA 79-0860] p0054 A79-34704
New opportunities for future small civil turbine engines - Overviews of the GATE studies
[SAE PAPER 790619] p0028 A79-36747
Wind turbines for electric utilities - Development status and economics
[AIAA PAPER 79-0965] p0148 A79-38888
Progress on Variable Cycle Engines
[AIAA PAPER 79-1312] p0036 A79-40759
Recent developments at ONERA in the field of structural analysis methods
[ONERA, TP NO. 1979-79] A79-49537
Commercial phosphoric acid fuel cell system technology development
p0150 A79-51809
The role of fuel cells in NASA's space power systems
p0056 A79-51810
Future Orbital Power Systems Technology Requirements
[NASA-CR-2058] p0052 N79-10122
Technology status: Batteries and fuel cells
p0052 N79-10132
Communications systems technology assessment study. Volume 2: Results
[NASA-CR-135224] p0095 N79-12273
Ion beam technology applications study --- ion impact, implantation, and surface finishing
[NASA-CR-159437] p0180 N79-12884
Preliminary power train design for a state-of-the-art electric vehicle (executive summary)
[NASA-CR-157625] p0188 N79-12968
A cross impact methodology for the assessment of US telecommunications system with application to fiber optics development: Executive summary
[NASA-CR-135209] p0096 N79-17071
Industrial ion source technology
[NASA-CR-159534] p0179 N79-19828
Study of an advanced General Aviation Turbine Engine (GATE)
[NASA-CR-159552] p0033 N79-21073
Evaluation of MOSTAS computer code for predicting dynamic loads in two bladed wind turbines
[NASA-TM-79101] p0137 N79-21549
Results from Symposium on Future Orbital power systems technology requirements
[NASA-TM-79125] p0053 N79-21911
Status of materials characterization studies
p0048 N79-24030
Premixed Prevaporized Combustor Technology Forum
[NASA-CR-2078] p0019 N79-24994
Advanced low emissions catalytic combustor program at Pratt and Whitney
p0021 N79-25012
Gas-turbine critical research and advanced technology support project
[NASA-TM-79139] p0139 N79-25498
Stirling engines for automobiles
[NASA-TM-79222] p0142 N79-28726
State-of-the-art of SiAlON materials --- conferences
[NASA-TM-79207] p0084 N79-30378

SUBJECT INDEX

Wind turbines for electric utilities: Development status and economics
[NASA-TM-79170] p0142 N79-30719
Silicon solar cells for space use: Present performance and trends
p0154 N79-32654

TECHNOLOGY TRANSFER

NASA gear research and its probable effect on rotorcraft transmission design
[NASA-TM-79292] p0116 N79-33477

TECHNOLOGY UTILIZATION

Energy conservation through sealing technology
p0118 A79-20700
Photovoltaic power systems for rural areas of developing countries
[NASA-TM-79097] p0135 N79-15411
A cross impact methodology for the assessment of US telecommunications system with application to fiber optics development, volume 1
[NASA-CR-135208] p0096 N79-18159
A cross impact methodology for the assessment of US telecommunications system with application to fiber optics development, volume 2
[NASA-CR-159511-VOL-2] p0096 N79-18160
Industrial potential, uses, and performance of sputtered and ion plated films
[NASA-TM-79107] p0157 N79-20527
Communications technology satellite: United States experiments and disaster communications applications
[NASA-TM-79109] p0044 N79-23999
Advanced low emissions catalytic combustor program at General Electric
p0021 N79-25011
Commercial phosphoric acid fuel cell system technology development
[NASA-TM-79169] p0139 N79-25500
National Aeronautics and Space Administration plans for space communication technology
[NASA-TM-79217] p0053 N79-28220

TECHNOLOGY (TECHNOLOGY)

Area scaling investigations of charging phenomena --- discharge pulse characteristics of Teflon thermal control tape
p0048 N79-24032
An investigation of the adhesive bonding of Teflon solar cell covers
[NASA-CR-159565] p0153 N79-26506

TELECOMMUNICATION

NT AIRCRAFT COMMUNICATION
NT BROADCASTING
NT DATA LINKS
NT RADIO COMMUNICATION
NT RADIO RELAY SYSTEMS
NT SPACE COMMUNICATION
NT SPACECRAFT COMMUNICATION
NT TELEPHONY
NT VIDEO COMMUNICATION
NT VOICE COMMUNICATION
Telecommunication service markets through the year 2000 in relation to millimeter wave satellite systems
p0095 A79-27398
VHF downlink communication system for SLAR data
p0045 A79-51097
Telecommunication service markets through the year 2000 in relation to millimeter wave satellite systems
[NASA-TM-79099] p0094 N79-16169
A cross impact methodology for the assessment of US telecommunications system with application to fiber optics development: Executive summary
[NASA-CR-135209] p0096 N79-17071
A cross impact methodology for the assessment of US telecommunications system with application to fiber optics development, volume 1
[NASA-CR-135208] p0096 N79-18159
A cross impact methodology for the assessment of US telecommunications system with application to fiber optics development, volume 2
[NASA-CR-159511-VOL-2] p0096 N79-18160
TELECONFERENCING
Design of a video teleconference facility for a synchronous satellite communications link
[NASA-TM-1376] p0094 N79-14275
TELEPHONY
Results of thin-route satellite communication system analyses including estimated service costs
p0095 A79-30395

TELEGRAPH THEORY

U NETWORK ANALYSIS
U NETWORK SYNTHESIS

TEMPERATURE

NT AMBIENT TEMPERATURE
NT ATMOSPHERIC TEMPERATURE
NT CRITICAL TEMPERATURE
NT GAS TEMPERATURE
NT HIGH TEMPERATURE
NT LOW TEMPERATURE
NT ROOM TEMPERATURE
NT SURFACE TEMPERATURE
NT TRANSITION TEMPERATURE

TEMPERATURE CONTROL

Low heat leak connector for cryogenic system
[NASA-CASE-XLE-02367-1] p0093 N79-21225
Description and orbit data of variable-conductance
heat-pipe system for the communications
technology satellite
[NASA-TF-1465] p0105 N79-30516

TEMPERATURE DEPENDENCE

Temperature and intensity dependence of the
performance of an electron-irradiated
(AlGa)As/GaAs solar cell
p0144 N79-32665

TEMPERATURE DISTRIBUTION

Velocity, temperature, and electrical conductivity
profiles in hydrogen-oxygen MHD duct flows
p0182 A79-26184

Ceramic coating effect on liner metal temperatures
of film-cooled annular combustor
[NASA-TF-1323] p0015 N79-14098

TEMPERATURE EFFECTS

Effect of inlet temperature on the performance of
a catalytic reactor
p0070 A79-11542

Effects of hydrothermal exposure on a
low-temperature cured epoxy
p0085 A79-15534

Hartmann flow with temperature-dependent physical
properties --- magnetohydrodynamics of liquid
metal
p0182 A79-15597

The magnetocaloric effect in dysprosium
p0185 A79-38402

Combined pressure and temperature distortion
effects on internal flow of a turbofan engine
[AIAA PAPER 79-1309] p0029 A79-39031

Experimental study of low temperature behavior of
aviation turbine fuels in a wing tank model
[NASA-CR-159615] p0091 N79-29355

TEMPERATURE FIELDS

U TEMPERATURE DISTRIBUTION

TEMPERATURE INDICATORS

U TEMPERATURE MEASURING INSTRUMENTS

TEMPERATURE INSTRUMENTS

U TEMPERATURE MEASURING INSTRUMENTS

TEMPERATURE INVERSIONS

Combined pressure and temperature distortion
effects on internal flow of a turbofan engine
[NASA-TM-79136] p0012 N79-23963

Effect of steady-state temperature distortion and
combined distortion on inlet flow to a turbofan
engine
[NASA-TM-79237] p0023 N79-30187

TEMPERATURE MEASUREMENT

Feasibility of determining flat roof heat losses
using aerial thermography
p0131 A79-51095

Fundamental mechanisms that influence the estimate
of heat transfer to gas turbine blades
[NASA-TM-79128] p0103 N79-20346

Commercial aircraft derived high resolution wind
and temperature data from the tropics for PGGE:
Implications for NASA
p0161 N79-20621

Inflight fuel tank temperature survey data
[NASA-CR-159569] p0009 N79-23940

Evaluation of miniature single-wire sheathed
thermocouples for turbine blade temperature
measurement
[NASA-TM-79173] p0110 N79-27480

TEMPERATURE MEASURING INSTRUMENTS

NT TEMPERATURE PROBES

Feasibility of determining flat roof heat losses
using aerial thermography
[NASA-TM-79152] p0131 N79-22590

TEMPERATURE PROBES

An in-place recalibration technique to extend the

temperature capability of capacitance-sensing,
rotor-blade-tip-clearance measurement systems
[SAE PAPER 781003] p0026 A79-25885

TEMPERATURE SENSORS

Analysis and preliminary design of optical sensors
for propulsion control --- temperature sensors
[NASA-CR-159519] p0180 N79-27975

TENSILE PROPERTIES

Transverse and longitudinal tensile properties at
760 C of several oxide dispersion strengthened
nickel-base alloys
p0078 A79-49531

TENSILE STRENGTH

Longitudinal shear behavior of several oxide
dispersion strengthened alloys
p0076 A79-14955

Some properties of an advanced boron
fiber
p0086 A79-21297

Some properties of an advanced boron
high strength, splittable fibers
[NASA-TM-79065] p0061 N79-16076

Transverse and longitudinal tensile properties at
760 C of several oxide dispersion strengthened
nickel-base alloys
[NASA-TM-79189] p0075 N79-30355

TENSILE TESTS

Metal spar/superhybrid shell composite fan blades
--- for application to turbofan engines
[NASA-CR-159594] p0067 N79-30295

TERNARY ALLOYS

NT ASTEROLOY (TRADEMARK)

TERNARY SYSTEMS

Normal state properties of the ternary molybdenum
sulfides
p0185 A79-27229

Low temperature normal state resistance of ternary
molybdenum sulfides
p0185 A79-27230

Reactively evaporated films of copper molybdenum
sulfide
p0185 A79-31973

TERNARY SYSTEMS (DIGITAL)

U DIGITAL SYSTEMS

TEST BEDS

U TEST EQUIPMENT

TEST CHAMBERS

NT PRESSURE CHAMBERS

NASA CF6 jet engine diagnostics program:
Long-term CF6-6D low-pressure turbine
deterioration
[NASA-CR-159618] p0039 N79-29191

TEST EQUIPMENT

Definition study for variable cycle engine testbed
engine and associated test program
[NASA-CR-159459] p0031 N79-13048

Fuel spray data with LDV --- solar laser
morphokinetic capabilities in combustion
research
p0019 N79-24997

Design and application of a test rig for
super-critical power transmission shafts
[NASA-CR-3155] p0122 N79-31603

Design and application of a test rig for
super-critical power transmission shafts
[NASA-CR-3155] p0122 N79-31603

TEST FACILITIES

NT ENGINE TESTING LABORATORIES

NT SUPERSONIC WIND TUNNELS

NT TRANSONIC WIND TUNNELS

Design study of superconducting magnets for a
combustion magnetohydrodynamic /MHD/ generator
p0098 A79-15305

A mobile apparatus for solar collector testing
[ASAE PAPER 79-DE-5] p0150 A79-47651

Preliminary summary of the ETF conceptual studies
[NASA-TM-78999] p0133 N79-11478

The NASA high pressure facility and turbine test rig
[NASA-TM-79054] p0015 N79-15050

Design and application of a test rig for
super-critical power transmission shafts
[NASA-CR-3155] p0122 N79-31603

TESTERS

U TEST EQUIPMENT

TESTING MACHINES

U TEST EQUIPMENT

TF-30 ENGINE

Combined pressure and temperature distortion
effects on internal flow of a turbofan engine
[AIAA PAPER 79-1309] p0029 A79-39031

THEOREMS

NT SIMILARITY THEOREM

THERMAL AGITATION

U THERMAL ENERGY

THERMAL CONDUCTIVITY

Wartmann flow with temperature-dependent physical properties --- magnetohydrodynamics of liquid metal

p0182 A79-15597

Thermal-conductivity measurements of tungsten-fiber-reinforced superalloy composites using a thermal-conductivity comparator [NASA-TP-1445]

p0063 N79-28234

THERMAL CONTROL COATINGS

NASA thermal barrier coatings - Summary and update

p0085 A79-21295

Effects of compositional changes on the performance of a thermal barrier coating system --- for aircraft gas turbine engines

p0077 A79-21299

Emission and absorptance of the National Aeronautics and Space Administration ceramic thermal barrier coating --- for gas turbine engine components

p0086 A79-27231

Thermal barrier coatings: Burner rig hot corrosion test results

p0073 N79-11179

NASA thermal barrier coatings: Summary and update [NASA-TM-79053]

p0015 N79-15048

Effect of thermal barrier coatings on the performance of steam and water-cooled gas turbine/steam turbine combined cycle system [NASA-TM-79057]

p0135 N79-17334

Area scaling investigations of charging phenomena --- discharge pulse characteristics of teflon thermal control tape

p0048 N79-24032

Industry tests of NASA ceramic thermal barrier coating --- for gas turbine engine applications [NASA-TP-1425]

p0022 N79-25023

Effects of yttrium, aluminum, and chromium concentrations in bond coatings on the performance of zirconia-yttria thermal barriers [NASA-TM-79206]

p0075 N79-29293

THERMAL CYCLING TESTS

Effects of compositional changes on the performance of a thermal barrier coating system --- for aircraft gas turbine engines

p0077 A79-21299

Development of surface coatings for air-lubricated, compliant journal bearings to 650 C

[ASLE PREPRINT 78-LC-3C-1] p0123 A79-23252

Effect of a chromium-containing fuel additive on hot corrosion

p0071 A79-26546

Static evaluation of surface coatings for compliant gas bearings in an oxidizing atmosphere to 650 C

p0088 A79-31957

Ultraviolet irradiation at elevated temperatures and thermal cycling in vacuum of FEP-A covered silicon solar cells

p0148 A79-40638

THERMAL DEGRADATION

Effect of thermal aging on the tribological properties of polyimide films and polyimide-bonded graphite fluoride films [NASA-TM-79045]

p0082 N79-15186

THERMAL EFFECTS

U TEMPERATURE EFFECTS

THERMAL EMISSION

NT THERMIONIC EMISSION

THERMAL ENERGY

Thermal energy storage for industrial waste heat recovery

p0145 A79-10101

NaOH-based high temperature heat-of-fusion thermal energy storage device

p0155 A79-10106

Storage systems for solar thermal power

p0145 A79-10108

Thermal storage for industrial process and reject heat

p0147 A79-21300

Mini-Brayton heat source assembly development [NASA-CR-159447]

p0151 N79-12554

Conceptual design of thermal energy storage systems for near term electric utility applications. Volume 1: Screening of concepts

[NASA-CR-159411-VOL-1] p0151 N79-13496

Thermal storage technologies for solar industrial

process heat applications

[NASA-TM-79130] p0136 N79-20498

Handbook of data on selected engine components for solar thermal applications

[NASA-TM-79027] p0139 N79-26476

Solar thermal power-conversion system

p0139 N79-26477

Power-conversion system component summation

p0140 N79-26483

Applications of thermal energy storage to process heat storage and recovery in the paper and pulp industry

[NASA-CR-159398] p0154 N79-30801

THERMAL ENERGY STORAGE

U HEAT STORAGE

THERMAL EXPANSION

Thermal expansion of some nickel and cobalt spinels and their solid solutions

p0186 A79-50233

A reduced volumetric expansion factor plot [NASA-TM-79240]

p0105 N79-31527

THERMAL FATIGUE

Exploratory thermal-mechanical fatigue results for Rene' 80 in ultrahigh vacuum

[NASA-CR-159444] p0079 N79-11180

Three-dimensional finite-element elastic analysis of a thermally cycled single-edge wedge geometry specimen

[NASA-TM-79026] p0172 N79-16644

High velocity burner rig oxidation and thermal fatigue behavior of Si3N4- and SiC base ceramics to 1370 deg C

[NASA-TM-79040] p0082 N79-16984

Measurement of transient strain and surface temperature on simulated turbine blades using noncontacting techniques

[NASA-TM-78982] p0126 N79-19415

Effect of grain orientation and coating on thermal fatigue resistance of a directionally solidified superalloy (MAR-M 247)

[NASA-TM-79129] p0127 N79-22565

THERMAL INSTABILITY

Mercury ion thruster research, 1978

[NASA-CR-159485] p0056 N79-16913

THERMAL INSULATION

Laboratory studies of electrical properties of insulating materials --- thermal insulation of spacecraft dielectrics

p0044 A79-20877

THERMAL MAPPING

Feasibility of determining flat roof heat losses using aerial thermography

[NASA-TM-79152] p0131 N79-22590

THERMAL POWER

U TURBOGENERATORS

THERMAL PROPERTIES

U THERMODYNAMIC PROPERTIES

THERMAL PROTECTION

Tests of NASA ceramic thermal barrier coating for gas-turbine engines

[NASA-TM-79116] p0017 N79-20118

A thermal control approach for a solar electric propulsion thrust subsystem [NASA-TM-79175]

p0043 N79-27236

THERMAL RADIATION

Introduction: Thermal Radiation in Industrial Flames

p0104 N79-22415

THERMAL RESISTANCE

Low-cycle fatigue of thermal-barrier coatings at 982 deg C

[NASA-TP-1322] p0014 N79-13046

THERMAL SHIELDING

U HEAT SHIELDING

THERMAL STABILITY

NT TEMPERATURE DEPENDENCE

Sound-suppressing structure with thermal relief [NASA-CASE-LEW-12658-1]

p0172 N79-14871

Boundary lubrication, thermal and oxidative stability of a fluorinated polyether and a perfluoropolyether triazine

[NASA-TM-79064] p0081 N79-15185

Effects of graphite fiber stability on the properties of FMR polyimide composites

[NASA-TM-79062] p0061 N79-16075

Resin/fiber thermo-oxidative interactions in FMR polyimide/graphite composites

- [NASA-TM-79093] p0062 N79-16920
Catalytic trimerization of aromatic nitriles and triaryl-s-triazine ring cross-linked high temperature resistant polymers and copolymers made thereby
[NASA-CASE-LEW-12053-2] p0083 N79-28307
- THERMAL STRESSES**
Effects of moisture profiles and laminate configuration on the hygro stress in advanced composites p0064 A79-24132
Apparatus and method for reducing thermal stress in a turbine rotor [NASA-CASE-LEW-12232-1] p0013 N79-10057
Thermal stress analysis of ceramic gas-path seal components for aircraft turbines [NASA-TP-1437] p0082 N79-21205
- THERMAL VACUUM TESTS**
High temperature dynamic modulus and damping of aluminum and titanium matrix composites p0065 A79-26132
- THERMIONIC CATHODES**
Diminide thermionic energy conversion with lanthanum-hexaboride electrodes p0146 A79-13098
Comment on the mechanism of operation of the impregnated tungsten cathode p0099 A79-42024
- THERMIONIC CONVERTERS**
Lithium and potassium heat pipes for thermionic converters p0145 A79-10113
Diminide thermionic energy conversion with lanthanum-hexaboride electrodes p0146 A79-13098
Optimize out-of-core thermionic energy conversion for nuclear electric propulsion p0146 A79-13099
Some properties of low-vapor-pressure braze alloys for thermionic converters p0076 A79-13100
Investigations of negative and positive cesium ion species [NASA-CR-159446] p0179 N79-18711
- THERMIONIC EMISSION**
Summary of the two year NASA program for active control of ATS-5/6 environmental charging --- with a thermionic electron source and a plasma source p0047 N79-24006
- THERMIONIC EMITTERS**
Diminide thermionic energy conversion with lanthanum-hexaboride electrodes p0146 A79-13098
- THERMIONIC REACTORS**
U ION ENGINES
- THERMOCOUPLES**
Thermocouples of molybdenum and iridium alloys for more stable vacuum-high temperature performance [NASA-CASE-LEW-12174-2] p0109 N79-14346
Evaluation of miniature single-wire sheathed thermocouples for turbine blade temperature measurement [NASA-TM-79173] p0110 N79-27480
- THERMODYNAMIC CYCLES**
NT BRAYTON CYCLE
NT RANKINE CYCLE
NT STIRLING CYCLE
Effect of steam addition on cycle performance of simple and recuperated gas turbines [NASA-TP-1440] p0137 N79-22626
- THERMODYNAMIC PROPERTIES**
NT CRITICAL TEMPERATURE
NT EMISSIVITY
NT ENTROPY
NT MELTING POINTS
NT THERMAL CONDUCTIVITY
NT THERMAL EXPANSION
NT THERMAL INSTABILITY
NT THERMAL STABILITY
NT THERMOPHYSICAL PROPERTIES
Alternative aviation turbine fuels p0090 A79-12378
Mini-BRU/BIPS foil bearing development [NASA-CR-159442] p0120 N79-11407
Prediction of properties of intraply hybrid composites [NASA-TM-79087] p0061 N79-16919
- WETAIR: A computer code for calculating thermodynamic and transport properties of air-water mixtures** [NASA-TP-1466] p0166 N79-23688
- THERMODYNAMICS**
NT COMBUSTION PHYSICS
Application of the principle of similarity fluid mechanics [NASA-TM-79258] p0105 N79-30515
- THERMOGRAMS**
U TEMPERATURE MEASURING INSTRUMENTS
- THERMOMECHANICAL TREATMENT**
Effects of thermomechanical processing on strength and toughness of Fe-12Ni reactive metal alloys at 77K p0078 A79-32600
- THERMOMECHANICS**
U THERMODYNAMICS
- THERMOMETRY**
U TEMPERATURE MEASUREMENT
- THERMOPHYSICAL PROPERTIES**
NT CRITICAL TEMPERATURE
NT EMISSIVITY
NT MELTING POINTS
NT TEMPERATURE DEPENDENCE
NT THERMAL CONDUCTIVITY
NT THERMAL STABILITY
Thermophysical property data: Who needs them? [NASA-TM-79241] p0090 N79-31403
A reduced volumetric expansion factor plot [NASA-TM-79240] p0105 N79-31527
- THERMOPHYSICS**
J THERMODYNAMICS
- THERMOSETTING RESINS**
NT EPOXY RESINS
NT PHENOLIC RESINS
- THERMOSTABILITY**
U THERMAL STABILITY
- THERMOTROPISM**
U ANISOTROPY
U TEMPERATURE EFFECTS
- THICKNESS RATIO**
Thin cells for space p0154 N79-32652
- THIN AIRFOILS**
Supersonic unstalled flutter --- aerodynamic loading of thin airfoils induced by cascade motion [NASA-TM-79001] p0002 N79-11000
- THIN FILMS**
Sputtering technology in solid film lubrication p0117 A79-16663
Application of ESCA to the determination of stoichiometry in sputtered coatings and interface regions --- X-ray photoelectron spectroscopy p0117 A79-16664
Superconducting properties of evaporated copper molybdenum sulfide films p0184 A79-20219
Low temperature normal state resistance of ternary molybdenum sulfides p0185 A79-27230
Industrial potential, uses, and performance of sputtered and ion plated films p0119 A79-30398
Reactively evaporated films of copper molybdenum sulfide p0185 A79-31973
Test results for electron beam charging of flexible insulators and composites --- solar array substrates, honeycomb panels, and thin dielectric films p0048 N79-24031
Sputtering in mercury ion thrusters [NASA-TM-79266] p0054 N79-31343
- THIN WALLED SHELLS**
Proof test criteria for thin walled pressure vessels p0123 A79-26985
- THREE DIMENSIONAL FLOW**
NT SECONDARY FLOW
An efficient user-oriented method for calculating compressible flow about three-dimensional inlets [AIAA PAPER 79-0081] p0005 A79-19524
Effects of inflow distortion profiles on fan tone noise calculated using a 3-D theory [AIAA PAPER 79-0577] p0175 A79-26911
Development of a three-dimensional turbulent duct flow analysis [NASA-CN-3029] p0106 N79-12366

- Modeling of premixing-prevaporizing fuel-air mixing passages
p0019 N79-24998
- THREE DIMENSIONAL MOTION**
NT SECONDARY FLOW
NT THREE DIMENSIONAL FLOW
- THRUST AUGMENTATION**
A summary of NASA/Air Force Full Scale Engine Research programs using the F100 engine
[AIAA PAPER 79-1308] p0030 A79-40488
- THRUST BEARINGS**
Self-acting shaft seals --- gas turbine engines
p0013 N79-11070
Operating characteristics of a cantilever-mounted resilient-pad gas-lubricated thrust bearing
[NASA-TF-1438] p0117 N79-22518
- THRUST CHAMBERS**
Development of sputtering process to deposit stoichiometric zirconia coatings for the inside wall of regeneratively cooled rocket thrust chambers
[NASA-CR-159412] p0056 N79-11115
Heat exchanger --- rocket combustion chambers and cooling systems
[NASA-CASE-LEW-12254-1] p0102 N79-13288
Heat exchanger and method of making --- bonding rocket chambers with a porous metal matrix
[NASA-CASE-LEW-12441-1] p0102 N79-13289
Structural analysis of cylindrical thrust chambers, volume 1
[NASA-CR-159522] p0057 N79-19073
Some effects of cyclic induced deformation in rocket thrust chambers
[NASA-TM-79112] p0103 N79-20337
Effect of low-stiffness closeout overwrap on rocket thrust-chamber life
[NASA-TF-1456] p0053 N79-23132
Development of sputtered techniques for thrust chambers
[NASA-CR-159637] p0080 N79-32326
- THRUST CONTROL**
Primary electric propulsion for future space missions
[AIAA 79-0881] p0055 A79-34773
Preliminary results of the mission profile life test of a 30 cm Hg bombardment thruster
[NASA-TM-79261] p0054 N79-33254
- THRUST MEASUREMENT**
SERT 2 1979 extended flight thruster system performance
[NASA-TM-79256] p0054 N79-33252
- THRUST REVERSAL**
Effect of forward velocity and crosswind on the reverse-thrust performance of a variable-pitch fan engine
[AIAA PAPER 79-0105] p0025 A79-23512
Effect of forward velocity and crosswind on the reverse-thrust performance of a variable-pitch fan engine
[NASA-TM-79059] p0015 N79-15049
- THRUSTORS**
U ROCKET ENGINES
- THYRISTORS**
Development and fabrication of improved power transistor switches
[NASA-CR-159524] p0100 N79-21273
- TILT**
U ALTITUDE (INCLINATION)
- TILTING**
U ALTITUDE (INCLINATION)
- TIME**
NT MTBF
- TIME FUNCTIONS**
Two-dimensional random surface model for asperity-contact in elastohydrodynamic lubrication
[NASA-TM-79006] p0115 N79-23430
- TIME MEASURING INSTRUMENTS**
NT TIMING DEVICES
- TIME RESPONSE**
Generalized computer-aided discrete time domain modeling and analysis of dc-dc converters
p0099 A79-10881
Simmer-enhanced flashlamp-pumped dye laser
p0112 A79-32981
- TIMERS**
U TIMING DEVICES
- TIMING DEVICES**
A cycle timer for testing electric vehicles
p0188 A79-37293
- TIN COMPOUNDS**
NT NIOBIUM STANNIDES
- TIP DRIVEN ROTORS**
An in-place recalibration technique to extend the temperature capability of capacitance-sensing, rotor-blade-tip-clearance measurement systems
[SAE PAPER 781003] p0026 A79-25885
Rotor redesign for a highly loaded 1800 ft/sec tip speed fan. 1: Aerodynamic and mechanical design report
[NASA-CR-159596] p0034 N79-26055
- TIP SPEED**
Tone noise of three supersonic helical tip speed propellers in a wind tunnel
p0175 A79-39801
- TIPS**
NT BLADE TIPS
- TITANIUM**
Titanium/beryllium laminates - fabrication, mechanical properties, and potential aerospace applications
p0064 A79-20836
High temperature dynamic modulus and damping of aluminum and titanium matrix composites
p0065 A79-26132
Friction and fracture of single-crystal silicon carbide in contact with itself and titanium
p0086 A79-32149
Supply of reactants for Redox bulk energy storage systems
[NASA-TM-78995] p0133 N79-11479
High temperature dynamic modulus and damping of aluminum and titanium matrix composites
[NASA-TM-79080] p0061 N79-16077
Evaluation of silicon carbide fiber/titanium composites
[NASA-TM-79232] p0064 N79-31349
- TITANIUM ALLOYS**
Influence of composition, annealing treatment, and texture on the fracture toughness of Ti-5Al-2.5Sn plate at cryogenic temperatures
p0077 A79-24262
Adherence of sputtered titanium carbides
p0078 A79-34997
Fabrication and testing of non-graphitic superhybrid composites
p0066 A79-43289
Improved adherence of sputtered titanium carbide coatings on nickel- and titanium-base alloys
[NASA-TF-1450] p0059 N79-22194
Titanium-alloy, metallic-fluid heat pipes for space service
[NASA-TM-79132] p0104 N79-22426
Plasma-sprayed coatings for lubrication of a titanium alloy in air at 430 deg C
[NASA-TF-1509] p0083 N79-29327
Fatigue behavior of SiC reinforced titanium composites
[NASA-TM-79223] p0064 N79-30296
- TITANIUM CARBIDES**
Use of a nitrogen-argon plasma to improve adherence of sputtered titanium carbide coatings on steel
p0119 A79-25103
Adherence of sputtered titanium carbides
p0078 A79-34997
Effect of nitrogen-containing plasma on adherence, friction, and wear of radiofrequency-sputtered titanium carbide coatings
[NASA-TF-1377] p0081 N79-15184
Adherence of sputtered titanium carbides
[NASA-TM-79117] p0074 N79-20220
Improved adherence of sputtered titanium carbide coatings on nickel- and titanium-base alloys
[NASA-TF-1450] p0059 N79-22194
- TITANIUM COMPOUNDS**
NT TITANIUM CARBIDES
- TOLERANCES (MECHANICS)**
NT IMPACT TOLERANCES
- TOLERANCES (PHYSIOLOGY)**
NT RADIATION TOLERANCE
- TOMOGRAPHY**
Digital enhancement of computerized axial tomograms
p0164 A79-11544
- TONE/NOISE**
U INTRAOCULAR PRESSURE
U PRESSURE MEASUREMENTS
- TOPOLOGY**
A new optimum topology switching dc-to-dc converter

- TOROIDAL PLASMAS**
 Microwave radiation measurements near the electron plasma frequency of the NASA Lewis Bumpy Torus plasma p0101 A79-10888
- Ion confinement and transport in a toroidal plasma with externally imposed radial electric fields [NASA-TP-1411] p0181 A79-14953 p0181 N79-19867
- TORSIONAL STRESS**
 Proposed design procedure for transmission shafting under fatigue loading p0117 A79-14950
- TOUGHNESS**
 High toughness-high strength iron alloy [NASA-CASE-LEW-12542-3] p0073 N79-19145
- TOWERS**
 Wind turbine generator application places unique demands on tower design and materials p0155 A79-20826
- TRACE CONTAMINANTS**
 Global sensing of gaseous and aerosol trace species using automated instrumentation on 747 airliners p0110 A79-15067
- TRACE ELEMENTS**
 NASA Global Atmospheric Sampling Program (GASP) data report for tapes VL0010 and VL0012 [NASA-TM-79061] p0157 N79-15450
- TRACKING (POSITION)**
 NT SATELLITE TRACKING
- TRACTION**
 Performance of a Nasvitis multiroller traction drive [NASA-TP-1378] p0113 N79-13369
 Traction drive performance prediction for the Johnson and Tevaarwerk traction model [NASA-TP-1530] p0116 N79-33475
- TRAILING EDGES**
 Trailing edge noise data with comparison to theory [AIAA PAPER 79-1524] p0176 A79-47340
- TRAILING-EDGE FLAPS**
 Variable area exhaust nozzle [NASA-CASE-LEW-12378-1] p0014 N79-14097
 Trailing edge noise data with comparison to theory [NASA-TM-79208] p0174 N79-27930
- TRAJECTORIES**
 NT PARTICLE TRAJECTORIES
 TRAJECTORY ANALYSIS
 Trajectories of charged particles in radial electric and uniform axial magnetic fields p0182 A79-41788
- TRANSCENDENTAL FUNCTIONS**
 NT LOGARITHMS
- TRANSDUCERS**
 NT DIGITAL TRANSDUCERS
 NT ELECTRONIC TRANSDUCERS
 NT PRESSURE SENSORS
 Adaptation of ion beam technology to microfabrication of solid state devices and transducers [NASA-CR-159439] p0186 N79-11921
- TRANSFER FUNCTIONS**
 Studies of the acoustic transmission characteristics of coaxial nozzles with inverted velocity profiles: Comprehensive data report --- nozzle transfer functions [NASA-CR-159628] p0177 N79-27933
- TRANSFER ORBITS**
 Low-thrust chemical orbit transfer propulsion [AIAA PAPER 79-1182] p0055 A79-39815
 Low-thrust chemical orbit transfer propulsion [NASA-TM-79190] p0043 N79-25129
- TRANSFORMERS**
 Description of a 2.3 kW power transformer for space applications p0099 A79-34991
 Description of a 2.3 kW power transformer for space applications [NASA-TM-79138] p0097 N79-23348
- TRANSIENT LOADS**
 NT GUST LOADS
 NT IMPACT LOADS
 Measurement of transient strain and surface temperature on simulated turbine blades using noncontacting techniques [NASA-TM-78982] p0126 N79-19415
- TRANSIENTS (SURGES)**
 U SURGES
- TRANSISTORS**
 Development and fabrication of improved power transistor switches [NASA-CR-159524] p0100 N79-21273
- TRANSITION METALS**
 NT CHROMIUM
 NT GOLD
 NT IRIIDIUM
 NT IRON
 NT MANGANESE
 NT MOLYBDENUM
 NT REFRACTORY METALS
 NT SILVER
 NT TITANIUM
 NT TUNGSTEN
 NT ZINC
- TRANSITION TEMPERATURE**
 Effects of hydrothermal exposure on a low-temperature cured epoxy p0085 A79-15534
- TRANSLATIONAL MOTION**
 NT SECONDARY FLOW
 NT THREE DIMENSIONAL FLOW
- TRANSMISSION**
 NT ACOUSTIC PROPAGATION
 NT CONVECTIVE HEAT TRANSFER
 NT DATA TRANSMISSION
 NT HEAT TRANSFER
 NT HEAT TRANSMISSION
 NT LIGHT TRANSMISSION
 NT MICROWAVE TRANSMISSION
 NT SATELLITE TRANSMISSION
 NT SOUND TRANSMISSION
 NT TELEPHONY
 NT WAVE PROPAGATION
- TRANSMISSION EFFICIENCY**
 Ground-to-space optical power transfer --- using laser propulsion for orbit transfer p0161 A79-17180
 Millimeter wave communication satellite concepts p0095 A79-29784
 Multistage depressed collector for dual node operation --- for travelling wave tubes [NASA-CASE-LEW-13282-1] p0098 N79-32463
- TRANSMISSION LINES**
 NT BEAM WAVEGUIDES
 NT FLUID TRANSMISSION LINES
 NT POWER LINES
- TRANSMISSIONS (MACHINE ELEMENTS)**
 Proposed design procedure for transmission shafting under fatigue loading p0117 A79-14950
 Diagnostics of wear in aeronautical systems p0120 A79-39805
 Conceptual design study of improved automotive gas turbine powertrain [NASA-CR-159580] p0189 N79-31088
- TRANSmitters**
 Life characteristics assessment of the communications technology satellite transmitter experiment package [NASA-TM-79181] p0044 N79-31264
- TRANSONIC COMPRESSORS**
 An off-design correlation of part span damper losses through transonic axial fan rotors [ASME PAPER 79-GT-6] p0028 A79-32329
- TRANSONIC FLOW**
 Performance of single-stage axial-flow transonic compressor with rotor and stator aspect ratios of 1.19 and 1.26, respectively, and with design pressure ratio of 1.82 [NASA-TP-1338] p0013 N79-10060
- TRANSONIC FLUTTER**
 Wind tunnel tests of a blade subjected to midchord torsional oscillation at high subsonic stall flutter conditions [NASA-TM-78998] p0002 N79-12016
- TRANSONIC INLETS**
 U SUPERSONIC INLETS
- TRANSONIC WIND TUNNELS**
 Low-turbulence high-speed wind tunnel for the determination of cascade shock losses [ASME PAPER 79-GT-129] p0039 A79-32398
- TRANSONICS**
 U TRANSONIC FLOW
- TRANSPARENCY**
 Aerospace Transparent Materials and Enclosures (12th) [AD-A065049] p0018 N79-23066

TRANSPARENT MATERIALS

U TRANSPARENCY

TRANSPORT AIRCRAFT

NT BOEING 747 AIRCRAFT

NT SHORT HAUL AIRCRAFT

Fuel conservative aircraft engine technology
p0025 A79-20078Energy efficient engine: Propulsion
system-aircraft integration evaluation
[NASA-CR-159488] p0032 A79-16850

TRANSPORT COEFFICIENTS

U TRANSPORT PROPERTIES

TRANSPORT PROPERTIES

NT CARRIER MOBILITY

NT DIFFUSION COEFFICIENT

NT ELECTRICAL RESISTIVITY

NT IONIC MOBILITY

NT MAGNETORESISTIVITY

NT SUPERCONDUCTIVITY

NT THERMAL CONDUCTIVITY

NT VISCOSITY

Experimental evidence of interhemispheric
transport from airborne carbon monoxide
measurements

p0158 A79-38942

Ion confinement and transport in a toroidal plasma
with externally imposed radial electric fields
[NASA-TP-1411] p0181 A79-19867METAL: A computer code for calculating
thermodynamic and transport properties of
air-water mixtures

[NASA-TP-1466] p0166 A79-23688

TRANSPORT THEORY

A summary of research on the NASA-Global
Atmospheric Sampling Program performed by the
Atmospheric Sciences Research Center --- ozone
transport theory
[NASA-CR-159614] p0159 A79-27716

TRANSPORTATION

NT SPACE TRANSPORTATION SYSTEM

TRANSPORTATION ENERGY

Response of lead-acid batteries to
chopper-controlled discharge --- for electric
vehicles

p0145 A79-10097

TRANSURANIUM ELEMENTS

NT PLUTONIUM 239

TRAVELING WAVE TUBES

Comments on measuring the overall and the
depressed collector efficiency in TWT's and
klystron amplifiers

p0099 A79-25118

Traveling wave tube circuit
[NASA-CASE-LEW-12013-1] p0102 A79-14339Efficiency enhancement of octave-bandwidth
traveling wave tubes by use of multistage
depressed collectors

[NASA-TP-1416] p0097 A79-17139

TWT design requirements for 30/20 GHz digital
communications' satellite

[NASA-TM-79119] p0097 A79-20316

Analytical prediction with multidimensional
computer programs and experimental verification
of the performance, at a variety of operating
conditions, of two traveling wave tubes with
depressed collectors

[NASA-TP-1449] p0097 A79-22375

Efficiency enhancement of dual-mode traveling wave
tubes at saturation and in the linear range by
use of spent-beam refocusing and multistage
depressed collectors

[NASA-TP-1486] p0098 A79-28420

Multistage depressed collector for dual mode
operation --- for travelling wave tubes

[NASA-CASE-LEW-13282-1] p0098 A79-32463

TREES (MATHEMATICS)

On the distribution of computation for sequential
decoding using the stack algorithm

p0096 A79-33793

TRIBOLOGY

Sputtering technology in solid film lubrication
p0117 A79-16663

TRIM (BALANCE)

U AERODYNAMIC BALANCE

TRIMERS

Catalytic trimerization of aromatic nitriles and
triaryl-s-triazine ring cross-linked high
temperature resistant polymers and copolymers
made thereby

[NASA-CASE-LEW-12053-2]

p0083 A79-28307

TRIPROPELLANTS

U LIQUID ROCKET PROPELLANTS

TROPOPAUSE

Sulfate and nitrate mixing ratios in the vicinity
of the tropopause
p0158 A79-49494

TROPOSPHERE

A summary of research on the NASA-Global
Atmospheric Sampling Program performed by the
Atmospheric Sciences Research Center --- ozone
transport theory
[NASA-CR-159614] p0159 A79-27716

TRUNNOLS

U SHAFTS (MACHINE ELEMENTS)

TRUSSES

Wind turbine generator application places unique
demands on tower design and materials
p0155 A79-20826

TUBE CATHODES

NT THERMIONIC CATHODES

TUBE GRIDS

Method for fabricating solar cells having
integrated collector grids
[NASA-CASE-LEW-12819-2] p0136 A79-18444

TUNGSTEN

Predicted inlet gas temperatures for tungsten
fiber reinforced superalloy turbine blades
p0025 A79-17029Mechanisms of boron fiber strengthening by thermal
treatment
p0065 A79-30396A proposed physical model for the impregnated
tungsten cathode based on Auger surface studies
of the Ba-O-W system
p0078 A79-39972Comment on the mechanism of operation of the
impregnated tungsten cathode
p0099 A79-42024Tungsten fiber reinforced FeCrAl: A first
generation composite turbine blade material
[NASA-TM-79094] p0063 A79-20187Thermal-conductivity measurements of
tungsten-fiber-reinforced superalloy composites
using a thermal-conductivity comparator
[NASA-TP-1445] p0063 A79-28234

TUNGSTEN ALLOYS

Tungsten fiber reinforced FeCrAl - A first
generation composite turbine blade material
p0065 A79-30397Interdiffusion behavior of tungsten or rhenium and
group 5 and 6 elements and alloys of the
periodic table. Part 2b: Appendices
[NASA-CR-134526] p0080 A79-33305

TURBINE BLADES

Ceramic blade attachments --- for turbine rotors
p0123 A79-12848Predicted inlet gas temperatures for tungsten
fiber reinforced superalloy turbine blades
p0025 A79-17029Increasing the FOD tolerance of composites --- gas
turbine engine blade foreign object damage
p0067 A79-20859An oxide dispersion strengthened alloy for gas
turbine blades
[AIAA 79-0763] p0077 A79-28276Evaluation of MOSTAS computer code for predicting
dynamic loads in two-bladed wind turbines
[AIAA 79-0733] p0005 A79-29007Tungsten fiber reinforced FeCrAl - A first
generation composite turbine blade material
p0065 A79-30397Thermal-structural mission analyses of air-cooled
gas turbine blades
[ASME PAPER 79-GT-19] p0027 A79-30553Fundamental mechanisms that influence the estimate
of heat transfer to gas turbine blades
p0099 A79-49526Evaluation of the cyclic behavior of aircraft
turbine disk alloys
[NASA-CR-159409] p0030 A79-10058Thermal-structural mission analyses of air-cooled
gas turbine blades
[NASA-TM-78963] p0126 A79-11433Evaluation of directionally solidified eutectic
superalloys for turbine blade applications
[NASA-CR-135151] p0079 A79-16948Design, fabrication and spin testing of ceramic
blade metal disk attachment

- [NASA-CR-159532] p0032 N79-17857
 TACT 1: A computer program for the transient thermal analysis of a cooled turbine blade or vane equipped with a coolant insert. 2. Programmers manual
 [NASA-TP-1391] p0103 N79-18288
 Turbojet blade vibration data acquisition design and feasibility testing
 [NASA-CR-159505] p0032 N79-18976
 Containment of composite fan blades
 [NASA-CR-158168] p0032 N79-18978
 Nonlinear equations of equilibrium for elastic helicopter or wind turbine blades undergoing moderate deformation
 [NASA-CR-159478] p0130 N79-19414
 Measurement of transient strain and surface temperature on simulated turbine blades using noncontacting techniques
 [NASA-TN-78982] p0126 N79-19415
 An oxide dispersion strengthened alloy for gas turbine blades
 [NASA-TN-79088] p0052 N79-20180
 Tungsten fiber reinforced FeCrAlY: A first generation composite turbine blade material
 [NASA-TN-79094] p0063 N79-20187
 Evaluation of an advanced directionally solidified gamma/gamma'-alpha Mo eutectic alloy
 [NASA-CR-159416] p0079 N79-20222
 Fundamental mechanisms that influence the estimate of heat transfer to gas turbine blades
 [NASA-TN-79128] p0103 N79-20346
 Evaluation of urethane for feasibility of use in wind turbine blade design
 [NASA-CR-159530] p0153 N79-20497
 Thermal stress analysis of ceramic gas-path seal components for aircraft turbines
 [NASA-TP-1437] p0082 N79-21205
 Evaluation of MOSTAS computer code for predicting dynamic loads in two bladed wind turbines
 [NASA-TN-79101] p0137 N79-21549
 Review and status of liquid-cooling technology for gas turbines
 [NASA-RP-1038] p0104 N79-22427
 Measuring unsteady pressure on rotating compressor blades
 [NASA-TN-79159] p0109 N79-22448
 Low-cost directionally-solidified turbine blades, volume 1
 [NASA-CR-159464] p0080 N79-24121
 Internally coated air-cooled gas turbine blading
 [NASA-CR-159574] p0034 N79-25018
 X-ray photoelectron spectroscopy study of nickel and nickel-base alloy surface alterations in simulated hot corrosion conditions with emphasis on eventual application to turbine blade corrosion
 [NASA-CR-159553] p0072 N79-25178
 Large horizontal axis wind turbine development
 [NASA-TN-79174] p0140 N79-26504
 Flow visualization of discrete-hole film cooling with spanwise injection over a cylinder
 [NASA-TP-1491] p0023 N79-27142
 Evaluation of miniature single-wire sheathed thermocouples for turbine blade temperature measurement
 [NASA-TN-79173] p0110 N79-27480
 The erosion/corrosion of small superalloy turbine rotors operating in the effluent of a PFB coal combustor
 [NASA-TN-79227] p0076 N79-30356
 Containment of composite fan blades
 [NASA-CR-159543] p0067 N79-31348
 Development of a plasma sprayed ceramic gas path seal for high pressure turbine applications
 [NASA-CR-159669] p0122 N79-31602
- TURBINE ENGINES**
 NT DUCTED FAN ENGINES
 NT GAS TURBINE ENGINES
 NT J-85 ENGINE
 NT JET ENGINES
 NT T-53 ENGINE
 NT T-63 ENGINE
 NT TF-30 ENGINE
 NT TURBOFAN ENGINES
 NT TURBOJET ENGINES
 NT TURBOPROP ENGINES
 High-freezing-point fuels used for aviation turbine engines
 [ASME PAPER 79-GT-141] p0090 A79-30555
- The GATE studies - Assessing the potential of future small general aviation turbine engines
 p0027 A79-30560
 New opportunities for future small civil turbine engines - Overviewing the GATE studies
 [SAE PAPER 790619] p0028 A79-36747
 Computer-aided analysis and design of the shape rolling process for producing turbine engine airfoils
 [NASA-CR-159455] p0012 N79-12087
 The NASA high pressure facility and turbine test rig
 [NASA-TN-79054] p0015 N79-15050
 High freezing point fuels used for aviation turbine engines
 [NASA-TN-79015] p0089 N79-15199
 The gate studies: Assessing the potential of future small general aviation turbine engines
 [NASA-TN-79075] p0016 N79-15958
 New opportunities for future small civil turbine engines: Overviewing the GATE studies
 [NASA-TN-79073] p0017 N79-16849
 Cold-air performance of free power turbine designed for 112-kilowatt automotive gas-turbine engine. 2: Effects of variable stator-vane-chord setting angle on turbine performance
 [NASA-TN-78993] p0017 N79-17859
 Composite seal for turbomachinery --- backings for turbine engine shrouds
 [NASA-CASE-LEW-12131-1] p0114 N79-18318
 CF6 jet engine performance improvement program. Task 1: Feasibility analysis
 [NASA-CR-159450] p0033 N79-21074
 JT8D revised high-pressure turbine cooling and other outer air seal program
 [NASA-CR-159551] p0033 N79-21076
 Self stabilizing sonic inlet
 [NASA-CASE-LEW-11890-1] p0011 N79-24976
 Advanced General Aviation Turbine Engine (GATE) concepts
 [NASA-CR-159603] p0034 N79-25017
 Computer-aided analysis and design of the shape rolling process for producing turbine engine airfoils
 [NASA-CR-135367] p0080 N79-26175
 Turbine engine altitude chamber and flight testing with liquid hydrogen
 [NASA-TN-79196] p0022 N79-27140
 Experimental study of low temperature behavior of aviation turbine fuels in a wing tank model
 [NASA-CR-159615] p0091 N79-29355
 Energy efficient engine flight propulsion system preliminary analysis and design report
 [NASA-CR-159487] p0035 N79-30189
- TURBINE PUMPS**
 Small, high-pressure, liquid oxygen turbopump
 [NASA-CR-159509] p0121 N79-17221
 Comparison of analysis and experiment for self-acting seals for liquid-oxygen turbopumps
 [NASA-TP-1443] p0115 N79-22519
- TURBINE WHEELS**
 The strainrange partitioning behavior of an advanced gas turbine disk alloy, AP2-10A
 [AIAA PAPER 79-1192] p0078 A79-38977
- TURBINES**
 NT AXIAL FLOW TURBINES
 NT GAS TURBINES
 NT SHROUDED TURBINES
 NT STEAM TURBINES
 Control and stabilization of the DOE/NASA Mod-1 two megawatt wind turbine generator
 p0156 A79-51780
 Design, fabrication, and test of a composite material wind turbine rotor blade
 [NASA-CR-135389] p0150 N79-10525
 Microprocessor control of a wind turbine generator
 [NASA-TN-79021] p0134 N79-12548
 Theory of low frequency noise transmission through turbines
 [NASA-CR-159457] p0033 N79-20117
 Evaluation of MOSTAS computer code for predicting dynamic loads in two bladed wind turbines
 [NASA-TN-79101] p0137 N79-21549
 The use of wind data with an operational wind turbine in a research and development environment
 [NASA-TN-73832] p0140 N79-26502
 Design, fabrication, and initial test of a fixture for reducing the natural frequency of the Mod-C wind turbine tower

- [NASA-TM-79200] p0142 N79-28727
- TURBOCHARGERS**
- U SUPERCHARGERS
- U TURBOCOMPRESSORS
- TURBOCOMPRESSORS**
- Axial-flow compressor turning angle and loss by inviscid-viscous interaction blade-to-blade computation [ASME PAPER 79-GT-5] p0006 A79-30504
- Experimental evaluation of the effect of inlet distortion on compressor blade vibrations p0128 A79-30558
- An off-design correlation of part span damper losses through transonic axial fan rotors [ASME PAPER 79-GT-6] p0028 A79-32329
- Effects of air injection on a turbocharged Teledyne Continental Motors TSIO-360-C engine [SAE PAPER 790607] p0028 A79-36760
- Combined pressure and temperature distortion effects on internal flow of a turbofan engine [AIAA PAPER 79-1309] p0029 A79-39031
- Apparatus and method for reducing thermal stress in a turbine rotor [NASA-CASE-LEW-12232-1] p0013 N79-10057
- Performance of single-stage axial-flow transonic compressor with rotor and stator aspect ratios of 1.19 and 1.26, respectively, and with design pressure ratio of 1.82 [NASA-TP-1338] p0013 N79-10060
- Analysis, design, fabrication and testing of the mini-Brayton rotating unit (Mini-BRU). Volume 1: Text and tables [NASA-CR-159441-VOL-1] p0120 N79-11408
- Analysis, design, fabrication and testing of the Mini-Brayton rotating unit (Mini-BRU). Volume 2: Figures and drawings [NASA-CR-159441-VOL-2] p0120 N79-11409
- Analysis of supersonic stall bending flutter in axial-flow compressor by actuator disk theory [NASA-TP-1345] p0003 N79-13003
- Effects of air injection on a turbocharged Teledyne Continental Motors TSIO-360-C engine [NASA-TM-79121] p0158 N79-20528
- Review of the AGARD S and M panel evaluation program of the NASA-Lewis SRP approach to high-temperature LCF life prediction p0023 N79-27179
- Wind turbines for electric utilities: Development status and economics [NASA-TM-79170] p0143 N79-30719
- Aerodynamic performance of 1.38-pressure-ratio, variable-pitch fan stage [NASA-TP-1502] p0024 N79-31213
- Effects of diffusion factor, aspect ratio and solidity on overall performance of 14 compressor middle stages --- the effects of varying both diffusion through the rotor and compressor blades and blade aspect ratio [NASA-TP-1523] p0038 N79-33210
- TURBOCONVERTERS**
- U TURBOGENERATORS
- TURBOELECTRIC CONVERSION**
- U TURBOGENERATORS
- TURBOFAN ENGINES**
- NT TP-30 ENGINE
- Impact behavior of filament-wound graphite/epoxy fan blades --- foreign object damage to turbofan engines p0025 A79-20880
- Effect of forward velocity and crosswind on the reverse-thrust performance of a variable-pitch fan engine [AIAA PAPER 79-0105] p0025 A79-23512
- Measured and predicted noise of the AVCO-Lycoming YF-102 turbofan engine [AIAA PAPER 79-0641] p0026 A79-26877
- Full-scale engine tests of bulk absorber acoustic inlet treatment [AIAA PAPER 79-0600] p0026 A79-26881
- Effects of inflow distortion profiles on fan tone noise calculated using a 3-D theory [AIAA PAPER 79-0577] p0175 A79-26911
- Noise from struts and splitters in turbofan exit ducts [AIAA PAPER 79-0637] p0178 A79-26923
- Evaluation of two inflow control devices for flight simulation of fan noise using a JT15D engine [AIAA PAPER 79-0654] p0026 A79-26926
- Analysis of radiation patterns of interaction tones generated by inlet rods in the JT15D engine [AIAA PAPER 79-0581] p0027 A79-26944
- Investigation of wing shielding effects on CTOL engine noise [AIAA PAPER 79-0669] p0011 A79-28970
- Characteristics of aeroelastic instabilities in turbomachinery - NASA full scale engine test results [AIAA 79-7011] p0027 A79-29386
- Effect of flight loads on turbofan engine performance deterioration p0027 A79-30559
- Preliminary QCGAT program test results --- Quiet, Clean General Aviation Turbofan [SAE PAPER 790596] p0028 A79-36729
- Test verification of a turbofan partial swirl afterburner [AIAA PAPER 79-1199] p0029 A79-38981
- Multivariable control altitude demonstration on the F100 turbofan engine [AIAA PAPER 79-1204] p0029 A79-39814
- A summary of NASA/Air Force Full Scale Engine Research programs using the F100 engine [AIAA PAPER 79-1308] p0030 A79-40488
- Energy efficient aircraft engines [AIAA PAPER 79-1861] p0030 A79-47918
- QCSSE - The key to future short-haul air transport --- Quiet, Clean, Short-Haul Experimental Engine program p0030 A79-50208
- Energy efficient engine preliminary design and integration study [NASA-CR-135396] p0012 N79-12084
- Effect of flight loads on turbofan engine performance deterioration [NASA-TM-79041] p0013 N79-12085
- Effect of forward velocity and crosswind on the reverse-thrust performance of a variable-pitch fan engine [NASA-TM-79059] p0015 N79-15049
- Preliminary QCGAT program test results [NASA-TM-79013] p0016 N79-15051
- Measured and predicted noise of the Avco-Lycoming YF-102 turbofan noise [NASA-TM-79069] p0016 N79-15957
- Analysis of radiation patterns of interaction tones generated by inlet rods in the JT15D engine [NASA-TM-79074] p0016 N79-15960
- Evaluation of two inflow control devices for flight simulation of fan noise using a JT15D engine [NASA-TM-79072] p0017 N79-15969
- Energy efficient engine: Propulsion system-aircraft integration evaluation [NASA-CR-159488] p0032 N79-16850
- Characteristics of aeroelastic instabilities in turbomachinery - NASA full scale engine test results [NASA-TM-79085] p0126 N79-17263
- Experimental clean combustor program, phase 3: Noise measurement addendum --- CF6-50 high bypass turbofan engine noise [NASA-CR-159458] p0177 N79-17656
- Combined pressure and temperature distortion effects on internal flow of a turbofan engine [NASA-TM-79136] p0012 N79-23963
- Effect of steady-state pressure distortion on flow characteristics entering a turbofan engine [NASA-TM-79134] p0019 N79-23969
- Low-cost directionally-solidified turbine blades, volume 1 [NASA-CR-159464] p0080 N79-24121
- Multivariable control altitude demonstration on the F100 turbofan engine [NASA-TM-79183] p0022 N79-25015
- Operating condition and geometry effects on low-frequency afterburner combustion instability in a turbofan at altitude [NASA-TP-1475] p0022 N79-25022
- NASA CF6 jet engine diagnostics program: Long-term CF6-6D low-pressure turbine deterioration [NASA-CR-159618] p0039 N79-29191
- Effect of steady-state temperature distortion and combined distortion on inlet flow to a turbofan engine [NASA-TM-79237] p0023 N79-30187

- A summary of NASA/Air Force full scale engine research programs using the F100 engine
[NASA-TM-79267] p0024 N79-30188
- Metal spar/superhybrid shell composite fan blades --- for application to turbofan engines
[NASA-CR-159594] p0067 N79-30295
- Experimental Clean Combustor Program (ECCP), phase 3 --- commercial aircraft turbofan engine tests with double annular combustor
[NASA-CR-173384] p0035 N79-31207
- CF6 jet engine performance improvement program. Short core exhaust nozzle performance improvement concept --- specific fuel consumption reduction
[NASA-CR-159564] p0038 N79-33206
- TURBOPANS**
- An off-design correlation of part span damper losses through transonic axial fan rotors
[ASME PAPER 79-GT-6] p0028 A79-32329
- Theoretical fan velocity distortions due to inlets and nozzles
p0006 A79-39810
- Aerodynamic performance of a 1.35-pressure ratio axial-flow fan stage
[NASA-TP-1299] p0002 N79-10022
- Aerodynamic and acoustic effects of eliminating core swirl from a full scale 7.6 stage pressure ratio fan (QF-5A)
[NASA-TM-78991] p0002 N79-11001
- Effects of inflow distortion profiles on fan tone noise calculated using a 3-D theory
[NASA-TM-79082] p0173 N79-16647
- Metal spar/superhybrid shell composite fan blades --- for application to turbofan engines
[NASA-CR-159594] p0067 N79-30295
- Containment of composite fan blades
[NASA-CR-159544] p0067 N79-31348
- TURBOGENERATORS**
- Large wind turbine generators --- NASA program status and potential costs
p0146 A79-15881
- Background and system description of the Mod 1 wind turbine generator
p0155 A79-20825
- Wind turbine generator application places unique demands on tower design and materials
p0155 A79-20826
- Fatigue impact on Mod-1 wind turbine design
p0156 A79-20827
- Wind-turbine-generator rotor-blade concepts with low-cost potential
p0147 A79-20828
- An operating 200 kW horizontal axis wind turbine
p0147 A79-20829
- Microprocessor control of a wind turbine generator
p0147 A79-21302
- Large horizontal axis wind turbine development
p0149 A79-46527
- Lewis Research Center studies of multiple large wind turbine generators on a utility network
p0149 A79-46547
- A 200-kW wind turbine generator conceptual design study
[NASA-TM-79032] p0135 N79-17333
- TURBOJET ENGINE CONTROL**
- Multivariable control altitude demonstration on the F100 turbofan engine
[AIAA PAPER 79-1204] p0029 A79-39814
- A summary of NASA/Air Force full scale engine research programs using the F100 engine
[NASA-TM-79267] p0024 N79-30188
- TURBOJET ENGINES**
- NT DUCTED FAN ENGINES
- NT J-85 ENGINE
- NT T-53 ENGINE
- NT T-55 ENGINE
- NT TF-30 ENGINE
- NT TURBOPAN ENGINES
- NT TURBOPROP ENGINES
- Characteristics of aeroelastic instabilities in turbomachinery - NASA full scale engine test results
[AIAA 79-7011] p0027 A79-29386
- Effect of shocks on film cooling of a full scale turbojet exhaust nozzle having an external expansion surface
[AIAA PAPER 79-1170] p0028 A79-38969
- Experimental evaluation of the effect of inlet distortion on compressor blade vibrations
[NASA-TM-79066] p0126 N79-16300
- Characteristics of aeroelastic instabilities in turbomachinery - NASA full scale engine test results
[NASA-TM-79085] p0126 N79-17263
- Turbojet blade vibration data acquisition design and feasibility testing
[NASA-CR-159505] p0032 N79-18976
- Parametric performance of a turbojet engine combustor using jet A and A diesel fuel
[NASA-TM-79089] p0017 N79-20114
- Identification and dual adaptive control of a turbojet engine
[NASA-TM-79145] p0093 N79-23257
- Effect of shocks on film cooling of a full scale turbojet exhaust nozzle having an external expansion surface
[NASA-TM-79157] p0018 N79-23966
- Effect of shocks on film cooling of a full scale turbojet exhaust nozzle having an external expansion surface
[NASA-TM-79157] p0018 N79-23966
- TURBOMACHINE BLADES**
- NT COMPRESSOR BLADES
- NT ROTOR BLADES (TUBOMACHINERY)
- NT STATOR BLADES
- NT TURBINE BLADES
- Synthesis of blade flutter vibratory patterns using stationary transducers
p0127 A79-10823
- Impact behavior of filament-wound graphite/epoxy fan blades --- foreign object damage to turbofan engines
p0025 A79-20880
- Characteristics of aeroelastic instabilities in turbomachinery - NASA full scale engine test results
[NASA-TM-79085] p0126 N79-17263
- TURBOMACHINERY**
- NT AXIAL FLOW TURBINES
- NT CENTRIFUGAL COMPRESSORS
- NT CENTRIFUGAL PUMPS
- NT GAS TURBINES
- NT SHROUDED TURBINES
- NT STEAM TURBINES
- NT TURBINE PUMPS
- NT TURBINES
- NT TURBOCOMPRESSORS
- NT TURBOFANS
- NT TURBOGENERATORS
- High speed smoke flow visualization for the determination of cascade shock losses
[AIAA PAPER 79-0042] p0005 A79-19495
- Elastomer mounted rotors - An alternative for smoother running turbomachinery
[ASME PAPER 79-GT-149] p0119 A79-32414
- Design problems of small turbomachinery
p0045 N79-22097
- Performance of two-stage fan with larger dampers on first-stage rotor
[NASA-TP-1399] p0018 N79-23967
- A calculation procedure for viscous flow in turbomachines, volume 1
[NASA-CR-159635] p0107 N79-30514
- TURBOPROP AIRCRAFT**
- Prop-fan propulsion - Its status and potential
[SAE PAPER 780995] p0026 A79-25880
- Wind tunnel performance of four energy efficient propellers designed for Mach 0.8 cruise --- Lewis 8x6 foot wind tunnel studies for noise reduction in high speed turboprop aircraft
[NASA-TM-79124] p0003 N79-20069
- TURBOPROP ENGINES**
- NT T-53 ENGINE
- Wind tunnel performance of four energy efficient propellers designed for Mach 0.8 cruise
[SAE PAPER 790573] p0028 A79-36759
- Tone noise of three supersonic helical tip speed propellers in a wind tunnel
p0175 A79-39801
- Energy efficient aircraft engines
[AIAA PAPER 79-1861] p0030 A79-47918
- TURBOPUMPS**
- U TURBINE PUMPS
- TURBOROTORS**
- U TURBINE WHEELS
- TURBOSHAPTS**
- Infrared suppressor effect on T63 turboshaft engine performance

[NASA-TM-78970] p0013 N79-11043
Design problems of small turbomachinery
[NASA-CR-159586] p0046 N79-22097
T700 power turbine rotor multiplane/multispeed
balancing demonstration
[NASA-CR-159586] p0122 N79-25392
Single shaft automotive gas turbine engine
characterization test
[NASA-CR-159654] p0189 N79-32129

TURBULENCE

NT ATMOSPHERIC TURBULENCE

NT HOMOGENEOUS TURBULENCE

NT LOW TURBULENCE

Decay of homogeneous turbulence from a given state
at higher Reynolds number
[NASA-TM-79011] p0102 N79-12361
Turbulence characteristics of compressor discharge
flows --- JT9D engine tests
p0019 N79-24995
Turbulence measurements in the compressor exit
flow of a General Electric CF6-50 engine
p0019 N79-24996

TURBULENCE EFFECTS

Turbulence effects on flame speed and flame
structure
[AIAA PAPER 79-0016] p0070 A79-19480
The free jet as a simulator of forward velocity
effects on jet noise
[NASA-CR-3056] p0176 N79-14873

TURBULENCE METERS

Experimental clean combustor program: Phase 3:
Turbulence measurement addendum
[NASA-CR-135422] p0031 N79-12088

TURBULENT BOUNDARY LAYER

Reduction of rotor-turbulence interaction noise in
static fan noise testing
[AIAA PAPER 79-0656] p0036 A79-26925
An experimental investigation of forced mixing of
a turbulent boundary layer in an annular diffuser
--- for boundary layer control
[NASA-TM-79171] p0004 N79-23920

TURBULENT DIFFUSION

Turbulence characteristics of compressor discharge
flows --- JT9D engine tests
p0019 N79-24995

TURBULENT FLOW

Comparison of a correlation term-discard closure
for decaying homogeneous turbulence with
experiment
p0106 A79-22424
Turbulence generated by the interaction of entropy
fluctuations with non-uniform mean flows
p0106 A79-45468
Trailing edge noise data with comparison to theory
[AIAA PAPER 79-1524] p0176 A79-47340
Development of a three-dimensional turbulent duct
flow analysis
[NASA-CR-3029] p0106 N79-12366
A three-dimensional turbulent compressible flow
model for ejector and fluted mixers
[NASA-CR-159467] p0100 N79-14325
Evaluation of two inflow control devices for
flight simulation of fan noise using a JT15D
engine
[NASA-TM-79072] p0017 N79-15969
Study of mean- and turbulent-velocity fields in a
large-scale turbine-vane passage
[NASA-CR-3067] p0032 N79-16853
Flow friction of the turbulent coolant flow in
cryogenic porous cables
[NASA-TM-79052] p0103 N79-20341
Full-coverage film cooling: 3-dimensional
measurements of turbulence structure and
prediction of recovery region hydrodynamics
[NASA-CR-3104] p0106 N79-22428
Heat transfer to a full-coverage, film-cooled
surface with compound-angle (30 deg and 45 deg)
hole injection
[NASA-CR-3103] p0107 N79-22429
Laser anemometer measurements at the exit of a
T63-C20 combustor
[NASA-CR-159623] p0107 N79-28456

TURBULENT JETS

Heat transfer from a row of jets impinging on
concave semi-cylindrical surface
p0108 A79-42890

TWO DIMENSIONAL BODIES

Two-dimensional random surface model for
asperity-contact in elastohydrodynamic lubrication

p0120 A79-39811
TWO DIMENSIONAL FLOW
A statistical theory of sound radiation from a
two-dimensional lined duct
[AIAA PAPER 79-1521] p0176 A79-46707
TWO PHASE FLOW
Two-phase choked flow of cryogenic fluids in
converging-diverging nozzles
[NASA-TP-1484] p0105 N79-29468
Application of the principle of similarity fluid
mechanics
[NASA-TM-79258] p0105 N79-30515

U

ULTRA SHORT WAVE RADIO EQUIPMENT

U VERY HIGH FREQUENCY RADIO EQUIPMENT

ULTRAHIGH FREQUENCIES

Global disaster satellite communications system
for disaster assessment and relief coordination
p0095 A79-30394

UHF coplanar-slot antenna for
aircraft-to-satellite data communications
[NASA-TM-79239] p0010 N79-31185

ULTRASONIC TESTS

Use of an ultrasonic-acoustic technique for
nondestructive evaluation of fiber composite
strength
p0064 A79-15545

Computer signal processing for ultrasonic
attenuation and velocity measurements for
material property characterizations
p0125 A79-39809

Definition of mutually optimum NDI and proof test
criteria for 2219 aluminum pressure vessels.
Volume 1: Methods
[NASA-CR-135445] p0125 N79-21410

Definition of mutually optimum NDI and proof test
criteria for 2219 aluminum pressure vessels.
Volume 2: Optimization and fracture studies
[NASA-CR-135446] p0125 N79-21411

Definition of mutually optimum NDI and proof test
criteria for 2219 aluminum pressure vessels.
Volume 3: Applications to rail defect evaluation
[NASA-CR-135447] p0125 N79-21412

ULTRASONICS

Computer signal processing for ultrasonic
attenuation and velocity measurements for
material property characterizations
[NASA-TM-79180] p0127 N79-24355

ULTRAVIOLET LASERS

Gain measurements of the Ca-Ie charge exchange
system --- for UV lasers
p0112 A79-19078

ULTRAVIOLET LIGHT

U ULTRAVIOLET RADIATION

ULTRAVIOLET RADIATION

Ultraviolet irradiation at elevated temperatures
and thermal cycling in vacuum of PEP-A covered
silicon solar cells
p0148 A79-40898

UV blocking filters for polymeric films
p0088 A79-51103

UNIVAC COMPUTERS

NT UNIVAC 1100 SERIES COMPUTERS

UNIVAC 1100 SERIES COMPUTERS

An expanded system simulation model for solar
energy storage (UNIVAC operation manual
revisions), volume 2
[NASA-CR-159602] p0166 N79-33882

UNMANNED SPACECRAFT

NT JUPITER PROBES

UNSTEADY FLOW

Unsteady flow in a supersonic cascade with
subsonic leading-edge locus
p0005 A79-16047
Unsteady vortical and entropic distortions of
potential flows round arbitrary obstacles
p0005 A79-19452
Scattering and distortion of the unsteady motion
on transversely sheared mean flows
p0106 A79-37140

UPPER ATMOSPHERE

NT MAGNETOSPHERE

UPWELLING

U UPWELLING WATER

UPWELLING WATER

A comparison of measured and calculated upwelling
radiance over water as a function of sensor

- altitude
p0162 A79-51096
- A comparison of measured and calculated upwelling
radiance over water as a function of sensor
altitude
[NASA-TN-79147] p0131 A79-22589
- URTHANES
Evaluation of urethane for feasibility of use in
wind turbine blade design
[NASA-CR-159530] p0153 A79-20497
- USER MANUALS (COMPUTER PROGRAMS)
User's manual for FRAC3D: Supplement to report on
stress analysis for structures with surface cracks
[NASA-CR-159401] p0129 A79-13406
- High speed cylindrical roller bearing analysis,
SKF computer program CYBEAN. Volume 2: User's
manual
[NASA-CR-159461] p0121 A79-17223
- User's guide to computer programs JET 5A and
CIVM-JET 5B to calculate the large
elastic-plastic dynamically-induced deformations
of multilayer partial and/or complete structural
rings
[NASA-CR-159484] p0129 A79-18343
- Simulation of fluidized bed coal combustors
[NASA-CR-159529] p0153 A79-20487
- Lewis hybrid computing system, user's manual
[NASA-TN-79111] p0165 A79-20752
- NASCAP user's manual, 1978
[NASA-CR-159417] p0100 A79-27398
- CFLP: Coupled Eulerian-Lagrangian Finite Element
program for high velocity impact. Part 2:
Program user's manual
[NASA-CR-159396] p0166 A79-29833
- An expanded system simulation model for solar
energy storage (UNIVAC operation manual
revisions), volume 2
[NASA-CR-159602] p0166 A79-33882
- SINWEST: A simulation model for wind and
photovoltaic energy storage systems (CDC user's
manual), volume 1
[NASA-CR-159607] p0166 A79-33883
- SINWEST: A simulation model for wind and
photovoltaic energy storage systems (cdc program
descriptions), volume 2
[NASA-CR-159608] p0167 A79-33884
- UTILITIES
Utility operational experience on the NASA/DOE
Mod-OA 200 kW Wind Turbine
p0149 A79-46537
- Photovoltaic power systems for rural areas of
developing countries
[NASA-TN-79097] p0135 A79-15411
- Utility operational experience on the NASA/DOE
MOD-OA 200-kW wind turbine
[NASA-TN-79084] p0136 A79-20494
- Large horizontal axis wind turbine development
[NASA-TN-79174] p0140 A79-26504
- UTILIZATION
NT COAL UTILIZATION
NT LASER APPLICATIONS
NT WASTE ENERGY UTILIZATION
NT WINDPOWER UTILIZATION
Applications of thermal energy storage to process
heat storage and recovery in the paper and pulp
industry
[NASA-CR-159398] p0154 A79-30801
- UV LASERS
U ULTRAVIOLET LASERS
- V
- V BAND
U EXTREMELY HIGH FREQUENCIES
- V/STOL AIRCRAFT
NT ROTARY WING AIRCRAFT
NT SHORT TAKEOFF AIRCRAFT
NT VERTICAL TAKEOFF AIRCRAFT
Performance of a V/STOL tilt nacelle inlet with
blowing boundary layer control
[AIAA PAPER 79-1163] p0006 A79-47347
- Recent applications of theoretical analysis to
V/STOL inlet design
p0006 A79-49530
- Theoretical fan velocity distortions due to inlets
and nozzles --- in V/STOL aircraft
[NASA-TN-79150] p0003 A79-23911
- Performance of a V/STOL tilt nacelle inlet with
blowing boundary layer control
- [NASA-TN-79176] p0004 A79-27093
- Recent applications of theoretical analysis to
V/STOL inlet design
[NASA-TN-79211] p0004 A79-29143
- VACUUM
Thermocouples of molybdenum and iridium alloys for
more stable vacuum-high temperature performance
[NASA-CASE-LEW-12174-2] p0109 A79-14346
- VACUUM APPARATUS
NT KNUDSEN GAGES
VACUUM GAGES
NT KNUDSEN GAGES
VACUUM TESTS
NT THERMAL VACUUM TESTS
Ultraviolet irradiation at elevated temperatures
and thermal cycling in vacuum of FEP-A covered
silicon solar cells
p0148 A79-40898
- VACUUM TUBE OSCILLATORS
NT KLYSTRONS
NT TRAVELING WAVE TUBES
VACUUM TUBES
NT KLYSTRONS
NT TRAVELING WAVE TUBES
VALIDITY
Spacecraft charging modeling development and
validation study
p0050 A79-24051
- VALVES
NT DAMPERS (VALVES)
VANES
NT GUIDE VANES
Cold-air performance of free power turbine
designed for 112-kilowatt automotive gas-turbine
engine 3: Effect of stator vane end clearances
on performance
[NASA-TN-78956] p0014 A79-13049
- Liquid oxygen/liquid hydrogen boost/vane pump for
the advanced orbit transfer vehicles auxiliary
propulsion system
[NASA-CR-159648] p0057 A79-31341
- VAPOR DEPOSITION
Superconducting properties of evaporated copper
molybdenum sulfide films
p0184 A79-20219
- Alternate methods of applying diffusants to
silicon solar cells --- screen printing of
thick-film paste materials and vapor phase
transport from solid sources
[NASA-CR-159508] p0153 A79-29603
- VAPOR PHASES
Condensation on a noncollapsing vapor bubble in a
subcooled liquid
[NASA-TN-79212] p0105 A79-27461
- VAPORIZING
NT COAL GASIFICATION
NT EVAPORATION
NT FILM BOILING
Effect of degree of fuel vaporization upon
emissions for a premixed prevaporized combustion
system
[AIAA PAPER 79-1320] p0071 A79-39036
- Mass spectrometric investigation of the
vaporization of sodium and potassium chromates -
Preliminary results
p0071 A79-45533
- Lean, premixed, prevaporized combustion for
aircraft gas turbine engines
[NASA-TN-79148] p0018 A79-23964
- Lean, premixed, prevaporized combustion for
aircraft gas turbine engines
[NASA-TN-79148] p0018 A79-23964
- Effect of degree of fuel vaporization upon
emissions for a premixed prevaporized combustion
system --- for gas turbine engines
[NASA-TN-79154] p0012 A79-23965
- Premixed Prevaporized Combustor Technology Forum
[NASA-CR-2078] p0019 A79-24994
- Effect of degree of fuel vaporization on emissions
for a premixed-prevaporized combustor system
p0020 A79-25003
- Mass spectrometric investigation of the
vaporization of sodium and potassium chromates:
Preliminary results
[NASA-TN-79210] p0069 A79-27279
- VAPORS
NT WATER VAPOR
Condensation on a noncollapsing vapor bubble in a
subcooled liquid

- VARIABLE AREA WINGS**
U TRAILING-EDGE FLAPS
VARIABLE CYCLE ENGINES
 Multivariable control altitude demonstration on the F100 turbofan engine [AIAA PAPER 79-1204] p0029 A79-39814
 Progress on Variable Cycle Engines [AIAA PAPER 79-1312] p0036 A79-40759
 Definition study of a Variable Cycle Experimental Engine (VCEE) and associated test program and test plan [NASA-CR-159419] p0031 A79-11042
 Definition study for variable cycle engine testbed engine and associated test program [NASA-CR-159459] p0031 A79-13448
 Premix fuels study applicable to duct burner conditions for a variable cycle engine [NASA-CR-159513] p0091 A79-20266
 Variable cycle engine technology program planning and definition study [NASA-CR-159539] p0034 A79-23084
- VARIABLE LIFT**
U LIFT
VARIABLE PITCH PROPELLERS
 Effect of forward velocity and crosswind on the reverse-thrust performance of a variable-pitch fan engine [AIAA PAPER 79-0105] p0025 A79-23512
 Aerodynamic performance of 1.38-pressure-ratio, variable-pitch fan stage [NASA-TF-1502] p0024 A79-31213
- VARIATIONAL PRINCIPLES**
 Recent developments at ONERA in the field of structural analysis methods [ONERA, TP NO. 1979-79] A79-49537
- VCE**
U VARIABLE CYCLE ENGINES
VELOCITY
 NT ACOUSTIC VELOCITY
 NT CRITICAL VELOCITY
 NT EXHAUST VELOCITY
 NT HIGH SPEED
 NT PROPAGATION VELOCITY
 NT ROTOR SPEED
 NT SUBSONIC SPEED
 NT SUPERSONIC SPEEDS
 NT TIP SPEED
 NT WIND VELOCITY
VELOCITY DISTRIBUTION
 Velocity, temperature, and electrical conductivity profiles in hydrogen-oxygen MHD duct flows p0182 A79-26184
 A jet exhaust noise prediction procedure for inverted velocity profile coannular nozzles [AIAA PAPER 79-0633] p0178 A79-28964
 Effects of geometric and flow-field variables on inverted-velocity-profile coaxial jet noise and source distributions [AIAA PAPER 79-0635] p0175 A79-32126
 Theoretical fan velocity distortions due to inlets and nozzles p0006 A79-39810
 The free jet as a simulator of forward velocity effects on jet noise [NASA-CR-3056] p0176 A79-14873
 Study of mean- and turbulent-velocity fields in a large-scale turbine-vane passage [NASA-CR-3067] p0032 A79-16853
 Theoretical fan velocity distortions due to inlets and nozzles --- in V/STOL aircraft [NASA-TM-79150] p0003 A79-23911
 Acoustic and aerodynamic performance investigation of inverted velocity profile coannular plug nozzles, comprehensive data report, volume 1 [NASA-CR-159575-VOL-1] p0177 A79-26884
 Acoustic and aerodynamic performance investigation of inverted velocity profile coannular plug nozzles, comprehensive data report, volume 2 [NASA-CR-159575-VOL-2] p0177 A79-26885
 Acoustic and aerodynamic performance investigation of inverted velocity profile coannular plug nozzles, comprehensive data report, volume 3 [NASA-CR-159575-VOL-3] p0177 A79-26886
 Studies of the acoustic transmission characteristics of coaxial nozzles with inverted velocity profiles: Comprehensive data report --- nozzle transfer functions [NASA-CR-159628] p0177 A79-27933
- Effect of rotor meridional velocity ratio on response to inlet radial and circumferential distortion [NASA-TP-1278] p0023 A79-28177
 Aerodynamic and acoustic investigation of inverted velocity profile coannular exhaust nozzle models and development of aerodynamic and acoustic prediction procedures, comprehensive data report, volume 1 [NASA-CR-159515] p0034 A79-30185
 Aerodynamic and acoustic investigation of inverted velocity profile coannular exhaust nozzle models and development of aerodynamic and acoustic prediction procedures, comprehensive data report, volume 2 [NASA-CR-159516] p0034 A79-30186
 Aerodynamic and acoustic investigation of inverted velocity profile coannular exhaust nozzle models and development of aerodynamic and acoustic prediction procedures [NASA-CR-3168] p0035 A79-31212
- VELOCITY FIELDS**
U VELOCITY DISTRIBUTION
VELOCITY MEASUREMENT
 Computer signal processing for ultrasonic attenuation and velocity measurements for material property characterizations p0125 A79-39809
 Computer signal processing for ultrasonic attenuation and velocity measurements for material property characterizations [NASA-TM-79180] p0127 A79-24359
- VELOCITY PROFILES**
U VELOCITY DISTRIBUTION
VENTURI TUBES
 Effect of swirler-mounted mixing venturi on emissions of flame-tube combustor using jet A fuel [NASA-TP-1393] p0015 A79-14099
 Performance of a multiple venturi fuel-air preparation system --- fuel injection for gas turbines p0020 A79-25000
- VERTICAL TAKEOFF AIRCRAFT**
 Effect of lip and centerbody geometry on aerodynamic performance of inlets for tilting-macelle VTOL aircraft [AIAA PAPER 79-03F1] p0025 A79-23509
 Theoretical study of VTOL tilt-macelle axisymmetric inlet geometries [NASA-TP-1380] p0003 A79-14996
 Effect of lip and centerbody geometry on aerodynamic performance of inlets for tilting-macelle VTOL aircraft [NASA-TM-79056] p0003 A79-14999
 Aerodynamic performance of axial-flow fan stage operated at nine inlet guide vane angles --- to be used on vertical lift aircraft [NASA-TP-1510] p0024 A79-31214
- VERY HIGH FREQUENCY RADIO EQUIPMENT**
 VHF downlink communication system for SLAR data p0045 A79-51097
- VIBRATION**
 NT FORCED VIBRATION
 NT SCGW EFFECTS
 NT RESONANT VIBRATION
 NT STRUCTURAL VIBRATION
 NT SUPERSONIC FLUTTER
 NT TRANSONIC FLUTTER
 Study of T53 engine vibration [NASA-CR-135449] p0030 A79-10061
- VIBRATION DAMPERS**
U VIBRATION ISOLATORS
VIBRATION DAMPING
 High temperature dynamic modulus and damping of aluminum and titanium matrix composites p0065 A79-31040
 Dynamic mechanical analysis of fiber reinforced composites p0065 A79-26132
 Nonsynchronous vibrations observed in a supercritical power transmission shaft [ASME PAPER 79-GT-146] p0123 A79-32412
 Space shuttle active-pogo-suppressor control design using linear quadratic regulator techniques [NASA-TP-1217] p0097 A79-14309
 T700 power turbine rotor multiplane/multispeed balancing demonstration [NASA-CR-159586] p0122 A79-25392

VIBRATION EFFECTS

NT POGO EFFECTS

VIBRATION ISOLATORS

Design and test of a squeeze-film damper for a flexible power transmission shaft p0123 A79-16011

Elastomer mounted rotors - An alternative for smoother running turbomachinery [ASME PAPER 79-GT-149] p0119 A79-32414

Development of procedures for calculating stiffness and damping of elastomers in engineering applications. Part 5: Elastomer performance limits and the design and test of an elastomer damper [NASA-CR-159552] p0122 W79-24373

Performance of two-stage fan with a first-stage rotor redesigned to account for the presence of a part-span damper [NASA-TP-1483] p0024 W79-30191

VIBRATION MEASUREMENT

Synthesis of blade flutter vibratory patterns using stationary transducers p0127 A79-10823

Experimental evaluation of the effect of inlet distortion on compressor blade vibrations [NASA-TM-79066] p0126 W79-16300

Turbojet blade vibration data acquisition design and feasibility testing [NASA-CR-159505] p0032 W79-18976

VIBRATION PROTECTION

U VIBRATION ISOLATORS

VIBRATION TESTS

High temperature dynamic modulus and damping of aluminum and titanium matrix composites p0065 A79-26132

VIDEO COMMUNICATION

Design of a video teleconference facility for a synchronous satellite communications link [NASA-TP-1376] p0094 W79-14275

VISCOSITY

Hartmann flow with temperature-dependent physical properties --- magnetohydrodynamics of liquid metal p0182 A79-15597

VISCOUS FLOW

NT BOUNDARY LAYER SEPARATION

NT SECONDARY FLOW

Axial-flow compressor turning angle and loss by inviscid-viscous interaction blade-to-blade computation [ASME PAPER 79-GT-5] p0006 A79-30504

A calculation procedure for viscous flow in turbomachines, volume 1 [NASA-CR-159635] p0107 W79-30514

VISUALIZATION OF FLOW

U FLOW VISUALIZATION

VOICE COMMUNICATION

NT TELEPHONE

Results of thin-route satellite communication system analyses including estimated service costs p0095 A79-30395

VOLATILIZATION

U VAPORIZING

VOLT-AMPERE CHARACTERISTICS

Factors affecting the open-circuit voltage and electrode kinetics of some iron/titanium/redox flow cells p0146 A79-11824

Discharge characteristics of 300 ampere-hour Ni-Zn traction cells [NASA-TM-79244] p0143 W79-31781

VOLTAGE

U ELECTRIC POTENTIAL

VOLTAGE BREAKDOWN

U ELECTRICAL FAULTS

VOLTAGE CONVERTERS (DC TO DC)

A general unified approach to modelling switching dc-to-dc converters in discontinuous conduction mode p0101 A79-10830

Generalized computer-aided discrete time domain modeling and analysis of dc-dc converters p0099 A79-10881

Power converter design optimization p0099 A79-10885

A new optimum topology switching dc-to-dc converter p0101 A79-10888

Modeling of switching regulator power stages with and without zero-inductor-current dwell time

Lightweight multiple output converter development [NASA-CR-159526] p0101 A79-49398

Analytical core loss calculations for magnetic materials used in high frequency high power converter applications [NASA-TM-79234] p0098 W79-31499

VOLTAGE GENERATORS

NT PHOTOVOLTAIC CELLS

VOLTAGE MEASUREMENT

U ELECTRICAL MEASUREMENT

VOLTAGE REGULATORS

Analysis of a parallel-arrayed power regulating system p0101 A79-49397

Modeling of switching regulator power stages with and without zero-inductor-current dwell time p0101 A79-49398

VOLUMETRIC ANALYSIS

A reduced volumetric expansion factor plot [NASA-TM-79240] p0105 W79-31527

VORTEX COLUMNS

U VORTICES

VORTEX DISTURBANCES

U VORTICES

VORTEX FLOW

U VORTICES

VORTEX GENERATION

U VORTEX GENERATORS

VORTEX GENERATORS

An experimental investigation of forced mixing of a turbulent boundary layer in an annular diffuser --- for boundary layer control [NASA-TM-79171] p0004 W79-23920

VORTEX TUBES

U VORTICES

VORTICES

Unsteady vortical and entropic distortions of potential flows round arbitrary obstacles p0005 A79-19452

Performance of a vortex-controlled diffuser in an annular swirl-can combustor at inlet Mach numbers up to 0.53 [NASA-TP-1452] p0017 W79-22099

VTOL AIRCRAFT

U VERTICAL TAKEOFF AIRCRAFT

W

WAFERS

Alternate methods of applying diffusants to silicon solar cells --- screen printing of thick-film paste materials and vapor phase transport from solid sources [NASA-CR-159508] p0153 W79-29603

High efficiency cell geometry p0143 W79-32653

WALL FLOW

Duct wall impedance control as an advanced concept for acoustic suppression enhancement --- engine noise reduction [NASA-CR-159425] p0176 W79-10842

WALL JETS

Heat transfer from a row of jets impinging on concave semi-cylindrical surface p0108 A79-42890

WANKEL ENGINES

A review of Curtiss-Wright rotary engine developments with respect to general aviation potential [SAE PAPER 790621] p0036 A79-36749

An overview of NASA research on positive displacement type general aviation engines [NASA-TM-79254] p0024 W79-31210

WARNING DEVICES

U WARNING SYSTEMS

WARNING SIGNALS

U WARNING SYSTEMS

WARNING SYSTEMS

Satellite communications for disaster relief operations [NASA-TM-78198] p0094 W79-27351

WASTE ENERGY UTILIZATION

Thermal energy storage for industrial waste heat recovery p0145 A79-10101

Analysis of a fuel cell on-site integrated energy system for a residential complex [AIAA PAPER 79-0990] p0147 A79-38192

- Applications of thermal energy storage to process heat and waste heat recovery in the iron and steel industry
[NASA-CN-159397] p0151 N79-11473
- Thermal storage for industrial process and reject heat
[NASA-TN-78994] p0134 N79-11481
- The role of thermal energy storage in industrial energy conservation
[NASA-TN-79122] p0137 N79-21550
- WASTES**
- WT INDUSTRIAL WASTES**
- WATER**
- WT SURFACE WATER**
- WATER COLOR**
- A comparison of measured and calculated upwelling radiance over water as a function of sensor altitude
p0162 A79-51096
- WATER CONTENT**
- U MOISTURE CONTENT**
- WATER COOLING**
- U LIQUID COOLING**
- WATER FLOW**
- Atomization of water jets and sheets in axial and swirling airflows
[NASA-TN-79043] p0102 N79-12362
- WATER INJECTION**
- Atomization of water jets and sheets in axial and swirling airflows
[ASME PAPER 79-GT-170] p0106 A79-30556
- WATER QUALITY**
- A comparison of measured and calculated upwelling radiance over water as a function of sensor altitude
p0162 A79-51096
- WATER VAPOR**
- An analysis of the first two years of GASP data --- Global Atmospheric Sampling Program
p0160 A79-15068
- WATER VEHICLES**
- WT SHIPS**
- WAVE ATTENUATION**
- WT ACOUSTIC ATTENUATION**
- WT SHOCK WAVE ATTENUATION**
- Modal propagation angles in ducts with soft walls and their connection with suppressor performance
[NASA-TN-79081] p0173 N79-16646
- WAVE OSCILLATORS**
- U OSCILLATORS**
- WAVE PROPAGATION**
- WT ACOUSTIC PROPAGATION**
- Modal propagation angles in a cylindrical duct with flow and their relation to sound radiation
[NASA-TN-79039] p0172 N79-15756
- Computation of atmospheric attenuation of sound for fractional-octave bands
[NASA-TF-1412] p0173 N79-17659
- WAVEFORMS**
- Computer signal processing for ultrasonic attenuation and velocity measurements for material property characterizations
[NASA-TN-79188] p0127 N79-24359
- Effect of positive pulse charge waveforms on cycle life of nickel-zinc cells
[NASA-TN-79215] p0142 N79-28728
- WAVEGUIDES**
- WT BEAM WAVEGUIDES**
- WEAR**
- Wear of seal materials used in aircraft propulsion systems
[NASA-TN-79003] p0073 N79-12204
- Friction and wear characteristics of iron-chromium alloys in contact with themselves and silicon carbide
[NASA-TF-1387] p0114 N79-14387
- The friction and wear of metals and binary alloys in contact with an abrasive grit of single-crystal silicon carbide
[NASA-TN-79131] p0075 N79-22274
- Effect of sterilization irradiation on friction and wear of ultrahigh-molecular-weight polyethylene
[NASA-TF-1462] p0082 N79-23216
- Two-dimensional random surface model for asperity-contact in elastohydrodynamic lubrication
[NASA-TN-79006] p0115 N79-23430
- Diagnostics of wear in aeronautical systems
[NASA-TN-79185] p0115 N79-24350
- Lubricating and wear mechanisms for a hemisphere sliding on polyimide-bonded graphite fluoride film
[NASA-TF-1524] p0084 N79-30381
- Surface chemistry of iron sliding in air and nitrogen lubricated with hexadecane and hexadecane containing dibenzyl-dithiolide
[NASA-TF-1545] p0059 N79-31346
- Ferrographic analysis of wear debris from full-scale bearing fatigue tests
[NASA-TF-1511] p0116 N79-31605
- WEAR INHIBITORS**
- The friction and wear properties of sputtered hard refractory compounds
p0085 A79-16666
- An IPS study of the adherence of refractory carbide, silicide, and boride RF-sputtered wear-resistant coatings --- X-ray photoelectron Spectroscopy of steel surfaces
p0085 A79-21022
- Development of surface coatings for air-lubricated, compliant journal bearings to 650 C
[ASLE PREPRINT 78-LC-3C-1] p0123 A79-23252
- Coatings for wear and lubrication
p0060 A79-27232
- Static evaluation of surface coatings for compliant gas bearings in an oxidizing atmosphere to 650 C
p0088 A79-31957
- Adherence of sputtered titanium carbides
[NASA-TN-79117] p0074 N79-20220
- The erosion/corrosion of small superalloy turbine rotors operating in the effluent of a PFB coal combustor
[NASA-TN-79227] p0076 N79-30356
- WEAR TESTS**
- Laser spectroscopy analysis in adhesion, friction and wear studies
p0110 A79-10992
- Development of surface coatings for air-lubricated, compliant journal bearings to 650 C
[ASLE PREPRINT 78-LC-3C-1] p0123 A79-23252
- Use of a nitrogen-argon plasma to improve adherence of sputtered titanium carbide coatings on steel
p0119 A79-25103
- Friction and fracture of single-crystal silicon carbide in contact with itself and titanium
p0086 A79-32149
- Friction and wear of single-crystal manganese-zinc ferrite
p0185 A79-34994
- Fretting wear of iron, nickel, and titanium under varied environmental conditions
p0078 A79-34995
- Diagnostics of wear in aeronautical systems
p0120 A79-39805
- The effect of nitrogen ion (N⁺) implantation on the friction and wear characteristics of iron
[NASA-TN-79029] p0073 N79-12201
- Fretting wear of iron, nickel, and titanium under varied environmental conditions
[NASA-TN-78972] p0073 N79-12203
- Effect of nitrogen-containing plasma on adherence, friction, and wear of radiofrequency-sputtered titanium carbide coating
[NASA-TF-1377] p0081 N79-15184
- Friction and wear of single-crystal manganese-zinc ferrite
[NASA-TF-78980] p0184 N79-16699
- Friction and wear with a single-crystal abrasive grit of silicon carbide in contact with iron base binary alloys in oil: Effects of alloying element and its content
[NASA-TF-1394] p0114 N79-17227
- Wear of aluminum and hypoeutectic aluminum-silicon alloys in boundary-lubricated pin-on disk sliding
[NASA-TF-1442] p0074 N79-21184
- Infrared analysis of polyethylene wear specimens using attenuated total reflection spectroscopy --- effects of radiation on the surface properties of materials for total joint prostheses
[NASA-TN-79228] p0083 N79-29329
- The erosion/corrosion of small superalloy turbine rotors operating in the effluent of a PFB coal combustor
[NASA-TN-79227] p0076 N79-30356

- Surface chemistry of iron sliding in air and nitrogen lubricated with hexadecane and hexadecane containing dibenzyl-dithiolide [NASA-TP-1545] p0059 N79-31346
- Evaluation and auger analysis of a zinc-dialkyl-dithiophosphate antiwear additive in several diester lubricants [NASA-TP-1544] p0084 N79-32359
- WEBS (SUPPORTS)**
Integrated gas turbine engine-nacelle [NASA-CASR-LZW-12389-3] p0014 N79-14096
- WEIGHT (MASS)**
WT STRUCTURAL WEIGHT
Development of advanced fuel cell system [NASA-CR-159443] p0151 N79-12553
- WEIGHT ANALYSIS**
A method to estimate weight and dimensions of large and small gas turbine engines [NASA-CR-159481] p0015 N79-15046
- WEIGHT FACTORS**
U WEIGHT (MASS)
WEIGHT MEASUREMENT
A method to estimate weight and dimensions of large and small gas turbine engines [NASA-CR-159481] p0015 N79-15046
- WEIGHTLESSNESS**
Axial jet mixing of ethanol in cylindrical containers during weightlessness [NASA-TP-1487] p0030 N79-28350
- Contoured tank outlets for draining of cylindrical tanks in low-gravity environment --- Lewis Research Center Zero Gravity Facility [NASA-TP-1492] p0105 N79-29467
- Combustion of porous solids at reduced gravitational conditions [NASA-CR-3197] p0072 N79-33288
- WELDED STRUCTURES**
WT STEEL STRUCTURES
- WELDING**
WT BRAZING
WT COLD WELDING
Interdiffusion behavior of tungsten or rhenium and group 5 and 6 elements and alloys of the periodic table. Part 2b: Appendices [NASA-CR-334526] p0080 N79-33305
- WETNESS**
U MOISTURE CONTENT
- WHEELS**
WT TURBINE WHEELS
- WHIRLING TESTS**
U SPIN TESTS
- WIGHTMAN THEORY**
J FIELD THEORY (PHYSICS)
- WIND (METEOROLOGICAL)**
An operating 200-kW horizontal axis wind turbine [NASA-TR-79034] p0135 N79-16357
- WIND EFFECTS**
Effect of forward velocity and crosswind on the reverse-thrust performance of a variable-pitch fan engine [AIAA PAPER 79-0105] p0025 A79-23512
- WIND PROFILES**
Commercial aircraft derived high resolution wind and temperature data from the tropics for FGGE: Implications for NASA p0161 N79-20621
- The use of wind data with an operational wind turbine in a research and development environment [NASA-TR-73832] p0140 N79-26502
- WIND TUNNEL TESTS**
High speed smoke flow visualization for the determination of cascade shock losses [AIAA PAPER 79-0042] p0005 A79-19495
- Aerodynamic performance of scarf inlets [AIAA PAPER 79-0380] p0005 A79-23510
- Wind tunnel performance of four energy efficient propellers designed for Mach 0.8 cruise [SAE PAPER 790573] p0028 A79-36759
- Tone noise of three supersonic helical tip speed propellers in a wind tunnel p0175 A79-39801
- Wind tunnel tests of a blade subjected to midchord torsional oscillation at high subsonic stall flutter conditions [NASA-TR-78998] p0002 N79-12016
- Effect of forward velocity and crosswind on the reverse-thrust performance of a variable-pitch fan engine [NASA-TR-79059] p0015 N79-15049
- Tone noise of three supersonic helical tip speed propellers in a wind tunnel at 0.8 Mach number [NASA-TR-79046] p0172 N79-15758
- Study of mean- and turbulent-velocity fields in a large-scale turbine-vane passage [NASA-CR-3067] p0032 N79-16853
- Wind tunnel performance of four energy efficient propellers designed for Mach 0.8 cruise --- Lewis 8x6 foot wind tunnel studies for noise reduction in high speed turboprop aircraft [NASA-TR-79124] p0003 N79-20069
- Tone noise of three supersonic helical tip speed propellers in a wind tunnel [NASA-TR-79167] p0174 N79-25840
- A throat-bypass stability-bleed system using relief valves to increase the transient stability of a mixed-compression inlet --- YF-12 aircraft inlet tests in the Lewis 10 by 10 ft supersonic wind tunnel [NASA-TP-1083] p0023 N79-28176
- WIND TUNNELS**
WT SUPERSONIC WIND TUNNELS
WT TRANSONIC WIND TUNNELS
WIND VELOCITY
Wind turbines for electric utilities: Development status and economics [NASA-TR-79170] p0142 N79-30719
- WINDING**
WT FILAMENT WINDING
WINDMILLS (WINDPOWERED MACHINES)
Design and operating experience on the U.S. Department of Energy Experimental Mod-C 100 kW Wind Turbine p0145 A79-10234
- DOE/NASA Mod-OA wind turbine performance p0145 A79-10235
- The application of hydraulics in the 2,000 kW wind turbine generator p0156 A79-27400
- Evaluation of HOSTAS computer code for predicting dynamic loads in two-bladed wind turbines [AIAA 79-0733] p0005 A79-29007
- WINDOWS (APERTURES)**
Holography through optically active windows [NASA-TP-1414] p0109 N79-17195
- WINDPOWER UTILIZATION**
SINWEST - A simulation model for wind energy storage systems
p0145 A79-10241
- Large wind turbine generators --- NASA program status and potential costs p0146 A79-15881
- Design, fabrication, and test of a composite material wind turbine rotor blade [NASA-CR-135389] p0150 N79-10525
- An expanded system simulation model for solar energy storage (UNIVAC operation manual revisions), volume 2 [NASA-CR-159602] p0166 N79-33882
- SINWEST: A simulation model for wind and photovoltaic energy storage systems (CDC user's manual), volume 1** [NASA-CR-159607] p0166 N79-33883
- SINWEST: A simulation model for wind and photovoltaic energy storage systems (cdc program descriptions), volume 2** [NASA-CR-159608] p0167 N79-33884
- WINDPOWERED GENERATORS**
Design and operating experience on the U.S. Department of Energy Experimental Mod-C 100 kW Wind Turbine p0145 A79-10234
- DOE/NASA Mod-OA wind turbine performance p0145 A79-10235
- Control of wind turbine generators connected to power systems p0146 A79-15574
- Large wind turbine generators --- NASA program status and potential costs p0146 A79-15881
- Background and system description of the Mod 1 wind turbine generator p0155 A79-20825
- Wind turbine generator application places unique demands on tower design and materials p0155 A79-20826
- Fatigue impact on Mod-1 wind turbine design p0156 A79-20827

Wind-turbine-generator rotor-blade concepts with low-cost potential p0147 A79-20828

An operating 200 kW horizontal axis wind turbine p0147 A79-20829

Microprocessor control of a wind turbine generator p0147 A79-21302

The application of hydraulics in the 2,000 kW wind turbine generator p0156 A79-17400

Wind turbines for electric utilities - Development status and economics [AIAA PAPER 79-0965] p0148 A79-28888

Large horizontal axis wind turbine development p0149 A79-46527

Utility operational experience on the NASA/DOE Mod-0 200 kW Wind Turbine p0149 A79-46537

Lewis Research Center studies of multiple large wind turbine generators on a utility network p0149 A79-46547

Control and stabilization of the DOE/NASA Mod-1 two megawatt wind turbine generator p0156 A79-51780

Microprocessor control of a wind turbine generator [NASA-TM-79021] p0134 A79-12548

Power train analysis for the DOE/NASA 100-kW wind turbine generator p0135 A79-16355

An operating 200-kW horizontal axis wind turbine [NASA-TJ-79034] p0135 A79-16357

A 200-kW wind turbine generator conceptual design study [NASA-TM-79032] p0135 A79-17333

Utility operational experience on the NASA/DOE MOD-0A 200-kW wind turbine [NASA-TM-79084] p0136 A79-20494

Evaluation of MOSTAS computer code for predicting dynamic loads in two bladed wind turbines [NASA-TM-79101] p0137 A79-21549

The use of wind data with an operational wind turbine in a research and development environment [NASA-TM-73832] p0140 A79-26502

Large horizontal axis wind turbine development [NASA-TM-79174] p0140 A79-26504

Safety considerations in the design and operation of large wind turbines [NASA-TM-79193] p0141 A79-28725

Design, fabrication, and initial test of a fixture for reducing the natural frequency of the Mod-0 wind turbine tower [NASA-TM-79200] p0142 A79-28727

MOD-2 failure mode and effects analysis [NASA-CR-159632] p0093 A79-30415

Wind turbines for electric utilities: Development status and economics [NASA-TM-79170] p0142 A79-30719

WING FLAPS

WT TRAILING-EDGE FLAPS

WING FLOW METHOD TESTS

Investigation of wing shielding effects on CTOL engine noise [AIAA PAPER 79-0669] p0011 A79-28970

Investigation of wing shielding effects on CTOL engine noise [NASA-TM-79078] p0127 A79-20390

WING LOADING

Wing aerodynamic loading caused by jet-induced lift associated with STOL-OTW configurations [AIAA PAPER 79-1664] p0006 A79-47346

Wing aerodynamic loading caused by jet-induced lift associated with STOL-OTW configurations [NASA-TM-79218] p0004 A79-28146

WING NACELLE CONFIGURATIONS

Assessment at full scale of nozzle/wing geometry effects on OTW aero-acoustic characteristics --- short takeoff aircraft noise [NASA-TM-79168] p0174 A79-25841

Wing aerodynamic loading caused by jet-induced lift associated with STOL-OTW configurations [NASA-TM-79218] p0004 A79-28146

WINGS

WT ROTARY WINGS

WT TIP DRIVEN ROTORS

Assessment at full scale of nozzle/wing geometry effects on OTW aeroacoustic characteristics --- Over The Wing STOL engine configurations p0175 A79-39802

Feasibility of wing shielding of the airplane interior from the shock noise generated by supersonic tip speed propellers [NASA-TM-79042] p0172 A79-15757

WORK HARDENING

NI STRAIN HARDENING

WORKING FLUIDS

Convective heat flux in a laser-heated thruster p0057 A79-22396

WRAPAROUND CONTACT SOLAR CELLS

U SOLAR CELLS

X

X BAND

U SUPERHIGH FREQUENCIES

X RAY SPECTROGRAPHY

U X RAY SPECTROSCOPY

X RAY SPECTROMETRY

U X RAY SPECTROSCOPY

X RAY SPECTROSCOPY

Application of ESCA to the determination of stoichiometry in sputtered coatings and interface regions --- X-ray photoelectron spectroscopy p0117 A79-16664

XENON

Inert gas ion source program [NASA-CR-159423] p0056 A79-10120

Y

YAW

Bilinear tangent yaw guidance [AIAA 79-1730] p0045 A79-45374

YAWMETERS

U YAW

YF-102 AIRCRAFT

U F-102 AIRCRAFT

YF-12 AIRCRAFT

A throat-bypass stability-bleed system using relief valves to increase the transient stability of a mixed-compression inlet --- YF-12 aircraft inlet tests in the Lewis 10 by 10 ft supersonic wind tunnel [NASA-TF-1083] p0023 A79-28176

YIELD

Use of refinery computer model to predict fuel production [NASA-TM-79203] p0089 A79-28349

YIELD STRENGTH

High toughness-high strength iron alloy [NASA-CASE-LEW-12542-3] p0073 A79-19145

YJ-85 ENGINE

U J-85 ENGINE

YOUNG MODULUS

U MODULUS OF ELASTICITY

YTTRIUM COMPOUNDS

WT YTTRIUM OXIDES

YTTRIUM OXIDES

Emission and absorptance of the National Aeronautics and Space Administration ceramic thermal barrier coating --- for gas turbine engine components p0086 A79-27231

An oxide dispersion strengthened alloy for gas turbine blades [AIAA 79-0763] p0077 A79-28276

Z

ZERO GRAVITY

U WEIGHTLESSNESS

ZINC

Friction and wear of single-crystal manganese-zinc ferrite p0185 A79-34994

Decay of the zincate concentration gradient at an alkaline zinc cathode after charging [NASA-TM-79106] p0137 A79-20520

ZINC ALLOYS

Anisotropic friction and wear of single-crystal manganese-zinc ferrite in contact with itself [NASA-TF-1339] p0113 A79-10425

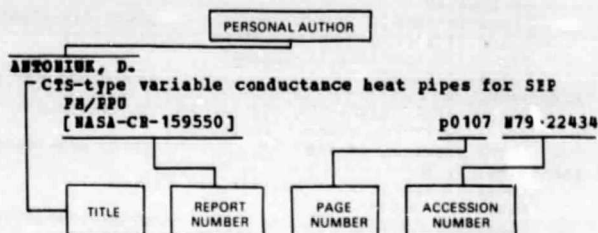
ZINC COMPOUNDS

Determination of the zincate diffusion coefficient and its application to alkaline battery problems p0070 A79-11547

Friction and wear of single-crystal manganese-zinc
ferrite
[NASA-TM-78980] p0184 N79-16699
Auger spectroscopy analysis of lubrication with
zinc dialkyldithiophosphate of several metal
combinations in sliding contact
[NASA-TP-1489] p0083 N79-27308
ZINC NICKEL BATTERIES
U NICKEL ZINC BATTERIES
ZINC SILVER BATTERIES
U SILVER ZINC BATTERIES
ZINC SILVER OXIDE BATTERIES
U SILVER ZINC BATTERIES
ZIRCONIUM COMPOUNDS
NT ZIRCONIUM OXIDES
Development of a plasma sprayed ceramic gas path
seal for high pressure turbine applications
[NASA-CR-159669] p0122 N79-31602
ZIRCONIUM OXIDES
Emission and absorptance of the National
Aeronautics and Space Administration ceramic
thermal barrier coating --- for gas turbine
engine components
p0086 A79-27231
Development of sputtering process to deposit
stoichiometric zirconia coatings for the inside
wall of regeneratively cooled rocket thrust
chambers
[NASA-CR-159412] p0056 N79-11115
Plasma-sprayed zirconia gas path seal technology:
A state-of-the-art review
[NASA-TM-79273] p0085 N79-33325

PERSONAL AUTHOR INDEX

Typical Personal Author Index Listing



Listings in this index are arranged alphabetically by personal author. The title of the document provides the user with a brief description of the subject matter. The report number helps to indicate the type of document listed (e.g. NASA report, translation, NASA contractor report). The page and accession numbers are located beneath and to the right of the title, e.g. p0107 N79-22434. Under any one author's name the accession numbers are arranged in sequence with the AIAA accession numbers appearing first.

A

ABBOTT, J. H.
Aerodynamic performance of scarf inlets
[AIAA PAPER 79-0380] p0005 A79-23510
Aerodynamic performance of scarf inlets
[NASA-TM-79055] p0003 N79-14998

ABRAHAM, K. H.
Feasibility study for a secondary Na/S battery
[NASA-CR-159469] p0152 N79-17330

ACKER, L. W.
Aerodynamic and acoustic effects of eliminating core swirl from a full scale 1.6 stage pressure ratio fan (QF-5A)
[NASA-TM-789911] p0002 N79-11001

ACURIO, J.
Materials and structural aspects of advanced gas-turbine helicopter engines
p0029 A79-39804
Materials and structural aspects of advanced gas-turbine helicopter engines
[NASA-TM-79100] p0001 N79-20008

ADAMCZYK, J. J.
Supersonic unstalled flutter
p0004 A79-12599
Unsteady flow in a supersonic cascade with subsonic leading-edge locus
p0005 A79-16047
Supersonic unstalled flutter
[NASA-TM-79001] p0002 N79-11000
Analysis of supersonic stall bending flutter in axial-flow compressor by actuator disk theory
[NASA-TP-1345] p0003 N79-13003
Supersonic unstalled flutter
p0023 N79-27181

ADAMO, R. C.
Laboratory studies of electrical properties of insulating materials
p0044 A79-20877

ADAMSON, A. N.
Integrated gas turbine engine-nacelle
[NASA-CASE-LEW-12389-3] p0014 N79-14096

ADAMSON, W. H.
Prop-fan propulsion - Its status and potential
[SAE PAPER 780995] p0026 A79-25880

ADUJA, K. K.
An impulse test technique with application to acoustic measurements
[AIAA PAPER 79-0679] p0178 A79-26890
Effects of simulated forward flight on jet noise, shock noise and internal noise
[AIAA PAPER 79-0615] p0178 A79-26936

The free jet as a simulator of forward velocity effects on jet noise
[NASA-CR-3056] p0176 N79-14873
Studies of the acoustic transmission characteristics of coaxial nozzles with inverted velocity profiles: Comprehensive data report
[NASA-CR-159628] p0177 N79-27933

AGERHAB, E.
Computer-aided analysis and design of the shape rolling process for producing turbine engine airfoils
[NASA-CR-159455] p0012 N79-12087
Computer-aided analysis and design of the shape rolling process for producing turbine engine airfoils
[NASA-CR-135367] p0080 N79-26175

ALEXANDER, A.
Interactive multi-mode blade impact analysis
[NASA-CR-159462] p0032 N79-17858

ALEXANDER, J. H.
Extension, validation and application of the NASCAP code
[NASA-CR-159595] p0100 N79-27397

ALEXOVICH, R. E.
Thermal anomalies of the transmitter experiment package on the communications technology satellite
[NASA-TP-1410] p0044 N79-21120
National Aeronautics and Space Administration plans for space communication technology
[NASA-TM-79217] p0053 N79-28220

ALGER, D. L.
Closed loop spray cooling apparatus
[NASA-CASE-LEW-11981-2] p0103 N79-2336

ALLAN, R. D.
Definition study of a Variable Cycle Experimental Engine (VCEE) and associated test program and test plan
[NASA-CR-159419] p0031 N79-11042

ALLARD, P. A.
Development of sputtered techniques for thrust chambers
[NASA-CR-159637] p0080 N79-32326

ALLEN, G. F.
Compressible flow across narrow passages: Comparison of theory and experiment for face seals
[NASA-TP-1346] p0113 N79-10424
Comparison of analysis and experiment for self-acting seals for liquid-oxygen turbo pumps
[NASA-TP-1443] p0115 N79-22519

ALSTON, W. B.
Stability of PNR-polyimide monomer solutions
p0086 A79-31041
Effects of graphite fiber stability on the properties of PNR polyimide composites
p0066 A79-43309
Effects of graphite fiber stability on the properties of PNR polyimide composites
[NASA-TM-79062] p0061 N79-16075
Resin/fiber thermo-oxidative interactions in PNR polyimide/graphite composites
[NASA-TM-79093] p0062 N79-16920
Stability of PNR-polyimide monomer solutions
[NASA-TM-79063] p0062 N79-16921

ALTAN, T.
Computer-aided analysis and design of the shape rolling process for producing turbine engine airfoils
[NASA-CR-159455] p0012 N79-12087
Computer-aided analysis and design of the shape rolling process for producing turbine engine airfoils
[NASA-CR-135367] p0080 N79-26175

ALTROVITZ, S.
Reactively evaporated films of copper molybdenum sulfide

- ALTEROVITZ, S. A. p0185 A79-31973
Superconducting properties of evaporated copper molybdenum sulfide films p0184 A79-20219
Critical current density in wire drawn and hydrostatically extruded Nb-Ti superconductors p0185 A79-20539
Hall effect and magnetoresistivity in the ternary molybdenum sulfides p0185 A79-21157
Critical current and scaling laws in evaporated two-phase Cu₂S-Mo₆S₈ p0185 A79-26375
Normal state properties of the ternary molybdenum sulfides p0185 A79-27229
Low temperature normal state resistance of ternary molybdenum sulfides p0185 A79-27230
Comparison of projected critical currents in PbMo₆S₈ and Nb₃Ge p0185 A79-28300
Electronic properties of PbMo₆S₈ and Cu₂Mo₆S₈ p0187 A79-41731
Indirect measurements of Fermi surface parameters of some chevrel phase materials p0185 A79-50231
- ANAGHOSSTOU, E.
Endurance testing of first generation /Eloek I/ commercial solar cell modules p0148 A79-41022
- ANAND, R.
Conceptual design of thermal energy storage systems for near term electric utility applications [NASA-CR-159577] p0155 A79-33560
- ANDERSON, D. M.
Effect of inlet temperature on the performance of a catalytic reactor p0070 A79-11542
- ANDERSON, N. E.
Performance of a Nasvytis multiroller traction drive [NASA-TF-1378] p0113 A79-13369
- ANDERSON, O. L.
Modeling of premixing-prevaporizing fuel-air mixing passages p0019 A79-24598
- ANDERSON, W. J.
The practical impact of elastohydrodynamic lubrication p0117 A79-11545
- ANGLIN, A. E., JR.
Transverse and longitudinal tensile properties at 760 C of several oxide dispersion strengthened nickel-base alloys p0078 A79-49531
Transverse and longitudinal tensile properties at 760 C of several oxide dispersion strengthened nickel-base alloys [NASA-TN-79189] p0075 A79-30355
- ANTOINE, A. C.
Evaluation of the application of some gas chromatographic methods for the determination of properties of synthetic fuels p007C A79-25917
Evaluation of the application of some gas chromatographic methods for the determination of properties of synthetic fuels [NASA-TN-79035] p0068 A79-16930
Comparison of the properties of some synthetic crudes with petroleum crudes [NASA-TN-79220] p0090 A79-31405
- ANTONIAK, D.
CIS-type variable conductance heat pipes for SEP FM/FPU [NASA-CR-159550] p0107 A79-22434
Heat pipe life and processing study [NASA-CR-159581] p0107 A79-25349
- ANZIC, G.
Determining potential 30/20 GHz domestic satellite system concepts and establishment of a suitable experimental configuration p0095 A79-27397
Determining potential 30/20 GHz domestic satellite system concepts and establishment of a suitable experimental configuration [NASA-TN-79092] p0094 A79-17072
- TWI design requirements for 30/20 GHz digital communications' satellite [NASA-TN-79119] p0097 A79-20316
- ARCELLA, F. G.
Interdiffusion behavior of tungsten or rhenium and group 5 and 6 elements and alloys of the periodic table. Part 2b: Appendices [NASA-CR-134526] p0080 A79-33305
- ARIAS, A.
Effect of oxygen-nitrogen ratio on sinterability of Sialons [NASA-TF-1382] p0082 A79-21204
Modules of rupture and oxidation resistance of S12.55A10.600.72N3.52 sialon [NASA-TF-1490] p0083 A79-27309
- ARMENTROUT, E. C.
Pressure instrumentation for gas turbine engines - A review of measurement technology [ASME PAPER 79-GT-148] p0110 A79-10800
- ARMSTRONG, W. H.
Structural analysis of cylindrical thrust chambers, volume 1 [NASA-CR-159522] p0057 A79-19073
- ARNOLD, W.
Mass drivers. 3: Engineering p0040 A79-32232
- ARON, P. R.
Area scaling investigations of charging phenomena p0048 A79-24032
- ARFASI, D. J.
Interactive debug program for evaluation and modification of assembly-language software [NASA-TF-1441] p0166 A79-21796
- AUKERMAN, C. A.
Plug cluster engine concept for in-space missions [AIAA PAPER 79-1179] p0055 A79-38972
- AULT, G. H.
Composites emerging for aeropropulsion applications p0066 A79-53720
- AYDELOTT, J. C.
Axial jet mixing of ethanol in cylindrical containers during weightlessness [NASA-TF-14487] p0090 A79-28350
- AYERS, J. W.
Design study of superconducting magnets for a combustion magnetohydrodynamic /MHD/ generator p0098 A79-15305

B

- BAKER, B. B.
Evaluation of high-contact-ratio spur gears with profile modification [NASA-TF-1458] p0115 A79-31604
- BADGLIN, E. H.
An introduction to a unified approach to flexible rotor balancing [ASME PAPER 79-GT-161] p0124 A79-32423
- BAHR, E. F.
Intraocular pressure reduction and regulation system [NASA-TN-79187] p0165 A79-28881
- BAGWELL, J. W.
An airborne meteorological data collection system using satellite relay /ASDAR/ p0010 A79-14949
- BAHR, D. H.
Social and economic impact of solar electricity at Schuchuli Village [NASA-TN-79194] p0139 A79-25501
- BAHR, D. W.
Experimental clean combustor program: Diesel no. 2 fuel addendum, phase 3 [NASA-CR-135413] p0091 A79-26221
Experimental Clean Combustor Program (ECCP), phase 3 [NASA-CR-135384] p0035 A79-21207
- BAILEY, D. A.
Study of mean- and turbulent-velocity fields in a large-scale turbine-vane passage [NASA-CR-3067] p0032 A79-16853
- BAILEY, E. H.
Infrared suppressor effect on T63 turboshaft engine performance [NASA-TN-78970] p0013 A79-11043
- BAILEY, M. H.
Rankine-cycle component characteristics p0140 A79-26478
Power-conversion system component summation p0140 A79-26483

- BAIR, V. L.**
Diminide thermionic energy conversion with lanthanum-hexaboride electrodes p0146 A79-13098
Some properties of low-vapor-pressure braze alloys for thermionic converters p0076 A79-13100
- BAKER, W. L.**
Workbook for estimating effects of accidental explosions in propellant ground handling and transport systems [NASA-CR-3023] p0091 N79-10226
- BANKS, B. A.**
Ion beam sputter deposition of fluoropolymers [NASA-CASE-LEW-13122-1] p0083 N79-24154
- BARAONA, C. E.**
Status of wraparound contact solar cells and arrays p0054 A79-10014
Preliminary evaluation of glass resin materials for solar cell cover use p0055 A79-40984
Modeling of thin, back-wall silicon solar cells p0143 N79-32650
- BARNA, G. J.**
Energy and cost savings results for advanced technology systems from the Cogeneration Technology Alternatives Study (CTAS) [AIAA PAPER 79-1000] p0149 A79-44225
Benefits of advanced technology in industrial cogeneration [NASA-TM-79160] p0138 N79-24444
Energy and cost saving results for advanced technology systems from the Cogeneration Technology Alternatives Study (CTAS) [NASA-TM-79213] p0141 N79-27665
- BARNES, P. E.**
Cam-operated pitch-change apparatus [NASA-CASE-LEW-13050-1] p0014 N79-14095
- BARNES, S. P.**
Carrier: Interference ratios for frequency sharing between satellite systems transmitting frequency modulated and digital television signals [NASA-TM-79265] p0094 N79-33379
- BARRENGER, J.**
An in-place recalibration technique to extend the temperature capability of capacitance-sensing, rotor-blade-tip-clearance measurement systems [SAE PAPER 781003] p0026 A79-25885
- BARTLETT, R. C.**
Summary of the two year NASA program for active control of ATS-5/6 environmental charging p0047 N79-24006
- BARTON, R. S.**
Control and stabilization of the DOE/NASA Mod-1 two megawatt wind turbine generator p0156 A79-51780
- BASKARONE, E.**
Flow in nonrotating passages of radial inflow turbines [NASA-CR-159679] p0035 N79-32212
- BAUNLISTER, K. J.**
Optimized multisectioned acoustic liners [AIAA PAPER 79-0182] p0174 A79-19581
Numerical spatial marching techniques in duct acoustics p0175 A79-25946
Condensation on a noncollapsing vapor bubble in a subcooled liquid p0100 A79-49535
Optimized multisectioned acoustic liners [NASA-TM-79028] p0172 N79-15759
Applications of velocity potential function to acoustic duct propagation and radiation from inlets using finite element theory [NASA-TM-79071] p0016 N79-15959
Condensation on a noncollapsing vapor bubble in a subcooled liquid [NASA-TM-79212] p0105 N79-27461
- BECHTEL, R. T.**
Preliminary results of the mission profile life test of a 30 cm Hg bombardment thruster [NASA-TM-79261] p0054 N79-33254
- BEEN, J.**
An economic analysis of a commercial approach to the design and fabrication of a space power system [AIAA 79-0914] p0055 A79-34737
- BEEN, J. F.**
The role of fuel cells in NASA's space power systems p0056 A79-51810
- An economic analysis of a commercial approach to the design and fabrication of a space power system [NASA-TM-79153] p0053 N79-2219J
The role of fuel cells in NASA's space power systems [NASA-TM-79182] p0053 N79-23133
- BEERS, B. L.**
First principles numerical model of avalanche-induced arc discharges in electron-irradiated dielectrics [NASA-CR-159560] p0101 N79-28418
- BEHREIN, E. A.**
Executive summary of Aircraft Icing Specialists Workshop p0004 N79-23914
- BEHRENDT, D. E.**
Some properties of an advanced boron fiber p0086 A79-21297
Some properties of an advanced boron fiber [NASA-TM-79065] p0061 N79-16076
- BELL, J. C.**
Stresses from arbitrary loads on a circular crack p0130 A79-27938
Stress analysis for structures with surface cracks [NASA-CR-159400] p0129 N79-13405
User's manual for FRAC3D: Supplement to report on stress analysis for structures with surface cracks [NASA-CR-159401] p0129 N79-13406
- BELL, W. F.**
Development of advanced fuel cell system [NASA-CR-159443] p0151 N79-12553
Strip cell test and evaluation program [NASA-CR-159652] p0154 N79-31784
- BENFOLD, S. E.**
The erosion/corrosion of small superalloy turbine rotors operating in the effluent of a PFB coal combustor [NASA-TM-79227] p0076 N79-30356
- BENFORD, S. E.**
The magnetocaloric effect in dysprosium p0185 A79-38402
- BENNETT, J. E.**
Preliminary evaluation of the role of K2S in MHD hot stream seed recovery [NASA-TM-79114] p0068 N79-20200
- BENSTEIN, E. E.**
Advanced General Aviation Turbine Engine (GATE) study [NASA-CR-159624] p0039 N79-29189
- BERCAN, B. W.**
Preliminary summary of the ETF conceptual studies [NASA-TM-78999] p0133 N79-11478
- BERNHARD, D. G.**
Free-piston regenerative hot gas hydraulic engine [NASA-CASE-LEW-12274-1] p0113 N79-10426
Stirling engines for automobiles [NASA-TM-79222] p0142 N79-28726
- BERKOFEC, F. D.**
Test results for electron beam charging of flexible insulators and composites p0048 N79-24031
Charging rates of metal-dielectric structures p0048 N79-24033
- BERKOWITZ, B. J.**
Conceptual design of thermal energy storage systems for near term electric utility applications. Volume 1: Screening of concepts [NASA-CR-159411-VOL-1] p0151 N79-13496
Conceptual design of thermal energy storage systems for near term electric utility applications. Volume 2: Appendices - screening of concepts [NASA-CR-159411-VOL-2] p0152 N79-13497
- BERLAD, A. L.**
Combustion of porous solids at reduced gravitational conditions [NASA-CR-3197] p0072 N79-33288
- BERNATOWICZ, D. T.**
A brief survey of the solar cell state-of-the-art p0052 N79-10130
- BHAT, G. K.**
Evaluation of the mechanical properties of electroslag refined Fe-12Ni alloys [NASA-CR-159394] p0079 N79-12202
- BHATT, R. T.**
Fatigue behavior of SiC reinforced titanium composites [NASA-TM-79223] p0064 N79-30296
- BHUSHAN, B.**
Development of surface coatings for

- air-lubricated, compliant journal bearings to 650 C
[ASLE PREPRINT 78-LC-3C-1] p0123 A79-23252
- Static evaluation of surface coatings for compliant gas bearings in an oxidizing atmosphere to 650 C
p0088 A79-31957
- BIFANO, W.**
NASA Lewis Research Center photovoltaic application experiments
[AIAA PAPER 78-1768] p0146 A79-13867
- BIFANO, W. J.**
Photovoltaic power systems for rural areas of developing countries
p0147 A79-26131
- Design and fabrication of a photovoltaic power system for the Papago Indian Village of Schuchuli /Gunsight/, Arizona
p0148 A79-41089
- Photovoltaic power systems for rural areas of developing countries
[NASA-TN-79097] p0135 A79-15411
- Description of photovoltaic village power systems in the United States and Africa
[NASA-TN-79149] p0138 A79-24443
- Social and economic impact of solar electricity at Schuchuli Village
[NASA-TN-79194] p0135 A79-25501
- BILL, R. C.**
An acoustic emission study of plastic deformation in polycrystalline aluminum
p0077 A79-19458
- Fretting wear of iron, nickel, and titanium under varied environmental conditions
p0078 A79-34995
- Fretting wear of iron, nickel, and titanium under varied environmental conditions
[NASA-TN-78972] p0073 A79-12203
- Wear of seal materials used in aircraft propulsion systems
[NASA-TN-79003] p0073 A79-12204
- Development of sprayed ceramic seal systems for turbine gas path sealing
[NASA-TN-79022] p0081 A79-12223
- Composite seal for turbomachinery
[NASA-CASE-LEW-12131-1] p0114 A79-18318
- Thermal stress analysis of ceramic gas-path seal components for aircraft turbines
[NASA-TN-79137] p0082 A79-21205
- Plasma-sprayed zirconia gas path seal technology: A state-of-the-art review
[NASA-TN-79273] p0085 A79-33325
- BILLINGS, R. W.**
The solid state remote power controller - Its status, use and perspective
p0095 A79-10896
- BIRCHENROUGH, A. G.**
Design and operating experience on the U.S. Department of Energy Experimental Mod-O 100 kW Wind Turbine
p0145 A79-10234
- BISHOP, A. R.**
Calculation of the three-dimensional flow field in supersonic inlets at angle of attack using a bicharacteristic method with discrete shock wave fitting
[AIAA PAPER 79-0379] p0025 A79-19698
- A computer program for the calculation of the flow field in supersonic mixed-compression inlets at angle of attack using the three-dimensional method of characteristics with discrete shock wave fitting
[NASA-TN-78947] p0002 A79-10023
- BIZON, P. T.**
Three-dimensional finite-element elastic analysis of a thermally cycled single-edge wedge geometry specimen
[NASA-TN-79026] p0172 A79-16644
- Effect of grain orientation and coating on thermal fatigue resistance of a directionally solidified superalloy (MAR-M 247)
[NASA-TN-79129] p0127 A79-22565
- BLANK, B. J.**
Wind tunnel performance of four energy efficient propellers designed for Mach 0.8 cruise
[SAE PAPER 790573] p0028 A79-36759
- Tone noise of three supersonic helical tip speed propellers in a wind tunnel
p0175 A79-39801
- Tone noise of three supersonic helical tip speed propellers in a wind tunnel at 0.8 Mach number
[NASA-TN-79046] p0172 A79-15758
- Wind tunnel performance of four energy efficient propellers designed for Mach 0.8 cruise
[NASA-TN-79124] p0003 A79-20069
- Aircraft icing
[NASA-CR-2086] p0004 A79-23912
- Tone noise of three supersonic helical tip speed propellers in a wind tunnel
[NASA-TN-79167] p0174 A79-25840
- BLANK, B. J.**
Dynamic analysis of a photovoltaic power system with battery storage capability
[NASA-TN-79209] p0142 A79-29599
- BLATT, R. R.**
Study of liquid and vapor flow into a Centaur capillary device
[NASA-CR-159657] p0108 A79-33432
- BLECH, R. A.**
Predicting dynamic performance limits for servosystems with saturating nonlinearities
[NASA-TN-1488] p0038 A79-28186
- BLOOMBERG, H. W.**
First principles numerical model of avalanche-induced arc discharges in electron-irradiated dielectrics
[NASA-CR-159560] p0101 A79-28418
- BLOOMER, H. R.**
Investigation of wing shielding effects on CTOL engine noise
[AIAA PAPER 79-0669] p0011 A79-28970
- Investigation of wing shielding effects on CTOL engine noise
[NASA-TN-79078] p0127 A79-20390
- BLOOMFIELD, H. S.**
Benefits of solar/fossil hybrid gas turbine systems
[ASME PAPER 79-GT-38] p0147 A79-30554
- Benefits of solar/fossil hybrid gas turbine systems
[NASA-TN-79083] p0134 A79-15410
- Solar thermal power-conversion system
p0139 A79-26477
- Brayton-cycle component characteristics
p0140 A79-26479
- Power-conversion system component summation
p0140 A79-26483
- BLOZY, J. I.**
Acoustic and aerodynamic performance investigation of inverted velocity profile coannular plug nozzles, comprehensive data report, volume 1
[NASA-CR-159575-VOL-1] p0177 A79-26884
- Acoustic and aerodynamic performance investigation of inverted velocity profile coannular plug nozzles, comprehensive data report, volume 2
[NASA-CR-159575-VOL-2] p0177 A79-26885
- Acoustic and aerodynamic performance investigation of inverted velocity profile coannular plug nozzles, comprehensive data report, volume 3
[NASA-CR-159575-VOL-3] p0177 A79-26886
- BOBULA, G. A.**
Effects of steady-state pressure distortion on the stall margin of a J85-21 turbojet engine
[NASA-TN-79123] p0018 A79-23968
- Effect of steady-state pressure distortion on flow characteristics entering a turbofan engine
[NASA-TN-79134] p0019 A79-23969
- Effect of steady-state temperature distortion and combined distortion on inlet flow to a turbofan engine
[NASA-TN-79237] p0023 A79-30187
- BOLDMAN, D.**
Trailing edge noise data with comparison to theory
[AIAA PAPER 79-1524] p0176 A79-47340
- Trailing edge noise data with comparison to theory
[NASA-TN-79208] p0174 A79-27930
- BOLDMAN, D. R.**
Wind tunnel tests of a blade subjected to midchord torsional oscillation at high subsonic stall flutter conditions
[NASA-TN-78998] p0002 A79-12016
- BOWEN, S.**
Mass drivers. 3: Engineering
p0040 A79-32232
- BOWLER, C. R. J.**
Control and stabilization of the DOE/NASA Mod-1 two megawatt wind turbine generator
p0156 A79-51780
- BOWLES, E. J.**
Use of an ultrasonic-acoustic technique for

- nondestructive evaluation of fiber composite strength
p0064 A79-15545
- Impact behavior of filament-wound graphite/epoxy fan blades
p0025 A79-20880
- BOWMAN, B. L.
Feasibility of determining flat roof heat losses using aerial thermography
p0131 A79-51095
- Feasibility of determining flat roof heat losses using aerial thermography
[NASA-TF-79152]
p0131 A79-22590
- BOYLE, E. J.
Effect of steam addition on cycle performance of simple and recuperated gas turbines
[NASA-TF-1440]
p0137 A79-22626
- BRAGINSKI, A. I.
Nb3Ge as a potential candidate material for 15- to 25-T magnets
p0186 A79-44548
- BRAINARD, W. A.
The friction and wear properties of sputtered hard refractory compounds
p0085 A79-16666
- An XPS study of the adherence of refractory carbide, silicide, and boride RF-sputtered wear-resistant coatings
p0085 A79-21022
- Use of a nitrogen-argon plasma to improve adherence of sputtered titanium carbide coatings on steel
p0119 A79-25103
- Adherence of sputtered titanium carbides
p0078 A79-34997
- Effect of nitrogen-containing plasma on adherence, friction, and wear of radiofrequency-sputtered titanium carbide coatings
[NASA-TF-1377]
p0081 A79-15184
- Adherence of sputtered titanium carbides
[NASA-TF-79117]
p0074 A79-20220
- Wear of aluminum and hypoeutectic aluminum-silicon alloys in boundary-lubricated pin-on disk sliding
[NASA-TF-1442]
p0074 A79-21184
- Improved adherence of sputtered titanium carbide coatings on nickel- and titanium-base alloys
[NASA-TF-1450]
p0055 A79-22194
- Adhesive material transfer in the erosion of an aluminum alloy
[NASA-TF-79165]
p0083 A79-27306
- Evaluation and auger analysis of a zinc-dialkyl-dithiophosphate antiwear additive in several diester lubricants
[NASA-TF-1544]
p0084 A79-32359
- BRALYNWATTE, W. E.
Combined pressure and temperature distortion effects on internal flow of a turbofan engine
[AIAA PAPER 79-1309]
p0029 A79-39031
- Combined pressure and temperature distortion effects on internal flow of a turbofan engine
[NASA-TF-79136]
p0012 A79-23963
- BRANDHORST, B. W.
Photon degradation effects in terrestrial solar cells
p0149 A79-41098
- Photon-degradation effects in terrestrial silicon solar cells
p0149 A79-42545
- BRANDHORST, B. W., JR.
Application of semiconductor diffusants to solar cells by screen printing
[NASA-CASE-LEW-12775-1]
p0133 A79-11468
- Back wall solar cell
[NASA-CASE-LEW-12236-2]
p0134 A79-14528
- The NASA Lewis Research Center program in space solar cell research and technology
p0143 A79-32641
- BRANTLEY, J. W.
Fabrication of J79 boron/aluminum compressor blades
[NASA-CR-159566]
p0034 A79-23970
- BREWE, E. E.
Effect of geometry on hydrodynamic film thickness
[ASME PAPER 78-LUE-24]
p0118 A79-23237
- BRIDEL, R.
Simultaneous measurements of ozone outside and inside cabins of two B-747 airliners and a Gates Learjet business jet
p0008 A79-27571
- NASA Global Atmospheric Sampling Program (GASP) data report for tapes V10007 and V10008
[NASA-TM-73784]
p0157 A79-17359
- BRINE, H.
Transmission seal development
[NASA-CR-135372]
p0120 A79-10423
- BRILLY, W. E.
Development of a three-dimensional turbulent duct flow analysis
[NASA-CR-3029]
p0106 A79-12366
- BRITSCH, W. E.
Effects of diffusion factor, aspect ratio and solidity on overall performance of 14 compressor middle stages
[NASA-TF-1523]
p0038 A79-33210
- BROCK, T. W.
Alternate methods of applying diffusants to silicon solar cells
[NASA-CR-159508]
p0153 A79-29602
- BRODER, J. D.
Ultraviolet irradiation at elevated temperatures and thermal cycling in vacuum of PEF-A covered silicon solar cells
p0148 A79-40898
- Photon degradation effects in terrestrial solar cells
p0149 A79-41098
- Photon-degradation effects in terrestrial silicon solar cells
p0149 A79-42545
- Ionized dopant concentrations at the heavily doped surface of a silicon solar cell
[NASA-TF-1347]
p0184 A79-13886
- BROWNSTEIN, L. E.
The 18 and 30 GHz fixed service communication satellite system study: Executive summary
[NASA-CR-159627-1]
p0096 A79-33373
- The 18 and 30 GHz fixed service communications satellite system study
[NASA-CR-159627-2]
p0096 A79-33374
- BRUNNER, S. E.
Feasibility study for a secondary Na/S battery
[NASA-CR-159469]
p0152 A79-17330
- BRUSCH, B. G.
Bilinear tangent yaw guidance
[AIAA 79-1730]
p0045 A79-45374
- BRUTON, W. E.
Lewis hybrid computing system, users manual
[NASA-TM-79111]
p0165 A79-20752
- BRUZZONE, C.
Solar-pumped lasers for space power transmission
[AIAA PAPER 79-1015]
p0112 A79-38202
- Design investigation of solar powered lasers for space applications
[NASA-CR-159554]
p0111 A79-26384
- BUCKLEY, D. H.
Auger spectroscopy analysis in adhesion, friction and wear studies
p0110 A79-10992
- Friction and fracture of single-crystal silicon carbide in contact with itself and titanium
p0086 A79-32149
- Friction and wear of single-crystal manganese-zinc ferrite
p0185 A79-34994
- Anisotropic friction and wear of single-crystal manganese-zinc ferrite in contact with itself
[NASA-TF-1339]
p0113 A79-10425
- Friction and transfer of copper, silver, and gold to iron in the presence of various adsorbed surface films
[NASA-TF-1392]
p0114 A79-14386
- Friction and wear characteristics of iron-chromium alloys in contact with themselves and silicon carbide
[NASA-TF-1387]
p0114 A79-14387
- Friction and wear of single-crystal manganese-zinc ferrite
[NASA-TM-78980]
p0184 A79-16699
- Friction and wear with a single-crystal abrasive grit of silicon carbide in contact with iron base binary alloys in oil: Effects of alloying element and its content
[NASA-TF-1394]
p0114 A79-17227
- The friction and wear of metals and binary alloys in contact with an abrasive grit of single-crystal silicon carbide
[NASA-TM-79131]
p0175 A79-22274

- Metal-dielectric interactions
[NASA-TM-79151] p0075 N79-25195
- Laser spectroscopy analysis of lubrication with zinc dialkylthiophosphate of several metal combinations in sliding contact
[NASA-TF-1489] p0083 N79-27308
- Anisotropic friction, deformation, and fracture of single-crystal silicon carbide at room temperature
[NASA-TF-1525] p0084 N79-30380
- BUDINIR, J.**
Active heat exchange system development for latent heat thermal energy storage
[NASA-CR-159479] p0153 N79-21554
- BUGGIE, A. E.**
Wind tunnel tests of a blade subjected to midchord torsional oscillation at high subsonic stall flutter conditions
[NASA-TM-78998] p0002 N79-12016
- BULZAN, D. L.**
Correlations of catalytic combustor performance parameters
p0070 A79-14956
- Correlations of catalytic combustor performance parameters
[NASA-TM-79014] p0134 N79-11480
- BUNDINGER, J. H.**
Multiple speed expandable bit synchronizer
[NASA-TM-79262] p0010 N79-33185
- BUNSAH, R. P.**
Superconducting properties of evaporated copper molybdenum sulfide films
p0184 A79-20219
- Reactively evaporated films of copper molybdenum sulfide
p0185 A79-31973
- BURGER, G. D.**
Study of blade aspect ratio on a compressor front stage aerodynamic and mechanical design report
[NASA-CR-159555] p0034 N79-23085
- BURGESS, G.**
T700 power turbine rotor multiplane/multispeed balancing demonstration
[NASA-CR-159586] p0122 N79-25392
- BURKHART, J. A.**
Design study of superconducting magnets for a combustion magnetohydrodynamic (MHD) generator
p0098 A79-15305
- BURLEY, B. B.**
Effect of lip and centerbody geometry on aerodynamic performance of inlets for tilting-nacelle VTOL aircraft
[AIAA PAPER 79-0381] p0025 A79-23509
- Effect of lip and centerbody geometry on aerodynamic performance of inlets for tilting-nacelle VTOL aircraft
[NASA-TM-79056] p0003 N79-14999
- BURKHISTER, L. C.**
A mobile apparatus for solar collector testing
[ASME PAPER 79-DE-5] p0150 A79-47651
- BURNEY, J. E.**
Intraocular pressure reduction and regulation system
[NASA-TM-79187] p0165 N79-28881
- BURNS, R. K.**
Energy and cost savings results for advanced technology systems from the Cogeneration Technology Alternatives Study (CTAS)
[AIAA PAPER 79-1000] p0149 A79-44225
- Benefits of advanced technology in industrial cogeneration
[NASA-TM-79160] p0138 N79-24444
- Energy and cost saving results for advanced technology systems from the Cogeneration Technology Alternatives Study (CTAS)
[NASA-TM-79213] p0141 N79-27665
- BURROUGHS, J. D.**
SINVEST: A simulation model for wind and photovoltaic energy storage systems (cdc program descriptions), volume 2
[NASA-CR-159608] p0167 N79-33894
- BUSCH, R.**
Development of sputtering process to deposit stoichiometric zirconia coatings for the inside wall of regeneratively cooled rocket thrust chambers
[NASA-CR-159412] p0056 N79-11115
- BUTZE, N. F.**
Wide range operation of advanced low NOx aircraft gas turbine combustors
[ASME PAPER 78-GT-128] p0024 A79-10792
- Parametric performance of a turbojet engine combustor using jet A and A diesel fuel
[NASA-TM-79089] p0017 N79-20114
- BYERS, D. C.**
Primary electric propulsion for future space missions
[AIAA 79-0881] p0055 A79-34773
- Primary electric propulsion for future space missions
[NASA-TM-79141] p0052 N79-22190
- Characteristics of primary electric propulsion systems
[NASA-TM-79255] p0053 N79-30290

C

- CABILL, K. J.**
Catalyst surfaces for the chromous/chromic redox couple
[NASA-CASE-LEW-13148-1] p0134 N79-14538
- CABILL, T. P.**
Wind-turbine-generator rotor-blade concepts with low-cost potential
p0147 A79-20828
- CAIRELLI, J. E.**
Ceramic applications in the advanced Stirling automotive engine
p0117 A79-12851
- CALFO, P. D.**
Measurement of transient strain and surface temperature on simulated turbine blades using noncontacting techniques
[NASA-TM-78982] p0126 N79-15415
- Effect of grain orientation and coating on thermal fatigue resistance of a directionally solidified superalloy (MAR-M 247)
[NASA-TM-79129] p0127 N79-22565
- CALOGERAS, J. E.**
Storage systems for solar thermal power
p0145 A79-10108
- CALVERT, G.**
Design, fabrication and spin testing of ceramic blade metal disk attachment
[NASA-CR-159532] p0032 N79-17857
- CALVERT, G. S.**
Ceramic blade attachments
p0123 A79-12848
- CAMERON, H. H.**
Stirling engine characteristics
p0140 N79-26480
- CARR, J. H.**
Applications of thermal energy storage to process heat storage and recovery in the paper and pulp industry
[NASA-CR-159398] p0154 N79-30801
- CARRUTHERS, W. D.**
Ceramic blade attachments
p0123 A79-12848
- CASSIDY, P.**
Design investigation of solar powered lasers for space applications
[NASA-CR-159554] p0111 N79-26384
- CASSIDY, J. J.**
The capabilities of the NASA charging analyzer program
p0047 N79-24011
- Charging analysis of the SCATHA satellite
p0049 N79-24012
- CASSIDY, J. J., III**
Extension, validation and application of the NASCAP code
[NASA-CR-159595] p0100 N79-27397
- NASCAP user's manual, 1978
[NASA-CR-159417] p0100 N79-27398
- CATALDO, R. L.**
Response of lead-acid batteries to chopper-controlled discharge
p0145 A79-10097
- CENKOS, H. A.**
Mechanical and chemical effects of ion-texturing biomedical polymers
[NASA-TM-79245] p0084 N79-31391
- CHANDERLIN, B.**
Energy efficient aircraft engines
[AIAA PAPER 79-1861] p0030 A79-47918
- Energy efficient aircraft engines
[NASA-TM-79204] p0022 N79-27141
- CHANIS, C. C.**
The effects of eccentricities on the fracture of

- off-axis fiber composites p0064 A79-15543
- Titanium/beryllium laminates - Fabrication, mechanical properties, and potential aerospace applications p0064 A79-20836
- CELFE/NASTRAN Code for the analysis of structures subjected to high velocity impact p0128 A79-21298
- Analysis/design of strip reinforced random composites /strip hybrids/ p0119 A79-24035
- Effects of moisture profiles and laminate configuration on the hygro stress in advanced composites p0064 A79-24132
- Analysis of high velocity impact on hybrid composite fan blades [AIAA 79-0783] p0128 A79-29027
- Mechanics of intraply hybrid composites - Properties, analysis and design p0065 A79-31033
- Fracture modes in off-axis fiber composites p0065 A79-31035
- CODSTRAN - Composite durability structural analysis p0128 A79-37292
- Fabrication and testing of non-graphitic superhybrid composites p0066 A79-43289
- Fracture modes in off-axis fiber composites [NASA-TN-79036] p0062 A79-12154
- CELFE/NASTRAN code for the analysis of structures subjected to high velocity impact [NASA-TN-79048] p0126 A79-15325
- CODSTRAN: Composite durability structural analysis [NASA-TN-79070] p0126 A79-15326
- Prediction of properties of intraply hybrid composites [NASA-TN-79087] p0061 A79-16919
- Fabrication and testing of nongraphitic superhybrid composites [NASA-TN-79102] p0063 A79-20188
- Analysis of high velocity impact on hybrid composite fan blades [NASA-TN-79133] p0127 A79-20398
- CHANG, G. C.
SINWEST - A simulation model for wind energy storage systems p0145 A79-10241
- CHAMIN, L. H.
Investigations of negative and positive cesium ion species [NASA-CR-159446] p0179 A79-18711
- CHARKEY, A.
Fabrication and testing of silver-hydrogen cells [NASA-CR-159490] p0152 A79-16375
- CHEN, T. L.
"H" downlink communication system for SLAE data p0045 A79-51097
VHF downline communication system for SLAE data [NASA-TN-79164] p0094 A79-23313
- CHEN, B.-K.
Chemically frozen multicomponent boundary layer theory of salt and/or ash deposition rates from combustion gases p0078 A79-50912
- CHEN, E. P.
Off-axis impact of unidirectional composites with cracks: Dynamic stress intensification [NASA-CR-159537] p0067 A79-30294
- CHEN, J. L. S.
Optimum dry-cooling sub-systems for a solar air conditioner [NASA-TN-79007] p0133 A79-11477
- CHEN, K. L.
A cross impact methodology for the assessment of US telecommunications system with application to fiber optics development: Executive summary [NASA-CR-135209] p0096 A79-17071
A cross impact methodology for the assessment of US telecommunications system with application to fiber optics development, volume 1 [NASA-CR-135208] p0096 A79-17071
A cross impact methodology for the assessment of US telecommunications system with application to fiber optics development, volume 2 [NASA-CR-159511-VOL-2] p0096 A79-18161
- CHEN, W. C.
A literature review on fatigue and creep interaction [NASA-CR-135305] p0130 A79-26429
- CHENNEY, E. C.
Ultrafine polybenzimidazole (PBI) fibers [NASA-CR-159644] p0067 A79-31350
- CHENG, H. S.
Experimental and analytical tools for evaluation of Stirling engine rod seal behavior [NASA-CR-159543] p0122 A79-23429
- CHENG, L. J.
High-energy electron-induced damage production at room temperature in aluminum-doped silicon p0154 A79-32662
- CHI, K. C.
Superconducting properties of evaporated copper molybdenum sulfide films p0184 A79-20219
Reactively evaporated films of copper molybdenum sulfide p0185 A79-31973
- CHIAPPETTA, L. M.
Modeling of premixing-prevaporizing fuel-air mixing passages p0019 A79-24998
- CHO, Y. C.
A statistical theory of sound radiation from a two-dimensional lined duct [AIAA PAPER 79-1521] p0176 A79-46707
- CHRISTIANSEN, W.
Solar-pumped lasers for space power transmission [AIAA PAPER 79-1015] p0112 A79-38202
Design investigation of solar powered lasers for space applications [NASA-CR-159554] p0111 A79-26384
- CHRISTNER, L.
Technology development for phosphoric acid fuel cell powerplant, phase 2 [NASA-CR-159572] p0153 A79-29604
- CHU, C. K.
Development and fabrication of improved power transistor switches [NASA-CR-159524] p0100 A79-21273
- CHUBB, D. L.
Gain measurements of the Ca-Xe charge exchange system p0112 A79-19078
- CIEPLUCH, C. C.
QCSSE - The key to future short-haul air transport p0030 A79-50208
- CIVINSKAS, K. C.
Infrared suppressor effect on T63 turboshaft engine performance [NASA-TN-78970] p0013 A79-11043
- CLARK, B. J.
Measured and predicted noise of the AVCO-Lycoming YF-102 turbofan engine [AIAA PAPER 79-0641] p0026 A79-26877
Measured and predicted noise of the Avco-Lycoming YF-102 turbofan noise [NASA-TN-79069] p0016 A79-15957
- CLARK, J. S.
Gas-turbine critical research and advanced technology support project [NASA-TN-79139] p0139 A79-25498
- CLATS, B. W.
Ceramic coating effect on liner metal temperatures of film-cooled annular combustor [NASA-TN-1323] p0015 A79-14098
- COFFINBERRY, G. A.
Fuel delivery system including heat exchanger means [NASA-CASE-LEW-12793-1] p0113 A79-11403
- COHEN, B. H.
NaOH-based high temperature heat-of-fusion thermal energy storage device p0155 A79-10106
Phase change thermal storage for a solar total energy system p0155 A79-17321
Development of a phase-change thermal storage system using modified anhydrous sodium hydroxide for solar electric power generation [NASA-CR-159465] p0153 A79-19454
- COHEN, S.
Mass drivers. 3: Engineering p0040 A79-32232
- COLBURN, B. L.
Analysis of a parallel-arrayed power regulating system p0101 A79-49397

COLB, G. L.

- A throat-bypass stability-bleed system using relief valves to increase the transient stability of a mixed-compression inlet
[NASA-TP-1083] p0023 79-28176

COLLINGS, E. W.

- Critical current density in wire drawn and hydrostatically extruded Nb-Ti superconductors
p0185 79-20539

CONRY, T. A.

- A comparison of measured and calculated upwelling radiance over water as a function of sensor altitude
p0162 79-51096

- A comparison of measured and calculated upwelling radiance over water as a function of sensor altitude
[NASA-TN-79147] p0131 79-22589

CONNOLLY, D. J.

- Traveling wave tube circuit
[NASA-CAGE-LEW-12013-1] p0102 79-10339

CONRAD, E. W.

- Turbine engine altitude chamber and flight testing with liquid hydrogen
[NASA-TN-79196] p0022 79-27140

CONRAD, G.

- Statistical study of supersonic compressors
p0039 79-21064

COOK, J. A.

- Evaluation of advanced regenerator systems
[NASA-CR-159422] p0188 79-12969

COOPER, L. P.

- Effect of degree of fuel vaporization upon emissions for a premixed prevaporized combustion system
[AIAA PAPER 79-1320] p0071 79-39036

- Effect of degree of fuel vaporization upon emissions for a premixed prevaporized combustion system
[NASA-TN-79154] p0012 79-23965

- Effect of degree of fuel vaporization on emissions for a premixed-prevaporized combustor system
p0020 79-25003

COPPA, A. P.

- Containment of composite fan blades
[NASA-CR-158168] p0032 79-18478

- Containment of composite fan blades
[NASA-CR-159544] p0067 79-31348

CORBETT, J. W.

- High-energy electron-induced damage production at room temperature in aluminum-doped silicon
p0154 79-32662

CORNFILL, B. W.

- Interactive multi-node blade impact analysis
[NASA-CR-159462] p0032 79-17858

COSGROVE, D. V.

- Effects of air injection on a turbocharged Teledyne Continental Motors TSIO-360-C engine
[SAE PAPER 792607] p0028 79-36760

- Effects of air injection on a turbocharged Teledyne Continental Motors TSIO-360-C engine
[NASA-TN-79121] p0158 79-20528

COLES, B. A.

- Evaluation of the cyclic behavior of aircraft turbine disk alloys
[NASA-CR-159409] p0030 79-10058

COY, J. J.

- Two-dimensional random surface model for asperity-contact in elastohydrodynamic lubrication
p0120 79-39811

- Two-dimensional random surface model for asperity-contact in elastohydrodynamic lubrication
[NASA-TN-79006] p0115 79-23430

- Comparison of predicted and measured elastohydrodynamic film thickness in a 20-millimeter-bore ball bearing
[NASA-TP-1542] p0116 79-32552

- Correlation of asperity contact-time fraction with elastohydrodynamic film thickness in a 20-millimeter-bore ball bearing
[NASA-TP-1547] p0116 79-33476

- NASA gear research and its probable effect on rotorcraft transmission design
[NASA-TN-79292] p0116 79-33477

CROUSE, J. E.

- High speed smoke flow visualization for the determination of cascade shock losses
[AIAA PAPER 79-0042] p0005 79-19495

- An off-design correlation of part span damper losses through transonic axial fan rotors
[ASME PAPER 79-GT-6] p0028 79-32329

CRUGHOLA, A.

- Effect of sterilization irradiation on friction and wear of ultrahigh-molecular-weight polyethylene
[NASA-TP-1462] p0082 79-23216

CSOHOH, A.

- Small, high-pressure, liquid oxygen turbopump
[NASA-CR-159509] p0121 79-17221

CUK, S.

- A general unified approach to modelling switching dc-to-dc converters in discontinuous conduction mode
p0101 79-10880

- A new optimum topology switching dc-to-dc converter
[NASA-CR-159509] p0101 79-10888

CULL, R.

- DOE photovoltaic tests and applications project
p0139 79-25492

CULLON, R.

- Test verification of a turbofan partial swirl afterburner
[AIAA PAPER 79-1199] p0029 79-38981

CULLON, R. E.

- Operating condition and geometry effects on low-frequency afterburner combustion instability in a turbofan at altitude
[NASA-TP-1475] p0022 79-25022

CUNHAM, W. S.

- Performance of two-stage fan with larger dampers on first-stage rotor
[NASA-TP-1399] p0018 79-23967

- Performance of two-stage fan having low-aspect-ratio first-stage rotor blading
[NASA-TP-1493] p0023 79-27143

CUNNINGHAM, R. E.

- Elastomer mounted rotors - An alternative for smoother running turbomachinery
[ASME PAPER 79-GT-149] p0119 79-32414

CURREN, A. E.

- Thermal anomalies of the transmitter experiment package on the communications technology satellite
[NASA-TP-1410] p0044 79-21120

- Life characteristics assessment of the communications technology satellite transmitter experiment package
[NASA-TN-79181] p0044 79-31264

CURRY, C. E.

- Study of an advanced General Aviation Turbine engine (GATE)
[NASA-CR-159558] p0033 79-21073

CUSANO, C.

- Elastohydrodynamic film thickness measurements of artificially produced surface dents and grooves
[ASLE PREPRINT 78-1C-1A-1] p0118 79-23267

- Elastohydrodynamic film thickness measurements of artificially produced nonsmooth surfaces
[NASA-TN-79214] p0115 79-28554

CUTRO, J. E.

- Properties and performance of fine-filament bronze-process Nb3Sn conductors
p0184 79-20529

CWYNAR, D. S.

- Lewis hybrid computing system, users manual
[NASA-TN-79111] p0165 79-20752

D

DABELLO, R. V.

- Epitaxial solar-cell fabrication, phase 2
[NASA-CR-135350] p0152 79-19446

DABNEY, D. E.

- Some heat transfer and hydrodynamic problems associated with superconducting cables (SPTL)
[NASA-TN-79023] p0102 79-15267

- Measurements of mixed convective heat transfer to low temperature helium in a horizontal channel
[NASA-TN-79158] p0104 79-23384

DABIEL, B. E.

- Measurements of admittances and characteristic combustion times of reactive gaseous propellant coaxial injectors
[NASA-CR-159542] p0072 79-23168

DABIEL, R. E.

- Nb3Ge as a potential candidate material for 15- to 25-T magnets
p0186 79-44548

- | | | | | | |
|--------------------|---|-----------------|---|---|-----------------|
| DANFELT, C. J. | Energy-state formulation of lumped volume dynamic equations with application to a simplified free piston Stirling engine | p0187 A79-49532 | Multivariable control altitude demonstration on the F100 turbofan engine
[NASA-TN-79183] | p0022 A79-25015 | |
| | Generation of linear dynamic models from a digital nonlinear simulation
[NASA-TF-1388] | p0001 A79-16796 | DEHSSLEN, R. G. | Decay of homogeneous turbulence from a given state at higher Reynolds number | p0105 A79-14952 |
| | Energy-state formulation of lumped volume dynamic equations with application to a simplified free piston Stirling engine
[NASA-TN-79197] | p0141 A79-27663 | | Comparison of a correlation term-discard closure for decaying homogeneous turbulence with experiment | p0106 A79-22424 |
| DARLOW, H. | Design and application of a test rig for super-critical power transmission shafts
[NASA-CR-3155] | p0122 A79-31603 | | Decay of homogeneous turbulence from a given state at higher Reynolds number
[NASA-TN-79011] | p0102 A79-12361 |
| DARLOW, H. S. | Design and test of a squeeze-film damper for a flexible power transmission shaft | p0123 A79-16011 | DELAAT, J. C. | Optically isolated logarithmic nanosensor capable of floating to 5 kilovolts
[NASA-TF-1527] | p0098 A79-32467 |
| | Nonsynchronous vibrations observed in a supercritical power transmission shaft
[ASME PAPER 79-GT-146] | p0123 A79-32412 | DELUCA, R. A. | Rotor fragment protection program: Statistics on aircraft gas turbine engine rotor failures that occurred in US commercial aviation during 1976
[NASA-CR-159474] | p0032 A79-18977 |
| | Elastomer mounted rotors - An alternative for smoother running turbomachinery
[ASME PAPER 79-GT-149] | p0115 A79-32414 | DELUGIS, P. | Polyimide prepreg material having improved tack retention
[NASA-CASE-LEW-12933-1] | p0059 A79-24061 |
| | An introduction to a unified approach to flexible rotor balancing
[ASME PAPER 79-GT-161] | p0124 A79-32423 | DELUGIS, P. | Effects of graphite fiber stability on the properties of PMR polyimide composites | p0066 A79-43305 |
| | Development of procedures for calculating stiffness and damping of elastomers in engineering applications. Part 5: Elastomer performance limits and the design and test of an elastomer damper
[NASA-CR-159552] | p0122 A79-24373 | | Effects of graphite fiber stability on the properties of PMR polyimide composites
[NASA-TN-79062] | p0061 A79-16075 |
| DATTA, T. | Optical, spin-resonance, and magnetoresistance studies of tetrathiatetracene/2-iodide/3 - The nature of the ground state | p0184 A79-10417 | | High char inside-modified epoxy matrix resins
[NASA-TN-79226] | p0063 A79-29240 |
| | High power phase locked laser oscillators
[NASA-CR-159630] | p0112 A79-32538 | | Curing agent for polyepoxides and epoxy resins and composites cured therewith
[NASA-CASE-LEW-13226-1] | p0059 A79-31345 |
| DATTON, J. A., JR. | Analytical prediction with multidimensional computer programs and experimental verification of the performance, at a variety of operating conditions, of two traveling wave tubes with depressed collectors
[NASA-TF-1449] | p0057 A79-22375 | DERUTE, R. S. | Laser balancing demonstration on a high-speed flexible rotor
[ASME PAPER 79-GT-56] | p0123 A79-32351 |
| DE WITT, K. J. | Resonance-tube ignition of aluminum | p0071 A79-46366 | | Experiments on multiplane balancing using a laser for material removal
[NASA-CR-3105] | p0121 A79-17228 |
| DEADHORE, D. L. | Effect of a chromium-containing fuel additive on hot corrosion | p0071 A79-26546 | DERGANCE, R. E. | Cryogenic propellant densification study
[NASA-CR-159438] | p0087 A79-12238 |
| | Airfoil cooling hole plugging by combustion gas impurities of the type found in coal derived fuels
[NASA-TN-79076] | p0089 A79-20265 | DERKACS, T. | Automated Plasma Spray (AFS) process feasibility study: Plasma spray process development and evaluation
[NASA-CR-159579] | p0092 A79-29382 |
| | An experimental, low-cost, silicon slurry/aluminide high-temperature coating for superalloys
[NASA-TN-79178] | p0075 A79-29292 | DEROCHER, W. L., JR. | Computer aided control of a mechanical arm | A79-50334 |
| DEAN, P. D. | An impulse test technique with application to acoustic measurements
[AIAA PAPER 79-0679] | p0178 A79-26890 | DESKIN, W. J. | A summary of NASA/Air Force Full Scale Engine Research programs using the F100 engine
[AIAA PAPER 79-1308] | p0030 A79-40488 |
| | Duct wall impedance control as an advanced concept for acoustic suppression enhancement
[NASA-CR-159425] | p0176 A79-10842 | | A summary of NASA/Air Force full scale engine research programs using the F100 engine
[NASA-TN-79267] | p0024 A79-30186 |
| | Studies of the acoustic transmission characteristics of coaxial nozzles with inverted velocity profiles: Comprehensive data report
[NASA-CR-159628] | p0177 A79-27933 | DICARLO, J. A. | High temperature dynamic modulus and damping of aluminum and titanium matrix composites | p0065 A79-26132 |
| DEBICARRI, D. J. | Fabrication and testing of silver-hydrogen cells
[NASA-CR-159490] | p0152 A79-16375 | | Mechanisms of boron fiber strengthening by thermal treatment | p0065 A79-30396 |
| DECKER, A. J. | Holography through optically active windows
[NASA-TF-1414] | p0109 A79-17195 | | High temperature dynamic modulus and damping of aluminum and titanium matrix composites
[NASA-TN-79080] | p0061 A79-16077 |
| | Simulated electronic heterodyne recording and processing of pulsed-laser holograms
[NASA-TF-1444] | p0111 A79-21329 | | Mechanisms of boron fiber strengthening by thermal treatment
[NASA-TN-79077] | p0062 A79-20186 |
| DEMOPF, R. L. | Multivariable control altitude demonstration on the F100 turbofan engine
[AIAA PAPER 79-1204] | p0029 A79-39814 | DICKMAN, R. A. | Lean, Preheated-Prevaporized (LPP) combustor conceptual design study
[NASA-CR-159629] | p0072 A79-31358 |
| | | | DICUS, J. | Synthesis of blade flutter vibratory patterns using stationary transducers | p0127 A79-10823 |
| | | | DIEDRICH, J. H. | An approach to optimum subsonic inlet design
[ASME PAPER 79-GT-51] | p0006 A79-3052 |

An approach to optimum subsonic inlet design
[NASA-TM-79051] p0002 N79-12020

DILLON, R. O.
Superconducting properties of evaporated copper
molybdenum sulfide films p0184 A79-20219

Reactively evaporated films of copper molybdenum
sulfide p0185 A79-31973

DITTMAR, J. E.
Tone noise of three supersonic helical tip speed
propellers in a wind tunnel p0175 A79-35801

Feasibility of wing shielding of the airplane
interior from the shock noise generated by
supersonic tip speed propellers p0172 N79-15757

Tone noise of three supersonic helical tip speed
propellers in a wind tunnel at 0.8 Mach number
[NASA-TM-79046] p0172 N79-15758

Tone noise of three supersonic helical tip speed
propellers in a wind tunnel [NASA-TM-79167] p0174 N79-25840

DOBLE, F. X.
Mini-BRU/EIPS foil bearing development
[NASA-CR-159442] p0120 N79-11407

Analysis, design, fabrication and testing of the
mini-Brayton rotating unit (Mini-BRU). Volume
1: Text and tables [NASA-CR-159441-VOL-1] p0120 N79-11408

Analysis, design, fabrication and testing of the
mini-Brayton rotating unit (Mini-BRU). Volume
2: Figures and drawings [NASA-CR-159441-VOL-2] p0120 N79-11409

DODDS, W. J.
Advanced low emissions catalytic combustor program
at General Electric p0021 N79-25011

Lean, Premixed-Prevaporized (LPP) combustor
conceptual design study [NASA-CR-159629] p0072 N79-31358

DOLAN, F. I.
Design, development, and test of a laser
velocimeter for a small 8:1 pressure ratio
centrifugal compressor [NASA-CR-134781] p0111 N79-27478

DOLLERIS, G. W.
Strain gage system evaluation program
[NASA-CR-159486] p0110 N79-19314

DONITZ, S.
Effect of parasitic plasma currents on solar-array
power output p0047 N79-24025

Neutralization tests on the SERT 2 spacecraft
[NASA-TM-79271] p0054 N79-33255

DONOFRUE, P.
Communications technology satellite: United
States experiments and disaster communications
applications [NASA-TM-79109] p0044 N79-23999

DONOVAN, R. L.
Development of single-cell protectors for sealed
silver-zinc cells [NASA-CR-159407] p0151 N79-12550

DONOVAN, R. E.
Wind turbines for electric utilities - Development
status and economics [AIAA PAPER 79-0965] p0148 A79-38888

Wind turbines for electric utilities: Development
status and economics [NASA-TM-79170] p0142 N79-30719

DONOVAN, R. E.
Large wind turbine generators p0146 A79-15881

DOE, T. A.
Determination of lubricant selection based on
elastohydrodynamic film thickness and traction
measurement [NASA-CR-159428] p0121 N79-14385

DOWSON, D.
Elastohydrodynamic lubrication of elliptical
contacts for materials of low elastic modulus.
II - Starved conjunction [ASME PAPER 78-LUB-1] p0118 A79-23229

DOYLE, V. L.
Experimental clean combustor program, phase 3:
Noise measurement addendum [NASA-CR-159458] p0177 N79-17656

DRAKE, S. E.
Three-dimensional finite-element elastic analysis
of a thermally cycled single-edge wedge geometry
specimen [NASA-TM-79026] p0172 N79-16644

DRENFIELD, E. L.
Effect of grain orientation and coating on thermal
fatigue resistance of a directionally solidified
superalloy (MAR-M 247) [NASA-TM-79129] p0127 N79-22565

DUDZINSKI, T.
Measurements of carbon monoxide, condensation
nuclei, and ozone on a B 747SP aircraft flight
around the world p0158 A79-31332

DUDZINSKI, T. J.
Airborne atmospheric sampling system p0012 A79-50333

NASA Global Atmospheric Sampling Program (GASP)
data report for tape V10009 [NASA-TM-79058] p0157 N79-15446

NASA Global Atmospheric Sampling Program (GASP)
data report for tapes V10010 and V10012
[NASA-TM-79061] p0157 N79-15450

Carbon monoxide measurement in the global
atmospheric sampling program [NASA-TP-1526] p0158 N79-31841

DURR, E. A.
Effects of flameholder blockage on emissions and
performance of lean premixed-prevaporized
combustors p0021 N79-25006

DURR, E. E.
Experimental study of the effects of flameholder
geometry on emissions and performance of lean
premixed combustors [AIAA PAPER 79-0187] p0070 A79-15586

DUGAN, J. F., JR.
Prop-fan propulsion - Its status and potential
[SAE PAPER 780995] p0026 A79-25880

DUNN, J. H.
Commercial synchronous alternating-current
generators p0140 N79-26482

DUSCHA, E. A.
Thermal energy storage for industrial waste heat
recovery p0145 A79-10101

Thermal storage for industrial process and reject
heat p0147 A79-21300

Thermal storage for industrial process and reject
heat [NASA-TM-78994] p0134 N79-11481

The role of thermal energy storage in industrial
energy conservation [NASA-TM-79122] p0137 N79-21550

DUSTIN, E. G.
A throat-bypass stability-bleed system using
relief valves to increase the transient
stability of a mixed-compression inlet
[NASA-TP-1083] p0023 N79-28176

DUTTA, S.
State-of-the-art of SiAlON materials
[NASA-TM-79207] p0084 N79-30378

E

EDSINGHE, E. W.
SINWEST - A simulation model for wind energy
storage systems p0145 A79-10241

SINWEST: A simulation model for wind and
photovoltaic energy storage systems (cdc program
descriptions), volume 2 [NASA-CR-159608] p0167 N79-33884

EDWARDS, D. E.
Modeling of premixing-prevaporizing fuel-air
mixing passages p0019 N79-24998

EISENHAJ, P. E.
Development of a three-dimensional turbulent duct
flow analysis [NASA-CR-3029] p0106 N79-12366

EKSTEDT, E. E.
Lean, premixed, prevaporized combustor conceptual
design study p0022 N79-25014

- Lean, Premixed-Prevaporized (LPP) combustor conceptual design study
[NASA-CR-159629] p0072 N79-31358
- ELLEN, J. H., JR.
Effects of arcing due to spacecraft charging on spacecraft survival
[NASA-CR-159593] p0100 N79-25312
- ENGLISH, G. W.
Trajectories of charged particles in radial electric and uniform axial magnetic fields
p0182 A79-41788
- ENGLUND, D. E.
Measuring unsteady pressure on rotating compressor blades
[NASA-TN-79159] p0105 N79-22448
- ENSIGN, C. E.
Interpolation and extrapolation of creep rupture data by the Minimum Commitment Method. I - Focal-point convergence. II - Oblique translation. III - Analysis of multiheats
p0077 A79-16038
- ERCEGOVICH, D. E.
Effect of swirler-mounted mixing venturi on emissions of flame-tube combustor using jet A fuel
[NASA-TP-1393] p0015 N79-14099
- ERNST, E. E.
Background and system description of the Mod 1 wind turbine generator
p0155 A79-20825
- ESINGER, A. W.
SINVEST: A simulation model for wind and photovoltaic energy storage systems (CIC user's manual), volume 1
[NASA-CR-159607] p0166 N79-33883
- ETSION, I.
Cantilever mounted resilient pad gas bearing
[NASA-CASE-LEW-12569-1] p0113 N79-10418
Self-stabilizing radial face seal
[NASA-CASE-LEW-12591-1] p0113 N79-12445
Hydrodynamic effects in a misaligned radial face seal
[NASA-CR-135228] p0121 N79-17226
- EVANS, J. C., JR.
Solar cells having integral collector grids
[NASA-CASE-LEW-12819-1] p0133 N79-11467
Application of semiconductor diffusants to solar cells by screen printing
[NASA-CASE-LEW-12775-1] p0133 N79-11468
Solar cell collector and method for producing same
[NASA-CASE-LEW-12552-2] p0133 N79-11472
Method for fabricating solar cells having integrated collector grids
[NASA-CASE-LEW-12819-2] p0136 N79-18444
- EWART, R. O.
Cryogenic propellant densification study
[NASA-CR-159438] p0087 N79-12238
- EWASHINKA, J. G.
Discharge characteristics of 300 ampere-hour Ni-Zn traction cells
[NASA-TN-79244] p0143 N79-31781
- F**
- FALCONER, P. D.
An analysis of the first two years of GASF data
p0160 A79-15068
A summary of research on the NASA-Global Atmospheric Sampling Program performed by the Atmospheric Sciences Research Center
[NASA-CR-159614] p0155 N79-27716
- FAN, B.
Sinner-enhanced flashlamp-pumped dye laser
p0112 A79-32981
- FAN, J. C. C.
Shallow-homojunction GaAs solar cells
p0144 N79-32666
- FASCHING, W. A.
CF6 jet engine performance improvement program. Task 1: Feasibility analysis
[NASA-CR-159450] p0033 N79-21074
CF6 jet engine performance improvement program. Short core exhaust nozzle performance improvement concept
[NASA-CR-159564] p0038 N79-33206
- FELBECK, D. E.
An acoustic emission study of plastic deformation in polycrystalline aluminum
p0077 A79-19458
- FELDER, S. F.
Intraocular pressure reduction and regulation system
[NASA-TN-79187] p0165 N79-28881
- FERRANTE, J.
The effect of nitrogen ion (N⁺) implantation on the friction and wear characteristics of iron
[NASA-TN-79029] p0073 N79-12201
Wear of aluminum and hypoeutectic aluminum-silicon alloys in boundary-lubricated pin-on disk sliding
[NASA-TP-1442] p0074 N79-21184
Evaluation and auger analysis of a zinc-dialkyl-dithiophosphate antiwear additive in several diester lubricants
[NASA-TP-1544] p0084 N79-32359
- FERTIS, D. G.
Evaluation of urethane for feasibility of use in wind turbine blade design
[NASA-CR-159530] p0153 N79-20497
- FESSLER, T. E.
METAIR: A computer code for calculating thermodynamic and transport properties of air-water mixtures
[NASA-TP-1466] p0166 N79-23688
- FETTEROFF, C. W.
Automated Plasma Spray (APS) process feasibility study: Plasma spray process development and evaluation
[NASA-CR-159579] p0092 N79-29382
- FIELD, B. B.
Alternate methods of applying diffusants to silicon solar cells
[NASA-CR-159508] p0153 N79-29603
- FIELDER, W. L.
The alkaline zinc electrode as a mixed potential system
[NASA-TN-79235] p0142 N79-29600
- FINE, L.
Mass drivers. 3: Engineering
p0040 N79-32232
- FINGER, R. W.
Proof test criteria for thin walled pressure vessels
p0123 A79-26985
- FINK, B. E.
Noise from struts and splitters in turbofan exit ducts
[AIAA PAPER 79-0637] p0178 A79-26923
- FIORENTINO, A. J.
Lean, premixed, prevaporized combustor conceptual design study
p0021 N79-25013
Lean, premixed, prevaporized fuel combustor conceptual design study
[NASA-CR-159647] p0035 N79-32211
- FIORITO, R. J.
Wide range operation of advanced low NOx aircraft gas turbine combustors
[ASME PAPER 78-GT-128] p0024 A79-10792
- FISHBACH, L. H.
Computerized systems analysis and optimization of aircraft engine performance, weight, and life cycle costs
[NASA-TN-79221] p0170 N79-29938
- FLEMING, D. F.
Stiffness of straight and tapered annular gas path seals
[ASME PAPER 78-LUB-18] p0118 A79-23235
Laser balancing demonstration on a high-speed flexible rotor
[ASME PAPER 79-GT-56] p0123 A79-32351
- FLORES, P. J.
Use of refinery computer model to predict fuel production
[NASA-TN-79203] p0089 N79-28349
- FORD, W. F.
Acceleration of linear and logarithmic convergence
p0168 A79-40494
- FORDYCE, J. S.
Technology status: Batteries and fuel cells
p0052 N79-10132
- FORESTIERI, A. P.
Endurance testing of first generation /Block I/ commercial solar cell modules
p0148 A79-41022
- FORNAN, R.
A proposed physical model for the impregnated tungsten cathode based on Auger surface studies of the Ba-O-W system
p0078 A79-39972

- Comment on the mechanism of operation of the
impregnated tungsten cathode
p0099 A79-42024
- FORSTH, J. B.**
Laser power conversion system analysis, volume 1
[NASA-CR-159523-VOL-1] p0112 W79-21334
Laser power conversion system analysis, volume 2
[NASA-CR-159523-VOL-2] p0112 W79-21335
Laser rocket system analysis
[NASA-CR-159521] p0112 W79-21337
- FORZINI, A.**
Heat exchanger and method of making
[NASA-CASR-LEW-12441-1] p0102 W79-13289
A heat exchanger and method of making
[NASA-CASR-LEW-12441-2] p0104 W79-21313
A heat exchanger and method of making
[NASA-CASR-LEW-12441-3] p0104 W79-23383
- FOX, T. A.**
Efficiency enhancement of octave-bandwidth
traveling wave tubes by use of multistage
depressed collectors
[NASA-TP-1416] p0097 W79-17139
Efficiency enhancement of dual-mode traveling wave
tubes at saturation and in the linear range by
use of spent-beam refocusing and multistage
depressed collectors
[NASA-TP-1486] p0098 W79-28420
- FRANKENFELD, J. B.**
High performance, high density hydrocarbon fuels
[NASA-CR-159480] p0091 W79-20267
- FRARY, J. L.**
Turbojet blade vibration data acquisition design
and feasibility testing
[NASA-CR-159505] p0032 W79-18976
- FRECHER, J. C.**
Materials and structural aspects of advanced
gas-turbine helicopter engines
p0029 A79-39804
Composites emerging for aeropropulsion applications
p0066 A79-53720
Materials and structural aspects of advanced
gas-turbine helicopter engines
[NASA-TM-79100] p0001 W79-20008
- FREDERICK, J. B.**
An acoustic emission study of plastic deformation
in polycrystalline aluminum
p0077 A79-19458
- FRIEDMAN, B.**
High-freezing-point fuels used for aviation
turbine engines
[ASME PAPER 79-GT-141] p0090 A79-30555
High freezing point fuels used for aviation
turbine engines
[NASA-TM-79015] p0089 W79-15199
- FRIEDMAN, P. P.**
Nonlinear equations of equilibrium for elastic
helicopter or wind turbine blades undergoing
moderate deformation
[NASA-CR-159478] p0130 W79-19414
- FRIEDBURG, G. C.**
Mass spectrometric investigation of the
vaporization of sodium and potassium chromates -
Preliminary results
p0071 A79-49533
The role of NaCl in flame chemistry, in the
deposition process, and in its reactions with
protective oxides as related to hot corrosion
p0071 A79-49534
Chemically frozen multicomponent boundary layer
theory of salt and/or ash deposition rates from
combustion gases
p0078 A79-50912
Mass spectrometric investigation of the
vaporization of sodium and potassium chromates:
Preliminary results
[NASA-TM-79210] p0069 W79-27279
The chemistry of sodium chloride involvement in
processes related to hot corrosion
[NASA-TM-79251] p0069 W79-31361
- FUCHIMORI, C. A.**
Evaluation of advanced regenerator systems
[NASA-CR-159422] p0188 W79-12969
- FUJII, H.**
Low-cost directionally-solidified turbine blades,
volume 1
[NASA-CR-159466] p0080 W79-24121
- FULLER, L. C.**
User's manual for PRESTO: A computer code for the
performance of regenerative steam turbine cycles
p0122 W79-25395
- FURMAN, E. B.**
Closed loop spray cooling apparatus
[NASA-CASR-LEW-11981-2] p0103 W79-20336
- FUSARO, R. L.**
A comparison of the lubricating mechanisms of
graphite fluoride and molybdenum disulfide films
p0085 A79-16659
Mechanisms of graphite fluoride/CF₄/n lubrication
p0086 A79-31249
Lubrication and failure mechanisms of molybdenum
disulfide films. 1: Effect of atmosphere
[NASA-TP-1343] p0081 W79-13158
Lubrication and failure mechanisms of molybdenum
disulfide films. 2: Effect of substrate
roughness
[NASA-TP-1379] p0081 W79-13159
Effect of thermal aging on the tribological
properties of polyimide films and
polyimide-bonded graphite fluoride films
[NASA-TM-79045] p0082 W79-15186
Lubricating and wear mechanisms for a hemisphere
sliding on polyimide-bonded graphite fluoride film
[NASA-TP-1524] p0084 W79-30381

G

- GAPPIN, W. O.**
JT8D and JT9D jet engine performance improvement
program. Task 1: Feasibility analysis
[NASA-CR-159449] p0033 W79-20116
JT8D revised high-pressure turbine cooling and
other outer air seal program
[NASA-CR-159551] p0033 W79-21076
- GAHT, R. P.**
Factors affecting the open-circuit voltage and
electrode kinetics of some iron/titanium/redox
flow cells
p0146 A79-11824
Supply of reactants for Redox bulk energy storage
systems
[NASA-TM-78995] p0133 W79-11479
- GALLAGHER, J. J.**
Millimeter wave satellite concepts. Volume 1:
Executive summary
[NASA-CR-159504] p0041 W79-26101
- GARDNER, W. B.**
Energy efficient engine flight propulsion system
preliminary analysis and design report
[NASA-CR-159487] p0035 W79-30189
- GARRETT, B. G.**
Social and economic impact of solar electricity at
Schuchull Village
[NASA-TM-79194] p0139 W79-25501
- GATZEL, B. S.**
Prop-fan propulsion - Its status and potential
[SAE PAPER 780995] p0026 A79-25880
- GAUGLER, R. L.**
Thermal-structural mission analyses of air-cooled
gas turbine blades
[ASME PAPER 79-GT-19] p0027 A79-30553
Thermal-structural mission analyses of air-cooled
gas turbine blades
[NASA-TM-78963] p0126 W79-11433
TACT 1: A computer program for the transient
thermal analysis of a cooled turbine blade or
vane equipped with a coolant insert. 2:
Programmers manual
[NASA-TP-1391] p0103 W79-18288
- GAUTHIER, D. J.**
Measurements of carbon monoxide, condensation
nuclei, and ozone on a B 747SP aircraft flight
around the world
p0158 A79-31332
Experimental evidence of interhemispheric
transport from airborne carbon monoxide
measurements
p0158 A79-38942
Aircraft cabin ozone measurements on B747-100 and
B747-SP aircraft: Correlations with atmospheric
ozone and ozone encounter statistics
[NASA-TM-79060] p0008 W79-15013
NASA Global Atmospheric Sampling Program (GASP)
data report for tapes VL0007 and VL0008
[NASA-TM-73784] p0157 W79-17359
- GAVALER, J. B.**
Nb₃Ge as a potential candidate material for 15- to
25-T magnets
p0186 A79-44548

- GEDRON, L.**
Description and orbit data of variable-conductance heat-pipe system for the communications technology satellite
[NASA-TN-1465] p0105 N79-30516
- GEDNEY, R. T.**
VHF downlink communication system for SLAS data
[NASA-TN-79164] p0094 N79-23313
- GEDWILL, H. A.**
Thermal barrier coatings: Burner rig hot corrosion test results
[NASA-TN-79005] p0073 N79-11179
- GELON, W.**
Advanced electrostatic ion thruster for space propulsion
[NASA-CN-159406] p0056 N79-14153
- GERBER, A. H.**
Survey of inorganic polymers
[NASA-CN-159563] p0087 N79-30377
- GRASSTIN, R.**
Fundamental of Gas Turbine combustion
[NASA-CN-1087] p0022 N79-25016
- GREUER, H. W.**
Wind-turbine-generator rotor-blade concepts with low-cost potential
p0147 A79-20828
- GIBALA, R.**
Some TEM observations of Al₂O₃ scales formed on NiCrAl alloys
[NASA-TN-79259] p0076 N79-33306
- GIGLIOTTI, E. F. I.**
Evaluation of an advanced directionally solidified gamma/gamma'-alpha Mo eutectic alloy
[NASA-CN-159416] p0079 N79-20222
- GILBERT, L. J.**
Control of wind turbine generators connected to power systems
p0146 A79-15574
Lewis Research Center studies of multiple large wind turbine generators on a utility network
p0149 A79-46547
- GILL, J. C.**
Study of an advanced General Aviation Turbine Engine (GATE)
[NASA-CN-159558] p0033 N79-21073
- GINER, J. D.**
Catalyst surfaces for the chromous/chromic redox couple
[NASA-CASE-LEW-13148-1] p0134 N79-14538
- GINTON, L. D.**
Atlas 5013 tank corrosion test
[NASA-CN-158760] p0050 N79-27234
- GITLOW, B.**
Development of advanced fuel cell system
[NASA-CN-159443] p0151 N79-12553
Strip cell test and evaluation program
[NASA-CN-159652] p0150 N79-31784
- GLASGOW, J. C.**
Design and operating experience on the U.S. Department of Energy Experimental Mod-O 100 kW Wind Turbine
p0145 A79-10234
Utility operational experience on the NASA/DOE Mod-OA 200 kW Wind Turbine
p0149 A79-46537
Utility operational experience on the NASA/DOE Mod-OA 200-kW wind turbine
[NASA-TN-79084] p0136 N79-20494
- GLASGOW, T. E.**
Longitudinal shear behavior of several oxide dispersion strengthened alloys
p0076 A79-14955
An oxide dispersion strengthened alloy for gas turbine blades
[AIAA 79-0763] p0077 A79-28276
An oxide dispersion strengthened alloy for gas turbine blades
[NASA-TN-79088] p0052 N79-20180
Bond strengths of reaction bonded silicon nitride prepared from dry attrition milled silicon powder
[NASA-TN-79230] p0084 N79-30379
- GLEASON, C. C.**
Experimental clean combustor program: Diesel no. 2 fuel addendum, phase 3
[NASA-CN-135413] p0091 N79-26221
Experimental Clean Combustor Program (ECCF), phase 3
[NASA-CN-135384] p0035 N79-31207
- GLUZEK, F.**
Liquid oxygen/liquid hydrogen boost/vane pump for the advanced orbit transfer vehicles auxiliary propulsion system
[NASA-CN-159648] p0057 N79-31341
- GNEDCO, A. J.**
Microprocessor control of a wind turbine generator
[NASA-TN-79021] p0147 A79-21302
Microprocessor control of a wind turbine generator
[NASA-TN-79021] p0134 N79-12548
- GODLEWSKI, H. P.**
Open-circuit voltage improvements in low-resistivity solar cells
p0143 N79-32649
- GOLD, R.**
Power train analysis for the DOE/NASA 100-kW wind turbine generator
[NASA-TN-78997] p0135 N79-16355
- GOLDSTEIN, H. E.**
Supersonic unstalled flutter
p0004 A79-12599
Unsteady flow in a supersonic cascade with subsonic leading-edge locus
p0005 A79-16047
Unsteady vortical and entropic distortions of potential flows round arbitrary obstacles
p0005 A79-19452
Scattering and distortion of the unsteady motion on transversely sheared mean flows
p0106 A79-37140
Turbulence generated by the interaction of entropy fluctuations with non-uniform mean flows
p0106 A79-45468
Supersonic unstalled flutter
[NASA-TN-79001] p0002 N79-11000
Supersonic unstalled flutter
p0023 N79-27181
- GOODYKOOTS, J. E.**
Experimental study of coaxial nozzle exhaust noise
[AIAA PAPER 79-0631] p0175 A79-28963
Effects of geometric and flow-field variables on inverted-velocity-profile coaxial jet noise and source distributions
[AIAA PAPER 79-0635] p0175 A79-32126
Experimental study of coaxial nozzle exhaust noise
[NASA-TN-79090] p0173 N79-20829
- GORDON, L. E.**
Storage systems for solar thermal power
p0145 A79-10108
SINWEST - A simulation model for wind energy storage systems
p0145 A79-10241
Thermal storage technologies for solar industrial process heat applications
[NASA-TN-79130] p0136 N79-20498
- GORLA, R. S. E.**
Comparison of predicted and measured elastohydrodynamic film thickness in a 20-millimeter-bore ball bearing
[NASA-TF-1542] p0116 N79-32552
- GORLAND, S.**
Results from Symposium on Future Orbital power systems technology requirements
[NASA-TN-79125] p0053 N79-22191
- GORRELL, W. L.**
Performance of two-stage fan having low-aspect-ratio first-stage rotor blading
[NASA-TF-1493] p0023 N79-27143
Performance of two-stage fan with a first-stage rotor redesigned to account for the presence of a part-span damper
[NASA-TF-1483] p0024 N79-30191
- GOULDIN, F. C.**
Turbulence effects on flame speed and flame structure
[AIAA PAPER 79-0016] p0070 A79-19480
- GRAHAM, H. W.**
Fundamental mechanisms that influence the estimate of heat transfer to gas turbine blades
p0099 A79-49526
Fundamental mechanisms that influence the estimate of heat transfer to gas turbine blades
[NASA-TN-79128] p0103 N79-20346
- GRAJER, H. A.**
Geosynchronous satellite operating anomalies caused by interaction with the local spacecraft environment
p0050 N79-24049

GRANT, H. P.

- Instrumentation for measuring the dynamic pressure on rotating compressor blades
[NASA-CR-159466] p0110 N79-12418
- Measuring unsteady pressure on rotating compressor blades
[NASA-TN-79159] p0109 N79-22448
- Turbulence characteristics of compressor discharge flows
p0019 N79-24995

GRAVES, B.

- Design and fabrication of the Mini-Brayton Recuperator (MBR)
[NASA-CR-159429] p0151 N79-11476

GRAY, D. E.

- Energy efficient engine preliminary design and integration study
[NASA-CR-135396] p0012 N79-12084

GRAY, S.

- Development of surface coatings for air-lubricated, compliant journal bearings to 650 C
[ASLE PREPRINT 78-LC-3C-1] p0123 A79-23252
- Static evaluation of surface coatings for compliant gas bearings in an oxidizing atmosphere to 650 C
p0088 A79-31957

GREENE, W.

- Lean, premixed, prevaporized fuel combustor conceptual design study
[NASA-CR-159647] p0035 N79-32211

GREYWALL, R. S.

- Velocity, temperature, and electrical conductivity profiles in hydrogen-oxygen MHD duct flows
p0182 A79-26184

GRIER, W.

- Laboratory studies of electrical properties of insulating materials
p0044 A79-20877

GRIER, W. T.

- Large space system - Charged particle environment interaction technology
[AIAA 79-0913] p0055 A79-34775
- Large space system: Charged particle environment interaction technology
[NASA-TN-79156] p0046 N79-22188
- Plasma Interaction Experiment (PIX) flight results
p0047 N79-24022
- High voltage surface-charged environment test results from space flight and ground simulation experiments
[NASA-TN-79184] p0043 N79-27235

GRIFFIN, D. G., JR.

- Wind-turbine-generator rotor-blade concepts with low-cost potential
p0147 A79-20828
- Design, fabrication, and test of a composite material wind turbine rotor blade
[NASA-CR-135389] p0150 N79-10525

GRINIS, R. H.

- Fatigue behavior of SiC reinforced titanium composites
[NASA-TN-79223] p0064 N79-30296

GROBMAN, J.

- Alternative aircraft fuels
p0090 A79-10824
- Alternative aviation turbine fuels
p0090 A79-12378

GROBMAN, J. S.

- Characteristics and combustion of future hydrocarbon fuels
p0090 A79-11599
- Impact of future fuel properties on aircraft engines and fuel systems
p0024 A79-11600
- Characteristics and combustion of future hydrocarbon fuels
p0089 N79-13196
- Impact of future fuel properties on aircraft engines and fuel systems
p0089 N79-13197

GROENEWEG, J. F.

- Effects of inflow distortion profiles on fan tone noise calculated using a 3-D theory
[AIAA PAPER 79-0577] p0175 A79-26911
- Effects of inflow distortion profiles on fan tone noise calculated using a 3-D theory
[NASA-TN-79082] p0173 N79-16647

GROSSBECK, D.

- Assessment at full scale of nozzle/wing geometry effects on OTW aeroacoustic characteristics
p0175 A79-39802
- Wing aerodynamic loading caused by jet-induced lift associated with STOL-OTW configurations
[AIAA PAPER 79-1664] p0006 A79-47346
- Assessment at full scale of nozzle/wing geometry effects on OTW aero-acoustic characteristics
[NASA-TN-79168] p0174 N79-25841
- Wing aerodynamic loading caused by jet-induced lift associated with STOL-OTW configurations
[NASA-TN-79218] p0004 N79-28146

GROSS, B.

- Mode I analysis of a cracked circular disk subject to a couple and a force
p0128 A79-15588
- Mode I analysis of a face cracked plate subjected to rotationally constrained end displacements
p0128 A79-21831
- Mode I crack surface displacements for a round compact specimen subject to a couple and force
p0129 A79-39812
- Mode I crack surface displacements for a round compact specimen subject to a couple and force
[NASA-TN-79096] p0161 N79-20572

GROVES, W. O.

- Method for the preparation of inorganic single crystal and polycrystalline electronic materials
[NASA-CASE-XLE-02545-1] p0184 N79-21910

GRUBER, R. P.

- Closed loop solar array-ion thruster system with power control circuitry
[NASA-CASE-LEW-12780-1] p0052 N79-20179

GUILLIAMS, B. P.

- Three-dimensional finite-element elastic analysis of a thermally cycled single-edge wedge geometry specimen
[NASA-TN-79026] p0172 N79-16644

GURSKI, G. S.

- Communications technology satellite: United States experiments and disaster communications applications
[NASA-TN-79109] p0044 N79-23999

GUSTAFSON, R. E.

- Design, fabrication, and test of a composite material wind turbine rotor blade
[NASA-CR-135389] p0150 N79-10525

GUSTAFSON, T. K.

- Simmer-enhanced flashlamp-pumped dye laser
p0112 A79-32981

GUSTAFSSON, U. E. C.

- Airborne atmospheric sampling system
p0012 A79-50333

GUTIERREZ, O. A.

- Effects of geometric and flow-field variables on inverted-velocity-profile coaxial jet noise and source distributions
[AIAA PAPER 79-0635] p0175 A79-32126

H

HAAS, J. E.

- Effect of rotor tip clearance and configuration on overall performance of a 12.77-centimeter tip diameter axial-flow turbine
[ASME PAPER 79-GT-42] p0027 A79-30521
- Effect of rotor tip clearance and configuration on overall performance of a 12.77-centimeter tip diameter axial-flow turbine
[NASA-TN-79025] p0002 N79-12015

HACKNEY, R. D.

- Multivariable control altitude demonstration on the F100 turbofan engine
[AIAA PAPER 79-1204] p0029 A79-39814
- Multivariable control altitude demonstration on the F100 turbofan engine
[NASA-TN-79183] p0022 N79-25015

HADEK, V.

- Optical, spin-resonance, and magnetoresistance studies of /tetrathiatetracene/2/iodide/3 - The nature of the ground state
p0184 A79-10417

HADT, W. P.

- Shaft seal assembly for high speed and high pressure applications
[NASA-CASE-LEW-11873-1] p0115 N79-22475

HADY, W. P.

- Compressible flow across narrow passages:

- Comparison of theory and experiment for face seals
[NASA-TF-1346] p0113 N79-10424
- Effect of sterilization irradiation on friction
and wear of ultrahigh-molecular-weight
polyethylene
[NASA-TP-1462] p0082 N79-23216
- HALFORD, G. E.**
The strainrange partitioning behavior of an
advanced gas turbine disk alloy, AF2-1DA
[AIAA PAPER 79-1192] p0078 A79-38977
- Strainrange partitioning behavior of the
nickel-base superalloys, Rene 80 and IN-100
p0126 N79-10480
- The strainrange partitioning behavior of an
advanced gas turbine disk alloy, AF2-1DA
[NASA-TM-79179] p0075 N79-23196
- Strainrange partitioning life predictions of the
long time metal properties council creep-fatigue
tests
[NASA-TM-79260] p0127 N79-31619
- HALL, E. W.**
Conceptual design of thermal energy storage
systems for near term electric utility
applications
[NASA-CR-159577] p0155 N79-33560
- HALL, R. M.**
High efficiency cell geometry p0143 N79-32653
- HALLER, J. A.**
Power-conversion system component summation
p0140 N79-26483
- HAMED, A.**
Flow in nonrotating passages of radial inflow
turbines
[NASA-CR-159679] p0035 N79-32212
- HAMROCK, B. J.**
Elastohydrodynamic lubrication of elliptical
contacts for materials of low elastic modulus.
II - Starved conjunction
[ASME PAPER 78-LUE-1] p0118 A79-23229
- Effect of geometry on hydrodynamic film thickness
[ASME PAPER 78-LUE-24] p0118 A79-23237
- HANLOSER, K. J.**
Test verification of a turbopan partial swirl
afterburner
[AIAA PAPER 79-1199] p0029 A79-38981
- HANNON, M. P.**
Some effects of cyclic induced deformation in
rocket thrust chambers
[AIAA 79-0911] p0054 A79-34736
- Some effects of cyclic induced deformation in
rocket thrust chambers
[NASA-TM-79112] p0103 N79-20337
- HANSEN, E. C.**
Axial-flow compressor turning angle and loss by
inviscid-viscous interaction blade-to-blade
computation
[ASME PAPER 79-GT-5] p0006 A79-30504
- HANSEN, I.**
Description of a 2.3 kW power transformer for
space applications p0099 A79-34991
- Description of a 2.3 kW power transformer for
space applications
[NASA-TM-79138] p0057 N79-23348
- HARE, R. C.**
Conceptual design of thermal energy storage
systems for near term electric utility
applications. Volume 1: Screening of concepts
[NASA-CR-159411-VOL-1] p0151 N79-13496
- Conceptual design of thermal energy storage
systems for near term electric utility
applications. Volume 2: Appendices - screening
of concepts
[NASA-CR-159411-VOL-2] p0152 N79-13497
- HART, F. E.**
Shear rupture of a directionally solidified
eutectic gamma/gamma-prime - alpha /Mo/ alloy
p0077 A79-21301
- Shear rupture of a directionally solidified
eutectic gamma/gamma-prime - alpha (Mo) alloy
[NASA-TM-79118] p0073 N79-12205
- HART, R. E.**
Photon degradation effects in terrestrial solar
cells p0149 A79-41098
- Photon-degradation effects in terrestrial silicon
solar cells p0149 A79-42545
- HART, R. E., JR.**
Temperature and intensity dependence of the
performance of an electron-irradiated
(AlGa)As/GaAs solar cell p0144 N79-32665
- HARTMAN, H. J.**
Supersonic unstalled flutter p0004 A79-12599
- Supersonic unstalled flutter
[NASA-TM-79001] p0002 N79-11000
- Supersonic unstalled flutter p0023 N79-27181
- HASTINGS, T. W.**
High performance, high density hydrocarbon fuels
[NASA-CR-159480] p0091 N79-20267
- HAUGLAND, E. J.**
Hall effect and magnetoresistivity in the ternary
molybdenum sulfides p0185 A79-21157
- HAUSZ, W.**
Conceptual design of thermal energy storage
systems for near term electric utility
applications. Volume 1: Screening of concepts
[NASA-CR-159411-VOL-1] p0151 N79-13496
- Conceptual design of thermal energy storage
systems for near term electric utility
applications. Volume 2: Appendices - screening
of concepts
[NASA-CR-159411-VOL-2] p0152 N79-13497
- Conceptual design of thermal energy storage
systems for near term electric utility
applications
[NASA-CR-159577] p0155 N79-33560
- HAWSTAD, P. E.**
Evaluation of ceramics for stator application:
Gas turbine engine report
[NASA-CR-159533] p0033 N79-21075
- HAWK, J. D.**
Theoretical fan velocity distortions due to inlets
and nozzles p0006 A79-39810
- Theoretical study of VTOL tilt-nacelle
axisymmetric inlet geometries
[NASA-TP-1380] p0003 N79-14996
- Theoretical fan velocity distortions due to inlets
and nozzles
[NASA-TM-79150] p0003 N79-23911
- Computer programs for calculating two-dimensional
potential flow through deflected nozzles
[NASA-TM-79144] p0004 N79-26019
- HAWKINS, C. E.**
Increased capabilities of the 30-cm diameter Hg
ion thruster
[AIAA 79-0910] p0055 A79-34774
- Increased capabilities of the 30-cm diameter Hg
ion thruster
[NASA-TM-79142] p0053 N79-22192
- HAYES, C. L.**
Ground-to-space optical power transfer p0161 A79-17180
- High power phase locked laser oscillators
[NASA-CR-159630] p0112 N79-32538
- HAYES, P. A.**
User's manual for FRAC3E: Supplement to report on
stress analysis for structures with surface cracks
[NASA-CR-159401] p0129 N79-13406
- HEIDLEY, D. W.**
Cross-linked polyvinyl alcohol and method of
making same
[NASA-CASE-LEW-13101-1] p0068 N79-14173
- HEIDLEBERG, L. J.**
Full-scale engine tests of bulk absorber acoustic
inlet treatment
[AIAA PAPER 79-0600] p0026 A79-26881
- Full-scale engine tests of bulk absorber acoustic
inlet treatment
[NASA-TM-79079] p0173 N79-16645
- HEIDMANN, H. P.**
Modal propagation angles in a cylindrical duct
with flow and their relation to sound radiation
[AIAA PAPER 79-0183] p0174 A79-19582
- Analysis of radiation patterns of interaction
tones generated by inlet rods in the JT15D engine
[AIAA PAPER 79-0581] p0027 A79-26944
- Modal propagation angles in a cylindrical duct
with flow and their relation to sound radiation
[NASA-TM-79030] p0172 N79-15756
- Analysis of radiation patterns of interaction
tones generated by inlet rods in the JT15D engine

- [NASA-TM-79074] p0016 N79-15960
- HEIGHWAY, J. E.**
Radar image processing of real aperture SAR data for the detection and identification of iceberg and ship targets p0131 A79-36537
- HEIN, G. F.**
Photovoltaic power systems for rural areas of developing countries p0147 A79-26131
Photovoltaic power systems for rural areas of developing countries [NASA-TM-79097] p0135 N79-15411
- HELLEN, J. A.**
Apparatus and method for reducing thermal stress in a turbine rotor [NASA-CASE-LEW-12232-1] p0013 N79-10057
Brayton-cycle component characteristics p0140 N79-26479
- HENDERICKS, E. C.**
Application of the principle of similarity fluid mechanics [NASA-TM-79258] p0105 N79-30515
- HENDERICKS, E. C.**
Some flow phenomena in a constant area duct with a Borda type inlet including the critical region [ASME PAPER 78-WA/HT-37] p0093 A79-19816
Some heat transfer and hydrodynamic problems associated with superconducting cables (SPTL) [NASA-TM-79023] p0102 N79-15267
Critical mass flux through short Borda type inlets of various cross sections [NASA-TM-79017] p0074 N79-20216
Flow friction of the turbulent coolant flow in cryogenic porous cables [NASA-TM-79052] p0103 N79-20341
Some aspects of a free jet phenomena to 105 L/D in a constant area duct [NASA-TM-79050] p0127 N79-20391
Measurements of mixed convective heat transfer to low temperature helium in a horizontal channel [NASA-TM-79158] p0104 N79-23384
Some flow characteristics of conventional and tapered high pressure drop simulated seals [NASA-TM-79192] p0104 N79-27460
Two-phase choked flow of cryogenic fluids in converging-diverging nozzles [NASA-TF-1484] p0105 N79-29468
Thermophysical property data: Who needs them? [NASA-TM-79241] p0090 N79-31403
Free jet phenomena in a 90 degree-sharp edge inlet geometry [NASA-TM-79229] p0105 N79-31526
A reduced volumetric expansion factor plot [NASA-TM-79240] p0105 N79-31527
- HENRY, R. E.**
Evaluation of directionally solidified eutectic superalloys for turbine blade applications [NASA-CR-135151] p0079 N79-16948
- HENRY, R. E.**
Evaluation of an advanced directionally solidified gamma/gamma'-alpha Ni eutectic alloy [NASA-CR-159416] p0079 N79-20222
- HENRELL, T. F.**
Bend strengths of reaction bonded silicon nitride prepared from dry attrition milled silicon [NASA-TM-79230] p0084 N79-30379
- HERMANN, A. H.**
Optical, spin-resonance, and magnetoresistance studies of /tetrathiatellurane/2/iodide/3 - The nature of the ground state p0184 A79-10417
- HERSCH, A. S.**
Effect of grazing flow on the acoustic impedance of Helmholtz resonators consisting of single and clustered orifices [NASA-CR-3177] p0178 N79-32056
- HERSCH, A. S.**
Acoustic behavior of a fibrous bulk material [AIAA PAPER 79-0599] p0178 A79-26910
- HESS, D. A.**
Turbojet blade vibration data acquisition design and feasibility testing [NASA-CR-159505] p0032 N79-18976
- HESS, J. L.**
An efficient user-oriented method for calculating compressible flow about three-dimensional inlets [AIAA PAPER 79-0081] p0005 A79-19524
- HESTER, D. D.**
Computer simulation of an aircraft engine fuel injection system [NASA-CR-157641] p0016 N79-15052
- HEYWOOD, J. B.**
Modelling turbulent flame ignition and blowout p0021 N79-25008
- HILL, R. J.**
Three-dimensional finite-element elastic analysis of cyclically cycled single-edge wedge geometry [NASA-TM-79026] p0172 N79-16644
- HILSEN, T. A.**
Millimeter wave communication satellite concepts p0095 A79-29784
Millimeter wave satellite concepts. Volume 1: Executive summary [NASA-CR-159504] p0041 N79-26101
Millimeter wave satellite concepts. Volume 2: Technical report [NASA-CR-159503] p0041 N79-26102
- HIRSCHBERG, H. H.**
Review of the Agard S6N panel evaluation program of the NASA-Lewis 'SRF' approach to high-temperature LCF life prediction p0128 A79-14954
Review of the AGARD S and M panel evaluation program of the NASA-Lewis SRF approach to high-temperature LCF life prediction p0023 N79-27179
- HO, P. F.**
Silicon solar cells for space use: Present performance and trends p0154 N79-32654
- HO, J. C.**
Properties and performance of fine-filament bronze-process Nb3Sn conductors p0184 A79-20529
- HODGE, P. E.**
Thermal barrier coatings: Burner rig hot corrosion test results [NASA-TM-79005] p0073 N79-11179
- HOFFMAN, A. C.**
Application of digital controls on the quiet clean short haul experimental engines [AIAA PAPER 79-1203] p0029 A79-38984
- HOFFMAN, H. W.**
Thermal energy storage for industrial waste heat recovery p0145 A79-10101
- HOFFMAN, J. D.**
Calculation of the three-dimensional flow field in supersonic inlets at angle of attack using a bicharacteristic method with discrete shock wave fitting [AIAA PAPER 79-0379] p0025 A79-19698
A computer program for the calculation of the flow field in supersonic mixed-compression inlets at angle of attack using the three-dimensional method of characteristics with discrete shock wave fitting [NASA-TM-78947] p0002 N79-10023
- HOLDEN, J. D.**
An analysis of the first two years of GASP data p0160 A79-15068
Aircraft cabin ozone measurements on B747-100 and B747-SF aircraft: Correlations with atmospheric ozone and ozone encounter statistics [NASA-TM-79060] p0008 N79-15013
NASA Global Atmospheric Sampling Program (GASP) data report for tape VL0009 [NASA-TM-79058] p0157 N79-15448
NASA Global Atmospheric Sampling Program (GASP) data report for tapes VL0010 and VL0012 [NASA-TM-79061] p0157 N79-15450
NASA Global Atmospheric Sampling Program (GASP) data report for tapes VL0007 and VL0008 [NASA-TM-73784] p0157 N79-17359
Procedures for estimating the frequency of commercial airline flights encountering high cabin ozone levels [NASA-TF-1560] p0008 N79-33171
- HOLLAND, L. D.**
Millimeter wave communication satellite concepts p0095 A79-29784
Millimeter wave satellite concepts. Volume 1: Executive summary [NASA-CR-159504] p0041 N79-26101

- Millimeter wave satellite concepts. Volume 2:
Technical report
[NASA-CR-159503] p0041 N79-26102
- HOLLANDA, R.
Evaluation of miniature single-wire sheathed thermocouples for turbine blade temperature measurement
[NASA-TN-79173] p0110 N79-27480
- HOLLOWAY, K. L.
Block 2 solar cell module environmental test program
[NASA-CR-159393] p0151 N79-13490
- HOLMS, A. G.
Numbers of center points appropriate to blocked response surface experiments
p0169 A79-49529
Numbers of center points appropriate to blocked response surface experiments
[NASA-TN-79201] p0168 N79-28970
- HOLWACH, J.
Sound-suppressing structure with thermal relief
[NASA-CASE-LEW-12658-1] p0172 N79-14871
- HONYAK, L.
Measured and predicted noise of the AVCO-Lycoming YF-102 turbofan engine
[AIAA PAPER 79-0641] p0026 A79-26877
Full-scale engine tests of bulk absorber acoustic inlet treatment
[AIAA PAPER 79-0600] p0026 A79-26881
Evaluation of two inflow control devices for flight simulation of fan noise using a JT15D engine
[AIAA PAPER 79-0654] p0026 A79-26926
Measured and predicted noise of the Avco-Lycoming YF-102 turbofan noise
[NASA-TN-79069] p0016 N79-15957
Evaluation of two inflow control devices for flight simulation of fan noise using a JT15D engine
[NASA-TN-79072] p0017 N79-15969
Full-scale engine tests of bulk absorber acoustic inlet treatment
[NASA-TN-79079] p0173 N79-16645
- HONG, H. Y.
Ion confinement and transport in a toroidal plasma with externally imposed radial electric fields
[NASA-TP-1411] p0181 N79-19867
- HORNELL, M. A.
Analysis of a parallel-arrayed power regulating system
p0101 A79-49397
- HOPPER, A. T.
User's manual for FEAC3D: Supplement to report on stress analysis for structures with surface cracks
[NASA-CR-159401] p0129 N79-13406
- HOPPIN, G. S., III
Low-cost directionally-solidified turbine blades, volume 1
[NASA-CR-159464] p0080 N79-24121
- HORTON, H. H.
Analysis of a parallel-arrayed power regulating system
p0101 A79-49397
- HOTCHKISS, G. B.
A mobile apparatus for solar collector testing
[ASME PAPER 79-DE-5] p0150 A79-47651
- HOWEN, P. L.
Development and fabrication of improved power transistor switches
[NASA-CR-159524] p0100 N79-21273
- HOWES, W. L.
Loudness of steady sounds - A new theory
p0176 A79-39975
Overall loudness of steady sounds according to theory and experiment
[NASA-EP-1001] p0163 N79-25753
- HOWLETT, E. A.
Progress on Variable Cycle Engines
[AIAA PAPER 79-1312] p0036 A79-40759
- HYCAJ, T. H.
Design study of superconducting magnets for a combustion magnetohydrodynamic /MHD/ generator
p0098 A79-15305
- HYCAK, P.
Heat transfer from a row of jets impinging on concave semi-cylindrical surface
p0108 A79-42890
- HSU, L.
Ionized dopant concentrations at the heavily doped surface of a silicon solar cell
[NASA-TP-1347] p0184 N79-13886
Internally coated air-cooled gas turbine blading
[NASA-CR-159574] p0034 N79-25018
- HSU, L. C.
Method of cross-linking polyvinyl alcohol and other water soluble resins
[NASA-CASE-LEW-13103-1] p0068 N79-14172
Cross-linked polyvinyl alcohol and method of making same
[NASA-CASE-LEW-13101-1] p0068 N79-14173
Three methods for in situ cross-linking of polyvinyl alcohol films for application as ion-conducting membranes in potassium hydroxide electrolyte
[NASA-TP-1407] p0059 N79-21128
In situ self cross-linking of polyvinyl alcohol battery separators
[NASA-CASE-LEW-12972-1] p0138 N79-25481
Electrochemical fluorination of trichloroethylene and N, N-dimethyltrifluoroacetamide
[NASA-TN-79188] p0059 N79-27242
Catalytic trimerization of aromatic nitriles and triaryl-s-triazine ring cross-linked high temperature resistant polymers and copolymers made thereby
[NASA-CASE-LEW-12053-2] p0083 N79-28307
- HSU, L.-C.
Electrochemical fluorination of trichloroethylene and N, N-dimethyltrifluoroacetamide
p0060 A79-49536
Electrochemical fluorination of trichloroethylene and N, N-dimethyltrifluoroacetamide
p0060 A79-49536
- HUANG, T. T.
An investigation of the initiation stage of hot corrosion in Ni-base alloys
[NASA-CR-159616] p0080 N79-25196
- HUCK, F. L.
Lean combustion limits of a confined premixed-prevaporized propane jet
[AIAA PAPER 79-0538] p0026 A79-25856
- HUMENIK, F. H.
Sulfate and nitrate mixing ratios in the vicinity of the tropopause
p0158 A79-49494
NASA Global Atmospheric Sampling Program (GASP) data report for tapes VL0007 and VL0008
[NASA-TN-79184] p0157 N79-17359
Parametric performance of a turbojet engine combustor using jet A and A diesel fuel
[NASA-TN-79089] p0017 N79-20114
- HUMPHREY, J. E.
Study of an advanced General Aviation Turbine Engine (GATE)
[NASA-CR-159558] p0033 N79-21073
- HURCZAK, H. L.
Communications technology satellite: United States experiments and disaster communications applications
[NASA-TN-79109] p0044 N79-23959
- HUNNICUTT, C. L.
An operating 200 kW horizontal axis wind turbine
p0147 A79-20829
An operating 200-kW horizontal axis wind turbine
[NASA-TN-79034] p0135 N79-16357
- HURLEY, I. J.
Applications of thermal energy storage to process heat storage and recovery in the paper and pulp industry
[NASA-CR-159398] p0154 N79-30801
- HURRELL, H. G.
A summary of NASA/Air Force Full Scale Engine Research programs using the F100 engine
[AIAA PAPER 79-1308] p0030 A79-40488
A summary of NASA/Air Force full scale engine research programs using the F100 engine
[NASA-TN-79267] p0024 N79-30188
- HURST, L. J.
An analytical and experimental study of sound propagation and attenuation in variable-area ducts
[NASA-CR-135392] p0177 N79-25845
- HWANG, H. C.
First principles numerical model of avalanche-induced arc discharges in electron-irradiated dielectrics
[NASA-CR-159560] p0101 N79-28418
- HWANG, H. H.
Control of wind turbine generators connected to power systems

- HYLAND, J. P.
Development of a plasma sprayed ceramic gas path seal for high pressure turbine applications
[NASA-CR-159669] p0146 A79-15574 p0122 N79-31602
- HYLAND, R. E.
Power-conversion system component summation p0140 N79-26483
- ICE, W. J.
Design and fabrication of a photovoltaic power system for the Papago Indian Village of Schubert / insight/, Arizona p0148 A79-41089
- IGNACZAK, L. R.
SENT 2 1979 extended flight thruster system performance
[NASA-TM-79256] p0054 N79-33252
- ILES, P. A.
Silicon solar cells for space use: Present performance and trends p0154 N79-32654
- INAMURA, M. S.
Development of single-cell protectors for sealed silver-zinc cells
[NASA-CR-159407] p0151 N79-12550
- INGERO, B. D.
Atomization of water jets and sheets in axial and swirling airflows
[ASME PAPER 79-GT-170] p0106 A79-30556
Atomization of water jets and sheets in axial and swirling airflows
[NASA-TM-79043] p0102 N79-12362
- INGRAM, L. S.
Definition of solder experiments for SpaceLab
[NASA-CR-159528] p0040 N79-20161
- INGUITE, G. T.
Effects of arcing due to spacecraft charging on spacecraft survival
[NASA-CR-159593] p0100 N79-25312
- INNS, R. P.
Generalized computer-aided discrete time domain modeling and analysis of dc-dc converters p0059 A79-10881
- JACK, J. R.
Feasibility of determining flat roof heat losses using aerial thermography p0331 A79-51095
Feasibility of determining flat roof heat losses using aerial thermography
[NASA-TM-79152] p0131 N79-22590
- JACKSON, M. E.
Evaluation of directionally solidified eutectic superalloys for turbine blade applications
[NASA-CR-135151] p0079 N79-16948
Evaluation of an advanced directionally solidified gamma/gamma'-alpha Mo eutectic alloy
[NASA-CR-159416] p0079 N79-20222
- JACOBSON, T. P.
Graphite-fiber-reinforced polyimide liners of various compositions in plain spherical bearings p0117 A79-16678
- JAMES, E. L.
Preliminary results of the mission profile life test of a 30 cm Hg bombardment thruster
[NASA-TM-79261] p0054 N79-33254
- JAMES, K. A.
Fiber optic sensors for military, industrial and commercial applications p0111 A79-38738
Analysis and preliminary design of optical sensors for propulsion control
[NASA-CR-159519] p0180 N79-27975
- JANARDAN, B. A.
Measurements of admittances and characteristic combustion times of reactive gaseous propellant coaxial injectors
[NASA-CR-159542] p0072 N79-23168
- JANETTE, D. C.
Evaluation of MOSTAS computer code for predicting dynamic loads in two-bladed wind turbines
[AIAA 79-0733] p0005 A79-29007
Evaluation of MOSTAS computer code for predicting dynamic loads in two bladed wind turbines
- [NASA-TM-79101] p0137 N79-21549
- JAWOROWSKI, A.
High-energy electron-induced damage production at room temperature in aluminum-doped silicon p0154 N79-32662
- JAY, A.
Effect of flight loads on turbofan engine performance deterioration p0027 A79-30559
Effect of flight loads on turbofan engine performance deterioration
[NASA-TM-79041] p0013 N79-12085
- JECHE, R. W.
Evaluation of silicon carbide fiber/titanium composites
[NASA-TM-79232] p0064 N79-1349
- JERACKI, E. J.
Wind tunnel performance of four energy efficient propellers designed for Mach 0.8 cruise
[SAE PAPER 790573] p0028 A79-36759
Tone noise of three supersonic helical tip speed propellers in a wind tunnel p0175 A79-39801
Tone noise of three supersonic helical tip speed propellers in a wind tunnel at 0.8 Mach number
[NASA-TM-79046] p0172 N79-15758
Wind tunnel performance of four energy efficient propellers designed for Mach 0.8 cruise
[NASA-TM-79124] p0003 N79-20069
Tone noise of three supersonic helical tip speed propellers in a wind tunnel
[NASA-TM-79167] p0174 N79-25840
- JIRBERG, E. J.
VHF downlink communication system for SLAR data p0045 A79-51097
VHF downlink communication system for SLAR data
[NASA-TM-79164] p0044 N79-23313
- JOHANNESSEN, E.
On the distribution of computation for sequential decoding using the stack algorithm p0096 A79-33793
- JOHNS, A. L.
Performance of a V/STOL tilt nacelle inlet with blowing boundary layer control
[AIAA PAPER 79-1163] p0006 A79-47347
Performance of a V/STOL tilt nacelle inlet with blowing boundary layer control
[NASA-TM-79176] p0004 N79-27093
- JOHNSEN, E. L.
Operating condition and geometry effects on low-frequency afterburner combustion instability in a turbofan at altitude p0022 N79-25022
[NASA-TF-1475]
- JOHNSON, E.
Characteristics of differential charging of ATS-6 p0049 N79-24008
- JOHNSON, E. A.
Conceptual design study of an Improved Gas Turbine (IGT) powertrain
[NASA-CR-15960-] p0189 N79-31087
Single shaft automotive gas turbine engine characterization test
[NASA-CR-159654] p0189 N79-32129
- JOHNSTON, E. A.
Variable area exhaust nozzle
[NASA-CASE-LEW-12378-1] p0014 N79-14097
- JOHNSTON, J. E.
High velocity burner rig oxidation and thermal fatigue behavior of Si3N4- and SiC base ceramics to 1370 deg C p0082 N79-16904
[NASA-TM-79040]
- JONES, C.
A review of Curtiss-Wright rotary engine developments with respect to general aviation potential
[SAE PAPER 790621] p0036 A79-36749
- JONES, S. W.
Elastomer mounted rotors - An alternative for smoother running turbomachinery
[ASME PAPER 79-GT-149] p0119 A79-32414
- JONES, W. L.
Evaluation of two inflow control devices for flight simulation of fan noise using a JT15D engine
[AIAA PAPER 79-0654] p0026 A79-26926
Evaluation of two inflow control devices for flight simulation of fan noise using a JT15D engine
[NASA-TM-79072] p0017 N79-15969

- JONES, W. R.**
Infrared analysis of polyethylene wear specimens using attenuated total reflection spectroscopy [NASA-TM-79228] p0083 79-29329
- JONES, W. R., JR.**
A study of various synthetic routes to produce a halogen-labeled traction fluid [NASA-TM-79024] p0059 79-11119
The effect of nitrogen ion (N⁺) implantation on the friction and wear characteristics of iron [NASA-TM-79029] p0073 79-12201
Boundary lubrication, thermal and oxidative stability of a fluorinated polyether and a perfluoropolyether triazine [NASA-TM-79064] p0081 79-15185
Effect of sterilization irradiation on friction and wear of ultrahigh-molecular-weight polyethylene [NASA-TM-1462] p0082 79-23216
Perrographic analysis of wear debris from full-scale bearing fatigue tests [NASA-TM-1511] p0116 79-31605
- JONES, W. S.**
Laser power conversion system analysis, volume 1 [NASA-CR-159523-VOL-1] p0112 79-21334
Laser power conversion system analysis, volume 2 [NASA-CR-159523-VOL-2] p0112 79-21335
Laser rocket system analysis [NASA-CR-159521] p0112 79-21337
- K**
- KAFKA, P. G.**
Effect of flight loads on turbofan engine performance deterioration p0027 79-30559
Effect of flight loads on turbofan engine performance deterioration [NASA-TM-79041] p0013 79-12085
- KAHOZ, P.**
A cross impact methodology for the assessment of US telecommunications system with application to fiber optics development, volume 1 [NASA-CR-135208] p0056 79-18159
A cross impact methodology for the assessment of US telecommunications system with application to fiber optics development, volume 2 [NASA-CR-159511-VOL-2] p0096 79-18160
- KAISER, J. E.**
An analytical and experimental study of sound propagation and attenuation in variable-area ducts [NASA-CR-135392] p0177 79-25845
- KANATH, G. S.**
Summary of GaAs Solar Cell Performance and Radiation Damage Workshop p0144 79-32669
- KAMI, S.**
Advanced electrostatic ion thruster for space propulsion [NASA-CR-159406] p0056 79-14153
- KANDEL, J. W.**
Determination of lubricant selection based on elastohydrodynamic film thickness and traction measurements [NASA-CR-159428] p0121 79-14385
- KANTOLA, R. A.**
Reduction of rotor-turbulence interaction noise in static fan noise testing [AIAA PAPER 79-0656] p0036 79-26925
Basic research in fan source noise: Inlet distortion and turbulence noise [NASA-CR-159451] p0177 79-14875
- KANURY, A. H.**
Feasibility study of liquid pool burning in reduced gravity [NASA-CR-159642] p0072 79-32303
- KAPLAN, D.**
Mass drivers. 3: Engineering p0040 79-32232
- KARINS, J. P.**
High-energy electron-induced damage production at room temperature in aluminum-doped silicon p0154 79-32662
- KASPER, R. J.**
Some effects of cyclic induced deformation in rocket thrust chambers [AIAA 79-0911] p0054 79-34736
Effect of low-stiffness clowout overwrap on rocket thrust-chamber life
- [NASA-TM-1456] p0053 79-23132
- KATZER, L. B.**
Applications of thermal energy storage to process heat and waste heat recovery in the iron and steel industry [NASA-CR-159397] p0151 79-11473
- KATZ, I.**
The decrease in effective photocurrents due to saddle points in electrostatic potentials near differentially charged spacecraft p0049 79-30140
The capabilities of the NASA charging analyzer program p0047 79-24011
Extension, validation and application of the NASCAP code [NASA-CR-159595] p0100 79-27397
- KATZER, R.**
Conceptual design of thermal energy storage systems for near term electric utility applications [NASA-CR-159577] p0155 79-33560
- KAUFMAN, A.**
Thermal-Structural mission analyses of air-cooled gas turbine blades [ASME PAPER 79-GT-19] p0027 79-30553
Thermal-structural mission analyses of air-cooled gas turbine blades [NASA-TM-78963] p0126 79-11433
Low-cycle fatigue of thermal-barrier coatings at 982 deg C [NASA-TM-1322] p0014 79-13046
- KAUFMAN, R. E.**
Industrial ion source technology [NASA-CR-159534] p0179 79-19828
Inert gas thrusters [NASA-CR-159527] p0057 79-26110
- KAUTZ, R. E.**
Determination of the zincate diffusion coefficient and its application to alkaline battery problems p0070 79-11547
Decay of the zincate concentration gradient at an alkaline zinc cathode after charging [NASA-TM-79106] p0137 79-20520
- KAYS, W. E.**
Full-coverage film cooling: 3-dimensional measurements of turbulence structure and prediction of recovery region hydrodynamics [NASA-CR-3104] p0106 79-22428
Heat transfer to a full-coverage, film-cooled surface with compound-angle (30 deg and 45 deg) hole injection [NASA-CR-3103] p0107 79-22429
- KAZ, I.**
Charging analysis of the SCATHA satellite p0049 79-24012
- KAZA, R. E. V.**
Evaluation of MOSTIAS computer code for predicting dynamic loads in two-bladed wind turbines [AIAA 79-0733] p0005 79-29007
Evaluation of MOSTIAS computer code for predicting dynamic loads in two bladed wind turbines [NASA-TM-79101] p0137 79-21549
- KAZABOFF, J. H.**
Heat exchanger and method of making [NASA-CASE-LEW-12441-1] p0102 79-13289
A heat exchanger and method of making [NASA-CASE-LEW-12441-2] p0104 79-21313
A heat exchanger and method of making [NASA-CASE-LEW-12441-3] p0104 79-23383
- KEDL, R. J.**
Thermal energy storage for industrial waste heat recovery p0145 79-10101
- KELLEY, R. L.**
Communications systems technology assessment study. Volume 2: Results [NASA-CR-135224] p0095 79-12273
- KELLY, D. L.**
Millimeter wave satellite concepts. Volume 1: Executive summary [NASA-CR-159504] p0041 79-26101
Millimeter wave satellite concepts. Volume 2: Technical report [NASA-CR-159503] p0041 79-26102
- KEMPKE, R. A.**
Effects of air injection on a turbocharged Teledyne Continental Motors TS10-360-C engine [SAE PAPER 790607] p0028 79-34760

- An overview of NASA research on positive displacement type general aviation engines
[AIAA PAPER 79-1824] p0038 A79-53750
- Effects of air injection on a turbocharged Teledyne Continental Motors TS10-360-C engine
[NASA-TN-79121] p0158 N79-20528
- An overview of NASA research on positive displacement type general aviation engines
[NASA-TN-79254] p0024 N79-31210
- KENNEDY, F. E.
Thermal stress analysis of ceramic gas-path seal components for aircraft turbines
[NASA-TN-1437] p0082 N79-21205
- KENNEDY, J. E.
Lean stability augmentation for premixing, prevaporizing combustors
[AIAA PAPER 79-1319] p0036 A79-39035
- Lean stability augmentation study
[NASA-CR-159536] p0071 N79-22244
- Lean stability augmentation study
p0021 N79-25007
- KENNEL, I. G.
Experimental investigation of a 0.15-scale model of an underfuselage normal-shock inlet
[NASA-CR-3049] p0006 N79-12014
- KERSLAKE, W. R.
SERT 2 1979 extended flight thruster system performance
[NASA-TN-79256] p0054 N79-33252
- Neutralization tests on the SERT 2 spacecraft
[NASA-TN-79271] p0054 N79-33255
- KHALIL, T.
A calculation procedure for viscous flow in turbomachinery, volume 1
[NASA-CR-159635] p0167 N79-30514
- KHANNA, S. K.
Optical, spin-resonance, and magnetoresistance studies of tetrathiatetracene/2-iodide/3 - The nature of the ground state
p0184 A79-10417
- KHATRI, B. K.
Communications systems technology assessment study. Volume 2: Results
[NASA-CR-135224] p0095 N79-12273
- KHATHONG, S.
Silicon solar cells for space use: Present performance and trends
p0154 N79-32654
- KHOSLA, P. K.
Filtering of non-linear instabilities
p0106 A79-32912
- KICKS, J. C.
Pressure instrumentation for gas turbine engines - A review of measurement technology
[ASME PAPER 78-ET-148] p0110 A79-10800
- KIESLING, J. W.
Communications systems technology assessment study. Volume 2: Results
[NASA-CR-135224] p0095 N79-12273
- KILLACKEY, J. J.
Design and fabrication of the Mini-Brayton Recuperator (MBR)
[NASA-CR-159429] p0151 N79-11476
- KILLBOT, J.
Combustion of porous solids at reduced gravitational conditions
[NASA-CR-3197] p0072 N79-33288
- KIM, H. K.
Heat transfer to a full-coverage, film-cooled surface with compound-angle (30 deg and 45 deg) hole injection
[NASA-CR-3103] p0107 N79-22429
- KIM, J.
Lean, premixed, prevaporized fuel combustor conceptual design study
[NASA-CR-159647] p0035 N79-32211
- KIM, Y. C.
Ion confinement and transport in a toroidal plasma with externally imposed radial electric fields
[NASA-TN-1411] p0181 N79-19867
- KING, G. W.
Development and fabrication of high strength alloy fibers for use in metal-metal matrix composites
[NASA-TN-79115] p0063 N79-22211
- KING, R. B.
Pattern recognition methods and air pollution source identification
p0156 A79-15079
- Commercial phosphoric acid fuel cell system technology development
p0150 A79-51809
- Commercial phosphoric acid fuel cell system technology development
[NASA-TN-79169] p0139 N79-25500
- KING, R. G.
Definition of mutually optimum NDI and proof test criteria for 2219 aluminum pressure vessels. Volume 1: Methods
[NASA-CR-135445] p0125 N79-21410
- Definition of mutually optimum NDI and proof test criteria for 2219 aluminum pressure vessels. Volume 2: Optimization and fracture studies
[NASA-CR-135446] p0125 N79-21411
- Definition of mutually optimum NDI and proof test criteria for 2219 aluminum pressure vessels. Volume 3: Applications to rail defect evaluation
[NASA-CR-135447] p0125 N79-21412
- KIRKPATRICK, A. R.
Applications of ion implantation to high performance, radiation tolerant silicon solar cells
p0143 N79-32648
- KISCH, J. J.
Lightweight multiple output converter development
[NASA-CR-159526] p0140 A79-20317
- KITA, J. P.
Wind turbine generator application of new design demands on tower design and materials
p0155 A79-20826
- KLADEN, J. L.
Three-dimensional finite-element elastic analysis of a thermally cycled single-edge wedge geometry specimen
[NASA-TN-79026] p0172 N79-16644
- KLECKNER, E. J.
High speed cylindrical roller bearing analysis, SKF computer program CYBEAN. Volume 1: Analysis
[NASA-CR-159460] p0121 N79-17222
- High speed cylindrical roller bearing analysis, SKF computer program CYBEAN. Volume 2: User's manual
[NASA-CR-159461] p0121 N79-17223
- KLEES, G. E.
A method to estimate weight and dimensions of large and small gas turbine engines
[NASA-CR-159481] p0015 N79-15046
- KLEIN, H. G.
Fabrication and testing of silver-hydrogen cells
[NASA-CR-159431] p0152 N79-16374
- KLOCHER, T. E.
Variation of solar cell sensitivity and solar radiation on tilted surfaces
p0148 A79-41023
- Evaluation of models to predict insolation on tilted surfaces
p0150 A79-53491
- Open-circuit voltage improvements in low-resistivity solar cells
p0143 N79-32649
- KNOTT, P. E.
Acoustic and aerodynamic performance investigation of inverted velocity profile coannular plug nozzles, comprehensive data report, volume 1
[NASA-CR-159575-VOL-1] p0177 N79-26884
- Acoustic and aerodynamic performance investigation of inverted velocity profile coannular plug nozzles, comprehensive data report, volume 2
[NASA-CR-159575-VOL-2] p0177 N79-26885
- Acoustic and aerodynamic performance investigation of inverted velocity profile coannular plug nozzles, comprehensive data report, volume 3
[NASA-CR-159575-VOL-3] p0177 N79-26886
- KNOWLES, G. R.
Active heat exchange system development for latent heat thermal energy storage
[NASA-CR-159479] p0153 N79-21554
- KOBAR, J. A.
Burn coal cleanly in a fluidized bed - The key is in the controls
p0071 A79-26374
- KOBAYASHI, H.
Effects of inflow distortion profiles on fan tone noise calculated using a 3-D theory
[NASA-TN-79082] p0173 N79-16647
- KOBAYASHI, H.
Effects of inflow distortion profiles on fan tone noise calculated using a 3-D theory

- [AIAA PAPER 79-0577] p0175 A79-26911
KOENIG, H. W.
 Preliminary QCGAT program test results [SAE PAPER 790596] p0028 A79-36729
 Preliminary QCGAT program test results [NASA-TM-79013] p0016 A79-15051
- KOPSEY, H. G.**
 Effect of rotor tip clearance and configuration on overall performance of a 12.77-centimeter tip diameter axial-flow turbine [ASME PAPER 79-GT-42] p0027 A79-30521
 Effect of rotor tip clearance and configuration on overall performance of a 12.77-centimeter tip diameter axial-flow turbine [NASA-TM-79025] p0002 A79-12015
 Cold-air performance of free power turbine designed for 112-kilowatt automotive gas-turbine engine 3: Effect of stator vane end clearances on performance [NASA-TM-78956] p0014 A79-13049
 Cold-air performance of free power turbine designed for 112-kilowatt automotive gas-turbine engine. 2: Effects of variable stator-vane-chord setting angle on turbine performance [NASA-TM-78993] p0017 A79-17859
- KOHL, P. J.**
 Mass spectrometric investigation of the vaporization of sodium and potassium chromates - Preliminary results p0071 A79-49533
 The role of NaCl in flame chemistry, in the deposition process, and in its reactions with protective oxides as related to hot corrosion p0071 A79-49534
 Chemically frozen multicomponent boundary layer theory of salt and/or ash deposition rates from combustion gases p0078 A79-50912
 Preliminary evaluation of the role of K2S in MHD hot stream seed recovery [NASA-TM-79114] p0068 A79-20200
 Mass spectrometric investigation of the vaporization of sodium and potassium chromates: Preliminary results [NASA-TM-79210] p0065 A79-27279
 The role of NaCl in flame chemistry, in the deposition process, and in its reactions with protective oxides as related to hot corrosion [NASA-TM-79225] p0065 A79-28258
 The chemistry of sodium chloride involvement in processes related to hot corrosion [NASA-TM-79251] p0065 A79-31361
- KOKOSZKA, E., JR.**
 Strain gage system evaluation program [NASA-CR-159486] p0110 A79-19314
- KOLECKI, J. C.**
 Effect of parasitic plasma currents on solar-array power output p0047 A79-24025
- KOLM, H.**
 Mass drivers. 3: Engineering p0040 A79-32232
- KOLM, H.**
 Mass drivers. 3: Engineering p0040 A79-32232
- KONATSU, G. K.**
 Ion beam technology applications study [NASA-CR-159437] p0180 A79-12884
- KORTOVICH, C. S.**
 A strainrange partitioning analysis of low cycle fatigue of coated and uncoated Rene 80 p0125 A79-10479
- KOSNAHL, H. G.**
 Comments on measuring the overall and the depressed collector efficiency in TWT's and klystron amplifiers p0099 A79-25118
 Analytical prediction with multidimensional computer programs and experimental verification of the performance, at a variety of operating conditions, of two traveling wave tubes with depressed collectors [NASA-TF-1449] p0097 A79-22375
 Multistage depressed collector for dual mode operation [NASA-CASE-LEW-13282-1] p0098 A79-32463
- KRAMARCHUK, I.**
 VHF downlink communication system for SLAR data p0045 A79-51097
 VHF downlink communication system for SLAR data [NASA-TM-79164] p0094 A79-23313
- KRAUTER, A. L.**
 Experimental and analytical tools for evaluation of Stirling engine rod seal behavior [NASA-CR-159543] p0122 A79-23429
- KRAWCZONK, W. E.**
 Ion confinement and transport in a toroidal plasma with externally imposed radial electric fields [NASA-TF-1411] p0181 A79-19867
- KRESSSEL, H.**
 Epitaxial solar-cell fabrication, phase 2 [NASA-CR-135350] p0152 A79-19448
- KROEGER, E.**
 Lithium and potassium heat pipes for thermionic converters p0145 A79-10113
- KROEGER, E. W.**
 Diminide thermionic energy conversion with lanthanum-hexaboride electrodes p0146 A79-13098
- KROSEL, S. E.**
 Generation of linear dynamic models from a digital nonlinear simulation [NASA-TF-1388] p0001 A79-16796
- KUIVINEN, D. E.**
 Ion chromatographic determination of sulfur in fuels p0070 A79-21222
 Ion chromatographic determination of sulfur in fuels [NASA-TM-78971] p0157 A79-17358
- KULESZ, J. J.**
 Workbook for estimating effects of accidental explosions in propellant ground handling and transport systems [NASA-CR-3023] p0091 A79-10226
- KURKOV, A.**
 Synthesis of blade flutter vibratory patterns using stationary transducers p0127 A79-10823
- KUZNETSOV, Y. V.**
 Some heat transfer and hydrodynamic problems associated with superconducting cables (SFTL) [NASA-TM-79023] p0102 A79-15267
 Measurements of mixed convective heat transfer to low temperature helium in a horizontal channel [NASA-TM-79158] p0104 A79-23384

L

- LAESSIG, H. E.**
 Effects of diffusion factor, aspect ratio and solidity on overall performance of 14 compressor middle stages [NASA-TF-1523] p0038 A79-33210
- LAHOTI, G. D.**
 Computer-aided analysis and design of the shape rolling process for producing turbine engine airfoils [NASA-CR-159455] p0012 A79-12087
 Computer-aided analysis and design of the shape rolling process for producing turbine engine airfoils [NASA-CR-135367] p0080 A79-26175
- LANABACHE, H.**
 Conceptual design of thermal energy storage systems for near term electric utility applications [NASA-CR-159577] p0155 A79-33560
- LANNECK, J. H.**
 Photon degradation effects in terrestrial solar cells p0149 A79-41098
 Photon-degradation effects in terrestrial silicon solar cells p0149 A79-42545
- LANATI, G. A.**
 Instrumentation for measuring the dynamic pressure on rotating compressor blades [NASA-CR-159466] p0110 A79-12418
 Measuring unsteady pressure on rotating compressor blades [NASA-TM-79159] p0109 A79-22448
- LARK, R. P.**
 Acoustic emission testing of composite vessels under sustained loading p0128 A79-11543
 Titanium/beryllium laminates - Fabrication, mechanical properties, and potential aerospace

- applications p0064 A79-20836
- Effects of moisture profiles and laminate configuration on the hygro stress in advanced composites p0064 A79-24132
- Fabrication and testing of non-graphitic superhybrid composites p0066 A79-43289
- Fabrication and testing of nongraphitic superhybrid composites [NASA-TM-79102] p0063 A79-20188
- LAWSON, R. S.
- A jet exhaust noise prediction procedure for inverted velocity profile coannular nozzles [AIAA PAPER 79-0631] p0178 A79-28964
- Aerodynamic and acoustic investigation of inverted velocity profile coannular exhaust nozzle models and development of aerodynamic and acoustic prediction procedures, comprehensive data report, volume 1 [NASA-CR-159515] p0034 A79-30185
- Aerodynamic and acoustic investigation of inverted velocity profile coannular exhaust nozzle models and development of aerodynamic and acoustic prediction procedures, comprehensive data report, volume 2 [NASA-CR-159516] p0034 A79-30186
- Aerodynamic and acoustic investigation of inverted velocity profile coannular exhaust nozzle models and development of aerodynamic and acoustic prediction procedures [NASA-CR-3168] p0035 A79-31212
- LAURE, J. L.
- Infrared analysis of polyethylene wear specimens using attenuated total reflection spectroscopy [NASA-TM-79228] p0083 A79-29329
- LAUVER, R. W.
- Effects of hydrothermal exposure on a low-temperature cured epoxy p0085 A79-15534
- Stability of PMR-polyimide monomer solutions p0086 A79-31041
- Characterization of PMR polyimides - of ester impurities with composite properties p0066 A79-43265
- Characterization of PMR polyimides: Correlation of ester impurities with composite properties [NASA-TM-79068] p0061 A79-16918
- Stability of PMR-polyimide monomer solutions [NASA-TM-79063] p0062 A79-16921
- LAYDEN, G. K.
- Development of SiAlON materials [NASA-CR-159675] p0067 A79-33258
- LAYS, E. J.
- Advanced General Aviation Turbine Engine (GATE) concepts [NASA-CR-159603] p0034 A79-25017
- LEAHY, E. C.
- Experimental investigation of a 0.15-scale model of an underfuselage normal-shock inlet [NASA-CR-30499] p0006 A79-12014
- LEAR, J. W.
- Development of single-cell protectors for sealed silver-zinc cells [NASA-CR-159407] p0151 A79-12550
- LEE, C. H.
- CELPE: Coupled Eulerian-Lagrangian Finite Element program for high velocity impact. Part 1: Theory and formulation [NASA-CR-159395] p0166 A79-29832
- CELPE: Coupled Eulerian-Lagrangian Finite Element program for high velocity impact. Part 2: Program user's manual [NASA-CR-159396] p0166 A79-29833
- LEE, D.
- Study of blade aspect ratio on a compressor front stage aerodynamic and mechanical design report [NASA-CR-159555] p0034 A79-23085
- LEE, F. C.
- Generalized computer-aided discrete time domain modeling and analysis of dc-dc converters p0095 A79-10881
- Input filter design for switching regulators p0101 A79-48653
- LEE, F. C. Y.
- Power converter design optimization p0099 A79-10885
- Modeling of switching regulator power stages with and without zero-inductor-current dwell time p0101 A79-49398
- LEE, Y. H.
- High-energy electron-induced damage production at room temperature in aluminum-doped silicon p0154 A79-32662
- LEFROIS, R. T.
- Active heat exchange system development for latent heat thermal energy storage [NASA-CR-159479] p0153 A79-21554
- LEHNHANN, R. P.
- Analysis of the impact of the use of broad specification fuels on combustors for commercial aircraft gas turbine engines [AIAA PAPER 79-1195] p0090 A79-38980
- LEHTINEN, E.
- Multivariable control altitude demonstration on the F100 turbofan engine [AIAA PAPER 79-1204] p0029 A79-39814
- Space shuttle active-pogo-suppressor control design using linear quadratic regulator techniques [NASA-TF-1217] p0097 A79-14709
- Multivariable control altitude demonstration on the F100 turbofan engine [NASA-TM-79183] p0022 A79-25015
- LEIBERCKI, R. P.
- Pattern recognition methods and air pollution source identification p0158 A79-15079
- LEIENCKI, R.
- The S-15-aircraft (Sambolot M-15) [NASA-TM-75586] p0013 A79-12063
- LEININGER, G.
- Identification and dual adaptive control of a turbojet engine [NASA-TM-79145] p0093 A79-23257
- LEWIS, E. C., JR.
- A cross impact methodology for the assessment of US telecommunications systems with application to fiber optics development: Executive summary [NASA-CR-135209] p0096 A79-17071
- A cross impact methodology for the assessment of U. telecommunications systems with application to fiber optics development, volume 1 [NASA-CR-135208] p0096 A79-18159
- A cross impact methodology for the assessment of US telecommunications systems with application to fiber optics development, volume 2 [NASA-CR-159511-VOL-2] p0096 A79-18160
- LEROY, R. E.
- Global disaster satellite communications system for disaster assessment and relief coordination p0095 A79-30394
- Global disaster satellite communications system for disaster assessment and relief coordination [NASA-TM-79105] p0044 A79-20176
- LEVINE, S. R.
- Thermal barrier coatings: Burner rig hot corrosion test results [NASA-TM-79005] p0073 A79-11179
- LEVI, E.
- Development of a three-dimensional turbulent duct flow analysis [NASA-CR-3029] p0106 A79-12366
- LEZBERG, E. A.
- Sulfate and nitrate mixing ratios in the vicinity of the tropopause p0158 A79-49494
- LIEBERMAN, E.
- High performance, high density hydrocarbon fuels [NASA-CR-159480] p0091 A79-20267
- LIEBERT, C. E.
- Emission and absorptance of the National Aeronautics and Space Administration ceramic thermal barrier coating p0086 A79-27231
- Tests of NASA ceramic thermal barrier coating for gas-turbine engines p0086 A79-34996
- Low-cycle fatigue of thermal-barrier coatings at 982 deg C [NASA-TF-1322] p0014 A79-13046
- Ceramic coating effect on liner metal temperatures of film-cooled annular combustor [NASA-TF-1323] p0015 A79-14098
- Tests of NASA ceramic thermal barrier coating for gas-turbine engines [NASA-TM-79116] p0017 A79-20118

- Industry tests of NASA ceramic thermal barrier coating
[NASA-TP-1425] p0022 N79-25023
- LIEBLEIN, S.
Evaluation of urethane for feasibility of use in wind turbine blade design
[NASA-CR-159530] p0153 N79-20497
- LIN, D. L.
First principles numerical model of avalanche-induced arc discharges in electron-irradiated dielectrics
[NASA-CR-159560] p0101 N79-28418
- LINDHOLM, P. A.
Design of high efficiency HLE solar cells for space and terrestrial applications
p0154 N79-32647
- LINDOW, R. G.
An airborne meteorological data collection system using satellite relay /ASDAR/
p0010 A79-14949
- LINDSTROM, L.
High-energy electron-induced damage productⁿ at room temperature in aluminum-doped silicon
p0154 N79-32662
- LINGSCHMIT, J. E.
Evaluation of advanced regenerator systems
[NASA-CR-159422] p0188 N79-12969
- LINN, G. T.
Hartmann flow with temperature-dependent physical properties
p0182 A79-15597
- LINSCOTT, R.
An operating 200 kW horizontal axis wind turbine
p0147 A79-20829
An operating 200-kW horizontal axis wind turbine
[NASA-TM-79034] p0135 N79-16357
- LIU, C. C.
Method and device for the detection of phenol and related compounds
[NASA-CASE-LEW-12513-1] p0065 N79-22235
- LOEWENTHAL, S. E.
Proposed design procedure for transmission shafting under fatigue loading
p0117 A79-14950
Filtration effects on ball bearing life and condition in a contaminated lubricant
[ASME PAPER 78-LUB-34] p0118 A79-23246
Performance of a Nasvitys multiroller traction drive
[NASA-TP-1378] p0113 N79-13369
Ferromagnetic analysis of wear debris from full-scale bearing fatigue tests
[NASA-TP-1511] p0116 N79-31605
- LOHMANN, R. P.
Progress on Variable Cycle Engines
[AIAA PAPER 79-1312] p0036 A79-40759
Analytical evaluation of the impact of broad specification fuels on high bypass turbofan engine combustors
[NASA-CR-159454] p0031 N79-13050
- LONGHURST, G. E.
Prediction of plasma properties in mercury ion thrusters
[NASA-CR-159448] p0056 N79-15152
- LONGWELL, J. P.
Alternative aircraft fuels
p0090 A79-10824
- LORENZ, C. P.
Space shuttle active-pogo-suppressor control design using linear quadratic regulator techniques
[NASA-TP-1217] p0057 N79-14309
- LORENZO, C. P.
Energy-state formulation of lumped volume dynamic equations with application to a simplified free piston Stirling engine
p0187 A79-49532
Energy-state formulation of lumped volume dynamic equations with application to a simplified free piston Stirling engine
[NASA-TM-79197] p0141 N79-27663
- LOW, J. E., JR.
Influence of composition, annealing treatment, and texture on the fracture toughness of Ti-5Al-2.5Sn plate at cryogenic temperatures
p0077 A79-24262
- LOWELL, C. E.
Effect of a chromium-containing fuel additive on hot corrosion
p0071 A79-26546
- Airfoil cooling hole plugging by combustion gas impurities of the type found in coal derived fuels
[NASA-TM-79076] p0089 N79-20265
- Gas-turbine critical research and advanced technology support project
[NASA-TM-79139] p0139 N79-25498
- The erosion/corrosion of small superalloy turbine rotors operating in the effluent of a PFB coal combustor
[NASA-TM-79227] p0076 N79-30356
- LUBOWSKI, J. P.
Characteristics of aeroelastic instabilities in turbomachinery - NASA full scale engine test results
[AIAA 79-7011] p0027 A79-24386
Experimental evaluation of the effect of inlet distortion on compressor blade vibrations
p0128 A79-30558
Experimental evaluation of the effect of inlet distortion on compressor blade vibrations
[NASA-TM-79066] p0126 N79-16300
Characteristics of aeroelastic instabilities in turbomachinery - NASA full scale engine test results
[NASA-TM-79085] p0126 1 9-17263
- LUDWIG, L. E.
Energy conservation through sealing technology
p0118 A79-20700
Gas path sealing in turbine engines
p0013 N79-11457
Self-acting shaft seals
p0013 N79-11070
Wear of seal materials used in aircraft propulsion systems
[NASA-TM-79003] p0073 N79-12204
Composite seal for turbomachinery
[NASA-CASE-LEW-12131-1] p0114 N79-18318
Shaft seal assembly for high speed and high pressure applications
[NASA-CASE-LEW-11873-1] p0115 N79-22475
- LUDKE, E. E.
CIS-type variable conductance heat pipes for SEP FM/FFU
[NASA-CR-159550] p0107 N79-22434
Heat pipe life and processing study
[NASA-CR-159581] p0107 N79-25349
- LUDWIG, R. W.
An approach to optimum subsonic inlet design
[ASME PAPER 79-GT-51] p0006 A79-30527
An approach to optimum subsonic inlet design
[NASA-TM-79051] p0002 N79-12020
- LYETTE, E.
MCD-2 failure mode and effects analysis
[NASA-CR-159632] p0093 N79-30415
- LYONS, V. J.
Effect of fuel/air nonuniformity on nitric oxide emissions
p0020 N79-25004

M

- MAAG, W. L.
Analysis of a fuel cell on-site integrated energy system for a residential complex
[AIAA PAPER 79-0990] p0147 A79-38192
Comparison of fuel-cell and diesel integrated energy systems and a conventional system for a 500-unit apartment
[NASA-TM-79037] p0134 N79-15403
Analysis of a fuel cell on-site integrated energy system for a residential complex
[NASA-TM-79161] p0137 N79-22624
- MACHRESON, D.
Advanced electrostatic ion thruster for space propulsion
[NASA-CR-159406] p0056 N79-14153
- MAISEL, J. E.
High temperature dynamic modulus and damping of aluminum and titanium matrix composites
p0065 A79-26132
High temperature dynamic modulus and damping of aluminum and titanium matrix composites
[NASA-TM-79080] p0061 N79-16077
- HAJJIGI, R. E.
Applications of velocity potential function to acoustic duct propagation and radiation from inlets using finite element theory
[NASA-TM-79071] p0016 N79-15959

- HALLAVARPU, R.**
Microwave radiation measurements near the electron plasma frequency of the NASA Lewis Sucky Torus plasma
p0181 A79-14953
- HALOY, J. E.**
A thermal control approach for a solar electric propulsion thrust subsystem
[NASA-TN-79175] p0043 A79-27236
- HARDILL, R. J.**
The decrease in effective photocurrents due to saddle points in electrostatic potentials near differentially charged spacecraft
p0049 A79-30140
- HASCAP** modelling of high-voltage power system interactions with space charged-particle environments
p0051 A79-39806
- Effects of bulk and surface conductivity on the potential developed by dielectrics exposed to electron beams
p0171 A79-50938
- HASCAP** modelling of high-voltage power system interactions with space charged-particle environments
[NASA-TN-79146] p0046 A79-24000
- The capabilities of the NASA charging analyzer program
p0047 A79-24011
- Charging analysis of the SCATHA satellite
p0049 A79-24012
- Extension, validation and application of the NAS-AP code
[NASA-CR-159595] p0100 A79-27397
- HAYI, R.**
Theory of low frequency noise transmission through turbines
[NASA-CR-159457] p0033 A79-20117
- HANSON, S. S.**
Interpolation and extrapolation of creep rupture data by the Minimum Commitment Method. I - Focal-point convergence. II - Oblique translation. III - Analysis of multiheats
p0077 A79-16038
- HANTHIEKS, R. A.**
Sputtering in mercury ion thrusters
[NASA-TN-79266] p0054 A79-31343
- HAYCO, R. A.**
Control of volume resistivity in inorganic organic separators
[NASA-TN-1439] p0069 A79-22246
- HARSHALL, R. L.**
An analytical and experimental study of sound propagation and attenuation in variable-area ducts
[NASA-CR-135392] p0177 A79-25845
- HARSIA, S. J.**
Ultraviolet irradiation at elevated temperatures and thermal cycling in vacuum of FEP-A covered silicon solar cells
p0148 A79-40898
- Preliminary evaluation of glass resin materials for solar cell cover use
p0055 A79-40984
- HARTHALES, J. G.**
Radar image processing of real aperture SLAR data for the detection and identification of iceberg and ship targets
p0131 A79-36537
- HARTIN, P. J.**
Applications of thermal energy storage to process heat storage and recovery in the paper and pulp industry
[NASA-CR-159398] p0154 A79-30801
- HARTIN, R. E.**
Development of advanced fuel cell systems
[NASA-CR-159443] p0151 A79-12553
- Strip cell test and evaluation program
[NASA-CR-159652] p0154 A79-31784
- Advanced technology light weight fuel cell program
[NASA-CR-159653] p0155 A79-33581
- HARTINELLI, R. M.**
Lightweight multiple output converter development
[NASA-CR-159526] p0100 A79-20317
- HARTINO, J. P.**
A cross impact methodology for the assessment of US telecommunications systems with application to fiber optics development: Executive summary
[NASA-CR-135209] p0096 A79-17071
- A cross impact methodology for the assessment of US telecommunications systems with application to fiber optics development, volume 1
[NASA-CR-135208] p0096 A79-18159
- A cross impact methodology for the assessment of US telecommunications systems with application to fiber optics development, volume 2
[NASA-CR-159511-VOL-2] p0096 A79-18160
- HASTE, J.**
NASA Lewis Research Center photovoltaic application experiments
[AIAA PAPER 78-1768] p0146 A79-13867
- HASKE, T. D.**
Advanced electrostatic ion thruster for space propulsion
[NASA-CR-159406] p0056 A79-14153
- HASICA, R. J.**
Thermal storage for industrial process and reject heat
p0147 A79-21300
- Thermal storage for industrial process and reject heat
[NASA-TN-78994] p0134 A79-11481
- The role of thermal energy storage in industrial energy conservation
[NASA-TN-79122] p0137 A79-21550
- HATAI, I. H.**
Automated Plasma Spray (APS) process feasibility study: Plasma spray process development and evaluation
[NASA-CR-159579] p0092 A79-29382
- HATHESCU, G. D.**
X-ray photoelectron spectroscopy study of nickel and nickel-base alloy surface alterations in simulated hot corrosion conditions with emphasis on eventual application to turbine blade corrosion
[NASA-CR-159553] p0072 A79-25178
- HATHOR, A. K.**
Active heat exchange system development for latent heat thermal energy storage
[NASA-CR-159479] p0153 A79-21554
- HATTA, R. K.**
Theory of low frequency noise transmission through turbines
[NASA-CR-159457] p0033 A79-20117
- HATTHEI, K. W.**
Applications of ion implantation to high performance, radiation tolerant silicon solar cells
p0143 A79-32648
- HAY, C. E.**
Determination of the zincate diffusion coefficient and its application to alkaline battery problems
p0070 A79-11547
- Decay of the zincate concentration gradient at an alkaline zinc cathode after charging
[NASA-TN-79106] p0137 A79-20520
- HAZARIS, G. A.**
Application of semiconductor diffusants to solar cells by screen printing
[NASA-CR-LEW-12775-1] p0133 A79-11468
- Open-circuit voltage improvements in low-resistivity solar cells
p0143 A79-32649
- HAZARIS, G. A., JR.**
Ionized dopant concentrations at the heavily doped surface of a silicon solar cell
[NASA-TN-1347] p0184 A79-13886
- HAZUN, R. J.**
Strain gage system evaluation program
[NASA-CR-159486] p0110 A79-19314
- MCARDLE, J. G.**
Measured and predicted noise of the AVCO-Lycoming YF-102 turbofan engine
[AIAA PAPER 79-0641] p0026 A79-26877
- Evaluation of two inflow control devices for flight simulation of fan noise using a JT15D engine
[AIAA PAPER 79-0654] p0026 A79-26926
- Analysis of radiation patterns of interaction tones generated by inlet rods in the JT15D engine
[AIAA PAPER 79-0581] p0027 A79-26944
- Measured and predicted noise of the Avco-Lycoming YF-102 turbofan engine
[NASA-TN-79069] p0016 A79-15957
- Evaluation of two inflow control devices for flight simulation of fan noise using a JT15D engine
[NASA-TN-79072] p0017 A79-15969

- MCCARTHY, J. P., JR.**
Engineering in the 21st century
[AAS PAPER 78-192] p0190 A79-21277
- MCDERMOTT, P. F.**
Some practical observations on the accelerated testing of Nickel-Cadmium Cells p0058 A79-51911
- MCDONALD, E.**
Development of a three-dimensional turbulent duct flow analysis
[NASA-CN-3029] p0106 A79-12366
- MCGARRON, E. J.**
Intraocular pressure reduction and regulation system
[NASA-TN-79187] p0165 A79-28881
- MCINERNEY, E. F.**
Survey of inorganic polymers
[NASA-CN-159563] p0087 A79-30377
- MCLALLIN, K. L.**
Cold-air performance of free power turbine designed for 112-kilowatt automotive gas-turbine engine 3: Effect of stator vane end clearances on performance
[NASA-TN-78955] p0014 A79-13049
Cold-air performance of free power turbine designed for 112-kilowatt automotive gas-turbine engine. 2: Effects of variable stator-vane-chord setting angle on turbine performance
[NASA-TN-78993] p0017 A79-17859
- MCPHERSON, D. A.**
Geosynchronous satellite operating anomalies caused by interaction with the local spacecraft environment p0050 A79-24049
- MCVEY, J. B.**
Lean stability augmentation for premixing, prevaporizing combustors
[AIAA PAPER 79-1319] p0036 A79-39035
Lean stability augmentation study
[NASA-CN-159536] p0071 A79-22244
Modeling of premixing-prevaporizing fuel-air mixing passages p0019 A79-24998
Lean Stability augmentation study p0021 A79-25007
- MEIER, G. B.**
An investigation of the initiation stage of hot corrosion in Ni-base alloys
[NASA-CN-159616] p0080 A79-25196
- MEIER, J. G.**
Fuel spray data with LDV p0019 A79-24997
- MELLISH, J. A.**
Advanced engine study for mixed-mode orbit-transfer vehicles
[NASA-CN-159491] p0057 A79-19074
- MERRILL, W.**
Identification and dual adaptive control of turbojet engine
[NASA-TN-79145] p0053 A79-23257
- MERRILL, W. C.**
An inverter/controller subsystem optimized for photovoltaic applications p0148 A79-11047
Dynamic analysis of a photovoltaic power system with battery storage capability
[NASA-TN-79209] p0142 A79-29599
- MESSINA, W. A.**
Definition of smolder experiments for Spacelab
[NASA-CN-159528] p0040 A79-20161
- MEULENBERG, A.**
Limiting process in shallow junction solar cells p0154 A79-32646
- MEVBS, G. E.**
Ground-to-space optical power transfer p0161 A79-17180
- MEYER, A. P.**
Development of advanced fuel cell system
[NASA-CN-159443] p0151 A79-12553
- MEYERS, J. E.**
Concepts for reducing exhaust emissions and fuel consumption of the aircraft piston engine
[SAE PAPER 790605] p0036 A79-36737
- MAO, D.**
Initial comparison of single cylinder Stirling engine computer model predictions with test results
[SAE PAPER 790327] p0119 A79-31368
- Initial comparison of single cylinder Stirling engine computer model predictions with test results
[NASA-TN-79044] p0188 A79-16721
- NICHOLS, C. J.**
Gain measurements of the Ca-Fe charge exchange system p0112 A79-19078
An electro-optic, high-voltage, transient probe
[NASA-TN-79019] p0103 A79-12414
- MIDDLEBROOK, R. D.**
A general unified approach to modelling switching dc-to-dc converters in discontinuous conduction mode p0101 A79-10880
A new optimum topology switching dc-to-dc converter p0101 A79-10888
- MIKKELSON, D. C.**
Wind tunnel performance of four energy efficient propellers designed for Mach 0.8 cruise
[SAE PAPER 790573] p0028 A79-36759
Wind tunnel performance of four energy efficient propellers designed for Mach 0.8 cruise
[NASA-TN-79124] p0003 A79-20069
- MILES, J. H.**
Dispersion of sound in a combustion duct by fuel droplets and soot particles
[NASA-TN-79236] p0174 A79-31002
- MILLER, E.**
Energy efficient aircraft engines
[AIAA PAPER 79-1861] p0030 A79-47918
Energy efficient aircraft engines
[NASA-TN-79204] p0022 A79-27141
- MILLER, B. A.**
Self stabilizing sonic inlet
[NASA-CASE-LEW-11890-1] p0011 A79-24976
- MILLER, L. J.**
Mini-BHU/BIPS foil bearing development
[NASA-CN-159442] p0120 A79-11407
- MILLER, E. A.**
Mass spectrometric investigation of the vaporization of sodium and potassium chromates - Preliminary results p0071 A79-49533
Mass spectrometric investigation of the vaporization of sodium and potassium chromates: Preliminary results
[NASA-TN-79210] p0069 A79-27279
- MINNUCCI, J. A.**
Applications of ion implantation to high performance, radiation tolerant silicon solar cells p0143 A79-32648
- MIRTECH, E. J.**
Adhesive bonding of ion beam textured metals and fluoropolymers p0060 A79-14798
Hydrogen hollow cathode ion source
[NASA-CASE-LEW-12940-1] p0181 A79-10894
Modification of the electrical and optical properties of polymers
[NASA-CASE-LEW-13027-1] p0081 A79-11216
Adhesive bonding of ion beam textured metals and fluoropolymers
[NASA-TN-79004] p0181 A79-12909
- MISKOLCZY, G.**
Lithium and potassium heat pipes for thermionic converters p0145 A79-10113
- HIYOSHI, K.**
Friction and fracture of single-crystal silicon carbide in contact with itself and titanium p0086 A79-32149
Friction and wear of single-crystal manganese-zinc ferrite p0185 A79-34994
Anisotropic friction and wear of single-crystal manganese-zinc ferrite in contact with itself
[NASA-TN-1339] p0113 A79-10425
Friction and wear characteristics of iron-chromium alloys in contact with themselves and silicon carbide
[NASA-TN-1387] p0114 A79-14387
Friction and wear of single-crystal manganese-zinc ferrite
[NASA-TN-78980] p0184 A79-16699
Friction and wear with a single-crystal abrasive grit of silicon carbide in contact with iron base binary alloys in oil: Effects of alloying

- element and its content
[NASA-TP-1394] p0114 N79-17227
- The friction and wear of metals and binary alloys
in contact with an abrasive grit of
single-crystal silicon carbide
[NASA-TM-79131] p0075 N79-22274
- Anisotropic friction, deformation, and fracture of
single-crystal silicon carbide at room temperature
[NASA-TP-1525] p0084 N79-30380
- MISIN, C. S.**
Ion chromatographic determination of sulfur in fuels
[NASA-TM-78971] p0070 A79-21222
- Ion chromatographic determination of sulfur in fuels
[NASA-TM-78971] p0157 N79-17358
- NOFFAT, R. J.**
Full-coverage film cooling: 3-dimensional
measurements of turbulence structure and
prediction of recovery region hydrodynamics
[NASA-CR-3104] p0106 N79-22428
- Heat transfer to a full-coverage, film-cooled
surface with compound-angle (30 deg and 45 deg)
hole injection
[NASA-CR-3103] p0107 N79-22429
- NOKADAN, R. G.**
Liquid oxygen/liquid hydrogen boost/vane pump for
the advanced orbit transfer vehicles auxiliary
propulsion system
[NASA-CR-159648] p0057 N79-31341
- NOSEGAMI, P. J.**
Computation of atmospheric attenuation of sound
for fractional-octave bands
[NASA-TP-1412] p0173 N79-17659
- NOONEY, P. M.**
High-energy electron-induced damage production at
room temperature in aluminum-doped silicon
p0154 N79-32662
- NOORE, R. D.**
Aerodynamic performance of a 1.35-pressure-ratio
axial-flow fan stage
[NASA-TP-1299] p0002 N79-10022
- Performance of single-stage axial-flow transonic
compressor with rotor and stator aspect ratios
of 1.19 and 1.26, respectively, and with design
pressure ratio of 1.82
[NASA-TP-1338] p0013 N79-10060
- Aerodynamic performance of 1.38-pressure-ratio,
variable-pitch fan stage
[NASA-TP-1502] p0024 N79-31213
- Aerodynamic performance of axial-flow fan stage
operated at nine inlet guide vane angles
[NASA-TP-1510] p0024 N79-31214
- NOORE, T. J.**
The use of ion beam cleaning to obtain high
quality cold welds with minimal deformation
p0119 A79-24121
- Evaluation of manufacturing processes for
boron/aluminum composites containing
0.2-mm-diameter boron fibers
[NASA-TM-79008] p0062 N79-12153
- Evaluation of a Brayton cycle recuperator after
21,000 hours of ground testing
[NASA-TM-79091] p0074 N79-20217
- MOORHEAD, P. E.**
Acoustic emission testing of composite vessels
under sustained loading
p0128 A79-11543
- Evaluation of manufacturing processes for
boron/aluminum composites containing
0.2-mm-diameter boron fibers
[NASA-TM-79008] p0062 N79-12153
- MORE, E. B.**
Design, fabrication, and test of a composite
material wind turbine rotor blade
[NASA-CR-135389] p0150 N79-10525
- MORGAN, L. L.**
Laser power conversion system analysis, volume 1
[NASA-CR-159523-VOL-1] p0112 N79-21334
- Laser power conversion system analysis, volume 2
[NASA-CR-159523-VOL-2] p0112 N79-21335
- MORRIS, J. F.**
Diinide thermionic energy conversion with
lanthanum-hexaboride electrodes
p0146 A79-13098
- Optimize out-of-core thermionic energy conversion
for nuclear electric propulsion
p0146 A79-13099
- Thermocouples of molybdenum and iridium alloys for
more stable vacuum-high temperature performance
[NASA-CASE-LEW-12174-2] p0109 N79-14346
- Titanium-alloy, metallic-fluid heat pipes for
space service
[NASA-TM-79132] p0104 N79-22426
- MOSLEY, P. K.**
Workbook for estimating effects of accidental
explosions in propellant ground handling and
transport systems
[NASA-CR-3023] p0091 N79-10226
- MOSINSKIS, G.**
Design and fabrication of the Mini-Brayton
Recuperator (NBR)
[NASA-CR-159429] p0151 N79-11476
- MOYER, D. W.**
Filtration effects on ball bearing life and
condition in a contaminated lubricant
[ASME PAPER 78-LUB-34] p0118 A79-23246
- MCZEIC, R. V.**
Control of wind turbine generators connected to
power systems
p0146 A79-15574
- MROZ, T. S.**
Rankine-cycle component characteristics
p0140 N79-26478
- Brayton-cycle component characteristics
p0140 N79-26479
- Speed reducers-increasers
p0140 N79-26481
- Power-conversion system component summation
p0140 N79-26483
- MUELLER, R. A.**
VHF downlink communication system for SLAR data
p0045 A79-51097
- VHF downlink communication system for SLAR data
[NASA-TM-79164] p0094 N79-23313
- MULARE, E. J.**
Lean, premixed, prevaporized combustion for
aircraft gas turbine engines
[AIAA PAPER 79-1318] p0029 A79-39034
- Lean, premixed, prevaporized combustion for
aircraft gas turbine engines
[NASA-TM-79148] p0018 N79-23964
- Lean, premixed, prevaporized combustion for
aircraft gas turbine engines
[NASA-TM-79148] p0018 N79-23964
- MULLALLY, J. E.**
Development of sputtered techniques for thrust
chambers
[NASA-CR-159637] p0080 N79-32326
- MUNGER, P.**
Studies of the acoustic transmission
characteristics of coaxial nozzles with inverted
velocity profiles: Comprehensive data report
[NASA-CR-159628] p0177 N79-27933
- MURPHY, G. C.**
Metal spar/superhybrid shell composite fan blades
[NASA-CR-159594] p0067 N79-30295
- MURRAY, G. L.**
Advanced General Aviation Turbine Engine (GATE)
concepts
[NASA-CR-159603] p0034 N79-25017
- MYERS, I. T.**
Primary electric propulsion for future space
missions
[AIAA 79-0881] p0055 A79-34773
- Primary electric propulsion for future space
missions
[NASA-TM-79141] p0052 N79-22190
- MYERS, R. W.**
UHF coplanar-slot antenna for
aircraft-to-satellite data communications
[NASA-TM-79239] p0010 N79-31185

N

NACHTIGALL, A. J.

- The strainrange partitioning behavior of an
advanced gas turbine disk alloy, AF2-1DA
[AIAA PAPER 79-1192] p0078 A79-38577
- Strainrange partitioning behavior of the
nickel-base superalloys, Rene 80 and IN-100
p0126 N79-10480
- Low-cycle fatigue of thermal-barrier coatings at
582 deg C
[NASA-TP-1322] p0014 N79-13046
- The strainrange partitioning behavior of an
advanced gas turbine disk alloy, AF2-1DA
[NASA-TM-79179] p0075 N79-23196
- NAGY, J.**
Evaluation of high-contact-ratio spur gears with

- profile modification
[NASA-TP-1454] p0115 N79-31604
- MAINWIGER, J. J.**
Effect of thermal barrier coatings on the performance of steam and water-cooled gas turbine/steam turbine combined cycle system
[NASA-TN-79057] p0135 N79-17334
Gas-turbine critical research and advanced technology support project
[NASA-TN-79139] p0139 N79-25498
- MANIKONG, D.**
Optimum dry-cooling sub-systems for a solar air conditioner
[NASA-TN-79007] p0133 N79-11477
- MANEVIC, J. E.**
Laboratory studies of electrical properties of insulating materials p0044 A79-20877
- NASH, D. G.**
Sound-suppressing structure with thermal relief
[NASA-CASE-LEW-12658-1] p0172 N79-14871
- NASTROM, G. D.**
An analysis of the first two years of GASF data p0160 A79-15068
Ozone in the upper troposphere from Gasf measurements p0160 A79-44810
- NASVYTIS, A. L.**
Performance of a Nasvytis multiroller traction drive
[NASA-TP-1378] p0113 N79-13369
- NATPEN, A. H.**
An analytical and experimental study of sound propagation and attenuation in variable-area ducts
[NASA-CN-135392] p0177 N79-25845
- NEICE, S.**
Design investigation of solar powered lasers for space applications
[NASA-CN-159554] p0111 N79-26384
- NEINER, G. H.**
A throat-bypass stability-bleed system using relief valves to increase the transient stability of a mixed-compression inlet
[NASA-TP-1083] p0023 N79-28176
- NELSON, D. P.**
Aerodynamic and acoustic investigation of inverted velocity profile coannular exhaust nozzle models and development of aerodynamic and acoustic prediction procedures, comprehensive data report, volume 1
[NASA-CN-159515] p0034 N79-30185
Aerodynamic and acoustic investigation of inverted velocity profile coannular exhaust nozzle models and development of aerodynamic and acoustic prediction procedures, comprehensive data report, volume 2
[NASA-CN-159516] p0034 N79-30186
Aerodynamic and acoustic investigation of inverted velocity profile coannular exhaust nozzle models and development of aerodynamic and acoustic prediction procedures
[NASA-CN-3168] p0035 N79-31212
- NELSON, L.**
Solar-pumped lasers for space power transmission
[AIAA PAPER 79-1015] p0112 A79-38202
Design investigation of solar powered lasers for space applications
[NASA-CN-159554] p0111 N79-26384
- NELSON, P. B.**
Evaluation of an advanced directionally solidified gamma/gamma'-alpha Mo eutectic alloy
[NASA-CN-159416] p0079 N79-20222
- NESETH, T. E.**
Operating characteristics of a cantilever-mounted resilient-pad gas-lubricated thrust bearing
[NASA-TP-1438] p0115 N79-22518
- NEWMAN, A.**
Design of high efficiency BLE solar cells for space and terrestrial applications p0154 N79-32647
- NEUMANN, R. E.**
Reynolds number, scale and frequency content effects on F-15 inlet instantaneous distortion
[AIAA PAPER 79-0104] p0005 A79-19533
- NEUSTADTER, R. E.**
DOE/NASA Mod-OA wind turbine performance p0145 A79-10235
The use of wind data with an operational wind turbine in a research and development environment
[NASA-TN-73832] p0140 N79-26502
- NEWELL, R. E.**
Experimental evidence of interhemispheric transport from airborne carbon monoxide measurements p0158 A79-38942
- NEWMAN, J.**
Mass drivers. 3: Engineering p0040 N79-32232
- NICHOLLS, J. A.**
Effect of fuel sprays on emissions p0020 N79-24999
- NIEDZWICKI, R. E.**
Gas-turbine critical research and advanced technology support project
[NASA-TN-79139] p0139 N79-25498
- NORED, D. L.**
Fuel conservative aircraft engine technology p0025 A79-20078
- NORTON, J. H.**
Rotor redesign for a highly loaded 1800 ft/sec tip speed fan. 1: Aerodynamic and mechanical design report
[NASA-CN-159596] p0034 N79-26055
- NOSEK, S. E.**
Ceramics for the advanced automotive gas turbine engine - A look at a single shaft design p0117 A79-12850
- NOTA-DONATO, J. J.**
Effect of low-stiffness closeout overlap on rocket thrust-chamber life
[NASA-TP-1456] p0053 N79-23132
- NOVAK, R. C.**
Increasing the FOD tolerance of composites p0067 A79-20859
- NOVOTNY, H.**
Optical, spin-resonance, and magnetoresistance studies of /tetrathiatetracene/2/iodide/3 - The nature of the ground state p0184 A79-10417
- NUGENT, J.**
Reynolds number, scale and frequency content effects on F-15 inlet instantaneous distortion
[AIAA PAPER 79-0104] p0005 A79-19533
- NYLAND, T.**
Measurements of carbon monoxide, condensation nuclei, and ozone on a B 747SP aircraft flight around the world p0158 A79-31332
- NYLAND, T. W.**
Airborne atmospheric sampling system p0012 A79-50333
- NASA Global Atmospheric Sampling Program (GASF)**
data report for tape VL0009
[NASA-TN-79058] p0157 N79-15448
NASA Global Atmospheric Sampling Program (GASF)
data report for tapes VL0010 and VL0012
[NASA-TN-79061] p0157 N79-15450
Condensation-nuclei (Aitken Particle) measurement system used in NASA global atmospheric sampling program
[NASA-TP-1415] p0157 N79-18479
- O**
- OBBERLY, C. E.**
Properties and performance of fine-filament bronze-process Nb3Sn conductors p0184 A79-20529
- OBBIEN, C. J.**
Plug cluster engine concept for in-space missions
[AIAA PAPER 79-1179] p0055 A79-38972
Unconventional nozzle tradeoff study
[NASA-CN-159520] p0057 N79-28224
- OBBIEN, H.**
Development of spiral-groove self-acting seals for helicopter engines
[NASA-CN-159622] p0122 N79-32551
- ODONWELL, E. E.**
Spacecraft charging modeling development and validation study p0050 N79-24051
- ODONWELL, P.**
NASA Lewis Research Center photovoltaic application experiments
[AIAA PAPER 78-1768] p0146 A79-13867
- OENHLEN, G.**
High-energy electron-induced damage production at room temperature in aluminum-doped silicon p0154 N79-32662

P

- OGLEBAY, J. C.
A thermal control approach for a solar electric propulsion thrust subsystem
[NASA-TN-79175] p0043 N79-27236
- OLSEN, R. C.
Operations of the ATS-6 ion engine p0049 N79-24007
- OLSEN, W.
Trailing edge noise data with comparison to theory [AIAA PAPER 79-1524] p0176 A79-47340
Trailing edge noise data with comparison to theory [NASA-TN-79208] p0174 N79-27930
- ONAT, E.
A method to estimate weight and dimensions of large and small gas turbine engines [NASA-CR-159481] p0015 N79-15046
- ONEILL, G. K.
Mass drivers. 3: Engineering p0040 N79-32232
- ONOPREICHUK, S.
The application of hydraulics in the 2,000 kW wind turbine generator p0156 A79-27400
- OPLINGER, J.
Conceptual design of thermal energy storage systems for near term electric utility applications [NASA-CR-159577] p0155 N79-33560
- ORANGE, T. W.
On the equivalence between semiempirical fracture analyses and R-curves p0129 A79-39813
On the equivalence between semiempirical fracture analyses and R-curves [NASA-TN-79127] p0103 N79-20338
- ORELL, H. E.
Synthesis of improved moisture resistant polymers [NASA-CR-159456] p0087 N79-18053
- ORHUP, H. J.
Study of an advanced General Aviation Turbine Engine (GATE) [NASA-CR-159558] p0033 N79-21073
- ORTEL, L. E.
The catalysis of nucleotide polymerization by compounds of divalent lead p0060 A79-32924
- OSBORN, W. H.
Aerodynamic performance of a 1.35-pressure-ratio axial-flow fan stage [NASA-TP-1299] p0002 N79-10022
Aerodynamic performance of 1.38-pressure-ratio, variable-pitch fan stage [NASA-TP-1502] p0024 N79-31213
Effects of diffusion factor, aspect ratio and solidity on overall performance of 14 compressor middle stages [NASA-TP-1523] p0038 N79-33210
- OSULLIVAN, G.
An inverter/controller subsystem optimized for photovoltaic applications p0148 A79-41047
- OTTENSON, D. A.
Application of ion chromatography to the study of hydrolysis of some halogenated hydrocarbons at ambient temperatures p0060 A79-14951
Ion chromatographic determination of sulfur in fuels p0070 A79-21222
Sulfate and nitrate mixing ratios in the vicinity of the tropopause p0158 A79-49494
Application of ion chromatography to the study of hydrolysis of some halogenated hydrocarbons at ambient temperatures [NASA-TN-79020] p0157 N79-12586
Ion chromatographic determination of sulfur in fuels [NASA-TN-78971] p0157 N79-17358
- OWENS, R. E.
Energy efficient engine: Propulsion system-aircraft integration evaluation [NASA-CR-159488] p0032 N79-16850
- OWENS, W. E.
Preliminary summary of the ETF conceptual studies [NASA-TN-78999] p0133 N79-11478
- OZERYANSKY, G. H.
Properties and performance of fine-filament bronze-process Nb3Sn conductors p0184 A79-20529
- PAPATHAKOS, L. C.
Global sensing of gaseous and aerosol trace species using automated instrumentation on 747 airliners p0110 A79-15067
- PARKER, D. E.
Design study and performance analysis of a high-speed multistage variable-geometry fan for a variable cycle engine [NASA-CR-159545] p0034 N79-25020
- PARKER, R. J.
Evaluation of CBS 600 carburized steel as a gear material [NASA-TP-1390] p0114 N79-14389
- PARKINSON, A. G.
An introduction to a unified approach to flexible rotor balancing [ASME PAPER 79-GT-161] p0124 A79-32423
- PARKS, D. E.
Effects of bulk and surface conductivity on the potential developed by dielectrics exposed to electron beams p0171 A79-50938
Charging analysis of the SCATHA satellite p0049 N79-24012
Extension, validation and application of the NASCAP code [NASA-CR-159595] p0100 N79-27397
- PARR, V. B.
Workbook for estimating effects of accidental explosions in propellant ground handling and transport systems [NASA-CR-3023] p0091 N79-10226
- PASION, A. J.
Inflight fuel tank temperature survey data [NASA-CR-159569] p0009 N79-23940
Design and evaluation of aircraft heat source systems for use with high-freezing point fuels [NASA-CR-159568] p0091 N79-24172
- PATCH, E. W.
Reduction of particulate carryover from a pressurized fluidized bed p0150 A79-49527
Reduction of particulate carryover from a pressurized fluidized bed p0150 A79-49527
Method for decomposing observed line shapes resulting from multiple causes - Application to plasma charge-exchange-neutral spectra p0182 A79-53867
Preliminary comparison of theory and experiment for a conical, pressurized-fluidized-bed coal combustor [NASA-TN-79137] p0137 N79-22623
Reduction of particulate carryover from a pressurized fluidized bed [NASA-TN-79216] p0141 N79-27664
- PATER, R. E.
Synthesis of improved moisture resistant polymers [NASA-CR-159510] p0087 N79-23218
- PEARSON, C. V.
Preliminary summary of the ETF conceptual studies [NASA-TN-78999] p0133 N79-11478
- PELOUCH, J. J., JR.
Space propulsion technology overview [AIAA 79-0860] p0054 A79-34704
Low-thrust chemical orbit transfer propulsion [AIAA PAPER 79-1182] p0055 A79-39815
Space propulsion technology overview [NASA-TN-79104] p0042 N79-20171
Low-thrust chemical orbit transfer propulsion [NASA-TN-79190] p0043 N79-25129
- PERKINS, F. J.
Global sensing of gaseous and aerosol trace species using automated instrumentation on 747 airliners p0110 A79-15067
Simultaneous measurements of ozone outside and inside cabins of two B-747 airliners and a Gates Learjet business jet p0008 A79-27571
Airborne atmospheric sampling system p0012 A79-50333
Aircraft cabin ozone measurements on B747-100 and B747-SP aircraft: Correlations with atmospheric ozone and ozone encounter statistics

- [NASA-TM-79060] p0008 N79-15013
Aircraft Icing
- p0161 N79-17418
Ozone contamination in aircraft cabins:
Objectives and approach
- p0008 N79-21022
Ozone Contamination in Aircraft Cabins: Summary
of recommendations
- p0008 N79-21026
Ozone Contamination in Aircraft Cabins: Post
workshop review of recommendations
- p0008 N79-21027
Ozone Contamination in Aircraft Cabins. Appendix
B: Overview papers. In-flight measurements
- p0008 N79-21029
- PERSSON, H.
Ion beam probing of electrostatic fields
[NASA-TM-79120] p0181 N79-20864
- PETERSEN, H. J.
Turbojet blade vibration data acquisition design
and feasibility testing
[NASA-CR-159505] p0032 N79-18976
- PETERSON, D. J.
Applications of thermal energy storage to process
heat and waste heat recovery in the iron and
steel industry
[NASA-CR-159397] p0151 N79-11473
- PETERSON, V. S.
Fine particulate capture device
[NASA-CASE-LEW-11583-1] p0109 N79-17192
- PETRASEK, D. W.
Predicted inlet gas temperatures for tungsten
fiber reinforced superalloy turbine blades
p0025 A79-17029
Tungsten fiber reinforced FeCrAlY - A first
generation composite turbine blade material
p0065 A79-30397
Tungsten fiber reinforced FeCrAlY: A first
generation composite turbine blade material
[NASA-TM-79094] p0063 N79-20187
Development and fabrication of high strength alloy
fibers for use in metal-metal matrix composites
[NASA-TM-79115] p0063 N79-22211
- PHILIPP, W. B.
Method of cross-linking polyvinyl alcohol and
other water soluble resins
[NASA-CASE-LEW-13103-1] p0068 N79-14172
Cross-linked polyvinyl alcohol and method of
making same
[NASA-CASE-LEW-13101-1] p0068 N79-14173
Three methods for in situ cross-linking of
polyvinyl alcohol films for application as
ion-conducting membranes in potassium hydroxide
electrolyte
[NASA-TP-1407] p0059 N79-21128
In situ self cross-linking of polyvinyl alcohol
battery separators
[NASA-CASE-LEW-12972-1] p0138 N79-25481
- PHILLIPS, B. R.
Resonance-tube ignition of aluminum
p0071 A79-46366
- PIAN, C. C. P.
Velocity, temperature, and electrical conductivity
profiles in hydrogen-oxygen MHD duct flows
p0182 A79-26184
Performance optimization of an MHD generator with
physical constraints
p0182 A79-51995
Evaluation of the ECAS open cycle MHD power plant
design
[NASA-TM-79012] p0136 N79-17335
Performance optimization of an MHD generator with
physical constraints
[NASA-TM-79172] p0138 N79-24446
MHD performance calculations with oxygen enrichment
[NASA-TM-79140] p0135 N79-25499
- PICKRELL, R. L.
An inverter/controller subsystem optimized for
photovoltaic applications
p0148 A79-41047
Dynamic analysis of a photovoltaic power system
with battery storage capability
[NASA-TM-79209] p0142 N79-29599
- PIERCE, W. S.
Influence of composition, annealing treatment, and
texture on the fracture toughness of
Ti-5Al-2.5Sn plate at cryogenic temperatures
p0077 A79-24262
- PINDROH, A.
Design investigation of solar powered lasers for
space applications
[NASA-CR-159554] p0111 N79-26384
- PINE, V. W.
First principles numerical model of
avalanche-induced arc discharges in
electron-irradiated dielectrics
[NASA-CR-159560] p0101 N79-28418
- PIRVICS, J.
High speed cylindrical roller bearing analysis,
SKF computer program CYBEAM. Volume 1: Analysis
[NASA-CR-159460] p0121 N79-17222
High speed cylindrical roller bearing analysis,
SKF computer program CYBEAM. Volume 2: User's
manual
[NASA-CR-159461] p0121 N79-17223
- PIUKO, R. J.
Control and stabilization of the DOE/NASA Mod-1
two megawatt wind turbine generator
p0156 A79-51780
- PLUMBLEE, H. E.
Studies of the acoustic transmission
characteristics of coaxial nozzles with inverted
velocity profiles: Comprehensive data report
[NASA-CR-159628] p0177 N79-27933
- PLUMBLEE, H. E., JR.
An impulse test technique with application to
acoustic measurements
[AIAA PAPER 79-0679] p0178 A79-26890
- POESCHL, R. L.
Advanced electrostatic ion thruster for space
propulsion
[NASA-CR-159406] p0056 N79-14153
- POLLACK, F. G.
Measurement of transient strain and surface
temperature on simulated turbine blades using
noncontacting techniques
[NASA-TM-78982] p0126 N79-19415
- POOLOS, M. P.
Critical mass flux through short Foria type inlets
of various cross sections
[NASA-TM-79017] p0074 N79-20216
- POORE, R.
MOD-2 failure mode and effects analysis
[NASA-CR-159632] p0093 N79-30415
- POPPEL, G. L.
Analysis and preliminary design of an optical
digital tip clearance sensor for propulsion
control
[NASA-CR-159434] p0031 N79-15053
- PORTER, T. R.
Evaluation of flawed composite structural
components under static and cyclic loading
[NASA-CR-135403] p0000 N79-26120
- POSTA, S. J.
An electro-optic, high-voltage, transient probe
[NASA-TM-79019] p0109 N79-12414
- POTONIDES, H. C.
Performance of a V/STOL tilt nacelle inlet with
blowing boundary layer control
[AIAA PAPER 79-1163] p0065 A79-47347
Performance of a V/STOL tilt nacelle inlet with
blowing boundary layer control
[NASA-TM-79176] p0004 N79-27093
- POWERS, E. J.
Ion confinement and transport in a toroidal plasma
with externally imposed radial electric fields
[NASA-TP-1411] p0181 N79-19867
- PRATT, R. W.
A summary of research on the NASA-Global
Atmospheric Sampling Program performed by the
Atmospheric Sciences Research Center
[NASA-CR-159614] p0159 N79-27716
- PROKOPIUS, P. E.
Commercial phosphoric acid fuel cell system
technology development
p0150 A79-51809
Commercial phosphoric acid fuel cell system
technology development
[NASA-TM-79169] p0139 N79-25500
- PURVIS, C. K.
Insulator edge voltage gradient effects in
spacecraft charging phenomena
p0048 A79-30139
Insulator edge voltage gradient effects in
spacecraft charging phenomena
[NASA-TM-78988] p0046 N79-11109

- Jupiter probe charging study
[NASA-TP-1263] p0046 N79-15149
Summary of the two year NASA program for active
control of ATS-5/6 environmental charging p0047 N79-24006
Comparison of NASCAP predictions with experimental
data p0047 N79-24013
Status of materials characterization studies p0048 N79-24030
Charging rates of metal-dielectric structures p0048 N79-24033
- PUTNEY, Z.**
An economic analysis of a commercial approach to
the design and fabrication of a space power system
[AIAA 79-0914] p0055 A79-34737
An economic analysis of a commercial approach to
the design and fabrication of a space power system
[NASA-TM-79153] p0053 N79-22193

Q

- QUENTMEYER, R. J.**
Some effects of cyclic induced deformation in
rocket thrust chambers p0054 A79-34736
[AIAA 79-0911]
Some effects of cyclic induced deformation in
rocket thrust chambers p0103 N79-20337
[NASA-TM-79112]
- QUICK, W. H.**
Fiber optic sensors for military, industrial and
commercial applications p0111 A79-38738
Analysis and preliminary design of optical sensors
for propulsion control p0180 N79-27975
[NASA-CR-159519]
- QUINNEY, D.**
Solar-pumped lasers for space power transmission
[AIAA PAPER 79-1015] p0112 A79-38202
Design investigation of solar powered lasers for
space applications p0111 N79-26384
[NASA-CR-159554]

R

- RADHAKRISHNAN, K.**
Modelling turbulent flame ignition and blowout p0021 N79-25008
- RAFTOPOULOS, D. D.**
Dispersion of sound in a combustion duct by fuel
droplets and soot particles p0174 N79-31002
[NASA-TM-79236]
- RAHNKE, C. J.**
Evaluation of advanced regenerator systems p0188 N79-12969
[NASA-CR-159422]
- RAJAN, R.**
Simulation of fluidized bed coal combustors p0153 N79-20487
[NASA-CR-159529]
- RAHNS, P.**
Efficiency enhancement of octave-bandwidth
traveling wave tubes by use of multistage
depressed collectors p0097 N79-17139
[NASA-TP-1416]
Analytical prediction with multidimensional
computer programs and experimental verification
of the performance, at a variety of operating
conditions, of two traveling wave tubes with
depressed collectors p0097 N79-22375
[NASA-TP-1449]
Efficiency enhancement of dual-mode traveling wave
tubes at saturation and in the linear range by
use of spent-beam refocusing and multistage
depressed collectors p0058 N79-28420
[NASA-TP-1486]
- RAHLEY, J. R.**
Wind turbines for electric utilities - Development
status and economics p0148 A79-38888
[AIAA PAPER 79-0965]
Wind turbines for electric utilities: Development
status and economics p0142 N79-30719
[NASA-TM-79170]
- RAMSEY, W. D.**
Inert gas ion source program p0056 N79-10120
[NASA-CR-159423]
- RATAJCZAK, A.**
NASA Lewis Research Center photovoltaic
application experiments p0146 A79-13867
[AIAA PAPER 78-1768]

- RATAJCZAK, A. F.**
Photovoltaic power systems for rural areas of
developing countries p0147 A79-26131
Design and fabrication of a photovoltaic power
system for the Papago Indian Village of
Schuchuli /Guasight/, Arizona p0148 A79-41089
Description and status of NASA-LeRC/DOE
photovoltaic applications systems experiments p0148 A79-41091
Photovoltaic power systems for rural areas of
developing countries p0135 N79-15411
[NASA-TM-79097]
Description of photovoltaic village power systems
in the United States and Africa p0138 N79-24443
[NASA-TM-79149]
Social and economic impact of solar electricity at
Schuchuli Village p0139 N79-25501
[NASA-TM-79194]
- RATAJCZAK, T.**
DOE photovoltaic tests and applications project p0139 N79-25492
- RAWLIN, V. K.**
Increased capabilities of the 30-cm diameter Hg
ion thruster p0055 A79-34774
[AIAA 79-0910]
Increased capabilities of the 30-cm diameter Hg
ion thruster p0053 N79-22192
[NASA-TM-79142]
Sputtering in mercury ion thrusters p0054 N79-31343
[NASA-TM-79266]
Reduced power processor requirements for the 30-cm
diameter Hg ion thruster p0054 N79-33253
[NASA-TM-79257]
- RAYL, G. J.**
UV blocking filters for polymeric films p0088 A79-51103
An investigation of the adhesive bonding of Teflon
solar cell covers p0153 N79-26506
[NASA-CR-159565]
- REED, K. E.**
Dynamic mechanical analysis of fiber reinforced
composites p0065 A79-31040
Dynamic mechanical analysis of fiber reinforced
composites p0061 N79-15157
[NASA-TM-79033]
- REEMSVIDER, D. C.**
Effect of forward velocity and crosswind on the
reverse-thrust performance of a variable-pitch
fan engine p0025 A79-23512
[AIAA PAPER 79-0105]
Effect of forward velocity and crosswind on the
reverse-thrust performance of a variable-pitch
fan engine p0015 N79-15049
[NASA-TM-79059]
- REID, L.**
Performance of single-stage axial-flow transonic
compressor with rotor and stator aspect ratios
of 1.19 and 1.26, respectively, and with design
pressure ratio of 1.82 p0013 N79-10060
[NASA-TP-1338]
Aerodynamic performance of axial-flow fan stage
operated at nine inlet guide vane angles p0024 N79-31214
[NASA-TP-1510]
- REID, R.**
Lightweight porous plastic plaque p0141 N79-28672
- REID, R. A.**
Factors affecting the open-circuit voltage and
electrode kinetics of some iron/titanium/redox
flow cells p0146 A79-11824
- REILLY, D. H.**
Safety considerations in the design and operation
of large wind turbines p0141 N79-28725
[NASA-TM-79193]
- REZY, B. J.**
Concepts for reducing exhaust emissions and fuel
consumption of the aircraft piston engine p0036 A79-36737
[SAE PAPER 790605]
- RICE, E. J.**
Modal propagation angles in a cylindrical duct
with flow and their relation to sound radiation p0174 A79-19582
[AIAA PAPER 79-0183]
Modal propagation angles in ducts with soft walls
and their connection with suppressor performance p0175 A79-26880
[AIAA PAPER 79-0624]

- Modal propagation angles in a cylindrical duct with flow and their relation to round radiation [NASA-TM-79030] p0172 N79-15756
- Modal propagation angles in ducts with soft walls and their connection with suppressor performance [NASA-TM-79081] p0173 N79-16646
- RICE, R. E.
NaOH-based high temperature heat-/f-fusion thermal energy storage device p0155 A79-10106
- Phase change thermal storage for a solar total energy system p0155 A79-17321
- Development of a phase-change thermal storage system using modified anhydrous sodium hydroxide for solar electric power generation [NASA-CR-159465] p0153 N79-19454
- RICE, W. J.
Indicated mean-effective pressure instrument [NASA-CASE-LEW-12661-1] p0109 N79-14345
- RICHARDS, T. E.
DOE/NASA Mod-OA wind turbine performance p0145 A79-10235
- RICHARDSON, J. H.
Causes of high pressure compressor deterioration in service [AIAA PAPER 79-1234] p0036 A79-40483
- RICHARDSON, R. D.
Design of a video teleconference facility for a synchronous satellite communications link [NASA-TP-1376] p0054 N79-14275
- RICKER, R. E.
Workbook for estimating effects of accidental explosions in propellant ground handling and transport systems [NASA-CR-3023] p0091 N79-10226
- RIO, R.
T700 power turbine rotor multiplane/multispeed balancing demonstration [NASA-CR-159586] p0122 N79-25392
- RIO, R. A.
Laser balancing demonstration on a high-speed flexible rotor [ASME PAPER 79-GT-56] p0123 A79-32351
- RISBERG, J. A.
Study of liquid and vapor flow into a Centaur capillary device [NASA-CR-159657] p0108 N79-33432
- RITTERMAN, P. F.
Hydrogen recombination in sealed nickel-cadmium aerospace cells p0057 A79-51907
- RITTNER, E.
Limiting process in shallow junction solar cells p0154 N79-32646
- ROBBINS, W. H.
Large horizontal axis wind turbine development p0149 A79-46527
- Utility operational experience on the NASA/DOE Mod-OA 200 kW Wind Turbine p0149 A79-46537
- Utility operational experience on the NASA/DOE Mod-OA 200-kW wind turbine [NASA-TM-79084] p0136 N79-20494
- Large horizontal axis wind turbine development [NASA-TM-79174] p0140 N79-26504
- ROBERTS, E., JR.
Digital enhancement of computerized axial tomograms p0164 A79-11544
- ROBERTS, P. E.
Wide range operation of advanced low NOx aircraft gas turbine combustors [ASME PAPER 78-GT-128] p0024 A79-10792
- ROBERTS, W. E.
High speed smoke flow visualization for the determination of cascade shock losses [AIAA PAPER 79-0042] p0005 A79-19495
- An off-design correlation of part span damper losses through transonic axial fan rotors [ASME PAPER 79-GT-6] p0028 A79-32329
- Low-turbulence high-speed wind tunnel for the determination of cascade shock losses [ASME PAPER 79-GT-129] p0039 A79-32398
- ROBINSON, J. W.
Potential mapping with charged-particle beams p0049 N79-24038
- Stable dielectric charge distributions from field enhancement of secondary emission p0049 N79-24046
- ROBINSON, P. H.
Epitaxial solar-cell fabrication, phase 2 [NASA-CR-135350] p0152 N79-19448
- ROBINSON, R. S.
Industrial ion source technology [NASA-CR-159534] p0179 N79-19828
- Physical processes in directed ion beam sputtering [NASA-CR-159567] p0182 N79-26943
- ROCHE, J. C.
The decrease in effective photocurrents due to saddle points in electrostatic potentials near differentially charged spacecraft p0049 A79-30140
- Large space system - Charged particle environment interaction technology [AIAA 79-0913] p0055 A79-34775
- NASCAP modelling of high-voltage power system interactions with space charged-particle environments p0051 A79-39806
- Large space system: Charged particle environment interaction technology [NASA-TM-79156] p0046 N79-22188
- NASCAP modelling of high-voltage power system interactions with space charged-particle environments [NASA-TM-79146] p0046 N79-24020
- The capabilities of the NASA charging analyzer program p0047 N79-24011
- Comparison of NASCAP predictions with experimental data p0047 N79-24013
- Charging rates of metal-dielectric structures p0048 N79-24033
- NASCAP modelling of environmental-charging-induced discharges in satellites [NASA-TM-79247] p0048 N79-31265
- ROFFE, G.
Experimental study of the effects of flameholder geometry on emissions and performance of lean premixed combustors [AIAA PAPER 79-0187] p0070 A79-19586
- Emission measurements for a lean premixed propane/air system at pressures up to 30 atmospheres [NASA-CR-159421] p0071 N79-10165
- Emissions measurements for a lean premixed propane/air system at pressures up to 30 atmospheres p0020 N79-25002
- ROHLIK, H. E.
Design problems of small turbomachinery p0046 N79-22097
- ROHY, D. A.
Fuel spray data with LDV p0019 N79-24997
- ROLAND, G. W.
Nb3Ge as a potential candidate material for 15- to 25-T magnets p0186 A79-44548
- ROMAN, R.
Hydrogen hollow cathode ion source [NASA-CASE-LEW-12940-1] p0181 N79-10894
- ROSEN, A.
Nonlinear equations of equilibrium for elastic helicopter or wind turbine blades undergoing moderate deformation [NASA-CR-159478] p0130 N79-19414
- Effects of arcing due to spacecraft charging on spacecraft survival [NASA-CR-159593] p0100 N79-25312
- ROSENBLUM, L.
Photovoltaic power systems for rural areas of developing countries p0147 A79-26131
- Photovoltaic power systems for rural areas of developing countries [NASA-TM-79097] p0135 N79-15411
- ROSENBLIEB, J. W.
Aircraft engine sump fire mitigation, phase 2 [NASA-CR-135379] p0121 N79-17219
- ROSENE, D. E.
Chemically frozen multicomponent boundary layer theory of salt and/or ash deposition rates from combustion gases p0078 A79-50912
- Experimental studies of the formation/deposition of sodium sulfate in/from combustion gases

- [NASA-CR-159612] p0072 N79-25183
Experimental studies of the formation/deposition
of sodium sulfate in/from combustion gases
[NASA-CR-159613] p0080 N79-25184
- ROSS, R. S.
Evaluation of urethane for feasibility of use in
wind turbine blade design
[NASA-CR-159530] p0153 N79-20497
- ROTHBERG, E.
Effects of bulk and surface conductivity on the
potential developed by dielectrics exposed to
electron beams
p0171 A79-50938
Extension, validation and application of the
NASCAP code
[NASA-CR-159525] p0100 N79-27397
- ROTH, J. E.
Microwave radiation measurements near the electron
plasma frequency of the NASA Lewis Bumpy Torus
plasma
p0181 A79-14953
Ion confinement and transport in a toroidal plasma
with externally imposed radial electric fields
[NASA-TP-1411] p0181 N79-19867
- ROWE, A. P.
The erosion/corrosion of small superalloy turbine
rotors operating in the effluent of a PFB coal
combustor
[NASA-TN-79227] p0076 N79-30356
- ROWNY, P. E.
Development of a phase-change thermal storage
system using modified anhydrous sodium hydroxide
for solar electric power generation
[NASA-CR-159465] p0153 N79-19454
- RUBIN, A. G.
Charging analysis of the SCATHA satellite
p0049 N79-24012
- RUBIN, S. G.
Filtering of non-linear instabilities
p0108 A79-32912
- RUDNY, R. A.
Characteristics and combustion of future
hydrocarbon fuels
p0090 A79-11599
Impact of future fuel properties on aircraft
engines and fuel systems
p0024 A79-11600
Effect of broadened-specification fuels on
aircraft engines and fuel systems
[AIAA 79-7008] p0027 A79-29383
Characteristics and combustion of future
hydrocarbon fuels
p0089 N79-13196
Impact of future fuel properties on aircraft
engines and fuel systems
p0089 N79-13197
Effect of broadened-specification fuels on
aircraft engines and fuel systems
[NASA-TN-79086] p0085 N79-16136
- RUMSTADLER, P. W., JR.
Design, development, and test of a laser
velocimeter for a small 8:1 pressure ratio
centrifugal compressor
[NASA-CR-134781] p0111 N79-27478
- RUSHMORE, W. L.
A three-dimensional turbulent compressible flow
model for ejector and fluted mixers
[NASA-CR-159467] p0100 N79-14325
- RUSSELL, L. E.
Flow visualization of discrete-hole film cooling
with spanwise injection over a cylinder
[NASA-TP-1491] p0023 N79-27142
- S
- SAGERNAN, G. D.
Energy and cost savings results for advanced
technology systems from the Cogeneration
Technology Alternatives Study (CTAS)
[AIAA PAPER 79-1000] p0149 A79-44225
Energy and cost saving results for advanced
technology systems from the Cogeneration
Technology Alternatives Study (CTAS)
[NASA-TN-79213] p0141 N79-27665
- SAGERNAN, D. A.
Effect of forward velocity and crosswind on the
reverse-thrust performance of a variable-pitch
fan engine
[AIAA PAPER 79-0105] p0025 A79-23512
- Effect of forward velocity and crosswind on the
reverse-thrust performance of a variable-pitch
fan engine
[NASA-TN-79059] p0015 N79-15049
- SALEH, C. T.
Metal spar/superhybrid shell composite fan blades
[NASA-CR-159594] p0067 N79-30295
- SALIK, J.
Adhesive material transfer in the erosion of an
aluminum alloy
[NASA-TN-79165] p0083 N79-27306
- SALIKUDDIN, S.
An impulse test technique with application to
acoustic measurements
[AIAA PAPER 79-0679] p0178 A79-26890
Studies of the acoustic transmission
characteristics of coaxial nozzles with inverted
velocity profiles: Comprehensive data report
[NASA-CR-159628] p0177 N79-27933
- SALLEH, G. P.
Causes of high pressure compressor deterioration
in service
[AIAA PAPER 79-1234] p0036 A79-40483
- SALTSMAN, J. F.
Strainrate partitioning life predictions of the
long time metal properties council creep-fatigue
tests
[NASA-TN-79260] p0127 N79-31619
- SALVINO, J. T.
Rotor fragment protection program: Statistics on
aircraft gas turbine engine rotor failures that
occurred in US commercial aviation during 1976
[NASA-CR-159474] p0032 N79-18977
- SALZMAN, J. A.
A comparison of measured and calculated upwelling
radiance over water as a function of sensor
altitude
p0162 A79-51096
A comparison of measured and calculated upwelling
radiance over water as a function of sensor
altitude
[NASA-TN-79147] p0131 N79-22589
- SANDERCOCK, D. E.
An off-design correlation of part span damper
losses through transonic axial fan rotors
[ASME PAPER 79-GT-6] p0028 A79-32329
Low-turbulence high-speed wind tunnel for the
determination of cascade shock losses
[ASME PAPER 79-GT-129] p0039 A79-32398
- SANDERS, W. L.
Effects of arcing due to spacecraft charging on
spacecraft survival
[NASA-CR-159593] p0100 N79-25312
- SANDERS, W. A.
High velocity burner rig oxidation and thermal
fatigue behavior of Si₃N₄- and SiC base ceramics
to 1370 deg C
[NASA-TN-79040] p0082 N79-16984
- SANGER, W. L.
Effect of rotor meridional velocity ratio on
response to inlet radial and circumferential
distortion
[NASA-TF-1278] p0023 N79-28177
- SANTHANAN, A. T.
Nb₃Ge as a potential candidate material for 15- to
25-T magnets
p0186 A79-44548
- SANTORO, G. J.
The hot corrosion of Co-25Cr-10Ni-5Ta-3Al-0.5Y
alloy /S-57/
p0076 A79-10420
- SARGISSON, D. F.
Integrated gas turbine engine-nacelle
[NASA-CASE-LEW-12389-3] p0014 N79-14096
- SATER, B. L.
The use of ion beam cleaning to obtain high
quality cold welds with minimal deformation
p0119 A79-24121
- SAULE, A. V.
Analysis of radiation patterns of interaction
tones generated by inlet rods in the JT15D engine
[AIAA PAPER 79-0581] p0027 A79-26944
Analysis of radiation patterns of interaction
tones generated by inlet rods in the JT15D engine
[NASA-TN-79074] p0016 N79-15960
- SAUNDERS, A. A., JR.
Application of digital controls on the quiet clean
short haul experimental engines
[AIAA PAPER 79-1203] p0029 A79-38984

- SCHENTLE, R. J.
VHF downlink communication system for SLAR data
[NASA-TM-79164] p0045 A79-51097
- SCHIFF, R.
VHF downlink communication system for SLAR data
[NASA-TM-79164] p0094 A79-23313
- SCHILLER, J. G.
Feasibility study for a secondary Na/S battery
[NASA-CR-159469] p0152 A79-17330
- SCHILLER, J. G.
Method and device for the detection of phenol and related compounds
[NASA-CASE-LEW-12513-1] p0065 A79-22235
- SCHNIDT, R. J.
First principles numerical model of avalanche-induced arc discharges in electron-irradiated dielectrics
[NASA-CR-159560] p0101 A79-28418
- SCHNORR, G. V.
The decrease in effective photocurrents due to saddle points in electrostatic potentials near differentially charged spacecraft
[NASA-TM-79177] p0049 A79-30140
- SCHNORR, G. V.
The capabilities of the NASA charging analyzer program
[NASA-TM-79177] p0047 A79-24011
- SCHNORR, G. V.
Charging analysis of the SCATHA satellite
[NASA-TM-79177] p0049 A79-24012
- SCHNORR, G. V.
Extension, validation and application of the EASCAP code
[NASA-CR-159595] p0100 A79-27357
- SCHULLER, F. T.
Operating characteristics of a large-bore roller bearing to speeds of 3 times 10 to the 6th power DM
[NASA-TF-1413] p0114 A79-18123
- SCHWAB, J. R.
Performance of a 14.9-kW laminated-frame dc series motor with chopper controller
[NASA-TM-79177] p0058 A79-26316
- SCHWAB, W. B.
Closed loop spray cooling apparatus
[NASA-CASE-LEW-11981-2] p0103 A79-20336
- SCHWALL, R. E.
Properties and performance of fine-filament bronze-process Nb3Sn conductors
[NASA-TM-79177] p0184 A79-20529
- SCHWARTZBERG, F. B.
Definition of mutually optimum NDI and proof test criteria for 2219 aluminum pressure vessels.
Volume 1: Methods
[NASA-CR-135445] p0125 A79-21410
- SCHWARTZBERG, F. B.
Definition of mutually optimum NDI and proof test criteria for 2219 aluminum pressure vessels.
Volume 2: Optimization and fracture studies
[NASA-CR-135446] p0125 A79-21411
- SCHWARTZBERG, F. B.
Definition of mutually optimum NDI and proof test criteria for 2219 aluminum pressure vessels.
Volume 3: Applications to rail defect evaluation
[NASA-CR-135447] p0125 A79-21412
- SCOLA, D. A.
Synthesis of improved moisture resistant polymers
[NASA-CR-159510] p0087 A79-23218
- SCOLA, D. A.
New high temperature cross linking monomers
[NASA-CR-159514] p0087 A79-29331
- SCUDDER, L. R.
Application of semiconductor diffusants to solar cells by screen printing
[NASA-CASE-LEW-12775-1] p0133 A79-11468
- SEIDEL, R. C.
Power train analysis for the DOE/NASA 100-kW wind turbine generator
[NASA-TM-78997] p0135 A79-16355
- SEIKEL, G. M.
Performance optimization of an MHD generator with physical constraints
[NASA-TM-79012] p0182 A79-51995
- SEIKEL, G. M.
Preliminary summary of the ETF conceptual studies
[NASA-TM-78999] p0133 A79-17478
- SEIKEL, G. M.
Evaluation of the ECAS open cycle MHD power plant design
[NASA-TM-79012] p0136 A79-17335
- SEIKEL, G. M.
Performance optimization of an MHD generator with physical constraints
[NASA-TM-79172] p0138 A79-24446
- SEIKEL, G. M.
MHD performance calculations with oxygen enrichment
[NASA-TM-79140] p0135 A79-25499
- SEKELY, B.
A cross impact methodology for the assessment of US telecommunications system with application to fiber optics development, volume 1
[NASA-CR-135208] p0096 A79-18159
- SEKELY, B.
A cross impact methodology for the assessment of US telecommunications system with application to fiber optics development, volume 2
[NASA-CR-159511-VOL-2] p0096 A79-18160
- SELLER, J. M., JR.
Ion beam technology applications study
[NASA-CR-159437] p0180 A79-12884
- SENGER, J. V.
Application of the principle of similarity fluid mechanics
[NASA-TM-79258] p0105 A79-30515
- SENAPATI, T. T.
Status review of PMR polyimides
[NASA-TM-79039] p0065 A79-37399
- SENAPATI, T. T.
Status review of PMR polyimides
[NASA-TM-79039] p0062 A79-12150
- SENAPATI, T. T.
Polyimide prepreg material having improved tack retention
[NASA-CASE-LEW-12933-1] p0059 A79-24061
- SENAPATI, T. T.
High char inide-modified epoxy matrix resins
[NASA-TM-79226] p0063 A79-29240
- SENAPATI, T. T.
Recent developments in PMR polyimides at NASA Lewis
[NASA-TM-79226] p0064 A79-30323
- SENAPATI, T. T.
Curing agent for polyepoxides and epoxy resins and composites cured therewith
[NASA-CASE-LEW-13226-1] p0059 A79-31345
- SENOVY, G. K.
Axial-flow compressor turning angle and loss by inviscid-viscous interaction blade-to-blade computation
[ASME PAPER 79-GT-5] p0006 A79-30504
- SHANNON, J. L., JR.
Influence of composition, annealing treatment, and texture on the fracture toughness of Ti-5Al-2.5Sn plate at cryogenic temperatures
[NASA-TM-79171] p0077 A79-24262
- SHAW, H. J.
An experimental investigation of forced mixing of a turbulent boundary layer in an annular diffuser
[NASA-TM-79171] p0064 A79-23920
- SHEIDLEY, D. W.
Method of cross-linking polyvinyl alcohol and other water soluble resins
[NASA-CASE-LEW-13103-1] p0068 A79-14172
- SHEIDLEY, D. W.
Formulated plastic separators for soluble electrode cells
[NASA-CASE-LEW-12358-1] p0135 A79-17313
- SHEIDLEY, D. W.
Control of volume resistivity in inorganic organic separators
[NASA-TM-1439] p0069 A79-22246
- SHEIDLEY, D. W.
Improved, low cost inorganic-organic separators for rechargeable silver-zinc batteries
[NASA-TF-1476] p0069 A79-25181
- SHEIDLEY, D. W.
In situ self cross-linking of polyvinyl alcohol battery separators
[NASA-CASE-LEW-12972-1] p0138 A79-25481
- SHEINKER, A. A.
A strainrange partitioning analysis of low cycle fatigue of coated and uncoated Rene 80
[NASA-CR-159444] p0129 A79-10479
- SHEINKER, A. A.
Exploratory thermal-mechanical fatigue results for Rene 80 in ultrahigh vacuum
[NASA-CR-159444] p0079 A79-11180
- SHEVCHENKO, O. A.
Measurements of mixed convective heat transfer to low temperature helium in a horizontal channel
[NASA-TM-79158] p0104 A79-23384
- SHEVCHENKO, O. A.
Some heat transfer and hydrodynamic problems associated with superconducting cables (SEPL)
[NASA-TM-79023] p0102 A79-15267
- SHENBROT, L. T.
Development of sprayed ceramic seal systems for turbine gas path sealing
[NASA-TM-79022] p0081 A79-12223
- SHENBROT, L. T.
Development of a plasma sprayed ceramic gas path seal for high pressure turbine applications
[NASA-CR-159669] p0122 A79-31602
- SHORT, F. R.
Study of an advanced General Aviation Turbine Engine (GATE)
[NASA-CR-159558] p0033 A79-21073
- SIDIK, S. M.
Two-dimensional random surface model for asperity-contact in elastohydrodynamic lubrication
[NASA-TM-79140] p0120 A79-39811

- Maximum likelihood estimation for life distributions with competing failure modes
[NASA-TM-79126] p0169 A79-23735
- SIEGEL, R.
Analysis of solidification interface shape during continuous casting of a slab
p0079 A79-52697
- Introduction: Thermal Radiation in Industrial Flames
p0104 A79-22415
- SIEVERS, G. K.
NASA research on general aviation power plants
[AIAA PAPER 79-0561] p0026 A79-25870
Preliminary QCGAT program test results
[SAE PAPER 790596] p0028 A79-36729
NASA research on general aviation power plants
[NASA-TM-79031] p0014 A79-12086
Preliminary QCGAT program test results
[NASA-TM-79013] p0016 A79-15051
- SIEWERT, E. D.
Fine particulate capture device
[NASA-CASE-LEW-11583-1] p0109 A79-17192
- SIGNORELLI, E. A.
Tungsten fiber reinforced FeCrAlY - A first generation composite turbine blade material
p0065 A79-30397
Tungsten fiber reinforced FeCrAlY: A first generation composite turbine blade material
[NASA-TM-79094] p0063 A79-20187
Evaluation of silicon carbide fiber/titanium composites
[NASA-TM-79232] p0064 A79-31349
- SIB, G. C.
Off-axis impact of unidirectional composites with cracks: Dynamic stress intensification
[NASA-CR-159537] p0067 A79-30294
Normal and radial impact of composites with embedded penny-shaped cracks
[NASA-CR-159538] p0130 A79-31627
- SIKORA, P. P.
Consolidation of Si₃N₄ by hot isostatic pressing
p0086 A79-32931
- SIMON, P. P.
A mobile apparatus for solar collector testing
[ASME PAPER 79-DE-5] p0150 A79-47651
A method for correlating performance data of a terrestrial solar cell array
[NASA-TM-79163] p0140 A79-26503
- SIMONIAU, V. J.
Some flow phenomena in a constant area duct with a Borda type inlet including the critical region
[ASME PAPER 78-WA/HT-37] p0093 A79-19816
Condensation on a noncollapsing vapor bubble in a subcooled liquid
p0100 A79-49535
Condensation on a noncollapsing vapor bubble in a subcooled liquid
[NASA-TM-79212] p0105 A79-27461
Two-phase choked flow of cryogenic fluids in converging-diverging nozzles
[NASA-TF-1484] p0105 A79-29468
- SIMONS, S. W.
Fuel cell on-site integrated energy system
parametric analysis of a residential complex
p0146 A79-14947
Analysis of a fuel cell on-site integrated energy system for a residential complex
[AIAA PAPER 79-0990] p0147 A79-38192
Commercial phosphoric acid fuel cell system technology development
p0150 A79-51809
Fuel cell on-site integrated energy system
parametric analysis of a residential complex
[NASA-TM-78490] p0188 A79-11955
Comparison of fuel-cell and diesel integrated energy systems and a conventional system for a 500-unit apartment
[NASA-TM-79037] p0134 A79-15403
Analysis of a fuel cell on-site integrated energy system for a residential complex
[NASA-TM-79161] p0137 A79-22624
Commercial phosphoric acid fuel cell system technology development
- [NASA-TM-79169] p0139 A79-25500
- SIMS, D. L.
Evaluation of the cyclic behavior of aircraft turbine disk alloys
[NASA-CR-159409] p0030 A79-10058
- SINCLAIR, J. H.
The effects of eccentricities on the fracture of off-axis fiber composites
p0064 A79-15543
Analysis/design of strip reinforced random composites /strip hybrids/
p0119 A79-24035
Effects of moisture profiles and laminate configuration on the hygro stress in advanced composites
p0064 A79-24132
Analysis of high velocity impact on hybrid composite fan blades
[AIAA 79-0783] p0128 A79-29027
Mechanics of intraply hybrid composites - Properties, analysis and design
p0055 A79-31033
Fracture modes in off-axis fiber composites
p0065 A79-31035
Fabrication and testing of non-graphitic superhybrid composites
p0066 A79-43289
Fracture modes in off-axis fiber composites
[NASA-TM-79036] p0062 A79-12154
Prediction of properties of intraply hybrid composites
[NASA-TM-79087] p0061 A79-16919
Fabrication and testing of nongraphitic superhybrid composites
[NASA-TM-79102] p0063 A79-20188
Analysis of high velocity impact on hybrid composite fan blades
[NASA-TM-79133] p0127 A79-20398
- SINK, L. W.
Low-cost directionally-solidified turbine blades, volume 1
[NASA-CR-159464] p0080 A79-24121
- SIVC, J. H.
Satellite communications for disaster relief operations
[NASA-TM-79198] p0094 A79-27351
- SIZEMONT, E. L.
Design, fabrication, and initial test of a fixture for reducing the natural frequency of the Rod-C wind turbine tower
[NASA-TM-79200] p0142 A79-28727
- SKRATT, J. P.
Laser power conversion system analysis, volume 1
[NASA-CR-159523-VOL-1] p0112 A79-21334
Laser power conversion system analysis, volume 2
[NASA-CR-159523-VOL-2] p0112 A79-21335
Laser rocket system analysis
[NASA-CR-159521] p0112 A79-21337
- SLIEPPE, R. L.
The catalysis of nucleotide polymerization by compounds of divalent lead
p0060 A79-32924
- SLIMBY, H. R.
Graphite-fiber-reinforced polyimide liners of various compositions in plain spherical bearings
p0117 A79-16678
Some loads limits and self-lubricating properties of plain spherical bearings with molded graphite fiber-reinforced polyimide liners to 320 C
[ASLE PREPRINT 78-LC-5C-2] p0118 A79-23251
Wide-temperature-spectrum self-lubricating coatings prepared by plasma spraying
p0119 A79-34993
Method of making bearing materials
[NASA-CASE-LEW-11930-4] p0062 A79-17916
Wide-temperature-spectrum self-lubricating coatings prepared by plasma spraying
[NASA-TM-79113] p0082 A79-20240
Plasma-sprayed coatings for lubrication of a titanium alloy in air at 430 deg C
[NASA-TF-1509] p0083 A79-29327
- SLOVSKI, J. A.
High speed smoke flow visualization for the determination of cascade shock losses
[AIAA PAPER 79-0042] p0005 A79-19495
Low-turbulence high-speed wind tunnel for the determination of cascade shock losses
[ASME PAPER 79-GT-129] p0039 A79-32398

- SHAKULA, P. K.**
Causes of high pressure compressor deterioration in service
[AIAA PAPER 79-1234] p0036 A79-40483
- SHALLEY, A.**
Design and application of a test rig for super-critical power transmission shafts
[NASA-CR-3155] p0122 N79-31603
- SHALLEY, A. J.**
Design and test of a squeeze-film damper for a flexible power transmission shaft
p0123 A79-16011
Elastomer mounted rotors - An alternative for smoother running turbomachinery
[ASME PAPER 79-GT-149] p0119 A79-32414
An introduction to a unified approach to flexible rotor balancing
[ASME PAPER 79-GT-161] p0124 A79-32423
Development of procedures for calculating stiffness and damping of elastomers in engineering applications. Part 5: Elastomer performance limits and the design and test of an elastomer damper
[NASA-CR-159552] p0122 N79-24373
- SHETANA, J.**
Life characteristics assessment of the communications technology satellite transmitter experiment package
[NASA-TM-79181] p0044 N79-31264
- SHIALEK, J.**
Some TEM observations of Al₂O₃ scales formed on NiCrAl alloys
[NASA-TM-79259] p0076 N79-33306
- SMITH, A. L.**
Analysis of the impact of the use of broad specification fuels on combustors for commercial aircraft gas turbine engines
[AIAA PAPER 79-1195] p0090 A79-38980
- SMITH, D. A.**
Acceleration of linear and logarithmic convergence
p0168 A79-40494
- SMITH, G. T.**
CODSTRAN - Composite durability structural analysis
p0128 A79-37292
CODSTRAN: Composite durability structural analysis
[NASA-TM-79070] p0126 N79-15326
- SMITH, J. J.**
NASA CF6 jet engine diagnostics program: Long-term CF6-6D low-pressure turbine deterioration
[NASA-CR-159618] p0039 N79-29191
- SMITH, J. M.**
Preliminary results in the NASA Lewis H₂-C₂ combustion MHD experiment
p0182 A79-39807
Performance optimization of an MHD generator with physical constraints
p0182 A79-51995
Performance of a vortex-controlled diffuser in an annular swirl-can combustor at inlet Mach numbers up to 0.53
[NASA-TP-1452] p0017 N79-22099
Preliminary results in the NASA Lewis H₂-C₂ combustion MHD experiment
[NASA-TM-79135] p0181 N79-22897
Performance optimization of an MHD generator with physical constraints
[NASA-TM-79172] p0138 N79-24446
- SMITH, K. O.**
Turbulence effects on flame speed and flame structure
[AIAA PAPER 79-0016] p0070 A79-19480
Performance characteristics of a slagging gasifier for MHD combustor systems
[NASA-TM-79195] p0142 N79-30720
- SMITH, R.**
Advanced General Aviation Turbine Engine (GATE) study
[NASA-CR-159624] p0035 N79-29189
- SMITH, S. R.**
X-ray photoelectron spectroscopy study of nickel and nickel-base alloy surface alterations in simulated hot corrosion conditions with emphasis on eventual application to turbine blade corrosion
[NASA-CR-159553] p0072 N79-25178
- SMITHRICK, J. J.**
Rapid, efficient charging of lead-acid and nickel-zinc traction cells
p0144 A79-10084
- Effect of positive pulse charge waveforms on cycle life of nickel-zinc cells
[NASA-TM-79215] p0142 N79-28728
- SNOW, D. W.**
Study of blade aspect ratio on a compressor front stage aerodynamic and mechanical design report
[NASA-CR-159555] p0034 N79-23085
- SNOW, W.**
Mass drivers. 3: Engineering
p0040 N79-32232
- SNYDER, C. E., JR.**
Boundary lubrication, thermal and oxidative stability of a fluorinated polyether and a perfluoropolyether triazine
[NASA-TM-79064] p0081 N79-15185
- SOCKOL, P. M.**
Axial-flow compressor turning angle and loss by inviscid-viscous interaction blade-to-blade computation
[ASME PAPER 79-GT-5] p0006 A79-30504
- SOEDER, R. H.**
Combined pressure and temperature distortion effects on internal flow of a turbofan engine
[AIAA PAPER 79-1309] p0029 A79-39031
Combined pressure and temperature distortion effects on internal flow of a turbofan engine
[NASA-TM-79136] p0012 N79-23963
Effect of steady-state pressure distortion on flow characteristics entering a turbofan engine
[NASA-TM-79134] p0019 N79-23969
Effect of steady-state temperature distortion and combined distortion on inlet flow to a turbofan engine
[NASA-TM-79237] p0023 N79-30187
- SOPRIN, T. G.**
Modal propagation angles in a cylindrical duct with flow and their relation to sound radiation
[AIAA PAPER 79-0183] p0174 A79-19582
Modal propagation angles in a cylindrical duct with flow and their relation to sound radiation
[NASA-TM-79030] p0172 N79-15756
- SOKOLOWSKI, D. E.**
Heat exchanger
[NASA-CASE-LEW-12252-1] p0102 N79-13288
- SOLTIS, D. G.**
Lewis Research Center program
p0137 N79-21576
- SOLTIS, R. F.**
A cycle timer for testing electric vehicles
p0188 A79-37293
- SOMMOANO, R. B.**
Optical, spin-resonance, and magnetoresistance studies of /tetrathiatetracene/2/iodide/3 - The nature of the ground state
p0184 A79-10417
- SOOHOO, J.**
High power phase locked laser oscillators
[NASA-CR-159630] p0112 N79-32538
- SOOHOO, J. P.**
Ground-to-space optical power transfer
p0161 A79-17180
- SOVEY, J. S.**
Ion beam sputtering of fluoropolymers
p0117 A79-14797
Adhesive bonding of ion beam textured metals and fluoropolymers
p0060 A79-14798
Hydrogen hollow cathode ion source
[NASA-CASE-LEW-12940-1] p0181 N79-10894
Modification of the electrical and optical properties of polymers
[NASA-CASE-LEW-13027-1] p0081 N79-11216
Adhesive bonding of ion beam textured metals and fluoropolymers
[NASA-TM-79004] p0181 N79-12909
Ion beam sputter deposition of fluoropolymers
[NASA-CASE-LEW-13122-1] p0083 N79-24154
- SPADACCINI, L. J.**
Autoignition of fuels
p0020 N79-25001
- SPALVINS, I.**
Sputtering technology in solid film lubrication
p0117 A79-16663
Coatings for wear and lubrication
p0060 A79-27232
Industrial potential, uses, and performance of sputtered and ion plated films
p0119 A79-30398

- Characterization of defect growth structures in ion plated films by scanning electron microscopy
[NASA-TM-79110] p0078 A79-34992
- Characterization of defect growth structure in ion plated films by scanning electron microscopy
[NASA-TM-79110] p0074 A79-20218
- Industrial potential, uses, and performance of sputtered and ion plated films
[NASA-TM-79107] p0157 A79-20527
- Survey of ion plating sources
[NASA-TM-79269] p0076 A79-31372
- SPILNER, R. L.**
User's guide to computer programs JET 5A and CIVM-JET 5B to calculate the large elastic-plastic dynamically-induced deformations of multilayer partial and/or complete structural rings
[NASA-CR-159484] p0129 A79-18343
- SPISE, E. W.**
Application of multispectral scanner data to the study of an abandoned surface coal mine
[NASA-TM-78912] p0131 A79-13472
- SPONG, E. D.**
Reynolds number, scale and frequency content effects on F-15 inlet instantaneous distortion
[AIAA PAPER 79-0104] p0005 A79-19533
- STABRYLLA, R. G.**
Fabrication of J79 boron/aluminum compressor blades
[NASA-CR-159566] p0034 A79-23970
- STAGLIANO, T. R.**
User's guide to computer programs JET 5A and CIVM-JET 5B to calculate the large elastic-plastic dynamically-induced deformations of multilayer partial and/or complete structural rings
[NASA-CR-159484] p0129 A79-18343
- STAHL, C. V., JR.**
Fatigue impact on Mod-1 wind turbine design
p0156 A79-20827
- STAID, P. S.**
Acoustic and aerodynamic performance investigation of inverted velocity profile coannular plug nozzles, comprehensive data report, volume 1
[NASA-CR-159575-VOL-1] p0177 A79-26884
- Acoustic and aerodynamic performance investigation of inverted velocity profile coannular plug nozzles, comprehensive data report, volume 2
[NASA-CR-159575-VOL-2] p0177 A79-26885
- Acoustic and aerodynamic performance investigation of inverted velocity profile coannular plug nozzles, comprehensive data report, volume 3
[NASA-CR-159575-VOL-3] p0177 A79-26886
- STAIGER, P. J.**
Evaluation of the ECAS open cycle MHD power plant design
[NASA-TM-79012] p0136 A79-17335
- MHD performance calculations with oxygen enrichment
[NASA-TM-79140] p0139 A79-25499
- STAIS, W. K.**
Energy conservation through sealing technology
p0118 A79-20700
- STAKOLICH, E. G.**
Effect of flight loads on turbofan engine performance deterioration
p0027 A79-30559
- Aerodynamic and acoustic effects of eliminating core swirl from a full scale 1.6 stage pressure ratio fan (QF-5A)
[NASA-TM-78991] p0002 A79-11001
- Effect of flight loads on turbofan engine performance deterioration
[NASA-TM-79041] p0013 A79-12085
- STANITE, J. D.**
Liquid oxygen/liquid hydrogen boost/vane pump for the advanced orbit transfer vehicles auxiliary propulsion system
[NASA-CR-159648] p0057 A79-31341
- STANKIEWICZ, W.**
TWT design requirements for 30/20 GHz digital communications' satellite
[NASA-TM-79115] p0097 A79-20316
- Analytical prediction with multidimensional computer programs and experimental verification of the performance, at a variety of operating conditions, of two traveling wave tubes with depressed collectors
[NASA-TP-1449] p0097 A79-22375
- Design of high-perveance confined-flow guns for periodic-permanent-magnet-focused tubes
[NASA-TP-1485] p0098 A79-27400
- STASKUS, J. V.**
Insulator edge voltage gradient effects in spacecraft charging phenomena
p0048 A79-30139
- Insulator edge voltage gradient effects in spacecraft charging phenomena
[NASA-TM-78588] p0046 A79-11109
- Test results for electron beam charging of flexible insulators and composites
p0048 A79-24031
- Area scaling investigations of charging phenomena
p0048 A79-24032
- Charging rates of metal-dielectric structures
p0048 A79-24033
- STATON, D. V.**
Study of an advanced General Aviation Turbine Engine (GATE)
[NASA-CR-159558] p0033 A79-21073
- STEARNS, C. A.**
Mass spectrometric investigation of the vaporization of sodium and potassium chromates - Preliminary results
p0071 A79-49533
- The role of NaCl in flame chemistry, in the deposition process, and in its reactions with protective oxides as related to hot corrosion
p0071 A79-49534
- Mass spectrometric investigation of the vaporization of sodium and potassium chromates: Preliminary results
[NASA-TM-79210] p0069 A79-27279
- The role of NaCl in flame chemistry, in the deposition process, and in its reactions with protective oxides as related to hot corrosion
[NASA-TM-79225] p0069 A79-28258
- The chemistry of sodium chloride involvement in processes related to hot corrosion
[NASA-TM-79251] p0069 A79-31361
- STECURA, S.**
Effects of compositional changes on the performance of a thermal barrier coating system
p0077 A79-21299
- Thermal barrier coatings: Burner rig hot corrosion test results
[NASA-TM-79005] p0073 A79-11179
- Effects of yttrium, aluminum, and chromium concentrations in bond coatings on the performance of zirconia-yttria thermal barriers
[NASA-TM-79206] p0075 A79-29293
- STEEN, P. G.**
The decrease in effective photocurrents due to saddle points in electrostatic potentials near differentially charged spacecraft
p0049 A79-30140
- The capabilities of the NASA charging analyzer program
p0047 A79-24011
- Charging analysis of the SCATBA satellite
p0049 A79-24012
- Extension, validation and application of the NASCAP code
[NASA-CR-159595] p0100 A79-27397
- STEINBERG, R.**
Automated meteorological data from commercial aircraft via satellite - Present experience and future implications
p0010 A79-17092
- Commercial aircraft derived high resolution wind and temperature data from the tropics for FGGE: Implications for NASA
p0161 A79-20621
- STEINKU, E. J.**
Aerodynamic performance of a 1.35-pressure-ratio axial-flow fan stage
[NASA-TP-1299] p0002 A79-10022
- STELIS, P. D.**
Low heat leak connector for cryogenic system
[NASA-CASE-XLE-02367-1] p0093 A79-21225
- STEPHENS, J. R.**
Effects of thermomechanical processing on strength and toughness of Fe-12Ni reactive metal alloys at 77K
p0078 A79-32600
- High toughness-high strength iron alloy
[NASA-CASE-LEW-12542-3] p0073 A79-19145
- Process for making a high toughness-high strength iron alloy
[NASA-CASE-LEW-12542-2] p0074 A79-22271

- STEPKA, P. S.**
Liquid-cooling technology for gas turbines -
Review and status p0116 A79-10038
NASA thermal barrier coatings - Summary and update p0065 A79-21295
The NASA high pressure facility and turbine test rig p0038 A79-21296
NASA thermal barrier coatings: Summary and update [NASA-TN-79053] p0015 W79-15048
The NASA high pressure facility and turbine test rig [NASA-TN-79054] p0015 W79-15050
Review and status of liquid-cooling technology for gas turbines [NASA-EP-1038] p0104 W79-22427
Industry tests of NASA ceramic thermal barrier coating [NASA-TP-1425] p0022 W79-25023
- STERN, A. B.**
Variable cycle engine technology program planning and definition study [NASA-CR-159539] p0034 W79-23084
- STETSON, A. E.**
Internally coated air-cooled gas turbine blading [NASA-CR-159574] p0034 W79-25018
- STEVENS, W.**
Performance of two-stage fan with larger dampers on first-stage rotor [NASA-TP-1399] p0018 W79-23967
- STEVENS, B. S.**
Aerodynamic and acoustic investigation of inverted velocity profile coannular exhaust nozzle models and development of aerodynamic and acoustic prediction procedures, comprehensive data report, volume 1 [NASA-CR-159515] p0034 W79-30185
Aerodynamic and acoustic investigation of inverted velocity profile coannular exhaust nozzle models and development of aerodynamic and acoustic prediction procedures, comprehensive data report, volume 2 [NASA-CR-159516] p0034 W79-30186
Aerodynamic and acoustic investigation of inverted velocity profile coannular exhaust nozzle models and development of aerodynamic and acoustic prediction procedures [NASA-CR-3166] p0035 W79-31212
- STEVENS, C. E.**
Reynolds number, scale and frequency content effects on F-15 inlet instantaneous distortion [AIAA PAPER 79-0104] p0005 A79-19533
- STEVENS, G.**
20/30 GHz satellite systems technology needs assessment p0095 A79-14548
Millimeter wave communication satellite concepts p0095 A79-29784
- STEVENS, G. E.**
Determining potential 30/20 GHz domestic satellite system concepts and establishment of a suitable experimental configuration p0095 A79-27397
Determining potential 30/20 GHz domestic satellite system concepts and establishment of a suitable experimental configuration [NASA-TN-79092] p0094 W79-17072
- STEVENS, J. E.**
Space environmental interactions with spacecraft surfaces [NASA-TN-79016] p0046 W79-15150
- STEVENS, H. J.**
Space environmental interactions with spacecraft surfaces [AIAA PAPER 79-0386] p0049 A79-23511
Insulator edge voltage gradient effects in spacecraft charging phenomena p0048 A79-30139
Large space system - Charged particle environment interaction technology [AIAA 79-0913] p0055 A79-34775
NASCAP modelling of high-voltage power system interactions with space charged-particle environments p0051 A79-39806
Insulator edge voltage gradient effects in spacecraft charging phenomena [NASA-TN-78988] p0046 W79-11109
Large space system: Charged particle environment interaction technology
- [NASA-TN-79156] p0046 W79-22188
NASCAP modelling of high-voltage power system interactions with space charged-particle environments [NASA-TN-79146] p0046 W79-24000
Interactions between spacecraft and the charged-particle environment p0047 W79-24021
Plasma Interaction Experiment (PII) flight results p0047 W79-24022
Computer and laboratory simulation of interactions between spacecraft surfaces and charged-particle environments [NASA-TN-79219] p0063 W79-29224
NASCAP modelling of environmental-charging-induced discharges in satellites [NASA-TN-79247] p0048 W79-31265
- STEVENS, W. G.**
Internally coated air-cooled gas turbine blading [NASA-CR-159574] p0034 W79-25018
- STEVENSON, S. E.**
Telecommunication service markets through the year 2000 in relation to millimeter wave satellite systems p0095 A79-27398
Telecommunication service markets through the year 2000 in relation to millimeter wave satellite systems [NASA-TN-79099] p0098 W79-16169
- STEWART, O. L.**
Development of sprayed ceramic seal systems for turbine gas path sealing [NASA-TN-79022] p0081 W79-12223
- STEWART, W. L.**
NASA research on general aviation power plants [AIAA PAPER 79-0561] p0026 A79-25870
NASA research on general aviation power plants [NASA-TN-79031] p0014 W79-12086
- STOCHL, R. J.**
Power-conversion system component summation p0140 W79-26483
Candidate power-conversion system cycles, appendix 2 p0140 W79-26484
- STOCKENHEE, P. J.**
Experimental study of low temperature behavior of aviation turbine fuels in a wing tank model [NASA-CR-159615] p0091 W79-29355
- STOCKER, H. L.**
Determining and improving labyrinth seal performance in current and advanced high performance gas turbines p0031 W79-11068
- STOCKMAN, W. O.**
An efficient user-oriented method for calculating compressible flow about three-dimensional inlets [AIAA PAPER 79-0081] p0005 A79-19524
An approach to optimum subsonic inlet design [ASME PAPER 79-GT-51] p0006 A79-30527
Recent applications of theoretical analysis to V/STOL inlet design p0006 A79-49530
An approach to optimum subsonic inlet design [NASA-TN-79051] p0002 W79-12020
Theoretical study of VTOL tilt-nacelle axisymmetric inlet geometries [NASA-TF-1380] p0003 W79-14996
Computer programs for calculating two-dimensional potential flow through deflected nozzles [NASA-TN-79144] p0004 W79-26019
Recent applications of theoretical analysis to V/STOL inlet design [NASA-TN-79211] p0004 W79-29143
- STONE, J. E.**
Experimental study of coaxial nozzle exhaust noise [AIAA PAPER 79-0631] p0175 A79-28963
Effects of geometric and flow-field variables on inverted-velocity-profile coaxial jet noise and source distributions [AIAA PAPER 79-0635] p0175 A79-32126
An improved method for predicting the effects of flight on jet mixing noise p0176 A79-39803
Experimental study of coaxial nozzle exhaust noise [NASA-TN-79090] p0173 W79-20829
Effects of geometric and flow-field variables on inverted-velocity-profile coaxial jet noise [NASA-TN-79095] p0173 W79-20830
An improved method for predicting the effects of flight on jet mixing noise

- [NASA-TM-79155] p0173 N79-24770
- STORTI, G.**
Thin cells for space p0154 N79-32652
- STOTLER, C. L.**
Containment of composite fan blades [NASA-CR-158168] p0032 N79-18978
Containment of composite fan blades [NASA-CR-159544] p0067 N79-31348
- STOTLER, C. L., JR.**
Integrated gas turbine engine-nacelle [NASA-CASE-LEW-12389-3] p0019 N79-14096
- STOVALL, T. E.**
User's manual for FRESTIC: A computer code for the performance of regenerative steam turbine cycles [NASA-CR-159540] p0122 N79-25395
- STRACK, W. C.**
The GATE studies - Assessing the potential of future small general aviation turbine engines p0027 A79-30560
New opportunities for future small civil turbine engines - Overviewing the GATE studies [SAE PAPER 790619] p0028 A79-36747
The gate studies: Assessing the potential of future small general aviation turbine engines [NASA-TM-79075] p0016 N79-15958
New opportunities for future small civil turbine engines: Overviewing the GATE studies [NASA-TM-79073] p0017 N79-16849
- STRAHAN, V. E.**
Fiber optic sensors for military, industrial and commercial applications p0111 A79-38738
Analysis and preliminary design of optical sensors for propulsion control [NASA-CR-159519] p0180 N79-27975
- STRAIGHT, D. M.**
Effect of shocks on film cooling of a full scale turbojet exhaust nozzle having an external expansion surface [AIAA PAPER 79-1170] p0028 A79-38969
Effect of shocks on film cooling of a full scale turbojet exhaust nozzle having an external expansion surface [NASA-TM-79157] p0018 N79-23966
Effect of shock on film cooling of a full scale turbojet exhaust nozzle having an external expansion surface [NASA-TM-79157] p0018 N79-23966
- STRICKLAND, D. J.**
First principles numerical model of avalanche-induced arc discharges in electron-irradiated dielectrics [NASA-CR-159560] p0101 N79-28418
- STUBBS, E. M.**
Ground-to-space optical power transfer p0161 A79-17180
- STUCKAS, K. J.**
Concepts for reducing exhaust emissions and fuel consumption of the aircraft piston engine [SAE PAPER 790605] p0036 A79-36737
- STURGESS, G. J.**
Advanced low emissions catalytic combustor program at Pratt and Whitney p0021 N79-25012
- TURNER, J. C.**
Optically isolated logarithmic nanometer capable of floating to 5 kilovolts [NASA-TF-1527] p0098 N79-32467
- SUGAWARA, K.**
Improved apparatus for trapped radical and other studies down to 1.5 K p0110 A79-20742
- SUGIHARA, K.**
Anomalous galvanomagnetic properties of graphite in strong magnetic fields p0185 A79-23633
- SULLIVAN, P. G.**
Elevated temperature properties of boron/aluminum composites [NASA-CR-159445] p0066 N79-16924
- SULLIVAN, T. J.**
Design study and performance analysis of a high-speed multistage variable-geometry fan for a variable cycle engine [NASA-CR-159545] p0034 N79-25020
- SULLIVAN, T. L.**
Wind-turbine-generator rotor-blade concepts with low-cost potential p0147 A79-20828
- Evaluation of MOSTAS computer code for predicting dynamic loads in two-bladed wind turbines [AIAA 79-0733] p0005 A79-29007
- Evaluation of MOSTAS computer code for predicting dynamic loads in two-bladed wind turbines [NASA-TM-79101] p0137 N79-21549
- Design, fabrication, and initial test of a fixture for reducing the natural frequency of the Mod-O wind turbine tower [NASA-TM-79200] p0142 N79-28727
- SUMNERFIELD, M.**
Definition of smolder experiments for Spacelab [NASA-CR-159528] p0040 N79-20161
- SUNDERBERG, G. E.**
The solid state remote power controller - Its status, use and perspective p0099 A79-10896
- SUTHERLAND, W. M.**
Atlas 5013 tank corrosion test [NASA-CR-158760] p0050 N79-27234
- SWARTZ, C. K.**
Preliminary evaluation of glass resin materials for solar cell cover use p0055 A79-40984
Radiation damage in high-voltage silicon solar cells p0144 N79-32658
Reverse annealing in radiation-damaged, silicon solar cells p0144 N79-32660
Temperature and intensity dependence of the performance of an electron-irradiated (AlGa)As/GaAs solar cell p0144 N79-32665
Annealing of radiation damage in 0.1- and 2-ohm-centimeter Silicon solar cells [NASA-TF-1559] p0144 N79-33572
- SYMONS, E. P.**
Contoured tank outlets for draining of cylindrical tanks in low-gravity environment [NASA-TF-1492] p0105 N79-29467
- SZANISZLO, A. J.**
The Advanced Low-Emissions Catalytic-Combustor Program: Phase I - Description and Status [ASME PAPER 79-GT-192] p0027 A79-30557
The advanced low-emissions catalytic-combustor program. Phase 1: Description and Status [NASA-TM-79049] p0015 N79-15047
- SZETELA, E. J.**
Analysis of the impact of the use of broad specification fuels on combustors for commercial aircraft gas turbine engines [AIAA PAPER 79-1195] p0090 A79-38980
Analytical evaluation of the impact of broad specification fuels on high bypass turbofan engine combustors [NASA-CR-159454] p0031 N79-13050

T

- TABAKOFF, W.**
A calculation procedure for viscous flow in turbomachines, volume 1 [NASA-CR-159635] p0107 N79-30514
Flow in nonrotating passages of radial inflow turbines [NASA-CR-159679] p0035 N79-32212
- TACINA, E. E.**
Performance of a multiple venturi fuel-air preparation system p0020 N79-25000
- TANNA, E. K.**
Effects of simulated forward flight on jet noise, shock noise and internal noise [AIAA PAPER 79-0615] p0178 A79-26936
The free jet as a simulator of forward velocity effects on jet noise [NASA-CR-1056] p0176 N79-14873
- TARI, U.**
Rotor redesign for a highly loaded 1800 ft/sec tip speed fan. 1: Aerodynamic and mechanical design report [NASA-CR-159596] p0034 N79-26055
- TAUSSIG, E.**
Solar-pumped lasers for space power transmission [AIAA PAPER 79-1015] p0112 A79-38202
Design investigation of solar powered lasers for space applications [NASA-CR-159554] p0111 N79-26384

- TAYLOR, C. H.**
Effect of geometry on hydrodynamic film thickness
[ASME PAPER 78-10B-24] p0118 A79-23237
- TAYLOR, J. B.**
Experimental clean combustor program: Phase 3:
Turbulence measurement addendum
[NASA-CR-135422] p0031 A79-12088
Turbulence measurements in the compressor exit
flow of a General Electric CP6-50 engine
p0019 A79-24996
- TAYLOR, W. P.**
High performance, high density hydrocarbon fuels
[NASA-CR-159480] p0091 A79-20267
- TECZA, J. A.**
Elastomer mounted rotors - An alternative for
smoother running turbomachinery
[ASME PAPER 79-GT-149] p0119 A79-32414
Development of procedures for calculating
stiffness and damping of elastomers in
engineering applications. Part 5: Elastomer
performance limits and the design and test of an
elastomer damper
[NASA-CR-159552] p0122 A79-24373
- TELK, C. L.**
High power phase locked laser oscillators
[NASA-CR-159630] p0112 A79-32538
- TERDAN, F. P.**
Primary electric propulsion for future space
missions
[AIAA 79-0881] p0055 A79-34773
Primary electric propulsion for future space
missions
[NASA-TM-79141] p0052 A79-22190
- TERREN, F.**
An economical approach to space power systems
p0052 A79-10139
- TESTER, B. J.**
Effects of simulated forward flight on jet noise,
shock noise and internal noise
[AIAA PAPER 79-0615] p0178 A79-26936
The free jet as a simulator of forward velocity
effects on jet noise
[NASA-CR-3056] p0176 A79-14873
- TEVAARWERK, J. L.**
Traction drive performance prediction for the
Johnson and Tevaarwerk traction model
[NASA-TP-1530] p0116 A79-33475
- TEW, R. C., JR.**
Initial comparison of single cylinder Stirling
engine computer model predictions with test
results
[SAE PAPER 790327] p0119 A79-31368
Baseline performance of the GPU 3 Stirling engine
[NASA-TM-79038] p0135 A79-16356
Initial comparison of single cylinder Stirling
engine computer model predictions with test
results
[NASA-TM-79044] p0188 A79-16721
- THALLER, L. B.**
Redox flow cell energy storage systems
[AIAA PAPER 79-0989] p0147 A79-38191
Recent advances in Redox flow cell storage systems
p0150 A79-51837
Redox flow cell energy storage systems
[NASA-TM-79143] p0138 A79-24442
Electrochemical cell for rebalancing REDOX flow
system
[NASA-CASE-LEW-13150-1] p0139 A79-26474
Recent advances in redox flow cell storage systems
[NASA-TM-79186] p0141 A79-26505
- THIENE, L. G.**
Initial comparison of single cylinder Stirling
engine computer model predictions with test
results
[SAE PAPER 790327] p0119 A79-31368
Baseline performance of the GPU 3 Stirling engine
[NASA-TM-79038] p0135 A79-16356
Initial comparison of single cylinder Stirling
engine computer model predictions with test
results
[NASA-TM-79044] p0188 A79-16721
Low-power baseline test results for the GPU 3
Stirling engine
[NASA-TM-79103] p0188 A79-27023
- THOMAS, R. E.**
Millimeter wave satellite concepts. Volume 1:
Executive summary
[NASA-CR-159504] p0041 A79-26101
- THOMAS, R. L.**
Large wind turbine generators
p0146 A79-15881
Large horizontal axis wind turbine development
p0149 A79-46527
Large horizontal axis wind turbine development
[NASA-TM-79174] p0140 A79-26504
- THOMAS, R. E.**
Millimeter wave satellite concepts. Volume 2:
Technical report
[NASA-CR-159503] p0041 A79-26102
- THOME, B. J.**
Design study of superconducting magnets for a
combustion magnetohydrodynamic /MHD/ generator
p0098 A79-15305
- TIERHANN, M.**
Measurements of carbon monoxide, condensation
nuclei, and ozone on a B 747SP aircraft flight
around the world
p0158 A79-31332
- TIERHANN, M. W.**
Airborne atmospheric sampling system
p0012 A79-50333
NASA Global Atmospheric Sampling Program (GASP)
data report for tape VL0009
[NASA-TM-79058] p0157 A79-15448
NASA Global Atmospheric Sampling Program (GASP)
data report for tapes VL0010 and VL0012
[NASA-TM-79061] p0157 A79-15450
Ozone measurement system for NASA global air
sampling program
[NASA-TP-1451] p0158 A79-22654
- TILLERY, D. G.**
Potential mapping with charged-particle beams
p0049 A79-24038
- TO, I. H.**
Liquid oxygen/liquid hydrogen boost/vane pump for
the advanced orbit transfer vehicles auxiliary
propulsion system
[NASA-CR-159648] p0057 A79-31341
- TODD, R. S.**
Effect of flight loads on turbofan engine
performance deterioration
p0027 A79-30559
Effect of flight loads on turbofan engine
performance deterioration
[NASA-TM-79041] p0013 A79-12085
- TODD, R. H., JR.**
Definition of mutually optimum NDI and proof test
criteria for 2219 aluminum pressure vessels.
Volume 1: Methods
[NASA-CR-135445] p0125 A79-21410
Definition of mutually optimum NDI and proof test
criteria for 2219 aluminum pressure vessels.
Volume 2: Optimization and fracture studies
[NASA-CR-135446] p0125 A79-21411
Definition of mutually optimum NDI and proof test
criteria for 2219 aluminum pressure vessels.
Volume 3: Applications to rail defect evaluation
[NASA-CR-135447] p0125 A79-21412
- TONAZIC, W. A.**
Ceramic applications in the advanced Stirling
automotive engine
p0117 A79-12851
- TOPICH, J. A.**
Adaptation of ion beam technology to
microfabrication of solid state devices and
transducers
[NASA-CR-159439] p0186 A79-11921
- TOTH, C., JR.**
Definition of mutually optimum NDI and proof test
criteria for 2219 aluminum pressure vessels.
Volume 2: Optimization and fracture studies
[NASA-CR-135446] p0125 A79-21411
Definition of mutually optimum NDI and proof test
criteria for 2219 aluminum pressure vessels.
Volume 3: Applications to rail defect evaluation
[NASA-CR-135447] p0125 A79-21412
- TOWNSEND, D. P.**
Evaluation of CBS 600 carburized steel as a gear
material
[NASA-TP-1390] p0114 A79-14389
Comparison of predicted and measured
elastohydrodynamic film thickness in a
20-millimeter-bore ball bearing
[NASA-TP-1542] p0116 A79-32552
NASA gear research and its probable effect on
rotorcraft transmission design
[NASA-TM-79292] p0116 A79-33477

- TOWSEND, D. P.**
Evaluation of high-contact-ratio spur gears with profile modification
[NASA-TP-1458] p0115 N79-31604
- TREADWAY, L. G.**
Atlas 5013 tank corrosion test
[NASA-CR-158760] p0050 N79-27234
- TRELA, W.**
Evaluation of ceramics for stator application: Gas turbine engine report
[NASA-CR-159533] p0033 N79-21075
- TRIMMER, D. H.**
Lewis Research Center studies of multiple large wind turbine generators on a utility network
p0149 N79-46547
- TRIMMER, J. E.**
Generalized computer-aided discrete time domain modeling and analysis of dc-dc converters
p0099 A79-10881
Power converter design optimization
p0099 A79-10885
Analytical core loss calculations for magnetic materials used in high frequency high power converter applications
[NASA-TN-79234] p0058 N79-31499
- TUCKER, J. E.**
Concepts for reducing exhaust emissions and fuel consumption of the aircraft piston engine
[SAE PAPER 790605] p0036 A79-36737
- TURNER, R. E.**
Atmospheric transformation of multispectral remote sensor data
[E79-10006] p0131 N79-12524
- U**
- URASEK, D. C.**
Effect of casing treatment on performance of a two-stage high-pressure-ratio fan
[NASA-TP-1409] p0017 N79-16852
Performance of two-stage fan with larger dampers on first-stage rotor
[NASA-TP-1399] p0018 N79-23967
Performance of two-stage fan having low-aspect-ratio first-stage rotor blading
[NASA-TP-1493] p0023 N79-27143
- V**
- VADYAK, J.**
Calculation of the three-dimensional flow field in supersonic inlets at angle of attack using a bicharacteristic method with discrete shock wave fitting
[AIAA PAPER 79-0379] p0025 A79-19698
A computer program for the calculation of the flow field in supersonic mixed-compression inlets at angle of attack using the three-dimensional method of characteristics with discrete shock wave fitting
[NASA-TN-78947] p0002 N79-10023
- VALID, R.**
Recent developments at ONERA in the field of structural analysis methods
[ONERA, TP NO. 1979-79] A79-49537
- VAN FOSSEN, G. J., JR.**
Liquid-cooling technology for gas turbines - Review and status
p0116 A79-10038
- VAN STONE, R. H.**
Influence of composition, annealing treatment, and texture on the fracture toughness of Ti-5Al-2.5Sn plate at cryogenic temperatures
p0077 A79-24262
- VANFOSSEN, G. J., JR.**
Review and status of liquid-cooling technology for gas turbines
[NASA-RF-1038] p0104 N79-22427
- VANNUCCI, R. D.**
Stability of PMR-polyimide monomer solutions
p0086 A79-31041
Characterization of PMR polyimides - Correlation of ester impurities with composite properties
p0066 A79-43265
Effects of graphite fiber stability on the properties of PMR polyimide composites
p0046 A79-43309
Effects of graphite fiber stability on the properties of PMR polyimide composites
- [NASA-TN-79062] p0061 N79-16075
Characterization of PMR polyimides: Correlation of ester impurities with composite properties
[NASA-TN-79068] p0061 N79-16918
Stability of PMR-polyimide monomer solutions
[NASA-TN-79063] p0062 N79-16921
High char yield-modified epoxy matrix resins
[NASA-TN-79226] p0063 N79-29240
- VARGAS, L. H.**
Workbook for estimating effects of accidental explosions in propellant ground handling and transport systems
[NASA-CR-3023] p0091 N79-10226
- VART, A.**
Use of an ultrasonic-acoustic technique for nondestructive evaluation of fiber composite strength
p0064 A79-15545
Computer signal processing for ultrasonic attenuation and velocity measurements for material property characterizations
p0125 A79-39809
Computer signal processing for ultrasonic attenuation and velocity measurements for material property characterizations
[NASA-TN-79180] p0127 N79-24359
A review of issues and strategies in nondestructive evaluation of fiber reinforced structural composites
[NASA-TN-79246] p0125 N79-29530
- VAUGHT, J. H.**
Study of an advanced General Aviation Turbine Engine (GATE)
[NASA-CR-159558] p0033 N79-21073
- VDOVIK, J. W.**
Definition study for variable cycle engine testbed engine and associated test program
[NASA-CR-159459] p0031 N79-13048
- VENKATARAMANI, K. S.**
Experimental study of the effects of flameholder geometry on emissions and performance of lean premixed combustors
[AIAA PAPER 79-0187] p0070 A79-19586
Emission measurements for a lean premixed propane/air system at pressures up to 30 atmospheres
[NASA-CR-159421] p0071 N79-10165
Premix fuels study applicable to duct burner conditions for a variable cycle engine
[NASA-CR-159513] p0091 N79-20266
Effects of flameholder geometry on emissions and performance of lean premixed combustors
p0021 N79-25005
- VOGLER, P. H.**
Millimeter wave satellite concepts. Volume 1: Executive summary
[NASA-CR-159504] p0041 N79-26101
Millimeter wave satellite concepts. Volume 2: Technical report
[NASA-CR-159503] p0041 N79-26102
- VON GLAHN, U.**
Assessment at full scale of nozzle/wing geometry effects on OTW aeroacoustic characteristics
p0175 A79-39802
Wing aerodynamic loading caused by jet-induced lift associated with STOL-OTW configurations
[AIAA PAPER 79-1664] p0006 A79-47346
- VON GLAHN, U. H.**
Correlation of combustor acoustic power levels inferred from internal fluctuating pressure measurements
p0025 A79-14796
- VONGLAHN, U.**
Assessment at full scale of nozzle/wing geometry effects on OTW aero-acoustic characteristics
[NASA-TN-79168] p0174 N79-25841
Wing aerodynamic loading caused by jet-induced lift associated with STOL-OTW configurations
[NASA-TN-79218] p0004 N79-28146
- VRANOS, A.**
Analytical evaluation of the impact of broad specification fuels on high bypass turbofan engine combustors
[NASA-CR-159454] p0031 N79-13050
- W**
- WALKER, B.**
Acoustic behavior of a fibrous bulk material

- [AIAA PAPER 79-0599] p0178 A79-26910
Effect of grazing flow on the acoustic impedance of Helmholtz resonators consisting of single and clustered orifices
[NASA-CR-3177] p0178 A79-32056
- WALKER, C. L.
Infrared suppressor effect on T63 turboshaft engine performance
[NASA-TN-78970] p0013 A79-11043
- WALKER, J. S.
Bartmann flow with temperature-dependent physical properties
p0182 A79-15597
- WALKER, H. S.
Properties and performance of fine-filament bronze-process Nb3Sn conductors
p0184 A79-20529
- WALLACE, R. W.
Millimeter wave communication satellite concepts
p0095 A79-29784
Millimeter wave satellite concepts. Volume 1: Executive summary
[NASA-CR-159504] p0041 A79-26101
Millimeter wave satellite concepts. Volume 2: Technical report
[NASA-CR-159503] p0041 A79-26102
- WALTER, J. L.
Evaluation of directionally solidified eutectic superalloys for turbine blade applications
[NASA-CR-135151] p0075 A79-16948
- WALTER, T. J.
Study of T53 engine vibration
[NASA-CR-135449] p0030 A79-10061
- WALTER, G. C.
Program for plasma-sprayed self-lubricating coatings
[NASA-CR-3163] p0087 A79-28315
- WANG, K. L.
High-energy electron-induced damage production at room temperature in aluminum-doped silicon
p0154 A79-32662
- WARD, J. W.
Advanced electrostatic ion thruster for space propulsion
[NASA-CR-159406] p0056 A79-14153
- WARREN, A. W.
SINWEST - A simulation model for wind energy storage systems
p0145 A79-10241
An expanded system simulation model for solar energy storage (technical report), volume 1
[NASA-CR-159601] p0166 A79-33881
An expanded system simulation model for solar energy storage (UNIVAC operation manual revisions), volume 2
[NASA-CR-159602] p0166 A79-33882
- SINWEST: A simulation model for wind and photovoltaic energy storage systems (CDC user's manual), volume 1
[NASA-CR-159607] p0166 A79-33883
- SINWEST: A simulation model for wind and photovoltaic energy storage systems (cdc program descriptions), volume 2
[NASA-CR-159608] p0167 A79-33884
- WARREN, J. R.
Evaluation of the cyclic behavior of aircraft turbine disk alloys
[NASA-CR-159409] p0030 A79-10058
- WARREN, R. E.
Reduction of rotor-turbulence interaction noise in static fan noise testing
[AIAA PAPER 79-0656] p0036 A79-26925
Basic research in fan source noise: Inlet distortion and turbulence noise
[NASA-CR-159451] p0177 A79-14875
- WARSHAW, R.
Commercial phosphoric acid fuel cell system technology development
p0150 A79-51809
Commercial phosphoric acid fuel cell system technology development
[NASA-TN-79169] p0139 A79-25500
- WATERS, W. J.
Effects of pressure and temperature on hot pressing a sialon
p0085 A79-11548
- WATSON, W. R.
A statistical theory of sound radiation from a two-dimensional lined duct
[AIAA PAPER 79-1521] p0176 A79-46707
- WEAK, J. D.
Ceramic coating effect on liner metal temperatures of film-cooled annular combustor
[NASA-TF-13223] p0015 A79-14098
- WEBB, D. E.
JT8D and JT9D jet engine performance improvement program. Task 1: Feasibility analysis
[NASA-CR-159449] p0033 A79-20116
- WEBB, J. A., JR.
Predicting dynamic performance limits for servosystems with saturating nonlinearities
[NASA-TF-1488] p0038 A79-28186
- WEBER, R. J.
NASA research on general aviation power plants
[AIAA PAPER 79-0561] p0026 A79-25870
NASA research on general aviation power plants
[NASA-TN-79031] p0014 A79-12086
- WEBER, R. E.
Rotor redesign for a highly loaded 1800 ft/sec tip speed fan. 1: Aerodynamic and mechanical design report
[NASA-CR-159596] p0034 A79-26055
- WEDEVEN, I. D.
Elastohydrodynamic film thickness measurements of artificially produced surface dents and grooves
[ASLE PREPRINT 78-LC-1A-1] p0118 A79-23267
- WEDEVEN, L. D.
Diagnostics of wear in aeronautical systems
p0120 A79-35805
Diagnostics of wear in aeronautical systems
[NASA-TN-79185] p0115 A79-24350
Elastohydrodynamic film thickness measurements of artificially produced nonsmooth surfaces
[NASA-TN-79214] p0115 A79-28554
- WEBER, G. E.
Whiskers, cones and pyramids created in sputtering by ion bombardment
[NASA-CR-159549] p0079 A79-20221
- WEIGAND, A. J.
Mechanical and chemical effects of ion-texturing biomedical polymers
[NASA-TN-79245] p0084 A79-31391
- WEILER, J.
Cross impact methodology for the assessment of US telecommunications system with application to fiber optics development, volume 1
[NASA-CR-135208] p0096 A79-18159
Cross impact methodology for the assessment of US telecommunications system with application to fiber optics development, volume 2
[NASA-CR-159511-VOL-2] p0096 A79-18160
- WEIN, D.
Mini-Brayton heat source assembly development
[NASA-CR-159447] p0151 A79-12554
- WEINBERG, I.
Ionized dopant concentrations at the heavily doped surface of a silicon solar cell
[NASA-TF-1347] p0184 A79-13886
Radiation damage in high-voltage silicon solar cells
p0144 A79-32658
Reverse annealing in radiation-damaged, silicon solar cells
p0144 A79-32660
Annealing of radiation damage in 0.1- and 2-cm-centimeter Silicon solar cells
[NASA-TF-1559] p0144 A79-33572
- WEISS, J. A.
Communications systems technology assessment study. Volume 2: Results
[NASA-CR-135224] p0095 A79-12273
- WEISER, V. G.
Photon degradation effects in terrestrial solar cells
p0149 A79-41098
Photon-degradation effects in terrestrial silicon solar cells
p0149 A79-42545
Open-circuit voltage improvements in low-resistivity solar cells
p0143 A79-32649
Radiation damage in high-voltage silicon solar cells
p0144 A79-32658
- WEINZEL, L. E.
Power train analysis for the DOE/NASA 100-kW wind turbine generator
[NASA-TN-78997] p0135 A79-16355
- WESTFALL, L. J.
Predicted inlet gas temperatures for tungsten fiber reinforced superalloy turbine blades

- Tungsten fiber reinforced FeCrAlY - A first generation composite turbine blade material
 [NASA-TM-79094] p0065 A79-30397
 Tungsten fiber reinforced FeCrAlY: A first generation composite turbine blade material
 [NASA-TM-79094] p0063 A79-20187
 Thermal-conductivity measurements of tungsten-fiber-reinforced superalloy composites using a thermal-conductivity comparator
 [NASA-TP-1445] p0063 A79-28234
- WESTINE, P. S.**
 Workbook for estimating effects of accidental explosions in propellant ground handling and transport systems
 [NASA-CR-3023] p0091 A79-10226
- WESTMORELAND, J. S.**
 Progress on Variable Cycle Engines
 [AIAA PAPER 79-1312] p0036 A79-40759
 Variable cycle engine technology program planning and definition study
 [NASA-CR-159539] p0034 A79-23084
- WHEELER, D. E.**
 Application of ESCA to the determination of stoichiometry in sputtered coatings and interface regions
 p0117 A79-16664
 An XPS study of the adherence of refractory carbide, silicide, and boride RF-sputtered wear-resistant coatings
 p0085 A79-21022
 Use of a nitrogen-argon plasma to improve adherence of sputtered titanium carbide coatings on steel
 p0119 A79-25103
 Adherence of sputtered titanium carbides
 p0078 A79-34997
 Effect of nitrogen-containing plasma on adherence, friction, and wear of radiofrequency-sputtered titanium carbide coatings
 [NASA-TP-1377] p0081 A79-15184
 Adherence of sputtered titanium carbides
 [NASA-TM-79117] p0074 A79-20220
 Improved adherence of sputtered titanium carbide coatings on nickel- and titanium-base alloys
 [NASA-TP-1450] p0055 A79-22194
 Surface chemistry of iron sliding in air and nitrogen lubricated with hexadecane and hexadecane containing dibenzyl-dithiolide
 [NASA-TP-1545] p0059 A79-31346
- WHIPPLE, E. C.**
 Operations of the ATS-6 ion engine
 p0049 A79-24007
 Characteristics of differential charging of ATS-6
 p0049 A79-24000
- WHITE, J. L.**
 Effect of flight loads on turbofan engine performance deterioration
 p0027 A79-30559
 Effect of flight loads on turbofan engine performance deterioration
 [NASA-TM-79041] p0013 A79-12085
- WHITEHEAD, G. T.**
 Microprocessor control of a wind turbine generator
 p0147 A79-21302
 Microprocessor control of a wind turbine generator
 [NASA-TM-79021] p0134 A79-12548
- WILBUR, P. J.**
 Mercury ion thruster research, 1978
 [NASA-CR-159485] p0056 A79-16913
- WILLIAMS, R. C.**
 Performance of a V/STOL tilt nacelle inlet with blowing boundary layer control
 [AIAA PAPER 79-1163] p0006 A79-47347
 Performance of a V/STOL tilt nacelle inlet with blowing boundary layer control
 [NASA-TM-79176] p0004 A79-27093
- WILLIS, E. A.**
 NASA research on general aviation power plants
 [AIAA PAPER 79-0561] p0026 A79-25870
 An overview of NASA research on positive displacement type general aviation engines
 [AIAA PAPER 79-1824] p0038 A79-53750
 NASA research on general aviation power plants
 [NASA-TM-79031] p0014 A79-12086
 An overview of NASA research on positive displacement type general aviation engines
 [NASA-TM-79254] p0024 A79-31210
- WILLIS, E. S.**
 QCSSE - The key to future short-haul air transport
 p0030 A79-50208
- WINDHILLER, J. E.**
 Design, fabrication, and initial test of a fixture for reducing the natural frequency of the Mod-0 wind turbine tower
 [NASA-TM-79200] p0142 A79-28727
- WINTA, E. A.**
 Predicted inlet gas temperatures for tungsten fiber reinforced superalloy turbine blades
 p0025 A79-17029
 Tungsten fiber reinforced FeCrAlY - A first generation composite turbine blade material
 p0065 A79-30397
 Tungsten fiber reinforced FeCrAlY: A first generation composite turbine blade material
 [NASA-TM-79094] p0063 A79-20187
 Thermal-conductivity measurements of tungsten-fiber-reinforced superalloy composites using a thermal-conductivity comparator
 [NASA-TP-1445] p0063 A79-28234
- WISANDER, D. W.**
 Plasma-sprayed coatings for lubrication of a titanium alloy in air at 430 deg C
 [NASA-TP-1509] p0083 A79-29327
- WISANDER, D. W.**
 Compressible flow across narrow passages: Comparison of theory and experiment for face seals
 [NASA-TP-1346] p0113 A79-10424
- WITHER, E. A.**
 User's guide to computer programs JET 5A and CIVM-JET 5B to calculate the large elastic-plastic dynamically-induced deformations of multilayer partial and/or complete structural rings
 [NASA-CR-159484] p0129 A79-18343
- WITMAN, E. E.**
 Aerospace Transparent Materials and Enclosures (12th)
 [AD-A065049] p0018 A79-23066
- WITZKE, W. E.**
 Effects of thermomechanical processing on strength and toughness of Fe-12Ni reactive metal alloys at 77K
 p0078 A79-32600
 High toughness-high strength iron alloy
 [NASA-CASE-LEW-12542-3] p0073 A79-19145
 Process for making a high toughness-high strength iron alloy
 [NASA-CASE-LEW-12542-2] p0074 A79-22271
- WOHLGEMUTH, J.**
 Thin cells for space
 p0154 A79-32652
- WOLF, B. A.**
 An operating 200 kW horizontal axis wind turbine
 p0147 A79-20829
 An operating 200-kW horizontal axis wind turbine
 [NASA-TM-79034] p0135 A79-16357
- WOLLSCHLAGER, J.**
 Liquid oxygen/liquid hydrogen boost/vane pump for the advanced orbit transfer vehicles auxiliary propulsion system
 [NASA-CR-159648] p0057 A79-31341
- WOODWARD, E. P.**
 Aerodynamic and acoustic effects of eliminating core swirl from a full scale 1.6 stage pressure ratio fan (QF-5A)
 [NASA-TM-78991] p0002 A79-11001
- WOOLAN, J. A.**
 Atomic hydrogen storage method and apparatus
 [NASA-CASE-LEW-12081-3] p0136 A79-18455
- WOOLAN, J. A.**
 Optical, spin-resonance, and magnetoresistance studies of tetrathiatetracene/2-iodide/3 - The nature of the ground state
 p0184 A79-10417
 Superconducting properties of evaporated copper molybdenum sulfide films
 p0184 A79-20219
 Properties and performance of fine-filament bronze-process Nb₃Sn conductors
 p0184 A79-20529
 Critical current density in wire drawn and hydrostatically extruded Nb-Ti superconductors
 p0185 A79-20539
 Improved apparatus for trapped radical and other studies down to 1.5 K
 p0110 A79-20742

- Hall effect and magnetoresistivity in the ternary molybdenum sulfides p0185 A79-21157
- Anomalous galvanomagnetic properties of graphite in strong magnetic fields p0185 A79-23633
- Critical current and scaling laws in evaporated two-phase Cu₂S/Mo₆S₈ p0185 A79-26375
- Normal state properties of the ternary molybdenum sulfides p0185 A79-27229
- Low temperature normal state resistance of ternary molybdenum sulfides p0185 A79-27230
- Comparison of projected critical currents in PbMo₆S₈ and Nb₃Ge p0185 A79-28300
- Reactively evaporated films of copper molybdenum sulfide p0185 A79-31973
- Electronic properties of PbMo₆S₈ and Cu₂Mo₆S₈ p0187 A79-41731
- Indirect measurements of Fermi surface parameters of some chevre phase materials p0185 A79-50231
- WRIGHT, D.**
20/30 GHz satellite system: technology needs assessment p0095 A79-14948
- WRIGHT, D. L.**
Results of thin-route satellite communication system analyses including estimated service costs p0095 A79-30395
Results of thin-route satellite communication system analyses including estimated service costs [NASA-TN-79098] p0054 A79-20300
- WRIGHT, C.**
Thin cells for space p0154 A79-32652
- WU, P. K. S.**
Convective heat flux in a laser-heated thruster p0057 A79-22396
- WU, B. W. H.**
User's guide to computer programs JET 5A and CIVM-JET 5B to calculate the large elastic-plastic dynamically-induced deformations of multilayer partial and/or complete structural rings [NASA-CN-159484] p0129 A79-18343
- Y**
- YANOVSKI, L. S.**
Flow friction of the turbulent coolant flow in cryogenic porous cables [NASA-TN-79052] p0103 A79-20341
- YAVUZKURT, S.**
Full-coverage film cooling: 3-dimensional measurements of turbulence structure and prediction of recovery region hydrodynamics [NASA-CN-3104] p0106 A79-22428
- YEE, S. T.**
Design, fabrication, and initial test of a fixture for reducing the natural frequency of the Mod-0 wind turbine tower [NASA-TN-79200] p0142 A79-28727
- YEE, T. K.**
Simmer-enhanced flashlamp-pumped dye laser p0112 A79-32981
- YEH, H. C.**
Effects of pressure and temperature on hot pressing a sialon p0085 A79-11548
Consolidation of Si₃N₄ by hot isostatic pressing p0086 A79-32931
- YEH, S. F. S.**
Optical, spin-resonance, and magnetoresistance studies of /tetrathiatetracene/2/iodide/3 - The nature of the ground state p0184 A79-10417
- YEROSHENKO, V. M.**
Some heat transfer and hydrodynamic problems associated with superconducting cables (SPTL) [NASA-TN-79023] p0102 A79-15267
Flow friction of the turbulent coolant flow in cryogenic porous cables [NASA-TN-79052] p0103 A79-20341
- Measurements of mixed convective heat transfer to low temperature helium in a horizontal channel [NASA-TN-79158] p0104 A79-23384
- YOUNG, L. E.**
Status of wraparound contact solar cells and arrays p0054 A79-10014
- YOUNG, S. G.**
A feasibility study of a diffusion barrier between Ni-Cr-Al coatings and nickel-based eutectic alloys p0077 A79-27233
- An experimental, low-cost, silicon slurry/aluminate high-temperature coating for superalloys [NASA-TN-79178] p0075 A79-29292
- YRASEK, D. C.**
Performance of two-stage fan with a first-stage rotor redesigned to account for the presence of a part-span damper [NASA-TF-1483] p0024 A79-30191
- YU, Y.**
Generalized computer-aided discrete time domain modeling and analysis of dc-dc converters p0099 A79-10881
Power converter design optimization p0099 A79-10885
Input filter design for switching regulators p0101 A79-48653
Modeling of switching regulator power stages with and without zero-inductor-current dwell time p0101 A79-49398
- Z**
- ZAFRAN, S.**
Ion beam technology applications study [NASA-CN-159437] p0180 A79-12884
- ZAICHIE, L. L.**
Flow friction of the turbulent coolant flow in cryogenic porous cables [NASA-TN-79052] p0103 A79-20341
- ZAPLATYNSKI, I.**
Thermal expansion of some nickel and cobalt spinels and their solid solutions p0186 A79-50233
Thermal barrier coatings: Burner rig hot corrosion test results [NASA-TN-79005] p0073 A79-11179
- ZARETSKY, E. V.**
Evaluation of CBS 600 carburized steel as a gear material [NASA-TF-1390] p0114 A79-14389
NASA gear research and its probable effect on rotorcraft transmission design [NASA-TN-79292] p0116 A79-33477
- ZEITLIN, B. A.**
Properties and performance of fine-filament bronze-process Nb₃Sn conductors p0184 A79-20529
- ZELAZNY, S. W.**
A three-dimensional turbulent compressible flow model for ejector and fluted mixers [NASA-CN-159467] p0100 A79-14325
- ZELLARS, G. E.**
A feasibility study of a diffusion barrier between Ni-Cr-Al coatings and nickel-based eutectic alloys p0077 A79-27233
The erosion/corrosion of small superalloy turbine rotors operating in the effluent of a PFB coal combustor [NASA-TN-79227] p0076 A79-30356
- ZERNUSSEN, B. O.**
Computer aided control of a mechanical arm A79-50334
- ZINER, B.**
A study of various synthetic routes to produce a halogen-labeled traction fluid [NASA-TN-79024] p0059 A79-11119
- ZINNERMAN, D. E.**
Laser anemometer measurements at the exit of a Te₃-C₂O combustor [NASA-CN-159623] p0107 A79-28456
- ZINNERMAN, W. F.**
Mini-Brayton heat source assembly development [NASA-CN-153447] p0151 A79-12554
- ZINN, B. T.**
Measurements of admittances and characteristic combustion times of reactive gaseous propellant coaxial injectors [NASA-CN-159542] p0072 A79-23168

ZOLEZZI, B. A.

PERSONAL AUTHOR INDEX

ZOLEZZI, B. A.

Study of an advanced General Aviation Turbine

Engine (GATE)

[NASA-CR-159558]

p0033 N79-21073

ZORZI, E. S.

Nonsynchronous vibrations observed in a

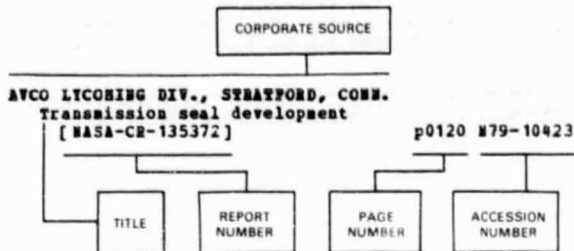
supercritical power transmission shaft

[ASME PAPER 79-GT-146]

p0123 A79-32412

CORPORATE SOURCE INDEX

Typical Corporate Source Index Listing



The title of the document is used to provide a brief description of the subject matter. The page number and NASA or AIAA accession number are included in each entry to assist the user in locating the abstract in the abstract section. If applicable, a report number is also included as an aid in identifying the document.

A

- ABACUS CONTROLS, INC., SOMERVILLE, N. J.**
An inverter/controller subsystem optimized for photovoltaic applications
p0148 A79-41047
- AEROJET LIQUID ROCKET CO., SACRAMENTO, CALIF.**
Plug cluster engine concept for in-space missions
[AIAA PAPER 79-1179] p0055 A79-38972
Advanced engine study for mixed-mode orbit-transfer vehicles
[NASA-CR-159491] p0057 N79-19074
Unconventional nozzle tradeoff study
[NASA-CR-159520] p0057 N79-28224
- AIR FORCE AERO PROPULSION LAB., WRIGHT-PATTESSON AFB, OHIO.**
Effect of rotor tip clearance and configuration on overall performance of a 12.77-centimeter tip diameter axial-flow turbine
[ASME PAPER 79-G1-42] p0027 A79-30521
- AIR FORCE FLIGHT DYNAMICS LAB., WRIGHT-PATTESSON AFB, OHIO.**
Aerospace Transparent Materials and Enclosures (12+h)
[AD-A065049] p0018 N79-23066
- AIR PRODUCTS AND CHEMICALS, INC., PHILADELPHIA, PA.**
Low heat leak connector for cryogenic system
[NASA-CASE-XLE-02367-1] p0093 N79-21225
- AIRSEARCH MFG. CO., PHOENIX, ARIZ.**
Mini-BRU/BIPS 1300 watt (sub) dynamic power conversion system development: Executive summary
[NASA-CR-159440] p0150 N79-10526
Mini-BRU/BIPS foil bearing development
[NASA-CR-159442] p0120 N79-11407
Analysis, design, fabrication and testing of the mini-Brayton rotating unit (Mini-BRU). Volume 1: Text and tables
[NASA-CR-159441-VOL-1] p0120 N79-11408
Analysis, design, fabrication and testing of the mini-Brayton rotating unit (MINI-BRU). Volume 2: Figures and drawings
[NASA-CR-159441-VOL-2] p0120 N79-11409
Low-cost directionally-solidified turbine blades, volume 1
[NASA-CR-159464] p0080 N79-2412
Conceptual design study of improved automotive gas turbine powertrain
[NASA-CR-159580] p0189 N79-31088
- AIRSEARCH MFG. CO., YORBAHUA, CALIF.**
Design and fabrication of the Mini-Brayton Recuperator (MBR)
[NASA-CR-159429] p0151 N79-11476

- ARMY AIR MOBILITY RESEARCH AND DEVELOPMENT LAB., CLEVELAND, OHIO.**
Effect of geometry on hydrodynamic film thickness
[ASME PAPER 78-LUB-24] p0118 A79-23237
Stability of PMR-polyimide monomer solutions
p0086 A79-31041
- ARMY AVIATION RESEARCH AND DEVELOPMENT COMMAND, CLEVELAND, OHIO.**
Fretting wear of iron, nickel, and titanium under varied environmental conditions
p0078 A79-34995
Effects of graphite fiber stability on the properties of PMR polyimide composites
p0066 A79-43309
Resin/fiber thermo-oxidative interactions in PMR polyimide/graphite composites
[NASA-TM-79093] p0062 N79-16520
Stability of PMR-polyimide monomer solutions
[NASA-TM-79063] p0062 N79-16921
Thermal stress analysis of ceramic gas-path seal components for aircraft turbines
[NASA-TP-1437] p0082 N79-21205
Performance of two-stage fan having low-aspect-ratio first-stage rotor blading
[NASA-TP-1493] p0023 N79-27143
- ARMY AVIATION RESEARCH AND DEVELOPMENT COMMAND, ST. LOUIS, MO.**
Wear of seal materials used in aircraft propulsion systems
[NASA-TM-79003] p0073 N79-12204
Lean, premixed, prevaporized combustion for aircraft gas turbine engines
[NASA-TM-79148] p0018 N79-23964
Lean, premixed, prevaporized combustion for aircraft gas turbine engines
[NASA-TM-79148] p0018 N79-23964
Effect of steady-state pressure distortion on flow characteristics entering a turbofan engine
[NASA-TM-79134] p0019 N79-23969
- ARMY PROPULSION LAB., ST. LOUIS, MO.**
Liquid-cooling technology for gas turbines - Review and status
p0116 A79-10038
- ARMY PROPULSION LAB., CLEVELAND, OHIO.**
Lean, premixed, prevaporized combustion for aircraft gas turbine engines
[AIAA PAPER 79-1318] p0029 A79-39034
- AUBURN UNIV., ALA.**
Analysis of a parallel-arrayed power regulating system
p0101 A79-49397
- AVCO LYCOMING DIV., STRATFORD, CONN.**
Transmission seal development
[NASA-CR-135372] p0120 N79-10423
Development of spiral-groove self-acting seals for helicopter engines
[NASA-CR-159622] p0122 N79-32551

B

- BATTELLE COLLEGE LABS., OHIO.**
Stresses from arbitrary loads on a circular crack
p0130 A79-27938
Computer-aided analysis and design of the shape rolling process for producing turbine engine airfoils
[NASA-CR-159455] p0012 N79-12087
Stress analysis for structures with surface cracks
[NASA-CR-159400] p0129 N79-13405
User's manual for FRAC3D: Supplement to report on stress analysis for structures with surface cracks
[NASA-CR-159401] p0129 N79-13406
Determination of lubricant selection based on elastohydrodynamic film thickness and traction

measurement
 [NASA-CR-159428] p0121 N79-14385
 Computer-aided analysis and design of the shape
 rolling process for producing turbine engine
 airfoils
 [NASA-CR-135367] p0080 N79-26175
BATTELLE MEMORIAL INST., COLUMBUS, OHIO.
 Critical current density in wire drawn and
 hydrostatically extruded Nb-Ti superconductors
 p0185 A79-20539
BATTELLE PACIFIC NORTHWEST LABS., RICHLAND, WASH.
 Development of sputtering process to deposit
 stoichiometric zirconia coatings for the
 inside wall of regeneratively cooled rocket
 thrust chambers
 [NASA-CR-159412] p0056 N79-11115
BOEING AEROSPACE CO., SEATTLE, WASH.
 Proof test criteria for thin walled pressure
 vessels
 p0123 A79-26985
 Evaluation of flawed composite structural
 components under static and cyclic loading
 [NASA-CR-135403] p0066 N79-26120
BOEING COMMERCIAL AIRPLANE CO., REMTON, WASH.
 Effect of flight loads on turbofan engine
 performance deterioration
 p0027 A79-30559
BOEING COMMERCIAL AIRPLANE CO., SEATTLE, WASH.
 Inflight fuel tank temperature survey data
 [NASA-CR-159569] p0009 N79-23940
 Design and evaluation of aircraft heat source
 systems for use with high-freezing point fuels
 [NASA-CR-159568] p0091 N79-24172
BOEING COMPUTER SERVICES, INC., SEATTLE, WASH.
 SIMWEST - A simulation model for wind energy
 storage systems
 p0145 A79-10241
 An expanded system simulation model for solar
 energy storage (technical report), volume 1
 [NASA-CR-159601] p0166 N79-33881
 An expanded system simulation model for solar
 energy storage (UNIVAC operation manual
 revisions), volume 2
 [NASA-CR-159602] p0166 N79-33882
 SIMWEST: A simulation model for wind and
 photovoltaic energy storage systems (CDC
 user's manual), volume 1
 [NASA-CR-159607] p0166 N79-33883
 SIMWEST: A simulation model for wind and
 photovoltaic energy storage systems (cdc
 program descriptions), volume 2
 [NASA-CR-159608] p0167 N79-33884
BOEING ENGINEERING AND CONSTRUCTION, SEATTLE, WASH.
 MOD-2 failure mode and effects analysis
 [NASA-CR-159632] p0093 N79-30415
 Applications of thermal energy storage to
 process heat storage and recovery in the paper
 and pulp industry
 [NASA-CR-159398] p0154 N79-30801
BOEING MILITARY AIRPLANE DEVELOPMENT, SEATTLE, WASH.
 A method to estimate weight and dimensions of
 large and small gas turbine engines
 [NASA-CR-159481] p0015 N79-15046
BOOZ-ALLEN AND HAMILTON, INC., CLEVELAND, OHIO.
 Preliminary power train design for a
 state-of-the-art electric vehicle (executive
 summary)
 [NASA-CR-157621] p0188 N79-12968

C

CALIFORNIA INST. OF TECH., PASADENA.
 A general unified approach to modelling
 switching dc-to-dc converters in discontinuous
 conduction mode
 p0101 A79-10880
 A new optimum topology switching dc-to-dc
 converter
 p0101 A79-10888
CALIFORNIA UNIV., BERKELEY.
 Simmer-enhanced flashlamp-pumped dye laser
 p0112 A79-32981
CALIFORNIA UNIV., LA JOLLA.
 Effects of bulk and surface conductivity on the
 potential developed by dielectrics exposed to
 electron beams
 p0171 A79-50938
CALIFORNIA UNIV., LOS ANGELES.
 Superconducting properties of evaporated copper
 molybdenum sulfide films
 p0184 A79-20219
 Reactively evaporated films of copper molybdenum
 sulfide
 p0185 A79-31973
CALIFORNIA UNIV., SAN DIEGO.
 Operations of the A1S-6 ion engine
 p0049 N79-24007
 Characteristics of differential charging of A1S-6
 p0049 N79-24008
CALIFORNIA UNIV. AT LOS ANGELES.
 Nonlinear equations of equilibrium for elastic
 helicopter or wind turbine blades undergoing
 moderate deformation
 [NASA-CR-159478] p0130 N79-19414
CARNEGIE-MELLON INST. OF RESEARCH, PITTSBURGH, PA.
 Evaluation of the mechanical properties of
 electrosag refined Fe-12Ni alloys
 [NASA-CR-159394] p0079 N79-12202
CARNEGIE-MELLON UNIV., PITTSBURGH, PA.
 Influence of composition, annealing treatment,
 and texture on the fracture toughness of
 Ti-5Al-2.5Sn plate at cryogenic temperatures
 p0077 A79-24262
CASE WESTERN RESERVE UNIV., CLEVELAND, OHIO.
 Interpolation and extrapolation of creep rupture
 data by the Minimum Commitment Method. I -
 Focal-point convergence. II - Oblique
 translation. III - Analysis of multiheats
 p0077 A79-16038
 Hall effect and magnetoresistivity in the
 ternary molybdenum sulfides
 p0185 A79-21157
 Adaptation of ion beam technology to
 microfabrication of solid state devices and
 transducers
 [NASA-CR-159439] p0185 N79-11921
 X-ray photoelectron spectroscopy study of nickel
 and nickel-base alloy surface alterations in
 simulated hot corrosion conditions with
 emphasis on eventual application to turbine
 blade corrosion
 [NASA-CR-159553] p0072 N79-25178
CELANESE RESEARCH CO., SUMMIT, N.J.
 Ultrafine polybenzimidazole (PBI) fibers
 [NASA-CR-159644] p0067 N79-31350
CINCINNATI UNIV., OHIO.
 A calculation procedure for viscous flow in
 turbomachines, volume 1
 [NASA-CR-159635] p0107 N79-30514
 Flow in nonrotating passages of radial inflow
 turbines
 [NASA-CR-159679] p0035 N79-32212
CLEVELAND STATE UNIV., OHIO.
 High temperature dynamic modulus and damping of
 aluminum and titanium matrix composites
 p0065 A79-26132
 Consolidation of Si3N4 by hot isostatic pressing
 p0086 A79-32931
COAST GUARD, WASHINGTON, D.C.
 Radar image processing of real aperture SLAR
 data for the detection and identification of
 iceberg and ship targets
 p0131 A79-36537
COLORADO STATE UNIV., FORT COLLINS.
 Prediction of plasma properties in mercury ion
 thrusters
 [NASA-CR-159448] p0056 N79-15152
 Mercury ion thruster research, 1978
 [NASA-CR-159485] p0056 N79-16913
 Industrial ion source technology
 [NASA-CR-159534] p0179 N79-19828
 Inert gas thrusters
 [NASA-CR-159527] p0057 N79-26110
 Physical processes in directed ion beam sputtering
 [NASA-CR-159567] p0182 N79-26943
CORSAT LABS., CLARKSBURG, MD.
 Limiting process in shallow junction solar cells
 p0154 N79-32646
CORSTOCK AND WESCOTT, INC., CAMBRIDGE, MASS.
 NaOH-based high temperature heat-of-fusion
 thermal energy storage device
 p0155 A79-10106
 Phase change thermal storage for a solar total
 energy system
 p0155 A79-17321
 Development of a phase-change thermal storage
 system using modified anhydrous sodium
 hydroxide for solar electric power generation

[NASA-CR-159465] p0153 N79-19454
CONTROL DATA CORP., MINNEAPOLIS, MINN.
 An analysis of the first two years of GASF data
 p0160 A79-15068
 Ozone in the upper troposphere from Gasp
 measurements p0160 A79-44810

COPPIN STATE COLL., BALTIMORE, MD.
 Some practical observations on the accelerated
 testing of Nickel-Cadmium Cells p0058 A79-51911

CORNELL UNIV., ITHACA, N. Y.
 Turbulence effects on flame speed and flame
 structure p0070 A79-19480
 [AIAA PAPER 79-0016]

CREANE, INC., HANOVER, N.H.
 Design, development, and test of a laser
 velocimeter for a small 8:1 pressure ratio
 centrifugal compressor p0111 N79-27478
 [NASA-CR-134781]

CURTIS-WRIGHT CORP., WOOD-RIDGE, N.J.
 A review of Curtiss-Wright rotary engine
 developments with respect to general aviation
 potential p0036 A79-36749
 [SAE PAPER 790621]

D

DAIMLER-BENZ A. G., STUTTGART (WEST GERMANY).
 Statistical study of supersonic compressors p0039 N79-21064

LAYTON UNIV. RESEARCH INST., OHIO.
 A cross impact methodology for the assessment of
 US telecommunications system with application
 to fiber optics development: Executive summary
 [NASA-CR-135209] p0096 N79-17071

A cross impact methodology for the assessment of
 US telecommunications system with application
 to fiber optics development, volume 1
 [NASA-CR-135208] p0096 N79-18159

A cross impact methodology for the assessment of
 US telecommunications system with application
 to fiber optics development, volume 2
 [NASA-CR-159511-VOL-2] p0096 N79-18160

DEPARTMENT OF ENERGY, WASHINGTON, D. C.
 SIMWEST - A simulation model for wind energy
 storage systems p0145 A79-10241

A method for correlating performance data of a
 terrestrial solar cell array p0140 A79-26503
 [NASA-TM-79163]

**DEPARTMENT OF THE AIR FORCE, WRIGHT-PATTERSON AFB,
 OHIO.**
 Properties and performance of fine-filament
 bronze-process Nb3Sn conductors p0184 A79-20529

DETROIT DIESEL ALLISON, INDIANAPOLIS, IND.
 Determining and improving labyrinth seal
 performance in current and advanced high
 performance gas turbines p0031 N79-11068

Study of an advanced General Aviation Turbine
 Engine (GATE) p0033 N79-21073
 [NASA-CR-159558]

Laser anemometer measurements at the exit of a
 T63-C20 combustor p0107 N79-28456
 [NASA-CR-159623]

Conceptual design study of an Improved Gas
 Turbine (IGT) powertrain p0189 N79-31087
 [NASA-CR-159604]

Single shaft automotive gas turbine engine
 characterization test p0189 N79-32129
 [NASA-CR-159654]

DOUGLAS AIRCRAFT CO., INC., LONG BEACH, CALIF.
 An efficient user-oriented method for
 calculating compressible flow about
 three-dimensional inlets p0005 A79-19524
 [AIAA PAPER 79-0081]

E

EIC, INC., NEWTON, MASS.
 Feasibility study for a secondary Na/S battery
 [NASA-CR-159464] p0152 N79-17330

ENERGY RESEARCH CORP., BETHEL, CONN.
 Fabrication and testing of silver-hydrogen cells
 [NASA-CR-159431] p0152 N79-16374
 Fabrication and testing of silver-hydrogen cells
 [NASA-CR-159490] p0152 N79-16375

ENERGY RESEARCH CORP., DANBURY, CONN.
 Technology development for phosphoric acid fuel
 cell powerplant, phase 2 p0153 N79-29604
 [NASA-CR-159572]

ENVIRONMENTAL RESEARCH INST. OF MICHIGAN, ANN ARBOR.
 Atmospheric transformation of multispectral
 remote sensor data p0131 N79-12524
 [E79-10006]

EXION RESEARCH AND ENGINEERING CO., LINDEN, N.J.
 High performance, high density hydrocarbon fuels
 [NASA-CR-159480] p0091 N79-20267

F

FARCHILD SPACE AND ELECTRONICS CO., GERRANTOWN, MD.
 Communications systems technology assessment
 study. Volume 2: Results p0095 N79-12273
 [NASA-CR-135224]

FLORIDA UNIV., GAINESVILLE.
 Design of high efficiency HLE solar cells for
 space and terrestrial applications p0154 N79-32647

FORD MOTOR CO., DEARBORN, MICH.
 Automotive Stirling engine development program
 [NASA-CR-159436] p0120 N79-11406
 Evaluation of advanced regenerator systems
 [NASA-CR-159422] p0188 N79-12969
 Evaluation of ceramics for stator application:
 Gas turbine engine report p0033 N79-21075
 [NASA-CR-159533]
 Conceptual design study of improved automobiles
 gas turbine powertrain p0189 N79-31068
 [NASA-CR-159580]

G

GENERAL APPLIED SCIENCE LABS., INC., WESTBURY, N. Y.
 Experimental study of the effects of flameholder
 geometry on emissions and performance of lean
 premixed combustors p0070 A79-19586
 [AIAA PAPER 79-0187]

Emission measurements for a lean premixed
 propane/air system at pressures up to 30
 atmospheres p0071 N79-10165
 [NASA-CR-159421]

Premix fuels study applicable to duct burner
 conditions for a variable cycle engine
 [NASA-CR-159513] p0091 N79-20266

Emissions measurements for a lean premixed
 propane/air system at pressures up to 30
 atmospheres p0020 N79-25002

Effects of flameholder geometry on emissions and
 performance of lean premixed combustors
 p0021 N79-25005

GENERAL DYNAMICS/CONVAIR, SAN DIEGO, CALIF.
 Bilinear tangent yaw guidance p0045 A79-45374
 [AIAA 79-1730]

Atlas 5013 tank corrosion test p0050 N79-27234
 [NASA-CR-158760]
 Study of liquid and vapor flow into a Centaur
 capillary device p0108 N79-33432
 [NASA-CR-159657]

GENERAL DYNAMICS/FORT WORTH, TEX.
 Experimental investigation of a 0.15-scale model
 of an underfuselage normal-shock inlet
 [NASA-CR-30499] p0006 N79-12014

GENERAL ELECTRIC CO., CINCINNATI, OHIO.
 Application of digital controls on the quiet
 clean short haul experimental engines
 [AIAA PAPER 79-1203] p0029 A79-38984

Definition study of a Variable Cycle
 Experimental Engine (VCEE) and associated test
 program and test plan p0031 N79-11042
 [NASA-CR-159419]

Fuel delivery system including heat exchanger
 means p0113 N79-11403
 [NASA-CASE-LEW-12793-1]

Experimental clean combustor program: Phase 3:
 Turbulence measurement addendum p0031 N79-12088
 [NASA-CR-135422]

Definition study for variable cycle engine
 testbed engine and associated test program
 [NASA-CR-159459] p0031 N79-13048
 Integrated gas turbine engine-nacelle
 [NASA-CASE-LEW-12389-3] p0014 N79-14096
 Variable area exhaust nozzle
 [NASA-CASE-LEW-12378-1] p0014 N79-14097

- Sound-suppressing structure with thermal relief
[NASA-CASE-LEW-12658-1] p0172 N79-14871
- Experimental clean combustor program, phase D:
Noise measurement addendum
[NASA-CR-159458] p0177 N79-17656
- CF6 jet engine performance improvement program.
Task 1: Feasibility analysis
[NASA-CR-159450] p0033 N79-21074
- Fabrication of J79 boron/aluminum compressor
blades
[NASA-CR-159566] p0034 N79-23970
- Turbulence measurements in the compressor exit
flow of a General Electric CF6-50 engine
p0019 N79-24996
- Advanced low emissions catalytic combustor
program at General Electric p0021 N79-25011
- Lean, premixed, prevaporized combustor
conceptual design study p0022 N79-25014
- Design study and performance analysis of a
high-speed multistage variable-geometry fan
for a variable cycle engine
[NASA-CR-159455] p0034 N79-25020
- Acoustic and aerodynamic performance
investigation of inverted velocity profile
coannular plug nozzles, comprehensive data
report, volume 1
[NASA-CR-159575-VOL-1] p0177 N79-26884
- Acoustic and aerodynamic performance
investigation of inverted velocity profile
coannular plug nozzles, comprehensive data
report, volume 2
[NASA-CR-159575-VOL-2] p0177 N79-26885
- Acoustic and aerodynamic performance
investigation of inverted velocity profile
coannular plug nozzles, comprehensive data
report, volume 3
[NASA-CR-159575-VOL-3] p0177 N79-26886
- Metal spar/superhybrid shell composite fan blades
[NASA-CR-159594] p0067 N79-30295
- Experimental Clean Combustor Program (ECCP),
phase 3
[NASA-CR-135384] p0035 N79-31207
- Containment of composite fan blades
[NASA-CR-159544] p0067 N79-31348
- Lean, Premixed-Prevaporized (LPP) combustor
conceptual design study
[NASA-CR-159629] p0072 N79-31358
- CF6 jet engine performance improvement program.
Short core exhaust nozzle performance
improvement concept
[NASA-CR-159564] p0038 N79-33206
- GENERAL ELECTRIC CO., EVANDEALE, OHIO.
Analysis and preliminary design of an optical
digital tip clearance sensor for propulsion
control
[NASA-CR-155434] p0031 N79-15053
- Theory of low frequency noise transmission
through turbines
[NASA-CR-159457] p0033 N79-20117
- Experimental clean combustor program: Diesel no.
2 fuel addendum, phase 3
[NASA-CR-135413] p0091 N79-26221
- NASA CF6 jet engine diagnostic program:
Long-term CF6-8D low-pressure turbine
deterioration
[NASA-CR-159618] p0039 N79-29191
- GENERAL ELECTRIC CO., PHILADELPHIA, PA.
Background and system description of the Mod 1
wind turbine generator p0155 A79-20825
- Wind turbine generator application places unique
demands on tower design and materials
p0155 A79-20826
- Fatigue impact on Mod-1 wind turbine design
p0156 A79-20827
- The application of hydraulics in the 2,000 kW
wind turbine generator p0156 A79-27400
- UV blocking filters for polymeric films
p0088 A79-51103
- Control and stabilization of the DOE/NASA Mod-1
two megawatt wind turbine generator
p0156 A79-51780
- Mini-Brayton heat source assembly development
[NASA-CR-159447] p0151 N79-12554
- Containment of composite fan blades
[NASA-CR-158168] p0032 N79-18978
- An investigation of the adhesive bonding of
Teflon solar cell covers
[NASA-CR-159565] p0153 N79-26506
- GENERAL ELECTRIC CO., SANTA BARBARA, CALIF.
Conceptual design of thermal energy storage
systems for near term electric utility
applications. Volume 1: Screening of concepts
[NASA-CR-159411-VOL-1] p0151 N79-13496
- Conceptual design of thermal energy storage
systems for near term electric utility
applications. Volume 2: Appendices -
screening of concepts
[NASA-CR-159411-VOL-2] p0152 N79-13497
- GENERAL ELECTRIC CO., SCHEMECTADY, N. Y.
Influence of composition, annealing treatment,
and texture on the fracture toughness of
Ti-5Al-2.5Sn plate at cryogenic temperatures
p0077 A79-24262
- Reduction of rotor-turbulence interaction noise
in static fan noise testing
[AIAA PAPER 79-0656] p0036 A79-26925
- Control and stabilization of the DOE/NASA Mod-1
two megawatt wind turbine generator
p0156 A79-51780
- Basic research in fan source noise: Inlet
distortion and turbulence noise
[NASA-CR-159451] p0177 N79-14875
- Evaluation of directionally solidified eutectic
superalloys for turbine blade applications
[NASA-CR-135151] p0079 N79-16548
- Evaluation of an advanced directionally
solidified gamma/gamma'-alpha Mo eutectic alloy
[NASA-CR-159416] p0079 N79-20222
- High efficiency cell geometry p0143 N79-32653
- Conceptual design of thermal energy storage
systems for near term electric utility
applications
[NASA-CR-159577] p0155 N79-33560
- GENERAL ELECTRIC CO., WEST LYNN, MASS.
QCSEE - The key to future short-haul air transport
p0030 A79-50208
- GEORGIA INST. OF TECH., ATLANTA.
Millimeter wave communication satellite concepts
p0095 A79-29784
- Measurements of admittances and characteristic
combustion times of reactive gaseous
propellant coaxial injectors
[NASA-CR-159542] p0072 N79-23168
- Millimeter wave satellite concepts. Volume 1:
Executive summary
[NASA-CR-159504] p0041 N79-26101
- Millimeter wave satellite concepts. Volume 2:
Technical report
[NASA-CR-159503] p0041 N79-26102
- GINER, INC., WALTHAM, MASS.
Catalyst surfaces for the chromous/chromic redox
couple
[NASA-CASE-LEW-13148-1] p0134 N79-14538
- GRUBMAN AEROSPACE CORP., BETHPAGE, N.Y.
Performance of a V-STOL tilt nacelle inlet with
blowing boundary layer control
[AIAA PAPER 79-1163] p0006 A79-47347

H

- HAMILTON STANDARD, WINDSOR LOCKS, CONN.
Interactive multi-mode blade impact analysis
[NASA-CR-159462] p0032 N79-17858
- HAMILTON STANDARD DIV., UNITED AIRCRAFT CORP.,
WINDSOR LOCKS, CONN.
Wind-turbine-generator rotor-blade concepts with
low-cost potential p0147 A79-20828
- HAWAII UNIV., HONOLULU.
Control of wind turbine generators connected to
power systems p0146 A79-15574
- HERSH ACOUSTICAL ENGINEERING, CHATSWORTH, CALIF.
Acoustic behavior of a fibrous bulk material
[AIAA PAPER 79-0599] p0178 A79-26910
- Effect of grazing flow on the acoustic impedance
of Helmholtz resonators consisting of single
and clustered orifices
[NASA-CR-3177] p0178 N79-32056
- HIBAN COLL., OHIO.
Geosynchronous satellite operating anomalies
caused by interaction with the local

spacecraft environment p0050 N79-24049

HOMBYWELL, INC., MINNEAPOLIS, MINN.
Active heat exchange system development for latent heat thermal energy storage [NASA-CR-159479] p0153 N79-21554

HOMIZONS RESEARCH, INC., CLEVELAND, OHIO.
Survey of inorganic polymers [NASA-CR-159563] p0087 N79-30377

HUGHES AIRCRAFT CO., CULVER CITY, CALIF.
Lightweight multiple output converter development [NASA-CR-159526] p0100 N79-20317

HUGHES AIRCRAFT CO., LOS ANGELES, CALIF.
The 18 and 30 GHz fixed service communication satellite system study: Executive summary [NASA-CR-159627-1] p0096 N79-33373
The 18 and 30 GHz fixed service communications satellite system study [NASA-CR-159627-2] p0096 N79-33374

HUGHES RESEARCH LABS., MALIBU, CALIF.
Advanced electrostatic ion thruster for space propulsion [NASA-CR-159406] p0056 N79-14153
Summary of GaAs Solar Cell Performance and Radiation Damage Workshop p0144 N79-32665

IBM WATSON RESEARCH CENTER, YOKTOWN HEIGHTS, N.Y.
Sinter-enhanced flashlamp-pumped dye laser p0112 A79-32981

IIT RESEARCH INST., CHICAGO, ILL.
Program for plasma-sprayed self-lubricating coatings [NASA-CR-3163] p0087 N79-28315

ILLINOIS UNIV., URBANA.
Bartmann flow with temperature-dependent physical properties p0182 A79-10097
Elastohydrodynamic film thickness measurements of artificially produced surface dents and grooves [ASME PREPRINT 78-LC-1A-1] p0118 A79-23267

INTERMAGNETICS GENERAL CORP., GUILDERLAND, N.Y.
Properties and performance of fine-filament bronze-process Nb3Sn conductors p0184 A79-20529

IOWA STATE UNIV. OF SCIENCE AND TECHNOLOGY, AMES.
Axial-flow compressor turning angle and loss by inviscid-viscous interaction blade-to-blade computation [ASME PAPER 79-GT-5] p0006 A79-30504

ISRAEL INST. OF TECH., HAIFA.
Hydrodynamic effects in a misaligned radial face seal [NASA-CR-135228] p0121 N79-17226

JET PROPULSION LAB., CALIFORNIA INST. OF TECH. PASADENA.
Optical, spin-resonance, and magnetoresistance studies of tetrathiatetracene/2-iodide/3 - The nature of the ground state p0184 A79-10417

JOINT INST. FOR ADVANCEMENT OF FLIGHT SCIENCES, HAMPTON, VA.
A statistical theory of sound radiation from a two-dimensional lined duct [AIAA PAPER 79-1521] p0176 A79-46707

KANAN AEROSPACE CORP., BLOOMFIELD, CONN.
Wind-turbine-generator rotor-blade concepts with low-cost potential p0147 A79-20828

KANAZAWA UNIV. (JAPAN).
Friction and fracture of single-crystal silicon carbide in contact with itself and titanium p0086 A79-32149

KANSAS UNIV., LAWRENCE.
A mobile apparatus for solar collector testing [ASME PAPER 79-DE-5] p0150 A79-47651

KULITH SEMI-CONDUCTOR PRODUCTS, INC., RIDGEFIELD, N. J.
Pressure instrumentation for gas turbine engines - A review of measurement technology

[ASME PAPER 78-GT-148] p0110 A79-10800

LEEDS UNIV. (ENGLAND).
Elastohydrodynamic lubrication of elliptical contacts for materials of low elastic modulus. II - Starved conjunction [ASME PAPER 78-LUB-1] p0118 A79-23229
Effect of geometry on hydrodynamic film thickness [ASME PAPER 78-LUB-24] p0118 A79-23237

LEHIGH UNIV., BETHLEHEM, PA.
Off-axis impact of unidirectional composites with cracks: Dynamic stress intensification [NASA-CR-159537] p0067 N79-30294
Normal and radial impact of composites with embedded penny-shaped cracks [NASA-CR-159538] p0130 N79-31627

LINCOLN LAB., MASS. INST. OF TECH., LEXINGTON.
Shallow-homojunction GaAs solar cells p0144 N79-32666

LOCKHEED AIRCRAFT SERVICE, INC., ONTARIO, CALIF.
An operating 200 kW horizontal axis wind turbine p0147 A79-20829

LOCKHEED-CALIFORNIA CO., BURBANK.
Experimental study of low temperature behavior of aviation turbine fuels in a wing tank model [NASA-CR-159615] p0091 N79-29355

LOCKHEED-GEORGIA CO., MARIETTA.
An impulse test technique with application to acoustic measurements [AIAA PAPER 79-0679] p0178 A79-26890
Effects of simulated forward flight on jet noise, shock noise and internal noise [AIAA PAPER 79-0615] p0178 A79-26936
Duct wall impedance control as an advanced concept for acoustic suppression enhancement [NASA-CR-159425] p0176 N79-10842
The free jet as a simulator of forward velocity effects on jet noise [NASA-CR-3056] p0176 N79-14873
Studies of the acoustic transmission characteristics of coaxial nozzles with inverted velocity profiles: Comprehensive data report [NASA-CR-159628] p0177 N79-27933

LOCKHEED MISSILES AND SPACE CO., HUNTSVILLE, ALA.
Structural analysis of cylindrical thrust chambers, volume 1 [NASA-CR-159522] p0057 N79-19073

CELFE: Coupled Eulerian-Lagrangian Finite Element program for high velocity impact. Part 1: Theory and formulation [NASA-CR-159395] p0166 N79-29832

CELFE: Coupled Eulerian-Lagrangian Finite Element program for high velocity impact. Part 2: Program user's manual [NASA-CR-159396] p0166 N79-29833

LOCKHEED MISSILES AND SPACE CO., PALO ALTO, CALIF.
Laser power conversion system analysis, volume 1 [NASA-CR-159523-VOL-1] p0112 N79-21334
Laser power conversion system analysis, volume 2 [NASA-CR-159523-VOL-2] p0112 N79-21335

LOCKHEED MISSILES AND SPACE CO., SUNNYVALE, CALIF.
Laser rocket system analysis [NASA-CR-159521] p0112 N79-21337

LUND UNIV. (SWEDEN).
On the distribution of computation for sequential decoding using the stack algorithm p0096 A79-33793

MES COMPUTING, INC., HUNTSVILLE, ALA.
Analysis of a parallel-arrayed power regulating system p0101 A79-49397

MAGNETIC CORP. OF AMERICA, WALTHAM, MASS.
Design study of superconducting magnets for a combustion magnetohydrodynamic /MHD/ generator p0098 A79-15305

MARTIN MARIETTA AEROSPACE, BETHESDA, MD.
Lean combustion limits of a confined premixed-prevaporized propane jet [AIAA PAPER 79-0538] p0026 A79-25856
Computer aided control of a mechanical arm A79-50334

MARTIN MARIETTA AEROSPACE, DENVER, COLO.
Definition of mutually optimum NDI and proof

- test criteria for 2219 aluminum pressure vessels. Volume 1: Methods [NASA-CR-135445] p0125 N79-21410
- Definition of mutually optimum NDI and proof test criteria for 2219 aluminum pressure vessels. Volume 2: Optimization and fracture studies [NASA-CR-135446] p0125 N79-21411
- Definition of mutually optimum NDI and proof test criteria for 2219 aluminum pressure vessels. Volume 3: Applications to rail defect evaluation [NASA-CR-135447] p0125 N79-21412
- MARTIN MARIETTA CORP., DENVER, COLO.**
- Cryogenic propellant densification study [NASA-CR-159438] p0087 N79-12238
- Development of single-cell protectors for sealed silver-zinc cells [NASA-CR-159407] p0151 N79-12550
- MASSACHUSETTS INST. OF TECH., CAMBRIDGE.**
- Alternative aircraft fuels p0090 N79-10824
- Experimental evidence of interhemispheric transport from airborne carbon monoxide measurements p0158 N79-38942
- User's guide to computer programs JET 5A and CIVM-JET 5B to calculate the large elastic-plastic dynamically-induced deformations of multilayer partial and/or complete structural rings [NASA-CR-159484] p0129 N79-18343
- Modelling turbulent flame ignition and blowout p0021 N79-25008
- MATHEMATICAL SCIENCES NORTHWEST, INC., BELLEVUE, WASH.**
- Design investigation of solar powered lasers for space applications [NASA-CR-159554] p0111 N79-26384
- MATHEMATICAL SCIENCES NORTHWEST, INC., SEATTLE, WASH.**
- Solar-pumped lasers for space power transmission [AIAA PAPER 79-1015] p0112 N79-38202
- MATSUSHITA ELECTRIC INDUSTRIAL CO. LTD., OSAKA (JAPAN).**
- Anomalous galvanomagnetic properties of graphite in strong magnetic fields p0185 N79-23633
- MCDONNELL-DOUGLAS CORP., ST. LOUIS, MO.**
- Reynolds number, scale and frequency content effects on F-15 inlet instantaneous distortion [AIAA PAPER 79-0104] p0005 N79-19533
- MECHANICAL TECHNOLOGY, INC., LATHAM, N. Y.**
- Design and test of a squeeze-film damper for a flexible power transmission shaft p0123 N79-16C11
- Development of surface coatings for air-lubricated, compliant journal bearings to 650 C [ASLE PREPRINT 79-TC-3C-1] p0123 N79-23252
- Static evaluation of surface coatings for compliant gas bearings in an oxidizing atmosphere to 650 C p0038 N79-31957
- Laser balancing demonstration on a high-speed flexible rotor [ASME PAPER 79-GT-56] p0123 N79-32351
- Nonsynchronous vibrations observed in a supercritical power transmission shaft [ASME PAPER 79-GT-146] p0123 N79-32412
- Elastomer mounted rotors - An alternative for smoother running turbomachinery [ASME PAPER 79-GT-149] p0119 N79-32414
- An introduction to a unified approach to flexible rotor balancing [ASME PAPER 79-GT-161] p0124 N79-32423
- Study of 153 engine vibration [NASA-CR-135449] p0030 N79-10061
- Experiments on multiplane balancing using a laser for material removal [NASA-CR-3105] p0121 N79-17228
- Development of procedures for calculating stiffness and damping of elastomers in engineering applications. Part 5: Elastomer performance limits and the design and test of an elastomer damper [NASA-CR-159552] p0122 N79-24373
- T700 power turbine rotor multiplane/multispeed balancing demonstration [NASA-CR-159586] p0122 N79-25392
- Conceptual design study of an automotive Stirling reference engine system [NASA-CR-159605] p0188 N79-29110
- Design and application of a test rig for super-critical power transmission shafts [NASA-CR-3105] p0122 N79-31603
- MICHIGAN UNIV., ANN ARBOR.**
- An acoustic emission study of plastic deformation in polycrystalline aluminum p0077 N79-19458
- Effect of fuel sprays on emissions p0020 N79-24999
- MINNESOTA UNIV., MINNEAPOLIS.**
- Investigations of negative and positive cesium ion species [NASA-CR-159446] p0179 N79-18711
- Whiskers, cones and pyramids created in sputtering by ion bombardment [NASA-CR-159549] p0079 N79-20221
- MONSANTO CO., ST. LOUIS, MO.**
- Method for the preparation of inorganic single crystal and polycrystalline electronic materials [NASA-CASE-XLE-02545-1] p184 N79-21910

N

- NATIONAL ACADEMY OF SCIENCES - NATIONAL RESEARCH COUNCIL, WASHINGTON, D. C.**
- Canilever mounted resilient pad gas bearing [NASA-CASE-LEW-12569-1] p0113 N79-10418
- NATIONAL AERONAUTICS AND SPACE ADMINISTRATION, WASHINGTON, D. C.**
- The M-15-aircraft (sawolot M-15) [NASA-TN-75596] p0013 N79-12063
- NATIONAL AERONAUTICS AND SPACE ADMINISTRATION. FLIGHT RESEARCH CENTER, EDWARDS, CALIF.**
- Reynolds number, scale and frequency content effects on F-15 inlet instantaneous distortion [AIAA PAPER 79-0104] p0005 N79-19533
- NATIONAL AERONAUTICS AND SPACE ADMINISTRATION. GODDARD SPACE FLIGHT CENTER, GREENBELT, MD.**
- Summary of the two year NASA program for active control of ATS-5/6 environmental charge p0047 N79-24005
- NATIONAL AERONAUTICS AND SPACE ADMINISTRATION. LANGLEY RESEARCH CENTER, LANGLEY STATION, VA.**
- A statistical theory of sound radiation from a two-dimensional lined duct [AIAA PAPER 79-1521] p0176 N79-46707
- NATIONAL AERONAUTICS AND SPACE ADMINISTRATION. MARSHALL SPACE FLIGHT CENTER, HUNTSVILLE, ALA.**
- Status of wraparound contact solar cells and arrays p0054 N79-10014
- NATIONAL AEROSPACE LAB., TOKYO (JAPAN).**
- Effects of inflow distortion profiles on fan tone noise calculated using a 3-D theory [AIAA PAPER 79-0577] p0175 N79-26911
- NAVAL AIR PROPULSION TEST CENTER, TRENTON, N.J.**
- Rotor fragment protection program: Statistics on aircraft gas turbine engine rotor failures that occurred in US commercial aviation during 1976 [NASA-CR-159474] p0032 N79-18977
- NAVAL WEAPONS SUPPORT CENTER, CAMMIE, IND.**
- Block 2 solar cell module environmental test program [NASA-CR-159393] p0151 N79-13493
- NEVADA ENGINEERING AND TECHNOLOGY CORP., LONG BEACH, CALIF.**
- Elevated temperature properties of boron/aluminum composites [NASA-CR-159445] p0066 N79-16924
- NEW JERSEY INST. OF TECHNOLOGY, NEWARK.**
- Heat transfer from a row of jets impinging on concave semi-cylindrical surface p0108 N79-42890
- NEW YORK STATE UNIV., ALBANY.**
- An analysis of the first two years of GASF data p0160 N79-15068
- NIELSEN ENGINEERING AND RESEARCH, INC., MOUNTAIN VIEW, CALIF.**
- High speed smoke flow visualization for the determination of cascade shock losses [AIAA PAPER 79-0042] p0005 N79-19495
- An off-design correlation of part span damper losses through transonic axial fan rotors

[ASME PAPER 79-GT-6] p0028 A79-32329
 Low-turbulence high-speed wind tunnel for the
 determination of cascade shock losses
 [ASME PAPER 79-GT-129] p0039 A79-32398
NOTRE DAME UNIV., IND.
 High speed smoke flow visualization for the
 determination of cascade shock losses
 [AIAA PAPER 79-0042] p0005 A79-19495
 Low-turbulence high-speed wind tunnel for the
 determination of cascade shock losses
 [ASME PAPER 79-GT-129] p0039 A79-32398
 Feasibility study of liquid pool burning in
 reduced gravity
 [NASA-CR-159642] p0072 N79-32303

O

OAK RIDGE NATIONAL LAB., TENN.
 Thermal energy storage for industrial waste heat
 recovery
 p0145 A79-10101
 User's manual for PRESTO: A computer code for
 the performance of regenerative steam turbine
 cycles
 [NASA-CR-159540] p0122 N79-25395
OPTICAL COATING LAB., INC., CITY OF INDUSTRY, CALIF.
 Silicon solar cells for space use: Present
 performance and trends
 p0154 N79-32654
OWENS-ILLINOIS, INC., TOLEDO, OHIO.
 Alternate methods of applying diffusants to
 silicon solar cells
 [NASA-CR-159508] p0153 N79-29603

P

PENNSYLVANIA STATE UNIV., UNIVERSITY PARK.
 Potential mapping with charged-particle beams
 p0049 N79-24038
 Stable dielectric charge distributions from
 field enhancement of secondary emission
 p0045 N79-24046
PITTSBURGH UNIV., PA.
 Method and device for the detection of phenol
 and related compounds
 [NASA-CASE-LEW-12513-1] p0069 N79-22235
 An investigation of the initiation stage of hot
 corrosion in Ni-base alloys
 [NASA-CR-159616] p0080 N79-25196
POLYTECHNIC INST. OF NEW YORK, FARMINGDALE.
 Filtering of non-linear instabilities
 p0108 A79-32912
PRATT AND WHITNEY AIRCRAFT, EAST HARTFORD, CONN.
 Effect of flight loads on turbofan engine
 performance deterioration
 p0027 A79-30559
 Analysis of the impact of the use of broad
 specification fuels on combustors for
 commercial aircraft gas turbine engines
 [AIAA PAPER 79-1195] p0090 A79-38980
 Instrumentation for measuring the dynamic
 pressure on rotating compressor blades
 [NASA-CR-159466] p0110 N79-12418
 Energy efficient engine: Propulsion
 system-aircraft integration evaluation
 [NASA-CR-159488] p0032 N79-16850
 Strain gage system evaluation program
 [NASA-CR-159486] p0110 N79-19314
PRATT AND WHITNEY AIRCRAFT, WEST PALM BEACH, FLA.
 Ceramic blade attachments
 p0123 A79-12848
PRATT AND WHITNEY AIRCRAFT GROUP, EAST HARTFORD, CONN.
 Modal propagation angles in a cylindrical duct
 with flow and their relation to sound radiation
 [AIAA PAPER 79-0183] p0174 A79-19582
 A jet exhaust noise prediction procedure for
 inverted velocity profile coannular nozzles
 [AIAA PAPER 79-0633] p0178 A79-28964
 Causes of high pressure compressor deterioration
 in service
 [AIAA PAPER 79-1234] p0036 A79-40483
 Progress on Variable Cycle Engines
 [AIAA PAPER 79-1312] p0036 A79-40759
 Energy efficient engine preliminary design and
 integration study
 [NASA-CR-135396] p0012 N79-12084
 Analytical evaluation of the impact of broad

specification fuels on high bypass turbofan
 engine combustors
 [NASA-CR-159454] p0031 N79-13050
**J18D and J19D jet engine performance improvement
 program. Task 1: Feasibility analysis**
 [NASA-CR-159449] p0033 N79-20116
**J18D revised high-pressure turbine cooling and
 other outer air seal program**
 [NASA-CR-159551] p0033 N79-21076
**Variable cycle engine technology program
 planning and definition study**
 [NASA-CR-159539] p0034 N79-23084
**Study of blade aspect ratio on a compressor
 front stage aerodynamic and mechanical design
 report**
 [NASA-CR-159555] p0034 N79-23085
**Turbulence characteristics of compressor
 discharge flows**
 p0019 N79-24995
**Advanced low emissions catalytic combustor
 program at Pratt and Whitney**
 p0021 N79-25012
**Lean, premixed, prevaporized combustor
 conceptual design study**
 p0021 N79-25013
**Rotor redesign for a highly loaded 1800 ft/sec
 tip speed fan. 1: Aerodynamic and mechanical
 design report**
 [NASA-CR-159596] p0034 N79-26055
**Aerodynamic and acoustic investigation of
 inverted velocity profile coannular exhaust
 nozzle models and development of aerodynamic
 and acoustic prediction procedures,
 comprehensive data report, volume 1**
 [NASA-CR-159515] p0034 N79-30185
**Aerodynamic and acoustic investigation of
 inverted velocity profile coannular exhaust
 nozzle models and development of aerodynamic
 and acoustic prediction procedures,
 comprehensive data report, volume 2**
 [NASA-CR-159516] p0034 N79-30186
**Energy efficient engine flight propulsion system
 preliminary analysis and design report**
 [NASA-CR-159487] p0035 N79-30189
**Fiber optic sensors for military, industrial and
 commercial applications**
 p0111 A79-38738
**Analysis and preliminary design of
 sensors for propulsion control**
 [NASA-CR-159519] p0180 N79-27975
High power phase locked laser oscillators
 [NASA-CR-159630] p0112 N79-32538
ROCKWELL INTERNATIONAL CORP., CANOGA PARK, CALIF.
Small, high-pressure, liquid oxygen turbopump
 [NASA-CR-159509] p0121 N79-17221
**Development of a plasma sprayed ceramic gas path
 seal for high pressure turbine applications**
 [NASA-CR-159669] p0122 N79-31602
**Lean, premixed, prevaporized fuel combustor
 conceptual design study**
 [NASA-CR-159647] p0035 N79-32211
**PRATT AND WHITNEY AIRCRAFT GROUP, WEST PALM BEACH,
 FLA.**
**Test verification of a turbofan partial swirl
 afterburner**
 [AIAA PAPER 79-1199] p0029 A79-38981
**Multivariable control altitude demonstration on
 the F100 turbofan engine**
 [AIAA PAPER 79-1204] p0029 A79-39814
**A summary of NASA/Air Force Full Scale Engine
 Research programs using the F100 engine**
 [AIAA PAPER 79-1308] p0030 A79-40488
**Evaluation of the cyclic behavior of aircraft
 turbine disk alloys**
 [NASA-CR-159409] p0030 N79-10058
**Design, fabrication and spin testing of ceramic
 blade metal disk attachment**
 [NASA-CR-159532] p0032 N79-17857
**Development of sputtered techniques for thrust
 chambers**
 [NASA-CR-159637] p0080 N79-32326
PRINCETON COMBUSTION RESEARCH LABS., INC., N.J.
Definition of smolder experiments for Spacelab
 [NASA-CR-159528] p0040 N79-20161
PURDUE UNIV., LAFAYETTE, IND.
**Calculation of the three-dimensional flow field
 in supersonic inlets at angle of attack using**

a bicharacteristic method with discrete shock wave fitting
[AIAA PAPER 79-0379] p0025 A79-19698
Lewis Research Center studies of multiple large wind turbine generators on a utility network
p0149 A79-46547

R

RCA LABS., PRINCETON, N. J.
Epitaxial solar-cell fabrication, phase 2
[NASA-CR-135350] p0152 N79-19448
ROCKET RESEARCH CORP., REDMOND, WASH.
Applications of thermal energy storage to process heat and waste heat recovery in the iron and steel industry
[NASA-CR-159397] p0151 N79-11473
ROCKWELL INTERNATIONAL CORP., ANAHEIM, CALIF.
Ground-to-space optical power transfer
p0161 A79-17180

S

SALK INSTITUTE FOR BIOLOGICAL STUDIES, SAN DIEGO, CALIF.
The catalysis of nucleotide polymerization by compounds of divalent lead
p0060 A79-32924
SCIENCE APPLICATIONS, INC., LA JOLLA, CALIF.
Spacecraft charging modeling development and validation study
p0050 N79-24051
SCIENCE APPLICATIONS, INC., VIENNA, VA.
First principles numerical model of avalanche-induced arc discharges in electron-irradiated dielectrics
[NASA-CR-159560] p0101 N79-28418
SHAKER RESEARCH CORP., BALLSTON LAKE, N. Y.
Turbojet blade vibration data acquisition design and feasibility testing
[NASA-CR-159505] p0032 N79-18976
Experimental and analytical tools for evaluation of Stirling engine rod seal behavior
[NASA-CR-159543] p0122 N79-23429
SKF INDUSTRIES, INC., KING OF PRUSSIA, PA.
Aircraft engine sump fire mitigation, phase 2
[NASA-CR-135379] p0121 N79-17219
High speed cylindrical roller bearing analysis, SKF computer program CYEFAN. Volume 1: Analysis
[NASA-CR-159460] p0121 N79-17222
High speed cylindrical roller bearing analysis, SKF computer program CYEFAN. Volume 2: User's manual
[NASA-CR-159461] p0121 N79-17223
SOLAR TURBINES INTERNATIONAL, SAN DIEGO, CALIF.
Wide range operation of advanced low NOx aircraft gas turbine combustors
[ASME PAPER 78-GT-128] p0024 A79-10792
Fuel spray data with LDV
p0019 N79-24997

Internally coated air-cooled gas turbine blading
[NASA-CR-159574] p0034 N79-25018
SOLAREX CORP., ROCKVILLE, MD.
An economic analysis of a commercial approach to the design and fabrication of a space power system
[AIAA 79-0914] p0055 A79-34737
Thin cells for space
p0154 N79-32652
SOUTHWEST RESEARCH INST., SAN ANTONIO, TEX.
Workbook for estimating effects of accidental explosions in propellant ground handling and transport systems
[NASA-CR-30233] p0091 N79-10226
SPIRE CORP., BEDFORD, MASS.
Applications of ion implantation to high performance, radiation tolerant silicon solar cells
p0143 N79-32648
SRI INTERNATIONAL CORP., MENLO PARK, CALIF.
Laboratory studies of electrical properties of insulating materials
p0044 A79-20877

STANFORD UNIV., CALIF.
Optical, spin-resonance, and magnetoresistance studies of α -tetrathiatetracene/2-iodide/3 - The nature of the ground state
p0184 A79-10417

Full-coverage film cooling: 3-dimensional measurements of turbulence structure and prediction of recovery region hydrodynamics
[NASA-CR-3104] p0106 N79-22428
Heat transfer to a full-coverage, film-cooled surface with compound-angle (30 deg and 45 deg) hole injection
[NASA-CR-3103] p0107 N79-22429
STATE UNIV. OF NEW YORK AT ALBANY.
A summary of research on the NASA-Global Atmospheric Sampling Program performed by the Atmospheric Sciences Research Center
[NASA-CR-159614] p0158 N79-27716
High-energy electron-induced damage production at room temperature in aluminum-doped silicon
p0154 N79-32662

STATE UNIV. OF NEW YORK AT STONY BROOK.
Combustion of porous solids at reduced gravitational conditions
[NASA-CR-3197] p0072 N79-33288
SUNDSTRAND CORP., ROCKFORD, ILL.
Liquid oxygen/liquid hydrogen boost/vane pump for the advanced orbit transfer vehicles auxiliary propulsion system
[NASA-CR-159648] p0057 N79-31341
SYRACUSE UNIV., N. Y.
A literature review on fatigue and creep interaction
[NASA-CR-135305] p0130 N79-26429
SYSTEMS CONTROL, INC., PALO ALTO, CALIF.
Multivariable control altitude demonstration on the F100 turbofan engine
[AIAA PAPER 79-1204] p0029 A79-39814
SYSTEMS SCIENCE AND SOFTWARE, LA JOLLA, CALIF.
The decrease in effective photocurrents due to saddle points in electrostatic potentials near differentially charged spacecraft
p0045 A79-30140
NASCAP modelling of high-voltage power system interactions with space charged-particle environments
p0051 A79-39806
Effects of bulk and surface conductivity on the potential developed by dielectrics exposed to electron beams
p0171 A79-50938
The capabilities of the NASA charging analyzer program
p0047 N79-24011
Charging analysis of the SCATHA satellite
p0049 N79-24012
Extension, validation and application of the NASCAP code
[NASA-CR-159595] p0100 N79-27397
NASCAP user's manual, 1978
[NASA-CR-159417] p0100 N79-27398

T

TECHNICAL MARKETING ASSOCIATES, INC., CONCORD, MASS.
Market definition studies for photovoltaic highway applications
[NASA-CR-159477] p0152 N79-19451
TECHNICAL REPORT SERVICES, ROCKY RIVER, OHIO.
Evaluation of urethane for feasibility of use in wind turbine blade design
[NASA-CR-159530] p0153 N79-20497
TECHNION RESEARCH AND DEVELOPMENT FOUNDATION LTD., HAIFA (ISRAEL).
Self-stabilizing radial face seal
[NASA-CR-LEW-12991-1] p0113 N79-12445
TEL-AVIV UNIV. (ISRAEL).
Electronic properties of PbMo6S8 and CuMo6S8
p0187 A79-41731
TELEDYNE CORP., TOLEDO, OHIO.
Advanced General Aviation Turbine Engine (GATE) study
[NASA-CR-159624] p0039 N79-29189
TELEDYNE CONTINENTAL MOTORS, MOBILE, ALA.
Concepts for reducing exhaust emissions and fuel consumption of the aircraft piston engine
[SAE PAPER 790605] p0036 A79-36737
Computer simulation of an aircraft engine fuel injection system
[NASA-CR-157641] p0016 N79-15052
TENNESSEE UNIV., KNOXVILLE.
Energy conservation through sealing technology
p0118 A79-20700
TEXAS A&M UNIV., COLLEGE STATION.

- Analysis of a parallel-arrayed power regulating system
p0101 A79-49397
- TEXAS INSTRUMENTS, INC., DALLAS.
A mobile apparatus for solar collector testing
[ASME PAPER 79-DE-5] p0150 A79-47651
- TEXTRON BELL AEROSPACE CO., BUFFALO, N. Y.
A three-dimensional turbulent compressible flow model for ejector and fluted mixers
[NASA-CR-159467] p0100 N79-14325
- THERMO ELECTRON CORP., WALTHAM, MASS.
Lithium and potassium heat pipes for thermionic converters
p0145 A79-10113
- TOLEDO UNIV., OHIO.
Evaluation of MOSIAS computer code for predicting dynamic loads in two-bladed wind turbines
[AIAA 79-0733] p0005 A79-29007
Resonance-tube ignition of aluminum
p0071 A79-46366
- TRIBON BEARING CO., CLEVELAND, OHIO.
Filtration effects on ball bearing life and condition in a contaminated lubricant
[ASME PAPER 78-LUB-34] p0118 A79-23246
- TRW DEFENSE AND SPACE SYSTEMS GROUP, REDONDO BEACH, CALIF.
Generalized computer-aided discrete time domain modeling and analysis of dc-dc converters
p0099 A79-10881
Power converter design optimization
p0099 A79-10885
Input filter design for switching regulators
p0101 A79-48653
Modeling of switching regulator power stages with and without zero-inductor-current dwell time
p0101 A79-49398
Ion beam technology applications study
[NASA-CR-159437] p0180 N79-12884
Synthesis of improved moisture resistant polymers
[NASA-CR-159456] p0087 N79-18053
CIS-type variable conductance heat pipes for SEF PM/FFU
[NASA-CR-159550] p0107 N79-22434
Effects of arcing due to spacecraft charging on spacecraft survival
[NASA-CR-159593] p0100 N79-25312
Heat pipe life and processing study
[NASA-CR-159581] p0107 N79-25349
- TRW, INC., CLEVELAND, OHIO.
A strainrange partitioning analysis of low cycle fatigue of coated and uncoated Rene 80
p0129 N79-10479
Exploratory thermal-mechanical fatigue results for Rene 80 in ultrahigh vacuum
[NASA-CR-159444] p0079 N79-11180
Automated Plasma Spray (AFS) process feasibility study: Plasma spray process development and evaluation
[NASA-CR-159579] p0092 N79-29382
- TRW SYSTEMS, REDONDO BEACH, CALIF.
Hydrogen recombination in sealed nickel-cadmium aerospace cells
p0057 A79-51907
- TULANE UNIV., NEW ORLEANS, LA.
Optical, spin-resonance, and magnetoresistance studies of /tetrathiatetracene/2/iodide/3 - The nature of the ground state
p0184 A79-10417
- UNITED AIR LINES, INC., SAN FRANCISCO, CALIF.
Airborne atmospheric sampling system
p0012 A79-50333
- UNITED TECHNOLOGIES CORP., EAST HARTFORD, CONN.
Prop-fan propulsion - Its status and potential
[SAE PAPER 780995] p0026 A79-25880
Development of advanced fuel cell system
[NASA-CR-159443] p0151 N79-12553
Aerodynamic and acoustic investigation of inverted velocity profile coannular exhaust nozzle models and development of aerodynamic and acoustic prediction procedures
[NASA-CR-3168] p0035 N79-31212
- UNITED TECHNOLOGIES CORP., SOUTH WINDSOR, CONN.
Strip cell test and evaluation program
[NASA-CR-159652] p0154 N79-31784
- Advanced technology light weight fuel cell program
[NASA-CR-159653] p0155 N79-33581
- UNITED TECHNOLOGIES CORP., WINDSOR LOCKS, CONN.
Design, fabrication, and test of a composite material wind turbine rotor blade
[NASA-CR-135389] p0150 N79-10525
Case-operated pitch-change apparatus
[NASA-CR-13050-1] p0014 N79-14095
- UNITED TECHNOLOGIES RESEARCH CENTER, EAST HARTFORD, CONN.
Increasing the FGD tolerance of composites
p0067 A79-20859
Noise from struts and splitters in turbofan exit ducts
[AIAA PAPER 79-0637] p0178 A79-26923
Analysis of the impact of the use of broad specification fuels on combustors for commercial aircraft gas turbine engines
[AIAA PAPER 79-1195] p0090 A79-38980
Lean stability augmentation for premixing, prevaporizing combustors
[AIAA PAPER 79-1319] p0036 A79-39035
Development of a three-dimensional turbulent duct flow analysis
[NASA-CR-3029] p0106 N79-12366
Study of mean- and turbulent-velocity fields in a large-scale turbine-vane passage
[NASA-CR-3067] p0032 N79-16853
Lean stability augmentation study
[NASA-CR-159536] p0071 N79-22244
Synthesis of improved moisture resistant polymers
[NASA-CR-159510] p0087 N79-23218
Modeling of premixing-prevaporizing fuel-air mixing passages
p0015 N79-24998
Autoignition of fuels
p0020 N79-25001
Lean Stability augmentation study
p0021 N79-25007
New high temperature cross linking monomers
[NASA-CR-159514] p0087 N79-29331
Development of SiAlON materials
[NASA-CR-159675] p0067 N79-33256
- UNIVERSITY COLL., LONDON (ENGLAND).
An introduction to a unified approach to flexible rotor balancing
[ASME PAPER 79-GT-161] p0124 A79-32423
- V
- VIRGINIA POLYTECHNIC INST. AND STATE UNIV., BLACKSBURG.
Input filter design for switching regulators
p0101 A79-48653
Modeling of switching regulator power stages with and without zero-inductor-current dwell time
p0101 A79-49398
An analytical and experimental study of sound propagation and attenuation in variable-area ducts
[NASA-CR-135392] p0177 N79-25845
- W
- WASHINGTON UNIV., SEATTLE.
Solar-pumped lasers for space power transmission
[AIAA PAPER 79-1015] p0112 A79-38202
- WEST VIRGINIA UNIV., MORGANTOWN.
Simulation of fluidized bed coal combustors
[NASA-CR-159529] p0153 N79-20487
- WESTINGHOUSE ATOMNUCLEAR LAB., PITTSBURGH, PA.
Interdiffusion behavior of tungsten or rhenium and group 5 and 6 elements and alloys of the periodic table. Part 2b: Appendices
[NASA-CR-134526] p0080 N79-33305
- WESTINGHOUSE ELECTRIC CORP., LIMA, OHIO.
The solid state remote power controller - Its status, use and perspective
p0099 A79-10896
- WESTINGHOUSE RESEARCH AND DEVELOPMENT CENTER, PITTSBURGH, PA.
Nb₃Ge as a potential candidate material for 15- to 25-T magnets
p0186 A79-44548
Development and fabrication of improved power transistor switches
[NASA-CR-159524] p0100 N79-21273

WICHITA STATE UNIV., KANS.

Properties and performance of fine-filament
bronze-process Nb3Sn conductors

p0184 A79-20529

Velocity, temperature, and electrical
conductivity profiles in hydrogen-oxygen MHD
duct flows

p0182 A79-26184

WILLIAMS RESEARCH CORP., WALLED LAKE, WICH.

Advanced General Aviation Turbine Engine (GATE)
concepts

[NASA-CR-159603]

p0034 N79-25017

X

TEROX ELECTRO-OPTICAL SYSTEMS, PASADENA, CALIF.

Inert gas ion source program

[NASA-CR-159423]

p0056 N79-10120

Y

YALE UNIV., NEW HAVEN, CONN.

Chemically frozen multicomponent boundary layer
theory of salt and/or ash deposition rates
from combustion gases

p0078 A79-50912

Experimental studies of the formation/deposition
of sodium sulfate in/from combustion gases

[NASA-CR-159612]

p0072 N79-25183

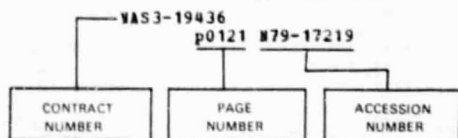
Experimental studies of the formation/deposition
of sodium sulfate in/from combustion gases

[NASA-CR-159613]

p0080 N79-25184

CONTRACT NUMBER INDEX

Typical Contract Number Index Listing



Listings in this index are arranged alphanumerically by contract number. Under each contract number, the accession numbers denoting documents that have been produced as a result of research done under that contract are arranged in ascending order with the /AA accession numbers appearing first. Preceding the accession number is the page number in the abstract section in which the citation may be found.

AF-AFOSR-78-3609
p0006 A79-30504
DA PROJ. 111-61102-AH-45
p01 A79-30514
DA PROJ. 111-62209-AH-76
p0107 N79-28456
DAHCO-75-C-0095
p0112 A79-32981
DE-A101-79ET20305
p0141 N79-28725
DE-A101-79ET20485
p0139 N79-25501
p0142 N79-29599
p0093 N79-30415
DE-A103-79ET11272
p0139 N79-25500
DE-A101-79ET20485
p0152 N79-19451
p0138 N79-24443
DEN3-2 p0093 N79-30415
DEN3-4 p0189 N79-32129
DEN3-8 p0188 N79-12969
DEN3-12
p0151 N79-13496
p0152 N79-13497
p0155 N79-33560
DEN3-22
p0122 N79-23429
DEN3-28
p0189 N79-31087
DEN3-32
p0188 N79-29110
DEN3-37
p0189 N79-31088
DEN3-38
p0153 N79-21554
DEN3-40
p0152 N79-19451
DEN3-42
p0166 N79-33881
p0166 N79-33882
p0166 N79-33883
p0167 N79-33884
DEN3-67
p0153 N79-29604
DEN3-00019
p0033 N79-21075
DOE TASK 64
p0185 A79-20539
DOE-40-666-77
p0122 N79-25395
DOT-FA79NA-1091
p0016 N79-15052
E(49-26)-1004
p0135 N79-16357
p0136 N79-20494
p0140 N79-26502
E(49-26)-1022
p0148 A79-41022
p0148 A79-41023
p0148 A79-41091
p0151 N79-13490
p0136 N79-17336
E(49-26)-1028
p0147 A79-21302
p0150 N79-10525

p0134 N79-12508
p0135 N79-16355
p0135 N79-17333
p0130 N79-19414
p0153 N79-20497
p0137 N79-21549
p0142 N79-30719
E(49-26)-1059
p0140 N79-26504
E(49-28)-1002
p0146 A79-11824
p0147 A79-38191
p0133 N79-11479
p0138 N79-24442
p0138 N79-24445
EC-77-A-31-1002
p0141 N79-26505
EC-77-A-31-1011
p0144 A79-10084
p0188 A79-37293
p0014 N79-13049
p0017 N79-17859
EC-77-A-31-1034
p0147 A79-21300
p0151 N79-11473
p0134 N79-11481
p0151 N79-13496
p0152 N79-13497
p0153 N79-19454
p0136 N79-20498
p0137 N79-21550
p0153 N79-21554
p0154 N79-30801
EC-77-A-31-1034-2
p0155 N79-33560
EC-77-A-31-1040
p0070 A79-11542
p0070 A79-14956
p0134 N79-11480
p0135 N79-16356
p0188 N79-16721
p0188 N79-27023
p0142 N79-28726
p0084 N79-30379
p0189 N79-31088
p0189 N79-32129
EC-77-A-31-1044
p0098 N79-26316
p0142 N79-28728
EC-77-A-31-1062
p0149 A79-44225
p0138 N79-24444
p0141 N79-27665
EC-77-A-31-10040
p0188 N79-29110
EC-77-C-01-5081
p0151 N79-11473
EC-77-C-01-5082
p0154 N79-30801
EC-77-C-02-4396
p0120 N79-11406
ED-77-A-31-1040
p0122 N79-23429
EF-77-A-01-2593
p0073 N79-11179
p0135 N79-17334

p0089 N79-20265
p0139 N79-25498
EF-77-A-01-2647
p0182 A79-26184
EF-77-A-01-2674
p0133 N79-11478
p0136 N79-17335
p0068 N79-20200
p0138 N79-24446
p0139 N79-25499
p0142 N79-30720
EPEI PROJ. RP1082-1
p0155 N79-33560
EX-76-A-29-1002
p0149 A79-42345
EX-76-A-29-1060
p0139 N79-26476
EX-76-A-31-1026
p0166 N79-33881
p0166 N79-33882
p0166 N79-33883
p0167 N79-33884
EX-76-I-01-1028
p0142 N79-28727
F04071-77-C-0166
p0050 N79-24049
F04701-77-C-0166
p0050 N79-24051
F33615-72-C-1739
p0130 A79-27938
F33615-76-C-2090
p0006 A79-30504
F44620-70-C-0042
p0186 A79-44548
GEORGIA TECH. PROJ. A-1855
p0041 N79-26101
p0041 N79-26102
JPL-954883
p0154 N79-32652
MIPR-W00953-77-MP09018
p0101 A79-10880
p0101 A79-10888
NASA ORDER C-1892-D
p0151 N79-13490
NASA ORDER C-7653
p0153 N79-20497
NASA ORDER C-8756
p0082 N79-23216
NASA ORDER C-10669-D
p0122 N79-25395
NASA ORDER C-41581-B
p0032 N79-18977
NASW-3199
p0013 N79-12063
NAS3-1960
p0101 A79-49398
NAS3-11175
p0108 A79-42890
NAS3-13231
p0080 N79-33305
NAS3-14336
p0106 N79-22428
p0107 N79-22429
NAS3-16824
p0123 A79-16011
p0123 A79-32412
p0124 A79-32423
p0122 N79-31603
NAS3-17760
p0130 A79-27938
NAS3-17790
p0125 N79-21410
p0125 N79-21411
p0125 N79-21412
NAS3-17800
p0121 N79-17221
NAS3-17830
p0129 N79-10479
NAS3-17853
p0036 A79-26925
p0177 N79-14875
NAS3-17860
p0111 N79-27478
NAS3-17863
p0178 A79-26923

NAS3-18021
p0029 A79-38984
NAS3-18029
p0151 N79-11476
NAS3-18517
p0150 N79-10526
p0120 N79-11407
p0120 N79-11408
p0120 N79-11409
NAS3-18520
p0123 A79-32351
p0121 N79-17228
p0122 N79-25392
NAS3-18541
p0151 N79-12554
NAS3-18546
p0122 N79-24373
NAS3-18553
p0177 N79-25845
NAS3-18906
p0123 A79-26985
NAS3-18908
p0128 A79-21298
p0166 N79-29832
p0166 N79-29833
NAS3-18916
p0100 N79-21273
NAS3-18937
p0161 A79-17180
NAS3-18941
p0067 A79-20859
NAS3-18943
p0034 N79-23970
NAS3-19154
p0045 A79-45374
NAS3-19401
p0152 N79-19448
NAS3-19427
p0123 A79-23252
p0088 A79-31957
NAS3-19432
p0151 N79-12550
NAS3-19436
p0121 N79-17219
NAS3-19690
p0101 A79-10880
p0099 A79-10881
p0099 A79-10885
p0101 A79-10888
NAS3-19709
p0066 N79-26120
NAS3-19711
p0079 N79-16948
NAS3-19712
p0067 N79-33258
NAS3-19715
p0123 A79-12848
p0032 N79-17857
NAS3-19721
p0056 N79-11115
NAS3-19728
p0057 A79-22396
NAS3-19736
p0031 N79-12088
p0177 N79-17656
p0091 A79-26221
p0035 N79-31207
NAS3-19745
p0178 A79-26910
p0178 N79-32056
NAS3-19752
p0032 N79-16853
NAS3-19755
p0036 A79-36737
p0016 N79-15052
NAS3-19773
p0150 N79-10525
NAS3-19777
p0177 N79-26884
p0177 N79-26885
p0177 N79-26886
NAS3-19778
p0151 N79-12553
NAS3-19780
p0152 N79-16374

CONTRACT NUMBER INDEX

NAS3-19856
p0106 N79-12366
NAS3-19885
p0098 A79-15305
NAS3-20027
p0033 N79-20117
NAS3-20030
p0036 A79-36749
NAS3-20040
p0067 N79-31350
NAS3-20041
p0034 N79-25020
NAS3-20042
p0154 N79-31784
NAS3-20045
p0120 N79-10423
NAS3-20048
p0036 A79-40759
NAS3-20050
p0178 A79-26936
p0176 N79-14873
NAS3-20056
p0031 N79-11068
NAS3-20058
p0155 A79-20825
p0155 A79-20826
p0156 A79-20827
p0156 A79-27400
p0156 A79-51780
NAS3-20061
p0178 A79-28964
p0036 A79-40759
p0034 N79-30185
p0034 N79-30186
p0035 N79-31212
NAS3-20068
p0121 N79-17222
p0121 N79-17223
NAS3-20071
p0176 N79-10842
NAS3-20073
p0080 N79-24121
NAS3-20079
p0066 N79-16924
NAS3-20091
p0032 N79-17858
NAS3-20092
p0108 N79-33432
NAS3-20101
p0056 N79-14153
NAS3-20102
p0101 A79-10880
p0101 A79-10888
p0101 A79-48653
NAS3-20109
p0057 N79-28224
NAS3-20110
p0095 A79-29784
p0041 N79-26101
p0041 N79-26102
NAS3-20112
p0092 N79-29382
NAS3-20118
p0032 N79-18978
p0067 N79-31348
NAS3-20233
p0186 A79-44548
NAS3-20270
p0145 A79-10113
NAS3-20296
p0110 N79-12418
NAS3-20298
p0110 N79-19314
NAS3-20364
p0095 A79-30395
p0095 A79-12273
p0094 A79-20300
NAS3-20365
p0096 A79-17071
p0096 A79-18159
p0096 A79-18160
NAS3-20367
p0030 N79-10058
NAS3-20370
p0079 N79-12202
NAS3-20372
p0112 N79-21337
NAS3-20376
p0112 N79-32538
NAS3-20377
p0080 N79-32326

NAS3-20380
p0012 N79-12087
p0080 N79-26175
NAS3-20383
p0079 N79-20222
NAS3-20393
p0056 N79-10120
NAS3-20394
p0091 N79-20267
NAS3-20401
p0057 N79-31341
NAS3-20402
p0067 N79-30295
NAS3-20483
p0131 N79-12524
NAS3-20497
p0091 N79-10226
NAS3-20579
p0153 N79-29603
NAS3-20582A
p0031 N79-13048
NAS3-20591
p0034 N79-26055
NAS3-20595
p0188 N79-12968
NAS3-20602
p0036 A79-40759
NAS3-20603
p0071 N79-10165
p0091 N79-20266
NAS3-20604
p0155 N79-33581
NAS3-20609
p0030 N79-10061
NAS3-20615
p0155 A79-10106
p0155 A79-17321
p0153 N79-19454
NAS3-20621
p0155 N79-33581
NAS3-20628
p0012 N79-12084
NAS3-20629
p0033 N79-21074
p0038 N79-33206
NAS3-20630
p0033 N79-20116
p0033 N79-21076
NAS3-20631
p0039 N79-29191
NAS3-20632
p0036 A79-40483
NAS3-20644
p0050 N79-27234
NAS3-20646
p0032 N79-16850
p0035 N79-30189
NAS3-20756
p0033 N79-21073
NAS3-20757
p0039 N79-29189
NAS3-20758
p0034 N79-25017
NAS3-20795
p0122 N79-32551
NAS3-20797
p0178 A79-26890
p0177 N79-27933
NAS3-20802
p0031 N79-13050
NAS3-20804
p0036 A79-39035
p0071 N79-22244
NAS3-20805
p0152 N79-16375
NAS3-20808
p0036 A79-36749
NAS3-20809
p0033 N79-23085
NAS3-20810
p0031 N79-11042
NAS3-20811
p0034 N79-23084
NAS3-20814
p0091 N79-29355
NAS3-20815
p0009 N79-23940
p0091 N79-24172
NAS3-20823
p0143 N79-32648

NAS3-20827
p0087 N79-28315
NAS3-21005
p0111 A79-38738
p0180 N79-27975
NAS3-21006
p0031 N79-15053
NAS3-21009
p0087 N79-29331
NAS3-21010
p0087 N79-23218
NAS3-21011
p0087 N79-18053
NAS3-21014
p0087 N79-12238
NAS3-21015
p0032 N79-18976
NAS3-21018
p0072 N79-32303
NAS3-21019
p0079 N79-11180
NAS3-21020
p0129 N79-13405
p0129 N79-13406
NAS3-21027
p0180 N79-12884
NAS3-21028
p0152 N79-17330
NAS3-21045
p0100 N79-20317
NAS3-21048
p0050 N79-24049
p0050 N79-24051
NAS3-21049
p0057 N79-19074
NAS3-21050
p0049 A79-30140
p0171 A79-50938
p0047 N79-24011
p0049 N79-24012
p0100 N79-27397
p0100 N79-27398
NAS3-21130
p0107 N79-22434
NAS3-21134
p0112 A79-38202
p0111 N79-26384
NAS3-21135
p0005 A79-19524
NAS3-21137
p0112 N79-21334
p0112 N79-21335
NAS3-21139
p0006 N79-12014
NAS3-21200
p0107 N79-25349
NAS3-21205
p0015 N79-15046
NAS3-21249
p0160 A79-44810
NAS3-21250
p0154 N79-32652
NAS3-21253
p0057 A79-51907
NAS3-21255
p0072 N79-31358
NAS3-21256
p0035 N79-32211
NAS3-21264
p0088 A79-51103
p0153 N79-26506
NAS3-21267
p0107 N79-28456
NAS3-21276
p0143 N79-32648
NAS3-21354
p0040 N79-20161
NAS3-21361
p0057 N79-19073
NAS3-21363
p0100 N79-25312
NAS3-21367
p0096 N79-33373
p0096 N79-33374
NAS3-21369
p0087 N79-30377
NAS3-21378
p0101 N79-28418
NAS3-21390
p0122 N79-31602

NAS3-21609
p0107 N79-30514
NAS7-100
p0184 A79-10417
NAS8-26752
p0101 A79-49397
NAS8-30820 A79-50334
NGL-5025
p0096 A79-33793
NGR-05-067-001
p0060 A79-32924
NGR-06-002-112
p0056 N79-15152
p0056 N79-16913
NGR-15-005-162
p0025 A79-19698
NGR-15-005-191
p0025 A79-19698
p0002 N79-10023
NGR-22-009-339
p0129 N79-18343
NGR-22-009-378
p0021 N79-25008
NGR-31-009-004
p0108 A79-42890
NGR-33-022-157
p0130 N79-26429
NGR-39-087-047
p0077 A79-24262
NSF ZWG-74-23778
p0182 A79-15597
NSG-1244
p0108 A79-32912
NSG-2151
p0112 A79-32981
NSG-3009
p0072 N79-25178
NSG-3011
p0057 N79-26110
NSG-3014
p0184 N79-13886
NSG-3018
p0154 N79-32647
NSG-3019
p0070 A79-19480
NSG-3033
p0006 A79-30504
NSG-3041
p0079 N79-20221
NSG-3051
p0072 N79-33288
NSG-3052
p0072 N79-23168
NSG-3066
p0035 N79-32212
NSG-3082
p0130 N79-19414
NSG-3086
p0179 N79-19828
p0182 N79-26943
NSG-3087
p0150 A79-47651
NSG-3094
p0179 N79-18711
NSG-3097
p0049 N79-24046
NSG-3107
p0078 A79-50912
NSG-3131
p0186 N79-11921
NSG-3133
p0005 A79-19495
p0028 A79-32329
NSG-3134
p0153 N79-20487
NSG-3138
p0159 N79-27716
NSG-3148
p0020 N79-24999
NSG-3150
p0049 N79-24007
p0049 N79-24008
NSG-3160
p0168 A79-40494
NSG-3166
p0049 N79-24038
NSG-3169
p0072 N79-25183
p0080 N79-25184
NSG-3179
p0067 N79-30294

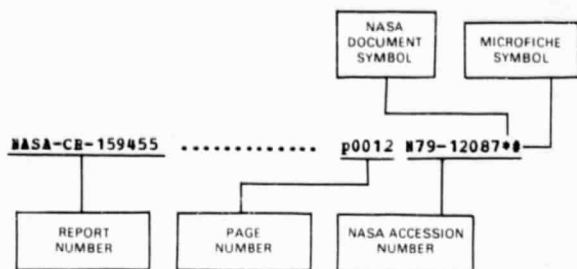
CONTRACT NUMBER INDEX

p0130 N79-31627
 NSG-3186 p0182 A79-26184
 NSG-3214 p0080 N79-25196
 NSG-5051 p0058 A79-51911
 NSG-7317 p0121 A79-17226
 N00140-73-C-005 p0031 N79-11068
 N00140-74-C-0759 p0031 N79-11068
 PROJECT SQUID p0085 A79-21295
 p0038 A79-21296
 R79AEG288 p0034 N79-25020
 W-7405-ENG-26 p0145 A79-10101
 p0122 N79-25355
 W-7405-ENG-92 p0185 A79-20539
 198-10 p0157 N79-18479
 p0158 N79-22654
 p0158 N79-31841
 p0008 N79-33171
 505-p4 p0022 N79-25022
 505-01 p0082 N79-21204
 p0166 N79-23688
 p0063 N79-28254
 505-01-12 p0067 N79-33258
 505-02-12 p0067 N79-31348
 505-03-22 p0031 N79-12088
 505-04 p0002 N79-10022
 p0013 N79-10060
 p0113 N79-10424
 p0014 N79-13046
 p0081 N79-13158
 p0081 N79-13159
 p0113 N79-13369
 p0015 N79-14098
 p0015 N79-14099
 p0017 N79-16852
 p0109 N79-17195
 p0173 N79-17659
 p0103 N79-18288
 p0114 N79-18323
 p0082 N79-21205
 p0111 N79-21329
 p0115 N79-22518
 p0018 N79-23967
 p0022 N79-25023
 p0023 N79-27142
 p0023 N79-27143
 p0023 N79-28177
 p0024 N79-30191
 p0084 N79-30381
 p0024 N79-31213
 p0024 N79-31214
 p0116 N79-31605
 p0038 N79-33210
 p0116 N79-33476
 505-04-22 p0034 N79-23085
 p0107 N79-28456
 505-04-42 p0122 N79-31602
 505-05 p0097 N79-14309
 p0003 N79-14996
 p0001 N79-16796
 p0166 N79-21798
 p0038 N79-29186
 506-10 p0082 N79-23216
 506-16 p0113 N79-10425
 p0114 N79-14386
 p0114 N79-14389
 p0081 N79-15184
 p0059 N79-21128
 p0074 N79-21184
 p0115 N79-22519
 p0083 N79-29327
 p0084 N79-30380
 p0059 N79-31346
 p0115 N79-31604
 p0084 N79-32359
 506-20 p0097 N79-17139
 p0097 N79-22375

p0098 N79-28420
 506-21 p0053 N79-23132
 p0090 N79-28350
 p0105 N79-29467
 p0105 N79-29468
 506-23 p0184 N79-13886
 p0046 N79-15149
 p0069 N79-22246
 p0098 N79-32467
 506-23-24 p0067 N79-31350
 506-25 p0181 N79-19867
 510-53-02 p0080 N79-24121
 510-55 p0003 N79-13003
 511-55-02 p0071 N79-22244
 p0072 N79-31358
 610-22 p0094 N79-14275
 p0044 N79-21120
 743-03 p0023 N79-28176
 778-11 p0137 N79-22626

REPORT/ACCESSION NUMBER INDEX

Typical Report/Accession Number Index Listing



Listings in this index are arranged alphanumerically by report number. The page number indicates the page in the abstract section in which the citation is located. The accession number denotes the number by which the citation is identified. An asterisk (*) indicates that the item is a NASA report. A pound sign (#) indicates that the item is available on microfiche. A plus sign (+) indicates a document that cannot be microfiched but for which one-to-one facsimile is available.

NAS PAPER 78-192 p0190 A79-21277**
 AD-A060452 p0016 N79-15052**
 AD-A065049 p0018 N79-23066 #
 AFFDL-TR-78-168 p0018 N79-23066 #
 AFGL-TR-79-0082 p0047 N79-24001**
 AIAA PAPER 78-1768 p0146 A79-13867**
 AIAA PAPER 79-0016 p0070 A79-19480**
 AIAA PAPER 79-0042 p0005 A79-19495**
 AIAA PAPER 79-0081 p0005 A79-19524**
 AIAA PAPER 79-0104 p0005 A79-19533**
 AIAA PAPER 79-0105 p0025 A79-23512**
 AIAA PAPER 79-0182 p0174 A79-19581**
 AIAA PAPER 79-0183 p0174 A79-19582**
 AIAA PAPER 79-0187 p0070 A79-19586**
 AIAA PAPER 79-0379 p0025 A79-19698**
 AIAA PAPER 79-0380 p0005 A79-23510**
 AIAA PAPER 79-0381 p0025 A79-23509**
 AIAA PAPER 79-0386 p0049 A79-23511**
 AIAA PAPER 79-0538 p0026 A79-25856**
 AIAA PAPER 79-0561 p0026 A79-25870**
 AIAA PAPER 79-0577 p0175 A79-26911**
 AIAA PAPER 79-0581 p0027 A79-26944**
 AIAA PAPER 79-0599 p0178 A79-26910**
 AIAA PAPER 79-0600 p0026 A79-26881**
 AIAA PAPER 79-0615 p0178 A79-26936**
 AIAA PAPER 79-0624 p0175 A79-26880**
 AIAA PAPER 79-0631 p0175 A79-28963**
 AIAA PAPER 79-0633 p0178 A79-28964**
 AIAA PAPER 79-0635 p0175 A79-32126**
 AIAA PAPER 79-0637 p0178 A79-26923**
 AIAA PAPER 79-0641 p0026 A79-26877**
 AIAA PAPER 79-0654 p0026 A79-26926**
 AIAA PAPER 79-0656 p0036 A79-26925**
 AIAA PAPER 79-0669 p0011 A79-28970**
 AIAA PAPER 79-0679 p0178 A79-26890**
 AIAA PAPER 79-0965 p0148 A79-38888**
 AIAA PAPER 79-0989 p0147 A79-38191**
 AIAA PAPER 79-0990 p0147 A79-38192**
 AIAA PAPER 79-1000 p0149 A79-44225**
 AIAA PAPER 79-1015 p0112 A79-38202**
 AIAA PAPER 79-1163 p0006 A79-47347**
 AIAA PAPER 79-1170 p0028 A79-38969**
 AIAA PAPER 79-1179 p0055 A79-36972**
 AIAA PAPER 79-1182 p0055 A79-39815**
 AIAA PAPER 79-1192 p0078 A79-38977**
 AIAA PAPER 79-1195 p0090 A79-38980**
 AIAA PAPER 79-1199 p0029 A79-38981**
 AIAA PAPER 79-1203 p0029 A79-38984**

AIAA PAPER 79-1204 p0029 A79-39814**
 AIAA PAPER 79-1234 p0036 A79-40483**
 AIAA PAPER 79-1308 p0030 A79-40488**
 AIAA PAPER 79-1309 p0029 A79-39031**
 AIAA PAPER 79-1312 p0036 A79-40759**
 AIAA PAPER 79-1318 p0029 A79-39034**
 AIAA PAPER 79-1319 p0036 A79-39035**
 AIAA PAPER 79-1320 p0071 A79-39036**
 AIAA PAPER 79-1521 p0176 A79-46707**
 AIAA PAPER 79-1524 p0176 A79-47340**
 AIAA PAPER 79-1664 p0006 A79-47346**
 AIAA PAPER 79-1824 p0038 A79-53750**
 AIAA PAPER 79-1861 p0030 A79-47918**
 AIAA 79-0733 p0005 A79-29007**
 AIAA 79-0763 p0077 A79-28276**
 AIAA 79-0783 p0128 A79-29027**
 AIAA 79-0860 p0054 A79-34704**
 AIAA 79-0881 p0055 A79-34773**
 AIAA 79-0910 p0055 A79-34774**
 AIAA 79-0911 p0054 A79-34736**
 AIAA 79-0913 p0055 A79-34775**
 AIAA 79-0914 p0055 A79-34737**
 AIAA 79-1730 p0045 A79-45374**
 AIAA 79-7008 p0027 A79-29383**
 AIAA 79-7011 p0027 A79-29386**
 AIAA-PAPER-79-0381 p0003 N79-14999**
 AIAA-PAPER-79-0641 p0016 N79-15957**
 AIAA-PAPER-79-2063 p0054 N79-33252**
 AIAA-PAPER-79-2064 p0054 N79-33255**
 AIAA-PAPER-79-2081 p0054 N79-33253**
 AIAA-78-1000 p0141 N79-27665**
 AIAA-79-0105 p0015 N79-15049**
 AIAA-79-1524 p0174 N79-27930**
 AIAA-79-1824 p0024 N79-31210**
 AIRESEARCH-21-2953-1 p0080 N79-24121**
 AIRESEARCH-31-2935-1 p0120 N79-11408**
 AIRESEARCH-31-2935-2 p0120 N79-11409**
 AIRESEARCH-31-2936 p0120 N79-11407**
 AIRESEARCH-31-2937 p0150 N79-10526**
 AIRESEARCH-78-14972 p0151 N79-11476**
 AL78P022-VOL-1 p0121 N79-17222**
 AL78P023-VOL-2 p0121 N79-17223**
 AL78T007 p0121 N79-17219**
 ASLE PREPRINT 78-LC-1A-1 p0118 A79-23267**
 ASLE PREPRINT 78-LC-3C-1 p0123 A79-23252**
 ASLE PREPRINT 78-LC-5C-2 p0118 A79-23251**
 ASME PAPER 78-GT-128 p0024 A79-10792**
 ASME PAPER 78-GT-148 p0110 A79-10800**
 ASME PAPER 78-LUE-1 p0118 A79-23229**
 ASME PAPER 78-LUE-18 p0118 A79-23235**
 ASME PAPER 78-LUE-24 p0118 A79-23237**
 ASME PAPER 78-LUE-34 p0118 A79-23246**
 ASME PAPER 78-WA/HT-37 p0093 A79-19816**
 ASME PAPER 79-DE-5 p0150 A79-47651**
 ASME PAPER 79-GT-5 p0006 A79-30504**
 ASME PAPER 79-GT-6 p0028 A79-32329**
 ASME PAPER 79-GT-19 p0027 A79-30553**
 ASME PAPER 79-GT-38 p0147 A79-30554**
 ASME PAPER 79-GT-42 p0027 A79-30521**
 ASME PAPER 79-GT-51 p0006 A79-30527**
 ASME PAPER 79-GT-56 p0123 A79-32351**
 ASME PAPER 79-GT-129 p0039 A79-32398**
 ASME PAPER 79-GT-141 p0090 A79-30555**
 ASME PAPER 79-GT-146 p0123 A79-32412**
 ASME PAPER 79-GT-149 p0119 A79-32414**
 ASME PAPER 79-GT-161 p0124 A79-32423**
 ASME PAPER 79-GT-170 p0106 A79-30556**
 ASME PAPER 79-GT-197 p0027 A79-30557**

REPORT/ACCESSION NUMBER INDEX

ASRL-TR-154-10	p0129	N79-18343**	DOE/NASA/1028-78/20	p0134	N79-12548**
AVRADCOM-TE-78-21	p0104	N79-22427**	DOE/NASA/1028-79/1	p0135	N79-17333**
AVRADCOM-TE-78-36	p0113	N79-13369**	DOE/NASA/1028-79/23	p0142	N79-30719**
AVRADCOM-TE-78-38 (PL)	p0013	N79-11043**	DOE/NASA/1028-79/24	p0142	N79-28727**
AVRADCOM-TE-78-41	p0015	N79-14099**	DOE/NASA/1034-78/3	p0134	N79-11481**
AVRADCOM-TE-78-42	p0082	N79-21205**	DOE/NASA/1034-79/1	p0137	N79-21550**
AVRADCOM-TE-78-47	p0073	N79-12204**	DOE/NASA/1034-79/2	p0136	N79-20498**
AVRADCOM-TE-78-48	p0115	N79-23430**	DOE/NASA/1040-78/4	p0134	N79-11480**
AVRADCOM-TE-78-49	p0023	N79-27143**	DOE/NASA/1040-78/5	p0135	N79-16356**
AVRADCOM-TE-78-52	p0081	N79-12223**	DOE/NASA/1040-78/30	p0188	N79-16721**
AVRADCOM-TE-78-54	p0002	N79-12015**	DOE/NASA/1040-79/6	p0188	N79-27023**
AVRADCOM-TE-78-59	p0073	N79-12203**	DOE/NASA/1040-79/8	p0084	N79-30379**
AVRADCOM-TE-78-62	p0061	N79-16075**	DOE/NASA/1044-79/2	p0098	N79-26316**
AVRADCOM-TE-78-63	p0062	N79-16921**	DOE/NASA/1044-79/3	p0142	N79-28728**
AVRADCOM-TE-79-4	p0001	N79-20008**	DOE/NASA/1059-79/2	p0140	N79-26504**
AVRADCOM-TE-79-6	p0062	N79-16920**	DOE/NASA/1060-78/1	p0139	N79-26476**
AVRADCOM-TE-79-10	p0024	N79-30191**	DOE/NASA/1062-79/1	p0138	N79-24444**
AVRADCOM-TE-79-12	p0018	N79-23968**	DOE/NASA/1062-79/2	p0141	N79-27665**
AVRADCOM-TE-79-18	p0018	N79-23964**	DOE/NASA/1892-78/1	p0151	N79-13490**
AVRADCOM-TE-79-18	p0018	N79-23964**	DOE/NASA/2593-78/3	p0073	N79-11179**
AVRADCOM-TE-79-19	p0019	N79-23969**	DOE/NASA/2593-78/4	p0135	N79-17334**
AVRADCOM-TE-79-20	p0116	N79-32552**	DOE/NASA/2593-79/1	p0089	N79-20265**
AVRADCOM-TE-79-26	p0116	N79-33476**	DOE/NASA/2593-79/6	p0139	N79-25498**
AVRADCOM-TE-79-47	p0085	N79-33325**	DOE/NASA/2674-78/1	p0133	N79-11478**
BCS-40159-1	p0166	N79-33881**	DOE/NASA/2674-78/2	p0136	N79-17335**
BCS-40180-2-REV	p0166	N79-33882**	DOE/NASA/2674-79/1	p0068	N79-20200**
BCS-40262-1	p0166	N79-33883**	DOE/NASA/2674-79/5	p0139	N79-25499**
BCS-40262-2	p0167	N79-33884**	DOE/NASA/2674-79/6	p0138	N79-24446**
C-081	p0142	N79-28727**	DOE/NASA/3082-78/1	p0142	N79-30720**
C-9180	p0126	N79-19415**	DOE/NASA/3082-78/1	p0130	N79-19414**
CASD-LVP-78-C78	p0050	N79-27234**	DOE/NASA/7653-79/1	p0153	N79-20497**
COMS-5082-1	p0154	N79-30801**	DOE/NASA/9773-78/1	p0150	N79-10525**
COMS/4396-3	p0120	N79-11406**	DOE/NASA/11272-79/1	p0139	N79-25500**
COMS/5031-1	p0151	N79-11473**	DOE/NASA/20305-79/3	p0141	N79-28725**
CREASE-TN-289	p0111	N79-27478**	DOE/NASA/20485-79/1	p0138	N79-24443**
C76-1555/501	p0112	N79-32538**	DOE/NASA/20485-79/2	p0140	N79-26503**
C79-386/501	p0180	N79-27975**	DOE/NASA/20485-79/3	p0139	N79-25501**
D-133	p0143	N79-32640**	DOE/NASA/20485-79/4	p0142	N79-29599**
DDA-EDR-9528	p0033	N79-21073**	D6-48097	p0091	N79-24172**
DDA-EDR-9719	p0189	N79-31087**	D6-48611	p0009	N79-23940**
DDA-EDR-9790	p0189	N79-32129**	D6146	p0087	N79-28315**
DDA-EN-79-A	p0107	N79-28456**	E-001	p0046	N79-24000**
DOC-78SDS4252	p0151	N79-12554**	E-003	p0131	N79-22589**
DOC-79SDS4218	p0153	N79-26506**	E-004	p0018	N79-23964**
DOE/NASA/0004-79/1	p0189	N79-32129**	E-004	p0018	N79-23964**
DOE/NASA/0008-78/4	p0188	N79-12969**	E-005	p0138	N79-24443**
DOE/NASA/0012-78/1-VOL-1	p0151	N79-13496**	E-006	p0003	N79-23911**
DOE/NASA/0012-78/1-VOL-2	p0152	N79-13497**	E-010	p0012	N79-23965**
DOE/NASA/0012-79/2	p0155	N79-33560**	E-011	p0173	N79-24770**
DOE/NASA/0019-78/1	p0033	N79-21075**	E-012	p0046	N79-22188**
DOE/NASA/0028-79/1	p0189	N79-31087**	E-013	p0018	N79-23966**
DOE/NASA/0032-79/1	p0188	N79-29110**	E-013	p0018	N79-23966**
DOE/NASA/0037-79/1	p0189	N79-31088**	E-014	p0104	N79-23384**
DOE/NASA/0038-79/1	p0153	N79-21554**	E-015	p0109	N79-22448**
DOE/NASA/0040-78/1	p0152	N79-19451**	E-016	p0138	N79-24444**
DOE/NASA/0042-79/1-VOL-1	p0166	N79-33881**	E-018	p0137	N79-22624**
DOE/NASA/0042-79/2-VOL-2	p0166	N79-33882**	E-023	p0140	N79-26503**
DOE/NASA/0042-79/3-VOL-1	p0166	N79-33883**	E-025	p0094	N79-23313**
DOE/NASA/0042-79/4-VOL-2	p0167	N79-33884**	E-026	p0022	N79-25016**
DOE/NASA/0067-79/1	p0153	N79-29604**	E-027	p0004	N79-23912**
DOE/NASA/0207-78/1	p0102	N79-15267**	E-028	p0083	N79-27306**
DOE/NASA/0207-79/1	p0103	N79-20341**	E-030	p0174	N79-25840**
DOE/NASA/0207-79/3	p0104	N79-23384**	E-031	p0174	N79-25841**
DOE/NASA/0615-79/1	p0153	N79-19454**	E-033	p0116	N79-33475**
DOE/NASA/1002-78/1	p0133	N79-11479**	E-034	p0139	N79-25500**
DOE/NASA/1002-78/2	p0138	N79-24445**	E-035	p0142	N79-30719**
DOE/NASA/1002-79/3	p0138	N79-24442**	E-036	p0138	N79-24446**
DOE/NASA/1002-79/4	p0141	N79-26505**	E-038	p0165	N79-28881**
DOE/NASA/1004-79/1	p0136	N79-20494**	E-039	p0140	N79-26504**
DOE/NASA/1004-79/16	p0140	N79-26502**	E-040	p0043	N79-27236**
DOE/NASA/1011-78/28	p0017	N79-17859**	E-042	p0053	N79-23133**
DOE/NASA/1011-78/29	p0014	N79-13049**	E-043	p0004	N79-27093**
DOE/NASA/1022-78/42	p0136	N79-17336**	E-045	p0075	N79-29292**
DOE/NASA/1028-72/2	p0137	N79-21549**	E-046	p0075	N79-23196**
DOE/NASA/1028-78/19	p0135	N79-16355**	E-048	p0127	N79-24359**
			E-049	p0044	N79-31264**
			E-050	p0022	N79-25015**
			E-051	p0043	N79-27235**
			E-052	p0115	N79-24350**
			E-053	p0141	N79-26505**
			E-057	p0059	N79-27242**
			E-058	p0075	N79-30355**
			E-059	p0043	N79-25129**
			E-060	p0053	N79-25131**
			E-062	p0022	N79-27140**
			E-064	p0104	N79-27460**
			E-067	p0141	N79-28725**

REPORT/ACCESSION NUMBER INDEX

E-06C	p0110	N79-27480**	E-9670	p0114	N79-14387**
E-071	p0139	N79-25501**	E-9673	p0113	N79-10425**
E-072	p0142	N79-30720**	E-9673-1	p0184	N79-16699**
E-075	p0141	N79-27663**	E-9681	p0081	N79-15184**
E-078	p0094	N79-27351**	E-9684	p0114	N79-14386**
E-082	p0168	N79-28970**	E-9688	p0114	N79-13046**
E-088	p0089	N79-28349**	E-9694	p0002	N79-10023**
E-089	p0022	N79-27141**	E-9697	p0082	N79-23216**
E-091	p0075	N79-29293**	E-9700	p0024	N79-31213**
E-092	p0084	N79-30378**	E-9713	p0052	N79-10122**
E-093	p0174	N79-27930**	E-9714	p0024	N79-31214**
E-094	p0142	N79-29599**	E-9715	p0081	N79-13159**
E-095	p0069	N79-27279**	E-9720	p0126	N79-11433**
E-096	p0004	N79-29143**	E-9728	p0097	N79-22375**
E-098	p0105	N79-7461**	E-9729	p0098	N79-27400**
E-100	p0142	N79-28728**	E-9730	p0013	N79-11043**
E-106	p0141	N79-27664**	E-9732	p0015	N79-14098**
E-107	p0053	N79-28220**	E-9735	p0044	N79-21120**
E-110	p0004	N79-28146**	E-9743	p0157	N79-17358**
E-111	p0063	N79-29224**	E-9745	p0073	N79-12203**
E-112	p0170	N79-29938**	E-9749	p0097	N79-17139**
E-115	p0090	N79-31405**	E-9754	p0181	N79-19867**
E-116	p0142	N79-28726**	E-9756	p0003	N79-14996**
E-118	p0064	N79-30296**	E-9762	p0015	N79-14099**
E-120	p0069	N79-28258**	E-9763	p0173	N79-17659**
E-123	p0063	N79-29240**	E-9765	p0114	N79-17227**
E-125	p0076	N79-30356**	E-9767	p0103	N79-18288**
E-130	p0083	N79-29329**	E-9769	p0046	N79-11109**
E-131	p0105	N79-31526**	E-9770	p0082	N79-21205**
E-132	p0084	N79-30379**	E-9774	p0002	N79-11001**
E-134	p0064	N79-31349**	E-9775	p0017	N79-17859**
E-141	p0142	N79-29600**	E-9777	p0134	N79-11481**
E-142	p0174	N79-31002**	E-9778	p0059	N79-21128**
E-143	p0023	N79-30187**	E-9779	p0133	N79-11479**
E-146	p0010	N79-31185**	E-9780	p0188	N79-11955**
E-148	p0105	N79-31527**	E-9782	p0002	N79-12016**
E-149	p0090	N79-31403**	E-9783	p0133	N79-11478**
E-151	p0143	N79-31781**	E-9785	p0002	N79-11000**
E-152	p0084	N79-31391**	E-9786	p0024	N79-30911**
E-153	p0125	N79-29530**	E-9787	p0073	N79-11179**
E-155	p0048	N79-31265**	E-9788	p0133	N79-11477**
E-161	p0069	N79-31361**	E-9789	p0073	N79-12204**
E-165	p0024	N79-31210**	E-9790	p0181	N79-12909**
E-166	p0053	N79-30290**	E-9792	p0062	N79-12153**
E-168	p0054	N79-33252**	E-9795	p0137	N79-22626**
E-169	p0054	N79-33253**	E-9796	p0102	N79-12361**
E-170	p0105	N79-30515**	E-9799	p0136	N79-17335**
E-171	p0076	N79-33306**	E-9800	p0016	N79-15961**
E-174	p0127	N79-31619**	E-9801	p0166	N79-23688**
E-175	p0054	N79-33254**	E-9802	p0016	N79-15051**
E-176	p0010	N79-33185**	E-9803	p0134	N79-11480**
E-180	p0094	N79-33379**	E-9804	p0089	N79-15199**
E-181	p0054	N79-31343**	E-9805	p0046	N79-15150**
E-183	p0024	N79-30188**	E-9806	p0115	N79-22519**
E-188	p0076	N79-31372**	E-9807	p0135	N79-17334**
E-191	p0054	N79-33255**	E-9808	p0109	N79-17195**
E-236	p0116	N79-33477**	E-9809	p0074	N79-21184**
E-1009	p0053	N79-22193**	E-9811	p0136	N79-17336**
E-8342	p0163	N79-25753**	E-9813	p0111	N79-21329**
E-8950	p0023	N79-28176**	E-9814	p0082	N79-21204**
E-8958	p0018	N79-23967**	E-9815	p0115	N79-22518**
E-8987	p0023	N79-28177**	E-9816	p0157	N79-18479**
E-8997	p0017	N79-16852**	E-9817	p0157	N79-12586**
E-9025	p0002	N79-10022**	E-9818	p0134	N79-12548**
E-9120	p0113	N79-10424**	E-9819	p0081	N79-12223**
E-9167	p0046	N79-15145**	E-9821	p0059	N79-11119**
E-9179-1	p0082	N79-15186**	E-9822	p0139	N79-26476**
E-9181-1	p0002	N79-12015**	E-9823	p0172	N79-15759**
E-9186	p0003	N79-13003**	E-9824	p0073	N79-12201**
E-9202	p0094	N79-14111**	E-9826	p0172	N79-15756**
E-9219	p0166	N79-21118**	E-9827	p0116	N79-31605**
E-9237	p0023	N79-27143**	E-9828	p0014	N79-12086**
E-9265-1	p0115	N79-23430**	E-9829	p0158	N79-22654**
E-9348	p0157	N79-17359**	E-9830	p0069	N79-22246**
E-9413	p0135	N79-16355**	E-9831	p0061	N79-15157**
E-9419	p0140	N79-26502**	E-9832	p0017	N79-22099**
E-9461	p0013	N79-10060**	E-9833	p0135	N79-16357**
E-9490	p0001	N79-16796**	E-9834	p0068	N79-16930**
E-9517	p0104	N79-22427**	E-9835	p0134	N79-15403**
E-9528	p0074	N79-20218**	E-9836	p0062	N79-12154**
E-9578	p0097	N79-14309**	E-9838	p0059	N79-22194**
E-9588	p0109	N79-12414**	E-9839	p0135	N79-16356**
E-9600	p0064	N79-13158**	E-9840	p0073	N79-12205**
E-9629	p0184	N79-13886**	E-9841	p0062	N79-12150**
E-9632	p0113	N79-13369**	E-9842	p0082	N79-16984**
E-9647	p0131	N79-13472**	E-9844	p0013	N79-12085**
E-9651	p0114	N79-11389**	E-9845	p0172	N79-15757**
E-9657	p0114	N79-18323**	E-9846	p0022	N79-25023**
E-9659	p0105	N79-29468**	E-9846-1	p0017	N79-20118**

REPORT/ACCESSION NUMBER INDEX

E-9847	p0102	N79-12362**	E-9956	p0059	N79-31346**
E-9848	p0188	N79-16721**	E-9957	p0137	N79-21550**
E-9853	p0015	N79-15047**	E-9958	p0018	N79-23968**
E-9854	p0172	N79-15758**	E-9960	p0003	N79-20069**
E-9857	p0126	N79-15325**	E-9961	p0053	N79-22191**
E-9860	p0002	N79-12020**	E-9962	p0169	N79-23735**
E-9861	p0172	N79-16644**	E-9963	p0103	N79-20338**
E-9862	p0015	N79-15048**	E-9965	p0084	N79-30381**
E-9863	p0015	N79-15050**	E-9966	p0103	N79-20346**
E-9865	p0003	N79-14998**	E-9968	p0127	N79-22565**
E-9866	p0003	N79-14999**	E-9969	p0105	N79-29467**
E-9867	p0127	N79-20391**	E-9970	p0136	N79-20498**
E-9868	p0074	N79-20216**	E-9971	p0083	N79-27309**
E-9870	p0053	N79-23132**	E-9972	p0158	N79-31841**
E-9872	p0157	N79-15448**	E-9973	p0075	N79-22274**
E-9873	p0015	N79-15049**	E-9974	p0104	N79-22426**
E-9874	p0157	N79-15450**	E-9976	p0097	N79-23348**
E-9875	p0008	N79-15013**	E-9977	p0115	N79-28554**
E-9876	p0083	N79-29327**	E-9979	p0127	N79-20398**
E-9877	p006	N79-16075**	E-9981	p0131	N79-22590**
E-9878	p0062	N79-16921**	E-9982	p0019	N79-23969**
E-9879	p0081	N79-15185**	E-9983	p0181	N79-22897**
E-9880	p0105	N79-30516**	E-9984	p0012	N79-23963**
E-9881	p0061	N79-16076**	E-9985	p0137	N79-22623**
E-9882	p0126	N79-16300**	E-9986	p0139	N79-25433**
E-9883	p0138	N79-24445**	E-9987	p0139	N79-25499**
E-9884	p0061	N79-16918**	E-9988	p0084	N79-30380**
E-9885	p0016	N79-15957**	E-9991	p0008	N79-33171**
E-9886	p0022	N79-25022**	E-9992	p0116	N79-37552**
E-9887	p0126	N79-15326**	E-9993	p0098	N79-31499**
E-9888	p0016	N79-15959**	E-9994	p0052	N79-22190**
E-9889	p0017	N79-15969**	E-9995	p0053	N79-22192**
E-9890	p0017	N79-16849**	E-9996	p0138	N79-24442**
E-9891	p0016	N79-15960**	E-9997	p0144	N79-33572**
E-9892	p0016	N79-15958**	E-9999	p0004	N79-26019**
E-9893	p0089	N79-20265**	E-10000	p0093	N79-23257**
E-9894	p0062	N79-20186**				
E-9895	p0127	N79-20390**	EPRI-EP1082-1-VOL-1	p0151	N79-13496**
E-9898	p0089	N79-13136**	EPRI-EP1082-1-VOL-2	p0152	N79-13497**
E-9899	p0173	N79-16645**				
E-9901	p0061	N79-16077**	ERIM-126100-3-F	p0131	N79-12524**
E-9902	p0173	N79-16646**				
E-9903	p0038	N79-28186**	EXXON/GRUS.1KWD.78	p0091	N79-20267**
E-9904	p0173	N79-16647**				
E-9905	p0134	N79-15410**	E79-10006	p0131	N79-12524**
E-9907	p0136	N79-20494**				
E-9908	p0126	N79-17263**	FAA-NA-78-156	p0016	N79-15052**
E-9909	p0083	N79-27308**				
E-9910	p0063	N79-28234**	FAA-RD-78-67	p0016	N79-15052**
E-9911	p0061	N79-16919**	FAA-RD-78-109	p0004	N79-23912**
E-9912	p0052	N79-20180**				
E-9912	p0098	N79-28420**	FCR-0398	p0151	N79-12553**
E-9913	p0017	N79-20114**	FCR-0945	p0154	N79-31784**
E-9914	p0173	N79-20829**	FCR-1017	p0155	N79-33581**
E-9915	p0074	N79-20217**				
E-9916	p0024	N79-17072**	FE-10179	p0032	N79-17857**
E-9917	p0062	N79-16920**	FE-11409	p0080	N79-32326**
E-9918	p0063	N79-20187**				
E-9919	p0173	N79-20830**	GASL-TR-250	p0071	N79-10165**
E-9920	p0161	N79-20572**				
E-9921	p0135	N79-15411**	GDC-NAS-79-001	p0108	N79-33432**
E-9922	p0094	N79-20300**				
E-9925	p0137	N79-21549**	GE78TME-60-VOL-1	p0151	N79-13496**
E-9926	p0063	N79-20188**	GE78TME-60-VOL-2	p0152	N79-13497**
E-9927	p0188	N79-27023**	GE79ET0101	p0155	N79-23560**
E-9928	p0042	N79-20171**				
E-9929	p0044	N79-20176**	HAC-REF-E1992-1	p0096	N79-33373**
E-9930	p0069	N79-25191**	HAC-REF-E1992-2	p0096	N79-33374**
E-9931	p0137	N79-20520**				
E-9932	p0157	N79-20527**	HI-78330	p0153	N79-21554**
E-9933	p0019	N79-24994**				
E-9934	p0098	N79-32467**	HRI-396	p0087	N79-30377**
E-9935	p0044	N79-23999**				
E-9937	p0090	N79-28350**	HSR-7383	p0150	N79-10525**
E-9938	p0165	N79-20752**				
E-9939	p0103	N79-20337**	IFSM-79-95	p0067	N79-30294**
E-9941	p0085	N79-33325**	IFSM-79-99	p0130	N79-31627**
E-9943	p0038	N79-33210**				
E-9944	p0084	N79-32359**	LG78ER0065	p0176	N79-14873**
E-9945	p0082	N79-20240**	LG78ER0243	p0176	N79-10842**
E-9946	p0023	N79-27142**				
E-9947	p0004	N79-23920**	LMSC-D564671-A	p0112	N79-21137**
E-9948	p0068	N79-20200**	LMSC-D673466-VOL-1	p0112	N79-21334**
E-9949	p0115	N79-31604**	LMSC-D673466-VOL-2	p0112	N79-21335**
E-9950	p0074	N79-20220**				
E-9951	p0063	N79-22211**	LMSC-HREC-TR-D497204-PT-1	p0166	N79-29832**
E-9952	p0097	N79-20316**	LMSC-HREC-TR-D497204-PT-2	p0166	N79-29833**
E-9953	p0181	N79-20864**	LMSC-HREC-TR-D568827-VOL-1	p0057	N79-19073**
E-9955	p0158	N79-20528**				

NASA-CR-3197	p0072	879-33288*
NASA-CR-134526	p0080	879-33305*
NASA-CR-134781	p0111	879-27478*
NASA-CR-135151	p0079	879-16948*
NASA-CR-135208	p0096	879-18159*
NASA-CR-135209	p0096	879-17071*
NASA-CR-135224	p0095	879-12273*
NASA-CR-135228	p0121	879-17226*
NASA-CR-135305	p0130	879-26429*
NASA-CR-135338	p0131	879-12524*
NASA-CR-135350	p0152	879-19448*
NASA-CR-135367	p0080	879-26175*
NASA-CR-135372	p0120	879-10423*
NASA-CR-135379	p0121	879-17219*
NASA-CR-135384	p0035	879-31207*
NASA-CR-135389	p0150	879-10525*
NASA-CR-135392	p0177	879-25845*
NASA-CR-135396	p0012	879-12084*
NASA-CR-135403	p0066	879-26120*
NASA-CR-135413	p0091	879-26221*
NASA-CR-135422	p0031	879-12088*
NASA-CR-135445	p0125	879-21410*
NASA-CR-135446	p0125	879-21411*
NASA-CR-135447	p0125	879-21412*
NASA-CR-135448	p0030	879-10061*
NASA-CR-157625	p0168	879-12968*
NASA-CR-157641	p0016	879-15052*
NASA-CR-158168	p0032	879-18978*
NASA-CR-158760	p0050	879-27234*
NASA-CR-159393	p0151	879-13490*
NASA-CR-159394	p0079	879-12202*
NASA-CR-159395	p0166	879-29832*
NASA-CR-159396	p0166	879-29833*
NASA-CR-159397	p0151	879-11473*
NASA-CR-159398	p0154	879-30801*
NASA-CR-159400	p0129	879-13405*
NASA-CR-159401	p0129	879-13406*
NASA-CR-159406	p0056	879-14153*
NASA-CR-159407	p0151	879-12550*
NASA-CR-159409	p0030	879-16058*
NASA-CR-159411-VOL-1	p0151	879-13496*
NASA-CR-159411-VOL-2	p0132	879-13497*
NASA-CR-159412	p0056	879-11115*
NASA-CR-159416	p0079	879-26222*
NASA-CR-159417	p0100	879-27398*
NASA-CR-159419	p0031	879-11042*
NASA-CR-159421	p0071	879-10165*
NASA-CR-159422	p0186	879-12969*
NASA-CR-159423	p0056	879-10120*
NASA-CR-159425	p0176	879-10812*
NASA-CR-159428	p0121	879-14355*
NASA-CR-159429	p0151	879-11476*
NASA-CR-159431	p0152	879-16374*
NASA-CR-159434	p0031	879-15053*
NASA-CR-159436	p0121	879-11406*
NASA-CR-159437	p0180	879-12884*
NASA-CR-159438	p0087	879-12230*
NASA-CR-159439	p0186	879-11921*
NASA-CR-159440	p0150	879-10526*
NASA-CR-159441-VOL-1	p0120	879-11408*
NASA-CR-159441-VOL-2	p0120	879-11409*
NASA-CR-159442-VOL-1	p0120	879-11407*
NASA-CR-159443	p0151	879-12553*
NASA-CR-159444	p0079	879-11180*
NASA-CR-159445	p0066	879-16924*
NASA-CR-159446	p0179	879-18711*
NASA-CR-159447	p0151	879-12554*
NASA-CR-159448	p0056	879-15152*
NASA-CR-159449	p0033	879-21160*
NASA-CR-159450	p0033	879-21070*
NASA-CR-159451	p0177	879-14875*
NASA-CR-159454	p0031	879-13050*
NASA-CR-159455	p0012	879-12087*
NASA-CR-159456	p0087	879-16053*
NASA-CR-159457	p0033	879-20117*
NASA-CR-159458	p0177	879-17656*
NASA-CR-159459	p0031	879-13048*
NASA-CR-159460	p0121	879-17222*
NASA-CR-159461	p0121	879-17223*
NASA-CR-159462	p0032	879-17858*
NASA-CR-159464	p0080	879-24121*
NASA-CR-159465	p0153	879-15454*
NASA-CR-159466	p0110	879-12418*
NASA-CR-159467	p0100	879-14141*
NASA-CR-159469	p0152	879-17300*
NASA-CR-159474	p0032	879-18977*
NASA-CR-159477	p0152	879-15451*
NASA-CR-159478	p0130	879-19414*
NASA-CR-159479	p0153	879-21754*

REPORT/ACCESSION NUMBER INDEX

NASA-CR-159480	p0091 N79-20267**	NASA-CR-159624	p0039 N79-29189**
NASA-CR-159481	p0015 N79-15046**	NASA-CR-159627-1	p0096 N79-33373**
NASA-CR-159484	p0129 N79-18343**	NASA-CR-159627-2	p0096 N79-33374**
NASA-CR-159485	p0056 N79-16913**	NASA-CR-159628	p0177 N79-27933**
NASA-CR-159486	p0110 N79-19314**	NASA-CR-159629	p0072 N79-31358**
NASA-CR-159487	p0035 N79-30189**	NASA-CR-159630	p0112 N79-32538**
NASA-CR-159488	p0032 N79-16850**	NASA-CR-159632	p0093 N79-30415**
NASA-CR-159490	p0152 N79-16375**	NASA-CR-159635	p0107 N79-30514**
NASA-CR-159491	p0057 N79-19074**	NASA-CR-159637	p0080 N79-32326**
NASA-CR-159503	p0041 N79-26102**	NASA-CR-159642	p0072 N79-32303**
NASA-CR-159504	p0041 N79-26101**	NASA-CR-159644	p0067 N79-31350**
NASA-CR-159505	p0032 N79-18976**	NASA-CR-159647	p0035 N79-32211**
NASA-CR-159508	p0153 N79-29603**	NASA-CR-159648	p0057 N79-31341**
NASA-CR-159509	p0121 N79-17221**	NASA-CR-159652	p0154 N79-31784**
NASA-CR-159510	p0087 N79-23218**	NASA-CR-159653	p0155 N79-33581**
NASA-CR-159511-VOL-2	p0096 N79-18160**	NASA-CR-159654	p0189 N79-32129**
NASA-CR-159513	p0091 N79-20266**	NASA-CR-159657	p0108 N79-33432**
NASA-CR-159514	p0087 N79-29331**	NASA-CR-159669	p0122 N79-31602**
NASA-CR-159515	p0034 N79-30185**	NASA-CR-159675	p0067 N79-33256**
NASA-CR-159516	p0034 N79-30186**	NASA-CR-159679	p0035 N79-32212**
NASA-CR-159519	p0180 N79-27975**		
NASA-CR-159520	p0057 N79-28224**	NASA-RP-1001	p0163 N79-25753**
NASA-CR-159521	p0112 N79-21337**	NASA-RP-1038	p0104 N79-22427**
NASA-CR-159522	p0057 N79-19073**		
NASA-CR-159523-VOL-1	p0112 N79-21334**	NASA-TN-73784	p0157 N79-17359**
NASA-CR-159523-VOL-2	p0112 N79-21335**	NASA-TN-73832	p0140 N79-26502**
NASA-CR-159524	p0100 N79-21273**	NASA-TN-75586	p0013 N79-12063**
NASA-CR-159526	p0100 N79-20317**	NASA-TN-78912	p0131 N79-13472**
NASA-CR-159527	p0057 N79-26110**	NASA-TN-78947	p0002 N79-10023**
NASA-CR-159528	p0040 N79-20161**	NASA-TN-78956	p0014 N79-13049**
NASA-CR-159529	p0153 N79-20467**	NASA-TN-78963	p0126 N79-11433**
NASA-CR-159530	p0153 N79-20497**	NASA-TN-78970	p0013 N79-11043**
NASA-CR-159532	p0032 N79-17857**	NASA-TN-78971	p0157 N79-17358**
NASA-CR-159533	p0033 N79-21075**	NASA-TN-78972	p0073 N79-12203**
NASA-CR-159534	p0179 N79-15828**	NASA-TN-78980	p0184 N79-16699**
NASA-CR-159536	p0071 N79-22244**	NASA-TN-78982	p0126 N79-19415**
NASA-CR-159537	p0067 N79-30294**	NASA-TN-78988	p0046 N79-11109**
NASA-CR-159538	p0130 N79-31627**	NASA-TN-78991	p0002 N79-11001**
NASA-CR-159539	p0034 N79-23084**	NASA-TN-78993	p0017 N79-17859**
NASA-CR-159540	p0122 N79-25395**	NASA-TN-78994	p0134 N79-11481**
NASA-CR-159542	p0072 N79-23168**	NASA-TN-78995	p0133 N79-11479**
NASA-CR-159543	p0122 N79-23429**	NASA-TN-78996	p0188 N79-11955**
NASA-CR-159544	p0067 N79-31348**	NASA-TN-78997	p0135 N79-16355**
NASA-CR-159545	p0034 N79-25020**	NASA-TN-78998	p0002 N79-12016**
NASA-CR-159549	p0079 N79-20221**	NASA-TN-78999	p0133 N79-11478**
NASA-CR-159550	p0107 N79-22434**	NASA-TN-79001	p0002 N79-11000**
NASA-CR-159551	p0033 N79-21076**	NASA-TN-79003	p0073 N79-12204**
NASA-CR-159552	p0122 N79-24373**	NASA-TN-79004	p0181 N79-12909**
NASA-CR-159553	p0072 N79-25178**	NASA-TN-79005	p0073 N79-11179**
NASA-CR-159554	p0111 N79-26384**	NASA-TN-79006	p0115 N79-23430**
NASA-CR-159555	p0034 N79-23285**	NASA-TN-79007	p0133 N79-11477**
NASA-CR-159556	p0033 N79-21073**	NASA-TN-79008	p0062 N79-12153**
NASA-CR-159560	p0101 N79-28418**	NASA-TN-79011	p0101 N79-12361**
NASA-CR-159563	p0087 N79-34377**	NASA-TN-79012	p0136 N79-17335**
NASA-CR-159564	p0038 N79-31206**	NASA-TN-79013	p0016 N79-15051**
NASA-CR-159565	p0153 N79-26506**	NASA-TN-79014	p0134 N79-11480**
NASA-CR-159566	p0034 N79-23970**	NASA-TN-79015	p0089 N79-15199**
NASA-CR-159567	p0162 N79-26943**	NASA-TN-79016	p0046 N79-15150**
NASA-CR-159568	p0091 N79-24172**	NASA-TN-79017	p0074 N79-20216**
NASA-CR-159569	p0009 N79-23940**	NASA-TN-79018	p0136 N79-17336**
NASA-CR-159572	p0153 N79-29604**	NASA-TN-79019	p0109 N79-12414**
NASA-CR-159574	p0034 N79-25018**	NASA-TN-79020	p0157 N79-12586**
NASA-CR-159575-VOL-1	p0177 N79-26884**	NASA-TN-79021	p0134 N79-12548**
NASA-CR-159575-VOL-2	p0177 N79-26885**	NASA-TN-79022	p0081 N79-12223**
NASA-CR-159575-VOL-3	p0177 N79-26886**	NASA-TN-79023	p0102 N79-15267**
NASA-CR-159577	p0155 N79-33560**	NASA-TN-79024	p0059 N79-11119**
NASA-CR-159579	p0092 N79-29382**	NASA-TN-79025	p0002 N79-12015**
NASA-CR-159580	p0189 N79-31088**	NASA-TN-79026	p0172 N79-16644**
NASA-CR-159581	p0107 N79-25349**	NASA-TN-79027	p0139 N79-26476**
NASA-CR-159586	p0122 N79-25392**	NASA-TN-79028	p0172 N79-15759**
NASA-CR-159593	p0100 N79-25312**	NASA-TN-79029	p0073 N79-12201**
NASA-CR-159594	p0067 N79-30295**	NASA-TN-79030	p0172 N79-15756**
NASA-CR-159595	p0100 N79-27397**	NASA-TN-79031	p0014 N79-12086**
NASA-CR-159596	p0034 N79-26055**	NASA-TN-79032	p0135 N79-17333**
NASA-CR-159601	p0166 N79-33881**	NASA-TN-79033	p0061 N79-15157**
NASA-CR-159602	p0156 N79-33882**	NASA-TN-79034	p0135 N79-16357**
NASA-CR-159603	p0034 N79-25017**	NASA-TN-79035	p0068 N79-16930**
NASA-CR-159604	p0169 N79-31087**	NASA-TN-79036	p0062 N79-12154**
NASA-CR-159605	p0178 N79-29110**	NASA-TN-79037	p0134 N79-15403**
NASA-CR-159607	p0166 N79-33883**	NASA-TN-79038	p0135 N79-16356**
NASA-CR-159608	p0178 N79-31088**	NASA-TN-79039	p0062 N79-12150**
NASA-CR-159612	p0071 N79-31839**	NASA-TN-79040	p0082 N79-16984**
NASA-CR-159613	p0094 N79-25184**	NASA-TN-79041	p0013 N79-12085**
NASA-CR-159614	p0156 N79-27716**	NASA-TN-79042	p0172 N79-15757**
NASA-CR-159615	p0091 N79-29355**	NASA-TN-79043	p0102 N79-12362**
NASA-CR-159616	p0080 N79-25196**	NASA-TN-79044	p0188 N79-16721**
NASA-CR-159618	p0049 N79-29191**	NASA-TN-79045	p0042 N79-15186**
NASA-CR-159622	p0122 N79-32557**	NASA-TN-79046	p0172 N79-15758**
NASA-CR-159623	p0107 N79-28456**	NASA-TN-79048	p0126 N79-15325**

REPORT/ACCESSION NUMBER INDEX

NASA-TM-79049	p0015	N79-15047**	NASA-TM-79139	p0139	N79-25498**
NASA-TM-79050	p0127	N79-20391**	NASA-TM-79140	p0139	N79-25499**
NASA-TM-79051	p0002	N79-12020**	NASA-TM-79141	p0052	N79-22190**
NASA-TM-79052	p0103	N79-20341**	NASA-TM-79142	p0053	N79-22192**
NASA-TM-79053	p0015	N79-15048**	NASA-TM-79143	p0138	N79-24442**
NASA-TM-79054	p0015	N79-15050**	NASA-TM-79144	p0004	N79-26019**
NASA-TM-79055	p0003	N79-14998**	NASA-TM-79145	p0093	N79-23257**
NASA-TM-79056	p0003	N79-14999**	NASA-TM-79146	p0046	N79-24000**
NASA-TM-79057	p0135	N79-17334**	NASA-TM-79147	p0131	N79-22589**
NASA-TM-79058	p0157	N79-15448**	NASA-TM-79148	p0018	N79-23964**
NASA-TM-79059	p0015	N79-15049**	NASA-TM-79148	p0018	N79-23964**
NASA-TM-79060	p0008	N79-15013**	NASA-TM-79149	p0138	N79-24443**
NASA-TM-79061	p0157	N79-15450**	NASA-TM-79150	p0003	N79-23911**
NASA-TM-79062	p0061	N79-16075**	NASA-TM-79151	p0075	N79-25195**
NASA-TM-79063	p0062	N79-16921**	NASA-TM-79152	p0131	N79-22590**
NASA-TM-79064	p0081	N79-15185**	NASA-TM-79153	p0053	N79-22193**
NASA-TM-79065	p0061	N79-16076**	NASA-TM-79154	p0012	N79-23965**
NASA-TM-79066	p0126	N79-16300**	NASA-TM-79155	p0173	N79-24770**
NASA-TM-79067	p0138	N79-24445**	NASA-TM-79156	p0046	N79-22188**
NASA-TM-79068	p0061	N79-16918**	NASA-TM-79157	p0018	N79-23966**
NASA-TM-79069	p0016	N79-15957**	NASA-TM-79157	p0018	N79-23966**
NASA-TM-79070	p0126	N79-15326**	NASA-TM-79158	p0104	N79-23384**
NASA-TM-79071	p0016	N79-15959**	NASA-TM-79159	p0109	N79-22448**
NASA-TM-79072	p0017	N79-15969**	NASA-TM-79160	p0138	N79-24444**
NASA-TM-79073	p0017	N79-16849**	NASA-TM-79161	p0137	N79-22624**
NASA-TM-79074	p0016	N79-15960**	NASA-TM-79163	p0140	N79-26503**
NASA-TM-79075	p0016	N79-15958**	NASA-TM-79164	p0094	N79-23313**
NASA-TM-79076	p0089	N79-20265**	NASA-TM-79165	p0083	N79-27306**
NASA-TM-79077	p0062	N79-20186**	NASA-TM-79167	p0174	N79-25840**
NASA-TM-79078	p0127	N79-20390**	NASA-TM-79168	p0174	N79-25841**
NASA-TM-79079	p0173	N79-16645**	NASA-TM-79169	p0139	N79-25500**
NASA-TM-79080	p0061	N79-16077**	NASA-TM-79170	p0142	N79-30719**
NASA-TM-79081	p0173	N79-16646**	NASA-TM-79171	p0004	N79-23920**
NASA-TM-79082	p0173	N79-16647**	NASA-TM-79172	p0138	N79-24446**
NASA-TM-79083	p0134	N79-15410**	NASA-TM-79173	p0110	N79-27480**
NASA-TM-79084	p0136	N79-20494**	NASA-TM-79174	p0140	N79-26504**
NASA-TM-79085	p0126	N79-17263**	NASA-TM-79175	p0043	N79-27238**
NASA-TM-79086	p0089	N79-16136**	NASA-TM-79176	p0004	N79-27093**
NASA-TM-79087	p0061	N79-16919**	NASA-TM-79177	p0098	N79-26316**
NASA-TM-79088	p0052	N79-20180**	NASA-TM-79178	p0075	N79-29292**
NASA-TM-79089	p0017	N79-20114**	NASA-TM-79179	p0075	N79-23196**
NASA-TM-79090	p0173	N79-20829**	NASA-TM-79180	p0127	N79-24359**
NASA-TM-79091	p0074	N79-20217**	NASA-TM-79181	p0044	N79-31264**
NASA-TM-79092	p0094	N79-17072**	NASA-TM-79182	p0053	N79-23133**
NASA-TM-79093	p0062	N79-16920**	NASA-TM-79183	p0022	N79-25015**
NASA-TM-79094	p0063	N79-20187**	NASA-TM-79184	p0043	N79-27235**
NASA-TM-79095	p0173	N79-20830**	NASA-TM-79185	p0115	N79-24350**
NASA-TM-79096	p0161	N79-20572**	NASA-TM-79186	p0141	N79-26505**
NASA-TM-79097	p0135	N79-15411**	NASA-TM-79187	p0165	N79-28861**
NASA-TM-79098	p0094	N79-20300**	NASA-TM-79188	p0059	N79-27242**
NASA-TM-79099	p0094	N79-16169**	NASA-TM-79189	p0075	N79-30355**
NASA-TM-79100	p0001	N79-20008**	NASA-TM-79190	p0043	N79-25129**
NASA-TM-79101	p0137	N79-21549**	NASA-TM-79191	p0053	N79-25131**
NASA-TM-79102	p0063	N79-20188**	NASA-TM-79192	p0104	N79-27460**
NASA-TM-79103	p0188	N79-27023**	NASA-TM-79193	p0141	N79-28725**
NASA-TM-79104	p0042	N79-20171**	NASA-TM-79194	p0139	N79-25501**
NASA-TM-79105	p0042	N79-20176**	NASA-TM-79195	p0142	N79-30720**
NASA-TM-79106	p0137	N79-20520**	NASA-TM-79196	p0022	N79-27140**
NASA-TM-79107	p0157	N79-20527**	NASA-TM-79197	p0141	N79-27663**
NASA-TM-79108	p0044	N79-23999**	NASA-TM-79198	p0094	N79-27351**
NASA-TM-79110	p0074	N79-20218**	NASA-TM-79200	p0142	N79-28727**
NASA-TM-79111	p0165	N79-20752**	NASA-TM-79201	p0168	N79-28970**
NASA-TM-79112	p0103	N79-20337**	NASA-TM-79203	p0089	N79-28349**
NASA-TM-79113	p0082	N79-20240**	NASA-TM-79204	p0022	N79-27141**
NASA-TM-79114	p0068	N79-20200**	NASA-TM-79206	p0075	N79-29293**
NASA-TM-79115	p0063	N79-22211**	NASA-TM-79207	p0084	N79-30378**
NASA-TM-79116	p0017	N79-20118**	NASA-TM-79208	p0174	N79-27930**
NASA-TM-79117	p0074	N79-20220**	NASA-TM-79209	p0142	N79-29599**
NASA-TM-79118	p0073	N79-12205**	NASA-TM-79210	p0069	N79-27279**
NASA-TM-79119	p0097	N79-20316**	NASA-TM-79211	p0004	N79-29143**
NASA-TM-79120	p0181	N79-20664**	NASA-TM-79212	p0105	N79-27461**
NASA-TM-79121	p0158	N79-20528**	NASA-TM-79213	p0141	N79-27665**
NASA-TM-79122	p0137	N79-21550**	NASA-TM-79214	p0115	N79-28554**
NASA-TM-79123	p0018	N79-23968**	NASA-TM-79215	p0142	N79-28728**
NASA-TM-79124	p0003	N79-20069**	NASA-TM-79216	p0141	N79-27664**
NASA-TM-79125	p0053	N79-22191**	NASA-TM-79217	p0053	N79-28220**
NASA-TM-79126	p0169	N79-23735**	NASA-TM-79218	p0004	N79-28146**
NASA-TM-79127	p0103	N79-20338**	NASA-TM-79219	p0063	N79-29224**
NASA-TM-79128	p0103	N79-20346**	NASA-TM-79220	p0090	N79-31405**
NASA-TM-79129	p0127	N79-22565**	NASA-TM-79221	p0170	N79-29938**
NASA-TM-79130	p0136	N79-20498**	NASA-TM-79222	p0142	N79-28726**
NASA-TM-79131	p0075	N79-22274**	NASA-TM-79223	p0064	N79-30296**
NASA-TM-79132	p0104	N79-22426**	NASA-TM-79225	p0069	N79-28258**
NASA-TM-79133	p0127	N79-20398**	NASA-TM-79226	p0063	N79-29240**
NASA-TM-79134	p0019	N79-23969**	NASA-TM-79227	p0076	N79-30356**
NASA-TM-79135	p0161	N79-22897**	NASA-TM-79228	p0083	N79-29329**
NASA-TM-79136	p0012	N79-23963**	NASA-TM-79229	p0105	N79-31526**
NASA-TM-79137	p0137	N79-22623**	NASA-TM-79230	p0084	N79-30379**
NASA-TM-79138	p0097	N79-23348**	NASA-TM-79232	p0064	N79-31349**

REPORT/ACCESSION NUMBER INDEX

NASA-TM-79234	p0098	N79-31499**	NASA-TP-1486	p0098	N79-28420**
NASA-TM-79235	p0142	N79-29600**	NASA-TP-1487	p0090	N79-28350**
NASA-TM-79236	p0174	N79-31002**	NASA-TP-1488	p0038	N79-28186**
NASA-TM-79237	p0023	N79-30187**	NASA-TP-1489	p0083	N79-27308**
NASA-TM-79239	p0010	N79-31185**	NASA-TP-1490	p0083	N79-27309**
NASA-TM-79240	p0105	N79-31527**	NASA-TP-1491	p0023	N79-27142**
NASA-TM-79241	p0090	N79-31403**	NASA-TP-1492	p0105	N79-29467**
NASA-TM-79244	p0143	N79-31781**	NASA-TP-1493	p0023	N79-27143**
NASA-TM-79245	p0084	N79-31391**	NASA-TP-1502	p0024	N79-31213**
NASA-TM-79246	p0125	N79-29530**	NASA-TP-1509	p0083	N79-29327**
NASA-TM-79247	p0048	N79-31265**	NASA-TP-1510	p0024	N79-31214**
NASA-TM-79251	p0069	N79-31361**	NASA-TP-1511	p0116	N79-31605**
NASA-TM-79254	p0024	N79-31210**	NASA-TP-1523	p0038	N79-33210**
NASA-TM-79255	p0053	N79-30290**	NASA-TP-1524	p0084	N79-30381**
NASA-TM-79256	p0054	N79-33252**	NASA-TP-1525	p0084	N79-30380**
NASA-TM-79257	p0054	N79-33253**	NASA-TP-1526	p0158	N79-31841**
NASA-TM-79258	p0105	N79-30515**	NASA-TP-1527	p0098	N79-32467**
NASA-TM-79259	p0076	N79-33306**	NASA-TP-1530	p0116	N79-33475**
NASA-TM-79260	p0127	N79-31619**	NASA-TP-1542	p0116	N79-32552**
NASA-TM-79261	p0054	N79-33254**	NASA-TP-1544	p0084	N79-32359**
NASA-TM-79262	p0010	N79-33185**	NASA-TP-1545	p0059	N79-31346**
NASA-TM-79265	p0094	N79-33379**	NASA-TP-1547	p0116	N79-33476**
NASA-TM-79266	p0054	N79-31343**	NASA-TP-1559	p0144	N79-33572**
NASA-TM-79267	p0024	N79-30188**	NASA-TP-1560	p0008	N79-33171**
NASA-TM-79269	p0076	N79-31372**			
NASA-TM-79271	p0054	N79-33255**	CNERRA, TP NO. 1979-79		A79-49537 *
NASA-TM-79273	p0085	N79-33325**			
NASA-TM-79292	p0116	N79-33477**	ORNL-5547	p0122	N79-25395**
NASA-TP-1083	p0023	N79-28176**	PCBL-FR-79-001	p0040	N79-20161**
NASA-TP-1217	p0097	N79-14309**	PRBL-77-CR-46	p0152	N79-19448**
NASA-TP-1263	p0046	N79-15149**			
NASA-TP-1278	p0023	N79-28177**	FWA-FR-10299	p0030	N79-10058**
NASA-TP-1299	p0002	N79-10022**			
NASA-TP-1322	p0014	N79-13046**	FWA-5500-18	p0012	N79-12084**
NASA-TP-1323	p0015	N79-14095**	FWA-5515-77	p0033	N79-21076**
NASA-TP-1338	p0013	N79-10060**	FWA-5518-38	p0033	N79-20116**
NASA-TP-1339	p0113	N79-10425**	FWA-5523-42	p0034	N79-26055**
NASA-TP-1343	p0081	N79-10158**	FWA-5550-8	p0025	N79-31212**
NASA-TP-1345	p0003	N79-13003**	FWA-5550-16-VCL-1	p0034	N79-30185**
NASA-TP-1346	p0113	N79-10424**	FWA-5550-17-VCL-2	p0034	N79-30186**
NASA-TP-1347	p0184	N79-13886**	FWA-5558-12	p0110	N79-12418**
NASA-TP-1376	p0094	N79-14275**	FWA-5565-15	p0031	N79-13050**
NASA-TP-1377	p0081	N79-15184**	FWA-5581-12	p0034	N79-23084**
NASA-TP-1378	p0113	N79-13369**	FWA-5583-25	p0034	N79-23085**
NASA-TP-1379	p0081	N79-13159**	FWA-5594-41	p0032	N79-16850**
NASA-TP-1380	p0003	N79-14996**	FWA-5594-41	p0035	N79-30189**
NASA-TP-1382	p0082	N79-21204**	FWA-5615-3	p0110	N79-19314**
NASA-TP-1387	p0114	N79-14387**	FWA-5626-12	p0035	N79-32211**
NASA-TP-1388	p0001	N79-16796**	FWA-5633-11	p0122	N79-31602**
NASA-TP-1390	p0114	N79-14389**			
NASA-TP-1391	p0103	N79-18288**	F78-683B	p0100	N79-20317**
NASA-TP-1392	p0114	N79-14386**			
NASA-TP-1393	p0015	N79-14099**	QPR-4	p0032	N79-18978**
NASA-TP-1394	p0114	N79-17227**			
NASA-TP-1399	p0018	N79-23967**	REFT-8	p0157	N79-15048**
NASA-TP-1407	p0059	N79-21128**	REFT-02-4778	p0091	N79-10126**
NASA-TP-1409	p0017	N79-16852**	REFT-791830-PT-5	p0122	N79-24373**
NASA-TP-1410	p0044	N79-21120**			
NASA-TP-1411	p0181	N79-19867**	RI/RD78-28	p0121	N79-17221**
NASA-TP-1412	p0173	N79-17659**			
NASA-TP-1413	p0114	N79-18323**	RRC-78-B-607	p0151	N79-11473**
NASA-TP-1414	p0109	N79-17195**			
NASA-TP-1415	p0157	N79-18479**	R77AEG450	p0032	N79-18978**
NASA-TP-1416	p0097	N79-17139**	R77AEG570	p0032	N79-20117**
NASA-TP-1425	p0022	N79-25023**	R78-912941-15	p0087	N79-23218**
NASA-TP-1437	p0082	N79-21205**	R78AEG319	p0177	N79-17656**
NASA-TP-1438	p0115	N79-22518**	R78AEG518	p0031	N79-15053**
NASA-TP-1439	p0069	N79-22246**	R78AEG529	p0031	N79-12088**
NASA-TP-1440	p0137	N79-22626**	R78AEG551	p0031	N79-13048**
NASA-TP-1441	p0166	N79-21798**	R78AEG568	p0031	N79-11042**
NASA-TP-1442	p0074	N79-21184**	R79-912997-39	p0067	N79-33256**
NASA-TP-1443	p0115	N79-22519**	R79AEG166-VCL-1	p0177	N79-26884**
NASA-TP-1444	p0111	N79-21329**	R79AEG166-VCL-2	p0177	N79-26885**
NASA-TP-1445	p0063	N79-28234**	R79AEG166-VCL-3	p0177	N79-26886**
NASA-TP-1449	p0097	N79-22375**	R79AEG197	p0067	N79-31348**
NASA-TP-1450	p0059	N79-22194**	R79AEG295	p0033	N79-21074**
NASA-TP-1451	p0156	N79-22654**	R79AEG356	p0039	N79-29191**
NASA-TP-1452	p0017	N79-22099**	R79AEG367	p0091	N79-26221**
NASA-TP-1456	p0053	N79-23132**	R79AEG376	p0072	N79-31358**
NASA-TP-1458	p0115	N79-21604**	R79AEG388	p0034	N79-23970**
NASA-TP-1462	p0082	N79-23216**	R79AEG410	p0035	N79-31267**
NASA-TP-1465	p0105	N79-30516**			
NASA-TP-1466	p0166	N79-23688**	SAE PAPER 780995	p0026	A79-25880*
NASA-TP-1475	p0022	N79-25022**	SAE PAPER 781003	p0026	A79-25885*
NASA-TP-1476	p0069	N79-25181**	SAE PAPER 790327	p0119	A79-31368*
NASA-TP-1483	p0024	N79-30191**	SAE PAPER 790573	p0119	A79-36759*
NASA-TP-1484	p0105	N79-29468**	SAE PAPER 790596	p0028	A79-36729*
NASA-TP-1485	p0098	N79-27400**			

REPORT/ACCESSION NUMBER INDEX

SAE PAPER 790605	p0036	A79-36737*	US-PATENT-APPL-SN-863770	p0136	N79-18444*
SAE PAPER 790607	p0028	A79-36760*	US-PATENT-APPL-SN-891244	p0011	N79-24976*
SAE PAPER 790619	p0028	A79-36747*	US-PATENT-APPL-SN-891370	p0052	N79-20179*
SAE PAPER 790621	p0036	A79-36749*	US-PATENT-APPL-SN-897829	p0138	N79-25481*
SAI-102-79-002	p0101	N79-28418**	US-PATENT-APPL-SN-899123	p0134	N79-14528*
SAR-1	p0072	N79-25183**	US-PATENT-APPL-SN-914260	p0139	N79-26474*
SAR-2	p0080	N79-25184**	US-PATENT-APPL-SN-950876	p0113	N79-10426**
SCG-90272R	p0096	N79-33374**	US-PATENT-APPL-SN-953391	p0181	N79-10894**
SCG-90275R	p0096	N79-33373**	US-PATENT-APPL-SN-958575	p0081	N79-11216**
SRC-TE-78-39	p0122	N79-23429**	US-PATENT-APPL-SN-961832	p0113	N79-12445**
SRC-TE-78-36	p0032	N79-18976**	US-PATENT-APPL-SN-964754	p0134	N79-14538**
SRD-78-186	p0177	N79-14875**	US-PATENT-APPL-SN-971473	p0068	N79-14173**
SRD-78-191	p0079	N79-20222**	US-PATENT-APPL-SN-971596	p0068	N79-14172**
SRD-78-158	p0079	N79-16548**	US-PATENT-CLASS-29-572	p0133	N79-11468*
SR79-R-4655-15	p0034	N79-25018**	US-PATENT-CLASS-29-572	p0133	N79-11472*
SSS-R-78-3739	p0100	N79-27398**	US-PATENT-CLASS-29-572	p0136	N79-18444*
SSS-E-79-3904	p0100	N79-27397**	US-PATENT-CLASS-29-578	p0136	N79-18444*
SU-HMT-27	p0106	N79-22428**	US-PATENT-CLASS-29-591	p0109	N79-17192*
SU-HMT-28	p0107	N79-22429**	US-PATENT-CLASS-55-118	p0109	N79-17192*
TELEDYNE-CAE-1600	p0039	N79-29189**	US-PATENT-CLASS-55-122	p0109	N79-17192*
TR-79-1	p0072	N79-32303**	US-PATENT-CLASS-55-127	p0109	N79-17192*
TR-251	p0091	N79-20266**	US-PATENT-CLASS-55-155	p0109	N79-17192*
TRB-101	p0153	N79-20497**	US-PATENT-CLASS-55-241	p0109	N79-17192*
TRW-ER-8019-1	p0092	N79-29382**	US-PATENT-CLASS-55-242	p0109	N79-17192*
TRW-ER-8028	p0079	N79-11180**	US-PATENT-CLASS-55-360	p0109	N79-17192*
TRW-30979-6003-RU-00	p0107	N79-22434**	US-PATENT-CLASS-55-407	p0109	N79-17192*
TRW-31781-6016-RU-00	p0087	N79-18053**	US-PATENT-CLASS-60-39.08	p0113	N79-11403*
TRW-32100-6009-RU-00	p0180	N79-12884**	US-PATENT-CLASS-60-39.14	p0013	N79-10057*
TRW-32937-6001-TU-00	p0107	N79-25349**	US-PATENT-CLASS-60-39.28R	p0113	N79-11403*
TRW-33631-6006-RU-00	p0100	N79-25312**	US-PATENT-CLASS-60-39.31	p0014	N79-14096*
UCLA-ENG-7718	p0130	N79-19414**	US-PATENT-CLASS-60-39.66	p0113	N79-11403*
UDR-TR-79-17	p0096	N79-17071**	US-PATENT-CLASS-60-226A	p0014	N79-14096*
UDR-TR-79-18-VOL-1	p0096	N79-18159**	US-PATENT-CLASS-60-226B	p0014	N79-14096*
UDR-TR-79-19-VOL-2	p0096	N79-18160**	US-PATENT-CLASS-60-267	p0102	N79-13288*
US-PATENT-APPL-SN-007083	p0073	N79-19145**	US-PATENT-CLASS-60-267	p0102	N79-13289*
US-PATENT-APPL-SN-009887	p0136	N79-18455**	US-PATENT-CLASS-62-268	p0103	N79-20326*
US-PATENT-APPL-SN-027557	p0059	N79-24061**	US-PATENT-CLASS-62-376	p0103	N79-20336*
US-PATENT-APPL-SN-032307	p0104	N79-23383**	US-PATENT-CLASS-62-514R	p0103	N79-20336*
US-PATENT-APPL-SN-041146	p0083	N79-24154**	US-PATENT-CLASS-73-115	p0109	N79-14345*
US-PATENT-APPL-SN-070771	p0059	N79-31345**	US-PATENT-CLASS-136-89	p0133	N79-11468*
US-PATENT-APPL-SN-073579	p0098	N79-32463**	US-PATENT-CLASS-136-89SC	p0133	N79-11467*
US-PATENT-APPL-SN-400857	p0093	N79-21225*	US-PATENT-CLASS-136-89SJ	p0134	N79-14528*
US-PATENT-APPL-SN-414042	p0109	N79-17192*	US-PATENT-CLASS-136-202	p0109	N79-14346*
US-PATENT-APPL-SN-430748	p0184	N79-21510*	US-PATENT-CLASS-136-236	p0109	N79-14346*
US-PATENT-APPL-SN-513346	p0014	N79-14095*	US-PATENT-CLASS-137-15.1	p0014	N79-14096*
US-PATENT-APPL-SN-552108	p0104	N79-14096*	US-PATENT-CLASS-137-15.1	p0011	N79-24976*
US-PATENT-APPL-SN-555846	p0102	N79-13289*	US-PATENT-CLASS-148-2	p0074	N79-22271*
US-PATENT-APPL-SN-559847	p0102	N79-13288*	US-PATENT-CLASS-148-6.3	p0136	N79-18444*
US-PATENT-APPL-SN-573029	p0014	N79-14097*	US-PATENT-CLASS-148-12.4	p0074	N79-22271*
US-PATENT-APPL-SN-667929	p0109	N79-14346*	US-PATENT-CLASS-148-12F	p0074	N79-22271*
US-PATENT-APPL-SN-702115	p0172	N79-14871*	US-PATENT-CLASS-148-188	p0133	N79-11468*
US-PATENT-APPL-SN-745766	p0113	N79-11403*	US-PATENT-CLASS-156-17	p0184	N79-21910*
US-PATENT-APPL-SN-753452	p0014	N79-14096*	US-PATENT-CLASS-165-146	p0102	N79-13289*
US-PATENT-APPL-SN-760771	p0134	N79-14528*	US-PATENT-CLASS-165-169	p0102	N79-13288*
US-PATENT-APPL-SN-768795	p0102	N79-10339*	US-PATENT-CLASS-165-169	p0102	N79-13289*
US-PATENT-APPL-SN-772167	p0069	N79-22235*	US-PATENT-CLASS-181-190	p0172	N79-14871*
US-PATENT-APPL-SN-776029	p0013	N79-10057*	US-PATENT-CLASS-181-213	p0172	N79-14871*
US-PATENT-APPL-SN-776146	p0135	N79-17313*	US-PATENT-CLASS-181-222	p0172	N79-14871*
US-PATENT-APPL-SN-792616	p0113	N79-10418*	US-PATENT-CLASS-181-293	p0172	N79-14871*
US-PATENT-APPL-SN-796263	p0083	N79-28307*	US-PATENT-CLASS-195-103.5R	p0069	N79-22235*
US-PATENT-APPL-SF-799026	p0133	N79-11468*	US-PATENT-CLASS-195-127	p0069	N79-22235*
US-PATENT-APPL-SN-801290	p0114	N79-18318*	US-PATENT-CLASS-204-11	p0069	N79-22235*
US-PATENT-APPL-SN-803822	p0074	N79-22271*	US-PATENT-CLASS-222-131	p0093	N79-21225*
US-PATENT-APPL-SN-803823	p0133	N79-11467*	US-PATENT-CLASS-239-127.1	p0102	N79-13288*
US-PATENT-APPL-SN-814006	p0115	N79-22475*	US-PATENT-CLASS-239-127.1	p0102	N79-13289*
US-PATENT-APPL-SN-829315	p0103	N79-20336*	US-PATENT-CLASS-239-265.39	p0014	N79-14097*
US-PATENT-APPL-SN-837796	p0109	N79-14345*	US-PATENT-CLASS-244-53B	p0011	N79-24976*
US-PATENT-APPL-SN-846346	p0133	N79-11472*	US-PATENT-CLASS-244-54	p0014	N79-14096*
US-PATENT-APPL-SN-853679	p0109	N79-14345*	US-PATENT-CLASS-250-352	p0103	N79-20336*
US-PATENT-APPL-SN-856462	p0104	N79-21513**	US-PATENT-CLASS-252-12.2	p0062	N79-17916*
US-PATENT-APPL-SN-860405	p0074	N79-22271*	US-PATENT-CLASS-260-37N	p0083	N79-28307*
US-PATENT-APPL-SN-860406	p0062	N79-17916*	US-PATENT-CLASS-260-42	p0083	N79-28307*
			US-PATENT-CLASS-260-53	p0083	N79-28307*
			US-PATENT-CLASS-277-62	p0115	N79-22475*
			US-PATENT-CLASS-277-96.1	p0115	N79-22475*
			US-PATENT-CLASS-301-82	p0102	N79-10339*
			US-PATENT-CLASS-308-DIG.1	p0113	N79-10418*
			US-PATENT-CLASS-308-DIG.8	p0062	N79-17916*
			US-PATENT-CLASS-308-DIG.9	p0062	N79-17916*
			US-PATENT-CLASS-308-56	p0113	N79-10418*
			US-PATENT-CLASS-308-9	p0113	N79-10418*
			US-PATENT-CLASS-308-78	p0062	N79-17916*
			US-PATENT-CLASS-308-87B	p0062	N79-17916*
			US-PATENT-CLASS-308-121	p0113	N79-10418*
			US-PATENT-CLASS-308-160	p0113	N79-10418*
			US-PATENT-CLASS-308-163	p0113	N79-10418*

REPORT/ACCESSION NUMBER INDEX

US-PATENT-CLASS-308-168	p0062	N79-17916*	US-PATENT-4,143,314	p0052	N79-20179*
US-PATENT-CLASS-308-171	p0062	N79-17916*	US-PATENT-4,145,058	p0115	N79-22475*
US-PATENT-CLASS-308-172	p0113	N79-10418*	US-PATENT-4,145,255	p0069	N79-22235*
US-PATENT-CLASS-313-22	p0103	N79-20336*	US-PATENT-4,146,109	p0074	N79-22271*
US-PATENT-CLASS-313-35	p0103	N79-20336*	US-PATENT-4,154,256	p0011	N79-24976*
US-PATENT-CLASS-315-3.5	p0102	N79-10339*	US-PATENT-4,154,912	p0138	N79-25481*
US-PATENT-CLASS-315-3.6	p0102	N79-10339*	US-PATENT-4,159,262	p0083	N79-28307*
US-PATENT-CLASS-323-15	p0052	N79-20179*	US-PATENT-4,159,366	p0139	N79-26474*
US-PATENT-CLASS-323-20	p0052	N79-20179*				
US-PATENT-CLASS-330-43	p0102	N79-10339*	OTEC/R78-912897-15	p0087	N79-29331**
US-PATENT-CLASS-357-15	p0133	N79-11467*	OTEC/R79-914104-18	p0071	N79-22244**
US-PATENT-CLASS-357-16	p0133	N79-11467*				
US-PATENT-CLASS-357-30	p0133	N79-11467*	WAWL-M-FR-74-005-PT-2	p0080	N79-33305**
US-PATENT-CLASS-357-30	p0134	N79-14528*				
US-PATENT-CLASS-357-65	p0133	N79-11467*	WQEC/C-78-224	p0151	N79-13490**
US-PATENT-CLASS-357-67	p0133	N79-11467*				
US-PATENT-CLASS-415-115	p0013	N79-10057*	WRC-78-113-15	p0034	N79-25017**
US-PATENT-CLASS-415-116	p0013	N79-10057*				
US-PATENT-CLASS-415-174	p0114	N79-18318*	IECS-2361	...	p0056	N79-10120**
US-PATENT-CLASS-415-200	p0014	N79-14096*				
US-PATENT-CLASS-415-200	p0114	N79-16318*				
US-PATENT-CLASS-415-201	p0014	N79-14096*				
US-PATENT-CLASS-416-157B	p0014	N79-14095*				
US-PATENT-CLASS-416-160	p0014	N79-14095*				
US-PATENT-CLASS-416-162	p0014	N79-14095*				
US-PATENT-CLASS-416-167	p0014	N79-14095*				
US-PATENT-CLASS-427-34	p0062	N79-17916*				
US-PATENT-CLASS-427-75	p0133	N79-11468*				
US-PATENT-CLASS-427-75	p0133	N79-11472*				
US-PATENT-CLASS-427-84	p0133	N79-11472*				
US-PATENT-CLASS-427-123	p0133	N79-11472*				
US-PATENT-CLASS-427-126	p0133	N79-11472*				
US-PATENT-CLASS-427-261	p0133	N79-11472*				
US-PATENT-CLASS-427-292	p0062	N79-17916*				
US-PATENT-CLASS-427-327	p0062	N79-17916*				
US-PATENT-CLASS-427-328	p0062	N79-17916*				
US-PATENT-CLASS-427-343	p0133	N79-11472*				
US-PATENT-CLASS-427-355	p0062	N79-17916*				
US-PATENT-CLASS-427-376B	p0062	N79-17916*				
US-PATENT-CLASS-427-376C	p0062	N79-17916*				
US-PATENT-CLASS-427-398A	p0133	N79-11472*				
US-PATENT-CLASS-427-399	p0133	N79-11472*				
US-PATENT-CLASS-429-15	p0139	N79-26474*				
US-PATENT-CLASS-429-33	p0135	N79-17313*				
US-PATENT-CLASS-429-101	p0135	N79-17313*				
US-PATENT-CLASS-429-101	p0139	N79-26474*				
US-PATENT-CLASS-429-253	p0138	N79-25481*				
US-PATENT-CLASS-526-7	p0138	N79-25481*				
US-PATENT-CLASS-526-9	p0138	N79-25481*				
US-PATENT-CLASS-528-126	p0083	N79-28307*				
US-PATENT-CLASS-528-127	p0083	N79-28307*				
US-PATENT-CLASS-528-128	p0083	N79-28307*				
US-PATENT-CLASS-528-221	p0083	N79-28307*				
US-PATENT-CLASS-528-223	p0083	N79-28307*				
US-PATENT-CLASS-528-225	p0083	N79-28307*				
US-PATENT-CLASS-528-227	p0083	N79-28307*				
US-PATENT-CLASS-528-229	p0083	N79-28307*				
US-PATENT-CLASS-528-331	p0083	N79-28307*				
US-PATENT-CLASS-528-336	p0083	N79-28307*				
US-PATENT-CLASS-528-337	p0083	N79-28307*				
US-PATENT-CLASS-528-338	p0083	N79-28307*				
US-PATENT-CLASS-528-342	p0083	N79-28307*				
US-PATENT-CLASS-544-193	p0083	N79-28307*				
US-PATENT-CLASS-2041-155B	p0069	N79-22235*				
US-PATENT-3,215,313	p0093	N75-21225*				
US-PATENT-3,429,756	p0184	N75-21910*				
US-PATENT-4,099,799	p0113	N79-10418*				
US-PATENT-4,104,084	p0133	N79-11467*				
US-PATENT-4,104,091	p0133	N79-11468*				
US-PATENT-4,104,873	p0113	N79-11403*				
US-PATENT-4,106,587	p0172	N79-14871*				
US-PATENT-4,107,919	p0102	N79-13288*				
US-PATENT-4,108,241	p0102	N79-13289*				
US-PATENT-4,111,041	p0109	N79-14346*				
US-PATENT-4,111,718	p0109	N79-14346*				
US-PATENT-4,117,669	p0013	N79-10057*				
US-PATENT-4,118,671	p0102	N79-10339*				
US-PATENT-4,122,214	p0133	N79-11472*				
US-PATENT-4,124,310	p0014	N79-14095*				
US-PATENT-4,131,486	p0134	N79-14528*				
US-PATENT-4,132,068	p0014	N79-14095*				
US-PATENT-4,132,069	p0014	N79-14096*				
US-PATENT-4,133,941	p0135	N79-17313*				
US-PATENT-4,134,744	p0109	N79-17192*				
US-PATENT-4,135,290	p0136	N79-16444*				
US-PATENT-4,135,851	p0114	N79-18318*				
US-PATENT-4,136,211	p0062	N79-17916*				
US-PATENT-4,141,224	p0103	N79-20336*				